VOLUME 29 / NUMBER 5
MARCH 8, 1991
ACC. NOS. N91-13399 TO N91-14272

STAR

AN ABSTRACT JOURNAL

Scientific and Technical Aerospace Reports

PRODUCED BY THE
SCIENTIFIC AND TECHNICAL
INFORMATION
DIVISION

NASA

NATIONAL AERONAUTICS AND SPACE ADMINISTRATION

***Scientific and Technical Aerospace Reports* (*STAR*)** is an abstract journal that provides comprehensive coverage of worldwide aerospace-related reports. It is a major product of the International Aerospace Database managed by the NASA Scientific and Technical Information (STI) Program. The coverage includes reports on aeronautics, space, and supporting disciplines. *STAR* lists current, publicly available reports entered into the NASA STI Database during the 2-week period preceding publication. An explanation of items that appear in each citation is given on the last page of each volume.

NASA sponsors a companion journal, *International Aerospace Abstracts* (*IAA*), that lists abstracts of the open literature on aerospace subjects available worldwide. *IAA* is available through the American Institute of Aeronautics and Astronautics.

Entries found in *STAR* and *IAA* are available through NASA's online service, RECON, as the International Aerospace Database and through DIALOG as the Aerospace Database.

Information on aerospace and related subjects is gathered by the NASA STI Program through national and international agreements and exchanges and is made available to the NASA community as well as to the public in many forms through various outlets. The section on NASA STI Program Products and Services contains additional information.

US ISSN 0036-8741

Volume 29 Number 5 / March 8, 1991

TABLE OF CONTENTS

AERONAUTICS For related information see also *Astronautics.*

01 AERONAUTICS (GENERAL) **613**

02 AERODYNAMICS **613**
Includes aerodynamics of bodies, combinations, wings, rotors, and control surfaces; and internal flow in ducts and turbomachinery. For related information see also *34 Fluid Mechanics and Heat Transfer.*

03 AIR TRANSPORTATION AND SAFETY **617**
Includes passenger and cargo air transport operations; and aircraft accidents. For related information see also *16 Space Transportation* and *85 Urban Technology and Transportation.*

04 AIRCRAFT COMMUNICATIONS AND NAVIGATION **618**
Includes digital and voice communication with aircraft; air navigation systems (satellite and ground based); and air traffic control. For related information see also *17 Space Communications, Spacecraft Communications, Command and Tracking* and *32 Communications and Radar.*

05 AIRCRAFT DESIGN, TESTING AND PERFORMANCE **619**
Includes aircraft simulation technology. For related information see also *18 Spacecraft Design, Testing and Performance* and *39 Structural Mechanics.* For land transportation vehicles see *85 Urban Technology and Transportation.*

06 AIRCRAFT INSTRUMENTATION **622**
Includes cockpit and cabin display devices; and flight instruments. For related information see also *19 Space craft Instrumentation* and *35 Instrumentation and Photography.*

07 AIRCRAFT PROPULSION AND POWER **623**
Includes prime propulsion systems and systems components, e.g., gas turbine engines and compressors; and onboard auxiliary power plants for aircraft. For related information see also *20 Spacecraft Propulsion and Power, 28 Propellants and Fuels,* and *44 Energy Production and Conversion.*

08 AIRCRAFT STABILITY AND CONTROL **624**
Includes aircraft handling qualities; piloting; flight controls; and autopilots. For related information see also *05 Aircraft Design, Testing and Performance.*

09 RESEARCH AND SUPPORT FACILITIES (AIR) **625**
Includes airports, hangars and runways; aircraft repair and overhaul facilities; wind tunnels; shock tubes; and aircraft engine test stands. For related information see also *14 Ground Support Systems and Facilities (Space).*

ASTRONAUTICS For related information see also *Aeronautics.*

12 ASTRONAUTICS (GENERAL) **626**
For extraterrestrial exploration see *91 Lunar and Planetary Exploration.*

13 ASTRODYNAMICS ..... **N.A.**
Includes powered and free-flight trajectories; and orbital and launching dynamics.

14 GROUND SUPPORT SYSTEMS AND FACILITIES (SPACE) ..... **N.A.**
Includes launch complexes, research and production facilities; ground support equipment, e.g., mobile transporters; and simulators. For related information see also *09 Research and Support Facilities (Air).*

15 LAUNCH VEHICLES AND SPACE VEHICLES ..... **N.A.**
Includes boosters; operating problems of launch/space vehicle systems; and reusable vehicles. For related information see also *20 Spacecraft Propulsion and Power.*

16 SPACE TRANSPORTATION ..... **N.A.**
Includes passenger and cargo space transportation, e.g., shuttle operations; and space rescue techniques. For related information see also *03 Air Transportation and Safety* and *18 Spacecraft Design, Testing and Performance.* For space suits see *54 Man/System Technology and Life Support.*

17 SPACE COMMUNICATIONS, SPACECRAFT COMMUNICATIONS, COMMAND AND TRACKING . **N.A.**
Includes telemetry; space communications networks; astronavigation and guidance; and radio blackout. For related information see also *04 Aircraft Communications and Navigation* and *32 Communications and Radar.*

N.A.—no abstracts were assigned to this category for this issue.

18 SPACECRAFT DESIGN, TESTING AND PERFORMANCE **627**
Includes satellites; space platforms; space stations; spacecraft systems and components such as thermal and environmental controls; and attitude controls. For life support systems see *54 Man/System Technology and Life Support.* For related information see also *05 Aircraft Design, Testing and Performance, 39 Structural Mechanics,* and *16 Space Transportation.*

19 SPACECRAFT INSTRUMENTATION **629**
For related information see also *06 Aircraft Instrumentation* and *35 Instrumentation and Photography.*

20 SPACECRAFT PROPULSION AND POWER **629**
Includes main propulsion systems and components, e.g., rocket engines; and spacecraft auxiliary power sources. For related information see also *07 Aircraft Propulsion and Power, 28 Propellants and Fuels, 44 Energy Production and Conversion,* and *15 Launch Vehicles and Space Vehicles.*

CHEMISTRY AND MATERIALS

23 CHEMISTRY AND MATERIALS (GENERAL) ..... **N.A.**

24 COMPOSITE MATERIALS **630**
Includes physical, chemical, and mechanical properties of laminates and other composite materials. For ceramic materials see *27 Nonmetallic Materials.*

25 INORGANIC AND PHYSICAL CHEMISTRY **633**
Includes chemical analysis, e.g., chromatography; combustion theory; electrochemistry; and photochemistry. For related information see also *77 Thermodynamics and Statistical Physics.*

26 METALLIC MATERIALS **635**
Includes physical, chemical, and mechanical properties of metals, e.g., corrosion; and metallurgy.

27 NONMETALLIC MATERIALS **637**
Includes physical, chemical, and mechanical properties of plastics, elastomers, lubricants, polymers, textiles, adhesives, and ceramic materials. For composite materials see *24 Composite Materials.*

28 PROPELLANTS AND FUELS **643**
Includes rocket propellants, igniters and oxidizers; their storage and handling procedures; and aircraft fuels. For related information see also *07 Aircraft Propulsion and Power, 20 Spacecraft Propulsion and Power,* and *44 Energy Production and Conversion.*

29 MATERIALS PROCESSING **644**
Includes space-based development of products and processes for commercial application. For biological materials see *55 Space Biology.*

ENGINEERING For related information see also *Physics.*

31 ENGINEERING (GENERAL) **644**
Includes vacuum technology; control engineering; display engineering; cryogenics; and fire prevention.

32 COMMUNICATIONS AND RADAR **646**
Includes radar; land and global communications; communications theory; and optical communications. For related information see also *04 Aircraft Communications and Navigation* and *17 Space Communications, Spacecraft Communications, Command and Tracking.* For search and rescue see *03 Air Transportation and Safety,* and *16 Space Transportation.*

33 ELECTRONICS AND ELECTRICAL ENGINEERING **650**
Includes test equipment and maintainability; components, e.g., tunnel diodes and transistors; microminiaturization; and integrated circuitry. For related information see also *60 Computer Operations and Hardware* and *76 Solid-State Physics.*

34 FLUID MECHANICS AND HEAT TRANSFER **655**
Includes boundary layers; hydrodynamics; fluidics; mass transfer and ablation cooling. For related information see also *02 Aerodynamics* and *77 Thermodynamics and Statistical Physics.*

35 INSTRUMENTATION AND PHOTOGRAPHY **661**
Includes remote sensors; measuring instruments and gauges; detectors; cameras and photographic supplies; and holography. For aerial photography see *43 Earth Resources and Remote Sensing.* For related information see also *06 Aircraft Instrumentation* and *19 Spacecraft Instrumentation.*

36 LASERS AND MASERS **665**
Includes parametric amplifiers. For related information see also *76 Solid-State Physics.*

37 MECHANICAL ENGINEERING **668**
Includes auxiliary systems (nonpower); machine elements and processes; and mechanical equipment.

38 QUALITY ASSURANCE AND RELIABILITY **673**
Includes product sampling procedures and techniques; and quality control.

39 STRUCTURAL MECHANICS **674**
Includes structural element design and weight analysis; fatigue; and thermal stress. For applications see *05 Aircraft Design, Testing and Performance* and *18 Spacecraft Design, Testing and Performance.*

GEOSCIENCES For related information see also *Space Sciences.*

42 GEOSCIENCES (GENERAL) **680**

43 EARTH RESOURCES AND REMOTE SENSING **680**
Includes remote sensing of earth resources by aircraft and spacecraft; photogrammetry; and aerial photography. For instrumentation see *35 Instrumentation and Photography.*

44 ENERGY PRODUCTION AND CONVERSION **682**
Includes specific energy conversion systems, e.g., fuel cells; global sources of energy; geophysical conversion; and windpower. For related information see also *07 Aircraft Propulsion and Power, 20 Spacecraft Propulsion and Power,* and *28 Propellants and Fuels.*

45 ENVIRONMENT POLLUTION **684**
Includes atmospheric, noise, thermal, and water pollution.

46 GEOPHYSICS **686**
Includes aeronomy; upper and lower atmosphere studies; ionospheric and magnetospheric physics; and geomagnetism. For space radiation see *93 Space Radiation.*

47 METEOROLOGY AND CLIMATOLOGY **689**
Includes weather forecasting and modification.

48 OCEANOGRAPHY **690**
Includes biological, dynamic, and physical oceanography; and marine resources. For related information see also *43 Earth Resources and Remote Sensing.*

LIFE SCIENCES

51 LIFE SCIENCES (GENERAL) **690**

52 AEROSPACE MEDICINE **694**
Includes physiological factors; biological effects of radiation; and effects of weightlessness on man and animals.

53 BEHAVIORAL SCIENCES **695**
Includes psychological factors; individual and group behavior; crew training and evaluation; and psychiatric research.

54 MAN/SYSTEM TECHNOLOGY AND LIFE SUPPORT **696**
Includes human engineering; biotechnology; and space suits and protective clothing. For related information see also *16 Space Transportation.*

55 SPACE BIOLOGY ..... **N.A.**
Includes exobiology; planetary biology; and extraterrestrial life.

MATHEMATICAL AND COMPUTER SCIENCES

59 MATHEMATICAL AND COMPUTER SCIENCES (GENERAL) ..... **N.A.**

60 COMPUTER OPERATIONS AND HARDWARE **698**
Includes hardware for computer graphics, firmware, and data processing. For components see *33 Electronics and Electrical Engineering.*

61 COMPUTER PROGRAMMING AND SOFTWARE **699**
Includes computer programs, routines, algorithms, and specific applications, e.g., CAD/CAM.

62 COMPUTER SYSTEMS **704**
Includes computer networks and special application computer systems.

63 CYBERNETICS **706**
Includes feedback and control theory, artificial intelligence, robotics and expert systems. For related information see also *54 Man/System Technology and Life Support.*

64 NUMERICAL ANALYSIS **708**
Includes iteration, difference equations, and numerical approximation.

65 STATISTICS AND PROBABILITY **711**
Includes data sampling and smoothing; Monte Carlo method; and stochastic processes.

66 SYSTEMS ANALYSIS **711**
Includes mathematical modeling; network analysis; and operations research.

67 THEORETICAL MATHEMATICS **711**
Includes topology and number theory.

PHYSICS For related information see also *Engineering.*

70 PHYSICS (GENERAL) **711**
For precision time and time interval (PTTI) see *35 Instrumentation and Photography;* for geophysics, astrophysics or solar physics see *46 Geophysics, 90 Astrophysics,* or *92 Solar Physics.*

71 ACOUSTICS **711**
Includes sound generation, transmission, and attenuation. For noise pollution see *45 Environment Pollution.*

72 ATOMIC AND MOLECULAR PHYSICS **713**
Includes atomic structure, electron properties, and molecular spectra.

73 NUCLEAR AND HIGH-ENERGY PHYSICS **714**
Includes elementary and nuclear particles; and reactor theory. For space radiation see *93 Space Radiation.*

74 OPTICS **715**
Includes light phenomena and optical devices. For lasers see *36 Lasers and Masers.*

75 PLASMA PHYSICS **717**
Includes magnetohydrodynamics and plasma fusion. For ionospheric plasmas see *46 Geophysics.* For space plasmas see *90 Astrophysics.*

76 SOLID-STATE PHYSICS **722**
Includes superconductivity. For related information see also *33 Electronics and Electrical Engineering* and *36 Lasers and Masers.*

77 THERMODYNAMICS AND STATISTICAL PHYSICS **728**
Includes quantum mechanics; theoretical physics; and Bose and Fermi statistics. For related information see also *25 Inorganic and Physical Chemistry* and *34 Fluid Mechanics and Heat Transfer.*

SOCIAL SCIENCES

80 SOCIAL SCIENCES (GENERAL) ..... **N.A.**
Includes educational matters.

81 ADMINISTRATION AND MANAGEMENT ..... **N.A.**
Includes management planning and research.

82 DOCUMENTATION AND INFORMATION SCIENCE **729**
Includes information management; information storage and retrieval technology; technical writing; graphic arts; and micrography. For computer documentation see *61 Computer Programming and Software.*

83 ECONOMICS AND COST ANALYSIS ..... **N.A.**
Includes cost effectiveness studies.

84 LAW, POLITICAL SCIENCE AND SPACE POLICY ..... **N.A.**
Includes NASA appropriation hearings; aviation law; space law and policy; international law; international cooperation; and patent policy.

85 URBAN TECHNOLOGY AND TRANSPORTATION **731**
Includes applications of space technology to urban problems; technology transfer; technology assessment; and surface and mass transportation. For related information see *03 Air Transportation and Safety, 16 Space Transportation,* and *44 Energy Production and Conversion.*

SPACE SCIENCES For related information see also *Geosciences.*

88 SPACE SCIENCES (GENERAL) **732**

89 ASTRONOMY **732**
Includes radio, gamma-ray, and infrared astronomy; and astrometry.

90 ASTROPHYSICS **733**
Includes cosmology; celestial mechanics; space plasmas; and interstellar and interplanetary gases and dust. For related information see also *75 Plasma Physics.*

91 LUNAR AND PLANETARY EXPLORATION **765**
Includes planetology; and manned and unmanned flights. For spacecraft design or space stations see *18 Spacecraft Design, Testing and Performance.*

92 SOLAR PHYSICS **767**
Includes solar activity, solar flares, solar radiation and sunspots. For related information see *93 Space Radiation.*

93 SPACE RADIATION **768**
Includes cosmic radiation; and inner and outer earth's radiation belts. For biological effects of radiation see *52 Aerospace Medicine.* For theory see *73 Nuclear and High-Energy Physics.*

GENERAL

Includes aeronautical, astronautical, and space science related histories, biographies, and pertinent reports too broad for categorization; histories or broad overviews of NASA programs.

99 GENERAL **769**

SUBJECT INDEX **I-1**

PERSONAL AUTHOR INDEX **I-61**

CORPORATE SOURCE INDEX **I-69**

CONTRACT NUMBER INDEX **I-81**

REPORT/ACCESSION NUMBER INDEX **I-85**

APPENDIX **A-1**

VOLUME 29 NUMBER 5 / MARCH 8, 1991

Scientific and Technical Aerospace Reports

A Semimonthly Publication of the National Aeronautics and Space Administration

01 AERONAUTICS (GENERAL)

N91-13399* National Aeronautics and Space Administration, Washington, DC.
AERONAUTICAL ENGINEERING: A CONTINUING BIBLIOGRAPHY WITH INDEXES (SUPPLEMENT 258)
Dec. 1988 167 p
(NASA-SP-7037(258); NAS 1.21:7037(258)) Avail: NTIS HC A08; NTIS standing order as PB89-914100, $11.50 domestic, $23.00 foreign CSCL 01B

This bibliography lists 536 reports, articles, and other documents introduced into the NASA scientific and technical information system in October 1990. Subject coverage includes: design, construction and testing of aircraft and aircraft engines; aircraft components, equipment and systems; ground support systems; and theoretical and applied aspects of aerodynamics and general fluid dynamics. Author

02 AERODYNAMICS

Includes aerodynamics of bodies, combinations, wings, rotors, and control surfaces; and internal flow in ducts and turbomachinery.

For related information see also *34 Fluid Mechanics and Heat Transfer.*

N91-13400*# National Aeronautics and Space Administration. Langley Research Center, Hampton, VA.
CLOSE-RANGE PHOTOGRAMMETRIC MEASUREMENT OF STATIC DEFLECTIONS FOR AN AEROELASTIC SUPERCRITICAL WING
Thomas A. Byrdsong, Richard R. Adams, and Maynard C. Sandford Washington Dec. 1990 93 p
(NASA-TM-4194; L-16720; NAS 1.15:4194) Avail: NTIS HC/MF A05 CSCL 01A

Close range photogrammetric measurements were made for the lower wing surface of a full span aspect ratio 10.3 aeroelastic supercritical research wing. The measurements were made during wind tunnel tests for quasi-steady pressure distributions on the wing. The tests were conducted in the NASA Langley Transonic Dynamics Tunnel at Mach numbers up to 0.90 and dynamic pressures up to 300 pounds per square foot. Deflection data were obtained for 57 locations on the wing lower surface using dual non-metric cameras. Representative data are presented as graphical overview to show variations and trends of spar deflection with test variables. Comparative data are presented for photogrammetric and cathetometric results of measurements for the wing tip deflections. A tabulation of the basic measurements is presented in a supplement to this report. Author

N91-13401*# National Aeronautics and Space Administration. Langley Research Center, Hampton, VA.
NAVIER-STOKES AND EULER SOLUTIONS FOR LEE-SIDE FLOWS OVER SUPERSONIC DELTA WINGS. A CORRELATION WITH EXPERIMENT
S. Naomi McMillin, James L. Thomas, and Earll M. Murman (Massachusetts Inst. of Tech., Cambridge.) Washington Dec. 1990 103 p Original contains color illustrations
(NASA-TP-3035; L-16751; NAS 1.60:3035) Avail: NTIS HC/MF A06; 19 functional color pages CSCL 01A

An Euler flow solver and a thin layer Navier-Stokes flow solver were used to numerically simulate the supersonic leeside flow fields over delta wings which were observed experimentally. Three delta wings with 75, 67.5, and 60 deg leading edge sweeps were computed over an angle-of-attack range of 4 to 20 deg at a Mach number 2.8. The Euler code and Navier-Stokes code predict equally well the primary flow structure where the flow is expected to be separated or attached at the leading edge based on the Stanbrook-Squire boundary. The Navier-Stokes code is capable of predicting both the primary and the secondary flow features for the parameter range investigated. For those flow conditions where the Euler code did not predict the correct type of primary flow structure, the Navier-Stokes code illustrated that the flow structure is sensitive to boundary layer model. In general, the laminar Navier-Stokes solutions agreed better with the experimental data, especially for the lower sweep delta wings. The computational results and a detailed re-examination of the experimental data resulted in a refinement of the flow classifications. This refinement in the flow classification results in the separation bubble with the shock flow type as the intermediate flow pattern between separated and attached flows. Author

N91-13402*# National Aeronautics and Space Administration. Langley Research Center, Hampton, VA.
EFFECT OF LOCATION OF AFT-MOUNTED NACELLES ON THE LONGITUDINAL AERODYNAMIC CHARACTERISTICS OF A HIGH-WING TRANSPORT AIRPLANE
William K. Abeyounis and James C. Patterson, Jr. (Vigyan Research Associates, Inc., Hampton, VA.) Washington Dec. 1990 98 p
(NASA-TP-3047; L-16743; NAS 1.60:3047) Avail: NTIS HC/MF A05 CSCL 01A

As part of a propulsion/airframe integration program at Langley Research Center, tests were conducted in the Langley 16-Foot Transonic Tunnel to determine the effects of locating flow-through mixed flow engine nacelles in several aft underwing positions on the longitudinal aerodynamics of a high wing transport airplane. D-shaped inlet nacelles were used in the test. Some configurations with antishock bodies and with nacelle toe-in were also tested. Data were obtained for a free stream Mach number range of 0.70 to 0.85 and a model angle-of-attack range from -2.5 to 4.0 degrees. Author

N91-13403 Stanford Univ., CA.
DEVELOPMENT AND EVALUATION OF CONTINUUM MODELS FOR TRANSLATIONAL-ROTATIONAL NONEQUILIBRIUM Ph.D. Thesis
Forrest Edward Lumpkin, III 1990 132 p
Avail: Univ. Microfilms Order No. DA9024344

It is assumed that continuum models for translational and rotational nonequilibrium may be developed independently and then applied to flows with combined translational-rotational nonequilibrium. The Burnett equations, obtained from the Chapman-Enskog expansion carried one order beyond Navier-Stokes, significantly improve computations of shock structure in monatomic gases where translational nonequilibrium alone exists. The Burnett equations are assumed to model translational nonequilibrium in diatomic gases. Alternative

constitutive relations which capture the essential features of the Burnett equations but are easier to implement are also presented and evaluated. The theoretical basis of Jeans' equation for rotational energy relaxation is reviewed. A more general model is developed from recent experimental measurements of rotational quantum transition rates. These rates are used in a solution of the master equation for a stationary gas in rotational nonequilibrium, and numerous such solutions are used to create the new rotational relaxation model. The above models are applied to the diatomic shock structure as a test case and are found to significantly improve the continuum description. The Burnett and simplified constitutive models are found to give shock thicknesses in close agreement with one another. The new rotational relaxation model based on transition rate data, in conjunction with either translational nonequilibrium model, is found to give good agreement with experimental shock thicknesses up to Mach 6. In a similar manner, Jeans' equation in conjunction with Lordi and Mates determinations of the rotational collision number Z(sub R) is found to under predict shock thicknesses at high Mach numbers. Modifications to the Lordi and Mates values of Z(sub R) are suggested which improve the agreement with experiment at high Mach numbers.

Dissert. Abstr.

N91-13404*# Georgia Inst. of Tech., Atlanta. Flight Mechanics and Control.

ANALYTICAL AERODYNAMIC MODEL OF A HIGH ALPHA RESEARCH VEHICLE WIND-TUNNEL MODEL

Jichang Cao, Frederick Garrett, Jr., Eric Hoffman, and Harold Stalford Sep. 1990 127 p

(Grant NAG1-959)

(NASA-CR-187362; NAS 1.26:187362) Avail: NTIS HC/MF A07 CSCL 01A

A 6 DOF analytical aerodynamic model of a high alpha research vehicle is derived. The derivation is based on wind-tunnel model data valid in the altitude-Mach flight envelope centered at 15,000 ft altitude and 0.6 Mach number with Mach range between 0.3 and 0.9. The analytical models of the aerodynamics coefficients are nonlinear functions of alpha with all control variable and other states fixed. Interpolation is required between the parameterized nonlinear functions. The lift and pitching moment coefficients have unsteady flow parts due to the time range of change of angle-of-attack (alpha dot). The analytical models are plotted and compared with their corresponding wind-tunnel data. Piloted simulated maneuvers of the wind-tunnel model are used to evaluate the analytical model. The maneuvers considered are pitch-ups, 360 degree loaded and unloaded rolls, turn reversals, split S's, and level turns. The evaluation finds that (1) the analytical model is a good representation at Mach 0.6, (2) the longitudinal part is good for the Mach range 0.3 to 0.9, and (3) the lateral part is good for Mach numbers between 0.6 and 0.9. The computer simulations show that the storage requirement of the analytical model is about one tenth that of the wind-tunnel model and it runs twice as fast. Author

N91-13405*# Wayne State Univ., Detroit, MI. Dept. of Mathematics.

ANALYSIS OF THE LEADING EDGE EFFECTS ON THE BOUNDARY LAYER TRANSITION Technical Report, 1 Mar. 1984 - 31 Aug. 1990

Pao-Liu Chow 24 Oct. 1990 32 p

(Grant NAG1-460)

(NASA-CR-187361; NAS 1.26:187361) Avail: NTIS HC/MF A03 CSCL 01A

A general theory of boundary layer control by surface heating is presented. Some analytical results for a simplified model, i.e., the optimal control of temperature fluctuations in a shear flow are described. The results may provide a clue to the effectiveness of the active feedback control of a boundary layer flow by wall heating. In a practical situation, the feedback control may not be feasible from the instrumentational point of view. In this case the vibrational control introduced in systems science can provide a useful alternative. This principle is briefly explained and applied to the control of an unstable wavepacket in a parallel shear flow.

Author

N91-13406*# National Aeronautics and Space Administration. Langley Research Center, Hampton, VA.

AERODYNAMIC EFFECT OF STRAKES ON TWO-DIMENSIONAL TAIL BOOM MODELS OF THE OH-58A AND THE OH-58D HELICOPTERS

Cynthia A. Crowell and Henry L. Kelley (Army Aerostructures Directorate, Hampton, VA.) Washington Dec. 1990 34 p

(DA Proj. 1L1-62211-A-47-A)

(NASA-TM-4248; L-16842; NAS 1.15:4248; AVSCOM-TR-90-B-010) Avail: NTIS HC/MF A03 CSCL 01A

During hover and low speed flight, helicopters experience significant aerodynamic forces on the tail boom caused by the wake from the main and tail rotors and by crosswinds. These effects were simulated during a study conducted in the Langley 14 by 22 Foot Subsonic Tunnel on a 136 percent scaled 2-D tail boom model with cross sections representative of those on the U.S. Army OH-58A and the OH-58D helicopters. The effects of longitudinal strakes attached to the cross sections were studied. To obtain the aerodynamic forces acting on the cross sections, the flow incidence range on the scaled models was varied from -45 to 90 degrees and the models were tested through a dynamic pressure range of 5 to 15 psf. The results of the OH-58A and the OH-58D configurations show a significant improvement at conditions which represent right sideward flight by reducing the adverse aerodynamic side force when the strakes are installed. These data were used to calculate a change in tail rotor power for the full scale flight vehicle and indicated approx. a 5 to 6 percent average savings in right sideward flight for the critical velocity range of 0 to 30 knots. Increases in the tail boom normal force were noted due to the strakes. The results indicate a potential for reducing the directional control and tail rotor thrust required in the critical hover and right sideward flight speed range with a calculated minimum increase to main rotor power required and an overall net improvement in power of 0.5 percent for both the OH-58A and OH-58D. Author

N91-13407 Georgia Inst. of Tech., Atlanta.

DEVELOPMENT OF A FULL POTENTIAL SOLVER FOR ROTOR AERODYNAMICS ANALYSIS Ph.D. Thesis

Devon S. Prichard 1990 210 p

Avail: Univ. Microfilms Order No. DA9031268

A computer program for calculating the unsteady, three-dimensional transonic potential flow about isolated rotor blades was developed. This method calculates the nearfield aerodynamics of arbitrarily shaped rotor blades by solving a conservative form of the unsteady full potential equations on a body-fitted grid. The application of this code to rotor flow problems was extended through the development of improved blade dynamics and farfield wake modeling, and incorporation of boundary layer modeling in the flow solution. Evaluation of the full potential solver applied to rotor problems and evaluations of the blade motion and boundary layer works are presented. Dissert. Abstr.

N91-13408*# National Aeronautics and Space Administration. Ames Research Center, Moffett Field, CA.

INDICIAL RESPONSE APPROACH DERIVED FROM NAVIER-STOKES EQUATIONS. PART 1: TIME-INVARIANT EQUILIBRIUM STATE

K. V. Truong and M. Tobak Oct. 1990 22 p

(NASA-TM-102856; A-90258; NAS 1.15:102856) Avail: NTIS HC/MF A03 CSCL 01A

The indicial response approach is recast in a form appropriate to the study of vortex induced oscillations phenomena. An appropriate form is demonstrated for the indicial response of the velocity field which may be derived directly from the Navier-Stokes equations. On the basis of the Navier-Stokes equations, it is demonstrated how a form of the velocity response to an arbitrary motion may be determined. To establish its connection with the previous work, the new approach is applied first to the simple situation wherein the indicial response has a time invariant

equilibrium state. Results for the aerodynamic response to an arbitrary motion are shown to confirm to the form obtained previously. Author

N91-13409# National Research Council of Canada, Ottawa (Ontario). Inst. for Aerospace Research.
THE IAR HIGH REYNOLDS NUMBER TWO-DIMENSIONAL TEST FACILITY: A DESCRIPTION OF EQUIPMENT AND PROCEDURES COMMON TO MOST 2-D AIRFOIL TESTS
R. D. Galway Jun. 1990 53 p
(AD-A226629; IAR-AN-66; NRC-32132) Avail: NTIS HC/MF A04 CSCL 14/2

Features and operational procedures are described which are common to the great majority of wind tunnel test projects conducted in the Two-Dimensional (2-D) Test Facility of the Institute of Aerospace Research (IAR) 1.5 m Trisonic Blowdown Wind Tunnel in Ottawa, Canada. The 'facility specific' aspects of tests performed in the above facility are described along with test reports for individual projects which concentrate on aspects which are specific to the particular model and test. The 2-D test facility as modernized by the commissioning of a new interchangeable 2-D test section module in early 1989 is described in detail. GRA

N91-13410*# Institute for Computer Applications in Science and Engineering, Hampton, VA.
LARGE-EDDY SIMULATION OF TRANSITIONAL CHANNEL FLOW Final Report
Ugo Piomelli and Thomas A. Zang (National Aeronautics and Space Administration. Langley Research Center, Hampton, VA.) Nov. 1990 15 p Submitted for publication
(Contract NAS1-18605)
(NASA-CR-187465; ICASE-90-80; NAS 1.26:187465) Avail: NTIS HC/MF A03 CSCL 01A

A large-eddy simulation (LES) of transition in plane channel flow was carried out. The LES results were compared with those of a fine direct numerical simulation (DNS), and with those of a coarse DNS that uses the same mesh as the LES, but does not use a residual stress model. While at the early stages of transition, LES and coarse DNS give the same results: the presence of the residual stress model was found to be necessary to predict accurately mean velocity and Reynolds stress profiles during the late stages of transition (after the second spike stage). The evolution of single Fourier modes is also predicted more accurately by the LES than by the DNS. As small scales are generated, the dissipative character of the residual stress starts to reproduce correctly the energy cascade. As transition progresses, the flow approaches its fully developed turbulent state, the subgrid scales tend towards equilibrium, and the model becomes more accurate. Author

N91-13411*# National Aeronautics and Space Administration. Langley Research Center, Hampton, VA.
SOME OBSERVATIONS ON THE HOUBOLT-RAINEY AND PEAK-HOLD METHODS OF FLUTTER ONSET PREDICTION
Robert V. Doggett, Jr. Nov. 1990 12 p
(NASA-TM-102745; NAS 1.15:102745) Avail: NTIS HC/MF A03 CSCL 01A

A subcritical response method for flutter onset prediction developed by Houbolt and Rainey in 1958 is compared with the Peak-Hold Method which was apparently first applied to flutter onset prediction by Sandford, Abel, and Gray in the early 1970's. The rational argument presented shows that the two methods are not different, but are actually the same. So, because there is an analytical foundation for the Houbolt-Rainey Method, then there is the same analytical foundation for the Peak-Hold Method. Further, it is suggested that, in applying Peak-Hold Method in cases where turbulence is used as the excitation force, the variation of the reciprocal of the response amplitude with the reciprocal of the dynamic pressure to be used to extrapolate to flutter onset rather than the variation with dynamic pressure which is the current practice because the linear trend which is predicted to occur for the former is easier to extrapolate to the flutter condition than the nonlinear trend predicted to occur for the latter. Author

N91-13412*# National Aeronautics and Space Administration. Langley Research Center, Hampton, VA.
SOME BUFFET RESPONSE CHARACTERISTICS OF A TWIN-VERTICAL-TAIL CONFIGURATION
Stanley R. Cole, Steven W. Moss, and Robert V. Doggett, Jr. Oct. 1990 25 p Prepared in cooperation with Arnold Engineering Development Center, Arnold Air Force Station, TN
(NASA-TM-102749; NAS 1.15:102749) Avail: NTIS HC/MF A03 CSCL 01A

A rigid, 1/6 size, full span model of an F-18 airplane was fitted with flexible vertical tails of two different levels of stiffness that were buffet tested in the Langley Transonic Dynamics Tunnel. Vertical tail buffet response results that were obtained over the range of angles of attack from -10 to 40 degs, and over the range of Mach numbers from 0.30 to 0.95 are presented. These results indicate the following: (1) the response occurs in the first bending mode; (2) the response increases with increasing dynamic pressure, but changes in response are not linearly proportional to the changes in dynamic pressure; (3) the response is larger at M = 0.30 than it is at the higher Mach numbers; (4) the maximum intensity of the buffeting is described as heavy to severe using an assessment criteria proposed by another investigator; and (5) the data at different dynamic pressures and for the different tails correlate reasonably well using the buffet excitation parameter derived from the dynamic analysis of buffeting. Author

N91-13413*# National Aeronautics and Space Administration. Langley Research Center, Hampton, VA.
INSTABILITY OF A SUPERSONIC SHOCK FREE ELLIPTIC JET
Roy S. Baty (Sandia National Labs., Albuquerque, NM.), John M. Seiner, and Michael K. Ponton 1990 14 p Presented at the 13th AIAA Aeroacoustics Conference, Tallahassee, FL, 22-24 Oct. 1990
(Contract NAG1-657; DE-AC04-76DP-00789)
(NASA-TM-103428; NAS 1.15:103428; DE91-001231; SAND-90-0179C; CONF-9010223-1) Avail: NTIS HC/MF A03 CSCL 01A

This paper presents a comparison of the measured and the computed spatial stability properties of an aspect ratio 2 supersonic shock free elliptic jet. The shock free nature of the elliptic jet provides an ideal test of validity of modeling the large scale coherent structures in the initial mixing region of noncircular supersonic jets with linear hydrodynamic stability theory. Both aerodynamic and acoustic data were measured. The data are used to compute the mean velocity profiles and to provide a description of the spatial composition of pressure waves in the elliptic jet. A hybrid numerical scheme is applied to solve the Rayleigh problem governing the inviscid linear spatial stability of the jet. The measured mean velocity profiles are used to provide a qualitative model for the cross sectional geometry and the smooth velocity profiles used in the stability analysis. Computational results are presented for several modes of instability at two jet cross sections. The acoustic measurements show that a varicose instability is the jet's perferred mode of motion. The stability analysis predicts that the Strouhal number varies linearly as a function of axial distance in the jet's initial mixing region, which is in good qualitative agreement with previous measurements. DOE

N91-13414# SRI International Corp., Menlo Park, CA.
SPANWISE AERODYNAMIC LOADS ON A ROTATING WIND TURBINE BLADE
C. P. Butterfield, D. Simms, W. Musial, and G. Scott Oct. 1990 6 p Presented at the Windpower '90, Washington, DC, 25-28 Sep. 1990
(Contract DE-AC02-83CH-10093)
(DE91-002101; SERI/TP-257-3983; CONF-9009107-4) Avail: NTIS HC/MF A02

Wind turbine performance and load predictions depend on accurate airfoil performance data. Wind tunnel test data are typically used which accurately describe two-dimensional airfoil performance characteristics. Usually these data are only available for a range of angles of attack from 0 to 15 deg, which excludes the stall characteristics. Airfoils on stall-controlled wind turbines operate in

deep stall in medium to high winds. Therefore it is very important to know how the airfoil will perform in these high load conditions. Butterfield et al. have shown that three-dimensional effects and rotation of the blade modify the two-dimensional performance of the airfoil. These effects are modified to different degrees throughout the blade span. The Solar Energy Research Institute (SERI) has conducted a series of tests to measure the spanwise variation of airfoil performance characteristics on a rotating wind turbine blade. Maximum lift coefficients were measured to be 200 percent greater than wind tunnel results at the 30 percent span. Stall characteristics were generally modified throughout the span. Lift characteristics were unmodified for low to medium angles of attack. This paper discusses these test results for four spanwise locations. DOE

N91-13415# Deutsche Forschungsanstalt fuer Luft- und Raumfahrt, Brunswick (Germany, F.R.). Abt. Flugmechanik der Drehfluegelflugzeuge.

ANALYTIC FORMULATIONS OF UNSTEADY PROFILE AERODYNAMICS AND ITS APPLICATION TO SIMULATION OF ROTORS

Berend vanderWall Mar. 1990 117 p In GERMAN; ENGLISH summary Report will also be announced as translation (ESA-TT-1244)
(DLR-FB-90-28; ISSN-0171-1342; ETN-91-98260; ESA-TT-1244) Avail: NTIS HC/MF A06; DLR, VB-PL-DO, Postfach 90 60 58, 5000 Cologne, Fed. Republic of Germany, HC 42 DM

A new way of modeling rotor aerodynamics is presented using a set of formulas describing the steady aerodynamic behavior of a profile. It offers the possibility to transfer the periodically changing velocities at the profile to an also periodically changing phase lag of angle of attack and dynamic stall effect directly in simulation. A model method is used for the description of blade dynamics. Induced velocities are formulated by a prescribed distorted spiral geometry, fitting well with measurements. Results show that this configuration is a good compromise between short calculation time requirements and accuracy of results, especially for higher harmonic control calculations. ESA

N91-13416# Aeronautical Research Inst. of Sweden, Stockholm. Dept. of Aerodynamics.

TRANSONIC WIND TUNNEL TESTS ON TWO-DIMENSIONAL AEROFOIL SECTIONS: DETERMINATION OF PRESSURE DISTRIBUTION AND DRAG FOR AN AEROFOIL OF TYPE SAAB 7301 IN FFA WIND TUNNEL S5

Goeran Ehn Dec. 1989 160 p
(Contract FMV-82223-72-004)
(FFA-TN-1989-47; ETN-91-98265) Avail: NTIS HC/MF A08

A symmetrical two dimensional airfoil model was investigated in a 0.25 sq m wind tunnel. The airfoil profile has a relative thickness of 12 percent at 40 percent of the chord. It is constructed to have shock free flow at the design Mach number M equals 0.7966, with a maximum local Mach number of M equals 1.104. The test program included airfoil pressure distribution measurements and wake drag measurements in the Mach number range M situated between 0.5 and 0.86 for angles of attack degrees alpha situated between -4 and 4. Boundary layer transition from laminar to turbulent was done by means of transition trips and was visualized by sublimation tests. The best agreement with the predicted C sub p curve is found for M equals 0.81 and alpha equals 0.2 degree. ESA

N91-13417# Aeronautical Research Inst. of Sweden, Stockholm. Dept. of Structures.

FE ANALYSES OF AIRCRAFT MODEL WITH INTERIOR TRIM

Peter Goeransson (Ingemanssons Ingenjoersbyraa A.B., Goteborg, Sweden) Sep. 1990 57 p Sponsored by Swedish Technical Board of Development Original contains color illustrations
(FFA-TN-1990-21; ETN-91-98267) Avail: NTIS HC/MF A04

A finite element (FE) analysis of the dynamic behavior of an aircraft fuselage with interior trim panels was performed. The FE model used is a half model of the fuselage shell, the trim panels, the acoustic cavity in between the two shells, and the interior acoustic cavity. For the present model, the eigenvalues and eigenmodes between 50 and 100 Hz are shown and observations regarding fluid structure interactions are made. The influence of the trim acoustic cavity is demonstrated through both a substantial resonance frequency shifting and an increased transmission. ESA

N91-13418 Messerschmitt-Boelkow-Blohm G.m.b.H., Munich (Germany, F.R.). Hubschrauber und Flugzeuge.

INFLUENCE OF THERMODYNAMICAL MODELIZATION FOR CHEMICALLY REACTING AIR FLOW Thesis - Tech. Univ. Munich [EINFLUSS THERMODYNAMISCHER MODELLIERUNGEN FUER STROEMUNGEN VON CHEMISCH REAGIERENDER LUFT]

R. Bareiss 7 May 1990 94 p In GERMAN
(MBB/FE122/S/PUB/400; ETN-91-98381) Copyright Avail: Fachinformationszentrum Karlsruhe 2, 7514 Eggenstein-Leopoldshaffen, Fed. Republic of Germany

As a heat protection system of an hypersonic aircraft takes a great part in its total mass, the flow field has to be known as exactly as possible for an optical design. The flow field is calculated numerically, because the simulation in wind channels is not possible in all flight ranges. The real gas effects, the flow chemical equilibrium, were already taken into consideration especially for flight heights inferior to 5 km. For greater flight heights, the chemical nonequilibrium effects are of interest. The influence of various modelizations on the flow and on the calculation time needed, was examined for three calculation cases: heat bath, perpendicular shock, and one-dimensional nozzle flow. The available models are essential for the calculation of chemical nonequilibrium flows. They confirm the importance of chemical nonequilibrium. For the modelization, it is shown that the exchange reactions are notably more important than the dissociation reactions. ESA

N91-13419# Sandia National Labs., Albuquerque, NM.

EFFECT OF BULK VISCOSITY IN LOW DENSITY, HYPERSONIC BLUNT BODY FLOWS

Walter H. Rutledge and Klaus A. Hoffmann (Texas Univ., Austin.) 1991 46 p Presented at the 29th AIAA Aerospace Sciences Conference, Reno, NV, 7-10 Jan. 1991
(Contract DE-AC04-76DP-00789)
(DE90-012756; SAND-90-1587C; CONF-910117-2) Avail: NTIS HC/MF A03

A computational fluids dynamics scheme is presented to solve the unsteady Thin-Layer Navier-Stokes (TLNS) equations over a blunt body at high altitude, high Mach number atmospheric reentry flow conditions. This continuum approach is directed to low density hypersonic flows by accounting for non-zero bulk viscosity effects in near frozen flow conditions. The TLNS equations are solved over an axisymmetric body at zero incidence relative to the free stream. The time dependent axisymmetric governing equations are transformed into a computational plane, then cast into weak conservative form and solved using a first-order fully implicit scheme in time with second-order flux vector splitting for spatial derivatives. The physical domain is defined over representative sphere and sphere/cone geometries using a body-fitted clustered algebraic grid within a fixed domain (i.e., shock capturing). At the present time, nonequilibrium thermo-chemistry effects are not modeled. Catalytic wall, ionization and radiation effects are also excluded from the current analysis. However, the significant difference from previous studies is the inclusion of the capability to model non-zero bulk viscosity effects. The importance of bulk viscosity is reviewed and blunt body flow field solutions are presented to illustrate the potential contribution of this phenomena at high altitude hypersonic conditions. The current technique is compared with experimental data and other approximate continuum solutions. A variety of test cases are also presented for a wide range of free stream Mach conditions. DOE

N91-13420*# National Aeronautics and Space Administration. Lewis Research Center, Cleveland, OH.

A STEADYING EFFECT OF ACOUSTIC EXCITATION ON TRANSITORY STALL

K. B. M. Q. Zaman 1991 17 p Proposed for presentation at the 29th Aerospace Sciences Meeting, Reno, NV, 7-10 Jan. 1991; sponsored by AIAA
(NASA-TM-103689; E-5908; NAS 1.15:103689; AIAA-91-0043)
Avail: NTIS HC/MF A03 CSCL 01A

The effect of acoustic excitation on a class of separated flows with a transitional boundary layer at the point of separation is considered. Experimental results on the flow over airfoils, a two-dimensional backward-facing step, and through large angle conical diffusers are presented. In all cases, the separated flow undergoes large amplitude fluctuations, much of the energy being concentrated at unusually low frequencies. In each case, an appropriate high frequency acoustic excitation is found to be effective in reducing the fluctuations substantially. The effective excitation frequency scales on the initial boundary layer thickness and the effect is apparently achieved through acoustic tripping of the separating boundary layer. Author

N91-13421*# National Aeronautics and Space Administration. Lewis Research Center, Cleveland, OH.
A REVIEW OF ICE ACCRETION DATA FROM A MODEL ROTOR ICING TEST AND COMPARISON WITH THEORY
Randall K. Britton (Sverdrup Technology, Inc., Brook Park, OH.) and Thomas H. Bond 1991 35 p Presented at the 29th Aerospace Sciences Meeting, Reno, NV, 7-10 Jan. 1991; sponsored by AIAA
(Contract NAS3-25266)
(NASA-TM-103712; E-5930; NAS 1.15:103712; AIAA-91-0661)
Avail: NTIS HC/MF A03 CSCL 01A

An experiment was conducted by the Helicopter Icing Consortium (HIC) in the NASA Lewis Icing Research Tunnel (IRT) in which a 1/6 scale fuselage model of a UH-60A Black Hawk helicopter with a generic rotor was subjected to a wide range of icing conditions. The HIC consists of members from NASA, Bell Helicopter, Boeing Helicopter, McDonnell Douglas Helicopters, Sikorsky Aircraft, and Texas A&M University. Data was taken in the form of rotor torque, internal force balance measurements, blade strain gage loading, and two dimensional ice shape tracings. A review of the ice shape data is performed with special attention given to repeatability and correctness of trends in terms of radial variation, rotational speed, icing time, temperature, liquid water content, and volumetric median droplet size. Moreover, an indepth comparison between the experimental data and the analysis of NASA's ice accretion code LEWICE is given. Finally, conclusions are drawn as to the quality of the ice accretion data and the predictability of the data base as a whole. Recommendations are also given for improving data taking technique as well as potential future work. Author

N91-13422*# Minnesota Univ., Minneapolis. Dept. of Aerospace Engineering and Mechanics.
TRANSONIC BLADE-VORTEX INTERACTIONS NOISE: A PARAMETRIC STUDY
A. S. Lyrintzis and Y. Xue 1990 37 p Presented at the 46th AHS Annual Forum, Washington, DC, 21-23 May 1990
(Grant NAG2-588)
(NASA-CR-187713; NAS 1.26:187713) Avail: NTIS HC/MF A03 CSCL 01A

Transonic Blade-Vortex Interactions (BVI) are simulated numerically and the noise mechanisms are investigated. The 2-D high frequency transonic small disturbance equation is solved numerically (VTRAN2 code). An Alternating Direction Implicit (ADI) scheme with monotone switches is used; viscous effects are included on the boundary and the vortex is simulated by the cloud-in-cell method. The Kirchoff method is used for the extension of the numerical 2-D near field aerodynamic results to the linear acoustic 3-D far field. The viscous effect (shock/boundary layer interaction) on BVI is investigated. The different types of shock motion are identified and compared. Two important disturbances with different directivity exist in the pressure signal and are believed to be related to the fluctuating lift and drag forces. Noise directivity for different cases is shown. The maximum radiation occurs at an angle between 60 and 90 deg below the horizontal for an airfoil fixed coordinate system and depends on the details of the airfoil shape. Different airfoil shapes are studied and classified according to the BVI noise produced. Author

N91-13423 Messerschmitt-Boelkow-Blohm G.m.b.H., Munich (Germany, F.R.). Military Aircraft Div.
GENERALIZED FLUX VECTORS FOR HYPERSONIC SHOCK CAPTURING
Albrecht Eberle, Manfred A. Schmatz, and Norbert C. Bissinger 24 Apr. 1990 14 p Presented at 28th Aerospace Sciences Meeting, Reno, NV, 8-11 Jan. 1990 Previously announced in IAA as A90-19829
(MBB/FE122/S/PUB/397; ETN-91-98380) Copyright Avail: Fachinformationszentrum Karlsruhe 2, 7514
Eggenstein-Leopoldshaffen, Fed. Republic of Germany

A powerful tool for updating characteristic methods to enable them to capture shocks of any strength, to represent leeside flows and to represent baseflows past vehicles cruising at hypersonic speed, is described. New split flux vectors were developed which guaranteed the perfect conservation of the total temperature. The nonconservative Euler equations are written with new variables: the sound velocity, an entropy function and the velocity vector. The obtained system was inverted so that the differentials of the flow variable were eliminated and a second transformation allowed to obtain and solve a free Riemann problem. A comparison of the results for a supercritical airfoil between nonconservative and homogeneous Riemann problems shows that the proposed solution has considerably lower enthalpy and entropy error margins. ESA

03 AIR TRANSPORTATION AND SAFETY

Includes passenger and cargo air transport operations; and aircraft accidents.

For related information see also *16 Space Transportation* and *85 Urban Technology and Transportation.*

N91-13424*# Boeing Commercial Airplane Co., Seattle, WA.
CIVIL TILTROTOR MISSIONS AND APPLICATIONS Final Report
Bill Clay, Paul Baumgaertner, Pete Thompson, Sam Meyer, Ron Reber, and Dennis Berry, ed. Jul. 1987 50 p Original contains color illustrations
(Contract NAS2-12393)
(NASA-CR-177452; NAS 1.26:177452; D6-53878) Avail: NTIS HC/MF A03; 8 functional color pages CSCL 01C

In 1983, an FAA-sponsored National Rotorcraft Program sought to identify improvements to the national interurban transportation networks and determined that conventional helicopters did not have the potential to satisfy requirements because of a lack of capacity, high operational costs, and high noise levels. Tiltrotors, it was felt offered a better potential to improve interurban air transport service. In 1985, the FAA proposed a joint civil tiltrotor study with NASA and DOD that would capitalize on development of the military V-22 tiltrotor and document the potential of the commercial tiltrotor transport market. The results of a study on the mission and application of a civil tiltrotor is presented. This study addresses national issues and includes a market summary. A technical summary provides information on six design configurations and potential risk areas are identified. The development of a National Plan for a tiltrotor transportation system is recommended including civil tiltrotor technology development, infrastructure planning and development, a flight technology demonstration plan, and near term actions. Author

N91-13425# National Transportation Safety Board, Washington, DC. Office of Aviation Safety.
AIRCRAFT ACCIDENT REPORT: ALOHA ISLANDAIR, INC., FLIGHT 1712, DE HAVILLAND TWIN OTTER, DHC-6-300, N707PV, HALAWA POINT, MOLOKAI, HAWAII, OCTOBER 28, 1989

25 Sep. 1990 43 p
(PB90-910405; NTSB/AAR-90/05) Avail: NTIS HC/MF A03 CSCL 01C

The crash of Aloha IslandAir flight 1712, a de Havilland Twin Otter DHC-6-300 near Halawa Bay, Molokai, Hawaii, on October 28, 1989, is explained. The safety issues discussed are surveillance of 14 CFR Part 135 operators by the Federal Aviation Administration, 14 CFR Part 135 operating procedures, flight following in the Hawaiian islands, weather, and crew training. Safety recommendations addressing these issues were made to the FAA, the National Weather Service, the Regional Airlines Association, and the Aircraft Owners and Pilots Association. Author

N91-13426# Loughborough Univ. of Technology (England). Dept. of Transport Technology.
AIRPORT STAND ASSIGNMENT MODEL
A. Marawa and N. J. Ashford Jun. 1990 106 p
(TT-9009; ISBN-0-904947-24-6; ETN-91-98357) Copyright Avail: NTIS HC/MF A06

Aircraft delay is outlined as a major source of diseconomy in the air transport system. Stand capacity deficiency is identified as one of its major causes. As physical expansion of stand capacity does not appear to be one of the obvious solutions, it is proposed to seek a cost effective way of managing and operating the existing capacity, and to develop a microcomputer simulation model as an innovative and effective technique to be used in the area of stand allocation, in order to significantly reduce aircraft delays and subsequently increase the overall stand capacity. ESA

N91-13427# Loughborough Univ. of Technology (England). Dept. of Transport Technology.
UK AIRLINES' COST STRUCTURE AND IMPLICATIONS OF AIR TRANSPORT SERVICES FRAGMENTATION. RESEARCH REPORT ON AIR TRANSPORT FRAGMENTATION
N. N. Ndoh Aug. 1990 47 p
(TT-9011; ISBN-0-904947-26-2; ETN-91-98358) Copyright Avail: NTIS HC/MF A03

It is proposed to determine the structure of United Kingdom airlines costs, using appropriate models, in order to readdress the arguments for and against fragmentation of air transport services, in particular within a metropolitan hub system of airports. The emphasis is on the supply of services rather than the demand for services. The full cost models estimated for United Kingdom scheduled airlines are attached in an appendix. ESA

04 AIRCRAFT COMMUNICATIONS AND NAVIGATION

Includes digital and voice communication with aircraft; air navigation systems (satellite and ground based); and air traffic control.

For related information see also *17 Space Communications, Spacecraft Communications, Command and Tracking* and *Communications and Radar.*

N91-13428*# Ohio State Univ., Columbus. ElectroScience Lab.
MODELLING AND PERFORMANCE ANALYSIS OF FOUR AND EIGHT ELEMENT TCAS Semiannual Report, Sep. 1989 - Mar. 1990
K. S. Sampath, R. G. Rojas, and W. D. Burnside Apr. 1990 86 p
(Grant NsG-1498)
(NASA-CR-187414; NAS 1.26:187414; ESL-TR-716199-15)
Avail: NTIS HC/MF A05 CSCL 17G

This semi-annual report describes the work performed during the period September 1989 through March 1990. The first section presents a description of the effect of the engines of the Boeing 737-200 on the performance of a bottom mounted eight-element traffic alert and collision avoidance system (TCAS). The second section deals exclusively with a four element TCAS antenna. The model obtained to simulate the four element TCAS and new algorithms developed for studying its performance are described. The effect of location on its performance when mounted on top of a Boeing 737-200 operating at 1060 MHz is discussed. It was found that the four element TCAS generally does not perform as well as the eight element TCAS III. Author

N91-13429# Georgia Inst. of Tech., Atlanta. Computer Engineering Research Lab.
GUIDANCE, NAVIGATION AND CONTROL. DIGITAL EMULATION TECHNOLOGY LABORATORY. VOLUME 2, TASK 2: SEEKER EMULATOR DEVELOPMENT Annual Report, FY90
Andrew M. Henshaw, Stephen R. Gieseking, and Roy W. Melton 22 Jul. 1990 60 p
(Contract DASG60-89-C-0142)
(AD-A225124; AR-0142-90-001-Vol-2) Avail: NTIS HC/MF A04 CSCL 15/3

A real-time Focal Plane Array Seeker Scene Emulator is described. Using real-time, positional updates, typically from the Parallel Function Processor, the Simple Seeker Scene Emulator (SSSE) can combine elements of a pre-computed database to form an image that is positionally and radiometrically correct. One problem issue with the SSSE is the use of pre-computed trajectories for the kill vehicle and targets. While this constraint is valid for many types of seeker testing, in some cases this should be avoided. Our goal with the ASSE is to avoid the use of canned scenarios, and additionally to provide: Wide Field of View, Closed-Loop Operation; Increased Fidelity Nuclear Effects Modeling; Multispectral Capability; Complex Threat Geometry and Dynamics; Dynamic Tailoring/Selection of Scene Scenario; and LATS Seeker Model Anchored to LETS Test Results. GRA

N91-13430# Georgia Inst. of Tech., Atlanta. Computer Engineering Research Lab.
GUIDANCE, NAVIGATION AND CONTROL. DIGITAL EMULATION TECHNOLOGY LABORATORY. VOLUME 3, TASK 3: SPECIAL STUDIES Annual Report, FY90
Cecil O. Alford and Phillip R. Bingham 23 Jul. 1990 53 p
(Contract DASG60-89-C-0142)
(AD-A225125; AR-0142-90-001-Vol-3) Avail: NTIS HC/MF A04 CSCL 15/3

Task 3 was set up with two objectives. The first was to establish interfaces between Georgia Tech and other programs such as LATS, LETS, AHAT and KDCE. Each of these programs requires specific interactions and data exchange with Georgia Tech. Some of these will eventually require an interface specification to define hardware and software boundaries between Georgia Tech and the other programs. The second objective of Task 3 is to resolve issues which were not anticipated in the original contract, but which needed resolution for the contract to move forward. These issues are sometimes quite difficult and beyond the resources of the contract. However, each issue is at least defined and evaluated in importance. GRA

N91-13431 Institute for Perception RVO-TNO, Soesterberg (Netherlands).
THE EFFECT OF STEREOSCOPIC PRESENTATION ON A SIMULATED AIR TRAFFIC CONTROL TASK Final Report
J. Walraven and A. D. Hekstra 1 Dec. 1989 25 p Original contains color illustrations Contains 3-D glasses as supplement
(IZF-1989-53; TD-89-4551; ETN-91-98304) Copyright Avail: Institute for Perception RVO-TNO, P.O. Box 23, 3769 ZG Soesterberg, Netherlands

Collision prediction in a simulated Air Traffic Control (ATC) task is compared for conditions in which the aircraft displacements on the radar display are shown in either two or three dimensions. The image separation required for stereoscopic (three-dimensional) viewing is achieved by both anaglyphic presentation (red-green glasses) and sequential field stereoscopy (electro-optical shutters). The stimuli consist of traffic scenarios that change in density and complexity. One of the aircraft is singled out to represent the one to be under control. The observer's task is to judge whether it was on a collision course or not. In the two-dimensional condition, the (necessary) altitude information is provided in numerical form. In the three-dimensional condition, experiments both with and

without numerical information are performed. The results indicate that stereoscopic information by itself, that is, without numerical altitude information, may already be sufficient for the task under consideration. However, in the condition with combined stereoscopic and numerical altitude information, the performance is not significantly better than in the two-dimensional condition employing numerical information only. Nevertheless, subjects preferred the stereoscopic display over the (normal) two-dimensional format. ESA

05 AIRCRAFT DESIGN, TESTING AND PERFORMANCE

Includes aircraft simulation technology.

For related information see also *18 Spacecraft Design, Testing and Performance* and *39 Structural Mechanics*.For land transportation vehicles see *85 Urban Technology and Transportation*.

N91-13432*# National Aeronautics and Space Administration. Langley Research Center, Hampton, VA.

CONCEPT DEVELOPMENT OF A MACH 4 HIGH-SPEED CIVIL TRANSPORT

Christopher S. Domack, Samuel M. Dollyhigh, Fred L. Beissner, Jr., Karl A. Geiselhart, Marvin E. McGraw, Jr., Elwood W. Shields, and Edward E. Swanson (Planning Research Corp., Hampton, VA.) Washington Dec. 1990 30 p

(NASA-TM-4223; L-16603; NAS 1.15:4223) Avail: NTIS HC/MF A03 CSCL 01C

A study was conducted to configure and analyze a 250 passenger, Mach 4 High Speed Civil Transport with a design range of 6500 n.mi. The design mission assumed an all-supersonic cruise segment and no community noise or sonic boom constraints. The study airplane was developed in order to examine the technology requirements for such a vehicle and to provide an unconstrained baseline from which to assess changes in technology levels, sonic boom limits, or community noise constraints in future studies. The propulsion, structure, and materials technologies utilized in the sizing of the study aircraft were assumed to represent a technology availability date of 2015. The study airplane was a derivative of a previously developed Mach 3 concept and utilized advanced afterburning turbojet engines and passive airframe thermal protection. Details of the configuration development, aerodynamic design, propulsion system, mass properties, and mission performance are presented. The study airplane was estimated to weigh approx. 866,000 lbs. Although an aircraft of this size is a marginally acceptable candidate to fit into the world airport infrastructure, it was concluded that the inclusion of community noise or sonic boom constraints would quickly cause the aircraft to grow beyond acceptable limits using the assumed technology levels. Author

N91-13433*# National Aeronautics and Space Administration. Langley Research Center, Hampton, VA.

A SEMIEMPIRICAL METHOD FOR OBTAINING FUSELAGE NORMAL AREAS FROM FUSELAGE MACH SLICED AREAS

Robert J. Mack and Kathy E. Needleman (Lockheed Engineering and Sciences Co., Hampton, VA.) Washington Dec. 1990 15 p

(NASA-TM-4228; L-16614; NAS 1.15:4228) Avail: NTIS HC/MF A03 CSCL 01C

An aircraft designed to meet low sonic boom or shaped ground overpressure signature requirements has a volume and lift equivalent area distribution which is in close agreement with the equivalent areas of a desired theoretical curve. Final-stage design modifications of the aircraft's geometry to meet this requirement are usually made through adjustments to the fuselage normal cross-section areas that are derived from the corresponding fuselage equivalent areas by iterative methods. The time required to obtain a good agreement between the desired low-boom area distribution and the conceptual aircraft total area distribution can be reduced by using a semi-empirical method which eliminates much of the final trial-and-error iteration previously employed. Fuselages from conceptual aircraft designed to generate low sonic boom ground overpressures at cruise Mach numbers of 2.0 and 3.0 were used as examples to examine the method's capabilities and limitations. Results indicated that the method has merit as a design tool consistent with other linear theory methods. Author

N91-13434# Advisory Group for Aerospace Research and Development, Neuilly-Sur-Seine (France). Guidance and Control Panel.

MISSILE INTERCEPTOR GUIDANCE SYSTEM TECHNOLOGY

Sep. 1990 159 p Lecture series held in Hamburg, Fed. Republic of Germany, 11-12 Oct. 1990; in Amsterdam, Netherlands, 15-16 Oct. 1990; and in Cambridge, MA, 25-26 Oct. 1990

(AGARD-LS-173; ISBN-92-835-0587-5) Copyright Avail: NTIS HC/MF A08; Non-NATO Nationals requests available only from AGARD/Scientific Publications Executive

Most operational interceptor tactical guidance systems are employing technologies which were developed more than two decades ago. Newer technologies have been slow to replace these mature technologies that meet the requirements; however, future interceptor guidance systems will have more demanding requirements and technological advances have great payoff potential. The guidance system technology fundamentals are presented which will serve as background so that theoretical advances in future and proposed systems can be both understood and appreciated. For individual titles, see N91-13435 through N91-13442.

N91-13435# Johns Hopkins Univ., Laurel, MD. Applied Physics Lab.

MODERN ROBUST CONTROL FOR MISSILE AUTOPILOT DESIGN

Robert T. Reichert and David J. Yost *In* AGARD, Missile Interceptor Guidance System Technology Sep. 1990 15 p (For primary document see N91-13434 05-05)

Copyright Avail: NTIS HC/MF A08; Non-NATO Nationals requests available only from AGARD/Scientific Publications Executive

The applicability of H(infinity) control to the design of automatic flight control systems for highly maneuverable, tail-controlled missiles is examined. The fundamentals of modern robust control analysis and synthesis are reviewed. Problem formulation with emphasis on selection of frequency domain weighting functions for design specifications and the role of modeling uncertainty are considered. An example problem is included as a tutorial overview of these methods. Author

N91-13436# Bodenseewerk Geraetetechnik G.m.b.H., Ueberlingen (Germany, F.R.). Intelligent Systems Div.

MIDCOURSE GUIDANCE TECHNOLOGIES FOR ADVANCED TACTICAL MISSILES SYSTEMS **c08**

Ulrich Hartmann *In* AGARD, Missile Interceptor Guidance System Technology Sep. 1990 27 p (For primary document see N91-13434 05-05)

Copyright Avail: NTIS HC/MF A08; Non-NATO Nationals requests available only from AGARD/Scientific Publications Executive

Midcourse guidance techniques can significantly improve operational aspects as well as overall performance of tactical missile systems. Operational requirements such as conformal carriage in the case of air-to-air missiles or canister launch in the case of ship-based systems can only be met by a lock-after-launch capability of the guidance system. On the other hand, seeker acquisition ranges may not be able to match the kinematic capabilities of the missile for a variety of reasons which may include adverse weather conditions and countermeasures. A number of operational aspects are addressed which are relevant to the design of midcourse guidance systems and the essential prerequisites for their application. Basic options of midcourse guidance, such as pure inertial, updated inertial, and aided inertial as well as the fundamental elements including inertial navigation and target prediction are discussed. Proper initialization and alignment of the guidance and navigation system are presented as further key issues. The alignment problem is defined and a number of methods

to achieve adequate alignment are described. A review of different techniques for the performance assessment and the most important criteria for handover from midcourse to terminal guidance is presented. Author

N91-13437# Hughes Aircraft Co., Canoga Park, CA.
FLIGHT CONTROL DESIGN ISSUES IN BANK-TO-TURN MISSILES **c08**
W. A. Kaufmann *In* AGARD, Missile Interceptor Guidance System Technology Sep. 1990 16 p Also presented at the Workshop on Bank-to-Turn Controlled Terminal Homing Missiles, 19-20 Sep. 1984 (For primary document see N91-13434 05-05)
Copyright Avail: NTIS HC/MF A08; Non-NATO Nationals requests available only from AGARD/Scientific Publications Executive

Design issues encountered in the synthesis of bank-to-turn autopilots are discussed for several proposed air-launched tactical guided missile configurations. Some approaches to dealing with these issues are also discussed. Much of the material was developed from experience gained in the design of an autopilot for a medium range air-to-air missile configuration incorporating an integral rocket-ramjet propulsion system. Therefore, emphasis is placed on that type of system. None of the bank-to-turn autopilots were flight tested, so only simulation results can be presented. The first issue discussed is why a designer would consider bank-to-turn control instead of the conventional skid-to-turn control used by most tactical missiles. The advantages and disadvantages of each approach are related to the performance of the airframe, propulsion, guidance, and autopilot subsystems. Several bank-to-turn control laws are presented. The relative merits of each are discussed with respect to the type of airframe, propulsion, and guidance required for the missile mission under consideration. Performance penalties are presented along with the advantages of including a skid-to-turn capability. Simulation studies have shown that some performance penalties may be incurred using bank-to-turn control for some types of missions, particularly for anti-air engagements, but these penalties are frequently small compared to other performance benefits derived from its utilization. These simulation studies and their results are discussed in appropriately general terms. Author

N91-13438# Electronique Marcel Dassault, Saint Cloud (France).
GUIDANCE SIMULATION MODEL OF ANTISEA-SKIMMER UTILIZATION FOR WEAPON SYSTEM DEFINITION **c08**
G. Vallas and F. Burel (Aerospatiale, Chatillon, France) *In* AGARD, Missile Interceptor Guidance System Technology Sep. 1990 32 p (For primary document see N91-13434 05-05)
Copyright Avail: NTIS HC/MF A08; Non-NATO Nationals requests available only from AGARD/Scientific Publications Executive

The way of quantifying the main parameters which size an antisea-skimmer missile by using numerical simulations is summarized. The ammunition-sizing can only be correctly defined when a sufficient number of iterations is achieved with the modelization tools, taking into account the specification of the threat and cost constraints. A method of evaluation of the main parameters is described and the primary function of the simulation during the various phases of the project is specified. Author

N91-13439# Royal Aerospace Establishment, Farnborough (England). Defensive Systems Dept.
ADVANCED MISSILE GUIDANCE **c08**
R. V. Lawrence *In* AGARD, Missile Interceptor Guidance System Technology Sep. 1990 9 p (For primary document see N91-13434 05-05)
Copyright Avail: NTIS HC/MF A08; Non-NATO Nationals requests available only from AGARD/Scientific Publications Executive

The problem of bringing a missile into collision with a moving target is discussed. The zero-control miss (ZCM) guidance concept is introduced. It is shown how errors in the estimates of the current system state and the future zero-control response of the system lead to errors in estimating the ZCM, and consequently how the missile suffers an aiming error. The missile generally suffers a miss, because of its limited ability to follow the changing error, due to restricted bandwidth and control saturation. Optimal control laws based on the ZCM are derived, and expressions for the idealized terminal miss obtained. The equations suggest how the target might choose an optimal evasion strategy to maximize the miss. This leads to some discussion of game theory, and the basis for multiple hypothesis guidance. Author

N91-13440# Draper (Charles Stark) Lab., Inc., Cambridge, MA.
MICRO BASED TECHNOLOGY: A NEW TOOL FOR MISSILE GUIDANCE SYSTEM DESIGN AND VISUALIZATION **c08**
Paul Zarchan *In* AGARD, Missile Interceptor Guidance System Technology Sep. 1990 16 p (For primary document see N91-13434 05-05)
Copyright Avail: NTIS HC/MF A08; Non-NATO Nationals requests available only from AGARD/Scientific Publications Executive

How simulation output can be generated and enhanced, in real time, with the computational horsepower and graphics visualization technology which is currently available with microcomputers is shown. Examples are presented which demonstrate how microcomputer based technology offers the designer a visualization which not only gives a deeper insight into the problem being solved, but in addition allows and encourages rapid iteration in order to get an acceptable design. Author

N91-13441# Draper (Charles Stark) Lab., Inc., Cambridge, MA.
INTERACTIONS BETWEEN BATTLE MANAGEMENT AND GUIDANCE LAW DESIGN FOR A STRATEGIC INTERCEPTOR **c08**
Owen L. Deutsch *In* AGARD, Missile Interceptor Guidance System Technology Sep. 1990 16 p (For primary document see N91-13434 05-05)
Copyright Avail: NTIS HC/MF A08; Non-NATO Nationals requests available only from AGARD/Scientific Publications Executive

The design of strategic interceptor systems presents many challenges. Considering a space-based system with orbiting interceptors, performance requirements may included near-zero miss distances, nearly complete coverage of many simultaneous threat launches, and successful interception against maneuvering targets. Cost constraints, on the other hand, will limit the interceptor weight and the numbers deployed. Also, the interceptor may operate at an acceleration disadvantage with respect to target, the range and time-to-go may not be precisely known, and there may be substantial prediction errors for the initial flyout. All of these factors conspire to place great importance on an integrated system design process that provides visibility into the interactions between battle management functions (e.g., sensor management, weapon-target assignment, and fire control) and the interceptor guidance law and component technologies. In particular, guidance-related issues must be taken into account in the weapon-target assignment and fire-control functions of the battle manager. As an example, the minimum time for lateral guidance (with limited acceleration capability) to null out heading errors resulting from prediction error must be accounted for in the timeline decisions of the assignment and fire-control processes. The battle manager may select assignments that avoid unfavorable engagement geometries, where possible. Finally, the fire control manager may select between different guidance laws based on engagement conditions. Once there is visibility into the existence and phenomenology of potential guidance problems, there may be easy opportunities for correction by system-level solutions. Author

N91-13442# Draper (Charles Stark) Lab., Inc., Cambridge, MA.
GUIDANCE METHODS FOR TACTICAL AND STRATEGIC MISSILES **c08**
Paul Zarchan *In* AGARD, Missile Interceptor Guidance System Technology Sep. 1990 16 p (For primary document see N91-13434 05-05)
Copyright Avail: NTIS HC/MF A08; Non-NATO Nationals requests available only from AGARD/Scientific Publications Executive

Methods of guidance which are applicable to both tactical and strategic missiles are reviewed. It is shown how the various guidance law technologies are related. 'Rules of thumb', which

were originally developed for the tactical world, are extended for application to the strategic world not only to gain insight but also to predict strategic interceptor fuel consumption and performance. Numerous examples are presented to clarify and illustrate concepts. Author

N91-13443*# North Carolina State Univ., Raleigh. Dept. of Mechanical and Aerospace Engineering.
THEORETICAL EVALUATION OF ENGINE AUXILIARY INLET DESIGN FOR SUPERSONIC V/STOL AIRCRAFT Final Technical Report
Michael A. Boles and Richard L. Heavner Aug. 1988 98 p
(Grant NAG3-608)
(NASA-CR-186610; NAS 1.26:186610) Avail: NTIS HC/MF A05 CSCL 01C

A higher order panel method is used to evaluate the potential flow of a two dimensional supersonic V/STOL inlet. A non-symmetric analytical inlet model is developed to closely match a wind tunnel model. The analytical inlet is analyzed for flow characteristics around the lower cowl lip and auxiliary inlets. The results are obtained from the output of a computer program that is based on the Hess Panel Method which determines source strengths of panels distributed over a three dimensional body. The analytical model was designed for the implementation of drooped/translated cowl lip and auxiliary inlets as flow improvement concepts. A 40 or 70 degree droop lip can be incorporated on the inlet to determine if these geometry modifications result in flow improvements which may reduce the propensity for flow separation on the interior portion of the lip. Auxiliary inlets are employed to decrease the mass flow over the inlet lip. Thus, the peak flow velocity is reduced at the lip which also lessens the likelihood of flow separation on the interior portion of the lip. A 2, 4, and 6 inch translated lip can be employed to also decrease mass flow over the inlet lower lip in the same manner as the auxiliary inlet. The performance results of the flow improvement concepts show that three possible inlet configurations provide a situation where separation is less likely to occur. A 70 degree droop lip maintains flow conditions such that attached flow over the lower cowl lip may exist for the entire angle of attack range studied. A 0 degree droop and translated lip combination provides similar results for the angle of attack range. The third configuration consists of a 0 degree droop and auxiliary inlet combination. This configuration provides slightly less favorable results than the other two, but still allows for conditions favorable to attached flow within the inlet. Author

N91-13444# Textron Bell Helicopter, Fort Worth, TX.
HELICOPTER STRUCTURAL INTEGRITY PROGRAM (HSIP). VOLUME 1: STRUCTURAL TEST REQUIREMENTS SPECIFICATION Final Report, Nov. 1988 - Dec. 1989
J. Martin, J. Fila, and D. Reisdorfer Jul. 1990 31 p
(Contract DAAJ02-88-C-0022)
(AD-A226520; BHT-699-099-319-Vol-1; USAAVSCOM-TR-90-D-15A) Avail: NTIS HC/MF A03 CSCL 01/3

This Structural Test Requirements Program is designed to provide the necessary ground test requirements to support the overall HSIP objectives. The Structural Test Requirements portion of the HSIP covers the ground tests which are required during the design development and qualification of rotary-wing/VTOL aircraft. The structural test requirements specification addresses composite and metallic components. Through a comprehensive survey of existing specifications and related documents for structural testing of rotary-wing/VTOL aircraft, key test technology elements such as static, fatigue, durability and damage tolerance were assessed for suitability to future aircraft systems, and evaluated for applicability into the test requirements specification. In cases where no adequate test requirements exist, this program has developed those requirements. A draft test specification was developed and presented to various representatives of the helicopter industry and government agencies at a Government/Industry Forum. Comments received from the forum participants were evaluated and incorporated, if appropriate, into a final revised specification. GRA

N91-13445*# National Aeronautics and Space Administration. Langley Research Center, Hampton, VA.
F-106B AIRPLANE ACTIVE CONTROL LANDING GEAR DROP TEST PERFORMANCE
William E. Howell, John R. McGehee, Robert H. Daugherty, and William A. Vogler (Lockheed Engineering and Sciences Co., Hampton, VA.) Nov. 1990 12 p
(NASA-TM-102741; NAS 1.15:102741) Avail: NTIS HC/MF A03 CSCL 01C

Aircraft dynamic loads and vibrations resulting from landing impact and from runway and taxiway unevenness are recognized as significant factors in causing fatigue damage, dynamic stress on the airframe, crew and passenger discomfort, and reduction of the pilot's ability to control the aircraft during ground operations. One potential method for improving operational characteristics of aircraft on the ground is the application of active control technology to the landing gears to reduce ground loads applied to the airframe. An experimental investigation was conducted on series-hydraulic active control nose gear. The experiments involved testing the gear in both passive and active control modes. Results of this investigation show that a series-hydraulic active control gear is feasible and that such a gear is effective in reducing the loads transmitted by the gear to the airframe during ground operations. Author

N91-13446*# Massachusetts Inst. of Tech., Cambridge. Technology Lab. for Advanced Composites.
COMPOSITE FUSELAGE TECHNOLOGY Annual Report, 7 Apr. 1989 - 6 Apr. 1990
Michael J. Graves and Paul A. Lagace Oct. 1990 25 p
(Grant NAG1-991)
(NASA-CR-187658; NAS 1.26:187658; TELAC-90-19) Avail: NTIS HC/MF A03 CSCL 01C

The overall objective is to identify and understand, via directed experimentation and analysis, the mechanisms which control the structural behavior of fuselages in their response to damage (resistance, tolerance, and arrest). A further objective is to develop straightforward design methodologies which can be employed by structural designers in preliminary design stages to make intelligent choices concerning the material, layup, and structural configuration so that a more efficient structure with structural integrity can be designed and built. Author

N91-13447*# Douglas Aircraft Co., Inc., Long Beach, CA. Advanced Aircraft Transports High Speed Civil Transport Group.
PROCEDURE FOR GENERATING GLOBAL ATMOSPHERIC ENGINE EMISSIONS DATA FROM FUTURE SUPERSONIC TRANSPORT AIRCRAFT. THE 1990 HIGH SPEED CIVIL TRANSPORT STUDIES
R. A. Sohn and J. W. Stroup Dec. 1990 37 p
(Contract NAS1-18378)
(NASA-CR-181882; NAS 1.26:181882) Avail: NTIS HC/MF A03 CSCL 01C

The input for global atmospheric chemistry models was generated for baseline High Speed Civil Transport (HSCT) configurations at Mach 1.6, 2.2, and 3.2. The input is supplied in the form of number of molecules of specific exhaust constituents injected into the atmosphere per year by latitude and by altitude (for 2-D codes). Seven exhaust constituents are currently supplied: NO, NO2, CO, CO2, H2O, SO2, and THC (Trace Hydrocarbons). An eighth input is also supplied, NO(x), the sum of NO and NO2. The number of molecules of a given constituent emitted per year is a function of the total fuel burned by a supersonic fleet and the emission index (EI) of the aircraft engine for the constituent in question. The EIs for an engine are supplied directly by the engine manufacturers. The annual fuel burn of a supersonic fleet is calculated from aircraft performance and economic criteria, both of which are strongly dependent on basic design parameters such as speed and range. The altitude and latitude distribution of the

emission is determined based on 10 Intern. Air Transport Assoc. (IATA) regions chosen to define the worldwide route structure for future HSCT operations and the mission flight profiles. Author

N91-13448# Aeronautical Research Inst. of Sweden, Stockholm. Dept. of Structures.
DAMAGE TOLERANCE ANALYSIS AND TESTING OF THE FIGHTER AIRCRAFT 37 VIGGEN
Bjoern Palmberg, Mats Olof Olsson, Per Olof Boman, and Anders F. Blom Aug. 1990 13 p Presented at the ICAS 1990, Stockholm, Sweden, 9-14 Sep. 1990
(Contract FMV-82250-89-156-73-001)
(FFA-TN-1990-35; ETN-91-98270) Avail: NTIS HC/MF A03

The Swedish fighter aircraft 37 Viggen was reassessed in terms of damage tolerance evaluation. Four versions of the main wing attachment frame and some components in the fin were subjected to detailed analyses and damage tolerance testing. It was necessary to perform very extensive finite element analyses, in order to get accurate stress distribution in critical sections for subsequent evaluation of three dimensional stress intensity factors. The stress analyses were mainly checked on the basis of traditional static and fatigue testing results available from the design phase of the aircraft. It was concluded that the methodology used is state of the art and that it has been successfully verified. Extension of the original design life may be possible. ESA

N91-13449*# Georgia Inst. of Tech., Atlanta. School of Aerospace Engineering.
PERIODIC TRIM SOLUTIONS WITH hp-VERSION FINITE ELEMENTS IN TIME Final Technical Report, 1 Jul. 1989 - 31 Dec. 1990
David A. Peters and Lin-Jun Hou 20 Dec. 1990 47 p
(Grant NAG1-1027)
(NASA-CR-187705; NAS 1.26:187705) Avail: NTIS HC/MF A01 CSCL 01C

Finite elements in time as an alternative strategy for rotorcraft trim problems are studied. The research treats linear flap and linearized flap-lag response both for quasi-trim and trim cases. The connection between Fourier series analysis and hp-finite elements for periodic a problem is also examined. It is proved that Fourier series is a special case of space-time finite elements in which one element is used with a strong displacement formulation. Comparisons are made with respect to accuracy among Fourier analysis, displacement methods, and mixed methods over a variety parameters. The hp trade-off is studied for the periodic trim problem to provide an optimum step size and order of polynomial for a given error criteria. It is found that finite elements in time can outperform Fourier analysis for periodic problems, and for some given error criteria. The mixed method provides better results than does the displacement method. Author

N91-13450 Physics and Electronics Lab. TNO, The Hague (Netherlands).
DESCRIPTION OF SEA WAVE MOTION AND ITS INFLUENCE ON THE ALTITUDE CONTROL OF SEA SKIMMING MISSILES Final Report
P. F. Ruizendaal Jan. 1990 45 p
(Contract A84/KM/080)
(FEL-89-A368; TD-89-4466; ETN-91-98296) Copyright Avail: Physics and Electronics Laboratory TNO, P.O. Box 96864, 2509 JG The Hague, Netherlands

The description and generation of sea wave motion is presented in order to examine the influence of this motion on the altitude performance of a low flying missile. A sea skimming missile is simulated with the 6 degrees of freedom Weapon Analysis and Simulation Program (WASP). It is concluded that the offline generation of a data file containing the sea wave elevations as a function of travelled distance can be used to simulate the sea surface as sensed by an altimeter aboard the missile. ESA

N91-13451# Royal Aerospace Establishment, Farnborough (England).
THE UNITED KINGDOM CONTRIBUTION TO THE AGARD FATIGUE-RATED FASTENER SYSTEMS PROGRAM
R. Cook 4 Sep. 1989 74 p
(RAE-TR-89046; RAE-MAT/STR-259; BR114106; ETN-91-98362)
Copyright Avail: NTIS HC/MF A04

The possible values of secondary bending stresses on bolted connections in aircraft wing structures are examined by means of different laboratory test specimens which were designed to determine fatigue performance of some fatigue rated fastener systems. The main objectives are to determine the fatigue life of joints in different materials, to establish the cost of the installed fastener systems, to identify the prime parameters involved in fastener system selection, to generate design data, and to develop a reference data for the comparison of test results produced in different countries using different specimen geometries. It was shown that fastener systems incorporating cold hole expansion or fasteners installed with high interference fits were significantly superior to fasteners installed with a clearance fit in plain holes under the same test conditions. The longest fatigue endurances were observed in joints which contained fastener systems with both cold expansion and a high degree of fastener interference. ESA

06 AIRCRAFT INSTRUMENTATION

Includes cockpit and cabin display devices; and flight instruments.

For related information see also *19 Spacecraft Instrumentation* and *35 Instrumentation and Photography*.

N91-13452*# Tennessee Univ. Space Inst., Tullahoma.
A FLIGHT EXPERT SYSTEM FOR ON-BOARD FAULT MONITORING AND DIAGNOSIS Final Report
Moonis Ali 31 Oct. 1990 52 p
(Grant NAG1-513)
(NASA-CR-187334; NAS 1.26:187334) Avail: NTIS HC/MF A04 CSCL 01D

An architecture for a flight expert system (FLES) to assist pilots in monitoring, diagnosing, and recovering from inflight faults is described. A prototype was implemented and an attempt was made to automate the knowledge acquisition process by employing a learning by being told methodology. The scope of acquired knowledge ranges from domain knowledge, including the information about objects and their relationships, to the procedural knowledge associated with the functionality of the mechanisms. AKAS (automatic knowledge acquisition system) is the constructed prototype for demonstration proof of concept, in which the expert directly interfaces with the knowledge acquisition system to ultimately construct the knowledge base for the particular application. The expert talks directly to the system using a natural language restricted only by the extent of the definitions in an analyzer dictionary, i.e., the interface understands a subset of concepts related to a given domain. In this case, the domain is the electrical system of the Boeing 737. Efforts were made to define and employ heuristics as well as algorithmic rules to conceptualize data produced by normal and faulty jet engine behavior examples. These rules were employed in developing the machine learning system (MLS). The input to MLS is examples which contain data of normal and faulty engine behavior and which are obtained from an engine simulation program. MLS first transforms the data into discrete selectors. Partial descriptions formed by those selectors are then generalized or specialized to generate concept descriptions about faults. The concepts are represented in the form of characteristic and discriminant descriptions, which are stored in the knowledge base and are employed to diagnose faults. MLS was successfully tested on jet engine examples. Author

N91-13453*# National Aeronautics and Space Administration. Hugh L. Dryden Flight Research Facility, Edwards, CA.
A PRELIMINARY LOOK AT TECHNIQUES USED TO OBTAIN AIRDATA FROM FLIGHT AT HIGH ANGLES OF ATTACK
Timothy R. Moes and Stephen A. Whitmore Dec. 1990 51 p Presented at the High Angle of Attack Technology Symposium, Hampton, VA, 30 Oct. - 1 Nov. 1990
(NASA-TM-101729; H-1674; NAS 1.15:101729) Avail: NTIS HC/MF A04 CSCL 01D

Flight research at high angles of attack has posed new problems for airdata measurements. New sensors and techniques for measuring the standard airdata quantities of static pressure, dynamic pressure, angle of attack, and angle of sideslip were subsequently developed. The ongoing airdata research supporting NASA's F-18 high alpha research program is updated. Included are the techniques used and the preliminary results. The F-18 aircraft was flown with three research airdata systems: a standard airdata probe on the right wingtip, a self-aligning airdata probe on the left wingtip, and a flush airdata system on the nose cone. The primary research goal was to obtain steady-state calibrations for each airdata system up to an angle of attack of 50 deg. This goal was accomplished and preliminary accuracies of the three airdata systems were assessed and are presented. An effort to improve the fidelity of the airdata measurements during dynamic maneuvering is also discussed. This involved enhancement of the aerodynamic data with data obtained from linear accelerometers, rate gyros, and attitude gyros. Preliminary results of this technique are presented. Author

07 AIRCRAFT PROPULSION AND POWER

Includes prime propulsion systems and systems components, e.g., gas turbine engines and compressors; and onboard auxilliary power plants for aircraft.

For related information see also *20 Spacecraft Propulsion and Power, 28 Propellants and Fuels,* and *44 Energy Production and Conversion.*

N91-13454# Air Force Systems Command, Wright-Patterson AFB, OH. Foreign Technology Div.
THE THIRD GENERATION OF SOVIET CIVILIAN-USE TURBOFAN ENGINES
Xiao Ming 19 Jun. 1990 7 p Transl. into ENGLISH from Guoji Hanghong (Peoples Republic of China), no. 7, 1982 p 41
(AD-A225392; FTD-ID(RS)T-0258-90) Avail: NTIS HC/MF A02 CSCL 21/5

At the beginning of the 1960s, the Soviet Union began to develop turbofan engines for civilian use. To date they have developed three generations: the first generation (1960 to 1970) - D-20P (used on Tu-124), D-30 (used on Tu-134), and NK-8-2U (used on Tu-154); the second generation (1970 to 1980) - D-30KU (used in I1-62M and Tu-154M), and NK-86 (used in I1-86); and the third generation (1980 to 1990) - D-36 (used in Yake-42), D-18T (used in An-124), D-90A (used in Tu-204 and I1-96-300). All third generation turbofans are high bypass ratio turbofans, and are representative of the current technological level of Soviet civilian turbofan engines. GRA

N91-13455*# National Aeronautics and Space Administration. Lewis Research Center, Cleveland, OH.
MEASUREMENTS AND PREDICTIONS OF A LIQUID SPRAY FROM AN AIR-ASSIST NOZZLE
Daniel L. Bulzan, Yeshayahou Levy, Suresh K. Aggarwal, and Susheel Chitre (Chicago Univ., IL.) 1991 12 p Presented at the 29th Aerospace Sciences Meeting, Reno, NV, 7-10 Jan. 1991; sponsored by ASAA
(NASA-TM-103640; E-5821; NAS 1.15:103640; AIAA-91-0692) Avail: NTIS HC/MF A03 CSCL 21E

Droplet size and gas velocity were measured in a water spray using a two-component Phase/Doppler Particle Analyzer. A complete set of measurements was obtained at axial locations from 5 to 50 cm downstream of the nozzle. The nozzle used was a simple axisymmetric air-assist nozzle. The sprays produced, using the atomizer, were extremely fine. Sauter mean diameters were less than 20 microns at all locations. Measurements were obtained for droplets ranging from 1 to 50 microns. The gas phase was seeded with micron sized droplets, and droplets having diameters of 1.4 microns and less were used to represent gas-phase properties. Measurements were compared with predictions from a multi-phase computer model. Initial conditions for the model were taken from measurements at 5 cm downstream. Predictions for both the gas phase and the droplets showed relatively good agreement with the measurements. Author

N91-13456*# National Aeronautics and Space Administration. Lewis Research Center, Cleveland, OH.
THERMAL AND STRUCTURAL ASSESSMENTS OF A CERAMIC WAFER SEAL IN HYPERSONIC ENGINES
Mike T. Tong (Sverdrup Technology, Inc., Brook Park, OH.) and Bruce M. Steinetz 1991 11 p Proposed for presentation at the 27th Joint Propulsion Conference, Sacramento, CA, 24-27 Jun. 1991; cosponsored by AIAA, ASME, SAE, and ASEE
(NASA-TM-103651; E-5840; NAS 1.15:103651) Avail: NTIS HC/MF A03 CSCL 21E

The thermal and structural performances of a ceramic wafer seal in a simulated hypersonic engine environment are numerically assessed. The effects of aerodynamic heating, surface contact conductance between the seal and its adjacent surfaces, flow of purge coolant gases, and leakage of hot engine flow path gases on the seal temperature were investigated from the engine inlet back to the entrance region of the combustion chamber. Finite element structural analyses, coupled with Weibull failure analyses, were performed to determine the structural reliability of the wafer seal. Author

N91-13457*# National Aeronautics and Space Administration. Lewis Research Center, Cleveland, OH.
AN AD100 IMPLEMENTATION OF A REAL-TIME STOVL AIRCRAFT PROPULSION SYSTEM
Peter J. Ouzts and Colin K. Drummond 1990 20 p Presented at the 4th Annual Conference of the Applied Dynamics International Users' Society of the Central/Northeastern Regions, Warren, MI, 1-2 Oct. 1990
(NASA-TM-103683; E-5901; NAS 1.15:103683) Avail: NTIS HC/MF A03 CSCL 21E

A real-time dynamic model of the propulsion system for a Short Take-Off and Vertical Landing (STOVL) aircraft was developed for the AD100 simulation environment. The dynamic model was adapted from a FORTRAN based simulation using the dynamic programming capabilities of the AD100 ADSIM simulation language. The dynamic model includes an aerothermal representation of a turbofan jet engine, actuator and sensor models, and a multivariable control system. The AD100 model was tested for agreement with the FORTRAN model and real-time execution performance. The propulsion system model was also linked to an airframe dynamic model to provide an overall STOVL aircraft simulation for the purposes of integrated flight and propulsion control studies. An evaluation of the AD100 system for use as an aircraft simulation environment is included. Author

N91-13458*# Cornell Univ., Ithaca, NY.
THEORY OF FINITE DISTURBANCES IN A CENTRIFUGAL COMPRESSION SYSTEM WITH A VANELESS RADIAL DIFFUSER Final Report
F. K. Moore Dec. 1990 68 p
(Grant NAG3-349)
(NASA-CR-187049; NAS 1.26:187049) Avail: NTIS HC/MF A04 CSCL 21E

A previous small perturbation analysis of circumferential waves in circumferential compression systems, assuming inviscid flow, is shown to be consistent with observations that narrow diffusers are more stable than wide ones, when boundary layer displacement effect is included. The Moore-Greitzer analysis for finite strength transients containing both surge and rotating stall in axial machines

is adapted for a centrifugal compression system. Under certain assumptions, and except for a new second order swirl, the diffuser velocity field, including resonant singularities, can be carried over from the previous inviscid linear analysis. Nonlinear transient equations are derived and applied in a simple example to show that throttling through a resonant value of flow coefficient must occur in a sudden surge-like drop, accompanied by a transient rotating wave. This inner solution is superseded by an outer surge response on a longer time scale. Surge may occur purely as result of circumferential wave resonance. Numerical results are shown for various parametric choices relating to throttle schedule and the characteristic slope. A number of circumferential modes considered simultaneously is briefly discussed. Author

08 AIRCRAFT STABILITY AND CONTROL

Includes aircraft handling qualities; piloting; flight controls; and autopilots.

For related information see also *05 Aircraft Design, Testing and Performance.*

N91-13459 Stanford Univ., CA.
INTEGRATED AERODYNAMIC AND CONTROL SYSTEM DESIGN OF OBLIQUE WING AIRCRAFT Ph.D. Thesis
Stephen James Morris 1990 270 p
Avail: Univ. Microfilms Order No. DA9024348

Improving the handling qualities of oblique wing aircraft is emphasized. This is accomplished by including aerodynamic configuration parameters as variables in the control system synthesis to provide additional degrees of freedom with which to further decouple the aircraft's response. Handling qualities are measured using a quadratic cost function identical to that considered in optimal control problems, but the controller architecture is not restricted to full state feedback. An optimization procedure is used to simultaneously solve for the aircraft configuration and control gains which maximize a handling qualities measure, while meeting imposed constraints on trim. In some designs, wing flexibility is also modeled and reduced order controllers are implemented. Oblique wing aircraft synthesized by this integrated design method show significant improvement in handling qualities when compared to the originally proposed closed loop aircraft. The integrated design synthesis method is then extended to show how handling qualities may be traded for other types of mission performance (drag, weight, etc.). Examples are presented which show how performance can be maximized while maintaining handling quality. Dissert. Abstr.

N91-13460*# National Aeronautics and Space Administration. Hugh L. Dryden Flight Research Facility, Edwards, CA.
INTEGRATED FLIGHT-PROPULSION CONTROL CONCEPTS FOR SUPERSONIC TRANSPORT AIRPLANES
Frank W. Burcham, Jr., Glenn B. Gilyard, and Paul A. Gelhausen Nov. 1990 18 p Presented at the Society of Automotive Engineers (SAE), Inc. Aerotech Conference, Long Beach, CA, 1-4 Oct. 1990 Prepared in cooperation with NASA-Ames Research Center, Moffett Field, CA
(NASA-TM-101728; H-1673; NAS 1.15:101728; SAE-901928)
Avail: NTIS HC/MF A03 CSCL 01C

Integration of propulsion and flight control systems will provide significant performance improvements for supersonic transport airplanes. Increased engine thrust and reduced fuel consumption can be obtained by controlling engine stall margin as a function of flight and engine operating conditions. Improved inlet pressure recovery and decreased inlet drag can result from inlet control system integration. Using propulsion system forces and moments to augment the flight control system and airplane stability can reduce the flight control surface and tail size, weight, and drag. Special control modes may also be desirable for minimizing community noise and for emergency procedures. The overall impact of integrated controls on the takeoff gross weight for a generic high speed civil transport is presented. Author

N91-13436# Bodenseewerk Geraetetechnik G.m.b.H., Ueberlingen (Germany, F.R.). Intelligent Systems Div.
MIDCOURSE GUIDANCE TECHNOLOGIES FOR ADVANCED TACTICAL MISSILES SYSTEMS
Ulrich Hartmann *In* AGARD, Missile Interceptor Guidance System Technology Sep. 1990 27 p (For primary document see N91-13434 05-05)
Copyright Avail: NTIS HC/MF A08; Non-NATO Nationals requests available only from AGARD/Scientific Publications Executive

N91-13437# Hughes Aircraft Co., Canoga Park, CA.
FLIGHT CONTROL DESIGN ISSUES IN BANK-TO-TURN MISSILES
W. A. Kaufmann *In* AGARD, Missile Interceptor Guidance System Technology Sep. 1990 16 p Also presented at the Workshop on Bank-to-Turn Controlled Terminal Homing Missiles, 19-20 Sep. 1984 (For primary document see N91-13434 05-05)
Copyright Avail: NTIS HC/MF A08; Non-NATO Nationals requests available only from AGARD/Scientific Publications Executive

N91-13438# Electronique Marcel Dassault, Saint Cloud (France).
GUIDANCE SIMULATION MODEL OF ANTISEA-SKIMMER UTILIZATION FOR WEAPON SYSTEM DEFINITION
G. Vallas and F. Burel (Aerospatiale, Chatillon, France) *In* AGARD, Missile Interceptor Guidance System Technology Sep. 1990 32 p (For primary document see N91-13434 05-05)
Copyright Avail: NTIS HC/MF A08; Non-NATO Nationals requests available only from AGARD/Scientific Publications Executive

N91-13439# Royal Aerospace Establishment, Farnborough (England). Defensive Systems Dept.
ADVANCED MISSILE GUIDANCE
R. V. Lawrence *In* AGARD, Missile Interceptor Guidance System Technology Sep. 1990 9 p (For primary document see N91-13434 05-05)
Copyright Avail: NTIS HC/MF A08; Non-NATO Nationals requests available only from AGARD/Scientific Publications Executive

N91-13440# Draper (Charles Stark) Lab., Inc., Cambridge, MA.
MICRO BASED TECHNOLOGY: A NEW TOOL FOR MISSILE GUIDANCE SYSTEM DESIGN AND VISUALIZATION
Paul Zarchan *In* AGARD, Missile Interceptor Guidance System Technology Sep. 1990 16 p (For primary document see N91-13434 05-05)
Copyright Avail: NTIS HC/MF A08; Non-NATO Nationals requests available only from AGARD/Scientific Publications Executive

N91-13441# Draper (Charles Stark) Lab., Inc., Cambridge, MA.
INTERACTIONS BETWEEN BATTLE MANAGEMENT AND GUIDANCE LAW DESIGN FOR A STRATEGIC INTERCEPTOR
Owen L. Deutsch *In* AGARD, Missile Interceptor Guidance System Technology Sep. 1990 16 p (For primary document see N91-13434 05-05)
Copyright Avail: NTIS HC/MF A08; Non-NATO Nationals requests available only from AGARD/Scientific Publications Executive

N91-13442# Draper (Charles Stark) Lab., Inc., Cambridge, MA.
GUIDANCE METHODS FOR TACTICAL AND STRATEGIC MISSILES
Paul Zarchan *In* AGARD, Missile Interceptor Guidance System Technology Sep. 1990 16 p (For primary document see N91-13434 05-05)
Copyright Avail: NTIS HC/MF A08; Non-NATO Nationals requests available only from AGARD/Scientific Publications Executive

09 RESEARCH AND SUPPORT FACILITIES (AIR)

Includes airports, hangars and runways; aircraft repair and overhaul facilities; wind tunnels; shock tubes; and aircraft engine test stands.

For related information see also *14 Ground Support Systems and Facilities (Space).*

N91-13461*# National Aeronautics and Space Administration. Langley Research Center, Hampton, VA.
CALIBRATION OF THE 13- BY 13-INCH ADAPTIVE WALL TEST SECTION FOR THE LANGLEY 0.3-METER TRANSONIC CRYOGENIC TUNNEL
Raymond E. Mineck and Acquilla S. Hill Washington Dec. 1990 111 p
(NASA-TP-3049; L-16787; NAS 1.60:3049) Avail: NTIS HC/MF A06 CSCL 14B

A 13 by 13 inch adaptive wall test section was installed in the 0.3 Meter Transonic Cryogenic Tunnel circuit. This new test section is configured for 2-D airfoil testing. It has four solid walls. The top and bottom walls are flexible and movable whereas the sidewalls are rigid and fixed. The wall adaptation strategy employed requires the test section wall shapes associated with uniform test section Mach number distributions. Calibration tests with the test section empty were conducted with the top and bottom walls linearly diverged to approach a uniform Mach number distribution. Pressure distributions were measured in the contraction cone, the test section, and the high speed diffuser at Mach numbers from 0.20 to 0.95 and Reynolds numbers from 10 to 100 x 10 (exp 6)/per foot. Author

N91-13462*# National Aeronautics and Space Administration. Langley Research Center, Hampton, VA.
WIND-TUNNEL SURVEY OF AN OSCILLATING FLOW FIELD FOR APPLICATION TO MODEL HELICOPTER ROTOR TESTING
Paul H. Mirick, M-Nabil H. Hamouda, and William T. Yeager, Jr. (Army Aerostructures Directorate, Hampton, VA.) Washington Dec. 1990 37 p
(DA Proj. 1L1-62211-A-47-AB)
(NASA-TM-4224; L-16757; NAS 1.15:4224; AVSCOM-TR-90-B-007) Avail: NTIS HC/MF A03 CSCL 14B

A survey was conducted of the flow field produced by the Airstream Oscillator System (AOS) in the Langley Transonic Dynamics Tunnel (TDT). The magnitude of a simulated gust field was measured at 15 locations in the plane of a typical model helicopter rotor when tested in the TDT using the Aeroelastic Rotor Experimental System (ARES) model. These measurements were made over a range of tunnel dynamic pressures typical of those used for an ARES test. The data indicate that the gust field produced by the AOS is non-uniform across the tunnel test section, but should be sufficient to excite a model rotor. Author

N91-13463*# Madison Magnetics, Inc., WI.
MAGNETIC SUSPENSION AND BALANCE SYSTEM ADVANCED STUDY, PHASE 2 Final Report, Jul. 1986 - May 1990
R. W. Boom, M. K. Abdelsalam, Y. M. Eyssa, and G. E. McIntosh Washington NASA Nov. 1990 224 p
(Contract NAS1-18279)
(NASA-CR-4327; NAS 1.26:4327) Avail: NTIS HC/MF A10 CSCL 14B

The design improvements for the system encompass 14 or 18 external superconductive coils mounted on a 8 x 8 foot wind tunnel, a superconductive model core magnet on a holmium mandrel to fit an F-16 model, model wings of permanent magnet material Nd2Fe14B, and fiber glass epoxy structure. The Magnetic Suspension and Balance System (MSBS) advanced design is confirmed by the successful construction and test of a full size superconductive model core solenoid with holmium mandrel. The solenoid is 75 cm long and 12.6 cm in diameter and produces 6.1 tesla for a hold time of 47 minutes. An integrated coil system design of a new compact configuration without specific coils for roll or pitch shows promise of simplicity; magnet reductions of 30 percent compared to the most recent 1985 design are possible. Author

N91-13464# Army Engineer Waterways Experiment Station, Vicksburg, MS. Geotechnical Lab.
LITERATURE REVIEW ON GEOTEXTILES TO IMPROVE PAVEMENTS FOR GENERAL AVIATION AIRPORTS Final Report
Dewey W. White, Jr. Oct. 1990 57 p Prepared in cooperation with Federal Aviation Administration, Washington, DC
(Contract DTFA01-89-Z-02029)
(DOT/FAA/RD-90/26) Avail: NTIS HC/MF A04

A literature search and review to obtain information on geotextile applications related to pavement construction are covered. This information was obtained for application to geotextiles in general aviation pavements. The study revealed that there are numerous design procedures available for using geotextiles in aggregate surface pavements and flexible pavement road construction. The state-of-the-art has not advanced to the point where design procedures for using geotextiles in paved airport construction are available. Construction/installation procedures are available for using geotextiles in aggregate surfaced pavements and flexible pavements for roads, and these may be used as an aid in recommending procedures for airport construction. Results of comprehensive tests by researchers indicate that geogrids have more potential than geotextiles for reinforcement of flexible pavements. Author

N91-13465# Federal Aviation Administration, Washington, DC.
LABORATORY INVESTIGATION OF THE USE OF GEOTEXTILES TO MITIGATE FROST HEAVE Final Report
Karen S. Henry (Army Cold Regions Research and Engineering Lab., Hanover, NH.) Aug. 1990 35 p
(DOT/FAA/RD-90/13; CRREL-90-6) Avail: NTIS HC/MF A03

Frost action beneath pavements can lead to several problems, including thaw weakening, which leads to cracking and subsequent pumping of fine soil particles onto the surface, as well as hazardous conditions caused by differential heaving. This study utilized data and frost-susceptible soil collected at Ravalli County Airport, Hamilton, Montant, to study the use of geotextiles to mitigate frost heave. The ability of geotectiles to reduce frost heave in subgrade material by creating a capillary break was assessed by inserting disks of fabric in soil samples and subjecting them to laboratory frost heave tests. Frost heave tests were also conducted to classify the frost-susceptibilities of soils at the airport. Soil moisture characteristics and unsaturated hydraulic conductivities were determined for soils tested as well as for one of the geotextiles used. Results of the laboratory investigation indicate that certain geotextiles show promise for use as capillary breaks. In laboratory tests, the presence of geotextiles led to the reduction of frost heave by amounts up to 60 percent. It is speculated that the capillary breaks action provided by the geotextile is attributable to the pore size and structure of the material and the surface properties of the fibers. Author

N91-13466*# National Aeronautics and Space Administration. Ames Research Center, Moffett Field, CA.
TURBULENCE AND PRESSURE LOSS CHARACTERISTICS OF THE INLET VANES FOR THE 80- BY 120-FT WIND TUNNEL
Michael R. Dudley Oct. 1990 23 p
(NASA-TM-102808; A-90123; NAS 1.15:102808) Avail: NTIS HC/MF A03 CSCL 14B

A series of wind tunnel investigations were conducted to determine the flow characteristics downstream of a set of wind tunnel inlet flow conditioning vanes. The purpose was to develop an understanding of the flow mechanisms that contributed to the pressure loss and turbulence generated by the vane set. The near-field characteristics and flow field development were investigated with a 1/3 scale two dimensional model of the vane set at near full-scale Reynolds numbers. In a second series of tests, the global flow field characteristics were investigated by

means of a 1/15 scale model of the full vane set and the 5:1 contraction leading to the model's test section. Scale effects due to Reynolds number mismatch were identified and their significance noted and accounted for when possible. Scaling parameters were adopted that allowed predictions to be made of the expected turbulence and pressure distributions in the full-scale wind tunnel test section, based on the small-scale test results. The predictions were found to be in good agreement with actual measurements made in the full-scale facility. Author

N91-13467*# National Aeronautics and Space Administration. Langley Research Center, Hampton, VA.
SIMULATION OF PRESSURE AND TEMPERATURE RESPONSES FOR THE 20 INCH SUPERSONIC WIND TUNNEL
Mark A. Motter Dec. 1990 53 p
(NASA-TM-102647; NAS 1.15:102647) Avail: NTIS HC/MF A04 CSCL 14B

A simulation of the pressure and temperature responses of the 20 inch Supersonic Wind Tunnel (SWT) is developed. The simulation models the tunnel system as a set of lumped parameter volumes connected by flow regulating elements such as valves and nozzles. Simulated transient responses of temperature and pressure for the five boundary points of the 20 inch SWT operating map are produced from their respective initial conditions, tunnel operating conditions, heater input power, and valve positions. Upon reaching steady state, a linearized model for each operating point is determined. Both simulated and actual tunnel responses are presented for comparison. Author

N91-13468 Institute for Perception RVO-TNO, Soesterberg (Netherlands).
SIMULATOR FLIGHT AS A SELECTION DEVICE: EFFECTS OF TEST ANXIETY ON SUBJECTIVE AND OBJECTIVE MEASURES OF PERFORMANCE Final Report
P. G. A. M. Jorna and R. T. B. Visser 15 Mar. 1990 21 p
(Contract A81/KM/126)
(IZF-1989-57; TD-89-4555; ETN-91-98306) Copyright Avail: Institute for Perception RVO-TNO, P.O. Box 23, 3769 ZG Soesterberg, Netherlands

The use of flight simulators as selection tools is discussed. Test procedures typically involve several flights in order to assess the trainability of an aspirant pilot. Performance is evaluated by an instructor and a positive grading is required to enter pilot training. The grading procedure as a selection tool, may confound situational stress responses with individual differences in information processing capacity. Situational or state-anxiety provoked by task demands and risk of failure could influence its validity by reducing the subjects' capacity for task-relevant information processing. The instances of anxiety are evaluated and their effects on flight performance studied by contrasting subjects with high and low levels of anxiety. Performance on these tests is evaluated by subjective instructor ratings and objective measures of flight control. ESA

12 ASTRONAUTICS (GENERAL)

For extraterrestrial exploration see *91 Lunar and Planetary Exploration.*

N91-13469# Air Force Systems Command, Wright-Patterson AFB, OH. Foreign Technology Div.
SPACE FLIGHT UNDERTAKINGS OF PRESENT-DAY CHINA (PHOTO CAPTIONS ON 65 SELECTED PAGES)
30 Apr. 1990 11 p Transl. into ENGLISH from Dang Dai Zhong Guo de Hangtian Shiye, Zhongguo Shehui Kexue Chubanshe (Beiging, China), 1986 7 p
(AD-A222816) Avail: NTIS HC/MF A03 CSCL 22/1

Photo captions (without photos) were translated and given for 65 pages of this book. E.R.

13 ASTRODYNAMICS

Includes powered and free-flight trajectories; and orbital and launching dynamics.

N91-13470*# Texas Univ., Austin. Center for Space Research.
MEASURING THE LENSE-THIRRING PRECESSION USING A SECOND LAGEOS SATELLITE Final Report
B. D. Tapley and I. Ciufolini (Consiglio Nazionale delle Ricerche, Frascati, Italy) 30 Sep. 1989 137 p
(Grant NAGw-1330)
(NASA-CR-186945; NAS 1.26:186945; CSR-89-3) Avail: NTIS HC/MF A07 CSCL 22A

A complete numerical simulation and error analysis was performed for the proposed experiment with the objective of establishing an accurate assessment of the feasibility and the potential accuracy of the measurement of the Lense-Thirring precession. Consideration was given to identifying the error sources which limit the accuracy of the experiment and proposing procedures for eliminating or reducing the effect of these errors. Analytic investigations were conducted to study the effects of major error sources with the objective of providing error bounds on the experiment. The analysis of realistic simulated data is used to demonstrate that satellite laser ranging of two Lageos satellites, orbiting with supplemental inclinations, collected for a period of 3 years or more, can be used to verify the Lense-Thirring precession. A comprehensive covariance analysis for the solution was also developed. Author

N91-13471# Nationaal Inst. voor Kernfysica en Hoge Energiefysica, Amsterdam (Netherlands).
LOCAL CLOSED ORBIT BUMPS IN AmPS
R. Maas Apr. 1990 31 p
(NIKHEF-K/AmPS/90-01; ETN-91-98324) Avail: NTIS HC/MF A03

It is shown that the regular Orbit Correction (OC) coils can be used to produce small corrections on the closed orbit in three areas where such corrections may be needed. Since the action of the OC is linear, the production of a local bump does not hamper the normal action of the OC. The two settings can simply be added. The total required strength should not exceed the rating of the coil (presumably phi max equals 1.0 mrad for both planes). ESA

N91-13472# Royal Aerospace Establishment, Farnborough (England).
ORBIT DETERMINATION AND ANALYSIS FOR AUREOLE 2 ROCKET AT 27:2 RESONANCE
A. N. Winterbottom 26 Feb. 1990 31 p
(RAE-TR-90018; RAE-SS-11; BR114653; ETN-91-98363)
Copyright Avail: NTIS HC/MF A03

Accurate orbits are computed on the basis of observations made during the time when the 27:2 resonance with the geopotential was affecting the orbit of the Aureole 2 rocket. Lumped geopotential harmonics of order 27 are evaluated from the changes they produce in the orbital inclination and eccentricity. It is shown that the resonance angle derivative increases quite steadily but is rather slower after the exact resonance. To obtain more precise values of the lumped harmonics than with the comprehensive models of the gravity field, a less eccentric orbit of considerably lower drag is necessary. ESA

14 GROUND SUPPORT SYSTEMS AND FACILITIES (SPACE)

Includes launch complexes, research and production facilities; ground support equipment, e.g., mobile transporters; and simulators.

For related information see also *09 Research and Support Facilities (Air).*

No abstracts in this category.

15 LAUNCH VEHICLES AND SPACE VEHICLES

Includes boosters; operating problems of launch/space vehicle systems; and reusable vehicles.

For related information see also *20 Spacecraft Propulsion and Power.*

No abstracts in this category.

16 SPACE TRANSPORTATION

Includes passenger and cargo space transportation, e.g., shuttle operations; and space rescue techniques.

For related information see also *03 Air Transportation and Safety* and *18 Spacecraft Design, Testing and Performance.* For space suits see *54 Man/System Technology and Life Support.*

No abstracts in this category.

17 SPACE COMM., SPACECRAFT COMM., COMMAND & TRACKING

Includes telemetry; space communications networks; astronavigation and guidance; and radio blackout.

For related information see also *04 Aircraft Communications and Navigation* and *32 Communications and Radar.*

No abstracts in this category.

18 SPACECRAFT DESIGN, TESTING AND PERFORMANCE

Includes satellites; space platforms; space stations; spacecraft systems and components such as thermal and environmental controls; and attitude controls.

For life support systems see *54 Man/System Technology and Life Support.* For related information see also *05 Aircraft Design, Testing and Performance, 39 Structural Mechanics,* and *16 Space Transportation.*

N91-13473*# National Aeronautics and Space Administration. Langley Research Center, Hampton, VA.
ANALYTICAL AND PHOTOGRAMMETRIC CHARACTERIZATION OF A PLANAR TETRAHEDRAL TRUSS
K. Chauncey Wu, Richard R. Adams, and Marvin D. Rhodes
Washington Dec. 1990 30 p
(NASA-TM-4231; L-16758; NAS 1.15:4231) Avail: NTIS HC/MF A03 CSCL 22B

Future space science missions are likely to require near-optical quality reflectors which are supported by a stiff truss structure. This support truss should conform closely with its intended shape to minimize its contribution to the overall surface error of the reflector. The current investigation was conducted to evaluate the planar surface accuracy of a regular tetrahedral truss structure by comparing the results of predicted and measured node locations. The truss is a 2-ring hexagonal structure composed of 102 equal-length truss members. Each truss member is nominally 2 meters in length between node centers and is comprised of a graphite/epoxy tube with aluminum nodes and joints. The axial stiffness and the length variation of the truss components were determined experimentally and incorporated into a static finite element analysis of the truss. From this analysis, the root mean square (RMS) surface error of the truss was predicted to be 0.11 mm (0004 in). Photogrammetry tests were performed on the assembled truss to measure the normal displacements of the upper surface nodes and to determine if the truss would maintain its intended shape when subjected to repeated assembly. Considering the variation in the truss component lengths, the measures rms error of 0.14 mm (0.006 in) in the assembled truss is relatively small. The test results also indicate that a repeatable truss surface is achievable. Several potential sources of error were identified and discussed. Author

N91-13474*# Spectra Research Systems, Inc., Huntsville, AL. Systems Technology Div.
TELEROBOTIC ON-ORBIT REMOTE FLUID RESUPPLY SYSTEM Final Report, May - Jul. 1989
17 Sep. 1990 79 p
(Contract NAS8-37743)
(NASA-CR-184052; NAS 1.26:184052; SRS/STD-TR90-89)
Avail: NTIS HC/MF A05 CSCL 22B

The development of a telerobotic on-orbit fluid resupply demonstration system is described. A fluid transfer demonstration system was developed which functionally simulates operations required to remotely transfer fluids (liquids or gases) from a servicing spacecraft to a receiving spacecraft through the use of telerobotic manipulations. The fluid system is representative of systems used by current or planned spacecraft and propulsion stages requiring on-orbit remote resupply. The system was integrated with an existing MSFC remotely controlled manipulator arm to mate/demate couplings for demonstration and evaluation of a complete remotely operated fluid transfer system. Author

N91-13475# Massachusetts Inst. of Tech., Cambridge. Lincoln Lab.
LOADING THE LES-9 WIDEBAND UHF TRANSPONDER
Bruce F. McGuffin 21 Jun. 1990 43 p
(Contract F19628-90-C-0002)
(AD-A226179; TR-882; ESD-TR-90-026) Avail: NTIS HC/MF A03 CSCL 22/2

This report describes results of a loading study performed for the LES-9 wideband UHF transponder. The study goal was to improve service quality, and increase satellite utilization by scheduling more concurrent users. Power-sharing models for LES-9 are developed using the time-domain model for nonlinear transponders. All nonsignal transponder output power is treated as noise, with power spectrum uniformly distributed across the transponder bandwidth. Compatible groups of users are found for LES-9, supporting common user terminal configurations. Based on the results of this study, it is recommended that all users be allowed to increase uplink power. GRA

N91-13476*# Jet Propulsion Lab., California Inst. of Tech., Pasadena.
AN APPLICATION OF MULTIATTRIBUTE DECISION ANALYSIS TO THE SPACE STATION FREEDOM PROGRAM. CASE STUDY: AUTOMATION AND ROBOTICS TECHNOLOGY EVALUATION

Jeffrey H. Smith, Richard R. Levin, and Elisabeth J. Carpenter 1 May 1990 196 p
(Contract NAS7-918)
(NASA-CR-187432; JPL-Publ-90-12; NAS 1.26:187432) Avail: NTIS HC/MF A09 CSCL 22B

The results are described of an application of multiattribute analysis to the evaluation of high leverage prototyping technologies in the automation and robotics (A and R) areas that might contribute to the Space Station (SS) Freedom baseline design. An implication is that high leverage prototyping is beneficial to the SS Freedom Program as a means for transferring technology from the advanced development program to the baseline program. The process also highlights the tradeoffs to be made between subsidizing high value, low risk technology development versus high value, high risk technology developments. Twenty one A and R Technology tasks spanning a diverse array of technical concepts were evaluated using multiattribute decision analysis. Because of large uncertainties associated with characterizing the technologies, the methodology was modified to incorporate uncertainty. Eight attributes affected the rankings: initial cost, operation cost, crew productivity, safety, resource requirements, growth potential, and spinoff potential. The four attributes of initial cost, operations cost, crew productivity, and safety affected the rankings the most. Author

N91-13477# Cincinnati Univ., OH. Dept. of Aerospace Engineering and Engineering Mechanics.
MULTIVARIABLE METHODS FOR THE DESIGN, IDENTIFICATION, AND CONTROL OF LARGE SPACE STRUCTURES. VOLUME 1: ESTIMATOR EIGENVALUE PLACEMENT IN POSITIVE REAL DESIGN Final Report, Jul. 1987 - Feb. 1989
G. L. Slater and M. D. McLaren Jul. 1989 36 p
(Contract F33615-86-C-3216)
(AD-A226525; WRDC-TR-90-3037-Vol-1) Avail: NTIS HC/MF A03 CSCL 22/2

The objective of this contract was to develop mathematical algorithms for the integration of structural dynamics and controls with particular reference to the design of large space structures. A numerical technique is presented to place the eigenvalues of the estimator in a positive real control environment. The estimator is based on a reduced-order model of the full system. The technique involves posing the problem as a constrained optimization problem. Two formulations are presented for solving the optimization problem, which differ in their objective functions and in the way constraints are handled. Examples are given illustrating the pole placement for estimators based on arbitrary second order model and on fourth and sixth order models of the DRAPER I tetrahedral truss structure. GRA

N91-13478# Cincinnati Univ., OH. Dept. of Aerospace Engineering and Engineering Mechanics.
MULTIVARIABLE METHODS FOR THE DESIGN, IDENTIFICATION, AND CONTROL OF LARGE SPACE STRUCTURES. VOLUME 3: A STUDY OF THE INTEGRATED CONTROL/STRUCTURE DESIGN OPTIMIZATION PROBLEM FOR LARGE FLEXIBLE STRUCTURES Final Report, Jul. 1987 - Feb. 1989
M. D. McLaren and G. L. Slater Jul. 1989 101 p
(Contract F33615-86-C-3216)
(AD-A226526; WRDC-TR-90-3037-Vol-3) Avail: NTIS HC/MF A06 CSCL 22/2

A comparison of optimal and suboptimal estimation applied to large flexible structures under perfect and imperfect model information conditions is presented. The filters estimate the modal positions and velocities of a simple pinned-pinned beam. Among the types of estimators investigated are full and reduce-order centralized estimators, reduced-order decentralized estimators, and one-mode and two-mode sensitivity-shaped estimators. The suboptimal estimators are shown to have lower position rms error values than the optimal estimator when 20 percent errors in the structural frequencies are present. The sensitivity-shaped estimators produce more accurate position estimates when velocity sensors are used that any of the reduced-order linear quadratic centralized or decentralized estimators. A method for choosing the gains of the sensitivity-shaped estimators is given. Robustness of the system is discussed using a proposed phase-shaping method and the Lyapunov method. The closed-loop system with the one-mode sensitivity-shaped filter is proven to be marginally stable with the former method and asymptotically stable with the latter method, provided controller gains satisfy requirements. GRA

N91-13479# Texas A&M Univ., College Station.
ANALYTICAL AND EXPERIMENTAL RESEARCH ON LARGE ANGLE MANEUVERS OF FLEXIBLE STRUCTURES Final Report, 1 Oct. 1988 - 31 Mar. 1990
John L. Junkins, Thomas C. Pollock, and Zahidul H. Rahman 4 May 1990 310 p
(Contract F49620-87-C-0078)
(AD-A226679; TAMURF-AERO-90-5-1; AFOSR-90-0919TR)
Avail: NTIS HC/MF A14 CSCL 22/1

New methods are presented for structural system identification and control of large angle maneuvers. Both analytical and experimental results are presented. Globally stable control laws for flexible body maneuvers are derived and validated experimentally. Stereo triangulation methods are proposed and tested experimentally for structural identification. GRA

N91-13480*# Colorado Univ., Boulder. Center for Space Structures and Controls.
COMPUTATIONAL METHODS AND SOFTWARE SYSTEMS FOR DYNAMICS AND CONTROL OF LARGE SPACE STRUCTURES Final Report
K. C. Park, C. A. Felippa, C. Farhat, and E. Pramono Jul. 1990 265 p
(Grant NAG1-756)
(NASA-CR-187669; NAS 1.26:187669; CU-CSSC-90-17) Avail: NTIS HC/MF A12 CSCL 22B

Two key areas of crucial importance to the computer-based simulation of large space structures are discussed. The first area involves multibody dynamics (MBD) of flexible space structures, with applications directed to deployment, construction, and maneuvering. The second area deals with advanced software systems, with emphasis on parallel processing. The latest research thrust in the second area involves massively parallel computers. Author

N91-13481*# National Aeronautics and Space Administration. Langley Research Center, Hampton, VA.
INTEGRATED LAUNCH AND EMERGENCY VEHICLE SYSTEM Patent Application
James A. Martin, inventor (to NASA) 31 Aug. 1990 17 p
(NASA-Case-LAR-13780-1; NAS 1.71:LAR-13780-1; US-Patent-Appl-SN-575737) Avail: NTIS HC/MF A03 CSCL 22B

A heavy launch vehicle is disclosed for placing a payload into a spatial earth orbit including an expendable, multi-container, propellant tank having a plurality of winged booster propulsion modules releasably disposed about one end thereof; and a payload supported by adapter structure at the other end. The preferred payload is an entry module adapted to be docked to a space station and used as a return vehicle for the space station crew, as scheduled, or in emergency situations. Alternately, the payload may include communication satellites, supplies, equipment and/or structural elements for the space station. The winged propulsion modules are released from the expendable propellant tank in pairs and return to Earth in a controlled glide, for safe landing at or near the launch site and prepared for reuse. The rocket engines for each propulsion module are dual-fuel, dual-mode engines and use methane-oxygen and hydrogen-oxygen, respectively, from the multi-containers of the propellant tank. When the propulsion modules are released from the expendable propellant tank, the rocket engines are pivotally moved into the module cargo bay for the return glide flight. NASA

N91-13482*# National Aeronautics and Space Administration. Marshall Space Flight Center, Huntsville, AL.
STANDARD REMOTE MANIPULATOR SYSTEM DOCKING TARGET AUGMENTATION FOR AUTOMATED DOCKING Patent Application
Richard Dabney, inventor (to NASA), Richard Howard, inventor (to NASA), and Thomas Bryan, inventor (to NASA) 20 Feb. 1990 12 p
(NASA-Case-MFS-28419-1; NAS 1.71:MFS-28419-1; US-Patent-Appl-SN-431538) Avail: NTIS HC/MF A03 CSCL 22B

A docking target is provided for use in automated docking of a first vehicle on which the target is located. The target comprising a pair of laterally extending arm portions lying in substantially the same plane and a central post extending outwardly from the plane of the arm portions. At least three reflectors are located on the target, two of the reflectors being located at the outboard ends of the arms portions and another reflector being located at the end of the central post. In an important embodiment, the reflectors comprise individual pieces of retroreflective tape. The reflectors, when viewed from the front of the target, are aligned along the longitudinal center line of the target, and can take a number of different shapes including circular or square. NASA

N91-13483*# National Aeronautics and Space Administration. Lyndon B. Johnson Space Center, Houston, TX.
ASSURED CREW RETURN VEHICLE Patent Application
Christopher J. Cerimele, inventor (to NASA), Robert C. Ried, inventor (to NASA), Wayne L. Peterson, inventor (to NASA), George A. Zupp, Jr., inventor (to NASA), Michael J. Stagnaro, inventor (to NASA), and Brian Ross, inventor (to NASA) 28 Dec. 1989 87 p
(NASA-Case-MSC-21536-1; NAS 1.71:MSC-21536-1; US-Patent-Appl-SN-458476) Avail: NTIS HC/MF A05

A return vehicle is disclosed for use in returning a crew to Earth from low earth orbit in a safe and relatively cost effective manner. The return vehicle comprises a cylindrically-shaped crew compartment attached to the large diameter of a conical heat sheild having a spherically rounded nose. On-board inertial navigation and cold gas control systems are used together with a de-orbit propulsion system to effect a landing near a preferred site on the surface of the Earth. State vectors and attitude data are loaded from the attached orbiting craft just prior to separation of the return vehicle. NASA

19 SPACECRAFT INSTRUMENTATION

For related information see also *06 Aircraft Instrumentation* and *35 Instrumentation and Photography.*

N91-13484*# University of Southern California, Marina del Rey. Inst. of Physics.
DEVELOPMENT OF MERCURIC IODIDE UNCOOLED X RAY DETECTORS AND SPECTROMETERS Final Report, period ending 30 Sep. 1989
Jan S. Iwanczyk 1 Nov. 1990 45 p
(Grant NAGw-1401)
(NASA-CR-185394; NAS 1.26:185394) Avail: NTIS HC/MF A03 CSCL 22B

The results obtained in the development of miniature, lowpower, light weight mercuric iodide, HgI2, x ray spectrometers for future space missions are summarized. It was demonstrated that HgI2 detectors can be employed in a high resolution x ray spectrometer, operating in a scanning electron microscope. Also, the development of HgI2 x ray detectors to augment alpha backscattering spectrometers is discussed. These combination instruments allow for the identification of all chemical elements, with the possible exception of hydrogen, and their respective concentrations. Additionally, further investigations of questions regarding radiation damage effects in the HgI2 x ray detectors are reported. Author

20 SPACECRAFT PROPULSION AND POWER

Includes main propulsion systems and components, e.g., rocket engines; and spacecraft auxilliary power sources.

For related information see also *07 Aircraft Propulsion and Power, 28 Propellants and Fuels, 44 Energy Production and Conversion,* and *15 Launch Vehicles and Space Vehicles.*

N91-13485*# Pratt and Whitney Aircraft, West Palm Beach, FL. Government Products Div.
ALL SHUTTLE CENTAUR ENGINE AND NOZZLE SUPPORT PLUG VIBRATION TESTING Final Report, Mar. 1985 - Jan. 1986
May 1987 83 p
(Contract NAS3-23791)
(NASA-CR-183201; NAS 1.26:183201; FR-19540-1) Avail: NTIS HC/MF A05 CSCL 21H

Loads applied to the RL10 engines while in flight in the orbiter payload bay are significantly different from the load environment experienced in Atlas and Titan/Centaur applications. To predict the engine loads, a NASTRAN analysis was conducted. As part of this effort a vibration test program was accomplished to provide input to the analysis, and to verify engine durability. This program was completed in two phases. The first phase provided data and characteristics which were used as input to the analysis. The second phase subjected the engine to limit loads, and included hot firings before and after the vibration test. The test hardware, performance, and results are described. Author

N91-13486*# Pratt and Whitney Aircraft, West Palm Beach, FL. Government Products Div.
RL10A-3-3B HIGH MIXTURE RATIO QUALIFICATION PROGRAM Final Report, Mar. 1985 - Jan. 1986
T. Vogel, D. Varella, and C. Smith May 1987 140 p
(Contract NAS3-22902)
(NASA-CR-183200; NAS 1.26:183200; FR-19435-1) Avail: NTIS HC/MF A07 CSCL 21H

The results of the high mixture ratio qualification testing of the RL10 engine for the Shuttle/Centaur program are presented. The objective of the engine qualification test was to demonstrate the suitability of the RL10A-3-3B engine for space vehicle flight by subjecting it to the testing specified in RL10A-3-3B Model Specification Number 2295 dated February 1986. The applicable section of the specification is presented. Due to payload volume advantages which can be achieved by increasing the operating mixture ratio of the RL10, a decision was made to qualify the engine to run at a higher mixture ratio. A program was created to qualify the RL10 engine for operation at 15,000 pounds thrust and a nominal 6.0 to 1 mixture ratio. This model of the engine was designated the RL10A-3-3B. The qualification program included three test series as follows: (1) hardware durability and limits test in which the engine completed 23 firings and 4605.7 seconds with 1588.7 seconds at less than 6.6 mixture ratio; (2) preliminary qualification test in which the engine completed 26 firings and 5750 seconds; and (3) qualification test in which the engine completed 26 hot firings and 5693.4 seconds with 905.9 seconds at 6.7 mixture ratio. Several changes in engine hardware were required for operation of the RL10A-3-3B engine in the Space Shuttle which include a duel pressure switch ignition, an oxidizer flow control, and helium plumbing changes. Author

N91-13487*# Pratt and Whitney Aircraft, West Palm Beach, FL. Government Products Div.
SHUTTLE CENTAUR ENGINE COOLDOWN EVALUATION AND EFFECTS OF EXPANDED INLETS ON START TRANSIENT Final Report, Aug. 1984 - Dec. 1985
May 1987 148 p
(Contract NAS3-22902)
(NASA-CR-183198; NAS 1.26:183198; FR-19545-1) Avail: NTIS HC/MF A07 CSCL 21H

As part of the integration of the RL10 engine into the Shuttle

Centaur vehicle, a satisfactory method of conditioning the engine to operating temperatures had to be established. This procedure, known as cooldown, is different from the existing Atlas Centaur due to vehicle configuration and mission profile differenced. The program is described, and the results of a Shuttle Centaur cooldown program are reported. Mission peculiarities cause substantial variation in propellant inlet conditions between the substantiated Atlas Centaur and Shuttle Centaur with the Shuttle Centaur having much larger variation in conditions. A test program was conducted to demonstrate operation of the RL10 engine over the expanded inlet conditions. As a result of this program, the Shuttle Centaur requirements were proven satisfactory. Minor configuration changes incorporated as a result of this program provide substantial reduction in cooldown propellant consumption. Author

N91-13488# Advisory Group for Aerospace Research and Development, Neuilly-Sur-Seine (France). Propulsion and Energetics Panel.
HAZARD STUDIES FOR SOLID PROPELLANT ROCKET MOTORS
Thomas L. Boggs, ed. and Ronald L. Derr, ed. Sep. 1990 205 p
(AGARD-AG-316; ISBN-92-835-0581-6) Copyright Avail: NTIS HC/MF A10; Non-NATO Nationals requests available only from AGARD/Scientific Publications Executive

This AGARDograph summarizes hazard studies for solid propellant rocket motors over the period 1984 to 1989. The AGARDograph presents concepts and methods for evaluating hazard risks associated with solid propellant rocket motors and the technology for minimizing potential damage due to these hazards. Author

N91-13489*# CHAM of North America, Inc., Huntsville, AL.
THRUST CHAMBER MODELING USING NAVIER-STOKES EQUATIONS: CODE DOCUMENTATION AND LISTINGS, VOLUME 2
P. L. Daley and S. F. Owens Dec. 1988 122 p
(Contract NAS8-36552)
(NASA-CR-183617; NAS 1.26:183617; CHAM-2008/3-A-Vol-2) Avail: NTIS HC/MF A06 CSCL 21H

A copy of the PHOENICS input files and FORTRAN code developed for the modeling of thrust chambers is given. These copies are contained in the Appendices. The listings are contained in Appendices A through E. Appendix A describes the input statements relevant to thrust chamber modeling as well as the FORTRAN code developed for the Satellite program. Appendix B describes the FORTRAN code developed for the Ground program. Appendices C through E contain copies of the Q1 (input) file, the Satellite program, and the Ground program respectively. Author

N91-13490# Los Alamos National Lab., NM.
THE BEHAVIOR OF FISSION PRODUCTS DURING NUCLEAR ROCKET REACTOR TESTS
Peter C. Bokor, William L. Kirk, and Richard J. Bohl 1991 13 p Presented at the 8th Symposium on Space Nuclear Power Systems, Albuquerque, NM, 6-10 Jan. 1991
(Contract W-7405-eng-36)
(DE91-001956; LA-UR-90-3544; CONF-910116-4) Avail: NTIS HC/MF A03

The experience base regarding fission product behavior developed during the Rover program, the nuclear rocket development program of 1955 to 1972, will be useful in planning a renewed nuclear rocket program. During the Rover program, 20 reactors were tested at the Nuclear Rocket Development Station in Nevada. Nineteen of these discharged effluent directly into the atmosphere; the last reactor tested, a non-flight-prototypic, fuel-element-testing reactor called the Nuclear Furnace (NF-1) was connected to an effluent cleanup system that removed fission products before the hydrogen coolant (propellant) was discharged to the atmosphere. In general, we are able to increase both test duration and fuel temperature during the test series. Therefore fission product data from the later part of the program are more interesting and more applicable to future reactors. We have collected fission product retention (and release) data reported in both formal and informal publications for six of the later reactor tests; five of these were Los Alamos reactors that were firsts of a kind in configuration or operating conditions. We have also, with the cooperation of Westinghouse, included fission product data from the NRX-A6 reactor, the final member of series of developmental reactors with the same basic geometry, but with significant design and fabrication improvements as the series continued. Table 1 lists the six selected reactors and the test parameters for each. DOE

N91-13491*# National Aeronautics and Space Administration. Lewis Research Center, Cleveland, OH.
JANNAF LIQUID ROCKET COMBUSTION INSTABILITY PANEL RESEARCH RECOMMENDATIONS
Mark D. Klem 1990 12 p Presented at the 27th JANNAF Combustion Meeting, Cheyenne, WY, 5-9 Nov. 1990
(NASA-TM-103653; E-5826; NAS 1.15:103653) Avail: NTIS HC/MF A03 CSCL 21H

The Joint Army, Navy, NASA, Air Force (JANNAF) Liquid Rocket Combustion Instability Panel was formed in 1988, drawing its members from industry, academia, and government experts. The panel was charted to address the needs of near-term engine development programs and to make recommendations whose implementation would provide not only sufficient data but also the analysis capabilities to design stable and efficient engines. The panel was also chartered to make long-term recommendations toward developing mechanistic analysis models that would not be limited by design geometry or operating regime. These models would accurately predict stability and thereby minimize the amount of subscale testing for anchoring. The panel has held workshops on acoustic absorbing devices, combustion instability mechanisms, instability test hardware, and combustion instability computational methods. At these workshops, research projects that would meet the panel's charter were suggested. The JANNAF Liquid Rocket Combustion Instability Panel's conclusions about the work that needs to be done and recommendations on how to approach it, based on evaluation of the suggested research projects, are presented. Author

23 CHEMISTRY AND MATERIALS (GENERAL)

No abstracts in this category.

24 COMPOSITE MATERIALS

Includes physical, chemical, and mechanical properties of laminates and other composite materials.
For ceramic materials see *27 Nonmetallic Materials.*

N91-13492*# National Aeronautics and Space Administration. Langley Research Center, Hampton, VA.
AN INVESTIGATION OF MICROSTRUCTURAL CHARACTERISTICS OF CONTACT-LENS POLYMERS
Jag J. Singh, Abe Eftekhari, Billy T. Upchurch, and Karen S. Burns (Old Dominion Univ., Norfolk, VA.) Washington Dec. 1990 12 p
(NASA-TP-3034; L-16817; NAS 1.60:3034) Avail: NTIS HC/MF A03 CSCL 11D

The free volume and gas permeability in several contact lens specimens were measured as part of a Space Commercialization Program. Free volume was measured using positron lifetime spectroscopy, while permeability for O2, N2, CO2 gases was measured using mass spectrometry and polarography. Permeability for all gases increases with the mean free volume cell size in the

test samples. As might be expected, the specimens with the highest free volume fraction also exhibit the lowest Rockwell Hardness Number. An interesting corollary is the finding that the presence of fluorine atoms in the lens chemical structure inhibits filling up of their free volume cells. This is expected to allow the lenses to breathe freely while in actual use. Author

N91-13493 Southampton Univ. (England).
EFFECTS OF TEMPERATURE ON ACOUSTICALLY-INDUCED STRAINS AND DAMAGE PROPAGATION IN CFRP PLATES Ph.D. Thesis
Stephen C. P. Galea 1989 359 p
Avail: Univ. Microfilms Order No. BRDX89581

The effect of temperature on the material elastic properties, acoustically-induced strains, damage initiation, damage propagation, and residual thermal strains of composite materials was investigated. An experimental rig, using the free-free beam technique, was built to attain accurate measurements of Young's modulus and loss factor or carbon fiber reinforced plastics (CFRP) beams in the temperature range -40 to 150 C. These results were then compared with measurements taken from a commercially available Dynamic Mechanical Thermal Analyzer. Using the finite element method a study was undertaken to determine the effect of temperature on the free vibration of clamped CFRP plates of various layups. Predictions of natural frequencies of two CFRP plates were then compared with experimentally determined values. CFRP plates subjected to broadband acoustic excitation of OSPL up to 160 dB showed no significant changes in the strain response with increasing temperature. Also predictions of RMS strains using the simple mode formulae agreed reasonably well with measured values for most OSPL and temperatures studied. A flexural fatigue apparatus, using a half-sine clamped cantilevered arrangement, was modified to allow flexural cyclic loading, when placed in an environmental chamber or oven, of CFRP coupons at various temperatures. Flexural fatigue results showed a considerable decrease in flexural fatigue resistance as temperatures were increased to 120 C. An optical microscopic analysis showed damage in CFRP appears to be in the form of translaminar cracking and delamination. Also an SEM analysis showed an increased propensity of fiber/matrix debonding under adverse conditions. A finite element analysis of the cantilevered coupon, under flexural and thermal loads, showed that large laminate residual thermal strains, as well as flexural strains, were present. Dissert. Abstr.

N91-13494*# College of William and Mary, Williamsburg, VA. Applied Science Program.
DAMAGE ASSESSMENT AND RESIDUAL COMPRESSION STRENGTH OF THICK COMPOSITE PLATES WITH THROUGH-THE-THICKNESS REINFORCEMENTS Semiannual Report, 1 Nov. 1989 - 1 Jun. 1990
Barry T. Smith Jun. 1990 11 p Presented at the Review of Progress in QNDE, San Diego, CA, 15-20 Jul. 1990; and Fiber-Tex 1990, Clemson, SC, 14 Aug. 1990
(Grant NAG1-1063)
(NASA-CR-187377; NAS 1.26:187377) Avail: NTIS HC/MF A03 CSCL 11D

Damage in composite materials was studied with through-the-thickness reinforcements. As a first step it was necessary to develop new ultrasonic imaging technology to better assess internal damage of the composite. A useful ultrasonic imaging technique was successfully developed to assess the internal damage of composite panels. The ultrasonic technique accurately determines the size of the internal damage. It was found that the ultrasonic imaging technique was better able to assess the damage in a composite panel with through-the-thickness reinforcements than by destructively sectioning the specimen and visual inspection under a microscope. Five composite compression-after-impact panels were tested. The compression-after-impact strength of the panels with the through-the-thickness reinforcements was almost twice that of the comparable panel without through-the-thickness reinforcement. Author

N91-13495*# National Aeronautics and Space Administration. Lewis Research Center, Cleveland, OH.
RELATIONSHIP BETWEEN VOIDS AND INTERLAMINAR SHEAR STRENGTH OF POLYMER MATRIX COMPOSITES
Kenneth J. Bowles and Stephen Frimpong 1991 20 p Proposed for presentation at the 36th International SAMPE Symposium and Exhibition, San Diego, CA, 15-18 Apr. 1991; sponsored by Society for the Advancement of Materials and Process Engineering
(NASA-TM-103643; E-5825; NAS 1.15:103643) Avail: NTIS HC/MF A03 CSCL 11D

The effect of voids on the interlaminar shear strength of a polyimide matrix composite system is described. The AS4 graphite/PMR-15 composite was chosen for study because this system can be readily processed by using the standard specified cure cycle to produce void-free composites and because preliminary work in this study had shown that the processing parameters of this resin matrix system can be altered to produce cured composites of varying void contents. Thirty-eight 12-ply unidirectional composite panels were fabricated for this study. A significant range of void contents (0 to 10 percent) was produced. The panels were mapped, ultrasonically inspected, and sectioned into interlaminar shear, flexure, and fiber content specimens. The density of each specimen was measured and interlaminar shear and flexure strength measurements were then made. The fiber content was measured last. The results of these tests were evaluated by using ultrasonic results, photomicrographs, statistical methods, theoretical relationships derived by other investigators, and comparison of the test data with the Integrated Composite Analyzer (ICAN) computer program developed at the Lewis Research Center for predicting composite ply properties. The testing is described in as much detail as possible in order to help others make realistic comparisons. Author

N91-13496# Texas A&M Univ., College Station. Center for Mechanics of Composites.
EXPERIMENTAL AND THEORETICAL DETERMINATION OF THE THERMOMECHANICAL RESPONSE OF INELASTIC STRUCTURAL MATERIALS TO HIGH ENERGY THERMAL INPUTS Final Technical Report
David H. Allen and M. S. Pilant Jul. 1990 297 p
(Contract F49620-86-K-0016)
(AD-A226671; CMC-5485-90-1; AFOSR-90-0922TR) Avail: NTIS HC/MF A13 CSCL 13/13

The general objective was to improve on existing theoretical models for predicting the response of inelastic aerospace structural components subjected to hostile thermal environments with emphasis on transient temperature conditions, radiation boundary conditions, extremely rapid heating rates, and possible phase change of the materials involved. For materials subjected to the conditions under study herein it is necessary to perform extremely complex experiments in order to determine the precise form of the theoretical constitutive equations. Finally, it is necessary to implement the resulting equations to boundary value problem solving algorithms in order to model the response of structural components with stress, strain, and temperature gradient fields. GRA

N91-13497# Babcock and Wilcox Co., Lynchburg, VA.
RESEARCH AND DEVELOPMENT OF A CERAMIC FIBER COMPOSITE HEAT EXCHANGER Final Report
W. P. Parks, Jr. Sep. 1989 337 p
(Contract DE-AC07-84ID-12536)
(DE90-017250; DOE/ID-12536/2) Avail: NTIS HC/MF A15

The Babcock and Wilcox Company has completed the Phase 2 study on the Advanced Heat Exchanger Project. Phase 2 addressed critical problems identified in the Phase 1 work. The major activity involved the development and characterization of oxide-oxide ceramic composites. Additional work included seal development and design review. Novel ceramic composite tubular materials were developed using filament winding of ceramic fibers in conjunction with sol-gel infiltration. Composites based on DuPont's PRD-166 fiber and zirconia matrices exhibited 53,000 psi strength at room temperature and 35,000 psi strength at 1100

C. Property characterization included creep, microstructure, density permeability, and porosity. Composites were tested in corrosive environments (NaCO3) and complex refuse combustion for up to 1000 hours with minor corrosion and no erosion. Scale-up to large tubular shapes was exhibited. Compatibility with two glass seal compositions was determined for up to 96 hours at 2000 F and 100 psia. Additional work needed to commercialize this technology was discussed. DOE

N91-13498# Oak Ridge National Lab., TN.
INFLUENCE OF OXIDE REINFORCEMENT MATERIALS ON HIGH-TEMPERATUE OXIDATION RESISTANCE OF Ni3Al MATRIX COMPOSITES
P. F. Tortorelli, J. H. DeVan, C. G. McKamey, and M. Howell 1990 7 p Presented at the Symposium on Composites, Orlando, FL, 15 Nov. 1990
(Contract DE-AC05-84OR-21400)
(DE91-001625; CONF-9011122-1) Avail: NTIS HC/MF A02

The oxidation resistance of Ni3Al-based metal matrix composites was studied in high-temperature air under isothermal and thermal cycling conditions as a function of the composition and form of oxide reinforcement material. The incorporation of oxide fibers Al2O3, HfO2, or Al2O3--ZrO2 or particles into the Ni3Al matrix led to oxidation rates significantly greater than that for the monolithic aluminide. The increase in susceptibility was primarily due to internal oxidation along the fiber- (or particle-) matrix interfaces and depended on the type of reinforcement material and its deposition in the matrix. The results suggest that the choice of reinforcement material and the method of materials processing will be important considerations in the design of oxidation-resistant Ni3Al composites. DOE

N91-13499# Lawrence Livermore National Lab., CA.
MULTIPHASE CARBON AND ITS PROPERTIES IN COMPLEX MIXTURES
M. vanThiel and F. H. Ree Sep. 1990 15 p Presented at the 12th European Conference on Thermophysical Properties, Vienna, Austria, 23-28 1990 Submitted for publication
(Contract W-7405-eng-48)
(DE91-001679; UCRL-JC-103870; CONF-900971-1) Avail: NTIS HC/MF A03

We describe some key features of a carbon three-phase equation of state and a high-pressure high temperature mixture model in which it is used. Electronic terms in the carbon model have been investigated with INFERNO (atom in a cell model). The Lindeman criterion for melting is rederived for the anisotropic structure of the graphite lattice. The curvature of the graphite melting line is constrained by the evidence for the positive slope of the diamond melting line. The importance of carbon is apparent from various experiments on shock generated mixtures. The model allows us to estimate the energy of carbon clusters produced in a detonating mixture. A cluster model with specific surface structure is used to predict this energy. DOE

N91-13500*# National Aeronautics and Space Administration. Lewis Research Center, Cleveland, OH.
COMPOSITE THERMAL BARRIER COATING Patent Application
Salvatore J. Grisaffe, inventor (to NASA) 31 Jul. 1990 12 p
(NASA-Case-LEW-14999-1; NAS 1.71:LEW-14999-1;
US-Patent-Appl-SN-560926) Avail: NTIS HC/MF A03 CSCL 11D

A composite thermal barrier coating for a substrate has a first layer which includes a first ceramic material and a second layer which includes a second ceramic material impregnated with a glass, the glass being a ternary eutectic. The glass may consist of about 14.6 weight percent Al203, about 23.3 weight percent CaO, and about 62.1 weight percent SiO2. The first and second ceramic materials may include yttria-stabilized zirconia. NASA

N91-13501# Lawrence Livermore National Lab., CA. Materials Test and Evaluation Section.
THREE POINT BEND CREEP TESTING OF CARBON/EPOXY
David S. Hiromoto 27 Jun. 1990 20 p
(Contract W-7405-eng-48)
(DE91-001083; UCRL-ID-104835) Avail: NTIS HC/MF A03

This study provides data to verify theoretical models for predicting and characterizing viscoelastic behavior of fiber composites. Since performing uninterrupted creep tests for years at a time was not feasible, creep behavior was accelerated with elevated temperatures. An improved method was developed and implemented for measuring specimen deflection within the tight confines of an environmental chamber. This proved to be critical to make this experiment a success. DOE

N91-13502*# National Aeronautics and Space Administration. Lewis Research Center, Cleveland, OH.
METHOD OF MAKING SINGLE CRYSTAL FIBERS Patent Application
Leonard J. Westfall, inventor (to NASA) 23 Aug. 1990 12 p
(NASA-Case-LEW-14921-1; NAS 1.71:LEW-14921-1;
US-Patent-Appl-SN-571059) Avail: NTIS HC/MF A03 CSCL 11D

Single crystal fibers are made from miniature extruded ceramic feed rods. A decomposable binder is mixed with powders to inform a slurry which is extruded into a small rod which may be sintered, either in air or in vacuum, or it may be used in the extruded and dried condition. A pair of laser beams focuses onto the tip of the rod to melt it thereby forming a liquid portion. A single crystal seed fiber of the same material as the feed rod contacts this liquid portion to establish a zone of liquid material between the feed rod and the single crystal seed fiber. The feed rod and the single crystal feed fiber are moved at a predetermined speed to solidify the molten zone onto the seed fiber while simultaneously melting additional feed rod. In this manner a single crystal fiber is formed from the liquid portion. NASA

N91-13503*# National Aeronautics and Space Administration. Lewis Research Center, Cleveland, OH.
METHOD OF MAKING CARBIDE/FLUORIDE/SILVER COMPOSITES Patent Application
Harold E. Sliney, inventor (to NASA) and Christopher Dellacorte, inventor (to NASA) 23 Aug. 1990 10 p
(NASA-Case-LEW-14902-1; NAS 1.71:LEW-14902-1;
US-Patent-Appl-SN-571058) Avail: NTIS HC/MF A02 CSCL 11D

A composition containing 30 to 70 percent chromium carbide, 5 to 20 percent soft noble metal, 5 to 20 percent metal fluorides, and 20 to 60 percent metal binder is used in a powdered metallurgy process for the production of self-lubricating components, such as bearings. The use of the material allows the self-lubricating bearing to maintain its low friction properties over an extended range of operating temperatures. NASA

N91-13504# Centre Technique des Industries Mecaniques, Nantes (France).
IMPACT BEHAVIOR OF COMPOSITE MATERIALS: EXPLORATORY RESEARCH Final Report [COMPORTEMENT AU CHOC DES MATERIAUX COMPOSITES: ETUDE EXPLORATOIRE]
A. Lemascon 11 Jan. 1989 25 p In FRENCH
(CETIM-101130; ETN-91-98329) Copyright Avail: NTIS HC/MF A03

The impact behavior of various composite materials is studied. Composite materials most often used in industry are shown to have very variable behavior properties. Much of the impact failure of these materials is due to the mediocre quality of many of the products. The impact testing methods and the materials tested are described. Test results are presented. It is concluded that the results obtained only permit comparisons within the experimental framework in which they were obtained. For the same type of impact, wide ranges of response are shown by the materials tested. The ruin phenomena are so different for the materials, that no comparisons can be made without further information concerning the fundamental damage mechanisms. ESA

N91-13505# Royal Armament Research and Development Establishment, Waltham Abbey (England).
WORK OF FRACTURE OF COMPOSITES IN AXIAL COMPRESSION: MEASUREMENT AND ORIGINS M.S. Thesis
N. J. Savage Apr. 1990 56 p
(RARDE-1/90; BR114657; ETN-91-98368) Copyright Avail: NTIS HC/MF A04

A test piece which can be used with Carbon Fiber Reinforced Plastics (CFRP) and Glass Reinforced Plastics (GRP) and allow controllable compression failure to be initiated or interrupted under various environmental conditions is designed. The contribution to the fracture of the different energy mechanisms is investigated. The material tested is an epoxy resin with a novolac additive and is typically used for aerospace applications. In GRP the formation and propagation of failure were strongly influenced by the radii left by the splitting saw used to cut the notch. In CFRP multiple kinks of about 40 microns in length appeared which pile up on top of one another. This effect was not observed in GRP because of the extensive splitting. ESA

25 INORGANIC AND PHYSICAL CHEMISTRY

Includes chemical analysis, e.g., chromatography; combustion theory; electrochemistry; and photochemistry.

For related information see also *77 Thermodynamics and Statistical Physics.*.

N91-13506*# Eloret Corp., Sunnyvale, CA.
COMPUTED POTENTIAL ENERGY SURFACES FOR CHEMICAL REACTIONS Semiannual Report, 1 Jan. - 30 Jun. 1990
Stephen P. Walch 1990 160 p
(Contract NCC2-478)
(NASA-CR-186877; NAS 1.26:186877) Avail: NTIS HC/MF A08 CSCL 21B

The objective was to obtain accurate potential energy surfaces (PES's) for a number of reactions which are important in the H/N/O combustion process. The interest in this is centered around the design of the SCRAM jet engine for the National Aerospace Plane (NASP), which was envisioned as an air-breathing hydrogen-burning vehicle capable of reaching velocities as large as Mach 25. Preliminary studies indicated that the supersonic flow in the combustor region of the scram jet engine required accurate reaction rate data for reactions in the H/N/O system, some of which was not readily available from experiment. The most important class of combustion reactions from the standpoint of the NASP project are radical recombinaton reactions, since these reactions result in most of the heat release in the combustion process. Theoretical characterizations of the potential energy surfaces for these reactions are presented and discussed. Y.S.

N91-13507# Cincinnati Univ., OH. Dept. of Chemistry.
ELECTROCATALYST SURFACES Final Report, Dec. 1986 - Nov. 1989
A. T. Hubbard Feb. 1990 33 p
(Contract GRI-5086-260-1404)
(PB90-252560; GRI-90/0121) Avail: NTIS HC/MF A03 CSCL 07D

Hydrocarbon reaction intermediates adsorbed at metallic catalyst surfaces were identified and quantitated by means of new surface spectroscopic and electrochemical methods, including Electron Energy-Loss Spectroscopy (EELS), Auger spectroscopy, surface InfraRed spectroscopy (IR), electron diffraction (LEED), and Cyclic Voltammetry. Investigated were catalyst surface structure, hydrocarbon molecular structure, modes of surface chemical bonding of adsorbed intermediates, and electrochemical oxidation of these intermediates as a function of the nature of the hydrocarbon solvent electrolyte, pH, temperature, catalyst elements, and adsorbable additives. Breakthroughs accomplished include: (1) first studies of hydrocarbon adsorbed intermediates at electrocatalyst surfaces by means of very difinitive EELS vibrational spectra; (2) first determinations of elemental analysis, purity, surface abundance, and molecular orientation of intermediates by Auger spectroscopy; (3) advances in surface IR spectroscopy permitting vibrational characterization of intermediates at high pressure; and (4) voltammetric studies revealing the nature of electrochemical reactions occurring at specific locations on the adsorbed molecule. Author

N91-13508# Princeton Univ., NJ. Dept. of Chemical Engineering.
[PHYSICAL PROPERTIES OF THERMOSETTING POLYMERS] Final Report No. 22, 1 Feb. 1984 - 30 Sep. 1990
John K. Gillham Sep. 1990 118 p
(Contract N00014-84-K-0021)
(AD-A225864) Avail: NTIS HC/MF A06 CSCL 07/6

Contributions to the following topics have been reported: (1) torsional pendulum/torsional braid analysis; (2) Time-Temperature-Transformation (TTT) cure diagram; (3) the glass transition Temperature (T sub g) as an index for monitoring cure; (4) anomalous behavior of thermosetting polymers: properties at room temperature vs. time and temperature of cure; (5) physical aging of thermosetting systems. GRA

N91-13509# Colorado State Univ., Fort Collins. Dept. of Chemical Engineering.
STUDY OF IMPROVED METHODS FOR PREDICTING CHEMICAL EQUILIBRIA Technical Progress Report, 1 Jul. 1989 - 31 Aug. 1990
Terry G. Lenz and John D. Vaughan 1990 6 p
(Contract DE-FG02-86ER-13582)
(DE91-000263; DOE/ER-13582/4) Avail: NTIS HC/MF A02

The objective of the research during the current and preceding periods has been to calculate thermodynamic properties (Delta H(sup o), Delta S(sup o), and Delta G(sup o)) of typical organic reactions in solution with sufficient accuracy to provide a viable alternative to expensive, time-consuming laboratory experimentation. The research has proceeded along five pathways. (1) Calculation of the thermodynamic properties Delta H(sub f)(sup o), C(sub p)(sup o), (H(sub o) minus H(sub o)(sup o))/T, and S(sup o) for reactants and products in the gas phase. Transformation of gas phase thermodynamic properties of reactants and products into condensed phase properties by use of observed vapor pressure data. (3) Experimental determination of x ray crystal structures, vapor and sublimation pressures, and calorimetric standard enthalpies of formation of large, relatively complicated reactants and products, such as Diels-Alder adducts of substituted anthracenes and substituted maleic anhydrides. (4) Experimental determination of equilibrium constants of Diels-Alder reactions of complicated, strained dienes and dienophiles over a range of temperatures in liquid solution. (5) Molecular dynamics study of pure liquids and liquid mixtures the to eventually permit a new activity coefficient models being developed. DOE

N91-13510*# California Univ., Los Angeles.
TRANSVERSE LIQUID FUEL JET BREAKUP, BURNING, AND IGNITION M.S. Thesis
Hsi-Shang Li 1990 101 p
(Contracts NCC2-374; DE-FG03-88ER-13910)
(NASA-CR-187423; NAS 1.26:187423) Avail: NTIS HC/MF A06 CSCL 21B

An analytical study of the breakup, burning, and ignition of liquid fuels injected transversely into a hot air stream is conducted. The non-reacting liquid jet breakup location is determined by the local sonic point criterion. Two models, one employing analysis of an elliptical jet cross-section and the other employing a two-dimensional blunt body to represent the transverse jet, were used for sonic point calculations. An auxiliary criterion based on surface tension stability is used as a separate means of determining the breakup location. For the reacting liquid jet problem, a diffusion flame supported by a one-step chemical reaction within the gaseous boundary layer is solved along the ellipse surface in subsonic cross flow. Typical flame structures and concentration profiles were calculated for various locations along the jet cross-section as a function of upstream Mach numbers. The integration reaction rate

along the jet cross-section is used to predict ignition position, which is found to be situated near the stagnation point. While a multi-step reaction is needed to represent the ignition process more accurately, the present calculation does yield reasonable predictions concerning ignition along a curved surface. Author

N91-13511# Instituto de Pesquisas Espaciais, Sao Jose dos Campos (Brazil).
SPRAY DEFLAGRATION M.S. Thesis [DEFLAGRACAO DE SPRAYS]
Thais Maia Araujo Jun. 1990 79 p In PORTUGUESE; ENGLISH summary
(INPE-5079-TDL/413) Avail: NTIS HC/MF A05

A review of the laminar flame theory, droplets evaporation and combustion, and an introduction to the spray combustion are presented. Furthermore, an analysis of the Williams' monodisperse spray deflagration theory is presented. Special attention is given to the criterion for spray homogeneous combustion, that is, the maximum droplet radius for this kind of spray burning. It is shown that this theory gives an incorrect variation of the radius r with ignition temperature. Therefore, a new expression for this variation is derived, based upon new hypothesis which avoids these problems. This new equation shows a better agreement with the experimental results. The flame region is analyzed by using Kirchhoff's transformation. Author

N91-13512# Naval Research Lab., Washington, DC.
A STUDY OF CONFINED DIFFUSION FLAMES Memorandum Report
J. L. Ellzey, K. J. Laskey (Grumman Aerospace Corp., Reston, VA.), and Elaine S. Oran 4 Sep. 1990 33 p Sponsored by ONR, Arlington, VA
(AD-A226552; NRL-MR-6704) Avail: NTIS HC/MF A03 CSCL 21/2

A numerical simulation of an axisymmetric confined diffusion flame formed between a H2 - N2 jet and coflowing air at 30 cm/s is presented in this paper. For the initial computations, the restrictions of the Burke Schumann theory are imposed and the results of the computation are compared with the analytical solution for flame location. For both the underventilated and overventilated flames, the results of the computations are in excellent agreement with the analytical solution. However, the flame behavior becomes more complex as the restrictions are relaxed. When variable diffusion coefficients and densities are included in the calculation, small radial velocities are induced and the flame interface is slightly distorted. When heat release is included, the flame is shorter and an unsteady mixing region forms at the fuel oxidizer interface. The instabilities are damped when viscous effects are included. Large scale instabilities form in the oxidizer region with a frequency of approximately 15 to 20 Hz when gravity is included in the calculation. GRA

N91-13513# Stanford Univ., CA. Dept. of Chemistry.
AMMONIA DECOMPOSITION ON SILICON SURFACES STUDIED USING TRANSMISSION FTIR SPECTROSCOPY
A. C. Dillon, P. Gupta, M. B. Robinson, A. S. Bracker, and Steven M. George 31 Jul. 1990 32 p Submitted for publication
(Contract N00014-86-K-0545)
(AD-A226625; SU-TR-13) Avail: NTIS HC/MF A03 CSCL 20/5

Fourier Transform Infrared (FTIR) transmission spectroscopy was used to monitor the decomposition of NH3 and ND3 on silicon surfaces. Experiments were performed in-situ in an ultra-high vacuum (UHV) chamber using high surface area porous silicon samples. The FTIR spectra revealed that NH3 (ND3) dissociatively adsorbs at 300 K to form SiH (SiD) and SiNH2 (SiND2) surface species. A comparison of the vibrational absorbances for the SiNH2 and Si2NH surface species indicated that the Si2NH species could account for less than or equal to 11 percent of the surface coverage at 300 K. The infrared absorbances of the SiN-H2 (SiN-D2) scissors mode at 1534 cu cm (1157 cu cm), the Si-H (SiD) stretch at 2077 cu cm (1510 cu cm) and the Si3-N stretches at 930 and 750 cm(exp -1) were employed to monitor the decomposition of the SiNH2 (SiND2) surface species. As the silicon surface was annealed to 700 K, the FTIR spectra revealed that the SiNH2 (SiND2) surface species gradually decomposed to produce Si3N species and additional SiH species. Above 680 D, the SiH surface species decreased concurrently with the desorption of H2 from the porous silicon surface. The uptake of surface species at various adsorption temperature was also monitored as a function of NH3 (ND3) exposure time. GRA

N91-13514# Stanford Univ., CA. Dept. of Chemistry.
PUBLICATIONS, PATENTS, PRESENTATIONS, HONORS, AND STUDENTS REPORT. KINETICS OF SEMICONDUCTOR PROCESSING CHEMISTRY: SiGe AND GaAs GROWTH ON SILICON SURFACES
Steven M. George Aug. 1990 15 p
(Contract N00014-90-J-1281)
(AD-A226639) Avail: NTIS HC/MF A03 CSCL 09/3

A listing is presented of articles presented to journals and symposia and graduate student reports. The following is a very brief sample of these articles: Laser Induced Desorption of H2 from Si(111)7x7; FTIR Studies of H2O and D2O Decomposition on Porous Silicon Surfaces; Ammonia Decomposition on Silicon Surfaces Studied Using Transmission FTIR Spectroscopy; FTIR Studies Reveal that Silicon Containing Laser Induced Desorption Products are Surface Reaction Intermediates. GRA

N91-13515*# Utah Univ., Salt Lake City. Dept. of Materials Science and Engineering.
FRICTION AND WEAR OF TPS FIBERS: A STUDY OF THE ADHESION AND FRICTION OF HIGH MODULUS FIBERS Final Report
Willard D. Bascom and Ilzoo Lee Nov. 1990 79 p
(Grant NAG2-444)
(NASA-CR-187666; NAS 1.26:187666) Avail: NTIS HC/MF A05 CSCL 07D

The adhesional and frictional forces between filaments in a woven fabric or felt, strongly influenced the processability of the fiber and the mechanical durability of the final product. Even though the contact loads between fibers are low, the area of contact is extremely small giving rise to very high stresses; principally shear stresses. One consequence of these strong adhesional and frictional forces is the resistance of fibers to slide past each other during weaving or when processed into nonwoven mats or felts. Furthermore, the interfiber frictional forces may cause surface damage and thereby reduce the fiber strength. Once formed into fabrics, flexural handling and manipulation of the material again causes individual filaments to rub against each other resulting in modulus, brittle fibers such as those used in thermal protection systems (TPS). The adhesion and friction of organic fibers, notably polyethylene terephthalate (PET) fibers, have been extensively studied, but there has been very little work reported on high modulus inorganic fibers. An extensive study was made of the adhesion and friction of flame drawn silica fibers in order to develop experimental techniques and a scientific basis for data interpretation. Subsequently, these methods were applied to fibers of interest in TPS materials. Author

N91-13516# Ames Lab., IA.
FUNDAMENTAL INVESTIGATIONS OF SUPPORTED MONOMETALLIC AND BIMETALLIC CATALYSTS BY PROTON MAGNETIC RESONANCE SPECTROSCOPY Ph.D. Thesis Iowa State Univ.
Xi Wu 21 Sep. 1990 410 p
(Contract W-7405-eng-82)
(DE91-000610; IS-T-1441) Avail: NTIS HC/MF A18

Proton magnetic resonance spectroscopy, or nuclear magnetic resonance (NMR) of hydrogen, has been applied to investigate silica-supported Group VIII monometallic and Group VIII-Group IB bimetallic catalysts and alumina- and silica-supported platinum-rhenium bimetallic catalysts. Two adsorbed states of hydrogen, i.e., irreversible and reversible hydrogen, on the surfaces of monometallic Ru, Pt, and Cu particles and bimetallic Ru-Group Ib, Pt-Group Ib, and Pt-Re particles were observed directly via

proton NMR. The same amounts of the irreversible hydrogen adsorbed on pure Ru catalysts were measured by both proton NMR and the volumetric technique. The electronic environments on surfaces of monometallic catalysts are sensitive to changes in metal dispersion, state of adsorbed hydrogen, and residual chlorine. Surface compositions for the Ru--Cu and Pt--Cu bimetallic catalysts were determined by NMR of adsorbed hydrogen. DOE

N91-13517# Oak Ridge National Lab., TN.
PROGRESS IN THE DETECTION OF SINGLE MOLECULES IN LEVITATED DROPLETS
W. B. Whitten, J. M. Ramsey, S. Arnold, and B. V. Bronk (Army Chemical Research and Development Center, Aberdeen Proving Ground, MD.) 1990 3 p Presented at the U.S. Army Chemical Research Development and Engineering Conference on Aerosols and Obscuration, Aberdeen, MD, 25-27 Jun. 1990
(Contract DE-AC05-84OR-21400)
(DE91-000612; CONF-9006277-1) Avail: NTIS HC/MF A01

This report briefly describes a method for the detection of single molecules of rhodamine-6G in levitated glycerine-water droplets by optical fluorescence. Laser induced fluorescence, photocounts, and volume determination of trapped droplets are employed in this method. For greater precision in droplet diameter, the positions of structural resonances in Mie scattering are measured as the droplet evaporates with fixed laser frequency. The resonances are identified by matching the experimental curves with calculations made with a FORTRAN program, averaged over the appropriate range of azimuthal angles and the droplet diameter calculated from the size parameter and the glycol refractive index. DOE

N91-13518# Ames Lab., IA.
ELECTROCATALYSIS OF ANODIC OXYGEN-TRANSFER REACTIONS AT MODIFIED LEAD DIOXIDE ELECTRODES Ph.D. Thesis
Yun-Lin Hsiao 21 Sep. 1990 183 p
(Contract W-7405-eng-82)
(DE91-000664; IS-T-1451) Avail: NTIS HC/MF A09

The electrocatalytic activities were compared for pure and chloride-doped beta-PbO2 (Cl-PbO2) films on gold and platinum substrates. Rate constants were increased significantly for oxidations of Mn(2+), toluene, benzyl alcohol, dimethylsulphoxide (DMSO), and benzaldehyde in acidic media by the incorporation of Cl(1-) into the oxide films. These reactions are concluded to occur by the electrocatalytic transfer of oxygen from H2O to the reaction products. Results of x ray diffraction studies indicate the Cl-PbO2 film continues to have the slightly distorted rutile structure of pure beta-PbO2 . The observed electrocatalytic phenomena are concluded to be the beneficial consequence of surface defects generated when Cl(1-) serves for charge compensation within the surface matrix and, thereby, increases the number of surface sites capable of adsorbing hydroxyl radicals which are transferred in the electrocatalytic O-transfer reactions. DOE

N91-13519# City Coll. of the City Univ. of New York, NY. Inst. for Physicochemical Hydrodynamics.
TOPICS IN PHYSICO-CHEMICAL HYDRODYNAMICS Progress Report, 1988 - 1989
Gregory Sivashinsky 1989 7 p
(Contract DE-FG02-88ER-13822)
(DE91-001674; DOE/ER-13822/T1) Avail: NTIS HC/MF A02

This paper discusses the following topics: theory of turbulent flame speed; flame extinction by periodic flow-field; influence of swirl on the structure and extinction of premixed flames; propagation and extinction of nonsteady spherical flame fronts; geometrically invariant formulation of intrinsic dynamics of premixed flames; nonlinear dynamics of oscillatory regime of premixed combustion; and pattern formation in premixed flames. DOE

N91-13520# Lawrence Livermore National Lab., CA. Center for Mass Spectrometry.
MATERIALS IMPURITY ANALYSIS BY MEANS OF NUCLEAR RESONANCE REACTIONS
R. S. Hornady Sep. 1990 11 p Presented at the 11th International Conference on the Application of Accelerators in Research and Industry, Denton, TX, 5-8 Nov. 1990 Submitted for publication
(Contract W-7405-eng-48)
(DE91-001758; UCRL-JC-104433; CONF-901116-22) Avail: NTIS HC/MF A03

An automated beam line for measurement of trace impurities in materials is installed on the FN tandem in the Center for Accelerator Mass Spectrometry, LLNL. The major purpose of the beam-line system is to determine the diffusion of water into glasses by use of the (19)F(p,alpha gamma)(16)O reaction. This study is stimulated by the radiation-waste-isolation program; however, the system is applicable to studies of other impurities in many material matrices. The target wheels, each of which holds twenty-four samples, can be changed in less than an hour. The beam-line control system both indexes the target wheel and controls the tandem energy as it steps through the requested measurement protocol. The tandem control system, in response to a request, adjusts the terminal potential and other transport elements to maintain constant spot size and location. DOE

N91-13521# Sandia National Labs., Albuquerque, NM. Process Research Div.
AN EXPLORATORY PROGRAM FOR USING HYDROUS METAL OXIDE ION EXCHANGERS AS FISCHER-TROPSCH CATALYSTS
A. W. Lynch, R. G. Dosch, and A. G. Sault 1990 8 p Presented at the Indirect Liquefaction Contractors Review, Pittsburgh, PA, 5-8 Nov. 1990
(Contract DE-AC04-76DP-00789)
(DE91-002341; SAND-90-2553C; CONF-901120-1) Avail: NTIS HC/MF A02

The purpose of this program is to investigate the potential of hydrous metal oxide (HMO) ion exchangers, invented at Sandia National Laboratories, as Fischer-Tropsch (F-T) catalysts. Metals known to be active in F-T synthesis (e.g., Fe, Co) were ion exchanged on hydrous metal oxide supports. Although HMO catalysts based on Zr, Nb, and Ta have been investigated in direct coal liquefaction studies, this effect focused on formulations based on the hydrous titanium oxide (HTO) system. The program has the goals of developing a catalyst with: (1) high activity; (2) selectively to fuel range or other useful products; and (3) better properties for use in slurry reactors. The program has three main tasks: (1) catalyst synthesis, to develop methods for preparing catalysts having desirable F-T properties; (2) characterization, to investigate catalysts proving to have desirable properties by a variety of analytical techniques to determine correlations between activity and material properties; and (3) testing to determine activity and selectivity of catalysts. This paper discussed results of activity testing of Ruhrchemie catalyst and some catalyst formulations prepared using ion exchange on hydrous titanium oxide and precipitation. For example, at 250 C the Ruhrchemie catalyst converts approximately 50 percent of the syngas feed to reaction products. In comparison, iron catalysts prepared by ion exchange and precipitation had conversions ranging from 20 to 50 percent over a temperature range of 250 to 275 C of the syngas feed. In addition, results are Auger surface analysis of Ruhrchemie catalyst are presented. DOE

26 METALLIC MATERIALS

Includes physical, chemical, and mechanical properties of metals, e.g., corrosion; and metallurgy.

N91-13522*# National Aeronautics and Space Administration. Langley Research Center, Hampton, VA.
OXIDATION CHARACTERISTICS OF Ti-25Al-10Nb-3V-1Mo INTERMETALLIC ALLOY
Terryl A. Wallace, Ronald K. Clark, Sankara N. Sankaran, and Karl E. Wiedemann (Analytical Services and Materials, Inc.,

Hampton, VA.) Washington Dec. 1990 18 p
(NASA-TP-3044; L-16808; NAS 1.60:3044) Avail: NTIS HC/MF A03 CSCL 11F

Static oxidation kinetics of the super-alpha 2 titanium-aluminide alloy Ti-25Al-10Nb-3V-1Mo (at. percent) were investigated in air over the temperature range of 650 to 1000 C using thermogravimetric analysis. The oxidation kinetics were complex at all exposure temperatures and displayed up to three distinct oxidation rates. Breakaway oxidation occurred after long exposure times at high temperatures. Oxidation products were determined using x ray diffraction techniques, electron microprobe analysis, and energy dispersive x ray analysis. Oxide scale morphology was examined by scanning electron microscopy of the surfaces and cross sections of oxidized specimens. The oxides during the parabolic stages were compact and multilayered, consisting primarily of TiO2 doped with Nb, a top layer of Al2O3, and a thin bottom layer of TiN. The transition between the second and third parabolic stage was found to be linked to the formation of a TiAl layer at the oxide-metal interface. Porosity was formed during the third stage, causing degradation of the oxide and the beginning of breakaway oxidation. Author

N91-13523# David Taylor Research Center, Bethesda, MD. Dept. Ship Materials Engineering.
INTELLIGENT PROCESSING FOR SPRAY METAL MANUFACTURING Research and Development Report, Oct. 1988 - Sep. 1989
Angela L. Moran and Dawn R. White Jun. 1990 20 p
(AD-A226499; DTRC/SME-90/54) Avail: NTIS HC/MF A03 CSCL 11/6

A program to implement real time sensing and control of spray formed preform conditions is underway at the David Taylor Research Center. The objective of the program is to develop sensor and control technology to monitor the critical process conditions and to modify parameters during the spray forming process to produce components with repeatable microstructural quality. This task has been divided into two phases, the first of which entails development of sensors and controls to monitor and correct simulated process conditions. In the second phase, the selected sensors and controls will be combined with actuators for integration with the DTRC equipment to allow for the production of nonsymmetric preforms. GRA

N91-13524# General Electric Co., Cincinnati, OH. Aircraft Engines Div.
RESEARCH AND DEVELOPMENT FOR IMPROVED TOUGHNESS ALUMINIDES Final Report, 1 Nov. 1985 - 31 Mar. 1989
B. J. Marquardt, G. K. Scarr, J. C. Chesnutt, C. G. Rhodes, and H. L. Fraser 11 Jun. 1990 179 p
(Contract F33615-85-C-5167; AF Proj. 2420)
(AD-A226627; WRDC-TR-89-4133) Avail: NTIS HC/MF A09 CSCL 11/6

The basic mechanisms which can improve the toughness of alloys based on the intermetallic compound Ti3Al was identified and examined. The improved properties offered by these alloys will increase their potential for application in rotating components and critical static parts in advanced aircraft engines. The program was conducted in two separate phases which addressed iterative alloy/processing studies as well as alloy scale up concerns. In the first phase of the program, the effects of solid solution alloying, tough second phase, and dispersoid additions were evaluated in parallel tasks. Subsequently, alloys were designed to make use of additive and/or synergistic effects by combining the various alloying and processing concepts. In the second phase of the program, three of the more promising compositions were selected for scale up and further microstructural and property evaluations. GRA

N91-13525# Ames Lab., IA.
SYNCHROTRON RADIATION PHOTOEMISSION STUDY OF METAL OVERLAYERS ON HYDROGENATED AMORPHOUS SILICON AT ROOM TEMPERATURE Ph.D. Thesis
Jonathan Pi 21 Sep. 1990 113 p
(Contract W-7405-eng-82)
(DE91-000740; IS-T-1409) Avail: NTIS HC/MF A06

In this dissertation, metals deposited on a hydrogenated amorphous silicon (a-Si:H) film at room temperature are studied. The purpose of this work is mainly understanding the electronic properties of the interface, using high-resolution synchrotron radiation photoemission techniques as a probe. Atomic hydrogen plays an important role in passivating dangling bonds of a-Si:H films, thus reducing the gap-state distribution. In addition, singly bonded hydrogen also reduces states at the top of the valence band which are now replaced by deeper Si-H bonding states. The interface is formed by evaporating metal on an a-Si:H film in successive accumulations at room temperature. Au, Ag, and Cr were chosen as the deposited metals. Undoped films were used as substrates. Since some unique features can be found in a-Si:H, such as surface enrichment of hydrogen diffused from the bulk and instability of the free surface, we do not expect the metals/a-Si:H interface to behave exactly as its crystalline counterpart. Metal deposits, at low coverages, are found to gather preferentially around regions deficient in hydrogen. As the thickness is increased, some Si atoms in those regions are likely to leave their sites to intermix with metal overlayers like Au and Cr. DOE

N91-13526# Ames Lab., IA.
REACTIONS OF THE EXCITED STATE OF POLYPYRIDYL CHROMIUM(III) ION Ph.D. Thesis Iowa State Univ.
Carl R. Steffan 21 Sep. 1990 176 p
(Contract W-7405-eng-82)
(DE91-000741; IS-T-1442) Avail: NTIS HC/MF A09

There has been much recent interest in the photochemistry and photophysics of transition metal polypyridine complexes due to the possibility of their use in solar energy conversion systems. The excited state of these compounds are known to undergo useful electron transfer and energy transfer reactions. This work attempts to elucidate the mechanism of the quenching of CrL3 (exp 3+) (where L = 2,2(prime)-bipyridine, 4,4(prime)-dimethyl-2,2(prime)-bipyridine, 1,10-phenanthroline, 5-chloro-1,10-phenanthroline, 5-methyl-1,10-phenanthroline) by oxalate ions in neutral pH. Evidence suggests an ion-pairing pre-equilibrium followed by rate limiting electron transfer to produce CrL3 (exp 2+) and CO2 (exp (minus)) can then react with ground state chromium(III) species to produce another mole of the reduced product or it can produce a secondary transient as in the case of phenanthroline and substituted phenanthroline complexes. The secondary transient reacts to produce CrL3 (exp 2+) in a subsequent reaction. DOE

N91-13527*# National Aeronautics and Space Administration. Langley Research Center, Hampton, VA.
METHOD AND APPARATUS FOR CHARACTERIZING RESIDUAL STRESS IN FERROMAGNETIC MATERIALS Patent Application
Min Namkung, inventor (to NASA), William T. Yost, inventor (to NASA), Peter W. Kushnick, inventor (to NASA), and John L. Grainger, inventor (to NASA) (AS&M, Inc., Hampton, VA.) 23 Jul. 1990 25 p
(NASA-Case-LAR-14239-1; NAS 1.71:LAR-14239-1;
US-Patent-Appl-SN-555864) Avail: NTIS HC/MF A03 CSCL 11F

The invention is a method and apparatus for characterizing residual uniaxial stress in a ferromagnetic test member by distinguishing between residual stresses resulting from positive (tension) forces and negative (compression) forces by using the distinct and known magnetoacoustic (MAC) and a magnetoacoustic emission (MAE) measurement circuit means. A switch permits the selective operation of the respective circuit means. NASA

N91-13528# Technical Research Centre of Finland, Espoo. Metals Lab.
CREEP AND CREEP FAILURE OF POWER PLANT STEELS
Pertti Auerkari, A. Neuvonen (Imatran Voima Oy, Helsinki, Finland), J. Jokinen, Jorma Salonen, and Reino Makinen May 1990

29 p In FINNISH; ENGLISH summary Sponsored by Finnish Metal and Engineering Industries
(VTT-RR-685; ISBN-951-38-3706-8; ISSN-0358-5077;
ETN-91-98273) Copyright Avail: NTIS HC/MF A03;
Government Printing Centre, P.O. Box 516, SF-00101 Helsinki, Finland, HC 40 Finnish marks

Numerical and analytical creep analysis of thick wall tubes is shown to agree reasonably well up to few percent of strain with experimental creep testing results of 1 Cr to 0.5 Mo steel tubes under internal pressure. Beyond this strain level a higher value of the creep exponent in the Norton creep law than that from uniaxial is needed to predict strains correctly. For detecting emerging creep damage the magnetic Barkhausen noise measurements showed some promise, when the measurements were performed with a calibration to a standard block. However, it is anticipated that the technique would work better in detecting creep cracks and therefore would exhibit more potential in replacing standard surface inspection methods like magnetic particle testing. ESA

N91-13529# Technical Research Centre of Finland, Espoo. Metals Lab.
BINDERS USED IN METAL INJECTION MOLDING
Jaako Salmi Jun. 1990 49 p In FINNISH; ENGLISH summmary Sponsored by Technology Development Industry
(VTT-RR-691; ISBN-951-38-3713-0; ISSN-0358-5077;
ETN-91-98274) Copyright Avail: NTIS HC/MF A03;
Government Printing Centre, P.O. Box 16, SF-00101 Helsinki, Finland, HC 40 Finnish marks

The structures of some components used in thermoplastic binder mixtures for metal injection molding and their effect on the properties of parts are described. Some physicochemical effects on debindering are presented, and an attempt is made to explain the difficulties in debindering and the behavior of some binders in the debindering process. According to the physicochemical study, the most important effects in the debindering process are temperature, pressure, vapor pressures of binder components, gas flow in the furnace and viscosity in the the binder mixture. ESA

N91-13530# Technical Research Centre of Finland, Espoo. Metals Lab.
MATERIAL DEGRADATION OF STEAM TURBINE ROTORS IN LONG TERM OPERATIONS
Ulla McNiven, Klaus Rahka, Rauno Rintamaa, and Pertti Auerkari Jun. 1990 44 p In FINNISH; ENGLISH summary
(VTT-RR-692; ISBN-951-38-3714-9; ISSN-0358-5077;
ETN-91-98275) Copyright Avail: NTIS HC/MF A03;
Government Printing Centre, P.O. Box 516, SF-00101 Helsinki, Finland HC 40 Finnish marks

The material property degradation of steam turbine rotors was investigated. The main factors limiting the life of the HP rotor are thermal fatigue and possibly creep fatigue. The result can be a catastrophic fracture, if the growing defects are not detected in time. Fatigue and/or stress corrosion limit the life time of LP rotors. The final result is again a fast fracture and the rotor will be destroyed if growing defects are not detected early enough. The state of material properties can be determined by nondestructive testing, material testing, by analyzing the service history and the damages. ESA

N91-13531# Technical Research Centre of Finland, Espoo. Metals Lab.
FABRICATION AND PROPERTIES OF POWDER METALLURGICALLY MANUFACTURED ALUMINUM PRODUCTS AND COMPOSITES
Antero Jokinen, Amar Mahiout, Klaus Rahka, and Simo-Pekka Hannula Aug. 1990 47 p In FINNISH; ENGLISH summary
(VTT-RR-699; ISBN-951-38-3781-5; ISSN-0358-5077;
ETN-91-98276) Copyright Avail: NTIS HC/MF A03;
Government Printing Centre, P.O. Box 516, SF-00101 Helsinki, Finland, HC 40 Finnish marks

Various processes for the hot extrusion of powder metallurgy aluminum alloys (corresponding to types P/M 2014 and P/M 7090) with or without silicon carbide particulate or whisker reinforcement were studied. The microstructure of the alloys was characterized and the tensile, fatigue and corrosion properties were determined and compared to those of conventionally manufactured wrought alloys I/M 2024 and I/M 7075. The results indicated that a good quality aluminum alloy bar can be produced by hot extrusion of P/M 2014 and P/M 7090 alloy powders. The microstructure of the products was fine and homogeneous and no porosity could be observed except in the bars extruded of loose powder. The tensile properties of the alloys were better than those of conventionally produced alloys. Especially the strength of the alloy P/M 7090-T6 was excellent. The fatigue resistance was better than that of the conventionally manufactured alloys. Further results are detailed: the addition of silicon carbide improved the elastic modulus of the alloy P/M 2014-T6 by over 50 percent; the corrosion resistance of the powder metallurgical alloys in 3.5 percent NaCl solution was better than that of conventionally manufactured alloys. ESA

N91-13532# Institut de Soudure, Paris (France).
STUDY OF THE METALLURGICAL EFFECTS OF HAMMERING BETWEEN PASSES DURING C-Mn WELD DEPOSITION Final Report [ETUDE DES CONSEQUENCES METALLURGIQUES DU MARTELAGE ENTRE PASSES DES DEPOTS DE NUANCE C-MN]
P. Roguin, R. Gaillard, and S. Debiez Mar. 1990 33 p In FRENCH Prepared in cooperation with Centre Technique des Industries Mecaniques, Nantes, France
(Contract CETIM-89-9003)
(CETIM-104850; IS-25101; ETN-91-98328) Copyright Avail: NTIS HC/MF A03

The tensile and thermal aging of three different types of Mn welds (0.8, 1.2 and 1.5 percent) is studied. Results of traction, compression, and aging tests show very little difference in behavior due to the Mn content. The effect of hammering at low temperatures (85 to 70C) is studied. The technique used greatly reduces the damage previously observed. Low manganese welds show a diminution in the intensity of aging. High manganese content welds owe their increased tensile strength to the colder welding treatment. Recommendations are made concerning the operational mode and the choice of manganese content in the welds. ESA

N91-13533# Centre Technique des Industries Mecaniques, Senlis (France).
MICROGRAPHIC ETCHING OF NITRIDED IRON AND STEEL LAYERS Final Report [ATTAQUES MICROGRAPHIQUES DES COUCHES NITRUREES]
J. Mongis, J. P. Peyre, and C. Tournier Jun. 1989 81 p In FRENCH
(CETIM-106470; ETN-91-98335) Copyright Avail: NTIS HC/MF A05

Four etching reagents are chosen and tested on four types of steel: nitrided ARMCO, XC 38, 35 CD4 and 30 CAD 612. Nital, Wells, Villela and Oberhoffer etching reagents are tried on these steel surfaces. The Wells and Villela reagents seem to be the best choice for studying the micrographic aspects of the combination layers of steels with low temperature carbonitriding. For the other types of steel and for the double phased structures these reagents highlight two phases for which the nature is hard to interpret along a traditional Fe, C, N format. Scanning electron microscopy must be used to better understand this ambiguous structure. ESA

27 NONMETALLIC MATERIALS

Includes physical, chemical, and mechanical properties of plastics, elastomers, lubricants, polymers, textiles, adhesives, and ceramic materials.

For composite materials see *24 Composite Materials.*

N91-13534*# Southwest Research Inst., San Antonio, TX.
MECHANICAL TESTING OF ADVANCED COATING SYSTEM, VOLUME 1 Final Report

T. A. Cruse, A. Nagy, and C. F. Popelar Jun. 1990 113 p
(Contract NCC3-89; SwRI Proj. 06-1778-001)
(NASA-CR-186725; NAS 1.26:186725) Avail: NTIS HC/MF A06 CSCL 11C

The Electron Beam Physical Vapor Deposition (EBPVD) coating material has a highly columnar microstructure, and as a result it was expected to have very low tensile strength. To be able to fabricate the required compression and tensile specimens, a substrate was required to provide structural integrity for the specimens. Substrate and coating dimensions were adjusted to provide sufficient sensitivity to resolve the projected loads carried by the EBPVD coating. The use of two distinctively different strain transducer systems, for tension and compression loadings, mandated two vastly different specimen geometries. Compression specimen and tensile specimen geometries are given. Both compression and tensile test setups are described. Data reduction mathematical models are given and discussed in detail as is the interpretation of the results. Creep test data is also given and discussed. E.R.

N91-13535*# Southwest Research Inst., San Antonio, TX.
FATIGUE TESTING OF PLASMA-SPRAYED THERMAL BARRIER COATINGS, VOLUME 2 Final Report
T. A. Cruse, A. Nagy, and C. F. Popelar Jul. 1990 21 p
(Contract NCC3-89; SwRI Proj. 06-1778-002)
(NASA-CR-186726; NAS 1.26:186726) Avail: NTIS HC/MF A03 CSCL 11C

A plasma sprayed thermal barrier coating for diesel engines were fatigue tested. Candidate thermal barrier coating materials were fatigue screened and a data base was generated for the selected candidate material. Specimen configurations are given for the bend fatigue tests, along with test setup, specimen preparation, test matrix and procedure, and data analysis. E.R.

N91-13536# Forschungszentrum Juelich G.m.b.H. (Germany, F.R.). Projektleitung Material- und Rohstofforschung.
RESIDUAL STRESSES IN CERAMICS [EIGENSPANNUNGEN IN KERAMIK]
W. Kollenberg, ed. 1990 177 p In GERMAN Presented at Seminar der Projektleitung Material- und Rohstooforschung im Forschungszentrum Juelich,Fed. Republic of Germany, 21-22 Sep. 1989
(Juel-Spez-550; ISSN-0343-7639; ETN-90-97354) Avail: NTIS HC/MF A09

Neutron diffraction and x ray diffraction methods were used to measure residual stresses in ceramics, metal ceramic laminated composites, metal ceramic composites, thin hard layers, to determine the influence of materials structure and production method of Al2O3 on the stress measurement as well as the influence of the texture of Al2O3 substrates on the fracture behavior under thermal loading, and to determine the elastic constants of ceramic materials for stress analysis. The blind-hole drilling technique for residual stress analysis was improved and compared with finite element method calculations. The ultrasonic technique and the acoustic microscope were used as nondestructive methods for the determination of mechanical stresses in ceramics. Residual stresses due to a phase transformation in materials as well as residual stresses in ceramic-metal soldered joints were calculated. For individual titles, see N91-13537 through N91-13549.

N91-13537# Dortmund Univ. (Germany, F.R.). Inst. fuer Festkoerperforschung.
USE OF NEUTRON DIFFRACTION METHODS FOR THE DETERMINATION OF MECHANICAL STRESSES IN METAL CERAMIC LAMINATED COMPOSITE MATERIALS [ANWENDUNG VON NEUTRONENBEUGUNGSVERFAHREN ZUR ERFASSUNG VON MECHANISCHEN SPANNUNGEN IN METALL-KERAMISCHEN SCHICHTVERBUNDWERKSTOFFEN]
W. Reimers, U. Selvadurai, and G. Eckold (Forschungszentrum Juelich G.m.b.H., Germany, F.R.) *In* Forschungszentrum Juelich G.m.b.H., Residual Stresses in Ceramics 1990 p 1-15 In GERMAN (For primary document see N91-13536 05-27)
Avail: NTIS HC/MF A09

Neutron diffraction measurements were performed on laminated composites, composed of a metallic substrate, an adhesive, and a ceramic superficial layer made of partly stabilized zirconium oxide, with a view to phase and stress analysis. Besides neutron diffraction methods, x ray diffraction and synchrotron diffraction methods were used to obtain data from different depths. The phase analyses show that, with a proper choice of the plasma spraying parameters, nearly identical phase compositions on different substrates can be produced. The stress analyses show that the segmentation of the layers induces the stresses in the superficial layer and hence globally in the composite partners only low residual stresses (below 40MPa) are present. ESA

N91-13538# Kernforschungszentrum G.m.b.H., Karlsruhe (Germany, F.R.). Inst. fuer Nukleare Festkoerperphysik.
DETERMINATION OF RESIDUAL STRESSES IN CERAMICS MATERIALS USING NEUTRON DIFFRACTION [BESTIMMUNG VON EIGENSPANNUNGEN IN KERAMISCHEN WERKSTOFFEN MITTELS NEUTRONENBEUGUNG]
L. Pintschovius *In* Forschungszentrum Juelich G.m.b.H., Residual Stresses in Ceramics 1990 p 17-24 In GERMAN (For primary document see N91-13536 05-27)
Avail: NTIS HC/MF A09

Residual stresses were determined in ceramic bending samples after creep tests using neutron diffraction. The first measurements were performed on bending samples made of Al2O3 and Si3N4, respectively, after a creep test, and allowed the quantitative determination of the different creep behavior with respect to compression or tensile load. The second series of measurements were performed on metal ceramic soldered joints, and allowed determination of the residual stresses due to the soldering process in the steel as well as in the ceramic (Si3N4, ZrO2). The present experience shows that despite the relatively large experimental effort, the determination of residual stresses in ceramic materials using neutron diffraction method is a worthwhile method. ESA

N91-13539# Karlsruhe Univ. (Germany, F.R.). Inst. fuer Werkstoffkunde.
RESIDUAL STRESSES ANALYSES IN CERAMICS AND METAL CERAMIC COMPOSITES USING X RAY METHODS [EIGENSPANNUNGSANALYSEN IN KERAMIKEN UND METALL-KERAMIK-VERBUNDEN MIT HILFE ROENTGENOGRAPHISCHER METHODEN]
B. Eigenmann and B. Scholtes *In* Forschungszentrum Juelich G.m.b.H., Residual Stresses in Ceramics 1990 p 25-35 In GERMAN (For primary document see N91-13536 05-27)
Avail: NTIS HC/MF A09

Some examples of residual stress analyses on soldered metal ceramic joints using x ray diffraction are presented. The measurements were combined with the removal of layers of material, allowing the determination of residual stress depth distributions. The use of x ray diffraction allows the separate determination of stress values of single phases in a multiphase structure. This procedure provides stresses of the first kind which are constant over larger volumes as well as stresses of the second kind resulting from the lightening of the grains of single phases against each other. ESA

N91-13540# Technische Univ., Hanover (Germany, F.R.). Inst. fuer Fertigungstechnik und Spannende Werkzeugmaschinen.
INFLUENCE OF MATERIALS STRUCTURE AND PRODUCTION METHOD OF Al2O3 CERAMIC ON THE X-RAY STRESS MEASUREMENT [EINFLUSS DES WERKSTOFFGEFUEGES UND DES HERSTELLUNGSVERFAHRENS VON AL2O3-KERAMIK AUF DIE ROENTGENOGRAPHISCHE SPANNUNGSMESSUNG]
E. Brinksmeier and H. Siemer *In* Forschungszentrum Juelich G.m.b.H., Residual Stresses in Ceramics 1990 p 37-46 In GERMAN (For primary document see N91-13536 05-27)
Avail: NTIS HC/MF A09

Using several Al2O3 ceramics the effects of the production method and the materials structure on the x ray diffraction stress analysis were experimentally and numerically investigated. The

cutting finishing of ceramic surfaces induces residual stresses in the machined boundary zone due to mechanical and thermal loading. It is shown that the x ray elasticity constants which represent the correlation between the measured crystal lattice deformation and the macroscopic stresses, depend clearly on the materials structure. The measurement conditions and the evaluation algorithms have to be adapted to the material to be analyzed. ESA

N91-13541# Technische Hochschule, Aachen (Germany, F.R.). Inst. fuer Werkstoffkunde.
THE X RAY ELASTIC CONSTANTS OF CERAMIC MATERIALS FOR THE DETERMINATION OF THE STRESSES FROM LATTICE EXPANSION MEASUREMENTS [DIE ROENTGENOGRAPHISCHEN ELASTIZITAETSKONSTANTEN KERAMISCHER WERKSTOFFE ZUR ERMITTLUNG DER SPANNUNGEN AUS GITTERDEHNUNGSMESSUNGEN]
H. Behnken and V. Hauk *In* Forschungszentrum Juelich G.m.b.H., Residual Stresses in Ceramics 1990 p 47-58 In GERMAN (For primary document see N91-13536 05-27)
Avail: NTIS HC/MF A09

The x ray elastic constants were calculated from single crystal coefficients using several model assumptions concerning the coupling of the crystallites among each other. These constants are required for the calculation of the stresses from x ray lattice expansions. A calculation method was developed to determine the effect of the heterogeneity of a material in the form of homogeneously distributed phases, of pores as well as laminated or fiber compounds. This method substantially reduces the measurement effort for the determination of the x ray elasticity constants. However, the knowledge of the elasticity coefficients of the single crystals of the ceramic materials as well as their dependence on the temperature remains absolutely necessary. ESA

N91-13542# Stiftung Inst. fuer Werkstofftechnik, Bremen (Germany, F.R.).
X RAY MEASUREMENTS OF RESIDUAL STRESSES IN THIN, HARD LAYERS [ROENTGENOGRAPHISCHE MESSUNG VON EIGENSPANNUNGEN IN DUENNEN, HARTEN SCHICHTEN]
T. Hirsch and P. Mayr *In* Forschungszentrum Juelich G.m.b.H., Residual Stresses in Ceramics 1990 p 59-77 In GERMAN (For primary document see N91-13536 05-27)
Avail: NTIS HC/MF A09

The status of the x ray measurement of residual stresses in both the film and substrate of materials coated with thin, hard layers made in vacuum or using vapor deposition is presented. These stresses depend on a large number of process parameters. The measurement problems occurring for small coating thicknesses and the concomitant small measuring volumes are discussed. As an example the influence of the coating parameters on the residual stresses of a vapor deposited TiN coating is discussed. The influence of residual stresses on the coating quality is not yet sufficient. ESA

N91-13543# Technische Univ., Clausthal-Zellerfeld (Germany, F.R.). Inst. fuer Metallkunde und Metallphysik.
THE INFLUENCE OF THE TEXTURE OF Al2O3 SUBSTRATES ON THE FRACTURE BEHAVIOR UNDER THERMAL LOADING [EINFLUSS DER TEXTUR VON AL2O3-SUBSTRATEN AUF DAS BRUCHVERHALTEN UNTER THERMISCHER SPANNUNG]
H. Klein (DODUCO G.m.b.H. und Co., Pforzheim, Germany, F.R.), B. Waibel, and Hans Joachim Bunge *In* Forschungszentrum Juelich G.m.b.H., Residual Stresses in Ceramics 1990 p 79-91 In GERMAN (For primary document see N91-13536 05-27)
Avail: NTIS HC/MF A09

The influence of the crystallographic texture on the thermal strength of polycrystalline Al2O3 substrates, coated at both sides with Cu foil, was investigated using x ray diffraction. It is shown that the preferential orientation of a Al2O3 base plane which can not technically be measured, can be determined by the measurement of five different so called Pol figures, using the orientation distribution function. The correlation between the breakdown of substrates under thermal cyclic loading and the sharpness of the texture was determined. ESA

N91-13544# Fraunhofer-Inst. fuer Betriebsfestigkeit, Darmstadt (Germany, F.R.).
DEVELOPMENT AND COMPUTER AIDED RESIDUAL STRESS MEASUREMENTS ON COATED SPECIMEN USING BLIND-HOLE DRILLING TECHNIQUE
P. Pantucek *In* Forschungszentrum Juelich G.m.b.H., Residual Stresses in Ceramics 1990 p 93-109 In GERMAN; ENGLISH summary (For primary document see N91-13536 05-27)
Avail: NTIS HC/MF A09

The blind-hole drilling technique for residual stress analysis was improved. The technique is now capable of a measuring depth of approximately 5 mm for the analysis of coated components, even in the presence of exterme stress gradients. The cutting is performed by a diamond cutter head, cleaned and cooled down by a special water-flush box with an intermittent low feed. A specially developed diamond bonding enables deformation-free cutting even in the most differing compounds with a high reproductibility of the hole geometry. The use of special software packages, containing interpolating as well as smoothing routines excludes possible subjective ratings and guarantees a reproducible and low cost analysis of the results. ESA

N91-13545# Max-Planck-Inst. fuer Metallforschung, Stuttgart (Germany, F.R.). Pulvermetallurgisches Lab.
RESIDUAL STRESSES IN Al2O3: COMPARISON BETWEEN ELECTROMECHANICAL MEASUREMENTS AND FINITE ELEMENT METHOD CALCULATIONS [EIGENSPANNUNGEN IN AL2O3: VERGLEICH VON ELEKTROMECHANISCHEN MESSUNGEN MIT FEM-RECHNUNGEN]
I. Buresch, A. Dutschk (Deutsche Forschungs- und Versuchsanstalt fuer Luft- und Raumfahrt, Stuttgart, Germany, F.R.), and H. Schubert *In* Forschungszentrum Juelich G.m.b.H., Residual Stresses in Ceramics 1990 p 111-122 In GERMAN (For primary document see N91-13536 05-27)
Avail: NTIS HC/MF A09

The thermally induced residual stresses in Al2O3 ceramics after cooling from sintering temperature were investigated. These stresses are due to the temperature difference between the fast cooling edge and the slowly cooling core. The residual stresses were measured using the blind-hole drilling technique. A finite element method for the calculation of the stress distribution in components with simple geometry was developed. The experimental residual stress distributions agree well with the numerical results. ESA

N91-13546# Fraunhofer Inst. fuer Werkstoffmechanik, Freiburg (Germany, F.R.).
DETERMINATION OF STRESSES IN CERAMICS USING ULTRASONIC METHODS: POSSIBILITIES AND LIMITATIONS [BESTIMMUNG VON SPANNUNGEN IN KERAMIKEN MITTELS ULTRASCHALLVERFAHREN: MOEGLICHKEITEN UND GRENZEN]
E. Schneider *In* Forschungszentrum Juelich G.m.b.H., Residual Stresses in Ceramics 1990 p 123-145 In GERMAN (For primary document see N91-13536 05-27)
Avail: NTIS HC/MF A09

The ultrasonic technique as a nondestructive method for the determination of mechanical stresses is presented. The ultrasonic stress analysis in ceramic components is still in an initial state. The first studies demonstrated the high potential of this method, due to the simple experimental setup and the suitability for automation. A significant limitation is imposed by the effect of the density: local change in the density of about + or - 2 percent have to be taken into account. Fundamental research of acoustoelastic effects in ceramics is necessary. ESA

N91-13547# Stiftung Inst. fuer Werkstofftechnik, Bremen (Germany, F.R.).
POSSIBILITIES OF STRESS MEASUREMENT ON CERAMIC MATERIALS USING ACOUSTIC MICROSCOPY [MOEGLICHKEITEN ZUR SPANNUNGSMESSUNG AN KERAMISCHEN WERKSTOFFEN MITTELS AKUSTISCHER MIKROSKOPIE]
H. Vetters and E. Matthaei *In* Forschungszentrum Juelich G.m.b.H., Residual Stresses in Ceramics 1990 p 147-152 In GERMAN (For primary document see N91-13536 05-27)
Avail: NTIS HC/MF A09

The use of the acoustic microscope as a nondestructive method for the measurement of stresses in ceramic materials is outlined. The measurement is based on the acoustoelastic effect, i.e., the change of the sound speeds due to lattice extensions. Several methods could be applied for the measurement and evaluation of stresses, but are not realized yet because of require further technical developments. The present method is suited to detailed analyses on thin layers. ESA

N91-13548# Forschungszentrum Juelich G.m.b.H. (Germany, F.R.).
POSSIBILITIES OF THE CALCULATION OF STRESSES AND RESIDUAL STRESSES IN MATERIALS WITH A PHASE TRANSFORMATION [MOEGLICHKEITEN DER BERECHNUNG VON SPANNUNGEN UND EIGENSPANNUNGEN IN WERKSTOFFEN MIT EINER PHASENUMWANDLUNG]
Hans P. Hougardy *In its* Residual Stresses in Ceramics 1990 p 153-162 In GERMAN (For primary document see N91-13536 05-27)
Avail: NTIS HC/MF A09

The possibility of calculating residual stresses due to a phase transformation in materials is discussed. The volumes of the different phases formed during the transformation have to be known very accurately. A calculation model developed for steels was transferred to the ceramics ZrO2. Additional difficulties are due to the fact that the anisotropy of the dilatation coefficient causes such high stresses that they affect the martensite formation. This imposes such small elements in a finite element calculation that large volume stress cannot be calculated due to the limited computer capacity. However, for a random grain distribution a large volume can be treated as quasi-isotropic, and hence the models developed for steels can be applied. ESA

N91-13549# Karlsruhe Univ. (Germany, F.R.). Inst. fuer Zuverlaessigkeit und Schadenskunde im Maschinenbau.
CALCULATIONS OF RESIDUAL STRESSES IN CERAMIC SOLDERED JOINTS [BERECHNUNGEN VON EIGENSPANNUNGEN IN KERAMIK/METALL-LOETVERBUNDEN]
O. Iancu and D. Munz *In* Forschungszentrum Juelich G.m.b.H., Residual Stresses in Ceramics 1990 p 163-170 In GERMAN (For primary document see N91-13536 05-27)
Avail: NTIS HC/MF A09

Residual stress fields in ceramic metal soldered joints were calculated using the finite element method with elastoplastic materials models. The global cooling history during the production process was taken into account. The comparison with measured stresses shows that the method is capable of the quantitative determination of residual stress fields. It is shown that tensile residual stresses in ceramics can be reduced by design measures, by the use of suitable pairing of materials and by a proper conduction of the production process. ESA

N91-13550# Maine Univ., Orono. Lab. for Surface Science and Technology.
INTERFACIAL CHEMISTRY OF TITANIUM FILMS DEPOSITED ON PMDA-ODA POLYIMIDE Technical Report, 1 Oct. 1989 - 30 Sep. 1990
W. N. Unertl 15 Aug. 1990 21 p Submitted for publication
Sponsored in part by IBM, Endicott, NY
(Contract N00014-89-J-1314)
(AD-A225730) Avail: NTIS HC/MF A03 CSCL 20/2

Titanium was evaporated onto 1,2,4,5-benzenetetracarboxylic anhydride (PMDA) and 1,4-oxydianiline (ODA) polyimide surfaces at room temperature up to total thickness of about five monolayers. The polyimide backbone is ruptured at both the oxygen ether linkage in the ODA and at the nitrogen imide linkage. The first fraction of a monolayer reacts with oxygen atoms in both the carbonyl and ether functionalities and forms a mixed oxide with titanium predominately in the Ti+3 oxidation state. Near one monolayer coverage, a carbide or mixed oxy-carbide species forms. Above one monolayer, nitrogen is strongly attacked and about fifty percent of the nitrogen reacts with titanium. The deposited titanium begins to take on metallic character only after the coverage has reached several monolayers. GRA

N91-13551# Massachusetts Inst. of Tech., Cambridge. Dept. of Chemistry.
THE SYNTHESIS OF STAR BLOCK COPOLYMERS BY CONTROLLED RING-OPENING METATHESIS POLYMERIZATION
G. C. Bazen and R. R. Schrock 6 Aug. 1990 23 p Submitted for publication
(Contract N00014-89-J-1542)
(AD-A225987; TR-9) Avail: NTIS HC/MF A03 CSCL 07/6

Living polymers made by adding norbornene to Mo(CH-t-Bu)(NAr)(O-t-Bu)2(NAr = N-2,6-C6H3-i-Pr2) react with 1,3-pentadienes and styrene to yield Mo(CHR)(NAr)(O-t-Bu(2 (R = CH=CHMe or Ph) and methylene capped polynorbornene. Both trans-1,3-pentadiene and styrene were found to be effective chain transfer agents, e.g., treating a mixture of Mo(CH-t-Bu)(NAr)(O-t-bu)2 and styrene (30 eq) at 40 min intervals with 10 portions of 80 eq of norbornene yielded an 80-mer with a PDI of 1.13 overall (1.07 for the main peak, approx. 95 percent of total). Analogous reactions involving 5,6-bis(trifluoromethyl)norbornadiene as the monomer gave a distribution of low molecular weight oligomers. GRA

N91-13552# Northwestern Univ., Evanston, IL. Dept. of Chemistry.
PBT, PBO-BASED HYBRID POLYMERS WITH NONLINEAR OPTICAL PROPERTIES OR HIGH ELECTRICAL CONDUCTIVITY Final Report, 1 Jul. 1988 - 30 Nov. 1989
Tobin J. Marks and Stephen H. Carr 6 Aug. 1990 25 p
(Contract F49620-88-C-0122; AF Proj. 2303)
(AD-A226646; AFOSR-90-1025TR) Avail: NTIS HC/MF A03 CSCL 07/6

This program has involved a combined synthetic, processing, and physicochemical study of multifunctional, high performance polymer systems rationally designed for certain unusual physical properties. In one thrust, the unique properties of the high modules/high strength macromolecules poly(p-phenylenebenzabisthiazole) (PBT) an poly (p-phenylenebisoxazolo) (PBO) were utilized to develop new kinds of electrically conductive polymeric and molecular/macromolecular hybrid materials. In the second thrust, several complementary approaches to the construction, evaluation, and fundamental understanding of new types of high performance nonlinear optical materials were pursued. Areas of emphasis have included chromophore functionalized glassy polymers, chromophore embedded crosslinkable matrices, inorganic/organic hybrid materials, crosslinked NLO films, the design of novel chromophores, and internally ordered polymeric NLO materials. Each research component has built upon past successes as well as upon strong on-going collaborations in laser optics and quantum theory. GRA

N91-13553# Lowell Univ., MA. Dept. of Chemistry.
A NEW APPROACH TO DESIGN OF CROSS-LINKED SECOND-ORDER NONLINEAR OPTICAL POLYMERS
Sukant Tripathy, Braja K. Mandal, and Jayant Kumer Sep. 1990 11 p
(Contract N00014-90-J-1148)
(AD-A226674; TR-18-ONR) Avail: NTIS HC/MF A03 CSCL 07/6

An integrated program for the development of novel macromolecular materials for nonlinear optics was established. Various aspects of molecular engineering and optics, viz., molecular design, synthesis, processing, characterization of linear and nonlinear optical properties, fabrication into desired forms and investigation of nonlinear phenomena, are emphasized. For example, based on p-extended donor-acceptor configuration a number of electroactive molecules which possess large molecular hyperpolarizabilities were developed. These molecules were incorporated into macromolecules as side groups or as components of the main chain. A set of macromolecules based on an epoxy structure were designed that permits orientation of the second order nonlinear optical elements and their subsequent vitrification by crosslinking. For second order application it is imperative that the system be noncentro-symmetric. This is brought about by electric field induced poling of the prepolymers based on an epoxy system. The active elements are azo dyes that are appropriately substituted with donor acceptor groups. GRA

N91-13554*# Texas Univ., San Antonio. Dept. of Mechanical Engineering.
A NONLINEAR VISCOELASTIC APPROACH TO DURABILITY PREDICTIONS FOR POLYMER BASED COMPOSITE STRUCTURES Interim Report
Hal F. Brinson and C. C. Hiel Nov. 1990 20 p
(Contract NCC2-678)
(NASA-CR-187653; NAS 1.26:187653; UTSA-DoE/ME-1) Avail: NTIS HC/MF A03 CSCL 11C

Current industry approaches for the durability assessment of metallic structures are briefly reviewed. For polymer based composite structures, it is suggested that new approaches must be adopted to include memory or viscoelastic effects which could lead to delayed failures that might not be predicted using current techniques. A durability or accelerated life assessment plan for fiber reinforced plastics (FRP) developed and documented over the last decade or so is reviewed and discussed. Limitations to the plan are outlined and suggestions to remove the limitations are given. These include the development of a finite element code to replace the previously used lamination theory code and the development of new specimen geometries to evaluate delamination failures. The new DCB model is reviewed and results are presented. Finally, it is pointed out that new procedures are needed to determine interfacial properties and current efforts underway to determine such properties are reviewed. Suggestions for additional efforts to develop a consistent and accurate durability predictive approach for FRP structures is outlined. Author

N91-13555# Oak Ridge National Lab., TN.
ADVANCED MATERIALS DEVELOPMENT PROGRAM: CERAMIC TECHNOLOGY FOR ADVANCED HEAT ENGINES PROGRAM PLAN, 1983--1993
Jul. 1990 66 p
(Contract DE-AC05-84OR-21400)
(DE91-000516; ORNL/M-1248) Avail: NTIS HC/MF A04

The purpose of the Ceramic Technology for Advanced Heat Engines (CTAHE) Project is the development of an industrial technology base capable of providing reliable and cost-effective high temperature ceramic components for application in advanced heat engines. There is a deliberate emphasis on industrial in the purpose statement. The project is intended to support the U.S. ceramic and engine industries by providing the needed ceramic materials technology. The heat engine programs have goals of component development and proof-of-concept. The CTAHE Project is aimed at developing generic basic ceramic technology and does not involve specific engine designs and components. The materials research and development efforts in the CTAHE Project are focused on the needs and general requirements of the advanced gas turbine and low heat rejection diesel engines. The CTAHE Project supports the DOE Office of Transportation Systems' heat engine programs, Advanced Turbine Technology Applications (ATTAP) and Heavy Duty Transport (HDT) by providing the basic technology required for development of reliable and cost-effective ceramic components. The heat engine programs provide the iterative component design, fabrication, and test development logic. DOE

N91-13556# Oak Ridge National Lab., TN.
OPTICAL CHARACTERIZATION TECHNIQUES APPLIED TO CERAMIC OXIDES Foreign Trip Report
M. M. Abraham 15 Oct. 1990 8 p
(Contract DE-AC05-84OR-21400)
(DE91-001526; ORNL/FTR-3783) Avail: NTIS HC/MF A02

The traveler was involved in a collaborative effort at the Clarendon Laboratory, Oxford University, to study tetragonal rare-earth phosphates and vanadates. Single crystals of these materials were grown and subsequently characterized by employing measurements of the magnetic susceptibility and specific heat. These magnetic studies revealed the presence not only of substitutional sites for various impurities, but also of specific orthorhombic impurity sites which were symmetrically oriented in the tetragonal host. The electronic energy levels of the rare-earth phosphates and vanadates were measured by optical and magnetic spectroscopy using state-of-the-art equipment, including superconducting-solenoidal magnets and dye lasers of different frequencies. DOE

N91-13557*# Calspan-State Univ. of New York Joint Venture, Buffalo, NY.
DEVELOPMENT OF BEM FOR CERAMIC COMPOSITES Annual Status Report No. 3, Jan. - Dec. 1990
D. P. Henry, P. K. Banerjee, and G. F. Dargush (State Univ. of New York, Buffalo.) 1990 129 p
(Grant NAG3-888)
(NASA-CR-187676; NAS 1.26:187676) Avail: NTIS HC/MF A07 CSCL 11C

Details on the progress made during the first three years of a five-year program towards the development of a boundary element code are presented. This code was designed for the micromechanical studies of advance ceramic composites. Additional effort was made in generalizing the implementation to allow the program to be applicable to real problems in the aerospace industry. The ceramic composite formulations developed were implemented in the three-dimensional boundary element computer code BEST3D. BEST3D was adopted as the base for the ceramic composite program, so that many of the enhanced features of this general purpose boundary element code could by utilized. Some of these facilities include sophisticated numerical integration, the capability of local definition of boundary conditions, and the use of quadratic shape functions for modeling geometry and field variables on the boundary. The multi-region implementation permits a body to be modeled in substructural parts; thus dramatically reducing the cost of the analysis. Furthermore, it allows a body consisting of regions of different ceramic matrices and inserts to be studied. Author

N91-13558*# National Aeronautics and Space Administration. Langley Research Center, Hampton, VA.
POLYMER/RIBLET COMBINATION FOR HYDRODYNAMIC SKIN FRICTION REDUCTION Patent Application
Dennis M. Bushnell, inventor (to NASA) and Jason C. Reed, inventor (to NASA) (Old Dominion Univ., Norfolk, VA.) 14 Aug. 1990 12 p
(NASA-Case-LAR-14271-1-CU; NAS 1.71:LAR-14271-1-CU; US-Patent-Appl-SN-567025) Avail: NTIS HC/MF A03 CSCL 11C

A process is disclosed for reducing skin friction and inhibiting the effects of liquid turbulence in a system involving the flow of a liquid along the surface of a body, e.g., a marine vehicle. This process includes injecting a drag reducing polymer into the valleys of adjacent, evenly spaced, longitudinal grooves extending along the length of the surface of the body, so that the rate of diffusion of the polymer from individual grooves into the liquid flow is predictably controlled by the groove dimensions. When the polymer has diffused over the tips of the grooves into the near wall region of the boundary layer, the polymer effectively reduces the turbulent

skin friction. A substantial drag reducing effect is achieved with less polymer than must be used to lower skin friction when the surface of the body is smooth. NASA

N91-13559*# National Aeronautics and Space Administration. Langley Research Center, Hampton, VA.
NOVEL POLYIMIDE MOLDING POWDER, COATING, ADHESIVE, AND MATRIX RESIN Patent Application
Terry L. St.Clair, inventor (to NASA) and Donald J. Progar, inventor (to NASA) 31 Jul. 1990 16 p
(NASA-Case-LAR-14163-1; NAS 1.71:LAR-14163-1; US-Patent-Appl-SN-560717) Avail: NTIS HC/MF A03 CSCL 11C

The invention is a polyimide prepared from 3,4'-oxydianiline (3,4'-ODA) and 4,4'-oxydiphthalic anhydride (ODPA), in 2-methoxyethyl ether (diglyme). The polymer was prepared in ultra high molecular weight and in a controlled molecular weight form which has a 2.5 percent offset is stoichiometry (excess diamine) with a 5.0 percent level of phthalic anhydride as an endcap. This controlled molecular weight form allows for greatly improved processing of the polymer for moldings, adhesive bonding, and composite fabrication. The higher molecular weight version affords tougher films and coatings. The overall polymer structure groups in the dianhydride, the diamine, and a metal linkage in the diamine affords adequate flow properties for making this polymer useful as a molding powder, adhesive, and matrix resin. NASA

N91-13560*# National Aeronautics and Space Administration. Langley Research Center, Hampton, VA.
PREPARATION OF POLYIMIDES FROM BIS(N-ISOPRENYL)S OF ARYL DIAMIDES Patent Application
Joseph G. Smith, Jr., inventor (to NASA) and Raphael M. Ottenbrite, inventor (to NASA) (Virginia Commonwealth Univ., Richmond.) 16 Aug. 1990 15 p
(NASA-Case-LAR-14330-1-CU; NAS 1.71:LAR-14330-1-CU; US-Patent-Appl-SN-568128) Avail: NTIS HC/MF A03 CSCL 11C

A process and polyimide product formed by the reaction of a bismaleimide with a bis(amidediene) is disclosed wherein the bis(amidediene) is formed by reacting an excess of an acid chloride with 1,4-N,N'-diisoprenyl 2,3,5,6-tetramethy1 benzene. NASA

N91-13561*# National Aeronautics and Space Administration. Langley Research Center, Hampton, VA.
METHYL SUBSTITUTED POLYIMIDES CONTAINING CARBONYL AND ETHER CONNECTING GROUPS Patent Application
Paul M. Hergenrother, inventor (to NASA) and Steven J. Havens, inventor (to NASA) (Lockheed Engineering and Sciences Co., Hampton, VA.) 28 Sep. 1990 19 p
(NASA-Case-LAR-14351-1; NAS 1.71:LAR-14351-1; US-Patent-Appl-SN-589571) Avail: NTIS HC/MF A03 CSCL 11C

Polyimides were prepared from the reaction of aromatic dianhydrides with novel aromatic diamines having carbonyl and ether groups connecting aromatic rings containing pendant methyl groups. The methyl substituent polyimides exhibit good solubility and form tough, strong films. Upon exposure to ultraviolet irradiation and/or heat, the methyl substituted polyimides crosslink to become insoluble. NASA

N91-13562*# National Aeronautics and Space Administration. Langley Research Center, Hampton, VA.
TISSUE SIMULATING GEL FOR MEDICAL RESEARCH Patent Application
John A. Companion, inventor (to NASA) (PRC Kentron, Inc., Hampton, VA.) 6 Oct. 1989 10 p
(NASA-Case-LAR-14036-1; NAS 1.71:LAR-14036-1; US-Patent-Appl-SN-418372) Avail: NTIS HC/MF A02 CSCL 11C

A tissue simulating gel and a method for preparing the tissue simulating gel are disclosed. The tissue simulating gel is prepared by a process using water, gelatin, ethylene gylcol, and a cross-linking agent. In order to closely approximate the characteristics of the type of tissue being simulated, other material has been added to change the electrical, sound conducting, and wave scattering properties of the tissue simulating gel. The result of the entire process is a formulation that will not melt at the elevated temperatures involved in hyperthermia medical research. Furthermore, the tissue simulating gel will not support mold or bacterial growth, is of a sufficient mechanical strength to maintain a desired shape without a supporting shell, and is non-hardening and non-drying. Substances were injected into the tissue simulating gel prior to the setting-up thereof just as they could be injected into actual tissue, and the tissue simulating gel is translucent so as to permit visual inspection of its interior. A polyurethane spray often used for coating circuit boards can be applied to the surface of the tissue simulating gel to give a texture similar to human skin, making the tissue simulating gel easier to handle and contributing to its longevity. NASA

N91-13563# Brown Univ., Providence, RI.
FRACTURE OF CERAMICS UNDER FARFIELD CYCLIC COMPRESSION
1990 5 p
(Contract DE-FG02-84ER-45167)
(DE90-008417; DOE/ER-45167/1) Avail: NTIS HC/MF A01

A DOE-funded research program was initiated in 1987 to examine the mechanics and mechanisms of fatigue crack growth in ceramics and ceramic composites at ambient temperature. In this program, several novel mechanistic processes associated with mechanical fatigue in a wide variety of brittle solids have been identified. DOE

N91-13564# Technische Hochschule, Darmstadt (Germany, F.R.). Fachbereich Physik.
THE EFFECT OF THE MOLECULAR STRUCTURE OF POLYMER AND LOW MOLECULAR LIQUID CRYSTALS ON THEIR ELECTRO-OPTICAL CHARACTERISTICS AT THE NEMATIC-ISOTROPIC PHASE TRANSITION Ph.D. Thesis [EINFLUSS DES MOLEKULAREN AUFBAUS POLYMERER UND NIEDERMOLEKULARER FLUESSIGKRISTALLE AUF ELEKTRO-OPTISCHE EIGENSCHAFTEN AM NEMATISCH-ISOTROPEN PHASENUEBERGANG]
Dietmar Jungbauer 1989 148 p In GERMAN
(ETN-91-98170) Avail: NTIS HC/MF A07

The electro-optical properties of low molecular and polymer liquid crystals in the neighborhood of the isotropic-nematic phase transition were studied as a function of their molecular structure. Theoretical approaches of the nematic-isotropic phase transition are discussed, especially the characteristic signs of the fluctuations following the phenomenological Landau-de Gennes theory. The important aspects of the nematic-isotropic phase transition (from calamitic to discotic mesogenes) of low molecular model systems and hence the special electro-optical behavior were determined. For side-chain polymers with calamitic mesogenes the influence of chain structure and length, as well as the effect of lateral instead of longitudinal connection of mesogene groups to the polymer main chain and of additional mesogene groups in the main chain on the electro-optical properties at the nematic-isotropic phase transition were examined. ESA

N91-13565# Rensselaer Polytechnic Inst., Troy, NY. Dept. of Materials Engineering.
MECHANISM OF MECHANICAL FATIGUE OF SILICA GLASS Progress Report
Minoru Tomozawa 1990 10 p
(Contract DE-FG02-85ER-45217)
(DE91-004053; DOE/ER-45217/T1) Avail: NTIS HC/MF A02

Research continued on the mechanism of mechanical fatigue of silica glass. Significant accomplishments this quarter include: strength increase of abraded glasses by thermal and chemical treatments was found best explained by crack tip blunting; fatigue was found to involve crack initiation in addition to crack propagation, and only water and ammonia were found capable of causing crack initiation from blunt crack tips at sub-critical stresses; water was

found to enter into silica glass during microhardness indentation as well as during slow crack growth in water-containing atmospheres at room temperature; water diffusion at low temperature showed anomalous phenomena including initial time dependences of solubility and apparent diffusion coefficient; glass containing water showed greater fatigue susceptibility and lower crack initiation stress than dry glass; fatigue of abraded silica glass showed effects of cyclic stress when tested by the rotation bending method while no cyclic stress effect was observed in reciprocal bending; and a new coating which can reduce fatigue of silica glass was developed. DOE

N91-13566*# National Aeronautics and Space Administration. Lewis Research Center, Cleveland, OH.
VINYL CAPPED ADDITION POLYIMIDES Patent Application
Raymond D. Vannucci, inventor (to NASA), Diane C. Malarik, inventor (to NASA), and Peter Delvigs, inventor (to NASA) 25 Oct. 1990 14 p
(NASA-Case-LEW-15027-1; NAS 1.71:LEW-15027-1; US-Patent-Appl-SN-603055) Avail: NTIS HC/MF A03 CSCL 11G

Polyimide resins having improved thermo-oxidative stability are provided having aromatic vinyl end-caps. The polyimides are prepared by the reaction of a mixture of monomers comprising (1) a diamine, (2) an ester of tetracarboxylic acid and (3) an aromatic vinyl compound in a molar ratio of 1:2:3 of n: (n + 1):2 when the aromatic vinyl compound contains nitrogen and in a ratio of (n + 1):n:2 when the aromatic vinyl compound does not contain nitrogen, wherein n ranges from about 5 to about 20. NASA

N91-13567# Technical Research Centre of Finland, Espoo. Metals Lab.
TESTING OF ENGINEERING CERAMICS, SUMMARY
Pertti Auerkari, Pentti Kauppinen, Tero Uuttu, Pekka H. Pankakoski, and Jorma Pitkanen Apr. 1990 24 p In FINNISH; ENGLISH summary Original contains color illustrations
(VTT-RR-678; ISBN-951-38-3619-3; ISSN-0358-5077; ETN-91-98272) Copyright Avail: NTIS HC/MF A03; Government Printing Centre, P.O. Box 516, SF-00101 Helsinki, Finland, HC 40 Finnish marks

Toughness often limits the use of engineering ceramics, when mechanical strength is the decisive factor in design. Relatively modest toughness means small critical defects, which are then easiest to account for by treating the resulting apparent strength as a statistical quantity. Methods to characterize strength so that the outcome is useful for designers is focused upon. Very sensitive and reliable nondestructive techniques are needed for quality control and in service inspections of ceramic components. No known method is without limitations, but the high frequency ultrasonic technique turned out to be very promising, with a potential sensitivity to detect flaws as small as 50 microns. This would be enough in many applications to replace simulated service testing. ESA

N91-13568 National Physical Lab., Teddington (England). Composite and Polymer Properties Branch.
DEVELOPMENT OF STANDARDS FOR ADVANCED POLYMER MATRIX COMPOSITES: A BPF/ACG OVERVIEW
Graham D. Sims Jul. 1990 37 p
(NPL-DMM(A)-8; ISSN-0959-2423; ETN-91-98372) Copyright Avail: National Physical Laboratory, Teddington, TW11 0LW, England

A review of developments standards of BPF/ACG (British Plastic Federation/Advanced Composite Group) is presented. A particular emphasis is put on the engineering properties required in design. An alternative description of the materials of interest is reinforced plastics/composites with fiber volume (Vf) greater than fifty per cent. Conclusions are given covering the current developments in standards for advanced polymer matrix composites, the initiatives towards international harmonization, the need, cost, and mechanism for validation, and the result of a survey for required standards. As most of the initially required test methods are already published or under development, the main effort should be directed towards publishing harmonized versions of these methods as validated ISO standards. A proposal for the funding of the first phase of the validation for ten test methods is included. It is directed at test methods for the basic in-plane properties of high volume fraction laminates. ESA

28 PROPELLANTS AND FUELS

Includes rocket propellants, igniters, and oxidizers; their storage and handling procedures; and aircraft fuels.

For related information see also *07 Aircraft Propulsion and Power, 20 Spacecraft Propulsion and Power,* and *44 Energy Production and Conversion.*

N91-13569*# Thiokol Corp., Brigham City, UT. Space Operations.
SUMMARY OF JAYGO MIXING AND FSM-1 APPLICATION OF CASTABLE INHIBITOR AND LINER Final Report
Kurt B. Evans Jun. 1990 23 p
(Contract NAS8-30490)
(NASA-CR-184030; NAS 1.26:184030; TWR-60551) Avail: NTIS HC/MF A03 CSCL 21I

Two JAYGO planetary mixers (12 and 42 gallon) are being qualified to mix STW5-3224 liner and STW5-3223 castable inhibitor. These mixers are an integral part of a mix process which allows for safe addition of the asbestos component. An essential part of the engineering evaluation (ETP-0347) of these mixers is the generation of static test fire data. Ultimately, these results will help confirm the adequacy of these mixers for production mixing of liner and inhibitor. (These data are not required for qualification of the Certification Test Plan CTP-0125). The details on the mixing, inhibiting, and sling-lining of JAYGO-mixed castable inhibitor and liner which were applied to the FSM-1 segments are presented. The objectives are the following: (1) to document processing events surrounding the JAYO mixing of castable inhibitor and liner, and the subsequent inhibiting and sling lining onto the FSM-1 segments; and (2) to substantiate the measured properties of these JAYGO-mixed materials (rheological and mechanical) and compare these properties to existing production database. Author

N91-13570*# Thiokol Corp., Brigham City, UT. Space Operations.
EVALUATION OF RAYTEK INFRARED PYROMETER FOR CONTINUOUS PROPELLANT TEMPERATURE MEASUREMENT Final Report
Mark D. Dykstra Mar. 1990 15 p
(Contract NAS8-30490)
(NASA-CR-184040; NAS 1.26:184040; TWR-60189) Avail: NTIS HC/MF A03 CSCL 21I

The primary purpose of this evaluation was to determine if the Raytek IR pyrometer that was installed in the 600 gallon propellant mixers could be used to provide a continuous, accurate, reliable measurement of the propellant temperature during mixing. The Raytek infrared sensor is not recommended to be used for controlling propellant temperature nor for inspection buy-off. The first part of the evaluation was to determine the accuracy of the sensor in measuring the propellant temperature. The second part was to determine the reliability of the air purge design in preventing contamination of the IR window. Author

N91-13571# Ballistic Research Labs., Aberdeen Proving Ground, MD.
THE MOLECULAR STRUCTURE OF THE HAN-BASED LIQUID PROPELLANTS Final Report, Jan. 1987 - Dec. 1989
Nathan Klein Aug. 1990 37 p
(AD-A226415; BRL-TR-3139) Avail: NTIS HC/MF A03 CSCL 21/9

The HAN-TEAN-water mixtures that are the gun propellants LGP1845 and LGP1846 are organized molecular aggregates separated by regions of unstructured water. Temperature, pressure and the presence of impurities or contaminants cause changes in

the microscopic organization of the mixtures. The size and structure of these aggregates control the physical and some of the chemical properties of the propellants, many of which are essential for proper gun performance. GRA

N91-13572# Oak Ridge National Lab., TN. Engineering Technology Div.
HIGH-ALCOHOL MICROEMULSION FUEL PERFORMANCE IN A DIESEL ENGINE
B. H. West, A. L. Compere, and W. L. Griffith 1990 34 p Presented at the 1990 SAE International Fuels and Lubricants Conference and Exposition, Tulsa, OK, 22-25 Oct. 1990
(Contract DE-AC05-84OR-21400)
(DE91-001617; CONF-9010205-2) Avail: NTIS HC/MF A03

Incidence of methanol use in diesel engines is increasing rapidly due to the potential to reduce both diesel particulate emissions and petroleum consumption. Because simple alcohols and conventional diesel fuel are normally immiscible, most tests to date have used neat to near-neat alcohol, or blends incorporating surfactants or other alcohols. Alcohol's poor ignition quality usually necessitates the use of often expensive cetane enhancers, full-time glow plugs, or spark assist. Reported herein are results of screening tests of clear microemulsion and micellar fuels which contain 10 to 65 percent C1-C4 alcohol. Ignition performance and NO emissions were measured for clear, stable fuel blends containing alcohols, diesel fuel, and additives such as alkyl nitrates, acrylic acids, and several vegetable oil derivatives. Using a diesel engine calibrated with reference fuels, cetane numbers for fifty four blends were estimated. The apparent cetane numbers ranged from around 20 to above 50 with the majority between 30 and 45. Emissions of nitric oxide were measured for a few select fuels and were found to be 10 to 20 percent lower than No. 2 diesel fuel. DOE

N91-13573# Los Alamos National Lab., NM.
ALL HOT SPOTS ARE NOT EQUAL
John B. Ramsay and Herbert P. Richter (Naval Weapons Center, China Lake, CA.) 1990 8 p Presented at the Physics of Explosives Technical Meeting, Saint Louis, France, Jun. 1990
(Contract W-7405-eng-36)
(DE91-002303; LA-UR-90-3413; CONF-9006286-1) Avail: NTIS HC/MF A02

Introduction of discontinuities increases the sensitivity of energetic material to initiation by shock waves. We have experimental evidence that the particular nature of these discontinuities significantly changes this sensitivity. The observations are preliminary, but they are significant in our understanding of heterogeneous initiation. Data from these studies, combined with literature data on the shock sensitivity of pressed explosives, show quantitatively different responses for materials with the three types of voids. In materials with the same porosity, damage creates the most sensitive material, but pressed explosives are affected less, and the addition of microballoons creates the smallest change in sensitivity. The analysis of these data employs an interesting, and as yet unexplored, representation of shock sensitivity as a function of density. DOE

N91-13574# Oak Ridge National Lab., TN.
CHARACTERIZATION OF ROCKET PROPELLANT COMBUSTION PRODUCTS: DESCRIPTION OF SAMPLING AND ANALYSIS METHODS FOR ROCKET EXHAUST CHARACTERIZATION STUDIES Interim Report
R. A. Jenkins, C. V. Thompson, T. M. Gayle, C. Y. Ma, and B. A. Tomkins 7 Jun. 1990 29 p Sponsored by Army Biomedical Research and Development Lab., Fort Detrick, MD
(Contract DE-AC05-84OR-21400)
(DE91-002536; ORNL-TM-11643) Avail: NTIS HC/MF A03

A systematic approach has been developed and experimentally validated for the sampling and chemical characterization of the rocket motor exhaust generated from the firing of scaled down test motors at the U.S. Army's Signature Characterization Facility (ASCF) at Redstone Arsenal in Huntsville, Alabama. The overall strategy was to sample and analyze major exhaust constituents in near real time, while performing off-site analyses of samples collected for the determination of trace constituents of the particulate and vapor phases. Initial interference studies were performed using atmospheric pressure burns of 1 g quantities of propellants in small chambers at Oak Ridge National Laboratory. Carbon monoxide and carbon dioxide were determined using non-dispersive infrared instrumentation. Hydrogen cyanide, hydrogen chloride, and ammonia determinations were made using ion selective electrode technology. Oxides of nitrogen were determined using chemiluminescence instrumentation. Airborne particulate mass concentration was determined using infrared forward scattering measurements and a tapered element oscillating microbalance, as well as conventional gravimetry. Particulate phase metals were determined by collection on Teflon membrane filters, followed by inductively coupled plasma and atomic absorption analysis. Particulate phase polynuclear aromatic hydrocarbons (PAH) and nitro-PAH were collected using high volume sampling on a two stage filter. Target species were extracted, and quantified by gas chromatography/mass spectrometry (GC/MS). Vapor phase species were collected on multi-sorbent resin traps, and subjected to thermal desorption GC/MS for analysis. DOE

29 MATERIALS PROCESSING

Includes space-based development of products and processes for commercial applications.
For biological materials see *55 Space Biology.*

N91-13575*# National Aeronautics and Space Administration, Washington, DC.
MICROGRAVITY STRATEGIC PLAN, 1990
1990 26 p
(NASA-TM-103448; NAS 1.15:103448) Avail: NTIS HC/MF A03 CSCL 22A

The mission of the NASA Microgravity program is to utilize the unique characteristics of the space environment, primarily the near absence of gravity, to understand the role of gravity in materials processing, and to demonstrate the feasibility of space production of improved materials that have high technological, and possible commercial, utility. The following five goals for the Microgravity Program are discussed: (1) Develop a comprehensive research program in fundamental sciences, materials science, and biotechnology for the purpose of attaining a structured understanding of gravity dependent physical phenomena in both Earth and non-Earth environments; (2) Foster the growth of interdisciplinary research community to conduct research in the space environment; (3) Encourage international cooperation for the purpose of conducting research in the space environment; (4) Utilize a permanently manned, multi-facility national microgravity laboratory in low-Earth orbit to provide a long-duration, stable microgravity environment; (5) Promote industrial applications of space research for the development of new, commercially viable products, services, and markets resulting from research in the space environment. Y.S.

31 ENGINEERING (GENERAL)

Includes vacuum technology; control engineering; display engineering; cryogenics; and fire prevention.

N91-13576# Minnesota Univ., Minneapolis. Dept. of Mechanical Engineering.
ANALYTICAL AND EXPERIMENTAL STUDIES FOR THERMAL PLASMA PROCESSING OF MATERIALS
1990 8 p
(Contract DE-FG02-85ER-13433)
(DE91-000599; DOE/ER-13433/T1) Avail: NTIS HC/MF A02

Work continued on thermal plasma processing of materials. This quarter, ceramic powders of carbides, aluminum nitride, oxides, solids solutions, magnetic and non magnetic spinels, superconductors, and composites have been successfully synthesized in a Triple DC Torch Plasma Jet Reactor (TTPR) and

in a single DC Plasma Jet Reactor. All the ceramic powders with the exception of AlN were synthesized using a novel injection method developed to overcome the problems associated with solid injection, in particular for the single DC plasma jet reactor, and to realize the benefits of gas phase reactions. Also, initial experiments have been performed for the deposition of diamond coatings on Si wafers using the TTPR with methane as the carbon source. Well faceted diamond crystallites were deposited on the surface of the wafers, forming a continuous one particle thick coating. For measuring temperature and velocity fields in plasma systems, enthalpy probes have been developed and tested. The validity has been checked by performing energy and mass flux balances in an argon plasma jet operated in argon atmosphere. Total Gibbs free energy minimization calculations using a quasi-equilibrium modification have been applied to simulate several chemical reactions. Plasma reactor modelling has been performed for the counter-flow liquid injection plasma synthesis experiment. Plasma diagnostics has been initiated to determine the pressure gradient in the coalesced part of the plasma jet. The pressure gradient drives the diffusion of chemical species which ultimately controls the chemical reactions. DOE

N91-13577# Oak Ridge Gaseous Diffusion Plant, TN. Computing and Telecommunications Div.
FLUID FLOW EFFECTS ON ELECTROPLATING
J. R. Kirkpatrick Sep. 1990 31 p
(Contract DE-AC05-84OT-21400)
(DE91-001087; K/CSD/TM-88) Avail: NTIS HC/MF A03

The effects of fluid flow patterns on the electroplating of rotating cylindrically symmetric objects are examined. Ways are outlined for preventing undesirable spiral patterns on the plated surface. Estimates are given for the diffusion boundary layer thickness for cylinders, disks, spheres, and cones. DOE

N91-13578# Oak Ridge National Lab., TN.
PERFORMANCE COMPARISON OF MAGNETIC REFRIGERATION CYCLES
F. C. Chen, G. L. Chen, R. W. Murphy, and V. C. Mei 1990 22 p Presented at the 6th International Cryocooler Conference, Plymouth, MA, 25-26 Oct. 1990
(Contract DE-AC05-84OR-21400)
(DE91-001520; CONF-901029-1) Avail: NTIS HC/MF A03

Magnetic refrigeration has been used for cryogenic cooling at temperatures near absolute zero for many years. In these cases, a single-step adiabatic demagnetization method that does not provide continuous refrigeration is commonly used. The possibilities of providing continuous cooling through magnetic refrigeration cycles and of extending the range of applications above near-absolute-zero temperatures have been investigated only in recent years. This paper reports the results of a parametric performance study of three magnetic refrigeration cycles using four rare-earth magnetic materials operating near their respective Curie temperatures. The thermodynamic cycles employed are the magnetic-equivalent Carnot, Ericsson, and ideal regenerative cycles, and the four magnetic materials are terbium, holmium, erbium, and thulium. Our findings show that the Carnot cycle is not possible for cases of temperature lift beyond 10 K for a magnetic field variation of 7 Tesla, that the performance and capacity of an ideal regenerative cycle are higher than that of the corresponding Ericsson cycle, and that the magnetocaloric effects of erbium and thulium seem to be too weak for practical applications. DOE

N91-13579# Society of Automotive Engineers of Japan, Tokyo.
THE 1990 JSAE (SOCIETY OF AUTOMATIVE ENGINEERS OF JAPAN, INC.) SPRING CONVENTION PROCEEDINGS 901
25 Apr. 1990 440 p In ENGLISH and JAPANESE Convention held in Tokyo, Japan, 15-16 May 1990
(DE91-715185; ETDE/JP-mf-1715185) Avail: NTIS (US Sales Only) HC/MF A19

Following is a summary of the 1990 Society of Automotive Engineers of Japan (JSAE) convention proceedings. Fundamental themes were the use of super computers, stress and vibration mode analyses through the use of the finite element method, and numerical analysis of in-cylinder flow. Simulation for aerodynamic characteristics was also applied. Themes of environment, comfort, safety, noise, vibration, and human engineering were emphasized. In the new fuel field, methanol ignitability in diesel engine and aldehyde analyzing method etc. were presented. In the material field, an alternative cooling medium for freon to be used in air conditioners, part corrosion resistance under exhausting conditions, laminated damping sheets and brake material were described. Maneuverability, contact patch temperature of tire tread, tires for ice and snow road, active control of vehicles and maneuvering stability were presented. DOE

N91-13580*# National Aeronautics and Space Administration. Lyndon B. Johnson Space Center, Houston, TX.
DUAL DIAPHRAGM TANK WITH TELLTALE DRAIN Patent Application
Wallace C. Tuthill, inventor (to NASA) 25 Oct. 1990 15 p
(NASA-Case-MSC-21703-1; NAS 1.71:MSC-21703-1; US-Patent-Appl-SN-603052) Avail: NTIS HC/MF A03 CSCL 13B

A fluid storage and expulsion system comprising a tank with an internal flexible diaphragm assembly of dual diaphragms in back-to-back relationship, at least one of which is provided with a patterned surface having fine edges such that the diaphragms are in contact along said edges without mating contact of surface areas to thereby form fluid channels which extend outwardly to the peripheral edges of the diaphragms. The interior wall of the tank at the juncture of tank sections is formed with a circumferential annular recess comprising an outer annular recess portion which forms a fluid collection chamber and an inner annular recess portion which accommodates the peripheral edge portions of the diaphragms and a sealing ring in clamped sealing relation therebetween. The sealing ring is perforated with radially extending passages which allow any fluid leaking or diffusing past a diaphragm to flow through the fluid channels between the diaphragms to the fluid collection chamber. Ports connectable to pressure fittings are provided in the tank sections for admission of fluids to opposite sides of the diaphragm assembly. A drain passage through the tank wall to the fluid collection chamber permits detection, analysis and removal of fluids in the collection chamber. NASA

N91-13581*# National Aeronautics and Space Administration. Pasadena Office, CA.
FLEXIBLE THERMAL APPARATUS FOR MOUNTING OF THERMOELECTRIC COOLER Patent Application
Jack A. Jones, inventor (to NASA), S. Walter Petrick, inventor (to NASA), and Steven Bard, inventor (to NASA) (Jet Propulsion Lab., California Inst. of Tech., Pasadena.) 31 Jul. 1990 10 p
(Contract NAS7-918)
(NASA-Case-NPO-17806-1-CU; NAS 1.71:NPO-17806-1-CU; US-Patent-Appl-SN-560908) Avail: NTIS HC/MF A02 CSCL 13B

A flexible heat transfer apparatus used to flexibly connect and thermally couple a thermoelectric cooler to an object to be cooled is disclosed. The flexible heat transfer apparatus consists of a pair of flexible corrugated sheets made from high thermal conductivity materials such as copper, aluminum, gold, or silver. The ridges of the corrugated sheets are oriented perpendicular to one another and bonded sandwich-fashion between three plates to define an upper section and a lower section. The upper section provides X flexure, the lower section provides Y flexure, and both sections together provide Z flexure. NASA

N91-13582# Los Alamos National Lab., NM.
SUPERFLUID STIRLING REFRIGERATOR- A NEW METHOD FOR COOLING BELOW 1 KELVIN
V. Kotsubo and G. W. Swift 1990 14 p Presented at the 6th International Cryocooler Conference, Plymouth, MA, 25-26 Oct. 1990 Submitted for publication
(Contract W-7405-eng-36)
(DE91-002311; LA-UR-90-3380; CONF-901029-2) Avail: NTIS HC/MF A03

We have invented and built a new type of cryocooler, which we call the superfluid Stirling refrigerator (SSR). The first prototype reached 0.6 K from a starting temperature of 1.2 K. The working fluid of the SSR is the (sup 3)He solute in a superfluid He(3) - He(4) solution. At low temperatures, the superfluid He(4) is in its quantum ground state, and therefore is thermodynamically inert, while the He(3) solute has the thermodynamic properties of a dense ideal gas. Thus, in principle, any refrigeration cycle that can use an ideal gas can also use the He(3) solute as working fluid. In our SSR prototype, bellows-sealed superleak pistons driven by a room-temperature camshaft work on the He(3) solute. Ultimately, we anticipate elimination of moving parts by analogy with pulse-tube refrigeration. DOE

N91-13583# Centre Technique des Industries Mecaniques, Senlis (France).
STUDY OF THE TIME AND EFFORT SIGNAL IN CUTTING OPERATIONS Final Report [ETUDE SIGNAL EFFORT-TEMPS EN DECOUPAGE]
E. Grosset, A. Maillard, C. Bouhelier, and J. Gasnier 1929 15 p In FRENCH
(CETIM-101580; ETN-91-98334) Copyright Avail: NTIS HC/MF A03

Perception and treatment of an effort signal by computer methods is discussed. An automatic control system used to measure the wear of machine tools and carry out quality control throughout the cutting process is described. The testing system is used to evaluate the performance of tools which have been vacuum plated. The system is used as part of the BRITE study, the goal of which is to develop an expert system for measuring the wear of tools used during drilling and perforation operations. ESA

N91-14035# Rutherford Appleton Lab., Chilton (England).
MINIATURE CLOSED CYCLE REFRIGERATORS
T. W. Bradshaw and A. H. Orlowska *In* AGARD, Applications of Superconductivity to Avionics Oct. 1990 7 p (For primary document see N91-14030 05-76)
Copyright Avail: NTIS HC/MF A08; Non-NATO Nationals requests available only from AGARD/Scientific Publications Executive

32 COMMUNICATIONS AND RADAR

Includes radar; land and global communications; communications theory; and optical communications.

For related information see also *04 Aircraft Communications and Navigation* and *17 Space Communications, Spacecraft Communications, Command and Tracking.* For search and rescue see *03 Air Transportation and Safety,* and *16 Space Transportation.*

N91-13584*# Georgia Inst. of Tech., Atlanta. School of Electrical Engineering.
PIONEER-VENUS RADIO OCCULTATION (ORO) DATA REDUCTION: PROFILES OF 13 cm ABSORPTIVITY Final Technical Report, 1 Jul. 1988 - 30 Sep. 1990
Paul G. Steffes 1990 63 p
(Grant NAG2-515)
(NASA-CR-186986; NAS 1.26:186986) Avail: NTIS HC/MF A04 CSCL 17B

In order to characterize possible variations in the abundance and distribution of subcloud sulfuric acid vapor, 13 cm radio occultation signals from 23 orbits that occurred in late 1986 and 1987 (Season 10) and 7 orbits that occurred in 1979 (Season 1) were processed. The data were inverted via inverse Abel transform to produce 13 cm absorptivity profiles. Pressure and temperature profiles obtained with the Pioneer-Venus night probe and the northern probe were used along with the absorptivity profiles to infer upper limits for vertical profiles of the abundance of gaseous H2SO4. In addition to inverting the data, error bars were placed on the absorptivity profiles and H2SO4 abundance profiles using the standard propagation of errors. These error bars were developed by considering the effects of statistical errors only. The profiles show a distinct pattern with regard to latitude which is consistent with latitude variations observed in data obtained during the occultation seasons nos. 1 and 2. However, when compared with the earlier data, the recent occultation studies suggest that the amount of sulfuric acid vapor occurring at and below the main cloud layer may have decreased between early 1979 and late 1986. Author

N91-13585*# National Aeronautics and Space Administration. Langley Research Center, Hampton, VA.
MODIFIED HILBERT TRANSFORM PAIR AND KRAMERS-KRONIG RELATIONS FOR COMPLEX PERMITTIVITIES
C. R. Cockrell Aug. 1990 21 p
(NASA-TM-102682; NAS 1.15:102682) Avail: NTIS HC/MF A03 CSCL 20N

Modified versions of the Hilbert transform pair and the Kramers-Kronig relations are derived for the complex permittivity of a plasma/dielectric medium which is singular at the frequency of the applied electric field equal to 0. Such a complex permittivity exists when the plasma/dielectric model allows a loss term but no restoring term. Permittivity, in which both loss and restoring terms are included, is shown to satisfy the standard Hilbert transform pair and, thus, the Kramers-Kronig relations. Y.S.

N91-13586# Instituto de Pesquisas Espaciais, Sao Jose dos Campos (Brazil).
S-BAND DIPLEXER FOR A TELECOMMUNICATION BOARD TRANSPONDER [DIPLEXADOR DE BANDA S PARA UM TRANSPONDER DE TELECOMUNICACOES DE BORDO]
Paulo MelloMarshall May 1988 9 p In PORTUGESE Presented at the 3rd Brazilian Symposium on Microwaves held 27-29 July 1988, Natal, Brazil Submitted for publication
(INPE-4540-PRE/1286) Avail: NTIS HC/MF A02

The project and performance parameters are described for an S band diplexer, developed for the Telecommunication Service transponder of a data collecting satellite of the Brazilian Complete Space Mission (MECB). The parameters for insertion loss, isolation, band noise limitation, and broadband match were optimized for the project. Transl. by B.G.

N91-13587# Instituto de Pesquisas Espaciais, Sao Jose dos Campos (Brazil).
RESTORATION OF SOLAR RADIO IMAGES: EVALUATION OF POOR CONDITIONS AND RESOLUTION BY REGULARIZATION TECHNIQUES [RESTAURACAO DE RADIOIMAGENS SOLARES: AVALIACAO DO MAU CONDICIONAMENTO E SOLUCAO POR TECNICAS DE REGULARIZACAO]
Nelson D. A. Mascarenhas, Edson A. Ribeiro, and Joaquim E. R. Costa May 1988 10 p In PORTUGESE Presented at the 1st Brazilian Symposium on Computer Graphics and Image Processing, 19-20 Apr. 1988, Petropolis, Brazil
(INPE-4557-PRE/1298) Avail: NTIS HC/MF A02

The problem of deconvolution of a degraded radio image by the antenna radiation pattern can be put in terms of an image restoration pattern. A computational model of regressive statistics is adopted. The problem is studied in poor quality by minimal estimates adapted from the scattering coefficient function of the Gaussian function that approximates the radiation pattern. The solution to the problem of poor quality is proposed in terms of regularization method use. Results are presented for simulated images and real images obtained from the Itapetinga Radio Astronomy Observatory, INPE. Transl. by BG

N91-13588# Naval Research Lab., Washington, DC. Plasma Physics Div.
NRL 1989 BEAM PROPAGATION STUDIES IN SUPPORT OF THE ATA MULTI-PULSE PROPAGATION EXPERIMENT Interim Report
Richard F. Hubbard, A. Wahab Ali, Jay P. Boris, Paul Boris, Richard F. Fernsler, Glenn Joyce, Elaine S. Oran, J. Michael Picone, Steven P. Slinker, and Ronald D. Taylor (Berkeley Research Association, Springfield, VA.) 31 Aug. 1990 40 p Presented at the 1989

Annual DARPA/SDIO/Services Charged Particle Beam Review, Monterey, CA, 18-21 Sep. 1989 Submitted for publication Sponsored in part by NSWC, Silver Spring, MD
(ARPA Order 4395)
(AD-A226443; NRL-MR-6677) Avail: NTIS HC/MF A03 CSCL 09/1

NRL theoretical and computational studies in support of the ATA Multi-Pulse Propagation Experiment (MPPE) are summarized in a series of papers which were presented at the 1989 Annual DARPA/SDIO/Services Charged Particle Beam Review. The six papers presented here were all written prior to the completion of the experiment. The first of these papers presents simulation results which modeled beam stability and channel evolution for an entire five pulse burst. The second paper describes a new air chemistry model used in the SARLAC propagation code and discusses the role of CO2 in speeding channel heating. An overview of NRL studies on beam propagation in reduced-density channels is provided in the next paper. The fourth paper describes hydrodynamic simulations of convective mixing in beam-generated channels using a new flux-corrected transport algorithm developed for NRL's Connection Machine. GRA

N91-13589# Syracuse Univ., NY. Dept. of Electrical and Computer Engineering.
RESONANCE REGION SCATTERING Final Report, Jun. 1989 - Feb. 1990
Xiaopu Yang and Ercument Arvas Jul. 1990 31 p
(Contract F30602-88-D-0027)
(AD-A226536; RADC-TR-90-155) Avail: NTIS HC/MF A03 CSCL 17/9

Using frequency derivative information, techniques were developed to predict the scattering from conductor and dielectric 2-D targets over a frequency band. Instead of computing a method of moments solution using a point approach, a rational function model is used to approximate the current as a function of frequency. The model coefficients are computed using frequency derivative information at one frequency within the band to improve efficiency of conventional moment method approaches. Results show that the model based approach gives excellent results over a limited frequency band, and is much more efficient than the conventional point by point approach. GRA

N91-13590# Pennsylvania State Univ., University Park. Communications and Space Sciences Lab.
[UTILIZATION OF THE HIPAS FACILITY FOR COOPERATIVE EXPERIMENTS RELATED TO IONOSPHERIC MODIFICATION] Final Report, 15 Jun. 1987 - 8 Aug. 1989
A. J. Ferraro and Alfred W. Wong 1989 175 p Prepared in cooperation with SAIC and the Univ. of California, Los Angeles
(Contract N00014-86-K-0677)
(AD-A226609) Avail: NTIS HC/MF A08 CSCL 20/14

The broad research objective of this program has been to investigate unique concepts for generating ULF, ELF, and VLF using the ionosphere as the wireless antenna. The Wireless Antenna or HF demodulation experiment was demonstrated in 1980 using the Arecibo observatory's heating facility. Modulation of the dynamo current system at that latitude was the major source for the wireless antenna. Some of the major experimental accomplishments are: excellent quality of generated ELF and VLF signals; determination of D-region electron density profiles at high latitudes for large sunspot numbers; slow beam steering to examine the structure of the electrojet current system mapped down into the D-region; determination of electrojet activity from ELF/VLF polarization characteristics; multiple VLF ionospheric sources (two-element VLF arrays); fast beam steering - the painting technique (a potential method of increasing ELF power); short range field measurements in Alaska with the Penn State Mobile Van; the stability of the current system to support bi-phase PSK and Quad-phase PSK to increase data rates. GRA

N91-13591# Naval Postgraduate School, Monterey, CA. Dept. of Administrative Sciences.
EXTREMELY HIGH FREQUENCY (EHF) LOW PROBABILITY OF INTERCEPT (LPI) COMMUNICATION APPLICATIONS M.S. Thesis
Robert W. Belcher Mar. 1990 81 p
(AD-A226653) Avail: NTIS HC/MF A05 CSCL 17/4

A Commander-in-Chief U.S. Pacific Fleet letter to the Chief of Naval Operations, dated September 12, 1989, contains a Command and Control Studies and Analysis Program (C2STAP) proposal for EHF line of sight communications. Several of the issues raised by the C2STAP proposal are addressed by providing: an analysis of the inherent advantages and disadvantages of communications in the EHF spectrum, an analysis of the current and projected future state of EHF technology with respect to potential military applications, a link analysis of an EHF LPI communications link in a specific tactical scenario, and a recommendation to upgrade the Integrated Refractive Effects Prediction System (IREPS) in order to provide an EHF LPI link assessment capability. Although many other applications are referred to, the feasibility practicality, and tactical benefit of EHF communication systems is addressed. GRA

N91-13592# Naval Postgraduate School, Monterey, CA. Dept. of Administrative Sciences.
ASSESSMENTS OF ATMOSPHERIC EFFECTS ON VHF AND UHF COMMUNICATIONS M.S. Thesis
Gary W. Culbertson Mar. 1990 83 p
(AD-A226661) Avail: NTIS HC/MF A05 CSCL 25/2

Nonstandard gradients of pressure, temperatures and humidity in the troposphere create refractive conditions that affect electromagnetic waves by either increasing or decreasing VHF and UHF communication ranges. The Naval Ocean Systems Center (NOSC) has developed the Integrated Refractive Effect Prediction System (IREPS) to assess refractive conditions for a point of interest and provide video display or printouts of how the refractive conditions will affect various EM transmissions. A research cruise was conducted from 1 to 8 November 1989 in the Eastern Pacific and included 31 rawinsonde launches. The data from rawinsondes was entered in IREPS PC Version 1.0 assess the refractive conditions. The IREPS generated refractive assessments where then compared to the GTE Sylvania Report and the Pacific Missile Test Center's Interim Procedure for Forecasting Refractivity Conditions (IPFRC). The results indicated that the GTE Sylvania climatology was not an accurate tool for assessing refractive condition at sea mainly because the GTE data set consisted of shore-based rawinsonde data. The IPFRC, based solely on synoptic weather parameters, obtained at 60 percent success rate in predicting the likelihood of the presence of refractive conditions. GRA

N91-13593# Lawrence Livermore National Lab., CA.
TEMPORAL SCATTERING AND RESPONSE SOFTWARE: USERS' MANUAL
Robert R. McLeod Sep. 1990 45 p
(Contract W-7405-eng-48)
(DE91-001760; UCRL-MA-104861) Avail: NTIS HC/MF A03

This manual gives complete information on how to use the TSAR electromagnetic analysis software. Included are descriptions of input files, the details of how these files affect the problem, and output data specifications. What is not included is the theory of the finite-difference time-domain (FDTD) algorithm or details of the TSAR implementation of it. This manual assumes that readers are sufficiently familiar with FDTD that they only need the how to knowledge presented here. For further information on the theory of operation of TSAR, see the papers reference in the bibliography. This is a reference, rather than a tutorial manual. To help new users become familiar with the TSAR software, a set of example problems is included with the TSAR distribution. DOE

N91-13594*# National Aeronautics and Space Administration. Pasadena Office, CA.
METHOD FOR PROVIDING A POLARIZATION FILTER FOR PROCESSING SYNTHETIC APERTURE RADAR IMAGE DATA Patent Application
Pascale C. Dubois, inventor (to NASA) and Jakob J. vanZyl, inventor (to NASA) (Jet Propulsion Lab., California Inst. of Tech., Pasadena.) 25 Jun. 1990 27 p
(Contract NAS7-918)
(NASA-Case-NPO-17904-1-CU; NAS 1.71:NPO-17904-1-CU; US-Patent-Appl-SN-544293) Avail: NTIS HC/MF A03 CSCL 17I

A polarization filter can maximize the signal-to-noise ratio of a polarimetric synthetic aperture radar (SAR) and help discriminate between targets or enhance image features, e.g., enhance contrast between different types of target. The method disclosed is based on the Stokes matrix/ Stokes vector representation, so the targets of interest can be extended targets, and the method can also be applied to the case of bistatic polarimetric radars. NASA

N91-13595*# National Aeronautics and Space Administration. Pasadena Office, CA.
PIPELINE SYNTHETIC APERTURE RADAR DATA COMPRESSION UTILIZING SYSTOLIC BINARY TREE-SEARCHED ARCHITECTURE FOR VECTOR QUANTIZATION Patent Application
Chi-Yung Chang, inventor (to NASA), Wai-Chi Fang, inventor (to NASA), and John C. Curlander, inventor (to NASA) (Jet Propulsion Lab., California Inst. of Tech., Pasadena.) 10 Jul. 1990 37 p
(Contract NAS7-918)
(NASA-Case-NPO-17941-1-CU; NAS 1.71:NPO-17941-1-CU; US-Patent-Appl-SN-550775) Avail: NTIS HC/MF A03 CSCL 17I

A system for data compression utilizing systolic array architecture for Vector Quantization (VQ) is disclosed for both full-searched and tree-searched. For a tree-searched VQ, the special case of a Binary Tree-Search VQ (BTSVQ) is disclosed with identical Processing Elements (PE) in the array for both a Raw-Codebook VQ (RCVQ) and a Difference-Codebook VQ (DCVQ) algorithm. A fault tolerant system is disclosed which allows a PE that has developed a fault to be bypassed in the array and replaced by a spare at the end of the array, with codebook memory assignment shifted one PE past the faulty PE of the array.
NASA

N91-13596*# National Aeronautics and Space Administration. Pasadena Office, CA.
MULTIPLE SYMBOL DIFFERENTIAL DETECTION Patent Application
D. Divsalar, inventor (to NASA) and M. Simon, inventor (to NASA) (Jet Propulsion Lab., California Inst. of Tech., Pasadena.) 31 Jul. 1990 24 p
(Contract NAS7-918)
(NASA-Case-NPO-17896-1-CU; NAS 1.71:NPO-17896-1-CU; US-Patent-Appl-SN-560691) Avail: NTIS HC/MF A03 CSCL 17B

A differential detection technique for multiple phase shift keying (MPSK) signals is provided which uses a multiple symbol observation interval on the basis of which a joint decision is made regarding the phase of the received symbols. In accordance with the invention, a first difference phase is created between first and second received symbols. Next the first difference phase is correlated with the possible values thereof to provide a first plurality of intermediate output signals. A second difference phase is next created between second and third received symbols. The second difference phase is correlated with plural possible values thereof to provide a second plurality of intermediate output signals. Next, a third difference phase is created between the first and third symbols. The third difference phase is correlated with plural possible values thereof to provide a third plurality of intermediate output signals. Each of the first plurality of intermediate outputs are combined with each of the second plurality of intermediate outputs and each of the third plurality of intermediate outputs to provide a plurality of possible output values. Finally, a joint decision is made by choosing from the plurality of possible output values the value which represents the best combined correlation of the first, second and third difference values with the possible values thereof.
NASA

N91-13597# Los Alamos National Lab., NM.
TRANSIONOSPHERIC PROPAGATION CODE (TIPC)
Robert Roussel-Dupre and Thomas A. Kelley Oct. 1990 83 p
(Contract W-7405-eng-36)
(DE91-002435; LA-11799-MS) Avail: NTIS HC/MF A05

The Transionospheric Propagation Code is a computer program developed at Los Alamos National Lab to perform certain tasks related to the detection of VHF signals following propagation through the ionosphere. The code is written in FORTRAN 77, runs interactively and was designed to be as machine independent as possible. A menu format in which the user is prompted to supply appropriate parameters for a given task has been adopted for the input while the output is primarily in the form of graphics. The user has the option of selecting from five basic tasks, namely transionospheric propagation, signal filtering, signal processing, delta times of arrival (DTOA) study, and DTOA uncertainty study. For the first task a specified signal is convolved against the impulse response function of the ionosphere to obtain the transionospheric signal. The user is given a choice of four analytic forms for the input pulse or of supplying a tabular form. The option of adding Gaussian-distributed white noise of spectral noise to the input signal is also provided. The deterministic ionosphere is characterized to first order in terms of a total electron content (TEC) along the propagation path. In addition, a scattering model parameterized in terms of a frequency coherence bandwidth is also available. In the second task, detection is simulated by convolving a given filter response against the transionospheric signal. The user is given a choice of a wideband filter or a narrowband Gaussian filter. It is also possible to input a filter response. The third task provides for quadrature detection, envelope detection, and three different techniques for time-tagging the arrival of the transionospheric signal at specified receivers. The latter algorithms can be used to determine a TEC and thus take out the effects of the ionosphere to first order. Task four allows the user to construct a table of DTOAs vs TECs for a specified pair of receivers.
DOE

N91-13598*# National Aeronautics and Space Administration. Lewis Research Center, Cleveland, OH.
REAL-TIME DATA COMPRESSION OF BROADCAST VIDEO SIGNALS Patent Application
Mary J. Shalkhauser, inventor (to NASA), Wayne A. Whyte, Jr., inventor (to NASA), and Scott P. Barnes, inventor (to NASA) (Hughes Aircraft Co., Canoga Park, CA.) 20 Jun. 1990 56 p
(NASA-Case-LEW-14945-1; NAS 1.71:LEW-14945-1; US-Patent-Appl-SN-540976) Avail: NTIS HC/MF A04

A non-adaptive predictor, a nonuniform quantizer, and a multi-level Huffman coder are incorporated into a differential pulse code modulation system for coding and decoding broadcast video signals in real time.
NASA

N91-13599# Lawrence Livermore National Lab., CA.
MPPE (MULTIPLE PULSE PROPAGATION EXPERIMENT) RESULTS
Frank W. Chambers, G. J. Caporaso, Y. P. Chong, F. J. Deadrick, G. Guethlein, W. M. Fawley, T. J. Orzechowski, V. L. Renbarger, D. Rogers, Jr., and J. T. Weir et al 1 Oct. 1990 7 p Presented at the 1990 Annual Charged Particle Beam Meeting, San Diego, CA, 11-14 Jun. 1990
(Contract W-7405-eng-48; DARPA Order 4395)
(DE91-001678; UCRL-JC-105200; CONF-9006228-4) Avail: NTIS HC/MF A02

The multiple pulse propagation experiment (MPPE) was conducted by the Beam Research Group of the Lawrence Livermore National Laboratory from September 1989, through January 1990, using the advanced test accelerator (ATA). This experiment represents the culmination of the three previous beam

propagation experiments conducted at the ATA over the past half decade. Highlights of this experiment were the multiple pulse operation of ATA, and the diagnosis of the beam propagation, and channel production at the higher repetition rates. A large database was collected on beam propagation in uniform gas and channels including m = 0 beam size and net current measurements; and m = 1 hose measurements. The generation and evolution of the electron beam driven channels was well documented. A key result of this experiment was that the beam was dominated by hose instability which limited propagation ranges. This report is organized into five sections. The experimental layout and beam parameters have been detailed in previous reports. First the beam initial conditions will be discussed in detail. Since beam injection parameters are ultimately the only variables one can specify in an atmospheric application, the control and documentation of the beam at the entrance to the gas is crucial. Next the beam lead pulse propagation in gas will be reported. Lead pulse results will be compared with past experiments. The density channel production and evolution will be briefly reported; an additional reference is available. Beam propagation in the channel will then be examined. Finally, conclusions will be presented. DOE

N91-13600# Norwegian Defence Research Establishment, Kjeller.
SAR DETECTION OF TOPOGRAPHY, VEGETATION AND INSTALLATIONS OVER LAND
Dan Johan Weydahl 21 May 1990 67 p In NORWEGIAN; ENGLISH summary
(FFI-90/7016; ISSN-0802-2437; ETN-91-98280) Avail: NTIS HC/MF A04

Detection of land features in SAR (Synthetic Aperture Radar) images is investigated. Effects caused by foreshortening, layover and shadow play an important role in high relief areas and may reduce interpretability drastically in SAR images. Other important factors are those which influence the backscatter coefficient. Slope and roughness of the terrain are in this respect especially significant concerning distributed targets. Point targets on the contrary, may largely be caused by human installations that often work like different kinds of reflectors. Classification in images can be improved by speckle reduction as well as using different texture measures together with the intensity. ESA

N91-13601 Physics and Electronics Lab. TNO, The Hague (Netherlands).
ELECTRONIC SCAN AT MILLIMETRE WAVE FREQUENCIES Final Report
J. Snieder Jun. 1990 127 p
(FEL-89-B258; TD-89-3875; ETN-91-98284) Copyright Avail: Physics and Electronics Laboratory TNO, P.O. Box 96864, 2509 JG The Hague, Netherlands

The possibilities of realizing phased array antennas in the mm wave region are reviewed. The use of discrete components and bulk material is discussed. The MMIC (Monolithic Microwave Integrated Circuits) techniques for the realization of phased array components are excluded from this report. A survey is given of the different electronic scan possibilities. PIN diode phase shifters and different types of ferrite phase shifters are discussed, including the principle functioning of these components as well as the advantages involved in their use. The availability of various ferrite materials for phase shifters is discussed. The requirements for phased array antennas and its phase shifters are given. A discussion of array element spacing, side lobe level and related power levels, effect of pulse repetition frequency and mutual coupling are presented. An attempt is made to correlate all the available information at cm wavelength (3 to 18 GHz) and to extrapolate it to mm wavelength. All the detailed properties of the phase shifters are included. The experimental results of mm wave phase shifters are given and compared with the extrapolated results given. ESA

N91-13602 Physics and Electronics Lab. TNO, The Hague (Netherlands).
MEASUREMENT RESULTS OF THE FEL-TNO PLANAR RECTANGULAR NEAR FIELD FACILITY (1978-1989) Final Report
J. G. vanHezewijk Nov. 1989 48 p
(FEL-89-B336; TD-89-4573; ETN-91-98288) Copyright Avail: Physics and Electronics Laboratory TNO, P.O. Box 96864, 2509 JG The Hague, Netherlands

Measurements performed with the rectangular planar near field facility of the Physics and Electronics Laboratory, TNO from 1978 to 1989 are described. Various types of antennas have been measured in this period. The radiation (both sum and difference) patterns of antennas with narrow main beams can be determined with great accuracy. This is true as well for antennas, which have dimensions, that are equal or slightly larger than the measurement frame of the near field scanner, or that have a broad main beam in one plane. The near field measurement facility offers the possibility to quickly detect defective radiating elements in a large array antenna. If a parameter, like the frequency of the scan-direction of the main beam, can be changed very quickly, more radiation patterns of an antenna can be determined during the time needed to perform one single near field measurement. The measurements presented give a good overview of the possibilites of the planar near field measurement technique. ESA

N91-13603 Physics and Electronics Lab. TNO, The Hague (Netherlands).
BSB RADAR PULSE CLASSIFICATION Final Report
P. P. Meiler and A. M. Wezenbeek Aug. 1990 46 p
(FEL-90-B023; TD-90-2780; ETN-91-98289) Copyright Avail: Physics and Electronics Laboratory TNO, P.O. Box 96864, 2509 JG The Hague, Netherlands

The Brain-State-in-a-Box (BSB) neural network is an auto-associative network. It is able to associate vectors with other vectors. Auto-association results in a system that has been taught to respond strongly to each input vector of a certain set of input vectors by returning this same vector multiplied its recollection strength, where vectors are bounded by the box. This gives the possibility for convergence to one vector of the taught set of vectors if the actual input vector is not known to the system. When radar signals are translated into vectors, the BSB network can be used for radar pulse classification. The whole process of classification together with its relation to other non neural algorithms is shown. ESA

N91-13604 Physics and Electronics Lab. TNO, The Hague (Netherlands).
PLANAR NEAR-FIELD MEASUREMENT OF NON-RECIPROCAL ANTENNAS Final Report
H. J. Visser Apr. 1990 18 p
(FEL-90-B092; TD-90-1227; ETN-91-98290) Copyright Avail: Physics and Electronics Laboratory TNO, P.O. Box 96864, 2509 JG The Hague, Netherlands

The transmission equation for a planar near field measurement configuration is derived for the situation in which the Antenna Under Test (AUT) is operated as a receiving antenna (usually the AUT is operated as a transmitting antenna). This transmission equation has the same form as that derived for the situation in which the AUT is acting as transmitting antenna. With this new derived equation and existing transmission equations it is possible to characterize non reciprocal antennas, provided that the probe used is completely characterized. ESA

N91-13605 Physics and Electronics Lab. TNO, The Hague (Netherlands).
COMPARISON OF SPECTRAL ESTIMATORS APPLICATION TO GROUND SENSOR SIGNALS Final Report
W. J. C. Beck Dec. 1988 80 p
(Contract A80/KL/138)
(FEL-1988-85; TD-89-0345; ETN-91-98293) Copyright Avail:

Physics and Electronics Laboratory TNO, P.O. Box 96684, 2509 JG The Hague, Netherlands

An overview of several spectrum estimation techniques with their mathematical background is presented. All methods have advantages and disadvantages, which have been summarized at the end of each chapter. The methods which fit best to one problem, depends on the nature of the signals involved and the specific application involved. Ingredients for an optimal choice of method are presented. An example of when Prony's method is applied to acoustic signals derived from moving vehicles at ranges of about 20 meters is presented. ESA

N91-13606 Physics and Electronics Lab. TNO, The Hague (Netherlands).
OBSERVATION WITH STAND-OFF RADARS Interim Report
G. P. deLoor Jun. 1990 33 p In DUTCH; ENGLISH summary
(Contract A87/KL/116)
(FEL-90-A022; TD-90-0046; ETN-91-98297) Copyright Avail: Physics and Electronics Laboratory TNO, P.O. Box 96864, 2509 JG The Hague, Netherlands

Some general aspects of the observation with stand-off radars (grazing angles under 10 deg) are discussed. The (optical) visibility (intervisiblity) of a target is not a guarantee for its actual observation since it can be hidden in its surroundings. In that case the use of clutter suppression is necessary, e.g. using a moving target indicator or a variation in the polarization. A target can also manifest itself through the clutter by changing its surroundings, e.g. by destroying the surrounding vegetation. Some problems requiring a closer study are indicated. ESA

N91-13607 Physics and Electronics Lab. TNO, The Hague (Netherlands).
FREQUENCY-DOMAIN ANALYSIS OF ONE-DIMENSIONAL ELECTROMAGNETIC SCATTERING BY LOSSY MEDIA Final Report
J. J. A. Klaasen May 1990 45 p
(Contract A86/K/012)
(FEL-90-A112; TD-90-1714; ETN-91-98300) Copyright Avail: Physics and Electronics Laboratory TNO, P.O. Box 96864, 2509 JG The Hague, Netherlands

A study performed to investigate the effect of a plane interface between two media with different electromagnetic properties, on the electromagnetic fields is described. Such an interface exists between an air/Earth or air/water boundary. The results of the study are presented. The incident field is assumed to be a uniform plane wave. The study addresses one-dimensional scattering problems. The analysis is performed in the s-domain, using the Laplace transform. Numerical results are presented for the scattering of nuclear electromagnetic pulse by the Earth's surface and the sea. ESA

N91-13608 Institute for Perception RVO-TNO, Soesterberg (Netherlands).
EVALUATION OF A SIMPLE METHOD FOR COLOR MONITOR RECALIBRATION Final Report
M. P. Lucassen and J. Walraven 8 Mar. 1990 18 p Sponsored by EEC
(Contract B89-10)
(IZF-1990-B-4; TD-90-0029; ETN-91-98316) Copyright Avail: Institute for Perception RVO-TNO, P.O. Box 23, 3769 ZG Soesterberg, Netherlands

An algorithm for recalibrating a color monitor's RGB input-output relations is evaluated. It requires only a single measurement on an appropriatly chosen reference stimulus. Three sets of data are obtained for evaluating the algorithm's error reduction power. These relate to different ways in which the monitor can get out of calibration. Slow (but cumulative) changes over time, fast changes due to gun interaction (resulting from changed stimulus conditions), and error introduced by a different setting of the monitor's brightness control are taken into consideration. The algorithm is found to be effective in dealing with instantaneous calibration changes (gun interaction, brightness control), and for keeping track of the slow changes that may finally necessitate a full recalibration of the monitor. ESA

33 ELECTRONICS AND ELECTRICAL ENGINEERING

Includes test equipment and maintainability; components, e.g., tunnel diodes and transistors; microminiaturization; and integrated circuitry.

For related information see also *60 Computer Operations and Hardware* and *76 Solid-State Physics.*

N91-13609*# Georgia Inst. of Tech., Atlanta.
A COMPLEX PERMITTIVITY AND PERMEABILITY MEASUREMENT SYSTEM FOR ELEVATED TEMPERATURES Semiannual Status Report, Jul. - Dec. 1989
Paul Friederich 4 Sep. 1990 125 p
(Grant NAG3-972)
(NASA-CR-186916; NAS 1.26:186916) Avail: NTIS HC/MF A06 CSCL 09C

The three goals of this research include: (1) to fully develop a method to measure the permittivity and permeability of special materials as a function of frequency in the range of 2.6 to 18 GHz, and of temperatures in the range of 25 to 1100 C; (2) to assist LeRC in setting up an in-house system for the measurement of high-temperature permittivity and permeability; and (3) to measure the complex permittivity and permeability of special materials as a function of frequency and temperature to demonstrate the capability of the method. The method chosen for characterizing the materials relies on perturbation of a resonant cavity with a small volume of sample material. Different field configurations in the cavity can be used to separate electric and magnetic effects. The cavity consists of a section of rectangular waveguide terminated at each end of a vertical slot iris. The center of one wall is a small hole through which the sample is introduced. Author

N91-13610# Office of Naval Research European Office, FPO New York, NY.
OVERVIEW OF EUROPEAN TECHNOLOGY IN COMPUTERS, TELECOMMUNICATIONS, AND ELECTRONICS
J. F. Blackburn May 1990 60 p
(PB90-215773; ONREUR-ESNIB-90-04) Avail: NTIS HC/MF A04 CSCL 09C

The emergence of the personal computer, the growing use of distributed systems, and the increasing demand for supercomputers and mini-supercomputers are causing a profound impact on the European computer market. An equally profound development in telecommunications is the integration of voice, data, and images in the public network systems - the Integrated Service Digital Network (ISDN). The programs being mounted in Europe to meet the challenges of these technologies are described. The Europe-wide trends and actions with respect to computers, telecommunications, and microelectronics are discussed, and the major European collaborative programs in these fields are described. Specific attention is given to the European Strategic Programme for Research and Development in Information (ESPRIT); Research in Advanced Communications for Europe (RACE); European Research Coordination Agency (Eureka) programs; Joint European Submicron Silicon Initiative (JESSI); and the recently combined programs Basic Research Industrial Technologies in Europe/European Research in Advanced Materials (BRITE/EURAM). Author

N91-13611# Military Academy, West Point, NY.
DESIGN OF INTEGRATED CMOS CIRCUITS FOR PARALLEL DETECTION AND STORAGE OF OPTICAL DATA Final Report Ph.D. Thesis
Andre Harding Sayles 13 Aug. 1990 178 p
(AD-A225702) Avail: NTIS HC/MF A09 CSCL 09/1

A CMOS circuit capable of storing optically transmitted data from a holographic read only memory (ROM) is described. The

investigation focuses on combining optical and electronic circuit technology to rapidly transfer data in parallel fashion from a ROM to an array of static random-access memory (SRAM) cells. The proposed optoelectronic SRAM cells have an optical detection component as well as electrical read and write functions. Development of the optoelectronic memory circuit is based on research in several areas. A design method is described which applies MOS inverter transfer characteristics to the six-transistor CMOS SRAM cell. Circuit diagrams, layouts, and models are presented for photodetection devices adapted to integrated CMOS circuits. These devices are fabricated in standard CMOS processes for silicon. Performance characteristics are provided for photodetection devices with different load circuits. The optical data transfer technology is extended to other systems in which high speed and parallelism are essential. An array of the optoelectronic cells and many related devices and circuits have been designed, fabricated, and tested. Simulation and experimental results are given for circuits applicable to optical detection and electronic storage of data. The optical data transfer concept has been verified with a 16-bit optoelectronic SRAM. Data contained in a parallel array of 16-bit optoelectronic SRAM. Data contained in a parallel array of 16 light beams with an average power of 3.35 microwatts per bit were successfully transferred to the SRAM. The Argon laser light pattern was formed by both a mask and a hologram. The storage of the optical information was verified by electrical addressing of each cell. This research is a fundamental component of a massively parallel optical-to-electronic data transfer system being developed. Data is to be transferred to a RAM from a page-oriented holographic ROM containing up to 10(exp 11) bits of volume-multiplexed data. GRA

N91-13612# California Univ., Davis. Dept. of Electrical Engineering and Computer Science.
OPTICAL SHARED MEMORY SYSTEM DEMONSTRATION MODEL Final Technical Report, Jun. - Nov. 1989
Stephen T. Kowel, N. Matloff, C. Eldering, P. Brinkley, T. Schubert, M. Landgraf, and R. Gosula Jul. 1990 42 p
(Contract F30602-88-D-0026; AF Proj. 5581)
(AD-A226431; RADC-TR-90-137) Avail: NTIS HC/MF A03
CSCL 09/5

This report discusses work performed on developing a system in which it is possible to optically read a VLSI memory into another VLSI device. Work was concentrated in the areas of: liquid crystal imaging of horizontal fields in integrated circuits, thin solid film integrated circuit structures for modulating light, simulation of system performance for a number of optically interconnect architectures, and construction of a working demonstration prototype. The construction of a prototype demonstrated that its possible to image a memory device using the horizontal fields above the integrated circuit. The liquid crystal approach and the thin solid film approach offer possibilities for the construction of a Single Transmitter Multiple Receiver (STMR) System and a Single Transmitter Single Receiver (STSR) System. Both systems offer advantages over electrically interconnect systems and in certain cases will provide a large speedup in computation. Appendices include the following topics: fixed optical interconnects for concurrent computing systems; electro-optic polymer materials and devices for global optical interconnects; high resolution imaging of a VLSI memory device using horizontal field modulated nematic liquid crystals. GRA

N91-13613# California Univ., Berkeley.
TIME DOMAIN FINITE DIFFERENCE ANALYSIS OF ANTENNAS Interim Report, Jun. 1988 - May 1989
Kenneth K. Mei Jul. 1990 51 p
(Contract F19628-88-K-0025)
(AD-A226534; RADC-TR-90-139) Avail: NTIS HC/MF A04
CSCL 09/1

The microstrip antenna is studied as an intermediate step to the development of a broadband type flare antenna, because the microstrip antennas have been well investigated so there are plenty of results available to check the time domain technique. In fact, the microstrip antennas have many advantages of their own, such as, lightweight, low profile, low fabrication costs, and ease for mass production. Despite their obvious disadvantages of narrow bandwidth and low power capacity, the microstrip antennas have found many areas of applications. GRA

N91-13614# Syracuse Univ., NY.
MAGNETIC FIELD EFFECT TRANSISTORS Final Technical Report, Feb. 1989 - Feb. 1990
Peter A. Dowben and James T. Spencer Jul. 1990 14 p
(Contract F30602-88-D-0027)
(AD-A226535; RADC-TR-90-158) Avail: NTIS HC/MF A03
CSCL 09/1

It was demonstrated that magnetic CrO2 can be selectively deposited on semiconductor substrates and polymide resin plastics with feature resolution smaller than micron. In addition, hard coatings were fabricated to protect active devices as well as developed new techniques for fabricating conventional devices such as p-n junctions, from organometallic and main group complexes. GRA

N91-13615# Consiglio Nazionale delle Ricerche, Frascati (Italy). Ist. di Fisica dello Spazio Interplanetario.
FUNDS REQUEST FOR 1990. THE CRYOGENIC GRAVITATIONAL ANTENNA (T = 2.0 K) ALTAIR [RICHIESTA DI FINANZIAMENTO PER IL 1990. ANTENNA GRAVITAZIONALE CRIOGENICA (T = 2.0 K) ALTAIR]
Feb. 1990 18 p In ITALIAN
(IFSI-90-2; ETN-90-97785) Avail: NTIS HC/MF A03

The cryostat for the resonant gravitational antenna ALTAIR (Advanced Low Temperature Antenna for Italian Research) is designed for temperatures of 2 K, obtained using superfluid helium. The cryogenic installation is described and design drawings are included. The listing and justification of 1990 funds extension request is presented. ESA

N91-13616# Consiglio Nazionale delle Ricerche, Frascati (Italy). Ist. di Fisica dello Spazio Interplanetario.
CRYOSTAT FOR THE GRAVITATIONAL ANTENNA ALTAIR [CRIOSTATO DELL'ANTENNA GRAVITAZIONALE ALTAIR]
P. Bonifazi, M. G. Castellano, M. Maiani, G. Martinelli, F. Tabacchioni, and M. Visco Feb. 1990 55 p In ITALIAN
(IFSI-90-3; ETN-90-97786) Avail: NTIS HC/MF A04

The cryostat for the resonant gravitational antenna ALTAIR (Advanced Low Temperature Antenna for Italian Research) is designed for temperatures less than 100 mK, obtained using a dilution technique with He3-He4 fluid. The cryogenic installation is described and design drawings are included. ESA

N91-13617# Sandia National Labs., Albuquerque, NM.
DYNAMIC HIGH-PRESSURE STUDIES OF AN ELECTROTHERMAL CAPILLARY
D. A. Benson and P. A. Cahill 1990 10 p Presented at the 27th JANNAF Combustion Meeting, Cheyenne, WY, 5-9 Nov. 1990
(Contract DE-AC04-76DP-00789)
(DE91-000966; SAND-90-2494C; CONF-9011119-1-Draft) Avail: NTIS HC/MF A02

This paper describes arc discharge tests conducted in a prepressurized, constant-volume pressure vessel to study arc behavior over a wide range of current densities, discharge durations, and initial vessel pressures. This method allows controlled access to a wider range of conditions than those previously studied in capillary tests. We have investigated aspects of the radiative heat transfer by calculating the material opacity and mean free paths of photons for conditions typical of arc diagnostics. We also performed one-dimensional Eulerian hydrodynamic calculations of the boundary layer behavior in the radiative diffusion approximation. These calculations, which describe the radial mass flow and heat transfer in the absence of turbulent flow effects, show the characteristic times for equilibrium of the high-pressure arc. Finally, we describe progress on a promising means for increasing the mass flux from the capillary

discharge through the use of chemically reactive media on the capillary walls. DOE

N91-13618# Oak Ridge National Lab., TN.
RADIATION EFFECTS ON JFETs (JUNCTION FIELD-EFFECT TRANSISTORS), MOSFETs, AND DIPOLAR TRANSISTORS, AS RELATED TO SSC CIRCUIT DESIGN
E. J. Kennedy, G. T. Alley, C. L. Britton, Jr., P. L. Skubic, B. Gray, and A. Wu (Tennessee Univ., Knoxville.) 1990 7 p Presented at the Symposium on Detector Research and Development for the Superconducting Super Collider, Fort Worth, TX, 15-18 Oct. 1990
(Contract DE-AC05-84OR-21400)
(DE91-001486; CONF-9010212-3) Avail: NTIS HC/MF A02

Some results of radiation effects on selected junction field-effect transistors, MOS field-effect transistors, and bipolar junction transistors are presented. The evaluations include dc parameters, as well as capacitive variations and noise evaluations. The tests are made at the low current and voltage levels (in particular, at currents less or equal to 1 mA) that are essential for the low-power regimes required by SSC circuitry. Detailed noise data are presented both before and after 5-Mrad (gamma) total-dose exposure. SPICE radiation models for three high-frequency bipolar processes are compared for a typical charge-sensitive preamplifier. DOE

N91-13619# Lawrence Livermore National Lab., CA.
RELATIVISTIC KYLSTRON SIMULATIONS USING RKTW2D
Robert D. Ryne and Simon S. Yu 19 Sep. 1990 5 p Presented at the Linear Accelerator Conference, Albuquerque, NM, 10-14 Sep. 1990 Submitted for publication
(Contract W-7405-eng-48)
(DE91-001747; UCRL-JC-103798; CONF-9009123-40) Avail: NTIS HC/MF A01

We are developing a two-dimensional, time-dependent computer code for the simulation of relativistic klystrons. We will discuss the main features of our code. We will also present an example simulation of a relativistic klystron with both a standing wave output cavity and a traveling wave output structure. DOE

N91-13620# Los Alamos National Lab., NM.
SEMI-CUSTOM INTEGRATED CIRCUIT AMPLIFIER AND LEVEL DISCRIMINATOR FOR NUCLEAR AND SPACE INSTRUMENTS
Sangkoo F. Hahn and Maureen M. Cafferty 1990 7 p Presented at the 1990 IEEE Nuclear Science Symposium, Arlington, VA, 23-27 Oct. 1990 Submitted for publication
(Contract W-7405-eng-36)
(DE91-001951; LA-UR-90-3576; CONF-9010220-2) Avail: NTIS HC/MF A02

An extra fast current feedback amplifier and a level discriminator are developed employing a dielectrically-isolated bipolar, semi-custom application specific integrated circuit (ASIC) process. These devices are specifically designed for instruments aboard spacecrafts or in portable packages requiring low power and weight. The amplifier adopts current feedback for a unity-gain bandwidth of 90 MHz while consuming 50 mW. The level discriminator uses a complementary output driver for balanced positive and negative response times. The power consumption of these devices can be programmed by external resistors for optimal speed and power trade-off. DOE

N91-13621*# National Aeronautics and Space Administration. Pasadena Office, CA.
SECONDARY Li BATTERY INCORPORATING 12-CROWN-4 ETHER Patent Application
Ganesan Nagasubramanian, inventor (to NASA) and Salvador DiStefano, inventor (to NASA) (Jet Propulsion Lab., California Inst. of Tech., Pasadena.) 11 Oct. 1990 16 p
(Contract NAS7-918)
(NASA-Case-NPO-17922-1-CU; NAS 1.71:NPO-17922-1-CU; US-Patent-Appl-SN-596139) Avail: NTIS HC/MF A03 CSCL 09A

A rechargeable lithium battery which utilizes a polyethylene oxide (PEO) solid polymeric electrolyte complexed with a lithium salt is disclosed. The conductivity is increased an order of magnitude and interfacial charge transfer resistance is substantially decreased by incorporating a minor amount of 12-Crown-4 ether in the PEO-lithium salt solid electrolyte film. Batteries containing the improved electrolyte permit operation at a lower temperature with improved efficiency. NASA

N91-13622*# National Aeronautics and Space Administration. Pasadena Office, CA.
DETECTION OF MULTIPLE-BIT ERRORS FROM SINGLE-ION TRACKS IN INTEGRATED CIRCUITS Patent Application
John A. Zoutendyk, inventor (to NASA) (Jet Propulsion Lab., California Inst. of Tech., Pasadena.) 23 Jul. 1990 17 p
(Contract NAS7-918)
(NASA-Case-NPO-18075-1-CU; NAS 1.71:NPO-18075-1-CU; US-Patent-Appl-SN-555865) Avail: NTIS HC/MF A03 CSCL 09C

A error detector and imaging system for multiple-bit errors from single-ion tracks in integrated circuits distinguishes between multiple bit errors caused by ion tracks which do not strike charge collection junctions having substantial capacitance and those that do on the basis of the sensitivity of the errors to changes in VDD. Data which do not occur during the time interval between successive read cycles, which do not occur at integral multiples of the read clock, whose recorded time tags are not greater than those of previous data or whose recorded address tags are not greater than those of previous data are discarded as bad data before further processing and display. NASA

N91-13623# Lawrence Livermore National Lab., CA.
COMPUTATIONAL AND EXPERIMENTAL PROGRESS ON LASER-ACTIVATED GAS AVALANCHE SWITCHES FOR BROADBAND, HIGH-POWER ELECTROMAGNETIC PULSE GENERATION
David J. Mayhall, Jick H. Yee, and Francesco Villa (Stanford Linear Accelerator Center, CA.) Sep. 1990 14 p Presented at the 1990 SPIE Symposium on Advances in Intelligent Systems, Boston, MA, 5-6 Nov. 1990 Submitted for publication
(Contract W-7405-eng-48)
(DE91-001763; UCRL-JC-103502; CONF-9011115-2) Avail: NTIS HC/MF A03

The gas avalanche switch, a high-voltage, picosecond-speed switch, has been proposed. The basic switch consists of pulse-charged electrodes, immersed in a high-pressure (7 to 800 atm) gas. An avalanche discharge is induced in the gas between the electrodes by ionization from a picosecond-scale laser pulse. The avalanching electrons move toward the anode, causing the applied voltage to collapse in picoseconds. This voltage collapse, if rapid enough, generates electromagnetic waves. A two-dimensional (2-D), finite difference computer code solves Maxwell's equations for transverse magnetic modes for rectilinear electrodes between parallel plate conductors, along with electron conservation equations for continuity, momentum, and energy. Collision frequencies for ionization and momentum and energy transfer to neutral molecules are assumed to scale linearly with neutral pressure. Electrode charging and laser-driven electron deposition are assumed to be instantaneous. Code calculations are done for a pulse generator geometry, consisting of an 0.7 mm wide by 0.8 mm high, beveled, rectangular center electrode between grounded parallel plates at 2 mm spacing in air. DOE

N91-13624# Los Alamos National Lab., NM.
COMPUTATION OF THE CURRENT DENSITY IN NONLINEAR MATERIALS SUBJECTED TO LARGE CURRENT PULSES
M. L. Hodgdon, R. S. Hixson, and W. M. Parsons 1990 4 p Presented at the 4th Biennial IEEE Conference on Electromagnetic Field Computation, Toronto, Ontario, 22-24 Oct. 1990
(Contract W-7405-eng-36)
(DE91-001950; LA-UR-90-3568; CONF-9010105-1) Avail: NTIS HC/MF A01

The finite element method and the finite difference method

are used to calculate the current distribution in two nonlinear conductors. The first conductor is a small ferromagnetic wire subjected to a current pulse that rises to 10,000 Amperes in 10 microseconds. Results from the transient thermal and transient magnetic solvers of the finite element code FLUX2D are used to compute the current density in the wire. The second conductor is a metal oxide varistor. Maxwell's equations, Ohm's law and the varistor relation for the resistivity and the current density of rho = alpha x j(exp -beta) are used to derive a nonlinear differential equation. The solutions of the differential equation are obtained by a finite difference approximation and a shooting method. The behavior predicted by these calculations is in agreement with experiments. DOE

N91-13625# Sandia National Labs., Albuquerque, NM.
SINGLE EVENT UPSET HARDENING TECHNIQUES
H. T. Weaver and W. T. Corbett 1990 5 p Presented at the American Nuclear Society Winter Meeting, Washington, DC, 11-15 Nov. 1990
(Contract DE-AC04-76DP-00789)
(DE91-002337; SAND-90-1725C; CONF-901101-43) Avail: NTIS HC/MF A01

Integrated circuit logic states are maintained by virtue of specific transistor combinations being either on (conducting) or off (nonconducting). High energy ion strikes on the microcircuit generate photocurrents whose primary detrimental effect is to make off transistors appear on, confusing the logic state and leading to single event upset (SEU). Protection against these soft errors is accomplished using either technology or circuit techniques, actions that generally impact yield and performance relative to unhardened circuits. We describe, and using circuit simulations analyze, a technique for hardening latches which requires combinations of technology and circuit modifications, but which provides SEU immunity without loss of speed. Specifically, a single logic state is hardened against SEU using technology methods and the information concerning valid states is then used to simplify hardened circuit design. The technique emphasizes some basic hardening concepts, ideas for which will be reviewed. DOE

N91-13626# Los Alamos National Lab., NM.
DUAL KLYSTRON MODULATOR
W. Joel D. Johnson and William E. Stein 1990 4 p Presented at the Linear Accelerator Conference, Albuquerque, NM, 10-14 Sep. 1990
(Contract W-7405-eng-36)
(DE91-002348; LA-UR-90-3440; CONF-9009123-47) Avail: NTIS HC/MF A01

The first phase of a 40 MeV upgrade at the Los Alamos Free-Electron Laser (FEL) experimental hall was completed during the summer of 1989. The second phase of this upgrade will be completed in November 1990. Because it was necessary to conserve facility space and expense, the concept of a dual klystron modulator was conceived. The novelty of this design is that a single switch tube and a single high voltage electronic circuit are used to simultaneously pulse two modulating-anode klystrons. In addition, this design configuration is amenable to extending the number of klystrons that are to be concurrently pulsed. In this short paper we report on this modulator design. DOE

N91-13627# Technische Hochschule, Darmstadt (Germany, F.R.).
THEORY AND PROCEDURE OF THE HIERARCHICAL DESIGN RULE CHECKING OF INTEGRATED CIRCUITS Ph.D. Thesis [THEORIE UND VERFAHREN DER HIERARCHISCHEN DESIGNREGELPRUEFUNG INTEGRIERTER SCHALTUNGEN]
Clemens Federschmidt 1989 130 p In GERMAN
(ETN-91-98173) Avail: NTIS HC/MF A07

A method for the hierarchical design rule checking, suitable for all layout design was developed with a view to Very Large Scale Integration (VLSI). A typical design of an integrated circuit, and the principle of the hierarchical design method are presented. A new method called HDRCV (Hierarchical Design Rule Checker of VLSI circuits) was developed; its properties are outlined. The definitions for the iteration checking of the single basic operations were deduced, and algorithms were developed. These algorithms were implemented and tested. The advantages of HDRCV as compared to other methods are discussed. ESA

N91-13628# Laboratoire d'Automatique et d'Analyse des Systemes, Toulouse (France). Composants Bipolaires.
EVALUATION AND FABRICATION OF GaAs INTEGRATED LOGIC CIRCUITS Ph.D. Thesis - Toulouse Univ.
Jean-Paul Vannel 1990 156 p In FRENCH; ENGLISH summary
(LAAS-90160; ETN-91-98214) Avail: NTIS HC/MF A08

The working principles and the state of art of integrated injection logic circuits are reviewed. A fine modeling allows to evaluate the potential performances and the optimization criteria for this family, based on GaAlAs/GaAs double heterojunction bipolar transistors. The fabrication sequences for the integrated injection logic circuits are described. Emphasis is given to the molecular beam epitaxy and the ion implantation. The high maximum current gains, measured for the elementary transistors in forward and reverse operations (250 and 400 respectively) and the effective gains measured in the four collector gates (between 16 and 4 according to the collector rank), simultaneously testify to the possibilities brought by the double heterojunction structure concerning the fan out and the noise immunity. The performances of this technology enhanced from the seven stage ring oscillator response, give a minimum propagation delay time about one nanosecond and a 1 pJ power delay product for a 20 micrometer design rule. Both agree with theoretical previsions. ESA

N91-13629# Laboratoire d'Automatique et d'Analyse des Systemes, Toulouse (France). Groupe Circuits et Composants a Effet de Champ.
DESIGN OF HIGH VOLTAGE PLANAR DEVICES USING SIPOS TECHNOLOGY Ph.D. Thesis - Inst. National des Sciences Appliquees de Toulouse
Denis Jaume 1990 153 p In FRENCH; ENGLISH summary
(LAAS-90237; ETN-91-98216) Avail: NTIS HC/MF A08

The use of a semi-insulating polycrystalline silicon (SIPOS) layer, in passive high voltage planar devices is discussed. The SIPOS characteristics are recalled and its effects, as well as the guard technique, are presented. The voltage capability of planar transistors in SIPOS technology is studied and design rules, to obtain breakdowm voltages in the range of 1000 and 1500 V, are established as a function of physical and geometrical parameters. This study is accomplished with the help of two dimensional numerical simulations. Test devices are realized by using low pressure chemical vapor deposition SIPOS planar technology with a multilayer passivation and a good agreement between numerical and experimental results is obtained. ESA

N91-13630# Ecole Centrale de Lyon (France).
INVESTIGATION AND DEVELOPMENT OF ISFET TYPE CHEMICAL SENSORS, SENSITIZED BY DIELECTRIC TYING Ph.D. Thesis [ETUDE ET MISE AU POINT DE CAPTEURS CHIMIQUES DE TYPE ISFET SENSIBILISES PAR GREFFAGE DU DIELECTRIQUE]
Hubert Perrot 1990 140 p In FRENCH Sponsored by the Region Rhone-Alps, France and Fondation Scientifique de Lyon et du Sud-Est
(ECL-90-18; ETN-91-98340) Avail: NTIS HC/MF A07

Ion Sensitive Field Effect Transistor (ISFET) general principles are presented including operational mode, mechanism parametrization, and membrane selection. The different characterization methods used (electrical, optoelectrochemical, optical and spectroscopic methods) are given. The development of various types of photosensitive layers is examined. The interface between the modified insulator/electrolyte is investigated, in order to explain the process involved, and to attain a better photosensitive layer characterization. Results obtained using these photosensitive layers are stated. Results are compared to those published by other laboratories. A possible swap of the insulating material used, for example silicon, for other materials is examined. ESA

N91-13631# Los Alamos National Lab., NM.
SMALL SIGNAL GAIN BASED ON ANALYTIC MODELS OF THIN INTENSE ELECTRON BEAMS
C. James Elliott, Brian D. McVey, and Mark Schmitt 1990 12 p Presented at the 12th International Free Electron Laser Conference, Paris, France, 17-21 Sep. 1990
(Contract W-7405-eng-36)
(DE91-001874; LA-UR-90-3595; CONF-9009166-9) Avail: NTIS HC/MF A03

The free-electron laser theory of the effective energy distribution and the small signal gain for a thin electron beam was developed. The assumption of thinness allows us to treat various transverse locations and electron beam trajectory angles as introducing phase shifts that have the same effect as those introduced by a change in energy of the electron. We have extended these ideas in five important ways. The first is the ability to treat electron beams with three different classes of matching or symmetry conditions: (1) electron beams with separate betatron matching in each plane; (2) those with aspect ratio matching; and (3) crossed matched beams. Manifestations of these symmetries include elliptical cross sections and electron beams that have modulated spatial profiles. Second, two emittance parameters for the electron beam are shown to consolidate into a single parameter that describes most of the energy variation of the effective energy distributions. Third, these calculations extend to energy distributions, angular distributions, and spatial distributions that all follow Gaussian profiles. Fourth, this model incorporates the description of the incident Gaussian optical beam and the above electron beam dynamics into a single influence function kernal. Fifth, three-dimensional profiles of the optical fields are computed. In this work the parameters of the incident optical beam are included. The resulting transverse dependence of the fields may be characterized by an optical beam radius. This optical beam width starts out large compared to the thin electron beam and then, in the example given, contracts to a size that becomes so small that the thin beam assumption is violated. DOE

N91-13632 Physics and Electronics Lab. TNO, The Hague (Netherlands).
GaAs MMIC MIXER FOR 8-12 GHz, BASED ON 0.5 MICROMETER GATE LENGTH D-MESFETS. VOLUME 1: DESIGN AND LAYOUT Final Report
T. C. Tieman and R. Grooters Jan. 1990 68 p Original contains color illustrations
(FEL-89-B277-Vol-1; TD-89-3879-Vol-1; ETN-91-98285)
Copyright Avail: Physics and Electronics Laboratory TNO, P.O. Box 96864, 2509 JG The Hague, Netherlands

A description is given of the design of an 8 to 12 GHz GaAs MMIC (Monolithic Microwave Integrated Circuit) mixer. The mixer consists of a dual FET (Field Effect Transistor) mixing element, active input and output matching and bias networks. The mixer is designed with the TriQuint HA process, which uses 0.5 micrometer gate length depletion mode MESFET devices. The design goals are a return loss better than -15 dB for the inputs and output and a conversion gain better than 0 dB. The complete circuit is biased with a symmetrical power supply of plus or minus 5 volts and has autobiasing through on chip bias networks. The total power consumption of the circuit is 350 mW. The dimensions of the chip are 1.4 by 1.4 mm. This report is of part one of two reports and gives an in depth description of the circuit design. Simulation results and chip layout are provided. A second report gives the measurements results and an evaluation of the results. ESA

N91-13633 Physics and Electronics Lab. TNO, The Hague (Netherlands).
DESIGN OF AN X-BAND PIN DIODE PHASE SHIFTER BY COMPUTER OPTIMIZATION Final Report
F. J. Klumpers Dec. 1989 66 p
(FEL-89-B286; TD-89-3869; ETN-91-98286) Copyright Avail: Physics and Electronics Laboratory TNO, P.O. Box 96864, 2509 JG The Hague, Netherlands

The design and experimental results of a four bit microstrip diode phase shifter in the frequency band of 9.0 to 10.0 GHz are presented. The phase shifter is built on an alumina substrate and the desired differential phase shift is reached by switching transmission lines by PIN diodes. The layout of the circuits is designed for minimum physical dimensions. Three circuits are made with good results. The circuit containing the 22.5 and 45 degree bits, gives an insertion loss of 0.75 dB and a maximum phase deviation of less than 3.5 degrees. The circuit containing the 90 and 180 degree bits, gives an insertion loss of 1.3 dB. The average phase shift of the 90 degree bit is not optimal (98 degrees) but the phase deviation in regard to the average phase shift is less than 1.7 degrees. The 180 degree bits gives a phase deviation of less than 4.5 degree. The four bit phase shifter shows good results for both insertion loss and differential phase shift, but has serious problems with input impedance match. ESA

N91-13634 Physics and Electronics Lab. TNO, The Hague (Netherlands).
FEASIBILITY TO STUDY OF A NON-RECIPROCAL LATCHED FERRITE PHASE SHIFTER IN THE 92-96 GHz BAND Final Report
F. A. Nennie Apr. 1990 17 p Original contains color illustrations
(FEL-90-B114; TD-90-1230; ETN-91-98291) Copyright Avail: Physics and Electronics Laboratory TNO, P.OO. Box 96864, 2509 JG The Hague, Netherlands

A non reciprocal latched lithium ferrite phase shifter developed at 92 to 96 GHz is described. A cylindrical lithium ferrite rod with a diameter of 1.27 mm and an axial hole of 0.25 mm is placed in the middle of a standard waveguide. Because of mechanical uncertainties a ferrite length of 10.0 mm is chosen. The average saturation differential phase shift at 92 to 96 GHz is 92.5 degrees. Over a 4 GHz frequency band the saturation differential phase shift is almost independent of frequency. The insertion loss of 1.5 to 2.5 dB can be improved. The rise time of the 90 percent saturation pulse is 100 nsec, the pulse length is 650 nsec and the fall time is 950 nsec. ESA

N91-13635 Physics and Electronics Lab. TNO, The Hague (Netherlands).
A DESIGN METHOD FOR AN X-BAND DIPLEXER Final Report
R. Overduin, J. C. Henkus, and P. J. Koomen Jun. 1990 50 p
(FEL-90-B176; TD-90-1726; ETN-91-98292) Copyright Avail: Physics and Electronics Laboratory TNO, P.O. Box 96864, 2509 JG The Hague, Netherlands

A detailed overview of a sequential method for the design of a passive X-band diplexer is presented. The method can be used to support future design activities in a similar field. Design steps and difficulties for diplexer design are dealt with in case only the computer program TOUCHSTONE is used. Predicted and measured performance of a realized diplexer are given. An overview of FORTRAN 77 programs is included. This software can be used for separate synthesis of low and highpass microstrip filters. ESA

N91-13636 Physics and Electronics Lab. TNO, The Hague (Netherlands).
TEST PROCEDURE FREQUENCY MULTIPLIER 583R936H03/H04 Final Report
G. J. M. Kemna and J. P. vanBezouwen Jul. 1990 51 p Original contains color illustrations
(Contract A88/KLu/631)
(FEL-90-A089; TD-90-1229; ETN-91-98299) Copyright Avail: Physics and Electronics Laboratory TNO, P.O. Box 96864, 2509 JG The Hague, Netherlands

A test and repair procedure to enable a frequency multiplier to be taken into service is described. The frequency multiplier is part of the low power radio frequency unit in the AM/APG-66 radar system of the F-16 fighter. The frequency multiplier systems design is described. By carrying out the described tests in the indicated sequence (i.e. the test procedure), the proper functioning of the device is thoroughly checked. ESA

N91-14040# TRW, Inc., Redondo Beach, CA. Space and Technology Group.
ANALOG SUPERCONDUCTIVE ELECTRONICS FOR AVIONICS
A. H. Silver and A. D. Smith *In* AGARD, Applications of Superconductivity to Avionics Oct. 1990 5 p (For primary document see N91-14030 05-76)
Copyright Avail: NTIS HC/MF A08; Non-NATO Nationals requests available only from AGARD/Scientific Publications Executive

N91-14041# Air Force Materials Lab., Wright-Patterson AFB, OH.
FABRICATION AND CHARACTERIZATION OF HIGH TEMPERATURE SUPERCONDUCTING THIN FILMS FOR SENSORS AND ELECTRONICS
P. M. Hemenger, T. L. Peterson, R. Fletcher, I. Maartense, P. T. Murray, and D. W. Chung (San Jose State Univ., CA.) *In* AGARD, Applications of Superconductivity to Avionics Oct. 1990 8 p (For primary document see N91-14030 05-76)
(Contract F33615-88-C-5423)
Copyright Avail: NTIS HC/MF A08; Non-NATO Nationals requests available only from AGARD/Scientific Publications Executive

N91-14044# Thomson SINTRA ASM (France).
SQUIDs DEVICES MADE FROM HIGH Tc SUPERCONDUCTORS: RESULTS AND PERSPECTIVES
Ronan Stephan *In* AGARD, Applications of Superconductivity to Avionics Oct. 1990 8 p (For primary document see N91-14030 05-76)
Copyright Avail: NTIS HC/MF A08; Non-NATO Nationals requests available only from AGARD/Scientific Publications Executive

N91-14046# American Superconductor Corp., Watertown, MA.
OXIDE SUPERCONDUCTOR COILS: PRESENT SUCCESSES, FUTURE CHALLENGES
Carl J. Russo *In* AGARD, Applications of Superconductivity to Avionics Oct. 1990 5 p (For primary document see N91-14030 05-76)
Copyright Avail: NTIS HC/MF A08; Non-NATO Nationals requests available only from AGARD/Scientific Publications Executive

34 FLUID MECHANICS AND HEAT TRANSFER

Includes boundary layers; hydrodynamics; fluidics; mass transfer; and ablation cooling.

For related information see also *02 Aerodynamics* and *77 Thermodynamics and Statistical Physics.*

N91-13637*# National Aeronautics and Space Administration. Langley Research Center, Hampton, VA.
COMPUTATIONAL FLUID DYNAMICS
1990 42 p Original contains color illustrations
(NASA-TM-101197; NAS 1.15:101197) Avail: NTIS HC/MF A03; 33 functional color pages CSCL 20D

An overview of recent activities at NASA Langley Research Center in the area of Computational Fluid Dynamics (CFD) is presented. The following subject topics are discussed: CFD, supercomputers, algorithm research, grid generation, transition and turbulence, and rarefied CFD. Y.S.

N91-13638*# National Aeronautics and Space Administration. Lewis Research Center, Cleveland, OH.
COMMENT ON LOCAL ENERGY TRANSFER AND NONLOCAL INTERACTIONS IN HOMOGENEOUS, ISOTROPIC TURBULENCE (PHYS. FLUIDS A2, 413 (1990))
Robert G. Deissler Aug. 1990 7 p
(NASA-TM-103263; E-5696; NAS 1.15:103263) Avail: NTIS HC/MF A02 CSCL 20D

It is argued that the low-Reynolds number results in the subject paper are not congruous with the data of Ling and Huang, and that the spectral transfer should be less local. Author

N91-13639*# MCAT Inst., San Jose, CA.
DEVELOPMENT OF A TIME-DEPENDENT INCOMPRESSIBLE NAVIER-STOKES SOLVER BASED ON A FRACTIONAL-STEP METHOD Final Report, 1 Oct. 1988 - 15 Feb. 1990
Moshe Rosenfeld Sep. 1990 11 p
(Contract NCC2-562)
(NASA-CR-182323; NAS 1.26:182323; MCAT-90-001) Avail: NTIS HC/MF A03 CSCL 20D

The main goals are the development, validation, and application of a fractional step solution method of the time-dependent incompressible Navier-Stokes equations in generalized coordinate systems. A solution method that combines a finite volume discretization with a novel choice of the dependent variables and a fractional step splitting to obtain accurate solutions in arbitrary geometries is extended to include more general situations, including cases with moving grids. The numerical techniques are enhanced to gain efficiency and generality. Y.S.

N91-13640*# Pennsylvania State Univ., University Park. Dept. of Aerospace Engineering.
REYNOLDS STRESS CLOSURE IN JET FLOWS USING WAVE MODELS Final Report
Philip J. Morris Sep. 1990 211 p
(Grant NAG1-657)
(NASA-CR-185717; NAS 1.26:185717) Avail: NTIS HC/MF A10 CSCL 20D

A collection of papers is presented. The outline of this report is as follows. Chapter three contains a description of a weakly nonlinear turbulence model that was developed. An essential part of the application of such a closure scheme to general geometry jets is the solution of the local hydrodynamic stability equation for a given jet cross-section. Chapter four describes the conformal mapping schemes used to map such geometries onto a simple computational domain. Chapter five describes a solution of a stability problem for circular, elliptic, and rectangular geometries. In chapter six linear models for the shock shell structure in non-circular jets is given. The appendices contain reprints of papers also published during this study including the following topics: (1) instability of elliptic jets; (2) a technique for predicting the shock cell structure in non-circular jets using a vortex sheet model; and (3) the resonant interaction between twin supersonic jets. Author

N91-13641 Iowa Univ., Iowa City.
NONLINEAR VISCOUS WAVES PRODUCED BY AN IMPULSIVELY MOVING PLATE Ph.D. Thesis
Shih-An Yang 1989 147 p
Avail: Univ. Microfilms Order No. DA9019988

The free-surface flow generated by an impulsively accelerating, surface-piercing, vertical plate was studied numerically as well as experimentally. The two-dimensional, unsteady Navier-Stokes equations are discretized using the finite-analytic scheme which incorporates the analytic solution into the locally linearized differential equations. The continuity equation and the dynamic boundary conditions on normal and tangential stresses at the free surface are applied to determine the pressure and two velocity components at the free surface. The kinematic boundary condition on the free surface provides the movement of the free surface. A series of experiments is carried out in an open channel with a constant water depth. The flat vertical plate is fixed on a towing carriage which is set off by suddenly dropping a weight bucket through a connecting steel cable in a pulley system. The free-surface profile ahead of the plate and the pressure distribution on the plate surface are measured. The flow field around the moving contact line is studied by applying the present numerical code. The contact angle between the free surface and the vertical plate is found to be very close to that formed by the free surface of a fluid contained in a rectangular tank which moves with the same constant acceleration. The velocity of the moving contact line is thereby derived as a function of the acceleration of the plate based on the principle of the conservation of mass. The

propagation of waves produced by a moving plate along the channel is also investigated numerically. The propagation speed of generated waves is close to that of shallow-water waves with small amplitudes. An empirical formula for the ultimate maximum wave amplitude is obtained as a function of the displacement and the acceleration of the plate. Dissert. Abstr.

N91-13642*# Institute for Computer Applications in Science and Engineering, Hampton, VA.
THE ROUTE TO CHAOS FOR THE KURAMOTO-SIVASHINSKY EQUATION Final Report
Demetrios T. Papageorgiou and Yiorgos Smyrlis, (California Univ., Los Angeles.) Oct. 1990 57 p Submitted for publication
(Contracts NAS1-18605; N00014-86-K-0691)
(NASA-CR-187461; NAS 1.26:187461; ICASE-90-78) Avail: NTIS HC/MF A04 CSCL 20D

The results of extensive numerical experiments of the spatially periodic initial value problem for the Kuramoto-Sivashinsky equation. This paper is concerned with the asymptotic nonlinear dynamics at the dissipation parameter decreases and spatio-temporal chaos sets in. To this end the initial condition is taken to be the same for all numerical experiments (a single sine wave is used) and the large time evolution of the system is followed numerically. Numerous computations were performed to establish the existence of windows, in parameter space, in which the solution has the following characteristics as the viscosity is decreased: a steady fully modal attractor to a steady bimodal attractor to another steady fully modal attractor to a steady trimodal attractor to a periodic attractor, to another steady fully modal attractor, to another periodic attractor, to a steady tetramodal attractor, to another periodic attractor having a full sequence of period-doublings (in parameter space) to chaos. Numerous solutions are presented which provide conclusive evidence of the period-doubling cascades which precede chaos for this infinite-dimensional dynamical system. These results permit a computation of the length of subwindows which in turn provide an estimate for their successive ratios as the cascade develops. A calculation based on the numerical results is also presented to show that the period doubling sequences found here for the Kuramoto-Sivashinsky equation, are in complete agreement with Feigenbaum's universal constant of 4,669201609.... Some preliminary work shows several other windows following the first chaotic one including periodic, chaotic, and a steady octamodal window; however, the windows shrink significantly in size to enable concrete quantitative conclusions to be made.
Author

N91-13643 Minnesota Univ., Minneapolis.
FREE-STREAM TURBULENCE AND CONCAVE CURVATURE EFFECTS ON HEATED, TRANSITIONAL BOUNDARY LAYERS, VOLUMES 1 AND 2 Ph.D. Thesis
Jungho Kim 1990 465 p
Avail: Univ. Microfilms Order No. DA9027345

The transition process on flat-plate and concave curved-wall boundary layers was investigated for various free-stream turbulence levels was performed. Where possible, sampling according to the intermittency function was made. Such sampling allowed segregation of the signal into two types of behavior, laminar-like and turbulent-like. Results show that for transition on a flat-plate, the two forms of boundary layer behavior, identified as laminar-like and turbulent-like, cannot be thought of as separate Blasius and fully-turbulent profiles, respectively. Thus, simple transition models in which the desired quantity is assumed to be an average, weighted on intermittency, of the theoretical laminar and fully turbulent values is not expected to be successful. Deviation of the flow identified as laminar-like from theoretical laminar behavior is shown to be due to recovery after the passage of a turbulent spot, while deviation of the flow identified as turbulent-like from the fully turbulent values is thought to be due to incomplete establishment of the fully turbulent power spectral distribution. For the curved-wall case with low free-stream turbulence intensity, the existence of Goertler vortices on the concave wall within both laminar and turbulent flows was established using liquid crystal visualization and spanwise velocity and temperature traverses. Transition was found to occur via a vortex breakdown mode. Predictions based on two-dimensional modeling of the flow over a concave wall with high free-stream turbulence levels, as on the pressure surface of a turbine blade, would seem to be adequate. Dissert. Abstr.

N91-13644*# California Univ., Los Angeles.
ANALYTICAL STUDY OF THE LIQUID PHASE TRANSIENT BEHAVIOR OF A HIGH TEMPERATURE HEAT PIPE M.S. Thesis
Gregory Lawrence Roche 1988 204 p
(Contract NCC2-374)
(NASA-CR-187426; NAS 1.26:187426) Avail: NTIS HC/MF A10 CSCL 20D

The transient operation of the liquid phase of a high temperature heat pipe is studied. The study was conducted in support of advanced heat pipe applications that require reliable transport of high temperature drops and significant distances under a broad spectrum of operating conditions. The heat pipe configuration studied consists of a sealed cylindrical enclosure containing a capillary wick structure and sodium working fluid. The wick is an annular flow channel configuration formed between the enclosure interior wall and a concentric cylindrical tube of fine pore screen. The study approach is analytical through the solution of the governing equations. The energy equation is solved over the pipe wall and liquid region using the finite difference Peaceman-Rachford alternating direction implicit numerical method. The continuity and momentum equations are solved over the liquid region by the integral method. The energy equation and liquid dynamics equation are tightly coupled due to the phase change process at the liquid-vapor interface. A kinetic theory model is used to define the phase change process in terms of the temperature jump between the liquid-vapor surface and the bulk vapor. Extensive auxiliary relations, including sodium properties as functions of temperature, are used to close the analytical system. The solution procedure is implemented in a FORTRAN algorithm with some optimization features to take advantage of the IBM System/370 Model 3090 vectorization facility. The code was intended for coupling to a vapor phase algorithm so that the entire heat pipe problem could be solved. As a test of code capabilities, the vapor phase was approximated in a simple manner. Author

N91-13645*# California Univ., Los Angeles. Dept. of Mechanical, Aerospace and Nuclear Engineering.
HEAT PIPE DYNAMIC BEHAVIOR
F. Issacci, G. L. Roche, D. B. Klein, and I. Catton Sep. 1988 123 p
(Contracts NCC2-374; NAG3-899; DNA001-C-0320)
(NASA-CR-187422; NAS 1.26:187422; UCLA-ENG-88-28) Avail: NTIS HC/MF A06 CSCL 20D

The vapor flow in a heat pipe was mathematically modeled and the equations governing the transient behavior of the core were solved numerically. The modeled vapor flow is transient, axisymmetric (or two-dimensional) compressible viscous flow in a closed chamber. The two methods of solution are described. The more promising method failed (a mixed Galerkin finite difference method) whereas a more common finite difference method was successful. Preliminary results are presented showing that multi-dimensional flows need to be treated. A model of the liquid phase of a high temperature heat pipe was developed. The model is intended to be coupled to a vapor phase model for the complete solution of the heat pipe problem. The mathematical equations are formulated consistent with physical processes while allowing a computationally efficient solution. The model simulates time dependent characteristics of concern to the liquid phase including input phase change, output heat fluxes, liquid temperatures, container temperatures, liquid velocities, and liquid pressure. Preliminary results were obtained for two heat pipe startup cases. The heat pipe studied used lithium as the working fluid and an annular wick configuration. Recommendations for implementation based on the results obtained are presented. Experimental studies were initiated using a rectangular heat pipe. Both twin beam laser holography and laser Doppler anemometry were investigated.

Preliminary experiments were completed and results are reported. Author

N91-13646# David Taylor Research Center, Bethesda, MD. Dept. of Ship Hydromechanics.
COMPUTATION OF INCOMPRESSIBLE FLOW AROUND THE DARPA SUBOFF BODIES Final Report
Joseph J. Gorski, Roderick M. Coleman, and Henry J. Haussling Jul. 1990 87 p Sponsored by DARPA and ONR
(AD-A226481; DTRC-90/016) Avail: NTIS HC/MF A05 CSCL 20/4

This report describes the application of the DTNS flow solvers, both axisymmetric (DTNSA) and three-dimensional (DTNS3D) versions, and the NUGGET grid generation code to the Defense Advanced Research Projects Agency (DARPA) SUBOFF bodies. GRA

N91-13647# Massachusetts Inst. of Tech., Cambridge. Dept. of Ocean Engineering.
FAR FIELD WAKE VELOCITY MEASUREMENTS WITH HOT FILM PROBES M.S. Thesis
Lewis Randall Grigg Jun. 1990 87 p
(Contract N00123-89-G-0580)
(AD-A226650) Avail: NTIS HC/MF A05 CSCL 20/4

An investigation into the feasibility of measuring wake velocity profiles in a towing tank using hot film probes was conducted. Results show that such a system is feasible, but care must be taken to minimize calibration errors due to the small velocity differences being measured. Included are calibration data and plots of wake profiles behind a sphere measured at the U.S. Naval Academy's Hydromechanics Laboratory and the MIT Ship Model Towing Tank. These plots show the effect of the presence of a free surface on the development of turbulent wake. Data collected using the hot film system can be used as an input to analytic wake algorithms, compared to wake prediction or visualization techniques. GRA

N91-13648*# Princeton Univ., NJ. Dept. of Chemical Engineering.
THE FLUID MECHANICS OF CONTINUOUS FLOW ELECTROPHORESIS Final Report, Sep. 1986 - Jul. 1990
D. A. Saville Nov. 1990 119 p
(Grant NAG8-597)
(NASA-CR-187647; NAS 1.26:187647) Avail: NTIS HC/MF A06 CSCL 20D

The overall objective is to establish theoretically and confirm experimentally the ultimate capabilities of continuous flow electrophoresis chambers operating in an environment essentially free of particle sedimentation and buoyancy. The efforts are devoted to: (1) studying the effects of particle concentration on sample conductivity and dielectric constant. The dielectric constant and conductivity were identified as playing crucial roles in the behavior of the sample and on the resolving power and throughput of continuous flow devices; and (2) improving the extant mathematical models to predict flow fields and particle trajectories in continuous flow electrophoresis. A dielectric spectrometer was designed and built to measure the complex dielectric constant of a colloidal dispersion as a function of frequency between 500 Hz and 200 kHz. The real part of the signal can be related to the sample's conductivity and the imaginary part to its dielectric constant. Measurements of the dielectric constants of several different dispersions disclosed that the dielectric constants of dilute systems of the sort encountered in particle electrophoresis are much larger than would be expected based on the extant theory. Experiments were carried out to show that, in many cases, this behavior is due to the presence of a filamentary structure of small hairs on the particle surface. A technique for producing electrokinetically ideal synthetic latex particles by heat treating was developed. Given the ubiquitous nature of hairy surfaces with both cells and synthetic particles, it was deemed necessary to develop a theory to explain their behavior. A theory for electrophoretic mobility of hairy particles was developed. Finally, the extant computer programs for predicting the structure of electro-osmotically driven flows were extended to encompass flow channels with variable wall mobilities. Author

N91-13649*# Institute for Computer Applications in Science and Engineering, Hampton, VA.
FLOW ESTABLISHMENT IN A GENERIC SCRAMJET COMBUSTOR Final Report
P. A. Jacobs, R. C. Rogers, E. H. Weidner, and R. D. Bittner (Analytical Services and Materials, Inc., Hampton, VA.) Oct. 1990 41 p Submitted for publication
(Contract NAS1-18605)
(NASA-CR-187467; ICASE-90-77; NAS 1.26:187467) Avail: NTIS HC/MF A03 CSCL 20D

The establishment of a quasi-steady flow in a generic scramjet combustor was studied for the case of a time varying inflow to the combustor. Such transient flow is characteristic of the reflected shock tunnel and expansion tube test facilities. Several numerical simulations of hypervelocity flow through a straight duct combustor with either a side wall step fuel injector or a centrally located strut injector are presented. Comparisons were made between impulsively started but otherwise constant flow conditions (typical of the expansion tube or tailored operations of the reflected shock tunnel) and the relaxing flow produced by the 'undertailored' operations of the reflected shock tunnel. Generally the inviscid flow features, such as the shock pattern and pressure distribution, were unaffected by the time varying inlet conditions and approached steady state in approx. the times indicated by experimental correlations. However, viscous features, such as heat transfer and skin friction, were altered by the relaxing inlet flow conditions. Author

N91-13650*# Institute for Computer Applications in Science and Engineering, Hampton, VA.
TOWARD THE LARGE-EDDY SIMULATION OF COMPRESSIBLE TURBULENT FLOWS Final Report
G. Erlebacher, M. Y. Hussaini, C. G. Speziale, and T. A. Zang (National Aeronautics and Space Administration. Langley Research Center, Hampton, VA.) Oct. 1990 46 p Submitted for publication
(Contract NAS1-18605)
(NASA-CR-187460; ICASE-90-76; NAS 1.26:187460) Avail: NTIS HC/MF A03 CSCL 20D

New subgrid-scale models for the large-eddy simulation of compressible turbulent flows are developed and tested based on the Favre-filtered equations of motion for an ideal gas. A compressible generalization of the linear combination of the Smagorinsky model and scale-similarity model, in terms of Favre-filtered fields, is obtained for the subgrid-scale stress tensor. An analogous thermal linear combination model is also developed for the subgrid-scale heat flux vector. The two dimensionless constants associated with these subgrid-scale models are obtained by correlating with the results of direct numerical simulations of compressible isotropic turbulence performed on a 96(exp 3) grid using Fourier collocation methods. Extensive comparisons between the direct and modeled subgrid-scale fields are provided in order to validate the models. A large-eddy simulation of the decay of compressible isotropic turbulence (conducted on a coarse 32(exp 3) grid) is shown to yield results that are in excellent agreement with the fine grid direct simulation. Future applications of these compressible subgrid-scale models to the large-eddy simulation of more complex supersonic flows are discussed briefly. Author

N91-13651*# Queensland Univ., Saint Lucia (Australia). Dept. of Mechanical Engineering
SHOCK TUNNEL STUDIES OF SCRAMJET PHENOMENA, SUPPLEMENT 5 Interim Report
R. Casey, R. J. Stalker, C. P. Brescianini, R. G. Morgan, P. A. Jacobs, M. Wendt, N. R. Ward, N. Akman, G. A. Allen, and K. Skinner Oct. 1990 200 p
(Grant NAGw-674)
(NASA-CR-182096-Suppl-5; NAS 1.26:182096-Suppl-5) Avail: NTIS HC/MF A09 CSCL 20D

A series of reports are presented on SCRAMjet studies, shock tunnel studies, and expansion tube studies. The SCRAMjet studies include: (1) Investigation of a Supersonic Combustion Layer; (2) Wall Injected SCRAMjet Experiments; (3) Supersonic Combustion with Transvers, Circular, Wall Jets; (4) Dissociated Test Gas Effects on SCRAMjet Combustors; (5) Use of Silane as a Fuel Additive for Hypersonic Thrust Production, (6) Pressure-length Correlations in Supersonic Combustion; (7) Hot Hydrogen Injection Technique for Shock Tunnels; (8) Heat Release - Wave Interaction Phenomena in Hypersonic Flows; (9) A Study of the Wave Drag in Hypersonic SCRAMjets; (10) Parametric Study of Thrust Production in the Two Dimensional SCRAMjet; (11) The Design of a Mass Spectrometer for use in Hypersonic Impulse Facilities; and (12) Development of a Skin Friction Gauge for use in an Impulse Facility. The shock tunnel studies include: (1) Hypervelocity flow in Axisymmetric Nozzles; (2) Shock Tunnel Development; and (3) Real Gas Efects in Hypervelocity Flows over an Inclined Cone. The expansion tube studies include: (1) Investigation of Flow Characteristics in TQ Expansion Tube; and (2) Disturbances in the Driver Gas of a Shock Tube. K.S.

N91-13652*# National Aeronautics and Space Administration. Ames Research Center, Moffett Field, CA.
TURBULENCE MODELING FOR SHARP-FIN-INDUCED SHOCK WAVE/TURBULENT BOUNDARY-LAYER INTERACTIONS
C. C. Horstman Oct. 1990 13 p Presented at the IUTAM Symposium on Separated Flows and Jets, Novosibirsk (USSR), 9-13 Jul. 1990
(NASA-TM-102828; A-90172; NAS 1.15:102828) Avail: NTIS HC/MF A03 CSCL 20D

Solutions of the Reynolds averaged Navier-Stokes equations are presented and compared with a family of experimental results for the 3-D interaction of a sharp fin induced shock wave with a turbulent boundary layer. Several algebraic and two equation eddy viscosity turbulence models are employed. The computed results are compared with experimental surface pressure, skin friction, and yaw angle data as well as the overall size of the interaction. Although the major feature of the flow fields are correctly predicted, several discrepancies are noted. Namely, the maximum skin friction values are significantly underpredicted for the strongest interaction cases. These and other deficiencies are discussed. Author

N91-13653*# National Aeronautics and Space Administration. Ames Research Center, Moffett Field, CA.
A LASER DOPPLER VELOCIMETER APPROACH FOR NEAR-WALL THREE-DIMENSIONAL TURBULENCE MEASUREMENTS
D. A. Johnson and J. D. Brown (Eloret Corp., Palo Alto, CA.) Oct. 1990 10 p Presented at the 5th International Symposium on Application of Laser Techniques in Fluid Mechanics, Lisbon, Portugal, 9-12 Jul. 1990
(NASA-TM-102841; A-90207; NAS 1.15:102841) Avail: NTIS HC/MF A02 CSCL 20D

A near-wall laser Doppler velocimeter approach is described that relies on a beam-turning probe which makes possible the direct measurement of the crossflow velocity at a grazing incident and the placement of optical components close to the flow region of interest regardless of test facility size. Other important elements of the approach are the use of digital frequency processing, an optically smooth measurement surface, and observation of the sensing volume at 90 degrees. The combination was found to dramatically reduce noise-in-signal effects caused by surface light scattering. Turbulent boundary-layer data to within 20 microns (y(sup+) approximately equal to 1) of the surface are presented which illustrate the potential of the approach. Author

N91-13654# Illinois Univ., Chicago. Dept. of Chemical Engineering.
TRANSPORT PROPERTIES OF DENSE FLUID MIXTURES USING NONEQUILIBRIUM MOLECULAR DYNAMICS
S. Murad Sep. 1990 37 p
(Contract DE-FG02-87ER-13769)
(DE91-000262; DOE/ER-13769/3) Avail: NTIS HC/MF A03

The main emphasis was on dense fluid mixtures, although in some cases work had to be done on pure fluids before mixtures could be studied in a meaningful way. A summary of the results is given. (1) An algorithm was developed and used to calculate the viscosity and thermal conductivity of continuous, or polydisperse mixtures with various distributions (e.g. linear, several Gaussian distributions including unsymmetric, etc.) using nonequilibrium molecular dynamics (NEMD). (2) A method was developed to calculate the thermal conductivity of nonspherical (rigid) molecules using NEMD. (3) The NEMD method for thermal conductivity of nonspherical molecules was used to have a careful look at the contributions due to internal rotational degrees of freedom in linear compounds such as chlorine, nitrogen, etc. (4) It has long been speculated that polar fluids exhibit heat induced birefringence, i.e., the molecules will tend to align themselves along the direction of an external heat field. Using nonequilibrium molecular dynamics this was conclusively confirmed. (5) A preliminary study was completed of the viscosity of homonuclear diatomics and their mixtures (e.g. N2, Cl2, etc.). (6) A study was completed of the various flexibility (vibrational) effects, such as bond bending, bond stretching etc., on linear and nonlinear model triatomics. To examine these effects in the preliminary study, the pressure second virial coefficients was examined. DOE

N91-13655# Westinghouse Savannah River Co., Aiken, SC.
THE EFFECT OF LONGITUDINAL SPACER RIBS ON THE MINIMUM PRESSURE DROP IN A HEATED ANNULUS
B. S. Johnston and J. M. Neff 1990 19 p Presented at the ASME Winter Annual Meeting, Dallas, TX, 25-30 Nov. 1990 Submitted for publication
(Contract DE-AC09-89SR-18035)
(DE91-000784; WSRC-MS-90-158; CONF-901194-4) Avail: NTIS HC/MF A03

When evaluating a heated flow passage for vulnerability to static flow excursions, special note should be taken of flow restrictions which might allow premature vapor generation. In this study, measurements of steady state pressure drop were made for the downward flow of water in a vertical annulus. The outer wall was uniformly heated to allow subcooled boiling. Minima in the pressure drop characteristics were compared for test sections with and without longitudinal spacer ribs. For a given power and inlet temperature, the minimum occurred at a higher flow rate in the ribbed test section. This is attributed to vapor generation at the ribs. The work cited in this document shows how a restriction in a heated channel can produce vapor which would not be observed in the absence of the restriction. In the present study, the effect of a flow restriction on the tendency to flow excursion is explored by finding demand curves for a heated annulus in subcooled boiling flow. The annulus is heated from the outside, and alternately equipped with and without longitudinal spacer ribs. These ribs separate the heated and unheated walls; in pressing against the heated wall they provide a means for premature vapor production. DOE

N91-13656*# State Univ. of New York, Buffalo. Dept. of Mechanical and Aerospace Engineering.
LARGE EDDY SIMULATIONS AND DIRECT NUMERICAL SIMULATIONS OF HIGH SPEED TURBULENT REACTING FLOWS Semiannual Report, 1 May - 30 Oct. 1990
Peyman Givi, Cyrus K. Madnia, and Craig J. Steinberger Oct. 1990 85 p
(Grant NAG1-1122)
(NASA-CR-187674; NAS 1.26:187674) Avail: NTIS HC/MF A05 CSCL 20D

This research is involved with the implementation of advanced computational schemes based on large eddy simulations (LES) and direct numerical simulations (DNS) to study the phenomenon of mixing and its coupling with chemical reactions in compressible turbulent flows. In the efforts related to LES, a research program to extend the present capabilities of this method was initiated for the treatment of chemically reacting flows. In the DNS efforts, the focus is on detailed investigations of the effects of compressibility, heat release, and non-equilibrium kinetics modelings in high speed

reacting flows. Emphasis was on the simulations of simple flows, namely homogeneous compressible flows, and temporally developing high speed mixing layers. Author

N91-13657*# National Aeronautics and Space Administration. Lyndon B. Johnson Space Center, Houston, TX.
VARIABLE ORIFICE FLOW REGULATOR Patent Application
Rollin Christianson, inventor (to NASA) 11 Apr. 1990 18 p
(NASA-Case-MSC-21549-1; NAS 1.71:MSC-21549-1; US-Patent-Appl-SN-507553) Avail: NTIS HC/MF A03 CSCL 20D

A flow regulator for high-pressure fluids at elevated temperatures includes a body having a flow passage extending between inlet and outlet openings. First and second orifice members are arranged in the flow passage so at least one of the orifice members can be moved transversely in relation to the flow passage between one operating position where the two orifice openings are aligned for establishing a maximum flow rate of fluids flowing through the flow passage and at least one other operating position in which the two openings are moderately misaligned with one another for establishing a predetermined reduced flow rate of fluids flowing through the flow passage. NASA

N91-13658*# National Aeronautics and Space Administration. Pasadena Office, CA.
MEASUREMENT OF WAVES IN FLOWS ACROSS A SURFACE Patent Application
James M. Kendall, Jr., inventor (to NASA) (Jet Propulsion Lab., California Inst. of Tech., Pasadena.) 16 Aug. 1990 16 p
(Contract NAS7-918)
(NASA-Case-NPO-17479-1-CU; NAS 1.71:NPO-17479-1-CU; US-Patent-Appl-SN-568127) Avail: NTIS HC/MF A03 CSCL 20D

A method and apparatus is disclosed for sensing wave flow across a surface wherein at least two pressure levels are sensed and combined to provide a representation of waves within the flow. In the preferred embodiment holes bored through the aircraft surface at an interval of one-half the wavelength of the flow being measured introduce pressure perturbations into a cavity so they may acoustically interfere. The interfering waveform is sensed by at least one microphone disposed in the cavity. NASA

N91-13659# California Univ., Los Angeles.
ENHANCEMENT OF CRITICAL HEAT FLUX IN TUBES USING STAGED TANGENTIAL FLOW INJECTION
1990 43 p
(Contract DE-FG03-85ER-13360)
(DE90-014935; DOE/ER-13360/T1) Avail: NTIS HC/MF A03

Significant enhancement in critical heat flux in tubes is possible by tangential injection of liquid. The enhancement depends on the ratio of momentum rate of the injected fluid to the momentum rate of the fluid exiting the tube, the tube length, injector to tube diameter ratio and on the density ratio of the liquid and vapor. In the reported experiments, critical heat fluxes as high as (vert bar)kw(vert bar)cm(exp 2) were obtained with up to about 50 percent enhancement over that for purely axial flow. DOE

N91-13660# Pittsburgh Energy Technology Center, PA.
A REVIEW OF INTERACTION MECHANISMS IN FLUID-SOLID FLOWS
G. Johnson, K. R. Rajagopal (Pittsburgh Univ., PA.), and M. Massoudi Sep. 1990 54 p
(DE91-000941; DOE/PETC/TR-90/9) Avail: NTIS HC/MF A04

Multiphase flows have become the subject of considerable attention because of their importance in many industrial applications, such as fluidized beds, pneumatic transport of solids, coal combustion, etc. Fundamental research into the nature of pneumatic transport has made significant progress in identifying key parameters controlling the characteristics of these processes. The emphasis of this study is on a mixture composed of spherical particles of uniform size and a linearly viscous fluid. Section 1 introduces our approach and the importance of this study. In Section 2, the dynamics of a single particle as studied in classical hydrodynamics and fluid dynamics is presented. This has been a subject of study for more than 200 years. In Section 3, we review the literature for the constitutive relations as given in multiphase studies, i.e., generalization of single particle and as given in literature concerning the continuum theories of mixtures or multicomponent systems. In Section 4, a comparison between these representations and the earlier approach, i.e., forces acting on a single particle will be made. The importance of flow regimes, particle concentration, particle size and shape, rotation of the particle, effect of solid walls, etc. are discussed. DOE

N91-13661# Edgerton, Germeshausen and Grier, Inc., Idaho Falls, ID.
HEAT EXCHANGER FOULING: PREDICTION, MEASUREMENT, AND MITIGATION
1989 10 p Presented at the 11th Annual Industrial Energy Technology Conference: Energy Strategies for the 1990s and Fall Conference of the Gulf Coast Cogeneration Association and Exposition, Houston, TX, 12-14 Sep. 1989
(Contract DE-AC07-76ID-01570)
(DE91-001997; EGG-M-89226; CONF-8909106-1) Avail: NTIS HC/MF A02

The US Department of Energy (DOE), Office of Industrial Programs (OIP) sponsors the development of innovative heat exchange systems. Fouling is a major and persistent cost associated with most industrial heat exchangers and nationally wastes an estimated 2.9 Quads per year. To predict and control fouling, three OIP projects are currently exploring heat exchanger fouling in specific industrial applications. A fouling probe has been developed to determine empirically the fouling potential of an industrial gas stream and to derive the fouling thermal resistance. The probe is a hollow metal cylinder capable of measuring the average heat flux along the length of the tube. The local heat flux is also measured by a heat flux meter embedded in the probe wall. The fouling probe has been successfully tested in the laboratory at flue gas temperatures up to 2200 F and a local heat flux up to 41,000 BTU/hr sq ft. The probe has been field tested at a coal-fired boiler plant. Future tests at a municipal waste incinerator are planned. Two other projects study enhanced heat exchanger tubes, specifically the effect of enhanced surface geometries on the tube bundle performance. Both projects include fouling in a liquid heat transfer fluid. Identifying and quantifying the factors affecting fouling in these enhanced heat transfer tubes will lead to techniques to mitigate fouling. DOE

N91-13662# Los Alamos National Lab., NM.
BIDIRECTIONAL SLAPPER DETONATORS IN SPHERICAL EXPLOSION SYSTEMS
Ernest C. Martinez Nov. 1990 11 p
(Contract W-7405-eng-36)
(DE91-002399; LA-11816-MS) Avail: NTIS HC/MF A03

A bidirectional slapper detonator has been proven effective for producing a spherically expanding shock wave. Two bridge foils are used to propel flyers in opposite directions, thereby initiating two explosive pellets, each embedded in one hemisphere of a spherical system. This detonation system produces a nearly perfect spherically expanding detonation front. DOE

N91-13663# Technische Hochschule, Darmstadt (Germany, F.R.). Fachbereich Mathematik.
THE COUPLING OF FINITE METHODS FOR TRANSPORT-DIFFUSION PROBLEMS Ph.D. Thesis [DIE KOPPLUNG FINITER METHODEN FUER TRANSPORT-DIFFUSIONS-PROBLEME]
Dietmar Albrecht 1989 163 p In GERMAN
(ETN-91-98172) Avail: NTIS HC/MF A08

Discretization methods for the treatment of transport diffusion problems in fluid mechanics are presented. The general formulation and theoretical fundamentals of a class of discretization methods for such problems are given. A semidiscrete approximation based on the horizontal line method was deducted. The formal description of the fully discrete transport diffusion algorithm is outlined, and

the classical concepts of consistency, convergence and stability are formulated. A concrete realization of the transport diffusion algorithm is illustrated by an example. A finite volume method with a novel control volume is introduced as an approximation. For the transport step, and an isoparametric finite element method for the diffusion step. The linear equation system resulting from the discretization is solved. ESA

N91-13664# Ecole Centrale de Lyon (France). Lab. de Mecanique des Fluides et Acoustique.
A MINIMIZATION METHOD ADAPTED TO THE FINITE ELEMENT TECHNIQUE FOR TURBULENT FLOW SIMULATION WITH NONLINEAR BOUNDARY CONDITIONS IN THE WALL VICINITY Ph.D. Thesis [METHODE DE MINIMISATION ADAPTEE A LA TECHNIQUE DES ELEMENTS FINIS POUR LA SIMULATION DES ECOULEMENTS TURBULENTS AVEC CONDITIONS AUX LIMITES NONLINEAIRES DE PROCHE PAROI]
Jose AlyesdaFontouraRodrigues 1990 163 p In FRENCH; ENGLISH summary
(ECL-90-016; ETN-91-98339) Avail: NTIS HC/MF A08

The minimization method is described for two dimensional turbulent flow. The governing equations of the system are time discretized by a semi-implicit scheme. The continuity constraint coupled with the momentum equation are solved by finite element with an iterative scheme based on an Uzawa algorithm and a minimal residue method. The minimization error technique for the calculus of boundary conditions is based on a minimal residue method. Three wall laws for turbulent boundary layers are tested: the classical logarithmic law of wall and two other laws derived for turbulent boundary layers developed under adverse pressure gradients. The calculated results for three basic test cases (backward facing step, flat and conical diffusers) and for a combustor dome are compared to experimental data. ESA

N91-13665# Ecole Centrale de Lyon (France). Lab. de Machines Thermiques.
MODELIZATION OF TWO PHASE TURBULENT JET UP TO ITS AUTO IGNITION IN VARIABLE PRESSURE AND TEMPERATURE ENVIRONMENTS Ph.D. Thesis [MODELISATION D'UN JET DIPHASIQUE TURBULENT JUSQU'A SON AUTO-INFLAMMATION DANS UNE ENCEINTE A PRESSION ET TEMPERATURE VARIABLES]
Gerard Fluzin 1990 178 p In FRENCH Original contains color illustrations
(ETN-91-98341) Avail: NTIS HC/MF A09

The direct model used for the modelization of the fuel injection in variable pressure and temperature environments is presented. The equations and the numerical method used for solving this problem are described. The code changes are given, with a view to representing as clearly as possible the experimentally observed phenomena. The auto ignition model is described. Experimental data are compared to calculation results. ESA

N91-13666# Loughborough Univ. of Technology (England). Dept. of Mathematical Sciences.
FRONTOGENESIS IN GRAVITY CURRENTS: THE EFFECT OF ENDWALLS AND DIFFUSION
A. Kay Jul. 1990 41 p
(MATHS-Rept-A-127; ETN-91-98349) Avail: NTIS HC/MF A03

The formation of gravity current fronts at the endwalls of a tank containing water with a linear horizontal density gradient is investigated. It was mathematically modeled, using the method of expansion in powers of the time since the initiation of the flow. A front was formed at each endwall, which was brought about by the deceleration of the flow as it approaches the endwall. The diffusion effect was to spread out at the deceleration region. A numerical solution of the vorticity and density equations is necessary to completely describe the front propagation. In the case of quadratic density profile, horizontal diffusion has no effect on the flow and has no influence on the density structure if this profile results from a quadratic salinity or temperature profile. The vertical diffusion effects are weak because of the small magnitudes of molecular diffusivities. ESA

N91-13667# Admiralty Research Establishment, Gosport (England).
TRANSITION CONTROL VIA BOUNDARY LAYER HEATING
D. J. Atkins and S. J. Pearce Jul. 1990 36 p
(ARE-TR-88503; BR114792; ETN-91-98359) Copyright Avail: NTIS HC/MF A03

A theoretical method for predicting flow transition on axisymmetric heated underwater bodies, based on linear stability, is described. A simple heated body experiment was carried out with a four to one ellipsoidal nose attached to a long cylinder in a water tunnel. The pressure coefficient was calculated by the Hess and Smith method. Heating was supplied by pumping hot water through a copper coil wound helically inside the nose. Intermittency measurements were made at some axial positions using glue on hot film probes. The turbulence intensity was measured in the empty tunnel. It is shown that transition was affected by model vibration and filtering the tunnel water. Heating the body surface also appeared to modify the Tollmein-Schlichting wave spectrum. ESA

N91-13668*# National Aeronautics and Space Administration. Lewis Research Center, Cleveland, OH.
HEAT TRANSFER DEVICE AND METHOD OF MAKING THE SAME Patent Application
Bruce A. Banks, inventor (to NASA) and James R. Gaier, inventor (to NASA) 30 Mar. 1990 11 p
(NASA-Case-LEW-14162-1; NAS 1.71:LEW-14162-1; US-Patent-Appl-SN-501893) Avail: NTIS HC/MF A03 CSCL 20D

Gas derived graphite fibers are generated by the decomposition of an organic gas. These fibers when joined with a suitable binder are used to make a high thermal conductivity composite material. The fibers may be intercalated. The intercalate can be halogen or halide salt, alkaline metal, or any other species which contributes to the electrical conductivity improvement of the graphite fiber. The heat transfer device may also be made of intercalated highly oriented pyrolytic graphite and machined, rather than made of fibers. NASA

N91-13669*# Institute for Computer Applications in Science and Engineering, Hampton, VA.
ZERO WAVENUMBER MODES OF A COMPRESSIBLE SUPERSONIC MIXING LAYER Final Report
T. L. Jackson and C. E. Grosch (Old Dominion Univ., Norfolk, VA.) Dec. 1990 13 p Submitted for publication
(Contract NAS1-18605)
(NASA-CR-187476; NAS 1.26:187476; ICASE-90-82) Avail: NTIS HC/MF A03 CSCL 20D

It is shown that there exists a family of supersonic neutral modes for a compressible mixing layer in an unbounded domain. These modes have zero wavenumber and frequency with nonzero phase speed. They are analogous to the supersonic neutral modes of the compressible vortex sheet found by Miles. The results presented give a more complete picture of the spectrum of the disturbances in this flow. Author

N91-13670# Idaho National Engineering Lab., Idaho Falls.
COHERENT ANTI-STOKES RAMAN SPECTROSCOPIC MEASUREMENT OF AIR ENTRAINMENT IN ARGON PLASMA JETS
J. R. Fincke, R. Rodriquez, and C. G. Pentecost 1990 6 p Presented at the Spring Meeting of the Materials Research Society, San Francisco, CA, 16-21 Apr. 1990
(Contract DE-AC07-76ID-01570)
(DE91-001936; EGG-M-89489; CONF-900466-91) Avail: NTIS HC/MF A02

The concentration and temperature of air entrained into an argon plasma jet has been measured using coherent anti-Stokes Raman spectroscopy (CARS). The flow field is characterized by a short region of well behaved laminar flow near the nozzle exit

followed by an abrupt transition to turbulence. Once the transition to turbulence occurs, air is rapidly entrained into the jet core. The location of the transition region is thought to be driven by the rapid cooling of the jet and the resulting increase in Reynolds number. DOE

N91-13671# Syracuse Univ., NY. Dept. of Chemical Engineering and Materials Science.
MECHANISMS OF GAS PERMEATION THROUGH POLYMER MEMBRANES Summary Technical Report, Sep. 1989 - Sep. 1990
S. Alexander Stern 1990 19 p
(Contract DE-FG02-87ER-13649)
(DE91-004190; DOE/ER-13649/4) Avail: NTIS HC/MF A03

The objective of the present study is to investigate the mechanisms by which gases are transported in and through polymer membranes, and the dependence of these mechanisms on pressure and temperature. Recent work has been focused on the permeation of gases through membranes made from glassy polymers, i.e., at temperatures below the glass transition of the polymers (Tg). During the past report period, a new theoretical model of gas solubility in glassy polymers was developed and tested with experimental data from the literature. This model describes satisfactorily the shape of solubility isotherms over wide ranges of pressure and temperatures, and is particularly useful for penetrant gases with ranges of pressure and temperatures, and is particularly useful for penetrant gases which plasticize (swell) glassy polymers. Work also continued on the behavior of light gases in poly (alkyl methacrylates). DOE

N91-13672# Imperial Coll. of Science and Technology, London (England). Dept. of Aeronautics.
WAVE BY WAVE ANALYSIS OF IN-LINE FORCE DATA FOR FIXED CYLINDERS IN REGULAR WAVES
Martin J. S. Davies Sep. 1989 19 p Sponsored by Dept. of Energy, London, England
(IC-Aero-89-02; ISSN-0308-7247; ETN-91-98369) Avail: NTIS HC/MF A03

The analysis of in line force data from experiments conducted on fixed cylinders in regular waves in the De Voorst wave flume is described. The in line force data was fitted to Morison's equation on a wave by wave basis, to obtain, Cd and Cm, using two different statistical assumptions. Predicted force signals and residual forces were calculated based on both assumptions and Fourier analyses of the residuals were performed. The results of the two methods were compared. Different ways of dealing with the mean force and velocity components were studied. The validity of comparing median and mean results was briefly examined. ESA

35 INSTRUMENTATION AND PHOTOGRAPHY

Includes remote sensors; measuring instruments and gages; detectors; cameras and photographic supplies; and holography.

For aerial photography see *43 Earth Resources and Remote Sensing.* For related information see also *06 Aircraft Instrumentation,* and *19 Spacecraft Instrumentation.*

N91-13673# National Aeronautical Lab., Bangalore (India). Structural Sciences Div.
CALIBRATION SET UP FOR LOAD CELLS
T. V. Govinda Rao, C. S. Venkatesh, and N. Shivashankar May 1989 35 p
(PD-ST-8917) Avail: NTIS HC/MF A03

The planning, designing, fabrication, and calibration of 30, 50, and 100 ton tension load cells and 30 ton shear load cells are described. The tension load cells are for monitoring the force developed by earth moving vehicles and the shear load cells are for monitoring the load that tipplers unload form platform to ground. The shear load cells were incorporated into a rotary wagon tippler. Author

N91-13674*# Morgan State Univ., Baltimore, MD. Dept. of Physics.
DATA REDUCTION OF DIGITIZED IMAGES PROCESSED FROM CALIBRATED PHOTOGRAPHIC AND SPECTROSCOPIC FILMS OBTAINED FROM TERRESTIAL, ROCKET AND SPACE SHUTTLE TELESCOPIC INSTRUMENTS Semiannual Report, 22 Aug. 1990
Ernest C. Hammond, Jr. Aug. 1990 90 p
(Grant NsG-5074)
(NASA-CR-187320; NAS 1.26:187320) Avail: NTIS HC/MF A05 CSCL 14B

The Microvax 2 computer, the basic software in VMS, and the Mitsubishi High Speed Disk were received and installed. The digital scanning tunneling microscope is fully installed and operational. A new technique was developed for pseudocolor analysis of the line plot images of a scanning tunneling microscope. Computer studies and mathematical modeling of the empirical data associated with many of the film calibration studies were presented. A gas can follow-up experiment which will be launched in September, on the Space Shuttle STS-50, was prepared and loaded. Papers were presented on the structure of the human hair strand using scanning electron microscopy and x ray analysis and updated research on the annual rings produced by the surf clam of the ocean estuaries of Maryland. Scanning electron microscopic work was conducted by the research team for the study of the Mossbauer and Magnetic Susceptibility Studies on NmNi(4.25)Fe(.85) and its Hydride. B.G.

N91-13675*# Thiokol Corp., Brigham City, UT. Space Operations.
TETHERING SOCKETS AND WRENCHES Final Report
E. P. Johnson Jul. 1990 12 p Revised
(Contract NAS8-30490)
(NASA-CR-184032; NAS 1.26:184032; TWR-60119-Rev-A; PEI-994) Avail: NTIS HC/MF A03 CSCL 14B

The tethering of sockets and wrenches was accomplished to improve the safety of working over motor segments. To accomplish the tethering of the sockets to the ratchets, a special design was implemented in which a groove was machined into each socket. Each socket was then fitted with a snap ring that can spin around the machined groove. The snap ring is tethered to the handle of the ratchet. All open end wrenches are also tethered to the ratchet or to the operator, depending upon the type. Tests were run to ensure that the modified tools meet torque requirements. The design was subsequently approved by Space Safety. Author

N91-13676*# Purdue Univ., West Lafayette, IN. School of Aeronautics and Astronautics.
A QUIET FLOW LUDWIEG TUBE FOR STUDY OF TRANSITION IN COMPRESSIBLE BOUNDARY LAYERS: DESIGN AND FEASIBILITY Semiannual Status Report, 1 May - 1 Nov. 1990
Steven P. Schneider Nov. 1990 24 p
(Grant NAG1-1133)
(NASA-CR-187374; NAS 1.26:187374) Avail: NTIS HC/MF A03 CSCL 14B

Since Ludwieg tubes have been around for many years, and NASA has already established the feasibility of creating quiet-flow wind tunnels, the major question addressed was the cost of the proposed facility. Cost estimates were obtained for major system components, and new designs which allowed fabrication at lower cost were developed. A large fraction of the facility cost comes from the fabrication of the highly polished quiet-flow supersonic nozzle. Methods for the design of this nozzle were studied at length in an attempt to find an effective but less expensive design. Progress was sufficient to show that a quality facility can be fabricated at a reasonable cost. Author

N91-13677*# Maryland Univ., College Park. Dept. of Mechanical Engineering.
[STUDY OF DESIGN KNOWLEDGE CAPTURE (DKC) SCHEMES IMPLEMENTED IN MAGNETIC BEARING APPLICATIONS] Final Report

Jan. 1990 33 p
(Grant NAG5-955)
(NASA-CR-187394; NAS 1.26:187394) Avail: NTIS HC/MF A03 CSCL 14B

A design knowledge capture (DKC) scheme was implemented using frame-based techniques. The objective of such a system is to capture not only the knowledge which describes a design, but also that which explains how the design decisions were reached. These knowledge types were labelled definitive and explanatory, respectively. Examination of the design process helped determine what knowledge to retain and at what stage that knowledge is used. A discussion of frames resulted in the recognition of their value to knowledge representation and organization. The FORMS frame system was used as a basis for further development, and for examples using magnetic bearing design. The specific contributions made by this research include: determination that frame-based systems provide a useful methodology for management and application of design knowledge; definition of specific user interface requirements, (this consists of a window-based browser); specification of syntax for DKC commands; and demonstration of the feasibility of DKC by applications to existing designs. It was determined that design knowledge capture could become an extremely valuable engineering tool for complicated, long-life systems, but that further work was needed, particularly the development of a graphic, window-based interface. Author

N91-13678 Council for National Academic Awards (England).
FIBRE-LINKED MINIATURE LASER TRANSIT ANEMOMETER FOR COMPLEX FLOW FIELDS Ph.D. Thesis
Sohail Hamid 1989 313 p
Avail: Univ. Microfilms Order No. BRDX89760

Laser anemometry has been shown to be a very successful optical measurement device. The non-intrusive nature of this technique made it possible to map the flow between the blade rows of a rotating machine which was previously impracticable. The initial designs of the laser anemometry systems have undergone much development and practical problems during the use of these systems still provide room for further development. Some of these problems were identified and solved by designing a miniaturized laser transit system. Miniaturization of the system was achieved by separating the optical head from the bulky and sensitive laser source and detectors. Keeping in view the measurement volume geometry of conventional systems, the optical parameters for the new system were selected. Emphasis was given to the use of optical components which were commercially available in the market. Regarding the arrangement of the optical components inside the system, different models were suggested. A compromise between the optical quality has to be made for practical limitations of cost and ease of operation. The operation of the probe was confirmed by measuring the flow in a simple duct and the blade rows of a rotating axial fan. The comparison of these results with those obtained using a commercial system show that the new probe is working with high accuracy. During near wall applications, some problems were revealed and the probe's performance was not found up to that standard as was expected. Suggestions were made which may improve the systems performance. Dissert. Abstr.

N91-13679*# Jet Propulsion Lab., California Inst. of Tech., Pasadena.
MILLIMETER-WAVE SENSOR IMAGE ENHANCEMENT
William J. Wilson and Helmut Suess 15 Sep. 1988 37 p Prepared in cooperation with Harry Diamond Labs., Adelphi, MD LIMITED REPRODUCIBILITY: More than 20% of this document may be affected by color photographs
(Contract NAS7-918)
(NASA-CR-187430; JPL-Publ-88-27; NAS 1.26:187430) Avail: NTIS HC/MF A03: 8 functional color pages CSCL 14B

Images of an airborne scanning radiometer operating at a frequency of 98 GHz were analyzed. The mm wave images were obtained using the JPL mm wave imaging sensor. The goal was to enhance the information content of these images and make their interpretation easier for human analysis. A visual interpretative approach was used for information extraction from the images. This included application of nonlinear transform techniques for noise reduction and for color, contrast, and edge enhancement. Results of the techniques on selected mm wave images are shown. Author

N91-13680# Lawrence Livermore National Lab., CA.
TWELVE SIGNALS MULTIPLEXED WITH THE LLNL OPTICAL STREAK CAMERA
R. A. Lerche and R. L. Griffith 28 Aug. 1990 4 p
(Contract W-7405-eng-48)
(DE91-000066; UCRL-ID-104836) Avail: NTIS HC/MF A01

At the Nova laser facility, the temporal history of incident and reflected laser energy is recorded on LLNL optical streak cameras. Currently, six cameras are used to record the incident 1.06 micron, incident 0.35 micron power of each of the ten Nova beams. Each camera records seven multiplexed signals: typically one signal from each of five beam lines, a fiducial pulse, and time mark generator signal. The optical signals are transported to the camera through optical fibers. The output end of each fiber is placed in the slit plane of the camera. The light exiting the fiber is focused to the streak camera photocathode by the streak camera relay lens. One camera can record a signal from each of the ten Nova beams plus a fiducial and time mark generator signal if the number of multiplexed channels can be increased from seven to twelve. This would allow one camera to record the same data that currently requires two cameras. At a savings of $150 per camera/CCD system, this represents a savings of $450K. Additionally, camera/CCD maintenance and operation complexity would be cut in half and three streak cameras would be freed for use in other experiments. Recent laboratory measurements suggest that the number of multiplexed signals per camera can indeed be increased from seven to twelve without noticeably increasing the crosstalk between signal channels. In this memorandum, recent work in which seven and twelve signals were multiplexed to one streak camera is described. The effect focusing has on the crosstalk channels and the effect wavelength has on focusing is described. DOE

N91-13681# Oak Ridge National Lab., TN. Applied Technology Div.
LASER-INDUCED FLUORESCENCE OF PHOSPHORS FOR REMOTE CRYOGENIC THERMOMETRY
D. L. Beshears, G. J. Capps, M. R. Cates, C. M. Simmons, and S. W. Schwenterly Oct. 1990 20 p Prepared for NASA. Marshall Space Flight Center
(Contract DE-AC05-84OR-21400)
(DE91-001733; ORNL/ATD-44) Avail: NTIS HC/MF A03

Remote cryogenic temperature measurements can be made by inducing fluorescence in phosphors with temperature-dependent emissions and measuring the emission lifetimes. The thermographic phosphor technique can be used for making precision, noncontact, cryogenic-temperature measurements in electrically hostile environments, such as high dc electric or magnetic fields. The National Aeronautics and Space Administration is interested in using these thermographic phosphors for mapping hot spots on cryogenic tank walls. Europium-doped lanthanum oxysulfide (La2O2S:Eu) and magnesium fluorogermanate doped with manganese (Mg4FGeO6:Mn) are suitable for low-temperature surface thermometry. Several emission lines, excited by a 337-nm ultraviolet laser, provide fluorescence lifetimes having logarithmic dependence with temperature from 4 to above 125 K. A calibration curve for both La2O2S:Eu and Mg4FGeO6:Mn is presented, as well as emission spectra taken at room temperature and 11 K. DOE

N91-13682# Los Alamos National Lab., NM.
OPERATION OF SILICON MICROSTRIP DETECTORS IN A HIGH RADIATION ENVIRONMENT
J. S. Kapustinsky, D. M. Alde, J. G. Boissevain, R. G. Jeppesen, D. W. Lane, M. J. Leitch, J. W. Lillberg, T. A. Lopez, P. L. McGaughey, and J. M. Moss et al 1990 4 p Presented at

the Symposium on Detector Research and Development for the Superconducting Super Collider, Fort Worth, TX, 15-18 Oct. 1990 Prepared in cooperation with Abilene Christian Univ., TX, Chicago Univ., IL, Fermi National Accelerator Lab., Batavia, IL, Lawrence Berkeley Lab., CA, Univ. of Northern Illinois, DeKalb, South Carolina Univ., Columbia, and Academia Sinica, Taipei
(Contract W-7405-eng-36)
(DE91-001953; LA-UR-90-3581; CONF-9010212-9) Avail: NTIS HC/MF A01

A Silicon Microstrip Spectrometer was recently installed and operated in an 800 GeV proton beamline at Fermilab as a major new component of experiment E789. The detectors received an estimated radiation exposure of up to 7.8 x 10(exp 12) minimum ionizing particles per cm(exp 2) over a period of two months. We report on the changes in detector performance that we have observed following preliminary data analysis. DOE

N91-13683*# National Aeronautics and Space Administration. Lyndon B. Johnson Space Center, Houston, TX.
VOLUMETRIC MEASUREMENT OF TANK VOLUME Patent Application
Richard T. Walter, inventor (to NASA), Paul VanBuskirk, inventor (to NASA) (Lockheed Engineering and Sciences Co., Houston, TX.), William Weber, inventor (to NASA), and Richard Froebel, inventor (to NASA) 28 Dec. 1989 18 p
(NASA-Case-MSC-21500-1; NAS 1.71:MSC-21500-1;
US-Patent-Appl-SN-458258) Avail: NTIS HC/MF A03 CSCL 14B

A method is disclosed for determining the volume of compressible gas in a system including incompressible substances in a zero-gravity environment consisting of measuring the change in pressure (delta P) for a known volume change rate (delta V/delta t) in the polytrophic region between isothermal and adiabatic conditions. The measurements are utilized in an idealized formula for determining the change in isothermal pressure (delta P sub iso) for the gas. From the isothermal pressure change (delta iso) the gas volume is obtained. The method is also applicable to determination of gas volume by utilizing work (W) in the compression process. In a passive system, the relationship of specific densities can be obtained. NASA

N91-13684*# National Aeronautics and Space Administration. Langley Research Center, Hampton, VA.
WATER COOLED STATIC PRESSURE PROBE Patent Application
Nicholas T. Lagen, inventor (to NASA) (George Washington Univ., Washington, DC.), John W. Eves, inventor (to NASA), Garland D. Reece, inventor (to NASA), and Steve K. Geissinger, inventor (to NASA) 31 Aug. 1990 18 p
(NASA-Case-LAR-14340-1-CU; NAS 1.71:LAR-14340-1-CU;
US-Patent-Appl-SN-575695) Avail: NTIS HC/MF A03 CSCL 14B

An improved static pressure probe containing a water cooling mechanism is disclosed. This probe has a hollow interior containing a central coolant tube and multiple individual pressure measurement tubes connected to holes placed on the exterior. Coolant from the central tube symmetrically immerses the interior of the probe, allowing it to sustain high temperature, in the region of 2500 F, supersonic jet flow indefinitely, while still recording accurate pressure data. The coolant exits the probe body by way of a reservoir attached to the aft of the probe. The pressure measurement tubes are joined to a single, larger manifold in the reservoir. This manifold is attached to a pressure transducer that records the average static pressure. NASA

N91-13685*# National Aeronautics and Space Administration. Lewis Research Center, Cleveland, OH.
PLUG-TYPE HEAT FLUX GAUGE AND METHOD OF PRODUCING SAME Patent Application
Curt H. Liebert, inventor (to NASA) and John Koch, Jr., inventor (to NASA) 31 May 1990 17 p
(NASA-Case-LEW-14967-1; NAS 1.71:LEW-14967-1;
US-Patent-Appl-SN-531433) Avail: NTIS HC/MF A03 CSCL 14B

A plug-type heat flux gauge formed in a material specimen and having a thermoplug integrally formed in the material specimen, and a method for making the same are disclosed. The thermoplug is surrounded by a concentric annulus, through which thermocouple wires are routed. The end of each thermocouple wire is welded to the thermoplug, with each thermocouple wire welded at a different location along the length of the thermoplug. The thermoplug and concentric annulus may be formed in the material specimen by electrical discharge machining and trepanning procedures. NASA

N91-13686*# National Aeronautics and Space Administration. Langley Research Center, Hampton, VA.
PASSIVE FETAL MONITORING SENSOR Patent Application
16 Jul. 1990 14 p
(NASA-Case-LAR-14088-1; NAS 1.71:LAR-14088-1;
US-Patent-Appl-SN-552670) Avail: NTIS HC/MF A03 CSCL 14B

The invention is an ambulatory, passive sensor for use in a fetal monitoring system. The invention incorporates piezoelectric polymer film combined with a metallic mounting plate fastened to a belt and electrically connected to a signal processing unit by means of a shielded cable. The purpose of the sensor is to receive pressure pulses emitted from a fetus inside an expectant mother and to provide means for filtering out pressure pulses arising from other sources, such as the maternal heart. NASA

N91-13687*# National Aeronautics and Space Administration. Langley Research Center, Hampton, VA.
DUAL STRAIN GAGE BALANCE SYSTEM FOR MEASURING LIGHT LOADS Patent Application
Paul W. Roberts, inventor (to NASA) 18 Sep. 1990 20 p
(NASA-Case-LAR-14419-1; NAS 1.71:LAR-14419-1;
US-Patent-Appl-SN-584018) Avail: NTIS HC/MF A03 CSCL 14B

A dual strain gage balance system for measuring normal and axial forces and pitching moment of a metric airfoil model imparted by aerodynamic loads applied to the airfoil model during wind tunnel testing includes a pair of non-metric panels being rigidly connected to and extending towards each other from opposite sides of the wind tunnel, and a pair of strain gage balances, each connected to one of the non-metric panels and to one of the opposite ends of the metric airfoil model for mounting the metric airfoil model between the pair of non-metric panels. Each strain gage balance has a first measuring section for mounting a first strain gage bridge for measuring normal force and pitching moment and a second measuring section for mounting a second strain gage bridge for measuring axial force. NASA

N91-13688*# Smithsonian Astrophysical Observatory, Cambridge, MA.
COMPLETE THE DEVELOPMENT AND CONSTRUCTION OF A SPACEBORNE HYDROGEN MASER CLOCK Final Report, 11 Aug. 1988 - 31 Jul. 1990
Robert F. C. Vessot 14 Sep. 1990 14 p
(Contract NAS8-37752)
(NASA-CR-184043; NAS 1.26:184043) Avail: NTIS HC/MF A03 CSCL 14B

The objective, to complete the development of an engineering model of a spaceborne hydrogen maser, was successfully achieved. A layout of the maser and detail drawings of the physics package was completed during the first 7 months of the contract. A computer model was made for the maser's thermal design. Using numerical computations, heater resistances were established for 7 temperature controlled zones. The physics package includes: a vacuum manifold that houses four sorption pumps capable of scavenging hydrogen for 4 years, a titanium vacuum tank housing the cavity, metallic seals for all vacuum joints, an RF dissociator within the vacuum envelope, a two-layer printed circuit solenoid and four layers of moly-permalloy magnetic shields. Problems were encountered and overcome in the procurements of the PC solenoid

and the magnetic shields. After completion of the fabrication of the maser's components, the maser was assembled using these parts and other components made available by SAO, NRL, and NASA from earlier development work. In March, 1990, the vacuum system was assembled, and by May the maser assembly was completed. The magnetic shielding was poor and the shields were removed, reannealed by a local vendor, and the maser was reassembled. The maser began tests in early June and has been oscillating since that time. The test results of the maser are very good and a life test of the maser is being conducted. It is anticipated that the development and construction of a maser to be tested in space under a new contract from NASA's Marshall Space Flight Center will continue. Author

N91-13689# Lawrence Livermore National Lab., CA.
OPERATION OF INDUCTIVELY COUPLED PLASMA SOURCE MASS SPECTROMETERS IN THE PEAK JUMPING MODE
G. Price Russ, III and Gerald F. Hunt 15 Mar. 1990 12 p
(Contract W-7405-eng-48)
(DE91-001766; UCRL-CR-104524) Avail: NTIS HC/MF A03

Operating any spectrometer in a peak-jumping rather than scanning mode improves the fraction of data collection time spent monitoring peaks of interest. This results in improved sensitivity. Several problems with the use of peak jumping with the VG Elemental Plasmaquad inductively coupled plasma source mass spectrometer (ICP-MS) are discussed. Software and hardware changes installed to overcome these limitations are presented. Of particular importance, is the identification of limitations on peak-jumping speed and the need for built in delays (less than 0.5 msec) to allow for the response time of the quadrupole's electronics. DOE

N91-13690# Lawrence Livermore National Lab., CA.
X RAY HOLOGRAPHY AT LAWRENCE LIVERMORE NATIONAL LABORATORY
J. Trebes, C. Annese, D. Birdsall, J. Brase, J. Gray, S. Lane, R. London, D. Matthews, D. Peters, and D. Pinkel et al 11 Oct. 1990 5 p Presented at the X Ray Microscopy Conference, London, England, 3-7 Sep. 1990 Submitted for publication
(Contract W-7405-eng-48)
(DE91-002673; UCRL-JC-104971; CONF-9009235-3) Avail: NTIS HC/MF A01

The x ray holography program at the Lawrence Livermore National Laboratory has two principal goals: (1) the development of x ray diffraction techniques for DNA sequence analysis, and (2) the development of x ray laser holography for structural analysis of intact biological cells and organelles. DNA sequence analysis will be accomplished by applying x ray diffraction techniques to determine the ensemble average of the sequence of labels along the individual elements of crystalline DNA. X ray laser holographic imaging will be accomplished by applying three dimensional x ray holography to elucidate the structure of few hundred angstrom objects such as 300 (Angstrom) chromatin fibers, nuclear pores and nucleic acid replication complexes in living cells. Existing laboratory x ray lasers will be utilized to produce flash x ray holograms of the biological structures. DOE

N91-13691*# National Aeronautics and Space Administration. John C. Stennis Space Center, Bay Saint Louis, MS.
PREDICTIVE SENSOR METHOD AND APPARATUS Patent Application
William L. Nail, inventor (to NASA), Thomas L. Koger, inventor (to NASA), and Vivien Cambridge, inventor (to NASA) (Sverdrup Technology, Inc., Bay Saint Louis, MS.) 7 Mar. 1990 14 p
(NASA-Case-SSC-00006-1; NAS 1.71:SSC-00006-1;
US-Patent-Appl-SN-489997) Avail: NTIS HC/MF A03 CSCL 14B

A predictive algorithm is used to determine, in near real time, the steady state response of a slow responding sensor such as hydrogen gas sensor of the type which produces an output current proportional to the partial pressure of the hydrogen present. A microprocessor connected to the sensor samples the sensor output at small regular time intervals and predicts the steady state response of the sensor in response to a perturbation in the parameter being sensed, based on the beginning and end samples of the sensor output for the current sample time interval. NASA

N91-13692*# National Aeronautics and Space Administration. Goddard Space Flight Center, Greenbelt, MD.
CONTROL SYSTEM FOR RULING BLAZED, ABERRATION CORRECTED DIFFRACTION GRATINGS Patent Application
Douglas B. Leviton, inventor (to NASA) 23 Aug. 1990 14 p
(NASA-Case-GSC-13240-1; NAS 1.71:GSC-13240-1;
US-Patent-Appl-SN-571344) Avail: NTIS HC/MF A03 CSCL 14E

The grooved surface of an aberration-corrected holographic model grating is sensed by utilizing the sensing head of a scanning tunneling microscope. The sensing head is mechanically connected to a blazing type stylus for replicating the groove pattern of the holographic model on a ruled grating blank. A ruling engine causes the sensing head not only to scan the surface of the holographic grating model but also drive a blazing type ruling stylus or an equivalent type device in accordance with an error signal resulting from a departure of a sensing tip from the top of the holographic model groove as a function of tunneling current. NASA

N91-13693*# National Aeronautics and Space Administration. Langley Research Center, Hampton, VA.
TRANSDUCER HOLDER AND METHOD OF MAKING Patent Application
John A. Companion, inventor (to NASA) (PRC Kentron, Inc., Hampton, VA.) 25 Sep. 1990 17 p
(NASA-Case-LAR-14027-1; NAS 1.71:LAR-14027-1;
US-Patent-Appl-SN-587880) Avail: NTIS HC/MF A03 CSCL 14B

The invention is a holder for supporting and acoustically coupling a transducer to a surface of a test object. The holder is formed in one piece in a suitable mold of a castable gel-like material having a determined acoustical impedance loss characteristic, the transducer being embedded in the holder as it is formed. The transducer is prepositioned within the mold at a determined angle N relative to the surface of the test object. The gel-like material may be composed of a solution of water and ethylene glycol in a collagen matrix. NASA

N91-13694* National Aeronautics and Space Administration. Langley Research Center, Hampton, VA.
REAL-TIME DYNAMIC HOLOGRAPHIC IMAGE STORAGE DEVICE Patent
Sharon S. LaFleur, inventor (to NASA) and Raymond C. Montgomery, inventor (to NASA) 3 Apr. 1990 8 p Filed 2 Mar. 1989
(NASA-Case-LAR-13989-1; US-Patent-4,913,534;
US-Patent-Appl-SN-318217; US-Patent-Class-350-3.64;
US-Patent-Class-350-320; US-Patent-Class-350-354;
Int-Patent-Class-G03H-1/02) Avail: US Patent and Trademark Office CSCL 14B

A real-time dynamic holographic image storage device uses four-wave mixing in a pair of photorefractive crystals. An oscillation is produced between the crystals which can be maintained indefinitely after the initial object beam is discontinued. The object beam produces an interference pattern in a first crystal to produce phase-conjugated object beam which is directed towards the second crystal. In the second crystal another interference pattern is created which produces a reconstructed object beam. The reconstructed object beam is directed back towards the first crystal. The interference patterns are produced by interaction of the object and phase-conjugated object beam with a read and write beam in each of the crystals. By manipulation of the ratio of the read and write beam intensities in at least one of the crystals, the phase-conjugate or reconstructed object beam output therefrom can be amplified to maintain stable oscillation between the two crystals.

Official Gazette of the U.S. Patent and Trademark Office

N91-14042# Honeywell, Inc., Minneapolis, MN.
APPLICATION OF HIGH-TEMPERATURE SUPERCONDUCTORS TO HIGH-PRECISION ACCELEROMETERS
James Lenz, Quark Chen, James McArdle, Tom Werner, and Wayne Castleman *In* AGARD, Applications of Superconductivity to Avionics Oct. 1990 7 p Sponsored by DARPA, Washington, DC and ONR, Washington, DC (For primary document see N91-14030 05-76)
Copyright Avail: NTIS HC/MF A08; Non-NATO Nationals requests available only from AGARD/Scientific Publications Executive

N91-14043# Naval Air Development Center, Warminster, PA.
SUPERCONDUCTING JOSEPHSON JUNCTION GYROSCOPE (JJG)
Francis A. Karwacki *In* AGARD, Applications of Superconductivity to Avionics Oct. 1990 4 p (For primary document see N91-14030 05-76)
Copyright Avail: NTIS HC/MF A08; Non-NATO Nationals requests available only from AGARD/Scientific Publications Executive

36 LASERS AND MASERS

Includes parametric amplifiers.
For related information see also *76 Solid-State Physics.*

N91-13695 Hull Univ. (England).
FOLDED RF-EXCITED CO2 WAVEGUIDE LASERS Ph.D. Thesis
Paul Edward Jackson 1988 337 p
Avail: Univ. Microfilms Order No. BRDX90143

Theoretical and experimental work on radio frequency (RF) excited CO2 waveguide lasers and amplifiers are described. The mode coupling losses at a bend in a folded waveguide were evaluated as a function of the selectable parameters to determine the low-loss folding geometries. The measured laser output power as a function of discharge conditions and mirror alignment for plane and curved mirror, and partial waveguide folded resonators are compared. The Z-fold laser output power is predicted by incorporating the known and estimated laser parameters into a Rigrod-type analysis. A simultaneous solution of the Rigrod equations predicting the laser powers for different intra-cavity gain lengths is used with the experimental data to derive the discharge and resonator parameters. Experiments related to laser efficiency and frequency stability are discussed briefly. These include an investigation into an automatic impedance matching scheme for dynamic optimization of the power transfer efficiency between RF generator and the laser head. In addition, theoretical and experimental studies of laser amplification are presented. The suitability of folded waveguide and non-waveguide structures for power amplification or pre-amplification is assessed to determine their applicability to coherent light detection and ranging device optical radar (LIDAR). Optical amplification of wideband transmitter and/or receiver signals is considered a favorable way of improving the discrimination of range and velocity determinations. Finally, as a result of this work, up to 53.4 Watts was output power in a high quality fundamental Gaussian beam obtained from a compact, sealed-off, Z-fold CO2 waveguide laser with a 115 cm discharge length, which implies a specific power performance of 0.46 W/cm. Efficiencies of up to 9.2 percent were also observed.
Dissert. Abstr.

N91-13696# Schwartz Electro-Optics, Inc., Concord, MA. Research Div.
CHROMIUM SENSITIZED GARNETS FOR MID-IR LASERS Final Technical Report, 30 Jan. 1988 - 29 Jan. 1990
Peter F. Moulton 29 Jan. 1990 26 p
(Contract F49620-88-C-0046; AF Proj. 3005)
(AD-A226630; AFOSR-90-0861TR) Avail: NTIS HC/MF A03 CSCL 09/3

The characteristics of chromium-sensitized solid state lasers operating in the mid-infrared wavelength region were studied. There was continued work on crystals doped with holmium and erbium, operating in the 2100 and 2800 nm regions. In addition, preliminary measurements were made on the laser performance of thulium around 2010 nm. For all these materials the effect of pump pulse length on output energy and overall efficiency was measured. A flashlamp-pumped Cr,Nd:GSGG slab laser was operated and characterized at 1061 and 1310 nm. Measurements included comparison of normal mode slope efficiencies, input-output vs. pump pulse length, characterization of thermal lensing and measurement of Q-switched performance at 1061 nm. Spectroscopic properties of GGG crystals doped with Ce4+ ions were measured, including absorption and emission spectra and fluorescence lifetime.
GRA

N91-13697# Lawrence Livermore National Lab., CA. Dept. of Electrical and Computer Engineering.
STUDY AND DEVELOPMENT OF TUNABLE, SINGLE MODE AlGaAs/GaAs LASERS Final Report
P. K. L. Yu and J. C. Liu (California Univ., San Diego, La Jolla.) Sep. 1990 23 p
(Contract W-7405-eng-48)
(DE91-001684; UCRL-CR-104625) Avail: NTIS HC/MF A03

Liquid phase epitaxy has been employed in this study to fabricate two-section wavelength tunable lasers. GaAs/AlGaAs and In GaAsP/InP material system have been used for fabricating the lasers. Both direct (butt) coupling and evanescent coupling approaches have been studied. The complications associated with the regrowth process have been responsible for poor laser performance. Some DBR gratings for three-section lasers have been made using the electron beam lithography at UCSD. A simple set up has been tested to measure the wavelength shift of GaAs/AlGaAs lasers. Also, a simple structure which avoids the regrowth process has been proposed for the two-section laser.
DOE

N91-13698# Lawrence Livermore National Lab., CA.
ULTRA-HIGH BRIGHTNESS (GREATER THAN 10(EXP 21) W/SQ CM) LASER FACILITY
M. D. Perry, E. M. Campbell, J. T. Hunt, C. Keane, A. Szoke, Gerard Mourou, P. Bado, and P. Maine (Rochester Univ., NY.) 21 Mar. 1990 44 p Presented at the Briefing for NAS Soviet Delegation Visit to Lawrence Livermore National Laboratory, Livermore, CA, 22 Mar. 1990
(Contract W-7405-eng-48)
(DE91-001685; UCRL-JC-103354; CONF-9003224-1) Avail: NTIS HC/MF A03

New short-pulse laser technology has made possible the production of extremely bright (greater than 10(exp 18) W/sq cm-sr) laser sources. The use of these new techniques on large scale Nd:Glass based laser systems would make it possible to produce 1000 TW (Petawatt) pulses. Such pulses would yield focused intensities exceeding 10(exp 21) W/sq cm corresponding to an electric field in excess of 100 e/sq a (sub 0) and an energy density equivalent to that of a 10 keV blackbody. Such a source would have important applications in x-ray laser research and lead to a fundamentally new class of experiments in atomic, nuclear, solid state, plasma and high-energy density physics. Such a facility could be constructed with existing 'chirped-pulse' technology. A one-year period of research addressing outstanding technical questions can extend the technology resulting in a more compact and cost effective design. For this reason, we are seeking a Director's Initiative grant in the amount of $590,000 for FY89 to investigate these issues. An equivalent amount in personnel and facilities would be provided by Y-Division. The study will include development of a 'chirped-pulse' front-end capable of producing laser pulses of 2 J at 1.053 micron with a 1 psec pulsewidth laser. Upon completion, this front-end will be installed on the Nova laser system in order to investigate propagation and compression issues associated with amplification of a chirped-pulse. Our goal is to demonstrate the production of 100 TW pulses using a portion of a Nova beamline.
DOE

N91-13699# Lawrence Livermore National Lab., CA.
FREE-ELECTRON LASER EXPERIMENTS IN THE MICROWAVE TOKAMAK EXPERIMENT
S. L. Allen, M. D. Brown, J. A. Byers, T. A. Casper, B. I. Cohen, R. H. Cohen, J. C. Cummings, M. E. Fenstermacher, J. H. Foote, and E. B. Hooper et al Aug. 1990 9 p Presented at the 13th International Conference on Plasma Physics and Controlled Nuclear Fusion Research, Arlington, VA, 1-6 Oct. 1990 Submitted for publication
(Contract W-7405-eng-48)
(DE91-001746; UCRL-JC-103458; CONF-901025-15) Avail: NTIS HC/MF A02

Microwave pulses have been injected from a free electron-laser (FEL) into the Microwave Tokamak Experiment (MTX) at up to 0.2 GW at 140 GHz in short pulses (10-ns duration) with O-mode polarization. The power transmitted through the plasma was measured in an experimental study of high power pulse propagation in the plasma; no nonlinear effects were found at this power level. Calculations indicate that nonlinear effects may be found at the higher power densities expected in future experiments. DOE

N91-13700# Los Alamos National Lab., NM. Isotope and Nuclear Chemistry Div.
ACTINIDE SPECIATION BY PHOTOTHERMAL SPECTROSCOPIES: INSTRUMENTATION DEVELOPMENT
J. M. Berg, C. D. Tait, D. E. Morris, and W. H. Woodruff 1990 8 p Presented at the Fall Meeting of the Materials Research Society, Boston, MA, 26-30 Nov. 1990
(Contract W-7405-eng-36)
(DE91-001854; LA-UR-90-3641; CONF-901105-18) Avail: NTIS HC/MF A02

Photoacoustic spectroscopy using pulsed laser excitation is being developed by a number of research groups as one of the most promising methods or studying speciation of actinides in solution at environmentally relevant concentrations. We present details of a number of hardware and software techniques we have implemented to improve the sensitivity of the method. Our approach is based on more extensive waveform analysis. While most signal processing techniques extract the analytical signal from only a small portion of the acoustic waveform produced in the detector by an absorption event, we describe two methods that use more of the waveform. Other methods of minimizing noise sources using both hardware and software are also described. DOE

N91-13701# Los Alamos National Lab., NM.
DIAGNOSTICS FOR HIGH-BRIGHTNESS BEAMS
Robert E. Shafer 1990 6 p Presented at the Linear Accelerator Conference, Los Alamos, NM, 9-14 Sep. 1990
(Contract W-7405-eng-36)
(DE91-001865; LA-UR-90-3564; CONF-9009123-43) Avail: NTIS HC/MF A02

Special techniques are required for beam diagnostics on high-brightness particle beams. Examples of high-brightness beams include low-emittance proton linacs (either pulsed or CW), electron linacs suitable for free-electron-laser applications, and future linear colliders. Non-interceptive and minimally-interceptive techniques for measuring beam current, position, profile, and transverse and longitudinal emittance will be reviewed. Included will be stripline, wire scanner, laser neutralization, beam-beam scattering, interceptive micrograting, spontaneous emission, optical transition radiation, and other techniques. DOE

N91-13702# Los Alamos National Lab., NM.
FIELD ERROR LOTTERY
C. James Elliott, Brian D. McVey, and David C. Quimby (Spectra Technology, Inc., Bellevue, WA.) 1990 29 p Presented at the 12th International Free Electron Laser Conference, Paris, France, 17-21 Sep. 1990
(Contract W-7405-eng-36)
(DE91-001875; LA-UR-90-3596; CONF-9009166-10) Avail: NTIS HC/MF A03

The level of field errors in an FEL is an important determinant of its performance. We have computed 3D performance of a large laser subsystem subjected to field errors of various types. These calculations have been guided by simple models such as SWOOP. The technique of choice is utilization of the FELEX free electron laser code that now possesses extensive engineering capabilities. Modeling includes the ability to establish tolerances of various types: fast and slow scale field bowing, field error level, beam position monitor error level, gap errors, defocusing errors, energy slew, displacement, and pointing errors. Many effects of these errors on relative gain and relative power extraction are displayed and are the essential elements of determining an error budget. The random errors also depend on the particular random number seed used in the calculation. The simultaneous display of the performance versus error level of cases with multiple seeds illustrates the variations attributable to stochasticity of this model. All these errors are evaluated numerically for comprehensive engineering of the system. In particular, gap errors are found to place requirements beyond mechanical tolerances of (plus minus)25(mu)m, and amelioration of these may occur by a procedure utilizing direct measurement of the magnetic fields at assembly time. DOE

N91-13703# Idaho National Engineering Lab., Idaho Falls.
HIGH PULSE RATE INTERFEROMETRY USING A RUBY LASER AND A CORDIN MODEL 360 CAMERA
V. A. Deason and J. S. Epstein 1990 9 p Presented at the 19th International Congress on High Speed Photography and Photonics, Cambridge, England, 16-22 Sep. 1990
(Contract DE-AC07-76ID-01570)
(DE91-001882; EGG-M-90380; CONF-9009248-3) Avail: NTIS HC/MF A02

This system was originally developed in support of a dynamic diffraction moire effort, but has obvious applications to other types of imaging, interferometry, and high speed optical measurement techniques. The system includes a holographic grade Apollo ruby laser and a Cordin model 330A high speed film camera. The laser has been modified to generate a train of 1 to 100 or more pulses having individual pulse energies of about 40 mJ and a pulse width under 50 ns. The separation between pulses is currently 8 microsec, but is expected to soon be reduced to about 1 microsec. The laser pulses are synchronized with the framing sync signals from the Cordin camera, so that an individual interferogram is recorded on each of the available frames (a maximum record length of 80 frames is possible). The system is currently configured as a diffraction moire interferometer that illuminates a specimen diffraction grating with a pair of laser beams. The resulting interferograms are recorded using the Cordin camera. The system and the experimental synchronization method are described and some representative experimental data are presented. DOE

N91-13704# Lawrence Livermore National Lab., CA.
AN INTERACTIVE PROGRAM FOR THE ANALYSIS AND DESIGN OF ADVANCED LASER TARGETS
Robert Thoe 18 Apr. 1990 69 p
(Contract W-7405-eng-48)
(DE91-002542; UCRL-ID-103856) Avail: NTIS HC/MF A04

Experiments are currently in progress testing the optical quality of cryogenic targets made using the beta-layering process. This process uses the heat liberated from decaying tritium to sublimate thick parts of the DT layer. This sublimated DT is subsequently condensed on a thinner part of the shell thereby tending to equalize the layer thickness. The uniformity and stability of the ice layer formed on the inside of these capsules is of fundamental importance. The experiments now being performed simply photograph a capsule through a pair of transparent windows in the dewar as the temperature is lowered below the triple point and finally the sublimation point of the DT mixture. The analysis of these photographs is made difficult by the strong refraction and multiple reflections of the light by the sapphire shell and the relatively weak refraction at the vacuum solid DT interface. Photographs thus far obtained show very little difference between an empty shell and a shell which is believed to be uniformly layered with hydrogen ice. The difficulty in interpreting these data has led to the establishment of an effort to simulate these

measurements by direct computational methods. The code which is the subject of this report is a simple ray tracing routine which allows the operator the freedom to enter as many as 50 different objects - light sources, opaque solids or surfaces, or transparent objects, placed anywhere in space. The program is written in Absoft FORTRAN for the Amiga, but the source code should compile without any major changes and run on any Macintosh. The next section gives a brief outline of how the calculation proceeds. This is followed by a presentation of some of the results obtained and a description of some additional features being implemented for future use. A listing of the source deck is added as an appendix. This source can be downloaded from the LEAF where it resides in my file space. DOE

N91-13705# General Atomic Co., San Diego, CA.
A MULTI-LASER SYSTEM FOR A FAST SAMPLING THOMSON SCATTERING DIAGNOSTIC
P. K. Trost, T. N. Carlstrom, J. C. DeBoo, C. M. Greenfield, C.-L. Hsieh, and R. T. Snider Oct. 1990 11 p Presented at the 8th Topical Conference on High-Temperature Plasma Diagnostics, Hyannis, MA, 7-10 May 1990 Submitted for publication
(Contract DE-AC03-89ER-51114; GA Proj. 3466)
(DE91-002708; GA-A-20095; CONF-900557-29) Avail: NTIS HC/MF A03

A multi-laser system is being developed for the DIII-D Thomson scattering diagnostic. This system combines the beams from up to eight Nd:YAG lasers onto a common beamline in which the beams are nearly parallel and are all focused into a small, common area within the desired scattering volume. Each laser can be fired at a constant rate (20 Hz per laser) for a high average repetition rate, or together in a burst, which will give very high sampling rates (10 to 20 kHz) for short periods. The burst mode will be triggerable by plasma events, which will allow study of transient phenomena, but will require non-periodic firing of the lasers. Beamline diagnostics include position sensitive detectors for computer controlled feedback alignment of the 35 m beamline, an image position detection system for monitoring the alignment of the collection lens to the scattering volume, and a 1-D reticon camera for divergence monitoring. The effects of the non-periodic firing of the lasers will be monitored with the reticon camera. DOE

N91-13706# General Atomic Co., San Diego, CA.
A SILICON AVALANCHE PHOTODIODE DETECTOR CIRCUIT FOR Nd:YAG LASER SCATTERING
C.-L. Hsieh, J. Haskovec, T. N. Carlstrom, J. C. DeBoo, C. M. Greenfield, R. T. Snider, and P. Trost Jun. 1990 19 p Presented at the 8th Topical Conference on High-Temperature Plasma Diagnostics, Hyannis, MA, 7-10 May 1990 Submitted for publication
(Contract DE-AC03-89ER-51114; GA Proj. 3466)
(DE91-002709; GA-A-20094; CONF-900557-31) Avail: NTIS HC/MF A03

A silicon avalanche photodiode with an internal gain of about 50 to 100 is used in a temperature controlled environment to measure the Nd:YAG laser Thomson scattered spectrum in the wavelength range from 700 to 1150 nm. A charge sensitive preamplifier was developed for minimizing the noise contribution from the detector electronics. Signal levels as low as 20 photoelectrons (S/N = 1) can be detected. Measurements show that both the signal and the variance of the signal vary linearly with the input light level over the range of interest, indicating Poisson statistics. The signal is processed using a 100 ns delay line and a differential amplifier which subtracts the low frequency background light component. The background signal is amplified with a computer controlled variable gain amplifier and is used for an estimate of the measurement error, calibration, and Z sub eff measurements of the plasma. The signal processing was analyzed using a theoretical model to aid the system design and establish the procedure for data error analysis. DOE

N91-13707# Lawrence Livermore National Lab., CA.
USE OF DOME (MENISCUS) LENSES TO ELIMINATE BIREFRINGENCE AND TENSILE STRESSES IN SPATIAL FILTERS FOR THE NOVA LASER
John H. Pitts, Demos T. Kyrazis, Lynn G. Seppala, and Stanley E. Bumpas 22 Oct. 1990 13 p Presented at the 22nd Annual Symposium on Optical Materials for High Power Lasers, Boulder, CO, 24-26 Oct. 1990 Submitted for publication
(Contract W-7405-eng-48)
(DE91-002784; UCRL-JC-104869; CONF-9010146-1) Avail: NTIS HC/MF A03

We document the concept and the design method for dome lenses that have a compressive pressure applied to the periphery. Dome (meniscus) lenses can eliminate both birefringence and tensile stresses if used in evacuated spatial filters where a pressure difference is present across the lenses. Calculations show that spatial filter birefringence is an insignificant 3 nm within the portion of a 740 mm Nova spatial filter dome lens illuminated by the laser beam. Membrane stresses are everywhere compressive, varying from -1.2 to -2.4 MPa, and are nearly uniform over the illuminated portion of the lens. Eliminating sources of birefringence on the Nova laser could increase the energy on target with Type II/Type II frequency conversion from approximately 50 percent to the approximately 70 percent level attainable with Type I/Type II frequency conversion. Eliminating tensile stresses may reduce the damage and catastrophic failure that has occurred in some Nova spatial filter input lenses. The major disadvantage of using dome lenses on Nova is the cost of new lenses which could range up to $50,000 per lens for the material and $20,000 per lens for finishing. DOE

N91-13708# Laboratoire d'Automatique et d'Analyse des Systemes, Toulouse (France).
DESIGN OF GaAlAs/GaAs GRIN-SCH SQW DIODE LASERS. ANALYSIS OF THE TEMPERATURE DEPENDENCE Ph.D. Thesis - Inst. National des Sciences Appliquees de Toulouse
Stephane Fourtine 1990 127 p In FRENCH: ENGLISH summary
(LAAS-90277; ETN-91-98217) Avail: NTIS HC/MF A07

A model for computer aided design of GaAlAs/GaAs quantum well GRIN-SCH (Graded Index-Separate Confinement Heterostructure) lasers diodes is developed. The methodology allows to predict, for any given structure, the gain current characteristic, the laser wavelength and the threshold current density. Temperature is introduced as a variable parameter. The two dimensional physical phenomena taking place in the quantum well and the recombinations in the well and in the confining layers are studied. Special attention is paid to the determination of the possible losses in the structure, depending on the quantum well composition and on the temperature. A systematic study leads to optimization criteria relative to the threshold current density and the temperature stability parameter. Experimental characterizations performed on quantum well diode lasers made by molecular beam epitaxy with 0, 15, and 20 percent aluminum composition in the well are presented. Comparison of theoretical and experimental results allows determination of the internal losses of the device thus giving an estimation of the quality of the structure. Characterizations of the laser wavelength, threshold current density, and parameters are shown to be in good agreement with the results predicted by the model. ESA

N91-13709# Lawrence Livermore National Lab., CA.
LASER PROGRAMS HIGHLIGHTS, JULY - AUGUST 1990
1990 18 p
(Contract W-7405-eng-48)
(DE91-001056; UCRL-ID-104374) Avail: NTIS HC/MF A03

Laser research at Lawrence Livermore National Laboratory (LLNL) is divided into five major programmatic areas: inertial confinement fusion (ICF), uranium atomic vapor laser isotope separation (U-AVLIS), special (plutonium) isotope separation (SIS), laser technology, and advanced applications. We have made important progress this past year in each of these areas. This report covers the current state of these 5 areas. DOE

37 MECHANICAL ENGINEERING

Includes auxiliary systems (nonpower); machine elements and processes; and mechanical equipment.

N91-13710 Newcastle-upon-Tyne Univ. (England).
EFFECT OF LUBRICATING OIL CHARACTERISTICS ON GEAR VIBRATIONS Ph.D. Thesis
P. A. B. A. R. Perera 1986 308 p
Avail: Univ. Microfilms Order No. BRDX89939

An extensive literature survey of the subject of gear dynamics is undertaken and the increasing recognition of the role of the lubricating oil film in this field, especially as a damping source, is highlighted. The oil film separating the mating surfaces of involute spur gears is analyzed assuming hydrodynamic conditions, rigid teeth (as far as the film shape is concerned), and pressure dependent viscosity. Gear tooth mesh stiffness is expressed as a function of the dynamic load and the position of contact. A simple model of a pair of spur gears is subjected to a transient response analysis and the behavior of the lubricating oil film observed. According to the motions of equivalent masses of the gears under these transient conditions, damping due to the oil film is determined. The numerical solutions obtained at various operating conditions are combined to form an approximate formula to predict the damping ratio in terms of the dynamic tooth load, rolling speed of the tooth surfaces and the viscosity of the lubricating oil. A digital computer simulation of the dynamic motion of the pair of gears is carried out incorporating the above damping ratio formula. The actual load sharing between the pairs of teeth is taken into account. The variations of the total maximum dynamic load and the maximum tooth load are studied under different nominal loads, contact ratios, oil viscosities, and pitch errors over a wide range of speeds covering the resonance area. The variations of the dynamic load, individual tooth load, mesh stiffness, and the oil film thickness during complete mesh cycles are also analyzed under different operating conditions to identify particular areas where high loads and minimum film thicknesses occur. Theoretical results are compared with the experimental results obtained on a back-to-back gear test rig. Dissert. Abstr.

N91-13711# Department of the Navy, Washington, DC.
SHEAVE ASSEMBLY Patent Application
Eldon N. Jorgensen, inventor (to Navy) 2 Apr. 1990 16 p
(AD-D014605; US-Patent-Appl-SN-507264; Navy-Case-71636)
Avail: NTIS HC/MF A03 CSCL 13/9

The disclosure describes a sheave that has the advantage of being able to be quickly coupled to a cable, and quickly decoupled from the cable. A further advantage is that the shaft of the pulley on which the cable rides is journaled at each end in side members that interlock when the sheave is in its closed position to support the shaft both from above the pulley, and from below. Other advantages include that the interlock is an arcuate T-shaped extension in the rotatable side member and a corresponding arcuate T-slot groove with which it engages in the stationary side member. The rotatable side member is affixed to the shaft of the pulley and is operable to rotate about the shaft from its closed and interlocked position to its open and disengaged position whereas the pulley is exposed such that the cable, cord or the like may be coupled or decoupled to the pulley. In the open position the side members only are connected by way of the pulley's shaft, whereas in the closed and load bearing position the side members additionally are supported to one another by the T-slot interlock that is both above and below the pulley. A slip ring lock is included to retain the side members in their interlocked position. GRA

N91-13712# Contraves Goerz Corp., Pittsburgh, PA.
THE IMPROVED THREE AXIS TEST TABLE (ITATT): PROGRAM STATUS AND RECOMMENDATION FOR COMPLETION Interim Report
Aug. 1990 254 p
(Contract F08635-89-C-0297)
(AD-A226508; TR-27824) Avail: NTIS HC/MF A12 CSCL 14/2

In May 1989 Contraves was awarded Phase 1 of the Improved Three-Axis Test Table (ITATT) program to develop the inner axis of what will eventually be the complete three axis ITATT. Phase 1 is a proof of principle research and development effort and is a cost plus incentive fee contract. Phase 2 is a firm fixed price not to exceed option that will incorporate the Phase 1 inner axis into new middle and outer taxes. Several critical ITATT technologies are being demonstrated in Phase 1 including: CFRP gimbals, roll rings, magnetic bearings, induction or A.C. motors, and back-to-back Inductosyn encoding. Based on a 1984 government funded design study, these technologies can be used to test table with 0.1 arc second pointing accuracy, which is a factor of ten improvement over current test tables. Contraves has worked diligently over the past 14 months to achieve the Phase 1 proof of principle objectives and has made significant progress. As of August 10, 1990, the baseline hardware is assembled, wired, integrated, and partially tested. GRA

N91-13713# Massachusetts Inst. of Tech., Cambridge. Dept. of Ocean Engineering.
MATERIAL AND MECHANICAL CHARACTERIZATIONS FOR BRAIDED COMPOSITE PRESSURE VESSELS M.S. Thesis
Brian Kent Antonio May 1990 118 p
(Contract N00123-89-G-0580)
(AD-A226640) Avail: NTIS HC/MF A06 CSCL 11/4

The materials studied include S-2 glass, carbon, and aramid (Kevlar) fiber reinforced epoxy composites (glass/epoxy, carbon/epoxy, and Kevlar/epoxy, respectively). Twelve material configurations are evaluated. Width-effects determination is conducted to examine the effect of cutting braided specimens from larger panels. Tensile strength and tensile modulus are measured on each material at room temperature and humidity, and on materials conditioned via exposure to a 560 F environment for one second but tested at room temperature and humidity. Resistance to slow and fast heat application (slow and fast cook-off, respectively) is examined to qualitatively determine material response. Additionally, a literature review of hygrothermo-mechanical effects is conducted. Width effects determination testing shows that as specimen width is increased average tensile strength increases sharply and levels off to a relatively constant value above a specimen width of 2 inches. Thus, the specimen width is set at 2 inches in the tensile test portion of the research. Mechanical property data are presented for the various material configurations. Braid angle is shown to have a strong influence on tensile properties in single ply braided composites. Single ply and dual ply S-2 glass/epoxy composites have higher tensile strength and tensile modulus than their Kevlar/epoxy counterparts of similar configuration. Combining Kevlar/epoxy and carbon/epoxy materials into a composite sandwich significantly improves the tensile properties of Kevlar/epoxy single ply and dual ply materials. GRA

N91-13714# Massachusetts Inst. of Tech., Cambridge. Dept. of Ocean Engineering.
TRITIUM METHOD OIL CONSUMPTION AND ITS RELATION TO OIL FILM THICKNESS IN A PRODUCTION DIESEL ENGINE M.S. Thesis
Richard M. Hartman Jun. 1990 86 p
(Contract N00123-89-G-0580)
(AD-A226649) Avail: NTIS HC/MF A05 CSCL 21/4

Oil consumption was measured in a modern production diesel engine using tritium as a radiotracer. The measurements were made primarily at two speeds and one load using first a single grade lubricant and then a multigrade lubricant. These values were then compared to oil flow rates up/down the liner which were based on film thickness traces of a sister engine under the same loads and speeds. The traces were obtained using the laser fluorescence technique. For the most part, it was discovered that there does not seem to exist a correlation between these flow rates and oil consumption. However, the traces do reveal that the crown land is dry on all four strokes and thus does not contribute to the engine's oil consumption. A larger data base is necessary

in order to accurately compare oil consumption to the film traces. GRA

N91-13715# Massachusetts Inst. of Tech., Cambridge. Dept. of Ocean Engineering.
ANALYSIS OF SINGLE AND MULTI-GRADE LUBRICANT FILM THICKNESS IN A DIESEL ENGINE M.S. Thesis
Mark Joseph Olechowski Jun. 1990 78 p
(Contract N00123-89-G-0580)
(AD-A226651) Avail: NTIS HC/MF A05 CSCL 11/8

Several recent experiments were made to attempt to determine the rheology of the lubricant in journal bearings of engines. A laser fluorescence technique in use at the Massachusetts Institute of Technology allows accurate data collection of the oil film thickness on the ring pack of a production diesel engine. The data collected from the Kubota EA300N IDI engine consisted of five different types of lubricant under the compression ring acts in a Newtonian manner independent of lubricant type or inertial effects. The difference between the types of lubricants appears to be the degree to which oil wets the ring with the single-grade oils wetting the ring more thoroughly than do the multigrades. A consistent linear relationship between the inlet wetting of the ring and the bearing number (a non-dimensional lift term) was found to exist for each stroke. Drag was also found to be inversely proportional to the amount of inlet wetting. GRA

N91-13716# Department of the Navy, Washington, DC.
HEAT ENGINE WITH CORRUGATED SHAPE MEMORY DRIVE BELT Patent Application
David Goldstein, inventor (to Navy) 19 Jul. 1990 9 p
(AD-D014640; US-Patent-Appl-SN-554509; Navy-Case-72787)
Avail: NTIS HC/MF A02 CSCL 13/9

An endless drive belt made of shape memory material is entrained about spaced pulleys, one of which projects into a thermal heating region within which the drive belt undergoes contraction to form corrugations therein through which variable spaced contact is established with said one of the pulleys to induce rotation thereof and movement of the belt. The belt expands as it moves out of the thermal heating region causing the corrugations to flatten out as the belt approaches the outer pulley. GRA

N91-13717# Consiglio Nazionale delle Ricerche, Frascati (Italy). Ist. di Fisica dello Spazio Interplanetario.
DESIGN OF A MECHANICAL MODULATOR FOR THE PLANETARY FOURIER SPECTROMETER EXPERIMENT OF THE MARS 94 MISSION [STUDIO DI UN PROGETTO DI UN MODULATORE MECCANICO PER L'ESPERIMENTO PLANETARY FOURIER SPECTROMETER DELLA MISSIONE MARS 94]
Paolo Baldetti Dec. 1989 40 p In ENGLISH and ITALIAN
(IFSI-89-22; ETN-90-97783) Avail: NTIS HC/MF A03

A 6 mm mirror is made to oscillate with the help of a piezoelectric transducer mechanically coupled to the mirror. Drawings are included. The assembly procedure and the transducer characteristics are included. ESA

N91-13718# Oak Ridge National Lab., TN.
RESULTS FROM THE SECOND YEAR OF OPERATION OF THE FEDERAL METHANOL FLEET AT OAK RIDGE NATIONAL LABORATORY
B. H. West, R. N. McGill, and S. L. Hillis (Tennessee Univ., Knoxville.) Sep. 1990 38 p
(Contract DE-AC05-84OR-21400)
(DE91-000543; ORNL/TM-11622) Avail: NTIS HC/MF A03

The Oak Ridge National Laboratory has completed its second year of operation of ten vehicles for the Federal Methanol Fleet Project; five of the vehicles are fueled with methanol. Over 56,000 miles were accumulated on the vehicles in the second year bringing the total to over 152,000 miles. Energy consumption for the methanol cars was slightly higher than that of the gasoline cars again this year, most likely as a result of shorter average trip lengths for the methanol gas. Iron and lead have accumulated at greater rates in the lubricating oil of the methanol cars. Driver's ratings of vehicles reflected some dissatisfaction with the cold-weather performance of the methanol cars, but the cars have no special provisions for cold weather starting, and the fuel vapor pressure has not been tailored to the season as at other test sites. Otherwise, drivers' opinions of the methanol cars have been favorable. DOE

N91-13719# Westinghouse Idaho Nuclear Co., Inc., Idaho Falls.
IMPROVED PLUG VALVE COMPUTER-AIDED DESIGN OF PLUG ELEMENT
J. J. Wordin Feb. 1990 36 p
(Contract DE-AC07-84ID-12435)
(DE91-001044; WINCO-1080) Avail: NTIS HC/MF A03

The purpose of this document is to present derivations of equations for the design of a plug valve and to present a computer program which performs the design calculations based on the derivations. The valve is based on a plug formed from a tractrix of revolution called a pseudosphere. It is of interest to be able to calculate various parameters for the plug for design purposes. For example, the surface area, volume, and center of gravity are important to determine friction and wear of the valve. A computer program in BASIC has been written to perform the design calculations. The appendix contains a computer program listing and verifications of results using approximation methods. A sample run is included along with necessary computer commands to run the program. DOE

N91-13720# Los Alamos National Lab., NM.
TRANSIONOSPHERIC PROPAGATION CALCULATIONS FOR THE OUTPUT OF TWO EMP (ELECTROMAGNETIC PULSE) SIMULATORS
Robert Roussel-Dupre Nov. 1990 41 p
(Contracts W-7405-eng-36; F62400-90-0034)
(DE91-001618; LA-11900-MS) Avail: NTIS HC/MF A03

The Los Alamos transionospheric propagation code (TIPC) was used to calculate the transionospheric signals corresponding to the computed output of two electromagnetic pulse (EMP) simulators, the NAVES II vertical polarization dipole and the TACAMO horizontal polarization dipole. The EMP calculations used as input to TIPC were performed by Mission Research Corporation. The 1986 International Reference Ionosphere code was used to generate vertical profiles of electron density over a twenty-four hour period for the geographical location of the NAVES II EMP simulator and for a solar content, used as input to TIPC, was calculated from the electron density profiles by integrating along a given line of sight. The maximum root mean square power densities to be expected in each of eight broadband receivers with bandwidths of 5 and 20 MHz centered at 200, 120, 80, and 40 MHz are presented. DOE

N91-13721*# Texas Univ., Austin. Dept. of Mechanical Engineering.
THE EFFECT OF INERTIAL COUPLING IN THE DYNAMICS AND CONTROL OF FLEXIBLE ROBOTIC MANIPULATORS Final Report
Delbert Tesar, Carol Cockrell Curran, and Philip Lee Graves Aug. 1988 166 p
(Grant NAG9-360)
(NASA-CR-187679; NAS 1.26:187679) Avail: NTIS HC/MF A08 CSCL 13I

A general model of the dynamics of flexible robotic manipulators is presented, including the gross motion of the links, the vibrations of the links and joints, and the dynamic coupling between the gross motions and vibrations. The vibrations in the links may be modeled using lumped parameters, truncated modal summation, a component mode synthesis method, or a mixture of these methods. The local link inertia matrix is derived to obtain the coupling terms between the gross motion of the link and the vibrations of the link. Coupling between the motions of the links results from the kinematic model, which utilizes the method of kinematic influence. The model is used to simulate the dynamics of a flexible space-based robotic manipulator which is attached to a spacecraft, and is free to move with respect to the inertial reference frame.

This model may be used to study the dynamic response of the manipulator to the motions of its joints, or to externally applied disturbances. Author

N91-13722*# Texas Univ., Austin. Dept. of Mechanical Engineering.
DYNAMIC MODELING, PROPERTY INVESTIGATION, AND ADAPTIVE CONTROLLER DESIGN OF SERIAL ROBOTIC MANIPULATORS MODELED WITH STRUCTURAL COMPLIANCE Final Report
Delbert Tesar, Sabri Tosunoglu, and Shyng-Her Lin Dec. 1990 359 p Sponsored in part by Cray Research, Inc.
(Contract NAG9-360; DE-FG02-86NE-37966)
(NASA-CR-187678; NAS 1.26:187678) Avail: NTIS HC/MF A16 CSCL 13I

Research results on general serial robotic manipulators modeled with structural compliances are presented. Two compliant manipulator modeling approaches, distributed and lumped parameter models, are used in this study. System dynamic equations for both compliant models are derived by using the first and second order influence coefficients. Also, the properties of compliant manipulator system dynamics are investigated. One of the properties, which is defined as inaccessibility of vibratory modes, is shown to display a distinct character associated with compliant manipulators. This property indicates the impact of robot geometry on the control of structural oscillations. Example studies are provided to illustrate the physical interpretation of inaccessibility of vibratory modes. Two types of controllers are designed for compliant manipulators modeled by either lumped or distributed parameter techniques. In order to maintain the generality of the results, neither linearization is introduced. Example simulations are given to demonstrate the controller performance. The second type controller is also built for general serial robot arms and is adaptive in nature which can estimate uncertain payload parameters on-line and simultaneously maintain trajectory tracking properties. The relation between manipulator motion tracking capability and convergence of parameter estimation properties is discussed through example case studies. The effect of control input update delays on adaptive controller performance is also studied. Author

N91-13723*# National Aeronautics and Space Administration. Lyndon B. Johnson Space Center, Houston, TX.
TWO FAULT TOLERANT TOGGLE-HOOK RELEASE Patent Application
Thomas Joseph Graves, inventor (to NASA) and Christopher William Brown, inventor (to NASA) (Boeing Aerospace Co., Seattle, WA.) 25 Oct. 1990 19 p
(NASA-Case-MSC-21671-1; NAS 1.71:MSC-21671-1; US-Patent-Appl-SN-603337) Avail: NTIS HC/MF A03 CSCL 13I

A coupling device is disclosed which is mechanically two fault tolerant for release. The device comprises a fastener plate and fastener body, each of which is attachable to a different one of a pair of structures to be joined. The fastener plate and body are coupled by an elongate toggle mounted at one end in a socket on the fastener plate for universal pivotal movement thereon. The other end of the toggle is received in an opening in the fastener body and adapted for limited pivotal movement therein. The toggle is adapted to be restrained by three latch hooks arranged in symmetrical equiangular spacing about the axis of the toggle, each hook being mounted on the fastener body for pivotal movement between an unlatching non-contact position with respect to the toggle and a latching position in engagement with a latching surface of the toggle. The device includes releasable lock means for locking each latch hook in its latching position whereby the toggle coupies the fastener plate to the fastener body and means for releasing the lock means to unlock each said latch hook from the latch position whereby the unlocking of at least one of the latch hooks from its latching position results in the decoupling of the fastener plate from the fastener body. NASA

N91-13724*# National Aeronautics and Space Administration. Pasadena Office, CA.
BILEVEL SHARED CONTROL FOR TELEOPERATORS Patent Application
Samad A. Hayati, inventor (to NASA) and Subramanian T. Venkataraman, inventor (to NASA) (Jet Propulsion Lab., California Inst. of Tech., Pasadena.) 11 May 1990 44 p
(Contract NAS7-918)
(NASA-Case-NPO-17800-1-CU; NAS 1.71:NPO-17800-1-CU; US-Patent-Appl-SN-522949) Avail: NTIS HC/MF A03 CSCL 13I

A shared system is disclosed for robot control including integration of the human and autonomous input modalities for an improved control. Autonomously planned motion trajectories are modified by a teleoperator to track unmodeled target motions, while nominal teleoperator motions are modified through compliance to accommodate geometric errors autonomously in the latter. A hierarchical shared system intelligently shares control over a remote robot between the autonomous and teleoperative portions of an overall control system. Architecture is hierarchical, and consists of two levels. The top level represents the task level, while the bottom, the execution level. In space applications, the performance of pure teleoperation systems depend significantly on the communication time delays between the local and the remote sites. Selection/mixing matrices are provided with entries which reflect how each input's signals modality is weighted. The shared control minimizes the detrimental effects caused by these time delays between earth and space. NASA

N91-13725*# Texas Univ., Austin. Computer and Vision Research Center.
POSITIONAL ESTIMATION TECHNIQUES FOR AN AUTONOMOUS MOBILE ROBOT Final Report
N. Nandhakumar and J. K. Aggarwal 1990 42 p
(Grant NAG9-361)
(NASA-CR-187689; NAS 1.26:187689) Avail: NTIS HC/MF A03 CSCL 13I

Techniques for positional estimation of a mobile robot navigation in an indoor environment are described. A comprehensive review of the various positional estimation techniques studied in the literature is first presented. The techniques are divided into four different types and each of them is discussed briefly. Two different kinds of environments are considered for positional estimation; mountainous natural terrain and an urban, man-made environment with polyhedral buildings. In both cases, the robot is assumed to be equipped with single visual camera that can be panned and tilted and also a 3-D description (world model) of the environment is given. Such a description could be obtained from a stereo pair of aerial images or from the architectural plans of the buildings. Techniques for positional estimation using the camera input and the world model are presented. Author

N91-13726# Lawrence Livermore National Lab., CA.
PENETRATION OF YAWED PROJECTILES
John E. Reaugh Oct. 1990 46 p
(Contract W-7405-eng-48)
(DE91-001084; UCRL-ID-104890) Avail: NTIS HC/MF A03

We used computer simulations and experiment to study the penetration of tungsten-alloy projectiles into a thick, armored steel target. These projectiles, with length-to-diameter ratios of 4, strike the target with severe yaws, up to 90 deg (side-on-impact), such as might be induced in an originally longer projectile by a multiple-spaced plate array. In this study, we focus on the terminal ballistics of these projectiles and ignore how the yaw was induced. We found that the minimum penetration depth occurs at 90 deg yaw. This case is well approximated by the two-dimensional plane-strain penetration of a side-on cylinder. The ratio of penetration depth to diameter, P:D, for this case is larger than that for a sphere because the plane-strain geometry lacks hoop stress, which is activated in axisymmetric geometry. A more surprising result of work is that the penetration at 60 deg yaw is only slightly deeper than that of the side-on impact. DOE

N91-13727# EG and G Rocky Flats, Inc., Golden, CO.
MATHEMATICAL MODELLING OF PART VOLTAGE AND WELD CURRENT IN RESISTANCE WELDERS
D. E. Destefan 11 Sep. 1990 18 p
(Contract DE-AC34-90DP-62349)
(DE91-002534; RFP-4218; DOE/OSTI-4500-R75) Avail: NTIS HC/MF A03

A mathematical model is presented to describe the part voltage and weld current that occur in a single-phase resistance welder. Developing an accurate model of part voltage and current is the first step toward understanding instrumentation, testing, calibration, and measurement requirements. Measurement requirements for dynamic part resistance, calculated from these basic process variables, can ultimately be determined using this analysis. This model utilizes electrical characteristics of the welder, power system, and parts, as well as geometric parameters of voltage-sensing wires to describe the resultant time functions. The complete equivalent circuit involves many resistive and inductive components in the welder primary and secondary circuits. These components are reduced to a simple equivalent circuit to obtain a closed-form solution for part voltage and weld current time functions. Actual measurements were acquired from a welder using a constant resistance load to verify accuracy of the model. Accuracy of the model is estimated to be within the measurement uncertainty and is, in general, approximately plus or minus 3 percent for current and plus or minus 5 percent for part voltage. Pertinent limitations of the model's accuracy and range of applications are also discussed briefly. DOE

N91-13728# Laboratoire d'Automatique et d'Analyse des Systemes, Toulouse (France).
MODELING AND CONTROL OF A REDUNDANT ROBOT MANIPULATOR COMPOSED OF SEVERAL STEWART PLATFORMS Ph.D. Thesis - Toulouse Univ.
Sylvie Charentus 1990 131 p In FRENCH; ENGLISH summary
(LAAS-90146; ETN-91-98213) Avail: NTIS HC/MF A07

Modeling of a robot manipulator composed of several Stewart platforms connected in series is discussed. From the mechanical point of view this robot possesses advantages of simplicity and rigidity but its structure of closed complex kinematic chain complicates modeling. Modeling consists of the calculation of transformations between generalized coordinates space, linked to the configuration, and operational coordinates space, linked to the end effector location. The singularities that characterize the workspace are then determined. Kinematic chains are studied topologically and geometrically. A vocabulary usable in robotics is developed. Stewart platform models are presented as an original solution to the direct geometric model which calculates operational coordinates from generalized coordinates. Robot modeling, composed of several Stewart platforms, is realizable if this structure is considered as a serial kinematic chain with several complex joints, each complex joint being a Stewart platform. As a practical application, the LC robot control, a prototype composed of four Stewart platforms built by Logabex company, is presented. ESA

N91-13729*# National Aeronautics and Space Administration. Marshall Space Flight Center, Huntsville, AL.
SOLDER DROSS REMOVAL APPARATUS Patent Application
Winston S. Webb, inventor (to NASA) (Honeywell, Inc., Minneapolis, MN.) 16 May 1990 12 p
(NASA-Case-MFS-28406-1; NAS 1.71:MFS-28406-1;
US-Patent-Appl-SN-524110) Avail: NTIS HC/MF A03 CSCL 13I

An automatic dross removal apparatus is disclosed for removing dross from the surface of a solder bath in an automated electric component handling system. A rotatable wiper blade is positioned adjacent the solder bath which skims the dross off of the surface prior to the dipping of a robot conveyed component into the bath. An electronic control circuit causes a motor to rotate the wiper arm one full rotational cycle each time a pulse is received from a robot controller as a component approaches the solder bath. NASA

N91-13730*# National Aeronautics and Space Administration. Lewis Research Center, Cleveland, OH.
POST CLAMP Patent Application
John K. Ramsey, inventor (to NASA) and Erwin M. Meyn, inventor (to NASA) 29 Sep. 1989 15 p
(NASA-Case-LEW-14862-1; NAS 1.71:LEW-14862-1;
US-Patent-Appl-SN-414816) Avail: NTIS HC/MF A03

A pair of spaced collars are mounted at right angles on a clamp body by retaining rings which enable the collars to rotate with respect to the clamp body. Mounting posts extend through aligned holes in the collars and clamp body. Each collar can be clamped onto the inserted post while the clamp body remains free to rotate about the post and collar. The clamp body is selectively clamped onto each post. NASA

N91-13731*# National Aeronautics and Space Administration. Marshall Space Flight Center, Huntsville, AL.
CANTILEVER CLAMP FITTING Patent Application
Patrick B. Melton, inventor (to NASA) (United Technologies Corp., Huntsville, AL.) 28 Dec. 1989 12 p
(NASA-Case-MFS-28328-1; NAS 1.71:MFS-28328-1;
US-Patent-Appl-SN-458065) Avail: NTIS HC/MF A03 CSCL 13I

A device is disclosed for sealing and clamping a cylindrical element which is to be attached to an object such as a wall, a pressurized vessel or another cylindrical element. The device includes a gland having an inner cylindrical wall, which is threaded at one end and is attached at a bendable end to a deformable portion, which in turn is attached to one end of a conical cantilever structure. The other end of the cantilever structure connects at a bendable area to one end of an outer cylindrical wall. The opposite end of cylindrical wall terminates in a thickened portion, the radially outer surface of which is adapted to accommodate a tool for rotating the gland. The terminal end of cylindrical wall also includes an abutment surface, which is adapted to engage a seal, which in turn engages a surface of a receiver. The receiver further includes a threaded portion for engagement with the threaded portion of gland whereby a tightening rotation of gland relative to receiver will cause relative movement between cylindrical walls and of gland. This movement causes a rotation of the conical structure and thus a bending action at bending area and at the bending end of the upper end of inner cylindrical wall. These rotational and bending actions result in a forcing of the deformable portion radially inwardly so as to contact and deform a pipe. This forcible contact creates a seal between gland and pipe, and simultaneously clamps the pipe in position. NASA

N91-13732*# National Aeronautics and Space Administration. Lewis Research Center, Cleveland, OH.
PROBE INSERTION APPARATUS WITH INFLATABLE SEAL Patent Application
Paul A. Trimarchi, inventor (to NASA) 23 Aug. 1990 17 p
(NASA-Case-LEW-14965-1; NAS 1.71:LEW-14965-1;
US-Patent-Appl-SN-571062) Avail: NTIS HC/MF A03 CSCL 13I

A sealing apparatus is disclosed for inserting a probe into a pressure vessel having an elongated opening includes a pair of resiliently deformable seals opposingly disposed in sealing engagement with each other. A retainer is connected to the pressure vessel around the elongated opening and holds the pair of seals rigidly to the pressure vessel. A wedge is engageable with the pair of seals and carries the probe, for longitudinally translating the probe in pressure vessel. NASA

N91-13733*# National Aeronautics and Space Administration. John C. Stennis Space Center, Bay Saint Louis, MS.
HYDRAULIC LIFTING DEVICE Patent Application
Kyle Terrell, inventor (to NASA) (Sverdrup Technology, Inc., Bay Saint Louis, MS.) 28 Jun. 1990 11 p
(NASA-Case-SSC-00008-1; NAS 1.71:SSC-00008-1;
US-Patent-Appl-SN-545178) Avail: NTIS HC/MF A03 CSCL 13I

A piston and cylinder assembly is disclosed which is constructed

of polyvinyl chloride that uses local water pressure to perform small lifting tasks. The chamber is either pressurized to extend the piston or depressurized to retract the piston. The present invention is best utilized for raising and lowering toilet seats.
NASA

N91-13734*# National Aeronautics and Space Administration. Goddard Space Flight Center, Greenbelt, MD.
DEVICE FOR APPLYING CONSTANT PRESSURE TO A SURFACE Patent Application
Eve Abrams, inventor (to NASA) 31 May 1990 10 p
(NASA-Case-GSC-13230-1; NAS 1.71:GSC-13230-1; US-Patent-Appl-SN-531374) Avail: NTIS HC/MF A02 CSCL 13I

A device for applying constant pressure to a surface is disclosed. The device includes a cylinder having a longitudinal axis greater than the diameter of the cylinder. A first wheel and a second wheel are coupled to each end, respectively, of the cylinder. The wheels have a diameter substantially greater than the diameter of the cylinder. An elastomeric covering surrounds the cylinder. The elastomeric covering has an outer diameter substantially greater than the diameter of the wheels. A handle is coupled to the wheels for rolling and applying pressure to the elastomeric covering.
NASA

N91-13735*# National Aeronautics and Space Administration. Goddard Space Flight Center, Greenbelt, MD.
ROBOT CABLE-COMPLIANT DEVICES Patent Application
James J. Kerley, Jr., inventor (to NASA) 13 May 1988 25 p
(NASA-Case-GSC-13127-1; NAS 1.71:GSC-13127-1; US-Patent-Appl-SN-193612) Avail: NTIS HC/MF A03 CSCL 20E

A cable-compliant robotic joint includes two U configuration cross-section brackets with their U cross-sections lying in different planes, one of the brackets being connected to a robot arm and the other to a tool. Additional brackets are displaced from the other brackets at corners of the robotic joint. All the brackets are connected by cable segments which lie in one or more planes which are perpendicular to the direction of tool travel as it approaches a work object. The compliance of the joint is determined by the cable segment characteristics, such as their length, material, angle, stranding, pre-twisting and pre-stressing.
NASA

N91-13736# Sandia National Labs., Albuquerque, NM.
TUBULAR LAP JOINTS FOR WIND TURBINE APPLICATIONS
E. D. Reedy, Jr. and T. R. Guess 1990 6 p Presented at the 14th Energy-Sources Technology Conference and Exhibition, Houston, TX, 20-24 Jan. 1991
(Contract DE-AC04-76DP-00789)
(DE91-001341; SAND-90-1978C; CONF-910104-1) Avail: NTIS HC/MF A02

A combined analytical/experimental study of the strength of thick-walled, adhesively bonded poly(methyl methacrylate) (PMMA)-to-aluminum and E-glass/epoxy composite-to-aluminum tubular lap joints under axial load has been conducted. Test results include strength and failure mode data. Moreover, strain gages placed along the length of the outer tubular adherend characterize load transfer from one adherend to the other. The strain gage data indicate that load transfer is nonuniform and that the relatively compliant PMMA has the shorter load transfer length. Strains determined by a finite element analysis of the tested joints are in excellent agreement with those measured. Calculated bond stresses are highest in the region of observed failure, and extensive bond yielding is predicted in the E-glass/epoxy composite-to-aluminum joint prior to joint failure.
DOE

N91-13737*# Ohio State Univ., Columbus. Dept. of Mechanical Engineering.
NON-LINEAR DYNAMIC ANALYSIS OF GEARED SYSTEMS Final Report Ph.D. Thesis
Rajendra Singh, Donald R. Houser, and Ahmet Kahraman Washington NASA Nov. 1990 245 p
(Grant NAG3-773)
(NASA-CR-4338; AVSCOM-TR-90-C-020; E-5718; NAS 1.26:4338) Avail: NTIS HC/MF A11 CSCL 13I

Under driving conditions, a typical geared system may be subjected to large dynamic loads. Also, the vibration level of the geared system is directly related to the noise radiated from the gear box. The steady state dynamic behavior of the system is examined in order to design reliable and quiet transmissions. The scope is limited to a system containing a spur gear pair with backlash and periodically time varying mesh stiffness, and rolling element bearings with clearance type nonlinearities. The internal static transmission error at the gear mesh, which is of importance from high frequency noise and vibration control view point, is considered in the formulation in sinusoidal or periodic form. A dynamic finite element model of the linear time invariant (LTI) system is developed. Effects of several system parameters, such as torsional and transverse flexibilities of the shafts and prime mover/load inertias, on free and forced vibration characteristics are investigated. Several reduced order LTI models are developed and validated by comparing their eigen solutions with the finite element model results. Using the reduced order formulations, a three degree of freedom dynamic model is developed which includes nonlinearities associated with radical clearances in the radial rolling element bearings, backlash between a spur gear pair and periodically varying gear mesh stiffness. As a limiting case, a single degree of freedom model of the spur gear pair with backlash is considered and mathematical conditions for tooth separation and back collision are defined. Both digital simulation technique and analytical models such as method of harmonic balance and the method of multiple scales were used to develop the steady state frequency response characteristics for various nonlinear and/or time varying cases.
Author

N91-13738# Institut de Soudure, Paris (France).
EVALUATION OF THE FUNCTIONAL PROPERTIES OF WELDS ON COLD FINISHED TUBES DEFINED AS NF A 49.541 Final Report [EVALUATION DES PROPRIETES D'EMPLOI DES SOUDURES SUR TUBES FINIS A FROID DEFINIS PAR LA NF A 49.541]
P. Roguin and R. Gaillard Nov. 1989 24 p In FRENCH Prepared in cooperation with Centre Technique des Industries Mecaniques, Nantes, France
(CETIM-104700; IS-24-288; ETN-91-98325) Copyright Avail: NTIS HC/MF A03

Comparisons are made between hot and cold finished tubes defined as NF A 49-541 of dimensions 89-5 and 48-4. Traction properties, and hardness and resilience figures are compared for the hot and cold finished tubes. These tests are carried out on the base metal, the assembled tube submitted to a conventional aging treatment at 250 C. The results show little difference in the behavior in the two different types of pipe. Aging of the cold finished tubes is not affected by a total flattening. The test results show these assemblies to be satisfactory as compared to hot finished tubes.
ESA

N91-13739# Institut de Soudure, Paris (France).
THE EFFECTS OF THERMAL TREATMENT AFTER WELDING ON THE FUNCTIONAL PROPERTIES OF ASSEMBLIES. FOLLOW-UP OF THE WORK ON Cr-Mo Final Report [EFFET DU TRAITEMENT THERMIQUE APRES SOUDAGE SUR LES PROPRIETES D'EMPLOIS DES ASSEMBLAGES. POURSUITE DES TRAVAUX SUR LES CR-MO. COMPLEMENT D'ETUDE SUR LES ZAT]
S. Debiez, P. Roguin, and R. Gaillard Mar. 1990 34 p In FRENCH Prepared in cooperation with Centre Technique des Industries Mecaniques, Nantes, France
(Contract CETIM-88-1352-B)
(CETIM-104720; IS-25-062; ETN-91-98326) Copyright Avail: NTIS HC/MF A03

The effect of thermal treatment after welding both on the functional properties and the resilience of assemblies is studied. Thermal treatment is shown to be of little value in 15 CD4-05 welds. If however such treatment is required to meet the code,

the temperature should not go beyond 680 C. At that temperature the various areas of the weld are homogenized and the resilience of the melted zone is increased. Resilience is shown to be better within the weld than within the neighboring region of base metal. ESA

N91-13740# Institut de Soudure, Paris (France).
STUDY OF THE TENSILE STRENGTH OF THE MELTED ZONE OF VERTICAL WELDS CARRIED OUT USING ELECTROSLAG WELDING ON C-Mn STEEL. FURTHER STUDY ON 80 mm THICK PLATE Final Report [ETUDE SUR LA TENANCITE DE LA ZONE FONDUE DES SOUDURES VERTICALES SOUS LAITIER AVEC GUIDE FIL FUSIBLE SUR ACIER C-MN. POURSUITE DE L'ETUDE SUR L'EPAISSEUR 80 MM]
R. Gaillard and P. Roguin Aug. 1989 27 p In FRENCH Prepared in cooperation with Centre Technique des Industries Mecaniques, Nantes, France
(Contract CETIM-88-1352-A)
(CETIM-104730; IS-28843; ETN-91-98327) Copyright Avail: NTIS HC/MF A03

A welding technique showing very satisfactory results on 30 mm thick plate is applied to 80 mm thick plate. Four types of welding rods are tried, a C-Mn, Mn-Mo, Mn-Ni-Mo and a steel E 36-4 without niobium. Very low impurity values are sought for in these rods. Good results are obtained. A 5 daJ/sq cm value can be guaranteed up to 20C using a Mn-Ni-Mo rod after heat treating the joint at 550C. The three dimensional structure shows little improvement over previous experiments. The increase in tensile strength is apparently due to the decrease in impurities alone. ESA

N91-13741# Institut de Soudure, Paris (France).
STUDY OF THE METALLURGICAL CONSEQUENCES OF HAMMERING BETWEEN PASSES TO COMPENSATE FOR THE WITHDRAWAL OF METAL CAUSED BY WELDING Final Report [ETUDE DES CONSEQUENCES METALLURGIQUES DU MARTELAGE ENTRE LES PASSES EXECUTE POUR COMPENSER LES RETRAITS DES SOUDURES]
Y. Darou, S. Debiez, and R. Gaillard Mar. 1989 54 p In FRENCH Prepared in cooperation with Centre Technique des Industries Mecaniques, Nantes, France
(Contract CETIM-86-3636)
(CETIM-104430; IS-23-284; ETN-91-98330) Copyright Avail: NTIS HC/MF A04

The technique of hammering between passes to compensate for the withdrawal of metal in welding is discussed. Two hammering intensities are studied, one capable of simply compensating for the welding withdrawal, the other capable of stretching the welded joint twice the amount that the original withdrawal contracted. For C-Mn alloys the hammering leads to thermotensile aging of the metal which greatly diminishes the tensile strength of the melted area. The amount of deterioration seems to depend on the composition of the weld alloy. Further research is needed to evaluate the effect of manganese content on fatigue of welded joints. ESA

N91-13742# Centre Technique des Industries Mecaniques, Saint Etienne (France).
BOLTED STRUCTURAL ASSEMBLIES: BIBLIOGRAPHIC ANALYSIS Final Report [ASSEMBLAGES VISSES STRUCTURAUX: SYNTHESE BIBLIOGRAPHIQUES]
A. Durand and R. Souvignet Jan. 1990 18 p In FRENCH
(CETIM-13N061; ETN-91-98333) Copyright Avail: NTIS HC/MF A03

Fatigue calculation and tightening parameters taken into consideration in assembling bolted structures are discussed. Thirty seven bibliographic sources are referred to in this survey of trends in bolted joint techniques. Ways in which to simplify calculation of tightening parameters are presented. Modeling of bolted joints is discussed. The bibliographic sources are listed under separate categories dealing with bolted structures, tightening, failure analysis and the influence of washers. The various bolting criteria applied to pressure vessels, nuclear power plants and lifting machines are considered separately. ESA

N91-14045# International Research and Development Co. Ltd., Fossway (England).
THE WORLD OF SUPERCONDUCTIVE MACHINERY
A. D. Appleton *In* AGARD, Applications of Superconductivity to Avionics Oct. 1990 10 p (For primary document see N91-14030 05-76)
Copyright Avail: NTIS HC/MF A08; Non-NATO Nationals requests available only from AGARD/Scientific Publications Executive

38 QUALITY ASSURANCE AND RELIABILITY

Includes product sampling procedures and techniques; and quality control.

N91-13743# Los Alamos National Lab., NM.
ANALYSIS OF BOND QUALITY BY RESONANT ULTRASOUND
William M. Visscher, Albert Migliori, and Raymond D. Dixon 1990 7 p Presented at the Review of Progress in Quantitative NDE, La Jolla, CA, 15-20 Jul. 1990 Submitted for publication
(Contract W-7405-eng-36)
(DE91-000439; LA-UR-90-2980; CONF-900791-3) Avail: NTIS HC/MF A02

Analysis of the response of small samples of materials to mechanical excitations at ultrasonic frequencies (resonant ultrasound spectroscopy, or RUS) can yield much information about the sample, including its geometry, density (densities, if composite), and elastic constants. In this paper, we sketch the experimental technique, the method by which the data can be analyzed, and extend the analysis to samples which comprise two different materials bonded together. In the latter case the technique can give information about the composition of the sample and bond integrity (i.e., whether or not displacements and stresses are continuous across the interface). Comparison of calculated with measured frequencies for a bonded sample will be made. DOE

N91-13744# Edgerton, Germeshausen and Grier, Inc., Idaho Falls, ID.
DESIGN RELIABILITY ENGINEERING
David Buden and R. Niall M. Hunt 1989 6 p Presented at the Winter Meeting of the American Nuclear Society and Nuclear Power and Technology Exhibit, San Francisco, CA, 26-30 Nov. 1989
(Contract DE-AC07-76ID-01570)
(DE91-001949; EGG-M-89285; CONF-891103-77) Avail: NTIS HC/MF A02

Improved design techniques are needed to achieve high reliability at minimum cost. This is especially true of space systems where lifetimes of many years without maintenance are needed and severe mass limitations exist. Reliability must be designed into these systems from the start. Techniques are now being explored to structure a formal design process that will be more complete and less expensive. The intent is to integrate the best features of design, reliability analysis, and expert systems to design highly reliable systems to meet stressing needs. Taken into account are the large uncertainties that exist in materials, design models, and fabrication techniques. Expert systems are a convenient method to integrate into the design process a complete definition of all elements that should be considered and an opportunity to integrate the design process with reliability, safety, test engineering, maintenance and operator training. DOE

N91-13745# Sandia National Labs., Albuquerque, NM.
ON THE DESIGN OF COMPONENT TEST PLANS BASED ON SYSTEM RELIABILITY OBJECTIVES
Robert G. Easterling, Floyd W. Spencer, and Mainak Mazumdar (Pittsburgh Univ., PA.) 1990 20 p Presented at the Annual Reliability and Maintainability Symposium, Orlando, FL, 29-31 Jan. 1991

(Contract DE-AC04-76DP-00789)
(DE90-017034; SAND-90-1064C; CONF-910102-1) Avail: NTIS HC/MF A03

Component test plans are often designed by allocating a system's reliability goal among the system's components, then designing individual component test plans suitable for demonstrating achievement of each component's reliability goal. One use of the resulting component test data is the calculation of estimated system reliability, based on a model linking the component reliabilities to system reliability. The statistical precision of this system estimate depends on the component test plans (numbers of each component tested and the type of tests, e.g., variables or attributes) and, hence, is determined by the component test planners. Because system reliability may be of considerable interest, we feel an integrated view of component testing is required to assure that the ensemble of component tests will provide an adequate system reliability estimate. This paper considers the case of a series system of different components and binomial component data. For the case of equal numbers of units tested of each component (which can be shown to minimize total cost, subject to the risk constraints) the O.C. envelope is readily derived and from this envelope component test plans that satisfy the specified risks can be derived from equations that involve the cumulative binomial distribution function. Existing tables pertaining to acceptance sampling plans based on the binomial distribution can be used to determine the required number of component tests. DOE

N91-13746# Brookhaven National Lab., Upton, NY.
DEGRADATION MODELING WITH APPLICATION TO AGING AND MAINTENANCE EFFECTIVENESS EVALUATIONS
P. K. Samanta, F. Hsu, M. Subduhi, and W. E. Vesely (Science Applications International Corp., La Jolla, CA.) 1990 20 p Presented at the 18th Water Reactor Safety Information Meeting, Gaithersburg, MD, 22-24 Oct. 1990
(Contract DE-AC02-76CH-00016)
(DE91-004004; BNL-NUREG-45309; CONF-9010185-10) Avail: NTIS HC/MF A03

This paper describes a modeling approach to analyze component degradation and failure data to understand the aging process of components. As used here, degradation modeling is the analysis of information on component degradation in order to develop models of the process and its implications. This particular modeling focuses on the analysis of the times of component degradations, and models how the rate of degradation changes with the age of the component. The methodology presented also discusses the effectiveness of maintenance as applicable to aging evaluations. The specific applications which are performed show quantitative models of component degradation rates and component failure rates from plant-specific data. The statistical techniques which are developed and applied allow aging trends to be effectively identified in the degradation and failure data. Initial estimates of the effectiveness of maintenance in limiting degradations from becoming failures also are developed. These results are important first steps in degradation modeling, and show that degradation can be modeled to identify aging trends. DOE

N91-13747 Physics and Electronics Lab. TNO, The Hague (Netherlands).
QUALITY OF EXPERT SYSTEMS: METHODS AND TECHNIQUES Final Report
J. H. J. Lenting (Limburg State Univ., Maastricht, Netherlands) and M. Perre Dec. 1989 80 p In DUTCH; ENGLISH summary
(Contract A89/K/602)
(FEL-89-A267; TD-89-3867; ETN-91-98294) Copyright Avail: Physics and Electronics Laboratory TNO, P.O. Box 96864, 2509 JG The Hague, Netherlands

The problems related to the quality of expert systems are examined. A method is presented which considers the development of expert systems as a (parallel) activation of modeling processes. The conceptual similarities between data bases and knowledge bases are stressed. As an implication the use of the Nyssens Information Analysis Method (NIAM) as a knowledge base specification method is proposed. The modularity and structure of knowledge bases was examined, together with the applicability of conventional testing methodologies in expert systems. It is demonstrated that the integration of data base theory and artificial intelligence is a step in the direction of a better quality control of expert systems. ESA

N91-13748 Physics and Electronics Lab. TNO, The Hague (Netherlands).
QUALITY OF EXPERT SYSTEMS: ALGORITHMS FOR INTEGRITY CONTROL Final Report
J. H. J. Lenting (Limburg State Univ., Maastricht, Netherlands) and M. Perre Mar. 1990 64 p In DUTCH; ENGLISH summary
(Contract A89/K/602)
(FEL-89-A312; TD-89-4578; ETN-91-98295) Copyright Avail: Physics and Electronics Laboratory TNO, P.O. Box 96864, 2504 JG The Hague, Netherlands

Algorithms for integrity control of knowledge bases were investigated with special emphasis on the computational efficiency. Algorithms for preserving consistency and integrity of the knowledge base were compared. The way in which a mapping can be performed between specifications made with ENIAM (Extended Nyssens Information Analysis Method) and an executable PROLOG program was examined, and a formal determination of the consistency and integrity of knowledge specifications was established. ESA

N91-13749# Centre Technique des Industries Mecaniques, Senlis (France).
SIGNAL PROCESSING USED IN THE ELECTROMAGNETIC INSPECTION OF LONG BODIES Final Report [TRAITEMENT DES SIGNAUX POUR LE CONTROLE ELECTROMAGNETIQUE DE PRODUITS LONGS]
A. Barbarin Jul. 1989 19 p In FRENCH
(CETIM-107270; ETN-91-98336) Copyright Avail: NTIS HC/MF A03

An experimental sensor able to carry out measurements and checks on cables up to 1000 meters long is described. The balancing software and the software used in the signal interpretation are presented. Results of a cable testing operation in which the number of anomalies recorded surpasses official selection criteria are demonstrated. Industrial applications of this cable testing technique are discussed. Anomaly localization and counting, linear density of broken strands analysis and identification of different types of signal are among the functions for which this cable testing machine is designed. ESA

39 STRUCTURAL MECHANICS

Includes structural element design and weight analysis; fatigue; and thermal stress.

For applications see *05 Aircraft Design, Testing and Performance* and *18 Spacecraft Design, Testing and Performance.*

N91-13750*# National Aeronautics and Space Administration. Langley Research Center, Hampton, VA.
FREE VIBRATIONS OF THIN-WALLED SEMICIRCULAR GRAPHITE-EPOXY COMPOSITE FRAMES
Ahmed K. Noor, Huey D. Carden, and Jeanne M. Peters (Joint Inst. for Advancement of Flight Sciences, Hampton, VA.) Washington Nov. 1990 43 p Original contains color illustrations
(Grant NAG1-730)
(NASA-TP-3010; L-16726; NAS 1.60:3010) Avail: NTIS HC/MF A03; 4 functional color pages CSCL 20K

A detailed study is made of the effects of variations in lamination and material parameters of thin walled composite frames on their vibrational characteristics. The structures considered are semicircular thin walled frames with I and J sections. The flanges

and webs of the frames are modelled by using 2-D shell and plate finite elements. A mixed formulation is used with the fundamental unknowns consisting of both the generalized displacements and stress resultants in the frames. The frequencies and modes predicted by the 2-D finite element model are compared with those obtained from experiments, as well as with the predictions of a 1-D thin walled beam finite element model. A detailed study is made of the sensitivity of the vibrational response to variations in the fiber orientation, material properties of the individual layers, and boundary conditions. Author

N91-13751*# National Aeronautics and Space Administration. Langley Research Center, Hampton, VA.
FAILURE BEHAVIOR OF GENERIC METALLIC AND COMPOSITE AIRCRAFT STRUCTURAL COMPONENTS UNDER CRASH LOADS
Huey D. Carden and Martha P. Robinson Washington Nov. 1990 48 p
(NASA-RP-1239; L-16744; NAS 1.61:1239) Avail: NTIS HC/MF A03 CSCL 20K

Failure behavior results are presented from crash dynamics research using concepts of aircraft elements and substructure not necessarily designed or optimized for energy absorption or crash loading considerations. To achieve desired new designs incorporating improved energy absorption capabilities often requires an understanding of how more conventional designs behave under crash loadings. Experimental and analytical data are presented which indicate some general trends in the failure behavior of a class of composite structures including individual fuselage frames, skeleton subfloors with stringers and floor beams without skin covering, and subfloors with skin added to the frame-stringer arrangement. Although the behavior is complex, a strong similarity in the static/dynamic failure behavior among these structures is illustrated through photographs of the experimental results and through analytical data of generic composite structural models. Author

N91-13752 California Univ., Los Angeles.
FRACTURE MECHANICS OF INTERFACE CRACKS BETWEEN DISSIMILAR ANISOTROPIC MATERIALS Ph.D. Thesis
Shiuh Chuan Her 1990 160 p
Avail: Univ. Microfilms Order No. DA9017661

The problem of an interface crack between two dissimilar anisotropic materials is examined under the assumption that the crack faces are separated. Two types of cracks, interior interface cracks and free edge interface cracks, are investigated. In the case of the interior interface crack, a global-local finite element method is employed. This hybrid method preserves much of the flexibility of the finite element method and is able to extract the stress singularities at the crack tip. A special crack tip element which accounts for the anisotropy and leads to highly accurate and economical solutions is developed. Numerical examples are presented to illustrate the accuracy and efficiency of the global-local finite element method. The free edge problem is three dimensional in character. The present method approaches the free edge interface crack problem in two steps. First, a simplified two dimensional version of the edge crack problem is solved. This procedure is then extended to solve the more complicated three dimensional free edge crack problem. For both cases, a system of Cauchy singular integral equations of the second kind is obtained. The equations are solved by taking advantage of the fact that the fundamental function of the integral equations is the weight function of the Jacobi polynomials. The problem of a symmetric graphite-epoxy composite under uniform axial extension is solved as a specific example and numerical results for the crack tip stress intensity factors are presented. Dissert. Abstr.

N91-13753 Liverpool Univ. (England).
A COMPARATIVE STUDY OF DUCTILE FRACTURE IN THE 2.25 PERCENT Cr-1 PERCENT Mo AND 9 PERCENT Cr-1 PERCENT Mo ALLOY STEELS Ph.D. Thesis
Jian Guo Zhang 1987 306 p
Avail: Univ. Microfilms Order No. BRDX89935

The influence of microstructural variations on the deformation and fracture behavior of 2.25Cr-1Mo and 9Cr-1Mo steel was investigated. In their standard conditions (S-conditions) the two steels differ primarily in their carbide distributions. The have similar strengths but different fracture characteristics in both tensile and impact tests. The effects of thermal aging on the microstructures produced by the standard heat treatments were in line with the results of the previous work. The sensitivity of the 2.25Cr-1Mo steel to aging embrittlement was confirmed as was the role played by phosphorus segregation, but there was little or no effect on ambient temperature tensile ductility. In contrast, the results for the 9Cr-1Mo steel confirmed that aging results in a decrease in tensile ductility and USE and an increase in ductile-to-brittle transition temperature (DBTT), associated with phosphorus segregation to carbide-matrix interfaces and/or prior austenite grain boundaries and at longer times the precipitation of the Laves phase. The nucleation of voids at carbides in each material was found to occur by decohesion of the particle-matrix interfaces over a large range of applied strain and appeared to be influenced significantly by precipitate size distribution in each material. The void nucleation behavior in the L-treated materials compared with that in the S-treated materials was rationalized in terms of the partitioning of strain and stress between the ferrite and the martensite in the two steels. The ease with which voids developed at carbides during straining correlated well with the changes in ductility. The growth of precipitate nucleated voids was found to be consistent with the Rice-Tracey model only if the values of the numerical constants are adjusted arbitrarily. Void coalescence occurred by the large inclusion nucleated voids becoming interlinked by the localized formation of voids at precipitates, forming a central crack at an applied strain of some 0.8 of the fracture strain. Dissert. Abstr.

N91-13754 Maryland Univ., College Park.
STUDY OF STATIC AND DYNAMIC FRACTURE USING STRAIN MEASUREMENTS Ph.D. Thesis
John Roland Berger 1990 221 p
Avail: Univ. Microfilms Order No. DA9030853

The analysis of strain fields surrounding both stationary and propagating cracks is presented. By using appropriate series expansions, relations are developed between the strain measured at a point and resistance strain gages, gage orientation is studied in order to optimize the gage response. Through proper orientation of the gage the contribution of the constant x-direction stress can be eliminated. For the analysis of dynamic crack propagation, two algorithms are presented which take advantage of either the temporal or spatial variations in the strain field. Combining these algorithms with the suggested gage orientations provides a means of analyzing dynamic fracture experiments for the propagation toughness-crack velocity relation as well as the arrest toughness. A dynamic test is analyzed to demonstrate the use of the techniques developed. Several issues involved in strain field analysis are presented. These include the extent of validity of the truncated series expansions for the strain field, the difficulty in extracting crack tip position from strains recorded by gages whose position was not optimized, and the propagation toughness with time, temperature, and position are determined. From this information details of the conditions at crack arrest are extracted. The propagation toughness-crack-velocity relation is then constructed. Dissert. Abstr.

N91-13755 Council for National Academic Awards (England).
FINITE ELEMENT AND BOUNDARY ELEMENT METHODS FOR ELASTOPLASTIC STRESS ANALYSIS OF TWO-DIMENSIONAL AND AXISYMMETRIC PROBLEMS Ph.D. Thesis
Imad Ahmed Husain 1989 444 p
Avail: Univ. Microfilms Order No. BRDX89763

Elastoplastic analysis of 2-dimensional and axisymmetric problems was performed using the finite element and boundary element techniques. The analysis is based upon a wide range of yield criteria and hardening rules so as to be suitable for most engineering materials. Many accuracy measures were employed with the boundary integral equation derivations, such as

isoparametric boundary elements, singular quadrature, corner models, finite difference schemes for internal stress evaluation, high-order integration cells, and the use of boundary integral expressions for domain loading terms. A programming package was developed with its own mesh generator and results plotter. The package was validated using several case studies including a benchmark test case recommended by NAFEMS. The finite element analysis of elastoplastic problems proved to be more stable and reliable than the corresponding boundary element analysis. Dissert. Abstr.

N91-13756*# Texas A&M Univ., College Station. Center for Mechanics of Composites.

EXPERIMENTAL OBSERVATIONS AND FINITE ELEMENT ANALYSIS OF THE INITIATION OF FIBER MICROBUCKLING IN NOTCHED COMPOSITE LAMINATES Final Report

E. Gail Guynn, Walter L. Bradley, and Ozden O. Ochoa 12 Nov. 1990 340 p

(Grant NAG1-659)

(NASA-CR-185354; NAS 1.26:185354) Avail: NTIS HC/MF A15 CSCL 20K

A better understanding of the factors that affect the semi-circular edge-notched compressive strength is developed, and the associated failure mode(s) of thermoplastic composite laminates with multidirectional stacking sequences are identified. The primary variables in this investigation are the resin nonlinear shear constitutive behavior, stacking sequence (orientation of plies adjacent to the 0 degree plies), resin-rich regions between the 0 degree plies and the off-axis supporting plies, fiber/matrix interfacial bond strength, and initial fiber waviness. Two thermoplastic composite material systems are used in this investigation. The materials are the commercial APC-2 (AS4/PEEK) and a poor interface experimental material, AU4U/PEEK, designed for this investigation. Notched compression specimens are studied at 21, 77, and 132 C. Geometric and material nonlinear two-dimensional finite element analysis is used to model the initiation of fiber microbuckling of both the ideal straight fiber and the more realistic initially wavy fiber. The effects of free surface, fiber constitutive properties, matrix constitutive behavior, initial fiber curvature, and fiber/matrix interfacial bond strength on fiber microbuckling initiation strain levels are considered. Author

N91-13757# EG and G Rocky Flats, Inc., Golden, CO.

SUPERPLASTIC DEFORMATION PROPERTIES OF Ti-6Al-4V

M. A. Zaccone and M. M. McDonald Aug. 1990 24 p

(Contract DE-AC34-90DP-62349)

(DE91-000503; RFP-4253) Avail: NTIS HC/MF A03

Superplastic forming of Ti-6Al-4V was investigated with three heats of material to examine the effects of extrinsic and intrinsic variables on strain rate sensitivity and flow stress. Tension tests with strain rate jumps and step strain rate tests were used to determine the effects of strain rate, strain, and temperature on strain rate sensitivity of Ti-6Al-4V. Superplastic forming of Ti-6Al-4V is strongly influenced by deformation temperature. The uniform elongation and the strain rate sensitivity were maximized at 900 C in the temperature range tested. In the strain rate range tested, strain rate sensitivity increased slightly as the strain rate decreased. In examining the results, it was apparent that at high strains, grain growth decreased strain rate sensitivity. This decrease was a strong function of temperature, which minimized at 875 C. The strong dependence of superplastic behavior on temperature can be related to relative amounts of alpha and beta in the microstructure, as shown in the model for superplastic deformation of Ti-6Al-4V. DOE

N91-13758# Naval Postgraduate School, Monterey, CA. Dept. of Mechanical Engineering.

CONSTRAINED VISCOELASTIC LAYER DAMPING OF THICK ALUMINUM PLATES: DESIGN, ANALYSIS, AND TESTING Progress Report, 1 Jun. 1989 - 31 May 1990

Michael J. Bateman, K. Steven Kim, and Young S. Shin May 1990 138 p Prepared for David Taylor Research Center, Bethesda, MD

(Contract N00167-90-WR-00300)

(AD-A226556; NPS69-90-05) Avail: NTIS HC/MF A07 CSCL 20/11

Modern naval warfare has been increasingly dependent upon the acoustic silencing of the participants. Constrained viscoelastic layer damping of vibrating elements is one method which can be used to meet acoustic silencing goals. This paper considers constrained viscoelastic layer damping treatments applied to a thick aluminum plate, including single layer, double layer, a milled pocket plate, and a milled floating element configuration. High modal damping values were obtained for each damping configuration. The Modal Strain Energy method, using finite element analysis to estimate modal loss factors, was investigated for use as a tool in constrained viscoelastic layer damping design. A comparison of experimentally measured frequency response and modal loss factors with those predicted by the modal strain energy method is presented to confirm the possible use of the modal strain energy method as a design tool. GRA

N91-13759*# Colorado Univ., Boulder. Coll. of Engineering.

CONSTRAINT TREATMENT TECHNIQUES AND PARALLEL ALGORITHMS FOR MULTIBODY DYNAMIC ANALYSIS Ph.D. Thesis

Jin-Chern Chiou Nov. 1990 190 p

(Grant NAG1-756)

(NASA-CR-187668; NAS 1.26:187668; CU-CSSC-90-26) Avail: NTIS HC/MF A09 CSCL 20K

Computational procedures for kinematic and dynamic analysis of three-dimensional multibody dynamic (MBD) systems are developed from the differential-algebraic equations (DAE's) viewpoint. Constraint violations during the time integration process are minimized and penalty constraint stabilization techniques and partitioning schemes are developed. The governing equations of motion, a two-stage staggered explicit-implicit numerical algorithm, are treated which takes advantage of a partitioned solution procedure. A robust and parallelizable integration algorithm is developed. This algorithm uses a two-stage staggered central difference algorithm to integrate the translational coordinates and the angular velocities. The angular orientations of bodies in MBD systems are then obtained by using an implicit algorithm via the kinematic relationship between Euler parameters and angular velocities. It is shown that the combination of the present solution procedures yields a computationally more accurate solution. To speed up the computational procedures, parallel implementation of the present constraint treatment techniques, the two-stage staggered explicit-implicit numerical algorithm was efficiently carried out. The DAE's and the constraint treatment techniques were transformed into arrowhead matrices to which Schur complement form was derived. By fully exploiting the sparse matrix structural analysis techniques, a parallel preconditioned conjugate gradient numerical algorithm is used to solve the systems equations written in Schur complement form. A software testbed was designed and implemented in both sequential and parallel computers. This testbed was used to demonstrate the robustness and efficiency of the constraint treatment techniques, the accuracy of the two-stage staggered explicit-implicit numerical algorithm, and the speed up of the Schur-complement-based parallel preconditioned conjugate gradient algorithm on a parallel computer. Author

N91-13760*# Colorado Univ., Boulder. Center for Space Structures and Controls.

A COMPUTATIONAL PROCEDURE FOR THE DYNAMICS OF FLEXIBLE BEAMS WITHIN MULTIBODY SYSTEMS Ph.D. Thesis Final Technical Report

Janice Diane Downer Nov. 1990 217 p

(Grant NAG1-756)

(NASA-CR-187667; NAS 1.26:187667; CU-CSSC-90-27) Avail: NTIS HC/MF A10 CSCL 20K

The dynamic analysis of three dimensional elastic beams which experience large rotational and large deformational motions are examined. The beam motion is modeled using an inertial reference for the translational displacements and a body-fixed reference for the rotational quantities. Finite strain rod theories are then defined

in conjunction with the beam kinematic description which accounts for the effects of stretching, bending, torsion, and transverse shear deformations. A convected coordinate representation of the Cauchy stress tensor and a conjugate strain definition is introduced to model the beam deformation. To treat the beam dynamics, a two-stage modification of the central difference algorithm is presented to integrate the translational coordinates and the angular velocity vector. The angular orientation is then obtained from the application of an implicit integration algorithm to the Euler parameter/angular velocity kinematical relation. The combined developments of the objective internal force computation with the dynamic solution procedures result in the computational preservation of total energy for undamped systems. The present methodology is also extended to model the dynamics of deployment/retrieval of the flexible members. A moving spatial grid corresponding to the configuration of a deployed rigid beam is employed as a reference for the dynamic variables. A transient integration scheme which accurately accounts for the deforming spatial grid is derived from a space-time finite element discretization of a Hamiltonian variational statement. The computational results of this general deforming finite element beam formulation are compared to reported results for a planar inverse-spaghetti problem. Author

N91-13761*# National Aeronautics and Space Administration. Langley Research Center, Hampton, VA.
A REVIEW OF NONLINEAR CONSTITUTIVE MODELS FOR METALS
David H. Allen (Texas A&M Univ., College Station.) and Charles E. Harris Dec. 1990 37 p
(NASA-TM-102727; NAS 1.15:102727) Avail: NTIS HC/MF A03 CSCL 20K

Over the past two decades a number of thermomechanical constitutive theories have been proposed for viscoplastic metals. These models are in most cases similar in that they utilize a set of internal state variables which provide locally averaged representations of microphysical phenomena such as dislocation rearrangement and grain boundary sliding. The state of development of several of these models is now at the point where accurate theoretical solutions can be obtained for a wide variety of structural problems at elevated temperatures. The fundamentals of viscoplasticity are briefly reviewed and a general framework is outlined. Several of the more prominent models are reviewed, and predictions from models are compared to experimental results. Author

N91-13762*# National Aeronautics and Space Administration. Ames Research Center, Moffett Field, CA.
GENERAL ROTORCRAFT AEROMECHANICAL STABILITY PROGRAM (GRASP): THEORY MANUAL
Dewey H. Hodges, A. Stewart Hopkins, Donald L. Kunz, and Howard E. Hinnant Oct. 1990 150 p Prepared in cooperation with Army Aviation Systems Command, Moffett Field, CA
(NASA-TM-102255; A-90014; NAS 1.15:102255; USAAVSCOM-TM-89-A-003) Avail: NTIS HC/MF A07 CSCL 20K

The general rotorcraft aeromechanical stability program (GRASP) was developed to calculate aeroelastic stability for rotorcraft in hovering flight, vertical flight, and ground contact conditions. GRASP is described in terms of its capabilities and its philosophy of modeling. The equations of motion that govern the physical system are described, as well as the analytical approximations used to derive them. The equations include the kinematical equation, the element equations, and the constraint equations. In addition, the solution procedures used by GRASP are described. GRASP is capable of treating the nonlinear static and linearized dynamic behavior of structures represented by arbitrary collections of rigid-body and beam elements. These elements may be connected in an arbitrary fashion, and are permitted to have large relative motions. The main limitation of this analysis is that periodic coefficient effects are not treated, restricting rotorcraft flight conditions to hover, axial flight, and ground contact. Instead of following the methods employed in other rotorcraft programs. GRASP is designed to be a hybrid of the finite-element method and the multibody methods used in spacecraft analysis. GRASP differs from traditional finite-element programs by allowing multiple levels of substructure in which the substructures can move and/or rotate relative to others with no small-angle approximations. This capability facilitates the modeling of rotorcraft structures, including the rotating/nonrotating interface and the details of the blade/root kinematics for various types. GRASP differs from traditional multibody programs by considering aeroelastic effects, including inflow dynamics (simple unsteady aerodynamics) and nonlinear aerodynamic coefficients. Author

N91-13763# Oak Ridge National Lab., TN. Engineering Technology Div.
POTENTIAL IMPACT OF ENHANCED FRACTURE-TOUGHNESS DATA ON PRESSURIZED-THERMAL-SHOCK ANALYSIS
T. L. Dickson and T. J. Theiss 1990 19 p Presented at the 18th Water Reactor Safety Information Meeting, Rockville, MD, 22-24 Oct. 1990
(Contract DE-AC05-84OR-21400)
(DE91-001493; CONF-9010185-2) Avail: NTIS HC/MF A03

The Heavy Section Steel Technology (HSST) Program is involved with the generation of enhanced fracture-initiation toughness and fracture-arrest toughness data of prototypic nuclear reactor vessel steels. These two sets of data are enhanced because they have distinguishing characteristics that could potentially impact PWR pressure vessel integrity assessments for the pressurized-thermal shock (PTS) loading condition which is a major plant-life extension issue to be confronted in the 1990's. Currently, the HSST Program is planning experiments to verify and quantify, for A533B steel, the distinguishing characteristic of elevated initiation-fracture toughness for shallow flaws which has been observed for other steels. Deterministic and probabilistic fracture-mechanics analyses were performed to examine the influence of the enhanced initiation and arrest fracture-toughness data on the cleavage fracture response of a nuclear reactor pressure vessel subjected to PTS loading. The results of the analyses indicated that application of the enhanced K(sub Ia) data does reduce the conditional probability of failure P(F(vert bar)E); however, it does not appear to have the potential to significantly impact the results of PTS analyses. The application of enhanced fracture-initiation-toughness data for shallow flaws also reduces P(F(vert bar)E), but it does appear to have a potential for significantly affecting the results of PTS analyses. The effect of including Type I warm prestress in probabilistic fracture-mechanics analyses is beneficial. The benefit is transient dependent and, in some cases, can be quite significant. DOE

N91-13764# Los Alamos National Lab., NM.
MESH CONSIDERATIONS FOR FINITE ELEMENT STRUCTURAL DYNAMIC APPLICATIONS
Ralph Robert Stevens Nov. 1990 24 p
(Contract W-7405-eng-36)
(DE91-001717; LA-11916-MS) Avail: NTIS HC/MF A03

Three factors relating to a finite element mesh and discretization scheme are discussed: the geometric accuracy of the node locations, the amount of warp of a quadrilateral shell element, and the directional biasing effect of similarly oriented triangular elements. These factors can have a significant effect on the accuracy of a finite element structural dynamic analysis. Two finite element models that illustrate these effects are described. DOE

N91-13765# Lawrence Livermore National Lab., CA. Computing and Mathematics Research Div.
A COMPARISON OF TWO NUMERICAL METHODS FOR SHOCKS IN ONE-DIMENSIONAL ELASTIC-PLASTIC SOLIDS
John A. Trangenstein Sep. 1990 37 p Presented at the Workshop on Viscous and Numerical Approximation of Shock Waves, Raleigh, NC, 23-25 May 1990 Submitted for publication
(Contract W-7405-eng-48)
(DE91-001741; UCRL-JC-105024; CONF-9005286-1) Avail: NTIS HC/MF A03

In this paper we compare and contrast a second-order Godunov

method with a second-order explicit finite element method for the dynamic response of one-dimensional elastic-plastic solids. We examine the numerical dissipation and dispersion of the two techniques, and compare their performance on problems describing the nonlinear response of an elastic-plastic bar. DOE

N91-13766*# National Aeronautics and Space Administration. Marshall Space Flight Center, Huntsville, AL.
TEST AND MODEL CORRELATION OF THE ATMOSPHERIC EMISSION PHOTOMETRIC IMAGER FIBERGLASS PEDESTAL
H. M. Lee, III and L. A. Barker Oct. 1990 62 p
(NASA-TM-103515; NAS 1.15:103515) Avail: NTIS HC/MF A04 CSCL 20K

The correlation is presented of the static loads testing and finite element modeling for the fiberglass pedestal used on the Atmospheric Emission Photometric Imaging (AEPI) experiment. This payload is to be launched in the space shuttle as part of the ATLAS-1 experiment. Strain gauge data from rosettes around the highly loaded base are compared to the same load case run for the Spacelab 1 testing done in 1981. Correlation of the model and test data was accomplished through comparison of the composite stress invariant using the expected flight loads for the ATLAS-1 mission. Where appropriate, the Tsai-Wu failure criteria was used in the development of the key margins of safety. Margins of safety are all positive for the pedestal and are reported. Author

N91-13767*# National Aeronautics and Space Administration. Pasadena Office, CA.
COMPOSITE PASSIVE DAMPING STRUTS FOR LARGE PRECISION STRUCTURES Patent Application
Benjamin P. Dolgin, inventor (to NASA) (Jet Propulsion Lab., California Inst. of Tech., Pasadena.) 31 Aug. 1990 16 p
(Contract NAS7-918)
(NASA-Case-NPO-17914-1-CU; NAS 1.71:NPO-17914-1-CU; US-Patent-Appl-SN-575697) Avail: NTIS HC/MF A03 CSCL 20K

In the field of viscoelastic dampers, a new strut design comprises a viscoelastic material sandwiched between multiple layers, some of which layers bear and dampen load force. In one embodiment, the layers are composite plies of opposing orientation. In another embodiment, the strut utilizes a viscoelastic layer sandwiched between V-shaped composite plies. In a third embodiment, a viscoelastic layer is sandwiched between sine-shaped plies. Strut strength is equal to or greater than conventional aluminum struts due to the unique high interlaminar shear ply design. NASA

N91-13768*# Aeronautical Research Inst. of Sweden, Stockholm. Dept. of Structures.
ON THE VARIATION IN CRACK-OPENING STRESSES AT DIFFERENT LOCATIONS IN A THREE-DIMENSIONAL BODY
R. G. Chermahini and Anders F. Blom Sep. 1990 29 p Sponsored by Defence Material Administration, Stockholm, Sweden
(Grant NAG1-529)
(NASA-CR-187722; NAS 1.26:187722; FFA-TN-1988-21; ETN-91-98263) Avail: NTIS HC/MF A03 CSCL 20K

Crack propagation and closure behavior of thin, and thick middle crack tension specimens under constant amplitude loading were investigated using a three dimensional elastic plastic finite element analysis of fatigue crack propagation and closure. In the thin specimens the crack front closed first on the exterior (free) surface and closed last in the interior during the unloading portion of cyclic loading; a load reduced displacement technique was used to determine crack opening stresses at specified locations in the plate from the displacements calculated after the seven cycle. All the locations were on the plate external surface and were located near the crack tip, behind the crack tip, at the centerline of the crack. With this technique, the opening stresses at the specified points were found to be 0.52, 0.42, and 0.39 times the maximum applied stress. ESA

N91-13769# Aeronautical Research Inst. of Sweden, Stockholm. Dept. of Structures.
ACCURATE AND RELIABLE COMPUTATION OF COMPLETE SOLUTIONS TO THE EQUATIONS OF LINEAR ELASTOMECHANICS ON THREE-DIMENSIONAL DOMAINS: COMPUTATION OF EDGE STRESS INTENSITY FUNCTIONS
Boerje Andersson, Urban Falk, and Ivo Babuska (Maryland Univ., College Park.) Aug. 1990 65 p Sponsored by Defence Material Administration, Stockholm, Sweden
(FFA-TN-1989-12; ETN-91-98264) Avail: NTIS HC/MF A04

Edge stress intensity functions are computed. It is shown how to derive accurate and reliable solutions to the equations of linear three dimensional elastomechanics. The numerical method used is the h p version of the finite element method. The exact solution which is regular inside the domain may have a singular behavior at edges and vertices. Close to vertices and edges the solution may be expanded in series characterized by eigenfunctions and intensity factors. The behavior of the solution close to smoothly curved edges is analyzed. The algorithms developed were implemented in the software STRIPE. ESA

N91-13770# Aeronautical Research Inst. of Sweden, Stockholm. Dept. of Structures.
ANALYSIS OF SHELLS AS 3D-ELASTICITY PROBLEMS USING THE p-VERSION OF THE FE METHOD
Rolf Jarlaas May 1990 26 p Sponsored by Defence Material Administration, Stockholm, Sweden
(FFA-TN-1990-25; ETN-91-98268) Avail: NTIS HC/MF A03

The structural responses of thick and thin shells are analyzed as fully three dimensional elasticity problems. In each finite element (FE) a local curvilinear coordinate system is introduced. The displacements in the directions of the three local axes are approximated with nonhomogeneous polynomials characterized by the couple (p, q). Blended mapping technique is used for exact geometry description of the domain studied in the benchmark example. ESA

N91-13771# Aeronautical Research Inst. of Sweden, Stockholm. Dept. of Structures.
ACCURATE AND RELIABLE DETERMINATION OF EDGE AND VERTEX STRESS INTENSITY FACTORS IN THREE-DIMENSIONAL ELASTOMECHANICS
Boerje Andersson, Urban Falk, and Ivo Babuska (Maryland Univ., College Park.) Jun. 1990 20 p Presented at the 17th International Congress of the Council of Aeronautical Sciences, Stockholm, Sweden, Sep. 1990 Sponsored by Defence Material Administration, Stockholm, Sweden
(FFA-TN-1990-28; ETN-91-98269) Avail: NTIS HC/MF A03

The way to derive accurate and reliable solutions to the equations of three dimensional elastomechanics in the domain of general shape is described. The h p version of the finite element is the numerical method employed. Close to edges and vertices the exact solution may be expanded in series. The terms in the series consist of unknown constants and functions which characterize the solution in areas where crack nucleation and propagation often take place. A new method is developed for edges that calculates the polynomial approximation to the modes' edge intensity functions. Vertex intensity factors and vertex edge intensity factors are defined. All intensity parameters can be determined with an error which decreases exponentially with increasing number of degrees of freedom. ESA

N91-13772# Aeronautical Research Inst. of Sweden, Stockholm. Dept. of Structures.
SPECTRUM FATIGUE TESTING: A LITERATURE SURVEY
Jonas Bogren Oct. 1990 33 p Sponsored by Defence Material Administration, Stockholm, Sweden
(FFA-TN-1990-40; ETN-91-98271) Avail: NTIS HC/MF A03

Topics related to spectrum fatigue testing are as follows: measuring of the fatigue loads, cycle counting methods, truncation and omission of loads, reconstitution of a loading sequence, systems for controlling a fatigue test and standardized stress time

histories. Prediction of fatigue and crack growth lives under spectrum loading is not discussed. ESA

N91-13773# Sandia National Labs., Albuquerque, NM.
A STRUCTURAL CONSTITUTIVE ALGORITHM BASED ON CONTINUUM DAMAGE MECHANICS FOR SOFTENING WITH SNAPBACK
M. K. Neilsen, Z. Chen, and H. L. Schreyer (New Mexico Univ., Albuquerque.) 1990 4 p Presented at the 3rd International Conference on Constitutive Laws for Engineering Materials: Theory and Application, Tucson, AZ, 7-12 Jan. 1991
(Contract DE-AC04-76DP-00789)
(DE90-015841; SAND-90-0957C; CONF-910120-1) Avail: NTIS HC/MF A01

A structural constitutive algorithm for elements with localized deformation zones is developed. The algorithm is based on the assumption that the material is described by an elastic-damage model. One- and two-dimensional problems are solved to demonstrate the effectiveness of the approach for generating solutions to strain-softening material problems that are not mesh dependent. DOE

N91-13774# Westinghouse Savannah River Co., Aiken, SC.
MECHANICAL PROPERTIES OF 1950'S VINTAGE TYPE 304 STAINLESS STEEL WELDMENT COMPONENTS
K. J. Stoner, R. L. Sindelar, N. G. Awadalla, J. R. Hawthorne, A. L. Hiser, and W. H. Cullen (Materials Engineering Associates, Inc., Lanham, MD.) 1990 9 p Presented at the 1990 Pressure Vessels and Piping Conference, Nashville, TN, 17-21 Jun. 1990 Submitted for publication
(Contract DE-AC09-89SR-18035)
(DE91-004328; WSRC-RP-89-959; CONF-900617-18) Avail: NTIS HC/MF A02

The primary coolant piping systems of the nuclear production reactors constructed in the 1950's at Savannah River Site are comprised of Type 304 stainless steel. A program has been completed which assessed the material properties of archival large diameter piping having approximately six years of service at temperatures between 25 and 125 C. An extensive database of mechanical properties was produced for examination of material variability and to provide properties for engineering analysis, including piping fracture resistance assessment. Tensile properties, Charpy-V notch ductility, and elastic-plastic fracture toughness were established for base metal, weld metal and weld heat-affected-zone (HAZ) materials. A total of 375 mechanical specimens representing ASTM L-C and C-L orientations were tested at temperatures of 25 or 125 C. The effect of dynamic loading on tensile and fracture toughness properties was also explored. The time-to-specimen maximum load (approx 80 milliseconds) was chosen to simulate a seismic loading event. The mechanical properties of the vintage piping material were found typical of those of recently-produced commercial melts of Type 304 stainless steel piping and are consistent with ASME Code Section II design values. The toughness properties of welds fabricated by the Metal Inert Gas (MIG) welding process (multipass, Type 308 stainless steel filler), were found similar to the base materials, yielding a high fracture resistance. Practical applications of the mechanical properties database in piping fracture assessments are illustrated with the methodology for an elastic-plastic analysis. DOE

N91-13775# Centre Technique des Industries Mecaniques, Senlis (France).
ANTIVIBRATION ISOLATION (A PRACTICAL GUIDEBOOK) Final Report [ISOLATION ANTI-VIBRATILE (GUIDE PRATIQUE)]
J. Brzezinski Oct. 1989 111 p In FRENCH
(CETIM-108220; ETN-91-98337) Copyright Avail: NTIS HC/MF A06

The main principles used in antivibration isolation are outlined. Uncoupling of movement is discussed. Impact isolation is considered separately. Antivibration suspension systems are outlined. Dimensional analysis of elastic suspension systems is investigated. Antivibration supports set directly upon foundations are discussed. The various types of antivibration isolating materials are described. Vibration measurement techniques are discussed. Units of measure, vectorial interpretation of harmonic vibration and characterization of isolator dynamics are described. ESA

N91-13776# Centre Technique des Industries Mecaniques, Senlis (France).
CALCULATIONS FOR STRUCTURES WITH NONLINEAR JOINTS Final Report [CALCUL DES STRUCTURES A APPUIS NON LINEAIRES]
M. Kadiri, D. Grolade, Y. Birembaut, and A. Naidon 21 Nov. 1988 109 p In FRENCH
(CETIM-108830; ETN-91-98338) Copyright Avail: NTIS HC/MF A06

An iterative algorithm is used in an E2D module of Castor to take the behavior of nonlinear joints into account. Tests carried out to better understand joint behavior and tests carried out on a Bride PN40 DN200 to validate the calculation method and the numerical and experimental results are described. The calculation method developed allows for elastic supports with independent rigidity and varying degrees of loading to be calculated. It is most applicable to bolted assemblies. Further development of the method needed to facilitate practical applications is discussed. ESA

N91-13777# Royal Aerospace Establishment, Farnborough (England).
SUSTAINED-LOAD CRACK GROWTH OF 8090 ALUMINIUM-LITHIUM ALLOY PLATE IN DRY AIR AT 50-200 C
S. P. Lynch 10 Jul. 1990 32 p Sponsored by Defence Science and Technology Organization, Melbourne, Australia, and Alcan International Labs., Banbury, England
(RAE-TR-90033; RAE-MAT/STR-288; BR114930; ETN-91-98365) Copyright Avail: NTIS HC/MF A03

The effects of test temperature, stress intensity factor, sodium impurities and aging condition on the short transverse creep cracking of precracked Al-Li-Cu-Mg-Zr alloy plates are studied. Several tests were carried out on two commercial 8090 plates aged 32 hours at 170 C. Three experimental Al-Li alloy plates, containing different trace amounts of sodium were studied and solution treated, quenched, naturally aged for several years and then artificially aged for 32 hours at 170 C. Some creep tests were carried out on two conventional aluminum alloy plates for comparison with the 8090 alloys. Significant rates of cracking were observed in 8090 alloys at temperatures as low as 60 C for low stress intensity factors. Metallographic and fractographic observations suggest that the presence of liquid, sodium rich impurity phases promote creep cracking in 8090 alloys. Creep cracking in conventional Al alloys is probably exacerbated by solid impurity phases. ESA

N91-13778# Southampton Univ. (England). Inst. of Sound and Vibration Research.
PRACTICAL CONSIDERATIONS FOR THE MEASUREMENT OF INTERNAL AND COUPLING LOSS FACTORS ON COMPLEX STRUCTURES
N. Lalor Jun. 1990 12 p
(ISVR-TR-182; ETN-91-98376) Avail: NTIS HC/MF A03

A solution to the difficulty in calibrating true subsystem energies from vibration measurements in statistical energy analysis is proposed. From measurements made on fully assembled structures, the following conclusions are obtained: internal loss factors can be directly calculated from subsystem energy injected power measurements without making any assumptions about the way in which power flows between subsystems; the accuracy of the calculated coupling loss factors can be considerably enhanced by using the fact that unconnected subsystems have zero coupling loss factors; for systems having three or more subsystems, there is a redundancy of information obtained via the consistency relationships and the resulting equalities, which involve triple products of coupling loss factors, allow an independent check on calculated values. It is suggested that an electrical analogy exists for vibrational power flow between subsystems. ESA

42 GEOSCIENCES (GENERAL)

N91-13779# Department of Energy, Washington, DC. Office of Energy Research.
SUMMARIES OF PHYSICAL RESEARCH IN THE GEOSCIENCES
Oct. 1990 145 p
(DE91-001043; DOE/ER-0474T) Avail: NTIS HC/MF A07

The Department of Energy supports research in the geosciences in order to provide a sound foundation of fundamental knowledge in those areas of the geosciences which are germane to the Department of Energy's many missions. The Division of Engineering and Geosciences, part of the Office of Basic Energy Sciences of the Office of Energy Research, supports the Geosciences Research Program. The participants in this program include Department of Energy laboratories, industry, universities, and other governmental agencies. The summaries in this document, prepared by the investigators, briefly describe the scope of the individual programs. The Geosciences Research Program includes research in geology, petrology, geophysics, geochemistry, solar physics, solar-terrestrial relationships, aeronomy, seismology, and natural resource modeling and analysis, including their various subdivisions and interdisciplinary areas. All such research is related either directly or indirectly to the Department of Energy's long-range technological needs. DOE

N91-13780# Lawrence Livermore National Lab., CA. Dept. of Physics.
ATMOSPHERIC AND GEOPHYSICAL SCIENCES DIVISION PROGRAM REPORT, 1988 - 1989
Jun. 1990 85 p
(Contract W-7405-eng-48)
(DE91-001057; UCRL-51444-88/89) Avail: NTIS HC/MF A05

In 1990, the Atmospheric and Geophysical Sciences Division begins its 17th year as a division. As the Division has grown over the years, its modeling capabilities have expanded to include a broad range of time and space scales ranging from hours to decades and from local to global. Our modeling is now reaching out from its atmospheric focus to treat linkages with the oceans and the land. In this report, we describe the Division's goal and organizational structure. We also provide tables and appendices describing the Division's budget, personnel, models, and publications. DOE

43 EARTH RESOURCES AND REMOTE SENSING

Includes remote sensing of earth resources by aircraft and spacecraft; photogrammetry; and aerial photography.

For instrumentation see *35 Instrumentation and Photography.*

N91-13781 Colorado Univ., Boulder.
A PHYSICAL PARAMETERIZATION OF SNOW ALBEDO FOR USE IN CLIMATE MODELS Ph.D. Thesis
Susan Elaine Marshall 1989 174 p
Avail: Univ. Microfilms Order No. DA9024849

The albedo of a natural snowcover is highly variable ranging from 90 percent for clean, new snow to 30 percent for old, dirty snow. This range is albedo represents a difference in surface energy absorption of 10 to 70 percent of incident solar radiation. Most general circulation models (GCMs) fail to calculate the surface snow albedo accurately, yet the results of these models are sensitive to the assumed value of the snow albedo. The current simple empirical parameterizations of snow albedo are replaced with a physically-based parameterization which is accurate yet efficient to compute. The parameterization is designed as a FORTRAN subroutine (called SNOALB) which can be easily implemented into model code. The subroutine requires less than 0.02 seconds of computer time (CRAY X-MP) per call and adds only one new parameter to the model calculations, the snow grain size. The snow grain size can be calculated according to one of the two methods offered. All other input variables to the subroutine are available from a climate model. The subroutine calculates a visible, near-infrared and solar snow albedo and offers a choice of two wavelengths at which the solar spectrum is separated into the visible and near-infrared components. The parameterization is incorporated into the National Center for Atmospheric Research (NCAR) Community Climate Model, version 1 (CCM1), and the results of a five-year, seasonal cycle, fixed hydrology experiment are compared to the current model snow albedo parameterization. The results show the SNOALB albedos to be comparable to the old CCM1 snow albedos for current climate conditions, with generally higher visible and lower near-infrared snow albedos using the new subroutine. However, this parameterization offers a greater predictability for climate change experiments outside the range of current snow conditions because it is physically-based and not tuned to current empirical results. Dissert. Abstr.

N91-13782*# Colorado Univ., Boulder. Cooperative Inst. for Research in Environmental Sciences.
SEA ICE-ATMOSPHERE INTERACTION: APPLICATION OF MULTISPECTRAL SATELLITE DATA IN POLAR SURFACE ENERGY FLUX ESTIMATES Progress Report
K. Steffen, A. Schweiger, J. Maslanik, J. Key, R. Weaver, and R. Barry Nov. 1990 37 p
(Grant NAGw-2158)
(NASA-CR-187376; NAS 1.26:187376) Avail: NTIS HC/MF A03 CSCL 08B

The application of multi-spectral satellite data to estimate polar surface energy fluxes is addressed. To what accuracy and over which geographic areas large scale energy budgets can be estimated are investigated based upon a combination of available remote sensing and climatological data sets. The general approach was to: (1) formulate parameterization schemes for the appropriate sea ice energy budget terms based upon the remotely sensed and/or in-situ data sets; (2) conduct sensitivity analyses using as input both natural variability (observed data in regional case studies) and theoretical variability based upon energy flux model concepts; (3) assess the applicability of these parameterization schemes to both regional and basin wide energy balance estimates using remote sensing data sets; and (4) assemble multi-spectral, multi-sensor data sets for at least two regions of the Arctic Basin and possibly one region of the Antarctic. The type of data needed for a basin-wide assessment is described and the temporal coverage of these data sets are determined by data availability and need as defined by parameterization scheme. The titles of the subjects are as follows: (1) Heat flux calculations from SSM/I and LANDSAT data in the Bering Sea; (2) Energy flux estimation using passive microwave data; (3) Fetch and stability sensitivity estimates of turbulent heat flux; and (4) Surface temperature algorithm. Author

N91-13783# Instituto de Pesquisas Espaciais, Sao Jose dos Campos (Brazil).
METHOD OF SELECTION OF TM/LANDSAT COLOR COMPOSITION FOR ANALYSIS OF LAND USE CLASSES M.S. Thesis [METODO DE SELECAO DE COMPOSICOES COLORIDAS TM/LANDSAT PARA ANALISE DE CLASSES DE USO DA TERRA]
Eliana Franco BuenoBucci Sep. 1990 135 p In PORTUGUESE; ENGLISH summary
(INPE-5119-TDL/421) Avail: NTIS HC/MF A07

The objective is to determine the color composites generated using digital processing (feature selection and radiometric enhancement) that enhance visual interpretation and improve the separability of land use classes in Conchal, Sao Paulo State. The procedure is based on a comparison among thematic classes, taking into consideration the following visual parameters such as shape, texture, color, and tone. A set of images was interpreted by different photointerpreters. The results from each interpreter were compared to the ground truth data, and then, a multiple comparison test (Scheffe) was applied. The results of the analysis

showed that the best color composites were 3B2G4R, enhanced by contrast stretch, 4I5H1S and 4I7H2S, enhanced by IHS/RGB transformation. The color parameter has the best performance. Citrus (8 years), pinus, and sugar cane (third stage) presented better separability among the land use classes analyzed. Author

N91-13784# Instituto de Pesquisas Espaciais, Sao Jose dos Campos (Brazil).

METHODOLOGICAL CONTRIBUTION UTILIZING TM/LANDSAT-5 IMAGERY IN GEOLOGIC MAPPING OF REGIONS WITH SIGNIFICANT VEGETATIVE COVER M.S. Thesis, 28 Nov. 1989 [CONTRIBUICAO METODOLOGICA A UTILIZACAO DE IMAGENS TM/LANDSAT-5 NO MAPEAMENTO GEOLOGICO DE REGIOES COM SIGNIFICATIVA COBERTURA VEGETAL]

Britaldo SilveiraSoaresFilho Sep. 1990 142 p In PORTUGUESE; ENGLISH summary
(INPE-5117-TDL/419) Avail: NTIS HC/MF A07

This work contributes to the methodological development of TM/LANDSAT-5 imagery application to geologic vegetation influence on the global and geologic information contents of multispectral/multitemporal images, selecting the best season for imagery acquisition and bands triplets with maximum information content, and defining a digital enhancements sequence. TM/LANDSAT imageries acquired in September 1985, October 1985, and May 1987, were used. Bands selection and information content analysis were done using multitemporal data and dry season imagery data subtracted by the vegetation class and vegetation plus mixture classes. Spatial and spectral attributes were treated and analyzed. Linear filtering applied to TM4 and to the first principal component was used to enhance spatial attributes. Both attributes were integrated by IHS merging and hybrid composition. As a result, the subtraction of vegetation and mixture classes showed the information ellipsoids along the gray line of the RGB cube, as demonstrated by the increase in variance values and correlation coefficients. The best triplets selected for soils and rocks discrimination were TM3-TM5-TM7 and TM1-TM5-TM7. The dry season imagery data were preferred because they show the best contribution of the vegetation to photogeologic interpretation and favor the soil and rock spectral approach.

Author

N91-13785# Beleidscommissie Remote Sensing, Delft (Netherlands).

THE RELATION BETWEEN TREE PHYSIOLOGY AND MULTISPECTRAL AND COLOR PHOTOGRAPHY: FIRST PHASE [RELATIE TUSSEN BOOMFYSIOLOGIE EN MULTISPECTRAAL- EN KLEURENFOTOGRAFFE: ERSTE FASE]

J. A. M. vandenAncker, D. C. vanderWerf, H. vanderVoet, W. Jans, and H. Relou (Instituut voor Bosbouw en Groenbeheer, Wageningen, Netherlands) Feb. 1990 201 p In DUTCH
(BCRS-89-39; ETN-90-97688) Avail: NTIS HC/MF A10

The relationship between the image of a tree on an aerial photograph and the real tree was investigated, and the feasibility of multispectral photography for the tree vitality monitoring was assessed. The image of a tree and its appearance in the field were compared. The choice of spectral bands for aerial photography, and the information provided by the photographic red edge are discussed. The representation of a tree crown on an aerial photograph is outlined with a view to the description of tree vitality. The spectral radiometric and geometric resolution of the color-infrared film and multispectral film-filter combinations were compared. The image processing system, the calibration and accuracy of aerial photographs, and correlation tests are discussed. The effects of acid rain in two forest stands were analyzed.

ESA

N91-13786# Technische Univ., Delft (Netherlands). Faculty of Geodesy.

STUDY OF STRATEGIES FOR THE DETERMINATION OF DEFORMATIONS FROM GLOBAL POSITIONING SYSTEM (GPS) MEASUREMENTS Thesis [ONDERZOEK NAAR STRATEGIEEN TER BEPALING VAN DEFORMATIES UIT GPS-METINGEN]

W. J. Kok May 1990 116 p In DUTCH
(ETN-91-98141) Avail: NTIS HC/MF A06

Strategies which can be used for the determination of deformations with a view to the extraction of natural gas are studied. Deformations are deduced from measurements of a network at several instants using a mathematical model consisting of a stochastic and a functional model: phase one is the adjustment of the network with the mathematical model per instant; phase two, in which the deformation parameters are determined can be subdivided into two strategies. The first starts from the adjusted coordinates at all instants, while the second starts from the observations at all instants. Each strategy can still be subdivided following the method used to determine the deformation parameters in the deformation model. ESA

N91-13787*# National Aeronautics and Space Administration. Pasadena Office, CA.

SYSTEM AND METHOD FOR MEASURING OCEAN SURFACE CURRENTS AT LOCATIONS REMOTE FROM LAND MASSES USING SYNTHETIC APERTURE RADAR Patent Application

Lawrence E. Young, inventor (to NASA) (Jet Propulsion Lab., California Inst. of Tech., Pasadena.) 14 Mar. 1990 22 p
(Contract NAS7-918)
(NASA-Case-NPO-17937-1-CU; NAS 1.71:NPO-17937-1-CU; US-Patent-Appl-SN-493190) Avail: NTIS HC/MF A03 CSCL 08F

A system for measuring ocean surface currents from an airborne platform is disclosed. A radar system having two spaced antennas wherein one antenna is driven and return signals from the ocean surface are detected by both antennas is employed to get raw ocean current data which are saved for later processing. There are a pair of global positioning system (GPS) systems including a first antenna carried by the platform at a first location and a second antenna carried by the platform at a second location displaced from the first antenna for determining the position of the antennas from signals from orbiting GPS navigational satellites. Data are also saved for later processing. The saved data are subsequently processed by a ground-based computer system to determine the position, orientation, and velocity of the platform as well as to derive measurements of currents on the ocean surface. NASA

N91-13788*# Stanford Univ., CA. Physics Lab.

GRADIOMETRY COEXPERIMENTS TO THE GRAVITY PROBE B AND STEP MISSIONS

M. Tapley, J. Breakwell, C. W. F. Everitt, R. vanPatten, and P. Worden 1990 7 p
(Contract NAS5-28067)
(NASA-CR-187704; NAS 1.26:187704) Avail: NTIS HC/MF A02 CSCL 08E

The Gravity Probe-B (GP-B) spacecraft, designed to test predictions of general relativity, will fly in the mid 1990s. It will carry four electrostatically suspended gyroscopes in a cryogenic environment and will have a drag-free control system to minimize disturbances on the gyroscopes. The Stanford Test of Equivalence Principle (STEP) spacecraft, to fly later, will carry a set of test masses under very similar conditions. The possibility of using differential measurements of the GP-B gyroscopes suspension forces and the STEP tests mass displacement readout to form single-axis gravity gradiometers is explored. It is shown that the noise in the suspension systems is sufficiently small in the relevant frequency range, and that enough information is collected to compensate for the spacecrafts' attitude motion. Finally, using Breakwell's flat-earth approximation, these experiments are compared to other geodesy experiments and predict the

contribution they can make to the knowledge of the Earth's geopotential. Author

N91-13789 Institute for Perception RVO-TNO, Soesterberg (Netherlands).
COLOUR SPECIFICATIONS FOR THE ELECTRONIC CHART DISPLAY AND INFORMATION SYSTEM (ECDIS) Final Report
J. Walraven and J. W. A. M. Alferdinck 5 Jun. 1990 35 p Original contains color illustrations
(Contract R87/KM/123)
(IZF-1990-A-19; TD-90-1609; ETN-91-98314) Copyright Avail: Institute for Perception RVO-TNO, P.O. Box 23, 3769 ZG Soesterberg, Netherlands

The problem of developing a color standard for the electronic sea chart is discussed. Due to the high (color coded) information content of the electronic chart, which shows much more than just hydrological features, a rather extensive color look up table is required. Using an analytical chart and a test pattern with representative graphical features, two color palettes are selected, for a daytime and a nighttime display, respectively. These two display modes may easily be modified (by varying screen luminance only) to accommodate intermediate ambient light levels as well. Each color palette is subdivided into foreground colors, both categories containing also some transparent colors. The individual colors are chosen such that the discriminability of foreground information (characters, symbols, tracks, etc.) is adequate at all foreground color combinations. ESA

N91-13790 Royal Netherlands Meteorological Inst., De Bilt. Dynamical Meteorology Dept.
THE USE OF SATELLITE DATA IN THE ECMWF ANALYSIS SYSTEM
Krisztina Labancz (Institute for Atmospheric Physics, Budapest, Hungary) 1990 15 p Sponsored by IAESTE
(KNMI-TR-123; ISSN-0169-1708; ETN-91-98318) Copyright Avail: Royal Netherlands Meteorological Institute, P.O. Box 201, 3730 AE De Bilt, Wilhelminalaan 10, Netherlands

A general survey of the use of satellite data is given. Quality control and selection of incoming observations are described. Data obtained from geostationary satellites are briefly outlined and a detailed description of polar orbiting satellite data is given. The radiance measurement instruments, the sensed parameters and the finally retrieved atmospheric profiles are studied. A brief description of the retrieval procedure, the quality controls and the data selection processes used by the ECMWF (European Centre for Medium Weather Forecasts) analysis system with regard to satellite sounding and radiance data, is given. The compact of satellite soundings and further developments are outlined. ESA

N91-13791# Technische Univ., Delft (Netherlands). Faculty of Aerospace Engineering.
REPORT BY THE SUBCOMMITEE ON INTERCOMPARISON AND MERGING OF GEODETIC DATA OF THE TOPEX/POSEIDON SCIENCE WORKING TEAM
K. F. Wakker May 1990 37 p
(LR-638; ETN-91-98320) Avail: NTIS HC/MF A03

During the first Topex/Poseidon (T/P) Science Definition Team (SDT) meeting at the NASA Jet Propulsion Laboratory (JPL) in November 1987, a Subcommitee on Intercomparison and Merging of Geodetic Data (SIMGD) was formed. Two new reference orbits were proposed. Operational orbit determination is to be performed. Recommendations on the T/P projects were made. A verification phase was fixed for the prelaunch T/P performance expectations. Recommendations were made on the altimeter calibration, the standardization of constants and models, and on the reference system, the gravity and tide models, the geoid and mean sea surface, the altimeter operations schedule, flags and land sea maps, crossover dataset, and data processing preparation. The reproduction of a summary sheet for the description of a terrestrial system attached to a set of station coordinates, is appended. ESA

44 ENERGY PRODUCTION AND CONVERSION

Includes specific energy conversion systems, e.g., fuel cells; global sources of energy; geophysical conversion; and windpower.

For related information see also *07 Aircraft Propulsion and Power, 20 Spacecraft Propulsion and Power,* and *28 Propellants and Fuels.*

N91-13792# Midwest Research Inst., Golden, CO. Solar Energy Research Inst.
SERI PHOTOVOLTAIC SUBCONTRACT REPORTS: ABSTRACTS AND DOCUMENT CONTROL INFORMATION Report, 1 Jan. - 31 Jul. 1990
Oct. 1990 17 p
(Contract DE-AC02-83CH-10093)
(DE90-000378; SERI/TP-211-3934) Avail: NTIS HC/MF A03

This report contains the document control information and abstracts for Solar Energy Research Institute (SERI) Photovoltaic (PV) Program Branch publications resulting from SERI's subcontracted PV research. The information is presented for reports published or distributed from January 1 through July 31, 1990. In the past, copies of the subcontractor reports were distributed to a broad spectrum of researchers in the field of photovoltaics at a considerable cost to the program. In an attempt to reduce costs and ensure that all researchers receive those current publications that are of specific interest to them, this report will outline these publications, organized by technology, on a regular basis. A list of additional publications and sources is included herein to provide the photovoltaic community with other sources of information. All of the documents represented here are available from the National Technical Information Service (NTIS) and can be purchased using the NTIS order form at the end of this document. Further information on a given subcontracted program may be obtained from the SERI technical monitor identified on each Document Control Page. DOE

N91-13793# Sandia National Labs., Albuquerque, NM.
STATUS OF CONCENTRATOR COLLECTOR AND HIGH-EFFICIENCY CONCENTRATOR CELL DEVELOPMENT
James M. Gee 1990 16 p Presented at the 5th International Photovoltaic Science and Engineering Conference, Kyoto, Japan, 26-30 Nov. 1990
(Contract DE-AC04-76DP-00789)
(DE91-001260; SAND-90-2598C; CONF-9011118-1) Avail: NTIS HC/MF A03

Photovoltaic concentrator collectors are an attractive option for utility-scale photovoltaic power plants. This paper reviews the current status of photovoltaic concentrator collector and cell development. Included in the review is a discussion of the economic motivation for concentrators, a summary of recent concentrator collector and cell development, and a description of a major new program to accelerate development and commercial introduction of concentrator collectors. DOE

N91-13794# Giner, Inc., Waltham, MA.
CORROSION-RESISTANT CATALYST SUPPORTS FOR PHOSPHORIC ACID FUEL CELLS
J. A. Kosek, C. C. Cropley, and A. B. LaConti 1990 5 p Presented at the Fuel Cell Seminar, Phoenix, AZ, 26-28 Nov. 1990
(Contracts DE-FG02-90ER-80861; DE-AC02-89ER-80807)
(DE91-001713; CONF-901106-2-Extd-Abst) Avail: NTIS HC/MF A01

High-surface-area carbon blacks such as Vulcan XC-72 (Cabot Corp.) and graphitized carbon blacks such as 2700 C heat-treated Black Pearls 2000 (HTBP) (Cabot Corp.) have found widespread applications as catalyst supports in phosphoric acid fuel cells (PAFCs). However, due to the operating temperatures and pressures being utilized in PAFCs currently under development, the carbon-based cathode catalyst supports suffer from corrosion, which decreases the performance and life span of a PAFC stack.

The feasibility of using alternative, low-cost, corrosion-resistant catalyst support (CRCS) materials as replacements for the cathode carbon support materials was investigated. The objectives of the program were to prepare high-surface-area alternative supports and to evaluate the physical characteristics and the electrochemical stability of these materials. The O2 reduction activity of the platinized CRCS materials was also evaluated. DOE

N91-13795# Sandia National Labs., Albuquerque, NM.
A THEORETICAL INVESTIGATION OF EFFECTIVE SURFACE RECOMBINATION VELOCITY IN AlGaAs/GaAs HETEROFACE SOLAR CELLS
James M. Gee and Timothy J. Drummond 1990 11 p Presented at the 5th International Photovoltaic Science and Engineering Conference, Kyoto, Japan, 26-30 Nov. 1990
(Contract DE-AC04-76DP-00789)
(DE91-001754; SAND-90-2597C; CONF-9011118-2) Avail: NTIS HC/MF A03

An AlGaAs window layer is used in high-efficiency GaAs solar cells to reduce carrier recombination at the front surface. Free surfaces of III-V semiconductors have a high density of surface states that serve as recombination sites and create a depletion region at the front surface. We have performed a theoretical investigation of front-surface recombination that includes the effect of a surface space-charge layer. It was found that the surface space-charge layer can have a profound effect on front-surface recombination for thin or lightly doped window layers. DOE

N91-13796*# National Aeronautics and Space Administration. Pasadena Office, CA.
THERMAL POWER TRANSFER SYSTEM USING APPLIED POTENTIAL DIFFERENCE TO SUSTAIN OPERATING PRESSURE DIFFERENCE Patent Application
Pradeep Bhandari, inventor (to NASA) and Toshio Fujita, inventor (to NASA) (Jet Propulsion Lab., California Inst. of Tech., Pasadena.) 16 Aug. 1990 14 p
(Contract NAS7-918)
(NASA-Case-NPO-18034-1-CU; NAS 1.71:NPO-18034-1-CU; US-Patent-Appl-SN-568130) Avail: NTIS HC/MF A03 CSCL 10B

A thermal power transfer system using a phase change liquid gas fluid in a closed loop configuration has a heat exchanger member connected to a gas conduit for inputting thermal energy into the fluid. The pressure in the gas conduit is higher than a liquid conduit that is connected to a heat exchanger member for outputting thermal energy. A solid electrolyte member acts as a barrier between the gas conduit and the liquid conduit adjacent a solid electrolyte member. The solid electrolyte member has the capacity of transmitting ions of a fluid through the electrolyte member. The ions can be recombined with electrons with the assistance of a porous electrode. An electrical field is applied across the solid electrolyte member to force the ions of the fluid from a lower pressure liquid conduit to the higher pressure gas conduit. NASA

N91-13797# Department of Energy, Washington, DC. Office of Coal, Nuclear, Electric and Alternate Fuels.
SOLAR COLLECTOR MANUFACTURING ACTIVITY, 1988
30 Nov. 1989 47 p
(DE90-003539; DOE/EIA-0174(88)) Avail: NTIS HC/MF A03

This report was prepared by the Energy Information Administration, the independent statistical and analytical agency within the U.S. Department of Energy in cooperation with the Office of Conservation and Renewable Energy. The report presents data on producer shipments and end uses obtained from manufacturers and importers of solar thermal collectors and photovoltaic modules. It provides annual data necessary for the Department of Energy to execute its responsibility to: (1) monitor activities and trends in the solar collector manufacturing industry, (2) prepare the national energy strategy, and (3) provide information on the size and status of the industry to interested groups such as the U.S. Congress, government agencies, the Solar Energy Research institute, solar energy specialists, manufacturers, and the general public. DOE

N91-13798# Edgerton, Germeshausen and Grier, Inc., Idaho Falls, ID.
SUPERCRITICAL BINARY GEOTHERMAL CYCLE EXPERIMENTS WITH MIXED-HYDROCARBON WORKING FLUIDS AND A NEAR-HORIZONTAL IN-TUBE CONDENSER
C. J. Bliem and G. L. Mines Dec. 1989 108 p
(Contract DE-AC07-76ID-01570)
(DE91-001815; EGG-EP-8800) Avail: NTIS HC/MF A06

The Heat Cycle Research Program, which is being conducted for the Department of Energy, has as its objective the development of the technology for effecting improved utilization of moderate temperature geothermal resources. Testing at the Heat Cycle Research Facility which was located at the DOE Geothermal Test Facility, East Mesa, California is presently being conducted to meet this objective. The testing effort discussed in this interim report involves a supercritical vaporization and counterflow in-tube condensing system with a near horizontal tube orientation. A previous report explored the supercritical heating, supersaturated turbine expansions and the condenser performance in the vertical orientation. This report presents a description of the test facility and results from a part of the program in which the condenser was oriented in a nearly horizontal orientation. Results of the experiments for the in-tube condenser in a nearly horizontal orientation are given for both pure and mixed-hydrocarbon working fluids. Although most of the data is for a completely active condenser in countercurrent flow, some data is available for a configuration in which half of the tubes were plugged and some data for cocurrent (parallel) flow is analyzed. The horizontal-oriented condenser behavior predicted by the Heat Transfer Research Institute computer codes used for correlation of the data was not in agreement with experimental results at this orientation. Some reasons for this difference are discussed. A special series of tests, conducted with propane and up to approximately 40 percent isopentane concentration, indicated that a close approach to 'integral' condensation has occurred as was the case with the horizontally oriented condenser (similar results were obtained for the vertical condenser). DOE

N91-13799# Idaho National Engineering Lab., Idaho Falls.
SECOND LAW ANALYSIS OF ADVANCED POWER GENERATION SYSTEMS USING VARIABLE TEMPERATURE HEAT SOURCES
C. J. Bliem and G. L. Mines 1990 8 p Presented at the ASME Winter Annual Meeting, Dallas, TX, 25-30 Nov. 1990
(Contract DE-AC07-76ID-01570)
(DE91-001818; EGG-M-90376; CONF-901194-6) Avail: NTIS HC/MF A02

Many systems produce power using variable temperature (sensible) heat sources. The Heat Cycle Research Program is currently investigating the potential improvements to such power cycles utilizing moderate temperature geothermal resources to produce electrical power. It has been shown that mixtures of saturated hydrocarbons (alkanes) or halogenated hydrocarbons operating with a supercritical Rankine cycle gave improved performance over boiling Rankine cycles with the pure working fluids for typical applications. Recently, in addition to the supercritical Rankine Cycle, other types of cycles have been proposed for binary geothermal service. This paper explores the limits on efficiency of a feasible plant and discusses the methods used in these advanced concept plants to achieve the maximum possible efficiency. The advanced plants considered appear to be approaching the feasible limit of performance so that the designer must weigh all considerations to fine the best plant for a given service. These results would apply to power systems in other services as well as to geothermal power plants. DOE

N91-13800# Sandia National Labs., Albuquerque, NM.
CARBON DIOXIDE REFORMING OF METHANE IN A SOLAR VOLUME-TRIC RECEIVER-REACTOR: THE CAESAR (CATALYTICALLY ENHANCED SOLAR ABSORPTION RECEIVER) PROJECT
Reiner Buck (Stuttgart Univ., Germany, F.R.), James F. Muir, Roy E. Hogan, and Russell D. Skocypec 1990 22 p Presented at

the 5th International Symposium on Solar High-Temperature Technologies, Davos, Switzerland, 27-31 Aug. 1990
(Contract DE-AC04-76DP-00789)
(DE91-002340; SAND-90-0884C; CONF-9008139-3) Avail: NTIS HC/MF A03

Solar reforming of methane with CO2 was demonstrated successfully with a direct absorption receiver/reactor on a parabolic dish capable of 150 kW solar power. The reactor, a volumetric absorber, consisted of a reticulated porous alumina foam disk coated with rhodium catalyst. The system was operated during both steady-state and solar transient (cloud passage) conditions. The total solar power absorbed reached values up to 97 kW and the maximum methane conversion was almost 70 percent. Receiver efficiencies ranged up to 85 percent and chemical efficiencies peaked at 54 percent. DOE

N91-13801# Aeronautical Research Inst. of Sweden, Stockholm. Dept. of Aerodynamics.
AIRFOIL DESIGN FOR VARIABLE RPM HORIZONTAL AXIS WIND TURBINES
Anders Bjoerck Jan. 1990 10 p Presented at EWEC 1989, Glasgow, Scotland
(Contract STEV-506-266-4)
(FFA-TN-1990-02; ETN-91-98266) Avail: NTIS HC/MF A02

The design criteria for new airfoils for a variable speed horizontal axis wind turbine are described. The two series of airfoils developed are characterized by high design lift coefficients in order to achieve small blade chords, high lift drag ratios for the airfoil sections designed for the outer part of the blade, performance insensitivity to surface roughness, and a gentle stall at an angle of attack in order to reduce excessive loads. Each series consists of airfoils with varying thickness to chord ratios for different radial stations. Interpolation between the two series is possible. ESA

N91-13802*# National Aeronautics and Space Administration. Lewis Research Center, Cleveland, OH.
SMALL PARTICLE SELECTIVE EMITTER Patent Application
Donald L. Chubb, inventor (to NASA) 30 Mar. 1990 14 p
(NASA-Case-LEW-14731-1; NAS 1.71:LEW-14731-1; US-Patent-Appl-SN-503486) Avail: NTIS HC/MF A03 CSCL 10C

This invention relates to a small particle selective emitter for converting thermal energy into narrow band radiation with high efficiency. The small particle selective emitter is used in combination with a photovoltaic array to provide a thermal to electrical energy conversion device. An energy conversion apparatus of this type is called a thermo-photovoltaic device. In the first embodiment, small diameter particles of a rare earth oxide are suspended in an inert gas enclosed between concentric cylinders. The rare earth oxides are used because they have the desired property of large emittance in a narrow wavelength band and small emittance outside the band. However, it should be emphasized that it is the smallness of the particles that enhances the radiation property. The small particle selective emitter is surrounded by a photovoltaic array. In an alternate embodiment, the small particle gas mixture is circulated through a thermal energy source. This thermal energy source can be a nuclear reactor, solar receiver, or combustor of a fossil fuel. NASA

N91-13803*# National Aeronautics and Space Administration. Lewis Research Center, Cleveland, OH.
THIN SOLAR CELL AND LIGHTWEIGHT ARRAY Patent Application
Henry W. Brandhorst, inventor (to NASA) and Irving Weinberg, inventor (to NASA) 20 Mar. 1990 14 p
(NASA-Case-LEW-14959-1; NAS 1.71:LEW-14959-1; US-Patent-Appl-SN-495969) Avail: NTIS HC/MF A03 CSCL 10A

A thin, lightweight solar cell utilizes front contact metallization. Both the front light receiving surface of the solar cell and the facing surface of the cover glass are recessed to accommodate this metallization. This enables the two surfaces to meet flush for an optimum seal. NASA

N91-13804* Sverdrup Technology, Inc., Cleveland, OH.
COMPARISON OF NASA LEWIS RESEARCH CENTER'S PERFORMANCE CODE'S PRESSURE-DROP MODEL PREDICTIONS TO STIRLING ENGINE WORKING-SPACE FLOW TEST DATA
Timothy J. Sullivan Dec. 1988 20 p
(Contracts NAS3-25266; DE-AI01-85CE-50112)
(NASA-CR-182215; DOE/NASA/5266-1; NAS 1.26:182215)
Avail: NTIS HC/MF A03 CSCL 10B

In support of DOE's Stirling Engine Highway Vehicle Systems program, the NASA Lewis Research Center's Stirling engine performance code's pressure-drop model was validated in this study. The validation was accomplished by comparing P-40 Stirling engine working-space pressure-drop prediction to experimental data for various steady flow test conditions. Details of the flow test rig and the working-space pressure-drop predictions are included. After making various improvements to the Stirling engine pressure-drop model, the comparison showed good agreement between the working-space pressure drop predictions and the flow rig data. Author

N91-13805# Department of Energy, Morgantown, WV. Office of Fossil Energy.
FUEL CELLS Technology Status Report
T. J. George and M. J. Mayfield Nov. 1990 67 p
(DE90-009686; DOE/METC-90-0268) Avail: NTIS HC/MF A04

This report summarizes the Fuel Cell program at the Department of Energy (DOE), Morgantown Energy Technology Center (METC) through mid-1990. A brief history of the Fuel Cell program is given. Options for fuel cell commercialization are reviewed. In particular, molten carbonate fuel cells, phosphoric acid and solid oxide fuel cells are discussed. DOE

N91-13806# Sandia National Labs., Albuquerque, NM.
EXPERIMENTS ON BENCH-SCALE HEAT-PIPE SOLAR RECEIVERS
Douglas R. Adkins 1990 8 p Presented at the 8th Symposium on Space Nuclear Power Systems, Albuquerque, NM, 6-9 Jan. 1991
(Contract DE-AC04-76DP-00789)
(DE90-013806; SAND-90-1779C; CONF-910116-1) Avail: NTIS HC/MF A02

Tests have been conducted on bench-scale heat-pipe solar receivers to explore methods of constructing wicks. The primary objective was to develop a wick structure that was easy to fabricate and was capable of transporting liquid sodium over long distances against hydrostatic and frictional pressure drops. One of the wicks tested in this program was able to lift sodium 45 cm by capillary pumping alone to cool a 3-cm times 10-cm area subjected to a 50 W/cm(exp 2) flux. DOE

45 ENVIRONMENT POLLUTION

Includes atmospheric, noise, thermal, and water pollution.

N91-13807*# Southwest Research Inst., San Antonio, TX.
SEPAC DATA ANALYSIS IN SUPPORT OF THE ENVIRONMENTAL INTERACTION PROGRAM Interim Report
Chin S. Lin 22 May 1990 51 p
(Contract NAS8-32488; NAGw-1231; SwRI Proj. 15-4865-009)
(NASA-CR-184028; NAS 1.26:184028) Avail: NTIS HC/MF A04 CSCL 13B

Injections of nonrelativistic electron beams from an isolated equipotential conductor into a uniform background of plasma and neutral gas were simulated using a two dimensional electrostatic particle code. The ionization effects of spacecraft charging are examined by including interactions of electrons with neutral gas. The simulations show that the conductor charging potential decreases with increasing neutral background density due to the production of secondary electrons near the conductor surface. In the spacecraft wake, the background electrons accelerated towards

the charged space craft produced an enhancement of secondary electrons and ions. Simulations run for longer times indicate that the spacecraft potential is further reduced and short wavelength beam-plasma oscillations appear. The results are applied to explain the space craft charging potential measured during the SEPAC experiments from Spacelab 1. A second paper is presented in which a two dimensional electrostatic particle code was used to study the beam radial expansion of a nonrelativistic electron beam injected from an isolated equipotential conductor into a background plasma. The simulations indicate that the beam radius is generally proportional to the beam electron gyroradius when the conductor is charged to a large potential. The simulations also suggest that the charge buildup at the beam stagnation point causes the beam radial expansion. From a survey of the simulation results, it is found that the ratio of the beam radius to the beam electron gyroradius increases with the square root of beam density and decreases inversely with beam injection velocity. This dependence is explained in terms of the ratio of the beam electron Debye length to the ambient electron Debye length. These results are most applicable to the SEPAC electron beam injection experiments from Spacelab 1, where high charging potential was observed.
Author

N91-13808*# Jet Propulsion Lab., California Inst. of Tech., Pasadena. Goldstone Deep Space Communications Complex.
ENVIRONMENTAL PROJECTS. VOLUME 12: FRIABLE ASBESTOS ABATEMENT, GDSCC
15 Jun. 1990 210 p
(NASA-CR-187636; JPL-Publ-87-4; NAS 1.26:187636) Avail: NTIS HC/MF A10 CSCL 13B

The Goldstone Deep Space Communications Complex (GDSCC) is part of the NASA Deep Space Network, one of the world's largest and most sensitive scientific telecommunications and radio navigation networks. Activities at the GDSCC are carried out in support of six large parabolic dish antennas. These activities may give rise to a variety of environmental hazards, particularly the danger of exposure of GDSCC personnel to asbestos fibers that have been shown to be responsible for such serious ailments as asbestosis, lung cancer, and mesothelioma. Asbestos-containing materials (ACM's) were used in the construction of many of the approximately 100 buildings and structures that were built at the GDSCC during a 30-year period from the 1950s through 1980s. The friable asbestos-abatement program at the GDSCC is presented which consists of text, illustrations, and tables that describe the friable asbestos abatement carried out at the GDSCC from December 21, 1988 through May 11, 1989. Author

N91-13809# Midwest Research Inst., Golden, CO. Solar Energy Research Inst.
CARBON DIOXIDE RELEASE FROM OCEAN THERMAL ENERGY CONVERSION (OTEC) CYCLES
Herbert J. Green and Peter R. Guenther (Scripps Institution of Oceanography, San Diego, CA.) Sep. 1990 12 p Presented at the 1st International Conference on Ocean Energy Recovery, Honolulu, HI, 28-30 Nov. 1989
(Contract DE-AC02-83CH-10093)
(DE89-009504; SERI/TP-253-3594; CONF-8911151-3) Avail: NTIS HC/MF A03

This paper presents the results of recent measurements of CO2 release from an open-cycle ocean thermal energy conversion (OTEC) experiment. Based on these data, the rate of short-term CO2 release from future open-cycle OTEC plants is projected to be 15 to 25 times smaller than that from fossil-fueled electric power plants. OTEC system that incorporate subsurface mixed discharge are expected to result in no long-term release. OTEC plants can significantly reduce CO2 emissions when substituted for fossil-fueled power generation. DOE

N91-13810# Oak Ridge National Lab., TN.
MANAGING THE GLOBAL COMMONS DECISION MAKING AND CONFLICT RESOLUTION IN RESPONSE TO CLIMATE CHANGE RESEARCH WORKSHOP
Steve Rayner, Wolfgang Naegeli (Tennessee Univ., Knoxville.), and Patricia Lund Jul. 1990 73 p Workshop held in Knoxville, TN, 1-4 Aug. 1989
(Contract DE-AC05-84OR-21400)
(DE91-001018; ORNL/TM-11619; CONF-8908254) Avail: NTIS HC/MF A04

A workshop was convened to develop a better understanding of decision-making matters concerning management of the global commons and to resolve conflicts in response to climate change. This workshop report does not provide a narrative of the proceedings. The workshop program is included, as are the abstracts of the papers that were presented. Only the introductory paper on social science research by William Riebsame and the closing summary by Richard Rockwell are reprinted here. This brief report focuses instead on the deliberations of the working groups that developed during the workshop. DOE

N91-13811# Brookhaven National Lab., Upton, NY.
A PRELIMINARY OCEAN ARM (ATMOSPHERIC RADIATION MEASUREMENTS) GUIDE FOR CLIMATIC EVALUATIONS
Robert M. Brown Jul. 1990 63 p
(Contract DE-AC02-76CH-00016)
(DE91-001120; BNL-45216) Avail: NTIS HC/MF A04

This guide was made to assist in the task of selecting sites for the Atmospheric Radiation Measurements (ARM) study. It is a preliminary attempt to provide mean annual and seasonal meteorological data that might be useful in initial climatic evaluations. It is not a finished product and will be added to in time to give other important information on parameters such as standard deviations, percent of means and times, and other variances. In order to cover the spectrum of climatic factors to be considered, this generalized climatic guide was established from various publications to provide a diversified set of basic meteorological data that exists. To comply with other site selection restrictions, namely, synergism with other programs and scientific and logistical viability, this guide covers only the United States, except for the material at the end on Koppens World Climate Classification. It is anticipated that a similar guide will be made to cover the world's climate at a later date. DOE

N91-13812# Oak Ridge National Lab., TN. Environmental Sciences Div.
ACIDIC DEPOSITION AND THE ENVIRONMENT
Charles T. Garten, Jr., Steven E. Lindberg, and Helga VanMiegroet 24 Oct. 1990 13 p Presented at the 4th International Conference on Acidic Deposition, Glasgow, Scotland, 16-21 Sep. 1990, and at a Preliminary Lecture on Metal Cycling and Global Change, Amsterdam, Netherlands, 18-19 Sep. 1990
(Contract DE-AC05-84OR-21400)
(DE91-002352; ORNL/FTR-3787) Avail: NTIS HC/MF A03

The travelers presented several papers at the Fourth International Conference on Acidic Deposition. These covered the following topics: atmospheric chemistry and deposition of airborne nitrogen compounds, soil solution chemistry in high-elevation spruce forests, and forest throughfall measurements for estimating total sulfur deposition to ecosystems. In addition, S. E. Lindberg was invited to organize and chair a conference session on Throughfall and Stemflow Experiments, and to present an invited lecture on Atmospheric Deposition and Canopy Interactions of Metals and Nitrogen in Forest Ecosystems: The Influence of Global Change, at the 110th Anniversary Celebration of the Free University of Amsterdam. DOE

N91-13813# Oak Ridge National Lab., TN. Environmental Sciences Div.
TERRESTRIAL ECOSYSTEMS AND CLIMATIC CHANGE
William R. Emanuel and David S. Schimel (Colorado State Univ., Fort Collins.) 1990 16 p Presented at the Workshop on Global Climate Feedbacks, Upton, NY, 3-6 Jun. 1990 Submitted for publication
(Contract DE-AC05-84OR-21400)
(DE91-001492; CONF-9006134-2) Avail: NTIS HC/MF A03

The structure and function of terrestrial ecosystems depend on climate, and in turn, ecosystems influence atmospheric

composition and climate. A comprehensive, global model of terrestrial ecosystem dynamics is needed. A hierarchical approach appears advisable given currently available concepts, data, and formalisms. The organization of models can be based on the temporal scales involved. A rapidly responding model describes the processes associated with photosynthesis, including carbon, moisture, and heat exchange with the atmosphere. An intermediate model handles subannual variations that are closely associated with allocation and seasonal changes in productivity and decomposition. A slow response model describes plant growth and succession with associated element cycling over decades and centuries. These three levels of terrestrial models are linked through common specifications of environmental conditions and constrain each other. DOE

N91-13814# Brookhaven National Lab., Upton, NY. Environmental Chemistry Div.
METHODS OF ANALYSIS FOR COMPLEX ORGANIC AEROSOL MIXTURES FROM URBAN EMISSION SOURCES OF PARTICULATE CARBON
M. A. Mazurek, L. M. Hildemann, G. R. Cass, and W. F. Rogge (California Inst. of Tech., Pasadena.) Apr. 1990 16 p Presented at the Symposium on Measurement of Airborne Compounds: Sampling, Analysis, and Data Interpretation, Washington, DC, 26-31 Aug. 1990 Submitted for publication
(Contract DE-AC02-76CH-00016; EPA-R-813277)
(DE91-001722; BNL-44441; CONF-9008162-1) Avail: NTIS HC/MF A03

Extractable organic compounds having between 6 to 40 carbon atoms comprise an important mass fraction of the fine particulate matter samples from major urban emission sources. Depending on the emission source type, this solvent-soluble fraction accounts for less than 20 to 100 percent of the total organic aerosol mass, as measured by quantitative high-resolution gas chromatography (HRGC) with flame ionization detection. In addition to total extract quantitation, HRGC can be applied to further analyses of the mass distributions of elutable organics present in the complex aerosol extract mixtures, thus generating profiles that serve as fingerprints for the sources of interest. This HRGC analytical method is applied to emission source samples that contain between 7 to 12,000 micrograms/filter organic carbon. It is shown to be a sensitive technique for analysis of carbonaceous aerosol extract mixtures having diverse mass loadings and species distributions. This study describes the analytical chemical methods that were applied to: the construction of chemical mass balances based on the mass of fine organic aerosol emitted for major urban sources of particulate carbon; and the generation of discrete emission source chemical profiles derived from chromatographic characteristics of the organic aerosol components. DOE

N91-13815# Lawrence Livermore National Lab., CA.
STRATOSPHERIC OZONE CONSERVATION BY ELECTRON ATTACHMENT TO CHLORINE ATOMS: THE NEGATIVE-ION CHEMISTRY
D. D.-M. Ho, K. T. Tsang, A. Y. Wong, and R. J. Siverson (California Univ., Los Angeles.) 12 Oct. 1990 17 p Presented at the International Workshop on Plasma Physics on Controlled Active Global Experiments, Varenna, Italy, 5-19 Sep. 1990
(Contract W-7405-eng-48)
(DE91-002951; UCRL-JC-105225; CONF-900960-1) Avail: NTIS HC/MF A03

Creating low-energy electrons in the stratosphere by photoelectric emission has the beneficial effect of suppressing ozone destruction by Cl. This is because Cl is converted to Cl(-), which is less reactive. Critical to the success of this scheme is the ability to attach most of the electrons to Cl(-) and its hydrates Cl(-)H2O. We found that this attachment efficiency is rather high. This is remarkable given the fact that the electron affinity of Cl(-) is less than that of NO3(-). Photodetachment of NO3(-) is the key factor that leads to this high efficiency. Computer calculations show that ozone increases with electron injection, and most of the electrons end up attaching to Cl(-)H2O. We also point out that 40 km, the altitude at which most of the ozone destruction occurs, is also the optimum altitude for injecting photoelectric electrons. DOE

N91-13816 Institut d'Aeronomie Spatiale de Belgique, Brussels.
AERONOMIC CHEMISTRY OF OZONE
Marcel Nicolet 1990 59 p Previously announced in IAA as A90-22085 Submitted for publication
(Aeronomica-Acta-A-355-1990; ISSN-0065-3713; ETN-91-98384)
Avail: Institut d'Aeronomie Spatiale de Belgique, 3 Avenue Circulaire, B-1180 Brussels, Belgium

Various parameters of the atmospheric chemistry of ozone are analyzed by using aeronomic equations in their general form. A general equation is written, which includes the production and destruction processes due to the action of hydrogen, nitrogen, halogen compounds or ultraviolet radiation. In the mesosphere, the transport conditions of water vapor, molecular hydrogen and atomic hydrogen at the upper boundary must be taken into consideration. In the stratosphere, the concentration ratios of OH, HO2, NO2, NO, Cl, ClO, Br and BrO must be determined and introduced in the equation. The effect of the transport terms of HNO3, HCl and HBr cannot be neglected in the lower stratosphere. To determine a reliable zone distribution, the sources must be known with sufficient accuracy and the dynamic transport from the lower stratosphere to the troposphere must be determined by considering photochemical influence. ESA

46 GEOPHYSICS

Includes aeronomy; upper and lower atmosphere studies; ionospheric and magnetospheric physics; and geomagnetism.

For space radiation see *93 Space Radiation.*

N91-13817*# Michigan Univ., Ann Arbor. Radiation Lab.
MESOSCALE MONITORING OF THE SOIL FREEZE/THAW BOUNDARY FROM ORBITAL MICROWAVE RADIOMETRY Final Report
Craig Dobson, Fawwaz T. Ulaby, Brian Zuerndorfer, and Anthony W. England 1 Feb. 1990 31 p
(Grant NAG5-852)
(NASA-CR-185901; NAS 1.26:185901; Rept-023921-1-F) Avail: NTIS HC/MF A03 CSCL 08M

A technique was developed for mapping the spatial extent of frozen soils from the spectral characteristics of the 10.7 to 37 GHz radiobrightness. Through computational models for the spectral radiobrightness of diurnally heated freesing soils, a distinctive radiobrightness signature was identified for frozen soils, and the signature was cast as a discriminant for unsupervised classification. In addition to large area images, local area spatial averages of radiobrightness were calculated for each radiobrightness channel at 7 meteorologic sites within the test region. Local area averages at the meteorologic sites were used to define the preliminary boundaries in the Freeze Indicator discriminate. Freeze Indicator images based upon Nimbus 7, Scanning Multichannel Microwave Radiometer (SMMR) data effectively map temporal variations in the freeze/thaw pattern for the northern Great Plains at the time scale of days. Diurnal thermal gradients have a small but measurable effect upon the SMMR spectral gradient. Scale-space filtering can be used to improve the spatial resolution of a freeze/thaw classified image. B.G.

N91-13818*# Florida State Univ., Tallahassee. Dept. of Geology.
NUMERICAL SOLUTION OF THE GEOELECTRODYNAMIC PROBLEM Progress Report
Joseph C. Cain 6 Sep. 1990 20 p
(Grant NAG5-1070)
(NASA-CR-186941; NAS 1.26:186941) Avail: NTIS HC/MF A03 CSCL 08G

The primary goal is to understand the sources of the near-Earth ambient magnetic field as observed by recent spacecraft surveys

and surface variational magnetic observations so as to determine the electrical properties of the crust and upper mantle. Also included is the structure and changes on a short time scale of the core field which must be separated and identified. The Magsat data collection interval provides an opportunity to compare the vector field projections of ionospheric currents computed from surface data above the ionosphere as does the POGO data for scalar projections. The limitation of Magsat is its sun-synchronous orbit, which only sampled low latitudes at dawn and dusk, whereas POGO, though only making observations of the scalar field, sampled all local times. Magsat operated at a lower altitude than POGO (down to 350 km) whereas the orbits of the three POGO spacecraft ranged up to 1500 km and were never lower than about 400 km. Y.S.

N91-13819*# University of Northern Colorado, Greeley.
REVIEW OF GEOGRAPHY INTERNSHIP OF CONVECTIVE WAVE PROJECT
Kurt R. Rademacher and Charles Collins 1990 13 p
(Grant NAG5-1115)
(NASA-CR-187022; NAS 1.26:187022) Avail: NTIS HC/MF A03 CSCL 08G

The internship of the author is examined in detail. The acquisition of the internship, the personnel of the project, the project itself, and the goals associated with it are described. The authors orientation to the internship, the project's operations, and the conclusion of the findings are also described. The overall goal of the project was to determine the effect of convective waves on wind speeds in the middle and upper troposphere, and how these waves affect the general circulation on a global scale. A more specific goal of the author was the satellite analysis of cloud street formations. This was done to determine frequency and areas in which cloud streets occur off the East Asian and North American coastlines. Author

N91-13820# National Center for Atmospheric Research, Boulder, CO.
[RESEARCH PROJECTS INCLUDING CLIMATE, ATMOSPHERIC CHEMISTRY, SOLAR-TERRESTRIAL PHYSICS, METROLOGY, AND STORM SYSTEMS] Annual Report, 1 Oct. 1988 - 30 Sep. 1989
Jul. 1990 54 p
(PB90-256306) Avail: NTIS HC/MF A04 CSCL 04A

NCAR's research includes climate, atmospheric chemistry, solar terrestrial physics, metrology, and storm systems. Author

N91-13821 Cornell Univ., Ithaca, NY.
FRACTALS AND CHAOTIC DYNAMICS IN TECTONICS: APPLICATIONS TO TOPOGRAPHY AND SEISMICITY Ph.D. Thesis
Jie Huang 1990 151 p
Avail: Univ. Microfilms Order No. DA9027136

Tectonics involves a composite of many intrinsically complex systems. Tectonic systems are highly irregular and heterogeneous, nevertheless they also exhibit order and correlation. Unifying properties can be found to better describe the complex shapes and processes in nature. The basic objective was to develop new geometric and dynamic descriptions of various tectonic phenomena within the framework of fractal geometry and nonlinear dynamics. Fractal analysis is first applied to the digitized topography for the states of Oregon and Arizona. Fourier spectrum approach is used to obtain maps of fractal dimension and roughness amplitude. Seismicity is another important manifestation of tectonics. The earthquake statistics associated with both the fractal distributions of fault geometries and fault plane heterogeneities are examined. First, earthquake sequences and their temporal and spatial relations are simulated by considering a self-similar, hierarchical fault zone. Assuming the difference between different distributions of heterogeneities and ambient stress levels. Finally, the question of whether seismicity in tectonically active regions is an example of deterministic chaos is addressed. The dynamical behavior of seismic faulting introduced by fault zone heterogeneities is explored using a simple spring-loaded system. Author

N91-13822 California Univ., San Diego.
PRECISION, ACCURACY, AND TECTONICS FROM THE GLOBAL POSITIONING SYSTEM Ph.D. Thesis
Kristine Marie Larson 1990 284 p
Avail: Univ. Microfilms Order No. DA9024009

The Global Positioning System, consisting of seven high quality navigational satellites, was utilized to measure crustal deformation in southern and central California. The data consists of 11 experiments conducted in southern and central California over 2.7 years. The major focus is to establish the inherent precision and accuracy of the Global Positioning System on baselines ranging from 50 to 350 kilometers in length. Short term precision is 3 to 5 mm in both horizontal components, with a length dependence of 1 part in 10(exp 8) for the east component. Vertical precision is length dependent. Precision assessed over 2 years is slightly degraded relative to the short-term precision results: 5 mm in both horizontal components, with a length dependence for the east of 1 part in 10(exp 8). Accuracy was determined by comparing GPX baseline evolutions with baseline estimates derived from very long baseline interferometry (VLBI), yielding 10 to 30 mm agreement in horizontal components, and better than 80 mm agreement in the vertical. Three geodetic networks were established for determination of present-day crustal deformation rates: a network in central California, and two offshore networks, located across the Santa Barbara Channel and the Gulf of Santa Catalina. Strain rates in central California and the Santa Barbara Channel agree with estimates from trilateration and triangulation. The mechanical behavior or the Salton Trough was studied. Shorelines caused by a lake in the trough over 500 years ago were used to evaluate four models of the Earth's elastic behavior: an elastic half-space, a layered elastic half-space, a flexure model, and a time dependent flexure model. Elastic models cannot adequately fit the shoreline data. The best-fitting model is the flexure model, with a maximum crustal thickness of 40 kilometers. Dissert. Abstr.

N91-13823 Kansas Univ., Lawrence.
A SOLAR CHRONOMETER FOR CLIMATE: ASTRONOMICAL AND GEOPHYSICAL EVIDENCE Ph.D. Thesis
Charles August Perry 1989 333 p
Avail: Univ. Microfilms Order No. DA9024200

The sun emits an entire spectrum of electromagnetic waves, charged particles, and magnetic force fields, each having a particular effect on the dynamics of the Earth. Various geophysical and astronomical data, on time scales of millions of years to minutes, exhibit cycles with features that appear to be interrelated. A method was developed that normalized the length of the many reported cycles representative of climatic change. The method involved the utilization of fundamental harmonics, which is the doubling of a basic cycle length. The distribution of the normalized geophysical and astronomical cycles displayed a central mode of approximately 11 years, with two side modes just within plus or minus one standard deviation. The relatively new field of helioseismology has revealed that the basic solar oscillations may be originating from a seismonuclear process deep within the Sun's core, producing a chronometer for solar activity. A mechanism for a solar chronometer is proposed based on relationships between properties of thermonuclear fusion, nuclear magnetic moment, and nuclear magnetic resonance. To test the hypothesis that solar fluctuations drive climate, a model for solar output was developed from relationships within the solar chronometer. Model output for several time frames was compared with data representative of climatic fluctuations. Magnetic intensity, solar output, and cycle length, basic principles of the solar chronometer, coupled with properties of the Pacific Ocean, enabled the development of a conceptual model for the occurrence of wet and dry patterns in the western United States. Also the El Nino/La Nina may be linked to the timing of the solar chronometer with the Pacific Ocean gyre. Dissert. Abstr.

N91-13824 Pennsylvania State Univ., University Park.
THE INFLUENCE OF THE SAMPLING TIME ON DIFFUSION MEASUREMENTS IN THE ATMOSPHERE Ph.D. Thesis

Richard Mark Eckman 1989 125 p
Avail: Univ. Microfilms Order No. DA9018206

A theory is developed to account for the influence of the sampling time on atmospheric diffusion. The developed general theory is too complex to use directly, so a simpler model containing an Eulerian spectrum is developed. This model is derived from the theory by assuming that the travel time T is small compared with the Lagrangian time scale and that the turbulence effecting the diffusion is within the inertial subrange. The model is primarily applicable to microscale diffusion, with maximum travel times on the order of hundreds or thousands of seconds. At large sampling times the model estimates of the horizontal diffusion parameter sigma(sub y) increase linearly with T. At small sampling times (i.e., relative diffusion) the estimates of sigma(sub y) are proportional to T(exp 3/2), which agrees with inertial-subrange theory. For a mean wind speed of about 5 m/sec and values of sigma(sub y) less than 100 m, the transition from the T(exp 3/2) growth to the linear growth occurs at a sampling time of about two minutes. Dissert. Abstr.

N91-13825# Instituto de Pesquisas Espaciais, Sao Jose dos Campos (Brazil).
THE IMPORTANCE OF FRACTURING IN THE PIMENTA BUENO-RO BASIN STRUCTURE: A STUDY OF THE MORPHOSTRUCTURAL ELEMENTS OF THE RUPTURE-DUCTILE CHARACTER THROUGH REMOTE SENSING TECHNIQUES AND PRODUCTS M.S. Thesis [A IMPORTANCIA DO FRATURAMENTO NO ARCABOUCO DA BACIA DE PIMENTA BUENO-RO: UM ESTUDO DAS FEICOES MORFOESTRUTURAIS DE CARATER RUPTIL-DUCTIL ATRAVES DE TECNICAS E PRODUTOS DE SENSORIAMENTO REMOTO]
Clayton deSouzaPontes Aug. 1989 261 p In PORTUGUESE; ENGLISH summary
(INPE-5004-TDL/398) Avail: NTIS HC/MF A12

The Pimenta Bueno sedimentary basin was studied with remote sensing techniques and images. A structural analysis was performed by statistical treatment over linear element of relief and drainage obtained from LANDSAT/TM images and radar mosaic in the scale of 1:250,000. Interpretation of the anisotropy drainage curves and interpretation of the magnetic lineaments in the whole area was also done. The main structural trends of fractures found in this area are: N85E-S80E, N10E-N10W, and N40-50E. The fractures in the range N85E-S80E were responsible for the control of paleozoic sedimentation in this basin. The drainage anisotropy analysis over the cretaceous sedimentation gave strong coherence with the most important regional lineaments, making the identification of highs and lows of the basement easy. Author

N91-13826# Idaho National Engineering Lab., Idaho Falls.
SIMULTANEOUS MEASUREMENT OF Ni-Al PARTICLE SIZE, VELOCITY, AND TEMPERATURE IN ATMOSPHERIC THERMAL PLASMAS
J. R. Fincke and W. D. Swank 1990 10 p Presented at the 3rd National Thermal Spray Conference and Exposition, Long Beach, CA, 21-24 May 1990
(Contract DE-AC07-76ID-01570)
(DE91-001935; EGG-M-89487; CONF-900520-1) Avail: NTIS HC/MF A02

A technique for simultaneously measuring particle size, velocity, and temperature has been applied to the in-flight characterization of a Ni-Al particles sprayed in a 28 kW plasma torch. The radial distribution of particle size, velocity, temperature and particle concentration were obtained at stand off distances between 63.5 and 88.9 mm. These measurements and their relationship to the characteristics of the resulting coating are discussed. Injection geometry dependent particle sizing and an apparent fracturing of the original particles into smaller particles was observed. A significant fraction of the largest particles observed did not appear to the molten. Particle behavior was found to be relatively insensitive to gas mixture and flow rate. DOE

N91-13827# Deutsche Forschungsanstalt fuer Luft- und Raumfahrt, Oberpfaffenhofen (Germany, F.R.). Abt. Umweltmeteorologie.
SIMULATION OF THE FORMATION AND TRANSPORT OF OZONE IN THE ATMOSPHERIC BOUNDARY LAYER Ph.D. Thesis - Ludwig-Maximilians-Univ.
Jutta Graf Jun. 1990 104 p In GERMAN; ENGLISH summary
Report will also be announced as translation (ESA-TT-1234)
(DLR-FB-90-25; ISSN-0171-1342; ETN-91-98259; ESA-TT-1234)
Avail: NTIS HC/MF A06; DLR, VB-PL-DO, Postfach 90 60 58, 5000 Cologne, Fed. Republic of Germany, HC 30 DM

A numerical model is presented to simulate chemical processes in the lower atmosphere, with special reference to the ozone formation. Only chemical reactions in the gas phase are taken into consideration. The model is used to simulate the ozone formation caused by motor car emissions in an urban area. The results illustrate the strong effects of hydrocarbon emissions on the ozone production. The combined effects of horizontal transport, vertical diffusion and chemical reactions are investigated on a larger scale. High ozone levels in nonindustrial areas are mainly due to the transport of ozone precursor substances. A real episode simulation shows the importance of the initial concentrations on the resulting ozone distribution. ESA

N91-13828# Norwegian Defence Research Establishment, Kjeller.
GRAVITY WAVES EXCITED BY FLOW OVER AN OBSTACLE
Oyvind Andreassen and Carl Erik Wasberg 29 Jun. 1990 14 p
(FFI-90/7017; ISSN-0802-2437; ETN-91-98281) Avail: NTIS HC/MF A03

Internal gravity waves generated when the airflow packets are lifted up and dropped again are studied and simulated with a 2-D model. The height of the obstacle which defines the lower boundary of the computational domain is described by a periodic function f(xi) of the horizontal coordinate, and the upper domain is considered open. Slip conditions are applied at the lower boundary. The computation domain is divided into two subdomains. Curvilinear coordinates, specified by f(xi) are used in the lower subdomain, whereas cartesian coordinates are used in the upper subdomain. The governing equations are solved separately in each subdomain by a spectral allocation method. The solutions are matched through the characteristic boundary conditions. Examples of waves generated by this method are presented. ESA

N91-13829# Royal Aerospace Establishment, Farnborough (England).
LONG PERSISTENCE EFFECTS OF GEOMAGNETIC ACTIVITY
Gordon L. Wrenn 3 Mar. 1990 11 p Presented at Solar Terrestrial Predictions Workshop, Sydney, Australia, Oct. 1989
(RAE-TM-SP-376; BR114645; ETN-91-98361) Copyright Avail: NTIS HC/MF A03

The identification of the physical processes which perturb the dynamic equilibrium of the charged particle populations in the terrestrial magnetosphere is investigated. A planetary index was used and it was proved that the introduction of a persistence factor for a derived index, a time weighted accumulation of recent values, gives a better correlation with an estimation of characteristic persistence times in order to establish the temporal response of observed effects in relation to available measures of geomagnetic activity. The analysis procedure was illustrated by results pertaining to ionospheric foF2, cold plasma concentration at geosynchronous orbit and ring current strength. ESA

N91-13830 Institut d'Aeronomie Spatiale de Belgique, Brussels.
ULTRAVIOLET ABSORPTION CROSS-SECTIONS OF PHOTOACTIVE SPECIES OF STRATOSPHERIC INTEREST. PART 1: THE HALOCARBONS
D. Gillotay and P. C. Simon 1990 177 p
(ETN-91-98385) Avail: Institut d'Aeronomie Spatiale de Belgique, 3 Avenue Circulaire, B-1180 Brussels, Belgium

Ultraviolet absorption cross section measurements of halogenated compounds of methane and ethane are carried out. Tables of values as function of temperature or of wavelength at

210 and 295K are presented for chloro and chlorofluoro methanes, ethanes and ethylenes and for brominated compounds. The parameters of the polynomial expression of the cross section as function of wavelength are given. The error budget of uncertainties for the optical path, pressure, impurities in the sample and absorbance is proposed. ESA

47 METEOROLOGY AND CLIMATOLOGY

Includes weather forecasting and modification.

N91-13831*# University of Northern Colorado, Greeley.
INTERANNUAL VARIATION OF SEASONAL MEANS AND SUBSEASONAL VARIABILITY OF CLOUD STREETS OFF THE EAST COAST OF NORTH AMERICA 1984-1987
Kurt R. Rademacher and Charles Collins 1990 17 p
(Grant NAG5-1115)
(NASA-CR-187021; NAS 1.26:187021) Avail: NTIS HC/MF A03 CSCL 04B

Convection waves are a strong function of the original forcing by convection in the boundary layer. This convection can take the form of random or 2-D spatial structure. When clouds are formed as a result of 2-D boundary layer forcing, they are called cloud streets. Convective waves may be important in the global momentum balance. Global circulation models presently overestimate wind speeds in the middle and upper troposphere, and do not account for convective waves. If the hypothesis that convective waves significantly contribute to momentum transport in the troposphere is correct, then climatology of cloud streets will help understand convective waves' role in the global momentum balance. If the hypothesis is incorrect, then cloud street climatology is still useful because cloud streets show areas where large amounts of sensible and latent heat are transferred from the ocean to the atmosphere. Interannual variation of seasonal means and subseasonal variability of cloud street occurrence off the east coast of North America is examined and compared. The months of Dec., Jan., and Feb. during 1984-85, 1985-86, and 1986-87 are examined along with each season. Author

N91-13832*# Texas A&M Univ., College Station. Dept. of Meteorology.
TROPICAL PACIFIC MOISTURE VARIABILITY: ITS DETECTION, SYNOPTIC STRUCTURE AND CONSEQUENCES IN THE GENERAL CIRCULATION Final Report, 6 Dec. 1986 - 31 Aug. 1990
James P. McGuirk Sep. 1990 125 p
(Contract NAS8-37284)
(NASA-CR-184045; NAS 1.26:184045) Avail: NTIS HC/MF A06 CSCL 04B

Satellite data analysis tools are developed and implemented for the diagnosis of atmospheric circulation systems over the tropical Pacific Ocean. The tools include statistical multi-variate procedures, a multi-spectral radiative transfer model, and the global spectral forecast model at NMC. Data include in-situ observations; satellite observations from VAS (moisture, infrared and visible) NOAA polar orbiters (including Tiros Operational Satellite System (TOVS) multi-channel sounding data and OLR grids) and scanning multichannel microwave radiometer (SMMR); and European Centre for Medium Weather Forecasts (ECHMWF) analyses. A primary goal is a better understanding of the relation between synoptic structures of the area, particularly tropical plumes, and the general circulation, especially the Hadley circulation. A second goal is the definition of the quantitative structure and behavior of all Pacific tropical synoptic systems. Finally, strategies are examined for extracting new and additional information from existing satellite observations. Although moisture structure is emphasized, thermal patterns are also analyzed. Both horizontal and vertical structures are studied and objective quantitative results are emphasized. Author

N91-13833*# Oregon State Univ., Corvallis. Dept. of Atmospheric Sciences.
CLOUD PROPERTIES AS DEDUCED FROM SATELLITE OBSERVATION Final Report
James A. Coakley, Jr. 1990 3 p
(Grant NAG1-935)
(NASA-CR-182851; NAS 1.26:182851) Avail: NTIS HC/MF A01 CSCL 04B

The three major accomplishments of this project are presented. The first was the simultaneous observations from both satellite and in situ aircraft of the effects of ship exhaust on cloud microphysics and the consequent changes in cloud reflectivity. Second, the satellite observations collected during the FIRE marine stratocumulus intensive field operation (IFO) were analyzed to reveal differences in the reflectivities of uniform and broken clouds. Third, the relationship between liquid water path and cloud reflectivity was examined. Author

N91-13834# National Severe Storms Lab., Norman, OK.
DOPLIGHT 1987 PROJECT SUMMARY
D. E. Forsyth, D. W. Burgess, C. A. Doswell, M. H. Jain, and L. E. Mooney Jun. 1990 195 p
(PB90-253584; NOAA-TM-ERL-NSSL-101) Avail: NTIS HC/MF A09 CSCL 04B

The primary purpose was to support warning operations. Secondary efforts were made to provide the National Weather Service staff Doppler experience; to develop radar warning products for distribution to the media; and to evaluate the utility of lightning cloud-to-ground strike location data. The project known as DOPLIGHT (DOPpler/LIGHTning) has continued yearly, with various improvements made to hardware and software capabilities. A separate Lightning Location Processor display for lightning ground flashes was added at the National Weather Service Forecast Office (NWSFO) in 1986. Experience with the lightning data continues to indicate further National Severe Storms Laboratory/NWSFO cooperative efforts in this area are needed. In response to these needs, an ambitious and much expanded DOPLIGHT '87 program was begun in the fall of 1986. A detailed description of the project and summaries of DOPLIGHT '87 are presented. Author

N91-13835 Washington Univ., Seattle.
A STUDY OF THE ICE-HAIL CHARGE SEPARATION MECHANISM USING A THUNDERSTORM ELECTRIFICATION MODEL WITH EXPLICIT MICROPHYSICS IN A KINEMATIC FRAMEWORK Ph.D. Thesis
Kent Weston Norville 1990 110 p
Avail: Univ. Microfilms Order No. DA9026013

A numerical model was developed for examining the thunderstorm electrification process assuming that the electrification is entirely due to non-inductive charge transfer between colliding ice crystals and hail. Since this ice-hail charge mechanism is very dependent on particle sizes and distributions, 78 categories of ice and 30 categories of drops are used in an explicit microphysical framework. To maintain simplicity, the electrification model has a kinematic structure; thus the temperature and velocity fields are input into the electrification model. These fields can be either calculated by a background model or retrieved from observation. The cloud model of Taylor (1989) was used to generate the temperature and velocity fields to examine the 19 July 1981 CCOPE thundercloud. Using these fields, the electrification model produced time-dependent ice particle concentrations, radar reflectivities, charge and vertical electric field distributions in good general agreement with those observed. The model produced a maximum electric field strength of 2.34 kV/cm, which is on the same order of that needed for lightning initiation, and occurred very close to the time of the observed discharge. Thus the ice-hail charge mechanism by itself seems capable of explaining the electrical development in storms such as the 19 July cloud. The details of the electrification depended on the liquid water content and the glaciation processes. Specifically, it was found that the locations of the charge centers were directly related to the interface between mixed-phase and completely glaciated cloud. The electrification was strongly dependent on the ice crystal

characteristics. The electrification was not sensitive to charge transfer critical diameter or the initial drop distribution. The electrification was sensitive to ice-ice sticking efficiency as predicted. Dissert. Abstr.

N91-13836 Colorado Univ., Boulder.
FRONTAL INTERACTIONS WITH OROGRAPHY: OBJECTIVE CROSS-SECTIONAL ANALYSIS OF ALPEX DATA Ph.D. Thesis
Craig Steven Hartsough 1989 209 p
Avail: Univ. Microfilms Order No. DA9024832

Cross-sectional analyses of data collected during the Alpine Experiment (ALPEX) are used to examine ageostrophic motions during a frontal interactions with the Alps. Dependent fields are represented on vertical cross-sections in isentropic coordinates using the Shapiro and Hastings objective analysis scheme. Ageostrophic motions and potential vorticity fields are determined from these analyzed fields using derivatives of the pressure and wind along isentropic surfaces. A 30-hour period on 4 to 5 March 1982 is examined, when a cold front progressed southward into the Alpine region. Rawinsonde data are reconstructed with splines to provide continuous approximations of the fields and to account for possible errors in the measurements. Diabatic heating is evaluated by integrating the continuity equation in isentropic coordinates. Moisture fields provide a qualitative assessment of the accuracy of the diabatic contribution to the ageostrophic motion. Dissert. Abstr.

N91-13837*# Maryland Univ., College Park. Atmospheric Lidar Observatory.
PROGRESS OF RESEARCH ON WATER VAPOR LIDAR Report, period ending 31 Jul. 1990
T. D. Wilkerson Nov. 1990 44 p
(Contract NCC1-25)
(NASA-CR-187673; NAS 1.26:187673; BN-1120) Avail: NTIS HC/MF A03 CSCL 04B

Research is described on several aspects of stimulated Raman scattering (SRS) of 532 nm laser light in H2, D2, and CH4. The goals of this work are to develop a more thorough understanding of nonlinear processes involving the Raman effect and four-wave mixing, and to find the best way to generate radiation at several wavelengths simultaneously, for lidar applications. Issues addressed are conversion efficiency, optimization of operating conditions (gas pressure, confocal parameter, etc.) and the distribution of output pulse energy over three Stokes components, the first anti-Stokes component, and the zeroth order (pump) wavelength. The described research and results constitute another step in the development of SRS applications for NASA's atmospheric lidar program. Author

N91-13838 Physics and Electronics Lab. TNO, The Hague (Netherlands).
LIDAR AS A SLANT PATH VISIO-CEILOMETER Final Report
G. J. Kunz (Technische Physische Dienst TNO-TH, Delft, Netherlands), L. A. Fontijn, and G. deLeeuw Jul. 1990 284 p In DUTCH; ENGLISH summary Original contains color illustrations
(Contract A89/KLu/654)
(FEL-90-A207; TD-90-2483; ETN-91-98302) Copyright Avail: Physics and Electronics Laboratory TNO, P.O. Box 96864, 2509 JG The Hague, Netherlands

The feasibility of an integrated lidar system for the measurement of the cloud base altitude as well as the horizontal and slant path visibility is discussed. The necessary background to design a dedicated lidar system for this purpose is described. These concepts are used to design systems for the measurement of cloud base altitudes up to levels higher than 2 km, as well as visibility (both horizontal and slant path). Based on safety and range requirements, the possibilities are reduced to two eye-safe systems in the UV and IR which both meet the demands on a slant path visio-ceilometer for airport use. Possibilities for wind measurements are discussed. A stand alone system is proposed to measure cloud cover. ESA

N91-13839# National Defence Research Establishment, Umea (Sweden).
EVALUATION OF A WIND PROFILE MODEL
Lennart Thaning, Goeran Arnoldsson, Hans Dahlquist, Gustav Grandin, and Eva Peterson Jun. 1990 44 p In SWEDISH; ENGLISH summary Sponsored by Swedish Air Force
(FOA-E-40045-4.5; ISSN-0281-9945; ETN-91-98379) Avail: NTIS HC/MF A03; National Defence Research Establishment, S-901 82 Umea, Sweden, HC 50 Swedish crowns

The possibility to diagnostically determine the wind profile up to 2000 m height, by using a stationary, balanced wind profile model based on the Taylor-Ekan solution, is evaluated. Profiles measured with sodar were used as input data and profiles measured with radar (balloon soundings) were used for verification. The measurements were performed by the Swedish Air Force at the wing in Karlsborg (Sweden) during 1987 and 1988. The main result of the evaluation is that the model does not give information enough about the wind above the highest sodar measurement, in order to be useful. The ensemble average for a long period, however, is reasonable. The deviation from a profile in equilibrium in each specific case, may be due to nonstationary phenomena, which could be caused by the horizontally nonhomogeneous conditions around Karlsborg. ESA

48 OCEANOGRAPHY

Includes biological, dynamic, and physical oceanography; and marine resources.

For related information see also *43 Earth Resources and Remote Sensing.*

N91-13840 Royal Netherlands Meteorological Inst., De Bilt. Div. of Oceanographic Research.
A PRIMITIVE EQUATION MODEL FOR THE EQUATORIAL PACIFIC
Marc A. F. Allaart and Arie Kattenberg 17 Apr. 1990 53 p
(KNMI-TR-124; ISSN-0169-1708; ETN-91-98319) Copyright Avail: Royal Netherlands Meteorological Institute, P.O. Box 201, 3730 AE De Bilt, Wilhelminalaan 10, Netherlands

The model described is a multilevel gridpoint model with variable horizontal resolution. The primitive equations for momentuum, heat and salt/fresh water balance are solved in a model of the region bounded by the latitudes + and - 29 degrees and realistic meridional land boundaries; the coastline of Central and South America and Australia on the other side. The model equations and the numerical solution techniques are given. Details of the computer code and implementation are presented. ESA

51 LIFE SCIENCES (GENERAL)

N91-13841*# Michigan State Univ., East Lansing. Dept. of Botany and Plant Pathology.
LOCALIZE AND IDENTIFY THE GRAVITY SENSING MECHANISM OF PLANTS Final Technical Report, Aug. 1980 - Oct. 1989
Robert S. Bandurski 19 Nov. 1990 18 p
(Grant NAGw-0097)
(NASA-CR-187411; NAS 1.26:187411) Avail: NTIS HC/MF A03 CSCL 06C

The machinery by which a plant transduces the gravity stimulus into a growth response is localized and identified at the cellular level. The fact that a plant grows unequally on the lower side of a horizontally placed stem implies that there must be an asymmetric distribution of some of the chemical substances involved in the growth response. The three most likely chemicals to cause this growth were determined to be potassium, calcium, or the growth hormone, indole-3-acetic acid (IAA). IAA was chosen for this study and the results present a fairly complete understanding of the transduction of the gravity stimulus. Author

N91-13842*# National Aeronautics and Space Administration, Washington, DC.
BIOLOGICAL LIFE SUPPORT TECHNOLOGIES: COMMERCIAL OPPORTUNITIES
Mark Nelson, ed. and Gerald Soffen, ed. (Space Biospheres Ventures, Oracle, AZ.) Nov. 1990 117 p Workshop held in Tucson, AZ, 30 Oct. - 1 Nov. 1989
(NASA-CP-3094; NAS 1.55:3094) Avail: NTIS HC/MF A06 CSCL 06C

The papers from the workshop on Biological Life Support Technologies: Commercial Opportunities are presented. The meeting attracted researchers in environmental and bioregenerative systems. The role of biological support technologies was evaluated in the context of the global environmental challenge on Earth and the space exploration initiative, with its goal of a permanent space station, lunar base, and Mars exploration. For individual titles, see N91-13843 through N91-13855.

N91-13843*# Paine (Thomas) Associates, Los Angeles, CA.
BIOSPHERES AND SOLAR SYSTEM EXPLORATION
Thomas O. Paine *In* NASA, Washington, Biological Life Support Technologies: Commercial Opportunities Nov. 1990 p 1-11 (For primary document see N91-13842 05-51)
Avail: NTIS HC/MF A06 CSCL 06C

The implications of biosphere technology is briefly examined. The exploration status and prospects of each world in the solar system is briefly reviewed, including the asteroid belt, the moon, and comets. Five program elements are listed as particularly critical for future interplanetary operations during the coming extraterrestrial century. They include the following: (1) a highway to Space (earth orbits); (2) Orbital Spaceports to support spacecraft assembly, storage, repair, maintenance, refueling, launch, and recovery; (3) a Bridge Between Worlds to transport cargo and crews to the moon and beyond to Mars; (4) Prospecting and Resource Utilization Systems to map and characterize the resources of planets, moons, and asteroids; and (5) Closed Ecology Biospheres. The progress in these five field is reviewed. E.R.

N91-13844*# Space Biospheres Ventures, Oracle, AZ. Dept. of Research and Development.
HISTORICAL OVERVIEW OF THE BIOSPHERE 2 PROJECT
John P. Allen *In* NASA, Washington, Biological Life Support Technologies: Commercial Opportunities Nov. 1990 p 12-22 (For primary document see N91-13842 05-51)
Avail: NTIS HC/MF A06 CSCL 06C

An extensive historical overview is given of the Biosphere 2 project. The overview begins in late 1969, as the moon landings commenced, when work began on ecological projects which laid the conceptual foundation for the current Biosphere 2 project. Continuing through to taking a complete functional suite of microbes together with their associated aquatic elements and an air volume and putting them inside a closed lab flask in which to measure the oxygen and CO2 levels, study energy flows and visually observe the changes therein. The laws of biospherics formulated by the author which can be tested in the Biosphere 2 project are listed. E.R.

N91-13845*# Space Biospheres Ventures, Oracle, AZ.
BIOSPHERE 2 TEST MODULE EXPERIMENTATION PROGRAM
Abigail Alling, Linda S. Leigh, Taber MacCallum, and Norberto Alvarez-Romo *In* NASA, Washington, Biological Life Support Technologies: Commercial Opportunities Nov. 1990 p 23-32 (For primary document see N91-13842 05-51)
Avail: NTIS HC/MF A06 CSCL 06C

The Biosphere 2 Test Module is a facility which has the capability to do either short or long term closures: five month closures with plants were conducted. Also conducted were investigations of specific problems, such as trace gas purification by bioregenerative systems by in-putting a fixed concentration of a gas and observing its uptake over time. In other Test Module experiments, the concentration of one gas was changed to observe what effects this has on other gases present or on the system. The science of biospherics which encompasses the study of closed biological systems provides an opening into the future in space as well as in the Earth's biosphere. E.R.

N91-13846*# Arizona Univ., Tucson. Environmental Research Lab.
SOIL BED REACTOR WORK OF THE ENVIRONMENTAL RESEARCH LAB. OF THE UNIVERSITY OF ARIZONA IN SUPPORT OF THE RESEARCH AND DEVELOPMENT OF BIOSPHERE 2
Robert Frye *In* NASA, Washington, Biological Life Support Technologies: Commercial Opportunities Nov. 1990 p 33-40 (For primary document see N91-13842 05-51)
Avail: NTIS HC/MF A06 CSCL 06C

Research at the Environmental Research Lab in support of Biosphere 2 was both basic and applied in nature. One aspect of the applied research involved the use of biological reactors for the scrubbing of trace atmospheric organic contaminants. The research involved a quantitative study of the efficiency of operation of Soil Bed Reactors (SBR) and the optimal operating conditions for contaminant removal. The basic configuration of a SBR is that air is moved through a living soil that supports a population of plants. Upon exposure to the soil, contaminants are either passively adsorbed onto the surface of soil particles, chemically transformed in the soil to usable compounds that are taken up by the plants or microbes as a metabolic energy source and converted to CO2 and water. Author

N91-13847*# Space Biospheres Ventures, Oracle, AZ. Dept. of Medical Operations.
BIOMEDICAL PROGRAM AT SPACE BIOSPHERES VENTURES
Roy Walford *In* NASA, Washington, Biological Life Support Technologies: Commercial Opportunities Nov. 1990 p 41-44 (For primary document see N91-13842 05-51)
Avail: NTIS HC/MF A06 CSCL 06C

There are many similarities and some important differences between potential health problems of Biosphere 2 and those of which might be anticipated for a space station or a major outpost on Mars. The demands of time, expense, and equipment would not readily allow medical evacuation from deep space for a serious illness or major trauma, whereas personnel can easily be evacuated from Biosphere 2 if necessary. Treatment facilities can be somewhat less inclusive, since distance would not compel the undertaking of heroic measures or highly complicated surgical procedures on site, and with personnel not fully trained for these procedures. The similarities are given between medical requirements of Biosphere 2 and the complex closed ecological systems of biospheres in space or on Mars. The major problems common to all these would seem to be trauma, infection, and toxicity. It is planned that minor and moderate degrees of trauma, including debridement and suturing of wounds, x ray study of fractures, will be done within Biosphere 2. Bacteriologic and fungal infections, and possibly allergies to pollen or spores are expected to be the commonest medical problem within Biosphere 2. E.R.

N91-13848*# National Aeronautics and Space Administration, Washington, DC.
THE NASA CELSS PROGRAM
Maurice M. Averner *In its* Biological Life Support Technologies: Commercial Opportunities Nov. 1990 p 45-46 (For primary document see N91-13842 05-51)
Avail: NTIS HC/MF A06 CSCL 06C

The NASA Controlled Ecological Life Support System (CELSS) program was initiated with the premise that NASA's goal would eventually include extended duration missions with sizable crews requiring capabilities beyond the ability of conventional life support technology. Currently, as mission duration and crew size increase, the mass and volume required for consumable life support supplies also increase linearly. Under these circumstances the logistics arrangements and associated costs for life support resupply will adversely affect the ability of NASA to conduct long duration missions. A solution to the problem is to develop technology for the recycling of life support supplies from wastes. The CELSS

concept is based upon the integration of biological and physico-chemical processes to construct a system which will produce food, potable water, and a breathable atmosphere from metabolic and other wastes, in a stable and reliable manner. A central feature of a CELSS is the use of green plant photosynthesis to produce food, with the resulting production of oxygen and potable water, and the removal of carbon dioxide. Author

N91-13849*# National Aeronautics and Space Administration. John F. Kennedy Space Center, Cocoa Beach, FL.
THE CELSS BREADBOARD PROJECT: PLANT PRODUCTION
William M. Knott *In* NASA, Washington, Biological Life Support Technologies: Commercial Opportunities Nov. 1990 p 47-52 (For primary document see N91-13842 05-51)
Avail: NTIS HC/MF A06 CSCL 06C

NASA's Breadboard Project for the Controlled Ecological Life Support System (CELSS) program is described. The simplified schematic of a CELSS is given. A modular approach is taken to building the CELSS Breadboard. Each module is researched in order to develop a data set for each one prior to its integration into the complete system. The data being obtained from the Biomass Production Module or the Biomass Production Chamber is examined. The other primary modules, food processing and resource recovery or waste management, are discussed briefly. The crew habitat module is not discussed. The primary goal of the Breadboard Project is to scale-up research data to an integrated system capable of supporting one person in order to establish feasibility for the development and operation of a CELSS. Breadboard is NASA's first attempt at developing a large scale CELSS. E.R.

N91-13850*# National Aeronautics and Space Administration. Ames Research Center, Moffett Field, CA.
CELSS RESEARCH AND DEVELOPMENT PROGRAM
David Bubenheim *In* NASA, Washington, Biological Life Support Technologies: Commercial Opportunities Nov. 1990 p 53-59 (For primary document see N91-13842 05-51)
Avail: NTIS HC/MF A06 CSCL 06C

Research in Controlled Ecological Life Support Systems (CELSS) conducted by NASA indicate that plant based systems are feasible candidates for human support in space. Ames has responsibility for research and development, systems integration and control, and space flight experiment portions of the CELSS program. Important areas for development of new methods and technologies are biomass production, waste processing, water purification, air revitalization, and food processing. For the plant system, the approach was to identify the flexibility and response time for the food, water, and oxygen production, and carbon dioxide consumption processes. Tremendous increases in productivity, compared with terrestrial agriculture, were realized. Waste processing research emphasizes recycle (transformation) of human wastes, trash, and inedible biomass to forms usable as inputs to the plant production system. Efforts to improve efficiency of the plant system, select new CELSS crops for a balanced diet, and initiate closed system research with the Crop Growth Research Chambers continue. The System Control and Integration program goal is to insure orchestrated system operation of the biological, physical, and chemical operation of the biological, physical, and chemical component processors of the CELSS. Space flight studies are planned to verify adequate operation of the system in reduced gravity or microgravity environments. Author

N91-13851*# Wolverton Environmental Services, Picayune, MS.
PLANTS AND THEIR MICROBIAL ASSISTANTS: NATURE'S ANSWER TO EARTH'S ENVIRONMENTAL POLLUTION PROBLEMS
B. C. Wolverton *In* NASA, Washington, Biological Life Support Technologies: Commercial Opportunities Nov. 1990 p 60-65 (For primary document see N91-13842 05-51)
Avail: NTIS HC/MF A06 CSCL 06C

The utilization of higher plants and their associated microorganisms to solve environmental pollution problems on Earth and in future space applications is briefly reviewed. If man is sealed inside closed facilities, he becomes a polluter of the environment. It is also common knowledge to most people that man cannot survive on Earth without green photosynthesizing plants and microorganisms. Therefore, it is vitally important to have a better understanding of the interactions of man with plants and microorganisms. Biosphere 2 and other related studies presently being conducted or planned, hopefully, will supply data that will help save planet Earth from impending environmental disaster. The development of means to utilize both air and water pollution as a nutrient source for growing green plants is examined. Author

N91-13852*# National Aeronautics and Space Administration. National Space Technology Labs., Bay Saint Louis, MS.
THE BIOHOME: A SPINOFF OF SPACE TECHNOLOGY
Anne Johnson *In* NASA, Washington, Biological Life Support Technologies: Commercial Opportunities Nov. 1990 p 66-71 (For primary document see N91-13842 05-51)
Avail: NTIS HC/MF A06 CSCL 06C

The discussion of the BioHome is prefaced with some information about the work done at the environmental lab over the past 15 years concerning environmental issues related to biological life support such as the use of water hyacinths for wastewater purification, artificial marshes, indoor polluted air revitalization, and the reduction of organic contaminants using a biological system comprised of plants and microorganisms. One of the main concerns, especially with respect to a closed environment, is whether or not these systems are expelling microorganisms into the air. Analyses are being conducted to determine the numbers and types of microbes that are emitted. The BioHome is a 650 sq ft habitat that will enable the evaluation of the efficiency of bioregenerative technology in a closed system. This BioHome system is described and its functions discussed. E.R.

N91-13853*# National Aeronautics and Space Administration. Goddard Space Flight Center, Greenbelt, MD.
EARTH OBSERVING SATELLITE: UNDERSTANDING THE EARTH AS A SYSTEM
Gerald Soffen *In* NASA, Washington, Biological Life Support Technologies: Commercial Opportunities Nov. 1990 p 72-87 (For primary document see N91-13842 05-51)
Avail: NTIS HC/MF A06 CSCL 06C

There is now a plan for global studies which include two very large efforts. One is the International Geosphere/Biosphere Program (IGBP) sponsored by the International Council of Scientific Unions. The other initiative is Mission to Planet Earth, an unbrella program for doing three kinds of space missions. The major one is the Earth Observation Satellite (EOS). EOS is large polar orbiting satellites with heavy payloads. Two will be placed in orbit by NASA, one by the Japanese and one or two by ESA. The overall mission measurement objectives of EOS are summarized: (1) the global distribution of energy input to and energy output from the Earth; (2) the structure, state variables, composition, and dynamics of the atmosphere from the ground to the mesopause; (3) the physical and biological structure, state, composition, and dynamics of the land surface, including terrestrial and inland water ecosystems; (4) the rates, important sources and sinks, and key components and processes of the Earth's biogeochemical cycles; (5) the circulation, surface temperature, wind stress, sea state, and the biological activity of the oceans; (6) the extent, type, state, elevation, roughness, and dynamics of glaciers, ice sheets, snow and sea ice, and the liquid equivalent of snow in the global cryosphere; (7) the global rates, amounts, and distribution of precipitation; and (8) the dynamic motions of the Earth (geophysics) as a whole, including both rotational dynamics and the kinematic motions of the tectonic plates. E.R.

N91-13854*# Space Industries, Inc., Houston, TX.
BUSINESS AND LIFE IN SPACE
Joseph Allen *In* NASA, Washington, Biological Life Support Technologies: Commercial Opportunities Nov. 1990 p 88-95

(For primary document see N91-13842 05-51)
Avail: NTIS HC/MF A06 CSCL 06C

The life support systems in the machine called the Space Shuttle is discussed and later about life support systems in a little cocoon that is far smaller than the shuttle; the more common term is a space suit. E.R.

N91-13855*# National Aeronautics and Space Administration. Lyndon B. Johnson Space Center, Houston, TX.
A PERSONAL HISTORY OF THE HUMAN EXPLORATION INITIATIVE WITH COMMENTARY ON THE PIVOTAL ROLE FOR LIFE SUPPORT RESEARCH
Wendell Mendell *In* NASA, Washington, Biological Life Support Technologies: Commercial Opportunities Nov. 1990 p 96-104
(For primary document see N91-13842 05-51)
Avail: NTIS HC/MF A06 CSCL 06C

The author relates the history of the human exploration initiative from a personal perspective from the 1961 J. F. Kennedy initiative to land a man on the moon up to 1986 when a memo was circulated from NASA Headquarters to its employees which stated as a major goal the expansion of the human presence beyond Earth into the solar system. The pivotal role of life support research is woven into this personalized history. E.R.

N91-13856*# Sverdrup Technology, Inc., Huntsville, AL. Materials and Processing Dept.
MICROBIAL ECOLOGY LABORATORY PROCEDURES MANUAL NASA/MSFC Final Report
Timothy L. Huff Sep. 1990 77 p
(Contract NAS8-37814)
(NASA-CR-184033; NAS 1.26:184033) Avail: NTIS HC/MF A05 CSCL 06C

An essential part of the efficient operation of any microbiology laboratory involved in sample analysis is a standard procedures manual. The purpose of this manual is to provide concise and well defined instructions on routine technical procedures involving sample analysis and methods for monitoring and maintaining quality control within the laboratory. Of equal importance is the safe operation of the laboratory. This manual outlines detailed procedures to be followed in the microbial ecology laboratory to assure safety, analytical control, and validity of results. Author

N91-13857*# National Aeronautics and Space Administration. Lyndon B. Johnson Space Center, Houston, TX.
BIOFILM MONITORING COUPON SYSTEM Patent Application
Richard L. Sauer, inventor (to NASA) and David T. Flanagan, inventor (to NASA) (Krug International, Houston, TX.) 14 Mar. 1990 15 p
(NASA-Case-MSC-21585-1; NAS 1.71:MSC-21585-1; US-Patent-Appl-SN-493529) Avail: NTIS HC/MF A03 CSCL 06C

An apparatus and method is disclosed for biofilm monitoring of a water distribution system which includes the mounting of at least one fitting in a wall port of a manifold in the water distribution system with a passage through the fitting in communication. The insertion of a biofilm sampling member is through the fitting with planar sampling surfaces of different surface treatment provided on linearly arrayed sample coupons of the sampling member disposed in the flow stream in edge-on parallel relation to the direction of the flow stream of the manifold under fluid-tight sealed conditions. The sampling member is adapted to be aseptically removed from or inserted in the fitting and manifold under a positive pressure condition and the fitting passage sealed immediately thereafter by appropriate closure means so as to preclude contamination of the water distribution system through the fitting. The apparatus includes means for clamping the sampling member and for establishing electrical continuity between the sampling surfaces and the system for minimizing electropotential effects. The apparatus may also include a plurality of fittings and sampling members mounted on the manifold to permit extraction of the sampling members in a timed sequence throughout the monitoring period. NASA

N91-13858# Oak Ridge National Lab., TN. Health and Safety Research Div.
INORGANIC CONCEPTS RELEVANT TO METAL BINDING, ACTIVITY, AND TOXICITY IN A BIOLOGICAL SYSTEM
James D. Hoeschele (Parke-Davis Pharmaceutical Co., Ann Arbor, MI.), James E. Turner, and M. Wendy England 1990 27 p Presented at the 4th International Workshop on QSAR in Environmental Toxicology, Veldhoven, Netherlands, 16-20 Sep. 1990
(Contract DE-AC05-84OR-21400)
(DE91-001489; CONF-9009278-1) Avail: NTIS HC/MF A03

The purpose of this paper is to review selected physical and inorganic concepts and factors which might be important in assessing and/or understanding the fact and disposition of a metal system in a biological environment. Hopefully, such inquiries will ultimately permit us to understand, rationalize, and predict differences and trends in biological effects as a function of the basic nature of a metal system and, in optimal cases, serve as input to a system of guidelines for the notion of 'Chemical Dosimetry'. The plan of this paper is to first review, in general terms, the basic principles of the Crystal Field Theory (CFT), a unifying theory of bonding in metal complexes. This will provide the necessary theoretical background for the subsequent discussion of selected concepts and factors. DOE

N91-13859# Brookhaven National Lab., Upton, NY.
CALCIFIED-TISSUE INVESTIGATIONS USING SYNCHROTRON X RAY MICROSCOPY
K. W. Jones, P. Spanne, G. Schidlovsky, Xue Dejun, R. S. Bockman, M. B. Rabinowitz, P. B. Hammond, R. L. Bornschein, and D. A. Hoeltzel (Columbia Univ., New York, NY.) Oct. 1990 8 p Presented at the X Ray Microscopy Conference, London, England, 3-7 Sep. 1990 Sponsored in part by Jaffin Foundation
(Contract DE-AC02-76CH-00016; NIEHS-ES0156611; NIH-RR-01838; NIH-CA-38645; NIH-H-08945; NIH-HD-17047; NIH-HD-20381; NIH-ES-00138; NIH-HD-18655)
(DE91-001729; BNL-44730; CONF-9009235-2) Avail: NTIS HC/MF A02

Synchrotron x ray microscopy (SXRM) in both emission and absorption modes has been used to examine elemental distributions in specimens of rat tibia, human deciduous teeth, and an orthopedic implant phantom. The work was performed with a spatial resolution of 8 microns for the emission work and 25 microns for the absorption work. The results illustrate the usefulness of SXRM for measurements of different types of calcified tissue. DOE

N91-13860*# National Aeronautics and Space Administration. Lyndon B. Johnson Space Center, Houston, TX.
THREE-DIMENSIONAL CELL TO TISSUE ASSEMBLY PROCESS Patent Application
David A. Wolf, inventor (to NASA), Ray P. Schwarz, inventor (to NASA), Marian L. Lewis, inventor (to NASA), John H. Cross, inventor (to NASA), and Mary H. Huls, inventor (to NASA) (Krug International, Houston, TX.) 2 Mar. 1989 55 p
(NASA-Case-MSC-21559-1; NAS 1.71:MSC-21559-1; US-Patent-Appl-SN-317776) Avail: NTIS HC/MF A04 CSCL 06C

The present invention relates a 3-dimensional cell to tissue and maintenance process, more particularly to methods of culturing cells in a culture environment, either in space or in a gravity field, with minimum fluid shear stress, freedom for 3-dimensional spatial orientation of the suspended particles and localization of particles with differing or similar sedimentation properties in a similar spatial region. NASA

52 AEROSPACE MEDICINE

Includes physiological factors; biological effects of radiation; and effects of weightlessness on man and animals.

N91-13861# Joint Publications Research Service, Arlington, VA.
JPRS REPORT: SCIENCE AND TECHNOLOGY. USSR: LIFE SCIENCES
P. S. Garayev and I. D. Aliyev 12 Oct. 1989 64 p
(JPRS-ULS-89-011) Avail: NTIS HC/MF A04

Numerous topics related to U.S.S.R. life science research are discussed. Topics covered include agricultural science, biochemistry, biotechnology, epidemiology, immunology, laser bioeffects, military medicine, pharmacology, physiology, and public health. Author

N91-13862*# National Aeronautics and Space Administration. Ames Research Center, Moffett Field, CA.
PHYSIOLOGICAL RESPONSES TO PROLONGED BED REST IN HUMANS: A COMPENDIUM OF RESEARCH, 1981-1988
Phuong B. Luu, Vanessa Ortiz, Paul R. Barnes (San Francisco State Univ., CA.), and John E. Greenleaf Jul. 1990 140 p
(NASA-TM-102249; A-90003; NAS 1.15:102249) Avail: NTIS HC/MF A07 CSCL 06S

Clinical observations and results form more basic studies that help to elucidate the physiological mechanisms of the adaptation of humans to prolonged bed rest. If the authors' abstract or summary was appropriate, it was included. In some cases a more detailed synopsis was provided under the subheadings of purpose, methods, results, and conclusions. Author

N91-13863# Advisory Group for Aerospace Research and Development, Neuilly-Sur-Seine (France). Aerospace Medical Panel.
ECHOCARDIOGRAPHY IN NATO AIRCREW
Oct. 1990 104 p
(AGARD-AR-297; AGARD-WG-13; ISBN-92-835-0593-X)
Copyright Avail: NTIS HC/MF A06; Non-NATO Nationals requests available only from AGARD/Scientific Publications Executive

The protocol is considered for a planned cross-sectional and a longitudinal study on echocardiography in NATO aircrew. It gives an overview of the procedures manual, technical manual, the echo data sheet, the software program, and the quality control manual. Included is the multinational protocol for the performance and reporting of echocardiograms. Author

N91-13864# John B. Pierce Foundation of Connecticut, New Haven.
THERMOREGULATORY CONSEQUENCES OF RESONANT MICROWAVE EXPOSURE Final Report, Aug. 1987 - Dec. 1989
Eleanor R. Adair Jun. 1990 89 p
(Contract F33615-87-C-0607; AF Proj. 7757)
(AD-A226540; USAFSAM-TR-90-7) Avail: NTIS HC/MF A05 CSCL 06/7

Four experiments were conducted in which it was shown that behavioral and autonomic thermo-regulatory responses are mobilized in an orderly fashion when squirrel monkeys undergo whole-body exposure at the resonant frequency, 450 MHz. The threshold for alteration of thermo-regulatory behavior is about 3 mW/sq cm, equivalent to an Specific Absorption Rate (SAR) of nearly 2 W/kg. Behavioral responses serve to regulate the skin temperature at the normally preferred level. Because of the deep penetration of the radiation at resonance, this regulation results in a stable hyperthermic offset or bias in the deep body temperature. This situation is identical to that which occurs during exercise. Although not yet studied, we presume that the magnitude of this offset will be a direct function of the energy deposited in the body or SAR. Autonomic response of peripheral vasodilation and sweating, manifested on the skin surface, are stimulated at SARs similar to the behavioral threshold, indicating the possibility that such responses could serve as auxiliary sensory cues to behavior. GRA

N91-13865*# National Aeronautics and Space Administration. Lyndon B. Johnson Space Center, Houston, TX.
PORTABLE DYNAMIC FUNDUS INSTRUMENT Patent Application
Gerald Taylor, inventor (to NASA), Richard Meehan, inventor (to NASA), Norwood Hunter, inventor (to NASA), Michael Caputo, inventor (to NASA) (Krug International, Houston, TX.), and C. Robert Gibson, inventor (to NASA) 29 Jun. 1990 21 p
(NASA-Case-MSC-21675-1; NAS 1.71:MSC-21675-1; US-Patent-Appl-SN-562095) Avail: NTIS HC/MF A03 CSCL 06C

A portable diagnostic image analysis instrument is disclosed for retinal funduscopy in which an eye fundus image is optically processed by a lens system to a CCD device which produces recordable and viewable output data and is simultaneously viewable on an electronic view finder. The fundus image is processed to develop a representation of the vessel or vessels from the output data. NASA

N91-13866# Brookhaven National Lab., Upton, NY.
A COMPUTER MODEL TO DETERMINE THE PRIMARY CONTRIBUTORS TO RELATIVE RADIATION DOSE RECEIVED BY ASTRONAUTS
O. W. Lazareth, M. Divadeenam, H. Ludewig, and J. R. Powell 1990 11 p Presented at the 8th Symposium on Space Nuclear Power Systems, Albuquerque, NM, 6-10 Jan. 1991
(Contract DE-AC02-76CH-00016)
(DE90-015681; BNL-44858; CONF-910116-2) Avail: NTIS HC/MF A03

This paper describes a computer model which was used to determine the relative radiation dose of protons of different energies. In the future, the model will be extended to calculate the dosage received by an astronaut during a specific mission to Mars, and within a spacecraft with specific materials and with a specific geometry. The framework for the calculations centered on the computer program HETC, a Monte Carlo transport code for computing the properties of high energy nucleon-meson cascades in matter. It is valid up to several hundred GeV. DOE

N91-13867# Wisconsin Univ., Madison. Dept. of Medical Physics.
DEVELOPMENT AND INITIAL CHARACTERIZATION OF A NUCLEAR MAGNETIC RESONANCE DOSIMETRY SYSTEM Ph.D. Thesis
David Michael Thomasson 1990 91 p Sponsored by National Cancer Inst., Bethesda, MD
(Contract DE-FG02-86ER-60417)
(DE91-001775; DOE/ER-60417/5) Avail: NTIS HC/MF A05

A high dose radiation dosimeter was developed employing NMR spectroscopic quantitation of the radiolytic products of methanol. Chemical shifts of product resonances relative to the solvent allow quantification using NMR techniques. Due to expected dynamic range limitations of NMR instrumentation, deuterated methanol is used with a presaturation suppression sequence to reduce the solvent proton signals. Methanol's (13)C-coupled proton resonances is used as an internal reference to normalize product signals otherwise subject to spectrometer variability. Data on reproducibility, dose response, and temporal stability were acquired. System reproducibility for a sample at 1 kGy is approximately 10 percent. The dose response is linear in the range between 200 Gy and 50 kGy. No significant signal degradation was observed during a six month period. Advantages of this type dosimeter system include ease of use, large dynamic range, and temporal stability. An additional characteristic of a methanol based system is the LET dependent response in the chemical yields of formaldehyde and ethylene glycol. DOE

N91-13868 National Physical Lab., Teddington (England). Div. of Radiation Science and Acoustics.
REVIEW OF UNCERTAINTIES IN THE USE OF NPL PRIMARY STANDARDS OF X RAY EXPOSURE FOR THE CALIBRATION OF SECONDARY STANDARDS IN TERMS OF EXPOSURE AND AIR KERMA

A. R. S. Marsh and C. Cross Dec. 1988 72 p
(NPL-RS(EXT)-109; ISSN-0143-7135; ETN-91-98373) Copyright Avail: National Physical Laboratory, Teddington, TW11 0LW, England

A review of the present values of accuracy or uncertainty was made. The numbers quoted should be considered as the base line from which future modifications are to be made. The systematic uncertainties associated with corrections to primary standards were re-examined, as well as those uncertainties associated with physical data and the intercomparison procedures. For random uncertainties in therapy level secondary standard calibration, the results from the last few calibration periods were analyzed, in order to obtain a more recent estimate of random uncertainty. For protection levels, random uncertainties were calculated on an accumulative basis. ESA

53 BEHAVIORAL SCIENCES

Includes psychological factors; individual and group behavior; crew training and evaluation; and psychiatric research.

N91-13869# New York Univ., New York. Neuromagnetism Lab.
COGNITIVE AND NEURAL BASES OF SKILLED PERFORMANCE Final Technical Report, 5 Sep. 1986 - 30 Nov. 1989
Lloyd Kaufman and Samuel J. Williamson 9 Aug. 1990 48 p
(Contract F49620-86-C-0131; AF Proj. 3484)
(AD-A226668; AFOSR-90-0918TR) Avail: NTIS HC/MF A03 CSCL 05/8

Major improvements were introduced for neuromagnetic studies by the installation of a magnetically shielded room and versatile gantry to hold our 5-sensor neuromagnetometer. Studies with this system verify that the strength of the 100-ms component of the cortical response to a tone is unaffected by tone frequency and intensity at suprathreshold levels, but we have shown that both the 100-ms and 180-ms components are affected by attention. Moreover, we have obtained evidence that auditory cortex in left and right hemispheres may have differing responses to a tone depending on the inter-stimulus interval. Neuronal sources of certain components of auditory-evoked responses are found to be displaced across cortex from the others, with a tonotopic representation for the 50-ms transient component apparently differing from the representation for the steady-state component, which has a similar apparent latency. Studies of spatial attention have revealed robust effects for latencies exceeding 200 ms, unlike for the auditory system, but some subjects show effects commencing as early as 100 ms. An investigation of the classic P300 response for both visual and auditory stimulation has been initiated with a more efficient paradigm, and early results provide evidence that the neuronal source is independent of sensory modality. To address the question of how much cortex is involved in producing an evoked field or potential, we have analyzed published data on intracortical voltage measurements in cat and monkey and found that the current dipole moment per square millimeter of cortical area is very much the same at moments of peak activity for long-latency response. For this we deduce that the area in human cortex typically ranges from 40 to 400 sq mm, based on the current dipole moments deduced from neuromagnetic data. Several technical developments were made during this period. GRA

N91-13870# Human Engineering Labs., Aberdeen Proving Ground, MD.
AN INDEXED BIBLIOGRAPHY ON TRACKING
Salvatore P. Schipani Jul. 1990 153 p
(AD-A226682; HEL-TN-6-90) Avail: NTIS HC/MF A08 CSCL 05/8

A bibliography about tracking and related literature, with corresponding documentation in the form of indexed author and subject listings is presented. Indexing was performed to enhance its utility as a reference. Topical subjects were distinguished after a review of citations revealed repeated mention. Generally, tracking is divided into compensatory tracking (such as driving a car while keeping the vehicle within the boundaries of the road) or pursuit tracking (such as aiming a gun at a moving target while keeping the gun sight directly on the target). This search was partly performed through computer inquiries using the National Technical Information Service's DIALOG Information Retrieval Service, and the PSYCINFO service of the American Psychological Association. Sources were also manually extracted, including journal articles, Government and private sector reports, conference proceedings, and books. In some instances, direct contact was made with author(s). GRA

N91-13871 Physics and Electronics Lab. TNO, The Hague (Netherlands).
STUDY SYSTEM CONCEPT FOR A PELOTONS PROCEDURE TRAINER (PEP-TRAINER) FOR THE WEAPON SYSTEMS YPR-PRAT, YPR-25 mm (EWS) AND LEOPARD 1-5 Final Report
J. C. P. Bol and G. Swiep Jul. 1990 50 p In DUTCH; ENGLISH summary
(Contract A89/KL/606)
(FEL-90-A084; TD-90-1224; ETN-91-98298) Copyright Avail: Physics and Electronics Laboratory TNO, P.O. Box 96864, 2506 JG The Hague, Netherlands

A system for procedure training for the guided weapon system YPR-PRAT, the 25 mm weapon system YPR-EWS and the tank system Leopard 1-5 is described. The starting points for the systems concept are the 'pelotons fire control trainer' developed by the Netherlands Army as well as the results of feasibility study. The systems concept of the novel PEP trainer is based on the use of a laser light source in combination with a CCD (Charged Coupled Device) sensor for the registration of a hit. The training system is based on a scaled target field containing stationary and moving targets. The concept of the PEP trainer has a generalized structure that can be used for different weapon systems. ESA

N91-13872 Institute for Perception RVO-TNO, Soesterberg (Netherlands).
TIME-SHARING PERFORMANCE AS A FACTOR FOR SUCCESS IN FLIGHT TRAINING: TEST DEVELOPMENT AND VALIDATION Final Report
P. G. A. M. Jorna 21 Dec. 1989 33 p
(Contract A81/KM/126)
(IZF-1989-58; TD-89-4556; ETN-91-98307) Copyright Avail: Institute for Perception RVO-TNO, P.O. Box 23, 3769 ZG Soesterberg, Netherlands

A test based on dual-task performance developed to investigate the trainability of aspirant pilots to perform under demanding conditions is described. The dual-task is a combination of a pursuit tracking task with preview and a Continuous Memory Task (CMT). Aspirant pilots practice the tracking task and are tested under single and dual task conditions. Dual-task performance is expected to be related to pilot aptitude as assessed by other criteria. Predictive validity is evaluated in a stepwise validation with increasing levels of pilot aptitude as assessed by traditional selection procedures. A flight simulator test and advanced flight training for the Lockheed Orion and Westland Lynx helicopter are used. Successful aspirants, now operational pilots, are characterized by their excellent performance under dual-task conditions as well as under single-task conditions, depending on how soon they failed in the selection and training process. Prior flying experience did not influence tracking performance and was not found to be a critical factor in predicting success in advanced or operational flight training. ESA

N91-13873 Institute for Perception RVO-TNO, Soesterberg (Netherlands).
VESTIBULO-OCULAR RESPONSES IN MAN TO +G SUB z HYPERGRAVITY Final Report
J. T. Marcus and C. R. vanHolten 21 Dec. 1989 19 p In DUTCH; ENGLISH summary Presented at AsMA Meeting, Washington, DC 8 May 1989 Previously announced in IAA as

A90-39645
(Contract A88/M/318)
(IZF-1989-59; TD-89-4557; ETN-91-98308) Copyright Avail: Institute for Perception RVO-TNO, P.O. Box 23, 3769 ZG Soesterberg, Netherlands

The influence of high G(sub z) gravito-inertial force on the vestibular system in man is investigated in a centrifuge (radius 4 m) with a freely swinging gondola. The subject is exposed to an acceleration of plus 2 G(sub z)/s, plus 3 G(sub z) for three minutes and a deceleration of minus 2 G(sub z)/s. The tests are carried out in two conditions in randomized order: facing forward and facing backward. Under these conditions the effective angular velocity in the plane on the vertical semicircular canals is opposed. Adding the slow phase velocity responses from these conditions yields the G(sub z) effect only; subtracting yields the angular velocity effect only. Vertical vestibular nystagmus is analyzed with five subjects. Results indicate that plus 3 G(sub z) induces a subject-dependent vertical nystagmus with slow phase downwards. The vestibular stimulation by G(sub z) could result in a false subjective perception of attitude, and could play a major role in spatial disorientation in flight. ESA

N91-13874 Institute for Perception RVO-TNO, Soesterberg (Netherlands).
ADAPTABLE DRIVER-CAR INTERFACING AND MENTAL WORKLOAD: A REVIEW OF THE LITERATURE Final Report
W. B. Verwey 26 Jan. 1990 41 p
(IZF-1990-B-3; TD-90-0018; ETN-91-98315) Copyright Avail: Institute for Perception RVO-TNO, P.O. Box 23, 3769 ZG Soesterberg, Netherlands

The design of an adaptive interface or dialog controller in a car equipped with a GIDS (Generic Intelligent Driver Support) system is discussed. A short review of human performance in multitask situations is given. Practice is assumed to be a major significance for mental workload reduction especially in tasks that are executed concurrently with similar tasks. Issues concerning the concept, prediction and assessment of mental workload are discussed. Distinction is made between mental workload assessment for the evaluation of GIDS systems and for the adaptation of the interface to the driver workload. Recommendations are given for workload assessment in evaluation studies. Literature on adaptive interfaces is reviewed. Distinctions are made between human and system initiated interface adaptation and between short-term and long-term adaptation. Recommendations regarding when and how to adapt the interface characteristics to driver workload are presented. ESA

54 MAN/SYSTEM TECHNOLOGY AND LIFE SUPPORT

Includes human engineering; biotechnology; and space suits and protective clothing.

For related information see also *16 Space Transportation.*

N91-13875*# California Univ., Davis. Dept. of Mechanical, Aeronautical, and Materials Engineering.
MODELING PILOT INTERACTION WITH AUTOMATED DIGITAL AVIONICS SYSTEMS: GUIDANCE AND CONTROL ALGORITHMS FOR CONTOUR AND NAP-OF-THE-EARTH FLIGHT Final Report, period ending 30 Sep. 1990
Ronald A. Hess 1990 121 p
(Grant NAG2-221)
(NASA-CR-186105; NAS 1.26:186105) Avail: NTIS HC/MF A06 CSCL 05H

A collection of technical papers are presented that cover modeling pilot interaction with automated digital avionics systems and guidance and control algorithms for contour and nap-of-the-earth flight. The titles of the papers presented are as follows: (1) Automation effects in a multiloop manual control system; (2) A qualitative model of human interaction with complex dynamic systems; (3) Generalized predictive control of dynamic systems; (4) An application of generalized predictive control to rotorcraft terrain-following flight; (5) Self-tuning generalized predictive control applied to terrain-following flight; and (6) Precise flight path control using a predictive algorithm. Author

N91-13876*# Jet Propulsion Lab., California Inst. of Tech., Pasadena.
GENERIC EXTRAVEHICULAR (EVA) AND TELEROBOT TASK PRIMITIVES FOR ANALYSIS, DESIGN, AND INTEGRATION. VERSION 1.0: REFERENCE COMPILATION FOR THE EVA AND TELEROBOTICS COMMUNITIES
Jeffrey H. Smith and Michael Drews 30 Mar. 1990 302 p
(Contract NAS7-918)
(NASA-CR-187429; JPL-Publ-90-10; NAS 1.26:187429) Avail: NTIS HC/MF A14 CSCL 05H

The results are described of an effort to establish commonality and standardization of generic crew extravehicular (crew-EVA) and telerobotic task analysis primitives used for the study of spaceborne operations. Although direct crew-EVA plans are the most visible output of spaceborne operations, significant ongoing efforts by a wide variety of projects and organizations also require tools for estimation of crew-EVA and telerobotic times. Task analysis tools provide estimates for input to technical and cost tradeoff studies. A workshop was convened to identify the issues and needs to establish a common language and syntax for task analysis primitives. In addition, the importance of such a syntax was shown to have precedence over the level to which such a syntax is applied. The syntax, lists of crew-EVA and telerobotic primitives, and the data base in diskette form are presented. Author

N91-13877# Ballistic Research Labs., Aberdeen Proving Ground, MD.
AN ALTERNATIVE TO SUPPRESSION: MODELING METHODOLOGY FOR ASSESSING INDIRECT EFFECTS OF WEAPONS AND HUMAN PERFORMANCE DEGRADATION
Ada W. Gilman Aug. 1990 51 p
(AD-A226518; BRL-TR-3131) Avail: NTIS HC/MF A04 CSCL 23/2

Performance of weapon systems and failure of well planned military operations can frequently be attributed to either a malfunction or limitation of the human element. Hence, an accurate quantification of weapons effects should include not only direct effects of weapons (physical destruction/degradation of targets and production of casualties) but also indirect effects. Most algorithms and equations used in military analysis today however do not consider indirect effects of weapons. Traditionally, the notion of suppression has been cited in such a context. The direct and psychological efforts of weapons are examined. A proposal for modeling them is presented. The difficulties in human performance degradation modeling in the context of modern warfare are discussed. An argument challenging the validity of continued usage of the traditional term suppression is presented. A definition of indirect effects of weapons is offered; a taxonomy of the relevant combat phenomenon is established. A modeling proposal on the quantification of indirect effects is described involving the establishment of five submodels representing several distinct elements of combat system: Individual/Personnel, Visual Detection, Immediate Physical Threat (Firing), Communication and Decision Making. GRA

N91-13878# Air Force Human Resources Lab., Wright-Patterson AFB, OH. Logistics and Human Factors Div.
THE POET REVEALED: A FUTURE FOR HUMAN-CENTERED DESIGN
Edward Boyle Sep. 1990 17 p Submitted for publication
(AD-A226648; AFHRL-TP-90-64) Avail: NTIS HC/MF A03 CSCL 23/2

Human centered design technology as it might operate in the future is described. A prototype on screen ergonomic technology is described in the form of a story. The objective of the paper is to introduce general readers to computer graphics man-modeling work being done by the Air Force Human Resources Laboratory's Logistics Systems Branch. GRA

N91-13879*# National Aeronautics and Space Administration. Lyndon B. Johnson Space Center, Houston, TX.
EMU HELMET MOUNTED DISPLAY Patent Application
Jose Marmolejo, inventor (to NASA), Stephen Smith, inventor (to NASA), Alan Plough, inventor (to NASA), Robert Clarke, inventor (to NASA), William McLean, inventor (to NASA), and Joseph Fournier, inventor (to NASA) (Hamilton Standard, Windsor Locks, CT.) 25 Sep. 1990 14 p
(NASA-Case-MSC-21460-1; NAS 1.71:MSC-21460-1; US-Patent-Appl-SN-587919) Avail: NTIS HC/MF A03 CSCL 05H

A helmet mounted display device is disclosed for projecting a display on a flat combiner surface located above the line of sight where the display is produced by two independent optical channels with independent LCD image generators. The display has a fully overlapped field of view on the combiner surface and the focus can be adjusted from a near field of four feet to infinity. NASA

N91-13880# Idaho National Engineering Lab., Idaho Falls. Human Factors Research Unit.
THE HUMAN FACTORS OF QUALITY AND QA IN R AND D ENVIRONMENTS
Susan G. Hill 1990 9 p Presented at the 17th Annual Conference of the American Society for Quality Control, Tucson, AZ, 9-12 Sep. 1990
(Contract DE-AC07-76ID-01570)
(DE91-001913; EGG-M-90048; CONF-9009153-3) Avail: NTIS HC/MF A02

Achieving quality is a human activity. It is therefore important to consider the human in the design, development and evaluation of work processes and environments in an effort to enhance human performance and minimize error. It is also important to allow for individual differences when considering human factors issues. Human Factors is the field of study which can provide information on integrating the human into the system. Human factors and quality are related for the customer of R and D work, R and D personnel who perform the work, and the quality professional who overviews the process of quality in the work. DOE

N91-13881 Institute for Perception RVO-TNO, Soesterberg (Netherlands).
THE EFFECT OF CONDENSATION IN CLOTHING ON HEAT TRANSFER Final Report
W. A. Lotens, F. J. G. vandeLinde, and G. Havenith 2 Apr. 1990 40 p
(Contract B87-63)
(IZF-1990-B-5; TD-90-0033; ETN-91-98317) Copyright Avail: Institute for Perception RVO-TNO, P.O. Box 23, 3769 ZG Soesterberg, Netherlands

A condensation theory is presented, that enables the calculation of the rate of vapor transfer with its associated effects on temperature and total heat transfer, inside a clothing ensemble consisting of underclothing, enclosed air, and outer garment. The model is experimentally tested by three experiments. Impermeable garments are worn by subjects with and without plastic foil around the skin, blocking sweat evaporation underneath the clothing. Comparison is made between heat loss in impermeable and semipermeable garments and the associated discomfort and strain. Subjects working in impermeable garments in cool and warm environments at two work rates, with and without external radiation, are tested until tolerance. The measured heat exchange and temperatures are calculated with satisfying accuracy using the model. Numerical analysis shows that for total heat loss the major determinants are vapor permeability of the outer garment, skin vapor concentration, air temperature and clothing insulation. In cold conditions the condensation mechanism may completely compensate for the lack of permeability of the clothing as far as heat dissipation is concerned. In hot conditions impermeable clothing is more stressful. ESA

N91-13882# Royal Aerospace Establishment, Farnborough (England).
A SUBJECTIVE RATING SCALE FOR ASSESSING PILOT WORKLOAD IN FLIGHT: A DECADE OF PRACTICAL USE
A. H. Roscoe and G. A. Ellis (British Aerospace Public Ltd. Co., Bristol, England) 5 Mar. 1990 19 p
(RAE-TR-90019; RAE-FM-6; BR114794; ETN-91-98364)
Copyright Avail: NTIS HC/MF A03

The design and development of a ten point rating scale by means of practicing pilots are developed. Effort was concentrated upon developing a comparative scale that could help to answer the important and practical question of whether the workload is appropriate for the primary task under consideration. The Cooper-Harper scale was used to assess handling qualities and the Bedford scale to estimate workload levels, the latter being augmented by recording the pilot heart rate. The scale was based on the concept of space capacity. The examples of various flight trials and workload studies realized by pilots showed their satisfaction of the Bedford scale. ESA

N91-13883# Southampton Univ. (England). Human Factors Research Unit.
MODELLING THE EFFECTS OF VIBRATION ON VISUAL PERFORMANCE
A. D. Davies and M. J. Griffin 1989 56 p
(ISVR-TR-171; ETN-91-98374) Avail: NTIS HC/MF A04

A model to account for and predict the effects of retinal image vibration on visual acuity is developed. It was assumed that the visual system performs a Fourier type analysis and that vibration may act primarily on the high spatial frequency region of the contrasty sensitivity function that was measured. A model of the blurring caused by image movement on the retina was developed using an exponential decay to represent the temporal characteristics of the retina. The usefulness of the temporal model as a predictor of target legibility during vibration is demonstrated. For sinusoidal single axis vibration performance during vibration is similar to performance with static images degraded to simulate legibility 18 degrees to 54 degrees after the modes of the vibration. The model can be applied to predicting the legibility of targets during multiple axis or random vibration provided that the maximum legibility points are identified. ESA

N91-13884# Southampton Univ. (England). Human Factors Research Unit.
EFFECTS OF ANTHROPOMETRIC AND POSTURAL VARIABLES ON THE TRANSMISSION OF WHOLE-BODY VERTICAL VIBRATION FROM SEAT-TO-HEAD
A. Messenger and M. J. Griffin Sep. 1989 125 p Sponsored by Ministry of Defence, London, England
(ISVR-TR-172; ETN-91-98375) Avail: NTIS HC/MF A06

Studies are conducted to obtain quantitative data relating systematic changes in selected postural variables to variations in vibration transmitted through the body. The effects of varying head angle in pitch, roll and yaw axes are investigated as well as those of varying pelvic and spinal posture. The results suggest that displays viewed frequently should be placed at or below eye level and directly in front of the observer. At low frequencies, significant correlations are found between transmittibility and body dimensions, but in all axes monitored at the head, partial correlation techniques did not indicate any particular body dimension as being consistently important. The systematic studies are applied to helicopter seat design and it is shown that overall static comfort in the lower back region are greater when lumbar support is present. ESA

55 SPACE BIOLOGY

Includes exobiology; planetary biology; and extraterrestrial life.

No abstracts in this category.

59 MATHEMATICAL AND COMPUTER SCIENCES (GENERAL)

No abstracts in this category.

60 COMPUTER OPERATIONS AND HARDWARE

Includes hardware for computer graphics, firmware, and data processing.

For components see *33 Electronics and Electrical Engineering.*

N91-13885*# Worcester Polytechnic Inst., MA.
FEASIBILITY STUDY, SOFTWARE DESIGN, LAYOUT AND SIMULATION OF A TWO-DIMENSIONAL FAST FOURIER TRANSFORM MACHINE FOR USE IN OPTICAL ARRAY INTERFEROMETRY
Valentin Boriakoff and Wei Chen Jul. 1990 74 p
(Grant NAG5-1138)
(NASA-CR-186922; NAS 1.26:186922) Avail: NTIS HC/MF A04 CSCL 09B

The NASA-Cornell Univ.-Worcester Polytechnic Institute Fast Fourier Transform (FFT) chip based on the architecture of the systolic FFT computation as presented by Boriakoff is implemented into an operating device design. The kernel of the system, a systolic inner product floating point processor, was designed to be assembled into a systolic network that would take incoming data streams in pipeline fashion and provide an FFT output at the same rate, word by word. It was thoroughly simulated for proper operation, and it has passed a comprehensive set of tests showing no operational errors. The black box specifications of the chip, which conform to the initial requirements of the design as specified by NASA, are given. The five subcells are described and their high level function description, logic diagrams, and simulation results are presented. Some modification of the Read Only Memory (ROM) design were made, since some errors were found in it. Because a four stage pipeline structure was used, simulating such a structure is more difficult than an ordinary structure. Simulation methods are discussed. Chip signal protocols and chip pinout are explained. Author

N91-13886# Department of the Navy, Washington, DC.
M-DIMENSIONAL COMPUTER MEMORY WITH M-1 DIMENSIONAL HYPERPLANE ACCESS Patent Application
Allen D. Parks, inventor (to Navy), James C. Perry, inventor (to Navy), and Albert P. Schuler, inventor (to Navy) 9 Jul. 1990 14 p
(AD-D014615; US-Patent-Appl-SN-551103; Navy-Case-72449)
Avail: NTIS HC A03/MF A01 CSCL 12/6

This invention relates generally to a computer memory and in particular to a m-dimensional computer memory with m-1 dimensional hyperplane access. Conventional computer memory is structurally linear in nature and its access can therefore only occur in a one directional linear manner. Thus, numerous accesses may be needed in order to reach required memory locations. Memory constructed in this way also has certain efficiency limitations in matrix and array processing applications. This is because software must be used to manipulate access data outside of memory in order to place it in proper form for processing and updating. In addition, when conventional memory is shared in a multiple processor environment, memory access control requires additional complexity in order to prevent access collision. GRA

N91-13887 Department of the Navy, Washington, DC.
SUPERCONDUCTING NEURAL NETWORK COMPUTER AND SENSOR ARRAY Patent
Harold H. Szu, inventor (to Navy) 24 Jul. 1990 9 p Filed 30 Sep. 1988
(AD-D014625; US-Patent-4,943,556; US-Patent-Appl-SN-252486; US-Patent-Class-505-1) Avail: US Patent and Trademark Office CSCL 12/6

This patent describes a combination of optical interconnect technology with superconducting material to form a superconducting neural network array. Superconducting material in a matrix has the superconducting current decreased in one filament of the matrix by interaction of the Cooper pairs with radiation controlled by a spatial light modulator. This decrease in current results in a switch of current, in a relative sense, to another filament in the matrix. This switching mechanism can be used in a digital or analog fashion in a superconducting computer application. GRA

N91-13888*# National Aeronautics and Space Administration. Pasadena Office, CA.
AUTO AND HETERO-ASSOCIATIVE MEMORY USING A 2-D OPTICAL LOGIC GATE Patent Application
Tien-Hsin Chao, inventor (to NASA) (Jet Propulsion Lab., California Inst. of Tech., Pasadena.) 16 Feb. 1990 17 p
(Contract NAS7-918)
(NASA-Case-NPO-17997-1-CU; NAS 1.71:NPO-17997-1-CU; US-Patent-Appl-SN-481013) Avail: NTIS HC/MF A03 CSCL 09B

An optical system for auto-associative and hetero-associative recall utilizing Hamming distance as the similarity measure between a binary input image vector V(sup k) and a binary image vector V(sup m) in a first memory array using an optical Exclusive-OR gate for multiplication of each of a plurality of different binary image vectors in memory by the input image vector. After integrating the light of each product V(sup k) x V(sup m), a shortest Hamming distance detection electronics module determines which product has the lowest light intensity and emits a signal that activates a light emitting diode to illuminate a corresponding image vector in a second memory array for display. That corresponding image vector is identical to the memory image vector V(sup m) in the first memory array for auto-associative recall or related to it, such as by name, for hetero-associative recall. NASA

N91-13889# Laboratoire d'Automatique et d'Analyse des Systemes, Toulouse (France). Groupe Decomposition, Hierarchisation, Parallelisme.
ABOUT TRANSIENT STABILITY OF POWER SYSTEMS: STATISTICAL PATTERN RECOGNITION APPROACH Ph.D. Thesis
Monsef Berbiche 1990 170 p In FRENCH; ENGLISH summary
(LAAS-90192; ETN-91-98215) Avail: NTIS HC/MF A08

On line transient stability assessment of power system by statistical pattern recognition is discussed. The approach enables the reduction of online computing time while maintaining an accuracy similar to those obtained by the conventional numerical integration approach. The main steps of the method are presented. To describe the transient machine behavior, a model based on Park transformation including voltage and speed regulators is considered. Two pattern vectors are derived from the transient behavior analysis. The pattern vector dimension is proportional to the number of machines. The pattern vector presents two types of information: a discriminant information for secure and non secure state separation and redundant information. In order to reduce the online time computation, some methods to select the discriminant features, and to achieve vector dimension reduction, are presented and compared. These results are applied to an eight machines system, and symmetrical three phase fault. The discriminant ability of the two patterns vectors is evaluated, using Bayes discriminant function and the k nearest neighbors rule. ESA

N91-13890*# National Aeronautics and Space Administration. Lyndon B. Johnson Space Center, Houston, TX.
PROGRAMMABLE REMAPPER WITH SINGLE FLOW ARCHITECTURE Patent Application
Timothy E. Fisher, inventor (to NASA) 30 Mar. 1990 24 p
(NASA-Case-MSC-21481-1; NAS 1.71:MSC-21481-1; US-Patent-Appl-SN-506136) Avail: NTIS HC/MF A03

The invention relates to image processing systems and methods and in particular to a machine which accepts a real time video image in the form of a matrix of picture elements (pixels) and remaps such image according to a selectable one of a plurality of mapping functions to create an output matrix of pixels. Such mapping functions, or transformations, may be any one of a number of different transformations depending on the objective of the user of the system. The system remaps input images from one coordinate system to another using a set of look-up tables for the data necessary for the transform. The transforms, which are operator selectable, are precomputed and loaded into massive look-up tables. Input pixels, via the look-up tables of any particular transform selected, are mapped into output pixels with the radiance information of the input pixels being appropriately weighted. An earlier embodiment of the system included two parallel processors: a collective processor which mapped multiple input pixels into a single output pixel and an interpolative processor. The interpolative processor performed an interpolation among pixels in the input image where a given input pixel may affect the value of many output pixels. Several advantages are provided over previous embodiments in that the two distinct processors are replaced by a single processor capable of performing both types of operations (collective and interpolative) with no more complexity. Previously, there has existed no image processor or 'remapper' that can operate with sufficient speed and flexibility to permit investigating different transformation patterns in real time. NASA

N91-13891# Norwegian Defence Research Establishment, Kjeller.
NDRE/TALL PROCESSOR ARCHITECTURE STUDY Final Report
Vidar S. Andersen, Robert H. MacDonald, Bjorn Rudberg, Bard Tokerud, and Knut Tvete 17 Jun. 1990 124 p
(FFI-90/7012; ETN-91-98279) Avail: NTIS HC/MF A06

An architecture suitable for real time image processing was studied. In parallel with the architecture studies, the detailed physical specification was carried out. The image processing algorithms were studied to give the exact processing power and communication requirements. Different candidates for the basic processing element were discussed. The proposed candidate, the INMOS transputer, was used. Different aspects of the proposed architecture were explained. The design phase was examined, in order to verify that the proposed architecture could be realized in hardware. Recommendations for the development of system software were given, and suggestions were made as to application programming. The conclusions of the Norwegian Defence Research Establishment (NDRE) were given. ESA

N91-13892 Physics and Electronics Lab. TNO, The Hague (Netherlands).
DEFINITION STUDY INTO THE REQUIREMENTS OF A DATA MODEM FOR THE SYSCOM NETWORK Final Report
P. P. Copeland May 1990 44 p
(Contract A87/KL/072)
(FEL-90-A116; TD-90-1234; ETN-91-98301) Copyright Avail: Physics and Electronics Laboratory TNO, P.O. Box 96864, 2509 JG The Hague, Netherlands

The functional requirements that need to be implemented in a development of a data modem in support of the SYSCOM (System Control and Management) project are described. The modem must be capable of supporting the transmission of data over the mobile tactical communications network ZODIAC, which operates in accordance with the requirements of EUROCOM Tactical Communications Systems (D/1). ESA

61 COMPUTER PROGRAMMING AND SOFTWARE

Includes computer programs, routines, alogorithms, and specific applications, e.g., CAD/CAM.

N91-13893*# Michigan Univ., Ann Arbor. Radiation Lab.
EXAMPLES OF FINITE ELEMENT MESH GENERATION USING SDRC IDEAS Technical Report, Feb. - Sep. 1990
John Zapp and John L. Volakis 1990 56 p
(Grant NAG2-541)
(NASA-CR-186962; NAS 1.26:186962; Rept-025921-16-T) Avail: NTIS HC/MF A04 CSCL 09B

IDEAS (Integrated Design Engineering Analysis Software) offers a comprehensive package for mechanical design engineers. Due to its multifaceted capabilities, however, it can be manipulated to serve the needs of electrical engineers, also. IDEAS can be used to perform the following tasks: system modeling, system assembly, kinematics, finite element pre/post processing, finite element solution, system dynamics, drafting, test data analysis, and project relational database. Author

N91-13894*# Southwest Research Inst., San Antonio, TX.
RESEARCH INTO ALTERNATIVE NETWORK APPROACHES FOR SPACE OPERATIONS Final Report
Antone L. Kusmanoff and Timothy J. Barton 27 Sep. 1990 205 p
(Grant NAG9-369; SwRI Proj. 05-2921)
(NASA-CR-187015; NAS 1.26:187015) Avail: NTIS HC/MF A10 CSCL 09B

The main goal is to resolve the interoperability problem of applications employing DOD TCP/IP (Department of Defence Transmission Control Protocol/Internet Protocol) family of protocols on a CCITT/ISO based network. The objective is to allow them to communicate over the CCITT/ISO protocol GPLAN (General Purpose Local Area Network) network without modification to the user's application programs. There were two primary assumptions associated with the solution that was actually realized. The first is that the solution had to allow for future movement to the exclusive use of the CCITT/ISO standards. The second is that the solution had to be software transparent to the currently installed TCP/IP and CCITT/ISO user application programs. Y.S.

N91-13895*# Southwest Research Inst., San Antonio, TX.
RESEARCH INTO SOFTWARE EXECUTIVES FOR SPACE OPERATIONS SUPPORT Final Report
Mark D. Collier 28 Sep. 1990 424 p
(Grant NAG9-340; SwRI Proj. 05-2881)
(NASA-CR-187013; NAS 1.26:187013) Avail: NTIS HC/MF A18 CSCL 09B

Research concepts pertaining to a software (workstation) executive which will support a distributed processing command and control system characterized by high-performance graphics workstations used as computing nodes are presented. Although a workstation-based distributed processing environment offers many advantages, it also introduces a number of new concerns. In order to solve these problems, allow the environment to function as an integrated system, and present a functional development environment to application programmers, it is necessary to develop an additional layer of software. This 'executive' software integrates the system, provides real-time capabilities, and provides the tools necessary to support the application requirements. Author

N91-13896 Florida Univ., Gainesville.
VERSION CONTROL AND MANAGEMENT IN COMPUTER-AIDED DESIGN DATABASES Ph.D. Thesis
Rafi Ahmed 1989 136 p
Avail: Univ. Microfilms Order No. DA9028488

There are essentially two characteristics of design objects which impact upon the iterative and probative nature of the design process. First, they are hierarchically formed assemblies of component objects. Second, they have several alternative

representations. A broad spectrum of modeling and operational issues related to these two aspects in computer-aided design databases is addressed. A formal treatment of datamodeling concepts is presented for design applications. A classification of composite object attributes into intrinsic interface and extrinsic internal assembly provides an insight into their behavior and functionality. The design process is studied with respect to these classes of attributes. Concepts of invariant attributes and value acquisition are found to be useful for developing a notion of version equivalence. A wide range of methodologies for version management and solutions for the related problems are discussed. The interdependence between composition and generalization graphs suggests that the effect of updates in these graphs on each other must be evaluated for maintaining consistency. A time complexity analysis of algorithms devised for this purpose shows a considerably improved performance when the stored, rather than the dynamically computed, transitive closures of these graphs are used. The proposed scheme and its related algorithms can determine an optimal storage organization based on significant units of clustering and expected frequency of retrieval and update operations. A multi-layer architecture is motivated by the accessibility and stability of versions they contain. The proposed protocols for sharing and transition of versions together with change notification provide a unifying framework for managing design in a cooperative CAD environment. Dissert. Abstr.

N91-13897# European Space Agency. European Space Research and Technology Center, ESTEC, Noordwijk (Netherlands). Thermal Control and Life Support Div.
ESATAN: USER MANUAL
Apr. 1990 444 p
(Contract ESA-4791/81/NL/DK(SC))
(ESA-PSS-03-105-Issue-1; ISSN-0379-4059; ETN-90-97994)
Copyright Avail: NTIS HC/MF A19

The ESATAN user manual provides a full description of the use and operation of the ESA Thermal Analyzer (ESATAN). The preprocessor, editor, SINDA to ESATAN translator and the syntax checker are described in detail. A complete list of the ESATAN library routines and their uses are given. ESA

N91-13898# Instituto de Pesquisas Espaciais, Sao Jose dos Campos (Brazil).
IMPLEMENTATION OF THE MAGINT-MAGGRAF CODE IN THE MICROVAX-3600 SYSTEM [IMPLEMENTACAO DO CODIGO MAGINT-MAGGRAF NO SISTEMA MICROVAX-3600]
Joaquim Paulino LeiteNeto, Carlos ShinyaShibata, and Antonio Montes Jan. 1990 57 p In PORTUGUESE; ENGLISH summary Presented at the 41st Annual Meeting of SBPC, Fortaleza, Brazil, 9-16 Jul. 1989
(INPE-5042-PRE/1575) Avail: NTIS HC/MF A04

An auxiliary code, named MAGGRAF, was developed and implemented on the MicroVAX-3600 system of the Plasma Laboratory at the Institute for Space Research, in order to perform the graphical output of the numerical results provided by the magnetic field calculation code MAGINT. A brief description of the graphical code, of the parameters which specify the different output options, and of the structure of the data file containing these parameters is presented. Some examples are shown to illustrate the versatility of the code, as well as the quality of the graphs. Author

N91-13899# Instituto de Pesquisas Espaciais, Sao Jose dos Campos (Brazil).
ANALYSIS OF PARALLELISM FOR NONLINEAR PROGRAMMING M.S. Thesis [ANALISE DE PARALELISMO PARA ALGORITMOS DE PROGRAMACAO NAO-LINEAR]
Ana Clara daMota Sep. 1990 88 p In PORTUGUESE; ENGLISH summary
(INPE-5121-TDL/422) Avail: NTIS HC/MF A05

A very brief survey of parallel architectures and general characteristics of parallel algorithms is given. Parallel algorithms are examined for solving unconstrained, constrained, and global optimization problems. Conjugate directions, Newton and Quasi-Newton methods (for unconstrained optimization), and two approaches, where parallelism can successfully be introduced were explored: A quadratic approximation method based on penalty function and a dual method (for constrained optimization), are presented for some of the main architectures of parallel computers. For global optimization, a parallel algorithm based on a stochastic approach was described. It is based on the idea of finding all the local minima in an efficient way. Author

N91-13900# Federal Aviation Administration, Atlantic City, NJ.
CONNECTIVITY ALTERNATIVES FOR REMOTE USERS OF THE MAINTENANCE PROCESSOR SUBSYSTEM (MPS) Final Report
Lori Adkisson, Dennis Steelman, Kurt Shallenberger, David Walters, and John Cherry Jul. 1990 40 p
(Contract T0704E)
(DOT/FAA/CT-90/16) Avail: NTIS HC/MF A03

Preliminary testing has shown that utilizing commercial off-the-shelf equipment to implement x.25 packet assembly and disassembly for remote maintenance monitoring terminal connectivity is far superior to the method described in EEM.6140.4. This approach yields an expected life cycle cost savings in excess of $37,000.00 per installation. Additionally, reliability, data transparency, and response time are improved, while space and cabling requirements are significantly reduced. This testing also showed potential for even greater cost savings and improved functionality by increasing the bandwidth and replacing the RS-232 standard connection with a V.35 connection. A follow-up report will be issued at the conclusion of tests conducted to determine the viability of this alternative when the communications load is increased significantly and the bandwidth changed accordingly. Author

N91-13901# Autometric Corp., Inc., Rome, NY.
ARCHITECTURE FOR ELECTRONIC IMAGERY INTEROPERABILITY Final Technical Report, Dec. 1988 - Jun. 1990
Ronald B. Haynes, Thomas A. Galayda, and Mary B. DeMatteo Aug. 1990 37 p
(Contract F30602-87-D-0086)
(AD-A226522; RADC-TR-90-257) Avail: NTIS HC/MF A03
CSCL 09/5

This report provides an overall description of an imagery interoperability architecture, being reviewed for implementation by the Office of the Secretary of Defense for Command, Control, Communications and Intelligence (OSD/C3I). The architecture furnishes the means for interoperability among digital electronic imagery reconnaissance assets of the United States and of its allies. It identifies programs designed to establish interoperability through standards, formats, and limited hardware and software development. These programs rely upon the unique properties of digital electronics used in new softcopy sensor exploitation systems as they replace traditional film based systems. GRA

N91-13902# Naval Postgraduate School, Monterey, CA. Dept. of Administrative Sciences.
COUPLING ARTIFICIAL INTELLIGENCE AND A SYSTEM DYNAMICS SIMULATION TO OPTIMIZE QUALITY ASSURANCE AND TESTING IN SOFTWARE DEVELOPMENT M.S. Thesis
Christopher E. Agan Mar. 1990 166 p
(AD-A226580) Avail: NTIS HC/MF A08 CSCL 12/5

The allocation of effort to quality assurance and testing is vitally important to the successful development and maintenance of a software system. There is no quantitative method for finding the right allocation policy. The most common methods include allocating fixed percentage of effort for all software projects or using allocations that have been used for similar projects in the past. The benefits of choosing the correct manpower allocation to suit a particular project can be substantial. Using the System Dynamics Model of Software Project Management an optimal quality assurance and testing level for project's development lifecycle can be found. The focus of this thesis is to design an

expert system that can be coupled with the model in order to find the optimal allocation of quality assurance and testing effort for a particular project. Two expert system modules were developed, that when coupled with the system dynamics model, will find optimum quality assurance and testing distributions for a software project. The expert system modules were then used to perform sensitivity analysis experiments on the results. GRA

N91-13903# Techplan Corp., San Diego, CA.
COORDINATES OF A LIFE-CYCLE MODEL FOR A SOFTWARE SYSTEM AND COMMUNICATING THE NEED FOR SOFTWARE TECHNOLOGY Final Report
Jul. 1990 29 p
(Contract N66001-87-D-0179)
(AD-A226592; NOSC/TD-1881) Avail: NTIS HC/MF A03
CSCL 12/5

On August 7 to 9, 1989, the Navy 6.2 Software Technology Project held a workshop meeting at the Naval Postgraduate School in Monterey, CA. Two parallel working groups were formed to address: (1) Evolving a consensus on the coordinates of a suitable software life-cycle model for the Navy; and (2) Communicating the need for software technology. The Working Meeting was opened by CDR Jane Van Fossen of the Office of Navy Technology who described the nature of software technology from a financial investment perspective. It was noted that software technology is a low profile budget item, with essentially no Navy 6.3A investment and a 6.2 budget that represents only about two million of the $430 million ONT budget. This level of investment in software technology seems inappropriate in light of the significance of software for major Navy systems. After CDR Van Fossen's remarks, the two working groups separated to pursue their respective topics. This report summarizes the efforts of these working groups. Working Group 1 accomplishments are summarized in Section 2. Working Group 2 accomplishments are summarized in Section 3. Working group participants are listed in Appendices A and B respectively. GRA

N91-13904*# North Carolina State Univ., Raleigh. Dept. of Computer Science.
SOFTWARE RELIABILITY THROUGH FAULT-AVOIDANCE AND FAULT-TOLERANCE Semiannual Technical Report No. 3, 1 Mar. - 31 Aug. 1990
Mladen A. Vouk and David F. McAllister 31 Aug. 1990 41 p
(Grant NAG1-983)
(NASA-CR-187646; NAS 1.26:187646) Avail: NTIS HC/MF A03
CSCL 09B

The use of back-to-back, or comparison, testing for regression test or porting is examined. The efficiency and the cost of the strategy is compared with manual and table-driven single version testing. Some of the key parameters that influence the efficiency and the cost of the approach are the failure identification effort during single version program testing, the extent of implemented changes, the nature of the regression test data (e.g., random), and the nature of the inter-version failure correlation and fault-masking. The advantages and disadvantages of the technique are discussed, together with some suggestions concerning its practical use. Author

N91-13905# Universiteit Twente, Enschede (Netherlands). Faculty of Applied Mathematics.
ALGORITHMS FOR FINDING AN OPTIMAL MATCHING BETWEEN A GIVEN STRING AND A STRING GENERATED BY A REGULAR GRAMMAR
S. M. Baas and P. vanSchaik (Department of Education, Netherlands) Dec. 1989 24 p
(MEMO-836; ISSN-0169-2690; ETN-90-98097) Avail: NTIS HC/MF A03

Procedures for comparing a given string Y with a family of strings obtainable from a regular grammar G by means of successive elementary productions are described. Symbols in a grammer are either terminal or non-terminal, including the start symbol. Elementary productions transform a non-terminal symbol into a string of terminal symbols, possibly closed by a single non-terminal symbol. If a string Z is the result of successive elementary productions from the start symbol and consists of terminal symbols only, it can be compared with the given string Y. The difference between Y and Z is expressed in terms of weighted elementary operations: deletions, insertions and substitutions. A matching between Y and Z is a transformation of Y into Z (or, equivalently Z into Y) by means of such elementary operations. The weight of a matching is the sum of the weights of the individual elementary matching operations involved. A minimum weight matching is found by standard dynamic programming. To do so a shortest path method in a directed graph in which the arc-lengths correspond with the weights of minimum weight matchings of elementary productions with substrings of Y is applied. It is shown that the problem can be solved in polynomial time by an algorithm including the shortest path method. ESA

N91-13906*# Softech, Inc., Houston, TX.
SECURITY FOR SAFETY CRITICAL SPACE BORNE SYSTEMS
Sue LeGrand 31 Dec. 1987 37 p Prepared in cooperation with Houston Univ., Clear Lake, TX
(Contract NCC9-16)
(NASA-CR-187656; NAS 1.26:187656) Avail: NTIS HC/MF A03
CSCL 09B

The Space Station contains safety critical computer software components in systems that can affect life and vital property. These components require a multilevel secure system that provides dynamic access control of the data and processes involved. A study is under way to define requirements for a security model providing access control through level B3 of the Orange Book. The model will be prototyped at NASA-Johnson Space Center. Author

N91-13907*# Computer Sciences Corp., Hampton, VA. Applied Technology Div.
PRESSURE VISUALIZATION (PREVIZ) PACKAGE VERSION 1.0 USER'S GUIDE
Bradford D. Bingel and Pamela J. Haley Nov. 1990 40 p
(Contract NAS1-19038)
(NASA-CR-187444; NAS 1.26:187444) Avail: NTIS HC/MF A03
CSCL 09B

The Pressure Visualization (PreViz) package is a software tool which merges a wireframe model of the test aircraft with pressure data represented as a series of displacement vectors normal to the aircraft's skin. The PreViz package automates much of the researcher's data reduction effort, reduces the time required to review large amounts of pressure data, presents the data more clearly than tabular listings, and provides a wireframe description for a black and white graphic suitable for a technical publication (the actual graphic images must be created by a local package since PreViz has no graphics capability). Although designed for pressure data, the PreViz package works equally well for any surface property (such as structural loading or skin temperature). Written in ANSI-standard FORTRAN 77 and self-contained, PreViz executes in UNIX, VAX/VMS, and CDC/NOS host environments. Author

N91-13908# Lawrence Livermore National Lab., CA.
IMAGE 3.3: TUTORIAL MANUAL
Robert R. McLeod and Michael J. Allison 1 Oct. 1990 15 p
(Contract W-7405-eng-48)
(DE91-001762; UCRL-MA-104860) Avail: NTIS HC/MF A03

This manual is a tutorial introduction to the image mesh-verification software for finite-difference time-domain (FDTD) grids. It assumes the reader is familiar with the FDTD method, the nature of its staggered spatial grid, and the general concepts of modelling physical objects in such a grid. If this is not the case, the reader is urged to refer to other publications and manuals to acquire this information. The TSAR and ANA user's manuals would be a good place to start. DOE

N91-13909# Idaho National Engineering Lab., Idaho Falls.
THE DESIGN OF A DISTRIBUTED IMAGE PROCESSING AND DISSEMINATION SYSTEM
Patrick Rafferty and Linn Hower 1990 9 p Presented at the GOMAC 1989: Government Microcircuit Applications Conference, Orlando, FL, 7-9 Nov. 1989
(Contract DE-AC07-76ID-01570)
(DE91-001835; EGG-M-89164; CONF-891159-5) Avail: NTIS HC/MF A02

The design and implementation of a distributed image processing and dissemination system was undertaken and accomplished as part of a prototype communication and intelligence (CI) system, the contingency support system (CSS), which is intended to support contingency operations of the Tactical Air Command. The system consists of six (6) Sun 3/180C workstations with integrated ITEX image processors and three (3) 3/50 diskless workstations located at four (4) system nodes (INEL, base, and mobiles). All 3/180C workstations are capable of image system server functions where as the 3/50s are image system clients only. Distribution is accomplished via both local and wide area networks using standard Defense Data Network (DDN) protocols (i.e., TCP/IP, et al.) and Defense Satellite Communication Systems (DSCS) compatible SHF Transportable Satellite Earth Terminals (TSET). Image applications utilize Sun's Remote Procedure Call (RPC) to facilitate the image system client and server relationships. The system provides functions to acquire, display, annotate, process, transfer, and manage images via an icon, panel, and menu oriented Sunview(trademark) based user interface. Image spatial resolution is 512 (times) 480 with 8-bits/pixel black and white and 12/24 bits/pixel color depending on system configuration. Compression is used during various image display and transmission functions to reduce the dynamic range of image data of 12/6/3/2 bits/pixel depending on the application. Image acquisition is accomplished in real-time or near-real-time by special purpose Itex image hardware. As a result all image displays are highly interactive with attention given to subsecond response time. DOE

N91-13910*# National Aeronautics and Space Administration. Marshall Space Flight Center, Huntsville, AL.
AN IMPROVED EXPLORATORY SEARCH TECHNIQUE FOR PURE INTEGER LINEAR PROGRAMMING PROBLEMS
F. R. Fogle Oct. 1990 130 p
(NASA-TM-103517; NAS 1.15:103517) Avail: NTIS HC/MF A07 CSCL 09B

The development is documented of a heuristic method for the solution of pure integer linear programming problems. The procedure draws its methodology from the ideas of Hooke and Jeeves type 1 and 2 exploratory searches, greedy procedures, and neighborhood searches. It uses an efficient rounding method to obtain its first feasible integer point from the optimal continuous solution obtained via the simplex method. Since this method is based entirely on simple addition or subtraction of one to each variable of a point in n-space and the subsequent comparison of candidate solutions to a given set of constraints, it facilitates significant complexity improvements over existing techniques. It also obtains the same optimal solution found by the branch-and-bound technique in 44 of 45 small to moderate size test problems. Two example problems are worked in detail to show the inner workings of the method. Furthermore, using an established weighted scheme for comparing computational effort involved in an algorithm, a comparison of this algorithm is made to the more established and rigorous branch-and-bound method. A computer implementation of the procedure, in PC compatible Pascal, is also presented and discussed. Author

N91-13911*# National Aeronautics and Space Administration. Lyndon B. Johnson Space Center, Houston, TX.
GENERAL METHOD OF PATTERN CLASSIFICATION USING THE TWO-DOMAIN THEORY Patent Application
Mark E. Rorvig, inventor (to NASA) 25 Sep. 1990 28 p
(NASA-Case-MSC-21737-1; NAS 1.71:MSC-21737-1; US-Patent-Appl-SN-587922) Avail: NTIS HC/MF A03 CSCL 09B

Human beings judge patterns (such as images) by complex mental processes, some of which may not be known, while computing machines extract features. By representing the human judgements with simple measurements and reducing them and the machine extracted features to a common metric space and fitting them by regression, the judgements of human experts rendered on a sample of patterns may be imposed on a pattern population to provide automatic classification. NASA

N91-13912# Idaho National Engineering Lab., Idaho Falls.
WORDPERFECT'S TOOLBOX: FORMATTING DOCUMENTS USING STYLES AND MACROS
William Edgar May 1990 5 p Presented at the Technical Communications Toolbox, Portland, OR, 12-13 Oct. 1990
(Contract DE-AC07-76ID-01570)
(DE91-001884; EGG-M-90394; CONF-9010239-1) Avail: NTIS HC/MF A01

An automated system for formatting documents provides the technical communicator with tools to increase productivity, provide consistent document appearance, and decrease hassle and error. This paper demonstrates such a system, which uses WordPerfect's styles and macros, and illustrates the keystrokes necessary to format procedures and tables. Levels of automation will be discussed, progressing from manual application of styles, to applying styles with macros, to repeating macros with the escape key and through a parent macro. DOE

N91-13913# Argonne National Lab., IL. Mathematics and Computer Science Div.
IMPLEMENTING AUTOMATIC DIFFERENTIATION EFFICIENTLY
David Juedes (Iowa State Univ. of Science and Technology, Ames.) and Andreas Griewank Oct. 1990 15 p
(Contract W-31-109-eng-38)
(DE91-002409; ANL/MCS-TM-140) Avail: NTIS HC/MF A03

The automatic differentiation of computer arithmetic has been investigated since before 1960. Most of this effort has been centered on the forward mode of derivative evaluation. Speelpenning, Iri and Kubota, and Horwedel et al. have all implemented the more efficient reverse mode of evaluating derivatives in their respective FORTRAN precompilers. The reverse mode requires information about a computation to be stored in order that derivatives may be calculated after the function evaluation has been completed. This additional storage cost may be prohibitive. The goals of our research have been to implement an automatic differentiation package that gracefully handles the storage issue and to generate a parallel implementation of derivative evaluation in the reverse mode. This paper discusses results of both research efforts, specifically those involving the ADOL-C package. DOE

N91-13914# Lawrence Livermore National Lab., CA.
COMPUTED TOMOGRAPHY SOFTWARE AND STANDARDS
S. G. Azevedo, H. E. Martz, M. F. Skeate, D. J. Schneberk, and G. P. Roberson 20 Feb. 1990 17 p
(Contract W-7405-eng-48)
(DE91-002573; UCRL-ID-105132) Avail: NTIS HC/MF A03

This document establishes the software design, nomenclature, and conventions for industrial Computed Tomography (CT) used in the Nondestructive Evaluation Section at Lawrence Livermore National Laboratory. It is mainly a users guide to the technical use of the CT computer codes, but also presents a proposed standard for describing CT experiments and reconstructions. Each part of this document specifies different aspects of the CT software organization. A set of tables at the end describes the CT parameters of interest in our project. DOE

N91-13915# Lawrence Livermore National Lab., CA. National Energy Research Supercomputer Center.
SOLVING THE FOKKER-PLANCK EQUATION ON A MASSIVELY PARALLEL COMPUTER

Arthur A. Mirin 16 Oct. 1990 4 p Presented at the US-Japan Workshop on Advances in Simulation Techniques Applied To Plasmas and Fusion, Los Angeles, CA, 26-28 Sep. 1990 Submitted for publication
(Contract W-7405-eng-48)
(DE91-002795; UCRL-JC-105217; CONF-9009269-3) Avail: NTIS HC/MF A01

The Fokker-Planck package FPPAC had been converted to the Connection Machine 2 (CM2). For fine mesh cases the CM2 outperforms the Cray-2 when it comes to time-integrating the difference equations. For long Legendre expansions the CM2 is also faster at computing the Fokker-Planck coefficients. DOE

N91-13916# Institut National Polytechnique, Grenoble (France). Lab. d'Informatique Fondamentale et d'Intelligence Artificielle.
SEMANTIC VALIDATION OF STRUCTURED THEORIES: APPLICATIONS TO A GENERIC PROGRAMMING LANGUAGE Ph.D. Thesis [VALIDATION SEMANTIQUE DANS LES THEORIES STRUCTUREES: APPLICATION A UN LANGAGE DE PROGRAMMATION GENERIQUE]
Pascal Drabik 1989 210 p In FRENCH; ENGLISH summary
(ETN-91-98207) Avail: NTIS HC/MF A10

The structured parameterized abstract data types in the algebraic framework are studied. These generic specifications are often linked by relations such as importation, parametrization, etc. Given a specification S1, which is parameterized by another specification S2, conditions described within S2 must hold within each instantiation of S1. In general, these verifications come to prove the validity of logical formulae within a particular theory. The semantic relations to be verified within the frame of a generic programming language are defined. The main features of the implementations are described. The implementation brings help to a user in order to achieve semantic validations using mainly a theorem prover. The need of reusability of proofs is stressed. The outlines of a proof environment using algebraic formalism are presented. ESA

N91-13917# Centre Technique des Industries Mecaniques, Saint Etienne (France).
ADENG, ADHESIVE BONDING TECHNOLOGY FOR ENGINEERING APPLICATIONS: COMPUTER AIDED DESIGN Final Report
P. Millet and J. P. Jeandreau Jun. 1989 12 p Prepared in cooperation with Oxford Polytechnic, England, and Pera, Melton Mowbray, Leicester, England
(Contract EEC-RI1B-0094-UK(H))
(CETIM-105070; ETN-91-98331) Copyright Avail: NTIS HC/MF A03

The possibility of incorporating an adhesively bonded joint design procedure into Computer Aided Design (CAD) programs is investigated. A more precise program of work to assess the economical and technical usefulness of developing a specific adhesive bonding CAD program was initiated. To determine the dimensioning methods, each configuration was studied using analytical calculation methods. For designing a bonded assembly, the choice of materials for the preparation of joint surfaces and a selection of adhesives were the basic items. The geometries used for the project (flat parts, disc, cylinder, ring) may be easily integrated into a CAD two-dimensional system on a microcomputer. In the case of irregular parts, the CAD three-dimensional system may define the geometry of the final assembly (calculating the joint system, determining the shape of parts, distortion of the joint under load). ESA

N91-13918# Loughborough Univ. of Technology (England). Dept. of Mathematical Sciences.
A GENERALIZED POLAK-RIBIERE ALGORITHM
K. M. Khoda, Y. Liu, and C. Storey Jul. 1990 21 p
(MATHS-Rept-A-128; ETN-91-98350) Avail: NTIS HC/MF A03

A conjugate gradient algorithm is developed in the case of multivariable, reasonably smooth function with real values and its practical and theoretical properties are discussed. With line searches satisfying the Wolfe-Powell conditions, the new algorithm is shown to be globally convergent and to have local quadratic convergence. All programs in the computational experiments were written in PASCAL under the UNIX environment and performed with double arithmetic precision. The results show that the presented algorithm is better than the Polak-Ribiere algorithm as regards the index of computational labor, which depends on the number of function and gradient evaluations and on problem dimension, and the computer processing unit time. ESA

N91-13919# Loughborough Univ. of Technology (England). Dept. of Mathematical Sciences.
ON UNCONSTRAINED CONJUGATE GRADIENT OPTIMIZATION METHODS AND THEIR INTERRELATIONSHIPS
Y. F. Hu and M. Storey Jul. 1990 37 p
(MATHS-Rept-A-129; ETN-91-98351) Avail: NTIS HC/MF A03

Connections between conjugate gradient algorithms and the corresponding two-dimensional Newton methods are investigated. All the conjugate gradient algorithms were implemented and used the same line search routine. The line searches were quite exact with at least one cubic interpolation, forced at each iteration. The algorithms were used on nine test functions, such as the extended Rosenbrock, Beale, Wood and Powell functions, the trigonometric function, the penalty function, the tridiagonal function, the extended Powell singular function and the matrix square root 2 function. The assumption, that the nearer a conjugate gradient algorithm is to its two-dimensional Newton counter part, the greater its efficiency will be, is verified by numerical experimentation. Geometrical interpretations and a generalization of the concepts of conjugacy are used to bring out connections between the studied methods. ESA

N91-13920# Loughborough Univ. of Technology (England). Dept. of Mathematical Sciences.
PROJECTED QUASI-NEWTON UPDATES
Y. F. Hu and C. Storey Sep. 1990 11 p
(MATHS-Rept-A-135; ETN-91-98355) Avail: NTIS HC/MF A03

The quasi-Newton updates used in optimization are derived by the minimization of appropriate matrix norms. Projected versions of the Greenstadt and BDFS updates are derived in an iterative manner. The current approximation to the inverse Hessian of the objective function was used in the calculations. The numerical implementations of algorithms based on various forms of these new formulae are under investigation. ESA

N91-13921# Helsinki Univ. of Technology, Espoo (Finland). Lab. of Information Processing Science.
METHODS FOR COMPUTER-AIDED DESIGN OF FREE-FORM OBJECTS Ph.D. Thesis
Charles Woodward Helsinki, Finland Finnish Academy of Technology May 1990 59 p Sponsored by Helsinki Univ. Foundation
(Ma-56; ISBN-951-666-313-3; ISSN-0355-2713; ETN-91-98277)
Avail: NTIS HC/MF A04

A set of B spline modeling and visualization methods was developed to support interactive free form shape design with the computer. The swinging method is described as a free form generalization of the standard rotational sweep. The projection curve method facilitates surface skimming construction by plane curve interaction. A variety of tools for local surface interaction is presented, including the B2 spline representation as an interface to smooth curve and surface interpolation. A complete algorithm for ray tracing parametric surfaces is described. The adaptive zero eye subdivision method is presented for efficient detection of ray intersection, with parametric surfaces. The overall amount of ray tracing computation is reduced by utilizing coherence properties with a novel method called shadow image buffers. The methods described form the core of a computer aided design system used in different industrial applications. ESA

N91-13922# Norwegian Defence Research Establishment, Kjeller.
CESAR MALU PROGRAM LIBRARY

Vidar S. Andersen and Halvor Bjordal 21 May 1990 57 p
(FFI-90/7010; ETN-91-98278) Avail: NTIS HC/MF A04

The routines of the complete CESAR (Computer for Experimental Synthetic Aperture Radar) MALU (Microprogrammable Arithmetic Logic Unit) program library for the ERS-1 SAR (Synthetic Aperture Radar) fast delivery algorithms are described. All the vector processing algorithms necessary to generate the fast delivery product of the SAR image from the ERS-1 satellite, using the CESAR processor are described. ESA

N91-13923# Norwegian Defence Research Establishment, Kjeller.

BAG: A PROGRAMMING LANGUAGE FOR THE CESAR BUFFER ADDRESS GENERATOR

Per Atle Valand 9 Aug. 1990 61 p
(FFI-90/7022; ISSN-0802-2437; ETN-91-98282) Avail: NTIS HC/MF A04

The high level language BAG (Buffer Address Generator) is described, together with the compiler. A users manual for programmers who wish to make CESAR (Computer for Experimental Synthetic Aperture Radar) address programs is presented. ESA

N91-13924# Norwegian Defence Research Establishment, Kjeller.

CESAR TRAP PROGRAM LIBRARY

Per Atle Valand 10 Aug. 1990 70 p
(FFI-90/7023; ISSN-0802-2437; ETN-91-98283) Avail: NTIS HC/MF A04

The CESAR (Computer for Experimental Synthetic Aperture Radar) trap runtime environment for the ERS-1 SAR (Synthetic Aperture Radar) fast delivery algorithms is described. All the trap programs and the runtime routines for the fast delivery product of the ERS-1 satellite using the CESAR processor are described. ESA

N91-13925 Physics and Electronics Lab. TNO, The Hague (Netherlands).

MULTISPECTRAL TARGET DETECTION USING IMAGE PROCESSING PROGRAMS DEVELOPED ON PC'S Final Report

A. Huygen and J. S. deVries Nov. 1989 168 p
(Contract R87/KL/097)
(FEL-89-B304; TD-89-3870; ETN-91-98287) Copyright Avail: Physics and Electronics Laboratory TNO, P.O. Box 96864, 2509 JG The Hague, Netherlands

A description and the source code is given of a set of computer programs for Personal Computers (PCs), which have been developed for the analysis of digital imagery obtained using sensors with different spectral bands. The programs specifically address the geometrical transformations necessary to overlay images from different sensors, and the restoration of striped images and multispectral analysis using two dimensional and three dimensional histograms. The programs are applied to imagery obtained using a FLIR (Forward Looking Infrared Detector) and two CCD cameras. ESA

N91-13926 National Physical Lab., Teddington (England). Div. of Electrical Science.

SOFTWARE MANAGEMENT GUIDELINES FOR AUTOMATED MEASURING SYSTEMS

E. J. Griffin, D. J. Bannister, D. W. Bradstreet, R. N. Clarke, M. G. Cox, L. Graver, T. E. Hodgetts, J. P. Ide, J. Luff, and G. R. Orford et al Jul. 1990 13 p
(NPL-DES-99; ISSN-0143-7305; ETN-91-98370) Copyright Avail: National Physical Laboratory, Teddington, TW11 0LW, England

Guidance is given for writing and controlling the use of computer programs and processing data for automated measuring systems. ESA

N91-13927 Politecnico di Milano (Italy). Dipt. di Elettronica.

AN OBJECT-ORIENTED LOGIC LANGUAGE FOR MODULAR SYSTEM SPECIFICATION

Angelo Morzenti and Pierluigi SanPietro Jun. 1990 30 p
Sponsored in part by CNR, and Ente Nazionale per l'Energia Elettrica
(Rept-90-027; ETN-91-98387) Avail: Politecnico di Milano, Piazzo Leonardo da Vinci 32, 20133 Milan, Italy

A first order logical language with temporal observers is described, which give the ability to determine the truth or falsity of propositions at time instants different from the current one. To describe a system, suitable classes were defined, which are sets of axioms, built up in the modular independent way, following information hiding principles and object oriented techniques. The language is suited to the specification of embedded and real time systems and provides an effective support to some validation activities, such as specification testing, simulation and property proof. Concepts like inheritance and genericity, and as expressive and intiative graphic notation are the particularities of this language. ESA

62 COMPUTER SYSTEMS

Includes computer networks and special application computer systems.

N91-13928*# Cornell Univ., Ithaca, NY. Dept. of Computer Science.

THE ISIS PROJECT: FAULT-TOLERANCE IN LARGE DISTRIBUTED SYSTEMS Semiannuel Status Report, 1 Jan. - 1 Jul. 1990

Kenneth P. Birman and Keith Marzullo 1 Jul. 1990 34 p
(Grant NAG2-593)
(NASA-CR-186625; NAS 1.26:186625) Avail: NTIS HC/MF A03 CSCL 09B

The semi-annual status report covers activities of the ISIS project during the second half of 1989. The project had several independent objectives: (1) At the level of the ISIS Toolkit, ISIS release V2.0 was completed, containing bypass communication protocols. Performance of the system is greatly enhanced by this change, but the initial software release is limited in some respects. (2) The Meta project focused on the definition of the Lomita programming language for specifying rules that monitor sensors for conditions of interest and triggering appropriate reactions. This design was completed, and implementation of Lomita is underway on the Meta 2.0 platform. (3) The Deceit file system effort completed a prototype. It is planned to make Deceit available for use in two hospital information systems. (4) A long-haul communication subsystem project was completed and can be used as part of ISIS. This effort resulted in tools for linking ISIS systems on different LANs together over long-haul communications lines. (5) Magic Lantern, a graphical tool for building application monitoring and control interfaces, is included as part of the general ISIS releases. Y.S.

N91-13929*# California Univ., San Diego, La Jolla. California Space Inst.

PARALLEL Ada BENCHMARKS FOR THE SVMS Final Report, Apr. 1989 - Apr. 1990

Philippe E. Collard 30 Mar. 1990 13 p
(Contract NCC2-603)
(NASA-CR-182453; NAS 1.26:182453; UCSD-90-1041) Avail: NTIS HC/MF A03 CSCL 09B

The use of parallel processing paradigm to design and develop faster and more reliable computers appear to clearly mark the future of information processing. NASA started the development of such an architecture: the Spaceborne VHSIC Multi-processor System (SVMS). Ada will be one of the languages used to program the SVMS. One of the unique characteristics of Ada is that it supports parallel processing at the language level through the tasking constructs. It is important for the SVMS project team to assess how efficiently the SVMS architecture will be implemented, as well as how efficiently Ada environment will be ported to the SVMS. AUTOCLASS II, a Bayesian classifier written in Common Lisp, was selected as one of the benchmarks for SVMS

configurations. The purpose of the R and D effort was to provide the SVMS project team with the version of AUTOCLASS II, written in Ada, that would make use of Ada tasking constructs as much as possible so as to constitute a suitable benchmark. Additionally, a set of programs was developed that would measure Ada tasking efficiency on parallel architectures as well as determine the critical parameters influencing tasking efficiency. All this was designed to provide the SVMS project team with a set of suitable tools in the development of the SVMS architecture. Y.S.

N91-13930*# Carnegie-Mellon Univ., Pittsburgh, PA. Dept. of Electrical and Computer Engineering.

VALIDATION ENVIRONMENT FOR AIPS/ALS: IMPLEMENTATION AND RESULTS Final Report, Nov. 1988 - Nov. 1990

Zary Segall, Daniel Siewiorek, Eddie Caplan, Alan Chung, Edward Czeck, and Dalibor Vrsalovic Washington NASA Nov. 1990 77 p

(Grant NAG1-190)

(NASA-CR-4340; NAS 1.26:4340) Avail: NTIS HC/MF A05 CSCL 09B

The work is presented which was performed in porting the Fault Injection-based Automated Testing (FIAT) and Programming and Instrumentation Environments (PIE) validation tools, to the Advanced Information Processing System (AIPS) in the context of the Ada Language System (ALS) application, as well as an initial fault free validation of the available AIPS system. The PIE components implemented on AIPS provide the monitoring mechanisms required for validation. These mechanisms represent a substantial portion of the FIAT system. Moreover, these are required for the implementation of the FIAT environment on AIPS. Using these components, an initial fault free validation of the AIPS system was performed. The implementation is described of the FIAT/PIE system, configured for fault free validation of the AIPS fault tolerant computer system. The PIE components were modified to support the Ada language. A special purpose AIPS/Ada runtime monitoring and data collection was implemented. A number of initial Ada programs running on the PIE/AIPS system were implemented. The instrumentation of the Ada programs was accomplished automatically inside the PIE programming environment. PIE's on-line graphical views show vividly and accurately the performance characteristics of Ada programs, AIPS kernel and the application's interaction with the AIPS kernel. The data collection mechanisms were written in a high level language, Ada, and provide a high degree of flexibility for implementation under various system conditions. Author

N91-13931# Oak Ridge National Lab., TN. Engineering and Mathematics Div.

SYNTHETIC MODELS OF DISTRIBUTED MEMORY PARALLEL PROGRAMS

David A. Poplawski (Michigan Technological Univ., Houghton.) Sep. 1990 38 p

(Contract DE-AC05-84OR-21400)

(DE91-001058; ORNL/TM-11634) Avail: NTIS HC/MF A03

This paper deals with the construction and use of simple synthetic programs that model the behavior of more complex, real parallel programs. Synthetic programs can be used in many ways: to construct an easily ported suite of benchmark programs; to experiment with alternate parallel implementations of a program without actually writing them; and to predict the behavior and performance of an algorithm on a new or hypothetical machine. Synthetic programs are constructed easily from scratch, from existing programs, and can even be constructed using nothing but information obtained from traces of the real program's execution. DOE

N91-13932# Edgerton, Germeshausen and Grier, Inc., Idaho Falls, ID.

TIGHTLY COUPLED SIMULATION UTILIZING THE EBR-II LMR: A REAL-TIME SUPERCOMPUTING AND AI ENVIRONMENT

Henry Makowitz, David G. Barber, Gail A. Cordes, Alan K. Powers, Robert Scott, Jr., Leonard W. Ward, John I. Sackett, Ronald W. King, Wayne K. Lehto, and Richard W. Lindsay (Argonne National Lab., IL.) et al 1990 6 p Presented at the Supercomputing in Nuclear Applications, Mito City, Japan, 12-16 Mar. 1990

(Contract DE-AC07-76ID-01570)

(DE91-001942; EGG-M-89448; CONF-900343-7) Avail: NTIS HC/MF A02

An integrated Supercomputing and AI environment utilizing a CRAY X-MP/216, a fiber-optic communications link, a distributed network of workstations and the Experimental Breeder Reactor II (EBR-II) liquid metal reactor (LMR) and its associated instrumentation and control system is being developed at the Idaho National Engineering Laboratory (INEL). This paper summarizes various activities that make up this supercomputing and AI environment. DOE

N91-13933# Argonne National Lab., IL. Computing and Telecommunications Div.

THE ADVANCED SOFTWARE DEVELOPMENT AND COMMERCIALIZATION PROJECT Progress Report

E. Gallopoulos, ed., T. R. Canfield, M. Minkoff, C. Mueller, E. Plaskacz, D. P. Weber, D. M. Anderson, I. U. Therios, S. Aslam, and R. Bramley (Illinois Univ., Urbana-Champaign.) et al Sep. 1990 44 p

(Contract W-31-109-eng-38; NSF CCR-90-00000)

(DE91-002956; ANL/TM-484) Avail: NTIS HC/MF A03

This is the first of a series of reports pertaining to progress in the Advanced Software Development and Commercialization Project, a joint collaborative effort between the Center for Supercomputing Research and Development of the University of Illinois and the Computing and Telecommunications Division of Argonne National Laboratory. The purpose of this work is to apply techniques of parallel computing that were pioneered by University of Illinois researchers to mature computational fluid dynamics (CFD) and structural dynamics (SD) computer codes developed at Argonne. The collaboration in this project will bring this unique combination of expertise to bear, for the first time, on industrially important problems. By so doing, it will expose the strengths and weaknesses of existing techniques for parallelizing programs and will identify those problems that need to be solved in order to enable wide spread production use of parallel computers. Secondly, the increased efficiency of the CFD and SD codes themselves will enable the simulation of larger, more accurate engineering models that involve fluid and structural dynamics. In order to realize the above two goals, we are considering two production codes that have been developed at ANL and are widely used by both industry and Universities. These are COMMIX and WHAMS-3D. The first is a computational fluid dynamics code that is used for both nuclear reactor design and safety and as a design tool for the casting industry. The second is a three-dimensional structural dynamics code used in nuclear reactor safety as well as crashworthiness studies. These codes are currently available for both sequential and vector computers only. Our main goal is to port and optimize these two codes on shared memory multiprocessors. In so doing, we shall establish a process that can be followed in optimizing other sequential or vector engineering codes for parallel processors. DOE

N91-13934*# Draper (Charles Stark) Lab., Inc., Cambridge, MA.

KNOWLEDGE REPRESENTATION INTO Ada PARALLEL PROCESSING Final Report

Tom Masotto, Carol Babikyan, and Richard Harper Jul. 1990 139 p Sponsored by Wright Research Development Center, Wright-Patterson AFB, OH

(Contract NAS1-18565)

(NASA-CR-187451; NAS 1.26:187451) Avail: NTIS HC/MF A07 CSCL 09B

The Knowledge Representation into Ada Parallel Processing project is a joint NASA and Air Force funded project to demonstrate the execution of intelligent systems in Ada on the Charles Stark Draper Laboratory fault-tolerant parallel processor (FTPP). Two applications were demonstrated - a portion of the adaptive tactical navigator and a real time controller. Both systems are implemented as Activation Framework Objects on the Activation Framework

intelligent scheduling mechanism developed by Worcester Polytechnic Institute. The implementations, results of performance analyses showing speedup due to parallelism and initial efficiency improvements are detailed and further areas for performance improvements are suggested. Author

63 CYBERNETICS

Includes feedback and control theory, artificial intelligence, robotics and expert systems.

For related information see also *54 Man/System Technology and Life Support.*

N91-13935*# Institute for Computer Applications in Science and Engineering, Hampton, VA.
DISSIPATIVE CONTROLLER DESIGNS FOR SECOND-ORDER DYNAMIC SYSTEMS Final Report
K. A. Morris and J. N. Juang (National Aeronautics and Space Administration. Langley Research Center, Hampton, VA.) Sep. 1990 17 p
(Contract NAS1-18605)
(NASA-CR-187452; NAS 1.26:187452; ICASE-90-65) Avail: NTIS HC/MF A03 CSCL 09B

The passivity theorem may be used to design robust controllers for structures with positive transfer functions. This result is extended to more general configurations using dissipative system theory. A stability theorem for robust, model-independent controllers of structures which lack collocated rate sensors and actuators is given. The theory is illustrated for non-square systems and systems with displacement sensors. Author

N91-13936 Arizona Univ., Tucson.
SPECIFICATIONS EXTRACTION AND SYNTHESIS: THEIR CORRELATIONS WITH PRELIMINARY DESIGN Ph.D. Thesis
Jagdish R. Umaretiya 1990 266 p
Avail: Univ. Microfilms Order No. DA9024654

Research applied towards the automation of the engineering design process is addressed, in particular the structural design process. Artificial Intelligence (AI) addresses the automation of complex and knowledge-intensive tasks such as the structural design process. It involves the development of the Knowledge Based Expert System (KBES). There are several tools, also known as expert shells, and languages available for the development of knowledge-based expert systems. A general purpose language, called LISP, is very popular among researchers in AI and is used as an environmental tool for the development of the KBES for the structural design process. The resulting system, called Expert-SEISD, is very generic in nature. The Expert-SEISD is composed of the user interface, inference engine, domain specific knowledge and data bases and the knowledge acquisition. The present domain of the Expert-SEISD encompasses the design of structural components such as beams and plates. The knowledge acquisition module is developed to facilitate the incorporation of new capabilities (knowledge or data) for beams, plates, and for new structural components. A decision-making model suitable for the specifications extraction and the preliminary design phases of the structural design process is proposed and developed based on the theory of fuzzy sets. The methods developed here are evaluated and compared with similar methods available in the literature. The new method, based on the union of fuzzy sets and contrast intensification, was found suitable for the proposed model. It was implemented as a separate module in the Expert-SEISD. A session with the Expert-SEISD is presented to demonstrate its capabilities of beam and plate designs and knowledge acquisition. Dissert. Abstr.

N91-13937 California Univ., Berkeley.
ROBUST DETERMINISTIC CONTROL FOR ROBOTIC MANIPULATORS Ph.D. Thesis
Chul Goo Kang 1989 132 p
Avail: Univ. Microfilms Order No. DA9028897

The development of a robust control scheme for singularly perturbed uncertain systems, and the application of the robust control to direct drive robotic manipulators are examined. In the case of direct drive robots, the nonlinear coupling among the links is significant, and the unmodeled dynamics such as parasitic actuator and sensor dynamics may not be negligible. To control this highly nonlinear system with unmodeled dynamics, a robust control is considered which eliminates the necessity for a precise identification process. The modeling process for a two degree of freedom (DOF) direct drive SCARA manipulator is discussed. For a class of singularly perturbed uncertain systems, an output feed-back control law (robust deterministic control) is proposed based mainly on information available about an uncertain reduced-order system. It is shown that the reduced-order system with the proposed controller possesses a stability property called global uniform attractivity. Furthermore, the global uniform attractivity of this control scheme is robust with respect to singular perturbations. The robust deterministic control scheme developed is applied to the tracking control of direct drive robotic manipulators. Inertia variations due to kinematic changes, unknown and time-varying payloads, Coriolis and centrifugal accelerations, and friction torques are considered as uncertainties. Parasitic actuator and sensor dynamics of the manipulator system are considered in the controller design and analysis by means of a singular perturbation technique. Simulation and experimental studies were conducted to evaluate the performance of the proposed deterministic control scheme. Dissert. Abstr.

N91-13938# Naval Postgraduate School, Monterey, CA.
APPLICATIONS OF NEURAL NETWORKS TO ADAPTIVE CONTROL M.S. Thesis
Russell W. Scott, II Dec. 1989 117 p
(AD-A225408) Avail: NTIS HC/MF A06 CSCL 23/3

The amount of a priori knowledge required to design some modern control systems is becoming prohibitive. Two current methods addressing this problem are robust control, in which the control design is insensitive to errors in system knowledge, and adaptive control, in which the control law is adjusted in response to a continually updated model of the system. This thesis examines the application of parallel distributed processing (neural networks) to the problem of adaptive control. The structure of neural networks is introduced, focusing on the Backpropagation paradigm. A general form of controller consistent with use in neural networks is developed and combined with a discussion of linear least squares parameter estimation techniques to suggest a structure for neural network adaptive controllers. This neural network adaptive control structure is then applied to a number of estimation and control problems using as a model the longitudinal motion of the A-4 aircraft. The purpose of this thesis is to develop and demonstrate a neural network adaptive control structure consistent with adaptive control theory. GRA

N91-13939*# Alabama Univ., Huntsville.
APPLICATIONS OF ARTIFICIAL INTELLIGENCE TO MISSION PLANNING Interim Report
Donnie R. Ford, John S. Rogers, and Stephen A. Floyd 7 Dec. 1990 55 p
(Grant NAG8-717)
(NASA-CR-184994; NAS 1.26:184994) Avail: NTIS HC/MF A04 CSCL 09B

The scheduling problem facing NASA-Marshall mission planning is extremely difficult for several reasons. The most critical factor is the computational complexity involved in developing a schedule. The size of the search space is large along some dimensions and infinite along others. It is because of this and other difficulties that many of the conventional operation research techniques are not feasible or inadequate to solve the problems by themselves. Therefore, the purpose is to examine various artificial intelligence (AI) techniques to assist conventional techniques or to replace them. The specific tasks performed were as follows: (1) to identify mission planning applications for object oriented and rule based programming; (2) to investigate interfacing AI dedicated hardware (Lisp machines) to VAX hardware; (3) to demonstrate how Lisp may be called from within FORTRAN programs; (4) to investigate

and report on programming techniques used in some commercial AI shells, such as Knowledge Engineering Environment (KEE); and (5) to study and report on algorithmic methods to reduce complexity as related to AI techniques. Author

N91-13940# Naval Postgraduate School, Monterey, CA. Dept. of Computer Science.
FLEXIBLE COOPERATION IN NON-STANDARD APPLICATION ENVIRONMENTS Progress Report, Apr. - Dec. 1989
Bernhard Holtkamp (Dortmund Univ., Germany, F.R.) Jan. 1990 27 p
(AD-A226486; NPS52-90-018) Avail: NTIS HC/MF A03 CSCL 12/7

The integration of preexisting systems into a single, heterogeneous, distributed non-standard application system in domains like office automation or computer-integrated manufacturing are regarded as cooperating systems. They are characterized through teamwork, distribution and the handling of complex data structures (e.g., multimedia data). Object-oriented database systems, providing for complex object management, represent one approach in support of such applications. They concentrate, however, on data modeling aspects and use more or less conventional transaction concepts, based on a global execution control. Hence, they only partially fulfill application requirements as they do not adequately cope with the autonomy that is often inherent to the system's components. As a consequence, we suggest S-transactions as an appropriate means for describing the cooperation of system components in terms of transactions and beyond. In this paper we outline the modeling of conventional transactions (flat or nested as well as distributed and design transactions) in terms of STDL, the S-transaction definition language. Beyond that we point out how to specify SAGAs and similar concepts. Finally we discuss the specification of non-linear but maybe acyclic or even cyclic cooperation structures. GRA

N91-13941*# National Aeronautics and Space Administration. Langley Research Center, Hampton, VA.
A DISCREPANCY WITHIN PRIMATE SPATIAL VISION AND ITS BEARING ON THE DEFINITION OF EDGE DETECTION PROCESSES IN MACHINE VISION
Daniel J. Jobson Sep. 1990 31 p
(NASA-TM-102739; NAS 1.15:102739) Avail: NTIS HC/MF A03 CSCL 09B

The visual perception of form information is considered to be based on the functioning of simple and complex neurons in the primate striate cortex. However, a review of the physiological data on these brain cells cannot be harmonized with either the perceptual spatial frequency performance of primates or the performance which is necessary for form perception in humans. This discrepancy together with recent interest in cortical-like and perceptual-like processing in image coding and machine vision prompted a series of image processing experiments intended to provide some definition of the selection of image operators. The experiments were aimed at determining operators which could be used to detect edges in a computational manner consistent with the visual perception of structure in images. Fundamental issues were the selection of size (peak spatial frequency) and circular versus oriented operators (or some combination). In a previous study, circular difference-of-Gaussian (DOG) operators, with peak spatial frequency responses at about 11 and 33 cyc/deg were found to capture the primary structural information in images. Here larger scale circular DOG operators were explored and led to severe loss of image structure and introduced spatial dislocations (due to blur) in structure which is not consistent with visual perception. Orientation sensitive operators (akin to one class of simple cortical neurons) introduced ambiguities of edge extent regardless of the scale of the operator. For machine vision schemes which are functionally similar to natural vision form perception, two circularly symmetric very high spatial frequency channels appear to be necessary and sufficient for a wide range of natural images. Such a machine vision scheme is most similar to the physiological performance of the primate lateral geniculate nucleus rather than the striate cortex. Author

N91-13942# Argonne National Lab., IL. Mathematics and Computer Science Div.
A TUTORIAL ON THE CONSTRUCTION OF HIGH-PERFORMANCE RESOLUTION/PARAMODULATION SYSTEMS
Ralph Butler (University of North Florida, Jacksonville.) and Ross Overbeek Sep. 1990 70 p
(Contract W-31-109-eng-38)
(DE91-001096; ANL-90/30) Avail: NTIS HC/MF A04

Over the past 25 years, researchers have written numerous deduction systems based on resolution and paramodulation. Of these systems, very few have been capable of generating and maintaining a formula database containing more than just a few thousand clauses. These few systems were used to explore mechanisms for rapidly extracting limited subsets of relevant clauses. We have written this tutorial to reflect some of the best ideas that have emerged and to cast them in a form that makes them easily accessible to students wishing to write their own high-performance systems. DOE

N91-13943# Lawrence Livermore National Lab., CA.
PROCEEDINGS OF THE WORKSHOP ON SOFTWARE TOOLS FOR DISTRIBUTED INTELLIGENT CONTROL SYSTEMS
Charles J. Herget, ed. Sep. 1990 290 p Workshop held in Pacifica, CA, 17-19 Jul. 1990
(Contract W-7405-eng-48)
(DE91-001755; CONF-9007134) Avail: NTIS HC/MF A13

The Workshop on Software Tools for Distributed Intelligent Control Systems was organized by Lawrence Livermore National Laboratory for the United States Army Headquarters Training and Doctrine Command and the Defense Advanced Research Projects Agency. The goals of the workshop were to identify the current state of the art in tools which support control systems engineering design and implementation, identify research issues associated with writing software tools which would provide a design environment to assist engineers in multidisciplinary control design and implementation, formulate a potential investment strategy to resolve the research issues and develop public domain code which can form the core of more powerful engineering design tools, and recommend test cases to focus the software development process and test associated performance metrics. Recognizing that the development of software tools for distributed intelligent control systems will require a multidisciplinary effort, experts in systems engineering, control systems engineering, and compute science were invited to participate in the workshop. In particular, experts who could address the following topics were selected: operating systems, engineering data representation and manipulation, emerging standards for manufacturing data, mathematical foundations, coupling of symbolic and numerical computation, user interface, system identification, system representation at different levels of abstraction, system specification, system design, verification and validation, automatic code generation, and integration of modular, reusable code. DOE

N91-13944*# National Aeronautics and Space Administration. Lyndon B. Johnson Space Center, Houston, TX.
SYSTEM AND METHOD FOR A GENERAL PURPOSE ARCHITECTURE FOR INTELLIGENT COMPUTER-AIDED TRAINING Patent Application
R. Bowen Loftin, inventor (to NASA), Lui Wang, inventor (to NASA), Paul Baffes, inventor (to NASA), and Grace C. Hua, inventor (to NASA) (Computer Sciences Corp., Houston, TX.) 28 Jun. 1990 99 p
(NASA-Case-MSC-21381-1; NAS 1.71:MSC-21381-1; US-Patent-Appl-SN-545235) Avail: NTIS HC/MF A05 CSCL 09B

An intelligent computer-aided training system having a general modular architecture is provided for use in a wide variety of training tasks and environments. It is comprised of a user interface which permits the trainee to access the same information available in

the task environment and serves as a means for the trainee to assert actions to the system; a domain expert which is sufficiently intelligent to use the same information available to the trainee and carry out the task assigned to the trainee; a training session manager for examining the assertions made by the domain expert and by the trainee for evaluating such trainee assertions and providing guidance to the trainee which are appropriate to his acquired skill level; a trainee model which contains a history of the trainee interactions with the system together with summary evaluative data; an intelligent training scenario generator for designing increasingly complex training exercises based on the current skill level contained in the trainee model and on any weaknesses or deficiencies that the trainee has exhibited in previous interactions; and a blackboard that provides a common fact base for communication between the other components of the system. Preferably, the domain expert contains a list of mal-rules which typifies errors that are usually made by novice trainees. Also preferably, the training session manager comprises an intelligent error detection means and an intelligent error handling means. The present invention utilizes a rule-based language having a control structure whereby a specific message passing protocol is utilized with respect to tasks which are procedural or step-by-step in structure. The rules can be activated by the trainee in any order to reach the solution by any valid or correct path. NASA

N91-13945# Lawrence Livermore National Lab., CA. Center for Accelerator Mass Spectroscopy.
SUCCESS WITH AN AUTOMATED COMPUTER CONTROL SYSTEM
M. L. Roberts and T. L. Moore Sep. 1990 11 p Presented at the 11th International Conference on the Application of Accelerators in Research and Industry, Denton, TX, 5-8 Nov. 1990
(Contract W-7405-eng-48)
(DE91-001759; UCRL-JC-104448; CONF-901116-23) Avail: NTIS HC/MF A03

LLNL has successfully implemented a distributed computer control system for automated operation of an FN tandem accelerator. The control system software utilized is the Thaumaturgic Automated Control Logic (TACL) written by the Continuous Electron Beam Accelerator Facility and co-developed with LLNL. Using TACL, accelerator components are controlled through CAMAC using a two-tiered structure. Analog control and measurement are at 12 or 16 bit precision as appropriate. Automated operation has been implemented for several nuclear analytical techniques including hydrogen depth profiling and accelerator mass spectrometry. An additional advantage of TACL lies in its expansion capabilities. Without disturbing existing control definitions and algorithms, additional control algorithms and display functions can be implemented quickly. DOE

N91-13946# Oak Ridge National Lab., TN.
AN APPLICATION OF OSCILLATION DAMPED MOTION FOR SUSPENDED PAYLOADS TO THE ADVANCED INTEGRATED MAINTENANCE SYSTEM
M. W. Noakes, B. J. Petterson, and J. C. Werner (Sandia National Labs., Albuquerque, NM.) 1990 7 p Presented at the American Nuclear Society Annual Meeting, Nashville, TN, 10-14 Jun. 1990
(Contracts DE-AC05-84OR-21400; DE-AC04-76DP-00789)
(DE91-002658; CONF-900608-51) Avail: NTIS HC/MF A02

Transportation of objects using overhead cranes can induce pendulum motion of the object, which usually must be damped or allowed to decay before the next process can take place. Recent work at Sandia National Laboratories (SNL) has shown that oscillation damped transport and swing-free stops are possible by properly programming the acceleration of the transporting crane. This paper reviews the theory associated with oscillation-damped trajectories for simply suspended objects and describes a specific, full-scale implementation of the damped oscillation methods for the Oak Ridge National Laboratory (ORNL) Advanced Integrated Maintenance System (AIMS). Hardware and software requirements and constraints for proper operation are discussed. Finally, test results and lessons learned are presented. DOE

N91-13947# Loughborough Univ. of Technology (England). Dept. of Mathematical Sciences.
ROBUST VARIABLE STRUCTURE CONTROL OF MODEL REFERENCE SYSTEMS
S. K. Spurgeon and R. J. Patton (York Univ., England) Aug. 1990 29 p
(MATHS-Rept-A-131; ETN-91-98352) Avail: NTIS HC/MF A03

A VSCS (Variable Structure Control System) design approach is used to create a system which exhibits parameter insensitivity with good disturbance rejection whilst allowing all command inputs, including those which act within the nominal input channels. Given a model with ideal response characteristics, the discontinuity surfaces are chosen to render the sliding dynamic mode minimally sensitive to those parameter variations which do not act within the nominal input channels. The possibility of forcing the error between the plant and model to zero and to ensure that the error system attains a sliding mode is demonstrated. It is proved that eigenstructure assignment can be used to modally shape a desired system response and so determine an ideal model while the pilot demand can be incorporated as a model input. ESA

N91-13948# Loughborough Univ. of Technology (England). Dept. of Mathematical Sciences.
ON HYPERPLANE DESIGN TECHNIQUES FOR DISCRETE-TIME VARIABLE STRUCTURE CONTROL SYSTEMS
S. K. Spurgeon Sep. 1990 18 p
(MATHS-Rept-A-133; ETN-91-98353) Avail: NTIS HC/MF A03

An uncertain discrete time system joining the state and control vectors with system uncertainty is considered, which exhibits a sliding mode and becomes insensitive to all parameter variations and external disturbances. The traditional hyperplane selection criteria to ensure asymptotic stability of the sliding motion for the nominal system pair is studied. It is shown that the usual parallel approach of the discrete time and continuous time cases is not always appropriate: a simple linear control structure coupled with a good hyperplane choice can provide a better performance than with a complicated nonlinear control configuration and an associated inappropriate sliding subspace. ESA

64 NUMERICAL ANALYSIS

Includes iteration, difference equations, and numerical approximation.

N91-13949*# Illinois Univ., Chicago.
EVALUATION OF EXPRESSIONS INVOLVING HIGHER ORDER DERIVATIONS
Robert Grossman May 1990 19 p
(Grant NAG2-513)
(NASA-CR-187319; NAS 1.26:187319) Avail: NTIS HC/MF A03 CSCL 12A

The local geometric properties of a nonlinear control system defined by vector fields E(sub 1),..., E(sub M) are determined by the algebraic properties of the iterated Lie brackets of the E(sub j)'s. The problem of rewriting expressions is examined involving the E(sub j)'s in terms of the D(sub mu)'s in such a way as to handle effectively any cancellation occurring due to commuting of the D(sub mu)'s. A data structure is introduced which allows us to organize the computation to take advantage of the symmetries in the expression and reduce the operation count. Author

N91-13950*# International Business Machines Corp., Yorktown Heights, NY.
THE SIMULTANEOUS INTEGRATION OF MANY TRAJECTORIES USING NILPOTENT NORMAL FORMS
Matthew A. Grayson and Robert Grossman (Chicago Univ., IL.) May 1990 12 p
(Grants NAG2-513; NSF DMS-89-04740)
(NASA-CR-187318; NAS 1.26:187318) Avail: NTIS HC/MF A03 CSCL 12A

Taylor's formula shows how to approximate a certain class of

functions by polynomials. The approximations are arbitrarily good in some neighborhood whenever the function is analytic and they are easy to compute. The main goal is to give an efficient algorithm to approximate a neighborhood of the configuration space of a dynamical system by a nilpotent, explicitly integrable dynamical system. The major areas covered include: an approximating map; the generalized Baker-Campbell-Hausdorff formula; the Picard-Taylor method; the main theorem; simultaneous integration of trajectories; and examples. Y.S.

N91-13951# Pittsburgh Univ., PA. Learning Research and Development Center.

THE MECHANISM OF RESTRUCTURING IN GEOMETRY

Stellan Ohlsson May 1990 24 p Submitted for publication
(Contract N00014-89-J-1681; NR Proj. RR0-4206)
(AD-A224740; UPITT/LRDC/ONR/KUL-90-04) Avail: NTIS HC/MF A03 CSCL 05/2

Restructuring consists of a change in the representation of the current search state, a process which breaks an impasse during problem solving by opening up new search paths. A corpus of 52 think-aloud protocols from the domain of geometry was scanned for evidence of restructuring. The data suggest that restructing is accomplished by re-parsing the geometric diagram. Knowledge and understanding in human learning (KUL) is an umbrella term for a loosely connected set of activities. The aim of KUL is to clarify the role of world knowledge in human thinking, reasoning, and problem solving. World knowledge consists of concepts and principles, and contrasts with facts (episodic knowledge) and with cognitive skills (procedural knowledge). The long term goal is consider six topics: the identification of concepts and principles of particular domains; the acquisition of the concepts and principles; the assessment of the acquisition of the concepts and principles; the process of encoding these concepts and principles in the brain; the utilization of the concepts and principles in performance and learning; and the acquisition and utilization of the concepts and principles by instruction (as opposed to episodic or procedural knowledge). GRA

N91-13952*# Institute for Computer Applications in Science and Engineering, Hampton, VA.

A FULLY SINC-GALERKIN METHOD FOR EULER-BERNOULLI BEAM MODELS Final Report

R. C. Smith, K. L. Bowers, and J. Lund (Montana State Univ., Bozeman.) Oct. 1990 45 p Submitted for publication
(Contract NAS1-18605)
(NASA-CR-187462; NAS 1.26:187462; ICASE-90-79) Avail: NTIS HC/MF A03 CSCL 12A

A fully Sinc-Galerkin method in both space and time is presented for fourth-order time-dependent partial differential equations with fixed and cantilever boundary conditions. The Sinc discretizations for the second-order temporal problem and the fourth-order spatial problems are presented. Alternate formulations for variable parameter fourth-order problems are given which prove to be especially useful when applying the forward techniques to parameter recovery problems. The discrete system which corresponds to the time-dependent partial differential equations of interest are then formulated. Computational issues are discussed and a robust and efficient algorithm for solving the resulting matrix system is outlined. Numerical results which highlight the method are given for problems with both analytic and singular solutions as well as fixed and cantilever boundary conditions. Author

N91-13953# Purdue Univ., West Lafayette, IN. Dept. of Statistics.

ON COMBINING SELECTION AND ESTIMATION IN THE SEARCH FOR THE LARGEST BINOMIAL PARAMETER

Shanti S. Gupta and Klaus J. Miescke (Illinois Univ., Urbana.) Jul. 1990 21 p
(Contract N00014-88-K-0170; NSF DMS-89-23071; NSF DMS-87-17799)
(AD-A226595; TR-90-33C) Avail: NTIS HC/MF A03 CSCL 12/3

For k greater or equal to 2 independent binomial populations, from which X sub i approximately equals to B(n sub i, theta sub i), i = 1,...,k, have been observed, the problem of selecting the population with the largest theta-value and simultaneously estimating the theta-parameter of the selected population is considered. Under several loss functions, Bayes decision rules are derived and studied for independent Beta-priors. A fixed sample size look ahead procedure is also considered. A numerical example is given to illustrate the performance of the procedures. GRA

N91-13954# Utrecht State Univ. (Netherlands). Dept. of Computer Science.

NEW TECHNIQUES FOR THE UNION-FIND PROBLEM

J. A. LaPoutre Aug. 1989 42 p Sponsored in part by EEC
(RUU-CS-89-12; ETN-90-98122) Avail: NTIS HC/MF A03

A new approach to a result which states that a program of up to n UNION and m FIND instructions can be executed in O(n + m.alpha(m,n)) time on a collection of n elements, where alpha(m,n) denotes the functional inverse of Akermann's function, is developed. It is proved that the time for the kth FIND can be limited to O(alpha(k,n)) worst case, while the total cost for the program of UNION's and m FIND's remains bounded by O(n + m.alph(m,n)). The technique is part of a family of algorithms that can achieve various tradeoffs in cost for the individual instructions. The new algorithms guarantee that FIND's are essentially O(1) worst case, within the optimal bound for the UNION-FIND problem as a whole. The algorithms run on a pointer machine and do not use any form of path compression. ESA

N91-13955# Oak Ridge National Lab., TN. Engineering Technology Div.

INTERPRETATION OF ENGINE CYCLE-TO-CYCLE VARIATION BY CHAOTIC TIME SERIES ANALYSIS

C. S. Daw and W. K. Kahl 1990 13 p Presented at the 1990 SAE International Fuels and Lubricants Conference and Exposition, Tulsa, OK, 22-25 Oct. 1990
(Contract DE-AC05-84OR-21400)
(DE91-000729; CONF-9010205-1) Avail: NTIS HC/MF A03

In this paper we summarize preliminary results from applying a new mathematical technique, chaotic time series analysis (CTSA), to cylinder pressure data from a spark-ignition (SI) four-stroke engine fueled with both methanol and iso-octane. Our objective is to look for the presence of deterministic chaos dynamics in peak pressure variations and to investigate the potential usefulness of CTSA as a diagnostic tool. Our results suggest that sequential peak cylinder pressures exhibit some characteristic features of deterministic chaos and that CTSA can extract previously unrecognized information from such data. DOE

N91-13956# Lawrence Livermore National Lab., CA.

NUMERICAL METHODS FOR BOUNDARY VALUE PROBLEMS IN DIFFERENTIAL-ALGEBRAIC EQUATIONS

Uri M. Ascher (British Columbia Univ., Vancouver.) and Linda R. Petzold 24 Sep. 1990 14 p Presented at the American Institute of Chemical Engineers Fall Annual Meeting, Chicago, IL, 11-16 Nov. 1990 Sponsored in part by NSERC Canada grant
(Contract W-7405-eng-48)
(DE91-001748; UCRL-JC-106088; CONF-901155-1) Avail: NTIS HC/MF A03

Differential-algebraic equation (DAE) boundary value problems arise in a variety of applications, including optimal control and parameter estimation for constrained systems. In this paper we survey these applications and explore some of the difficulties associated with solving the resulting DAE systems. For finite difference methods, the need to maintain stability in the differential part of the system often necessitates the use of methods based on symmetric discretizations. However, these methods can suffer from instability and loss of accuracy when applied to certain DAE systems. We describe a new class of methods, Projected Implicit Runge-Kutta Methods, which overcomes these difficulties. We give convergence and stability results, and present numerical experiments which illustrate the effectiveness of the new methods. DOE

N91-13957# Los Alamos National Lab., NM. Center for Nonlinear Studies.
VORTEX COLLAPSE FROM A VIEWPOINT OF COMPLEX-TIME SINGULARITY
Yoshifumi Kimura 1990 21 p Presented at the 10th Annual Conference on Nonlinear Science: The Next Decade, Los Alamos, NM, 5-9 May 1990
(Contract W-7405-eng-36)
(DE91-001852; LA-UR-90-3664; CONF-9005237-7) Avail: NTIS HC/MF A03

When collisions of point vortices occur under certain initial and parametrical conditions, a singularity appears on the real time axis. If some of the conditions are deviated from the collapse ones, the singularity splits to a (or some) complex-conjugate pair(s). Recently a scaling law between a deviation of an initial condition and a resulted shift of the position of singularity from the real point was proposed for a system of point vortices. This scaling law is verified using the collisions of three and four point vortices. DOE

N91-13958# Colorado Univ., Boulder. Applied Mathematics Program.
AN ASYMPTOTIC SYMMETRY OF THE RAPIDLY FORCED PENDULUM
Yi-Hua Chang and Harvey Segur (State Univ. of New York, Buffalo.) Sep. 1990 26 p
(Contract DE-FG02-86ER-25021)
(DE91-001868; DOE/ER-25021/T1) Avail: NTIS HC/MF A03

The inhomogeneous differential equation x" + sin x = delta sin (t + t(sub 0))/epsilon describes the motion of a sinusoidally forced pendulum. The orbits that connect the two saddle points of the unforced (delta = 0) pendulum, (x = pi) and (x = -pi), are called separatrices. If epsilon = Omicron(1), then one can use Melnikov's method to show that these separatrices can split for weak forcing (delta much less than 1), and that the perturbed motion is chaotic. If epsilon is much less than 1, Melnikov's method fails because the perturbation term is not analytic in epsilon at epsilon = 0. In this paper we show that for delta much less than 1 and epsilon much less than 1, the solution of the perturbed problem exhibits a symmetry to all orders in an asymptotic expansion. From the asymptotic expansion it follows that the separatrices split by an amount that is at most transcendentally small. This proof differs from that of Holmes, Marsden and Scheurle. DOE

N91-13959# Oak Ridge National Lab., TN. Mathematical Sciences Section.
COMPUTING THE EIGENVALUES AND EIGENVECTORS OF A GENERAL MATRIX BY REDUCTION TO GENERAL TRIDIAGONAL FORM
J. J. Dongarra, G. A. Geist, and C. H. Romine Sep. 1990 15 p
(Contract DE-AC05-84OR-21400)
(DE91-002523; ORNL/TM-11669) Avail: NTIS HC/MF A03

This paper describes programs to reduce a nonsymmetric matrix to tridiagonal form, compute the eigenvalues of the tridiagonal matrix, improve the accuracy of an eigenvalue, and compute the corresponding eigenvector. DOE

N91-13960# Grenoble-1 Univ. (France). Lab. de Genie Informatique.
LOGICS FOR THE DESCRIPTION OF PROCESSES AND THEIR PROPERTIES: EXPRESSIVITY AND DECIDABILITY Ph.D. Thesis
Ahmed Bouajjani 1989 92 p In FRENCH; ENGLISH summary
(ETN-91-98200) Avail: NTIS HC/MF A05

Decidability and expressivity of propositional mu-calculi with linear and branching time models is discussed. The logic for the description of regular processes and their properties called LSP is presented. LSP is a branching time mu-calculus that can be viewed as an extension of a process algebra for regular processes. This logic and its extensions are shown to be adequate and expressive for strong bisimulation. Decidability of LSP by reduction to the emptiness problem of Rabin automata on infinite trees is demonstrated. LSP is compared to both branching and linear time logics. LSP is shown to be equivalent to the propositional mu-calculus of Kozen and more expressive than the class of the omega-regular languages and is shown to give a translation associating with any formula of a linear time logic an equivalent formula of LSP. ESA

N91-13961# Loughborough Univ. of Technology (England). Dept. of Mathematical Sciences.
A GLOBAL CONVERGENCE RESULT FOR CONJUGATE GRADIENT METHODS
Y. F. Hu and C. Storey Jul. 1990 10 p Revised
(MATHS-Rept-A-134; ETN-91-98354) Avail: NTIS HC/MF A02

The problems of search direction are investigated. The different parameters of the search direction are studied, such as the Fletcher-Reeves and Polak-Ribiere parameters. Numerical experiences show that conjugate gradient methods using the latter are generally more efficient than those using the former; global convergence was shown, while the other does not have this property even with exact line searches. A combination of both methods assures global convergence of the algorithm and seems always to restrict the parameter to be non negative. It is proved that a more general convergence theorem can be used, which allows this parameter to be negative. ESA

N91-13962# Lawrence Livermore National Lab., CA.
LATTICE BOLTZMANN METHODS FOR SOME 2-D NONLINEAR DIFFUSION EQUATIONS: COMPUTATIONAL RESULTS
Bracy H. Elton, Garry H. Rodrigue, and C. David Levermore (Arizona Univ., Tucson.) 1990 18 p Presented at the Workshop on Asymptotic Analysis and Numerical Solution of PDEs, Argonne, IL, 26-28 Feb. 1990 Submitted for publication
(Contract W-7405-eng-48; NSF DMS-89-14420)
(DE91-004175; UCRL-JC-104691) Avail: NTIS HC/MF A03

In this paper we examine two lattice Boltzmann methods (that are a derivative of lattice gas methods) for computing solutions to two two-dimensional nonlinear diffusion equations of the form (d/dt)u=v(d/dx)D(u)(d/dx)u+(d/dy)D(u)(d/dy)u where d=partial derivative and u=u(vector-x,t), vector-x is an element of R(sup 2), v is a constant, and D(u) is a nonlinear term that arises from a Chapman-Enskog asymptotic expansion. In particular, we provide computational evidence supporting recent results showing that the methods are second order convergent (in the L(sub 1)-norm), conservative, conditionally monotone finite difference methods. Solutions computed via the lattice Boltzmann methods are compared with those computed by other explicit, second order, conservative, monotone finite difference methods. Results are reported for both the L(sub 1)- and L(sub (infinity))-norms. DOE

N91-13963 Politecnico di Milano (Italy). Dipt. di Elettronica.
ON THE INVERTIBILITY OF LESLIE SYSTEMS
Simona Muratori and Sergio Rinaldi 1990 16 p
(Rept-90-006; ETN-91-98386) Avail: Politecnico di Milano, Piazzo Leonardo da Vinci 32, 20133 Milan, Italy

The reconstruction of the stocking rate of exploited renewable resources from an output time series is considered. The resource was described by a linear age structured model of the Leslie type and the measured output was a linear and a positive combination of the number of individual in each reproductive class. A general invertibility condition based on the zeros of the transfer function system is used. Although the zeros of a linear system are in general (n minus 1), where n is the maximum age of the population, it is proved that the invertibility of this system can be checked by determining the module of the roots of a polynomial of a smaller degree. Two particular cases were analyzed: the total number of fertile individuals at the beginning of the year and the total number of newly born individuals at the end of the reproduction season. It is shown that in the first case the system is invertible. ESA

65 STATISTICS AND PROBABILITY

Includes data sampling and smoothing; Monte Carlo method; and stochastic processes.

N91-13964# Universiteit Twente, Enschede (Netherlands). Faculty of Applied Mathematics.
DIRECT MODELING OF WHITE NOISE IN STOCHASTIC SYSTEMS
Arunabha Bagchi and Ravi Mazundar (Quebec Univ., Verdun.) Jun. 1990 34 p
(MEMO-865; ISSN-0169-2690; ETN-90-98107) Avail: NTIS HC/MF A03

The line of development that led to a direct modeling of white noise in stochastic systems is explained. The mathematical theory of finitely additive white noise and some recent results on modeling the state process with white noise input are presented. Likelihood ratio plays a central role throughout the paper study. ESA

66 SYSTEMS ANALYSIS

Includes mathematical modeling; network analysis; and operations research.

N91-13965# Technische Hochschule, Darmstadt (Germany, F.R.). Fachbereich Mathematik.
CLASSES OF PRIORS IN GAMES AND DECISION MODELS Ph.D. Thesis
June M. Parker 1989 90 p
(ETN-91-98171) Avail: NTIS HC/MF A05

The use of prior information in two person zero sum games was investigated. Two person zero sum games with spaces of mixed strategies for player 1 are studied; of prime importance to player 2 is the knowledge that the game is strictly determined. Three types of classes of priors were examined and results which facilitate the application of strategies to classes of priors of these forms are discussed. Complementary results for minimax testing of hypotheses concerning classes of priors defined by convex combinations are given. ESA

67 THEORETICAL MATHEMATICS

Includes topology and number theory.

N91-13966*# Institute for Computer Applications in Science and Engineering, Hampton, VA.
REGULARIZED CHAPMAN-ENSKOG EXPANSION FOR SCALAR CONSERVATION LAWS Final Report
Steven Schochet and Eitan Tadmor (Tel-Aviv Univ., Israel) Oct. 1990 19 p Prepared in cooperation with Michigan Univ., Ann Arbor
(Contract NAS1-18605)
(NASA-CR-187441; ICASE-90-68; NAS 1.26:187441) Avail: NTIS HC/MF A03 CSCL 12A

Rosenau has recently proposed a regularized version of the Chapman-Enskog expansion of hydrodynamics. This regularized expansion resembles the usual Navier-Stokes viscosity terms at law wave-numbers, but unlike the latter, it has the advantage of being a bounded macroscopic approximation to the linearized collision operator. The behavior of Rosenau regularization of the Chapman-Enskog expansion (RCE) is studied in the context of scalar conservation laws. It is shown that thie RCE model retains the essential properties of the usual viscosity approximation, e.g., existence of traveling waves, monotonicity, upper-Lipschitz continuity..., and at the same time, it sharpens the standard viscous shock layers. It is proved that the regularized RCE approximation converges to the underlying inviscid entropy solution as its mean-free-path epsilon approaches 0, and the convergence rate is estimated. Author

70 PHYSICS (GENERAL)

For precision time and time interval (PTTI) see *35 Instrumentation and Photography;* for geophysics, astrophysics or solar physics see *46 Geophysics, 90 Astrophysics,* or *92 Solar Physics.*

N91-13967*# Alabama Univ., Huntsville. Center for Microgravity and Materials Research.
VISCOSITY MEASUREMENTS AT HIGH TEMPERATURE AND HIGH PRESSURE: A NOVEL TECHNIQUE
Wei-qing Jin, J. Iwan D. Alexander, and Franz Rosenberger [1989] 12 p
(Grant NAG8-790)
(NASA-CR-187239; NAS 1.26:187239) Avail: NTIS HC/MF A03 CSCL 20C

The extensive numerical modelling of transport phenomena was performed for the melt growth of mercury cadmium telluride. To increase the fidelity of modelling the kinematic viscosity of liquid Hg(1-x)Cd(x)Te was determined at various compositions in the range of x between 0 and 0.2 and at temperatures around and below the respective melting point. The phase diagram of Hg(1-x)Cd(x)Te shows that for this range the melting point varies from 670 C for pure HgTe to 790 C at x=0.2. The vapor pressure above the melt varies correspondingly from 15 to about 40 atm. Hence, the measurement of viscosities in this system requires a technique that allows for combinations of high temperatures and pressures. In addition, a closed isothermal system is required. The high pressure melt container must also be inert to molten Hg(1-x)Cd(x)Te to avoid possible errors from contamination of the liquid. A novel technique that largely circumvents the above experimental problems is described. Its theory is also presented. Y.S.

N91-13968 National Physical Lab., Teddington (England). Div. of Electrical Science.
INVESTIGATION OF THE UNIFORMITY OF THE MAGNETIC FIELD AND FLUX DENSITY IN THE NPL PERMEAMETER
A. E Drake and C. Ager Aug. 1990 26 p
(NPL-DES-101; ISSN-0143-7305; ETN-91-98371) Copyright Avail: National Physical Laboratory, Teddington, TW11 0LW, England

The errors that would be introduced into the determination of the direct current magnetic properties of materials measured in the permeameter, when using a Hall effect probe to sense the magnetic field strength, are ascertained. The variation of the magnetic field strength and magnetic flux density over the length of the magnetizing coil of the permeameter is determined for test specimens of typical materials. ESA

71 ACOUSTICS

Includes sound generation, transmission and attenuation. For noise pollution see *45 Environmental Pollution.*

N91-13969# Florida State Univ., Tallahassee. Dept. of Mathematics.
COMPUTATION OF BROADBAND MIXING NOISE FROM TURBOMACHINERY Semiannual Progress Report, 1 Mar. - 31 Aug. 1990
Christopher Tam 31 Aug. 1990 2 p
(Contract N00014-89-J-1836)
(AD-A226559) Avail: NTIS HC/MF A01 CSCL 20/1

This paper discusses the phenomena of dispersion and spurious acoustic radiation in calculating propeller noise using finite difference approximation. Dispersion effect here is global in nature and could cause large distortion of the radiated acoustic waveform as the waves propagate away from the propeller. GRA

N91-13970# Idaho National Engineering Lab., Idaho Falls.
ULTRASOUND GENERATION THROUGH A FIBER OPTIC DELIVERY SYSTEM USING PULSED LASER ENERGY
Nancy M. Carlson and John A. Johnson 1990 10 p Presented

at the Review of Progress in Quantitative NDE, La Jolla, CA, 15-20 Jul. 1990
(Contract DE-AC07-76ID-01570)
(DE91-001914; EGG-M-90086; CONF-900791-7) Avail: NTIS HC/MF A02

Short duration laser pulses can generate high frequency, broadband ultrasound in a material without contacting the surface. For these noncontacting techniques to be useful on the shop floor, in remote applications, and in harsh environments, a dependable delivery system must be developed. Fiber optic techniques have been used to deliver either moderate laser energy for a large number of pulses or a large laser energy for a few pulses for the purpose of generating acoustic waves. However, transmitting high energy pulses continuously through a fiber is required for practical sensing systems. Fiber optics systems are currently used for a long duration pulses (of the order of milliseconds) in laser welding applications; e.g., a welding systems developed for manufacture of headlamps uses a fiber optic delivery system. The key to the success of this welding systems is the coupling technique used to deliver laser power to the fiber. Because the pulse duration is on the order of several milliseconds, the power density in the fiber is several orders of magnitude below the power densities required for ultrasonic applications. DOE

N91-13971*# Wisconsin Univ., Milwaukee.
HEARING IN THREE DIMENSIONS: SOUND LOCALIZATION
Frederic L. Wightman and Doris J. Kistler [1990] 18 p
(Contract NCC2-542; NIH-P01-NS-12732)
(NASA-CR-187706; NAS 1.26:187706) Avail: NTIS HC/MF A03 CSCL 20A

The ability to localize a source of sound in space is a fundamental component of the three dimensional character of the sound of audio. For over a century scientists have been trying to understand the physical and psychological processes and physiological mechanisms that subserve sound localization. This research has shown that important information about sound source position is provided by interaural differences in time of arrival, interaural differences in intensity and direction-dependent filtering provided by the pinnae. Progress has been slow, primarily because experiments on localization are technically demanding. Control of stimulus parameters and quantification of the subjective experience are quite difficult problems. Recent advances, such as the ability to simulate a three dimensional sound field over headphones, seem to offer potential for rapid progress. Research using the new techniques has already produced new information. It now seems that interaural time differences are a much more salient and dominant localization cue than previously believed. Author

N91-13972*# Coe Engineering, Inc., Mountain View, CA.
AN ASSESSMENT OF WIND TUNNEL TEST DATA ON FLEXIBLE THERMAL PROTECTION MATERIALS AND RESULTS OF NEW FATIGUE TESTS OF THREADS
Charles F. Coe Apr. 1985 70 p
(Contract NAS2-11420)
(NASA-CR-177466; NAS 1.26:177466) Avail: NTIS HC/MF A04 CSCL 20A

Advanced Flexible Reusable Surface Insulation (AFRSI) was developed as a replacement for the low-temperature (white) tiles on the Space Shuttle. The first use of the AFRSI for an Orbiter flight was on the OMS POD of Orbiter (OV-099) for STS-6. Post flight examination after STS-6 showed that damage had occurred to the AFRSI during flight. The failure anomaly between previous wind-tunnel tests and STS-6 prompted a series of additional wind tunnel tests to gain an insight as to the cause of the failure. An assessment of all the past STS-6 wind tunnel tests pointed out the sensitivity of the test results to scaling of dynamic loads due to the difference of boundary layer thickness, and the material properties as a result of exposure to heating. The thread component of the AFRSI was exposed to fatigue testing using an apparatus that applied pulsating aerodynamic loads on the threads similar to the loads caused by an oscillating shock. Comparison of the mean values of the number-of-cycles to failure showed that the history of the thread was the major factor in its performance. The thread and the wind tunnel data suggests a mechanism of failure for the AFRSI. Author

N91-13973# Brown Univ., Providence, RI.
SURFACES AND THIN FILMS STUDIED BY PICOSECOND ULTRASONICS Annual Progress Report, 1 Dec. 1989 - 30 Nov. 1990
Humphrey J. Maris and Jan Tauc 1990 10 p
(Contract DE-FG02-86ER-45267)
(DE91-004167; DOE/ER-45267/4) Avail: NTIS HC/MF A02

This research supported by grant FG02-86ER45367 is the study of the properties of solids by means of the picosecond technique. In this research we investigate both fundamental problems in phonon physics and lattice dynamics, and we also apply the technique to the non-destructive evaluation of thin-film microstructures. In the experiments a picosecond light pulse is absorbed at a surface, thereby generating an elastic pulse. This strain pulse propagates through the sample, and is detected at a later time by means of a time-delayed probe light pulse. During the past year our research has been concentrated in three main areas. We have made an extensive series of measurements of ultrasonic attenuation as a function of frequency and temperature in glasses. We have succeeded in generating and detecting surface acoustic waves in microstructures with surface gratings and dot arrays, and have performed several experiments to study the structure of thin films and surface layers. The third area is the investigation of heat flow from metal films into dielectric crystals, and the possible observation of second sound. Also included is the proposal for next years work. DOE

N91-13974# Southampton Univ. (England). Inst. of Sound and Vibration Research.
THE PREDICTION AND MEASUREMENT OF THE ONE-PARAMETER BEHAVIOUR OF HORNS
K. R. Holland, F. J. Fahy, and C. L. Morfey Apr. 1990 59 p
(ISVR-TR-185; ETN-91-98377) Avail: NTIS HC/MF A04

A one parameter mathematical loudspeaker horn model is described on the basis of the momentum and continuity equations with reference to the Webster equation. Axial pressure phase distribution and normalized transfer impedence were obtained in the case of rectangular exponential or axisymmetric horns made of aluminum or glass fiber. A method was developed for measuring the throat impedance of horns using an impedance tube. The results show a good agreement with the model predictions. The one parameter modeling of horns can result in the accurate prediction of throat inpedance provided wave front shapes within the horn are taken into account. The prediction of the sound field radiated by the horn is only possible with this method if transverse pressure variations are not present. ESA

N91-13975# Southampton Univ. (England). Inst. of Sound and Vibration Research.
ADAPTIVE INVERSE FILTERS FOR STEREOPHONIC SOUND REPRODUCTION
P. A. Nelson, H. Hamada (Tokyo Denki Univ., Japan), and S. J. Elliott Jul. 1990 52 p
(ISVR-TR-187; ETN-91-98378) Avail: NTIS HC/MF A04

A general theoretical basis for the design of adaptive digital filters for the equalization of the response of multichannel sound reproduction systems is described. The formulation used was a generalization of the Atal-Shroeder cross talk canceller. The use of a least square approach to the digital filter design, combined with appropriate modeling delays, allowed the effective equalization of nonminimum phase components in the transmission path. A stochastic gradient algorithm is presented which facilitates the adoption of the digital filters to the optimal solution, providing the possibility of the design of the filters 'in situ' in a given listening space. Some experimental results appear at very low frequencies if the response of the filters are an exponential form. ESA

72 ATOMIC AND MOLECULAR PHYSICS

Includes atomic structure, electron properties, and molecular spectra.

N91-13976*# Fermi National Accelerator Lab., Batavia, IL.
AXIONS AND SN 1987A: AXION TRAPPING
Adam Burrows, M. Ted Ressell, and Michael S. Turner (Chicago Univ., IL.) Jul. 1990 33 p
(Grant NAGw-1340)
(NASA-CR-186467; NAS 1.26:186467;
FERMILAB-Pub-90/81-Rev) Avail: NTIS HC/MF A03 CSCL 20H

If an axion of mass between about 10(exp -3) and 10 eV exists, axion emission would have significantly affected the cooling of the nascent neutron star associated with SN 1987A. For an axion of mass greater than about 10(exp -2) eV axions would, like neutrinos, have a mean-free path that is smaller than the size of a neutron star, and thus would become trapped and radiated from an axion sphere. The trapping regime is treated by using numerical models of the initial cooling of a hot neutron star that incorporate a diffusion approximation for axion-energy transport. The axion opacity due to inverse nucleon-nucleon, axion bremsstrahlung is computed; and then the numerical models are used to calculate the integrated axion luminosity, the temperature of the axion sphere, and the effect of axion emission on the neutrino bursts detected by the Kamiokande II (KII) and Irvine-Michigan-Brookhaven (IMB) water-Cherenkov detectors. The larger the axion mass, the stronger the trapping and the smaller the axion luminosity. The estimate of the axion mass is confirmed above which trapping is so strong that axion emission does not significantly affect the neutrino burst. Based upon the neutrino-burst duration - the most sensitive barometer of axion cooling - it is concluded that for an axion mass greater than about 3 eV axion emission would not have had a significant effect on the neutrino bursts detected by KII and IMB. It is strongly suggested that an axion with mass in the interval 10(exp -3) to 3 eV is excluded by the observation of neutrinos from SN 1987A. Author

N91-13977# Sandia National Labs., Albuquerque, NM.
THE ROLE OF CHEMICAL INTERACTIONS IN ION-SOLID PROCESSES
Brian W. Dodson 1990 22 p Presented at the 7th International Conference on Ion Beam Modification of Materials, Knoxville, TN, 9-14 Sep. 1990
(Contract DE-AC04-76DP-00789)
(DE91-000763; SAND-90-2440C; CONF-900936-11) Avail: NTIS HC/MF A03

Computer simulation of low-energy ion-solid processes has greatly broadened in scope in recent years. In particular, realistic descriptions of the ion-solid and solid-solid interactions can now be utilized. The molecular dynamics technique, in which the equations of motion of the interacting atoms are numerically integrated, can now be used to characterize ion-solid interactions in a range of model material systems. Despite practical limitations of this procedure, a number of substantial results have appeared. The available results are examined to investigate the qualitative influence that chemical interactions have on low-energy ion-solid processes. DOE

N91-13978# Lawrence Livermore National Lab., CA. Div. of Chemistry and Materials Science.
REAL-SPACE MULTIPLE SCATTERING THEORY CALCULATIONS OF LEED (LOW-ENERGY ELECTRON DIFFRACTION) INTENSITIES FOR STEPPED SURFACES
X.-G. Zhang, P. J. Rous, M. A. VanHove, J. M. MacLaren, A. Gonis, and G. A. Somorjai (California Univ., Berkeley. Lawrence Berkeley Lab.) 25 Jul. 1990 7 p Presented at the 3rd International Conference on the Structure of Surfaces, Milwaukee, WI, 9-12 Jul. 1990 Submitted for publication
(Contracts W-7405-eng-48; DE-AC03-76SF-00098)
(DE91-000810; UCRL-JC-104938; CONF-9007131-3) Avail: NTIS HC/MF A02

We use a newly developed real-space multiple scattering theory (RS-MST) to calculate low-energy electron diffraction (LEED) intensities from stepped surfaces. In this calculation the electron wavefunctions are expanded in terms of an angular momentum basis, utilizing the property of removal invariance of systems with semi-infinite periodicity. This strongly reduces the dependence of the calculation on the interlayer spacing and thus opens up the possibility of treating more open surfaces. This includes in particular stepped surfaces, to which conventional methods cannot be applied. Applications of the formalism to various stepped surfaces are presented. In particular, the results for Cu(311) and (331) surfaces obtained from both the layer doubling and RS-MST methods are compared. In addition, numerical techniques which can improve the convergence as well as the speed of the RS-MST approach are discussed. DOE

N91-13979# Tennessee Univ., Knoxville. Dept. of Physics.
ELEMENTARY PARTICLE INTERACTIONS Report, 1 Oct. 1989 - 30 Sep. 1990
W. M. Bugg, G. T. Condo, T. Handler, E. L. Hart, B. F. L. Ward, F. E. Close, and L. G. Christophorou Oct. 1990 72 p
(Contract DE-AS05-76ER-03956)
(DE91-001220; DOE/ER-03956/9) Avail: NTIS HC/MF A04

This report discusses freon bubble chamber experiments exposed to (mu)(sup +) and neutrinos, photon-proton interactions; shower counter simulations; SLD detectors at the Stanford Linear Collider, and the detectors at the Superconducting Super Collider; elementary particle interactions; physical properties of dielectric materials used in high energy physics detectors; and nuclear physics. DOE

N91-13980# Sandia National Labs., Albuquerque, NM.
APPLICATION OF PARALLEL COMPUTING TO THE MONTE CARLO SIMULATION OF ELECTRON SCATTERING IN SOLIDS: A RAPID METHOD FOR PROFILE DECONVOLUTION
A. D. Romig, Jr., S. J. Plimpton, J. R. Michael, R. L. Myklebust, and D. E. Newbury (National Inst. of Standards and Technology, Gaithersburg, MD.) 1990 19 p Presented at the 12th International Congress for Electron Microscopy, Seattle, WA, 12-18 Aug. 1990
(Contract DE-AC04-76DP-00789)
(DE91-001227; SAND-90-2549C; CONF-900877-9) Avail: NTIS HC/MF A03

X-ray microanalysis by analytical electron microscopy (AEM) has proven to be a powerful tool for characterizing the spatial distribution of solute elements in materials. True compositional variations over spatial scales smaller than the actual resolution for microanalysis can be determined if the measured composition profile is deconvoluted. Explicit deconvolutions of such data, via conventional techniques such as Fourier transforms, are not possible due to statistical noise in AEM microanalytical data. Hence, the method of choice is to accomplish the deconvolution via iterative convolutions. In this method, a function describing the assumed true composition profile, calculated by physically permissible thermodynamic and kinetic modeling, is convoluted with the x-ray generation function and the result compared to the measured composition profile. If the measured and calculated profiles agree within experimental error, it is assumed that the true compositional profile has been determined. If the measured and calculated composition profiles are in disagreement, the assumptions in the physical model are adjusted and the convolution process repeated. To employ this procedure it is necessary to calculate the x-ray generation function explicitly. While a variety of procedures are available for calculating this function, the most accurate procedure is to use Monte Carlo modeling of electron scattering. DOE

N91-13981# Lawrence Livermore National Lab., CA. High Temperature Physics Div.
INNER-SHELL IONIZATION OF LITHIUM-LIKE CHROMIUM IONS
D. A. Vogel, P. Beiersdorfer, R. E. Marrs, K. L. Wong, and R. Zasadzinski 7 Sep. 1990 7 p Presented at the 5th International Conference on the Physics of Highly-Charged Ions, Giessen, Fed.

Republic of Germany, 10-14 Sep. 1990 Submitted for publication
(Contract W-7405-eng-48)
(DE91-001749; UCRL-JC-104991; CONF-900923-3) Avail: NTIS HC/MF A02

We have used high-resolution x ray spectroscopy to investigate inner-shell ionization of Cr(21+) ions by electron impact using the Electron Beam Ion Trap at Lawrence Livermore Laboratory. Our measurements indicate that inner-shell ionization enhances the intensity of the radiative transition 1s2sS(sup 3)(sub 1) yields 1s(sup 2)S(sup 1)(sub 0). DOE

N91-13982# California Univ., Berkeley. Lawrence Berkeley Lab. Exploratory Studies Group.
INFLUENCE OF COLLECTIVE EFFECTS ON THE PERFORMANCE OF HIGH-LUMINOSITY COLLIDERS
Michael S. Zisman Apr. 1990 49 p Presented at the Workshop on Beam Dynamics Issues of High Luminosity Asymmetric Collider Rings, Berkeley, CA, 12-16 Feb. 1990
(Contract DE-AC03-76SF-00098)
(DE91-001797; LBL-28820; CONF-9002128-3) Avail: NTIS HC/MF A03

The design of a high-luminosity electron-positron collider to study B physics is a challenging task from many points of view. In this paper we consider the influence of collective effects on the machine performance; most of our findings are generic, in the sense that they depend rather weakly on the details of the machine design. Both single-bunch and coupled-bunch instabilities are described and their effects are estimated based upon an example machine design (APIARY-IV). In addition, we examine the possibility of emittance growth from intrabeam scattering and calculate the beam lifetime from both Touschek and gas scattering. We find that the single-bunch instabilities should not lead to difficulty, and that the emittance growth is essentially negligible. At a background gas pressure of 10 nTorr, beam lifetimes of only a few hours are expected. Multibunch growth rates are very severe, even when using an optimized RF system consisting of single-cell, room-temperature RF cavities with geometrical shapes typical of superconducting cavities. Thus, a powerful feedback system will be required. In terms of collective effects, it does not appear. DOE

N91-13983# Argonne National Lab., IL.
ATOMIC AND MOLECULAR THEORY
Mitio Inokuti 1990 38 p Presented at the Physical and Chemical Mechanisms in Molecular Radiation Biology Conference, Woods Hole, MA, 4-7 Sep. 1990
(Contract W-31-109-eng-38)
(DE91-004475; CONF-9009267-2) Avail: NTIS HC/MF A03

The multifaceted role of theoretical physics in understanding the earliest stages of radiation action is discussed. Scientific topics chosen for the present discourse include photoabsorption, electron collisions, and ionic collisions, and electron transport theory. Connections of atomic and molecular physics with condensed-matter physics are also discussed. The present article includes some historical perspective and an outlook for the future. DOE

N91-13984 Max-Planck-Inst. fuer Physik und Astrophysik, Garching (Germany, F.R.). Werner-Heisenberg Inst. fuer Physik.
PROSPECTS OF CsJ(Tl)-PHOTODIODE DETECTORS FOR LOW LEVEL SPECTROSCOPY
U. Kilgus, R. Kotthaus, and E. Lange Jul. 1990 46 p Submitted for publication
(MPI-PAE/Exp.El-228; ETN-91-98382) Copyright Avail: Fachinformationszentrum Karlsruhe 2, 7514 Eggenstein-Leopoldshafen, Fed. Republic of Germany

The possibilities of CsJ(Tl) PD (photodiode) detectors are investigated for the spectroscopy of rare events such as the detection of low level radioactivity and very rare nuclear decay modes, like double beta decay of some even-even nuclei. The PDs were directly coupled to the crystal surfaces which were sanded and polished with Al2O3 powder immersed in ethylenglycol or with an H2O wetted tissue. The diodes were selected for extra low dark currents. Measurements show that scintillation light yields slowly vary with temperature and time so that excellent long time stability could be expected. A systematic investigation of inherent crystal radioactivity was possible due to the improved energy resolution obtained with big crystals. Six alpha-active radionuclides of the Th-decay-chain were identified. The total alpha activity varies from crystal to crystal between 2.4 and 5.5 decays per h and cc. ESA

73 NUCLEAR AND HIGH-ENERGY PHYSICS

Includes elementary and nuclear particles; and reactor theory.

For space radiation see *93 Space Radiation.*

N91-13985*# National Aeronautics and Space Administration. Langley Research Center, Hampton, VA.
INCLUSIVE INELASTIC SCATTERING OF HEAVY IONS AND NUCLEAR CORRELATIONS
Francis A. Cucinotta, Lawrence W. Townsend, John W. Wilson, and Govind S. Khandelwal (Old Dominion Univ., Norfolk, VA.) Washington Nov. 1990 22 p
(NASA-TP-3026; L-16793; NAS 1.60:3026) Avail: NTIS HC/MF A03 CSCL 20H

Calculations of inclusive inelastic scattering distributions for heavy ion collisions are considered within the high energy optical model. Using ground state sum rules, the inclusive projectile and complete projectile-target inelastic angular distributions are treated in both independent particle and correlated nuclear models. Comparisons between the models introduced are made for alpha particles colliding with He-4, C-12, and O-16 targets and protons colliding with O-16. Results indicate that correlations contribute significantly, at small momentum transfers, to the inelastic sum. Correlation effects are hidden, however, when total scattering distributions are considered because of the dominance of elastic scattering at small momentum transfers. Author

N91-13986# Edgerton, Germeshausen and Grier, Inc., Idaho Falls, ID. Strategic Defense Initiative Organization.
SP-100 FROM GROUND DEMONSTRATION TO FLIGHT VALIDATION
David Buden 1989 3 p Presented at the Winter Meeting of the American Nuclear Society (ANS) and Nuclear Power and Technology Exhibit, San Francisco, CA, 26-30 Nov. 1989
(Contract DE-AC07-76ID-01570)
(DE91-001869; EGG-M-89286; CONF-891103-78) Avail: NTIS HC/MF A01

The SP-100 program is in the midst of developing and demonstrating the technology of a liquid metal cooled, fast reactor using thermoelectric thermal-to-electric conversion devices for space power applications in the range of 10s to 100s of kilowatts. The current Ground Engineering System (GES) design and development phase will demonstrate the readiness of the technology building blocks and the system to proceed to flight system validation. This phase includes the demonstration of a 2.4 MW thermal reactor in the Nuclear Assembly Test (NAT) and aerospace subsystem in the Integrated Assembly Test (IAT). The next phase in the SP-100 development, now being planned, is to be a flight demonstration of the readiness of the technology to be incorporated into future military and civilian missions. DOE

N91-13987# Idaho National Engineering Lab., Idaho Falls.
UNIQUE FEATURES OF SPACE REACTORS
David Buden 1990 7 p Presented at the American Nuclear Society Topical Meeting on Safety of Non-Commercial Nuclear Reactor Research and Irradiation Facilities, Boise, ID, 30 Sep. - 3 Oct. 1990
(Contract DE-AC07-76ID-01570)
(DE91-001910; EGG-M-90309; CONF-900917-24) Avail: NTIS HC/MF A02

Space reactors are designed to meet a unique set of requirements; they must be sufficiently compact to be launched in a rocket to their operational location, operate for many years without maintenance and servicing, operate in extreme environments, and reject heat by radiation to space. To meet these restrictions, operating temperatures are much greater than in terrestrial power plants, and the reactors tend to have a fast neutron spectrum. Currently, a new generation of space reactor power plants is being developed. The major effort is in the SP-100 program, where the power plant is being designed for seven years of full power, and no maintenance operation at a reactor outlet operating temperature of 1350 K. DOE

N91-13988# Los Alamos National Lab., NM.
A LINEAR ACCELERATOR IN THE SPACE: THE BEAM EXPERIMENT ABOARD ROCKET
Patrick G. OShea, Thomas A. Butler, Michael T. Lynch, Kenneth F. McKenna, Morris B. Pongratz, and Thomas J. Zaugg 1990 4 p Presented at the Linear Accelerator Conference, Albuquerque, NM, 10-14 Sep. 1990
(Contract W-7405-eng-36)
(DE91-002347; LA-UR-90-3441; CONF-9009123-46) Avail: NTIS HC/MF A01

On July 13, 1989 the BEAM experiment Aboard Rocket (BEAR) linear accelerator was successfully launched and operated in space. The flight demonstrated that a neutral hydrogen beam could be successfully propagated in an exoatmospheric environment. The accelerator, which was the result of an extensive collaboration between Los Alamos National Laboratory and industrial partners, was designed to produce a 10 mA (equivalent), 1 MeV neutral hydrogen beam in 50 micro-sec pulses at 5 Hz. The major components were a 30 keV H(-) injector a 1 MeV radio frequency quadrupole, two 425 Mhz RF amplifiers, a gas cell neutralizer, beam optics, vacuum system and controls. The design was strongly constrained by the need for a lightweight rugged system that would survive the rigors of launch and operate autonomously. Following the flight the accelerator was recovered and operated again on the laboratory. DOE

N91-13989# Texas A&M Univ., College Station. Dept. of Physics.
HIGH ENERGY PHYSICS PROGRAM AT TEXAS A&M UNIVERSITY Annual Report, 1 Apr. 1990 - 31 Mar. 1991
Oct. 1990 107 p
(Contract DE-AS05-81ER-40039)
(DE91-001639; DOE/ER-40039/46) Avail: NTIS HC/MF A06

The Texas A&M high energy physics program has achieved significant mile-stones in each of its research initiatives. We are participating in two major operating experiments, CDF and MACRO; the development of two new detector technologies, liquid scintillating fiber calorimetry and knife-edge chambers; and two SSC detector proposals, SDC and TEXAS/EMPACT. We have developed prototypes of a liquid-scintillator fiber calorimeter system, in which internally reflecting channels are imbedded in a lead matrix and filled with liquid scintillator. This approach combines the performance features of fiber calorimetry and the radiation hardness of liquid scintillator, and is being developed for forward calorimetry in TEXAS/EMPACT. A new element in this program is the inclusion of a theoretical high energy physics research program being carried out by D. Nanopoulos and C. Pope. D. Nanopoulos has succeeded in building a string-derived model that unifies all known interactions: flipped SU(5), which is the leading candidate for a TOE. The impact of this work on string phenomenology certainly has far reaching consequences. C. Pope is currently working on some generalizations of the symmetries of string theory, known as W algebras. These are expected to have applications in two- dimensional conformal field theory, two-dimensional extensions of gravity and topological gravity, and W-string theory. The following report presents details of the accomplishments of the Texas A&M program over the past year and the proposed plan of research for the coming year. DOE

N91-13990# Sandia National Labs., Albuquerque, NM.
MULTIPLEXER/AMPLIFIER TEST RESULTS FOR SP-100
Donald B. King, Spencer Michael Luker, and Rodger Ryan (General Electric Co., San Jose, CA.) 1990 5 p Presented at the 8th Symposium on Space Nuclear Power Systems, Albuquerque, NM, 6-10 Jan. 1991
(Contract DE-AC04-76DP-00789)
(DE91-004504; SAND-90-2730C; CONF-910116-7) Avail: NTIS HC/MF A01

Multiplexer and amplifier systems must be designed with transistors that can perform satisfactorily over ten years to a total gamma dose of 120E6 rads and a total neutron fluence of 1.6E15 nvt for the SP-100 reactor system. Series of gamma and neutron tests have been completed to measure transistor degradation as a function of total dose, fluence, and temperature. Test results indicate that modest increases in temperature result in substantial improvement of transistor performance at a neutron flux of 8E8 n/cm(exp 2)/s. DOE

74 OPTICS

Includes light phenomena; and optical devices.
For lasers see *36 Lasers and Masers.*

N91-13991*# College of William and Mary, Williamsburg, VA. Dept. of Physics.
INJECTION EFFICIENCY OF BOUND MODES Ph.D. Thesis
Claudio Oliveira Egalon Washington NASA Nov. 1990 127 p
(Contract NAS1-18347)
(NASA-CR-4333; NAS 1.26:4333) Avail: NTIS HC/MF A07 CSCL 20F

Previous work on efficiency of light injection into the core of a fiber from a thin film and a bulk distribution of sources in the cladding have used the fields of a weakly guiding fiber. This approximation simplifies the analysis of the power efficiency by introducing universal values for the eigenvalues of different fibers with the same V-number, but cannot predict accurately the behavior of the injected light into a fiber with arbitrary differences in indices of refraction. The exact field solution was used in the expressions of the power efficiency, p sub eff, and its behavior as a function of the fiber parameter was analyzed. Weakly guiding results obtained previously are confirmed. However, P sub eff does not always increase with the V-number but with the difference in the indices of refraction, eta sub core-eta sub clad. For the bulk distribution it was found that P sub eff increases with the wavelength, lambda, and decreases with the fiber core radius, a, i.e., it decreases with the V-number. However, for the thin film, the P sub eff remains almost constant with lambda and the fiber core radius. Author

N91-13992# University of North Texas, Denton. Dept. of Mathematics.
THE DESIGN OF PHASE-ONLY FILTERS FOR OPTICAL CORRELATIONS Final Report, Jun. 1986 - Dec. 1989
Robert R. Kallman Jul. 1990 114 p
(Contract F08635-86-K-0139)
(AD-A225641; AFATL-TR-90-63) Avail: NTIS HC/MF A06 CSCL 20/6

In 1984 to 1985 the design of phase-only filters was formulated for optical correlators as a complicated nonlinear nondifferentiable optimization question in a very large number of variables. The first objective of this program was to find effective mathematical tools for the solution of this class of optimization problems and to implement them in computer codes. The phase-only filters designed by the techniques developed during the course of this program can be packed with a great deal of information, give good target recognition in the presence of large amounts of additive zero mean Gaussian noise, and objectively perform up to two orders of magnitude better in target recognition and discrimination than filters designed by other techniques. These desirable characteristics continue to hold even after the phase-only filters have been

optimally discretized for implementation in actual devices. The second goal of the program was to use the mathematical tools and computer codes developed herein for phase-only filter design when a warm target resides in a warm background and the average temperature of the target and the average temperature of the background are close. GRA

N91-13993# Massachusetts Inst. of Tech., Cambridge. Research Lab. of Electronics.
DISTORTION-FREE X RAY MASK TECHNOLOGY Quarterly Technical Report, 11 Jun. - 11 Sep. 1990
Henry I. Smith 11 Sep. 1990 6 p
(Contract N00014-90-K-2018)
(AD-A226524) Avail: NTIS HC/MF A02 CSCL 20/11

The objective of this research project is to develop a closed-loop, feedback-controlled, robust system for reliably achieving zero stress in tungsten (W) films sputtered onto various x ray mask shop. Our system for controlling stress in sputtered W films is based on the measurement of resonant frequency. Since resonant frequency depends on both the thickness and the stress of the W films, if the thickness is known, the stress is easily calculated. We have set up an rf sputtering system, a fixture for driving the membrane into oscillation, and optical means of detecting the membrane motion. GRA

N91-13994# Edgerton, Germeshausen and Grier, Inc., Idaho Falls, ID.
COMMUNICATION SYSTEM TEST FOR IMAGE TRANSMISSION
Frank J. Kocsis and Bernard A. Rando 1989 5 p Presented at the Nuclear Information and Records Management Association Symposium, Minneapolis, MN, 27-30 Aug. 1989
(Contract DE-AC07-76ID-01570)
(DE91-001890; EGG-M-89227; CONF-890870-2) Avail: NTIS HC/MF A01

This paper and corresponding NIRMA presentation deals with the testing of the installed network for the transmission of record indexing information and associated images. Details cover the fiber optic and networking specifications, type and volume of record data transmitted, time and communication specifications for the system, and optical test equipment utilized. DOE

N91-13995*# National Aeronautics and Space Administration. Pasadena Office, CA.
HIGH-GAIN AlGaAs/GaAs DOUBLE HETEROJUNCTION DARLINGTON PHOTOTRANSISTORS FOR OPTICAL NEURAL NETWORKS Patent Application
Jae H. Kim, inventor (to NASA) and Steven H. Lin, inventor (to NASA) (Jet Propulsion Lab., California Inst. of Tech., Pasadena.) 11 Oct. 1990 20 p
(Contract NAS7-918)
(NASA-Case-NPO-18101-1-CU; NAS 1.71:NPO-18101-1-CU; US-Patent-Appl-SN-596133) Avail: NTIS HC/MF A03 CSCL 20F

High-gain MOCVD-grown (metal-organic chemical vapor deposition) AlGaAs/GaAs/AlGaAs n-p-n double heterojunction bipolar transistors (DHBTs) and Darlington phototransistor pairs are provided for use in optical neural networks and other optoelectronic integrated circuit applications. The reduced base doping level used herein results in effective blockage of Zn out-diffusion, enabling a current gain of 500, higher than most previously reported values for Zn-diffused-base DHBTs. Darlington phototransistor pairs of this material can achieve a current gain of over 6,000, which satisfies the gain requirement for optical neural network designs, which advantageously may employ neurons comprising the Darlington phototransistor pair in series with a light source. NASA

N91-13996*# National Aeronautics and Space Administration. Lewis Research Center, Cleveland, OH.
MONOLITHIC mm-WAVE PHASE SHIFTER USING OPTICALLY ACTIVATED SUPERCONDUCTING SWITCHES Patent Application
Robert R. Romanofsky, inventor (to NASA) and Kul B. Bhasin, inventor (to NASA) 25 Sep. 1990 16 p
(NASA-Case-LEW-14878-1; NAS 1.71:LEW-14878-1; US-Patent-Appl-SN-587921) Avail: NTIS HC/MF A03 CSCL 20F

A phase shifter is disclosed having a reference path and a delay path, light sources, and superconductive switches. Each of the superconductive switches is terminated in a virtual short circuit, which may be a radial stub. Switching between the reference path and delayed path is accomplished by illuminating the superconductive switches connected to the desired path, while not illuminating the superconductive switches connected to the other path. NASA

N91-13997*# National Aeronautics and Space Administration. Lyndon B. Johnson Space Center, Houston, TX.
OPTICAL JOINT CORRELATION FOR REAL-TIME TRACKING Patent Application
Richard D. Juday, inventor (to NASA) 31 Jul. 1990 18 p
(NASA-Case-MSC-21509-1; NAS 1.71:MSC-21509-1; US-Patent-Appl-SN-560924) Avail: NTIS HC/MF A03 CSCL 20F

A method for tracking an object in a sequence of images is described. Such sequence of images may, for example, be a sequence of television frames. The object in the current frame is correlated with the object in the previous frame to obtain the relative location of the object in the two frames. An optical joint transform correlator apparatus is provided to carry out the process. Such joint transform correlator apparatus forms the basis for laser eye surgical apparatus where an image of the fundus of an eyeball is stabilized and forms the basis for the correlator apparatus to track the position of the eyeball caused by involuntary movement. With knowledge of the eyeball position, a surgical laser can be precisely pointed toward a position on the retina. NASA

N91-13998*# National Aeronautics and Space Administration. Pasadena Office, CA.
MOTION DETECTION, NOVELTY FILTERING, AND TARGET TRACKING USING AN INTERFEROMETRIC TECHNIQUE WITH A GaAs PHASE CONJUGATE MIRROR Patent Application
Li-Jen Cheng, inventor (to NASA) and Tsuen-Hsi Liu, inventor (to NASA) (Jet Propulsion Lab., California Inst. of Tech., Pasadena.) 16 Aug. 1990 17 p
(Contract NAS7-918)
(NASA-Case-NPO-17784-1-CU; NAS 1.71:NPO-17784-1-CU; US-Patent-Appl-SN-568129) Avail: NTIS HC/MF A03 CSCL 20F

A method and apparatus is disclosed for detecting and tracking moving objects in a noise environment cluttered with fast-and slow-moving objects and other time-varying background. A pair of phase conjugate light beams carrying the same spatial information commonly cancel each other out through an image subtraction process in a phase conjugate interferometer, wherein gratings are formed in a fast photo-refractive phase conjugate mirror material. In the steady state, there is no output. When the optical path of one of the two phase conjugate beams is suddenly changed, the return beam loses its phase conjugate nature and the inter-ferometer is out of balance, resulting in an observable output. The observable output lasts until the phase conjugate nature of the beam has recovered. The observable time of the output signal is roughly equal to the formation time of the grating. If the optical path changing time is slower than the formation time, the change of optical path becomes unobservable, because the index grating can follow the change. Thus, objects traveling at speeds which result in a path changing time which is slower than the formation time are not observable and do not clutter the output image view. NASA

N91-13999*# National Aeronautics and Space Administration. Marshall Space Flight Center, Huntsville, AL.
WIDE ACCEPTANCE ANGLE, HIGH CONCENTRATION RATIO, OPTICAL COLLECTOR Patent Application
Mark Arthur Kruer, inventor (to NASA) (TRW Defense and Space

Systems Group, Redondo Beach, CA.) 30 Mar. 1990 15 p
(NASA-Case-MFS-28295-1; NAS 1.71:MFS-28295-1;
US-Patent-Appl-SN-503408) Avail: NTIS HC/MF A03 CSCL 20F

The invention is directed to an optical collector requiring a wide acceptance angle, and a high concentration ratio. The invention is particularly adapted for use in solar collectors of cassegrain design. The optical collector system includes a parabolic circular concave primary mirror and a hyperbolic circular convex secondary mirror. The primary mirror includes a circular hole located at its center wherein a solar collector is located. The mirrored surface of the secondary mirror has three distinct zones: a center circle, an on-axis annulus, and an off-axis section. The parabolic shape of the primary mirror is chosen so that the primary mirror reflects light entering the system on-axis onto the on-axis annulus. A substantial amount of light entering the system off-axis is reflected by the primary mirror onto either the off-axis section or onto the center circle. Subsequently, the off-axis sections reflect the off-axis light toward the solar collector. Thus, off-axis light is captured which would otherwise be lost to the system. The novelty of the system appears to lie in the configuration of the primary mirror which focuses off-axis light onto an annular portion of the secondary mirror to enable capture thereof. This feature results in wide acceptance angle and a high concentration ratio, and also compensates for the effects of non-specular reflection, and enables a cassegrain configuration to be used where such characteristics are required. NASA

N91-14000*# National Aeronautics and Space Administration. Lyndon B. Johnson Space Center, Houston, TX.
THREE DIMENSIONAL MOIRE PATTERN ALIGNMENT Patent Application
Richard D. Juday, inventor (to NASA) 28 Jun. 1990 24 p
(NASA-Case-MSC-21416-1; NAS 1.71:MSC-21416-1;
US-Patent-Appl-SN-545177) Avail: NTIS HC/MF A03

An apparatus is disclosed for determining three dimensional positioning relative to a predetermined point utilizing moire interference patterns such that the patterns are complementary when viewed on axis from the predetermined distance. Further, the invention includes means for determining rotational positioning in addition to three dimensional translational positioning. NASA

N91-14001*# National Aeronautics and Space Administration. Goddard Space Flight Center, Greenbelt, MD.
LASER OPTICAL DISK POSITION ENCODER WITH ACTIVE HEADS Patent Application
Eric P. Osborne, inventor (to NASA) 30 Mar. 1990 57 p
(NASA-Case-GSC-13175-1; NAS 1.71:GSC-13175-1;
US-Patent-Appl-SN-506636) Avail: NTIS HC/MF A04 CSCL 20F

An angular position encoder is provided that minimizes the effects of eccentricity and other misalignments between the disk and the read stations by employing heads which incorporate beam steering optics with the ability to actively track the disk in directions along the disk radius and normal to its surface. The device adapts features prevalent in optical disk technology toward the application of angular position sensing. A reflective disk and the principles of interferometry are employed. The servo-controlled steering optics move so as to acquire a track on the disk lying at a predetermined radius and distance below the head, and then adjust position and orientation in order to maintain the view of the disk track as required. Thus, the device is actively self-aligning. NASA

N91-14002*# National Aeronautics and Space Administration. Ames Research Center, Moffett Field, CA.
APPARATUS FOR PRECISION FOCUSING AND POSITIONING OF A BEAM WAIST ON A TARGET Patent Application
Dana H. Lynch, inventor (to NASA), William D. Gunter, inventor (to NASA), and Kenneth W. McAlister, inventor (to NASA) (Army Research and Technology Labs., Moffett Field, CA.) 31 May 1990 29 p
(NASA-Case-ARC-11916-1-SB; NAS 1.71:ARC-11916-1-SB;
US-Patent-Appl-SN-531373) Avail: NTIS HC/MF A03

The invention relates to optical focussing apparatus and, more particularly, to optical apparatus for focussing a highly collimated Gaussian beam which provides independent and fine control over the focus waist diameter, the focus position both along the beam axis and transverse to the beam, and the focus angle. A beam focusing and positioning apparatus provides focusing and positioning for the waist of a waisted beam at a desired location on a target such as an optical fiber. The apparatus includes a first lens, having a focal plane f(sub 1), disposed in the path of an incoming beam and a second lens, having a focal plane f(sub 2) and being space downstream from the first lens by a distance at least equal to f(sub 1) + 10 f(sub 2), which cooperates with the first lens to focus the waist of the beam on the target. A rotatable optical device, disposed upstream of the first lens, adjusts the angular orientation of the beam waist. The transverse position of the first lens relative to the axis of the beam is varied to control the transverse position of the beam waist relative to the target (a fiber optic as shown) while the relative axial positions of the lenses are varied to control the diameter of the beam waist and to control the axial position of the beam waist. Mechanical controllers C(sub 1), C(sub 2), C(sub 3), C(sub 4), and C(sub 5) control the elements of the optical system. How seven adjustments can be made to correctly couple a laser beam into an optical fiber is illustrated. Prior art systems employing optical techniques to couple a laser beam into an optical fiber or other target simply do not provide the seven necessary adjustments. The closest known prior art, a Newport coupler, provides only two of the seven required adjustments. NASA

N91-14003 Institute for Perception RVO-TNO, Soesterberg (Netherlands).
MULTI-SCALE CONTRAST ENHANCEMENT WITH APPLICATIONS TO IMAGE FUSION Final Report
A. Toet 6 Feb. 1990 22 p
(Contract A87/D/149)
(IZF-1990-A-9; TD-90-0022; ETN-91-98309) Copyright Avail: Institute for Perception RVO-TNO, P.O. Box 23, 3769 ZG Soesterberg, Netherlands

A method used to merge images from different sensing modalities for visual display is outlined. The method produces a fused image by nonlinear recombination of the RoLP (Ratio of Low-Pass) pyramidal decompositions of the original images. The appearance of merged images that are produced by this scheme is highly dependent on the contrast and mean luminance of the input images. It is shown that nonlinear multiplication of the successive layers of a RoLP pyramid results in a contrast enhanced image representation which is highly invariant for changes in the global luminance characteristics of the original image. Application of this nonlinear multiplication procedure in the image fusion process results in composite images that appear highly independent of changes in lighting and luminance gradients in the input images. The method is tested by merging different degraded versions of parallel registered thermal forward looking infrared detectors and visual (CCD) images. ESA

75 PLASMA PHYSICS

Includes magnetohydrodynamics and plasma fusion.

For ionospheric plasmas see *46 Geophysics*. For space plasmas see *90 Astrophysics*.

N91-14004# Lawrence Livermore National Lab., CA.
HYLIFE-2 INERTIAL CONFINEMENT FUSION REACTOR DESIGN
Ralph W. Moir Oct. 1990 19 p Presented at the 9th Topical Meeting on Technology of Fusion Energy, Oak Brook, IL, 7-11 Oct. 1990
(Contract W-7405-eng-48)
(DE91-000792; UCRL-JC-103816; CONF-901007-6) Avail: NTIS HC/MF A03

The HYLIFE-II inertial fusion power plant design study uses a liquid fall, in the form of jets to protect the first structural wall

from neutron damage, x rays, and blast to provide a 30-y lifetime. HYLIFE-I used liquid lithium. HYLIFE-II avoids the fire hazard of lithium by using a molten salt composed of fluorine, lithium, and beryllium (Li2BeF4) called Flibe. Access for heavy-ion beams is provided. Calculations for assumed heavy-ion beam performance show a nominal gain of 70 at 5 MJ producing 350 MJ, about 5.2 times less yield than the 1.8 GJ from a driver energy of 4.5 MJ with gain of 400 for HYLIFE-I. The nominal 1 GWe of power can be maintained by increasing the repetition rate by a factor of about 5.2, from 1.5 to 8 Hz. A higher repetition rate requires faster re-establishment of the jets after a shot, which can be accomplished in part by decreasing the jet fall height and increasing the jet flow velocity. Multiple chambers may be required. In addition, although not considered for HYLIFE-I, there is undoubtedly liquid splash that must be forcibly cleared because gravity is too slow, especially at high repetition rates. Splash removal can be accomplished by either pulsed or oscillating jet flows. The cost of electricity is estimated to be 0.09 $/kW h in constant 1988 dollars, about twice that of future coal and light water reactor nuclear power. The driver beam cost is about one-half the total cost. DOE

N91-14005# Naval Research Lab., Washington, DC. Plasma Physics Div.

NRL COMPACT ACCELERATOR THEORY STUDIES

Richard F. Hubbard, A. Wahab Ali, Glenn Joyce, J. Krall, F. Mako, P. Serafim (Northeastern Univ., Boston, MA.), S. P. Slinker, P. Sprangle, and C. M. Tang 31 Aug. 1990 44 p

(AD-A226537; NRL-MR-6681) Avail: NTIS HC/MF A03 CSCL 20/7

NRL compact accelerator theory studies in support of the Spiral Line Induction Accelerator (SLIA) and the Recirculating Linear Accelerator (RLA) are summarized in a series of short papers. The first of these papers describes the ELBA 3-D beam simulation code, a particle code which was used to model beam stability and transport in both accelerators. The second paper presents and analytical model for the dangerous three-wave electromagnetic instability and defines parameter regimes for the SLIA where the instability can be completely stabilized. ELBA simulations of the SLIA in the various stability regimes, described by the analytical mode, are described in the next paper. The fourth paper includes additional ELBA simulations of beam transport in the SLIA, demonstrating that high eccentricity equilibria can lead to serious emittance growth. The effects of axisymmetric ion channel motion on beam transport in the RLA are discussed in the next paper. The sixth paper describes ELBA simulations of erosion and off-axis drifts in both straight and curved sections of the RLA. The final paper discusses the various atomic and surface plasma processes which may occur in compact accelerators. GRA

N91-14006# New York Univ., New York. Inst. of Mathematical Sciences.

PLASMA PROPERTIES Annual Progress Report, 1990

Harold Weitzner Aug. 1990 44 p

(Contract DE-FG02-86ER-53223)

(DE91-001361; DOE/ER-53223/146) Avail: NTIS HC/MF A03

The topics of active research in the calendar year 1989 included: RF induced plasma transport, not only for its effects on the mean particle distribution function but also as a means to enhance confinement of particles and to eliminate relatively cold alpha particle ash; thorough statistical analysis of tokamak data; improved neoclassical transport analysis; deeper analysis of two-fluid Braginskii transport in a tokamak; modelling of the plasma edge and wall interaction problem; reformulation of ballooning mode stability analysis in particularly strong and general terms; MHD modelling of tokamak phenomena, such as H-mode transition, and giant sawteeth, description of highly elongated tokamaks; and analysis of edge plasma RF antenna interactions. Our basic plasma physics studies include: statistical mechanics of Coulomb gases in bounded domains; theory of MHD instabilities with flow; numerical scheme for kinetic equations with nontrivial collision operators, and heat flow in particle simulations induced by discreteness effects. In addition, there is a modest space plasma physics effort funded by non-DOE sources. The studies of heating of the solar corona are strongly affected by work from the fusion program. Equally, work on ballooning modes led to work in magnetotail instabilities and additional solar corona heating mechanisms. We except to keep some research effort in this area. We do not include in this proposal plans for any new work in this field. DOE

N91-14007# Lawrence Livermore National Lab., CA. Plasma Physics Research Inst.

STIMULATED RAMAN SCATTER FROM LASER-PRODUCED PLASMAS: MERELY NONLINEAR OR ALSO CHAOTIC

R. Paul Drake and Steven H. Batha 21 Aug. 1990 10 p Presented at the 1990 Summer Workshop on Nonlinear and Chaotic Phenomena in Plasmas, Solids, and Fluids, Edmonton, Alberta, 16-27 Jul. 1990

(Contract W-7405-eng-48)

(DE91-001742; UCRL-JC-104150; CONF-9007136-5) Avail: NTIS HC/MF A03

Stimulated Raman scattering in plasmas is a three-wave instability with important practical consequences for laser fusion. Most studies of this process to date have focused on its threshold. Even the linear-theory threshold poses interesting problems; and observed thresholds have been difficult to interpret. However, with increasing evidence that this instability often becomes absolute, it has become appropriate to examine saturation mechanisms as well. A number of such mechanisms are discussed here, one of which has been reported to have a chaotic regime. DOE

N91-14008# Los Alamos National Lab., NM.

CONFINEMENT AND HEATING STUDIES OF FIELD-REVERSED CONFIGURATIONS

Robert E. Chrien 1990 21 p Presented at the Workshop on Physics of Alternative Magnetic Confinement Schemes, Varenna, Italy, 15-24 Oct. 1990

(Contract W-7405-eng-36)

(DE91-001965; LA-UR-90-3516; CONF-9010209-4) Avail: NTIS HC/MF A03

Confinement studies of field-reversed configurations (FRCs) have been actively pursued during the past ten years with the larger and longer-lived FRCs produced in the FRX-C and FRX-C/LSM devices. Confinement measurements have included the global FRC quantities and, in some cases, profiles of electron temperature and density. The inferred confinement times and transport coefficients are used for comparison with transport models as well as to find the best operating conditions in the experiment. Global power flow modelling shows that energy confinement during the equilibrium phase is usually dominated by particle losses, with a substantial secondary contribution from electron thermal conduction. Particle losses in present kinetic FRCs are strongly influenced by open field line confinement, which complicates the study of transport mechanisms. The electron thermal conduction is observed to be anomalous, as in other plasma devices. The bulk electrical resistivity is also anomalous and shows no evidence of classical Spitzer scaling. Recently, the resistive anomaly has been shown to correlate with tilt-like magnetic perturbations observed with Mirnov coils. FRC confinement studies have also been extended to a higher temperature regime during magnetic compression heating. In these experiments, translated FRCs are compressed by increasing the external magnetic flux up to a factor of seven on a time scale between the radial Alfven time and the FRC lifetime. Electron and ion temperatures up to 0.4 keV and 1.6 keV, respectively have been obtained. Confinement times scale roughly as r(exp 2) during compression. DOE

N91-14009# Los Alamos National Lab., NM.

MAGNETIC TURBULENT ELECTRON TRANSPORT IN A REVERSED FIELD PINCH

Kurt F. Schoenberg and Ronald W. Moses, Jr. 1990 22 p Presented at the International School of Plasma Physics, Varenna, Italy, 15-24 Oct. 1990

(Contract W-7405-eng-36)

(DE91-001898; LA-UR-90-3512; CONF-9010230-6) Avail: NTIS HC/MF A03

A model of magnetic turbulent electron transport is presented. The model, based on the thermal conduction theory of Rechester and Rosenbluth, entails a Boltzmann description of electron dynamics in the long mean-free-path limit and quantitatively describes the salient features of superthermal electron measurements in the RFP edge plasma. Included are predictions of the mean superthermal electron energy, current density, and power flux asymmetry. A discussion of the transport model, the assumptions implicit in the model, and the relevance of this work to more general issue of magnetic turbulent transport in toroidal systems is presented. DOE

N91-14010# Los Alamos National Lab., NM.
MEASUREMENT OF MAGNETIC FLUCTUATIONS ON ZT-40(M)
Guthrie Miller 1990 13 p Presented at the International School of Plasma Physics, Varenna, Italy, 15-24 Oct. 1990
(Contract W-7405-eng-36)
(DE91-001899; LA-UR-90-3511; CONF-9010230-5) Avail: NTIS HC/MF A03

The mathematical basis for experimental measurement of magnetic fluctuations in a Reversed Field Pinch is reviewed. A quasi-static drift model is introduced as the frame-work for analysis of the five-fixed-probe technique. The extrapolation of edge-measured (rvec B)(sub r) fluctuations into the plasma is discussed. Correlations between magnetic and other fluctuations expected from a quasi-static model are derived and transport-relevant correlations are discussed. Data from ZT-40(M) are presented. DOE

N91-14011# Los Alamos National Lab., NM.
KINETIC AND ELECTROMAGNETIC TRANSPORT PROCESSES IN TOROIDAL DEVICES
Ronald W. Moses, Jr. and K. F. Schoenberg 1990 13 p Presented at the International School of Plasma Physics, Varenna, Italy, 15-19 Oct. 1990
(Contract W-7405-eng-36)
(DE91-001901; LA-UR-90-3589; CONF-9010230-7) Avail: NTIS HC/MF A03

A brief review of transport processes in toroidal devices is presented. Particular attention is given to radial transport of power by the Poynting's vector and kinetic electron flow. This work is primarily focused on the Reversed Field Pinch (RFP) which holds the added complexity of a dynamo process that sustains poloidal current in the edge region, where the toroidal field is reversed. The experimental observation of superthermal unidirectional electrons in the plasma edge of ZT-40M and HBTX1C is noted, and the rapid, nonclassical ion heating in RFPs is taken account of. Radial transport parallel to fluctuating magnetic field lines is deemed a likely candidate for both electromagnetic and kinetic energy transport. Two models are discussed and compared. It is concluded that electromagnetic transport using a local Ohm's law best describes nonclassical ion heating, and the transport of kinetic energy by long mean free path electrons best represents the half-Maxwellian of electrons observed in the edge of several RFPs. A nonlocal Ohm's law is essential for the kinetic electron model. DOE

N91-14012# Oak Ridge National Lab., TN. Controlled Fusion Atomic Data Center.
ASSESSMENT OF ION-ATOM COLLISION DATA FOR MAGNETIC FUSION PLASMA EDGE MODELLING
R. A. Phaneuf 1990 23 p Presented at the IAEA Atomic and Molecular Data for Fusion Edge Plasmas Conference, Vienna, Austria, 24-26 Sep. 1990
(Contract DE-AC05-84OR-21400)
(DE91-001920; CONF-9009283-1) Avail: NTIS HC/MF A03

Cross-section data for ion-atom collision processes which play important roles in the edge plasma of magnetically-confined fusion devices are surveyed and reviewed. The species considered include H, He, Li, Be, C, O, Ne, Al, Si, Ar, Ti, Cr, Fe, Ni, Cu, Mo, W and their ions. The most important ion-atom collision processes occurring in the edge plasma are charge-exchange reactions. Excitation and ionization processes are also considered. The scope is limited to atomic species and to collision velocities corresponding to plasma ion temperatures in the 2 to 200 eV range. Sources of evaluated or recommended data are presented where possible, and deficiencies in the data base are indicated. DOE

N91-14013# Idaho National Engineering Lab., Idaho Falls.
MEASUREMENT OF AIR ENTRAINMENT IN PLASMA JETS
J. R. Fincke, R. Rodriquez, and C. G. Pentecost 1990 6 p Presented at the 3rd National Thermal Spray Conference and Exposition, Long Beach, CA, 21-24 May 1990
(Contract DE-AC07-76ID-01570)
(DE91-001943; EGG-M-89488; CONF-900520-1) Avail: NTIS HC/MF A02

The concentration and temperature of air entrained into argon and helium plasma jets has been measured using coherent anti-Stokes Raman spectroscopy (CARS). The argon plasma flow field is characterized by a short region of well behaved laminar flow near the nozzle exit followed by an abrupt transition to turbulence. Once the transition of turbulence occurs, air is rapidly mixed into the jet core. The location of the transition region is determined by the rapid cooling of the jet and the resulting increase in Reynolds number. In contrast, the helium plasma flow field never exceeds a Reynolds number of 200 and remains laminar. The entrainment process in this case is controlled by molecular diffusion rather than turbulent mixing. DOE

N91-14014# Los Alamos National Lab., NM.
TWO-FLUID SIMULATIONS OF THE REVERSED-FIELD PINCH
R. A. Nebel 1990 21 p Presented at the International School of Plasma Physics, Varenna, Italy, 15-19 Oct. 1990
(Contract W-7405-eng-36)
(DE91-001961; LA-UR-90-3534; CONF-9010230-2) Avail: NTIS HC/MF A03

Two fluid and transport effects have recently been incorporated into the 3-D MHD code (Debs) originally developed by Schnack and coworkers. These include the Hall effect, diamagnetic drift effects, Braginskii viscosity and anisotropic thermal conduction. Incorporation of these effects required the development of new semi-implicit operators in order to provide numerical stability. Both anisotropic thermal conduction and parallel viscosity make the equations extremely stiff and require some care in formulation in order to avoid matrix conditioning problems. In general, these new concerns favor using simple isotropic operators (such as nabla(exp 2)) over the less dispersive but exact anisotropic semi-implicit operators. These numerical formulations will be discussed in detail. Accuracy and poisoning checks also will be presented. Results indicate that a number of new phenomena are present in these extended equations. For instance, the dynamo effect is seen to emerge from the Hall terms rather than the MHD terms if the viscosity is large. The observed relaxation is also much more robust than its MHD counterpart. Resistive wall instabilities are seen to lock nonlinearly to the wall if the edge viscosity is large but not to lock if the viscosity is small. Similarly, resistive g-modes are also very sensitive to the amount of viscosity present. The significant factor in all of these phenomena appears to be the parallel viscosity. DOE

N91-14015# Los Alamos National Lab., NM.
CONFINEMENT PROPERTIES OF THE RFP (REVERSED FIELD PINCH)
P. G. Weber, K. F. Schoenberg, J. C. Ingraham, Guthrie Miller, C. P. Munson, M. M. Pickrell, G. A. Wurden, H. Y. W. Tsui, Ch. P. Ritz, and R. F. Ellis (Maryland Univ., College Park.) 1990 18 p Presented at the International School of Plasma Physics, Varenna, Italy, 14-24 Oct. 1990
(Contract W-7405-eng-36)
(DE91-002322; LA-UR-90-3457; CONF-9010230-3) Avail: NTIS HC/MF A03

Research in ZT-40M has been focused on elucidating the confinement properties of the Reversed Field Pinch (RFP). Recent improvements in diagnostic capability have permitted measurement

of radial profiles, as well as a detailed study of the edge plasma. The emerging confinement picture for ZT-40M has several ingredients: Typically 0.3 of the Ohmic input power to ZT-40M is available to drive fluctuations. Evidence points to this fluctuational power heating the ions. Approximately one quarter of the input power is lost through radiation, with metal impurities playing a key role. Magnetic fluctuations in ZT-40M are at the percent level, as measured in the edge plasma. Extrapolating these data to small radii shows stochasticity in the core plasma. Suprathermal electrons are measured in the edge plasma. These electrons originate in the core, and transport to the edge along the fluctuating magnetic field lines. Under typical conditions, these electrons constitute the major electron energy loss channel in ZT-40M. Electrostatic fluctuations dominate the edge electron particle flux, but not the electron thermal flux. The major ion loss process is charge exchange, with smaller contributions from conduction and convection. In examining these observations, and the parametric dependences of confinement, a working model for RFP confinement emerges. An overview of this model, together with implications for the multi-mega-ampere ZTH experiment will be presented. DOE

N91-14016# Lawrence Livermore National Lab., CA.
COMPACT IGNITION TOKAMAK PROJECT: LOCALIZABILITY OF ELECTRON-CYCLOTRON HEATING POWER
Gary R. Smith 25 Oct. 1990 5 p
(Contract W-7405-eng-48)
(DE91-002571; UCRL-ID-105222) Avail: NTIS HC/MF A01

Estimates of the localizability of electron-cyclotron heating power are made for the Compact Ignition Tokamak. A particular heating scenario is examined, namely, the fundamental O-mode, injected nearly perpendicular to the toroidal magnetic field. The absorption depth due to finite T(sub e) is very small, about 1 cm, near the q = 2 surface. Absorption is even better localized near q = 1. Several issues that might lead to degraded localizability are reviewed. Use of an intense, pulsed microwave source is the only issue with a possibly significant impact. DOE

N91-14017# Oak Ridge National Lab., TN.
INTERNATIONAL THERMONUCLEAR EXPERIMENTAL REACTOR PHYSICS BASIS
N. A. Uckan and D. E. Post (Princeton Univ., NJ.) 1990 20 p Presented at the 9th Topical Meeting on Technologyof Fusion Energy, Oak Brook, 7-11 Oct. 1990
(Contracts DE-AC05-84OR-21400; DE-AC02-76CH-03073)
(DE91-002646; CONF-901007-23) Avail: NTIS HC/MF A03

The physics basis of ITER has been developed from an assessment of the present knowledge of tokamak physics with allowance for improvements in that knowledge during the design and construction phases of ITER. The assessment has been carried out by the ITER design team in collaboration with the international fusion program, including participation by the experimental teams of all of the major toroidal experiments. The physics basis consists of guidelines for energy confinement, operational limits, power and particle control, disruptions, current drive and heating, alpha particle physics, and plasma control. The ITER physics group has worked with the engineering groups to implement these guidelines. In addition, a preliminary design for the plasma diagnostics for ITER has been developed and an operational program has been planned. In many cases, the physics issues have not been fully resolved, and a physics R and D program has been developed to complete the physics basis for ITER. DOE

N91-14018# Oak Ridge National Lab., TN.
ITER CONFINEMENT CAPABILITY
N. A. Uckan and J. T. Hogan 1990 15 p Presented at the 9th Topical Meeting on Technology of Fusion Energy, Oak Brook, IL, 7-11 Oct. 1990
(Contract DE-AC05-84OR-21400)
(DE91-002647; CONF-901007-24) Avail: NTIS HC/MF A03

The confinement capability of ITER was examined for a number of operational scenarios. The reference ITER physics baseline scenario (I = 22 MA) allows ignited burn under H-mode conditions tau(sub E)(H-mode) is approximately 2 times tau(sub E)(L-mode). At higher currents (I = 25 to 28 MA) at which ITER can operate for limited pulse duration, there is an increased ignition margin if low-q operation proves acceptable. About a factor of 2 reduction in helium ash concentration (from the baseline value of 10 to 5 percent) in the reference ITER scenario has about the same impact on ignition capability as increasing the plasma current by about 15 percent (from the baseline value of 22 MA to greater than or equal to 25 MA). It might be possible to further optimize the ignition capability of ITER if some of the limits on operational boundaries can be relaxed by tailoring plasma profiles. DOE

N91-14019# Oak Ridge National Lab., TN.
DEPENDENCE OF CIT (COMPACT IGNITION TOKAMAK) PF (POLOIDAL FIELD) COIL CURRENTS ON PROFILE AND SHAPE PARAMETERS USING THE CONTROL MATRIX
D. J. Strickler, Y.-K. M. Peng, S. C. Jardin, and N. Pomphrey (Princeton Univ., NJ.) 1990 18 p Presented at the 9th Topical Meeting on Technology of Fusion Energy, Oak Brook, IL, 7-11 Oct. 1990
(Contract DE-AC05-84OR-21400)
(DE91-002650; CONF-901007-25) Avail: NTIS HC/MF A03

The plasma shaping flexibility of the Compact Ignition Tokamak (CIT) poloidal field (PF) coil set is demonstrated through MHD equilibrium calculations of optimal PF coil current distributions and their variation with poloidal beta, internal inductance, plasma 95 percent elongation, and 95 percent triangularity. Calculations of the magnetic stored energy are used to compare solutions associated with various plasma parameters. The Control Matrix (CM) equilibrium code, together with the nonlinear equation and numerical optimization software packages HYBRD, and VMCON, respectively, are used to find equilibrium coil current distributions for fixed divertor geometry, volt-seconds, and plasma profiles in order to isolate the dependence on individual parameters. A reference equilibrium and coil current distribution are chosen, and correction currents dI are determined using the CM equilibrium method to obtain other specified plasma shapes. The reference equilibrium is the kappa = 2 divertor at beginning of flattop (BOFT) with a minimum stored energy solution for the coil current distribution. The pressure profile function is fixed. DOE

N91-14020# Lawrence Livermore National Lab., CA.
A RAPID RELATIVISTIC DISTORTED WAVE APPROACH FOR CALCULATING CROSS SECTIONS FOR IONIZATION OF HIGHLY CHARGED IONS
Hong Lin Zhang and Douglas H. Sampson (Pennsylvania State Univ., University Park.) 22 Oct. 1990 18 p
(Contracts W-7405-eng-48; DE-FG02-85ER-53208; N00014-88-K-2021)
(DE91-002667; UCRL-CR-105109) Avail: NTIS HC/MF A03

The rapid relativistic distorted wave method of Zhang et al., for excitation, which uses the atomic structure data of Sampson et al., has been extended to ionization. In this approach the same Dirac-Fock-Slater potential evaluated using a single mean configuration is used in calculating the orbitals of all electrons bound and free. Values for the cross sections Q for ionization of various ions have been calculated and generally good agreement is obtained with other recent relativistic calculations. When results are expressed in terms of the reduced ionization cross section Q(sub R), which is proportional to I(exp 2)Q, they are close to the non-relativistic Coulomb-Born-Exchange values of Moores et al., for hydrogenic ions except for high Z and/or high energies. This suggests that fits of the Q(sub R) to simple functions of the impact electron energy in threshold units with coefficients that are quite slowly varying functions of an effective Z can probably be made. This would be convenient for plasma modeling applications. DOE

N91-14021# Lawrence Livermore National Lab., CA.
FAST Pb-GLASS NEUTRON-TO-LIGHT CONVERTER FOR ICF (INERTIAL CONFINEMENT FUSION) TARGET BURN HISTORY MEASUREMENTS
R. A. Lerche, M. D. Cable, and D. W. Phillion Presented at the

8th Topical Conference on High-Te Sep. 1990 Presented at the 8th Topical Conference on High-temperature Plasma Diagnostics, Hyannis, MA, 6-10 May 1990 (For primary document see
(Contract W-7405-eng-48)
(DE91-002670; UCRL-JC-103281; CONF-900557-26) Avail: NTIS HC/MF A03

We are developing a streak camera based instrument to diagnose the fusion reaction rate (burn history) within laser-driven ICF targets filled with D-T fuel. Recently, we attempted measurements using the 16.7 MeV gamma ray emitted in the T(d,gamma)He(5) fusion reaction. Pb glass which has a large cross section for pair production acts as a gamma-ray-to-light converter. Gamma rays interact within the glass to form electron-positron pairs that produce large amounts (1000 photons/gamma ray) of prompt (less than 10 ps) Cerenkov light as they slow down. In our experimental instrument, an f/10 Cassegrain telescope optically couples light produced within the converter to a streak camera having 20-ps resolution. Experiments using high-yield (10(exp 13) D-T neutrons), direct-drive targets at Nova produced good signals with widths of 200 ps. Time-of-flight measurements show the signals to be induced by neutrons rather than gamma rays. The Pb glass appears to act as a fast neutron-to-light converter. We continue to study the interactions process and the possibility of using the 16.7 MeV gamma rays for burn time measurements. DOE

N91-14022# General Atomic Co., San Diego, CA.
A 15 MeV PROTON DIANOSTIC FOR DIII-D
Hau Duong and W. W. Heidbrink (California Univ., Irvine.) Oct. 1990 11 p Presented at the 8th Topical Conference on High-Temperature Plasma Diagnostics, Hyannis, MA, 7-10 May 1990 Submitted for publication
(Contract DE-AC03-89ER-51114; GA Proj. 3466)
(DE91-002717; GA-A-20111; CONF-900557-32) Avail: NTIS HC/MF A03

A 15 MeV proton diagnostic that is patterned after the ASDEX proton probe is presently being fabricated for the DIII-D tokamak. A bellows assembly inserts a silicon detector into the vacuum for plasma operation and retracts it for baking. The detector preamplifier is situated in a reentrant tube (at atmosphere) beside the detector; electrically, the whole assembly is referenced to vessel potential. Orbit calculations in realistic magnetic field geometries predict a proton detection efficiency of O x 10 (exp -7). The diagnostic will be used for burnup studies at high (beta) and particle transport studies in the H-mode. DOE

N91-14023# General Atomic Co., San Diego, CA.
HIGH SPATIAL AND TEMPORAL RESOLUTION VISIBLE SPECTROSCOPY OF THE PLASMA EDGE IN DIII-D
P. Gohil, K. H. Burrell, R. J. Groebner, and R. P. Seraydarian Oct. 1990 11 p Presented at the 8th Topical Conference on High-Temperature Plasma Diagnostics, Hyannis, MA, 7-10 May 1990 Submitted for publication
(Contract DE-AC03-89ER-51114; GA Proj. 3466)
(DE91-002718; GA-A-20105; CONF-900557-23) Avail: NTIS HC/MF A03

In DIII-D, visible spectroscopic measurements of the He II 468.6 nm and C VI 529.2 nm Doppler broadened spectral lines, resulting from charge exchange recombination interactions between beam neutral atoms and plasma ions, are performed to determine ion temperatures, and toroidal and poloidal rotation velocities. The diagnostics system comprises 32 viewing chords spanning a typical minor radius of 63 cm across the midplane, of which 16 spatial chords span 11 cm of the plasma edge just within the separatrix. A temporal resolution of 260 msec per time slice can be obtained as a result of using MCP phosphors with short decay times and fast camera readout electronics. Results from this system will be used in radial electric field comparisons with theory at the L-H transition and ion transport analysis. DOE

N91-14024# General Atomic Co., San Diego, CA.
A COMPACT, LOW COST, 7 CHANNEL POLYCHROMATOR FOR THOMSON SCATTERING MEASUREMENTS
T. N. Carlstrom, J. C. DeBoo, R. Evanko, C. M. Greenfield, C.-L. Hsieh, R. T. Snider, and P. Trost Oct. 1990 12 p Presented at the 8th Topical Conference on High-Temperature Plasma Diagnostics, Hyannis, MA, 7-10 May 1990 Submitted for publication
(Contract DE-AC03-89ER-51114; GA Proj. 3466)
(DE91-002719; GA-A-20098; CONF-900557-24) Avail: NTIS HC/MF A03

A seven channel polychromator, utilizing high performance interference filters, was tested for use in the multi-Nd:YAG laser Thomson scattering system for the DIII-D tokamak. Unique features of this polychromator are the combination of high throughput, easy alignment, flexibility, compact size, and low cost when compared with other alternatives. Light is introduced to the polychromator (f/1.75) via a fiber optic bundle which permits the use of small (3.0 cm dia) optics and leads to a compact design, an important design consideration for multiple polychromator systems. The light is cascaded through a series of different bandpass interference filters and relay lenses which are mounted on two precision parallel rails in such a way that alignment is trivial. The relay lenses are positioned directly in front of the filters so that light reflected from the filter passes through the lens twice. This leads to an efficient, compact design and reduces the angle of incidence (4 deg) and the cone angle of light (4.5 deg) seen by the filter, an important factor for narrowband (3.0 nm) filters. The transmission was optimized for 700 to 1100 nm by using broadband coatings throughout. The output images of each channel (2.3 mm dia) can be directly coupled to large format (3 nm dia) RCA silicon avalanche photodiode detectors, avoiding the losses caused by fiber optic coupling. DOE

N91-14025# General Atomic Co., San Diego, CA.
A REAL-TIME DIGITAL CONTROL, DATA ACQUISITION AND ANALYSIS SYSTEM FOR THE DIII-D MULTIPULSE THOMSON SCATTERING DIAGNOSTIC
C. M. Greenfield, G. L. Campbell, T. N. Carlstrom, J. C. DeBoo, C.-L. Hsieh, R. T. Snider, and P. K. Trost Oct. 1990 13 p Presented at the 8th Topical Conference on High-Temperature Plasma Diagnostics, Hyannis, MA, 7-10 May 1990 Submitted for publication
(Contract DE-AC03-89ER-51114; GA Proj. 3466)
(DE91-002720; GA-A-20097; CONF-900557-25) Avail: NTIS HC/MF A03

A VME-based real time computer systems for laser control, data acquisition and analysis for the DIII-D multipulse Thomson scattering diagnostic is described. The laser control task requires precise timing of up to 8 Nd:YAG lasers, each with an average firing rate of 20 Hz. A cpu module in real time multiprocessing computer system will operate the lasers with evenly staggered laser pulses or in a 'burst mode', where all available (fully charged) lasers can be fired at 50 to 100 msec intervals upon receipt of an external event trigger signal. One of more cpu modules, along with a LeCroy FERA (Fast Encoding and Readout ADC) system, will perform real time data acquisition and analysis. Partial electron temperature and density profiles will be available for plasma feedback control within 1 msec following each laser pulse. The VME-based computer system consists of 2 or more target processor modules (25 MHz Motorola 68030) running the VMEexec real time operating system connected to a Unix based Host system (also a 68030). All real time software is fully interrupt driven to maximize system efficiency. Operator interaction and (non real-time) data analysis takes place on a MicroVAX 3400 connected via DECnet. DOE

N91-14026# KMS Fusion, Inc., Ann Arbor, MI.
EXPERIMENTAL DEVELOPMENT, TESTING, AND RESEARCH WORK IN SUPPORT OF THE INERTIAL CONFINEMENT FUSION PROGRAM Annual Technical Report, Oct. 1988 - Sep. 1989
Douglas J. Drake, ed., Ruth Luckhardt, ed., Sandra Moyer, ed., Charles J. Armentrout, ed., Raymond L. Downs, ed., and Kent Moncur, ed. 28 Feb. 1990 309 p

(Contract DE-AC03-87DP-10560)
(DE91-002770; DOE/DP-10560/8; KMSF-U-2339) Avail: NTIS HC/MF A14

This report discusses: cryogenic technology; polymer shell fabrication; glass shell fabrication and characterization; coating technology; development of characterization techniques; laser technology; and plasma research and instrumentation. DOE

N91-14027# Technische Hochschule, Darmstadt (Germany, F.R.). Fachbereich Physik.
IONIZATION DEGREE OF CLASSICAL, DENSE, AND HIGHLY CONDENSED PLASMAS Ph.D. Thesis [IONISATIONSGRAD KLASSISCHER, DICHTER UND HOCHVERDICHTETER PLASMEN]
Susanne Pfalzner 1989 94 p In GERMAN
(ETN-91-98174) Avail: NTIS HC/MF A05

Models for the calculation of the ionization degree were investigated, and simple methods for the determination of the ionization degree were developed. The determination of the ionization degree of classical plasmas using the Saha equation is outlined. The statistical Thomas-Fermi (TF) model for the determination of the ionization degree of highly condensed plasmas is discussed. The effect of the ion temperature on the ionization degree was investigated. The effect of the density on the ionization potential in the TF model is outlined with a view to the calculation of the ionization degree in very high density plasmas. Local thermal ionization equilibrium in high density plasmas is discussed. ESA

N91-14028# Argonne National Lab., IL.
MODELING AND ANALYSIS OF SURFACE ROUGHNESS EFFECTS ON SPUTTERING, REFLECTION, AND SPUTTERED PARTICLE TRANSPORT
J. N. Brooks and D. N. Ruzic (Illinois Univ., Urbana.) 1990 17 p Presented at the 9th Plasma Surface Interactions in Controlled Fusion Devices Conference, Bournemouth, England, 20-25 May 1990
(Contract W-31-109-eng-38)
(DE91-004429; CONF-900505-10) Avail: NTIS HC/MF A03

The microstructure of the redeposited surface in tokamaks may affect sputtering and reflection properties and subsequent particle transport. This subject has been studied numerically using coupled models/codes for near-surface plasma particle kinetic transport (WBC code) and rough surface sputtering (fractal-TRIM). The coupled codes provide an overall Monte Carlo calculation of the sputtering cascade resulting from an initial flux of hydrogen ions. Beryllium, carbon, and tungsten surfaces are analyzed for typical high recycling, oblique magnetic field, divertor conditions. Significant variations in computed sputtering rates are found with surface roughness. Beryllium exhibits high D-T and self-sputtering coefficients for the plasma regime studied (T(sub e) = 30-75 eV). Carbon and tungsten sputtering is significantly lower. DOE

76 SOLID-STATE PHYSICS

Includes superconductivity.

For related information, see also *33 Electronics and Electrical Engineering* and *36 Lasers and Masers.*

N91-14029*# Alabama Univ., Huntsville. Center for Microgravity and Materials Research.
DEFINITION STUDY FOR TEMPERATURE CONTROL IN ADVANCED PROTEIN CRYSTAL GROWTH Final Report, 14 Mar. - 30 Sep. 1990
Thomas A. Nyce, Franz Rosenberger, Jennifer W. Sowers, and Lisa A. Monaco 30 Sep. 1990 27 p
(Grant NAG8-824)
(NASA-CR-187346; NAS 1.26:187346) Avail: NTIS HC/MF A03 CSCL 20L

Some of the technical requirements for an expedient application of temperature control to advanced protein crystal growth activities are defined. Lysozome was used to study the effects of temperature ramping and temperature gradients for nucleation/dissolution and consecutive growth of sizable crystals and, to determine a prototype temperature program. The solubility study was conducted using equine serum albumin (ESA) which is an extremely stable, clinically important protein due to its capability to bind and transport many different small ions and molecules. Author

N91-14030# Advisory Group for Aerospace Research and Development, Neuilly-Sur-Seine (France). Avionics Panel.
APPLICATIONS OF SUPERCONDUCTIVITY TO AVIONICS
Oct. 1990 164 p Meeting held in Bath, England, 7-8 May 1990
(AGARD-CP-481; ISBN-92-835-0586-7) Copyright Avail: NTIS HC/MF A08; Non-NATO Nationals requests available only from AGARD/Scientific Publications Executive

Recent advances in developing high temperature superconductors have renewed interest in the entire superconductivity field. Modern techniques in materials preparation are making it possible to fabricate a number of new superconducting components which promise significant improvements in the performance of avionics systems. The almost daily revelation of advances in this area attests to its importance as an emerging technology. Device scientists and avionics engineers explore the possibilities for exploiting all aspects of superconductivity in avionics systems. For individual titles, see N91-14031 through N91-14048.

N91-14031# Royal Signals and Radar Establishment, Malvern (England).
PROGRESS IN HIGH Tc SUPERCONDUCTORS
R. G. Humphreys, N. G. Chew, S. W. Goodyear, J. A. Edwards, J. S. Satchell, and S. E. Blenkinsop *In* AGARD, Applications of Superconductivity to Avionics Oct. 1990 7 p (For primary document see N91-14030 05-76)
Copyright Avail: NTIS HC/MF A08; Non-NATO Nationals requests available only from AGARD/Scientific Publications Executive

The high temperature superconductor materials are introduced, and their properties relating to applications reviewed, with particular reference to the prospects for fabrication of devices. Recent results on the factors relating to the growth of smooth high quality YBa2Cu3O7 thin films are presented. Author

N91-14032# Royal Military Coll. of Canada, Kingston (Ontario). Dept. of Science.
PHYSICS AND APPLICATIONS OF LOW TEMPERATURE SUPERCONDUCTIVITY
D. C. Baird *In* AGARD, Applications of Superconductivity to Avionics Oct. 1990 25 p (For primary document see N91-14030 05-76)
Copyright Avail: NTIS HC/MF A08; Non-NATO Nationals requests available only from AGARD/Scientific Publications Executive

A historically-based introduction to low temperature superconductivity is provided. Those aspects of the basic physics that underlie the practical applications of superconductors and that are significant for understanding the properties of the new high temperature superconductors are emphasized. Author

N91-14033# Laboratoire Central de Recherches Thomson-CSF, Orsay (France).
HIGH TEMPERATURE SUPERCONDUCTING THIN FILMS FOR MICROELECTRONICS: PREPARATION AND PROPERTIES
G. Creuzet, R. Cabanel, and A. Schuhl *In* AGARD, Applications of Superconductivity to Avionics Oct. 1990 8 p (For primary document see N91-14030 05-76)
Copyright Avail: NTIS HC/MF A08; Non-NATO Nationals requests available only from AGARD/Scientific Publications Executive

The discovery of high temperature superconductors (HTSC) has generated a great deal of activity, both fundamental and towards applications. For the latter, low current devices appear to be particularly interesting. The fundamental building block of superconducting electronics is the Josephson junction, in which two superconducting electrodes are isolated by a thin metallic (SNS) or insulating (SIS) barrier. Due to the extreme low value of the coherence length in these compounds, one has to achieve

very thin (a few nm) barriers with sharp interfaces with the superconducting material. This leads first to the major challenge of producing HTSC epitaxial films controlled at the atomic level. For HTSC thin film preparation, reasonable good films are now available routinely using the laser ablation technique. In particular, these films present high frequency characteristics which are good enough to develop superconducting components like microstrips for delay lines. For Josephson junction electronics, the requirements, especially for the barrier thickness control, are much more ambitious. In this context, molecular beam epitaxy, and furthermore atomic layer epitaxy, appear to be very promising.
Author

N91-14034# American Superconductor Corp., Watertown, MA.
SUCCESS CRITERIA FOR OXIDE SUPERCONDUCTOR WIRES: MEASURING THE PRESENT, PREDICTING THE FUTURE
Carl J. Russo *In* AGARD, Applications of Superconductivity to Avionics Oct. 1990 7 p (For primary document see N91-14030 05-76)
Copyright Avail: NTIS HC/MF A08; Non-NATO Nationals requests available only from AGARD/Scientific Publications Executive

Successful application of oxide superconductor wires to large-scale applications requires: high critical current in long lengths at high fields; adequate mechanical properties for handling; a process technology scalable to production quantities; corrosion resistance; adequate strength at low temperatures in high fields; superconducting joints; cryostability; and low ac losses. The present state of conductor development is discussed in terms of several figures of merit. Historical data is evaluated, technology challenges is investigated, and predictions for the future of oxide superconductor wire development are examined. Author

N91-14035# Rutherford Appleton Lab., Chilton (England).
MINIATURE CLOSED CYCLE REFRIGERATORS c31
T. W. Bradshaw and A. H. Orlowska *In* AGARD, Applications of Superconductivity to Avionics Oct. 1990 7 p (For primary document see N91-14030 05-76)
Copyright Avail: NTIS HC/MF A08; Non-NATO Nationals requests available only from AGARD/Scientific Publications Executive

A closed cycle cooler suitable for long-life space applications is described. The development heritage and the mechanical design are described and the inherently long life-time characteristics of the cooler are explained. Many types of cooler were developed from the original concept; those developed at the Rutherford Appleton Laboratory (RAL) are the main focus. Author

N91-14036# Birmingham Univ. (England). Dept. of Electronic and Electrical Engineering.
PASSIVE MICROWAVE DEVICES USING HIGH TEMPERATURE SUPERCONDUCTORS
M. J. Lancaster, T. S. M. Maclean, Z. Wu, C. E. Gough, and N. McN. Alford *In* AGARD, Applications of Superconductivity to Avionics Oct. 1990 6 p (For primary document see N91-14030 05-76)
Copyright Avail: NTIS HC/MF A08; Non-NATO Nationals requests available only from AGARD/Scientific Publications Executive

Passive microwave devices that benefit from the inclusion of a superconducting element are listed. Three devices out of the list; a superconducting loop antenna, a superconducting filter, and a cavity resonator were designed, built, and tested. The advantages of each of these components are reviewed and results of their performance are presented. Author

N91-14037# Laboratoire Central de Recherches Thomson-CSF, Orsay (France).
MICROWAVE SUPERCONDUCTING ELECTRONIC DEVICES
P. Hartemann *In* AGARD, Applications of Superconductivity to Avionics Oct. 1990 7 p (For primary document see N91-14030 05-76)
Copyright Avail: NTIS HC/MF A08; Non-NATO Nationals requests available only from AGARD/Scientific Publications Executive

The present and future applications of superconductors to the small-scale microwave electronics are reviewed by taking into account the results obtained with the conventional superconductors and the potentialities of the new high-temperature superconductors. The signal transmission by superconductive planar waveguides is surveyed. Then the effect of the electrode thickness on the propagation loss and velocity along superconductive microstrip waveguides is pointed out. The use of Josephson junctions in mixers or amplifiers or generators of periodic signals is considered. Examples of signal processing devices including linear or nonlinear superconducting elements are given. Their main characteristics are compared to those feasible by other techniques. Author

N91-14038# Laboratoire Central de Recherches Thomson-CSF, Orsay (France).
HIGH Tc SUPERCONDUCTORS FOR MICROWAVE FILTERS
J. C. Mage and D. Dieumegard *In* AGARD, Applications of Superconductivity to Avionics Oct. 1990 8 p (For primary document see N91-14030 05-76)
Copyright Avail: NTIS HC/MF A08; Non-NATO Nationals requests available only from AGARD/Scientific Publications Executive

Passive microwave components will probably be the first application of high Tc superconductors. Devices such as multi-pole filters, delay lines, transversal filters with improved performances can easily be developed as soon as reliable high quality superconducting thin films are available. The basic constituent of these devices is a microwave line which consists of a superconducting layer deposited on a dielectric substrate then patterned. At the present time, the accurate characterization of both superconducting and dielectric materials is the main topic of the research activities in cooperation with the improvement of deposition techniques. Author

N91-14039# Hitachi Ltd., Tokyo (Japan). Superconducting Electronics Research Center.
THE STATUS-QUO AND PROSPECT OF SUPERCONDUCTING DIGITAL DEVICES
Ushio Kawabe *In* AGARD, Applications of Superconductivity to Avionics Oct. 1990 12 p (For primary document see N91-14030 05-76)
Copyright Avail: NTIS HC/MF A08; Non-NATO Nationals requests available only from AGARD/Scientific Publications Executive

Superconducting digital devices, featuring high-speed, small size, and low power dissipation, are expected to be one of key components of future computer system. Currently, research and development are continued to demonstrate the possibility of the superconducting computer system above 1 GHz clock using highly reliable Nb/AlO(x)/Nb Josephson junctions with small size and high current density and further to explore new digital devices capable with higher speeds and higher levels of integration. The striking feature is that superconducting digital devices have a small switching energy below 0.1 fJ and that they can be connected with a lossless superconducting wiring. From this good performance, a giga-scale integration type parallel-processing computer is promising through the heat flux and cooling power in cryogenic environment are taken into consideration. The status-quo and prospect of superconducting digital devices are discussed.
Author

N91-14040# TRW, Inc., Redondo Beach, CA. Space and Technology Group.
ANALOG SUPERCONDUCTIVE ELECTRONICS FOR AVIONICS c33
A. H. Silver and A. D. Smith *In* AGARD, Applications of Superconductivity to Avionics Oct. 1990 5 p (For primary document see N91-14030 05-76)
Copyright Avail: NTIS HC/MF A08; Non-NATO Nationals requests available only from AGARD/Scientific Publications Executive

Superconductive electronics may solve critical problems in avionic sensors and signal processing. This results from both fundamental considerations such as low RF loss and power dissipation, flux quantization, and the Josephson effect. Because new physical mechanisms can be applied, new device configurations can be employed. This presentation describes the state-of-the-art and project near-term applications. Examples of

high leverage superconductive technology in analog signal processing, analog-to-digital converters, low noise receivers, and phased array components are presented. Both high temperature copper-oxides and low temperature metallic superconductors are discussed. Author

N91-14041# Air Force Materials Lab., Wright-Patterson AFB, OH.
FABRICATION AND CHARACTERIZATION OF HIGH TEMPERATURE SUPERCONDUCTING THIN FILMS FOR SENSORS AND ELECTRONICS **c33**
P. M. Hemenger, T. L. Peterson, R. Fletcher, I. Maartense, P. T. Murray, and D. W. Chung (San Jose State Univ., CA.) *In* AGARD, Applications of Superconductivity to Avionics Oct. 1990 8 p (For primary document see N91-14030 05-76)
(Contract F33615-88-C-5423)
Copyright Avail: NTIS HC/MF A08; Non-NATO Nationals requests available only from AGARD/Scientific Publications Executive

Superconducting thin films of YBa2Cu3O(x-7) that do not require post-annealing were deposited on SrTiO3 substrates using laser ablation. The electrical, magnetic, optical, and structural properties of the films were analyzed in order to identify and control the processing parameters which lead to optimization of the material's properties. The laser deposition process using an ArF excimer laser to grow high temperature superconducting (HTS) films is described. Detailed characterization of the films using ac magnetic susceptibility measurements is emphasized, because this technique is valuable as a screening tool. In one temperature scan from 4.2 to 125 K the critical temperature, Tc, the width of the transition, the presence of additional superconducting phases, the film's response to magnetic fields, and the critical current, Jc, are obtained. The susceptibility results are correlated with transport measurements of Jc(T) and Tc(R = 0). Process control is essential when fabricating HTS materials for avionics applications. A process optimized to produce the best properties for one particular application such as high Jc, for interconnects will probably not be an optimal process for producing sensor material. High current-carrying capability is generally not important for sensors, but rather good optical properties and low noise characteristics. The material requirements will also differ depending upon the type of sensor, e.g., bolometric or non-equilibrium. Some applications will require more stringent control of surface morphology, grain structure, and crystallographic orientation than will other applications. For these reasons a parametric study of the process is required in order to fabricate material with properties optimized for each application. Author

N91-14042# Honeywell, Inc., Minneapolis, MN.
APPLICATION OF HIGH-TEMPERATURE SUPERCONDUCTORS TO HIGH-PRECISION ACCELEROMETERS **c35**
James Lenz, Quark Chen, James McArdle, Tom Werner, and Wayne Castleman *In* AGARD, Applications of Superconductivity to Avionics Oct. 1990 7 p Sponsored by DARPA, Washington, DC and ONR, Washington, DC (For primary document see N91-14030 05-76)
Copyright Avail: NTIS HC/MF A08; Non-NATO Nationals requests available only from AGARD/Scientific Publications Executive

Superconducting materials offer unique capabilities to high-precision acceleration sensing. Two specific aspects are shielding of magnetic fields and magnetic levitation due to the Meissner Effect. The basic configuration and operation of accelerometers using superconducting materials are reviewed. Physical properties such as conductivity, permeability, trapped magnetic flux, and material uniformity are correlated to shielding and levitation performance. Measurements of these properties for the YBaCuO superconductors are included. Author

N91-14043# Naval Air Development Center, Warminster, PA.
SUPERCONDUCTING JOSEPHSON JUNCTION GYROSCOPE (JJG) **c35**
Francis A. Karwacki *In* AGARD, Applications of Superconductivity to Avionics Oct. 1990 4 p (For primary document see N91-14030 05-76)
Copyright Avail: NTIS HC/MF A08; Non-NATO Nationals requests available only from AGARD/Scientific Publications Executive

A multi-year effort to develop a Josephson Junction Gyroscope (JJG) is described. The goal is to develop a small solid-state gyroscope that utilizes the phase coherence of Cooper-paired electrons to measure applied rotation. The research is divided into a low temperature proof of concept, high temperature material research, Josephson junction development, and the development of an experimental test facility. Author

N91-14044# Thomson SINTRA ASM (France).
SQUIDs DEVICES MADE FROM HIGH Tc SUPERCONDUCTORS: RESULTS AND PERSPECTIVES **c33**
Ronan Stephan *In* AGARD, Applications of Superconductivity to Avionics Oct. 1990 8 p (For primary document see N91-14030 05-76)
Copyright Avail: NTIS HC/MF A08; Non-NATO Nationals requests available only from AGARD/Scientific Publications Executive

After a brief presentation of magnetic sensoring, results are presented, dealing with thick superconductive films where the intergranular native weak-links were used. The potential of high temperature superconductors (HTSCs) in SQUID magnetometry is introduced with emphasis on the utilization of thin films. Author

N91-14045# International Research and Development Co. Ltd., Fossway (England).
THE WORLD OF SUPERCONDUCTIVE MACHINERY **c37**
A. D. Appleton *In* AGARD, Applications of Superconductivity to Avionics Oct. 1990 10 p (For primary document see N91-14030 05-76)
Copyright Avail: NTIS HC/MF A08; Non-NATO Nationals requests available only from AGARD/Scientific Publications Executive

The development of superconducting machinery has been in progress since the early 1960's. A summary of the progress which was made to date together with a view on the likely developments in the future is presented. The bulk of the work in respect of rotating machinery was on dc homopolar motors and generators, and ac generators; the superconducting components are the stationary field windings of the dc machines and the rotating dc field windings of the ac machines. The bulk of the work on superconducting ac generators was directed towards the requirements of large central power stations. However some of the earliest investigations were in respect to aircraft generators and this application continues to be of interest. Although some work was undertaken on inside out generators in which the dc field winding was stationary, all of the current activity is in respect to the more conventional geometry. In the early 1980s it was discovered that by producing ultra fine wires of niobium titanium, these liquid helium cooled superconductors could carry current at power frequencies without prohibitive losses which had previously been the case. This discovery and the subsequent production of these wires in France and later in Japan enabled work to proceed on superconducting transformers and on totally superconducting ac generators. The next events in this rapidly evolving technology were the discoveries in late 1986 and early 1987 that a non metallic material was superconducting at temperatures in excess of 90 K. The great significance of this development is that these ceramic materials could be cooled with liquid nitrogen instead of liquid helium and the ramifications of this upon design and cost are immense. The likely impact of this discovery on electrical power equipment is discussed. Author

N91-14046# American Superconductor Corp., Watertown, MA.
OXIDE SUPERCONDUCTOR COILS: PRESENT SUCCESSES, FUTURE CHALLENGES **c33**
Carl J. Russo *In* AGARD, Applications of Superconductivity to Avionics Oct. 1990 5 p (For primary document see N91-14030 05-76)
Copyright Avail: NTIS HC/MF A08; Non-NATO Nationals requests available only from AGARD/Scientific Publications Executive

Coils are a fundamental building block for large-scale

applications. Successful application of oxide superconductor coils in these applications requires: high quality, superconducting-oxide wire forms; an insulation technology compatible with processing; a mandrel material compatible with processing and operational requirements; a compatible, high-strength, mechanical-support material; ability to maintain superconducting properties while being strained; and compatibility with other subsystems which are part of the application. The present state of coil development is discussed in terms of several applications. Predictions for the future of oxide superconductor coils is examined in terms of several figures of merit and anticipated operational criteria. Author

N91-14047# Varian Associates, Palo Alto, CA.
A LIQUID NITROGEN COOLED SUPERCONDUCTIVE ELECTRON BEAM FOCUSING SYSTEM FOR IMPROVED PERFORMANCE ECM HELIX TRAVELING WAVE TUBES
M. C. Green *In* AGARD, Applications of Superconductivity to Avionics Oct. 1990 6 p (For primary document see N91-14030 05-76)
Copyright Avail: NTIS HC/MF A08; Non-NATO Nationals requests available only from AGARD/Scientific Publications Executive

In avionics, the focus of attention in recent years has been upon the development of solid state devices for low-level signal processing. Device development based upon the new high-temperature superconductors has mirrored this, with concentration upon thin film systems as a basis for the eventual fabrication of delay lines, resonators and the like. However, large numbers of avionics systems, particularly in the electronic countermeasures (ECM) area, employ traveling wave tubes (TWTs) as final power amplifiers. Broadband ECM helix TWTs utilizing periodic permanent magnet (PPM) focusing systems are particularly suitable for the application of superconductive focusing systems, since despite the relatively low magnetic fields employed along the electron beam axis in a typical PPM stack, the PPM configuration is limited to less-than-optimum axial fields by the local saturation of polepiece material between the adjacent ring magnets of the stack. In a typical I-J band ECM helix TWT, the axial field does not exceed 2.5 KG despite the use of exotic polepiece materials, which in turn means a lower-than-optimum perveance electron beam. This impacts adversely upon TWT bandwidth, stability, and gain. The relatively low field requirement for this application means that a solenoidal field generated by a high-temperature superconductor flux trap is potentially practical with today's level of materials development. Author

N91-14048# Naval Surface Weapons Center, Silver Spring, MD. Dept. of Research and Technology.
SYNTHESIS AND CHARACTERIZATION OF HIGH TEMPERATURE SUPERCONDUCTOR MATERIALS
W. A. Ferrando, A. P. Divecha, S. D. Karmarkar, A. N. Mansour, and P. W. Hesse *In* AGARD, Applications of Superconductivity to Avionics Oct. 1990 10 p Sponsored by NRL (For primary document see N91-14030 05-76)
Copyright Avail: NTIS HC/MF A08; Non-NATO Nationals requests available only from AGARD/Scientific Publications Executive

High temperature superconductors are oxides and, therefore, inherently brittle. A process involving thermal decomposition of silver nitrate in the presence of YBa2Cu307 (123) powder was developed which shows promise for synthesis of fine diameter wires. The silver deposits uniformly on the 123 powder as indicated by optical and scanning electron microscopy. The composite powder can be formed into rods via drawing and swaging through conical converging dies. Finer diameter wires were produced by slurry extrusion of the composite powder in a polymeric vehicle. The current carrying capacity, Jc, continues to rise due to better understanding of the Ag/superconductor interface. Jc values of a typical wire has now reached 400 A/sq cm at 77 K and zero magnetic field, with a superconducting transition temperature of 93 K. In addition, the AgN03 decomposition process can be employed with fine HTS powder and ethylene glycol as a suitable vehicle to produce an adherent, stable high temperature superconducting paint. The composition, chemistry, and uniformity of dispersion of Ag was investigated by x ray diffraction, x ray photoelectron spectroscopy, and scanning electron microscopy. Author

N91-14049*# Jet Propulsion Lab., California Inst. of Tech., Pasadena.
TOTAL-DOSE RADIATION EFFECTS DATA FOR SEMICONDUCTOR DEVICES (1989 SUPPLEMENT)
Keith E. Martin, James R. Coss, Charles A. Goben, David C. Shaw, Sam Farmanesh, Michael M. Davarpanah, LeRoy H. Craft, and William E. Price 15 Feb. 1990 214 p
(Contract NAS7-918)
(NASA-CR-187431; JPL-Publ-89-17; NAS 1.26:187431) Avail: NTIS HC/MF A10 CSCL 20L

Steady state, total dose radiation test data are provided for electronic designers and other personnel using semiconductor devices in a radiation environment. The data are presented in graphic and narrative formats. Two primary radiation source types were used: Cobalt-60 gamma rays and a Dynamitron electron accelerator capable of delivering 2.5 MeV electrons at a steady rate. Author

N91-14050*# National Aeronautics and Space Administration. Lewis Research Center, Cleveland, OH.
AN X RAY PHOTOELECTRON SPECTROSCOPY STUDY OF Au(x)In(y) ALLOYS
Douglas T. Jayne, Navid S. Fatemi (Sverdrup Technology, Inc., Brook Park, OH.), and Victor G. Weizer Nov. 1990 18 p Presented at the 37th Annual National Symposium, Toronto, Ontario, 8-12 Oct. 1990; sponsored by the American Vacuum Society
(Contract NAS3-25266; NAG3-696)
(NASA-TM-103659; E-5745; NAS 1.15:103659) Avail: NTIS HC/MF A03 CSCL 20L

Four gold-indium alloys were studied by x ray photoelectron spectroscopy. The binding energies and intensity ratios of the Au 4f7/2 and In 3d5/2 core levels were determined for the bulk alloy compositions of Au(10 percent In), Au3In, AuIn, and AuIn2. These values were determined for the native oxides on the materials, for the surfaces prepared by ion bombardment to remove the oxide and for surfaces scraped in-situ with a ceramic tool to expose the bulk composition. These results furnish calibration values that allow determination of the composition of thin films of this alloy system. In addition the binding energies add to the data base for understanding the effect of alloying on core level binding energies. As an illustration, these results are used to determine the composition of a series of alloy films formed by incongruent evaporation of an alloy charge. Author

N91-14051# State Univ. of New York, Stony Brook. Dept. of Physics.
EXPERIMENTAL STUDIES OF JOSEPHSON EFFECT Final Technical Report, 15 Mar. 1984 - 30 Sep. 1989
James Lukens 6 Sep. 1990 31 p
(Contract N00014-84-C-0261)
(AD-A226548) Avail: NTIS HC/MF A03 CSCL 20/10

During the course of this contract, research has been conducted in three distinct areas, all involving the Josephson effect: (1) development of Josephson junction arrays as tunable sources of microwave through submillimeter radiation; (2) conformation of general relativistic effects, equivalent to the red shift, for charged particles; and (3) studies of the quantum mechanics of macroscopic variables, in particular of the flux linking a SQUID. GRA

N91-14052# Parke Mathematical Labs., Inc., Carlisle, MA.
SIGNAL PROCESSING DEVELOPMENT Annual Report, Jan. - Dec. 1984
T. B. Barrett, R. Marshall, J. Bloom, C. Comer, J. Caulfield, C. Warde, and M. Salour Nov. 1989 99 p
(Contract F19628-84-C-0008; AF Proj. 4600)
(AD-A226593; RADC-TR-89-229) Avail: NTIS HC/MF A05 CSCL 20/2

This electron microscope has been applied to the study of the

growth of thin epitaxial films on silicon substrates. The study of the nature of platinum-silicide films formed by heating evaporated platinum films on these substrates is discussed. The use of ultra high vacuum systems together with a residual gas analyzer (RGA) is discussed as they relate to the preparation of silicides, a dielectric layer of silicon monoxide is evaporated and an ion beam implanter is used to form a special buried layer as a step toward silicon devices. Synthesis and single crystal growth of indium phosphide in a one-step in-situ process at high ambient pressures is discussed. Analysis of heat transfer by convection, conduction, and radiation in a closed pressure vessel is given. A set of source modules and NOS procedures have been prepared to permit easy access to a 3-dimensional, non-isotrophic ray-tracing program (the Jones - Stephenson program). This system is designed to be run on a CDC CYBER computer system or equivalent using the operating system. GRA

N91-14053*# National Aeronautics and Space Administration. Langley Research Center, Hampton, VA.
THEORETICAL TEMPERATURE-DEPENDENT BRANCHING RATIOS AND LASER THRESHOLDS OF THE (5)I7 YIELDS (5)I8 LEVELS OF Ho3(+) IN TEN GARNETS Interim Report, Apr. 1989 - Apr. 1990
Clyde A. Morrison, Elizabeth D. Filer, Norman P. Barnes, and Gregory A. Turner (Harry Diamond Labs., Adelphi, MD.) Sep. 1990 32 p
(NASA-TM-103429; NAS 1.15:103429; AD-A226664; HDL-TR-2185) Avail: NTIS HC/MF A03 CSCL 08/7

This report presents a comparative study of triply ionized holmium in ten garnets. The point charge model of crystal fields is used to predict the energy levels of Ho3+ in YAG, LaLuGG, GdScAG, YScAG, GdGG, GDScGG, YGG, LuGG, LuAG and GdAG. The magnetic and electric dipole transition probabilities are used to predict theoretical temperature dependent branching ratios and laser thresholds of a quasi four level laser for each of these garnets. GRA

N91-14054# Rochester Univ., NY. Lab. for Laser Energetics.
ULTRAFAST OPTICAL ELECTRONICS CENTER Final Technical Report, 1 Nov. 1986 - 31 Mar. 1990
Gerard Mourou 28 Aug. 1990 73 p
(Contract F49620-87-C-0016)
(AD-A226669; AFOSR-90-0916TR) Avail: NTIS HC/MF A04 CSCL 09/5

The work done under the URI had the mission to bridge ultrafast optics with high-speed electronic and photonics. Ultrashort optical pulses have been used to study of fundamental processes taking place in the femtosecond and picosecond timescales in bulk and layered semiconductors, metals, and superconductors. Under this contract electron velocity overshoot in GaAs was time-resolved for the first time. Using short optical and electrical pulses, both sequential and resonant tunneling transport were investigated. The high-frequency properties of high-Tc superconductors in the 10 to 100 GHz range were studied. Time-resolved thermo-modulation was used to investigate the electron phonon interaction in metals. This URI also had an important technological impact. Novel techniques and devices were demonstrated. In particular, time-domain reflectometry, based on electrooptic sampling to test devices and circuits at room and cryogenic temperatures was developed. We test HEMT, PBT, heterostructure transistor prescaler, NMOS silicon multiplexer, and GaAs power amplifier MMIC. Broadband electronic requires a complete understanding of normal and superconducting transmission lines. Extensive work has been done in this area. A time-temperature of the first high-energy electron diffraction technique was also demonstrated and used to determine the surface temperature of the first monolayers in crystals. GRA

N91-14055*# Alabama Univ., Huntsville. Center for Microgravity and Materials Research.
MORPHOLOGICAL STABILITY AND KINETICS IN CRYSTAL GROWTH FROM VAPORS Final Report, 20 Jan. 1989 - 19 Jul. 1990
Franz Rosenberger Jul. 1990 115 p
(Grant NAG1-972)
(NASA-CR-187650; NAS 1.26:187650) Avail: NTIS HC/MF A06 CSCL 20L

The following topics are discussed: (1) microscopy image storage and processing system; (2) growth kinetics and morphology study with carbon tetrabromide; (3) photothermal deflection vapor growth setup; (4) bridgman growth of iodine single crystals; (5) vapor concentration distribution measurement during growth; and (6) Monte Carlo modeling of anisotropic growth kinetics and morphology. A collection of presentations and publications of these results are presented. Author

N91-14056# Sandia National Labs., Albuquerque, NM.
BAND-GAP NARROWING AND III-V HETEROSTRUCTURE FETS (FIELD-EFFECT TRANSISTORS)
David R. Myers, J. A. Lott, J. F. Klem, C. P. Tigges, and J. R. Lowney (National Inst. of Standards and Technology, Gaithersburg, MD.) 1990 5 p Presented at the International Electron Device Conference, San Francisco, CA, 10-12 Dec. 1990
(Contract DE-AC04-76DP-00789)
(DE91-000401; SAND-90-1911C; CONF-901244-1) Avail: NTIS HC/MF A01

We calculate the magnitude of band-gap narrowing for GaAs-based alloys, and have included these results into one-dimensional heterojunction device models for strained In(sub 0.15)Ga(sub 0.85)As quantum-well MODulation-doped Field-Effect Transistors (MODFETs). Equivalent rigid shifts of as much as 1.2 MeV are obtained for the valence band of depleted p-type Al(sub 0.15)Ga(sub 0.85)As doped at 5 x 10(exp 18)/cm(exp 3). Our simulations suggest that band-gap narrowing is most significant for p-channel MODFETs. The predicted effect of band-gap narrowing in p-channel MODFETs is the formation of parasitic conduction in the low-mobility parent dopant region. The parasitic conduction would reduce the intrinsic gain. DOE

N91-14057# Washington Univ., Seattle. Dept. of Physics.
STATUS OF LATTICE FIELD THEORY CALCULATIONS
Stephen R. Sharpe 1990 22 p Presented at the PASCOS 1990, Boston, MA, 1990
(Contract DE-AS06-88ER-40423)
(DE91-001141; DOE/ER-40423/10-P90; CONF-9003221-1)
Avail: NTIS HC/MF A03

This report briefly discusses the following topics: overview of all present calculations; reliability criteria for quenched calculation; quenched versus full QCD, and difficulties facing full QCD; results for the quenched pion wavefunction; results for the quenched hadron spectrum; results for quenched B(sub K); a new method for calculating the surface tension; the non-pertubative upper bound on the Higgs mass; and the TERAFLOP machine. DOE

N91-14058# Minnesota Univ., Minneapolis. Dept. of Chemistry.
VARIATIONAL TRANSITION STATE THEORY
Donald G. Truhlar 1990 4 p
(Contract DE-FG02-86ER-13579)
(DE91-001253; DOE/ER-13579/22) Avail: NTIS HC/MF A01

In recent years our research group has made a systematic effort to study the validity of transition state theory (TST). We have found that the conventional theory is sometimes remarkably accurate, but in many other cases it leads to large errors. Fortunately we have found that a much more reliable theory that has many of the advantages of conventional TST can also be formulated, and it can be applied to practical problems with an effort that is much closer to that required for conventional transition state theory than to that required for quantal dynamics calculations. The two most important features in the improved approach to transition state theory are the variational determination of the transition state and the incorporation of tunneling contributions by multidimensional semiclassical approximations. DOE

N91-14059# Ames Lab., IA.
OPTICAL PROPERTIES AND ELECTRONIC STRUCTURES OF d- AND f-ELECTRON METALS AND ALLOYS, Ag-In, Ni-Cu, AuGa2, PtGa2, BETA'-NiAl, BETA'-CoAl, CeSn3, AND LaSn3 Ph.D. Thesis
Kwang Joo Kim 17 Oct. 1990 109 p
(Contract W-7405-eng-82)
(DE91-001597; IS-T-1495) Avail: NTIS HC/MF A06

Optical properties and electronic structures of disordered Ag(1-x)In(x)(x = 0.0, 0.04, 0.08, 0.12) and Ni(1-x)Cu(x) (x = 0.0, 0.1, 0.3, 0.4) alloys and ordered AuGa2, PtGa2, beta'-NiAl, beta'-CoAl, CeSn(3), and LaSn(sub 3) have been studied. The complex dielectric functions have been determined for Ag(1-x)In(x), Ni(1-x)Cu(x), AuGa2, and PtGa2 in the 1.2-5.5 eV region and for CeSn3 and LaSn3 in the 1.5-4.5 eV region using spectroscopic ellipsometry. Self-consistent relativistic band calculations using the linearized-augmented-plane-wave method have been performed for AuGa2, PtGa2, beta'-NiAl, beta'-CoAl, CeSn3, and LaSn3 to interpret the experimental optical spectra. DOE

N91-14060# California Univ., Berkeley. Lawrence Berkeley Lab. Physics Div.
X RAY AND CHARGED PARTICLE DETECTION WITH CsI(Tl) LAYER COUPLED TO a-Si:H PHOTODIODE LAYERS
I. Fujieda, G. Cho, J. Drewery, T. Gee, T. Jing, S. N. Kaplan, V. Perez-Mendez, D. Wildermuth, and R. A. Street (Xerox Palo Alto Research Center, CA.) Oct. 1990 11 p Presented at the IEEE Symposium on Nuclear Science, Washington, DC, 19-23 Oct. 1990 Submitted for publication
(Contract DE-AC03-76SF-00098)
(DE91-001798; LBL-29477; CONF-9010226-1) Avail: NTIS HC/MF A03

A compact real-time X ray and charged particle imager with digitized position output can built either by coupling a fast scintillator to a photodiode array or by forming one on a photodiode array directly. CsI(Tl) layers 100 to 1000 microns thick were evaporated on glass substrates from a crystal CsI(Tl). When coupled to a crystalline Si or amorphous silicon (a-Si:H) photodiode and exposed to calibrated X ray pulses, their light yields and speed were found to be comparable to those of a crystal CsI(Tl). Single beta particle detection was demonstrated with this combination. The light spread inside evaporated CsI(Tl) was suppressed by its columnar structure. Scintillation detection gives much larger signals than direct X ray detection due to the increased energy deposition in the detector material. Fabrication of monolithic type X-ray sensors consisting of CsI + a-Si:H photodiodes is discussed. DOE

N91-14061# Oak Ridge National Lab., TN.
ION-INDUCED DAMAGE AND AMORPHIZATION IN Si
O. W. Holland and C. W. White 1990 25 p Presented at the 7th International Conference on Ion Beam Modification of Materials, Knoxville, TN, 9-14 Sep. 1990
(Contract DE-AC05-84OR-21400)
(DE91-002358; CONF-900936-17) Avail: NTIS HC/MF A03

Ion-induced damage growth in high-energy, self-ion irradiated Si was studied using electron microscopy and Rutherford backscattering spectroscopy. The results show that there is a marked variation in the rate of damage growth, as well as the damage morphology, along the path of the ion. Near the ion End-Of-Range (EOR), damage increases monotonically with ion fluence until a buried amorphous layer is formed, while damage growth saturates at a low level in the region ahead. The morphology of the damage in the saturated region is shown to consist predominantly of simple defect clusters such as the divacancy. Damage growth remains saturated ahead of the EOR until expansion of the buried amorphous layer encroaches into the region. A homogeneous growth model is presented which accounts for damage saturation, and accurately predicts the dose-rate dependence of the saturation level. Modifications of the model are discussed which are needed to account for the rapid growth in the EOR region and near the interface of the buried amorphous layer. Two important factors contributing to rapid damage growth are identified. Spatial separation of the Frenkel defect pairs (i.e., interstitials and vacancies) due to the momentum of the interstitials is shown to greatly impact damage growth near the EOR, while uniaxial strain in the interfacial region of the amorphous layer is identified as an important factor contributing to growth at that location. DOE

N91-14062# Washington Univ., Saint Louis, MO. Dept. of Physics.
NON-EMPIRICAL INTERATOMIC POTENTIALS FOR TRANSITION METALS, ALLOYS, AND SEMICONDUCTORS
1990 10 p
(Contract DE-FG02-84ER-45130)
(DE91-002396; DOE/ER-45130/5) Avail: NTIS HC/MF A02

Progress has been made on several fronts in the development and application of simplified energy and force functionals. These elucidate the basic features of bulk and defect structures, and are being coded in a form which can be used in atomistic simulations of materials properties. The main categories of materials which we have treated are transition metals, semiconductors, and aluminum alloys. We have analyzed the basic form of the angular dependence of the interatomic forces in these materials. We have then applied this understanding to the structures of polytetrahedrally packed transition metal compounds, icosahedral phase in the Ti-Mn system, and complex phases in Al-transition metal alloys. A force code for use in atomistic simulations of Si has also been developed. The Principal Investigator has completed a major review article on interatomic potentials for Solid State Physics: Advances in Research and Applications. The significance of the research accomplishment has also been recognized by several invited lectures, as well as solicitation to write an article entitled Cohesion (physics) for the upcoming new edition of the McGraw-Hill Encyclopedia of Science and Technology. DOE

N91-14063# Lawrence Livermore National Lab., CA.
SUBNANOSECOND, HIGH VOLTAGE PHOTOCONDUCTIVE SWITCHING IN GaAs
Robert L. Druce, Michael D. Pocha, Kenneth L. Griffin, and B. Jim OBannon (Rockwell International Corp., Anaheim, CA.) 1990 14 p Presented at the OPTCON 1990: SPIE Symposium on Laser Science and Applications of Optics, Optically Activate Switching Conference, Boston, MA, 4-9 Nov. 1990 Submitted for publication
(Contract W-7405-eng-48)
(DE91-002671; UCRL-JC-104969; CONF-9011125-3) Avail: NTIS HC/MF A03

We are conducting research on the switching properties of photoconductive materials to explore their potential for generating high-power microwaves (HPM) and for high rep-rate switching. We have investigated the performance of Gallium Arsenide (GaAs) in linear mode (the conductivity of the device follows the optical pulse) as well as an avalanche-like mode (the optical pulse only controls switch closing). Operating in the linear mode, we have observed switch closing times of less than 200 ps with a 100 ps duration laser pulse and opening times of less than 400 ps at several kV/cm fields using neutron irradiated GaAs. In avalanche and lock-on modes, high fields are switched with lower laser pulse energies, resulting in higher efficiencies; but with measurable switching delay and jitter. We are currently investigating both large area (1 cm(sup 2)) and small area (less than 1 mm(sup 2)) switches illuminated by AlGaAs laser diodes at 900 nm and Nd:YAG lasers at 1.06 microns. DOE

N91-14064# Rochester Univ., NY. Dept. of Physics and Astronomy.
FLUX FLOW PINNING AND RESISTIVE BEHAVIOR IN SUPERCONDUCTING NETWORKS Annual Progress Report No. 2, 1 May 1990 - 30 Apr. 1991
Stephen Teitel Oct. 1990 9 p
(Contract DE-FG02-89ER-14017)
(DE91-002756; DOE/ER-14017/2) Avail: NTIS HC/MF A02

The behavior was studied of superconducting networks in terms of XY and Coulomb gas models. The dynamics of frustrated

Josephson junction arrays was simulated, with a view toward understanding the effects of vortex correlations on flux flow resistance. Randomness was introduced, and its effects on the superconducting transition, and vortex mobility, were studied. A 3-D network was simulated to study the effects of vortex line entanglement in high temperature superconductors. Preliminary calculations are in progress. The 2-D classical Coulomb gas where charges map onto vortices in the superconducting network, was simulated. The melting transitions of ordered charge (vortex) lattices were studied, and clear evidence was found that these transitions do not have the critical behavior expected from standard symmetry analysis. DOE

N91-14065# Technische Hochschule, Darmstadt (Germany, F.R.). Fachbereich Physik.
INFLUENCE OF THE DELOCALIZED EXCITATION PROCESS ON THE DETERMINATION OF FOREIGN ATOM POSITIONS USING THE CHANNELING EFFECT Ph.D. Thesis [EINFLUSS DES DELOKALISIERTEN ANREGUNGSPROZESSES BEI DER BESTIMMUNG VON FREMDATOMPOSITIONEN MIT HILFE DES CHANNELING EFFEKTS]
Dirk vonHugo 1989 95 p In GERMAN Sponsored by DFG
(ETN-91-98175) Avail: NTIS HC/MF A05

The excitation process of inner shells (K,L) of crystal atoms by electrons with an energy of around 100 keV was treated theoretically. The calculation of the cross section for inner shell excitation by the beam electrons was strongly simplified since it only took into account scattering processes leading to the emission of a characteristic x ray quantum. This method makes it possible to calculate the measurement results from the so-called ALCHEMI (Atom Location by Channeling Enhanced Microanalysis) experiments. The determined dependence of the x ray intensity on the electron beam conditions, the position of the atom and its excitation characteristic allow the calculation of the influence of delocalization. Experimental observations which cannot be understood due to the supposition of strict localization, can be interpreted using the present model. ESA

N91-14066*# National Aeronautics and Space Administration. Goddard Space Flight Center, Greenbelt, MD.
METHOD OF FABRICATING GERMANIUM AND GALLIUM ARSENIDE DEVICES Patent Application
Murzban Jhabvala, inventor (to NASA) 31 Aug. 1990 10 p
(NASA-Case-GSC-13265-1; NAS 1.71:GSC-13265-1;
US-Patent-Appl-SN-575694) Avail: NTIS HC/MF A02

A method of semiconductor diode fabrication is disclosed which relies on the epitaxial growth of a precisely doped thickness layer of gallium arsenide or germanium on a semi-insulating or intrinsic substrate, respectively, of gallium arsenide or germanium by either molecular beam epitaxy (MBE) or by metal-organic chemical vapor deposition (MOCVD). The method involves: depositing a layer of doped or undoped silicon dioxide on a germanium or gallium arsenide wafer or substrate, selectively removing the silicon dioxide layer to define one or more surface regions for a device to be fabricated thereon, growing a matched epitaxial layer of doped germanium or gallium arsenide of an appropriate thickness using MBE or MOCVD techniques on both the silicon dioxide layer and the defined one or more regions; and etching the silicon dioxide and the epitaxial material on top of the silicon dioxide to leave a matched epitaxial layer of germanium or gallium arsenide on the germanium or gallium arsenide substrate, respectively, and upon which a field effect device can thereafter be formed. NASA

77 THERMODYNAMICS AND STATISTICAL PHYSICS

Includes quantum mechanics; theoretical physics; and Bose and Fermi statistics.

For related information see also *25 Inorganic and Physical Chemistry* and *34 Fluid Mechanics and Heat Transfer.*

N91-14067# Virginia Polytechnic Inst. and State Univ., Blacksburg. Inst. of High Energy Physics.
NEW PHASES OF D GREATER THAN OR EQUAL TO 2 CURRENT AND DIFFEOMORPHISM ALGEBRAS IN PARTICLE PHYSICS
Chia-Hsiung Tze Sep. 1990 57 p Presented at the 5th Symmetries in Science: Algebraic Structures, Their Representations, Realizations and Physical Applications, Voralberg, Austria, 30 Jul. - 3 Aug. 1990 Submitted for publication
(Contract DE-AS05-80ER-10713)
(DE91-001515; CONF-9007181-1) Avail: NTIS HC/MF A04

We survey some global results and open issues of current algebras and their canonical field theoretical realization in D greater than or equal to 2 dimensional spacetime. We assess the status of the representation theory of their generalized Kac-Moody and diffeomorphism algebras. Particular emphasis is put on higher dimensional analogs of fermi-bose correspondence, complex analyticity and the phase entanglements of anyonic solitons with exotic spin and statistics. DOE

N91-14068# California Univ., Berkeley. Lawrence Berkeley Lab.
U1(PRIME) DARK MATTER AND R-PARITY VIOLATION Ph.D. Thesis
David Ernest Brahm Apr. 1990 71 p Prepared in cooperation with California Univ., Berkeley
(Contract DE-AC03-76SF-00098; NSF PHY-85-15857)
(DE91-001792; LBL-28841; UCB-PTH-90/10) Avail: NTIS HC/MF A05

Attempts to understand physics beyond the Standard Model must face many phenomenological constraint, from recent Z(sup (degree)) data, neutral current measurements, cosmology and astrophysics, neutrino experiments, tests of lepton-and baryon-number conservation and CP violation, and many other ongoing experiments. The most interesting models are those which are allowed by current data, but offer predictions which can soon be experimentally confirmed or refuted. Two classes of such models are explored in this dissertation. The first, containing an extra U1(prime) gauge group, has a dark matter candidate which could soon be detected. The second, incorporating supersymmetry with R-parity violation, predicts rare Z(sup (degree)) decays at LEP; some of these models can already be ruled out by LEP data and gluino searches at the Tevatron. DOE

N91-14069# Los Alamos National Lab., NM. Theoretical Div.
ALGORITHMIC INFORMATION CONTENT, CHURCH-TURING THESIS, PHYSICAL ENTROPY, AND MAXWELL'S DEMON
Wojciech H. Zurek 1990 24 p Presented at the NATO/Advanced Study Institute on Information Dynamics Conference, Irsee, German Democratic Republic, Jun. 1990
(Contract W-7405-eng-36)
(DE91-001804; LA-UR-90-3702; CONF-9006288-1) Avail: NTIS HC/MF A03

Measurements convert alternative possibilities of its potential outcomes into the definiteness of the 'record' - data describing the actual outcome. The resulting decrease of statistical entropy has been, since the inception of the Maxwell's demon, regarded as a threat to the second law of thermodynamics. For, when the statistical entropy is employed as the measure of the useful work which can be extracted from the system, its decrease by the information gathering actions of the observer would lead one to believe that, at least from the observer's viewpoint, the second law can be violated. I show that the decrease of ignorance does not necessarily lead to the lowering of disorder of the measured physical system. Measurements can only convert uncertainty

(quantified by the statistical entropy) into randomness of the outcome (given by the algorithmic information content of the data). The ability to extract useful work is measured by physical entropy, which is equal to the sum of these two measures of disorder. So defined physical entropy is, on the average, constant in course of the measurements carried out by the observer on an equilibrium system. DOE

N91-14070# Los Alamos National Lab., NM. Center for Nonlinear Studies.
CHAOS AND ORDER IN NON-INTEGRABLE MODEL FIELD THEORIES
David K. Campbell and Michel Peyrard (Dijon Univ., France) 1989 51 p Presented at the AIP Chaos Conference, Woodsaw, 24 Jul. 1989 Submitted for publication
(Contract W-7405-eng-36)
(DE91-002313; LA-UR-90-3373; CONF-8907226-1) Avail: NTIS HC/MF A04

We illustrate the presence of chaos and order in non-integrable, classical field theories, which we view as many-degree-of-freedom Hamiltonian nonlinear dynamical systems. For definiteness, we focus on the phi(exp 4) theory and compare and contrast it with the celebrated integrable sine-Gordon equation. We introduce and investigate two specific problems: the interactions of solitary 'kink'-like waves in non-integrable theories; and the existence of stable 'breather' solutions - spatially-localized, time-periodic nonlinear waves - in the phi(exp 4) theory. For the former problem we review the rather well developed understanding, based on a combination of computational simulations and heuristic analytic models, of the presence of a sequence of resonances in the kink-antikink interactions as a function of the relative velocity of the interaction. For the latter problem we discuss first the case of the continuum (chi)(sup 4) theory. We discuss the multiple-scale asymptotic perturbation theory arguments which first suggested the existence of phi(exp 4) breathers, then the subsequent discovery of terms 'beyond-all-orders' in the perturbation expansion which destroy the putative breather, and finally, the recent rigorous proofs of the non-existence of breathers in the continuum theory. We then present some very recent numerical results on the existence of breathers in discrete phi(exp 4) theories which show an intricate interweaving of stable and unstable breather solutions on finite discrete lattices. We develop a heuristic theoretical explanation of the regions of stability and instability. DOE

N91-14071# Johns Hopkins Univ., Baltimore, MD. Dept. of Physics and Astronomy.
RESEARCH IN THEORETICAL PHYSICS Annual Progress Report, 1 Apr. 1990 - 31 Mar. 1991
G. Domokos and S. Kovesi-Domokos Oct. 1990 14 p
(Contract DE-FG02-85ER-40211)
(DE91-002458; DOE/ER-40211/6) Avail: NTIS HC/MF A03

In this report we describe a research undertaken approximately three years ago: in it we investigate possible signatures of physics not described by the Standard Model of electroweak and strong interactions. The source of such data is signals obtained from observations of point sources in the sky, typically x ray binary stars, but also some others, such as the CRAB nebula. DOE

N91-14072# Oak Ridge National Lab., TN. Engineering Physics and Mathematics Div.
LINEAR VS NONLINEAR AND INFINITE VS FINITE: AN INTERPRETATION OF CHAOS
V. Protopopescu Oct. 1990 10 p
(Contract DE-AC05-84OR-21400)
(DE91-002522; ORNL/TM-11667) Avail: NTIS HC/MF A02

An example of a linear infinite-dimensional system is presented that exhibits deterministic chaos and thus challenges the presumably unquestionable connection between chaos and nonlinearity. Via this example, the roles of, and relationships between, linearity, nonlinearity, infinity and finiteness in the occurrence of chaos are investigated. The analysis of these complementary but related aspects leads to a new interpretation of chaos as the manifestation of incompressible information and a conjecture about the nonexistence of operationally accessible linear systems. DOE

N91-14073# California Univ., Berkeley. Lawrence Berkeley Lab. Earth Sciences Div.
COUPLED TRANSPORT PROCESSES IN SEMIPERMEABLE MEDIA. PART 2: NUMERICAL METHOD AND RESULTS
Janet S. Jacobsen and Chalon L. Carnahan Apr. 1990 36 p
(Contract DE-AC03-76SF-00098)
(DE91-004140; LBL-25619-Pt-2) Avail: NTIS HC/MF A03

A numerical simulator has been developed to investigate the effects of coupled processes on heat and mass transport in semipermeable media. The governing equations on which the simulator is based were derived using the thermodynamics of irreversible processes. The equations are nonlinear and have been solved numerically using the n-dimensional Newton's method. As an example of an application, the numerical simulator has been used to investigate heat and solute transport in the vicinity of a heat source buried in a saturated clay-like medium, in part to study solute transport in bentonite packing material surrounding a nuclear waste canister. The coupled processes considered were thermal filtration, thermal osmosis, chemical osmosis and ultrafiltration. In the simulations, heat transport by coupled processes was negligible compared to heat conduction, but pressure and solute migration were affected. Solute migration was retarded relative to the uncoupled case when only chemical osmosis was considered. When both chemical osmosis and thermal osmosis were included, solute migration was enhanced. DOE

80 SOCIAL SCIENCES (GENERAL)

Includes educational matters.

No abstracts in this category.

81 ADMINISTRATION AND MANAGEMENT

Includes management planning and research.

No abstracts in this category.

82 DOCUMENTATION AND INFORMATION SCIENCE

Includes information management; information storage and retrieval technology; technical writing; graphic arts; and micrography.

For computer documentation see *61 Computer Programming and Software.*

N91-14074# Syracuse Univ., NY. School of Information Studies.
FEDERAL INFORMATION INVENTORY/LOCATOR SYSTEMS: FROM BURDEN TO BENEFIT Final Report
Charles R. McClure, Ann Bishop, Philip Doty, and Pierette Bergeron 27 Jul. 1990 104 p Sponsored by General Services Administration, Regulatory Information Service Center and Office of Management and Budget, Office of Information and Regulatory Affairs
Avail: NTIS HC/MF A06

There is wide agreement across the various stakeholders (Federal mission agencies, Federal information dissemination

agencies, OMB-OIRA, Congress, public advocacy groups, the library/information science community, the general public, and the private sector) that some form of an inventory/locator system for government information is both desirable and feasible. Given this context, it was the intent to review the existing policy system regarding inventory/locator systems, clarify the objectives and uses for such systems, and discuss issues and criteria related to how such systems can best meet the needs of both government agencies and the general public. Author

N91-14075 Texas Univ., Austin.
INFORMATION SYSTEMS SUPPORTED END-USER INTERACTION: IMPACTS ON INTER- AND INTRA-ORGANIZATIONAL CONNECTIVITY AND COOPERATIVE BEHAVIOR Ph.D. Thesis
Francis Woomin Wu 1989 250 p
Avail: Univ. Microfilms Order No. DA9017007

An Executive Information Systems Leadership Model is proposed with emphasis on executive involvement in facilitating internal and external connectivity and interactivity to achieve organizational and social integration. Four components of this leadership models are explained: (1) cooperative culture; (2) multi-dimensional social structure; (3) motivation for communication across groups; and (4) catalysts which stimulate collective action. Four hypotheses are derived from this model to propose the integrative role of the executive and its interaction with information technology. These four hypotheses are tested in all cases with substantial empirical support. The integrative role of the executive information systems leadership, the dynamics of social interaction within and across organizations, and the changes in organizational and social connectivity, participative culture, and cooperative behavior are examined to better understand the impacts of end-user computing from organizational and social integration perspective. Dissert. Abstr.

N91-14076# Advisory Group for Aerospace Research and Development, Neuilly-Sur-Seine (France). Technical Information Panel.
LIST OF STANDARDS TO ACCOMPANY MANUAL OF DOCUMENTATION PRACTICES APPLICABLE TO DEFENCE-AEROSPACE SCIENTIFIC AND TECHNICAL INFORMATION. ADDENDUM
Oct. 1990 49 p
(AGARD-AG-235-Add; ISBN-92-835-0583-2) Copyright Avail: NTIS HC/MF A03; Non-NATO Nationals requests available only from AGARD/Scientific Publications Executive

This addendum to the Manual of Documentation Practices Applicable to Defence-Aerospace Scientific and Technical Information, originally published in five volumes from 1978 to 1982, contains lists of standards applicable to information work, grouped by field of application and by nation. Author

N91-14077# Instituto de Pesquisas Espaciais, Sao Jose dos Campos (Brazil).
SWEEPING-VECTOR CONVERSION FOR POLYGONAL DATA [CONVERSAO VARREDURA-VETOR PARA DADOS POLIGONAIS]
Guaraci Jose Erthal Jun. 1988 11 p In PORTUGESE Presented at the 1st Brazilian Symposium on Computer Graphics and Image Processing, 19-20 Apr. 1988, Petropolis, Brazil
(INPE-4558-PRE/1299) Avail: NTIS HC/MF A03

The Geological Information System has as its objective the integration of space information distribution. A combination of satellite imagery data (sweeping format) with data mapping (traditional storage in vector format) requires, inevitably, procedures for conversion of the format to the other and vice-versa. The required procedures depend on the format utilized for manipulation of the data and available entry and exit arrangement. The objective is to increase the different propositions for data conversion by sweeping format, for the formal vector and insertion into the project version 2.1 of the Geographic Information System, developed by INPE. Transl. by B.G.

N91-14078# Instituto de Pesquisas Espaciais, Sao Jose dos Campos (Brazil). Dept. de Processamento de Imagens.
GEORELATIONAL DATA MODEL: A CONCEPTUAL VISION OF A GEOGRAPHICAL INFORMATION SYSTEM [MODELO DE DADOS GEO-RELACIONAL: UMA VISAO CONCEITUAL DE UM SISTEMA GEOGRAFICO DE INFORMACOES]
Guaraci Jose Erthal, Diogenes SalasAlves, and Gilberto CamaraNeto Jun. 1988 11 p In PORTUGESE Presented at the 1st Brazilian Symposium on Computer Graphics and Image Processing, 19-20 Apr. 1988, Petropolis, Brazil
(INPE-4612-PRE/1335) Avail: NTIS HC/MF A03

The geo-relational data model, conceptual framework of the INPE Geographic Information System, is described. The model permits management, in a united manner, of a great diversity of cartographic information through abstractions and operators (applications) and forsees someday the tools for incorporating the data bank relative to the system. Transl. by B.G.

N91-14079*# National Aeronautics and Space Administration. Langley Research Center, Hampton, VA.
TECHNICAL COMMUNICATIONS IN AEROSPACE: AN ANALYSIS OF THE PRACTICES REPORTED BY US AND EUROPEAN AEROSPACE ENGINEERS AND SCIENTISTS
Thomas E. Pinelli, Rebecca O. Barclay, John M. Kennedy, and Myron Glassman (Old Dominion Univ., Norfolk, VA.) Sep. 1990 10 p Presented at the International Professional Communication Conference, Guilford, England, 14 Sep. 1990 Sponsored in part by AF, Washington, DC
(NASA-TM-103441; NAS 1.15:103441; AD-A226503; SAF/AQT-SR-90-013; USAF-STINFO-CONTRIB-90/7) Avail: NTIS HC/MF A02 CSCL 05/2

Two pilot studies were conducted that investigated the technical communications practices of U.S. and European aerospace engineers and scientists. Both studies had the same five objectives: (1) solicit opinions regarding the importance of technical communications; (2) determine the use and production of technical communications; (3) seek views about the appropriate content of an undergraduate course in technical communications; (4) determine use of libraries, information centers, and online database; (5) determine use and importance of computer and information technology to them. A self-administered questionnaire was mailed to randomly selected aerospace engineers and scientists, with a slightly modified version sent to European colleagues. Their responses to selected questions are presented in this paper. GRA

N91-14080# Advisory Group for Aerospace Research and Development, Neuilly-Sur-Seine (France).
AGARD HIGHLIGHTS 90/2, PART 2
Sep. 1990 131 p In ENGLISH and FRENCH Presented at Delegues Nationaux AGARD de l'Industrie Aerospatiale Francaise et du Complexe, Toulouse, France, 29 Mar. 1990
(AD-A226532) Avail: NTIS HC/MF A07; Non-NATO Nationals requests available only from AGARD/Scientific Publications Executive CSCL 01/3

Various aerospace research facilities and/or organizations in the vicinity of Toulouse are discussed. Partial contents are as follows: The Toulouse Research Center and the Fauga-Mauzac Test Center of the French National Aerospace Research Agency (ONERA); Toulouse Aeronautical Test Center of ONERA; Toulouse Research and Studies Center of ONERA; The prime contractor and his subcontractors and subcontracting (A strategic element in Aerospatiale policy); and The Toulouse Space Center. GRA

N91-14081# Department of Energy, Oak Ridge, TN. Office of Scientific and Technical Information.
ENERGY DATA BASE
Leota S. Kane, ed. and Deborah E. Cutler, ed. Sep. 1990 47 p
(DE90-009278; DOE/OSTI-4649) Avail: NTIS HC/MF A03

To aid in the processing of bibliographic citations (including cataloging information, subject content indicators and abstracts), data are encoded in a format specific to the Office of Scientific

and Technical Information (OSTI). This format allows for computer storage, manipulation, and retrieval using both online and offline systems. Expansion of OSTI's data files to include nonnuclear information is relatively recent, beginning in 1974. OSTI's selection and announcement of technical information now represents a broad spectrum of energy-related fields following current research and development interest in both the domestic and the international arenas. To make the database as comprehensive as possible, current as well as background information is included. As part of its responsibility to build and maintain this database, OSTI accepts data on magnetic tape and floppy diskettes; OSTI's responsibility also includes dissemination of this technical information on magnetic tape as well. Each outgoing tape represents a two-week period of input to the database and may vary from 5000 to 14,000 records per tape. These tapes or diskettes, their format, and data content are described in this document. DOE

N91-14082# Oak Ridge National Lab., TN. Metals and Ceramics Div.
REPORT OF FOREIGN TRAVEL
Richard A. Strehlow 19 Oct. 1990 10 p
(Contract DE-AC05-84OR-21400)
(DE91-001732; ORNL/FTR-3800) Avail: NTIS HC/MF A02

Terminological requirements in information management was but one of the principal themes of the 2nd Congress on Terminology and Knowledge Engineering. The traveler represented the American Society for Testing and Materials' Committee on Terminology, of which he is the Chair. The traveler's invited workshop emphasized terminology standardization requirements in databases of material properties as well as practical terminology standardizing methods. The congress included six workshops in addition to approximately 82 lectures and papers from terminologists, artificial intelligence practitioners, and subject specialists from 18 countries. There were approximately 292 registrants from 33 countries who participated in the congress. The congress topics were broad. Examples were the increasing use of International Standards Organization (ISO) Standards in legislated systems such as the USSR Automated Data Bank of Standardized Terminology, the enhanced Physics Training Program based on terminology standardization in Physics in the Chinese province of Inner Mongolia, and the technical concept dictionary being developed at the Japan Electronic Dictionary Research Institute, which is considered to be the key to advanced artificial intelligence applications. The more usual roles of terminology work in the areas of machine translation, indexing protocols, knowledge theory, and data transfer in several subject specialties were also addressed, along with numerous special language terminology areas. DOE

N91-14083# European Space Agency, Paris (France). Legal Affairs.
CATALOGUE OF ESA PATENTS
P. A. Kallenbach, comp. and B. Battrick, ed. Jul. 1990 36 p
Original contains color illustrations
(ESA-SP-1131; ISBN-100-05-1131; ISSN-0379-6566;
ETN-91-98345) Copyright Avail: NTIS HC/MF A03; EPD, ESTEC, Noordwijk, Netherlands, HC 20 Dutch guilders

The July 1990 catalog is presented. Subjects covered are antennas, astronomy, attitude and control, communication equipment, communication systems, data processing, environment control, life support, measurement and control, mechanical engineering, metallic materials, power supplies, propulsion remote sensing, spacecraft systems and test facilities. ESA

N91-14084# Westinghouse Savannah River Co., Aiken, SC.
DATABASE MANAGEMENT SYSTEM FOR INSTRUMENT DATA MANAGEMENT
Charles P. Tatum 1990 5 p Presented at the 1990 Computer Symposium, Pittsburgh, Oct. - Nov. 1990 Submitted for publication
(Contract DE-AC09-89SR-18035)
(DE91-004300; WSRC-RP-90-186; CONF-9010256-1) Avail: NTIS HC/MF A01

Data from many measuring devices throughout the Savannah River Site (SRS) is transmitted to a central location for processing as a vital component in the SRS emergency preparedness and response program. The data processing is currently accomplished using VAX-based FORTRAN programs with the data stored in Digital's Record Management System (RMS) files which is shared using global COMMON. A program is underway to store and process this data using a Structured Query Language (SQL)-based Database Management System (DBMS). The advantages of replacing the current system with one using an SQL-based DBMS are discussed. DOE

N91-14085# Royal Signals and Radar Establishment, Malvern (England).
THE SWORD MODEL OF MULTILEVEL SECURE DATABASES
A. W. Wood Jun. 1990 11 p
(RSRE-90008; BR114552; ETN-91-98367) Copyright Avail: NTIS HC/MF A03

A multilevel secure database management system is described, which provides confidentiality and integrity to the user without introducing problems of signalling channels and interference. To eliminate these problems, data in SWORD is stored in tables with a proper name. Insertion or deletion of rows in a table are permitted only to users whose clearance equals the table class and only users whose clearance dominate the table class may perform read and update operations. To avoid resticting the ability to insert and delete data, a trusted path mechanism was added, which is a user interface which acts faithfully on behalf of human users. Rows made up of data which are of different sensitivity levels may therefore be inserted and retrieved. ESA

83 ECONOMICS AND COST ANALYSIS

Includes cost effectiveness studies.

No abstracts in this category.

84 LAW, POLITICAL SCIENCE AND SPACE POLICY

Includes NASA appropriation hearings; aviation law; space law and policy; international law; international cooperation; and patent policy.

No abstracts in this category.

85 URBAN TECHNOLOGY AND TRANSPORTATION

Includes applications of space technology to urban problems; technology transfer; technology assessment; and surface and mass transportation.

For related information see also *03 Air Transportation and Safety, 16 Space Transportation,* and *44 Energy Production and Conversion.*

N91-14086# Instituto de Pesquisas Espaciais, Sao Jose dos Campos (Brazil).
UTILIZATION OF IHS TRANSFORMATION FOR INTEGRATION OF IMAGES OF DIFFERING RESOLUTIONS: URBAN LAND USE STUDY [UTILIZACAO DE TRANSFORMACAO IHS PARA INTEGRACAO DE IMAGENS DE DIFERENTES RESOLUCOES: ESTUDO DO USO DO SOLO URBANO]
Luciano VieiraDutra, Celina Foresti, Paulo Roberto Meneses, and Maria deLourdesNevesdeOliveiraKurkdjian Jun. 1988 10 p In

PORTUGESE Presented at the 1st Brazilian Symposium on Computer Graphics and Image Processing, 19-20 Apr. 1988, Petropolis, Brazil
(INPE-4606-PRE/1329) Avail: NTIS HC/MF A02

A methodology is presented for combining images of different resolutions, utilizing color packet transformation (IHS transformation). The result and evaluation of the techniques for the terrestrial resources survey is presented for the area of Alphaville, Baueri, Sao Paulo state. Transl. by B.G.

88 SPACE SCIENCES (GENERAL)

N91-14087*# National Aeronautics and Space Administration. Ames Research Center, Moffett Field, CA.
PERFORMANCE OF MULTIPLEXED Ge:Ga DETECTOR ARRAYS IN THE FAR INFRARED
Jam Farhoomand (Sterling Federal Systems, Inc., Palo Alto, CA.) and Craig McCreight Oct. 1990 26 p
(NASA-TM-102275; A-90053; NAS 1.15:102275) Avail: NTIS HC/MF A03 CSCL 03B

The performance of two multi-element, multiplexed Ge:Ga linear arrays under low-background conditions was investigated. The on-focal switching is accomplished by MOSFET switches, and the integrated charge is made available through MOSFET source followers. The tests were conducted at 106 microns, and the radiation on the detectors was confined to a spectral window 1.25 microns wide using a stack of cold filters. At 4.2 K, the highest responsivity was 584 A/W, the noise equivalent power was 1.0 x 10(exp -16) W/square root of Hz, and the read noise was 6100 electrons/sample. A detailed description of the test setup and procedure is presented. Author

89 ASTRONOMY

Includes radio, gamma-ray, and infrared astronomy, and astrometry.

N91-14088*# Ohio State Univ., Columbus. Dept. of Astronomy.
GROUND-BASED STUDIES OF EMISSION-LINE VARIABILITY: RECENT RESULTS FOR NGC 5548 AND FUTURE PLANS
Bradley M. Peterson 1990 10 p Presented at the Variability of Active Galaxies Conference, Heidelberg, Fed. Republic of Germany, 3-5 Sep. 1990 Submitted for publication
(Grants NAG5-1366; NSF AST-89-15258)
(NASA-CR-180433; NAS 1.26:180433) Avail: NTIS HC/MF A02 CSCL 03A

Ever since emission-line variability was first detected in AGNs, it has been clearly understood that light-travel time effects in the broadline region (BLR) afford a tool for studying the structure of these spatially unresolved regions. However, only within the last few years has the observational problem become well defined in terms of the sampling rates and quality of data necessary to address the problem correctly. The amount of data required to extract structural information about the BLR from the continuum and emission-line light curves is so considerable that the most promising approach seemed to be to combine the observational efforts. The goal was to work together to produce a large, high-quality database which would then be released to individual investigators for more complete analysis. The cornerstone of this effort, was a joint NASA/ESA/SERC program to monitor the spectrum of NGC 5548 every four days with IUE from December 1988 through August 1988. A concurrent ground-based program was organized in an effort to enhance the scientific return on the project by extending the wavelength coverage and providing higher spectral resolution and signal to noise ratios than would be possible with IUE. It also turned out that the temporal resolution of the ground-based program was somewhat better than the temporal resolution of the IUE program, and the temporal baseline is longer and continues to grow. The database and initial results are presented by Peterson et al., (1991). The important results of the ground-based program are summarized, some additional applications of the existing data are described, and a few comments are made on what can be done in the future to expand on this work. Author

N91-14089*# Missouri Univ., Saint Louis. Dept. of Physics.
AN ADP PROPOSAL TO STUDY THE FORMATION AND EVOLUTION OF DUST-EMBEDDED CLUSTERS Final Report
Bruce A. Wilking 12 Sep. 1990 8 p
(Grant NAG5-1157)
(NASA-CR-186793; NAS 1.26:186793) Avail: NTIS HC/MF A02 CSCL 03A

Using high resolution and high sensitivity IRAS data at 12 and 25 microns low mass stars were studied which have recently formed in the Ophiuchus, Corona Australis, and IC1396 dark clouds. The successful application of these techniques to the Rho Ophiuchi infrared cluster is briefly described. The status of research performed is also presented. Author

N91-14090*# Louisiana State Univ., Baton Rouge. Dept. of Physics and Astronomy.
A CRITICAL REVIEW OF CHARGED PARTICLE ASTRONOMY AT SATURN: THE EVIDENCE FOR CO-ORBITING MATERIAL IN THE INNER SATELLITE SYSTEM Final Report, 1 Jul. 1988 - 30 Nov. 1989
John P. Wefel and John F. Cooper 15 Oct. 1990 37 p
(Grant NAG2-528)
(NASA-CR-187348; NAS 1.26:187348) Avail: NTIS HC/MF A03 CSCL 03A

The charged particle observations from Pioneer and Voyager at Saturn were reassessed with a view towards providing limits on the amount of unseen dust and debris that may exist in the Saturnian system. Such estimates are crucial for planning the Cassini tour of Saturn. The data from Pioneer 11 and Voyager were reviewed, intercompared, and correlated with model predictions to set limits on the matter distribution. Author

N91-14091 Michigan Univ., Ann Arbor.
THE LARGE-SCALE SPACE DISTRIBUTION OF EMISSION-LINE GALAXIES Ph.D. Thesis
Gregory Scott Aldering 1990 174 p
Avail: Univ. Microfilms Order No. DA9023505

The utility of surveys of emission-line galaxies (ELGs) are investigated as an efficient means of studying the space distribution of galaxies on scales between 50 and 500/h Mpc. The motiviation for, and execution of, a narrowband filter survey for ELGs are described. The initial survey results are encouraging, with 32 candidate ELGs being detected within a region of 0.25 square degrees. A fast focal-reducing camera, capable of imaging a 20 x 20 min field onto a TI 800 x 800 CCD on the McGraw-Hill 1.3 meter telescope, was built to improve the efficiency of this survey. The design, construction, and testing of this instrument are discussed. Using newly discovered ELGs from the IRAS Faint Source Survey, the integral and differential counts are examined in an attempt to detect the galaxy underdensity caused by the Bootes Void. Finding the results ambiguous, a redshift survey of IRAS Faint Source Survey galaxies in the Bootes Void was begun. From this survey, the density contrast of the Bootes Void was determined. The fact that the Bootes Void continues to have such a large deficit of galaxies when examined with a filled survey, presents problems for the currently popular Cold Dark Matter cosmogonical model, both in its unbiased and biased forms. In addition, the presence of a sizable population of galaxies in the Bootes Void adds additional weight to the argument that galaxies are biased tracers of the mass distribution, and that some types of galaxies are more biased than others. Dissert. Abstr.

N91-14092 Pennsylvania State Univ., University Park.
A STUDY OF ACTIVE REGIONS ON RS CVn STARS Ph.D. Thesis
Derek Laszlo Buzasi 1989 274 p
Avail: Univ. Microfilms Order No. DA9018191

Intense observational scrutiny was combined with theoretical modeling efforts for three regular RS CVn stellar systems, II Peg, UX Ari, and HR 1099. Observational analysis consisted of application of the technique of spectral subtraction to yield excess emission profiles for these stars; these profiles were considered indicative of extraphotospheric activity. The subtraction technique was applied to the H alpha, H beta, Ca II H, Ca II K, and Ca II infrared triplet lines, and the resulting fluxes were examined for correlations with phase and with each other. An analysis of the velocity information present in the line profiles was also attempted. Theoretical work consisted of the application of radiative transfer models to stellar plage and prominence models in an attempt to determine the physical nature of the active regions on these stars. The radiative transfer models were also used to test the limits of validity of the spectral subtraction technique itself. Author

N91-14093 Massachusetts Univ., Amherst.
RADIO OBSERVATIONS OF SEVERAL INTERSTELLAR MOLECULES Ph.D. Thesis
Young Chol Minh 1990 244 p
Avail: Univ. Microfilms Order No. DA9022722

Observations of rotational transitions are presented for several interstellar molecules whose formation may be related to grain processes and their implications are discussed for interstellar chemistry. Instellar hydrogen sulfide was observed at fractional abundances f(H2S) is approximately 10(exp -9) relative to H2 towards cold, dark clouds, while its abundance is enhanced by a factor of 1000 in the Orion hot core and the plateau. H2S may be evaporating from the grain mantles in the hot core, and even in the cold, dark clouds, grain surface reactions may be responsible for the gas-phase H2S abundances. An upper limit was derived for the HDS abundance (HDS)/(H2S) is less than or equal to 6 x 10(exp -4) in the Orion hot core. H2CS ortho-to-para ratios were observed to be approximately 1.8 towards TMC-1, which may suggest that H2SC is in equilibrium with the expected grain temperature and gas-grain exchanges are taking place effectively in cold, dark clouds. A ratio of approximately 3, the statistical value, was derived for Orion (3N1E) and NGC7538, and approximately 2 for Orion (KL). Upper limits were derived for the ethyl cyanide column densities of approximately 3 x 10(exp 12)/sq cm toward TMC-1 and L134N. Together with the detection for vinyl cyanide, there may be no necessity of invoking grain surface synthesis for these highly saturated species in cold clouds, but the desorption processes seem to be quite inefficient for these heavy molecules. Finally, HOCO+ was surveyed as a tracer of interstellar CO2 towards many galactic sources, and derived f(HOCO+) approximately 10(exp -8) to 10(exp -9) in the Galactic center and less than or equal to 10(exp -10) for cold dark clouds. The observed abundance of HOCO+ in the Galactic center is approximately 3 and approximately 1 orders of magnitude larger than that predicted by ion-molecule chemistry and shock chemistry, respectively. UV photolysis of grain mantles may produce CO2 efficiently, resulting in a large abundance of HOCO+ in the Galactic center. Dissert. Abstr.

N91-14094# Consiglio Nazionale delle Ricerche, Frascati (Italy). Ist. di Fisica dello Spazio Interplanetario.
METHODOLOGY TO TREAT STELLAR IMAGES [METODOLOGIA DI ELABORAZIONE DELLE IMMAGINI STELLARI]
Vittorio Formisano and Valeria Loschiavo Nov. 1989 32 p In ITALIAN
(IFSI-89-21; ETN-90-97782) Avail: NTIS HC/MF A03

The Plot10 software developed to treat stellar images on a Force computer is described. The original CCD (Charge Coupled Device) images are 384 by 576 pixels while the screen is 1024 by 1024 pixels with 16 colors. After each step there is a return to the PDOS operating system. The organization of the computer memory over 7 megabytes is described. The program is written in FORTRAN with some assembler routines. Example images are presented. ESA

N91-14095# European Space Agency, Paris (France).
FIRST: FAR INFRARED AND SUBMILLIMETRE SPACE TELESCOPE
Brigitte Kaldeich, ed. Jul. 1990 44 p Original contains color illustrations
(ESA-BR-69; ISBN-92-9092-055-6; ETN-91-98348) Copyright Avail: NTIS HC/MF A03

FIRST, which will open up the last major part of the electric spectrum, is compared to other projects, such as the NASA Kuiper Airborne Observatory (KAO). The methods for astronomical detection, such as the direct detection method and the heterodyne method are evaluated. The mission concept is described. The main scientific themes are reviewed. A few of the most important areas to which FIRST will make major contributions are mentioned: interstellar spectroscopy, interstellar matter in galaxies, highly luminous infrared galaxies and the evolution of quasars, stellar and solar formation and evolution. The imaging photometer and the heterodyne receivers are described. ESA

N91-14096*# National Aeronautics and Space Administration. Marshall Space Flight Center, Huntsville, AL.
VARIABLE MAGNIFICATION GLANCING INCIDENCE X RAY TELESCOPE Patent Application
Richard Hoover, inventor (to NASA) 28 Jun. 1990 22 p
(NASA-Case-MFS-28013-2; NAS 1.71:MFS-28013-2; US-Patent-Appl-SN-545220) Avail: NTIS HC/MF A03

A multispectral glancing incidence x ray telescope is disclosed, which capable of broadband, high resolution imaging of solar and stellar x ray and extreme ultraviolet radiation sources includes a primary optical system which focuses the incoming radiation to a primary focus. Two or more ellipsoidal mirrors are positioned behind the primary focus at an inclination to the optical axis, each mirror having a concave surface coated with a multilayer synthetic microstructure coating to reflect a desired wavelength. The ellipsoidal mirrors are segments of respective ellipsoids having a common first focus coincident with the primary focus. A detector such as an x ray sensitive photographic film is positioned at the second focus of each of the ellipsoids so that each of the ellipsoidal mirrors may reflect the image at the first focus to the detector. In one embodiment the mirrors are inclined at different angles and has its respective second focus at a different location, separate detectors being located at the respective second focus. The mirrors are arranged so that the magnification and field of view differ, and a solenoid activated arm may withdraw at least one mirror from the beam to select the mirror upon which the beam is to impinge so that selected magnifications and fields of view may be detected. NASA

90 ASTROPHYSICS

Includes cosmology; celestial mechanics; space plasmas; and interstellar and interplanetary gases and dust.

For related information see also *75 Plasma Physics*.

N91-14097*# Utah State Univ., Logan. Dept. of Physics
[INSTELLAR GAS EXPERIMENT (IGE): TESTING INTERSTELLAR GAS PARTICLES TO PROVIDE INFORMATION ON THE PROCESSES OF NUCLEOSYNTHESIS IN THE BIG BANG STARS AND SUPERNOVA] Final Report
Don Lind [1985] 19 p
(Grant NAG1-702)
(NASA-CR-186713; NAS 1.26:186713) Avail: NTIS HC/MF A03 CSCL 03B

The Interstellar Gas Experiment (IGE) is designed to collect particles of the interstellar gas - a wind of interstellar media particles moving in the vicinity of the solar system. These particles will be returned to earth where the isotopic ratios of the noble gases among these particles will be measured. IGE was designed and programmed to expose 7 sets of six copper-beryllium metallic collecting foils to the flux of neutral interstellar gas particles which penetrate the heliosphere to the vicinity of the earth's orbit. These particles are trapped in the collecting foils and will be returned to

earth for mass-spectrographic analysis when Long Duration Exposure Facility (LDEF) on which IGE was launched, is recovered. Y.S.

N91-14098*# Lunar and Planetary Inst., Houston, TX.
PROCEEDINGS OF A WORKSHOP ON COSMOGENIC NUCLIDE PRODUCTION RATES
Peter A. J. Englert, ed., Robert C. Reedy, ed., and Rolf Michel, ed. Jul. 1989 124 p Workshop held in Vienna, Austria, 25-26 Jul. 1989; sponsored in part by San Jose State Univ. and The University of Vienna
(Contract NASw-4066)
(NASA-CR-185349; NAS 1.26:185349; LPI-TR-90-05) Avail: NTIS HC/MF A06 CSCL 03B

Abstracts of reports from the proceedings are presented. The presentations were divided into discussion topics. The following general topic areas were used: (1) measured cosmogenic noble gas and radionuclide production rates in meteorite and planetary surface samples; (2) cross-section measurements and simulation experiments; and (3) interpretation of sample studies and simulation experiments. Author

N91-14099*# Lunar and Planetary Inst., Houston, TX.
ABSTRACTS FOR THE INTERNATIONAL WORKSHOP ON METEORITE IMPACT ON THE EARLY EARTH
Sep. 1990 70 p Workshop held in Perth, Australia, 21-22 Sep. 1990; sponsored in part by Barringer Crater Company, IUGS Commission on Comparative Planetology; and Meteoritical Society
(Contract NASw-4066)
(NASA-CR-185355; NAS 1.26:185355; LPI-CONTRIB-746) Avail: NTIS HC/MF A04 CSCL 03B

This volume contains abstracts that were accepted for presentation at the International Workshop on Meteorite Impact on the Early Earth, September 21-22, 1990, in Perth, Western Australia. The effects these impacts had on the young Earth are emphasized and a few of the topics covered are as follows: impact induced hot atmosphere, crater size and distribution, late heavy bombardment, terrestrial mantle and crust, impact damage, continental growth, volcanism, climate catastrophes, shocked quartz, and others. K.S.

N91-14100*# National Aeronautics and Space Administration. Ames Research Center, Moffett Field, CA.
THE INTERSTELLAR MEDIUM IN EXTERNAL GALAXIES: SUMMARIES OF CONTRIBUTED PAPERS
David J. Hollenbach, ed. and Harley A. Thronson, Jr., ed. (Wyoming Univ., Laramie.) Washington Jul. 1990 431 p Second conference held in the Grand Teton National Park, WY, 3-7 Jul. 1989; sponsored by NASA, NSF, and Wyoming Univ.
(NASA-CP-3084; A-90075; NAS 1.55:3084) Avail: NTIS HC/MF A19 CSCL 03B

The Second Wyoming Conference entitled, The Interstellar Medium in External Galaxies, was held on July 3 to 7, 1989, to discuss the current understanding of the interstellar medium in external galaxies and to analyze the basic physical processes underlying interstellar phenomena. The papers covered a broad range of research on the gas and dust in external galaxies and focused on such topics as the distribution and morphology of the atomic, molecular, and dust components; the dynamics of the gas and the role of the magnetic field in the dynamics; elemental abundances and gas depletions in the atomic and ionized components; cooling flows; star formation; the correlation of the nonthermal radio continuum with the cool component of the interstellar medium; the origin and effect of hot galactic halos; the absorption line systems seen in distant quasars; and the effect of galactic collisions. For individual titles, see N91-14101 through N91-14240.

N91-14101*# Leiden Univ. (Netherlands).
THE EXTRAGALACTIC RADIATION FIELD AND SHARP EDGES TO HI DISKS IN GALAXIES
Philip Richard Maloney *In* NASA, Ames Research Center, The Interstellar Medium in External Galaxies: Summaries of Contributed Papers Jul. 1990 p 1-3 (For primary document see N91-14100 05-90)
Avail: NTIS HC/MF A19 CSCL 03B

Observations of neutral hydrogen (HI) are widely used as a probe of the interstellar medium in galaxies and of galactic kinematics and dynamics. The 21-cm line can be used to determine galactic rotation curves far beyond the optical disk, and is one of the prime sources of evidence for the existence of dark haloes in spiral galaxies. However, a recent attempt to measure the 21-cm emission from NGC 3198 to very low column densities (N sub H approx. equals 5 times 10 to the 18th power) found that the HI disk is very sharply truncated at a column density of a few times 10 to the 19th power (Sancisi 1989, private communication). This discovery reinforces the earlier suggestion (Briggs et al. 1980) that extended, low-column density envelopes of neutral hydrogen are not common around galaxies. Here the author suggests that the sharp edge seen in the HI disk in NGC 3198 is consistent with a model in which a self-gravitating neutral HI disk is photoionized by the extragalactic radiation field. The possibility that the extragalactic background would produce sharp edges to HI disks was first suggested by Silk and Sunyaev (1976). Author

N91-14102*# Toledo Univ., OH. Dept. of Physics and Astronomy.
A COMPARISON OF UV SURFACE BRIGHTNESS AND HI SURFACE DENSITIES FOR SPIRAL GALAXIES
S. R. Federman and C. Strom *In* NASA, Ames Research Center, The Interstellar Medium in External Galaxies: Summaries of Contributed Papers Jul. 1990 p 4-5 (For primary document see N91-14100 05-90)
Avail: NTIS HC/MF A19 CSCL 03B

Shaya and Federman (1987) suggested that the ambient ultraviolet flux at 1000 A permeating a spiral galaxy controls the neutral hydrogen (HI) surface density in the galaxy. They found that the atomic envelopes surrounding small molecular clouds, because of their great number, provide the major contribution to the HI surface density over the stellar disk. The increase in HI surface density with later Hubble types was ascribed to the stronger UV fields from more high-mass stars in later Hubble types. These hypotheses are based on the observations of nearby diffuse interstellar clouds, which show a sharp atomic-to-molecular transition (Savage et al. 1977), and on the theoretical framework introduced by Federman, Glassgold, and Kwan (1979). Atomic envelopes around interstellar clouds in the solar neighborhood arise when a steady state is reached between photodissociation of H2 and the formation of H2 on grains. The photodissociation process involves photons with wavelengths between 912 A and 1108 A. Shaya and Federman used H-alpha flux as an approximate measure for the far UV flux and made their comparisons based on averages over Hubble type. Here, researchers compare, on an individual basis, UV data obtained with space-borne and balloon-borne instruments for galaxies with measurements of HI surface density (Warmels 1988a, b). The comparisons substantiate the conclusion of Shaya and Federman that the far UV field controls the HI content of spiral galaxies. Author

N91-14103*# Colorado Univ., Boulder. Dept. of Astrophysics, Planetary, and Atmospheric Science.
NGC 1058: GAS MOTIONS IN AN EXTENDED, QUIESCENT SPIRAL DISK
Margaret Murray Hanson, John M. Dickey, and George Helou (California Inst. of Tech., Pasadena.) *In* NASA, Ames Research Center, The Interstellar Medium in External Galaxies: Summaries of Contributed Papers Jul. 1990 p 6-7 (For primary document see N91-14100 05-90)
Avail: NTIS HC/MF A19 CSCL 03B

Researchers investigate in detail the motion of gas in the galaxy NGC 1058 using the very large array (VLA) to map the emission in the 21-cm line. This galaxy is so nearly face-on that the contribution to the line width due to the variation of the rotational velocity across the D-array beam is small compared with the random z-motion of the gas. Researchers confirm results of earlier

studies (Lewis 1987, A. and A. Suppl., 63, 515; van der Kruit and Shostak 1984, A. and A., 134, 258) of the galaxy's total neutral hydrogen (HI) and kinematics, including the fact that the rotation curve drops faster than Keplerian at the outer edge of the disk, which is interpreted as a fortuitous twist of the plane of rotation in the outer disk. However, their very high velocity resolution (2.58 km s(exp -1) after Hanning smoothing) coupled with good spatial resolution, allows researchers to measure more accurately the line width, and even to some extent its shape, throughout the disk. One of the most interesting results of this study is the remarkable constancy of the line width in the outer disk. From radius 90 to 210 seconds the Gaussian velocity dispersion (sigma sub nu) of the 21-cm line has a mean value of 5.7 km s(exp -1) (after correcting for the spectral resolution) with a dispersion of less than 0.9 km s(exp -1) (after correcting for the spectral resolution) with a dispersion of less than 0.9 km s(exp -1). Translating this directly into a kinetic temperature (Doppler temperature): T sub Dopp equals 121K (sigma sub mu exp 2/(km s(exp -1) (exp 2) gives 4000 K, with a dispersion of less than 1500 K over the outer disk. This constancy is observed even when comparing the spiral arms versus inter-arm regions, which in the radius range from 100 to 150 seconds the surface density modulates (defined as the ratio N sub peak -N sub trough/N sub peak + N sub trough) from 0.5 to 0.25 in the range 150 to 200 seconds. Author

N91-14104*# Leiden Univ. (Netherlands).
NEUTRAL HYDROGEN IN THE STARBURST GALAXY NGC3690/IC694
E. Tolstoy, John M. Dickey, and F. P. Israel *In* NASA, Ames Research Center, The Interstellar Medium in External Galaxies: Summaries of Contributed Papers Jul. 1990 p 8-11 (For primary document see N91-14100 05-90)
Avail: NTIS HC/MF A19 CSCL 03B

Researchers made observations of the neutral hydrogen (HI) emission structure surrounding the very deep absorption peak (observed earlier by Dickey (1986)) in the galaxy pair NGC3690/IC694. This galaxy pair is highly luminous in the far infrared, and known to exhibit extensive star formation as well as nuclear activity. Knowledge of the spatial distribution and velocity structure of the HI emission is of great importance to the understanding of the dynamics of the interaction and the resulting environmental effects on the galaxies. Author

N91-14105*# Kapteyn Astronomical Lab., Groningen (Netherlands).
HIGH VELOCITY GAS IN EXTERNAL GALAXIES
J. Kamphuis, J. M. vanderHulst, and R. Sancisi *In* NASA, Ames Research Center, The Interstellar Medium in External Galaxies: Summaries of Contributed Papers Jul. 1990 p 12-14 (For primary document see N91-14100 05-90)
Avail: NTIS HC/MF A19 CSCL 03B

Two nearby, nearly face-on spiral galaxies, M 101 and NGC 6946, observed in the HI with the Westerbork Synthesis Radio Telescope (WSRT) as part of a program to search for high velocity gas in other galaxies, are used to illustrate the range of properties of high velocity gas in other galaxies found thusfar. Author

N91-14106*# California Inst. of Tech., Pasadena. Dept. of Astronomy.
A SCALING LAW OF RADIAL GAS DISTRIBUTION IN DISK GALAXIES
Zhong Wang *In* NASA, Ames Research Center, The Interstellar Medium in External Galaxies: Summaries of Contributed Papers Jul. 1990 p 15-17 (For primary document see N91-14100 05-90)
Avail: NTIS HC/MF A19 CSCL 03B

Based on the idea that local conditions within a galactic disk largely determine the region's evolution time scale, researchers built a theoretical model to take into account molecular cloud and star formations in the disk evolution process. Despite some variations that may be caused by spiral arms and central bulge masses, they found that many late-type galaxies show consistency with the model in their radial atomic and molecular gas profiles. In particular, researchers propose that a scaling law be used to generalize the gas distribution characteristics. This scaling law may be useful in helping to understand the observed gas contents in many galaxies. Their model assumes an exponential mass distribution with disk radius. Most of the mass are in atomic gas state at the beginning of the evolution. Molecular clouds form through a modified Schmidt Law which takes into account gravitational instabilities in a possible three-phase structure of diffuse interstellar medium (McKee and Ostriker, 1977; Balbus and Cowie, 1985); whereas star formation proceeds presumably unaffected by the environmental conditions outside of molecular clouds (Young, 1987). In such a model both atomic and molecular gas profiles in a typical galactic disk (as a result of the evolution) can be fitted simultaneously by adjusting the efficiency constants. Galaxies of different sizes and masses, on the other hand, can be compared with the model by simply scaling their characteristic length scales and shifting their radial ranges to match the assumed disk total mass profile sigma tot(r). Author

N91-14107*# Iowa State Univ. of Science and Technology, Ames.
RADIAL PROFILES OF GAS IN LATE-TYPE DISK GALAXIES
Curtis Struck-Marcell *In* NASA, Ames Research Center, The Interstellar Medium in External Galaxies: Summaries of Contributed Papers Jul. 1990 p 18-20 (For primary document see N91-14100 05-90)
Avail: NTIS HC/MF A19 CSCL 03B

The azimuthally averaged neutral hydrogen (HI) distribution, and the total gas density distribution derived from HI and CO observations (N sub H2 = 2.8 x 10(exp 20) I sub CO) as a function of radius in several nearby, early-type disks are examined. Author

N91-14108*# Harvard-Smithsonian Center for Astrophysics, Cambridge, MA.
DISK MASS DENSITIES IN EDGE-ON SPIRAL GALAXIES
Michael P. Rupen *In* NASA, Ames Research Center, The Interstellar Medium in External Galaxies: Summaries of Contributed Papers Jul. 1990 p 21-22 (For primary document see N91-14100 05-90)
Avail: NTIS HC/MF A19 CSCL 03B

Very Large Array (VLA) observations of the neutral hydrogen (HI) gas in two nearby edge-on spirals (NGC 4565 and NGC 891) successfully resolve the thickness of the gas layers in both disks over a wide range in radii. The combination of B, C, and D array data produces a 4 arcsec (approx. 200 pc) beam and 21 km s(exp -1) velocity resolution, combined with sensitivity to structures as large as 18 arcmin (approx. 54 kpc). These observations directly constrain the mid-plane disk mass densities, under the assumption of an equilibrium between the thermal pressure of the gas and the gravitational attraction of the disk. The results of a preliminary analysis are given regarding the z-velocity dispersion of the gas, the mass-to-light ratio of the disk in NGC 4565, and the roles of atomic and molecular gases. The data also allow a detailed study of the HI in these galaxies; in general their brightness temperature distributions seem similar to that in the Milky Way. Both galaxies show asymmetric HI extensions beyond the optical disk. In NGC 4565 the extension is a surprisingly abrupt warp, which may bend back to parallel the galactic plane; the velocity structure implies the warp is continuous around the disk. Author

N91-14109*# National Radio Astronomy Observatory, Charlottesville, VA.
A SURVEY OF THE PROPERTIES OF EARLY-TYPE GALAXIES
Joel N. Bregman, M. S. Roberts, and D. E. Hogg *In* NASA, Ames Research Center, The Interstellar Medium in External Galaxies: Summaries of Contributed Papers Jul. 1990 p 23-25 (For primary document see N91-14100 05-90)
Avail: NTIS HC/MF A19 CSCL 03B

A compilation of the properties of elliptical and early disk galaxies was completed. In addition to material from the literature, such as Infrared Astronomy Satellite (IRAS) fluxes, the compilation

includes recent measurements of HI and CO, as well as a review of the x ray properties by Forman and Jones. The data are used to evaluate the gas content of early systems and to search for correlations with x ray emission. The interstellar medium in early-type galaxies is generally dominated by hot interstellar gas (T approx. 10 to the 7th power K; c.f. the review by Fabbiano 1989 and references therein). In addition, a significant fraction of these galaxies show infrared emission (Knapp, et al., 1989), optical emission lines, and visible dust. Sensitive studies in HI and CO of a number of these galaxies have been completed recently, resulting in several detections, particularly of the later types. Researchers wish to understand the connection among these different forms of the interstellar medium, and to examine the theoretical picture of the fate of the hot gas. To do so, they compiled observations of several forms of interstellar matter for a well-defined sample of early-type galaxies. Here they present a statistical analysis of this data base and discuss the implications of the results. Author

N91-14110*# Princeton Univ., NJ.
INTERGALACTIC HI IN THE NGC5018 GROUP
P. Guhathakurta, G. R. Knapp, Jacqueline H. vanGorkom, and D.-W. Kim (Smithsonian Astrophysical Observatory, Cambridge, MA.) *In* NASA, Ames Research Center, The Interstellar Medium in External Galaxies: Summaries of Contributed Papers Jul. 1990 p 26-28 (For primary document see N91-14100 05-90)
Avail: NTIS HC/MF A19 CSCL 03B

The cold interstellar and intergalactic medium is in the small group of galaxies whose brightest member is the elliptical galaxy NGC5018. Researchers' attention was first drawn to this galaxy as possibly containing cold interstellar gas by the detection by the Infrared Astronomy Satellite (IRAS) of emission at lambda 60 microns and lambda 100 microns at an intensity of about 1 Jy (Knapp et al. 1989), which is relatively strong for an elliptical (Jura et al. 1987). These data showed that the temperature of the infrared emission is less than 30K and that its likely source is therefore interstellar dust. A preliminary search for neutral hydrogen (HI) emission from this galaxy using the Very Large Array (VLA) showed that there appears to be HI flowing between NGC5018 and the nearby Sc galaxy NGC5022 (Kim et al. 1988). Since NGC5018 has a well-developed system of optical shells (cf. Malin and Carter 1983; Schweizer 1987) this observation suggests that NGC5018 may be in the process of forming its shell system by the merger of a cold stellar system with the elliptical, as suggested by Quinn (1984). Researchers describe follow-up HI observations of improved sensitivity and spatial resolution, and confirm that HI is flowing between NCG5022 and NGC5018, and around NGC5018. The data show, however, that the HI bridge actually connects NGC5022 and another spiral in the group, MCG03-34-013, both spatially and in radial velocity, and that in doing so it flows through and around NGC5018, which lies between the spiral galaxies. This is shown by the total HI map, with the optical positions of the above three galaxies labelled. Author

N91-14111*# Illinois Univ., Urbana. Dept. of Astronomy.
HI AND FIR EMISSION FROM S0 GALAXIES
Paul B. Eskridge and Richard W. Pogge (McDonald Observatory, Austin, TX.) *In* NASA, Ames Research Center, The Interstellar Medium in External Galaxies: Summaries of Contributed Papers Jul. 1990 p 29-32 (For primary document see N91-14100 05-90)
Avail: NTIS HC/MF A19 CSCL 03B

A large body of work has accumulated in recent years which throws into disarray the traditional assumption that S0 systems are inert, non-starforming galaxies with uniform, old stellar populations. The copious 21-cm data have been recently reviewed and assessed by Wardle and Knapp (1986). This work showed that roughly a third of the several hundred observed S0's contain detectable amounts of neutral hydrogen (HI). More recently, Pogge and Eskridge (1987) have shown that a significant fraction of HI-rich systems also exhibit H alpha emission. Thronson et al. (1989) report detection of CO line emission from two thirds of the S0's in their sample. Both of these last papers, however, report on fairly small data sets (approx. 20 objects each). From co-added Infrared Astronomy Satellite (IRAS) data, Knapp et al. (1989) report that roughly two thirds of a sample of several hundred S0's are detected at 60 and 100 microns. Work by Bally and Thronson (1989) and Walsh et al. (1989) has shown that, while a large number of S0's follow a relation between radio continuum and far infrared radiation (FIR) emission similar to that found for spirals, significant numbers of both radio-bright, and FIR-bright S0's exist. Clearly, a large number of factors are involved in determining the state of the interstellar medium in S0 galaxies. The class is probably heterogeneous, suggesting that large data samples are required to sort out various sorts of objects. The 21 cm and FIR samples are the two largest currently available. It is therefore of interest to compare the two and see where this leads. The following results are already clear: HI and FIR flux data can be used to isolate strong candidates for systems which have gained their HI gas via accretion; a rough power-law relationship exists for galaxies which are undergoing relatively normal star-forming activity; a heterogeneous class of galaxies with strong FIR emission compared to their HI emission exists. Further work is required to determine the various physical processes responsible for this last class. Author

N91-14112*# Harvard-Smithsonian Center for Astrophysics, Cambridge, MA.
THE HOT AND COLD INTERSTELLAR MATTER OF EARLY TYPE GALAXIES AND THEIR RADIO EMISSION
Dong-Woo Kim and Giuseppina Fabbiano *In* NASA, Ames Research Center, The Interstellar Medium in External Galaxies: Summaries of Contributed Papers Jul. 1990 p 33-36 (For primary document see N91-14100 05-90)
Avail: NTIS HC/MF A19 CSCL 03B

Over the last few years, the knowledge of the interstellar matter (ISM) of early type galaxies has increased dramatically. Many early type galaxies are now known to have ISM in three different phases: cold (neutral hydrogen (HI), dust and molecular material), warm (ionized) and hot (S-ray emitting) gas. Early type galaxies have smaller masses of cold ISM (10 to the 7th power - 10 to the 8th power solar mass; Jura et al. 1987) than later type spiral galaxies, while they have far more hot gas (10 to the 9th power - 10 to the tenth power solar mass; Forman et al. 1985, Canizares et al. 1987). In order to understand the relationship between the different phases of the ISM and the role of the ISM in fueling radio continuum sources and star formation, researchers compared observational data from a wide range of wavelengths. Author

N91-14113*# National Aeronautics and Space Administration. Ames Research Center, Moffett Field, CA.
PHYSICAL CONDITIONS IN PHOTODISSOCIATION REGIONS: APPLICATION TO GALACTIC NUCLEI
M. G. Wolfire (Chicago Univ., IL.), A. G. G. M. Tielens, and David J. Hollenbach *In its* The Interstellar Medium in External Galaxies: Summaries of Contributed Papers Jul. 1990 p 37-39 (For primary document see N91-14100 05-90)
Avail: NTIS HC/MF A19 CSCL 03B

Infrared and sub-millimeter observations are used in a simple procedure to determine average physical properties of the neutral interstellar medium in Galactic photodissociation regions as well as in ensembles of clouds which exist in the nuclei of luminous infrared galaxies. The relevant observations include the Infrared Astronomy Satellite (IRAS) infrared continuum measurements, infrared spectroscopy of the fine-structure lines of SiII 35 microns, OI 63 microns, and CII 158 microns, and the 2.6 mm CO (J=1-0) rotational transition. The diagnostic capabilities of the OI 145 microns line is also addressed. Researchers attribute these emission lines as well as the continuum to the atomic/molecular photodissociation region on the surfaces of molecular clouds which are illuminated by strong ultraviolet fields. They use the theoretical photodissociation region models of Tielens and Hollenbach (1985, Ap. J., 291, 722) to construct simple diagrams which utilize line ratios and line to continuum ratios to determine the average gas density n, the average incident far-ultraviolet flux G sub o, and the temperature of the atomic gas T. Author

N91-14114*# National Aeronautics and Space Administration. Ames Research Center, Moffett Field, CA.
FAR-INFRARED SPECTROSCOPY OF NGC 6946, IC 342, AND ARP 299
Steven D. Lord, David J. Hollenbach, Sean W. J. Colgan (California Univ., Santa Cruz.), Michael R. Haas, Robert H. Rubin, and Edwin F. Erickson *In its* The Interstellar Medium in External Galaxies: Summaries of Contributed Papers Jul. 1990 p 40-41 (For primary document see N91-14100 05-90)
Avail: NTIS HC/MF A19 CSCL 03B

Researchers investigated the physical conditions in the infrared bright galaxies NGC 6946, IC 342, and Arp 299 through measurements of far-infrared emission lines from Si II, O I, C II, and O III using the facility Cooled Grating Spectrometer on the Kuiper Airborne Observatory. These data are interpreted using our theoretical models for photodissociation regions and H II regions. For the central 45 inches of these galaxies, researchers determined that the dominant excitation mechanism for the far infrared radiation (FIR) lines is far ultraviolet radiation (FUR) radiation from young stars, and the authors derived the total mass, density, and temperature of the warm atomic gas and the typical sizes, number densities, and filling factors for the interstellar clouds. Author

N91-14115*# Chicago Univ., IL.
NEUTRAL ATOMIC ABSORPTION LINES AND FAR-UV EXTINCTION: POSSIBLE IMPLICATIONS FOR DEPLETIONS AND GRAIN PARAMETERS
Daniel E. Welty *In* NASA, Ames Research Center, The Interstellar Medium in External Galaxies: Summaries of Contributed Papers Jul. 1990 p 42-44 (For primary document see N91-14100 05-90)
(Contract NAG5-255; NAG5-286; CW-0001-85)
Avail: NTIS HC/MF A19 CSCL 03B

Researchers examine nine lines of sight within the Galaxy and one in the Large Magellanic Cloud (LMC) for which data on both neutral atomic absorption lines (Snow 1984; White 1986; Welty, Hobbs, and York 1989) and far UV extinction (Bless and Savage 1972; Jenkins, Savage, and Spitzer 1986) are available, in order to test the assumption that variations in gamma/alpha will cancel in taking ratios of the ionization balance equation, and to try to determine to what extent that assumption has affected the aforementioned studies of depletions and grain properties. Author

N91-14116*# Princeton Univ. Observatory, NJ.
EMPIRICAL RELATIONSHIPS BETWEEN GAS ABUNDANCES AND UV SELECTIVE EXTINCTION
Charles L. Joseph *In* NASA, Ames Research Center, The Interstellar Medium in External Galaxies: Summaries of Contributed Papers Jul. 1990 p 45-46 (For primary document see N91-14100 05-90)
Avail: NTIS HC/MF A19 CSCL 03B

Several studies of gas-phase abundances in lines of sight through the outer edges of dense clouds are summarized. These lines of sight have 0.4 less than E(B-V) less than 1.1 and have inferred spatial densities of a few hundred cm(-3). The primary thrust of these studies has been to compare gaseous abundances in interstellar clouds that have various types of peculiar selective extinction. To date, the most notable result has been an empirical relationship between the CN/Fe I abundance ratio and the depth of the 2200 A extinction bump. It is not clear at the present time, however, whether these two parameters are linearly correlated or the data are organized into two discrete ensembles. Based on 19 samples and assuming the clouds form discrete ensembles, lines of sight that have a CN/Fe I abundance ratio greater than 0.3 (dex) appear to have a shallow 2.57 plus or minus 0.55 bump compared to 3.60 plus or minus 0.36 for other dense clouds and compared to the 3.6 Seaton (1979) average. The difference in the strength of the extinction bump between these two ensembles is 1.03 plus or minus 0.23. Although a high-resolution IUE survey of dense clouds is far from complete, the few lines of sight with shallow extinction bumps all show preferential depletion of certain elements, while those lines of sight with normal 2200 A bumps do not. Ca II, Cr II, and Mn II appear to exhibit the strongest preferential depletion compared to S II, P II, and Mg II. Fe II and Si II depletions also appear to be enhanced somewhat in the shallow-bump lines of sight. It should be noted that Copernicus data suggest all elements, including the so-called nondepletors, deplete in diffuse clouds (Snow and Jenkins 1980, Joseph 1988). Those lines of sight through dense clouds that have normal 2200 A extinction bumps appear to be extensions of the depletions found in the diffuse interstellar medium. That is, the overall level of depletion is enhanced, but the element-to-element abundances are similar to those in diffuse clouds. In a separate study, the abundances of neutral atoms were studied in a dense cloud having a shallow 2200 A bump and in one with a normal strength bump. Author

N91-14117*# Massachusetts Univ., Amherst.
THE FCRAO EXTRAGALACTIC CO SURVEY: GLOBAL PROPERTIES OF GALAXIES
J. S. Young, M. Claussen, Nicholas A. Devereux, Y. Huang, J. D. Kenney, Patricia M. Knezek, L. Tacconi, L. Tacconi-Garman, F. P. Schloerb, and P. Viscuso et al *In* NASA, Ames Research Center, The Interstellar Medium in External Galaxies: Summaries of Contributed Papers Jul. 1990 p 47-49 Prepared in cooperation with Five-College Astronomy Dept., Amherst, MA (For primary document see N91-14100 05-90)
Avail: NTIS HC/MF A19 CSCL 03B

Since stars form in molecular clouds, a critical element in studies of galaxy evolution is knowledge of the molecular content of a large sample of galaxies. To this end, researchers undertook a survey of CO emission from galaxies using the Fire College Radio Astronomy Observatory (FCRAO) 14-m millimeter telescope at 115 GHz. The aim was to better understand the differences found among and within galaxies with regard to the efficiency of star and cloud formation. The galaxies observed as part of the FCRAO Extragalactic CO Survey were selected on the basis of their optical or infrared properties. The galaxies observed thus far are (1) brighter than B sub T (sub o)=12.5 in the blue, or (2) brighter than 20 Jy at 100 microns. From major axis CO observations at 45 seconds resolution and spacing in over 200 galaxies, researchers determined the CO radial distributions, and derived global CO fluxes (cf. Kenney and Young 1988); H2 masses were derived using the conversion factor N(H2)/I sub CO=2.8 times 10 to the 20th power cm(-2)/K km s(-1)) (Bloemen et al. 1986). Here, researchers concentrate on the global galaxy properties within the sample. Neutral hydrogen (HI) masses for the sample galaxies were taken from Huchtmeier et al. (1983), blue luminosities and morphological types were taken from RC2. IR luminosities, colors, dust temperatures and dust masses were determined from coadded Infrared Astronomy Satellite (IRAS) data (Young et al. 1989). They have chosen to first compare absolute luminosities and masses in order to determine the slope and scatter in each correlation; next they investigate luminosity independent ratios in order to intercompare large and small galaxies. Author

N91-14118*# Stockholm Observatory (Sweden).
A SURVEY OF GALAXIES IN CO
Torsten Elfhag *In* NASA, Ames Research Center, The Interstellar Medium in External Galaxies: Summaries of Contributed Papers Jul. 1990 p 50-52 (For primary document see N91-14100 05-90)
Avail: NTIS HC/MF A19 CSCL 03B

A large survey of galaxies in the CO (J=1-0) line is presented. Among different types of active galaxies, within the sample, the detection rate is found to be: Starbursts (15 percent), Liners (60 percent), Seyferts (30 percent). A look at the subsample that is located within 40 Mpc (Ho = 75 km s(-1) Mpc(-1) regarding local density of galaxies reveals no substantial difference between detections and non-detections. Author

N91-14119*# Massachusetts Univ., Amherst.
THE RATIO OF MOLECULAR TO ATOMIC GAS IN SPIRAL GALAXIES AS A FUNCTION OF MORPHOLOGICAL TYPE

Patricia M. Knezek and Judith S. Young *In* NASA, Ames Research Center, The Interstellar Medium in External Galaxies: Summaries of Contributed Papers Jul. 1990 p 53-55 Previously announced in IAA as A90-19542 Prepared in cooperation with Five-College Astronomy Dept., Amherst, MA (For primary document see N91-14100 05-90)
Avail: NTIS HC/MF A19 CSCL 03B

In order to gain an understanding of the global processes which influence cloud and star formation in disk galaxies, it is necessary to determine the relative amounts of atomic, molecular, and ionized gas both as a function of position in galaxies and from galaxy to galaxy. With observations of the CO distributions in over 200 galaxies now completed as part of the Five College Radio Astronomy Observatory (FCRAO) Extragalactic CO Survey (Young et al. 1989), researchers are finally in a position to determine the type dependence of the molecular content of spiral galaxies, along with the ratio of molecular to atomic gas as a function of type. Do late type spirals really have more gas than early types when the molecular gas content is included. Researchers conclude that there is more than an order of magnitude decrease in the ratio of molecular to atomic gas mass as a function of morphological type from Sa-Sd; an average Sa galaxy has more molecular than atomic gas, and an average Sc has less. Therefore, the total interstellar gas mass to blue luminosity ratio, M sub gas/L sub B, increases by less than a factor of two as a function of type from Sa-Sd. The dominant effect found is that the phase of the gas in the cool interstellar medium (ISM) varies along the Hubble sequence. Researchers suggest that the more massive and centrally concentrated galaxies are able to achieve a molecular-dominated ISM through the collection of more gas in the potential. That gas may then form molecular clouds when a critical density is exceeded. The picture which these observations support is one in which the conversion of atomic gas to molecular gas is a global process which depends on large scale dynamics (cf Wyse 1986). Among interacting and merging systems, researchers find considerable scatter in the M(H2)/M(HI) ratio, with the mean ratio similar to that in the early type galaxies. The high global ratio of molecular to atomic gas could result from the removal of HI gas, the enhanced conversion of HI into H2, or both. Author

N91-14120*# Tokyo Univ. (Japan). Inst. of Astronomy.
CIRCUMNUCLEAR MOLECULAR GAS IN STARBURST AND SEYFERT GALAXIES
Yoshiaki Taniguchi, Osamo Kameya, and Naomasa Nakai (Nobeyema Solar Radio Observatory, Japan) *In* NASA, Ames Research Center, The Interstellar Medium in External Galaxies: Summaries of Contributed Papers Jul. 1990 p 56-58 (For primary document see N91-14100 05-90)
Avail: NTIS HC/MF A19 CSCL 03B

In order to investigate circumnuclear molecular gaseous contents and their relation to the nuclear activity, researchers made a search for circumnuclear (12)CO (J=1-0) emission from 28 starburst-nucleus galaxies (SBNs) and 12 Seyfert galaxies with the recession velocities less than 5000 km/s, using the Nobeyama Radio Observatory 45-m telescope. The full half-power beam width of 17 arcsec covers a region of less than about 5 kpc in diameter for the sample galaxies. The circumnuclear CO emission was detected from twelve SBNs (one is marginal) and four Seyfert galaxies. The main results and conclusions are summarized. Researchers derived the circumnuclear surface density of molecular gas which is corrected for inclination of the galaxies. This analysis shows that the surface density spans a wide range over two orders of magnitude. Further, there is no significant difference in the surface densities between types 1 and 2 Seyfert galaxies. Thus, we may conclude that the circumnuclear molecular content is not a key parameter producing the dichotomy of the Seyfert galaxies. It is also shown that there is no significant difference in the circumnuclear surface densities of molecular gas among the Seyfert, starburst, and normal galaxies. This implies that the circumnuclear gaseous content is not a key parameter determining which activity occurs in nuclei. We may conclude that more centrally condensed (i.e., less than 10 - 100 pc in diameter) gas components play an essential role on the occurrence of nuclear activities. Comparing results with the previous ones, researchers deduced radial distribution of surface density of molecular gases. They cannot obtain evidence for strong central concentration of molecular gas in the sample Seyfert galaxies except for NGC 3227. This is consistent with the previous result by Blitz, Mathieu, and Bally (1986). Comparing the CO emission line profiles with the previous ones taken with the larger beams, researchers discovered circumnuclear components of molecular gases. In particular, they found that molecular gas clouds may be absent in the SE of the nucleus of NGC 7469 where the high-excitation emitting region is discovered by Heckman et al. (1986). It is suggested that the nuclear activity (strong radiation and/or wind) may destruct the molecular clouds in that region. Author

N91-14121*# Maryland Univ., College Park.
HIGH RESOLUTION CO IMAGES OF SEYFERT GALAXIES
M. Meixner, R. Puchalsky, L. Blitz, and M. Wright (California Univ., Berkeley.) *In* NASA, Ames Research Center, The Interstellar Medium in External Galaxies: Summaries of Contributed Papers Jul. 1990 p 59-61 Previously announced in IAA as A90-32188 (For primary document see N91-14100 05-90)
Avail: NTIS HC/MF A19 CSCL 03B

The CO (J = 1-0) emission of three Seyfert galaxies, NGC 3227, NGC 7469, and NGC 5033 was imaged. The CO emission in NGC 3227 and NGC 7469 appears as compact structures centered on the active nuclei, containing substantial fractions of the single-dish flux. In NGC 3227, 10 percent of the CO flux detected by the interferometer is contained within the ionized narrow-line region. The unresolved molecular gas concentrations in the nucleus of NGC 3227 imply a CO mass of 65 million solar masses concentrated within a diameter less than 50 pc. The CO emission in NGC 5033 is not detected at this resolution, implying a CO structure size of 20 to 60 arcsec. Continuum emission at 2.7 mm is not detected in any of the three galaxies. In the center of NGC 7469, the H2 mass is comparable to the dynamical mass. Kinematic studies of the detected gas reveal a rotational motion of the gas in NGC 3227 and NGC 7469, allowing identification of the gas in NGC 7469 with a nuclear starburst. These data are consistent with the idea that interactions between galaxies cause gas to concentrate in their nuclei thereby feeding starburst and Seyfert activity. Author

N91-14122*# Owens Valley Radio Observatory, Pasadena, CA.
APERTURE SYNTHESIS CO OBSERVATIONS OF THE INNER DISK OF NGC 1068
P. Planesas, N. Z. Scoville, and S. T. Myers *In* NASA, Ames Research Center, The Interstellar Medium in External Galaxies: Summaries of Contributed Papers Jul. 1990 p 62-64 (For primary document see N91-14100 05-90)
Avail: NTIS HC/MF A19 CSCL 03B

NGC 1068 is probably the nearest galaxy with both a high rate of star formation and a high luminosity active nucleus. About one-half of the total IR luminosity originates in a disk approximately 30 seconds in size, which has been taken as evidence for a high rate of massive star formation (Telesco et al. 1984). Previous CO line observations have shown the existence of a ring at the outer boundary of the inner disk (Myers and Scoville 1987). Although these observations have proved that this ring is extremely rich in molecular gas (as suggested by Scoville et al. 1983), the angular resolution (approx. 6 seconds) was not high enough to resolve its structure. New aperture synthesis observations of the CO (J=1 to 0) emission in the inner disk of NGC 1068 have been carried out with the Owens Valley Radio Observatory (OVRO) mm Interferometer. The new receivers installed for the 88/89 season have allowed researchers to obtain a high sensitivity map of the CO emission. The molecular cloud ring has been resolved and continuum as well as line emission from the nucleus of the galaxy have been detected. Author

N91-14123*# Wisconsin Univ., Madison.
CO APERTURE SYNTHESIS OF NGC 4038/9 (ARP 244)
S. A. Stanford, D. B. Sanders, A. I. Sargent, and N. Z. Scoville

(California Inst. of Tech., Pasadena.) *In* NASA, Ames Research Center, The Interstellar Medium in External Galaxies: Summaries of Contributed Papers Jul. 1990 p 65-67 (For primary document see N91-14100 05-90)
Avail: NTIS HC/MF A19 CSCL 03B

Researchers present high-resolution (approx. 6 seconds) CO observations of the merging galaxies NGC 4038/9 made with the Owens Valley Radio Observatory (OVRO) Millimeter Wave Interferometer. The CO observations of Arp 244 were obtained between April and June 1988 using the OVRO Millimeter Wave Interferometer. Two fields with phase centers near the NGC 4039 nucleus and near the NGC 4038 nucleus were observed. The size of the synthesized beam is approximately 6.5 x 7 seconds at PA=72 degrees. The rms in a single cleaned channel map is 0.06 Jy beam(exp -1), corresponding to a brightness temperature of 0.12 K over the synthesized beam. Contour maps of the integrated CO intensity for both interferometer fields are shown. Three CO concentrations are evident. Two are centered near the nuclei of NGC 4038 and NGC 4039, closely correlated with H alpha and radio continuum maxima. A third CO emission region lies about 25 seconds northeast of the NGC 4039 nucleus. A number of radio continuum, H alpha, and 10 micron emission knots appear in this region. The total integrated intensity at the northern nuclear source, 302 K km/s, leads to a molecular mass of 8.3 by 10 to the 8th power solar mass assuming a Galactic CO to H2 conversion factor of 3.0 x 10 to the 20th power H2 cm(-2) (K km/s)(-1). The integrated CO intensity of the southern nuclear source leads to a molecular mass of 2.4 x 10 to the 8th solar mass. The extranuclear CO concentration contains 1.2 x 10 to the 9th power solar mass of molecular gas, extending over 170 km/s, and is resolved in a number of channels. Its large size, mass, and morphology strongly suggest that it is an agglomeration of several clumps. Author

N91-14124*# Massacnusetts Inst. of Tech., Cambridge. Center for Astrophysics.
OBSERVATIONS OF CO IN THE MAGELLANIC IRREGULAR GALAXY NGC 55
Andreas Heithausen and Ralf-Juergen Dettmar (Lowell Observatory, Flagstaff, AZ.) *In* NASA, Ames Research Center, The Interstellar Medium in External Galaxies: Summaries of Contributed Papers Jul. 1990 p 68-70 Sponsored in part by Deutsche Forschungsgemeinschaft (For primary document see N91-14100 05-90)
Avail: NTIS HC/MF A19 CSCL 03B

The content of molecular gas in galaxies, mainly H2, is one of the key observations necessary for the understanding of star formation processes and history. As the CO molecule is the most widely distributed molecule after H2 and has easily observable mm lines, it is used as a tracer for the molecular gas. CO was detected towards the direction where the H alpha and 6 cm radio continuum emission is strongest (Hummel et al. 1986). Here, researchers present the Gaussian line parameters in tabular form. The distribution of CO corresponds well with the intense HI cloud near the bar of NGC 55. The extent of the CO cloud is about 975 pc perpendicular to the major axis. As the radio continuum and the H alpha emission also peaks in this region, it is most probably associated with the star forming region in NGC 55. Assuming that the molecular gas is in virial equilibrium, researchers derive a mass of about 8 times 10(exp 7) solar magnitude. The molecular mass found indicates that the conversion factor for the molecular mass in Irr galaxies as inferred from CO line emission is indeed higher by up to a factor of 20 compared to the canonical value for the Galaxy. Author

N91-14125*# Max-Planck-Inst. fuer Physik und Astrophysik, Garching (Germany, F.R.). Inst. fuer Extraterrestrische Physik.
OBSERVATIONS OF CO ISOTOPIC EMISSION AND THE FAR-INFRARED CONTINUUM OF CENTAURUS A Abstract Only
A. Eckart, M. Cameron, H. Rothermel, W. Wild, H. Zinnecker, M. Olberg, G. Rydbeck, and T. Wiklind (Onsala Space Observatory, Sweden) *In* NASA, Ames Research Center, The Interstellar Medium in External Galaxies: Summaries of Contributed Papers Jul. 1990 p 71 (For primary document see N91-14100 05-90)
Avail: NTIS HC/MF A19 CSCL 03B

Researchers present maps of the CO-12(1=0) line and the 100 micron and 50 micron far-infrared emission of Centaurus A, as well as measurements of the CO-12(2-1), CO-13(1-0), and the C-18O(1-0) lines at selected positions. The observations were taken with the Swedish-ESO Submillimeter Telescope (SEST) and the CPC instrument on board the Infrared Astronomy Satellite (IRAS). The millimeter data show that the bulk molecular material is closely associated with the dust lane and contained in a disk of about 180 seconds diameter and a total molecular mass of about 2 x 10 to the 8th power solar mass. The total molecular mass of the disk and bulge is of the order of 3 x 10 to the 8th power solar mass. The molecular gas in the nucleus is warm with a kinetic temperature of the order of 15 K and a number density of 10 to the 3rd power to 3 x 10 to the 4th power cm(-3). Absorption features in the CO-12 and CO-13 lines against the nuclear continuum emission indicate that the properties of giant molecular clouds are comparable to those of the Galaxy. The far-infrared data show that to a good approximation the dust temperature is constant across the dust lane at a value of about 42 K. The ratio between the far-infrared luminosity and the total molecular mass is 18 solar luminosity/solar mass and close to the mean value obtained for isolated galaxies. A comparison of the CO-12(1-0) and the far-infrared data indicates that a considerable amount of the far-infrared emission is not intimately associated with massive star formation. Author

N91-14126*# Massachusetts Univ., Amherst. Dept. of Physics and Astronomy.
THE CO-12 AND CO-13 J=2-1 AND J=1-0 OBSERVATIONS OF HOT AND COLD GALAXIES
Shuding Xie, F. Peter Schloerb, and Judith Young *In* NASA, Ames Research Center, The Interstellar Medium in External Galaxies: Summaries of Contributed Papers Jul. 1990 p 72-74 (For primary document see N91-14100 05-90)
Avail: NTIS HC/MF A19 CSCL 03B

Researchers observed the nuclear regions of the galaxies NGC 2146 and IC 342 in CO-12 and CO-13 J=1-0 and J=2-1 lines using the Five College Radio Astronomy Observatory (FCRAO) 14m telescope. NGC 2146 is a peculiar Sab spiral galaxy. Its complex optical morphology and strong nuclear radio continuum emission suggest that it is experiencing a phase of violent activity and could have a polar ring which may have resulted from an interaction. IC 342 is a nearby luminous Scd spiral galaxy. Strong CO, infrared and radio continuum emission from the nuclear region of IC 342 indicate enhanced star-forming activity, and interferometric CO-12 J=1-0 observations reveal a bar-like structure centered on the nucleus, along the dark lane in the NS direction. These two galaxies are selected based on their different dust temperatures and star formation efficiencies (SFE) as derived from the Infrared Astronomy Satellite (IRAS) S sub 60 mu/S sub 100 mu flux density ratio and L sub IR/M(H2), respectively, with a relatively high SFE and dust temperature of 45 K in NGC 2146 and a relatively low SFE and dust temperature of 35 K in IC 342. The data from the different CO-12 and CO-13 lines are used to study the physical conditions in the molecular clouds in the galaxies. Researchers also consider the radiative transfer to determine whether a warm and optically thin gas component exists in these galaxies, as has been suggested in the case of M82 (Knapp et al. 1980), and whether the warm gas is related to the dust properties. Since optically thin CO-12 gas is rarely detected in our own Galaxy (except in outflow sources), to confirm its existence in external galaxies is very important in understanding the molecular content of external galaxies and its relationship to star formation activity. The present CO-12 J=2-1 and CO-13 J=2-1 and J=1-0 data for NGC 2146 are the first detections of this galaxy to our knowledge. The CO-12 J=1-0 distribution in NGC 2146 has been measured as part of the FCRAO Extragalactic Survey. For the well-studied IC 342, the data are compared with 30m observations and other available data. Researchers present the observed results. Author

N91-14127*# Onsala Space Observatory (Sweden).
THE MOLECULAR CLOUD CONTENT OF EARLY TYPE GALAXIES
Tommy Wiklind and Christian Henkel (Max-Planck-Inst. fuer Radioastronomie, Bonn, Germany, F.R.) *In* NASA, Ames Research Center, The Interstellar Medium in External Galaxies: Summaries of Contributed Papers Jul. 1990 p 75-77 (For primary document see N91-14100 05-90)
Avail: NTIS HC/MF A19 CSCL 03B

A survey of the CO content of early type galaxies led to 24 new detections, mostly lenticular galaxies. The galaxies, which are situated in both the Northern and Southern Hemispheres, were selected as being far-IR luminous compared to their blue luminosity, and situated at distances less than about 50 Mpc (H sub o=100 km/s Mpc(-1). Results for some early galaxies (NGC 404, NGC 3593 and NGC 4369 are given. Author

N91-14128*# Arizona Univ., Tucson.
CS J = 2 YIELDS 1 EMISSION TOWARD THE CENTRAL REGION OF M82
C. E. Walker, C. K. Walker, J. E. Carlstrom (California Univ., Berkeley.), and R. N. Martin *In* NASA, Ames Research Center, The Interstellar Medium in External Galaxies: Summaries of Contributed Papers Jul. 1990 p 78-80 (For primary document see N91-14100 05-90)
Avail: NTIS HC/MF A19 CSCL 03B

M82 is an irregular (Type II) galaxy located at a distance of approximately 3.5 Mpc. Its unusual appearance and high luminosity, particularly in the infrared, has led many astronomers to classify it as a starburst galaxy. This interpretation is supported by the observation of a large number of radio continuum sources within the central arcminute of the galaxy. These sources are thought to be associated with supernova remnants. The starburst in the central region of the galaxy is believed to have been triggered by tidal interaction with either M81 or the HI cloud surrounding the M81 group. High angular resolution CO-12 J=1 to 0 maps by Nakai (1984) and Lo et al. (1987) indicate the existence of a 400 to 450 pc rotating ring of molecular material about the central region of M82. Red- and blue-shifted absorption components of the HI and OH lines measured by Weliachew et al. (1984) provided the first evidence for the presence of the ring. Many astronomers, each using a different angular resolution, have compared CO-12 J=1 to 0, J=2 to 1, and J=3 to 2 emission and concluded that a large fraction of the CO emission is optically thin. Additional observations suggest that the molecular material toward the center of M82 is clumpy and dense. Unlike the lower rotational transitions of CO, CS is excited only at relatively high densities, n sub H sub 2 greater than or equal to 10(exp 4) cm(-3). It is in clouds with these densities that stars are expected to form. This makes CS an excellent probe of star formation regions. Researchers observed the CS J=2 to 1 transition (97.981 GHz) toward 52 positions in M82 using the National Radio Astronomy Observatory (NRAO) 12 m telescope. Author

N91-14129*# Edinburgh Univ. (Scotland). Dept. of Astronomy.
HIGH RESOLUTION SUB-MILLIMETRE MAPPING OF STARBURST GALAXIES: COMPARISON WITH CO EMISSION
P. A. Smith, P. W. J. L. Brand, Phil J. Puxley, C. M. Mountain, and Naomasa Nakai (Nobeyema Solar Radio Observatory, Japan) *In* NASA, Ames Research Center, The Interstellar Medium in External Galaxies: Summaries of Contributed Papers Jul. 1990 p 81-83 Submitted for publication (For primary document see N91-14100 05-90)
Avail: NTIS HC/MF A19 CSCL 03B

Researchers present first results from a program of submillimeter continuum mapping of starburst galaxies, and comparison of their dust and CO emission. This project was prompted by surprising results from the first target, the nearby starburst M82, which shows in the dust continuum a morphology quite unlike that of its CO emission, in contrast to what might be expected if both CO and dust are accurately tracing the molecular hydrogen. Possible explanations for this striking difference are discussed. In the light of these results, the program has been extended to include sub-mm mapping of the nearby, vigorously star forming spirals, M83 and Maffei 2. The latter were also observed extensively in CO, in order to study excitation conditions in its central regions. The James Clerk Maxwell Telescope was used in these studies. Author

N91-14130*# Texas Univ., Austin.
HIGH SPATIAL RESOLUTION 100 MICRON OBSERVATIONS OF THE M83 BAR
B. J. Smith, Dan F. Lester, and P. M. Harvey *In* NASA, Ames Research Center, The Interstellar Medium in External Galaxies: Summaries of Contributed Papers Jul. 1990 p 84-85 (For primary document see N91-14100 05-90)
Avail: NTIS HC/MF A19 CSCL 03B

A program of high spatial resolution far-infrared observations of galaxies using the Kuiper Airborne Observatory (KAO), was conducted to better understand the role of star formation, the general interstellar radiation field, and non-thermal activity in powering the prodigious far-infrared luminosities seen in spiral and interacting galaxies. Here, researchers present observations of the central region of the well-known barred spiral M83 (NGC 5236). The resultant channel 3 scans for M83 and IRC + 10216, after co-addition and smoothing, are shown. These data show that M83 is extended at 100 microns compared to a point source. A simple Gaussian deconvolution of the M83 data with the point source profile from IRC+10216 gives a full width half maximum (FWHM) of about 19 seconds for M83. By comparison with IRC+10216, researchers obtain a flux for the unresolved component in M83 of about 110 Jy. This is about 1/6 the total flux for M83 (Rice et al. 1988) and about 1/2 the PSC flux. The M83 and IRC+10216 profiles in the cross-scan direction (SE-NW) were also compared, and show that M83 is extended in this direction as well, with a width of about 18 seconds. A comparison of the different channel profiles for M83 and IRC+10216 shows that there is an asymmetry in the M83 data, in that the maximum in the profiles shifts from southeast to northwest as channel number increases. This corresponds to the extension in the bar seen in the CO data. Thus the far-infrared emission in the central region of M83 tends to trace the CO bar. The new 100 micron data is also compared with previous H alpha observations from the literature, to determine how well the far-infrared traces the stellar structure, the star formation as measured by H alpha, and the optical colors.
Author

N91-14131*# Tata Inst. of Fundamental Research, Bombay (India).
FAR-INFRARED OBSERVATIONS OF CIRCINUS AND NGC 4945 GALAXIES
R. S. Bisht, S. K. Ghosh, K. V. K. Iyengar, T. N. Rengarajan, S. N. Tandon, and R. P. Verma *In* NASA, Ames Research Center, The Interstellar Medium in External Galaxies: Summaries of Contributed Papers Jul. 1990 p 86-88 (For primary document see N91-14100 05-90)
Avail: NTIS HC/MF A19 CSCL 03B

Circinus and NGC 4945 are two galaxies luminous in the infrared and are characterized by compact non thermal radio nuclei, deep silicate absorption features and unusually strong water vapor maser luminosities. Moorwood and Glass (1984) have observed these galaxies extensively in the 1 to 20 micron range. In the far-infrared, observations up to 100 microns are available from the Infrared Astronomy Satellite (IRAS). In order to study the cool dust component of these galaxies, researchers observed them at 150 microns using the Tata Institute of Fundamental Research (TIFR) 100 cm balloon-borne telescope. Here, they report observations along with deconvolved maps at 50 and 100 microns obtained from the Chopped Photometric Channel (CPC) on board IRAS.
Author

N91-14132*# Lancaster Polytechnic, Preston (England). School of Physics and Astronomy.
THE 3 MICRON SPECTRUM OF NGC 4565
A. J. Adamson and D. C. B. Whittet (York Univ., Toronto, Ontario) *In* NASA, Ames Research Center, The Interstellar Medium in

External Galaxies: Summaries of Contributed Papers Jul. 1990 p 89-91 (For primary document see N91-14100 05-90)
Avail: NTIS HC/MF A19 CSCL 03B

Researchers spectrum of NGC 4565 is essentially featureless. The absence of the 3.0 micron feature (Tau 3.0 less than 0.05) implies that the extinction to the nucleus does not arise to a significant degree in molecular clouds. Researchers deduce Tau 3.0/A sub V less than 0.01, compared with approx. 0.022 for GC-IRS7. These results support the conclusion (McFadzean et al. 1989) that the 3.0 micron absorption in the GC-IR sources is due to the presence of ice in a (probably single) foreground molecular cloud. The 3.4 micron feature is also weak or absent in the researchers spectrum of NGC 4565 (Tau 3.4 less than or equal to 0.07), hence, Tau 3.4/A sub V less than or equal to 0.016, compared with approx. 0.008 towards GC-IRS7. The absence of the feature in NGC 4565 at the signal-to-noise level of the current observations is consistent with a probable moderate degree of extinction towards the nucleus. The observations of NGC 4565 provide a useful comparison for studies of dust in the Galaxy. Limits have been set on the strengths of the 3.0 and 3.4 micron features in NGC 4565. The absence of 3.0 micron absorption is significant, and supports the view that the feature at this wavelength in the Galactic Centre is due to water-ice absorption in a foreground molecular cloud. The non-detection of the 3.4 micron absorption is less surprising and provides indirect support for the association between this feature and the diffuse interstellar medium. The current spectrum probably represents the best that can be achieved with a single-detector instrument within reasonable integration times. It will clearly be of interest in the future to obtain spectra of higher signal-to-noise, as a positive detection of the 3.4 micron feature in an external galaxy, even at a low level, would be of considerable astrophysical significance. Author

N91-14133*# Lawrence Livermore National Lab., CA. Inst. of Geophysics and Planetary Physics.
SPATIAL ANALYSIS OF IRAS OBSERVATIONS OF NEARBY SPIRALS
Roger Ball and R. Y. Lo (Illinois Univ., Urbana.) *In* NASA, Ames Research Center, The Interstellar Medium in External Galaxies: Summaries of Contributed Papers Jul. 1990 p 95-96 (For primary document see N91-14100 05-90)
Avail: NTIS HC/MF A19 CSCL 03B

The unbiased survey of the infrared sky carried out by the Infrared Astronomy Satellite (IRAS) satellite has greatly accelerated advances in understanding the dust component of our own and external galaxies. However, most extragalactic studies to date have been based on the IRAS Point Source Catalog (PSC), which has two serious limitations. First, in sources where a significant fraction of the flux is extended, significant errors may result from using PSC fluxes in comparative studies, and these errors could be systematic if the tendency to be non-pointlike depends on physical properties of the galaxy. Additionally, use of PSC fluxes rules out any direct investigation of the spatial distribution of the IRAS emission from disks in external galaxies. Since work on the Galactic IRAS results has shown that very different physical processes can make varying contributions to the observed flux, it is important to look at a wide sample of galaxies with some spatial resolution to study the relative dominance of these processes under a variety of conditions. Here, researchers report on work they are doing to carry out this program for many nearby spirals, using an analysis package that was developed for this purpose. Researchers carried out analysis for a sample of 121 nearby spirals. The fraction of the flux contained in a point source varies from 0 to 1 across the sample, all of which are well resolved at their nominal optical diameters. There is no evidence that the galaxies of smaller angular size are less likely to be resolved by IRAS at this level. The program gives results which are quite repeatable from scan to scan; the fraction f (point source flux over total flux) at 60 microns has typical errors of 0.03 when different scans are combined. Approximately two-thirds of the sample have more flux in the extended than in the nuclear component. There is a tendency for earlier-type spirals to be less centrally concentrated, but this effect is slight and the degree of variation is large for all types. Barred spirals are also found across the spectrum of f, but are much more likely to have little or no nuclear emission. Author

N91-14134*# Yerkes Observatory, Williams Bay, WI.
CONTRIBUTION OF COOL DUST TO THE FIR BRIGHTNESS DISTRIBUTION OF NGC 6946 Sc(s)2
Greg Engargiola and D. A. Harper *In* NASA, Ames Research Center, The Interstellar Medium in External Galaxies: Summaries of Contributed Papers Jul. 1990 p 97-99 (For primary document see N91-14100 05-90)
Avail: NTIS HC/MF A19 CSCL 03B

A few galaxies have been observed at submillimeter wavelengths (Stark et al., 1988; Eales, Wynn-Williams, and Duncan, 1988). These observations do not support the hypothesis that there exist substantial amounts of cool dust generating submillimeter radiation in excess of predictions from modified blackbody curves of the form (1/lambda)exp 1.5 B sub v (v, T) fit to total 100 and 160 micron fluxes. However, researchers find relatively cold dust (approx. 17 to 23 degrees K) at several interarm locations in the central 5 minute by 5 minute region of NGC 6946 Sc(s)II. Since molecular gas is the predominate constituent of the interstellar medium (ISM) in this region, such low dust temperatures are indicative of quiescent molecular clouds and low star formation rates. Based on the contribution of cool grains to the 160 micron surface brightness distribution, regions of low star formation activity can be identified. A 1/lambda exp 1.5 emissivity law is assumed for this analysis. Researchers assumed a two temperature grain model in an effort to decompose the far infrared surface brightness distribution of NGC 6946 into contributions from cool, quiescent and active, star forming regions. This model has some validity; although an oversimplification of the dust energetics, researchers find from it that, where giant HII regions are sparse, a significant fraction of the 160 micron emission is emitted by a cool grain component which the Infrared Astronomy Satellite (IRAS) could barely detect. Author

N91-14135*# Pennsylvania State Univ., University Park. Dept. of Astronomy.
FAR INFRARED LUMINOSITY FUNCTIONS OF NORMAL GALAXIES
Takashi Isobe and Eric D. Feigelson *In* NASA, Ames Research Center, The Interstellar Medium in External Galaxies: Summaries of Contributed Papers Jul. 1990 p 100-102 Sponsored in part by JPL and Zaccheus Daniel Foundation (For primary document see N91-14100 05-90)
Avail: NTIS HC/MF A19 CSCL 03B

Researchers constructed a volume limited sample of 443 optically selected nearby galaxies from the Zwicky catalog to study far infrared luminosity functions. Schechter function fits and integrated luminosity densities are calculated. Comparing the resulting infrared spectrum with the infrared spectrum for interstellar matter in the solar neighborhood, researchers find most of the infrared emission is due to dust heated by the interstellar radiation field, except at 60 micron emission where star forming regions contribute significantly. Author

N91-14136*# Space Telescope Science Inst., Baltimore, MD.
EVIDENCE AGAINST A SIMPLE TWO-COMPONENT MODEL FOR THE FAR-INFRARED EMISSION FROM GALAXIES
Stephen A. Eales and Nicholas A. Devereux (Five-College Astronomy Dept., Amherst, MA.) *In* NASA, Ames Research Center, The Interstellar Medium in External Galaxies: Summaries of Contributed Papers Jul. 1990 p 103-104 (For primary document see N91-14100 05-90)
Avail: NTIS HC/MF A19 CSCL 03B

Two of the first Infrared Astronomy Satellite (IRAS) results were that galaxies have a wide range of values for the ratio of 60 micron to 100 micron flux density (0.2 less than or equal to S sub 60/S sub 100 less than or equal to 1.0) and that this ratio is correlated with L sub fir, L sub b, L sub fir being the total far-infrared luminosity and L sub b being the luminosity at visible wavelengths (de Jong et al. 1984; Soifer et al. 1984). From these results arose

the following simple model for the far-infrared emission from galaxies (de Jong et al. 1984), which has remained the standard model ever since. In this model, the far-infrared emission comes from two dust components: warm dust (T approx. equals 50 K) intermingled with, and heated by, young massive OB stars in molecular clouds and HII regions, and colder dust (T approx. equals 20 K) associated with the diffuse atomic hydrogen in the interstellar medium and heated by the general interstellar radiation field. As the number of young stars in a galaxy increases, S sub 60/S sub 100 increases, because there is a greater proportion of warm dust, and so does L sub fir/L sub b, because most of the radiation from the young stars is absorbed by the dust, leading to a swifter increase in far-infrared emission than in visible light. Although this model explains the basic IRAS results, it is inelegant. It uses two free parameters to fit two data (the 60 and 100 micron flux densities)-and there are now several observations that contradict it. Despite these major problems with the two-component model, it is not clear what should be put in its place. When considering possible models for the far-infrared emission from galaxies, the observational evidence for our own galaxy must be considered. Researchers suspect that the study by Boulanger and Perault (1988) of the far-infrared properties of the local interstellar medium may be particularly relevant. They showed that molecular clouds are leaky - that most of the light from OB stars in molecular clouds does not heat the dust in the clouds, but instead leaks out. The consequence of this is that that while most of the far-infrared emission from the solar neighborhood is from dust associated with diffuse HI, this dust is mostly heated by young stars. Author

N91-14137*# National Aeronautics and Space Administration. Goddard Space Flight Center, Greenbelt, MD.

EMISSION FROM SMALL DUST PARTICLES IN DIFFUSE AND MOLECULAR CLOUD MEDIUM

J. P. Bernard (Paris XI Univ., Orsay, France) and X. Desert *In* NASA, Ames Research Center, The Interstellar Medium in External Galaxies: Summaries of Contributed Papers Jul. 1990 p 105-107 (For primary document see N91-14100 05-90)

Avail: NTIS HC/MF A19 CSCL 03B

Infrared Astronomy Satellite (IRAS) observations of the whole galaxy has shown that long wavelength emission (100 and 60 micron bands) can be explained by thermal emission from big grains (approx 0.1 micron) radiating at their equilibrium temperature when heated by the InterStellar Radiation Field (ISRF). This conclusion has been confirmed by continuum sub-millimeter observations of the galactic plane made by the EMILIE experiment at 870 microns (Pajot et al. 1986). Nevertheless, shorter wavelength observations like 12 and 25 micron IRAS bands, show an emission from the galactic plane in excess with the long wavelength measurements which can only be explained by a much hotter particles population. Because dust at equilibrium cannot easily reach high temperatures required to explain this excess, this component is thought to be composed of very small dust grains or big molecules encompassing thermal fluctuations. Researchers present here a numerical model that computes emission, from Near Infrared Radiation (NIR) to Sub-mm wavelengths, from a non-homogeneous spherical cloud heated by the ISRF. This model fully takes into account the heating of dust by multi-photon processes and back-heating of dust in the Visual/Infrared Radiation (VIS-IR) so that it is likely to describe correctly emission from molecular clouds up to large A sub v and emission from dust experiencing temperature fluctuations. The dust is a three component mixture of polycyclic aromatic hydrocarbons, very small grains, and classical big grains with independent size distributions (cut-off and power law index) and abundances. Author

N91-14138*# National Aeronautics and Space Administration. Ames Research Center, Moffett Field, CA.

VERY SMALL GRAINS IN THE MILKY WAY AND EXTERNAL GALAXIES

L. Luan, M. W. Werner, C. Heiles, and K. Sellgren (Hawaii Univ., Honolulu.) *In its* The Interstellar Medium in External Galaxies: Summaries of Contributed Papers Jul. 1990 p 108-110 Sponsored in part by IPAC (For primary document see N91-14100 05-90)

(Contract NCA2-279)

Avail: NTIS HC/MF A19 CSCL 03B

These studies of the infrared colors of reflection nebulae, HL HI clouds, HII regions and external galaxies have shown the following results. Different classes of objects locate in different regions on the R vs F sub v (60)/F sub v (100) diagram. This is determined both by differences in dust properties and by differences in the illuminating radiation field. For example, HL clouds and reflection nebulae almost have the same behavior since both are in the diffuse Interstellar Medium (ISM) and can be expected to have similar grain populations; the small difference in their infrared colors can be explained by the difference of the illuminating radiation field. On the other hand, the dramatic difference of R=vF sub v (12)/F sub v (far IR) between HII region and diffuse ISM may be due to the destruction of the Very Small Grain (VSG) component in the HII regions, although radiation transfer effects may play a part as well. The ratio R=vF sub v (12)/F sub v (far IR) is approximately constant in normal spiral galaxies. This implies that the mass ratio b=Mass (VSG)/Mass (dust) does not vary greatly from one galaxy to another. Author

N91-14139*# National Aeronautics and Space Administration. Goddard Space Flight Center, Greenbelt, MD.

A MODEL FOR THE INFRARED EMISSION FROM AN OB STAR CLUSTER ENVIRONMENT

D. Leisawitz *In* NASA, Ames Research Center, The Interstellar Medium in External Galaxies: Summaries of Contributed Papers Jul. 1990 p 111-112 (For primary document see N91-14100 05-90)

Avail: NTIS HC/MF A19 CSCL 03B

Researchers developed an interactive radiative transfer code that predicts the infrared emission from an HII region containing diffuse ionized and atomic gas and dense molecular clouds. This model complements the investigation of the redistribution of OB star luminosity in the interstellar medium (Leisawitz and Hauser 1988, Ap. J., 332, 954). The model can be used as a diagnostic tool to probe the radiation field and matter density in an HII region, place constraints on the proximity and orientation of an illuminated molecular cloud with respect to the ionizing stars, test for the presence of small, transiently heated dust grains, and determine whether the dust-to-gas ratio is normal. Predictions of the model agree qualitatively and quantitatively with observations of blister-type HII regions ionized by well-studied OB clusters in which the distribution of dense neutral material is known. This is illustrated by a model for Infrared Astronomy Satellite (IRAS) observations of the region around NGC 7380 (S142). Researchers plan to use the model in a survey of regions of massive star formation in the outer Galaxy to study OB stars embedded to various degrees in their parental molecular clouds. Author

N91-14140*# National Aeronautics and Space Administration. Ames Research Center, Moffett Field, CA.

IRAS OBSERVATIONS OF THE ISM IN THE GAMMA CAS REFLECTION NEBULA

Richard H. Buss, Jr. and Michael W. Werner *In its* The Interstellar Medium in External Galaxies: Summaries of Contributed Papers Jul. 1990 p 113-115 (For primary document see N91-14100 05-90)

Avail: NTIS HC/MF A19 CSCL 03B

Mid-infrared emission from other galaxies originates both from interstellar grains heated by diffuse starlight and local excitation of grains by hot OB stars. Thus, a detailed examination of the Infrared Astronomy Satellite (IRAS) data from a B star interacting with the interstellar medium (ISM) could provide insight into infrared (IR) emission processes in external galaxies. Researchers have therefore used IRAS data to study the B0 IVe star gamma Cas and its surroundings, which they find to exhibit evidence of grain heating, destruction, and possible star formation. Author

N91-14141*# Wyoming Univ., Laramie. Infrared Observatory.
PEERING BEYOND IRAS: THE 100 TO 350 MICRON DUST EMISSION FROM GALAXIES
Harley A. Thronson, Jr., Deidre A. Hunter, Sean Casey, Greg Engargiola, and D. A. Harper (Yerkes Observatory, Williams Bay, WI.) *In* NASA, Ames Research Center, The Interstellar Medium in External Galaxies: Summaries of Contributed Papers Jul. 1990 p 116-119 (For primary document see N91-14100 05-90)
(Grant NAG2-134)
Avail: NTIS HC/MF A19 CSCL 03B

Several arguments can be made to study the continuum emission from dust in galaxies at wavelengths between the cutoff of the Infrared Astronomy Satellite (IRAS) survey (about 100 microns) and the shortest wavelength that is commonly accessible from the ground (about 350 microns). Some theoretical work (see the summary by Cox and Mezger 1989) indicates that there are very cool (T sub d less than or equal to 25 K) components to the dust emission that emit primarily at wavelengths between 100 and 250 microns. In fact, a significant fraction of the total luminosity, representing a large fraction of the dust mass in some types of galaxies, is emitted at long far-infrared wavelengths. In such cases, the cool dust must play a major role in regulation of the energy balance of the Interstellar Medium (ISM) and in shielding the cores of neutral clouds. Author

N91-14142*# Princeton Univ., NJ.
FAR-INFRARED EMISSION FROM DUSTY ELLIPTICALS
Duncan Walsh and Jill Knapp *In* NASA, Ames Research Center, The Interstellar Medium in External Galaxies: Summaries of Contributed Papers Jul. 1990 p 120-122 (For primary document see N91-14100 05-90)
(Grant NSF AST-86-02698)
Avail: NTIS HC/MF A19 CSCL 03B

The incidence of dust lanes in elliptical galaxies has been estimated at approx. 40 percent by Sadler and Gerhard (1985), although the observed fraction is lower because of inclination effects. A similar percentage of ellipticals has been detected by the Infrared Astronomy Satellite (IRAS) at 100 microns (Knapp et al. 1989); these have far-infrared colors expected for emission from cool dust (S sub 60 micron/S sub 100 micron approx. 1/3). For the far-infrared detected galaxies, neither L sub 100 microns/L sub B nor L sub 60 microns/L sub 100 microns are very dependent on dust content, suggesting that the source of the infrared luminosity is the same in both cases; and hence that dust is responsible even when not detected optically. Despite this indication, L sub 100 microns does not prove to be a good indicator of the quantity of cool interstellar matter in elliptical galaxies, as measured by the mass of neutral hydrogen. There even exist several examples of ellipticals with dust, strong 100 micron flux density and sensitive limits on HI mass (Walsh et al. in preparation). Chief reasons for the lack of correlation include the existence of other important sources of far-IR power in ellipticals, such as nonthermal continuum emission extending from longer wavelengths in flat spectrum radio sources (Golombek, Miley and Neugebauer 1988); and the fact that far-infrared luminosity per unit dust mass is extremely sensitive to the temperature of the ambient radiation field, which is not accurately known. In addition to having their appearance distorted by dust, several ellipticals also show such features as shells, box-shaped isophotes or inner disks. These may be signatures of past mergers, which could also add to the ISM content of the system. Author

N91-14143*# Naval Research Lab., Washington, DC. Center for Space Research.
OBSERVATIONS OF THE GALACTIC PLANE BY THE ZODIACAL INFRARED PROJECT
L. J. Rickard, S. W. Stemwedel, and S. D. Price (Air Force Geophysics Lab., Hanscom AFB, MA.) *In* NASA, Ames Research Center, The Interstellar Medium in External Galaxies: Summaries of Contributed Papers Jul. 1990 p 123-125 (For primary document see N91-14100 05-90)
Avail: NTIS HC/MF A19 CSCL 03B

The two rocket flights of the Zodiacal Infrared Project (ZIP), flown 18 August 1980 and 31 July 1981, were intended to provide data on the near-infrared thermal emission of the interplanetary dust cloud over a broad range of ecliptic coordinates (latitudes -60 to +85 degrees, solar elongation angles 22 to 90 degrees and 140 to 180 degrees). In addition, their multiple crossings of the Galactic plane provided low resolution spectral data (delta lambda/lambda ranging from 1. to 0.1, for effective wavelengths from 3 to 30 microns) for most of the first quadrant (longitudes 30 to 100 degrees). Examples are displayed. Having made a thorough reanalysis of the calibration of the ZIP database, researchers present the salient features of the Galactic plane as observed by ZIP. The binned, in-plane data, corrected for zodiacal emission, generally show an exponential decrease with increasing longitude. The fitted exponential scale-length is 0.038/degree, and can be inverted to derive a radial density profile. Channel ratios are converted to temperatures by using model spectra in which thermal emitters with emissivity approx. 1/lambda are convolved with the filter responses. The results for channels 5 (11 microns) and 12 (21 microns) are shown, along with similarly derived temperatures from Infrared Astronomy Satellite (IRAS) 12 microns and 25 microns data. The ZIP data show little variation with longitude, consistent with IRAS results. A narrow spectral feature at 13 microns appears consistently in data for the plane (uncorrected for zodiacal emission). However, this is strongly contaminated by calibration problems for channel 8. Researchers suggest that residual emission at 13 microns arises from the (NeII) line at 12.8 microns. Author

N91-14144*# Joint Inst. for Lab. Astrophysics, Boulder, CO.
THE INFRARED CONTINUUM SPECTRUM OF X RAY ILLUMINATED MOLECULAR GAS Abstract Only
G. Mark Voit *In* NASA, Ames Research Center, The Interstellar Medium in External Galaxies: Summaries of Contributed Papers Jul. 1990 p 126 (For primary document see N91-14100 05-90)
Avail: NTIS HC/MF A19 CSCL 03B

In starburst galaxies, active galaxies, and the mysterious ultraluminous infrared galaxies, x rays are likely to interact with molecular gas and dust, thereby inducing infrared emission. X ray heated thermal dust will emit the IR continuum, and x ray photoelectrons will excite an IR emission-line spectrum. Here, researchers model the IR continuum emission characteristic of some selected x ray spectral fluxes, in particular the x ray bremsstrahlung characteristic of supernova and stellar wind bubble shocks in dense media and the power law spectra characteristic of active galactic nuclei. These models are part of a larger project to determine the complete IR spectra, lines plus continuum, of x ray sources embedded in molecular gas. They modeled the thermal emission from grains by calculating a grain temperature/size/composition distribution function, f(T,a,Comp.), which accounts for temperature fluctuations by averging over all grain thermal histories. In determining the grain thermal distribution, researchers account for both direct grain heating (by x ray absorption and subsequent electron energy deposition) and indirect grain heating (by absorption of the UV emission stimulated by non-thermal photo- and Auger electrons in the gas phase). We let the grain size distribution be proportional to a(exp -3.5), and they consider two types of grain composition: graphites, which we assume to be pure carbon, and silicates, which contain all other depleted heavy elements. They derive the grain composition distribution function from solar abundances and interstellar depletion data. Author

N91-14145*# Five-College Astronomy Dept., Amherst, MA.
A COMPARISON OF THE RADIAL DISTRIBUTION OF MOLECULAR GAS AND NON-THERMAL RADIO CONTINUUM IN SPIRAL DISKS
Nicholas A. Devereux and J. S. Young *In* NASA, Ames Research Center, The Interstellar Medium in External Galaxies: Summaries of Contributed Papers Jul. 1990 p 127-129 (For primary document see N91-14100 05-90)
Avail: NTIS HC/MF A19 CSCL 03B

The present study includes 65 spiral galaxies selected from the Five College Radio Astronomy Observatory (FCRAO) Extragalactic CO Survey for which the major axis distributions of CO emission and 1.49 GHz radio continuum emission are well determined. The radial distribution of the CO emission has been measured with the FCRAO at positions along the major axis that are spaced by one half power beam width (HPBW) (45 seconds). The radial profile of the 1.49 GHz radio continuum emission was constructed by determining the radio emission at the location of the CO measurements from the 1.49 GHz maps of Condon (1987). Large, greater than a factor of ten, radially decreasing gradients in the star formation efficiency are observed for a small percentage, approx. 10 percent, of the spirals in this sample. The majority of spirals, however, are associated with small gradients in the star formation efficiency that do not systematically increase or decrease with radius. That the star formation efficiency does not systematically decrease with radius tends to argue against a global dynamical mechanism, such as a spiral density wave, for being the dominant mechanism triggering disk star formation for the majority of spirals in this sample. The results tend to support the view that the star formation in spiral disks is dominated by a local process that depends more on the molecular cloud properties than the dynamical structure of a galaxy. Author

N91-14146*# Illinois Univ., Urbana. Dept. of Astronomy.
A RELATIONSHIP BETWEEN THE INTEGRATED CO INTENSITY AND THE RADIO CONTINUUM EMISSION IN SPIRAL GALAXIES
D. S. Adler, R. J. Allen, and K. Y. Lo *In* NASA, Ames Research Center, The Interstellar Medium in External Galaxies: Summaries of Contributed Papers Jul. 1990 p 130-132 (For primary document see N91-14100 05-90)
Avail: NTIS HC/MF A19 CSCL 03B

In an effort to determine the role played by cosmic ray electrons and interstellar radiation fields on the collapse of molecular clouds, a survey was begun to investigate the relationship between the radio continuum brightness emission and the integrated CO intensity in spiral galaxies. The investigation was done on two scales; a global galaxy to galaxy comparison of integrated disk values, and a ring-averaged study over the disks of individual galaxies. For the large-scale survey, radio continuum flux densities integrated over the full disk at 1.49 GHz were taken from Condon (1987) and the total CO fluxes were taken from Verter (1985). The galaxies with values included in the two catalogs are displayed. It can be seen that a good correlation exists between the integrated CO emission and radio continuum emission. Author

N91-14147*# Tata Inst. of Fundamental Research, Bombay (India).
RADIO CONTINUUM AND FAR-INFRARED EMISSION OF SPIRAL GALAXIES: IMPLICATIONS OF CORRELATIONS
T. N. Rengarajan and K. V. K. Iyengar *In* NASA, Ames Research Center, The Interstellar Medium in External Galaxies: Summaries of Contributed Papers Jul. 1990 p 133-135 (For primary document see N91-14100 05-90)
Avail: NTIS HC/MF A19 CSCL 03B

Researchers present a study extending the correlation seen between radio continuum and far-infrared emissions from spiral galaxies to a lower frequency of 408 MHz and also as a function of radio spectral index. The tight correlation seen between the two luminosities is then used to constrain several parameters governing the emissions such as the changes in star formation rate and mass function, frequency of supernovae that are parents of the interstellar electrons and factors governing synchrotron radio emission. Author

N91-14148*# Tokyo Univ., Mitake (Japan). Inst. of Astronomy.
CIRCUMNUCLEAR IONIZED GAS IN STARBURST NUCLEI
Yoshiaki Taniguchi *In* NASA, Ames Research Center, The Interstellar Medium in External Galaxies: Summaries of Contributed Papers Jul. 1990 p 137-139 (For primary document see N91-14100 05-90)
Avail: NTIS HC/MF A19 CSCL 03B

In order to study kinematical properties of starburst nuclei (SBNs), researchers made high-resolution spectroscopy of fifteen SBNs in the H alpha region using an intensified Reticon system attached to the coude focus of the 188-cm reflector at the Okayama Astrophysical Observatory. The instrumental resolution is 21 km s(-1) Full Width Half Maximum (FWHM) at lambda sub H alpha. As for the archetypical SBN, Mrk 538 (=NGC 7714), researchers present high-resolution emission line profiles of several species of ions such as (OIII), (NII), (SII), and (OII). Main results and conclusions are summarized. It has been known that emission-line profiles of SBNs are symmetrical and narrow. However, this high-resolution spectroscopy shows that the observed emission-line profiles of the SBNs have the following asymmetrical patterns; blueward, redward, and double-peaked. It is known that such features have been observed for narrow line regions (NLRs) of active galactic nuclei (AGNs). There is no remarkable correlation between the asymmetry index and the reddening indicator such as a Balmer decrement. Thus the line asymmetry is not attributed to inhomogeneous obscuration in the emitting regions. The observed FWHMs of the H alpha emission lines cover a range from 85 km s(-1) to 318 km s(-1) and are slightly larger than those of (NII) lambda 6584A emission except for the double-peaked SBNs. The FWHMs of H alpha emission show a good correlation with sin i (i is an inclination angle of galaxy). This correlation means that the FWHMs of the SBNs suffer significantly from rotational broadening. Mrk 52 is an anomalous SBN because it has narrow emission line widths for its high inclination angle (cf. Taniguchi 1987). From the above correlation, it is estimated that the intrinsic (i.e., rotation free) FWHMs of H alpha emission are about 50 km s(-1). Author

N91-14149*# Princeton Univ., NJ. Inst. for Advanced Study.
IMAGING SPECTROPHOTOMETRY OF THE NUCLEAR OUTFLOW OF NGC 1068
Gerald Cecil *In* NASA, Ames Research Center, The Interstellar Medium in External Galaxies: Summaries of Contributed Papers Jul. 1990 p 140-142 Sponsored in part by NSF (For primary document see N91-14100 05-90)
(Contract NAS8-32902)
Avail: NTIS HC/MF A19 CSCL 03B

This observational program (in conjunction with R. B. Tully (IfA, Honolulu), and J. Bland (Rice U., Houston)) aims to constrain the kinematic organization and dominant excitation mechanisms of ionized gas in active galaxies. More generally, researchers are interested in the dynamics of radiative, supersonic flows in the Interstellar Medium (ISM). Imaging Fabry-Perot interferometers and low-noise Charge Coupled Devices (CCDs) are used for complete spatial coverage of the complex gas distribution in circumnuclear narrow-line regions (NLRs). Extranuclear emission line widths in NLRs can exceed 3000 km s(-1), so to avoid inter-order confusion researchers use an etalon of 4000 km s(-1) free spectral range to map (N II) lambda lambda 6548, 6583 and H alpha. To maximize spatial resolution, researchers select nearby active systems independent of luminosity but known to possess interesting morphologies and/or high-velocity extranuclear ionized gas. Monochromatic images Full Width Half Maximum (FWHM) approx. 65 km s(-1) have thus far been obtained in 1 second or better seeing at the U. Hawaii 2.2m, CFH 3.6m, and CTIO 4.0m telescopes. These are stacked into grids of line profiles, of spectrophotometric quality, at sub-arcsecond increments across a 3 second field. To handle the approx. 20,000 to 300,000 useful spectra that arise from a typical night's work, researchers have developed a complete analysis and reduction package for VAX and Sun image workstations. Reduction involves parametrization of approx. 10 to the 8th raw data points to a few maps (e.g., velocities of each kinematic subsystem, continuum-free line fluxes) containing approx. 10 to the 5th pixels. Researchers identify kinematic and structural symmetries by examining these maps and the point to point variations of the synthesized line profiles. The combination of monochromatic images and full spatial sampling of line profiles has allowed them to isolate such symmetries and has led to reliable kinematic deprojections. Author

N91-14150*# Rice Univ., Houston, TX.
LARGE SCALE EXCITATION OF THE ISM IN NGC 1068
J. Sokolowski, Jonathan Bland, G. N. Cecil, and R. B. Tully (Hawaii Univ., Honolulu.) *In* NASA, Ames Research Center, The Interstellar Medium in External Galaxies: Summaries of Contributed Papers Jul. 1990 p 143-145 (For primary document see N91-14100 05-90)
Avail: NTIS HC/MF A19 CSCL 03B

Researchers have shown that photoionization by the continuum of the hidden Seyfert I nucleus in NGC 1068 can have a significant effect on the ionization state and energetics of this disk's Interstellar Medium (ISM). Photoionization models with appropriate power law spectra can produce (NII) lambda lambda 6538, 6584/H alpha line ratios of 1.25 for ionization parameters Q approx. 10 (exp -12). However the data indicate large regions where the (NII)/H alpha ratio is 1 to 3. Since the abundances are known to be solar, there must be additional heating sources. Hardening of the incident radiation field by intervening absorption should be able to raise T sub e, thereby raising the (NII)/H alpha ratio. Heating with moderate efficiency by the intense starburst ring should also be a significant factor in raising the temperature of the ISM. The photoionization models with additional heating predict enhanced emission from other forbidden lines including (OII) lambda 3727 and (SII) lambda 6731. Author

N91-14151*# National Aeronautics and Space Administration. Ames Research Center, Moffett Field, CA.
MULTIBAND OBSERVATIONS OF CYGNUS A: A STUDY OF PRESSURE BALANCE IN THE CORE OF A POWERFUL RADIO GALAXY
Chris Carilli, Sam Conner, John Dreher, and Rick Perley (National Radio Astronomy Observatory, Socorro, NM.) *In its* The Interstellar Medium in External Galaxies: Summaries of Contributed Papers Jul. 1990 p 146-148 (For primary document see N91-14100 05-90)
Avail: NTIS HC/MF A19 CSCL 03B

Cygnus A is a powerful double radio source associated with a giant elliptical galaxy at the center of a poor cluster of galaxies. The radio source also sits within the core radius of a dense, cooling flow, x ray emitting cluster gas. Optical spectroscopy and narrow band imaging have revealed copious amounts of narrow line emission from the inner 20 kpc of the associated galaxy. Researchers assume H sub o = 75 km sec (-1) Mpc(-1). Discussed here are the pressures in the three components of the Interstellar Medium (ISM) (i.e., the radio, x ray, and line emitting fluids) within a radius of about 15 kpc of the active nucleus of the Cygnus A galaxy. Author

N91-14152*# Lowell Observatory, Flagstaff, AZ.
IONIZED INTERSTELLAR FROTH IN IRREGULAR GALAXIES
Deidre A. Hunter and John S. Gallagher, III (Association of Univ. for Research in Astronomy, Inc., Baltimore, MD.) *In* NASA, Ames Research Center, The Interstellar Medium in External Galaxies: Summaries of Contributed Papers Jul. 1990 p 149-150 (For primary document see N91-14100 05-90)
Avail: NTIS HC/MF A19 CSCL 03B

The warm interstellar medium of galaxies is a complicated place. It is often full of holes, neutral and ionized loops and shells, and diffuse ionized gas. Deep H alpha images of Magellanic-type irregular galaxies also reveal complex spatial structures consisting of loops and filaments in the interstellar gas outside of the boundaries of traditional HII regions. Researchers refer to these ionized structures as froth. Such structures could mark paths over which newly produced heavy elements are dispersed in irregular galaxies, and they could be the signatures of a feedback process related to star formation. In order to investigate the physical nature of the froth, researchers obtained narrow-band images and high and low dispersion spectra from Kitt Peak National Observatory (KPNO) and deep blue-passband plates from the Canada-France-Hawaii Observatory (CFHO). Author

N91-14153*# York Univ., Toronto (Ontario).
Ar/S
Marshall L. McCall, Chris Stevenson, and Douglas L. Welch (McMaster Univ., Hamilton, Ontario) *In* NASA, Ames Research Center, The Interstellar Medium in External Galaxies: Summaries of Contributed Papers Jul. 1990 p 151-153 (For primary document see N91-14100 05-90)
Avail: NTIS HC/MF A19 CSCL 03B

Near-infrared spectroscopy at high altitude and low humidity has been carried out to accurately measure (Ar III) lambda 7136 and (S III) lambda 9069 in the extreme metal-poor dwarf irregular galaxy IZw18. The ratio of the abundance of argon to the abundance of sulfur is within about 0.2 dex of the value for the solar neighborhood. Since n(Ar)/n(S) appears to be a universal constant, the line ratio (AR III) lambda 7136/(S III) lambda 9069 may be a useful diagnostic of temperature in cool, metal-rich HII regions. Author

N91-14154*# Texas Univ., Austin. Dept. of Astronomy.
SPATIALLY RESOLVED OPTICAL AND NEAR INFRARED SPECTROSCOPY OF I Zw 18
Evan D. Skillman and R. C. Kennicutt, Jr. (Arizona Univ., Tucson.) *In* NASA, Ames Research Center, The Interstellar Medium in External Galaxies: Summaries of Contributed Papers Jul. 1990 p 154-156 Sponsored in part by Robert A. Welch Foundation (For primary document see N91-14100 05-90)
(Grant NSF AST-86-13257)
Avail: NTIS HC/MF A19 CSCL 03B

For a long time, I Zw 18 has been recognized as the lowest abundance extra-galactic HII region (with the possible recent exception of SBS 0335-052; Izotov 1989). As such, it is important for many studies, including the determination of the primordial helium abundance. Recent imaging studies of I Zw 18 have revealed a more complex structure to I Zw 18 than the simple two-component model previously assumed. This has given rise to concern about the reliability of chemical abundance measurements derived for I Zw 18. Researchers have obtained long-slit spectra covering the wavelength range lambda 3650 to lambda 10,000, which allow us to measure physical parameters and chemical abundances as a function of position. With these new data we can investigate the SE component, which has not been studied previously, and we can address some of the concerns about abundance uncertainties. Author

N91-14155*# Washington Univ., Seattle.
OPTICAL AND NEAR-IR STUDY OF LMC HII REGION N11AB
Myung Gyoon Lee *In* NASA, Ames Research Center, The Interstellar Medium in External Galaxies: Summaries of Contributed Papers Jul. 1990 p 157-159 (For primary document see N91-14100 05-90)
Avail: NTIS HC/MF A19 CSCL 03B

N11 (DEM 34), complex HII region located about 4 degrees from the center of the LMC bar, is a very interesting giant interstellar shell. It has a complicated structure and motion. It is located on the edge of an HI concentration. This is the progress report of the study of its two components, A and B at the optical and near-IR wavelengths to investigate stars, dust and ionized gas associated with them. N11A is a compact high-excitation blob and N11B is a bright HII region in this complex, which embeds OB association Lucke-Hodge 10. Author

N91-14156*# Washington Univ., Seattle.
HII REGIONS IN DWARF IRREGULAR GALAXIES OF THE LOCAL GROUP
Paul Hodge and Myung Gyoon Lee *In* NASA, Ames Research Center, The Interstellar Medium in External Galaxies: Summaries of Contributed Papers Jul. 1990 p 160-162 (For primary document see N91-14100 05-90)
Avail: NTIS HC/MF A19 CSCL 03B

Deep, narrowband H alpha Charge Coupled Device (CCD) surveys of HII regions were carried out in several dwarf irregular galaxies in and near the local group. Data are now complete for these galaxies: NGC 6822, GR 8, IC 10, IC 1613, Sextans A, Sextans B, and Sag Irr. Observations are complete for DDO 47, 53, 167, 168 and 187. Details of some of the results for the

surveys completed so far are discussed. For NGC 6822, CCD survey at H alpha resulted in the detection of 145 HII regions in the local group irregular galaxy NGC 6822. Most of them are newly detected, faint surface-brightness objects. Positions, maps and dimensions are being published elsewhere. For GR 8, a deep narrowband H alpha imaging of the nearby dwarf irregular galaxy GR 8 revealed a total of 32 HII regions. Positions, H alpha luminosities, and sizes of these objects were determined. The H alpha luminosity function has the same shape as that for more luminous galaxies, except for size of sample effects. Most HII regions detected are at the very low luminosity end of the general luminosity function. For IC 10, a deep CCD narrowband H alpha imaging of the local group dwarf irregular galaxy IC 10 revealed a total of 144 HII regions. Positions, H alpha luminosities, and sizes of these objects were determined. The H alpha luminosity function has the same shape as that for more luminous galaxies. Author

N91-14157*# Bentley Coll., Boston, MA.
HII REGIONS IN IC 1613: THE ISM IN A NEARBY DWARF IRREGULAR GALAXY
Jill S. Price, Stephen F. Mason, and Craig A. Gullixson (Lowell Observatory, Flagstaff, AZ.) *In* NASA, Ames Research Center, The Interstellar Medium in External Galaxies: Summaries of Contributed Papers Jul. 1990 p 163-165 (For primary document see N91-14100 05-90)
Avail: NTIS HC/MF A19 CSCL 03B

IC 1613, a nearby (725 kpc distant) dwarf irregular galaxy, has always been known to contain large, ring-shaped HII regions in its northeast corner. A new H alpha image has been obtained using the Bell Labs Charge Coupled Device (CCD) camera, an RCA 320 X 512 pixel-thinned, back-illuminated CCD, an H alpha filter of central wavelength 6562 A and width (full width half maximum) of 30 A, and the 42 inch telescope at Lowell Observatory. The low resolution images exhibit many new, faint features.
Author

N91-14158*# Rice Univ., Houston, TX.
DIFFERENCES IN THE SIZE-INTERNAL VELOCITY RELATION OF GALACTIC AND EXTRAGALACTIC HII REGIONS
C. R. ODell *In* NASA, Ames Research Center, The Interstellar Medium in External Galaxies: Summaries of Contributed Papers Jul. 1990 p 166-168 (For primary document see N91-14100 05-90)
Avail: NTIS HC/MF A19 CSCL 03B

The nature of the size-internal velocity relation in extragalactic HII regions is examined in order to improve their use as distance determinants. The relation between the linear size and the internal velocity was compared for HII regions in the Galaxy and in external galaxies. Data for the former are from the researcher's own studies at high spatial resolution, while the latter have been the subject of spectroscopy that includes almost the entire objects. The Galactic HII regions are corrected to values of the internal velocity that would be observed if they were at extragalactic distances. A very different size-internal velocity relation was found for the two types of objects in the sense that the extragalactic objects are some ten times larger at the same internal velocity. This is interpreted to mean that the extragalactic HII regions are actually complexes of small HII regions comparable in size to their Galactic counterparts. Author

N91-14159*# Arizona Univ., Tucson.
A STUDY OF HII REGIONS IN SPIRAL GALAXIES USING MULTIOBJECT SPECTROSCOPY
Dennis Zaritsky, Richard Elston (Kitt Peak National Observatory, Tucson, AZ.), and J. M. Hill *In* NASA, Ames Research Center, The Interstellar Medium in External Galaxies: Summaries of Contributed Papers Jul. 1990 p 169-171 Sponsored in part by NSF (For primary document see N91-14100 05-90)
Avail: NTIS HC/MF A19 CSCL 03B

Multiobject spectroscopy results of HII regions in nearby late-type spiral galaxies are given. Results include excitation measurements, log ((O III)/H beta), for 81 regions in M 101, 30 regions in NGC 2403, and 13 regions in M 51. Researchers conclude that late-type spirals can be classified into two distinct populations, examine possible causes of this division, and derive metallicity gradients for these galaxies. M 51 appears to have an anomalously shallow abundance gradient. Author

N91-14160*# Lowell Observatory, Flagstaff, AZ.
THE DIFFUSE IONIZED INTERSTELLAR MEDIUM PERPENDICULAR TO THE PLANE OF NGC 891
Ralf-Juergen Dettmar, Jean Keppel, Morton S. Roberts (National Radio Astronomy Observatory, Charlottesville, VA.), and John S. Gallagher, III *In* NASA, Ames Research Center, The Interstellar Medium in External Galaxies: Summaries of Contributed Papers Jul. 1990 p 172-173 Sponsored in part by DFG (For primary document see N91-14100 05-90)
Avail: NTIS HC/MF A19 CSCL 03B

In an attempt to study the structure and the properties of the diffuse ionized interstellar medium perpendicular to the plane of disk galaxies researchers obtained H alpha images and spectra of NGC 891. Perhaps the most remarkable property of the H alpha emission line in NGC 891 is its extension out of the plane of the galaxy: researchers are able to measure the H alpha line out to more than 30 seconds (1.4 kpc) from the midplane. This means that the ionized hydrogen extends at least four times higher than the neutral hydrogen layer. An anomalously large scale-height for the ionized gas of approx. equals 1 kpc is also found in the Milky Way. The echelle spectra show a changing ratio of NII to H alpha. This excludes the possibility that the large scaleheight of the emission is due to scattering of disk emission by dust high above the plane. The z-extent of the H alpha emission is confirmed by the imaging result. The large z-extent of the ionized gas is confined to the inner half of the visible disk. In this inner region the H alpha distribution also shows a filamentary structure of the diffuse ionized medium. These filaments, sticking out of the plane, originate in HII regions in the plane. The H alpha image also shows a large scale asymmetry if the NE and SW parts of the disk are compared. The NE part is more prominent and extended in H alpha. The same asymmetry is also seen in the radio continuum distribution. This correlation between the diffuse ionized medium and the distribution of relativistic electrons is one example of a relation between star formation processes in the disk and the various components of the halo. Thermal filaments or spurs which are related to HII regions are also known in the Galaxy. These filamentary structures perpendicular to the galactic planes may represent the chimneys which result in the supernova dominated model of the Interstellar Medium by Norman and Ikeuchi (1989).
Author

N91-14161*# Catholic Univ. of America, Washington, DC. Dept. of Physics.
HOT INTERSTELLAR GAS AND IONIZATION OF EMBEDDED CLOUDS
K.-P. Cheng and F. Bruhweiler *In* NASA, Ames Research Center, The Interstellar Medium in External Galaxies: Summaries of Contributed Papers Jul. 1990 p 175-176 (For primary document see N91-14100 05-90)
Avail: NTIS HC/MF A19 CSCL 03B

Researchers present detailed photoionization calculations for the instellar cloud in which the Sun is embedded. They consider the EUV radiation field with contribution from discrete stellar sources and from a thermal bremsstrahlung-radiative recombination spectrum emitted from the surrounding 10 to the 6th power k coronal substrate. They establish lower limits to the fractional ionization of hydrogen and helium of 0.17 and 0.29 respectively. The high He ionization fraction results primarily from very strong line emission below 500 A originating in the surrounding coronal substrate while the H ionization is dominated by the EUV radiation from the discrete stellar sources. The dual effects of thermal conduction and the EUV spectrum of the 10 to the 6th k plasma on ionization in the cloud skin are explored. The EUV radiation field and Auger ionization have insignificant effects on the resulting ionic column densities of Si IV, C IV, N V and O VI through the cloud skin. Calculations show that the abundances of these species are dominated by collisional ionization in the thermal conduction

front. Because of a low charge exchange rate with hydrogen, the ionic column density ratios of N (CIII)/N (CII) and N (NII)/N (NI) are dominated by the EUV radiation field in the local interstellar medium. These ratios should be important diagnostics for the EUV radiation field and serve as surrogate indicators of the interstellar He and H ionization fraction respectively. Spacecraft such as Lyman which is designed to obtain high resolution spectral data down to the Lyman limit at 912 A could sample interstellar lines of these ions. Author

N91-14162*# Virginia Univ., Charlottesville. Dept. of Astronomy.

RADIATIVE THERMAL CONDUCTION FRONTS

Kazimierz J. Borkowski, Steven A. Balbus, and Carl C. Fristrom *In* NASA, Ames Research Center, The Interstellar Medium in External Galaxies: Summaries of Contributed Papers Jul. 1990 p 177-179 (For primary document see N91-14100 05-90)

Avail: NTIS HC/MF A19 CSCL 03B

The discovery of the O VI interstellar absorption lines in our Galaxy by the Copernicus observatory was a turning point in our understanding of the Interstellar Medium (ISM). It implied the presence of widespread hot (approx. 10 to the 6th power K) gas in disk galaxies. The detection of highly ionized species in quasi-stellar objects' absorption spectra may be the first indirect observation of this hot phase in external disk galaxies. Previous efforts to understand extensive O VI absorption line data from our Galaxy were not very successful in locating the regions where this absorption originates. The location at interfaces between evaporating ISM clouds and hot gas was favored, but recent studies of steady-state conduction fronts in spherical clouds by Ballet, Arnaud, and Rothenflug (1986) and Bohringer and Hartquist (1987) rejected evaporative fronts as the absorption sites. Researchers report here on time-dependent nonequilibrium calculations of planar conductive fronts whose properties match well with observations, and suggest reasons for the difference between the researchers' results and the above. They included magnetic fields in additional models, not reported here, and the conclusions are not affected by their presence. Author

N91-14163*# Cornell Univ., Ithaca, NY. Center for Radiophysics and Space Research.

ENERGY INPUT AND HI SPIN TEMPERATURES IN LOW PRESSURE REGIONS

E. Corbelli and E. E. Salpeter *In* NASA, Ames Research Center, The Interstellar Medium in External Galaxies: Summaries of Contributed Papers Jul. 1990 p 180-181 (For primary document see N91-14100 05-90)

Avail: NTIS HC/MF A19 CSCL 03B

Two recent (unpublished) HI emission/absorption studies carried out with good sensitivity using the Arecibo 21 cm beam are discussed. One study (Colgan, Salpeter and Terzian) looked for high velocity clouds of our own Galaxy in absorption in the directions of 63 of the brightest continuum sources reachable with the Arecibo telescope. HI emission mapping in the neighborhood of these directions was also carried out. The other study (Corbelli and Schneider) looked for absorption along lines of sight to about 50 weaker sources which pass within a few diameters of nearby disk galaxies. Neither study detected any absorption. Author

N91-14164*# California Inst. of Tech., Pasadena.

THE INTERSTELLAR HALO OF SPIRAL GALAXIES: NGC 891

Shrinivas R. Kulkarni, R. J. Rand, and J. Jeff Hester *In* NASA, Ames Research Center, The Interstellar Medium in External Galaxies: Summaries of Contributed Papers Jul. 1990 p 182-184 (For primary document see N91-14100 05-90)

Avail: NTIS HC/MF A19 CSCL 03B

Researchers have detected the Warm Ionized Medium (WIM) phase in the galaxy NGC 891. They found that the radial distribution of the WIM follows the molecular or young star distribution - an expected dependence. The amount of the WIM in this galaxy exceeds that in our Galaxy. The major surprize is the large thickness of the WIM phase - about 9 kpc instead 3 kpc as in our Galaxy. Clearly, this is the most significant result of the observations. The presence of low ionization gas at high z as well as at large galactocentric radii (where young stars are rare) is an important clue to the origin of the halo and observations such as the one reported here provide important data on this crucial question. In particular, the ionization of gas at high absolute z implies that either the UV photons manage to escape from the disk of the galaxy or that the extragalactic UV background plays an important role. The bulk of the WIM in spiral galaxies is a result of star-formation activity and thus these results can be understood by invoking a high star formation rate in NGC 891. Only the concerted action of supernovae can get the gas to the large z-heights as is observed in this galaxy. Support for this view comes from our detection of many worms i.e., bits and pieces of supershells in the form of kilo-parsec long vertical filaments. Researchers also saw a 600-pc size supershell located nearly one kpc above the plane of the galaxy. Author

N91-14165*# Harvard-Smithsonian Center for Astrophysics, Cambridge, MA.

THE ONSET OF GALACTIC WINDS IN EARLY-TYPE GALAXIES

W. Forman, C. Jones, W. Tucker, and L. P. David *In* NASA, Ames Research Center, The Interstellar Medium in External Galaxies: Summaries of Contributed Papers Jul. 1990 p 185-187 (For primary document see N91-14100 05-90)

Avail: NTIS HC/MF A19 CSCL 03B

Researchers report on a program using Einstein x ray observations of the x ray spectra and surface brightness profiles (or extents) of a large sample of early-type (elliptical and SO) galaxies for which the goal is to determine the critical optical luminosity for which galactic winds are important. For galaxies in which the x ray emission is dominated by hydrostatic coronae, the x ray spectra will be relatively soft (characterized by a temperature of approx. 10 to the 7th power K), while for galaxies with a galactic wind, the emission will be dominated by the spectrally harder discrete sources (since the x ray emission from the wind is essentially negligible). In this new sample of 180 galaxies, there are 28 early type galaxies with sufficient counts to obtain a spectrum with the Einstein Image Proportional Counter (IPC). This sample more than doubles the total number of early-type galaxies in earlier compilations (Forman, Jones, and Tucker 1985; Canizares et al. 1987). The new spectral observations will help determine the critical optical luminosity for the onset of galactic winds which is important for understanding the chemical evolution of galaxies and of the intergalactic medium. The implications of galactic winds for the heavy element enrichment and energy content of the intracluster medium are discussed. Author

N91-14166*# Mullard Radio Astronomy Observatory, Cambridge (England).

THE ENVIRONMENTS OF DOUBLE RADIOGALAXIES

Steve Rawlings *In* NASA, Ames Research Center, The Interstellar Medium in External Galaxies: Summaries of Contributed Papers Jul. 1990 p 188-190 (For primary document see N91-14100 05-90)

Avail: NTIS HC/MF A19 CSCL 03B

Discussed here are simple methods by which the densities and pressures of the gas confining double radiogalaxies can be estimated from optical and x ray data. By applying these methods to an unbiased sample of nearby (z less than 0.5) double radiogalaxies, the author quantifies the empirical relation between the external confining pressure and the internal pressure of the lobes as inferred from the minimum energy argument. This relation is explained by an analytic model in which the lobes are statically confined by ambient material pre-heated in the bow-shock of the advancing radiosource. Such a model allows one to estimate source expansion speeds from a combination of radio and environmental data, and estimate properties of the environment from radio data alone, providing expansion speeds can be estimated from multifrequency observations. Author

N91-14167*# Joint Inst. for Lab. Astrophysics, Boulder, CO.
ORIGIN AND DYNAMICS OF EMISSION LINE CLOUDS IN COOLING FLOW ENVIRONMENTS
Michael Loewenstein *In* NASA, Ames Research Center, The Interstellar Medium in External Galaxies: Summaries of Contributed Papers Jul. 1990 p 191-192 (For primary document see N91-14100 05-90)
Avail: NTIS HC/MF A19 CSCL 03B

The author suggests that since clouds are born co-moving in a turbulent intra-cluster medium (ICM), the allowed parameter space can now be opened up to a more acceptable range. Large-scale motions can be driven in the central parts of cooling flows by a number of mechanisms including the motion of the central and other galaxies, and the dissipation of advected, focussed rotational and magnetic energy. In addition to the velocity width paradox, two other paradoxes (Heckman et al. 1989) can be solved if the ICM is turbulent. Firstly, the heating source for the emission line regions has always been puzzling - line luminosities are extremely high for a given (optical or radio) galaxy luminosity compared to those in non-cooling flow galaxies, therefore a mechanism peculiar to cooling flows must be at work. However most, if not all, previously suggested heating mechanisms either fail to provide enough ionization or give the wrong line ratios, or both. The kinetic energy in the turbulence provides a natural energy source if it can be efficiently converted to cloud heat. Researchers suggest that this can be done via magneto-hydrodynamic waves through plasma slip. Secondly, while the x ray observations indicate extended mass deposition, the optical line emission is more centrally concentrated. Since many of the turbulence-inducing mechanisms are strongest in the central regions of the ICM, so is the method of heating. In other words material is dropping out everywhere but only being lit up in the center. Author

N91-14168*# Michigan Univ., Ann Arbor. Dept. of Astronomy.
NARROW BAND IMAGES OF SUSPECTED COOLING FLOW GALAXIES
Susana Deustua and Greg Bothun *In* NASA, Ames Research Center, The Interstellar Medium in External Galaxies: Summaries of Contributed Papers Jul. 1990 p 193-195 (For primary document see N91-14100 05-90)
Avail: NTIS HC/MF A19 CSCL 03B

Narrow-band (H alpha and (NII)) charge coupled device (CCD) images of elliptical galaxies suspected of having cooling flows are discussed. Researchers find evidence of optical emission from cool gas which is most likely associated with a cooling flow. At least 4 galaxies (NGC 3998, NGC 4203, NGC 4550 and NGC 4697) show emission of (NII) and/or H alpha within the central 20 seconds, a fraction consistent with results from Phillips et al. (1987) and Caldwell (1984). In these four, (NII) lambda 6584A emission is stronger than H alpha (which is often in absorption e.g., as seen in long slit spectra of NGC4697). From long slit spectra of these galaxies, Deustua and Teske (1989) infer electron densities, N sub e, of order 1.2x10 to the 3rd power cm(-3) assuming T = 10 to the 4th power K for the optically emitting gas. NGC 2685, NGC 3489 appear to have emission in (NII); NGC 4636 may also, but, is difficult to see in the data (Demoulin-Ulrich, Butcher and Boksenberg (1984) did not see emission from this galaxy). NGC 4472, NGC 4473, NGC 4365, NGC 4638 and NGC 4649 show no emission. Author

N91-14169*# Colorado Univ., Boulder. Center for Astrophysics and Space Astronomy.
OPTICAL EMISSION FROM COOLING FLOWS IN DISTANT X RAY CLUSTERS OF GALAXIES
Megan Donahue, John T. Stocke, G. Mark Voit, and Isabella Gioia (Harvard-Smithsonian Center for Astrophysics, Cambridge, MA.) *In* NASA, Ames Research Center, The Interstellar Medium in External Galaxies: Summaries of Contributed Papers Jul. 1990 p 196-197 (For primary document see N91-14100 05-90)
Avail: NTIS HC/MF A19 CSCL 03B

Although the Einstein satellite detected cooling flows in the x ray emission from clusters of galaxies 10 years ago, the understanding of these flows remains incomplete. The x ray emitting gas in the centers of these clusters is so dense that its cooling time is shorter than a Hubble time. Thus gas may cool and flow into the center of the cluster. This cooling gas is thermally unstable and should quickly become inhomogeneous. Optical filamentation (1-100 kpc scales) often appears near the centers of nearby clusters containing cooling flows, usually within the central galaxies accreting the gas. Indeed, only clusters with well-developed cooling flows seem to possess highly luminous, emission-line nebulae. Researchers present here some results of preliminary observational and theoretical studies of this class of emission-line objects. Researchers observed a complete, x ray selected sample of 25 distant clusters of galaxies extracted from the Einstein Extended Medium Sensitivity Survey. They discovered luminous extended H alpha emission in 10 of these clusters. Thus at least 40 percent of the clusters in the sample contain cool gas. If we crudely compare the sample to that of Arnaud (1988), in which approx. 40 percent of his 104 x ray clusters have cooling flows, the result implies that cooling flows may actually be a more common phenomenon in the past than in the present. The connection between the cooling flow and the H alpha emission is a mystery. The straightforward calculation of 1 (photoionization) to 3 (shocks) recombinations per H atom in the cooling flow gives mass infall rates 3 to 100 times greater than M derived from x ray observations. Researchers have made some preliminary theoretical calculations in an attempt to resolve this problem. Author

N91-14170*# Harvard-Smithsonian Center for Astrophysics, Cambridge, MA.
GAS FLOWS IN ELLIPTICAL GALAXIES
L. P. David, W. Forman, and C. Jones *In* NASA, Ames Research Center, The Interstellar Medium in External Galaxies: Summaries of Contributed Papers Jul. 1990 p 198-200 (For primary document see N91-14100 05-90)
Avail: NTIS HC/MF A19 CSCL 03B

In preparation for the next generation of x ray telescopes, researchers have begun a program investigating the evolving x ray properties of elliptical galaxies. Their galaxy models consist of a modified King profile for the luminous portion of the galaxy and can include an isothermal dark halo comprising 90 percent of the total mass. The stellar population is assumed to form at a rate which decreases exponentially on a dynamical time scale with a Salpeter initial mass function. Stellar mass loss occurs instantaneously as stars evolve off the main sequence. All stars more massive than 8 solar mass produce type II supernovae, while less massive stars loss mass through a planetary nebulae. The evolving rate of type I supernovae is normalized to a fraction, gamma sub sn I, of Tammann's (1974) value. All of this information is then incorporated into a one-dimensional hydrodynamics code to determine the evolving dynamical state of the interstellar medium. Author

N91-14171*# Institute of Astronomy, Cambridge (England).
STRIPPING OF GAS AND DUST FROM THE ELLIPTICAL GALAXY M86
D. A. White, A. C. Fabian, W. Forman, C. Jones, and C. Stern (Harvard-Smithsonian Center for Astrophysics, Cambridge, MA.) *In* NASA, Ames Research Center, The Interstellar Medium in External Galaxies: Summaries of Contributed Papers Jul. 1990 p 201-202 (For primary document see N91-14100 05-90)
Avail: NTIS HC/MF A19 CSCL 03B

Past observations of the x ray morphology of M86 have revealed that the galaxy is experiencing ram-pressure stripping due to its large velocity (1500 km s(-1)) relative to the intracluster medium of Virgo (Forman et al. 1979, Fabian, Schwartz, and Forman 1980). Observations indicate that the x ray emitting gas in the plume of M86 is still being produced from the continual heating of gas and dust stripped from nearer the galaxy's center. Researchers obtained two-dimensional Infrared Astronomy Satellite (IRAS) images of M86 which have revealed that there are two spatially separated regions of emission, one at 60 microns and the other at 100 microns of the IRAS wavebands. The 100 microns emission, presumably from cool dust (at approximately 20 K), appears to be located near the center of the galaxy together with

HI (detected by Bregman, Roberts and Giovanelli 1988), while the 60 microns emission appears to lie more than 3 arcminutes away from the optical center in a direction slightly south of the center of the plume. Optical images produced by scanning U.K. Schmidt plates, reveal asymmetric isophotal contours along the major axis of the galaxy (first reported by Nulsen and Carter in 1987, which they propose as excess emission due to star formation). This excess optical emission is co-incident with the direction of the 60 micron infra-red emission. Author

N91-14172*# Virginia Univ., Charlottesville. Dept. of Astronomy.

ISM STRIPPING FROM CLUSTER GALAXIES AND INHOMOGENEITIES IN COOLING FLOWS

Noam Soker, Joel N. Bregman (National Radio Astronomy Observatory, Charlottesville, VA.), and Craig L. Sarazin *In* NASA, Ames Research Center, The Interstellar Medium in External Galaxies: Summaries of Contributed Papers Jul. 1990 p 203 (For primary document see N91-14100 05-90)

Avail: NTIS HC/MF A19 CSCL 03B

Analyses of the x ray surface brightness profiles of cluster cooling flows suggest that the mass flow rate decreases towards the center of the cluster. It is often suggested that this decrease results from thermal instabilities, in which denser blobs of gas cool rapidly and drop below x ray emitting temperatures. If the seeds for the thermal instabilities are entropy perturbations, these perturbations must enter the flow already in the nonlinear regime. Otherwise, the blobs would take too long to cool. Here, researchers suggest that such nonlinear perturbations might start as blobs of interstellar gas which are stripped out of cluster galaxies. Assuming that most of the gas produced by stellar mass loss in cluster galaxies is stripped from the galaxies, the total rate of such stripping is roughly M sub Interstellar Matter (ISM) approx. 100 solar mass yr(-1). It is interesting that the typical rates of cooling in cluster cooling flows are M sub cool approx. 100 solar mass yr(-1). Thus, it is possible that a substantial portion of the cooling gas originates as blobs of interstellar gas stripped from galaxies. The magnetic fields within and outside of the low entropy perturbations can help to maintain their identities, both by suppressing thermal conduction and through the dynamical effects of magnetic tension. One significant question concerning this scenario is: Why are cooling flows seen only in a fraction of clusters, although one would expect gas stripping to be very common. It may be that the density perturbations only survive and cool efficiently in clusters with a very high intracluster gas density and with the focusing effect of a central dominant galaxy. Inhomogeneities in the intracluster medium caused by the stripping of interstellar gas from galaxies can have a number of other effects on clusters. For example, these density fluctuations may disrupt the propagation of radio jets through the intracluster gas, and this may be one mechanism for producing Wide-Angle-Tail radio galaxies. Author

N91-14173*# Alabama Univ., Huntsville.

ACCOUNTING FOR THE DISPERSION IN THE X RAY PROPERTIES OF EARLY-TYPE GALAXIES

Raymond E. White, III and Craig L. Sarazin (Virginia Univ., Charlottesville.) *In* NASA, Ames Research Center, The Interstellar Medium in External Galaxies: Summaries of Contributed Papers Jul. 1990 p 204-205 (For primary document see N91-14100 05-90)

Avail: NTIS HC/MF A19 CSCL 03B

The x ray luminosities of early-type galaxies are correlated with their optical (e.g., blue) luminosities (L sub X approx. L sub B exp 1.6), but the x ray luminosities exhibit considerable scatter for a given optical luminosity L sub B. This dispersion in x ray luminosity is much greater than the dispersion of other properties of early-type galaxies (for a given L sub B), such as luminosity scale-length, velocity dispersion, color, and metallicity. Here, researchers consider several possible sources for the dispersion in x ray luminosity. Some of the scatter in x ray luminosity may result from stellar population variations between galaxies with similar L sub B. Since the x ray emitting gas is from accumulated stellar mass loss, the L sub X dispersion may be due to variations in integrated stellar mass loss rates. Another possible cause of the L sub X dispersion may be variations in the amount of cool material in the galaxies; cool gas may act as an energy sink for the hot gas. Infrared emission may be used to trace such cool material, so researchers look for a correlation between the infrared emission and the x ray emission of early-type galaxies at fixed L sub B. Velocity dispersion variations between galaxies of similar L sub B may also contribute to the L sub X dispersion. The most likely a priori source of the dispersion in L sub X is probably the varying amount of ram-pressure stripping in a range of galaxy environments. The hot gaseous halos of early-type galaxies can be stripped in encounters with other galaxies or with ambient cluster gas if the intracluster gas is sufficiently dense. Researchers find that the most likely cause of dispersion in the x ray properties of early type galaxies is probably the ram-pressure stripping of gaseous halos from galaxies. For a sample of 81 early-type galaxies with x ray luminosities or upper limits derived from Einstein Observatory observations (CFT) researchers calculated the cumulative distribution of angular distances between the x ray sample members and bright galaxies from the Revised Shapley - Ames catalog. Collectively, galaxies with low x ray luminosities (for a given L sub B) tend to be in denser environments than galaxies with higher x ray luminosities. Author

N91-14174*# Northwestern Univ., Evanston, IL. Dept. of Physics and Astronomy.

SEARCH FOR COLD GAS IN CLUSTERS WITH AND WITHOUT COOLING FLOWS

D. A. Grabelsky and M. P. Ulmer *In* NASA, Ames Research Center, The Interstellar Medium in External Galaxies: Summaries of Contributed Papers Jul. 1990 p 206-210 (For primary document see N91-14100 05-90)

Avail: NTIS HC/MF A19 CSCL 03B

The dominant galaxy in each of approx. 40 clusters was studied using co-added Infrared Astronomy Satellite (IRAS) survey data, and 11 of these galaxies were observed for CO (J=1 to 0) emission with the 12 m telescope at Kitt Peak. Half of the galaxies in the sample are in clusters reported to have cooling flows while the other half are not. Six of the galaxies appear to have been detected by IRAS at fairly low flux levels, in addition to one previously known strong detection; all seven have reported cooling flows. No detectable CO emission (to 2 to 3 mK) was found in any of the 11 galaxies observed. Assuming accretion rates of approx. 100 Solar Mass yr(-1), the star formation rates and efficiencies in these galaxies must be quite high in order to render the CO undetectable. At the same time, the infrared luminosities of these galaxies is unremarkable, suggesting that the correlation between star formation efficiency and infrared luminosity found for spirals may not hold for cooling flows. Author

N91-14175*# National Aeronautics and Space Administration. Marshall Space Flight Center, Huntsville, AL.

AN INFRARED JET IN CENTAURUS A (NGC 5128): EVIDENCE FOR INTERACTION BETWEEN THE ACTIVE NUCLEUS AND THE INTERSTELLAR MEDIUM

Marshall Joy, P. M. Harvey, E. V. Tollestrup, P. J. McGregor, and A. R. Hyland (Mount Stromlo and Siding Spring Observatory, Canberra, Australia) *In* NASA, Ames Research Center, The Interstellar Medium in External Galaxies: Summaries of Contributed Papers Jul. 1990 p 211-213 (For primary document see N91-14100 05-90)

Avail: NTIS HC/MF A19 CSCL 03B

In the present study, higher resolution near infrared images of the visually-obscured central region of Centaurus A were obtained in order to investigate the effects of the active nucleus on the surrounding galaxy. Researchers present J(1.25 microns), H(1.65 microns), and K(2.2 microns) images of the central 40 seconds of the galaxy, taken with the Univ. of Texas InSb array camera on the Anglo Australian 3.9 meter telescope. These images reveal a jet extending approx. 10 arcseconds to the northeast of the nucleus at the same position angle as the x ray and radio jets. The infrared jet is most prominent at the shortest wavelength (1.25 microns), where its brightness surpasses that of the nucleus. The blue

appearance of the infrared jet is remarkable considering the heavy obscuration that is evident at visual wavelengths. The amount of reddening in the vicinity of the jet is determined from the measured colors of the stellar core of the galaxy, and this value is used to generate an extinction-corrected energy distribution. In contrast to previously studied optical and infrared jets in active nuclei, the short-wavelength prominence of the Cen A jet indicates that it cannot be attributed to synchrotron emission from a beam of relativistic electrons. The remaining viable mechanisms involve an interaction between the interstellar medium and the active nucleus: the infrared radiation from the jet may be due to emission from interstellar gas that has been entrained and heated by the flow of relativistic particles from the nucleus; alternatively, luminous blue stars may have been created by compression of interstellar material by the relativistic plasma. To investigate these proposed mechanisms, near-infrared spectroscopic studies of Cen A are in progress to look for collisionally excited molecular hydrogen emission lines and recombination lines from ionized gas. Author

N91-14176*# Columbia Univ., New York, NY.
NGC 4438: RAM PRESSURE SWEEPING OF A TIDALLY DISRUPTED GALAXY
J. E. Hibbard and Jacqueline H. vanGorkom (National Radio Astronomy Observatory, Socorro, NM.) *In* NASA, Ames Research Center, The Interstellar Medium in External Galaxies: Summaries of Contributed Papers Jul. 1990 p 214-216 (For primary document see N91-14100 05-90)
Avail: NTIS HC/MF A19 CSCL 03B

NGC 4438 is the highly HI deficient peculiar spiral in the center of the Virgo cluster. Observations are given of the neutral hydrogen emission obtained with the Very Large Array (VLA) in the D-array configuration. These observations map out the total HI as determined from single dish measurements, and show the hydrogen to be confined to a region about one third the size of the optical disk and displaced to the side of the galaxy opposite M87. The hydrogen content of the galaxy is over an order of magnitude less than that expected for a galaxy of its type. The data suggest that the HI deficiency is a result of ram pressure stripping of the gas in the outer regions of the galaxy by the hot intracluster medium after being tidally perturbed. Author

N91-14177*# Columbia Univ., New York, NY.
NGC 3312: A VICTIM OF RAM PRESSURE SWEEPING
P. M. McMahon, O.-G. Richter, Jacqueline H. vanGorkom, and H. C. Ferguson (Johns Hopkins Univ., Baltimore, MD.) *In* NASA, Ames Research Center, The Interstellar Medium in External Galaxies: Summaries of Contributed Papers Jul. 1990 p 217-220 (For primary document see N91-14100 05-90)
Avail: NTIS HC/MF A19 CSCL 03B

Researchers are undertaking a volume limited survey of the Hydra I cluster in neutral hydrogen using the National Radio Astronomy Observatory's Very Large Array (VLA). The main purpose is to study the effects of a dense environment on the gaseous component of the galaxies. Observational evidence has been accumulating recently that ram pressure sweeping does occur in the centers of clusters, but it is possible that tidal interactions play a role as well. Results of high resolution HI imaging of NGC 3312, the large peculiar spiral near the cluster center are presented. Hydra I (= A1060) is the nearest rich cluster beyond Virgo and, as such, presents a unique opportunity to do a complete survey of a cluster. It is similar to the Virgo cluster in many of its general physical characteristics, such as size, x ray luminosity, velocity dispersion, and galaxy content (high spiral fraction). However, Hydra I appears to be more regular and relaxed. This is evident in the x ray distribution in its central region, which is radially symmetric and centered on the dominant galaxy, NGC 3311, a cD-like elliptical. The observed x ray luminosity implies a central gas density of 4.5 x 10 to the 3rd power cm(-3). Gallagher (1978) argued from optical images of NGC 3312 that this galaxy might be an ideal candidate to directly study effects of the ram pressure process; it might currently be undergoing stripping of its interstellar medium. The researchers' data are consistent with this suggestion, but other origins of the peculiar appearance cannot yet be ruled out. Author

N91-14178*# Royal Greenwich Observatory, Hailsham (England).
THE VIOLENT INTERSTELLAR MEDIUM IN MESSIER 31
Elias Brinks, Robert Braun (National Radio Astronomy Observatory, Socorro, NM.), and Stephen W. Unger *In* NASA, Ames Research Center, The Interstellar Medium in External Galaxies: Summaries of Contributed Papers Jul. 1990 p 221-223 (For primary document see N91-14100 05-90)
Avail: NTIS HC/MF A19 CSCL 03B

Taurus observations in the line of H alpha and Very Large Array (VLA) HI mapping of the HII complex No. 722 in M31, reveal what seems to be a spherical cavity 330 pc in diameter blown out by a stellar association of over 20(exp 6) years old. Evidence of induced star formation which was initiated less than 5(exp 6) years ago is present in the form of bright HII emission and numerous O, B and Wolf-Rayet stars which are found within the shell surrounding the cavity. The energy necessary to create the HI shell is estimated to be about 5(exp 51) erg. Author

N91-14179*# California Univ., Berkeley.
SUPERNOVA REMNANTS AND DIFFUSE IONIZED GAS IN M31
Rene Walterbos and Robert Braun (National Radio Astronomy Observatory, Socorro, NM.) *In* NASA, Ames Research Center, The Interstellar Medium in External Galaxies: Summaries of Contributed Papers Jul. 1990 p 224-226 (For primary document see N91-14100 05-90)
Avail: NTIS HC/MF A19 CSCL 03B

Researchers have compiled an initial list of radio/optical supernova remnants (SNRs) in M31, by searching for radio identifications of emission-line sources with a high (SII)/H alpha ratio (greater than 0.60). The (SII) filter included both sulfur lines and the H alpha filter did not include (NII). This search revealed 11 SNRs, of which only two were known. In addition, researchers detected radio emission from 3 SNRs that were identified in previous optical surveys (D'Odorico et al., 1980), but that were outside the charge coupled device (CCD) fields. The 14 objects only include the most obvious candidates, but a full search is in progress and the researchers expect to find several more SNRs. Also not all optical SNRs show detectable radio emission and a pure optical list of SNR candidates based only on the ratio of (SII)/H alpha emission contains many more objects. Two conclusions are apparent. First, the radio properties of the SNRs in M31 are quite similar to those of Galactic SNRs as is illustrated. The brightnesses are not systematically lower as has been suggested in the past (Dickel and D'Odorico, 1984). Second, the slope of the relation is close to -2; this slope is expected from the intrinsic dependence between surface brightness and diameter. The radio luminosity of the SNRs does not seem to depend strongly on diameter, or age, contrary to model predictions. Selection effects, however, play an important role in these plots. The CCD images show widespread diffuse ionized gas with a ratio of (SII)/H alpha that is higher than that of discrete HII regions. Discrete HII regions typically show ratios between 0.2 to 0.3, while the diffuse gas in the arms consistently shows ratios of 0.5. Researchers can trace this gas across the spiral arms to emission measures below 5 pc cm (-6). Its properties seem to be similar to that of the diffuse gas in the solar neighborhood. Author

N91-14180*# National Aeronautics and Space Administration. Ames Research Center, Moffett Field, CA.
EVOLUTION OF A SUPERBUBBLE BLASTWAVE IN A MAGNETIZED MEDIUM
Katia M. Ferriere, Ellen G. Zweibel (Colorado Univ., Boulder.), and Mordecai-Mark MacLow *In its* The Interstellar Medium in External Galaxies: Summaries of Contributed Papers Jul. 1990 p 227-228 (For primary document see N91-14100 05-90)
(Grant NAGw-766)
Avail: NTIS HC/MF A19 CSCL 03B

Researchers investigate the effects of interstellar magnetic fields on the evolution and structure of interstellar superbubbles,

using both analytic and numerical magnetohydrodynamic (MHD) calculations. These cavities of hot gas, surrounded by shells of cold dense material preceded by a shock wave result from the combined action of stellar winds and supernova explosions in OB associations. If the medium in which a superbubble goes off is homogeneous and unmagnetized, the blast wave expands isotropically. As the interstellar gas flows through the shock, it cools significantly and gets strongly compressed such that thermal pressure remains approximately equal to ram pressure. Hence, the swept up material is confined to a very thin shell. However, if the ambient medium is permeated by a uniform magnetic field B sub o approx. 3 mu G (typical value for the interstellar matter (ISM)), the configuration loses its spherical symmetry, and, due to magnetic pressure, the shell of swept up material does not remain thin. Researchers found the following qualitative differences: (1) Except in the immediate vicinity of the magnetic poles, the shell is supported by magnetic pressure. (2) The refraction of field lines at the shock and the thermal pressure gradient along the shell both contribute to accelerating the gas toward the equator. The resulting mass flux considerably decreases the column density at the magnetic poles. (3) Away from the poles, magnetic tension in the shell causes the field lines (particularly the inner boundary) to elongate in the direction of B sub o. In contrast, the shock wave radius increases with increasing theta. (4) The reduced inertia of a parcel in the polar neighborhood makes it easier to decelerate, and accounts for the dimple which appears at the poles in numerical simulations. This dimple also results from the necessity to call on intermediate shocks in order to insure a smooth transition between a purely thermal shock at the poles and a magnetic shock in the rest of the shell. (5) The shock wave propagates faster than in the absence of magnetic field, except near the poles where the reduced mass of the shell allows it to be more efficiently decelerated. Author

N91-14181*# National Aeronautics and Space Administration. Goddard Space Flight Center, Greenbelt, MD.

INFRARED ANALYSIS OF LMC SUPERBUBBLES

Fran Verter and Eli Dwek *In* NASA, Ames Research Center, The Interstellar Medium in External Galaxies: Summaries of Contributed Papers Jul. 1990 p 229-231 (For primary document see N91-14100 05-90)

Avail: NTIS HC/MF A19 CSCL 03B

Researchers are analyzing three superbubbles in the Large Magellanic Cloud (LMC), cataloged by Meaburn (1980) as LMC-1, LMC-4 (a.k.a. Shapley Constellation III), and LMC-5. Superbubbles are the largest infrared sources in the disks of external galaxies. Their expansion requires multiple supernovae from successive generations of star formation. In LMC superbubbles, the grains swept up by shocks and winds represent an interstellar medium (ISM) whose abundances are quite different from the Galaxy. By applying the Dwek (1986) grain model, we can derive the composition and size spectrum of the grains. The inputs to this model are the dust emission in the four Infrared Astronomy Satellite (IRAS) bands and the interstellar radiation field (ISRF) that provides the heating. The first step in the project is to derive the ISRF for star-forming regions on the periphery of superbubbles. Researchers are doing this by combining observations at several wavelengths to determine the energy budget of the region. They will use a UV image to trace the ionizing stellar radiation that escapes, an H alpha image to trace the ionizing stellar radiation that is absorbed by gas, and the four IRAS images to trace the stellar radiation, both ionizing and non-ionizing, that is absorbed by dust. This multi-wavelength approach has the advantages that we do not have to assume the shape of the IMF or the extinction of the source. Author

N91-14182*# Illinois Univ., Urbana-Champaign. National Center for Supercomputing Applications.

MAGNETIC COLLIMATION OF PROTOSTELLAR WINDS INTO BIPOLAR OUTFLOWS

Michael L. Norman and James M. Stone *In* NASA, Ames Research Center, The Interstellar Medium in External Galaxies: Summaries of Contributed Papers Jul. 1990 p 232-234 (For primary document see N91-14100 05-90)

Avail: NTIS HC/MF A19 CSCL 03B

Researchers describe self-consistent 2-D magnetohydrodynamic (MHD) simulations of the collimation of an isotropic protostellar wind into bipolar outflows by magnetic stresses in the ambient medium. A variety of ambient field strengths, wind luminosities, and density profiles were studied. Collimation occurs when the energy of the magnetic field swept up by the expanding bubble approaches the bubble thermal energy. Measured axial and radial expansion rates are in good agreement with the analytical predictions of Konigl (1982). Author

N91-14183*# National Aeronautics and Space Administration. Ames Research Center, Moffett Field, CA.

MHD SHOCKS IN THE ISM

D. F. Chernoff, David J. Hollenbach, and Christopher F. Mckee (California Univ., Berkeley.) *In its* The Interstellar Medium in External Galaxies: Summaries of Contributed Papers Jul. 1990 p 235-237 (For primary document see N91-14100 05-90)

Avail: NTIS HC/MF A19 CSCL 03B

Researchers survey shock solutions of a partially ionized gas with a magnetic field. The gas is modeled by interacting neutral, ion, electron and charged grain components. They employ a small neutral-ion chemical network to follow the dissociation and ionization of the major species. Cooling by molecular hydrogen (rotational, vibrational and dissociation), grains and dipole molecules is included. There are three basic types of solutions (C, C asterisk, and J) and some more complicated flows involving combinations of the basic types. The initial preshock conditions cover hydrogen nuclei densities of 1 less than n less than 10(exp 10) cm(-3) and shock velocities of 5 less than v(sub s) less than 60 km/s. The magnetic field is varied over 5 decades and the sensitivity of the results to grain parameters, UV and cosmic ray fluxes is ascertained. The parameter space is quite complicated, but there exist some simple divisions. When the initial ionization fraction is small (chi sub i less than 10(-5)), there is a sharp transition between fully C solutions at low velocity and strong J solutions at high velocity. When the initial ionization fraction is larger, C asterisk and/or very weak J shocks are present at low velocities in addition to the C solutions. The flow again changes to strong J shocks at high velocities. When the ionization fraction is large and the flow is only slightly greater than the bulk Alfven velocity, there is a complicated mixture of C, C asterisk and J solutions. Author

N91-14184*# National Aeronautics and Space Administration. Ames Research Center, Moffett Field, CA.

WHAT SORT OF STANDARD CANDLE IS ORION FOR STUDYING MOLECULAR HYDROGEN LINE EMISSION IN GALAXIES

Michael Burton and Phil J. Puxley (Hawaii Univ., Honolulu.) *In its* The Interstellar Medium in External Galaxies: Summaries of Contributed Papers Jul. 1990 p 238-240 (For primary document see N91-14100 05-90)

Avail: NTIS HC/MF A19 CSCL 03B

The total shocked and fluorescent molecular hydrogen 1-0 S(1) line luminosities from Orion have been measured to be about 2.5 solar luminosity and about 2.0 solar luminosity, respectively. The implications for using Orion to study the interstellar medium in galaxies is discussed. Author

N91-14185*# Joint Astronomy Centre, Hilo, HI.

H2 LINE EMISSION IN THREE SEYFERT NUCLEI: EVIDENCE AGAINST UV-EXCITATION

T. R. Geballe *In* NASA, Ames Research Center, The Interstellar Medium in External Galaxies: Summaries of Contributed Papers Jul. 1990 p 241-242 (For primary document see N91-14100 05-90)

Avail: NTIS HC/MF A19 CSCL 03B

Line emission from vibrationally excited molecular hydrogen has been detected in a considerable number of active galactic nuclei (AGNs), including those generally believed to contain

compact and luminous central engines (e.g., Seyfert nuclei) and those in which the luminosity is believed to arise from massive bursts of star formation (starburst nuclei). In most of these AGNs, only the bright 1-0 S(1) line (rest wavelength 2.12 microns) has been searched for and detected to date. Line-emitting H2 can be excited directly either by energetic collisions created by shock waves or by absorption of UV radiation. Each of these excitation mechanisms has been clearly identified in galactic and extragalactic regions. In active galactic nuclei strong sources of UV and (in some case) x rays are present. If the nuclear molecular matter is quiescent (i.e., isolated from the active nucleus and not set into motion by episodes of star formation) the H2 line emission will be dominated by fluorescence, or possibly by thermal emission due to heating by x rays (Krolik, this conference). However, it is expected or indeed observed that a significant fraction of the interstellar medium in and near these nuclei is undergoing rapid motions; either generated by the central engine or by a nuclear starburst, which are capable of producing strong shock phenomena in nearby molecular gas. Thus, a priori it is not obvious which mechanism is responsible for the H2 line emission from the nucleus of an active galaxy. Author

N91-14186*# California Univ., Berkeley. Dept. of Physics.
LYMAN ALPHA RADIATION IN EXTERNAL GALAXIES
David A. Neufeld and Christopher F. McKee *In* NASA, Ames Research Center, The Interstellar Medium in External Galaxies: Summaries of Contributed Papers Jul. 1990 p 243-245 (For primary document see N91-14100 05-90)
(Grant NSF AST-86-15177)
Avail: NTIS HC/MF A19 CSCL 03B

The Ly alpha line of atomic hydrogen is often a luminous component of the radiation emitted by distant galaxies. Except for those galaxies which have a substantial central source of non-stellar ionizing radiation, most of the Ly alpha radiation emitted by galaxies is generated within regions of the interstellar medium which are photoionized by starlight. Conversely, much of the energy radiated by photoionized regions is carried by the Ly alpha line. Only hot, massive stars are capable of ionizing hydrogen in the interstellar medium which surrounds them, and because such stars are necessarily short-lived, Ly alpha emission traces regions of active star formation. Researchers argue that the strength of the Ly alpha emission observed from external galaxies may be used to estimate quantitatively the dust content of the emitting region, while the Ly alpha line profile is sensitive to the presence of shock waves. Interstellar dust particles and shock waves are intimately associated with the process of star formation in two senses. First, both dust particles and shock waves owe their existence to stellar activity; second, they may both serve as agents which facilitate the formation of stars, shocks by triggering gravitational instabilities in the interstellar gas that they compress, and dust by shielding star-forming molecular clouds from the ionizing and dissociative effects of external UV radiation. By using Ly alpha observations as a probe of the dust content in diffuse gas at high redshift, we might hope to learn about the earliest epochs of star formation. Author

N91-14187*# Lowell Observatory, Flagstaff, AZ.
OBSERVATIONS OF EXTENDED AND COUNTERROTATING DISKS OF IONIZED GAS IN S0 GALAXIES
Ralf-Juergen Dettmar, Marlies Jullien-Dettmar, and Andreas Barteldrees (Max-Planck-Inst. fuer Radioastronomie, Bonn, Germany, F.R.) *In* NASA, Ames Research Center, The Interstellar Medium in External Galaxies: Summaries of Contributed Papers Jul. 1990 p 246-248 (For primary document see N91-14100 05-90)
(Contracts DFG-DE-385/1-1; DFG-DE-385/2-1)
Avail: NTIS HC/MF A19 CSCL 03B

While many E/S0 galaxies have been found to show emission line spectra in their nuclear regions, the question of the presence and nature of extended disks of ionized gas in these galaxies has been addressed only in recent years. Typically the ionized gas is detected in the inner region on a scale of approx. 1 kpc (e.g., Phillips et al. 1986, Caldwell 1984). Here researchers present evidence that the disks of ionized gas of at least some S0 galaxies are much more extended than previously believed. In addition, with the detection of the counterrotation of gas and stars in NGC 7007 they strengthen the basis for arguments that the source of gas in S0 galaxies is external Author

N91-14188*# Commissariat a l'Energie Atomique, Saclay (France). Service d'Astrophysique.
THE GRAVITATIONAL WAKEFIELD OF A MOLECULAR CLOUD IN A DISK GALAXY Abstract Only
M. Tagger, R. Pellat, and J. F. Sygnet (Institut d'Astrophysique, Paris, France) *In* NASA, Ames Research Center, The Interstellar Medium in External Galaxies: Summaries of Contributed Papers Jul. 1990 p 249 (For primary document see N91-14100 05-90)
Avail: NTIS HC/MF A19 CSCL 03B

A molecular cloud (considered as a point macroparticle) represents a clump of increased mass density moving in the disk of a galaxy. Its presence generates a gravitational polarization of the disk, somewhat analogous to the polarization of a dielectric medium by a test charged particle. This means that the cloud travels along with a wakefield (a region of increased mass density) which is the collective response of the stars and gas to the perturbing mass. It can represent many times the mass of the cloud, and emits spiral density waves which propagate away. In terms of statistical mechanics, this wakefield will appear as an increased two-particle correlation function which is the equivalent of the Debye sphere in a plasma - despite the absence here of negative charges. At short distances clouds will thus interact through their own gravitational field amplified by their wakefields, which might thus strongly affect their collisionality. Researchers present a calculation of this wakefield and discuss its importance in the collisional dynamics of molecular clouds. Author

N91-14189*# Washington State Univ., Pullman. Dept. of Pure and Applied Mathematics.
THE EFFECT OF SUSPENDED PARTICLES ON JEAN'S CRITERION FOR GRAVITATIONAL INSTABILITY Abstract Only
David J. Wollkind and Kemble R. Yates (Southern Oregon Coll., Ashland.) *In* NASA, Ames Research Center, The Interstellar Medium in External Galaxies: Summaries of Contributed Papers Jul. 1990 p 250-251 (For primary document see N91-14100 05-90)
Avail: NTIS HC/MF A19 CSCL 03B

The effect that the proper inclusion of suspended particles has on Jeans' criterion for the self-gravitational instability of an unbounded nonrotating adiabatic gas cloud is examined by formulating the appropriate model system, introducing particular physically plausible equations of state and constitutive relations, performing a linear stability analysis of a uniformly expanding exact solution to these governing equations, and exploiting the fact that there exists a natural small material parameter for this problem given by N sub 1/n sub 1, the ratio of the initial number density for the particles to that for the gas. The main result of this investigation is the derivation of an altered criterion which can substantially reduce Jeans' original critical wavelength for instability. It is then shown that the existing discrepancy between Jeans' theoretical prediction using and actual observational data relevant to the Andromeda nebula M31 can be accounted for by this new criterion of assuming suspended particles of a reasonable grain size and distribution to be present. Author

N91-14190*# Colorado Univ., Boulder.
VIRIAL THEOREM ANALYSIS OF THE STRUCTURE AND STABILITY OF MAGNETIZED CLOUDS
Ellen G. Zweibel *In* NASA, Ames Research Center, The Interstellar Medium in External Galaxies: Summaries of Contributed Papers Jul. 1990 p 252-254 Previously announced in IAA as A90-20294 Submitted for publication (For primary document see N91-14100 05-90)
(Grants NAGw-91; NSF R11-87-22796; NSF ATM-25-06632)
Avail: NTIS HC/MF A19 CSCL 03B

The tensor virial theorem is used to analyze the structure and stability of self-gravitating, magnetized spheroids surrounded by a low-density medium with pressure and magnetic field. Analytical expressions are developed for the effect of a weak field and calculate critical states when the effect of the field is arbitrarily strong, comparing the results with full magnetohydrostatic calculations. This analysis suggests that a magnetic field may prevent gravitational collapse but may also be destabilizing, depending on its degree of concentration within the cloud.
Author

N91-14191*# Niigata Univ. (Japan). Faculty of Education.
EVOLUTION OF MAGNETIZED, ROTATING, ISOTHERMAL CLOUDS
Kohji Tomisaka *In* NASA, Ames Research Center, The Interstellar Medium in External Galaxies: Summaries of Contributed Papers Jul. 1990 p 255-257 (For primary document see N91-14100 05-90)
Avail: NTIS HC/MF A19 CSCL 03B

Molecular cloud cores, in which star formation process now proceeds, are often found with elongated shape. This suggests that the core collapsed preferentially along the direction parallel to the global magnetic field and/or parallel to the cloud's initial angular momentum. Actually the magnetic field strength in the cloud has been measured recently with the Zeeman splitting (Goodman et al. 1989). The authors indicate the magnetic field of 10 to 30 mu G exists in the cloud. Further, the observation of polarization in the near IR from background stars shows that the magnetic field runs perpendicularly to the major axis of the cloud (Tamura et al. 1987). As for the angular momentum, the rotation rate of 0.2 to 6 kms s(exp -1) pc(exp -1) is reported (Goldsmith and Arquilla 1984) in 16 dark cloud regions. If the cloud collapses from the diffuse cloud with density n approx. 1 cm (exp -3) with strictly conserving the angular momentum which was shared from the galactic rotation, the rotation rate of the cloud will be x mega sub j = const approx. 3(n/1000 cm exp -3) exp 2/3 km s(exp -1) pc (exp -1) (Mouschovias 1987). The evolution of the rotating magnetized cloud is discussed here.
Author

N91-14192*# Minnesota Univ., Minneapolis.
INFRARED POLARIMETRY AND THE MAGNETIC FIELD IN EXTERNAL GALAXIES
Terry Jay Jones *In* NASA, Ames Research Center, The Interstellar Medium in External Galaxies: Summaries of Contributed Papers Jul. 1990 p 258-259 (For primary document see N91-14100 05-90)
Avail: NTIS HC/MF A19 CSCL 03B

Here researchers report for the first time infrared polarimetry of the normal edge on spiral NGC 4565 and the interacting pair NGC 3690/IC 694 (Arp 299). These observations, as well as previous observations, were made with the Minnesota Infrared Polarimeter on the Space Infrared Telescope Facility during the past year. The goal is to explore the magnetic field geometry in these galaxies and to determine the extent to which the field is ordered and uniform.
Author

N91-14193*# York Univ., Toronto (Ontario).
POLARIZATION IN THE LAGOON NEBULA
Marshall L. McCall, Michael G. Richer, and N. Visvanathan (Mount Stromlo and Siding Spring Observatory, Canberra, Australia) *In* NASA, Ames Research Center, The Interstellar Medium in External Galaxies: Summaries of Contributed Papers Jul. 1990 p 260-262 (For primary document see N91-14100 05-90)
Avail: NTIS HC/MF A19 CSCL 03B

A V-band polarimetric survey of stars associated with the Lagoon nebula was conducted. The data were combined with existing photometric and spectroscopic observations in order to investigate the alignment of magnetic field lines with identifiable symmetry axes and to evaluate the nature of dust in the immediate vicinity. Although stars are not in general highly polarized, electric vectors align with the minor axis of the Lagoon nebula, perpendicular to the major axis of the spatial distribution of massive stars. The observations indicate that the collapse of the molecular cloud progenitor was inhibited along directions perpendicular to magnetic field lines. Considering the low polarization efficiency and the high ratio of total to selective extinction, smaller grains of intranebular dust appear to have been destroyed.
Author

N91-14194*# Space Telescope Science Inst., Baltimore, MD.
GRANULARITY IN THE MAGNETIC FIELD STRUCTURE OF M83
R. J. Allen and S. Sukumar (Illinois Univ., Urbana.) *In* NASA, Ames Research Center, The Interstellar Medium in External Galaxies: Summaries of Contributed Papers Jul. 1990 p 263-265 (For primary document see N91-14100 05-90)
(Grant NSF AST-87-15905)
Avail: NTIS HC/MF A19 CSCL 03B

Researchers recently reported Very Large Array (VLA) 20 cm continuum polarization observations of the bright, nearly face-on southern spiral galaxy M83 (NGC 5236) at a spatial resolution of 2 kpc (Sukumar and Allen 1989). The strongest linearly-polarized emission is found in two giant arcs, with typical lengths of about 30 kpc, which are situated roughly opposite each other in the dark outer regions of the galaxy at a radius of 12 kpc from the center. These regions of high polarized intensity (and hence highly-uniform magnetic field) do not coincide with any prominent spiral-arm tracers, in contrast to the expectations of simple models for the large-scale compression of magnetic field in density-wave shock fronts. From a comparison of the data with previous results at 6 cm, the authors concluded that the low polarization in the central regions of the galaxy is a result of disorder in the interstellar magnetic field. The most likely cause of this disorder is the greater star formation activity observed in the inner parts of the galaxy. The intrinsic direction of the magnetic field in the outer parts of the galaxy has also recently been determined on a length scale of 6.5 kpc from a comparison of the VLA 20 cm results with 6.3 cm observations obtained earlier with the Effelsberg telescope (Sukumar et al. 1989). There is very little Faraday rotation in the regions of the highly-polarized arcs of emission. The magnetic field in these polarized arcs is parallel to the general spiral arm structure seen in the usual optical tracers (dust, HII regions) in the bright inner parts of the galaxy disk. The maximum observed polarization at 2 kpc resolution is about 50 percent.
Author

N91-14195*# California Univ., Santa Cruz.
THERMAL INSTABILITIES IN PROTOGALACTIC CLOUDS
S. D. Murray and D. N. C. Lin *In* NASA, Ames Research Center, The Interstellar Medium in External Galaxies: Summaries of Contributed Papers Jul. 1990 p 267-268 (For primary document see N91-14100 05-90)
Avail: NTIS HC/MF A19 CSCL 03B

The means by which a protogalaxy can fragment to form the first generation of stars and globular clusters remains an important problem in astrophysics. Gravitational instabilities grow on timescales too long to drive fragmentation before the background density grows by many orders of magnitude (see Murray and Lin 1989a, and references therein). Thermal instability provides a much more likely mechanism. After its initial collapse, a protogalactic cloud is expected to be shock heated to its virial temperature approx. 10(exp 6) K. Cooling by H and He+ below 10(exp 6) K has a negative slope, so that the cloud is subject to strong thermal instabilities. Density enhancements may then grow rapidly, fragmenting the protogalaxy as it cools to lower temperatures. The role of dynamical effects upon the growth of perturbations is considered here. The method used is similar to that used in Murray and Lin (1989a; see also the Erratum to appear September 15), which examined the growth of thermal instabilities with a one-dimensional Lagrangian hydrodynamics code, written for spherical symmetry. Perturbed regions therefore take the form of shells. The dynamical variables are integrated explicitly, while the temperature, ionization fraction, and molecular fraction are integrated implicitly, and account is taken for non-equilibrium values of these quantities.
Author

N91-14196*# National Radio Astronomy Observatory, Socorro, NM.

HIGH BRIGHTNESS NEUTRAL HYDROGEN IN M31: A NEW PROBE OF INTERSTELLAR PRESSURE

Robert Braun and Rene Walterbos (California Univ., Berkeley.) *In* NASA, Ames Research Center, The Interstellar Medium in External Galaxies: Summaries of Contributed Papers Jul. 1990 p 269-271 (For primary document see N91-14100 05-90)

Avail: NTIS HC/MF A19 CSCL 03B

An observational parameter of our own Galaxy, the peak brightness temperature of neutral hydrogen in emission, was determined almost twenty years ago (Burton 1970). This quantity, although possessing a degree of local variations, has a remarkably consistent peak value of 125 K towards spiral arm segments with a few isolated peaks extending to 135 K, once sufficient spatial and velocity resolution are used (less than or equal to 70 pc, less than or equal to 5 km/s) to resolve the emission peaks. The higher spatial and velocity resolution of more recent surveys has not led to the detection of higher brightnesses. For many years this remarkable observational result has received little attention, primarily because similar data for other galaxies, which would allow a meaningful comparison and analysis, did not exist. Recently this situation has changed. A Westerbork survey of M33 (Deul and Van der Hulst 1987, and private comm.) with 40 pc x 8 km/s resolution has revealed consistent peak values of only 95 plus or minus 5 K (although there is still some question of whether the velocity resolution was sufficient in this case), while a Very Large Array (VLA) survey of M31 (Braun 1989a) with 35 pc x 5 km/s resolution has shown consistent peak values but at a temperature of 155 to 165 K. It has become clear that although peak HI brightness seems to be a well-defined quantity within individual galaxies (with a degree of local variation) there are very significant differences in this quantity amongst different galaxies. Researchers embarked on an observational program directed at a sample of 11 nearby galaxies: NGC 55, 247, 7793, 3031, 2366, 2403, 4236, 4826, 4736, 4244, and 5457. They hope to determine the gas properties and phases as a function of both galaxy type and position within the galaxies utilizing high resolution HI observations and optical narrow band imagery and spectroscopy which are now underway. Author

N91-14197*# Ecole Normale Superieure, Paris (France).

CO OBSERVATIONS OF SOUTHERN MERGERS

F. Casoli, C. Dupraz, and F. Combes *In* NASA, Ames Research Center, The Interstellar Medium in External Galaxies: Summaries of Contributed Papers Jul. 1990 p 273-275 (For primary document see N91-14100 05-90)

Avail: NTIS HC/MF A19 CSCL 03B

There are good reasons to believe that the formation of some elliptical galaxies result from the merging of two disk galaxies, as Toomre and Toomre first suggested (1972, Ap. J. 178, 623). Such a process strongly enhances the star-formation activity of the system, thus consuming its molecular gas. This might account for the low cold-gas content of elliptical galaxies compared to that of spirals. Researchers present here CO(1-0) and CO(2-1) observations of a sequence of three objects, NGC 1614, NGC 3256, and NGC 7252, that present characteristic features of merger remnants: single body and extended tidal tails. NGC 3256 and 7252 even exhibit the r(exp 1/4) radial light distribution that is the signature of elliptical galaxies, which indicates that their stellar bodies are in late stages of relaxation. Both NGC 1614 and NGC 3256 undergo extended bursts of star formation revealed by their large far-infrared luminosities, and by the presence in the near-infrared spectrum of the 3.28 microns feature (Morwood: 1986, A. A. 166, 4) attributed to polycyclic aromatic hydrocarbons. On the other hand, NGC 7252 has a milder activity of star formation, as suggested by a lower infrared luminosity, and thus seems to have gone past the starburst phase. The CO data were collected with the Swedish-ESO 15 m Submillimeter Telescope (SEST) (beamsize = 43 seconds at 115 GHz, 23 seconds at 230 GHz). For NGC 7252, researchers have only observed the central position in CO-12(1-0). The spectrum is displayed together with an HI spectrum obtained with the Nancay radiotelescope. Researchers mapped NGC 1614 and NGC 3256 in CO-12(1-0) and CO-12(2-1), and also observed the nucleus of NGC 3256 in CO-13(1-0). The various CO spectra obtained towards the nuclei of both galaxies are presented. Characteristics of the galaxies are gathered, with luminosities and masses in solar units and temperatures in Kelvins. Author

N91-14198*# Iowa State Univ. of Science and Technology, Ames. Dept. of Physics.

STAR FORMATION ON THE LEADING EDGE OF A RING-LIKE DENSITY WAVE IN ARP 143

P. N. Appleton *In* NASA, Ames Research Center, The Interstellar Medium in External Galaxies: Summaries of Contributed Papers Jul. 1990 p 276-278 (For primary document see N91-14100 05-90)

Avail: NTIS HC/MF A19 CSCL 03B

NGC 2445 is a member of the pair of interacting galaxies Arp 143 (=VV117) and has been classified as an irregular ring galaxy by deVaucouleurs et al. (1976). Although not obviously a classical ring galaxy from its optical appearance, it nevertheless shows many of the symptoms of a collisional off-center ring galaxy in the early stages of development. Optically the galaxy shows a rough ring of super-giant HII regions distributed asymmetrically with respect to the nucleus with most of the emission concentrated on the western side of the galaxy. Researchers mapped the HI emission in this system (with F. Ghigo and J. van Gorkom; NRAO) and the observations show that the disk of NGC 2445 is characterized by a large-scale banana-shaped HI wave with its peak to the west of the nucleus. Nearing-IR imaging (with E. I. Robson and A. J. Adamson; Lancs. Polytechnic, U.K.) demonstrates that, like the HI, the underlying population of old stars is very asymmetrically distributed with the bulk of the stars concentrated to the western side of the galaxy. Author

N91-14199*# Netherlands Foundation for Radio Astronomy, Dwingelo.

A MULTI-WAVELENGTH STUDY OF THE PECULIAR GALAXY NGC 2976

L. J. Tacconi, J. M. vanderHulst, and P. R. Wesselius (Groningen Rijksuniv., Netherlands) *In* NASA, Ames Research Center, The Interstellar Medium in External Galaxies: Summaries of Contributed Papers Jul. 1990 p 279-280 (For primary document see N91-14100 05-90)

Avail: NTIS HC/MF A19 CSCL 03B

Researchers are currently studying NGC 2976 at many wavelengths to investigate the extent to which an interaction with M81 may have affected the star formation history of this galaxy. Here, researchers present observations of NGC 2976 made at 50 microns with the high resolution (CPC) instrument onboard Infrared Astronomy Satellite (IRAS) at 21-cm (both HI line and radio continuum) with the Westerbork Synthesis Radio Telescope (WSRT) and in the H alpha line with the Kitt Peak National Observatory (KPNO) 36 inch telescope. The far infrared emission is not centrally peaked as in other spirals (e.g., Wainscoat et al. 1987), but has obvious intensity peaks near the ends of the disk. The ionized gas as inferred from the H alpha observations, is largely confined to two large, symmetrically placed emission regions near the ends of the disk. Finally, the HI and 21-cm radio continuum emission also exhibit this strongly double-peaked structure. At all of the above wavelengths the emission peaks are roughly coincident and lie approx. 1.2 minutes to the NW and approx. 1.1 minutes to the SE of the optical center of this galaxy. Author

N91-14200*# Johns Hopkins Univ., Baltimore, MD.

THE MORPHOLOGY-DENSITY RELATION FOR DWARF GALAXIES

H. C. Ferguson and A. Sandage (Carnegie Institution of Washington, DC.) *In* NASA, Ames Research Center, The Interstellar Medium in External Galaxies: Summaries of Contributed Papers Jul. 1990 p 281-283 (For primary document see N91-14100 05-90)

Avail: NTIS HC/MF A19 CSCL 03B

The morphology-density relation is examined for dwarf galaxies

with absolute magnitudes -18 less than or equal to M sub B sub T less than or equal to -12.5, based on a deep photographic survey of nearby groups and clusters of galaxies. Results are given. Compared to dwarf ellipticals, dwarf irregulars form a more extended population in nearby clusters, and may in fact be entirely absent from the cluster cores. The spatial distribution of dwarf ellipticals in clusters depends on luminosity and the presence or absence of nucleation. Nucleated dE's and non-nucleated dE's fainter than M sub B sub T approx. -13.5 are concentrated toward the centers of clusters like the giant E and S0 galaxies. In contrast, non-nucleated dE's brighter than M sub B sub T approx. -14.5 are distributed like the spirals and irregulars. The intrinsic shapes of the bright non-nucleated dE's are similar to those of the dwarf irregulars, suggesting a possible evolutionary connection between these two classes of galaxies. Author

N91-14201*# California Inst. of Tech., Pasadena.
UNBOUND MOLECULAR COMPLEXES IN M33
Christine D. Wilson *In* NASA, Ames Research Center, The Interstellar Medium in External Galaxies: Summaries of Contributed Papers Jul. 1990 p 285-287 (For primary document see N91-14100 05-90)
Avail: NTIS HC/MF A19 CSCL 03B

The HI content of the nearby spiral galaxy M33 (d approx. 0.8 Mpc) has been the subject of many detailed studies (most recently Deul and van der Hulst 1987), but similar data on the molecular gas component has been lacking. This galaxy is currently undergoing vigorous high-mass star formation, as evidenced by the many OB associations and HII regions, and so is expected to possess at least some molecular gas. Interferometric studies have detected molecular clouds similar to Galactic Giant Molecular Clouds (GMCs) (Boulanger et al. 1988; Wilson et al. 1988). Researchers have recently mapped the nuclear region of M33 in the CO J=1-0 line with a 12 m telescope (half power beam width 55 inches approx. 210 pc) out to a radius of 3.5 minutes in order to trace the detailed distribution of the molecular gas. The resulting map reveals six large complexes with diameters of 200 to 400 pc. Interferometer observations of these regions have resolved them into individual molecular clouds similar to Galactic GMCs (Wilson et al. 1988). The complexes shown are much larger than individual Galactic GMCs (Sanders, Scoville, and Solomon 1985), but are somewhat smaller on average than the large associations seen in the grand-design spiral galaxy M51 (Rand and Kulkarni 1989). If we extend the velocity-diameter relation observed for Galactic GMCs to these larger structures, the predicted velocity widths are a factor of 1.5 to 3 times greater than the observed full-width half-maximum velocities (13 to 29 km (s-1). The peak brightness temperatures are approx. 0.2 K, at least a factor of 10 lower than what is observed for Galactic GMCs. If these large structures are made up of objects similar to Galactic GMCs, the area filling factor of the small clouds is roughly 10 percent. These results suggest that these complexes are not very large GMCs, but rather are associations of many individual GMCs or GMCs embedded in a diffuse gas component. Author

N91-14202*# California Inst. of Tech., Pasadena. Infrared Processing and Analysis Center.
DEEP NARROW BAND IMAGERY OF THE DIFFUSE ISM IN M33
J. Jeff Hester and Shrinivas R. Kulkarni *In* NASA, Ames Research Center, The Interstellar Medium in External Galaxies: Summaries of Contributed Papers Jul. 1990 p 288-290 (For primary document see N91-14100 05-90)
Avail: NTIS HC/MF A19 CSCL 03B

Very deep narrow band images were obtained for several fields in the local group spiral galaxy M33 using a wide field reimaging Charge Coupled Device (CCD) camera on the 1.5 m telescope at Palomar Observatory. The reimaging system uses a 306 mm collimator and a 58 mm camera lens to put a 16 minute by 16 minute field onto a Texas Instruments 800 x 800 pixel CCD at a resolution of 1.2 arcseconds pixel (-1). The overall system is f/1.65. Images were obtained in the light of H alpha (S II) lambda lambda 6717, 6731, (O III) lambda 5007, and line-free continuum bands 100A wide, centered at 6450A and 5100A. Assuming a distance of 600 kpc to M33 (Humphreys 1980, Ap. J., 241, 587), this corresponds to a linear scale of 3.5 pc pixel (-1), and a field size of 2.8 kpc x 2.8 kpc. Researchers discuss the H alpha imagery of a field centered approx. equal to 8 minutes NE of the nucleus, including the supergiant HII region complex NGC 604. Two 2000 second H alpha images and two 300 second red continuum images were obtained of two slightly offset fields. The fields were offset to allow for discrimination between real emission and possible artifacts in the images. All images were resampled to align them with one of the H alpha frames. The continuum images were normalized to the line images using the results of aperture photometry on a grid of stars in the field, then the rescaled continuum data were directly subtracted from the line data. Author

N91-14203*# Illinois Univ., Urbana.
A HIGH RESOLUTION CO MAP OF M51
D. S. Adler, K. Y. Lo, and R. J. Allen *In* NASA, Ames Research Center, The Interstellar Medium in External Galaxies: Summaries of Contributed Papers Jul. 1990 p 291-292 (For primary document see N91-14100 05-90)
Avail: NTIS HC/MF A19 CSCL 03B

Observations of the CO (1-0) emission in two fields of M51 were taken with the Berkeley-Illinois-Maryland Array at Hat Creek, California from May 1988 to February 1989. When combined with two previously observed fields (Lo et al. 1988), a complete map of the central 5 minute x 4 minute at a resolution of 7 seconds x 10 seconds was obtained. The project is part of an ongoing high-resolution survey of the molecular, atomic, and ionized gas distributions in nearby spiral galaxies. The two recently observed fields can be compared to the results of the interferometric study of Vogel et al. (1988 - hereafter VKS). Since the shortest spacing in the current survey is shorter than that of VKS, researchers expect to see more of the extended emission. This is evident when comparing the width of the spiral arms in each survey; ours are a bit broader. While some of the peaks in this region correspond to the peaks in VKS, several of them do not. These discrepancies are probably because of the low signal to noise inherent in observations of this nature. Single-dish maps are currently being readied for inclusion with the interferometer data. These will help fill the short-spacing hole in the UV plane, and serve to recover the flux missing from the interferometer maps. Author

N91-14204*# California Inst. of Tech., Pasadena.
M51: MOLECULAR SPIRAL ARMS, GMAS AND SUPERCLOUDS
Richard J. Rand and Shrinivas R. Kulkarni *In* NASA, Ames Research Center, The Interstellar Medium in External Galaxies: Summaries of Contributed Papers Jul. 1990 p 293-295 (For primary document see N91-14100 05-90)
Avail: NTIS HC/MF A19 CSCL 03B

Researchers present an aperture synthesis image of M51 in the CO 1 to 0 line at 9 seconds x 7 seconds resolution made with the Owens Valley Millimeter Interferometer. The image is a mosaic of 30 one-arcminute fields. The image shows narrow spiral arms which are coincident with the optical dust lanes and non-thermal radio emission, but are offset from the ridges of H alpha emission. Many dense concentrations of CO emission, termed Giant Molecular Associations (GMAs), are seen both along and between the arms. The typical GMA mass is about 3 times 10(exp 7) solar mass. Most of the on-arm GMAs appear to be gravitationally bound. These GMAs consist of several spectral components (Molecular Superclouds) with typical mass 10(exp 7) solar mass, which also appear to be bound. The observed streaming motions in the GMAs are consistent with density wave theory. The interarm GMAs are not gravitationally bound, and are likely to be due to a secondary compression of the density wave. Author

N91-14205*# Princeton Univ. Observatory, NJ.
DISSOCIATION AND IONIZATION OF MOLECULAR GAS IN THE SPIRAL ARMS OF M51
J. F. Lees and K. Y. Lo (Illinois Univ., Urbana.) *In* NASA, Ames

Research Center, The Interstellar Medium in External Galaxies: Summaries of Contributed Papers Jul. 1990 p 296-297 (For primary document see N91-14100 05-90)
(Grant NSF AST-87-15905)
Avail: NTIS HC/MF A19 CSCL 03B

Researchers derive the star formation rate and efficiency in the arm and interarm regions of M51 from observations of the molecular (Lo et al. 1987) and ionized (van der Hulst et al. 1988) phases of the interstellar medium, and show that the HI observations of Tilanus and Allen (1989) are consistent with dissociation of molecular gas by these young, massive stars if n sub H greater than or equal to 200 cm (-2). However, these stars are not able to dissociate or ionize all the gas, and at least 60 percent must remain molecular in the interarm regions. The efficiency of star formation in M51 seems to be similar to that in the Galaxy, and does not appear to be enhanced in the spiral arms. Therefore, the effect of the strong density wave may be only to concentrate the gas, and hence the young stars, to the arm regions. Author

N91-14206*# Kapteyn Astronomical Lab., Groningen (Netherlands).
SPIRAL STRUCTURE OF M51: STREAMING MOTIONS ACROSS THE SPIRAL ARMS
R. P. J. Tilanus and R. J. Allen (Space Telescope Science Inst., Baltimore, MD.) *In* NASA, Ames Research Center, The Interstellar Medium in External Galaxies: Summaries of Contributed Papers Jul. 1990 p 298-300 (For primary document see N91-14100 05-90)
Avail: NTIS HC/MF A19 CSCL 03B

The atomic hydrogen (HI) and the H alpha emission line in the grand-design spiral galaxy M51 have been observed with the Westerbork Synthesis Radio Telescope and the Taurus Fabry-Perot imaging spectrometer, respectively. Across the inner spiral arms significant tangential and radial velocity gradients are detected in the H alpha emission after subtraction of the axi-symmetric component of the velocity field. The shift is positive on the inside and negative on the outside of the northern arm. Across the southern arm this situation is reversed. The direction of the shifts is such that the material is moving inward and faster compared to circular rotation in both arms, consistent with the velocity perturbations predicted by spiral density wave models for gas downstream of a spiral shock. The observed shifts amount to 20 to 30 km (s-1), corresponding to streaming motions of 60 to 90 km (s-1) in the plane of the disk (inclination angle 20 degrees). Comparable velocity gradients have also been observed by Vogel et al. in the CO emission from the inner northern arm of M51. The streaming motions in M51 are about 2 to 3 times as large as the ones found in HI by Rots in M81, and successfully modelled by Visser with a self-consistent density wave model. Researchers have not been able to detect conclusively streaming motions in the HI emission from the arms, perhaps due to the relatively poor angular resolution (approx. 15 seconds) of the HI observations.
Author

N91-14207*# Aerospace Corp., Los Angeles, CA. Space Sciences Lab.
HIGH SPATIAL-RESOLUTION IRAS IMAGES OF M51
R. Canterna, John A. Hackwell, and Gary L. Grasdalen (Wyoming Univ., Laramie.) *In* NASA, Ames Research Center, The Interstellar Medium in External Galaxies: Summaries of Contributed Papers Jul. 1990 p 301-303 (For primary document see N91-14100 05-90)
Avail: NTIS HC/MF A19 CSCL 03B

High spatial-resolution (approx. equal to 30 seconds) images of M51 in the four Infrared Astronomy Satellite (IRAS) bands (12, 25, 60, and 100 microns) have been obtained. The spatial variation in flux in all four bands is coincident with the spiral features seen in H alpha and 6 cm with a few exceptions. In the nuclear region (4 minutes) the position of the peak of maximum intensity shifts in relation to the visual nucleus: it is coincident with the nucleus at 12 microns, shifts approximately 45 seconds to south-southwest, and is 45 seconds northwest of the nucleus at 60 and 100 microns. Author

N91-14208*# Arizona Univ., Tucson.
ARE BARS ESSENTIAL FOR STARBURSTS IN NON-INTERACTING GALAXIES Abstract Only
Stephen M. Pompea and G. H. Rieke *In* NASA, Ames Research Center, The Interstellar Medium in External Galaxies: Summaries of Contributed Papers Jul. 1990 p 305-306 (For primary document see N91-14100 05-90)
Avail: NTIS HC/MF A19 CSCL 03B

Analyzed here are the 1.6 and 2.2 micron images of a sample of galaxies that are classified as unbarred by the Revised Shapley-Ames Catalog. These galaxies have characteristic properties of nuclear starbursts and are examined through near infrared imaging in a search for hidden bars. Researchers selected a sample of 36 galaxies from the Revised Shapley-Ames Catalog that have far infrared luminosities greater than 10(exp 10) solar luminosity and hot Infrared Astronomy Satellite (IRAS) colors between 60 and 100 microns, indicative of nuclear starbursts, but are not classified as Seyfert 1 or 2. Their determination of the presence of a bar relies primarily on an analysis of the 2 micron image using the Galaxy Surface Photometry (GASP) package (Cawson, 1983). The GASP analysis programs determine the galaxy surface brightness and ellipticity profiles as well as the position angle and the center coordinates of the ellipses. To test the way that GASP will characterize the surface brightness of barred galaxies, two galaxies with known bars, NGC 1068 and NGC 2523, were imaged with the 2 micron camera and analyzed with GASP. Fifteen of the sample that are not clearly barred from optical data and are isolated were imaged at 1.6 and 2.2 microns; 9 of these do not appear to have bars. Strong bars therefore do not appear to be an absolute requirement for high infrared luminosity in isolated galaxies. Author

N91-14209*# Virginia Univ., Charlottesville.
ASPECTS OF THE INTERSTELLAR MEDIUM IN STARBURST GALAXIES
Michael N. Fanelli *In* NASA, Ames Research Center, The Interstellar Medium in External Galaxies: Summaries of Contributed Papers Jul. 1990 p 307-308 (For primary document see N91-14100 05-90)
Avail: NTIS HC/MF A19 CSCL 03B

Researchers are engaged in a multifaceted program to investigate the stellar content and star formation history of actively star-forming galaxies. A large body of stellar spectra have been examined to identify spectral features characteristic of specific stellar types. These spectral diagnostics are then calibrated in terms of temperature (spectral type), gravity (luminosity class) and metallicity. The spectral data is compiled into a stellar library whose members represent specific locations in the HR diagram. Through the use of population synthesis techniques, both optimizing and evolutionary approaches, the stellar luminosity function in composite populations can be determined by analysis of their integrated light. Researchers have concentrated on the ultraviolet wavelength region (lambda lambda 1200 to 3200), utilizing the International Ultraviolet Explorer (IUE) archives supplemented by additional observations. In the optical, virtually all stars will contribute to the integrated light. In the ultraviolet however, cool stars will produce negligible flux due to their steep ultraviolet-to-visual continua, greatly simplifying the investigation of the hot component in a composite population. The researchers' initial stellar library has been applied to several blue compact galaxies, (BCGs), a class of starburst galaxy which is UV luminous. BCGs possess a complex interstellar medium which affects the emergent stellar continuum in several ways. This presents a challenge to the stellar analysis but affords insight into the properties of the gas and dust from which the massive OB stars have formed. The optimizing synthesis method solves for the stellar luminosity function and extinction simultaneously. This therefore provides an independent measure of the extinction affecting the hot population component. Despite the rise of the reddening law

towards the ultraviolet, BCGs are found to be brighter in the ultraviolet than expected. Author

N91-14210*# Arizona Univ., Tucson.
GRAVITATIONAL STAR FORMATION THRESHOLDS AND GAS DENSITY IN THREE GALAXIES
M. S. Oey and R. C. Kennicutt, Jr. *In* NASA, Ames Research Center, The Interstellar Medium in External Galaxies: Summaries of Contributed Papers Jul. 1990 p 309-311 (For primary document see N91-14100 05-90)
Avail: NTIS HC/MF A19 CSCL 03B

It has long been held that the star formation rate (SFR) may be described as a power law of the gas density, p(exp n), as given by Schmidt (1959). However, this relation has as yet remained poorly defined and is likewise poorly understood. In particular, most studies have been investigations of global gas and star formation properties of galaxies, due to lack of adequate high-resolution data for detailed studies of individual galaxies. The three spiral galaxies in this study have published maps of both H2 (as traced by CO), and HI, thereby enabling the authors to investigate the relationship between total gas surface density and SFR. The purpose of the present investigation is the comparison of spatially-resolved total surface gas density in three galaxies (NGC 6946, M51, and M83) to sigma sub c as given by the above model. CO, HI and H alpha data for NGC 6946 were taken from Tacconi-Garman (1988), and for M51 and M83 from Lord (1987). The authors used a CO-H2 conversion of N(H2)/I sub CO(exp cos i = 2.8 x 10(exp 20) atoms cm(-2)/(K kms(-1), and summed the H2 and HI data for each galaxy to obtain the total hydrogen gas density. This total was then multiplied by a factor of 1.36 to include the contribution of helium to the total surface gas density. The authors assumed distances to NGC 6946, M51, and M83 to be 6.0, 9.6, and 8.9 Mpc respectively, with inclination angles of 30, 20, and 26 degrees. H alpha flux was used as the measure of SFR for NGC 6946, and SFR for the remaining two galaxies was taken directly from Lord as computed from H alpha measurements. The results of these full-disk studies thus show a remarkable correlation between the total gas density and the threshold densities given by the gravitational stability criterion. In particular, the threshold density appears to mark a lower boundary to the range of gas densities in these galaxies, which may have consequence in determining appropriate models for star formation and gas dynamics. More evidence is required to verify this result, and the authors are currently undertaking a high-resolution study of the nearby spiral M33 and other galaxies to further investigate this problem. Author

N91-14211*# Wyoming Univ., Laramie.
ONE-DIMENSIONAL CLOUD FLUID MODEL FOR PROPAGATING STAR FORMATION
Timothy N. Titus and Curtis Struck-Marcell (Iowa State Univ. of Science and Technology, Ames.) *In* NASA, Ames Research Center, The Interstellar Medium in External Galaxies: Summaries of Contributed Papers Jul. 1990 p 312-313 (For primary document see N91-14100 05-90)
(Grant NAGw-1009)
Avail: NTIS HC/MF A19 CSCL 03B

The aim of this project was to study the propagation of star formation (SF) with a self-consistent deterministic model for the interstellar gas. The questions of under what conditions does star formation propagate in this model and what are the mechanisms of the propagation are explored. Here, researchers used the deterministic Oort-type cloud fluid model of Scalo and Struck-Marcell (1984, also see the review of Struck-Marcell, Scalo and Appleton 1987). This cloud fluid approach includes simple models for the effects of cloud collisional coalescence or disruption, collisional energy dissipation, and cloud disruption and acceleration as the result of young star winds, HII regions and supernovae. An extensive one-zone parameter study is presented in Struck-Marcell and Scalo (1987). To answer the questions above, researchers carried out one-dimensional calculations for an annulus within a galactic disk, like the so-called solar neighborhood of the galactic chemical evolution. In the calculations the left-hand boundary is set equal to the right hand boundary. The calculation is obviously idealized; however, it is computationally convenient to study the first order effects of propagating star formation. The annulus was treated as if it were at rest, i.e., in the local rotating frame. This assumption may remove some interesting effects of a supersonic gas flow, but was necessary to maintain a numerical stability in the annulus. The results on the one-dimensional propagation of SF in the Oort cloud fluid model follow: (1) SF is propagated by means of hydrodynamic waves, which can be generated by external forces or by the pressure generated by local bursts. SF is not effectively propagated via diffusion or variation in cloud interaction rates without corresponding density and velocity changes. (2) The propagation and long-range effects of SF depend on how close the gas density is to the critical threshold value, i.e., on the susceptibility of the medium. Author

N91-14212*# Canadian Inst. for Theoretical Astrophysics, Toronto (Ontario).
STAR FORMATION IN PROTO DWARF GALAXIES
A. Noriega-Crespo, P. Bodenheimer, D. N. C. Lin, and G. Tenorio-Tagle (Max-Planck-Inst. fuer Astrophysik, Garching, Germany, F.R.) *In* NASA, Ames Research Center, The Interstellar Medium in External Galaxies: Summaries of Contributed Papers Jul. 1990 p 314-316 Sponsored in part by Toronto Univ. and Natural Sciences and Engineering Research Council, Canada (For primary document see N91-14100 05-90)
(Grant NSF AST-87-17867)
Avail: NTIS HC/MF A19 CSCL 03B

The effects of the onset of star formation on the residual gas in primordial low-mass Local-Group dwarf spheroidal galaxies is studied by a series of hydrodynamical simulations. The models have concentrated on the effect of photoionization. The results indicate that photoionization in the presence of a moderate gas density gradient can eject most of the residual gas on a time scale of a few 10 to the 7th power years. High central gas density combined with inefficient star formation, however, may prevent mass ejection. The effect of supernova explosions is discussed briefly. Author

N91-14213*# Edinburgh Univ. (Scotland). Dept. of Astronomy.
INFRARED SPECTROSCOPY OF THE DWARF STARBURST GALAXY HENIZE 2-10
P. R. Blanco and P. J. Puxley (Hawaii Univ., Honolulu.) *In* NASA, Ames Research Center, The Interstellar Medium in External Galaxies: Summaries of Contributed Papers Jul. 1990 p 317 (For primary document see N91-14100 05-90)
Avail: NTIS HC/MF A19 CSCL 03B

Researchers present 1.2 to 2.2 micron spectra of the nucleus of Henize 2 to 10, taken at United Kingdom Infrared Telescope (UKIRT) with the cool grating spectrometer 2 (CGS 2). This galaxy displays strong line emission from interstellar H (+) (1.282 and 2.166 microns) and (Fe (+)) (1.256 and 1.644 microns), in common with other star-forming galaxy nuclei. However, the 1 to 0 S(1) line of molecular hydrogen at 2.122 micron is not detected - the upper limit of 0.15 (3 sigma) for the value of the flux ratio I sub 1-os(1)/I sub Br gamma is much lower than the typical values of 0.4 to 0.9 measured in a sample of 28 non-interacting starburst galaxies. From the Pa beta/Br gamma line ratio researchers derive a total extinction of A sub v approx. 4 mag. The de-reddened H (+) and (Fe (+) line fluxes are used to estimate the total ionizing luminosity and the average supernova rate in the central 150 pc of He 2 to 10. By comparison of these estimates with existing Infrared Astronomy Satellite (IRAS) and radio continuum data, researchers are able to set limits on the range of stellar masses present in this unevolved (less than 10(exp 7) year old) starburst nucleus. Possible reasons for the low H2/H+ line ratios observed in young starburst systems (He 2 to 10, NGC 7714, IIZw40; e.g., Moorwood and Oliva 1988) are briefly discussed. Author

N91-14214*# York Univ., Toronto (Ontario).
SMALL-SCALE STAR FORMATION AT LOW METALLICITY
Marshall L. McCall, Robert Hill, and Jayanne English (Toronto Univ., Ontario) *In* NASA, Ames Research Center, The Interstellar

Medium in External Galaxies: Summaries of Contributed Papers Jul. 1990 p 318-320 Previously announced in IAA as A90-39893 (For primary document see N91-14100 05-90)
Avail: NTIS HC/MF A19 CSCL 03B

Massive star formation in a low metallicity environment is investigated by studying the morphology of small HII regions in the Small Magellanic Cloud. A classification scheme based upon the symmetry of form in the light of H-alpha is proposed to make possible an examination of the properties of blister candidates with respect to nebulas embedded in a more uniform medium. A new diagnostic of size is developed to derive quantitative information about the ionized gas and ionizing stars. The asymmetrical surface-brightness distribution of many HII regions demonstrates that massive stars often form at the edge of dense neutral clouds. However, the existence of many symmetrical nebulas with similar sizes, luminosities, and surface brightnesses shows that massive star formation often occurs within these clouds. Nevertheless, the statistics of the two different forms indicate that the rate of massive star formation declines less steeply with radius across host clouds than in the Milky Way, suggesting that external triggering may play a larger role in initiating star formation.
Author

N91-14215*# Five-College Astronomy Dept., Amherst, MA.
GLOBAL AND RADIAL VARIATIONS IN THE EFFICIENCY OF MASSIVE STAR FORMATION AMONG GALAXIES
Lori E. Allen and Judith S. Young *In* NASA, Ames Research Center, The Interstellar Medium in External Galaxies: Summaries of Contributed Papers Jul. 1990 p 321-324 (For primary document see N91-14100 05-90)
Avail: NTIS HC/MF A19 CSCL 03B

In order to determine the regions within galaxies which give rise to the most efficient star formation and to test the hypothesis that galaxies with high infrared luminosities per unit molecular mass are efficiently producing high mass stars, researchers have undertaken an H alpha imaging survey in galaxies whose CO distributions have been measured as part of the Five College Radio Astronomy Observatory (FCRAO) Extragalactic CO Survey. From these images researchers have derived global H alpha fluxes and distributions for comparison with far infrared radiation (FIR) fluxes and CO fluxes and distributions. Here, researchers present results on the global massive star formation efficiency (SFE = L sub H sub alpha/M(H2)) as a function of morphological type and environment, and on the radial distribution of the SFE within both peculiar and isolated galaxies. On the basis of comparison of the global L sub H sub alpha/M(H2) and L sub FIR/M(H2) for 111 galaxies, researchers conclude that environment rather than morphological type has the strongest effect on the global efficiency of massive star formation. Based on their study of a small sample, they find that the largest radial gradients are observed in the interacting/peculiar galaxies, indicating that environment affects the star formation efficiency within galaxies as well. Author

N91-14216*# Owens Valley Radio Observatory, Pasadena, CA.
MOLECULAR GAS AND STAR FORMATION IN THE CENTERS OF VIRGO SPIRALS
Blaise Canzian *In* NASA, Ames Research Center, The Interstellar Medium in External Galaxies: Summaries of Contributed Papers Jul. 1990 p 325-328 (For primary document see N91-14100 05-90)
Avail: NTIS HC/MF A19 CSCL 03B

The CO and H alpha flux distributions for a sample of Virgo spirals were mapped out in an attempt to understand the coupling between gas dynamics and star formation in spiral galaxies. A broad range of morphological types were observed (types Sab through Scd) under the hypothesis that the gas dynamics is most influential in determining the overall appearance of a spiral galaxy. Only non-barred spirals were considered so that the well-studied but complicated properties of bars and their role in inducing star formation would not be a factor. All galaxies were chosen from the Virgo cluster to eliminate uncertainties due to distance errors. Since the dynamical seat of a spiral is at its center, it was expected that the dynamics of the central region would influence global properties of the rest of the disk. This could happen through the existence or absence of an inner Lindblad resonance (according to the degree of central concentration of mass) to modulate swing amplification of spiral waves, or the persistence of an oval distortion to initiate an instability which leads to spiral structure. Author

N91-14217*# Observatoire de Paris-Meudon (France).
NEAR-INFRARED MAPPING OF SPIRAL BARRED GALAXIES
P. Gallais, D. Rouan, and F. Lacombe *In* NASA, Ames Research Center, The Interstellar Medium in External Galaxies: Summaries of Contributed Papers Jul. 1990 p 329-330 (For primary document see N91-14100 05-90)
Avail: NTIS HC/MF A19 CSCL 03B

In external galaxies, near-infrared emission originates from stellar populations, hot dust, free-free emission from H+ regions, gaseous emission, non-thermal nucleus if any. Because of the low extinction compared to the visible, infrared wavelengths are useful to probe regions obscured by dust such as central parts where starburst phenomena can occur because of the large quantity of matter. The results presented were obtained with a 32 x 32 InSb charge injection device (CID) array cooled at 4K, at the f/36 cassegrain focus of the 3m60 Canada-France-Hawaii telescope with a spatial resolution of 0.5 inches per pixel. The objects presented are spiral barred galaxies mapped at J(1.25 microns), H(1.65 microns) and K(2.2 microns). The non-axisymetric potential due to the presence of a bar induces dynamical processes leading to the confinement of matter and peculiar morphologies. Infrared imaging is used to study the link between various components. Correlations with other wavelengths ranges and 2-colors diagrams ((J-H), (H-K)) lead to the identification of star forming regions, nucleus. Maps show structures connected to the central core. The question is, are they flowing away or toward the nucleus. Observations of M83 lead to several conclusions. The star forming region, detected in the visible and the infrared cannot be very compact and must extend to the edge of the matter concentration. The general shape of the near-infrared emission and the location of radio and 10 micron peaks suggest the confinement of matter between the inner Linblad resonances localized from CO measurements about 100 and 400 pc. The distribution of color indices in the arc from southern part to the star forming region suggests an increasing amount of gas and a time evolution eventually triggered by supernova explosions. Close to the direction of the bar, a bridge-like structure connects the arc to the nucleus with peculiar color indices. Perhaps, this structure can be linked to a height velocity component seen in UV and we can attribute it to a jet and/or a matter flow along the bar toward the nucleus, fuelling it. NGC 1068 is the nearest Seyfert 2 galaxy. It has been a subject of many studies at all wavelengths. This object was mapped at J, H, K, L and M, and in polaro-imagery. Results are given. Author

N91-14218*# Mount Stromlo and Siding Spring Observatory, Canberra (Australia).
HIGH-MASS STAR FORMATION IN SOUTHERN DISK GALAXIES
Michael A. Dopita, J. R. Forster (Wild, Paul Observatory, Narrabri, Australia), and Lilia Ferrario *In* NASA, Ames Research Center, The Interstellar Medium in External Galaxies: Summaries of Contributed Papers Jul. 1990 p 331-333 (For primary document see N91-14100 05-90)
Avail: NTIS HC/MF A19 CSCL 03B

As part of a major study of the physical processes of star formation and the evolution of galactic discs, the detailed distribution of high-mass star formation within southern late-type spirals and Magellanic-type galaxies is being measured by means of narrow-band imaging in Ha and the continuum, spectroscopic studies of prominent HII regions identified in the Ha images, and by radio mapping in neutral hydrogen and the continuum. The radio mapping will be undertaken with the Southern Hemisphere's first large, multi-frequency synthesis array, the Australia Telescope. Some optical imaging and spectroscopic data has already been acquired; the optical data and some preliminary results are described. Author

N91-14219*# Washington Univ., Seattle.
STARBURST OUTFLOWS FROM NEARBY GALAXIES
William H. Waller *In* NASA, Ames Research Center, The Interstellar Medium in External Galaxies: Summaries of Contributed Papers Jul. 1990 p 334-336 (For primary document see N91-14100 05-90)
Avail: NTIS HC/MF A19 CSCL 03B

Starburst outflows from NGC 5461, 1569 and M82 are discussed. The Sc I galaxy, M101, is reknowned for the kpc-size superassociations of star clusters and HII regions that dominate its spiral arms. NGC 5461 is one of the brightest of these superassociations, rivaling the Large Magellanic Cloud in H alpha luminosity. The NGC 5461 superassociation is dominated by a single unresolved HII region of outstanding luminosity (approx. 1000 Orion nebulae). Detailed examination of corresponding continuum images indicates that only the southern plume has any sort of stellar counterpart. The other plumes are clearly diffuse with no underlying hot stars. An image of NGC 1569 is discussed. Besides showing the peculiar arm noted by Zwicky (1971) and the filamentary extensions to the North and South (as noted by Hodge 1974), this image also reveals two arc-like features of diffuse ionized gas to the South. Both arcs are concentric with the bright center of the galaxy - where the super star clusters, A and B are located. The inner arc (Arc 1) appears to follow the same curve as the SW arm thus suggesting that the two features represent limb-brightened fragments of vast superbubble that was blown out by a central starburst sometime in the past. As the classic starburst galaxy, M82 displays all the luminous hallmarks of intense high-mass star formation and outflow activity. The diffuse H alpha and x ray emitting gas along the minor axis provides especially good evidence for a bipolar outflow of hot gas which is shock heating the swept-up interstellar medium (ISM) to temperatures of approx. 10(exp 4) K. An image shows the H alpha emission within the disk and along the minor axis. Another image shows the same field in the light of near-infrared. Both figures are based on charge coupled device images taken with the McGraw-Hill 1.3 m telescope (Waller 1989). The longer wavelength emission clearly shows a more extended morphology along the major axis. The morphological discrepancy is most likely due to the greater obscuration by dust suffered by the H alpha photons. A third image shows the map of visual extinction that researchers derive from a pixel-by-pixel comparison of the (SIII) and H alpha fluxes. The greatest extinctions are evident along an arc that includes two especially obscured regions on opposite sides of the bursting nucleus. Author

N91-14220*# California Univ., Berkeley.
DENSE GAS AND HII REGIONS IN THE STARBURST GALAXY NGC 253
J. E. Carlstrom, James M. Jackson, Paul T. P. Ho, and J. L. Turner (California Univ., Los Angeles.) *In* NASA, Ames Research Center, The Interstellar Medium in External Galaxies: Summaries of Contributed Papers Jul. 1990 p 337-339 (For primary document see N91-14100 05-90)
(Grant NSF AST-87-14721)
Avail: NTIS HC/MF A19 CSCL 03B

The energetic activity in the nuclear barred region of NGC 253 is attributable to a burst of star formation. NGC 253 is in many ways a twin of the prototypical starburst galaxy M82; the strong non-thermal radio continuum, high far-infrared luminosity, and bright molecular emission of the central 1 Kpc parallel the morphology of the M82 starburst. Furthermore, the filamentary low ionization optical emission and extended x ray emission along the minor axis in NGC 253 is similar to a scaled down version of the well developed galactic bipolar wind in M82. The infrared luminosity of NGC 253, 3(exp 10) solar luminosity, is comparable to M82 but is emitted from a smaller region (Telesco and Harper 1980). This suggests that the NGC 253 starburst may be more intense and at an earlier evolutionary stage than M82. However, the presence of a non-stellar AGN in NGC 253 may complicate the comparison (Turner and Ho, 1985). Researchers used the Hat Creek millimeter interferometer to map emission from the J = 1 to 0 transitions of HCN and HCO(+) as well as 3 mm continuum emission, toward the nuclear region of NGC 253. The HCO(+) and continuum observations are sensitive to spatial scales from 6 to 45 seconds. The 2 minute field of view comfortably includes the entire starburst region (about 40 seconds; 650 pc). Because the longer baseline HCN observations are not yet complete, they are only sensitive to spatial scales from 15 to 45 seconds.
Author

N91-14221*# National Aeronautics and Space Administration. Goddard Space Flight Center, Greenbelt, MD.
A NEAR INFRARED SPECTROSCOPIC STUDY OF THE INTERSTELLAR GAS IN THE STARBURST CORE OF M82
Dan F. Lester, John Carr, Marshall Joy, and Niall Gaffney (McDonald Observatory, Austin, TX.) *In* NASA, Ames Research Center, The Interstellar Medium in External Galaxies: Summaries of Contributed Papers Jul. 1990 p 340-342 (For primary document see N91-14100 05-90)
Avail: NTIS HC/MF A19 CSCL 03B

Researchers used the McDonald Observatory Infrared Grating Spectrometer, to complete a program of spatially resolved spectroscopy of M82. The inner 300 pc of the starburst was observed with 4 inch (50 pc) resolution. Complete J, H and K band spectra with resolution 0.0035 micron (lambda/delta lambda=620 at K) were measured at the near-infrared nucleus of the galaxy. Measurements of selected spectral features including lines of FeII, HII and H2 were observed along the starburst ridge-line, so the relative distribution of the diagnostic features could be understood. This information was used to better define the extinction towards the starburst region, the excitation conditions in the gas, and to characterize the stellar populations there.
Author

N91-14222*# California Univ., Berkeley. Dept. of Astronomy.
CLUES TO GALAXY ACTIVITY FROM RICH CLUSTER SIMULATIONS
August E. Evrard *In* NASA, Ames Research Center, The Interstellar Medium in External Galaxies: Summaries of Contributed Papers Jul. 1990 p 343-345 (For primary document see N91-14100 05-90)
Avail: NTIS HC/MF A19 CSCL 03B

New simulations of rich cluster evolution are used to evaluate the first infall hypothesis of Gunn and Dressler - the idea that the enhanced fraction of active galaxies seen in high redshift clusters is due to a one-time burst of star formation triggered by the rapid rise in external pressure as a galaxy plows into the hot intracluster medium (ICM). Using three-dimensional simulations which contain both baryonic gas and collisionless dark material, local static pressure histories for test orbits of galaxies are generated and a simple trigger threshold based on dP/dt/P sub ISM is applied to define an active fraction of the population. The results lend qualitative and quantitative support to the first infall interpretation.
Author

N91-14223*# National Aeronautics and Space Administration. Marshall Space Flight Center, Huntsville, AL.
CENTRAL STAR FORMATION IN S0 GALAXIES
L. L. Dressel, R. W. OConnell (Virginia Univ., Charlottesville.), and C. M. Telesco *In* NASA, Ames Research Center, The Interstellar Medium in External Galaxies: Summaries of Contributed Papers Jul. 1990 p 346-348 (For primary document see N91-14100 05-90)
(Grant NSF AST-88-18606)
Avail: NTIS HC/MF A19 CSCL 03B

As a class, S0 galaxies are characterized by a lack of resolved bright stars in the disk. However, several lines of evidence support the hypothesis that a high rate of star formation is occurring at the centers of some S0 galaxies. Many of the warmest, most powerful far infrared sources in nearby bright galaxies occur in S0 galaxies. (Dressel 1988, Ap. J., 329, L69). The ratios of radio continuum flux to far infrared flux for these S0 galaxies are comparable to the ratios found for spiral galaxy disks and for star-burst galaxies. Very Large Array (VLA) maps of some of these S0 galaxies show that the radio continuum emission originates in the central few kiloparsecs. It is diffuse or clumpy, unlike the

radio sources in active S0 galaxies, which are either extremely compact or have jet-lobe structures. Imaging of some of these galaxies at 10.8 microns shows that the infrared emission is also centrally concentrated. Many of the infrared-powerful S0 galaxies are Markarian galaxies. In only one case in this sample is the powerful ultraviolet emission known to be generated by a Seyfert nucleus. Optical spectra of the central few kiloparsecs of these S0 galaxies generally show deep Balmer absorption lines characteristic of A stars, and H beta emission suggestive of gas heated by O stars. A key question to our understanding of these galaxies is whether they really are S0 galaxies, or at least would have been recognized as S0 galaxies before the episode of central star formation began. Some of Nilson's classifications (used here) have been confirmed by Sandage or de Vaucouleurs and collaborators from better plates; some of the galaxies may be misclassified Sa galaxies (the most frequent hosts of central star formation); some are apparently difficult to classify because of mixed characteristics, faint non-S0 features, or peculiarities. More optical imaging is needed to characterize the host galaxies and to study the evolution of their star-forming regions. Author

N91-14224*# National Radio Astronomy Observatory, Socorro, NM.

CURRENT STAR FORMATION IN S0 GALAXIES: NGC 4710

J. M. Wrobel *In* NASA, Ames Research Center, The Interstellar Medium in External Galaxies: Summaries of Contributed Papers Jul. 1990 p 349-351 (For primary document see N91-14100 05-90)

Avail: NTIS HC/MF A19 CSCL 03B

Elliptical (E) and lenticular (S0) galaxies lack the substantial interstellar medium (ISM) found in the star-forming spiral galaxies. However, significant numbers of E and S0 galaxies are known to contain detectable amounts of interstellar matter (e.g., Jura 1988). Thus, it is worth investigating whether these galaxies are currently able to form stars from their ISM, or whether they should be consigned to the dustbin of inert objects (Thronson and Bally 1987). The results strongly imply that current star formation is responsible for NGC 4710's far infrared and radio continuum properties. If this is indeed the case, then one expects this star formation to be fueled by molecular gas, which is presumably dominated by H2 and can be traced by the CO-12 J=1 to 0 line. Both Kenney and Young (1988) and Sage and Wrobel (1989) have detected such an emission line from NGC 4710, and infer the presence of more than 10(exp 8) solar mass of H2. The origin of the molecular gas in NGC 4710 remains a mystery. The galaxy is very deficient in HI (Kenney and Young, in preparation), suggesting that it originally was a spiral galaxy from which the outer, mainly atomic, gas was stripped by the ram pressure of the Virgo Cluster's intracluster medium, leaving only a central interstellar medium (ISM) rich in molecular gas. Alternatively, the CO may have originated via stellar mass loss with subsequent cooling, cooling flows, or capture from a gas-rich companion. Information on the morphology and kinematics of the CO can be compared with that of the galaxy's other gases and stars to distinguish among these various possible origins for the molecular gas. Major axis CO mapping with single dishes indicate an unresolved source. Thus, a millimeter array is currently being used to image NGC 4710 in CO to provide the needed morphological and kinematical data. Author

N91-14225*# Princeton Univ. Observatory, NJ.

INTERPRETING THE CONVERGENCE OF LYMAN SERIES ABSORPTION LINES

Edward B. Jenkins *In* NASA, Ames Research Center, The Interstellar Medium in External Galaxies: Summaries of Contributed Papers Jul. 1990 p 353-355 (For primary document see N91-14100 05-90)

(Grant NAG5-616)

Avail: NTIS HC/MF A19 CSCL 03B

Spectra of quasars at high z often show absorption at the Lyman limit from intervening gas systems at intermediate z having N(H) approx. greater than 10(exp 7) cm(-2). In some circumstances, N(H) can be determined by measuring the strength of the Lyman limit absorption or the damping wings of Lyman - alpha. With a spectrum taken at low wavelength resolution, say, lambda/delta lambda approx. 10(exp 3), it is usually not possible to distinguish individual Lyman series lines near the limit, yet one can still discern how rapidly the average intensity drops off as the limit is approached from the long wavelength side. The purpose here is to point out the information which is available from measurements of this series convergence. Author

N91-14226*# National Radio Astronomy Observatory, Socorro, NM.

RADIO CONTINUUM OBSERVATIONS OF THE QUASAR-GALAXY PAIR 3C 232-NGC 3067

Eric Haxthausen, Chris Carilli, and Jacqueline H. vanGorkom *In* NASA, Ames Research Center, The Interstellar Medium in External Galaxies: Summaries of Contributed Papers Jul. 1990 p 356-358 (For primary document see N91-14100 05-90)

Avail: NTIS HC/MF A19 CSCL 03B

The quasar-galaxy pair 3C 232-NGC 3067 is well known to show absorption by gas associated with the foreground galaxy against the background quasar (see Stocke et al. this volume). Observations by Carilli, van Gorkom, and Stocke (Nature 338, 134, 1989) found that the absorbing gas is located in a long tail of gas which extends from the galaxy toward the quasar and beyond (in projection). Though the HI observations of NGC 3067 indicate that the galaxy has been severely disturbed, there is no obvious candidate in the field which could cause such a disturbance, leading to the conclusion that the system has undergone a recent merger. The radio continuum observations of this system were designed to study the nature of this highly disturbed galaxy. New continuum observations confirm the notion that NGC 3067 is a highly disturbed system, and, in particular, the notion that the western half of the galaxy extends only 1/2 as far in radius as the eastern half. This disturbance must have occurred recently, since the galactic rotation would smooth out the observed asymmetry in about 10(exp 8) years. Researchers are left with the problem that there are no obvious candidates which could have caused such a disturbance. Author

N91-14227*# Colorado Univ., Boulder. Center for Astrophysics and Space Astronomy.

PROBING THE INTERSTELLAR MEDIUM OF EXTERNAL GALAXIES USING QUASAR ABSORTION LINES: THE 3C 232/NGC 3067 SYSTEM

John T. Stocke, James Case, Megan Donahue, J. Michael Shull, and Theodore P. Snow *In* NASA, Ames Research Center, The Interstellar Medium in External Galaxies: Summaries of Contributed Papers Jul. 1990 p 359-361 (For primary document see N91-14100 05-90)

Avail: NTIS HC/MF A19 CSCL 03B

Quasar absorption lines offer unique opportunities to probe the interstellar medium of external galaxies. Researchers present new optical and UV absorption line spectroscopy of the quasar 3C232 (z=0.55) revealing new detail in the foreground absorption system due to the bright, spiral galaxy NGC 3067 (cz=1420 km/s). Specifically, the spectra show evidence for two and possibly three separate absorption components in CaII and Na I spanning approx. 150 km/s. The original HI detection of Haschick and Burke (1975) corresponds to the strongest of these metal systems which exhibits doublet ratios consistent with saturation in both CaII and Na I. Due to the recent detection in HI emission of a tidal tail or finger of HI extending from the western edge of NGC 3067 through the position of 3C 232 (Carilli, van Gorkom and Stocke, 1989), the morphology of the HI absorber is now known and is not either a warped disk nor a spherical halo as had been proposed. New deep continuum and H alpha imaging provides a sensitive upper limit on the the ionizing continuum impinging upon this cloud (and thus a limit on the intensity of the extragalactic ionizing radiation field). Together with the observed UV spectrum of 3C 232, the optical emission line ratios and the deep H alpha imaging set a minimum distance between the quasar and the HI cloud disregarding redshift information. This limit strains the non-cosmological redshift interpretation for 3C 232 -- and this

quasar is one of the original 5 3C quasars found to be too close to NGC galaxies as if by chance (Burbidge, Burbidge, Solomon and Strittmatter, 1972). Author

N91-14228*# California Univ., San Diego. Center for Astrophysics and Space Sciences.
DETECTION OF A z=0.0515, 0.0522 ABSORPTION SYSTEM IN THE QSO S4 0248+430 DUE TO AN INTERVENING GALAXY
Donna S. Womble, Vesa T. Junkkarinen, Ross D. Cohen, and E. Margaret Burbidge *In* NASA, Ames Research Center, The Interstellar Medium in External Galaxies: Summaries of Contributed Papers Jul. 1990 p 362-364 (For primary document see N91-14100 05-90)
(Contract NAS5-29293)
Avail: NTIS HC/MF A19 CSCL 03B

In some of the few cases where the line of sight to a Quasi-Stellar Object (QSO) passes near a galaxy, the galaxy redshift is almost identical to an absorption redshift in the spectrum of the QSO. Although these relatively low redshift QSO-galaxy pairs may not be typical of the majority of the narrow heavy-element QSO absorption systems, they provide a direct measure of column densities in the outer parts of galaxies and some limits on the relative abundances of the gas. Observations are presented here of the QSO S4 0248+430 and a nearby anonymous galaxy (Kuhr 1977). The 14 second separation of the line of sight to the QSO (z sub e = 1.316) and the z=0.052 spiral galaxy, (a projected separation of 20 kpc ((h sub o = 50, q sub o = 0)), makes this a particularly suitable pair for probing the extent and content of gas in the galaxy. Low resolution (6A full width half maximum), long slit charge coupled device (CCD) spectra show strong CA II H and K lines in absorption at the redshift of the galaxy (Junkkarinen 1987). Higher resolution spectra showing both Ca II H and K and Na I D1 and D2 in absorption and direct images are reported here. Author

N91-14229*# Texas Univ., Austin.
HIGH SPATIAL RESOLUTION STUDIES OF GALAXIES IN THE FAR IR: OBSERVATIONS WITH THE KAO, AND THE PROMISE OF SOFIA
Dan F. Lester and P. M. Harvey *In* NASA, Ames Research Center, The Interstellar Medium in External Galaxies: Summaries of Contributed Papers Jul. 1990 p 365-367 (For primary document see N91-14100 05-90)
Avail: NTIS HC/MF A19 CSCL 03B

NASA, in collaboration with the West German Science Ministry (BMFT), plans a larger airborne telescope as a successor to the Kuipper Airborne Observatory (KAO) that will achieve these goals. The Stratospheric Observatory for Infrared Astronomy (SOFIA) is entering the final stages of Phase B review with targeted new start early in the next decade. SOFIA is a 2.7 m diameter telescope that is carried in a Boeing 747SP. In addition to having 3 times the spatial resolution of the KAO, and 10 times the light gathering power, it will incorporate improvements over the KAO in lower optical emissivity and better telescope tracking stability. The thin primary mirror will equilibrate quickly to ambient temperature at an altitude which, accompanied by airflow improvements across the telescope cavity, will result in better image quality. The sensitivity of SOFIA will allow us to see a large number of typical bright galactic HII regions in local group galaxies. The spatial resolution of 8 seconds (full width half maximum Airy disk) at 100 microns will allow these regions to be measured independently, if they are distributed similarly to those in our own galaxy. At this spatial resolution, the disks of normal galaxies will be easily resolved out to distances of several hundred Mpc. This portion of space includes many of the superluminous galaxies discovered by the Infrared Astronomy Satellite (IRAS), and this spatial scale is relevant for studies of the morphology of regions of interaction among the majority of these galaxies that are members of colliding pairs. Author

N91-14230*# Max-Planck-Inst. fuer Extraterrestrische Physik, Garching (Germany, F.R.).
HIGH ANGULAR RESOLUTION mm- AND SUBmm-OBSERVATIONS OF DENSE MOLECULAR GAS IN M82
W. Wild, Andreas Eckart, Reinhard Genzel, Andrew I. Harris, James M. Jackson, D. T. Jaffe, J. B. Lugten (Hawaii Univ., Honolulu.), and J. Stutzki *In* NASA, Ames Research Center, The Interstellar Medium in External Galaxies: Summaries of Contributed Papers Jul. 1990 p 368-370 (For primary document see N91-14100 05-90)
Avail: NTIS HC/MF A19 CSCL 03B

Researchers observed CO(7-6), CO(3-2), HCN(3-2) and HCO+(3-2) line emission toward the starburst nucleus of M82 and have obtained an upper limit to H13CN(3-2). These are the first observations of the CO(7-6), HCN(3-2) and HCO+(3-2) lines in any extragalactic source. Researchers took the CO(7-6) spectrum in January 1988 at the Infrared Telescope Facility (IRTF) with the Max Planck Institute for Extraterrestrial Physics/Univ. of California, Berkeley 800 GHz Heterodyne Receiver. In March 1989 researchers used the Institute for Radio Astronomy in the Millimeter range (IRAM) 30 m telescope to observe the CO(3-2) line with the new MPE 350 GHz Superconductor Insulator Superconductor (SIS) receiver and the HCN(3-2) and HCO+(3-2) lines with the (IRAM) 230 GHz SIS receiver (beam 12' FWHM, Blundell et al. 1988). The observational parameters are summarized. Author

N91-14231*# Ecole Normale Superieure, Paris (France).
THE MOLECULAR SPIRAL ARMS OF NGC 6946
F. Casoli, F. Clausset, F. Viallefond, F. Combes, and F. Boulanger *In* NASA, Ames Research Center, The Interstellar Medium in External Galaxies: Summaries of Contributed Papers Jul. 1990 p 371-372 (For primary document see N91-14100 05-90)
Avail: NTIS HC/MF A19 CSCL 03B

High resolution observations of molecules in external galaxies are essential to understanding physical processes leading to the formation of stars. One question is whether there is a spiral structure in the molecular gas, but it was not possible to resolve the spiral arms of external galaxies until the advent of large millimeter-wave telescopes. With the Institute for Radio Astronomy in the Millimeter Range (IRAM) 30 m telescope, researchers are carrying through the mapping of NGC 6946 in the CO-12(1-0) and (2-1) lines. This galaxy is a large, gas-rich Scd spiral with a strong star formation activity. NGC 6946 is well studied at radio and optical wavelengths, so that it is possible to compare the location of the spiral arms tracers: HI ridge, HII regions and molecular clouds. The disk CO emission is very contrasted (no lines for some positions, 1 K in CO(1-0) for some others) and correlated with the optical spiral arms: this clearly shows up in a figure which presents superimposed contours of CO(2-1) integrated emissivity and of H alpha line emission. The agreement is very good, and there is no displacement across the arm between the CO, HI and H alpha ridges of emission. The arms are barely resolved by the 23 inch beam and the molecular contrast averaged over the map is about 4. The CO(2-1) maxima are closer to the position of the HII regions than those of CO(1-0), which could be due to variations of excitation conditions. The CO excitation in the disk of NGC 6946 is low: when all data are convolved to the same resolution of 23 inches the CO(2-1) lines are about 0.45 times fainter than the CO(1-0) ones, while in the nucleus they have roughly the same intensity. This suggests that in the disk of NGC 6946 most of the CO emission comes from cold optically thick gas located in cloud envelopes rather than from cloud cores. The molecular and atomic component in the observed regions of NGC 6946 seems to be organized in large gaseous complexes. Author

N91-14232*# Netherlands Foundation for Radio Astronomy, Dwingelo.
THE MOLECULAR SPIRAL ARMS OF NGC 6946
L. J. Tacconi and S. Xie (Massachusetts Univ., Amherst.) *In* NASA, Ames Research Center, The Interstellar Medium in External

Galaxies: Summaries of Contributed Papers Jul. 1990 p 373-374 (For primary document see N91-14100 05-90)
Avail: NTIS HC/MF A19 CSCL 03B

From CO-12(J=1 to 0) observations at 45 seconds resolution Tacconi and Young (1989) have found evidence for enhancements in both the CO emissivity and the massive star formation efficiency (MSFE) on optical spiral arms of the bright spiral galaxy NGC 6946. In the optically luminous and well-defined spiral arm in the NE quadrant, there are enhancements in both the H2 surface density and MSFE relative to the interarm regions. In contrast, a poorly defined arm in the SW shows no arm-interarm contrast in the MSFE. To further investigate the molecular gas content of these two spiral arms, researchers have made CO-12 J=2 to 1 and 3 to 2 observations with the James Clerk Maxwell Telescope. In the J=2 to 1 line, they made observations of the NE and SW spiral arm and interarm regions in 4 x 9 10 seconds spaced grids (36 points per grid). Because of decreased sensitivity in the J=3 to 2 line, they were limited to mapping the two arm regions in 2 x 3 10 seconds spaced grids (6 points per grid). The centers of each of the grids lie 2.4 minutes to the NE and 2.3 minutes to the SW of the nucleus of NGC 6946. With the CO J=2 to 1 data researchers are able to fully resolve the two observed spiral arms in NGC 6946. In both cases the CO emission is largely confined to the optical spiral arm regions with the peak observed T asterisk sub A being up to 4 times higher on the spiral arms than in the interarm regions. Researchers are currently estimating massive star formation efficiencies on and off the spiral arms through direct comparison of the CO maps with an H alpha image. They are also comparing the CO J=2 to 1 data with an HI map made at similar resolution. Thus, they will be able to determine structure in all components of the IS on scales of less than 20 inches.
Author

N91-14233*# Nobeyema Solar Radio Observatory (Japan).
CO MAPPING OF THE NUCLEAR REGION OF NGC 6946 AND IC 342 WITH NOBEYAMA MILLIMETER ARRAY
Sumio Ishizuki (Tokyo Univ., Japan), Ryohei Kawabe, Sachiko K. Okumura, Koh-Ichiro Morita, and Masato Ishiguro *In* NASA, Ames Research Center, The Interstellar Medium in External Galaxies: Summaries of Contributed Papers Jul. 1990 p 375-377 (For primary document see N91-14100 05-90)
Avail: NTIS HC/MF A19 CSCL 03B

CO observations of nearby galaxies with nuclear active star forming regions (and starburst galaxies) with angular resolutions around 7 seconds revealed that molecular bars with a length of a few kiloparsecs have been formed in the central regions of the galaxies. The molecular bar is interpreted as part of shock waves induced by an oval or barred potential field. By shock dissipation or dissipative cloud-cloud collisions, the molecular gas gains an infall motion and the nuclear star formation activity is fueled. But the distribution and kinematics of the molecular gas in the nuclear regions, which are sites of active star formation, remain unknown. Higher angular resolutions are needed to investigate the gas in the nuclear regions. Researchers made aperture synthesis observations of the nuclear region of the late-type spiral galaxies NGC 6946 and IC 342 with resolutions of 7.6 seconds x 4.2 seconds (P.A. = 147 deg) and 2.4 seconds x 2.3 seconds (P.A. = 149 deg), respectively. The distances to NGC 6496 and IC 342 are assumed to be 5.5 Mpc and 3.9 Mpc, respectively. Researchers have found 100-300 pc nuclear gas disk and ring inside a few kpc molecular gas bars. Researchers present the results of the observations and propose a possible mechanism of active star formation in the nuclear region.
Author

N91-14234*# Institut de Radio Astronomie Millimetrique, Grenoble (France).
CO EXCITATION IN FOUR IR LUMINOUS GALAXIES
Simon J. E. Radford, P. M. Solomon (State Univ. of New York, Stony Brook.), and Dennis Downes *In* NASA, Ames Research Center, The Interstellar Medium in External Galaxies: Summaries of Contributed Papers Jul. 1990 p 378-380 (For primary document see N91-14100 05-90)
Avail: NTIS HC/MF A19 CSCL 03B

The correlation between the CO and far infrared luminosities of spiral galaxies is well established. The luminosity ration, L sub FIR/L sub CO in IR luminous active galaxies is, however, systematically five to ten times higher than in ordinary spirals and molecular clouds in our Galaxy. Furthermore, the masses of molecular hydrogen in luminous galaxies are large, M (H2) approx. equals 10(exp 10) solar magnitude, which indicates the observed luminosity ratios are due to an excess of infrared output, rather than a deficiency of molecular gas. These large amounts of molecular gas may fuel luminous galaxies through either star formation or nuclear activity. This interpretation rests on applying the M (H2)/L sub CO ratio calibrated in our Galaxy to galaxies with strikingly different luminosity ratios. But are the physical conditions of the molecular gas different in galaxies with different luminosity ratios. And, if so, does the proportionality between CO and H2 also vary among galaxies. To investigate these questions researchers observed CO (2 to 1) and (1 to 0) emission from four luminous galaxies with the Institute for Radio Astronomy in the Millimeter range (IRAM) 30 m telescope. Researchers conclude that most of the CO emission from these Arp 193, Arp 220, and Mrk 231 arises in regions with moderate ambient densities similar to the clouds in the Milky Way molecular ring. The emission is neither from dense hot cloud cores nor from the cold low density gas characteristic of the envelopes of dark clouds.
Author

N91-14235*# Instituto de Radioastronomia, Granada (Spain).
CS IN NEARBY GALAXIES: DISTRIBUTION, KINEMATICS, AND MULTILEVEL STUDIES
R. Mauersberger and Christian Henkel (Max-Planck-Inst. fuer Radioastronomie, Bonn, Germany, F.R.) *In* NASA, Ames Research Center, The Interstellar Medium in External Galaxies: Summaries of Contributed Papers Jul. 1990 p 381-383 (For primary document see N91-14100 05-90)
Avail: NTIS HC/MF A19 CSCL 03B

As a result of observations at the Institute for Radio Astronomy in the Millimeter Range (IRAM) 30-m telescope, maps of the distribution of the J = 2-1 transition of CS toward the galaxies IC 342 and NGC 253 are presented. The distribution of the CS emission from NGC 253 is consistent with the CO 1-0 line. The distribution of the CS emission from IC 342, however, resembles more that seen in the CO 3-2 line. For the first time, the detection of the isotopic substitution C-34S is reported toward an external galaxy: The C-34S 2-1 line has been detected toward NGC 253 and M 82 and the C-34S line has been detected tentatively toward M 82. Also for the first time, extragalactic CS has been observed in the 3-2 (toward NGC 253, IC 342 and M 82) and 5-4 (NGC 253 and IC 342) transitions.
Author

N91-14236*# Max-Planck-Inst. fuer Extraterrestrische Physik, Garching (Germany, F.R.).
SPATIAL VARIATION OF THE PHYSICAL CONDITIONS OF MOLECULAR GAS IN GALAXIES
James M. Jackson, Andreas Eckart, Wolfgang Wild, Reinhard Genzel, Andrew I. Harris, Dennis Downes, D. T. Jaffe, and Paul T. P. Ho (Smithsonian Astrophysical Observatory, Cambridge, MA.) *In* NASA, Ames Research Center, The Interstellar Medium in External Galaxies: Summaries of Contributed Papers Jul. 1990 p 384-385 (For primary document see N91-14100 05-90)
Avail: NTIS HC/MF A19 CSCL 03B

Multi-line studies of CO-12, CO-13, C-18O, HCN, and HCO(+) at 3 mm, 1.3 mm, and 0.8 mm using the Institute for Radio Astronomy in the Millimeter range (IRAM) 30 m telescope, with the IRAM superconductor insulator superconductor (SIS) receivers and the Max Planck Institute for External Physics (MPE) 350 GHz SIS receiver, show that the densities and temperatures of molecular gas in external galaxies change significantly with position. CO-12 measures the densities and temperature of diffuse interclump molecular gas, but not the bulk of the molecular gas. Simple one-component models, with or without external heating, cannot account for the weakness of the CO-12 J = 3 to 2 line relative to J = 2 to 1 and J = 1 to 0. CO-12 does not trace the bulk of the molecular gas, and optical depth effects obviate a

straightforward interpretation of CO-12 data. Instead, researchers turned to the optically thin CO isotopes and other molecular species. Isotopic CO lines measure the bulk of the molecular gas, and HCN and HCO(+) pick out denser regions. Researchers find a warm ridge of gas in IC 342 (Eckart et al. 1989), denser gas in the starburst nucleus of IC 342, and a possible hot-spot in NGC 2903. In IC 342, NGC 2146, and NGC 6764, the CO-13 J = 2 to 1 line is subthermally populated, implying gas densities less than or equal to 10(exp 4) cm(-3). Author

N91-14237*# Max-Planck-Inst. fuer Radioastronomie, Bonn (Germany, F.R.).
DETECTION OF CO EMISSION IN HYDRA 1 CLUSTER GALAXIES
W. K. Huchtmeier *In* NASA, Ames Research Center, The Interstellar Medium in External Galaxies: Summaries of Contributed Papers Jul. 1990 p 386-388 (For primary document see N91-14100 05-90)
Avail: NTIS HC/MF A19 CSCL 03B

A survey of bright Hydra cluster spiral galaxies for the CO(1-0) transition at 115 GHz was performed with the 15m Swedish-ESO submillimeter telescope (SEST). Five out of 15 galaxies observed have been detected in the CO(1-0) line. The largest spiral galaxy in the cluster, NGC 3312, got more CO than any spiral of the Virgo cluster. This Sa-type galaxy is optically largely distorted and disrupted on one side. It is a good candidate for ram pressure stripping while passing through the cluster's central region. A comparison with global CO properties of Virgo cluster spirals shows a relatively good agreement with the detected Hydra cluster galaxies. Author

N91-14238*# Mullard Radio Astronomy Observatory, Cambridge (England).
NON-STELLER LIGHT FROM HIGH-REDSHIFT RADIOGALAXIES
Steve Rawlings and Stephen A. Eales (Space Telescope Science Inst., Baltimore, MD.) *In* NASA, Ames Research Center, The Interstellar Medium in External Galaxies: Summaries of Contributed Papers Jul. 1990 p 389-391 (For primary document see N91-14100 05-90)
Avail: NTIS HC/MF A19 CSCL 03B

With the aid of a new IRCAM image of 3C356, researchers question the common assumption that radiosource-stimulated starbursts are responsible for the extended optical emission aligned with radio structures in high-redshift radiogalaxies. They propose an alternative model in which the radiation from a hidden luminous quasar is beamed along the radio axis and illuminates dense clumps of cool gas to produce both extended narrow emission line regions and, by Thomson scattering, extended optical continua. Simple observational tests of this model are possible and necessary if we are to continue to accept that the color, magnitude and shape evolution of radiogalaxies are controlled by the active evolution of stellar populations. Author

N91-14239*# Kapteyn Astronomical Lab., Groningen (Netherlands).
CO DISTRIBUTION IN SOUTHERN S0 GALAXIES
Hugo vanWoerden and Linda Tacconi (Netherlands Foundation for Radio Astronomy, Dwingelo.) *In* NASA, Ames Research Center, The Interstellar Medium in External Galaxies: Summaries of Contributed Papers Jul. 1990 p 392-394 (For primary document see N91-14100 05-90)
Avail: NTIS HC/MF A19 CSCL 03B

With the Swedish ESO Submillimeter Telescope (SEST), researchers observed 7 S0 galaxies at 2.6 mm, and detected CO emission in five. Observing four offset positions per galaxy at greater than or equal to 40 seconds from the center, they find significantly extended CO emission in almost all cases. The (lower limits to) H2 masses of several times 10(exp 8) solar magnitude amount to 0.2-0.3 times the HI mass in 4 or 5 galaxies. Author

N91-14240*# Rice Univ., Houston, TX.
THE HAWAII IMAGING FABRY-PEROT INTERFEROMETER (HIFI)
Jonathan Bland, Gerald Cecil, and Brent Tully (Hawaii Univ., Honolulu.) *In* NASA, Ames Research Center, The Interstellar Medium in External Galaxies: Summaries of Contributed Papers Jul. 1990 p 395-396 (For primary document see N91-14100 05-90)
(Contract NAS8-32902; NSF AST-88-18900)
Avail: NTIS HC/MF A19 CSCL 03B

At Mauna Kea Observatory, researchers conducted optical, imaging spectrophotometric studies of selected active galaxies using both the Canada-France-Hawaii 3.6m and University of Hawaii 2.2m telecopes (Tully, Bland and Cecil 1988). To maximize spatial resolution, researchers select galaxies independent of luminosity but known to possess interesting morphologies or high-velocity, extranuclear ionized gas (Walker 1968; Rubin and Ford 1968). They study both the large-scale patterns produced in IR-luminous, starburst systems (e.g., M82, NGC 253, NGC 6240) and those with compact, but spatially extended, circumnuclear, narrow line regions (e.g., M51, NGC 1068, NGC 4151). Current studies are restricted to the optical (SII), (NII) and (OIII) lines and the brightest Balmer recombination lines. These lines are, in principle, sufficient to constrain the dynamical structure and dominant excitation mechanism of the ionized component. Author

N91-14241 Maine Univ., Orono.
A COMBINED N-BODY AND HYDRODYNAMIC CODE FOR MODELING DISK GALAXIES Ph.D. Thesis
Michael Christopher Schroeder 1989 297 p
Avail: Univ. Microfilms Order No. DA9023869

A combined N-body and hydrodynamic computer code for the modeling of two dimensional galaxies is described. The N-body portion of the code is used to calculate the motion of the particle component of a galaxy, while the hydrodynamics portion of the code is used to follow the motion and evolution of the fluid component. A complete description of the numerical methods used for each portion of the code is given. Additionally, the proof tests of the separate and combined portions of the code are presented and discussed. Finally, a discussion of the topics researched with the code and results obtained is presented. These include: the measurement of stellar relaxation times in disk galaxy simulations; the effects of two-armed spiral perturbations on stable axisymmetric disks; the effects of the inclusion of an instellar medium (ISM) on the stability of disk galaxies; and the effect of the inclusion of stellar evolution on disk galaxy simulations. Author

N91-14242 Colorado Univ., Boulder.
THE EVOLUTION OF COMETS AND THE DETECTABILITY OF EXTRA-SOLAR OORT CLOUDS Ph.D. Thesis
Sol Alan Stern 1989 322 p
Avail: Univ. Microfilms Order No. DA9024872

According the standard theory, comets are natural products of solar system formation, ejected to the Oort Cloud by gravitational scattering events during the epoch of giant planet formation. Stored far from the Sun for billions of years, comets almost certainly contain a record of the events which occurred during (and perhaps even before) the epoch of planetary formation. Two themes are examined of the evolutionary processes that affect comets in the Oort Cloud, and a search for evidence of Extra-Solar Oort Clouds (ESOCs). With regard to cometary evolution in the Oort Cloud, it was found that luminous O stars and supernovae have heated the surface layers of all comets on numerous occasions to 20 to 30 K and perhaps once to 50 K. Interstellar medium (ISM) interactions blow small grains out of the Oort Clouds, and erode the upper few hundred g/cu cm of material from cometary surfaces. The findings presented contradict the standard view that comets do not undergo physical change in the Oort Cloud. A logical consequence of the intimate connection between the Oort Cloud and our planetary system is that the detection of comet clouds around other stars would strongly indicate the sites of extant extra-solar planetary systems. A search was conducted for infrared

IR emission from debris in ESOCs. After examining 17 stars using the Infrared Astronomical Satellite data base, only upper limits on ESOC emission could be set. Author

N91-14243 Colorado Univ., Boulder.
SPECTRUM FORMATION IN SN1987A Ph.D. Thesis
Yueming Xu 1989 212 p
Avail: Univ. Microfilms Order No. DA9024881

Techniques were developed for modeling the spectra at wavelengths from gamma ray to infrared that emerges from the late-time envelope of Supernova 1987A. The theory of spectrum formation was applied to infer the interior properties of SN1987A from the observed spectra. It was assumed that the late-time emission of SN1987A was powered by the gamma rays resulting from Co-56 decay. An analytic method was developed to calculate the Comptonization of gamma rays in a gas with photoabsorptions. The spectra of gamma rays and x rays was calculated for a stratified envelope model of SN1987A by use of Monte Carlo simulations. The technique for calculating the energy degradation spectrum of the fast electrons resulting from gamma ray Comptonizations were improved. The Bethe approximation was used to estimate the fractions of the fast electron energies deposited to heat, excitations, and ionization of the envelope material, and the resultant source spectrum of the line emissions was derived. The detailed properties of the scattering and line trapping were analyzed by use of the Sobolev approximation. Hydrogen is photo-ionized from the n = 2 state, which is overpopulated because of the Lyman alpha trapping. The hydrogen recombination was calculated in the Case C approximation (optically thick Lyman and Balmer lines and no direct recombination to the n = 2 state). It was found that the line trapping and the charge transfer between hydrogen and heavy elements are important processes for the ionization equilibrium of the envelope material. The calculation showed that the heavy elements must be mixed macroscopically, not microscopically, into the hydrogen-rich envelope. The emergent spectrum at the wavelengths of ultraviolet to infrared was calculated by Monte Carlo simulations and showed how photons of wavelength less than 2000 A would split, redistributing their luminosity to the wavelength range is greater than or equal to approximately 3000 A. Dissert. Abstr.

N91-14244 Minnesota Univ., Minneapolis.
THE STELLAR CONTENT OF M101 Ph.D. Thesis
Cynthia Anne Blaha 1989 245 p
Avail: Univ. Microfilms Order No. DA9019053

Photographic plates of spiral galaxy M101 were obtained through U, B, V, and R filters and scanned with the automated plate scanner. Scanner data taken with four threshold levels were reconstructed into images and matched between plates to obtain a comprehensive set of brightnesses and colors for the M101 images. Photoelectric measurements and CCD observations were made to provide the photometric calibrations transforming instrumental image diameters into apparent brightnesses. Profile information was used to separate the images into sets of foreground stars and background galaxies in the outer regions of the plates and stellar and nonstellar objects within M101. Data sets of the brightest stars in our own galaxy and the Magellanic Clouds were analyzed to determine the U, B, and V luminosity distributions and initial mass functions of these populations and were used for comparison with the M101 results. The observed apparent magnitude and color ranges of the stellar images within M101 corresponded to an evolved population of B through G supergiants with an absolute magnitude range of -8 to -10 and progenitor masses of 30 to 60 stellar mass. Many of the previously identified brightest blue supergiant candidates were classified as nonstellar and may be compact clusters or multiple systems, thus questioning their use as extragalactic distance indicators. A slight flattening in the slope of the luminosity function with increasing galactocentric distance was noted and the overall luminosity function corrected for contamination effects had a slope of 0.9 to 1.0, implying a steeper luminosity function for M101 than found in other galaxies. Crowding and saturation of images in the spiral arms prevent a complete count of the number of supergiants in M101. Dissert. Abstr.

N91-14245 Texas Univ., Austin.
PROPERTIES OF THE MAGELLANIC-TYPE GALAXIES Ph.D. Thesis
Stephen Charles Odewahn 1989 577 p
Avail: Univ. Microfilms Order No. DA9016945

Studies of the photometric, kinematic, and dynamical properties of the Magellanic type galaxies are undertaken in order to ascertain the systematic properties of the late stages of spiral structure in the Hubble sequence. Statistical analysis of large optical and radio data sets, contained in the newly completed Third Reference Catalog of Bright Galaxies, as well as a general survey of the largest Magellanic type galaxies on the Palomar and UK Schmidt Photographic Surveys, are used to determine properties such as mean color, frequency of bar formation, intrinsic shape, and the abundance of physically associated neighbor galaxies. Detailed photometric studies of a few select Magellanic galaxies are carried out using photographic and new-technology CCD area detectors. Studies of these same systems are conducted using the technique of Fabry-Perot interferometry in order to map the two dimensional ionized gas velocity fields. These galaxies are predominantly barred, with the center of the stellar bar often displaced from the photometric center of the galaxy disk. The dynamical consequences of such an asymmetric mass distribution are modeled using a simple prolate spheroid and exponential disk potential field and compared directly with observational data from the photometric and kinematic investigations. A systematic search is made for matter trapping and gas streaming motions caused by the bar and its associated stable Lagrangian points. Finally, a series of recent theoretical studies, as well as a set of original N-body numerical calculations, are used to explore the origin and dynamical evolution of these intriguing galaxies. Dissert. Abstr.

N91-14246 Massachusetts Univ., Amherst.
MOLECULAR OUTFLOWS IN THE L1641 REGION OF ORION Ph.D. Thesis
James Arthur Morgan 1990 207 p
Avail: Univ. Microfilms Order No. DA9022724

Little is known about the interaction between molecular outflows associated with young stellar objects and the parent molecular cloud that produced them. This is because molecular outflows are a recently discovered phenomenon and, so, have not had their global properties studied in great detail and molecular clouds were not mapped to sufficiently high spatial resolution to resolve the interaction. The interaction between molecular outflows and the L1641 molecular cloud is addressed by both identifying and mapping all the molecular outflows as well as the detailed structure of the cloud. Candidate molecular outflows were found from single point 12-CO observations of young stellar objects identified from the IRAS survey data. The candidate sources were then mapped to confirm their molecular outflow nature. From these maps, molecular outflow characteristics such as their morphology, orientation, and energetics were determined. In addition, the Orion molecular cloud was mapped to compare directly with the molecular outflows. The molecular outflows identified were found to have rising infrared spectra, radio continuum emission that suggests a stellar wind or optically thick H II region, and molecular line strengths that indicate that they are embedded within a very dense environment. The lack of an optical counterpart for many molecular outflows suggests that they occur at the earliest stages of stellar evolution. The lack of an optical counterpart for many molecular outflows suggest that they occur at the earliest stages of stellar evolution. The orientations of the molecular outflows appear to lie in no preferred direction and they have shapes that indicate that the molecular cloud is responsible for determining their direction and collimation. Author

N91-14247 Columbia Univ., New York, NY.
RELATIVISTIC EFFECTS IN MILLISECOND PULSARS AND ACTIVE GALACTIC NUCLEI Ph.D. Thesis

Kai-You Chen 1989 99 p
Avail: Univ. Microfilms Order No. DA9020504

Rapidly rotating neutron stars and the accretion disks around super-massive black holes at the nuclei of active galaxies were studied relativistically. The light curves of radiation from antipodal caps of rapidly rotating neutron stars were calculated with and without gravity. The light curves are found to depend strongly on the rotation speed and on the emission spectrum, and could become quite sharp. Gravity generally flattens the light curves; however, it does so less for rapidly rotating neutrons stars and can never flatten them enough to explain the absence of pulsations from low-mass x ray binary (LMXB's), the putative progenitors of millisecond pulsars. Spectral analysis of radiation from rapidly rotating neutron stars must take rotation effects into account; in LMXB's, pulses are expected to be sharpest for the hardest x rays. Line profiles for a Keplerian disk are calcuated, including relativistic effects. An excellent fit was found between the resulting double-peaked, asymmetric profiles and the observed H alpha line of an active galactic nucleus (AGN), Arp 102B. It was concluded that the line profile of Arp 102B shows the most convincing direct kinematic evidence for rotation in any AGN. A self-consistent model of a line-emitting accretion disk is presented which accounts for the observed properties of a small class of AGN's. The prime objects are Arp 102B and 3C 390.3, broad-line radio galaxies with double-peaked emission lines. The combination of ion torus and thin disk accounts for several additional properties of Arp 102B and 3C 390.3. The far-infrared peaks at 25 microns are in agreement with the predicted synchrotron self-absorption turnover for an ion torus. The outer radius of the hot ion torus, which is identified with the measured inner radius of the line-emitting thin disk, is consistent with the theoretical location of the onset of the Lightman-Eardley instability. Dissert. Abstr.

N91-14248 California Univ., Berkeley.
THE PHOTOEVAPORATION OF INTERSTELLAR CLOUDS Ph.D. Thesis
Frank Bertoldi 1989 215 p
Avail: Univ. Microfilms Order No. DA9028741

The dynamics of the photoevaporation of interstellar clouds and its consequences for the structure and evolution of H II regions are studied. An approximate analytical solution for the evolution of photoevaporating clouds is derived under the realistic assumption of axisymmetry. The effects of magnetic fields are taken into account in an approximate way. The evolution of a neutral cloud subjected to the ionizing radiation of an OB star has two distinct stages. When a cloud is first exposed to the radiation, the increase in pressure due to the ionization at the surface of the cloud leads to a radiation-driven implosion: an ionization front drives a shock into the cloud, ionizes part of it and compresses the remaining into a dense globule. The initial implosion is followed by an equilibrium cometary stage, in which the cloud maintains a semistationary comet-shaped configuration; it slowly evaporates while accelerating away from the ionizing star until the cloud has been completely ionized, reaches the edge of the H II region, or dies. Expressions are derived for the cloud mass-loss rate and acceleration. To investigate the effect of the cloud photoevaporation on the structure of H II regions, the evolution of an ensemble of clouds of a given mass distribution is studied. It is shown that the compressive effect of the ionizing radiation can induce star formation in clouds that were initially gravitationally stable, both for thermally and magnetically supported clouds.
Dissert. Abstr.

N91-14249 Catholic Univ. of America, Washington, DC.
IONIZATION IN THE LOCAL INTERSTELLAR AND INTERGALACTIC MEDIA Ph.D. Thesis
Kwang-Ping Cheng 1990 104 p
Avail: Univ. Microfilms Order No. DA9027626

Detailed photoionization calculations for the local interstellar medium (LISM) and the intergalactic medium (IGM) are presented. Constraints in the LISM are imposed by H I column density derived from IUE and Copernicus data toward nearby B stars and hot white dwarfs. The EUV radiation field is modeled including contributions from discrete stellar sources and from a thermal bremsstrahlung-radiative recombination spectrum emitted from the surrounding 10(exp 6) K coronal substrate. Lower limits to the fractional ionization of hydrogen and helium of 0.17 and 0.30 respectively are established. The derived limits have important implications for the interpretation of the H I and He I backscattering results. The high He ionization fraction results primarily from very strong line emission below 500 A originating in the surrounding coronal substrate while the H ionization is dominated by the EUV radiation from the discrete stellar sources. The dual effects of thermal conduction and the EUV spectrum of the 10(exp 6) K plasma on ionization in the cloud skin are explored. The EUV radiation field and Auger ionization have insignificant effects on the resulting ionic column densities of Si IV, C IV, N V and O VI through the cloud skin. Calculations show that the abundances of these species are dominated by collisional ionization in the thermal conduction front. Because of a low charge exchange rate with hydrogen, the ionic column density ratios of N(C III)/N(C II) and N(N II)/N(N I) are dominated by the EUV radiation field in the local interstellar medium. These ratios should be important diagnostics for the EUV radiation field and serve as surrogate indicators of the interstellar He and H ionization fraction respectively. The same photoionization model is applied to the intergalactic medium. By combining calculation results with existing observation results, constraints are placed on the physical conditions in both the hot substrate and the clouds of the IGM.
Dissert. Abstr.

N91-14250# Delaware Univ., Newark.
PARTICLE THEORY AND COSMOLOGY Progress Report
1990 24 p
(Contract DE-AC02-78ER-05007)
(DE91-004189; DOE/ER-05007/27) Avail: NTIS HC/MF A03

The overall objective of the research supported by this contract is to further our understanding of the basic building blocks of matter as well as the role fundamental interactions play in cosmology and astrophysics. Astrophysical data, such as from high energy cosmic rays and large scale structure of the universe, are employed to constrain particle physics theories. Particle collisions at Tevatron and higher (SSC) energies are also under investigation. During the past year a systematic reanalysis of the correlation between solar activity and the solar neutrino flux was undertaken. The conclusion seems to be that the Homestake experimental data show a correlation at a significant level, supporting the hypothesis that the neutrino possesses a magnetic moment. A separate, but related, theoretical investigation of electromagnetic properties of elementary particles has led to the discovery of a class of models in which the neutrino is endowed with an appreciable magnetic moment while it remains small. Altogether members of the group have been co-authors of 28 papers during the grant year on topics ranging from fermion masses to the role of ultra-high energy hadronic interactions in cosmic ray physics. DOE

91 LUNAR AND PLANETARY EXPLORATION

Includes planetology; and manned and unmanned flights.
For spacecraft design or space stations see *18 Spacecraft Design, Testing and Performance.*

N91-14251*# National Aeronautics and Space Administration. Langley Research Center, Hampton, VA.
SINGLE LAUNCH LUNAR HABITAT DERIVED FROM AN NSTS EXTERNAL TANK
Charles B. King, Ansel J. Butterfield, Warren D. Hypes (Bionetics Corp., Hampton, VA.), John E. Nealy, and Lisa C. Simonsen Washington Dec. 1990 34 p
(NASA-TM-4212; L-16764; NAS 1.15:4212) Avail: NTIS HC/MF A03 CSCL 06K

A concept for using the spent external tank from a National Space Transportation System (NSTS) to derive a lunar habitat is

described. The external tank is carried into low Earth orbit where the oxygen tank-intertank subassembly is separated from the hydrogen tank, berthed to Space Station Freedom and the subassembly outfitted as a 12-person lunar habitat using extravehicular activity (EVA) and intravehicular activity (IVA). A single launch of the NSTS orbiter can place the external tank in LEO, provide orbiter astronauts for disassembly of the external tank, and transport the required subsystem hardware for outfitting the lunar habitat. An estimate of the astronauts' EVA and IVA is provided. The liquid oxygen intertank modifications utilize existing structures and openings for man access without compromising the structural integrity of the tank. The modifications include installation of living quarters, instrumentation, and an airlock. Feasibility studies of the following additional systems include micrometeoroid and radiation protection, thermal control, environmental control and life support, and propulsion. The converted lunar habitat is designed for unmanned transport and autonomous soft landing on the lunar surface without need for site preparation. Lunar regolith is used to fill the micrometeoroid shield volume for radiation protection using a conveyer. The lunar habitat concept is considered to be feasible by the year 2000 with the concurrent development of a space transfer vehicle and a lunar lander for crew changeover and resupply. Author

N91-14252*# Lunar and Planetary Inst., Houston, TX.
PROCEEDINGS OF THE MEVTV WORKSHOP ON THE EVOLUTION OF MAGMA BODIES ON MARS
P. Mouginis-Mark, ed. and J. Holloway, ed. Jan. 1990 64 p
Workshop held in San Diego, CA, 15-17 Jan. 1990
(Contract NASw-4066)
(NASA-CR-187357; NAS 1.26:187357; LPI-TR-90-04) Avail: NTIS HC/MF A04 CSCL 03B

The workshop focused on many of the diverse approaches related to the evolution of magma bodies on Mars that have been pursued during the course of the Mars Evolution of Volcanism, Tectonism, and Volatiles (MEVTV) Program. Approximately 35 scientists from the Mars volcanology, petrology, geochemistry, and modeling communities attended. Segments of the meeting concentrated of laboratory analyses and investigations of SNC meteorites, the interpretation of Viking Orbiter and Lander datasets, and the interpretation of computer codes that model volcanic and tectonic processes on Mars. Abstracts of these reports are presented. Author

N91-14253 Colorado Univ., Boulder.
THE ORIGIN AND EVOLUTION OF THE URANIAN DUST RINGS Ph.D. Thesis
Joshua Edwards Colwell 1989 179 p
Avail: Univ. Microfilms Order No. DA9024822

The numerous dust bands discovered by Voyager 2 at Uranus have lifetimes on the order of 100 years against orbital decay by exospheric drag. A system of low optical depth rings of 10 meter to 1 km sized bodies (moonlet belts) are proposed as continuing sources of the dust particles. The ring system is modeled as a Markov Chain consisting of states through which dust particle evolve with time. Physical processes included in the model are orbit decay by exospheric drag and Poynting-Robertson light drag; destruction of grains by meteoroid impact; transport of dust through the classical rings and moonlet belts; creation of dust particles from meteoroid impacts onto rings, moons, and moonlet belts; liberation of regolith material through ring and moonlet belt particle collisions; and sweepup of ejecta by ring and moonlet belt particles. The optical depth profiles for the main rings from Voyager 2 Photopolarimeter Subsystem (PPS) occultation observation are used in modeling the transport of dust through the rings. Simulations of the Uranus ring system show that this model reproduces the observed characteristics of the Uranus dust rings. The moonlet belt model is applied to the rings of Jupiter, Saturn, and Neptune, and is capable of reproducing some of the observed characteristics of those ring systems. The moonlet belt objects fit on a collisionally derived power-law size distribution with the other components of the ring moon systems. Since the rings and moonlet belts have lifetimes due to viscous spreading less than the age of the solar system, a net model of planetary rings emerges in which the rings are continually created from the disruption of small satellites by meteoroid bombardment. Dissert. Abstr.

N91-14254*# Massachusetts Inst. of Tech., Cambridge. Dept. of Earth, Atmospheric, and Planetary Sciences.
MARS TECTONICS AND VOLCANISM Final Technical Report, 1 June. 1987 - 31 May 1990
Sean C. Solomon 30 Oct. 1990 67 p
(Grants NAGw-1077; NAGw-1937)
(NASA-CR-187351; NAS 1.26:187351) Avail: NTIS HC/MF A04 CSCL 03B

The focus of this research was on three broad areas: (1) the relation between lithospheric stress in the vicinity of a growing volcano and the evolution of eruption characteristics and tectonic faulting; (2) the relation between elastic lithosphere thickness and thermal structure; and (3) a synthesis of constraints on heat flow and internal dynamics on Mars. The two reports presented are: (1) Heterogeneities in the Thickness of the Elastic Lithosphere of Mars--Constraints on Heat Flow and Internal Dynamics; and (2) State of Stress, Faulting, and Eruption Characteristics of Large Volcanoes on Mars. Author

N91-14255*# Desert Research Inst., Reno, NV. Biological Sciences Center.
EXOBIOLOGY SITE SELECTION FOR FUTURE MARS MISSIONS: MARTIAN PALEOLAKE SEDIMENTS AND TERRESTRIAL ANALOGS Final Report, 15 Nov. 1988 - 14 Nov. 1989
Robert A. Wharton, Jr. Nov. 1989 69 p
(Contract NCC2-577)
(NASA-CR-187358; NAS 1.26:187358) Avail: NTIS HC/MF A04 CSCL 03B

This research was conducted to establish the scientific framework for the exobiological study of sediments on Mars and to encourage the selection of these sedimentary deposits as sampling sites for future Mars missions. A study was completed on the Antarctic Dry Valley Lakes (terrestrial analogs of the purported Martian paleolakes) and their sediments that allowed the development of quantitative models relating environmental factors to the nature of the biological community and sediment forming processes. The publications presented include: (1) Diversity of micro-fungi isolated in an Antarctic dry valley; (2) Lake Hoare, Antarctica--sedimentation through a thick perennial ice cover; (3) The possibility of life on Mars during a water-rich past; (4) An Antarctic research outpost as a model for planetary exploration; (5) Early Martian environments--the Antarctic and other terrestrial analogs; (6) Lipophilic pigments from the benthos of a perennially ice-covered Antarctic lake; and (7) Perennially ice-covered Lake Hoare, Antarctica-physical environment, biology, and sedimentation. Author

N91-14256*# Arkansas Coll., Batesville.
KINETICS OF HYDROGEN RELEASE FROM LUNAR SOIL Final Report, 1 May - 31 Oct. 1990
Roberta Bustin Oct. 1990 23 p
(Grant NAG9-474)
(NASA-CR-187363; NAS 1.26:187363) Avail: NTIS HC/MF A03 CSCL 03B

With increasing interest in a lunar base, there is a need for extensive examination of possible lunar resources. Hydrogen will be needed on a lunar base for many activities including providing fuel, making water, and serving as a reducing agent in the extraction of oxygen from its ores. Previous studies have shown the solar wind has implanted hydrogen in the lunar regolith and that hydrogen is present not only in the outer layer of soil but to considerable depths, depending on the sampling site. If this hydrogen is to be mined and used on the lunar surface, a number of questions need to be answered. How much energy must be expended in order to release the hydrogen from the soil. What temperatures must be attained, and how long must the soil be heated. This study was undertaken to provide answers to practical questions such as these. Hydrogen was determined using a Pyrolysis/GC

technique in which hydrogen was released by heating the soil sample contained in a quartz tube in a resistance wire furnace, followed by separation and quantitative determination using a gas chromatograph with a helium ionization detector. Heating times and temperatures were varied, and particle separates were studied in addition to bulk soils. The typical sample size was 10 mg of lunar soil. All of the soils used were mature soils with similar hydrogen abundances. Pre-treatments with air and steam were used in an effort to find a more efficient way of releasing hydrogen. Author

N91-14257# Instituto de Pesquisas Espaciais, Sao Jose dos Campos (Brazil).
CENTIMETER EMISSION VARIATION OF VENUS: ITS SECOND PHASE M.S. Thesis, 2 Oct. 1989 [VARIACAO DA EMISSAO CENTIMETRICA DE VENUS SEGUNDO SUA FASE]
Lineu FernandoDelCiampo Sep. 1990 97 p In PORTUGUESE; ENGLISH summary
(INPE-5122-TDL/423) Avail: NTIS HC/MF A05

The radio emission from the planet Venus, at wavelengths smaller than 10 centimeters, presents some fluctuations in the brightness temperature. The reasons for those fluctuations are still inconclusive. During 1988, Venus was relatively closer to the Earth than in the preceeding years and also presented large phase angle changes along the year. This exceptional orbital configuration allowed to program an extensive series of observations with the scope of finding out if there is any fluctuation in the planetary brightness temperature associated to its phase. For this program the 13.7 m antenna of the Itapetinga Radio Observatory was used, the observations being carried out in 22 GHz and 43 GHz. The observational results of Venus brightness temperature, from March to October 1988, which shows some fluctuations in this temperature are presented. The results of observations suggest that the variation of the brightness temperature is probably due to the phase angle of the planet. This temperature variation may be due to variations in the abundance of SO2, H2O, and gaseous H2SO4 which are the main absorbers in those wavelengths. Author

N91-14258# Los Alamos National Lab., NM. Space Science and Technology.
ELEMENTAL MAPPING OF PLANETARY SURFACES USING GAMMA RAY SPECTROSCOPY
Robert C. Reedy 1990 9 p Presented at the 7th International Symposium on Capture Gamma Ray Spectroscopy and Related Topics, Pacific Grove, CA, 14-19 Oct. 1990
(Contract W-7405-eng-36)
(DE91-001877; LA-UR-90-3503; CONF-901057-4) Avail: NTIS HC/MF A02

The gamma rays escaping from a planet can be used to map the concentrations of various elements in its surface. In a planet, the high-energy particles in the galactic cosmic rays induce a cascade of particles that includes many neutrons. The gamma rays are made by the nuclear excitations induced by these cosmic ray particles and their secondaries (especially capture or inelastic-scattering reactions induced by neutrons) and decay of the naturally-occurring radioelements. After a short history of planetary gamma-ray spectroscopy and its applications, the gamma-ray spectrometer planned for the Mars Observer mission is presented. The results of laboratory experiments that simulate the cosmic-ray bombardments of planetary surfaces or measure cross sections for the production of gamma rays and the status of the theoretical calculations for the processes that make and transport neutrons and gamma rays will be reviewed. The emphasis here is on studies of Mars and on new ideas, concepts, and problems that have arisen over the last decade, such as Doppler broadening and peaks from neutron scattering with germanium nuclei in a high-resolution gamma-ray spectrometer. DOE

N91-14259*# National Aeronautics and Space Administration. Lewis Research Center, Cleveland, OH.
DESIGN CONSIDERATIONS FOR LUNAR BASE PHOTOVOLTAIC POWER SYSTEMS
J. Mark Hickman, Henry B. Curtis, and Geoffrey A. Landis 1990 10 p Presented at the 21st Photovoltaic Specialists Conference, Kissimmee, FL, 21-25 May 1990; sponsored by IEEE
(NASA-TM-103642; E-5823; NAS 1.15:103642) Avail: NTIS HC/MF A02 CSCL 03B

A survey was made of factors that may affect the design of photovoltaic arrays for a lunar base. These factors, which include the lunar environment and system design criteria, are examined. A photovoltaic power system design with a triangular array geometry is discussed and compared to a nuclear reactor power systems and a power system utilizing both nuclear and solar power sources. Author

92 SOLAR PHYSICS

Includes solar activity, solar flares, solar radiation and sunspots.

For related information see *93 Space Radiation.*

N91-14260# National Geophysical Data Center, Boulder, CO.
SOLAR-GEOPHYSICAL DATA NUMBER 550, JUNE 1990. PART 1: (PROMPT REPORTS). DATA FOR MAY, APRIL 1990 AND LATE DATA
H. E. Coffey Jun. 1990 151 p
(PB90-258799; SGD-550-Pt-1) Avail: NTIS HC/MF A08 CSCL 03B

The major areas covered include: (1) Detailed index for 1989 to 1990; (2) Data for May 1990 - solar-terrestrial environment, IUWDS alert periods (advance and worldwide) solar activity indices, solar flares, solar radio emission, Stanford mean solar magnetic field; (3) Data for April 1990 - solar active regions, sudden ionospheric disturbances, solar radio spectral observations, cosmic ray measurements by neutron monitor, geomagnetic indices; and (4) Late data - geomagnetic indices - geomagnetic activity indices March 1990. Author

N91-14261# National Geophysical Data Center, Boulder, CO.
SOLAR-GEOPHYSICAL DATA NUMBER 550, JUNE 1990. PART 2: (COMPREHENSIVE REPORTS). DATA FOR DECEMBER 1989 AND MISCELLANEOUS
H. E. Coffey Jun. 1990 98 p
(PB90-258807; SGD-550-Pt-2) Avail: NTIS HC/MF A05 CSCL 03B

The major areas covered include: (1) Detailed index for 1989 to 1990; (2) Data for December 1989 - solar flares, solar radio bursts at fixed frequencies, interplanetary solar particles and plasma, solar x ray radiation from GOES satellite, mass ejections from the sun, active prominence and filaments; (3) miscellaneous data - Meudon carte synoptique - Carrington rotations 1820 to 1821 September to October 1989, interplanetary solar plasma - IMP-8 solar wind July to November 1989. Author

N91-14262# National Geophysical Data Center, Boulder, CO.
SOLAR-GEOPHYSICAL DATA NUMBER 549, MAY 1990. PART 1: (PROMPT REPORTS). DATA FOR APRIL, MARCH, 1990, AND LATE DATA
H. E. Coffey May 1990 165 p
(PB90-251224; SGD-549-Pt-1) Avail: NTIS HC/MF A08 CSCL 03B

The major areas covered include: (1) Data for April 1990 - solar-terrestrial environment, IUWDS alert periods, solar activity indices, solar flares, solar radio emission, and Stanford mean solar magnetic field; (2) Data for March 1990 - solar active regions, sudden ionospheric disturbances, pioneer XII interplanetary magnetic field magnitudes, solar radio spectral observations, geomagnetic indices, and radio propagation indices; (3) Late data - Nancay interferometric chart Mar 90, geomagnetic activity indices Feb 90, sudden commencements Dec. 1989 to Jan. 1990, pioneer XII solar wind data 1989, and forbush decreases Mt. Washington 1954 to 1990. Author

N91-14263# National Geophysical Data Center, Boulder, CO.
SOLAR-GEOPHYSICAL DATA NUMBER 549, MAY 1990. PART 2: (COMPREHENSIVE REPORTS). DATA FOR NOVEMBER 1989 AND MISCELLANEOUS
H. E. Coffey May 1990 102 p
(PB90-251232; SGD-549-Pt-2) Avail: NTIS HC/MF A06 CSCL 03B

The major areas covered include: solar flares; solar radio bursts at fixed frequencies; interplanetary solar particles and plasma; solar x ray radiation from GOES satellite graphs; mass ejections from the sun; active prominences and filaments. Author

N91-14264# Los Alamos National Lab., NM.
LABORATORY SPECTRA OF AMORPHOUS AND CRYSTALLINE OLIVINE: AN APPLICATION TO COMET HALLEY IR SPECTRUM
A. Blanco, V. Orofino, E. Bussoletti, S. Fonti, L. Colangeli (Cassino Univ., Italy), and J. R. Stephens 1990 8 p Presented at the IAU Colloquium: Origin and Evolution of Interplanetary Dust, Kyoto, Japan, 27-30 Aug. 1990
(Contract W-7405-eng-36)
(DE91-002307; LA-UR-90-3395; CONF-9008164-1) Avail: NTIS HC/MF A02

Among the various silicates proposed as components of cosmic dust grains, olivine is considered one of the most likely materials. In this work we present the infrared spectra of three different types of olivine grains: crystalline, amorphous, and synthetic (also amorphous). While the first and second sample derive from the same natural mineral, the third one has been prepared in laboratory according to the relative cosmic abundances of the elements. The experiment data are used to fit the emission feature observed in the comet Halley spectrum between 8 and 13 microns. Satisfactory results are obtained by using synthetic olivine mixed with a small amount (5 percent) of crystalline grains. DOE

93 SPACE RADIATION

Includes cosmic radiation; and inner and outer earth's radiation belts.

For biological effects of radiation see *52 Aerospace Medicine*. For theory see *73 Nuclear and High-Energy Physics*.

N91-14265*# National Aeronautics and Space Administration. Langley Research Center, Hampton, VA.
SPACE RADIATION DOSE ANALYSIS FOR SOLAR FLARE OF AUGUST 1989
John E. Nealy, Lisa C. Simonsen, Herbert H. Sauer (National Oceanic and Atmospheric Administration, Boulder, CO.), John W. Wilson, and Lawrence W. Townsend Washington Dec. 1990 9 p
(NASA-TM-4229; L-16812; NAS 1.15:4229) Avail: NTIS HC/MF A02 CSCL 03B

Potential dose and dose rate levels to astronauts in deep space are predicted for the solar flare event which occurred during the week of August 13, 1989. The Geostationary Operational Environmental Satellite (GOES-7) monitored the temporal development and energy characteristics of the protons emitted during this event. From these data, differential fluence as a function of energy was obtained in order to analyze the flare using the Langley baryon transport code, BRYNTRN, which describes the interactions of incident protons in matter. Dose equivalent estimates for the skin, ocular lens, and vital organs for 0.5 to 20 g/sq cm of aluminum shielding were predicted. For relatively light shielding (less than 2 g/sq cm), the skin and ocular lens 30-day exposure limits are exceeded within several hours of flare onset. The vital organ (5 cm depth) dose equivalent is exceeded only for the thinnest shield (0.5 g/sq cm). Dose rates (rem/hr) for the skin, ocular lens, and vital organs are also computed. Author

N91-14266# Ballistic Research Labs., Aberdeen Proving Ground, MD.
FEASIBILITY OF COSMIC-RAY MUON INTENSITY MEASUREMENTS FOR TUNNEL DETECTION Final Report, Feb. 1989 - Feb. 1990
Aivars Celmins Jun. 1990 40 p
(AD-A223355; BRL-TR-3110) Avail: NTIS HC/MF A03 CSCL 17/8

Subsurface cosmic-ray muon intensity depends on the amount of material above the point of reference and is therefore influenced by anomalies in rock density. Because such anomalies might be caused by geological structures (e.g. ore bodies), cosmic-ray intensity measurements have been used for geophysical exploration. Recently, cosmic-ray muon intensity measurements have been also proposed as a method to detect tunnels. The feasibility of this application depends on the type of radiation detection apparatus (it must fit into a bore hole) and on the magnitude of the signal by a tunnel. If the signal is too weak, then the required observation times are estimated for a projected bore-hole radiation detector and for tunnels with a 2 m diameter. The estimates show that a reasonable upper bound for the detector depth is about 30 to 40 m if the observations are to be used in a tomographic reconstruction of the density field. The required observation times at that depth are of the order of days. The upper bound for the depth of detectable tunnels is less than the quoted bound for the detector depth. It might be possible to use the method at greater depths if special data interpretation techniques are developed that take into account prior knowledge about the tunnel, e.g. its anticipated direction. GRA

N91-14267 New Hampshire Univ., Durham.
TEMPORAL VARIATIONS OF COSMIC RAYS IN THE HELIOSPHERE Ph.D. Thesis
Ping Ping Chih 1989 107 p
Avail: Univ. Microfilms Order No. DA9022637

Temporal variations of cosmic rays in the heliosphere are investigated analytically. A perturbation approach is presented to solve the diffusion equation for energetic particle transport in the solar wind. A linear response of the cosmic ray number density to variations in the spatial diffusion coefficient is computed based on the convection-diffusion equation. As the simplest cases to study, the 11-year variation and a Forbush decrease, the assumptions are made that the solar-cycle variation arises from an 11-year sinusoidal variation of the diffusion coefficient at the Sun which propagates out through the heliosphere; and a Forbush decrease arises from the passage of an interplanetary traveling disturbance characterized by a sudden decrease of the diffusion coefficient. The predicted solar-cycle variation exhibits a hysteresis effect in which high-energy particles respond before low-energy particles. The predicted Forbush decrease profiles exhibit precursors, sudden decreases, and gradual approximate energy independent recoveries arising from a decay of the propagating disturbance. For high energy particles the time-dependent solution for a Forbush decrease in spherical coordinates is obtained by solving a steady state equation and then substituting the time dependent variation of the diffusion coefficient. It is found that the response function is similar to the Forbush decrease for a delta-function disturbance. Investigation of the response function in terms of the time-dependent Forbush decrease in spherical coordinates results in the determination of the characteristic timescale of it decay, which increases with increasing distance from the Sun.
Dissert. Abstr.

N91-14268 California Univ., Berkeley.
AN IMAGING AND SPECTROSCOPIC STUDY OF LOW AND INTERMEDIATE POWER RADIO GALAXIES Ph.D. Thesis
Kathleen Ann Ebneter 1989 259 p
Avail: Univ. Microfilms Order No. DA9028811

A search for 'features' (departures from elliptical symmetry) was conducted in a sample of 85 nearby, low, and intermediate power radio galaxies selected from the B2 and 3CR catalogs, and in a comparison sample of 159 optically-selected, early-type galaxies. Charge coupled device (CCD) images of the galaxies

were processed using a technique which involves division by a purely elliptical model image, constructed from the best fit surface photometry profiles for a given object. In addition, CCD spectra were obtained of approximately 2/3 of the galaxies in the radio sample, to investigate the stellar populations found in those galaxies. With a small number of exceptions, the radio galaxies were found to have integrated absorption line spectra which are indistinguishable from those of normal, giant elliptical galaxies. The three exceptions show strong Balmer absorption features suggestive of a relatively young stellar population. Radio-loud ellipticals were found to show higher rates of isophotal disturbances than radio-quiet ellipticals. In addition, radio-loud ellipticals in low galaxy density environments had a higher incidence of high-surface-brightness isophotal disturbances and strong nuclear emission lines than those in high galaxy density environments. The evidence suggests that there are two classes of radio galaxies which are distinguished primarily by the local galaxy density of their environment. Class A galaxies are found in regions of low galaxy density; and Class B galaxies are found in regions of high galaxy density. The possible reasons for this distinction between the two classes, and the influence of galactic mergers on the evolution of radio sources, are discussed. Dissert. Abstr.

N91-14269# Lawrence Livermore National Lab., CA. Physics Dept.
ANALYSIS OF GAMMA RAY BURST SPECTRA WITH CYCLOTRON LINES
Vincent Kargatis (Rice Univ., Houston, TX.) and Edison P. Liang 26 Sep. 1990 8 p Presented at the Los Alamos Workshop on Gamma-Ray Bursts, Taos, NM, 30 Jul. - 2 Aug. 1990
(Contract W-7405-eng-48)
(DE91-001745; UCRL-JC-106057; CONF-9007101-1) Avail: NTIS HC/MF A02

Motivated by the recent developments in the cyclotron resonance upscattering of soft photons or CUSP model of Gamma Ray Burst (GRB) continuum spectra, we revisit a select database of GRBs with credible cyclotron absorption features. We measure the break energy of the continuum, the slope below the break, and deduce the soft photon energy or the electron beam Lorentz factor cutoff. We study the correlation (or lack of) between various parameters in the context of the CUSP model. One surprise result is that there appears to be marginal correlation between the break energy and the spectral index below the break. DOE

N91-14270# Los Alamos National Lab., NM.
GAMMA RAY BURSTS FROM COMET NEUTRON STAR MAGNETOSPHERE INTERACTION, FIELD TWISTING AND E(SUB PARALLEL) FORMATION
Stirling A. Colgate 1990 8 p Presented at the Los Alamos Workshop on Gamma-Ray Bursts, Taos, NM, 29 Jul. - 3 Aug. 1990
(Contract W-7405-eng-36)
(DE91-002320; LA-UR-90-3461; CONF-9007101-2) Avail: NTIS HC/MF A02

The problem of a comet in a collision trajectory with a magnetized neutron star is discussed. The question addressed in this paper is whether the comet interacts strongly enough with a magnetic field such as to capture at a large radius or whether in general the comet will escape a magnetized neutron star. DOE

99 GENERAL

N91-14271*# National Aeronautics and Space Administration. Goddard Space Flight Center, Greenbelt, MD.
COBE'S SEARCH FOR STRUCTURE IN THE BIG BANG
Gerald Soffen, ed., Gene Guerny, ed., Thomas Keating, ed., Karen Moe, ed., Walter Sullivan, ed., and Walt Truszkowski, ed. 1989 280 p Original contains color illustrations
(NASA-TM-102976; NAS 1.15:102976) Avail: NTIS HC/MF A13; 32 functional color pages CSCL 05D

The launch of Cosmic Background Explorer (COBE) and the definition of Earth Observing System (EOS) are two of the major events at NASA-Goddard. The three experiments contained in COBE (Differential Microwave Radiometer (DMR), Far Infrared Absolute Spectrophotometer (FIRAS), and Diffuse Infrared Background Experiment (DIRBE)) are very important in measuring the big bang. DMR measures the isotropy of the cosmic background (direction of the radiation). FIRAS looks at the spectrum over the whole sky, searching for deviations, and DIRBE operates in the infrared part of the spectrum gathering evidence of the earliest galaxy formation. By special techniques, the radiation coming from the solar system will be distinguished from that of extragalactic origin. Unique graphics will be used to represent the temperature of the emitting material. A cosmic event will be modeled of such importance that it will affect cosmological theory for generations to come. EOS will monitor changes in the Earth's geophysics during a whole solar color cycle. Author

N91-14272 Max-Planck-Inst. fuer Aeronomie, Katlenburg-Lindau (Germany, F.R.).
[ACTIVITIES REPORT OF THE MAX-PLANCK INSTITUTE FOR AERONOMY] Annual Report, 1989 [MAX-PLANCK-INSTITUT FUER AERONOMIE, JAHRESBERICHT 1989]
H. Schwentek, A. Macke, and S. Deutsche Apr. 1990 169 p In GERMAN Original contains color illustrations
(ETN-91-98383) Copyright Avail: Fachinformationszentrum Karlsruhe 2, 7514 Eggenstein-Leopoldshaffen, Fed. Republic of Germany

Very interesting data were obtained, and new phenomena discovered during the work carried out by the Institute for the Soviet Spatial Sonde PHOBOS. The instruments developed by the Institute for the Spatial Sonde Galileo worked satisfactorily. The institute is also involved in the Voyager 2 mission to Neptune. In the field of ionosphere research, the improvement of the heating installation was started. The STARE (Scandinavian Twin Auroral Radar Experiment) system was improved in cooperation with Finland. Four payloads in rockets started successfully for the ROSE project. The atmospheric research works are being pursued in cooperation with Norway, and with the development of the lidar system. Measurements of trace gases in the middle atmosphere were carried out in the framework of the RASMUS (Rocket Air Sampler for Mesosphere and Upper Stratosphere) system. The MAS (Millimeterwave Atmospheric Sonde) instrument was completed and delivered as part of the ATLAS (Atmospheric Laboratory for Application and Science) Shuttle mission. ESA

Typical Subject Index Listing

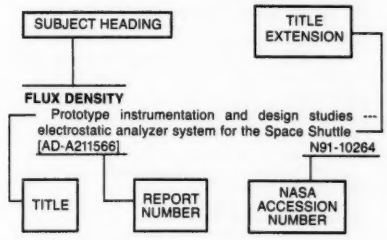

The subject heading is a key to the subject content of the document. Titles, report numbers, and accession numbers of pertinent documents are provided under each subject heading. When the title is insufficiently descriptive of the document content, a title extension has been added, separated from the title by three hyphens. The report number helps to indicate the type of document cited (e.g., NASA report, NASA translation, NASA contractor report). The NASA accession number is the number by which the document abstracts are arranged in this journal and by which the document is sold or requested. The titles, with title extensions if present, are arranged under each subject heading in ascending accession number order. The subject headings have been selected from the latest revision of the *NASA Thesaurus* (NASA SP-7064).

A

ABERRATION
Control system for ruling blazed, aberration corrected diffraction gratings
[NASA-CASE-GSC-13240-1] N91-13692

ABSORPTION CROSS SECTIONS
Ultraviolet absorption cross-sections of photoactive species of stratospheric interest. Part 1: The halocarbons
[ETN-91-98385] N91-13830

ABSORPTION SPECTRA
Chromium sensitized garnets for mid-IR lasers
[AD-A226630] N91-13696
Neutral atomic absorption lines and far-UV extinction: Possible implications for depletions and grain parameters N91-14115
Radiative thermal conduction fronts N91-14162
Energy input and HI spin temperatures in low pressure regions N91-14163
Interpreting the convergence of Lyman series absorption lines N91-14225
Detection of a z=0.0515, 0.0522 absorption system in the QSO S4 0248+430 due to an intervening galaxy N91-14228

ABSORPTIVITY
Pioneer-Venus radio occultation (ORO) data reduction: Profiles of 13 cm absorptivity
[NASA-CR-186986] N91-13584

ABSTRACTS
Managing the Global Commons Decision Making and Conflict Resolution in Response to Climate Change Research Workshop
[DE91-001018] N91-13810
Physiological responses to prolonged bed rest in humans: A compendium of research, 1981-1988
[NASA-TM-102249] N91-13862
List of standards to accompany manual of documentation practices applicable to defence-aerospace scientific and technical information. Addendum
[AGARD-AG-235-ADD] N91-14076
Proceedings of a Workshop on Cosmogenic Nuclide Production Rates
[NASA-CR-185349] N91-14098
Abstracts for the International Workshop on Meteorite Impact on the Early Earth
[NASA-CR-185355] N91-14099
Proceedings of the MEVTV Workshop on The Evolution of Magma Bodies on Mars
[NASA-CR-187357] N91-14252

ABUNDANCE
Radio observations of several interstellar molecules N91-14093
Empirical relationships between gas abundances and UV selective extinction N91-14116
Spatially resolved optical and near infrared spectroscopy of I Zw 18 N91-14154

AC GENERATORS
The world of superconductive machinery N91-14045

ACCELERATION STRESSES (PHYSIOLOGY)
Vestibulo-ocular responses in man to +G sub z hypergravity
[IZF-1989-59] N91-13873

ACCELERATION TOLERANCE
Vestibulo-ocular responses in man to +G sub z hypergravity
[IZF-1989-59] N91-13873

ACCELEROMETERS
A preliminary look at techniques used to obtain airdata from flight at high angles of attack
[NASA-TM-101729] N91-13453
Application of high-temperature superconductors to high-precision accelerometers N91-14042

ACCESS CONTROL
Security for safety critical space borne systems
[NASA-CR-187656] N91-13906

ACCRETION DISKS
Relativistic effects in millisecond pulsars and active galactic nuclei N91-14247

ACCUMULATORS
Status of concentrator collector and high-efficiency concentrator cell development
[DE91-001260] N91-13793

ACCURACY
Evaluation of a simple method for color monitor recalibration
[IZF-1990-B-4] N91-13608

ACID RAIN
Acidic deposition and the environment
[DE91-002352] N91-13812

ACIDITY
Acidic deposition and the environment
[DE91-002352] N91-13812

ACOUSTIC EXCITATION
A steadying effect of acoustic excitation on transitory stall
[NASA-TM-103689] N91-13420

ACOUSTIC FREQUENCIES
The prediction and measurement of the one-parameter behaviour of horns
[ISVR-TR-185] N91-13974

ACOUSTIC IMPEDANCE
Transducer holder and method of making
[NASA-CASE-LAR-14027-1] N91-13693

ACOUSTIC MICROSCOPES
Possibilities of stress measurement on ceramic materials using acoustic microscopy N91-13547

ACOUSTIC PROPERTIES
Adaptive inverse filters for stereophonic sound reproduction
[ISVR-TR-187] N91-13975

ACRYLIC RESINS
Mechanisms of gas permeation through polymer membranes
[DE91-004190] N91-13671

ACTINIDE SERIES COMPOUNDS
Actinide speciation by photothermal spectroscopies: Instrumentation development
[DE91-001854] N91-13700

ACTIVE CONTROL
Analysis of the leading edge effects on the boundary layer transition
[NASA-CR-187361] N91-13405
F-106B airplane active control landing gear drop test performance
[NASA-TM-102741] N91-13445
Success with an automated computer control system
[DE91-001759] N91-13945

ACTIVE GALACTIC NUCLEI
High resolution CO images of Seyfert Galaxies N91-14121
Circumnuclear ionized gas in starburst nuclei N91-14148
H2 line emission in three Seyfert nuclei: Evidence against UV-excitation N91-14185
Relativistic effects in millisecond pulsars and active galactic nuclei N91-14247

ACTIVE GALAXIES
A survey of galaxies in CO N91-14118
The infrared continuum spectrum of x ray illuminated molecular gas N91-14144
Imaging spectrophotometry of the nuclear outflow of NGC 1068 N91-14149
Clues to galaxy activity from rich cluster simulations N91-14222
CO excitation in four IR luminous galaxies N91-14234

ADA (PROGRAMMING LANGUAGE)
Parallel Ada benchmarks for the SVMS
[NASA-CR-182453] N91-13929
Validation environment for AIPS/ALS: Implementation and results
[NASA-CR-4340] N91-13930
Knowledge representation into Ada parallel processing
[NASA-CR-187451] N91-13934

ADAPTATION
Physiological responses to prolonged bed rest in humans: A compendium of research, 1981-1988
[NASA-TM-102249] N91-13862

ADAPTIVE CONTROL
Dynamic modeling, property investigation, and adaptive controller design of serial robotic manipulators modeled with structural compliance
[NASA-CR-187678] N91-13722
Applications of neural networks to adaptive control
[AD-A225408] N91-13938

ADAPTIVE FILTERS
Adaptive inverse filters for stereophonic sound reproduction
[ISVR-TR-187] N91-13975

ADDITION RESINS
Vinyl capped addition polyimides
[NASA-CASE-LEW-15027-1] N91-13566

ADDITIVES
Electrocatalysis of anodic oxygen-transfer reactions at modified lead dioxide electrodes
[DE91-000664] N91-13518
High-alcohol microemulsion fuel performance in a diesel engine
[DE91-001617] N91-13572

ADDRESSING
BAG: A programming language for the CESAR buffer address generator
[FFI-90/7022] N91-13923

ADHESION
Interfacial chemistry of titanium films deposited on PMDA-ODA polyimide
[AD-A225730] N91-13550

ADHESIVE BONDING
Friction and wear of TPS fibers: A study of the adhesion and friction of high modulus fibers
[NASA-CR-187666] N91-13515
Novel polyimide molding powder, coating, adhesive, and matrix resin
[NASA-CASE-LAR-14163-1] N91-13559
Tubular lap joints for wind turbine applications
[DE91-001341] N91-13736
ADENG, adhesive bonding technology for engineering applications: Computer aided design
[CETIM-105070] N91-13917

ADIABATIC CONDITIONS
Volumetric measurement of tank volume
[NASA-CASE-MSC-21500-1] N91-13683
ADJUSTING
Apparatus for precision focusing and positioning of a beam waist on a target
[NASA-CASE-ARC-11916-1-SB] N91-14002
ADSORPTION
Electrocatalyst surfaces
[PB90-252560] N91-13507
AERIAL PHOTOGRAPHY
The relation between tree physiology and multispectral and color photography: First phase
[BCRS-89-39] N91-13785
AEROACOUSTICS
Instability of a supersonic shock free elliptic jet
[NASA-TM-103428] N91-13413
AERODYNAMIC BALANCE
A review of ice accretion data from a model rotor icing test and comparison with theory
[NASA-TM-103712] N91-13421
Periodic trim solutions with hp-version finite elements in time
[NASA-CR-187705] N91-13449
AERODYNAMIC CHARACTERISTICS
Analytical aerodynamic model of a high alpha research vehicle wind-tunnel model
[NASA-CR-187362] N91-13404
FE analyses of aircraft model with interior trim
[FFA-TN-1990-21] N91-13417
AERODYNAMIC COEFFICIENTS
Airfoil design for variable RPM horizontal axis wind turbines
[FFA-TN-1990-02] N91-13801
AERODYNAMIC CONFIGURATIONS
Concept development of a Mach 4 high-speed civil transport
[NASA-TM-4223] N91-13432
Theoretical evaluation of engine auxiliary inlet design for supersonic V/STOL aircraft
[NASA-CR-186610] N91-13443
Airfoil design for variable RPM horizontal axis wind turbines
[FFA-TN-1990-02] N91-13801
AERODYNAMIC HEATING
Analysis of the leading edge effects on the boundary layer transition
[NASA-CR-187361] N91-13405
AERODYNAMIC INTERFERENCE
Effect of location of aft-mounted nacelles on the longitudinal aerodynamic characteristics of a high-wing transport airplane
[NASA-TP-3047] N91-13402
AERODYNAMIC LOADS
Spanwise aerodynamic loads on a rotating wind turbine blade
[DE91-002101] N91-13414
Test and model correlation of the atmospheric emission photometric imager fiberglass pedestal
[NASA-TM-103515] N91-13766
AERODYNAMIC NOISE
Transonic blade-vortex interactions noise: A parametric study
[NASA-CR-187713] N91-13422
AERODYNAMIC STABILITY
General Rotorcraft Aeromechanical Stability Program (GRASP): Theory manual
[NASA-TM-102255] N91-13762
AERODYNAMIC STALLING
Spanwise aerodynamic loads on a rotating wind turbine blade
[DE91-002101] N91-13414
A steadying effect of acoustic excitation on transitory stall
[NASA-TM-103689] N91-13420
AERODYNAMICS
Aeronautical engineering: A continuing bibliography with indexes (supplement 258)
[NASA-SP-7037(258)] N91-13399
A preliminary look at techniques used to obtain airdata from flight at high angles of attack
[NASA-TM-101729] N91-13453
AEROELASTICITY
Close-range photogrammetric measurement of static deflections for an aeroelastic supercritical wing
[NASA-TM-4194] N91-13400
Some observations on the Houbolt-Rainey and peak-hold methods of flutter onset prediction
[NASA-TM-102745] N91-13411
Wind-tunnel survey of an oscillating flow field for application to model helicopter rotor testing
[NASA-TM-4224] N91-13462
General Rotorcraft Aeromechanical Stability Program (GRASP): Theory manual
[NASA-TM-102255] N91-13762
AERONAUTICAL ENGINEERING
Aeronautical engineering: A continuing bibliography with indexes (supplement 258)
[NASA-SP-7037(258)] N91-13399
AGARD highlights 90/2, part 2
[AD-A226532] N91-14080
AERONOMY
Aeronomic chemistry of ozone
[AERONOMICA-ACTA-A-355-1990] N91-13816
Activities report of the Max-Planck Institute for Aeronomy
[ETN-91-98383] N91-14272
AEROSOLS
Methods of analysis for complex organic aerosol mixtures from urban emission sources of particulate carbon
[DE91-001722] N91-13814
AEROSPACE ENGINEERING
Space flight undertakings of present-day china (photo captions on 65 selected pages)
[AD-A222816] N91-13469
Technical communications in aerospace: An analysis of the practices reported by US and European aerospace engineers and scientists
[NASA-TM-103441] N91-14079
AEROSPACE ENVIRONMENTS
Development of mercuric iodide uncooled x ray detectors and spectrometers
[NASA-CR-185394] N91-13484
Microgravity strategic plan, 1990
[NASA-TM-103448] N91-13575
Unique features of space reactors
[DE91-001910] N91-13987
AEROSPACE MEDICINE
Biomedical program at Space Biospheres Ventures N91-13847
AEROSPACE SYSTEMS
Design reliability engineering
[DE91-001949] N91-13744
Technical communications in aerospace: An analysis of the practices reported by US and European aerospace engineers and scientists
[NASA-TM-103441] N91-14079
AGARD highlights 90/2, part 2
[AD-A226532] N91-14080
AEROSPACE VEHICLES
Experimental and theoretical determination of the thermomechanical response of inelastic structural materials to high energy thermal inputs
[AD-A226671] N91-13496
AGING (MATERIALS)
Physical properties of thermosetting polymers
[AD-A225864] N91-13508
Degradation modeling with application to aging and maintenance effectiveness evaluations
[DE91-004004] N91-13746
AGING (METALLURGY)
Study of the metallurgical effects of hammering between passes during C-Mn weld deposition
[CETIM-104850] N91-13532
Study of the metallurgical consequences of hammering between passes to compensate for the withdrawal of metal caused by welding
[CETIM-104430] N91-13741
A comparative study of ductile fracture in the 2.25 percent Cr-1 percent Mo and 9 percent Cr-1 percent Mo alloy steels N91-13753
Sustained-load crack growth of 8090 aluminium-lithium alloy plate in dry air at 50-200 C
[RAE-TR-90033] N91-13777
AGRICULTURE
JPRS Report: Science and technology. USSR: Life sciences
[JPRS-ULS-89-011] N91-13861
AIR FLOW
Influence of thermodynamical modelization for chemically reacting air flow
[MBB/FE122/S/PUB/400] N91-13418
Coherent anti-Stokes Raman spectroscopic measurement of air entrainment in argon plasma jets
[DE91-001936] N91-13670
Gravity waves excited by flow over an obstacle
[FFI-90/7017] N91-13828
Measurement of air entrainment in plasma jets
[DE91-001943] N91-14013
AIR LAUNCHING
Flight control design issues in bank-to-turn missiles N91-13437
AIR POLLUTION
Acidic deposition and the environment
[DE91-002352] N91-13812
Methods of analysis for complex organic aerosol mixtures from urban emission sources of particulate carbon
[DE91-001722] N91-13814
Cloud properties as deduced from satellite observation
[NASA-CR-182851] N91-13833
AIR PURIFICATION
The NASA CELSS program N91-13848
CELSS research and development program N91-13850
The BioHome: A spinoff of space technology N91-13852
AIR SEA ICE INTERACTIONS
Sea ice-atmosphere interaction: Application of multispectral satellite data in polar surface energy flux estimates
[NASA-CR-187376] N91-13782
AIR TO AIR MISSILES
Flight control design issues in bank-to-turn missiles N91-13437
AIR TRAFFIC CONTROL
The effect of stereoscopic presentation on a simulated air traffic control task
[IZF-1989-53] N91-13431
AIR TRANSPORTATION
Civil tiltrotor missions and applications
[NASA-CR-177452] N91-13424
UK airlines' cost structure and implications of air transport services fragmentation. Research report on air transport fragmentation
[TT-9011] N91-13427
AIR WATER INTERACTIONS
Interannual variation of seasonal means and subseasonal variability of cloud streets off the east coast of North America 1984-1987
[NASA-CR-187021] N91-13831
AIRBORNE EQUIPMENT
High spatial resolution studies of galaxies in the far IR: Observations with the KAO, and the promise of SOFIA N91-14229
AIRBORNE SURVEILLANCE RADAR
Modelling and performance analysis of four and eight element TCAS
[NASA-CR-187414] N91-13428
AIRCRAFT
Airport stand assignment model
[TT-9009] N91-13426
AIRCRAFT ACCIDENT INVESTIGATION
Aircraft accident report: Aloha IslandAir, Inc., Flight 1712, de Havilland Twin Otter, DHC-6-300, N707PV, Halawa Point, Molokai, Hawaii, October 28, 1989
[PB90-910405] N91-13425
AIRCRAFT ACCIDENTS
Aircraft accident report: Aloha IslandAir, Inc., Flight 1712, de Havilland Twin Otter, DHC-6-300, N707PV, Halawa Point, Molokai, Hawaii, October 28, 1989
[PB90-910405] N91-13425
AIRCRAFT CONFIGURATIONS
Some buffet response characteristics of a twin-vertical-tail configuration
[NASA-TM-102749] N91-13412
Civil tiltrotor missions and applications
[NASA-CR-177452] N91-13424
Concept development of a Mach 4 high-speed civil transport
[NASA-TM-4223] N91-13432
A semiempirical method for obtaining fuselage normal areas from fuselage Mach sliced areas
[NASA-TM-4228] N91-13433
AIRCRAFT CONSTRUCTION MATERIALS
The United Kingdom contribution to the AGARD fatigue-rated fastener systems program
[RAE-TR-89046] N91-13451
AIRCRAFT CONTROL
A flight expert system for on-board fault monitoring and diagnosis
[NASA-CR-187334] N91-13452
Integrated aerodynamic and control system design of oblique wing aircraft N91-13459
Modeling pilot interaction with automated digital avionics systems: Guidance and control algorithms for contour and nap-of-the-Earth flight
[NASA-CR-186105] N91-13875
AIRCRAFT DESIGN
Effect of location of aft-mounted nacelles on the longitudinal aerodynamic characteristics of a high-wing transport airplane
[NASA-TP-3047] N91-13402
Concept development of a Mach 4 high-speed civil transport
[NASA-TM-4223] N91-13432
A semiempirical method for obtaining fuselage normal areas from fuselage Mach sliced areas
[NASA-TM-4228] N91-13433
Integrated aerodynamic and control system design of oblique wing aircraft N91-13459
Integrated flight-propulsion control concepts for supersonic transport airplanes
[NASA-TM-101728] N91-13460

AIRCRAFT ENGINES
An AD100 implementation of a real-time STOVL aircraft propulsion system
[NASA-TM-103683] N91-13457
AIRCRAFT EQUIPMENT
Modelling and performance analysis of four and eight element TCAS
[NASA-CR-187414] N91-13428
A flight expert system for on-board fault monitoring and diagnosis
[NASA-CR-187334] N91-13452
AIRCRAFT GUIDANCE
Modeling pilot interaction with automated digital avionics systems: Guidance and control algorithms for contour and nap-of-the-Earth flight
[NASA-CR-186105] N91-13875
AIRCRAFT MANEUVERS
Robust variable structure control of model reference systems
[MATHS-REPT-A-131] N91-13947
AIRCRAFT MODELS
FE analyses of aircraft model with interior trim
[FFA-TN-1990-21] N91-13417
AIRCRAFT STRUCTURES
Failure behavior of generic metallic and composite aircraft structural components under crash loads
[NASA-RP-1239] N91-13751
AIRFOIL PROFILES
Calibration of the 13- by 13-inch adaptive wall test section for the Langley 0.3-meter transonic cryogenic tunnel
[NASA-TP-3049] N91-13461
AIRFOILS
The IAR high Reynolds number two-dimensional test facility: A description of equipment and procedures common to most 2-D airfoil tests
[AD-A226629] N91-13409
Spanwise aerodynamic loads on a rotating wind turbine blade
[DE91-002101] N91-13414
Transonic wind tunnel tests on two-dimensional aerofoil sections: Determination of pressure distribution and drag for an aerofoil of type SAAB 7301 in FFA wind tunnel S5
[FFA-TN-1989-47] N91-13416
A steadying effect of acoustic excitation on transitory stall
[NASA-TM-103689] N91-13420
Dual strain gage balance system for measuring light loads
[NASA-CASE-LAR-14419-1] N91-13687
Airfoil design for variable RPM horizontal axis wind turbines
[FFA-TN-1990-02] N91-13801
AIRGLOW
Procedure for generating global atmospheric engine emissions data from future supersonic transport aircraft. The 1990 high speed civil transport studies
[NASA-CR-181882] N91-13447
AIRLINE OPERATIONS
UK airlines' cost structure and implications of air transport services fragmentation. Research report on air transport fragmentation
[TT-9011] N91-13427
AIRPORT PLANNING
Airport stand assignment model
[TT-9009] N91-13426
AIRPORTS
Literature review on geotextiles to improve pavements for general aviation airports
[DOT/FAA/RD-90/26] N91-13464
ALBEDO
A physical parameterization of snow albedo for use in climate models N91-13781
ALCOHOLS
High-alcohol microemulsion fuel performance in a diesel engine
[DE91-001617] N91-13572
ALGEBRA
Logics for the description of processes and their properties: Expressivity and decidability
[ETN-91-98200] N91-13960
New phases of D greater than or equal to 2 current and diffeomorphism algebras in particle physics
[DE91-001515] N91-14067
ALGORITHMS
Modelling and performance analysis of four and eight element TCAS
[NASA-CR-187414] N91-13428
Multivariable methods for the design, identification, and control of large space structures. Volume 1: Estimator Eigenvalue placement in positive real design
[AD-A226525] N91-13477
NRL 1989 beam propagation studies in support of the ATA multi-pulse propagation experiment
[AD-A226443] N91-13588
Evaluation of a simple method for color monitor recalibration
[IZF-1990-B-4] N91-13608
Analytical study of the liquid phase transient behavior of a high temperature heat pipe
[NASA-CR-187426] N91-13644
Transport properties of dense fluid mixtures using nonequilibrium molecular dynamics
[DE91-000262] N91-13654
Predictive sensor method and apparatus
[NASA-CASE-SSC-00006-1] N91-13691
Quality of expert systems: Algorithms for integrity control
[FEL-89-A312] N91-13748
Study of static and dynamic fracture using strain measurements N91-13754
Constraint treatment techniques and parallel algorithms for multibody dynamic analysis
[NASA-CR-187668] N91-13759
A computational procedure for the dynamics of flexible beams within multibody systems
[NASA-CR-187667] N91-13760
A structural constitutive algorithm based on continuum damage mechanics for softening with snapback
[DE90-015841] N91-13773
Calculations for structures with nonlinear joints
[CETIM-108830] N91-13776
Sea ice-atmosphere interaction: Application of multispectral satellite data in polar surface energy flux estimates
[NASA-CR-187376] N91-13782
Modeling pilot interaction with automated digital avionics systems: Guidance and control algorithms for contour and nap-of-the-Earth flight
[NASA-CR-186105] N91-13875
Analysis of parallelism for nonlinear programming
[INPE-5121-TDL/422] N91-13899
Algorithms for finding an optimal matching between a given string and a string generated by a regular grammar
[MEMO-836] N91-13905
An improved exploratory search technique for pure integer linear programming problems
[NASA-TM-103517] N91-13910
A generalized Polak-Ribiere algorithm
[MATHS-REPT-A-128] N91-13918
On unconstrained conjugate gradient optimization methods and their interrelationships
[MATHS-REPT-A-129] N91-13919
Synthetic models of distributed memory parallel programs
[DE91-001058] N91-13931
A tutorial on the construction of high-performance resolution/paramodulation systems
[DE91-001096] N91-13942
The simultaneous integration of many trajectories using nilpotent normal forms
[NASA-CR-187318] N91-13950
A fully Sinc-Galerkin method for Euler-Bernoulli beam models
[NASA-CR-187462] N91-13952
New techniques for the union-find problem
[RUU-CS-89-12] N91-13954
A global convergence result for conjugate gradient methods
[MATHS-REPT-A-134] N91-13961
Algorithmic information content, Church-Turing thesis, physical entropy, and Maxwell's demon
[DE91-001804] N91-14069
ALIGNMENT
Post clamp
[NASA-CASE-LEW-14862-1] N91-13730
Three dimensional moire pattern alignment
[NASA-CASE-MSC-21416-1] N91-14000
ALLOYING
Research and development for improved toughness aluminides
[AD-A226627] N91-13524
ALLOYS
Band-gap narrowing and III-V heterostructure FETs (Field-Effect Transistors)
[DE91-000401] N91-14056
Optical properties and electronic structures of d- and f-electron metals and alloys, Ag-In, Ni-Cu, AuGa2, PtGa2, beta'-NiAl, beta'-CoAl, CeSn3, and LaSn3
[DE91-001597] N91-14059
ALPINE METEOROLOGY
Frontal interactions with orography: Objective cross-sectional analysis of ALPEX data N91-13836
ALPS MOUNTAINS (EUROPE)
Frontal interactions with orography: Objective cross-sectional analysis of ALPEX data N91-13836
ALTERNATING DIRECTION IMPLICIT METHODS
Analytical study of the liquid phase transient behavior of a high temperature heat pipe
[NASA-CR-187426] N91-13644
ALTERNATIVES
Connectivity alternatives for remote users of the Maintenance Processor Subsystem (MPS)
[DOT/FAA/CT-90/16] N91-13900
ALTITUDE CONTROL
Description of sea wave motion and its influence on the altitude control of sea skimming missiles
[FEL-89-A368] N91-13450
ALUMINIDES
Oxidation characteristics of Ti-25Al-10Nb-3V-1Mo intermetallic alloy
[NASA-TP-3044] N91-13522
Research and development for improved toughness aluminides
[AD-A226627] N91-13524
ALUMINUM
Tubular lap joints for wind turbine applications
[DE91-001341] N91-13736
Constrained viscoelastic layer damping of thick aluminum plates: Design, analysis, and testing
[AD-A226556] N91-13758
Composite passive damping struts for large precision structures
[NASA-CASE-NPO-17914-1-CU] N91-13767
The prediction and measurement of the one-parameter behaviour of horns
[ISVR-TR-185] N91-13974
ALUMINUM ALLOYS
Influence of oxide reinforcement materials on high-temperatue oxidation resistance of Ni3Al matrix composites
[DE91-001625] N91-13498
Fabrication and properties of powder metallurgically manufactured aluminum products and composites
[VTT-RR-699] N91-13531
Superplastic deformation properties of Ti-6Al-4V
[DE91-000503] N91-13757
Sustained-load crack growth of 8090 aluminium-lithium alloy plate in dry air at 50-200 C
[RAE-TR-90033] N91-13777
Simultaneous measurement of Ni-Al particle size, velocity, and temperature in atmospheric thermal plasmas
[DE91-001935] N91-13826
Non-empirical interatomic potentials for transition metals, alloys, and semiconductors
[DE91-002396] N91-14062
ALUMINUM GALLIUM ARSENIDES
Study and development of tunable, single mode AlGaAs/GaAs lasers
[DE91-001684] N91-13697
Design of GaAlAs/GaAs GRIN-SCH SQW diode lasers. Analysis of the temperature dependence
[LAAS-90277] N91-13708
A theoretical investigation of effective surface recombination velocity in AlGaAs/GaAs heteroface solar cells
[DE91-001754] N91-13795
Band-gap narrowing and III-V heterostructure FETs (Field-Effect Transistors)
[DE91-000401] N91-14056
ALUMINUM OXIDES
Influence of oxide reinforcement materials on high-temperatue oxidation resistance of Ni3Al matrix composites
[DE91-001625] N91-13498
Influence of materials structure and production method of Al2O3 ceramic on the x-ray stress measurement N91-13540
The influence of the texture of Al2O3 substrates on the fracture behavior under thermal loading N91-13543
Residual stresses in Al2O3: Comparison between electromechanical measurements and finite element method calculations N91-13545
AMMONOLYSIS
Ammonia decomposition on silicon surfaces studied using transmission FTIR spectroscopy
[AD-A226625] N91-13513
AMORPHOUS MATERIALS
Ion-induced damage and amorphization in Si
[DE91-002358] N91-14061
Laboratory spectra of amorphous and crystalline olivine: An application to comet Halley IR spectrum
[DE91-002307] N91-14264
AMORPHOUS SILICON
Synchrotron radiation photoemission study of metal overlayers on hydrogenated amorphous silicon at room temperature
[DE91-000740] N91-13525
X ray and charged particle detection with CsI(Tl) layer coupled to a-Si:H photodiode layers
[DE91-001798] N91-14060
AMPLIFIERS
Multiplexer/amplifier test results for SP-100
[DE91-004504] N91-13990

AMPS (SATELLITE PAYLOAD)
Local closed orbit bumps in AmPS
[NIKHEF-K/AMPS/90-01] N91-13471
ANALOGIES
Auto and hetero-associative memory using a 2-D optical logic gate
[NASA-CASE-NPO-17997-1-CU] N91-13888
ANALYSIS (MATHEMATICS)
Wave by wave analysis of in-line force data for fixed cylinders in regular waves
[IC-AERO-89-02] N91-13672
ANDROMEDA GALAXY
The violent interstellar medium in Messier 31
N91-14178
Supernova remnants and diffuse ionized gas in M31
N91-14179
The effect of suspended particles on Jean's criterion for gravitational instability N91-14189
ANGLE OF ATTACK
Analytic formulations of unsteady profile aerodynamics and its application to simulation of rotors
[DLR-FB-90-28] N91-13415
A preliminary look at techniques used to obtain airdata from flight at high angles of attack
[NASA-TM-101729] N91-13453
ANGULAR DISTRIBUTION
Inclusive inelastic scattering of heavy ions and nuclear correlations
[NASA-TP-3026] N91-13985
ANGULAR RESOLUTION
High angular resolution mm- and submm-observations of dense molecular gas in M82 N91-14230
ANNUAL VARIATIONS
Interannual variation of seasonal means and subseasonal variability of cloud streets off the east coast of North America 1984-1987
[NASA-CR-187021] N91-13831
ANNULAR FLOW
The effect of longitudinal spacer ribs on the minimum pressure drop in a heated annulus
[DE91-000784] N91-13655
ANTARCTIC REGIONS
Exobiology site selection for future Mars missions: Martian paleolake sediments and terrestrial analogs
[NASA-CR-187358] N91-14255
ANTENNA ARRAYS
Modelling and performance analysis of four and eight element TCAS
[NASA-CR-187414] N91-13428
Electronic scan at millimetre wave frequencies
[FEL-89-B258] N91-13601
Measurement results of the FEL-TNO planar rectangular near field facility (1978-1989)
[FEL-89-B336] N91-13602
ANTENNA DESIGN
Measurement results of the FEL-TNO planar rectangular near field facility (1978-1989)
[FEL-89-B336] N91-13602
Planar near-field measurement of non-reciprocal antennas
[FEL-90-B092] N91-13604
System and method for measuring ocean surface currents at locations remote from land masses using synthetic aperture radar
[NASA-CASE-NPO-17937-1-CU] N91-13787
ANTENNA RADIATION PATTERNS
Modelling and performance analysis of four and eight element TCAS
[NASA-CR-187414] N91-13428
Restoration of solar radio images: Evaluation of poor conditions and resolution by regularization techniques
[INPE-4557-PRE/1298] N91-13587
Planar near-field measurement of non-reciprocal antennas
[FEL-90-B092] N91-13604
ANTHROPOMETRY
Effects of anthropometric and postural variables on the transmission of whole-body vertical vibration from seat-to-head
[ISVR-TR-172] N91-13884
ANTIAIRCRAFT MISSILES
Missile Interceptor Guidance System Technology
[AGARD-LS-173] N91-13434
ANTIMISSILE DEFENSE
Guidnace simulation model of antisea-skimmer utilization for weapon system definition N91-13438
Interactions between battle management and guidance law design for a strategic interceptor N91-13441
Guidance methods for tactical and strategic missiles
N91-13442
ANXIETY
Simulator flight as a selection device: Effects of test anxiety on subjective and objective measures of performance
[IZF-1989-57] N91-13468
APEXES
Accurate and reliable computation of complete solutions to the equations of linear elastomechanics on three-dimensional domains: Computation of edge stress intensity functions
[FFA-TN-1989-12] N91-13769
Accurate and reliable determination of edge and vertex stress intensity factors in three-dimensional elastomechanics
[FFA-TN-1990-28] N91-13771
APPLICATION SPECIFIC INTEGRATED CIRCUITS
Semi-custom integrated circuit amplifier and level discriminator for nuclear and space instruments
[DE91-001951] N91-13620
APPLICATIONS PROGRAMS (COMPUTERS)
Thrust chamber modeling using Navier-Stokes equations: Code documentation and listings, volume 2
[NASA-CR-183617] N91-13489
Development of BEM for ceramic composites
[NASA-CR-187676] N91-13557
Relativistic kylstron simulations using RKTW2D
[DE91-001747] N91-13619
A design method for an X-band diplexer
[FEL-90-B176] N91-13635
Improved plug valve computer-aided design of plug element
[DE91-001044] N91-13719
Comparison of NASA Lewis Research Center's performance code's pressure-drop model predictions to Stirling engine working-space flow test data
[NASA-CR-182215] N91-13804
NDRE/TAII processor architecture study
[FFI-90/7012] N91-13891
Examples of finite element mesh generation using SDRC IDEAS
[NASA-CR-186962] N91-13893
CESAR MALU program library
[FFI-90/7010] N91-13922
Applications of artificial intelligence to mission planning
[NASA-CR-184994] N91-13939
Dependence of CIT (compact ignition tokamak) PF (poloidal field) coil currents on profile and shape parameters using the control matrix
[DE91-002650] N91-14019
ARC DISCHARGES
Dynamic high-pressure studies of an electrothermal capillary
[DE91-000966] N91-13617
ARCHITECTURE (COMPUTERS)
An interactive program for the analysis and design of advanced laser targets
[DE91-002542] N91-13704
Superconducting neural network computer and sensor array
[AD-D014625] N91-13887
About transient stability of power systems: Statistical pattern recognition approach
[LAAS-90192] N91-13889
Programmable remapper with single flow architecture
[NASA-CASE-MSC-21481-1] N91-13890
NDRE/TAII processor architecture study
[FFI-90/7012] N91-13891
Version control and management in computer-aided design databases N91-13896
Architecture for electronic imagery interoperability
[AD-A226522] N91-13901
The design of a distributed image processing and dissemination system
[DE91-001835] N91-13909
Computed tomography software and standards
[DE91-002573] N91-13914
Parallel Ada benchmarks for the SVMS
[NASA-CR-182453] N91-13929
Flexible cooperation in non-standard application environments
[AD-A226486] N91-13940
System and method for a general purpose architecture for intelligent computer-aided training
[NASA-CASE-MSC-21381-1] N91-13944
Success with an automated computer control system
[DE91-001759] N91-13945
A real-time digital control, data acquisition and analysis system for the DIII-D multipulse Thomson scattering diagnostic
[DE91-002720] N91-14025
ARGON
Ar/S N91-14153
ARGON PLASMA
Coherent anti-Stokes Raman spectroscopic measurement of air entrainment in argon plasma jets
[DE91-001936] N91-13670
Measurement of air entrainment in plasma jets
[DE91-001943] N91-14013
ARITHMETIC AND LOGIC UNITS
CESAR MALU program library
[FFI-90/7010] N91-13922
ARRAYS
Superconducting neural network computer and sensor array
[AD-D014625] N91-13887
ARTIFICIAL INTELLIGENCE
Coupling artificial intelligence and a system dynamics simulation to optimize quality assurance and testing in software development
[AD-A226580] N91-13902
Tightly coupled simulation utilizing the EBR-II LMR: A real-time supercomputing and AI environment
[DE91-001942] N91-13932
Specifications extraction and synthesis: Their correlations with preliminary design N91-13936
Applications of artificial intelligence to mission planning
[NASA-CR-184994] N91-13939
A tutorial on the construction of high-performance resolution/paramodulation systems
[DE91-001096] N91-13942
Proceedings of the Workshop on Software Tools for Distributed Intelligent Control Systems
[DE91-001755] N91-13943
Report of foreign travel
[DE91-001732] N91-14082
ARTIFICIAL SATELLITES
Orbit determination and analysis for Aureole 2 rocket at 27:2 resonance
[RAE-TR-90018] N91-13472
The use of satellite data in the ECMWF analysis system
[KNMI-TR-123] N91-13790
ASBESTOS
Summary of JAYGO mixing and FSM-1 application of castable inhibitor and liner
[NASA-CR-184030] N91-13569
Environmental projects. Volume 12: Friable asbestos abatement, GDSCC
[NASA-CR-187636] N91-13808
ASSEMBLY LANGUAGE
BAG: A programming language for the CESAR buffer address generator
[FFI-90/7022] N91-13923
ASSOCIATIVE PROCESSING (COMPUTERS)
BSB radar pulse classification
[FEL-90-B023] N91-13603
ASTRONAUTS
A computer model to determine the primary contributors to relative radiation dose received by astronauts
[DE90-015681] N91-13866
ASTRONOMICAL MODELS
Axions and SN 1987A: Axion trapping
[NASA-CR-186467] N91-13976
U1(prime) dark matter and R-parity violation
[DE91-001792] N91-14068
The large-scale space distribution of emission-line galaxies N91-14091
Gas flows in elliptical galaxies N91-14170
One-dimensional cloud fluid model for propagating star formation N91-14211
A combined N-body and hydrodynamic code for modeling disk galaxies N91-14241
Properties of the Magellanic-type galaxies
N91-14245
Ionization in the local interstellar and intergalactic media N91-14249
ASTRONOMICAL PHOTOGRAPHY
Methodology to treat stellar images
[IFSI-89-21] N91-14094
ASTRONOMICAL PHOTOMETRY
FIRST: Far Infrared and Submillimetre Space Telescope
[ESA-BR-69] N91-14095
The stellar content of M101 N91-14244
ASTRONOMY
A solar chronometer for climate: Astronomical and geophysical evidence N91-13823
ASTROPHYSICS
Thermal instabilities in protogalactic clouds
N91-14195
ASYMMETRY
Localize and identify the gravity sensing mechanism of plants
[NASA-CR-187411] N91-13841
ASYMPTOTIC SERIES
An asymptotic symmetry of the rapidly forced pendulum
[DE91-001868] N91-13958
ATMOSPHERIC BOUNDARY LAYER
Review of geography internship of convective wave project
[NASA-CR-187022] N91-13819

Simulation of the formation and transport of ozone in the atmospheric boundary layer
[DLR-FB-90-25] N91-13827
Gravity waves excited by flow over an obstacle
[FFI-90/7017] N91-13828
Interannual variation of seasonal means and subseasonal variability of cloud streets off the east coast of North America 1984-1987
[NASA-CR-187021] N91-13831

ATMOSPHERIC CHEMISTRY
NRL 1989 beam propagation studies in support of the ATA multi-pulse propagation experiment
[AD-A226443] N91-13588
Atmospheric and geophysical sciences division program report, 1988 - 1989
[DE91-001057] N91-13780
Acidic deposition and the environment
[DE91-002352] N91-13812
Stratospheric ozone conservation by electron attachment to chlorine atoms: The negative-ion chemistry
[DE91-002951] N91-13815
Aeronomic chemistry of ozone
[AERONOMICA-ACTA-A-355-1990] N91-13816
Research projects including climate, atmospheric chemistry, solar-terrestrial physics, metrology, and storm systems
[PB90-256306] N91-13820
Simulation of the formation and transport of ozone in the atmospheric boundary layer
[DLR-FB-90-25] N91-13827

ATMOSPHERIC CIRCULATION
Review of geography internship of convective wave project
[NASA-CR-187022] N91-13819
Interannual variation of seasonal means and subseasonal variability of cloud streets off the east coast of North America 1984-1987
[NASA-CR-187021] N91-13831
Tropical Pacific moisture variability: Its detection, synoptic structure and consequences in the general circulation
[NASA-CR-184045] N91-13832
Frontal interactions with orography: Objective cross-sectional analysis of ALPEX data N91-13836

ATMOSPHERIC COMPOSITION
Terrestrial ecosystems and climatic change
[DE91-001492] N91-13813
Stratospheric ozone conservation by electron attachment to chlorine atoms: The negative-ion chemistry
[DE91-002951] N91-13815
Historical overview of the Biosphere 2 project N91-13844
Biosphere 2 test module experimentation program N91-13845

ATMOSPHERIC DIFFUSION
The influence of the sampling time on diffusion measurements in the atmosphere N91-13824

ATMOSPHERIC EFFECTS
Assessments of atmospheric effects on VHF and UHF communications
[AD-A226661] N91-13592

ATMOSPHERIC GENERAL CIRCULATION MODELS
A physical parameterization of snow albedo for use in climate models N91-13781

ATMOSPHERIC MODELS
Utilization of the HIPAS facility for cooperative experiments related to ionospheric modification
[AD-A226609] N91-13590
The influence of the sampling time on diffusion measurements in the atmosphere N91-13824
Simulation of the formation and transport of ozone in the atmospheric boundary layer
[DLR-FB-90-25] N91-13827
A study of the ice-hail charge separation mechanism using a thunderstorm electrification model with explicit microphysics in a kinematic framework N91-13835

ATMOSPHERIC PHYSICS
Atmospheric and geophysical sciences division program report, 1988 - 1989
[DE91-001057] N91-13780
Research projects including climate, atmospheric chemistry, solar-terrestrial physics, metrology, and storm systems
[PB90-256306] N91-13820

ATMOSPHERIC RADIATION
A preliminary ocean ARM (Atmospheric Radiation Measurements) guide for climatic evaluations
[DE91-001120] N91-13811

ATMOSPHERIC REFRACTION
Assessments of atmospheric effects on VHF and UHF communications
[AD-A226661] N91-13592

ATOMIC EXCITATIONS
Influence of the delocalized excitation process on the determination of foreign atom positions using the channeling effect
[ETN-91-98175] N91-14065

ATOMIC THEORY
Atomic and molecular theory
[DE91-004475] N91-13983

ATOMIZERS
Measurements and predictions of a liquid spray from an air-assist nozzle
[NASA-TM-103640] N91-13455

ATOMS
Influence of the delocalized excitation process on the determination of foreign atom positions using the channeling effect
[ETN-91-98175] N91-14065

ATTITUDE (INCLINATION)
Gradiometry coexperiments to the gravity probe B and step missions
[NASA-CR-187704] N91-13788

ATTITUDE GYROS
A preliminary look at techniques used to obtain airdata from flight at high angles of attack
[NASA-TM-101729] N91-13453

AUTOMATIC CONTROL
An application of multiattribute decision analysis to the Space Station Freedom program. Case study: Automation and robotics technology evaluation
[NASA-CR-187432] N91-13476
Standard remote manipulator system docking target augmentation for automated docking
[NASA-CASE-MFS-28419-1] N91-13482
Study of the time and effort signal in cutting operations
[CETIM-101580] N91-13583
Positional estimation techniques for an autonomous mobile robot
[NASA-CR-187689] N91-13725
Solder dross removal apparatus
[NASA-CASE-MFS-28406-1] N91-13729

AUTOMATIC FLIGHT CONTROL
Modern robust control for missile autopilot design N91-13435

AUTOMATIC PILOTS
Missile Interceptor Guidance System Technology
[AGARD-LS-173] N91-13434
Modern robust control for missile autopilot design N91-13435
Flight control design issues in bank-to-turn missiles N91-13437

AUTOMOBILES
Advanced Materials Development Program: Ceramic Technology for Advanced Heat Engines program plan, 1983--1993
[DE91-000516] N91-13555
The 1990 JSAE (Society of Automative Engineers of Japan, Inc.) Spring Convention Proceedings 901
[DE91-715185] N91-13579
Results from the second year of operation of the Federal Methanol Fleet at Oak Ridge National Laboratory
[DE91-000543] N91-13718
Adaptable driver-car interfacing and mental workload: A review of the literature
[IZF-1990-B-3] N91-13874

AUTONOMOUS NAVIGATION
Positional estimation techniques for an autonomous mobile robot
[NASA-CR-187689] N91-13725

AUTONOMY
Bilevel shared control for teleoperators
[NASA-CASE-NPO-17800-1-CU] N91-13724

AUTOREGRESSIVE PROCESSES
Comparison of spectral estimators application to ground sensor signals
[FEL-1988-85] N91-13605

AVALANCHE DIODES
A silicon avalanche photodiode detector circuit for Nd:YAG laser scattering
[DE91-002709] N91-13706

AVIONICS
Applications of Superconductivity to Avionics
[AGARD-CP-481] N91-14030
Analog superconductive electronics for avionics N91-14040
Fabrication and characterization of high temperature superconducting thin films for sensors and electronics N91-14041
A liquid nitrogen cooled superconductive electron beam focusing system for improved performance ECM helix traveling wave tubes N91-14047

AZO COMPOUNDS
A new approach to design of cross-linked second-order nonlinear optical polymers
[AD-A226674] N91-13553

B

B STARS
IRAS observations of the ISM in the gamma CAS reflection nebula N91-14140

BACKGROUND RADIATION
COBE's search for structure in the Big Bang
[NASA-TM-102976] N91-14271

BACKSCATTERING
SAR detection of topography, vegetation and installations over land
[FFI-90/7016] N91-13600

BACKWARD FACING STEPS
A steadying effect of acoustic excitation on transitory stall
[NASA-TM-103689] N91-13420

BALLISTIC MISSILES
A linear accelerator in the space: The beam experiment aboard rocket
[DE91-002347] N91-13988

BALLOON SOUNDING
Evaluation of a wind profile model
[FOA-E-40045-4.5] N91-13839

BALMER SERIES
The Hawaii Imaging Fabry-Perot Interferometer (HIFI) N91-14240
Spectrum formation in SN1987A N91-14243

BAND STRUCTURE OF SOLIDS
Optical properties and electronic structures of d- and f-electron metals and alloys, Ag-In, Ni-Cu, AuGa2, PtGa2, beta'-NiAl, beta'-CoAl, CeSn3, and LaSn3
[DE91-001597] N91-14059

BARIUM OXIDES
Progress in high Tc superconductors N91-14031

BARRED GALAXIES
Are bars essential for starbursts in non-interacting galaxies N91-14208
Near-infrared mapping of spiral barred galaxies N91-14217

BATHS
Solder dross removal apparatus
[NASA-CASE-MFS-28406-1] N91-13729

BAYES THEOREM
Parallel Ada benchmarks for the SVMS
[NASA-CR-182453] N91-13929

BEACON COLLISION AVOIDANCE SYSTEM
Modelling and performance analysis of four and eight element TCAS
[NASA-CR-187414] N91-13428

BEAM INJECTION
MPPE (Multiple Pulse Propagation Experiment) results
[DE91-001678] N91-13599
SEPAC data analysis in support of the environmental interaction program
[NASA-CR-184028] N91-13807
Injection efficiency of bound modes
[NASA-CR-4333] N91-13991

BEAM INTERACTIONS
Diagnostics for high-brightness beams
[DE91-001865] N91-13701

BEAM LEADS
MPPE (Multiple Pulse Propagation Experiment) results
[DE91-001678] N91-13599

BEAMS (SUPPORTS)
A computational procedure for the dynamics of flexible beams within multibody systems
[NASA-CR-187667] N91-13760
Specifications extraction and synthesis: Their correlations with preliminary design N91-13936

BED REST
Physiological responses to prolonged bed rest in humans: A compendium of research, 1981-1988
[NASA-TM-102249] N91-13862

BEDS (GEOLOGY)
Exobiology site selection for future Mars missions: Martian paleolake sediments and terrestrial analogs
[NASA-CR-187358] N91-14255

BELTS
Heat engine with corrugated shape memory drive belt
[AD-D014640] N91-13716

BEND TESTS
Three point bend creep testing of carbon/epoxy
[DE91-001083] N91-13501
Fatigue testing of plasma-sprayed thermal barrier coatings, volume 2
[NASA-CR-186726] N91-13535

BENZENE
Interfacial chemistry of titanium films deposited on PMDA-ODA polyimide
[AD-A225730] N91-13550

BERNOULLI THEOREM
A fully Sinc-Galerkin method for Euler-Bernoulli beam models
[NASA-CR-187462] N91-13952

BETA PARTICLES
X ray and charged particle detection with CsI(Tl) layer coupled to a-Si:H photodiode layers
[DE91-001798] N91-14060
BIBLIOGRAPHIES
Aeronautical engineering: A continuing bibliography with indexes (supplement 258)
[NASA-SP-7037(258)] N91-13399
Bolted structural assemblies: Bibliographic analysis
[CETIM-13N061] N91-13742
Spectrum fatigue testing: A literature survey
[FFA-TN-1990-40] N91-13772
SERI photovoltaic subcontract reports: Abstracts and document control information
[DE90-000378] N91-13792
An indexed bibliography on tracking
[AD-A226682] N91-13870
BIMETALS
Fundamental investigations of supported monometallic and bimetallic catalysts by proton magnetic resonance spectroscopy
[DE91-000610] N91-13516
BINARY MIXTURES
Transport properties of dense fluid mixtures using nonequilibrium molecular dynamics
[DE91-000262] N91-13654
BINARY STARS
Research in theoretical physics
[DE91-002458] N91-14071
BINAURAL HEARING
Adaptive inverse filters for stereophonic sound reproduction
[ISVR-TR-187] N91-13975
BINDERS (MATERIALS)
Method of making single crystal fibers
[NASA-CASE-LEW-14921-1] N91-13502
Method of making carbide/fluoride/silver composites
[NASA-CASE-LEW-14902-1] N91-13503
Binders used in metal injection molding
[VTT-RR-691] N91-13529
Heat transfer device and method of making the same
[NASA-CASE-LEW-14162-1] N91-13668
BINOMIALS
On combining selection and estimation in the search for the largest binomial parameter
[AD-A226595] N91-13953
BIOCHEMISTRY
JPRS Report: Science and technology. USSR: Life sciences
[JPRS-ULS-89-011] N91-13861
BIOGEOCHEMISTRY
Earth observing satellite: Understanding the Earth as a system N91-13853
BIOINSTRUMENTATION
Cognitive and neural bases of skilled performance
[AD-A226668] N91-13869
BIOLOGICAL EFFECTS
Inorganic concepts relevant to metal binding, activity, and toxicity in a biological system
[DE91-001489] N91-13858
Thermoregulatory consequences of resonant microwave exposure
[AD-A226540] N91-13864
BIOMAGNETISM
Cognitive and neural bases of skilled performance
[AD-A226668] N91-13869
BIOMASS
The CELSS breadboard project: Plant production N91-13849
CELSS research and development program N91-13850
BIOMEDICAL DATA
Biomedical program at Space Biospheres Ventures N91-13847
BIOREACTORS
Soil bed reactor work of the Environmental Research Lab. of the University of Arizona in support of the research and development of Biosphere 2 N91-13846
BIOSPHERE
Biological Life Support Technologies: Commercial Opportunities
[NASA-CP-3094] N91-13842
Biospheres and solar system exploration N91-13843
Historical overview of the Biosphere 2 project N91-13844
Biosphere 2 test module experimentation program N91-13845
Soil bed reactor work of the Environmental Research Lab. of the University of Arizona in support of the research and development of Biosphere 2 N91-13846
Biomedical program at Space Biospheres Ventures N91-13847
Plants and their microbial assistants: Nature's answer to Earth's environmental pollution problems N91-13851
BIOTECHNOLOGY
JPRS Report: Science and technology. USSR: Life sciences
[JPRS-ULS-89-011] N91-13861
BIPOLAR TRANSISTORS
Radiation effects on JFETs (Junction Field-Effect Transistors), MOSFETs, and dipolar transistors, as related to SSC circuit design
[DE91-001486] N91-13618
Evaluation and fabrication of GaAs integrated logic circuits
[LAAS-90160] N91-13628
High-gain AlGaAs/GaAs double heterojunction Darlington phototransistors for optical neural networks
[NASA-CASE-NPO-18101-1-CU] N91-13995
BIPOLARITY
Magnetic collimation of protostellar winds into bipolar outflows N91-14182
BIREFRINGENCE
Use of dome (meniscus) lenses to eliminate birefringence and tensile stresses in spatial filters for the Nova laser
[DE91-002784] N91-13707
BIREFRINGENT FILTERS
Use of dome (meniscus) lenses to eliminate birefringence and tensile stresses in spatial filters for the Nova laser
[DE91-002784] N91-13707
BISMALEIMIDE
Preparation of polyimides from bis(N-isoprenyl)s of aryl diamides
[NASA-CASE-LAR-14330-1-CU] N91-13560
BIT ERROR RATE
Detection of multiple-bit errors from single-ion tracks in integrated circuits
[NASA-CASE-NPO-18075-1-CU] N91-13622
BLACK HOLES (ASTRONOMY)
A survey of galaxies in CO N91-14118
BLADE-VORTEX INTERACTION
Transonic blade-vortex interactions noise: A parametric study
[NASA-CR-187713] N91-13422
BLOCK COPOLYMERS
The synthesis of star block copolymers by controlled ring-opening metathesis polymerization
[AD-A225987] N91-13551
BLOWDOWN WIND TUNNELS
The IAR high Reynolds number two-dimensional test facility: A description of equipment and procedures common to most 2-D airfoil tests
[AD-A226629] N91-13409
BLUNT BODIES
Effect of bulk viscosity in low density, hypersonic blunt body flows
[DE90-012756] N91-13419
BLURRING
Modelling the effects of vibration on visual performance
[ISVR-TR-171] N91-13883
BODY KINEMATICS
Constraint treatment techniques and parallel algorithms for multibody dynamic analysis
[NASA-CR-187668] N91-13759
BOEING 737 AIRCRAFT
A flight expert system for on-board fault monitoring and diagnosis
[NASA-CR-187334] N91-13452
BOLTED JOINTS
Bolted structural assemblies: Bibliographic analysis
[CETIM-13N061] N91-13742
Calculations for structures with nonlinear joints
[CETIM-108830] N91-13776
BOLTZMANN TRANSPORT EQUATION
Lattice Boltzmann methods for some 2-D nonlinear diffusion equations: Computational results
[DE91-004175] N91-13962
BONDING
Electrocatalyst surfaces
[PB90-252560] N91-13507
Dual diaphragm tank with telltale drain
[NASA-CASE-MSC-21703-1] N91-13580
Analysis of bond quality by resonant ultrasound
[DE91-000439] N91-13743
BONES
Calcified-tissue investigations using synchrotron x ray microscopy
[DE91-001729] N91-13859
BOOLEAN ALGEBRA
An object-oriented logic language for modular system specification
[REPT-90-027] N91-13927
BOREHOLES
Development and computer aided residual stress measurements on coated specimen using blind-hole drilling technique N91-13544
BOSONS
Axions and SN 1987A: Axion trapping
[NASA-CR-186467] N91-13976
BOUNDARIES
A minimization method adapted to the finite element technique for turbulent flow simulation with nonlinear boundary conditions in the wall vicinity
[ECL-90-016] N91-13664
BOUNDARY CONDITIONS
Development of a time-dependent incompressible Navier-Stokes solver based on a fractional-step method
[NASA-CR-182323] N91-13639
A fully Sinc-Galerkin method for Euler-Bernoulli beam models
[NASA-CR-187462] N91-13952
BOUNDARY ELEMENT METHOD
Development of BEM for ceramic composites
[NASA-CR-187676] N91-13557
Finite element and boundary element methods for elastoplastic stress analysis of two-dimensional and axisymmetric problems N91-13755
BOUNDARY LAYER CONTROL
Analysis of the leading edge effects on the boundary layer transition
[NASA-CR-187361] N91-13405
The IAR high Reynolds number two-dimensional test facility: A description of equipment and procedures common to most 2-D airfoil tests
[AD-A226629] N91-13409
BOUNDARY LAYER FLOW
Transonic blade-vortex interactions noise: A parametric study
[NASA-CR-187713] N91-13422
Computation of incompressible flow around the DARPA SUBOFF bodies
[AD-A226481] N91-13646
Turbulence modeling for sharp-fin-induced shock wave/turbulent boundary-layer interactions
[NASA-TM-102828] N91-13652
A laser Doppler velocimeter approach for near-wall three-dimensional turbulence measurements
[NASA-TM-102841] N91-13653
BOUNDARY LAYER TRANSITION
Analysis of the leading edge effects on the boundary layer transition
[NASA-CR-187361] N91-13405
Transition control via boundary layer heating
[ARE-TR-88503] N91-13667
BOUNDARY LAYERS
Development of a full potential solver for rotor aerodynamics analysis N91-13407
Fluid flow effects on electroplating
[DE91-001087] N91-13577
BOUNDARY VALUE PROBLEMS
Numerical methods for boundary value problems in differential-algebraic equations
[DE91-001748] N91-13956
BRACKETS
Robot cable-compliant devices
[NASA-CASE-GSC-13127-1] N91-13735
BRANCHING (MATHEMATICS)
The route to chaos for the Kuramoto-Sivashinsky equation
[NASA-CR-187461] N91-13642
Logics for the description of processes and their properties: Expressivity and decidability
[ETN-91-98200] N91-13960
BRANCHING (PHYSICS)
Theoretical temperature-dependent branching ratios and laser thresholds of the (5)I7 yields (5)I8 levels of Ho3(+) in ten garnets
[NASA-TM-103429] N91-14053
BRAZIL
Utilization of IHS transformation for integration of images of differing resolutions: Urban land use study
[INPE-4606-PRE/1329] N91-14086
BREADBOARD MODELS
The CELSS breadboard project: Plant production N91-13849
BREEDER REACTORS
Tightly coupled simulation utilizing the EBR-II LMR: A real-time supercomputing and AI environment
[DE91-001942] N91-13932
BREMSSTRAHLUNG
The infrared continuum spectrum of x ray illuminated molecular gas N91-14144
BRIDGMAN METHOD
Morphological stability and kinetics in crystal growth from vapors
[NASA-CR-187650] N91-14055
BRIGHTNESS
Ultra-high brightness (greater than 10(exp 21) W/sq cm) laser facility
[DE91-001685] N91-13698
A comparison of UV surface brightness and HI surface densities for spiral galaxies N91-14102

The FCRAO extragalactic CO survey: Global properties of galaxies N91-14117
The onset of galactic winds in early-type galaxies N91-14165
An infrared jet in Centaurus A (NGC 5128): Evidence for interaction between the active nucleus and the interstellar medium N91-14175
Are bars essential for starbursts in non-interacting galaxies N91-14208

BRIGHTNESS DISTRIBUTION
Contribution of cool dust to the FIR brightness distribution of NGC 6946 Sc(s)2 N91-14134

BRIGHTNESS TEMPERATURE
High brightness neutral hydrogen in M31: A new probe of interstellar pressure N91-14196
Centimeter emission variation of Venus: Its second phase
[INPE-5122-TDL/423] N91-14257

BRITTLENESS
Synthesis and characterization of high temperature superconductor materials N91-14048

BROADBAND
Loading the LES-9 wideband UHF transponder
[AD-A226179] N91-13475
Computational and experimental progress on laser-activated gas avalanche switches for broadband, high-power electromagnetic pulse generation
[DE91-001763] N91-13623
Computation of broadband mixing noise from turbomachinery
[AD-A226559] N91-13969
Ultrasound generation through a fiber optic delivery system using pulsed laser energy
[DE91-001914] N91-13970
Ultrafast optical electronics center
[AD-A226669] N91-14054

BROADCASTING
Real-time data compression of broadcast video signals
[NASA-CASE-LEW-14945-1] N91-13598

BUBBLE CHAMBERS
Elementary particle interactions
[DE91-001220] N91-13979

BUBBLES
Infrared analysis of LMC superbubbles N91-14181

BUCKLING
Experimental observations and finite element analysis of the initiation of fiber microbuckling in notched composite laminates
[NASA-CR-185354] N91-13756

BUDGETING
Coordinates of a life-cycle model for a software system and communicating the need for software technology
[AD-A226592] N91-13903

BUFFETING
Some buffet response characteristics of a twin-vertical-tail configuration
[NASA-TM-102749] N91-13412

BUNCHING
Influence of collective effects on the performance of high-luminosity colliders
[DE91-001797] N91-13982

BURNING TIME
Fast Pb-glass neutron-to-light converter for ICF (Inertial Confinement Fusion) target burn history measurements
[DE91-002670] N91-14021

C

CABLES (ROPES)
Sheave assembly
[AD-D014605] N91-13711

CALCIUM
Calcified-tissue investigations using synchrotron x ray microscopy
[DE91-001729] N91-13859

CALCULUS
Implementing automatic differentiation efficiently
[DE91-002409] N91-13913

CALCULUS OF VARIATIONS
Variational transition state theory
[DE91-001253] N91-14058

CALIBRATING
A preliminary look at techniques used to obtain airdata from flight at high angles of attack
[NASA-TM-101729] N91-13453
Calibration of the 13- by 13-inch adaptive wall test section for the Langley 0.3-meter transonic cryogenic tunnel
[NASA-TP-3049] N91-13461
Evaluation of a simple method for color monitor recalibration
[IZF-1990-B-4] N91-13608
Far field wake velocity measurements with hot film probes
[AD-A226650] N91-13647
Calibration set up for load cells
[PD-ST-8917] N91-13673
Data reduction of digitized images processed from calibrated photographic and spectroscopic films obtained from terrestial, rocket and space shuttle telescopic instruments
[NASA-CR-187320] N91-13674
Practical considerations for the measurement of internal and coupling loss factors on complex structures
[ISVR-TR-182] N91-13778
Review of uncertainties in the use of NPL primary standards of x ray exposure for the calibration of secondary standards in terms of exposure and air kerma
[NPL-RS(EXT)-109] N91-13868
An x ray photoelectron spectroscopy study of Au(x)In(y) alloys
[NASA-TM-103659] N91-14050

CALIFORNIA
Precision, accuracy, and tectonics from the Global Positioning System N91-13822

CAMERAS
Deep narrow band imagery of the diffuse ISM in M33 N91-14202

CANTILEVER MEMBERS
Cantilever clamp fitting
[NASA-CASE-MFS-28328-1] N91-13731

CAPILLARY TUBES
Dynamic high-pressure studies of an electrothermal capillary
[DE91-000966] N91-13617

CARBIDES
Interfacial chemistry of titanium films deposited on PMDA-ODA polyimide
[AD-A225730] N91-13550

CARBON
Multiphase carbon and its properties in complex mixtures
[DE91-001679] N91-13499
CS in nearby galaxies: Distribution, kinematics, and multilevel studies N91-14235

CARBON DIOXIDE
Carbon dioxide reforming of methane in a solar volume-TRIC receiver-reactor: The CAESAR (Catalytically Enhanced Solar Absorption Receiver) project
[DE91-002340] N91-13800
Carbon dioxide release from Ocean Thermal Energy Conversion (OTEC) cycles
[DE89-009504] N91-13809

CARBON DIOXIDE LASERS
Folded RF-excited CO2 waveguide lasers N91-13695

CARBON FIBER REINFORCED PLASTICS
Effects of temperature on acoustically-induced strains and damage propagation in CFRP plates N91-13493
Work of fracture of composites in axial compression: Measurement and origins
[RARDE-1/90] N91-13505

CARBON MONOXIDE
The Interstellar Medium in External Galaxies: Summaries of contributed papers
[NASA-CP-3084] N91-14100
A survey of galaxies in CO N91-14118
Circumnuclear molecular gas in starburst and Seyfert galaxies N91-14120
High resolution CO images of Seyfert Galaxies N91-14121
Aperture synthesis CO observations of the inner disk of NGC 1068 N91-14122
Observations of CO in the Magellanic irregular galaxy NGC 55 N91-14124
The CO-12 and CO-13 J=2-1 and J=1-0 observations of hot and cold galaxies N91-14126
High resolution sub-millimetre mapping of starburst galaxies: Comparison with CO emission N91-14129
A comparison of the radial distribution of molecular gas and non-thermal radio continuum in spiral disks N91-14145
A relationship between the integrated CO intensity and the radio continuum emission in spiral galaxies N91-14146
CO observations of southern mergers N91-14197
A high resolution CO map of M51 N91-14203
M51: Molecular spiral arms, GMAs and superclouds N91-14204
Global and radial variations in the efficiency of massive star formation among galaxies N91-14215
The molecular spiral arms of NGC 6946 N91-14232
CO excitation in four IR luminous galaxies N91-14234
Spatial variation of the physical conditions of molecular gas in galaxies N91-14236
Detection of CO emission in Hydra 1 cluster galaxies N91-14237
CO distribution in southern S0 galaxies N91-14239

CARBON 13
Development and initial characterization of a nuclear magnetic resonance dosimetry system
[DE91-001775] N91-13867

CARBONYL COMPOUNDS
Methyl substituted polyimides containing carbonyl and ether connecting groups
[NASA-CASE-LAR-14351-1] N91-13561

CARNOT CYCLE
Performance comparison of magnetic refrigeration cycles
[DE91-001520] N91-13578

CARRIER DENSITY (SOLID STATE)
A theoretical investigation of effective surface recombination velocity in AlGaAs/GaAs heteroface solar cells
[DE91-001754] N91-13795

CASSEGRAIN OPTICS
Wide acceptance angle, high concentration ratio, optical collector
[NASA-CASE-MFS-28295-1] N91-13999

CASTING
Novel polyimide molding powder, coating, adhesive, and matrix resin
[NASA-CASE-LAR-14163-1] N91-13559

CASTINGS
Transducer holder and method of making
[NASA-CASE-LAR-14027-1] N91-13693

CATALOGS
List of standards to accompany manual of documentation practices applicable to defence-aerospace scientific and technical information. Addendum
[AGARD-AG-235-ADD] N91-14076

CATALOGS (PUBLICATIONS)
Catalogue of ESA patents
[ESA-SP-1131] N91-14083

CATALYSTS
Fundamental investigations of supported monometallic and bimetallic catalysts by proton magnetic resonance spectroscopy
[DE91-000610] N91-13516
An exploratory program for using hydrous metal oxide ion exchangers as Fischer-Tropsch catalysts
[DE91-002341] N91-13521
Corrosion-resistant catalyst supports for phosphoric acid fuel cells
[DE91-001713] N91-13794
Carbon dioxide reforming of methane in a solar volume-TRIC receiver-reactor: The CAESAR (Catalytically Enhanced Solar Absorption Receiver) project
[DE91-002340] N91-13800

CATHODES
Corrosion-resistant catalyst supports for phosphoric acid fuel cells
[DE91-001713] N91-13794
Fuel cells
[DE90-009686] N91-13805

CATHODIC COATINGS
Corrosion-resistant catalyst supports for phosphoric acid fuel cells
[DE91-001713] N91-13794

CAUCHY PROBLEM
Generalized flux vectors for hypersonic shock capturing
[MBB/FE122/S/PUB/397] N91-13423

CAVITIES
Measurement of waves in flows across a surface
[NASA-CASE-NPO-17479-1-CU] N91-13658
The violent interstellar medium in Messier 31 N91-14178
Evolution of a superbubble blastwave in a magnetized medium N91-14180

CAVITY RESONATORS
A complex permittivity and permeability measurement system for elevated temperatures
[NASA-CR-186916] N91-13609
Relativistic kylstron simulations using RKTW2D
[DE91-001747] N91-13619
Influence of collective effects on the performance of high-luminosity colliders
[DE91-001797] N91-13982

CELLS (BIOLOGY)
X ray holography at Lawrence Livermore National Laboratory
[DE91-002673] N91-13690
Three-dimensional cell to tissue assembly process
[NASA-CASE-MSC-21559-1] N91-13860

CENTAUR LAUNCH VEHICLE
All Shuttle Centaur engine and nozzle support plug vibration testing
[NASA-CR-183201] N91-13485
RL10A-3-3B high mixture ratio qualification program
[NASA-CR-183200] N91-13486

Shuttle Centaur engine cooldown evaluation and effects of expanded inlets on start transient
[NASA-CR-183198] N91-13487

CENTRIFUGAL COMPRESSORS
Theory of finite disturbances in a centrifugal compression system with a vaneless radial diffuser
[NASA-CR-187049] N91-13458

CENTRIFUGING STRESS
Vestibulo-ocular responses in man to +G sub z hypergravity
[IZF-1989-59] N91-13873

CERAMIC COATINGS
Residual stresses in ceramics
[JUEL-SPEZ-550] N91-13536
X ray measurements of residual stresses in thin, hard layers N91-13542
Development and computer aided residual stress measurements on coated specimen using blind-hole drilling technique N91-13544

CERAMIC MATRIX COMPOSITES
Development of BEM for ceramic composites
[NASA-CR-187676] N91-13557

CERAMICS
Thermal and structural assessments of a ceramic wafer seal in hypersonic engines
[NASA-TM-103651] N91-13456
Research and development of a ceramic fiber composite heat exchanger
[DE90-017250] N91-13497
Composite thermal barrier coating
[NASA-CASE-LEW-14999-1] N91-13500
Method of making single crystal fibers
[NASA-CASE-LEW-14921-1] N91-13502
Residual stresses in ceramics
[JUEL-SPEZ-550] N91-13536
Use of neutron diffraction methods for the determination of mechanical stresses in metal ceramic laminated composite materials N91-13537
Determination of residual stresses in ceramics materials using neutron diffraction N91-13538
Residual stresses analyses in ceramics and metal ceramic composites using x ray methods N91-13539
The x ray elastic constants of ceramic materials for the determination of the stresses from lattice expansion measurements N91-13541
Determination of stresses in ceramics using ultrasonic methods: Possibilities and limitations N91-13546
Possibilities of stress measurement on ceramic materials using acoustic microscopy N91-13547
Calculations of residual stresses in ceramic soldered joints N91-13549
Optical characterization techniques applied to ceramic oxides
[DE91-001526] N91-13558
Development of BEM for ceramic composites
[NASA-CR-187676] N91-13557
Fracture of ceramics under farfield cyclic compression
[DE90-008417] N91-13563
Testing of engineering ceramics, summary
[VTT-RR-678] N91-13567
Analytical and experimental studies for thermal plasma processing of materials
[DE91-000599] N91-13576
An x ray photoelectron spectroscopy study of Au(x)In(y) alloys
[NASA-TM-103659] N91-14050

CEREBRAL CORTEX
Cognitive and neural bases of skilled performance
[AD-A226668] N91-13869

CESIUM IODIDES
X ray and charged particle detection with CsI(Tl) layer coupled to a-Si:H photodiode layers
[DE91-001798] N91-14060

CETANE
High-alcohol microemulsion fuel performance in a diesel engine
[DE91-001617] N91-13572

CHANNEL FLOW
Large-eddy simulation of transitional channel flow
[NASA-CR-187465] N91-13410

CHAOS
The route to chaos for the Kuramoto-Sivashinsky equation
[NASA-CR-187461] N91-13642
Fractals and chaotic dynamics in tectonics: Applications to topography and seismicity N91-13821
Chaos and order in non-integrable model field theories
[DE91-002313] N91-14070
Linear vs nonlinear and infinite vs finite: An interpretation of chaos
[DE91-002522] N91-14072

CHAPMAN-ENSKOG THEORY
Lattice Boltzmann methods for some 2-D nonlinear diffusion equations: Computational results
[DE91-004175] N91-13962
Regularized Chapman-Enskog expansion for scalar conservation laws
[NASA-CR-187441] N91-13966

CHARACTERIZATION
Laboratory investigation of the use of geotextiles to mitigate frost heave
[DOT/FAA/RD-90/13] N91-13465
Method and apparatus for characterizing residual stress in ferromagnetic materials
[NASA-CASE-LAR-14239-1] N91-13527
High Tc superconductors for microwave filters N91-14038

CHARGE COUPLED DEVICES
Twelve signals multiplexed with the LLNL optical streak camera
[DE91-000066] N91-13680
Portable dynamic fundus instrument
[NASA-CASE-MSC-21675-1] N91-13865
HII regions in dwarf irregular galaxies of the local group N91-14156
Deep narrow band imagery of the diffuse ISM in M33 N91-14202

CHARGE TRANSFER
Secondary Li battery incorporating 12-crown-4 ether
[NASA-CASE-NPO-17922-1-CU] N91-13621
A study of the ice-hail charge separation mechanism using a thunderstorm electrification model with explicit microphysics in a kinematic framework N91-13835
Assessment of ion-atom collision data for magnetic fusion plasma edge modelling
[DE91-001920] N91-14012
Spectrum formation in SN1987A N91-14243

CHARGED PARTICLES
NRL 1989 beam propagation studies in support of the ATA multi-pulse propagation experiment
[AD-A226443] N91-13588
A critical review of charged particle astronomy at Saturn: The evidence for co-orbiting material in the inner satellite system
[NASA-CR-187348] N91-14090

CHARTS
Colour specifications for the Electronic Chart Display and Information System (ECDIS)
[IZF-1990-A-19] N91-13789

CHEMICAL ANALYSIS
Actinide speciation by photothermal spectroscopies: Instrumentation development
[DE91-001854] N91-13700
Microbial ecology laboratory procedures manual NASA/MSFC
[NASA-CR-184033] N91-13856

CHEMICAL BONDS
Inorganic concepts relevant to metal binding, activity, and toxicity in a biological system
[DE91-001489] N91-13858
The role of chemical interactions in ion-solid processes
[DE91-000763] N91-13977

CHEMICAL COMPOSITION
Progress in high Tc superconductors N91-14031
Synthesis and characterization of high temperature superconductor materials N91-14048

CHEMICAL EQUILIBRIUM
Study of improved methods for predicting chemical equilibria
[DE91-000263] N91-13509

CHEMICAL EVOLUTION
The onset of galactic winds in early-type galaxies N91-14165

CHEMICAL PROPERTIES
The molecular structure of the HAN-based liquid propellants
[AD-A226415] N91-13571

CHEMICAL REACTIONS
Influence of thermodynamical modelization for chemically reacting air flow
[MBB/FE122/S/PUB/400] N91-13418
Computed potential energy surfaces for chemical reactions
[NASA-CR-186877] N91-13506
Electrocatalyst surfaces
[PB90-252560] N91-13507
Reactions of the excited state of polypyridyl chromium(III) ion
[DE91-000741] N91-13526
The synthesis of star block copolymers by controlled ring-opening metathesis polymerization
[AD-A225987] N91-13551
The role of chemical interactions in ion-solid processes
[DE91-000763] N91-13977
Variational transition state theory
[DE91-001253] N91-14058

CHEMICAL REACTORS
Carbon dioxide reforming of methane in a solar volume-TRIC receiver-reactor: The CAESAR (Catalytically Enhanced Solar Absorption Receiver) project
[DE91-002340] N91-13800

CHIPS (ELECTRONICS)
Feasibility study, software design, layout and simulation of a two-dimensional fast Fourier transform machine for use in optical array interferometry
[NASA-CR-186922] N91-13885

CHLORINE
Stratospheric ozone conservation by electron attachment to chlorine atoms: The negative-ion chemistry
[DE91-002951] N91-13815

CHROMIUM
Reactions of the excited state of polypyridyl chromium(III) ion
[DE91-000741] N91-13526
Chromium sensitized garnets for mid-IR lasers
[AD-A226630] N91-13696
Inner-shell ionization of lithium-like chromium ions
[DE91-001749] N91-13981

CHROMIUM ALLOYS
The effects of thermal treatment after welding on the functional properties of assemblies. Follow-up of the work on Cr-Mo
[CETIM-104720] N91-13739

CHROMIUM CARBIDES
Method of making carbide/fluoride/silver composites
[NASA-CASE-LEW-14902-1] N91-13503

CHROMIUM COMPOUNDS
Reactions of the excited state of polypyridyl chromium(III) ion
[DE91-000741] N91-13526

CHROMIUM STEELS
Creep and creep failure of power plant steels
[VTT-RR-685] N91-13528
A comparative study of ductile fracture in the 2.25 percent Cr-1 percent Mo and 9 percent Cr-1 percent Mo alloy steels N91-13753

CHRONOMETERS
A solar chronometer for climate: Astronomical and geophysical evidence N91-13823

CITIES
Utilization of IHS transformation for integration of images of differing resolutions: Urban land use study
[INPE-4606-PRE/1329] N91-14086

CITRUS TREES
Method of selection of TM/LANDSAT color composition for analysis of land use classes
[INPE-5119-TDL/421] N91-13783

CIVIL AVIATION
Aircraft accident report: Aloha IslandAir, Inc., Flight 1712, de Havilland Twin Otter, DHC-6-300, N707PV, Halawa Point, Molokai, Hawaii, October 28, 1989
[PB90-910405] N91-13425
The third generation of Soviet civilian-use turbofan engines
[AD-A225392] N91-13454

CLADDING
Injection efficiency of bound modes
[NASA-CR-4333] N91-13991

CLAMPS
Post clamp
[NASA-CASE-LEW-14862-1] N91-13730
Cantilever clamp fitting
[NASA-CASE-MFS-28328-1] N91-13731

CLASSES
Classes of priors in games and decision models
[ETN-91-98171] N91-13965

CLASSIFICATIONS
Mesoscale monitoring of the soil freeze/thaw boundary from orbital microwave radiometry
[NASA-CR-185901] N91-13817
General method of pattern classification using the two-domain theory
[NASA-CASE-MSC-21737-1] N91-13911

CLIMATE
A preliminary ocean ARM (Atmospheric Radiation Measurements) guide for climatic evaluations
[DE91-001120] N91-13811
Terrestrial ecosystems and climatic change
[DE91-001492] N91-13813

CLIMATE CHANGE
Managing the Global Commons Decision Making and Conflict Resolution in Response to Climate Change Research Workshop
[DE91-001018] N91-13810
Terrestrial ecosystems and climatic change
[DE91-001492] N91-13813
Research projects including climate, atmospheric chemistry, solar-terrestrial physics, metrology, and storm systems
[PB90-256306] N91-13820

A solar chronometer for climate: Astronomical and geophysical evidence N91-13823
CLOCKS
Complete the development and construction of a spaceborne hydrogen maser clock [NASA-CR-184043] N91-13688
CLOSED CYCLES
Miniature closed cycle refrigerators N91-14035
CLOSED ECOLOGICAL SYSTEMS
Biological Life Support Technologies: Commercial Opportunities [NASA-CP-3094] N91-13842
Historical overview of the Biosphere 2 project N91-13844
Biosphere 2 test module experimentation program N91-13845
Soil bed reactor work of the Environmental Research Lab. of the University of Arizona in support of the research and development of Biosphere 2 N91-13846
Biomedical program at Space Biospheres Ventures N91-13847
The NASA CELSS program N91-13848
The CELSS breadboard project: Plant production N91-13849
CELSS research and development program N91-13850
The BioHome: A spinoff of space technology N91-13852
CLOSURE LAW
Reynolds stress closure in jet flows using wave models [NASA-CR-185717] N91-13640
CLOTHING
The effect of condensation in clothing on heat transfer [IZF-1990-B-5] N91-13881
CLOUD HEIGHT INDICATORS
Lidar as a slant path visio-ceilometer [FEL-90-A207] N91-13838
CLOUD PHYSICS
Cloud properties as deduced from satellite observation [NASA-CR-182851] N91-13833
CLOUDS (METEOROLOGY)
Interannual variation of seasonal means and subseasonal variability of cloud streets off the east coast of North America 1984-1987 [NASA-CR-187021] N91-13831
Cloud properties as deduced from satellite observation [NASA-CR-182851] N91-13833
CLUTTER
Motion detection, novelty filtering, and target tracking using an interferometric technique with a GaAs phase conjugate mirror [NASA-CASE-NPO-17784-1-CU] N91-13998
CMOS
Design of integrated CMOS circuits for parallel detection and storage of optical data [AD-A225702] N91-13611
Feasibility study, software design, layout and simulation of a two-dimensional fast Fourier transform machine for use in optical array interferometry [NASA-CR-186922] N91-13885
COATING
X ray measurements of residual stresses in thin, hard layers N91-13542
Novel polyimide molding powder, coating, adhesive, and matrix resin [NASA-CASE-LAR-14163-1] N91-13559
COATINGS
Mechanical testing of advanced coating system, volume 1 [NASA-CR-186725] N91-13534
Analytical and experimental studies for thermal plasma processing of materials [DE91-000599] N91-13576
Magnetic field effect transistors [AD-A226535] N91-13614
COBALT ISOTOPES
Spectrum formation in SN1987A N91-14243
CODING
Laser optical disk position encoder with active heads [NASA-CASE-GSC-13175-1] N91-14001
COGNITION
Cognitive and neural bases of skilled performance [AD-A226668] N91-13869
COGNITIVE PSYCHOLOGY
The mechanism of restructuring in geometry [AD-A224740] N91-13951
COILS
Oxide superconductor coils: Present successes, future challenges N91-14046
COLD GAS
Narrow band images of suspected cooling flow galaxies N91-14168
Optical emission from cooling flows in distant x ray clusters of galaxies N91-14169
Search for cold gas in clusters with and without cooling flows N91-14174
Non-steller light from high-redshift radiogalaxies N91-14238
COLD WORKING
Evaluation of the functional properties of welds on cold finished tubes defined as NF A 49.541 [CETIM-104700] N91-13738
COLLAPSE
Vortex collapse from a viewpoint of complex-time singularity [DE91-001852] N91-13957
COLLECTION
Instellar Gas Experiment (IGE): Testing interstellar gas particles to provide information on the processes of nucleosynthesis in the big bang stars and supernova [NASA-CR-186713] N91-14097
COLLIMATION
Magnetic collimation of protostellar winds into bipolar outflows N91-14182
COLLISION AVOIDANCE
Modelling and performance analysis of four and eight element TCAS [NASA-CR-187414] N91-13428
COLLISIONS
Advanced missile guidance N91-13439
Gamma ray bursts from comet neutron star magnetosphere interaction, field twisting and E(sub parallel) formation [DE91-002320] N91-14270
COLLOIDS
The fluid mechanics of continuous flow electrophoresis [NASA-CR-187647] N91-13648
COLOR
Evaluation of a simple method for color monitor recalibration [IZF-1990-B-4] N91-13608
Method of selection of TM/LANDSAT color composition for analysis of land use classes [INPE-5119-TDL/421] N91-13783
Utilization of IHS transformation for integration of images of differing resolutions: Urban land use study [INPE-4606-PRE/1329] N91-14086
COLOR CODING
Colour specifications for the Electronic Chart Display and Information System (ECDIS) [IZF-1990-A-19] N91-13789
COLOR PHOTOGRAPHY
The relation between tree physiology and multispectral and color photography: First phase [BCRS-89-39] N91-13785
COLOR TELEVISION
Evaluation of a simple method for color monitor recalibration [IZF-1990-B-4] N91-13608
COMBAT
Interactions between battle management and guidance law design for a strategic interceptor N91-13441
COMBUSTIBLE FLOW
Thrust chamber modeling using Navier-Stokes equations: Code documentation and listings, volume 2 [NASA-CR-183617] N91-13489
Topics in physico-chemical hydrodynamics [DE91-001674] N91-13519
Large eddy simulations and direct numerical simulations of high speed turbulent reacting flows [NASA-CR-187674] N91-13656
COMBUSTION
Computed potential energy surfaces for chemical reactions [NASA-CR-186877] N91-13506
COMBUSTION PHYSICS
Spray deflagration [INPE-5079-TDL/413] N91-13511
COMBUSTION PRODUCTS
Procedure for generating global atmospheric engine emissions data from future supersonic transport aircraft. The 1990 high speed civil transport studies [NASA-CR-181882] N91-13447
Characterization of rocket propellant combustion products: Description of sampling and analysis methods for rocket exhaust characterization studies [DE91-002536] N91-13574
COMBUSTION STABILITY
JANNAF liquid rocket combustion instability panel research recommendations [NASA-TM-103653] N91-13491
COMETARY MAGNETOSPHERES
Gamma ray bursts from comet neutron star magnetosphere interaction, field twisting and E(sub parallel) formation [DE91-002320] N91-14270
COMETS
The evolution of comets and the detectability of Extra-Solar Oort Clouds N91-14242
Gamma ray bursts from comet neutron star magnetosphere interaction, field twisting and E(sub parallel) formation [DE91-002320] N91-14270
COMMAND AND CONTROL
Extremely High Frequency (EHF) Low Probability of Intercept (LPI) communication applications [AD-A226653] N91-13591
Research into software executives for space operations support [NASA-CR-187013] N91-13895
Architecture for electronic imagery interoperability [AD-A226522] N91-13901
COMMUNICATION
Information systems supported end-user interaction: Impacts on inter- and intra-organizational connectivity and cooperative behavior N91-14075
COMMUNICATION CABLES
Signal processing used in the electromagnetic inspection of long bodies [CETIM-107270] N91-13749
COMMUNICATION NETWORKS
Overview of European technology in computers, telecommunications, and electronics [PB90-215773] N91-13610
Research into alternative network approaches for space operations [NASA-CR-187015] N91-13894
Architecture for electronic imagery interoperability [AD-A226522] N91-13901
The design of a distributed image processing and dissemination system [DE91-001835] N91-13909
The ISIS project: Fault-tolerance in large distributed systems [NASA-CR-186625] N91-13928
Tightly coupled simulation utilizing the EBR-II LMR: A real-time supercomputing and AI environment [DE91-001942] N91-13932
Communication system test for image transmission [DE91-001890] N91-13994
COMPACT GALAXIES
Aspects of the interstellar medium in starburst galaxies N91-14209
COMPENSATORY TRACKING
An indexed bibliography on tracking [AD-A226682] N91-13870
COMPILERS
Implementing automatic differentiation efficiently [DE91-002409] N91-13913
COMPLEX COMPOUNDS
Inorganic concepts relevant to metal binding, activity, and toxicity in a biological system [DE91-001489] N91-13858
COMPLEX SYSTEMS
Modeling pilot interaction with automated digital avionics systems: Guidance and control algorithms for contour and nap-of-the-Earth flight [NASA-CR-186105] N91-13875
COMPONENT RELIABILITY
On the design of component test plans based on system reliability objectives [DE90-017034] N91-13745
COMPOSITE MATERIALS
Impact behavior of composite materials: Exploratory research [CETIM-101130] N91-13504
Residual stresses in ceramics [JUEL-SPEZ-550] N91-13536
Residual stresses analyses in ceramics and metal ceramic composites using x ray methods N91-13539
Advanced Materials Development Program: Ceramic Technology for Advanced Heat Engines program plan, 1983--1993 [DE91-000516] N91-13555
Development of BEM for ceramic composites [NASA-CR-187676] N91-13557
Fracture of ceramics under farfield cyclic compression [DE90-008417] N91-13563
Heat transfer device and method of making the same [NASA-CASE-LEW-14162-1] N91-13668
COMPOSITE STRUCTURES
Damage assessment and residual compression strength of thick composite plates with through-the-thickness reinforcements [NASA-CR-187377] N91-13494
Relationship between voids and interlaminar shear strength of polymer matrix composites [NASA-TM-103643] N91-13495
A nonlinear viscoelastic approach to durability predictions for polymer based composite structures [NASA-CR-187653] N91-13554
Material and mechanical characterizations for braided composite pressure vessels [AD-A226640] N91-13713

Free vibrations of thin-walled semicircular graphite-epoxy composite frames
[NASA-TP-3010] N91-13750

COMPRESSED GAS
Computational and experimental progress on laser-activated gas avalanche switches for broadband, high-power electromagnetic pulse generation
[DE91-001763] N91-13623

COMPRESSIBLE BOUNDARY LAYER
A quiet flow Ludwieg tube for study of transition in compressible boundary layers: Design and feasibility
[NASA-CR-187374] N91-13676

COMPRESSIBLE FLOW
Heat pipe dynamic behavior
[NASA-CR-187422] N91-13645
Toward the large-eddy simulation of compressible turbulent flows
[NASA-CR-187460] N91-13650
Large eddy simulations and direct numerical simulations of high speed turbulent reacting flows
[NASA-CR-187674] N91-13656
Zero wavenumber modes of a compressible supersonic mixing layer
[NASA-CR-187476] N91-13669

COMPRESSION TESTS
Mechanical testing of advanced coating system, volume 1
[NASA-CR-186725] N91-13534

COMPUTATIONAL FLUID DYNAMICS
Large-eddy simulation of transitional channel flow
[NASA-CR-187465] N91-13410
Thrust chamber modeling using Navier-Stokes equations: Code documentation and listings, volume 2
[NASA-CR-183617] N91-13489
Computational fluid dynamics
[NASA-TM-101197] N91-13637
Toward the large-eddy simulation of compressible turbulent flows
[NASA-CR-187460] N91-13650
The coupling of finite methods for transport-diffusion problems
[ETN-91-98172] N91-13663
The advanced software development and commercialization project
[DE91-002956] N91-13933

COMPUTATIONAL GRIDS
Development of a time-dependent incompressible Navier-Stokes solver based on a fractional-step method
[NASA-CR-182323] N91-13639
Toward the large-eddy simulation of compressible turbulent flows
[NASA-CR-187460] N91-13650
Finite element and boundary element methods for elastoplastic stress analysis of two-dimensional and axisymmetric problems N91-13755
Mesh considerations for finite element structural dynamic applications
[DE91-001717] N91-13764
Examples of finite element mesh generation using SDRC IDEAS
[NASA-CR-186962] N91-13893

COMPUTER AIDED DESIGN
Theory and procedure of the hierarchical design rule checking of integrated circuits
[ETN-91-98173] N91-13627
Design of an X-band PIN diode phase shifter by computer optimization
[FEL-89-B286] N91-13633
Study of Design Knowledge Capture (DKC) schemes implemented in magnetic bearing applications
[NASA-CR-187394] N91-13677
Design of GaAlAs/GaAs GRIN-SCH SQW diode lasers. Analysis of the temperature dependence
[LAAS-90277] N91-13708
Improved plug valve computer-aided design of plug element
[DE91-001044] N91-13719
Version control and management in computer-aided design databases N91-13896
ADENG, adhesive bonding technology for engineering applications: Computer aided design
[CETIM-105070] N91-13917
Methods for computer-aided design of free-form objects
[MA-56] N91-13921
Specifications extraction and synthesis: Their correlations with preliminary design N91-13936

COMPUTER AIDED TOMOGRAPHY
Computed tomography software and standards
[DE91-002573] N91-13914

COMPUTER ASSISTED INSTRUCTION
Development and computer aided residual stress measurements on coated specimen using blind-hole drilling technique N91-13544
System and method for a general purpose architecture for intelligent computer-aided training
[NASA-CASE-MSC-21381-1] N91-13944

COMPUTER DESIGN
About transient stability of power systems: Statistical pattern recognition approach
[LAAS-90192] N91-13889

COMPUTER GRAPHICS
Micro based technology: A new tool for missile guidance system design and visualization N91-13440
The poet revealed: A future for human-centered design
[AD-A226648] N91-13878
Research into software executives for space operations support
[NASA-CR-187013] N91-13895
Implementation of the MAGINT-MAGGRAF code in the microVAX-3600 system
[INPE-5042-PRE/1575] N91-13898
Methods for computer-aided design of free-form objects
[MA-56] N91-13921
Georelational data model: A conceptual vision of a geographical information system
[INPE-4612-PRE/1335] N91-14078

COMPUTER INFORMATION SECURITY
Security for safety critical space borne systems
[NASA-CR-187656] N91-13906
The SWORD model of multilevel secure databases
[RSRE-90008] N91-14085

COMPUTER NETWORKS
Research into alternative network approaches for space operations
[NASA-CR-187015] N91-13894
The design of a distributed image processing and dissemination system
[DE91-001835] N91-13909

COMPUTER PROGRAM INTEGRITY
The SWORD model of multilevel secure databases
[RSRE-90008] N91-14085

COMPUTER PROGRAMMING
WordPerfect's toolbox: Formatting documents using styles and macros
[DE91-001884] N91-13912
Validation environment for AIPS/ALS: Implementation and results
[NASA-CR-4340] N91-13930
A tutorial on the construction of high-performance resolution/paramodulation systems
[DE91-001096] N91-13942
Methodology to treat stellar images
[IFSI-89-21] N91-14094

COMPUTER PROGRAMS
Navier-Stokes and Euler solutions for lee-side flows over supersonic delta wings. A correlation with experiment
[NASA-TP-3035] N91-13401
Development of a full potential solver for rotor aerodynamics analysis N91-13407
Transonic blade-vortex interactions noise: A parametric study
[NASA-CR-187713] N91-13422
An AD100 implementation of a real-time STOVL aircraft propulsion system
[NASA-TM-103683] N91-13457
Relationship between voids and interlaminar shear strength of polymer matrix composites
[NASA-TM-103643] N91-13495
Computed potential energy surfaces for chemical reactions
[NASA-CR-186877] N91-13506
Temporal scattering and response software: Users' manual
[DE91-001760] N91-13593
Transionospheric Propagation Code (TIPC)
[DE91-002435] N91-13597
Data reduction of digitized images processed from calibrated photographic and spectroscopic films obtained from terrestial, rocket and space shuttle telescopic instruments
[NASA-CR-187320] N91-13674
Study of Design Knowledge Capture (DKC) schemes implemented in magnetic bearing applications
[NASA-CR-187394] N91-13677
An interactive program for the analysis and design of advanced laser targets
[DE91-002542] N91-13704
A physical parameterization of snow albedo for use in climate models N91-13781
DOPLIGHT 1987 project summary
[PB90-253584] N91-13834
Echocardiography in NATO aircrew
[AGARD-AR-297] N91-13863
A computer model to determine the primary contributors to relative radiation dose received by astronauts
[DE90-015681] N91-13866
Research into software executives for space operations support
[NASA-CR-187013] N91-13895
ESATAN: User manual
[ESA-PSS-03-105-ISSUE-1] N91-13897
Implementation of the MAGINT-MAGGRAF code in the microVAX-3600 system
[INPE-5042-PRE/1575] N91-13898
Security for safety critical space borne systems
[NASA-CR-187656] N91-13906
Pressure visualization (PreViz) package version 1.0 user's guide
[NASA-CR-187444] N91-13907
Image 3.3: Tutorial manual
[DE91-001762] N91-13908
Computed tomography software and standards
[DE91-002573] N91-13914
A generalized Polak-Ribiere algorithm
[MATHS-REPT-A-128] N91-13918
CESAR trap program library
[FFI-90/7023] N91-13924
Software management guidelines for automated measuring systems
[NPL-DES-99] N91-13926
Synthetic models of distributed memory parallel programs
[DE91-001058] N91-13931
The advanced software development and commercialization project
[DE91-002956] N91-13933
The design of phase-only filters for optical correlations
[AD-A225641] N91-13992
NRL compact accelerator theory studies
[AD-A226537] N91-14005
A real-time digital control, data acquisition and analysis system for the DIII-D multipulse Thomson scattering diagnostic
[DE91-002720] N91-14025
Variational transition state theory
[DE91-001253] N91-14058
Sweeping-vector conversion for polygonal data
[INPE-4558-PRE/1299] N91-14077
A model for the infrared emission from an OB star cluster environment N91-14139
A combined N-body and hydrodynamic code for modeling disk galaxies N91-14241

COMPUTER STORAGE DEVICES
Design of integrated CMOS circuits for parallel detection and storage of optical data
[AD-A225702] N91-13611

COMPUTER SYSTEMS DESIGN
Success with an automated computer control system
[DE91-001759] N91-13945

COMPUTER SYSTEMS PROGRAMS
The ISIS project: Fault-tolerance in large distributed systems
[NASA-CR-186625] N91-13928

COMPUTER TECHNIQUES
Superconducting neural network computer and sensor array
[AD-D014625] N91-13887
System and method for a general purpose architecture for intelligent computer-aided training
[NASA-CASE-MSC-21381-1] N91-13944
New techniques for the union-find problem
[RUU-CS-89-12] N91-13954

COMPUTER VISION
Positional estimation techniques for an autonomous mobile robot
[NASA-CR-187689] N91-13725
A discrepancy within primate spatial vision and its bearing on the definition of edge detection processes in machine vision
[NASA-TM-102739] N91-13941

COMPUTERIZED SIMULATION
Analytical aerodynamic model of a high alpha research vehicle wind-tunnel model
[NASA-CR-187362] N91-13404
Guidance, navigation and control. Digital emulation technology laboratory. Volume 3, Task 3: Special studies
[AD-A225125] N91-13430
Flight control design issues in bank-to-turn missiles N91-13437
Micro based technology: A new tool for missile guidance system design and visualization N91-13440
Description of sea wave motion and its influence on the altitude control of sea skimming missiles
[FEL-89-A368] N91-13450
Measurements and predictions of a liquid spray from an air-assist nozzle
[NASA-TM-103640] N91-13455
Simulation of pressure and temperature responses for the 20 Inch Supersonic Wind Tunnel
[NASA-TM-102647] N91-13467

Thrust chamber modeling using Navier-Stokes equations: Code documentation and listings, volume 2
[NASA-CR-183617] N91-13489
A study of confined diffusion flames
[AD-A226552] N91-13512
Restoration of solar radio images: Evaluation of poor conditions and resolution by regularization techniques
[INPE-4557-PRE/1298] N91-13587
NRL 1989 beam propagation studies in support of the ATA multi-pulse propagation experiment
[AD-A226443] N91-13588
Relativistic kylstron simulations using RKTW2D
[DE91-001747] N91-13619
Computation of incompressible flow around the DARPA SUBOFF bodies
[AD-A226481] N91-13646
Complete the development and construction of a spaceborne hydrogen maser clock
[NASA-CR-184043] N91-13688
An interactive program for the analysis and design of advanced laser targets
[DE91-002542] N91-13704
Penetration of yawed projectiles
[DE91-001084] N91-13726
A computer model to determine the primary contributors to relative radiation dose received by astronauts
[DE90-015681] N91-13866
Implementation of the MAGINT-MAGGRAF code in the microVAX-3600 system
[INPE-5042-PRE/1575] N91-13898
Coupling artificial intelligence and a system dynamics simulation to optimize quality assurance and testing in software development
[AD-A226580] N91-13902
The advanced software development and commercialization project
[DE91-002956] N91-13933
Two-fluid simulations of the reversed-field pinch
[DE91-001961] N91-14014

COMPUTERS
Flexible cooperation in non-standard application environments
[AD-A226486] N91-13940

CONCENTRATORS
Status of concentrator collector and high-efficiency concentrator cell development
[DE91-001260] N91-13793

CONCURRENT PROCESSING
The poet revealed: A future for human-centered design
[AD-A226648] N91-13878

CONDENSED MATTER PHYSICS
Atomic and molecular theory
[DE91-004475] N91-13983

CONDENSERS (LIQUEFIERS)
Supercritical binary geothermal cycle experiments with mixed-hydrocarbon working fluids and a near-horizontal in-tube condenser
[DE91-001815] N91-13798

CONDENSING
Supercritical binary geothermal cycle experiments with mixed-hydrocarbon working fluids and a near-horizontal in-tube condenser
[DE91-001815] N91-13798
The effect of condensation in clothing on heat transfer
[IZF-1990-B-5] N91-13881

CONDUCTING POLYMERS
PBT, PBO-based hybrid polymers with nonlinear optical properties or high electrical conductivity
[AD-A226646] N91-13552

CONDUCTIVE HEAT TRANSFER
Two-fluid simulations of the reversed-field pinch
[DE91-001961] N91-14014
Radiative thermal conduction fronts N91-14162

CONDUCTIVITY
The fluid mechanics of continuous flow electrophoresis
[NASA-CR-187647] N91-13648

CONFERENCES
Missile Interceptor Guidance System Technology
[AGARD-LS-173] N91-13434
The 1990 JSAE (Society of Automative Engineers of Japan, Inc.) Spring Convention Proceedings 901
[DE91-715185] N91-13579
Applications of Superconductivity to Avionics
[AGARD-CP-481] N91-14030
Proceedings of a Workshop on Cosmogenic Nuclide Production Rates
[NASA-CR-185349] N91-14098
The Interstellar Medium in External Galaxies: Summaries of contributed papers
[NASA-CP-3084] N91-14100
Proceedings of the MEVTV Workshop on The Evolution of Magma Bodies on Mars
[NASA-CR-187357] N91-14252

CONFINEMENT
A study of confined diffusion flames
[AD-A226552] N91-13512
Plasma properties
[DE91-001361] N91-14006
Confinement and heating studies of field-reversed configurations
[DE91-001965] N91-14008
Confinement properties of the RFP (reversed field pinch)
[DE91-002322] N91-14015
ITER confinement capability
[DE91-002647] N91-14018

CONFORMAL MAPPING
Reynolds stress closure in jet flows using wave models
[NASA-CR-185717] N91-13640

CONJUGATE GRADIENT METHOD
A generalized Polak-Ribiere algorithm
[MATHS-REPT-A-128] N91-13918
On unconstrained conjugate gradient optimization methods and their interrelationships
[MATHS-REPT-A-129] N91-13919
A global convergence result for conjugate gradient methods
[MATHS-REPT-A-134] N91-13961

CONSERVATION
Stratospheric ozone conservation by electron attachment to chlorine atoms: The negative-ion chemistry
[DE91-002951] N91-13815

CONSERVATION LAWS
Regularized Chapman-Enskog expansion for scalar conservation laws
[NASA-CR-187441] N91-13966

CONSTRUCTION
Complete the development and construction of a spaceborne hydrogen maser clock
[NASA-CR-184043] N91-13688

CONSTRUCTION MATERIALS
Literature review on geotextiles to improve pavements for general aviation airports
[DOT/FAA/RD-90/26] N91-13464

CONTACT LENSES
An investigation of microstructural characteristics of contact-lens polymers
[NASA-TP-3034] N91-13492

CONTAMINATION
Biofilm monitoring coupon system
[NASA-CASE-MSC-21585-1] N91-13857

CONTINUOUS SPECTRA
The infrared continuum spectrum of x ray illuminated molecular gas N91-14144

CONTINUUM MECHANICS
A structural constitutive algorithm based on continuum damage mechanics for softening with snapback
[DE90-015841] N91-13773
Chaos and order in non-integrable model field theories
[DE91-002313] N91-14070

CONTINUUM MODELING
Development and evaluation of continuum models for translational-rotational nonequilibrium N91-13403

CONTINUUMS
A comparison of the radial distribution of molecular gas and non-thermal radio continuum in spiral disks N91-14145
A relationship between the integrated CO intensity and the radio continuum emission in spiral galaxies N91-14146
Radio continuum and far-infrared emission of spiral galaxies: Implications of correlations N91-14147
Radio continuum observations of the quasar-galaxy pair 3C 232-NGC 3067 N91-14226

CONTRACTION
Study of the metallurgical consequences of hammering between passes to compensate for the withdrawal of metal caused by welding
[CETIM-104430] N91-13741

CONTROL SIMULATION
Intelligent processing for spray metal manufacturing
[AD-A226499] N91-13523

CONTROL SYSTEMS DESIGN
Integrated aerodynamic and control system design of oblique wing aircraft N91-13459
Materials impurity analysis by means of nuclear resonance reactions
[DE91-001758] N91-13520
Version control and management in computer-aided design databases N91-13896
Tightly coupled simulation utilizing the EBR-II LMR: A real-time supercomputing and AI environment
[DE91-001942] N91-13932
Applications of neural networks to adaptive control
[AD-A225408] N91-13938
Proceedings of the Workshop on Software Tools for Distributed Intelligent Control Systems
[DE91-001755] N91-13943
System and method for a general purpose architecture for intelligent computer-aided training
[NASA-CASE-MSC-21381-1] N91-13944
Success with an automated computer control system
[DE91-001759] N91-13945
Robust variable structure control of model reference systems
[MATHS-REPT-A-131] N91-13947

CONTROL THEORY
Flight control design issues in bank-to-turn missiles N91-13437
Advanced missile guidance N91-13439
Integrated flight-propulsion control concepts for supersonic transport airplanes
[NASA-TM-101728] N91-13460
Analytical and experimental research on large angle maneuvers of flexible structures
[AD-A226679] N91-13479
Modeling pilot interaction with automated digital avionics systems: Guidance and control algorithms for contour and nap-of-the-Earth flight
[NASA-CR-186105] N91-13875
Robust deterministic control for robotic manipulators N91-13937
On hyperplane design techniques for discrete-time variable structure control systems
[MATHS-REPT-A-133] N91-13948

CONTROL VALVES
Improved plug valve computer-aided design of plug element
[DE91-001044] N91-13719

CONTROLLABILITY
Integrated aerodynamic and control system design of oblique wing aircraft N91-13459

CONTROLLED FUSION
Assessment of ion-atom collision data for magnetic fusion plasma edge modelling
[DE91-001920] N91-14012

CONTROLLERS
Guidance, navigation and control. Digital emulation technology laboratory. Volume 2, Task 2: Seeker emulator development
[AD-A225124] N91-13429
Dynamic modeling, property investigation, and adaptive controller design of serial robotic manipulators modeled with structural compliance
[NASA-CR-187678] N91-13722
Solder dross removal apparatus
[NASA-CASE-MFS-28406-1] N91-13729
Knowledge representation into Ada parallel processing
[NASA-CR-187451] N91-13934
Dissipative controller designs for second-order dynamic systems
[NASA-CR-187452] N91-13935
Apparatus for precision focusing and positioning of a beam waist on a target
[NASA-CASE-ARC-11916-1-SB] N91-14002

CONVECTION CURRENTS
Review of geography internship of convective wave project
[NASA-CR-187022] N91-13819

CONVECTIVE HEAT TRANSFER
Interannual variation of seasonal means and subseasonal variability of cloud streets off the east coast of North America 1984-1987
[NASA-CR-187021] N91-13831

CONVERGENCE
A generalized Polak-Ribiere algorithm
[MATHS-REPT-A-128] N91-13918
A global convergence result for conjugate gradient methods
[MATHS-REPT-A-134] N91-13961
Regularized Chapman-Enskog expansion for scalar conservation laws
[NASA-CR-187441] N91-13966
Interpreting the convergence of Lyman series absorption lines N91-14225

CONVEXITY
Wide acceptance angle, high concentration ratio, optical collector
[NASA-CASE-MFS-28295-1] N91-13999

COOLERS
Flexible thermal apparatus for mounting of thermoelectric cooler
[NASA-CASE-NPO-17806-1-CU] N91-13581

COOLING
Shuttle Centaur engine cooldown evaluation and effects of expanded inlets on start transient
[NASA-CR-183198] N91-13487
Origin and dynamics of emission line clouds in cooling flow environments N91-14167
Narrow band images of suspected cooling flow galaxies N91-14168

Optical emission from cooling flows in distant x ray clusters of galaxies N91-14169
COOLING FLOWS (ASTROPHYSICS)
ISM stripping from cluster galaxies and inhomogeneities in cooling flows N91-14172
Search for cold gas in clusters with and without cooling flows N91-14174
COPPER OXIDES
Progress in high Tc superconductors N91-14031
CORNERS
Robot cable-compliant devices
[NASA-CASE-GSC-13127-1] N91-13735
CORRECTION
Local closed orbit bumps in AmPS
[NIKHEF-K/AMPS/90-01] N91-13471
CORRELATION
A survey of the properties of early-type galaxies N91-14109
Radio continuum and far-infrared emission of spiral galaxies: Implications of correlations N91-14147
CORRELATORS
The design of phase-only filters for optical correlations
[AD-A225641] N91-13992
CORROSION RESISTANCE
Research and development of a ceramic fiber composite heat exchanger
[DE90-017250] N91-13497
Corrosion-resistant catalyst supports for phosphoric acid fuel cells
[DE91-001713] N91-13794
COSMIC BACKGROUND EXPLORER SATELLITE
COBE's search for structure in the Big Bang
[NASA-TM-102976] N91-14271
COSMIC DUST
An ADP proposal to study the formation and evolution of dust-embedded clusters
[NASA-CR-186793] N91-14089
A critical review of charged particle astronomy at Saturn: The evidence for co-orbiting material in the inner satellite system
[NASA-CR-187348] N91-14090
The Interstellar Medium in External Galaxies: Summaries of contributed papers
[NASA-CP-3084] N91-14100
Intergalactic HI in the NGC5018 group N91-14110
Observations of CO isotopic emission and the far-infrared continuum of Centaurus A N91-14125
The CO-12 and CO-13 J=2-1 and J=1-0 observations of hot and cold galaxies N91-14126
The 3 micron spectrum of NGC 4565 N91-14132
Contribution of cool dust to the FIR brightness distribution of NGC 6946 Sc(s)2 N91-14134
Far infrared luminosity functions of normal galaxies N91-14135
Evidence against a simple two-component model for the far-infrared emission from galaxies N91-14136
Emission from small dust particles in diffuse and molecular cloud medium N91-14137
Very small grains in the Milky Way and external galaxies N91-14138
A model for the infrared emission from an OB star cluster environment N91-14139
IRAS observations of the ISM in the gamma CAS reflection nebula N91-14140
Peering beyond IRAS: The 100 to 350 micron dust emission from galaxies N91-14141
Far-infrared emission from dusty ellipticals N91-14142
The infrared continuum spectrum of x ray illuminated molecular gas N91-14144
Optical and near-IR study of LMC HII region N11AB N91-14155
The diffuse ionized interstellar medium perpendicular to the plane of NGC 891 N91-14160
Stripping of gas and dust from the elliptical galaxy M86 N91-14171
Infrared analysis of LMC superbubbles N91-14181
Lyman alpha radiation in external galaxies N91-14186
Polarization in the Lagoon nebula N91-14193
M51: Molecular spiral arms, GMAs and superclouds N91-14204
Laboratory spectra of amorphous and crystalline olivine: An application to comet Halley IR spectrum
[DE91-002307] N91-14264
COSMIC GASES
High velocity gas in external galaxies N91-14105
A scaling law of radial gas distribution in disk galaxies N91-14106
The ratio of molecular to atomic gas in spiral galaxies as a function of morphological type N91-14119
Observations of CO in the Magellanic irregular galaxy NGC 55 N91-14124
The infrared continuum spectrum of x ray illuminated molecular gas N91-14144
Imaging spectrophotometry of the nuclear outflow of NGC 1068 N91-14149
Radiative thermal conduction fronts N91-14162
ISM stripping from cluster galaxies and inhomogeneities in cooling flows N91-14172
Accounting for the dispersion in the x ray properties of early-type galaxies N91-14173
NGC 3312: A victim of ram pressure sweeping N91-14177
Observations of extended and counterrotating disks of ionized gas in S0 galaxies N91-14187
COSMIC RAYS
A relationship between the integrated CO intensity and the radio continuum emission in spiral galaxies N91-14146
MHD shocks in the ISM N91-14183
Elemental mapping of planetary surfaces using gamma ray spectroscopy
[DE91-001877] N91-14258
Feasibility of cosmic-ray muon intensity measurements for tunnel detection
[AD-A223355] N91-14266
Temporal variations of cosmic rays in the heliosphere N91-14267
COSMOLOGY
Proceedings of a Workshop on Cosmogenic Nuclide Production Rates
[NASA-CR-185349] N91-14098
Particle theory and cosmology
[DE91-004189] N91-14250
COST EFFECTIVENESS
Assured crew return vehicle
[NASA-CASE-MSC-21536-1] N91-13483
Software reliability through fault-avoidance and fault-tolerance
[NASA-CR-187646] N91-13904
COST ESTIMATES
Heat exchanger fouling: Prediction, measurement, and mitigation
[DE91-001997] N91-13661
A quiet flow Ludwieg tube for study of transition in compressible boundary layers: Design and feasibility
[NASA-CR-187374] N91-13676
COST REDUCTION
Connectivity alternatives for remote users of the Maintenance Processor Subsystem (MPS)
[DOT/FAA/CT-90/16] N91-13900
COUNTER ROTATION
Observations of extended and counterrotating disks of ionized gas in S0 galaxies N91-14187
COUPLED MODES
Folded RF-excited CO2 waveguide lasers N91-13695
COUPLES
Two fault tolerant toggle-hook release
[NASA-CASE-MSC-21671-1] N91-13723
COUPLING
The effect of inertial coupling in the dynamics and control of flexible robotic manipulators
[NASA-CR-187679] N91-13721
COWLINGS
Theoretical evaluation of engine auxiliary inlet design for supersonic V/STOL aircraft
[NASA-CR-186610] N91-13443
CRAB NEBULA
Research in theoretical physics
[DE91-002458] N91-14071
CRACK ARREST
Composite fuselage technology
[NASA-CR-187658] N91-13446
CRACK CLOSURE
On the variation in crack-opening stresses at different locations in a three-dimensional body
[NASA-CR-187722] N91-13768
CRACK INITIATION
Mechanism of mechanical fatigue of silica glass
[DE91-004053] N91-13565
CRACK PROPAGATION
Composite fuselage technology
[NASA-CR-187658] N91-13446
Work of fracture of composites in axial compression: Measurement and origins
[RARDE-1/90] N91-13505
Fracture of ceramics under farfield cyclic compression
[DE90-008417] N91-13563
Use of dome (meniscus) lenses to eliminate birefringence and tensile stresses in spatial filters for the Nova laser
[DE91-002784] N91-13707
Study of static and dynamic fracture using strain measurements N91-13754
Potential impact of enhanced fracture-toughness data on pressurized-thermal-shock analysis
[DE91-001493] N91-13763
On the variation in crack-opening stresses at different locations in a three-dimensional body
[NASA-CR-187722] N91-13768
Sustained-load crack growth of 8090 aluminium-lithium alloy plate in dry air at 50-200 C
[RAE-TR-90033] N91-13777
CRACK TIPS
Fracture mechanics of interface cracks between dissimilar anisotropic materials N91-13752
On the variation in crack-opening stresses at different locations in a three-dimensional body
[NASA-CR-187722] N91-13768
CRACKS
Mechanism of mechanical fatigue of silica glass
[DE91-004053] N91-13565
Fracture mechanics of interface cracks between dissimilar anisotropic materials N91-13752
CRANES
An application of oscillation damped motion for suspended payloads to the advanced integrated maintenance system
[DE91-002658] N91-13946
CRASHES
Aircraft accident report: Aloha IslandAir, Inc., Flight 1712, de Havilland Twin Otter, DHC-6-300, N707PV, Halawa Point, Molokai, Hawaii, October 28, 1989
[PB90-910405] N91-13425
CRASHWORTHINESS
Failure behavior of generic metallic and composite aircraft structural components under crash loads
[NASA-RP-1239] N91-13751
CRAY COMPUTERS
Tightly coupled simulation utilizing the EBR-II LMR: A real-time supercomputing and AI environment
[DE91-001942] N91-13932
CREEP ANALYSIS
Creep and creep failure of power plant steels
[VTT-RR-685] N91-13528
CREEP PROPERTIES
Creep and creep failure of power plant steels
[VTT-RR-685] N91-13528
Determination of residual stresses in ceramics materials using neutron diffraction N91-13538
Fracture of ceramics under farfield cyclic compression
[DE90-008417] N91-13563
CREEP TESTS
Three point bend creep testing of carbon/epoxy
[DE91-001083] N91-13501
Creep and creep failure of power plant steels
[VTT-RR-685] N91-13528
Sustained-load crack growth of 8090 aluminium-lithium alloy plate in dry air at 50-200 C
[RAE-TR-90033] N91-13777
CRITICAL FLOW
Enhancement of critical heat flux in tubes using staged tangential flow injection
[DE90-014935] N91-13659
CROSS FLOW
Aerodynamic effect of strakes on two-dimensional tail boom models of the OH-58A and the OH-58D helicopters
[NASA-TM-4248] N91-13406
A laser Doppler velocimeter approach for near-wall three-dimensional turbulence measurements
[NASA-TM-102841] N91-13653
CROSSLINKING
A new approach to design of cross-linked second-order nonlinear optical polymers
[AD-A226674] N91-13553
Methyl substituted polyimides containing carbonyl and ether connecting groups
[NASA-CASE-LAR-14351-1] N91-13561
Tissue simulating gel for medical research
[NASA-CASE-LAR-14036-1] N91-13562
CROSSTALK
Adaptive inverse filters for stereophonic sound reproduction
[ISVR-TR-187] N91-13975
CRUSTAL FRACTURES
Precision, accuracy, and tectonics from the Global Positioning System N91-13822
CRYOGENIC COOLING
Performance comparison of magnetic refrigeration cycles
[DE91-001520] N91-13578
Superfluid Stirling refrigerator: A new method for cooling below 1 Kelvin
[DE91-002311] N91-13582
CRYOGENIC EQUIPMENT
An interactive program for the analysis and design of advanced laser targets
[DE91-002542] N91-13704
CRYOGENIC FLUID STORAGE
Laser-induced fluorescence of phosphors for remote cryogenic thermometry
[DE91-001733] N91-13681

CRYOGENICS
Funds request for 1990. The cryogenic gravitational antenna (T = 2.0 K) ALTAIR
[IFSI-90-2] N91-13615
Cryostat for the gravitational antenna ALTAIR
[IFSI-90-3] N91-13616
Laser-induced fluorescence of phosphors for remote cryogenic thermometry
[DE91-001733] N91-13681
Gradiometry coexperiments to the gravity probe B and step missions
[NASA-CR-187704] N91-13788
Experimental development, testing, and research work in support of the inertial confinement fusion program
[DE91-002770] N91-14026
The world of superconductive machinery N91-14045
CRYOSTATS
Funds request for 1990. The cryogenic gravitational antenna (T = 2.0 K) ALTAIR
[IFSI-90-2] N91-13615
Cryostat for the gravitational antenna ALTAIR
[IFSI-90-3] N91-13616
CRYSTAL DEFECTS
Ion-induced damage and amorphization in Si
[DE91-002358] N91-14061
Influence of the delocalized excitation process on the determination of foreign atom positions using the channeling effect
[ETN-91-98175] N91-14065
CRYSTAL GROWTH
Optical characterization techniques applied to ceramic oxides
[DE91-001526] N91-13556
Signal processing development
[AD-A226593] N91-14052
Morphological stability and kinetics in crystal growth from vapors
[NASA-CR-187650] N91-14055
CRYSTAL LATTICES
The x ray elastic constants of ceramic materials for the determination of the stresses from lattice expansion measurements N91-13541
Surfaces and thin films studied by picosecond ultrasonics
[DE91-004167] N91-13973
Real-space multiple scattering theory calculations of LEED (Low-Energy Electron Diffraction) intensities for stepped surfaces
[DE91-000810] N91-13978
Status of lattice field theory calculations
[DE91-001141] N91-14057
Influence of the delocalized excitation process on the determination of foreign atom positions using the channeling effect
[ETN-91-98175] N91-14065
CRYSTAL OSCILLATORS
Real-time dynamic holographic image storage device
[NASA-CASE-LAR-13989-1] N91-13694
CRYSTAL STRUCTURE
Influence of materials structure and production method of Al2O3 ceramic on the x-ray stress measurement N91-13540
CRYSTAL SURFACES
Ammonia decomposition on silicon surfaces studied using transmission FTIR spectroscopy
[AD-A226625] N91-13513
Real-space multiple scattering theory calculations of LEED (Low-Energy Electron Diffraction) intensities for stepped surfaces
[DE91-000810] N91-13978
CRYSTALS
A study of the ice-hail charge separation mechanism using a thunderstorm electrification model with explicit microphysics in a kinematic framework N91-13835
Theoretical temperature-dependent branching ratios and laser thresholds of the (5)I7 yields (5)I8 levels of Ho3(+) in ten garnets
[NASA-TM-103429] N91-14053
CUES
Hearing in three dimensions: Sound localization
[NASA-CR-187706] N91-13971
CULTURE TECHNIQUES
Three-dimensional cell to tissue assembly process
[NASA-CASE-MSC-21559-1] N91-13860
CURING
Physical properties of thermosetting polymers
[AD-A225864] N91-13508
CURRENT AMPLIFIERS
Semi-custom integrated circuit amplifier and level discriminator for nuclear and space instruments
[DE91-001951] N91-13620
CURRENT DENSITY
Computation of the current density in nonlinear materials subjected to large current pulses
[DE91-001950] N91-13624
The status-quo and prospect of superconducting digital devices N91-14039
CURRENT DISTRIBUTION
Computation of the current density in nonlinear materials subjected to large current pulses
[DE91-001950] N91-13624
CURVES (GEOMETRY)
Methods for computer-aided design of free-form objects
[MA-56] N91-13921
CYCLIC HYDROCARBONS
Emission from small dust particles in diffuse and molecular cloud medium N91-14137
CO observations of southern mergers N91-14197
CYCLIC LOADS
On the variation in crack-opening stresses at different locations in a three-dimensional body
[NASA-CR-187722] N91-13768
CYCLOTRON RESONANCE
Free-electron laser experiments in the microwave tokamak experiment
[DE91-001746] N91-13699
Analysis of gamma ray burst spectra with cyclotron lines
[DE91-001745] N91-14269
CYLINDERS
Composite fuselage technology
[NASA-CR-187658] N91-13446
CYLINDRICAL BODIES
Wave by wave analysis of in-line force data for fixed cylinders in regular waves
[IC-AERO-89-02] N91-13672

D

D REGION
Utilization of the HIPAS facility for cooperative experiments related to ionospheric modification
[AD-A226609] N91-13590
DAMAGE
Effects of temperature on acoustically-induced strains and damage propagation in CFRP plates N91-13493
DAMAGE ASSESSMENT
Damage tolerance analysis and testing of the fighter aircraft 37 Viggen
[FFA-TN-1990-35] N91-13448
Hazard studies for solid propellant rocket motors
[AGARD-AG-316] N91-13488
Damage assessment and residual compression strength of thick composite plates with through-the-thickness reinforcements
[NASA-CR-187377] N91-13494
DAMPING
Composite passive damping struts for large precision structures
[NASA-CASE-NPO-17914-1-CU] N91-13767
DARK MATTER
U1(prime) dark matter and R-parity violation
[DE91-001792] N91-14068
The large-scale space distribution of emission-line galaxies N91-14091
DATA ACQUISITION
S-band diplexer for a telecommunication board transponder
[INPE-4540-PRE/1286] N91-13586
Operation of inductively coupled plasma source mass spectrometers in the peak jumping mode
[DE91-001766] N91-13689
DATA BASE MANAGEMENT SYSTEMS
Flexible cooperation in non-standard application environments
[AD-A226486] N91-13940
Communication system test for image transmission
[DE91-001890] N91-13994
Database management system for instrument data management
[DE91-004300] N91-14084
The SWORD model of multilevel secure databases
[RSRE-90008] N91-14085
DATA BASES
Version control and management in computer-aided design databases N91-13896
Georelational data model: A conceptual vision of a geographical information system
[INPE-4612-PRE/1335] N91-14078
Technical communications in aerospace: An analysis of the practices reported by US and European aerospace engineers and scientists
[NASA-TM-103441] N91-14079
Energy Data Base
[DE90-009278] N91-14081
Report of foreign travel
[DE91-001732] N91-14082
Ground-based studies of emission-line variability: Recent results for NGC 5548 and future plans
[NASA-CR-180433] N91-14088
A survey of the properties of early-type galaxies N91-14109
DATA COMPRESSION
Pipeline synthetic aperture radar data compression utilizing systolic binary tree-searched architecture for vector quantization
[NASA-CASE-NPO-17941-1-CU] N91-13595
Real-time data compression of broadcast video signals
[NASA-CASE-LEW-14945-1] N91-13598
DATA LINKS
Tightly coupled simulation utilizing the EBR-II LMR: A real-time supercomputing and AI environment
[DE91-001942] N91-13932
DATA MANAGEMENT
Version control and management in computer-aided design databases N91-13896
Database management system for instrument data management
[DE91-004300] N91-14084
DATA PROCESSING
The use of satellite data in the ECMWF analysis system
[KNMI-TR-123] N91-13790
Software management guidelines for automated measuring systems
[NPL-DES-99] N91-13926
DATA REDUCTION
Data reduction of digitized images processed from calibrated photographic and spectroscopic films obtained from terrestial, rocket and space shuttle telescopic instruments
[NASA-CR-187320] N91-13674
DATA STORAGE
M-dimensional computer memory with M-1 dimensional hyperplane access
[AD-D014615] N91-13886
Implementing automatic differentiation efficiently
[DE91-002409] N91-13913
DATA STRUCTURES
Flexible cooperation in non-standard application environments
[AD-A226486] N91-13940
Evaluation of expressions involving higher order derivations
[NASA-CR-187319] N91-13949
DATA TRANSMISSION
Overview of European technology in computers, telecommunications, and electronics
[PB90-215773] N91-13610
Definition study into the requirements of a data modem for the SYSCOM network
[FEL-90-A116] N91-13892
Research into alternative network approaches for space operations
[NASA-CR-187015] N91-13894
Communication system test for image transmission
[DE91-001890] N91-13994
DECISION MAKING
Multiple symbol differential detection
[NASA-CASE-NPO-17896-1-CU] N91-13596
Managing the Global Commons Decision Making and Conflict Resolution in Response to Climate Change Research Workshop
[DE91-001018] N91-13810
DECISION THEORY
An application of multiattribute decision analysis to the Space Station Freedom program. Case study: Automation and robotics technology evaluation
[NASA-CR-187432] N91-13476
On combining selection and estimation in the search for the largest binomial parameter
[AD-A226595] N91-13953
Classes of priors in games and decision models
[ETN-91-98171] N91-13965
DECOMPOSITION
Synthesis and characterization of high temperature superconductor materials N91-14048
DECOUPLING
Two fault tolerant toggle-hook release
[NASA-CASE-MSC-21671-1] N91-13723
DEEP SPACE NETWORK
Environmental projects. Volume 12: Friable asbestos abatement, GDSCC
[NASA-CR-187636] N91-13806
DEFLAGRATION
Spray deflagration
[INPE-5079-TDL/413] N91-13511
DEFLECTION
Close-range photogrammetric measurement of static deflections for an aeroelastic supercritical wing
[NASA-TM-4194] N91-13400

Three point bend creep testing of carbon/epoxy
[DE91-001083] N91-13501

DEFORMATION
Cantilever clamp fitting
[NASA-CASE-MFS-28328-1] N91-13731
Probe insertion apparatus with inflatable seal
[NASA-CASE-LEW-14965-1] N91-13732
Superplastic deformation properties of Ti-6Al-4V
[DE91-000503] N91-13757
A structural constitutive algorithm based on continuum damage mechanics for softening with snapback
[DE90-015841] N91-13773
Study of strategies for the determination of deformations from Global Positioning System (GPS) measurements
[ETN-91-98141] N91-13786

DEGRADATION
Degradation modeling with application to aging and maintenance effectiveness evaluations
[DE91-004004] N91-13746

DELAY
Airport stand assignment model
[TT-9009] N91-13426

DELTA WINGS
Navier-Stokes and Euler solutions for lee-side flows over supersonic delta wings. A correlation with experiment
[NASA-TP-3035] N91-13401

DEMODULATION
Utilization of the HIPAS facility for cooperative experiments related to ionospheric modification
[AD-A226609] N91-13590

DENSE PLASMAS
Ionization degree of classical, dense, and highly condensed plasmas
[ETN-91-98174] N91-14027

DENSITY (NUMBER/VOLUME)
The morphology-density relation for dwarf galaxies
N91-14200

DENSITY DISTRIBUTION
Radial profiles of gas in late-type disk galaxies
N91-14107
Ionization in the local interstellar and intergalactic media N91-14249

DEPLETION
A theoretical investigation of effective surface recombination velocity in AlGaAs/GaAs heteroface solar cells
[DE91-001754] N91-13795
Neutral atomic absorption lines and far-UV extinction: Possible implications for depletions and grain parameters N91-14115
Empirical relationships between gas abundances and UV selective extinction N91-14116

DEPOLARIZATION
Use of dome (meniscus) lenses to eliminate birefringence and tensile stresses in spatial filters for the Nova laser
[DE91-002784] N91-13707

DEPOSITION
Analytical and experimental studies for thermal plasma processing of materials
[DE91-000599] N91-13576

DESIGN ANALYSIS
Modern robust control for missile autopilot design
N91-13435
An application of multiattribute decision analysis to the Space Station Freedom program. Case study: Automation and robotics technology evaluation
[NASA-CR-187432] N91-13476
Design reliability engineering
[DE91-001949] N91-13744
On the design of component test plans based on system reliability objectives
[DE90-017034] N91-13745
Constrained viscoelastic layer damping of thick aluminum plates: Design, analysis, and testing
[AD-A226556] N91-13758
Design considerations for lunar base photovoltaic power systems
[NASA-TM-103642] N91-14259

DESORPTION
Radio observations of several interstellar molecules
N91-14093

DESTRUCTIVE TESTS
Impact behavior of composite materials: Exploratory research
[CETIM-101130] N91-13504

DETECTION
Transionospheric Propagation Code (TIPC)
[DE91-002435] N91-13597
A silicon avalanche photodiode detector circuit for Nd:YAG laser scattering
[DE91-002709] N91-13706
Detection of CO emission in Hydra 1 cluster galaxies
N91-14237

DETECTORS
Intelligent processing for spray metal manufacturing
[AD-A226499] N91-13523

DETERMINANTS
Differences in the size-internal velocity relation of galactic and extragalactic HII regions N91-14158

DETONATION
Multiphase carbon and its properties in complex mixtures
[DE91-001679] N91-13499
All hot spots are not equal
[DE91-002303] N91-13573

DETONATORS
Bidirectional slapper detonators in spherical explosion systems
[DE91-002399] N91-13662

DEUTERIUM
Fast Pb-glass neutron-to-light converter for ICF (Inertial Confinement Fusion) target burn history measurements
[DE91-002670] N91-14021

DEUTERIUM COMPOUNDS
Ammonia decomposition on silicon surfaces studied using transmission FTIR spectroscopy
[AD-A226625] N91-13513

DIAGNOSIS
Portable dynamic fundus instrument
[NASA-CASE-MSC-21675-1] N91-13865

DIAMAGNETISM
Application of high-temperature superconductors to high-precision accelerometers N91-14042

DIAMINES
Vinyl capped addition polyimides
[NASA-CASE-LEW-15027-1] N91-13566

DIAMONDS
Analytical and experimental studies for thermal plasma processing of materials
[DE91-000599] N91-13576

DIAPHRAGMS (MECHANICS)
Dual diaphragm tank with telltale drain
[NASA-CASE-MSC-21703-1] N91-13580

DIATOMIC GASES
Development and evaluation of continuum models for translational-rotational nonequilibrium N91-13403

DIELECTRIC PROPERTIES
Optical properties and electronic structures of d- and f-electron metals and alloys, Ag-In, Ni-Cu, AuGa2, PtGa2, beta'-NiAl, beta'-CoAl, CeSn3, and LaSn3
[DE91-001597] N91-14059

DIELECTRICS
Modified Hilbert transform pair and Kramers-Kronig relations for complex permittivities
[NASA-TM-102682] N91-13585
Investigation and development of ISFET type chemical sensors, sensitized by dielectric tying
[ECL-90-18] N91-13630
The fluid mechanics of continuous flow electrophoresis
[NASA-CR-187647] N91-13648

DIELS-ALDER REACTIONS
Study of improved methods for predicting chemical equilibria
[DE91-000263] N91-13509

DIESEL ENGINES
Advanced Materials Development Program: Ceramic Technology for Advanced Heat Engines program plan, 1983--1993
[DE91-000516] N91-13555
Analysis of single and multi-grade lubricant film thickness in a diesel engine
[AD-A226651] N91-13715

DIESEL FUELS
High-alcohol microemulsion fuel performance in a diesel engine
[DE91-001617] N91-13572

DIFFERENTIAL EQUATIONS
Numerical methods for boundary value problems in differential-algebraic equations
[DE91-001748] N91-13956

DIFFERENTIAL PULSE CODE MODULATION
Real-time data compression of broadcast video signals
[NASA-CASE-LEW-14945-1] N91-13598

DIFFRACTION PATTERNS
Three dimensional moire pattern alignment
[NASA-CASE-MSC-21416-1] N91-14000

DIFFUSERS
A steadying effect of acoustic excitation on transitory stall
[NASA-TM-103689] N91-13420

DIFFUSION
Polymer/riblet combination for hydrodynamic skin friction reduction
[NASA-CASE-LAR-14271-1-CU] N91-13558
Frontogenesis in gravity currents: The effect of endwalls and diffusion
[MATHS-REPT-A-127] N91-13666
Mechanisms of gas permeation through polymer membranes
[DE91-004190] N91-13671

DIFFUSION COEFFICIENT
A study of confined diffusion flames
[AD-A226552] N91-13512

DIFFUSION FLAMES
A study of confined diffusion flames
[AD-A226552] N91-13512

DIFFUSION THEORY
The coupling of finite methods for transport-diffusion problems
[ETN-91-98172] N91-13663

DIGITAL ELECTRONICS
Architecture for electronic imagery interoperability
[AD-A226522] N91-13901

DIGITAL FILTERS
Adaptive inverse filters for stereophonic sound reproduction
[ISVR-TR-187] N91-13975

DIGITAL NAVIGATION
Guidance, navigation and control. Digital emulation technology laboratory. Volume 3, Task 3: Special studies
[AD-A225125] N91-13430

DIGITAL SIMULATION
Guidance, navigation and control. Digital emulation technology laboratory. Volume 2, Task 2: Seeker emulator development
[AD-A225124] N91-13429

DIMENSIONAL ANALYSIS
Antivibration isolation (a practical guidebook)
[CETIM-108220] N91-13775

DIPLEXERS
S-band diplexer for a telecommunication board transponder
[INPE-4540-PRE/1286] N91-13586
A design method for an X-band diplexer
[FEL-90-B176] N91-13635

DIPPING
Solder dross removal apparatus
[NASA-CASE-MFS-28406-1] N91-13729

DISCONTINUITY
All hot spots are not equal
[DE91-002303] N91-13573
Robust variable structure control of model reference systems
[MATHS-REPT-A-131] N91-13947

DISCRIMINATORS
Semi-custom integrated circuit amplifier and level discriminator for nuclear and space instruments
[DE91-001951] N91-13620

DISK GALAXIES
A scaling law of radial gas distribution in disk galaxies
N91-14106
Radial profiles of gas in late-type disk galaxies
N91-14107
A survey of the properties of early-type galaxies
N91-14109
The diffuse ionized interstellar medium perpendicular to the plane of NGC 891 N91-14160
Radiative thermal conduction fronts N91-14162
Energy input and HI spin temperatures in low pressure regions N91-14163
The gravitational wakefield of a molecular cloud in a disk galaxy N91-14188
CO observations of southern mergers N91-14197
High-mass star formation in southern disk galaxies
N91-14218
High spatial resolution studies of galaxies in the far IR: Observations with the KAO, and the promise of SOFIA
N91-14229
A combined N-body and hydrodynamic code for modeling disk galaxies N91-14241

DISPERSING
Accounting for the dispersion in the x ray properties of early-type galaxies N91-14173

DISPLACEMENT
Periodic trim solutions with hp-version finite elements in time
[NASA-CR-187705] N91-13449

DISPLAY DEVICES
Colour specifications for the Electronic Chart Display and Information System (ECDIS)
[IZF-1990-A-19] N91-13789
Multi-scale contrast enhancement with applications to image fusion
[IZF-1990-A-9] N91-14003

DISSIPATION
Dissipative controller designs for second-order dynamic systems
[NASA-CR-187452] N91-13935

DISSOCIATION
MHD shocks in the ISM N91-14183
Dissociation and ionization of molecular gas in the spiral arms of M51 N91-14205

DISTANCE
Auto and hetero-associative memory using a 2-D optical logic gate
[NASA-CASE-NPO-17997-1-CU] N91-13888
Differences in the size-internal velocity relation of galactic and extragalactic HII regions N91-14158
DISTRIBUTED PARAMETER SYSTEMS
Proceedings of the Workshop on Software Tools for Distributed Intelligent Control Systems
[DE91-001755] N91-13943
DISTRIBUTED PROCESSING
Research into software executives for space operations support
[NASA-CR-187013] N91-13895
The design of a distributed image processing and dissemination system
[DE91-001835] N91-13909
Synthetic models of distributed memory parallel programs
[DE91-001058] N91-13931
DISTRIBUTION (PROPERTY)
The effect of suspended particles on Jean's criterion for gravitational instability N91-14189
DISTRIBUTION FUNCTIONS
On the design of component test plans based on system reliability objectives
[DE90-017034] N91-13745
DOCUMENTS
WordPerfect's toolbox: Formatting documents using styles and macros
[DE91-001884] N91-13912
DOPED CRYSTALS
Electrocatalysis of anodic oxygen-transfer reactions at modified lead dioxide electrodes
[DE91-000664] N91-13518
DOPPLER EFFECT
Comparison of spectral estimators application to ground sensor signals
[FEL-1988-85] N91-13605
High spatial and temporal resolution visible spectroscopy of the plasma edge in DIII-D
[DE91-002718] N91-14023
DOPPLER RADAR
DOPLIGHT 1987 project summary
[PB90-253584] N91-13834
DOSIMETERS
Development and initial characterization of a nuclear magnetic resonance dosimetry system
[DE91-001775] N91-13867
Review of uncertainties in the use of NPL primary standards of x ray exposure for the calibration of secondary standards in terms of exposure and air kerma
[NPL-RS(EXT)-109] N91-13868
DRAG REDUCTION
Polymer/riblet combination for hydrodynamic skin friction reduction
[NASA-CASE-LAR-14271-1-CU] N91-13558
Gradiometry coexperiments to the gravity probe B and step missions
[NASA-CR-187704] N91-13788
DRAINAGE
Dual diaphragm tank with telltale drain
[NASA-CASE-MSC-21703-1] N91-13580
DROP SIZE
Measurements and predictions of a liquid spray from an air-assist nozzle
[NASA-TM-103640] N91-13455
DROP TESTS
F-106B airplane active control landing gear drop test performance
[NASA-TM-102741] N91-13445
DROPS (LIQUIDS)
Measurements and predictions of a liquid spray from an air-assist nozzle
[NASA-TM-103640] N91-13455
Progress in the detection of single molecules in levitated droplets
[DE91-000612] N91-13517
DUCTILITY
A comparative study of ductile fracture in the 2.25 percent Cr-1 percent Mo and 9 percent Cr-1 percent Mo alloy steels N91-13753
DURABILITY
Composite thermal barrier coating
[NASA-CASE-LEW-14999-1] N91-13500
A nonlinear viscoelastic approach to durability predictions for polymer based composite structures
[NASA-CR-187653] N91-13554
DUST
The origin and evolution of the Uranian dust rings N91-14253
DWARF GALAXIES
Ar/S N91-14153
HII regions in dwarf irregular galaxies of the local group N91-14156
HII regions in IC 1613: The ISM in a nearby dwarf irregular galaxy N91-14157
The morphology-density relation for dwarf galaxies N91-14200
Star formation in proto dwarf galaxies N91-14212
Infrared spectroscopy of the dwarf starburst galaxy Henize 2-10 N91-14213
DYNAMIC CONTROL
Computational methods and software systems for dynamics and control of large space structures
[NASA-CR-187669] N91-13480
DYNAMIC LOADS
Effect of lubricating oil characteristics on gear vibrations N91-13710
Non-linear dynamic analysis of geared systems
[NASA-CR-4338] N91-13737
DYNAMIC MODELS
An AD100 implementation of a real-time STOVL aircraft propulsion system
[NASA-TM-103683] N91-13457
Effect of lubricating oil characteristics on gear vibrations N91-13710
Dynamic modeling, property investigation, and adaptive controller design of serial robotic manipulators modeled with structural compliance
[NASA-CR-187678] N91-13722
Dissipative controller designs for second-order dynamic systems
[NASA-CR-187452] N91-13935
DYNAMIC PRESSURE
Some observations on the Houbolt-Rainey and peak-hold methods of flutter onset prediction
[NASA-TM-102745] N91-13411
A preliminary look at techniques used to obtain airdata from flight at high angles of attack
[NASA-TM-101729] N91-13453
Pressure visualization (PreViz) package version 1.0 user's guide
[NASA-CR-187444] N91-13907
DYNAMIC PROGRAMMING
Algorithms for finding an optimal matching between a given string and a string generated by a regular grammar
[MEMO-836] N91-13905
DYNAMIC RESPONSE
A computational procedure for the dynamics of flexible beams within multibody systems
[NASA-CR-187667] N91-13760
A comparison of two numerical methods for shocks in one-dimensional elastic-plastic solids
[DE91-001741] N91-13785
Robust variable structure control of model reference systems
[MATHS-REPT-A-131] N91-13947
DYNAMIC STRUCTURAL ANALYSIS
Multivariable methods for the design, identification, and control of large space structures. Volume 1: Estimator Eigenvalue placement in positive real design
[AD-A226525] N91-13477
Multivariable methods for the design, identification, and control of large space structures. Volume 3: A study of the integrated control/structure design optimization problem for large flexible structures
[AD-A226526] N91-13478
Computational methods and software systems for dynamics and control of large space structures
[NASA-CR-187669] N91-13480
The effect of inertial coupling in the dynamics and control of flexible robotic manipulators
[NASA-CR-187679] N91-13721
Constraint treatment techniques and parallel algorithms for multibody dynamic analysis
[NASA-CR-187668] N91-13759
A computational procedure for the dynamics of flexible beams within multibody systems
[NASA-CR-187667] N91-13760
General Rotorcraft Aeromechanical Stability Program (GRASP): Theory manual
[NASA-TM-102255] N91-13762
Mesh considerations for finite element structural dynamic applications
[DE91-001717] N91-13764
The advanced software development and commercialization project
[DE91-002956] N91-13933
DYNAMIC TESTS
Coupling artificial intelligence and a system dynamics simulation to optimize quality assurance and testing in software development
[AD-A226580] N91-13902
DYNAMICAL SYSTEMS
The route to chaos for the Kuramoto-Sivashinsky equation
[NASA-CR-187461] N91-13642
Chaos and order in non-integrable model field theories
[DE91-002313] N91-14070

E

E GLASS
Tubular lap joints for wind turbine applications
[DE91-001341] N91-13736
EARTH (PLANET)
Abstracts for the International Workshop on Meteorite Impact on the Early Earth
[NASA-CR-185355] N91-14099
EARTH ATMOSPHERE
Managing the Global Commons Decision Making and Conflict Resolution in Response to Climate Change Research Workshop
[DE91-001018] N91-13810
EARTH CRUST
Numerical solution of the geoelectrodynamic problem
[NASA-CR-186941] N91-13818
EARTH ENVIRONMENT
Terrestrial ecosystems and climatic change
[DE91-001492] N91-13813
EARTH IONOSPHERE
Transionospheric Propagation Code (TIPC)
[DE91-002435] N91-13597
EARTH MAGNETOSPHERE
Utilization of the HIPAS facility for cooperative experiments related to ionospheric modification
[AD-A226609] N91-13590
EARTH MANTLE
Numerical solution of the geoelectrodynamic problem
[NASA-CR-186941] N91-13818
EARTH OBSERVATIONS (FROM SPACE)
Earth observing satellite: Understanding the Earth as a system N91-13853
EARTH OBSERVING SYSTEM (EOS)
Earth observing satellite: Understanding the Earth as a system N91-13853
COBE's search for structure in the Big Bang
[NASA-TM-102976] N91-14271
EARTH ORBITS
Assured crew return vehicle
[NASA-CASE-MSC-21536-1] N91-13483
EARTH RESOURCES
Managing the Global Commons Decision Making and Conflict Resolution in Response to Climate Change Research Workshop
[DE91-001018] N91-13810
EARTH SURFACE
Frequency-domain analysis of one-dimensional electromagnetic scattering by lossy media
[FEL-90-A112] N91-13607
Earth observing satellite: Understanding the Earth as a system N91-13853
EARTHQUAKES
Fractals and chaotic dynamics in tectonics: Applications to topography and seismicity N91-13821
ECCENTRICITY
Laser optical disk position encoder with active heads
[NASA-CASE-GSC-13175-1] N91-14001
ECHOCARDIOGRAPHY
Echocardiography in NATO aircrew
[AGARD-AR-297] N91-13863
ECLIPSING BINARY STARS
A study of active regions on RS CVn stars N91-14092
ECOLOGY
Microbial ecology laboratory procedures manual NASA/MSFC
[NASA-CR-184033] N91-13856
ECOSYSTEMS
Acidic deposition and the environment
[DE91-002352] N91-13812
Terrestrial ecosystems and climatic change
[DE91-001492] N91-13813
CELSS research and development program N91-13850
EDGE DETECTION
Millimeter-wave sensor image enhancement
[NASA-CR-187430] N91-13679
A discrepancy within primate spatial vision and its bearing on the definition of edge detection processes in machine vision
[NASA-TM-102739] N91-13941
EDGE LOADING
Accurate and reliable computation of complete solutions to the equations of linear elastomechanics on three-dimensional domains: Computation of edge stress intensity functions
[FFA-TN-1989-12] N91-13769
Accurate and reliable determination of edge and vertex stress intensity factors in three-dimensional elastomechanics
[FFA-TN-1990-28] N91-13771
EDGES
The extragalactic radiation field and sharp edges to HI disks in galaxies N91-14101

EDUCATION
System and method for a general purpose architecture for intelligent computer-aided training
[NASA-CASE-MSC-21381-1] N91-13944
EIGENVALUES
Computing the eigenvalues and eigenvectors of a general matrix by reduction to general tridiagonal form
[DE91-002523] N91-13959
EIGENVECTORS
Computing the eigenvalues and eigenvectors of a general matrix by reduction to general tridiagonal form
[DE91-002523] N91-13959
ELASTIC BARS
A comparison of two numerical methods for shocks in one-dimensional elastic-plastic solids
[DE91-001741] N91-13765
ELASTIC PROPERTIES
Effects of temperature on acoustically-induced strains and damage propagation in CFRP plates N91-13493
Experimental and theoretical determination of the thermomechanical response of inelastic structural materials to high energy thermal inputs
[AD-A226671] N91-13496
The x ray elastic constants of ceramic materials for the determination of the stresses from lattice expansion measurements N91-13541
Possibilities of stress measurement on ceramic materials using acoustic microscopy N91-13547
Accurate and reliable computation of complete solutions to the equations of linear elastomechanics on three-dimensional domains: Computation of edge stress intensity functions
[FFA-TN-1989-12] N91-13769
Analysis of shells as 3D-elasticity problems using the p-version of the FE method
[FFA-TN-1990-25] N91-13770
Accurate and reliable determination of edge and vertex stress intensity factors in three-dimensional elastomechanics
[FFA-TN-1990-28] N91-13771
ELASTIC SCATTERING
Progress in the detection of single molecules in levitated droplets
[DE91-000612] N91-13517
ELASTOMERS
Device for applying constant pressure to a surface
[NASA-CASE-GSC-13230-1] N91-13734
ELASTOPLASTICITY
Finite element and boundary element methods for elastoplastic stress analysis of two-dimensional and axisymmetric problems N91-13755
ELECTRIC BATTERIES
Secondary Li battery incorporating 12-crown-4 ether
[NASA-CASE-NPO-17922-1-CU] N91-13621
ELECTRIC CONTACTS
Thin solar cell and lightweight array
[NASA-CASE-LEW-14959-1] N91-13803
ELECTRIC CURRENT
Mathematical modelling of part voltage and weld current in resistance welders
[DE91-002534] N91-13727
ELECTRIC DISCHARGES
Computational and experimental progress on laser-activated gas avalanche switches for broadband, high-power electromagnetic pulse generation
[DE91-001763] N91-13623
ELECTRIC FIELDS
Laser-induced fluorescence of phosphors for remote cryogenic thermometry
[DE91-001733] N91-13681
ELECTRIC POTENTIAL
Mathematical modelling of part voltage and weld current in resistance welders
[DE91-002534] N91-13727
ELECTRIC POWER SUPPLIES
Second law analysis of advanced power generation systems using variable temperature heat sources
[DE91-001818] N91-13799
ELECTRIC PULSES
Computation of the current density in nonlinear materials subjected to large current pulses
[DE91-001950] N91-13624
ELECTRIC SWITCHES
Computational and experimental progress on laser-activated gas avalanche switches for broadband, high-power electromagnetic pulse generation
[DE91-001763] N91-13623
ELECTRIC WELDING
Mathematical modelling of part voltage and weld current in resistance welders
[DE91-002534] N91-13727
ELECTRICAL MEASUREMENT
A complex permittivity and permeability measurement system for elevated temperatures
[NASA-CR-186916] N91-13609
ELECTRICAL RESISTANCE
Mathematical modelling of part voltage and weld current in resistance welders
[DE91-002534] N91-13727
ELECTRICAL RESISTIVITY
PBT, PBO-based hybrid polymers with nonlinear optical properties or high electrical conductivity
[AD-A226646] N91-13552
Computation of the current density in nonlinear materials subjected to large current pulses
[DE91-001950] N91-13624
Heat transfer device and method of making the same
[NASA-CASE-LEW-14162-1] N91-13668
ELECTRICITY
Small particle selective emitter
[NASA-CASE-LEW-14731-1] N91-13802
ELECTRIFICATION
A study of the ice-hail charge separation mechanism using a thunderstorm electrification model with explicit microphysics in a kinematic framework N91-13835
ELECTRO-OPTICS
The effect of the molecular structure of polymer and low molecular liquid crystals on their electro-optical characteristics at the nematic-isotropic phase transition
[ETN-91-98170] N91-13564
Design of integrated CMOS circuits for parallel detection and storage of optical data
[AD-A225702] N91-13611
Ultrafast optical electronics center
[AD-A226669] N91-14054
ELECTROCATALYSTS
Electrocatalyst surfaces
[PB90-252560] N91-13507
Electrocatalysis of anodic oxygen-transfer reactions at modified lead dioxide electrodes
[DE91-000664] N91-13518
ELECTROCHEMICAL OXIDATION
Electrocatalyst surfaces
[PB90-252560] N91-13507
ELECTRODES
Electrocatalysis of anodic oxygen-transfer reactions at modified lead dioxide electrodes
[DE91-000664] N91-13518
ELECTROLYTES
Secondary Li battery incorporating 12-crown-4 ether
[NASA-CASE-NPO-17922-1-CU] N91-13621
Thermal power transfer system using applied potential difference to sustain operating pressure difference
[NASA-CASE-NPO-18034-1-CU] N91-13796
ELECTROMAGNETIC ABSORPTION
Probing the interstellar medium of external galaxies using quasar absortion lines: The 3C 232/NGC 3067 system N91-14227
ELECTROMAGNETIC FIELDS
Frequency-domain analysis of one-dimensional electromagnetic scattering by lossy media
[FEL-90-A112] N91-13607
Field error lottery
[DE91-001875] N91-13702
ELECTROMAGNETIC PULSES
Transionospheric Propagation Code (TIPC)
[DE91-002435] N91-13597
Computational and experimental progress on laser-activated gas avalanche switches for broadband, high-power electromagnetic pulse generation
[DE91-001763] N91-13623
Transionospheric propagation calculations for the output of two EMP (Electromagnetic Pulse) simulators
[DE91-001618] N91-13720
Ultrafast optical electronics center
[AD-A226669] N91-14054
ELECTROMAGNETIC SCATTERING
Resonance region scattering
[AD-A226536] N91-13589
Frequency-domain analysis of one-dimensional electromagnetic scattering by lossy media
[FEL-90-A112] N91-13607
Real-space multiple scattering theory calculations of LEED (Low-Energy Electron Diffraction) intensities for stepped surfaces
[DE91-000810] N91-13978
ELECTROMAGNETIC WAVE TRANSMISSION
Assessments of atmospheric effects on VHF and UHF communications
[AD-A226661] N91-13592
Temporal scattering and response software: Users' manual
[DE91-001760] N91-13593
ELECTROMECHANICS
Residual stresses in Al2O3: Comparison between electromechanical measurements and finite element method calculations N91-13545
ELECTRON ATTACHMENT
Stratospheric ozone conservation by electron attachment to chlorine atoms: The negative-ion chemistry
[DE91-002951] N91-13815
ELECTRON BEAMS
MPPE (Multiple Pulse Propagation Experiment) results
[DE91-001678] N91-13599
Small signal gain based on analytic models of thin intense electron beams
[DE91-001874] N91-13631
Diagnostics for high-brightness beams
[DE91-001865] N91-13701
SEPAC data analysis in support of the environmental interaction program
[NASA-CR-184028] N91-13807
Inner-shell ionization of lithium-like chromium ions
[DE91-001749] N91-13981
A liquid nitrogen cooled superconductive electron beam focusing system for improved performance ECM helix traveling wave tubes N91-14047
ELECTRON CYCLOTRON HEATING
Free-electron laser experiments in the microwave tokamak experiment
[DE91-001746] N91-13699
Compact Ignition Tokamak project: Localizability of electron-cyclotron heating power
[DE91-002571] N91-14016
ELECTRON DIFFRACTION
Real-space multiple scattering theory calculations of LEED (Low-Energy Electron Diffraction) intensities for stepped surfaces
[DE91-000810] N91-13978
ELECTRON ENERGY
A multi-laser system for a fast sampling Thomson scattering diagnostic
[DE91-002708] N91-13705
A compact, low cost, 7 channel polychromator for Thomson scattering measurements
[DE91-002719] N91-14024
ELECTRON MICROSCOPES
Control system for ruling blazed, aberration corrected diffraction gratings
[NASA-CASE-GSC-13240-1] N91-13692
Signal processing development
[AD-A226593] N91-14052
ELECTRON MICROSCOPY
Ion-induced damage and amorphization in Si
[DE91-002358] N91-14061
ELECTRON SCATTERING
Application of parallel computing to the Monte Carlo simulation of electron scattering in solids: A rapid method for profile deconvolution
[DE91-001227] N91-13980
ELECTRON TRANSFER
Reactions of the excited state of polypyridyl chromium(III) ion
[DE91-000741] N91-13526
Magnetic turbulent electron transport in a reversed field pinch
[DE91-001898] N91-14009
Kinetic and electromagnetic transport processes in toroidal devices
[DE91-001901] N91-14011
Optical properties and electronic structures of d- and f-electron metals and alloys, Ag-in, Ni-Cu, AuGa2, PtGa2, beta'-NiAl, beta'-CoAl, CeSn3, and LaSn3
[DE91-001597] N91-14059
ELECTRON TUNNELING
Control system for ruling blazed, aberration corrected diffraction gratings
[NASA-CASE-GSC-13240-1] N91-13692
ELECTRON-POSITRON PAIRS
Influence of collective effects on the performance of high-luminosity colliders
[DE91-001797] N91-13982
ELECTRONIC CONTROL
Solder dross removal apparatus
[NASA-CASE-MFS-28406-1] N91-13729
ELECTRONIC COUNTERMEASURES
Extremely High Frequency (EHF) Low Probability of Intercept (LPI) communication applications
[AD-A226653] N91-13591
A liquid nitrogen cooled superconductive electron beam focusing system for improved performance ECM helix traveling wave tubes N91-14047
ELECTRONIC EQUIPMENT
Connectivity alternatives for remote users of the Maintenance Processor Subsystem (MPS)
[DOT/FAA/CT-90/16] N91-13900
Applications of Superconductivity to Avionics
[AGARD-CP-481] N91-14030
ELECTRONS
A relationship between the integrated CO intensity and the radio continuum emission in spiral galaxies N91-14146

ELECTROPHORESIS
The fluid mechanics of continuous flow electrophoresis
[NASA-CR-187647] N91-13648
ELECTROPLATING
Fluid flow effects on electroplating
[DE91-001087] N91-13577
ELECTROSLAG WELDING
Study of the tensile strength of the melted zone of vertical welds carried out using electroslag welding on C-Mn steel. Further study on 80 mm thick plate
[CETIM-104730] N91-13740
ELECTROSTATICS
Thin solar cell and lightweight array
[NASA-CASE-LEW-14959-1] N91-13803
Confinement properties of the RFP (reversed field pinch)
[DE91-002322] N91-14015
ELEMENTARY PARTICLE INTERACTIONS
Elementary particle interactions
[DE91-001220] N91-13979
ELEMENTARY PARTICLES
U1(prime) dark matter and R-parity violation
[DE91-001792] N91-14068
ELLIPTICAL GALAXIES
A survey of the properties of early-type galaxies N91-14109
Intergalactic HI in the NGC5018 group N91-14110
Far-infrared emission from dusty ellipticals N91-14142
Multiband observations of Cygnus A: A study of pressure balance in the core of a powerful radio galaxy N91-14151
The onset of galactic winds in early-type galaxies N91-14165
Narrow band images of suspected cooling flow galaxies N91-14168
Gas flows in elliptical galaxies N91-14170
Stripping of gas and dust from the elliptical galaxy M86 N91-14171
NGC 4438: Ram pressure sweeping of a tidally disrupted galaxy N91-14176
CO observations of southern mergers N91-14197
Current star formation in S0 galaxies: NGC 4710 N91-14224
An imaging and spectroscopic study of low and intermediate power radio galaxies N91-14268
ELLIPTICITY
Instability of a supersonic shock free elliptic jet
[NASA-TM-103428] N91-13413
EMBEDDED COMPUTER SYSTEMS
An object-oriented logic language for modular system specification
[REPT-90-027] N91-13927
EMBEDDING
Transducer holder and method of making
[NASA-CASE-LAR-14027-1] N91-13693
EMERGENCIES
Integrated launch and emergency vehicle system
[NASA-CASE-LAR-13780-1] N91-13481
EMISSION
Carbon dioxide release from Ocean Thermal Energy Conversion (OTEC) cycles
[DE89-009504] N91-13809
Observations of CO isotopic emission and the far-infrared continuum of Centaurus A N91-14125
The CO-12 and CO-13 J=2-1 and J=1-0 observations of hot and cold galaxies N91-14126
High resolution sub-millimetre mapping of starburst galaxies: Comparison with CO emission N91-14129
Evidence against a simple two-component model for the far-infrared emission from galaxies N91-14136
Optical and near-IR study of LMC HII region N11AB N91-14155
Energy input and HI spin temperatures in low pressure regions N91-14163
The onset of galactic winds in early-type galaxies N91-14165
The violent interstellar medium in Messier 31 N91-14178
A high resolution CO map of M51 N91-14203
Detection of CO emission in Hydra 1 cluster galaxies N91-14237
EMISSION SPECTRA
Chromium sensitized garnets for mid-IR lasers
[AD-A226630] N91-13696
Far-infrared spectroscopy of NGC 6946, IC 342, and Arp 299 N91-14114
Observations of the galactic plane by the zodiacal infrared project N91-14143
An infrared jet in Centaurus A (NGC 5128): Evidence for interaction between the active nucleus and the interstellar medium N91-14175
H2 line emission in three Seyfert nuclei: Evidence against UV-excitation N91-14185
Observations of extended and counterrotating disks of ionized gas in S0 galaxies N91-14187
Relativistic effects in millisecond pulsars and active galactic nuclei N91-14247
An imaging and spectroscopic study of low and intermediate power radio galaxies N91-14268
EMISSIVITY
Contribution of cool dust to the FIR brightness distribution of NGC 6946 Sc(s)2 N91-14134
Observations of the galactic plane by the zodiacal infrared project N91-14143
The molecular spiral arms of NGC 6946 N91-14232
EMITTANCE
Passive fetal monitoring sensor
[NASA-CASE-LAR-14088-1] N91-13686
Peering beyond IRAS: The 100 to 350 micron dust emission from galaxies N91-14141
Dense gas and HII regions in the starburst galaxy NGC 253 N91-14220
EMITTERS
Small particle selective emitter
[NASA-CASE-LEW-14731-1] N91-13802
EMULSIONS
High-alcohol microemulsion fuel performance in a diesel engine
[DE91-001617] N91-13572
ENERGY ABSORPTION
Failure behavior of generic metallic and composite aircraft structural components under crash loads
[NASA-RP-1239] N91-13751
A physical parameterization of snow albedo for use in climate models N91-13781
ENERGY BANDS
Optical properties and electronic structures of d- and f-electron metals and alloys, Ag-In, Ni-Cu, AuGa2, PtGa2, beta'-NiAl, beta'-CoAl, CeSn3, and LaSn3
[DE91-001597] N91-14059
ENERGY BUDGETS
Sea ice-atmosphere interaction: Application of multispectral satellite data in polar surface energy flux estimates
[NASA-CR-187376] N91-13782
Peering beyond IRAS: The 100 to 350 micron dust emission from galaxies N91-14141
ENERGY CONSERVATION
Heat exchanger fouling: Prediction, measurement, and mitigation
[DE91-001997] N91-13661
ENERGY CONSUMPTION
Semi-custom integrated circuit amplifier and level discriminator for nuclear and space instruments
[DE91-001951] N91-13620
ENERGY CONVERSION
Heat engine with corrugated shape memory drive belt
[AD-D014640] N91-13716
Small particle selective emitter
[NASA-CASE-LEW-14731-1] N91-13802
ENERGY DISTRIBUTION
Small signal gain based on analytic models of thin intense electron beams
[DE91-001874] N91-13631
ENERGY GAPS (SOLID STATE)
Band-gap narrowing and III-V heterostructure FETs (Field-Effect Transistors)
[DE91-000401] N91-14056
ENERGY POLICY
Solar collector manufacturing activity, 1988
[DE90-003539] N91-13797
ENERGY TECHNOLOGY
Spanwise aerodynamic loads on a rotating wind turbine blade
[DE91-002101] N91-13414
Summaries of physical research in the geosciences
[DE91-001043] N91-13779
Energy Data Base
[DE90-009278] N91-14081
ENERGY TRANSFER
Comment on local energy transfer and nonlocal interactions in homogeneous, isotropic turbulence (Phys. Fluids A2, 413 (1990))
[NASA-TM-103263] N91-13638
ENGINE AIRFRAME INTEGRATION
Effect of location of aft-mounted nacelles on the longitudinal aerodynamic characteristics of a high-wing transport airplane
[NASA-TP-3047] N91-13402
ENGINE DESIGN
JANNAF liquid rocket combustion instability panel research recommendations
[NASA-TM-103653] N91-13491
ENGINE FAILURE
A flight expert system for on-board fault monitoring and diagnosis
[NASA-CR-187334] N91-13452
ENGINE INLETS
Theoretical evaluation of engine auxiliary inlet design for supersonic V/STOL aircraft
[NASA-CR-186610] N91-13443
Shuttle Centaur engine cooldown evaluation and effects of expanded inlets on start transient
[NASA-CR-183198] N91-13487
ENGINE PARTS
Heat engine with corrugated shape memory drive belt
[AD-D014640] N91-13716
ENGINE TESTS
All Shuttle Centaur engine and nozzle support plug vibration testing
[NASA-CR-183201] N91-13485
RL10A-3-3B high mixture ratio qualification program
[NASA-CR-183200] N91-13486
Shuttle Centaur engine cooldown evaluation and effects of expanded inlets on start transient
[NASA-CR-183198] N91-13487
ENGINEERING DRAWINGS
ADENG, adhesive bonding technology for engineering applications: Computer aided design
[CETIM-105070] N91-13917
ENGINES
The third generation of Soviet civilian-use turbofan engines
[AD-A225392] N91-13454
ENTRAINMENT
Coherent anti-Stokes Raman spectroscopic measurement of air entrainment in argon plasma jets
[DE91-001936] N91-13670
Measurement of air entrainment in plasma jets
[DE91-001943] N91-14013
ENTROPY
Algorithmic information content, Church-Turing thesis, physical entropy, and Maxwell's demon
[DE91-001804] N91-14069
ENVIRONMENT EFFECTS
Managing the Global Commons Decision Making and Conflict Resolution in Response to Climate Change Research Workshop
[DE91-001018] N91-13810
Acidic deposition and the environment
[DE91-002352] N91-13812
ENVIRONMENT POLLUTION
Plants and their microbial assistants: Nature's answer to Earth's environmental pollution problems N91-13851
ENVIRONMENT PROTECTION
Acidic deposition and the environment
[DE91-002352] N91-13812
ENVIRONMENTAL ENGINEERING
Biological Life Support Technologies: Commercial Opportunities
[NASA-CP-3094] N91-13842
ENVIRONMENTAL TESTS
Development of mercuric iodide uncooled x ray detectors and spectrometers
[NASA-CR-185394] N91-13484
ENVIRONMENTS
Modelization of two phase turbulent jet up to its auto ignition in variable pressure and temperature environments
[ETN-91-98341] N91-13665
EPIDEMIOLOGY
JPRS Report: Science and technology. USSR: Life sciences
[JPRS-ULS-89-011] N91-13861
EPITAXY
Signal processing development
[AD-A226593] N91-14052
Method of fabricating germanium and gallium arsenide devices
[NASA-CASE-GSC-13265-1] N91-14066
EPOXY COMPOUNDS
A new approach to design of cross-linked second-order nonlinear optical polymers
[AD-A226674] N91-13553
EPOXY RESINS
Material and mechanical characterizations for braided composite pressure vessels
[AD-A226640] N91-13713
EQUATIONS OF MOTION
Vortex collapse from a viewpoint of complex-time singularity
[DE91-001852] N91-13957
The role of chemical interactions in ion-solid processes
[DE91-000763] N91-13977
EQUATIONS OF STATE
Multiphase carbon and its properties in complex mixtures
[DE91-001679] N91-13499
Temporal variations of cosmic rays in the heliosphere N91-14267

EQUATORIAL REGIONS
A primitive equation model for the equatorial Pacific [KNMI-TR-124] N91-13840
ERROR ANALYSIS
Measuring the Lense-Thirring precession using a second Lageos satellite [NASA-CR-186945] N91-13470
Pioneer-Venus radio occultation (ORO) data reduction: Profiles of 13 cm absorptivity [NASA-CR-186986] N91-13584
Detection of multiple-bit errors from single-ion tracks in integrated circuits [NASA-CASE-NPO-18075-1-CU] N91-13622
ERRORS
Periodic trim solutions with hp-version finite elements in time [NASA-CR-187705] N91-13449
Field error lottery [DE91-001875] N91-13702
ERS-1 (ESA SATELLITE)
CESAR MALU program library [FFI-90/7010] N91-13922
ESCAPE SYSTEMS
Assured crew return vehicle [NASA-CASE-MSC-21536-1] N91-13483
ESTIMATING
The environments of double radiogalaxies N91-14166
ETCHING
Micrographic etching of nitrided iron and steel layers [CETIM-106470] N91-13533
Method of fabricating germanium and gallium arsenide devices [NASA-CASE-GSC-13265-1] N91-14066
ETHERS
Methyl substituted polyimides containing carbonyl and ether connecting groups [NASA-CASE-LAR-14351-1] N91-13561
Secondary Li battery incorporating 12-crown-4 ether [NASA-CASE-NPO-17922-1-CU] N91-13621
EULER EQUATIONS OF MOTION
Navier-Stokes and Euler solutions for lee-side flows over supersonic delta wings. A correlation with experiment [NASA-TP-3035] N91-13401
Generalized flux vectors for hypersonic shock capturing [MBB/FE122/S/PUB/397] N91-13423
EULER-LAGRANGE EQUATION
The influence of the sampling time on diffusion measurements in the atmosphere N91-13824
EUROPE
Overview of European technology in computers, telecommunications, and electronics [PB90-215773] N91-13610
EUROPEAN SPACE AGENCY
Catalogue of ESA patents [ESA-SP-1131] N91-14083
EVAPORATION RATE
The effect of condensation in clothing on heat transfer [IZF-1990-B-5] N91-13881
EVEN-EVEN NUCLEI
Prospects of CsJ(Tl)-photodiode detectors for low level spectroscopy [MPI-PAE/EXP.EL-228] N91-13984
EXCITATION
Some observations on the Houbolt-Rainey and peak-hold methods of flutter onset prediction [NASA-TM-102745] N91-13411
Reactions of the excited state of polypyridyl chromium(III) ion [DE91-000741] N91-13526
Imaging spectrophotometry of the nuclear outflow of NGC 1068 N91-14149
Large scale excitation of the ISM in NGC 1068 N91-14150
CO excitation in four IR luminous galaxies N91-14234
EXHAUST EMISSION
Procedure for generating global atmospheric engine emissions data from future supersonic transport aircraft. The 1990 high speed civil transport studies [NASA-CR-181882] N91-13447
Methods of analysis for complex organic aerosol mixtures from urban emission sources of particulate carbon [DE91-001722] N91-13814
EXHAUST GASES
Procedure for generating global atmospheric engine emissions data from future supersonic transport aircraft. The 1990 high speed civil transport studies [NASA-CR-181882] N91-13447
Characterization of rocket propellant combustion products: Description of sampling and analysis methods for rocket exhaust characterization studies [DE91-002536] N91-13574
Cloud properties as deduced from satellite observation [NASA-CR-182851] N91-13833
EXOBIOLOGY
Exobiology site selection for future Mars missions: Martian paleolake sediments and terrestrial analogs [NASA-CR-187358] N91-14255
EXPERIMENT DESIGN
Analysis of bond quality by resonant ultrasound [DE91-000439] N91-13743
EXPERT SYSTEMS
A flight expert system for on-board fault monitoring and diagnosis [NASA-CR-187334] N91-13452
Study of the time and effort signal in cutting operations [CETIM-101580] N91-13583
Bilevel shared control for teleoperators [NASA-CASE-NPO-17800-1-CU] N91-13724
Design reliability engineering [DE91-001949] N91-13744
Quality of expert systems: Methods and techniques [FEL-89-A267] N91-13747
Quality of expert systems: Algorithms for integrity control [FEL-89-A312] N91-13748
Adaptable driver-car interfacing and mental workload: A review of the literature [IZF-1990-B-3] N91-13874
General method of pattern classification using the two-domain theory [NASA-CASE-MSC-21737-1] N91-13911
Tightly coupled simulation utilizing the EBR-II LMR: A real-time supercomputing and AI environment [DE91-001942] N91-13932
Knowledge representation into Ada parallel processing [NASA-CR-187451] N91-13934
Specifications extraction and synthesis: Their correlations with preliminary design N91-13936
Proceedings of the Workshop on Software Tools for Distributed Intelligent Control Systems [DE91-001755] N91-13943
EXPLOSIONS
Bidirectional slapper detonators in spherical explosion systems [DE91-002399] N91-13662
Evolution of a superbubble blastwave in a magnetized medium N91-14180
Star formation in proto dwarf galaxies N91-14212
EXPLOSIVES
Multiphase carbon and its properties in complex mixtures [DE91-001679] N91-13499
All hot spots are not equal [DE91-002303] N91-13573
EXPULSION
Dual diaphragm tank with telltale drain [NASA-CASE-MSC-21703-1] N91-13580
EXTERNAL TANKS
Single launch lunar habitat derived from an NSTS external tank [NASA-TM-4212] N91-14251
EXTINCTION
Neutral atomic absorption lines and far-UV extinction: Possible implications for depletions and grain parameters N91-14115
Empirical relationships between gas abundances and UV selective extinction N91-14116
EXTRACTION
General method of pattern classification using the two-domain theory [NASA-CASE-MSC-21737-1] N91-13911
EXTRATERRESTRIAL MATTER
The large-scale space distribution of emission-line galaxies N91-14091
The hot and cold interstellar matter of early type galaxies and their radio emission N91-14112
EXTRATERRESTRIAL RADIATION
Space radiation dose analysis for solar flare of August 1989 [NASA-TM-4229] N91-14265
EXTRAVEHICULAR ACTIVITY
Generic extravehicular (EVA) and telerobot task primitives for analysis, design, and integration. Version 1.0: Reference compilation for the EVA and telerobotics communities [NASA-CR-187429] N91-13876
EXTREME ULTRAVIOLET RADIATION
Variable magnification glancing incidence x ray telescope [NASA-CASE-MFS-28013-2] N91-14096
Hot interstellar gas and ionization of embedded clouds N91-14161
Ionization in the local interstellar and intergalactic media N91-14249
EXTREMELY HIGH FREQUENCIES
Extremely High Frequency (EHF) Low Probability of Intercept (LPI) communication applications [AD-A226653] N91-13591
EXTREMELY LOW FREQUENCIES
Utilization of the HIPAS facility for cooperative experiments related to ionospheric modification [AD-A226609] N91-13590
EXTRUDING
Method of making single crystal fibers [NASA-CASE-LEW-14921-1] N91-13502
Fabrication and properties of powder metallurgically manufactured aluminum products and composites [VTT-RR-699] N91-13531
EYE (ANATOMY)
Portable dynamic fundus instrument [NASA-CASE-MSC-21675-1] N91-13865

F

F-16 AIRCRAFT
Test procedure frequency multiplier 583R936H03/H04 [FEL-90-A089] N91-13636
F-18 AIRCRAFT
A preliminary look at techniques used to obtain airdata from flight at high angles of attack [NASA-TM-101729] N91-13453
F-106 AIRCRAFT
F-106B airplane active control landing gear drop test performance [NASA-TM-102741] N91-13445
FABRICATION
Relationship between voids and interlaminar shear strength of polymer matrix composites [NASA-TM-103643] N91-13495
Novel polyimide molding powder, coating, adhesive, and matrix resin [NASA-CASE-LAR-14163-1] N91-13559
Fuel cells [DE90-009686] N91-13805
Applications of Superconductivity to Avionics [AGARD-CP-481] N91-14030
Progress in high Tc superconductors N91-14031
Fabrication and characterization of high temperature superconducting thin films for sensors and electronics N91-14041
Method of fabricating germanium and gallium arsenide devices [NASA-CASE-GSC-13265-1] N91-14066
FABRY-PEROT INTERFEROMETERS
The Hawaii Imaging Fabry-Perot Interferometer (HIFI) N91-14240
FACILITIES
Environmental projects. Volume 12: Friable asbestos abatement, GDSCC [NASA-CR-187636] N91-13808
FAILURE ANALYSIS
Thermal and structural assessments of a ceramic wafer seal in hypersonic engines [NASA-TM-103651] N91-13456
Hazard studies for solid propellant rocket motors [AGARD-AG-316] N91-13488
Effects of temperature on acoustically-induced strains and damage propagation in CFRP plates N91-13493
Impact behavior of composite materials: Exploratory research [CETIM-101130] N91-13504
A nonlinear viscoelastic approach to durability predictions for polymer based composite structures [NASA-CR-187653] N91-13554
Failure behavior of generic metallic and composite aircraft structural components under crash loads [NASA-RP-1239] N91-13751
Experimental observations and finite element analysis of the initiation of fiber microbuckling in notched composite laminates [NASA-CR-185354] N91-13756
On the variation in crack-opening stresses at different locations in a three-dimensional body [NASA-CR-187722] N91-13768
An assessment of wind tunnel test data on flexible thermal protection materials and results of new fatigue tests of threads [NASA-CR-177466] N91-13972
FAR FIELDS
Far field wake velocity measurements with hot film probes [AD-A226650] N91-13647
FAR INFRARED RADIATION
Performance of multiplexed Ge:Ga detector arrays in the far infrared [NASA-TM-102275] N91-14087
HI and FIR emission from S0 galaxies N91-14111
Far-infrared spectroscopy of NGC 6946, IC 342, and Arp 299 N91-14114

Far-infrared observations of Circinus and NGC 4945 galaxies N91-14131
Far infrared luminosity functions of normal galaxies N91-14135
Evidence against a simple two-component model for the far-infrared emission from galaxies N91-14136
Peering beyond IRAS: The 100 to 350 micron dust emission from galaxies N91-14141
Far-infrared emission from dusty ellipticals N91-14142
Radio continuum and far-infrared emission of spiral galaxies: Implications of correlations N91-14147
A multi-wavelength study of the peculiar galaxy NGC 2976 N91-14199
Are bars essential for starbursts in non-interacting galaxies N91-14208
Central star formation in S0 galaxies N91-14223
Current star formation in S0 galaxies: NGC 4710 N91-14224
CO excitation in four IR luminous galaxies N91-14234
COBE's search for structure in the Big Bang [NASA-TM-102976] N91-14271

FAR ULTRAVIOLET RADIATION
A comparison of UV surface brightness and HI surface densities for spiral galaxies N91-14102
Far-infrared spectroscopy of NGC 6946, IC 342, and Arp 299 N91-14114
Neutral atomic absorption lines and far-UV extinction: Possible implications for depletions and grain parameters N91-14115

FAST FOURIER TRANSFORMATIONS
Feasibility study, software design, layout and simulation of a two-dimensional fast Fourier transform machine for use in optical array interferometry [NASA-CR-186922] N91-13885

FAST NUCLEAR REACTORS
SP-100 from ground demonstration to flight validation [DE91-001869] N91-13986

FASTENERS
The United Kingdom contribution to the AGARD fatigue-rated fastener systems program [RAE-TR-89046] N91-13451
Two fault tolerant toggle-hook release [NASA-CASE-MSC-21671-1] N91-13723

FATIGUE (MATERIALS)
The United Kingdom contribution to the AGARD fatigue-rated fastener systems program [RAE-TR-89046] N91-13451
Mechanism of mechanical fatigue of silica glass [DE91-004053] N91-13565

FATIGUE TESTS
Fatigue testing of plasma-sprayed thermal barrier coatings, volume 2 [NASA-CR-186726] N91-13535
Spectrum fatigue testing: A literature survey [FFA-TN-1990-40] N91-13772

FAULT TOLERANCE
Pipeline synthetic aperture radar data compression utilizing systolic binary tree-searched architecture for vector quantization [NASA-CASE-NPO-17941-1-CU] N91-13595
Two fault tolerant toggle-hook release [NASA-CASE-MSC-21671-1] N91-13723
Software reliability through fault-avoidance and fault-tolerance [NASA-CR-187646] N91-13904
The ISIS project: Fault-tolerance in large distributed systems [NASA-CR-186625] N91-13928
Validation environment for AIPS/ALS: Implementation and results [NASA-CR-4340] N91-13930
Knowledge representation into Ada parallel processing [NASA-CR-187451] N91-13934

FEASIBILITY ANALYSIS
Feasibility to study of a non-reciprocal latched ferrite phase shifter in the 92-96 GHz band [FEL-90-B114] N91-13634

FEEDBACK AMPLIFIERS
Semi-custom integrated circuit amplifier and level discriminator for nuclear and space instruments [DE91-001951] N91-13620

FEEDBACK CONTROL
Analysis of the leading edge effects on the boundary layer transition [NASA-CR-187361] N91-13405
Multivariable methods for the design, identification, and control of large space structures. Volume 1: Estimator Eigenvalue placement in positive real design [AD-A226525] N91-13477
Multivariable methods for the design, identification, and control of large space structures. Volume 3: A study of the integrated control/structure design optimization problem for large flexible structures [AD-A226526] N91-13478
Thermal power transfer system using applied potential difference to sustain operating pressure difference [NASA-CASE-NPO-18034-1-CU] N91-13796
Distortion-free x ray mask technology [AD-A226524] N91-13993

FERRITES
Feasibility to study of a non-reciprocal latched ferrite phase shifter in the 92-96 GHz band [FEL-90-B114] N91-13634

FERROMAGNETIC MATERIALS
Method and apparatus for characterizing residual stress in ferromagnetic materials [NASA-CASE-LAR-14239-1] N91-13527
Computation of the current density in nonlinear materials subjected to large current pulses [DE91-001950] N91-13624

FETUSES
Passive fetal monitoring sensor [NASA-CASE-LAR-14088-1] N91-13686

FIBER COMPOSITES
Research and development of a ceramic fiber composite heat exchanger [DE90-017250] N91-13497
A nonlinear viscoelastic approach to durability predictions for polymer based composite structures [NASA-CR-187653] N91-13554
Development of standards for advanced polymer matrix composites: A BPF/ACG overview [NPL-DMM(A)-8] N91-13568
Material and mechanical characterizations for braided composite pressure vessels [AD-A226640] N91-13713
Experimental observations and finite element analysis of the initiation of fiber microbuckling in notched composite laminates [NASA-CR-185354] N91-13756

FIBER OPTICS
Ultrasound generation through a fiber optic delivery system using pulsed laser energy [DE91-001914] N91-13970
Injection efficiency of bound modes [NASA-CR-4333] N91-13991
Communication system test for image transmission [DE91-001890] N91-13994
Apparatus for precision focusing and positioning of a beam waist on a target [NASA-CASE-ARC-11916-1-SB] N91-14002

FIBERS
Friction and wear of TPS fibers: A study of the adhesion and friction of high modulus fibers [NASA-CR-187666] N91-13515

FIELD COILS
Dependence of CIT (compact ignition tokamak) PF (poloidal field) coil currents on profile and shape parameters using the control matrix [DE91-002650] N91-14019

FIELD EFFECT TRANSISTORS
Magnetic field effect transistors [AD-A226535] N91-13614
Radiation effects on JFETs (Junction Field-Effect Transistors), MOSFETs, and dipolar transistors, as related to SSC circuit design [DE91-001486] N91-13618
Investigation and development of ISFET type chemical sensors, sensitized by dielectric tying [ECL-90-18] N91-13630
GaAs MMIC mixer for 8-12 GHz, based on 0.5 micrometer gate length D-MESFETS. Volume 1: Design and layout [FEL-89-B277-VOL-1] N91-13632
Band-gap narrowing and III-V heterostructure FETs (Field-Effect Transistors) [DE91-000401] N91-14056
Performance of multiplexed Ge:Ga detector arrays in the far infrared [NASA-TM-102275] N91-14087

FIELD OF VIEW
EMU helmet mounted display [NASA-CASE-MSC-21460-1] N91-13879
Variable magnification glancing incidence x ray telescope [NASA-CASE-MFS-28013-2] N91-14096

FIELD THEORY (ALGEBRA)
Evaluation of expressions involving higher order derivations [NASA-CR-187319] N91-13949

FIELD THEORY (PHYSICS)
A solar chronometer for climate: Astronomical and geophysical evidence N91-13823
Status of lattice field theory calculations [DE91-001141] N91-14057
New phases of D greater than or equal to 2 current and diffeomorphism algebras in particle physics [DE91-001515] N91-14067
Chaos and order in non-integrable model field theories [DE91-002313] N91-14070

FIGHTER AIRCRAFT
Damage tolerance analysis and testing of the fighter aircraft 37 Viggen [FFA-TN-1990-35] N91-13448

FILM THICKNESS
Tritium method oil consumption and its relation to oil film thickness in a production diesel engine [AD-A226649] N91-13714
Analysis of single and multi-grade lubricant film thickness in a diesel engine [AD-A226651] N91-13715

FINITE DIFFERENCE THEORY
Time domain finite difference analysis of antennas [AD-A226534] N91-13613
Analytical study of the liquid phase transient behavior of a high temperature heat pipe [NASA-CR-187426] N91-13644
Heat pipe dynamic behavior [NASA-CR-187422] N91-13645
Image 3.3: Tutorial manual [DE91-001762] N91-13908
A generalized Polak-Ribiere algorithm [MATHS-REPT-A-128] N91-13918
Numerical methods for boundary value problems in differential-algebraic equations [DE91-001748] N91-13956
Lattice Boltzmann methods for some 2-D nonlinear diffusion equations: Computational results [DE91-004175] N91-13962

FINITE ELEMENT METHOD
FE analyses of aircraft model with interior trim [FFA-TN-1990-21] N91-13417
Composite fuselage technology [NASA-CR-187658] N91-13446
Damage tolerance analysis and testing of the fighter aircraft 37 Viggen [FFA-TN-1990-35] N91-13448
Periodic trim solutions with hp-version finite elements in time [NASA-CR-187705] N91-13449
Thermal and structural assessments of a ceramic wafer seal in hypersonic engines [NASA-TM-103651] N91-13456
Effects of temperature on acoustically-induced strains and damage propagation in CFRP plates N91-13493
Residual stresses in Al2O3: Comparison between electromechanical measurements and finite element method calculations N91-13545
A nonlinear viscoelastic approach to durability predictions for polymer based composite structures [NASA-CR-187653] N91-13554
The coupling of finite methods for transport-diffusion problems [ETN-91-98172] N91-13663
A minimization method adapted to the finite element technique for turbulent flow simulation with nonlinear boundary conditions in the wall vicinity [ECL-90-016] N91-13664
Fracture mechanics of interface cracks between dissimilar anisotropic materials N91-13752
Finite element and boundary element methods for elastoplastic stress analysis of two-dimensional and axisymmetric problems N91-13755
Experimental observations and finite element analysis of the initiation of fiber microbuckling in notched composite laminates [NASA-CR-185354] N91-13756
A computational procedure for the dynamics of flexible beams within multibody systems [NASA-CR-187667] N91-13760
General Rotorcraft Aeromechanical Stability Program (GRASP): Theory manual [NASA-TM-102255] N91-13762
Mesh considerations for finite element structural dynamic applications [DE91-001717] N91-13764
A comparison of two numerical methods for shocks in one-dimensional elastic-plastic solids [DE91-001741] N91-13765
Test and model correlation of the atmospheric emission photometric imager fiberglass pedestal [NASA-TM-103515] N91-13766
On the variation in crack-opening stresses at different locations in a three-dimensional body [NASA-CR-187722] N91-13768
Accurate and reliable computation of complete solutions to the equations of linear elastomechanics on three-dimensional domains: Computation of edge stress intensity functions [FFA-TN-1989-12] N91-13769
Analysis of shells as 3D-elasticity problems using the p-version of the FE method [FFA-TN-1990-25] N91-13770

Accurate and reliable determination of edge and vertex stress intensity factors in three-dimensional elastomechanics
[FFA-TN-1990-28] N91-13771
Examples of finite element mesh generation using SDRC IDEAS
[NASA-CR-186962] N91-13893

FINITE VOLUME METHOD
The coupling of finite methods for transport-diffusion problems
[ETN-91-98172] N91-13663

FINS
Damage tolerance analysis and testing of the fighter aircraft 37 Viggen
[FFA-TN-1990-35] N91-13448

FIRE CONTROL
Study system concept for a pelotons procedure trainer (PEP-trainer) for the weapon systems YPR-PRAT, YPR-25 mm (EWS) and Leopard 1-5
[FEL-90-A084] N91-13871

FISCHER-TROPSCH PROCESS
An exploratory program for using hydrous metal oxide ion exchangers as Fischer-Tropsch catalysts
[DE91-002341] N91-13521

FISSION PRODUCTS
The behavior of fission products during nuclear rocket reactor tests
[DE91-001956] N91-13490

FITTING
Cantilever clamp fitting
[NASA-CASE-MFS-28328-1] N91-13731

FLAME PROPAGATION
Topics in physico-chemical hydrodynamics
[DE91-001674] N91-13519

FLAMES
Spray deflagration
[INPE-5079-TDL/413] N91-13511
Topics in physico-chemical hydrodynamics
[DE91-001674] N91-13519

FLAPS (CONTROL SURFACES)
Periodic trim solutions with hp-version finite elements in time
[NASA-CR-187705] N91-13449

FLEXIBILITY
Calibration of the 13- by 13-inch adaptive wall test section for the Langley 0.3-meter transonic cryogenic tunnel
[NASA-TP-3049] N91-13461

FLEXIBLE BODIES
A computational procedure for the dynamics of flexible beams within multibody systems
[NASA-CR-187667] N91-13760

FLEXIBLE SPACECRAFT
Multivariable methods for the design, identification, and control of large space structures. Volume 1: Estimator Eigenvalue placement in positive real design
[AD-A226525] N91-13477
Multivariable methods for the design, identification, and control of large space structures. Volume 3: A study of the integrated control/structure design optimization problem for large flexible structures
[AD-A226526] N91-13478
Analytical and experimental research on large angle maneuvers of flexible structures
[AD-A226679] N91-13479
Computational methods and software systems for dynamics and control of large space structures
[NASA-CR-187669] N91-13480

FLIGHT CONTROL
Missile Interceptor Guidance System Technology
[AGARD-LS-173] N91-13434
Flight control design issues in bank-to-turn missiles N91-13437
Integrated aerodynamic and control system design of oblique wing aircraft N91-13459
Integrated flight-propulsion control concepts for supersonic transport airplanes
[NASA-TM-101728] N91-13460

FLIGHT CREWS
Echocardiography in NATO aircrew
[AGARD-AR-297] N91-13863

FLIGHT SAFETY
Security for safety critical space borne systems
[NASA-CR-187656] N91-13906

FLIGHT SIMULATION
An AD100 implementation of a real-time STOVL aircraft propulsion system
[NASA-TM-103683] N91-13457

FLIGHT SIMULATORS
Simulator flight as a selection device: Effects of test anxiety on subjective and objective measures of performance
[IZF-1989-57] N91-13468
Time-sharing performance as a factor for success in flight training: Test development and validation
[IZF-1989-58] N91-13872

FLIGHT TRAINING
Aircraft accident report: Aloha IslandAir, Inc., Flight 1712, de Havilland Twin Otter, DHC-6-300, N707PV, Halawa Point, Molokai, Hawaii, October 28, 1989
[PB90-910405] N91-13425

FLOATING POINT ARITHMETIC
Guidance, navigation and control. Digital emulation technology laboratory. Volume 3, Task 3: Special studies
[AD-A225125] N91-13430

FLOW CHARACTERISTICS
Turbulence and pressure loss characteristics of the inlet vanes for the 80- by 120-ft wind tunnel
[NASA-TM-102808] N91-13466

FLOW COEFFICIENTS
Theory of finite disturbances in a centrifugal compression system with a vaneless radial diffuser
[NASA-CR-187049] N91-13458

FLOW DISTRIBUTION
Navier-Stokes and Euler solutions for lee-side flows over supersonic delta wings. A correlation with experiment
[NASA-TP-3035] N91-13401
Influence of thermodynamical modelization for chemically reacting air flow
[MBB/FE122/S/PUB/400] N91-13418
A steadying effect of acoustic excitation on transitory stall
[NASA-TM-103689] N91-13420
Theory of finite disturbances in a centrifugal compression system with a vaneless radial diffuser
[NASA-CR-187049] N91-13458
Calibration of the 13- by 13-inch adaptive wall test section for the Langley 0.3-meter transonic cryogenic tunnel
[NASA-TP-3049] N91-13461
Wind-tunnel survey of an oscillating flow field for application to model helicopter rotor testing
[NASA-TM-4224] N91-13462
Turbulence and pressure loss characteristics of the inlet vanes for the 80- by 120-ft wind tunnel
[NASA-TM-102808] N91-13466
Simulation of pressure and temperature responses for the 20 Inch Supersonic Wind Tunnel
[NASA-TM-102647] N91-13467
Thrust chamber modeling using Navier-Stokes equations: Code documentation and listings, volume 2
[NASA-CR-183617] N91-13489
Topics in physico-chemical hydrodynamics
[DE91-001674] N91-13519
Nonlinear viscous waves produced by an impulsively moving plate N91-13641
The fluid mechanics of continuous flow electrophoresis
[NASA-CR-187647] N91-13648
Flow establishment in a generic scramjet combustor
[NASA-CR-187467] N91-13649
Turbulence modeling for sharp-fin-induced shock wave/turbulent boundary-layer interactions
[NASA-TM-102828] N91-13652
Zero wavenumber modes of a compressible supersonic mixing layer
[NASA-CR-187476] N91-13669
Coherent anti-Stokes Raman spectroscopic measurement of air entrainment in argon plasma jets
[DE91-001936] N91-13670

FLOW EQUATIONS
Lattice Boltzmann methods for some 2-D nonlinear diffusion equations: Computational results
[DE91-004175] N91-13962

FLOW MEASUREMENT
A laser Doppler velocimeter approach for near-wall three-dimensional turbulence measurements
[NASA-TM-102841] N91-13653
Measurement of waves in flows across a surface
[NASA-CASE-NPO-17479-1-CU] N91-13658

FLOW REGULATORS
Variable orifice flow regulator
[NASA-CASE-MSC-21549-1] N91-13657

FLOW STABILITY
Instability of a supersonic shock free elliptic jet
[NASA-TM-103428] N91-13413
Reynolds stress closure in jet flows using wave models
[NASA-CR-185717] N91-13640
Zero wavenumber modes of a compressible supersonic mixing layer
[NASA-CR-187476] N91-13669

FLOW VELOCITY
Enhancement of critical heat flux in tubes using staged tangential flow injection
[DE90-014935] N91-13659
Tritium method oil consumption and its relation to oil film thickness in a production diesel engine
[AD-A226649] N91-13714
Gravity waves excited by flow over an obstacle
[FFI-90/7017] N91-13828
Optical emission from cooling flows in distant x ray clusters of galaxies N91-14169

FLUE GASES
Heat exchanger fouling: Prediction, measurement, and mitigation
[DE91-001997] N91-13661

FLUID FLOW
A review of interaction mechanisms in fluid-solid flows
[DE91-000941] N91-13660
Supercritical binary geothermal cycle experiments with mixed-hydrocarbon working fluids and a near-horizontal in-tube condenser
[DE91-001815] N91-13798
Lattice Boltzmann methods for some 2-D nonlinear diffusion equations: Computational results
[DE91-004175] N91-13962

FLUID JETS
Transverse liquid fuel jet breakup, burning, and ignition
[NASA-CR-187423] N91-13510

FLUID MANAGEMENT
Telerobotic on-orbit remote fluid resupply system
[NASA-CR-184052] N91-13474

FLUID MECHANICS
Effect of bulk viscosity in low density, hypersonic blunt body flows
[DE90-012756] N91-13419

FLUID PRESSURE
The effect of longitudinal spacer ribs on the minimum pressure drop in a heated annulus
[DE91-000784] N91-13655
Thermal power transfer system using applied potential difference to sustain operating pressure difference
[NASA-CASE-NPO-18034-1-CU] N91-13796

FLUTTER ANALYSIS
Some observations on the Houbolt-Rainey and peak-hold methods of flutter onset prediction
[NASA-TM-102745] N91-13411

FLUX DENSITY
Investigation of the uniformity of the magnetic field and flux density in the NPL permeameter
[NPL-DES-101] N91-13968

FLUX PINNING
Flux flow pinning and resistive behavior in superconducting networks
[DE91-002756] N91-14064

FLUX QUANTIZATION
Analog superconductive electronics for avionics N91-14040

FLUX VECTOR SPLITTING
Generalized flux vectors for hypersonic shock capturing
[MBB/FE122/S/PUB/397] N91-13423

FLYING PLATFORMS
System and method for measuring ocean surface currents at locations remote from land masses using synthetic aperture radar
[NASA-CASE-NPO-17937-1-CU] N91-13787

FOCUSING
Apparatus for precision focusing and positioning of a beam waist on a target
[NASA-CASE-ARC-11916-1-SB] N91-14002
A liquid nitrogen cooled superconductive electron beam focusing system for improved performance ECM helix traveling wave tubes N91-14047

FOKKER-PLANCK EQUATION
Solving the Fokker-Planck equation on a massively parallel computer
[DE91-002795] N91-13915

FOLDING
Folded RF-excited CO2 waveguide lasers N91-13695

FORBUSH DECREASES
Temporal variations of cosmic rays in the heliosphere N91-14267

FORCE DISTRIBUTION
A semiempirical method for obtaining fuselage normal areas from fuselage Mach sliced areas
[NASA-TM-4228] N91-13433

FORMAT
WordPerfect's toolbox: Formatting documents using styles and macros
[DE91-001884] N91-13912
Sweeping-vector conversion for polygonal data
[INPE-4558-PRE/1299] N91-14077

FORTRAN
A physical parameterization of snow albedo for use in climate models N91-13781

FOULING
Heat exchanger fouling: Prediction, measurement, and mitigation
[DE91-001997] N91-13661

FOURIER ANALYSIS
Periodic trim solutions with hp-version finite elements in time
[NASA-CR-187705] N91-13449

Design of a mechanical modulator for the planetary Fourier spectrometer experiment of the MARS 94 mission
[IFSI-89-22] N91-13717
Modelling the effects of vibration on visual performance
[ISVR-TR-171] N91-13883

FOURIER TRANSFORMATION
Comparison of spectral estimators application to ground sensor signals
[FEL-1988-85] N91-13605

FRACTALS
Fractals and chaotic dynamics in tectonics: Applications to topography and seismicity N91-13821

FRACTOGRAPHY
Mechanical properties of 1950's vintage Type 304 stainless steel weldment components
[DE91-004328] N91-13774

FRACTURE MECHANICS
Advanced Materials Development Program: Ceramic Technology for Advanced Heat Engines program plan, 1983--1993
[DE91-000516] N91-13555
Mechanism of mechanical fatigue of silica glass
[DE91-004053] N91-13565
A comparative study of ductile fracture in the 2.25 percent Cr-1 percent Mo and 9 percent Cr-1 percent Mo alloy steels N91-13753

FRACTURE STRENGTH
Research and development for improved toughness aluminides
[AD-A226627] N91-13524
The influence of the texture of Al2O3 substrates on the fracture behavior under thermal loading N91-13543
Testing of engineering ceramics, summary
[VTT-RR-678] N91-13567
Potential impact of enhanced fracture-toughness data on pressurized-thermal-shock analysis
[DE91-001493] N91-13763

FRACTURES (MATERIALS)
Work of fracture of composites in axial compression: Measurement and origins
[RARDE-1/90] N91-13505

FRACTURING
Fracture of ceramics under farfield cyclic compression
[DE90-008417] N91-13563
Study of static and dynamic fracture using strain measurements N91-13754
The importance of fracturing in the Pimenta Bueno-Ro Basin structure: A study of the morphostructural elements of the rupture-ductile character through remote sensing techniques and products
[INPE-5004-TDL/398] N91-13825

FRAGMENTATION
UK airlines' cost structure and implications of air transport services fragmentation. Research report on air transport fragmentation
[TT-9011] N91-13427

FRAMES
Free vibrations of thin-walled semicircular graphite-epoxy composite frames
[NASA-TP-3010] N91-13750

FRAMES (DATA PROCESSING)
Study of Design Knowledge Capture (DKC) schemes implemented in magnetic bearing applications
[NASA-CR-187394] N91-13677

FREE ELECTRON LASERS
Dual klystron modulator
[DE91-002348] N91-13626
Small signal gain based on analytic models of thin intense electron beams
[DE91-001874] N91-13631
Free-electron laser experiments in the microwave tokamak experiment
[DE91-001746] N91-13699
Field error lottery
[DE91-001875] N91-13702

FREE FLOW
Free-stream turbulence and concave curvature effects on heated, transitional boundary layers, volumes 1 and 2 N91-13643

FREE JETS
Instability of a supersonic shock free elliptic jet
[NASA-TM-103428] N91-13413

FREE WING AIRCRAFT
Free-stream turbulence and concave curvature effects on heated, transitional boundary layers, volumes 1 and 2 N91-13643

FREEZING
Mesoscale monitoring of the soil freeze/thaw boundary from orbital microwave radiometry
[NASA-CR-185901] N91-13817

FREON
Elementary particle interactions
[DE91-001220] N91-13979

FREQUENCIES
Resonance region scattering
[AD-A226536] N91-13589

FREQUENCY ANALYZERS
Frequency-domain analysis of one-dimensional electromagnetic scattering by lossy media
[FEL-90-A112] N91-13607

FREQUENCY MULTIPLIERS
Test procedure frequency multiplier 583R936H03/H04
[FEL-90-A089] N91-13636

FREQUENCY RANGES
A complex permittivity and permeability measurement system for elevated temperatures
[NASA-CR-186916] N91-13609
Gradiometry coexperiments to the gravity probe B and step missions
[NASA-CR-187704] N91-13788

FREQUENCY SHIFT
Comparison of spectral estimators application to ground sensor signals
[FEL-1988-85] N91-13605

FRICTION
Friction and wear of TPS fibers: A study of the adhesion and friction of high modulus fibers
[NASA-CR-187666] N91-13515

FRICTION REDUCTION
Polymer/riblet combination for hydrodynamic skin friction reduction
[NASA-CASE-LAR-14271-1-CU] N91-13558

FROST
Laboratory investigation of the use of geotextiles to mitigate frost heave
[DOT/FAA/RD-90/13] N91-13465

FUEL CELLS
Fuel cells
[DE90-009686] N91-13805

FUEL COMBUSTION
Procedure for generating global atmospheric engine emissions data from future supersonic transport aircraft. The 1990 high speed civil transport studies
[NASA-CR-181882] N91-13447
Transverse liquid fuel jet breakup, burning, and ignition
[NASA-CR-187423] N91-13510

FUEL CONSUMPTION
Guidance methods for tactical and strategic missiles N91-13442
Tritium method oil consumption and its relation to oil film thickness in a production diesel engine
[AD-A226649] N91-13714
Results from the second year of operation of the Federal Methanol Fleet at Oak Ridge National Laboratory
[DE91-000543] N91-13718

FUEL INJECTION
Transverse liquid fuel jet breakup, burning, and ignition
[NASA-CR-187423] N91-13510
Modelization of two phase turbulent jet up to its auto ignition in variable pressure and temperature environments
[ETN-91-98341] N91-13665

FUEL OILS
Tritium method oil consumption and its relation to oil film thickness in a production diesel engine
[AD-A226649] N91-13714

FUEL TESTS
High-alcohol microemulsion fuel performance in a diesel engine
[DE91-001617] N91-13572

FUELS
Results from the second year of operation of the Federal Methanol Fleet at Oak Ridge National Laboratory
[DE91-000543] N91-13718

FUSELAGES
FE analyses of aircraft model with interior trim
[FFA-TN-1990-21] N91-13417
A review of ice accretion data from a model rotor icing test and comparison with theory
[NASA-TM-103712] N91-13421
A semiempirical method for obtaining fuselage normal areas from fuselage Mach sliced areas
[NASA-TM-4228] N91-13433
Composite fuselage technology
[NASA-CR-187658] N91-13446

FUSION REACTORS
HYLIFE-2 inertial confinement fusion reactor design
[DE91-000792] N91-14004

FUZZY SETS
Specifications extraction and synthesis: Their correlations with preliminary design N91-13936

G

GALACTIC CLUSTERS
Intergalactic HI in the NGC5018 group N91-14110
Multiband observations of Cygnus A: A study of pressure balance in the core of a powerful radio galaxy N91-14151
The onset of galactic winds in early-type galaxies N91-14165
Origin and dynamics of emission line clouds in cooling flow environments N91-14167
Optical emission from cooling flows in distant x ray clusters of galaxies N91-14169
Stripping of gas and dust from the elliptical galaxy M86 N91-14171
ISM stripping from cluster galaxies and inhomogeneities in cooling flows N91-14172
Accounting for the dispersion in the x ray properties of early-type galaxies N91-14173
Search for cold gas in clusters with and without cooling flows N91-14174
NGC 4438: Ram pressure sweeping of a tidally disrupted galaxy N91-14176
NGC 3312: A victim of ram pressure sweeping N91-14177
The morphology-density relation for dwarf galaxies N91-14200
Clues to galaxy activity from rich cluster simulations N91-14222
Detection of CO emission in Hydra 1 cluster galaxies N91-14237

GALACTIC COSMIC RAYS
Elemental mapping of planetary surfaces using gamma ray spectroscopy
[DE91-001877] N91-14258

GALACTIC EVOLUTION
The FCRAO extragalactic CO survey: Global properties of galaxies N91-14117
A survey of galaxies in CO N91-14118
The onset of galactic winds in early-type galaxies N91-14165
Properties of the Magellanic-type galaxies N91-14245
An imaging and spectroscopic study of low and intermediate power radio galaxies N91-14268

GALACTIC NUCLEI
Physical conditions in photodissociation regions: Application to galactic nuclei N91-14113
The 3 micron spectrum of NGC 4565 N91-14132
Large scale excitation of the ISM in NGC 1068 N91-14150
An infrared jet in Centaurus A (NGC 5128): Evidence for interaction between the active nucleus and the interstellar medium N91-14175
Infrared spectroscopy of the dwarf starburst galaxy Henize 2-10 N91-14213

GALACTIC RADIATION
HI and FIR emission from S0 galaxies N91-14111
The FCRAO extragalactic CO survey: Global properties of galaxies N91-14117
Circumnuclear molecular gas in starburst and Seyfert galaxies N91-14120
Evidence against a simple two-component model for the far-infrared emission from galaxies N91-14136
Peering beyond IRAS: The 100 to 350 micron dust emission from galaxies N91-14141
Optical emission from cooling flows in distant x ray clusters of galaxies N91-14169
CO excitation in four IR luminous galaxies N91-14234

GALACTIC ROTATION
Evolution of magnetized, rotating, isothermal clouds N91-14191

GALACTIC STRUCTURE
Properties of the Magellanic-type galaxies N91-14245

GALAXIES
The large-scale space distribution of emission-line galaxies N91-14091
Radio observations of several interstellar molecules N91-14093
The Interstellar Medium in External Galaxies: Summaries of contributed papers
[NASA-CP-3084] N91-14100
The extragalactic radiation field and sharp edges to HI disks in galaxies N91-14101
NGC 1058: Gas motions in an extended, quiescent spiral disk N91-14103
Neutral hydrogen in the starburst galaxy NGC3690/IC894 N91-14104
HI and FIR emission from S0 galaxies N91-14111
The hot and cold interstellar matter of early type galaxies and their radio emission N91-14112
Far-infrared spectroscopy of NGC 6946, IC 342, and Arp 299 N91-14114
The FCRAO extragalactic CO survey: Global properties of galaxies N91-14117
Aperture synthesis CO observations of the inner disk of NGC 1068 N91-14122

CO aperture synthesis of NGC 4038/9 (ARP 244) N91-14123
Observations of CO isotopic emission and the far-infrared continuum of Centaurus A N91-14125
The molecular cloud content of early type galaxies N91-14127
CS J = 2 yields 1 emission toward the central region of M82 N91-14128
High spatial resolution 100 micron observations of the M83 bar N91-14130
Far-infrared observations of Circinus and NGC 4945 galaxies N91-14131
The 3 micron spectrum of NGC 4565 N91-14132
Spatial analysis of IRAS observations of nearby spirals N91-14133
Contribution of cool dust to the FIR brightness distribution of NGC 6946 Sc(s)2 N91-14134
Far infrared luminosity functions of normal galaxies N91-14135
Evidence against a simple two-component model for the far-infrared emission from galaxies N91-14136
Emission from small dust particles in diffuse and molecular cloud medium N91-14137
IRAS observations of the ISM in the gamma CAS reflection nebula N91-14140
Peering beyond IRAS: The 100 to 350 micron dust emission from galaxies N91-14141
Differences in the size-internal velocity relation of galactic and extragalactic HII regions N91-14158
The diffuse ionized interstellar medium perpendicular to the plane of NGC 891 N91-14160
Radiative thermal conduction fronts N91-14162
Energy input and HI spin temperatures in low pressure regions N91-14163
Stripping of gas and dust from the elliptical galaxy M86 N91-14171
Accounting for the dispersion in the x ray properties of early-type galaxies N91-14173
Search for cold gas in clusters with and without cooling flows N91-14174
NGC 4438: Ram pressure sweeping of a tidally disrupted galaxy N91-14176
NGC 3312: A victim of ram pressure sweeping N91-14177
What sort of standard candle is Orion for studying molecular hydrogen line emission in galaxies N91-14184
Lyman alpha radiation in external galaxies N91-14186
Observations of extended and counterrotating disks of ionized gas in S0 galaxies N91-14187
Infrared polarimetry and the magnetic field in external galaxies N91-14192
High brightness neutral hydrogen in M31: A new probe of interstellar pressure N91-14196
Gravitational star formation thresholds and gas density in three galaxies N91-14210
Global and radial variations in the efficiency of massive star formation among galaxies N91-14215
Clues to galaxy activity from rich cluster simulations N91-14222
Central star formation in S0 galaxies N91-14223
Radio continuum observations of the quasar-galaxy pair 3C 232-NGC 3067 N91-14226
Probing the interstellar medium of external galaxies using quasar absortion lines: The 3C 232/NGC 3067 system N91-14227
Detection of a z=0.0515, 0.0522 absorption system in the QSO S4 0248+430 due to an intervening galaxy N91-14228
High spatial resolution studies of galaxies in the far IR: Observations with the KAO, and the promise of SOFIA N91-14229
CS in nearby galaxies: Distribution, kinematics, and multilevel studies N91-14235
CO distribution in southern S0 galaxies N91-14239
The Hawaii Imaging Fabry-Perot Interferometer (HIFI) N91-14240
Properties of the Magellanic-type galaxies N91-14245

GALERKIN METHOD
A fully Sinc-Galerkin method for Euler-Bernoulli beam models
[NASA-CR-187462] N91-13952

GALLIUM ARSENIDE LASERS
Study and development of tunable, single mode AlGaAs/GaAs lasers
[DE91-001684] N91-13697
Design of GaAlAs/GaAs GRIN-SCH SQW diode lasers. Analysis of the temperature dependence
[LAAS-90277] N91-13708

GALLIUM ARSENIDES
Publications, patents, presentations, honors, and students report. Kinetics of semiconductor processing chemistry: SiGe and GaAs growth on silicon surfaces
[AD-A226639] N91-13514
Evaluation and fabrication of GaAs integrated logic circuits
[LAAS-90160] N91-13628
Motion detection, novelty filtering, and target tracking using an interferometric technique with a GaAs phase conjugate mirror
[NASA-CASE-NPO-17784-1-CU] N91-13998
Ultrafast optical electronics center
[AD-A226669] N91-14054
Band-gap narrowing and III-V heterostructure FETs (Field-Effect Transistors)
[DE91-000401] N91-14056
Subnanosecond, high voltage photoconductive switching in GaAs
[DE91-002671] N91-14063
Method of fabricating germanium and gallium arsenide devices
[NASA-CASE-GSC-13265-1] N91-14066

GAME THEORY
Advanced missile guidance N91-13439
Classes of priors in games and decision models
[ETN-91-98171] N91-13965

GAMMA RAY BURSTS
Analysis of gamma ray burst spectra with cyclotron lines
[DE91-001745] N91-14269
Gamma ray bursts from comet neutron star magnetosphere interaction, field twisting and E(sub parallel) formation
[DE91-002320] N91-14270

GAMMA RAY SPECTRA
Elemental mapping of planetary surfaces using gamma ray spectroscopy
[DE91-001877] N91-14258
Analysis of gamma ray burst spectra with cyclotron lines
[DE91-001745] N91-14269

GAMMA RAY SPECTROMETERS
Elemental mapping of planetary surfaces using gamma ray spectroscopy
[DE91-001877] N91-14258

GAMMA RAYS
Radiation effects on JFETs (Junction Field-Effect Transistors), MOSFETs, and dipolar transistors, as related to SSC circuit design
[DE91-001486] N91-13618
Multiplexer/amplifier test results for SP-100
[DE91-004504] N91-13990
Fast Pb-glass neutron-to-light converter for ICF (Inertial Confinement Fusion) target burn history measurements
[DE91-002670] N91-14021
Spectrum formation in SN1987A N91-14243
Elemental mapping of planetary surfaces using gamma ray spectroscopy
[DE91-001877] N91-14258

GARNETS
Chromium sensitized garnets for mid-IR lasers
[AD-A226630] N91-13696
Theoretical temperature-dependent branching ratios and laser thresholds of the (5)I7 yields (5)I8 levels of Ho3(+) in ten garnets
[NASA-TM-103429] N91-14053

GAS ANALYSIS
Signal processing development
[AD-A226593] N91-14052

GAS CHROMATOGRAPHY
Methods of analysis for complex organic aerosol mixtures from urban emission sources of particulate carbon
[DE91-001722] N91-13814

GAS COMPOSITION
High resolution CO images of Seyfert Galaxies N91-14121

GAS DENSITY
The extragalactic radiation field and sharp edges to HI disks in galaxies N91-14101
Radial profiles of gas in late-type disk galaxies N91-14107
Disk mass densities in edge-on spiral galaxies N91-14108
Circumnuclear molecular gas in starburst and Seyfert galaxies N91-14120
The environments of double radiogalaxies N91-14166
NGC 3312: A victim of ram pressure sweeping N91-14177
Gravitational star formation thresholds and gas density in three galaxies N91-14210
Star formation in proto dwarf galaxies N91-14212
Dense gas and HII regions in the starburst galaxy NGC 253 N91-14220
High angular resolution mm- and submm-observations of dense molecular gas in M82 N91-14230
The molecular spiral arms of NGC 6946 N91-14232
Spatial variation of the physical conditions of molecular gas in galaxies N91-14236

GAS DETECTORS
Predictive sensor method and apparatus
[NASA-CASE-SSC-00006-1] N91-13691

GAS DISSOCIATION
MHD shocks in the ISM N91-14183
Dissociation and ionization of molecular gas in the spiral arms of M51 N91-14205

GAS DYNAMICS
Development and evaluation of continuum models for translational-rotational nonequilibrium N91-13403
Molecular gas and star formation in the centers of Virgo spirals N91-14216

GAS FLOW
Heat pipe dynamic behavior
[NASA-CR-187422] N91-13645
Gas flows in elliptical galaxies N91-14170
Evolution of a superbubble blastwave in a magnetized medium N91-14180

GAS HEATING
Stripping of gas and dust from the elliptical galaxy M86 N91-14171

GAS IONIZATION
Ionization degree of classical, dense, and highly condensed plasmas
[ETN-91-98174] N91-14027
The interstellar halo of spiral galaxies: NGC 891 N91-14164
Dissociation and ionization of molecular gas in the spiral arms of M51 N91-14205

GAS JETS
Reynolds stress closure in jet flows using wave models
[NASA-CR-185717] N91-13640

GAS PRESSURE
The environments of double radiogalaxies N91-14166

GAS TRANSPORT
Mechanisms of gas permeation through polymer membranes
[DE91-004190] N91-13671
Simulation of the formation and transport of ozone in the atmospheric boundary layer
[DLR-FB-90-25] N91-13827

GASEOUS DIFFUSION
An investigation of microstructural characteristics of contact-lens polymers
[NASA-TP-3034] N91-13492
Lattice Boltzmann methods for some 2-D nonlinear diffusion equations: Computational results
[DE91-004175] N91-13962

GASES
Mechanisms of gas permeation through polymer membranes
[DE91-004190] N91-13671

GATES (CIRCUITS)
GaAs MMIC mixer for 8-12 GHz, based on 0.5 micrometer gate length D-MESFETS. Volume 1: Design and layout
[FEL-89-B277-VOL-1] N91-13632
Auto and hetero-associative memory using a 2-D optical logic gate
[NASA-CASE-NPO-17997-1-CU] N91-13888

GEAR TEETH
Effect of lubricating oil characteristics on gear vibrations N91-13710
Non-linear dynamic analysis of geared systems
[NASA-CR-4338] N91-13737

GEARS
Effect of lubricating oil characteristics on gear vibrations N91-13710

GELS
Tissue simulating gel for medical research
[NASA-CASE-LAR-14036-1] N91-13562

GEOCHEMISTRY
Summaries of physical research in the geosciences
[DE91-001043] N91-13779

GEODESY
Gradiometry coexperiments to the gravity probe B and step missions
[NASA-CR-187704] N91-13788
Report by the Subcommitee on Intercomparison and Merging of Geodetic Data of the Topex/Poseidon science working team
[LR-638] N91-13791
Precision, accuracy, and tectonics from the Global Positioning System N91-13822

GEODYNAMICS
Summaries of physical research in the geosciences
[DE91-001043] N91-13779

GEOELECTRICITY
Numerical solution of the geoelectrodynamic problem
[NASA-CR-186941] N91-13818

GEOGRAPHIC INFORMATION SYSTEMS
Sweeping-vector conversion for polygonal data
[INPE-4558-PRE/1299] N91-14077

Georelational data model: A conceptual vision of a geographical information system
[INPE-4612-PRE/1335] N91-14078

GEOLOGICAL FAULTS
The importance of fracturing in the Pimenta Bueno-Ro Basin structure: A study of the morphostructural elements of the rupture-ductile character through remote sensing techniques and products
[INPE-5004-TDL/398] N91-13825

GEOLOGICAL SURVEYS
Methodological contribution utilizing TM/LANDSAT-5 imagery in geologic mapping of regions with significant vegetative cover
[INPE-5117-TDL/419] N91-13784
Sweeping-vector conversion for polygonal data
[INPE-4558-PRE/1299] N91-14077

GEOLOGY
Summaries of physical research in the geosciences
[DE91-001043] N91-13779
Methodological contribution utilizing TM/LANDSAT-5 imagery in geologic mapping of regions with significant vegetative cover
[INPE-5117-TDL/419] N91-13784

GEOMAGNETISM
Numerical solution of the geoelectrodynamic problem
[NASA-CR-186941] N91-13818
Long persistence effects of geomagnetic activity
[RAE-TM-SP-376] N91-13829
Solar-geophysical data number 550, June 1990. Part 1: (Prompt reports). Data for May, April 1990 and late data
[PB90-258799] N91-14260
Solar-geophysical data number 549, May 1990. Part 1: (Prompt reports). Data for April, March, 1990, and late data
[PB90-251224] N91-14262

GEOMETRIC ACCURACY
Mesh considerations for finite element structural dynamic applications
[DE91-001717] N91-13764

GEOMETRY
The mechanism of restructuring in geometry
[AD-A224740] N91-13951

GEOPHYSICS
Summaries of physical research in the geosciences
[DE91-001043] N91-13779
Atmospheric and geophysical sciences division program report, 1988 - 1989
[DE91-001057] N91-13780
A solar chronometer for climate: Astronomical and geophysical evidence N91-13823
Earth observing satellite: Understanding the Earth as a system N91-13853
Solar-geophysical data number 549, May 1990. Part 1: (Prompt reports). Data for April, March, 1990, and late data
[PB90-251224] N91-14262
Solar-geophysical data number 549, May 1990. Part 2: (Comprehensive reports). Data for November 1989 and miscellaneous
[PB90-251232] N91-14263

GEOPOTENTIAL
Gradiometry coexperiments to the gravity probe B and step missions
[NASA-CR-187704] N91-13788

GEOSTROPHIC WIND
Frontal interactions with orography: Objective cross-sectional analysis of ALPEX data N91-13836

GEOTECHNICAL FABRICS
Literature review on geotextiles to improve pavements for general aviation airports
[DOT/FAA/RD-90/26] N91-13464
Laboratory investigation of the use of geotextiles to mitigate frost heave
[DOT/FAA/RD-90/13] N91-13465

GEOTHERMAL ENERGY UTILIZATION
Supercritical binary geothermal cycle experiments with mixed-hydrocarbon working fluids and a near-horizontal in-tube condenser
[DE91-001815] N91-13798
Second law analysis of advanced power generation systems using variable temperature heat sources
[DE91-001818] N91-13799

GEOTHERMAL RESOURCES
Supercritical binary geothermal cycle experiments with mixed-hydrocarbon working fluids and a near-horizontal in-tube condenser
[DE91-001815] N91-13798
Second law analysis of advanced power generation systems using variable temperature heat sources
[DE91-001818] N91-13799

GERMANIUM
Method of fabricating germanium and gallium arsenide devices
[NASA-CASE-GSC-13265-1] N91-14066

GIMBALS
The Improved Three Axis Test Table (ITATT): Program status and recommendation for completion
[AD-A226508] N91-13712

GLASS
Materials impurity analysis by means of nuclear resonance reactions
[DE91-001758] N91-13520
Thin solar cell and lightweight array
[NASA-CASE-LEW-14959-1] N91-13803

GLASS FIBER REINFORCED PLASTICS
Work of fracture of composites in axial compression: Measurement and origins
[RARDE-1/90] N91-13505

GLASS FIBERS
Friction and wear of TPS fibers: A study of the adhesion and friction of high modulus fibers
[NASA-CR-187666] N91-13515
Test and model correlation of the atmospheric emission photometric imager fiberglass pedestal
[NASA-TM-103515] N91-13766
The prediction and measurement of the one-parameter behaviour of horns
[ISVR-TR-185] N91-13974

GLASS LASERS
Ultra-high brightness (greater than 10(exp 21) W/sq cm) laser facility
[DE91-001685] N91-13698

GLASS TRANSITION TEMPERATURE
Physical properties of thermosetting polymers
[AD-A225864] N91-13508

GLIDE LANDINGS
Integrated launch and emergency vehicle system
[NASA-CASE-LAR-13780-1] N91-13481

GLOBAL POSITIONING SYSTEM
Study of strategies for the determination of deformations from Global Positioning System (GPS) measurements
[ETN-91-98141] N91-13786
System and method for measuring ocean surface currents at locations remote from land masses using synthetic aperture radar
[NASA-CASE-NPO-17937-1-CU] N91-13787
Precision, accuracy, and tectonics from the Global Positioning System N91-13822

GLOBULAR CLUSTERS
Thermal instabilities in protogalactic clouds N91-14195

GOLD ALLOYS
An x ray photoelectron spectroscopy study of Au(x)In(y) alloys
[NASA-TM-103659] N91-14050

GOVERNMENTS
Federal information inventory/locator systems: From burden to benefit N91-14074

GRADIENTS
Frontogenesis in gravity currents: The effect of endwalls and diffusion
[MATHS-REPT-A-127] N91-13666

GRAIN SIZE
The effect of suspended particles on Jean's criterion for gravitational instability N91-14189

GRAPHITE
Corrosion-resistant catalyst supports for phosphoric acid fuel cells
[DE91-001713] N91-13794

GRAPHITE-EPOXY COMPOSITES
Composite fuselage technology
[NASA-CR-187658] N91-13446
Three point bend creep testing of carbon/epoxy
[DE91-001083] N91-13501
Free vibrations of thin-walled semicircular graphite-epoxy composite frames
[NASA-TP-3010] N91-13750

GRAPHS (CHARTS)
Implementation of the MAGINT-MAGGRAF code in the microVAX-3600 system
[INPE-5042-PRE/1575] N91-13898

GRATINGS (SPECTRA)
Control system for ruling blazed, aberration corrected diffraction gratings
[NASA-CASE-GSC-13240-1] N91-13692

GRAVITATION
Measuring the Lense-Thirring precession using a second Lageos satellite
[NASA-CR-186945] N91-13470
Frontogenesis in gravity currents: The effect of endwalls and diffusion
[MATHS-REPT-A-127] N91-13666
Gravitational star formation thresholds and gas density in three galaxies N91-14210

GRAVITATIONAL COLLAPSE
Virial theorem analysis of the structure and stability of magnetized clouds N91-14190

GRAVITATIONAL EFFECTS
Orbit determination and analysis for Aureole 2 rocket at 27:2 resonance
[RAE-TR-90018] N91-13472
Localize and identify the gravity sensing mechanism of plants
[NASA-CR-187411] N91-13841
The effect of suspended particles on Jean's criterion for gravitational instability N91-14189
Relativistic effects in millisecond pulsars and active galactic nuclei N91-14247

GRAVITATIONAL FIELDS
Three-dimensional cell to tissue assembly process
[NASA-CASE-MSC-21559-1] N91-13860
The gravitational wakefield of a molecular cloud in a disk galaxy N91-14188

GRAVITATIONAL PHYSIOLOGY
Localize and identify the gravity sensing mechanism of plants
[NASA-CR-187411] N91-13841
Vestibulo-ocular responses in man to +G sub z hypergravity
[IZF-1989-59] N91-13873

GRAVITATIONAL WAVE ANTENNAS
Funds request for 1990. The cryogenic gravitational antenna (T = 2.0 K) ALTAIR
[IFSI-90-2] N91-13615
Cryostat for the gravitational antenna ALTAIR
[IFSI-90-3] N91-13616

GRAVITROPISM
Localize and identify the gravity sensing mechanism of plants
[NASA-CR-187411] N91-13841

GRAVITY PROBE B
Gradiometry coexperiments to the gravity probe B and step missions
[NASA-CR-187704] N91-13788

GRAVITY WAVES
Gravity waves excited by flow over an obstacle
[FFI-90/7017] N91-13828

GRID GENERATION (MATHEMATICS)
Computation of incompressible flow around the DARPA SUBOFF bodies
[AD-A226481] N91-13646
Mesh considerations for finite element structural dynamic applications
[DE91-001717] N91-13764
Examples of finite element mesh generation using SDRC IDEAS
[NASA-CR-186962] N91-13893

GROOVES
Sheave assembly
[AD-D014605] N91-13711

GROUND SUPPORT EQUIPMENT
Ground-based studies of emission-line variability: Recent results for NGC 5548 and future plans
[NASA-CR-180433] N91-14088

GROUND TESTS
Helicopter structural integrity program (HSIP). Volume 1: Structural test requirements specification
[AD-A226520] N91-13444
SP-100 from ground demonstration to flight validation
[DE91-001869] N91-13986

GROUND TRUTH
Method of selection of TM/LANDSAT color composition for analysis of land use classes
[INPE-5119-TDL/421] N91-13783

GUIDANCE (MOTION)
Guidance, navigation and control. Digital emulation technology laboratory. Volume 2, Task 2: Seeker emulator development
[AD-A225124] N91-13429
Guidance, navigation and control. Digital emulation technology laboratory. Volume 3, Task 3: Special studies
[AD-A225125] N91-13430

GUN PROPELLANTS
The molecular structure of the HAN-based liquid propellants
[AD-A226415] N91-13571

GUST LOADS
Wind-tunnel survey of an oscillating flow field for application to model helicopter rotor testing
[NASA-TM-4224] N91-13462

GYROSCOPES
Superconducting Josephson Junction Gyroscope (JJG) N91-14043

H

H ALPHA LINE
A multi-wavelength study of the peculiar galaxy NGC 2976 N91-14199
Spiral structure of M51: Streaming motions across the spiral arms N91-14206

Global and radial variations in the efficiency of massive star formation among galaxies N91-14215
The molecular spiral arms of NGC 6946 N91-14231

H I REGIONS
Very small grains in the Milky Way and external galaxies N91-14138
Star formation on the leading edge of a ring-like density wave in Arp 143 N91-14198
The molecular spiral arms of NGC 6946 N91-14231

H II REGIONS
Far-infrared spectroscopy of NGC 6946, IC 342, and Arp 299 N91-14114
Evidence against a simple two-component model for the far-infrared emission from galaxies N91-14136
Very small grains in the Milky Way and external galaxies N91-14138
A model for the infrared emission from an OB star cluster environment N91-14139
Ionized interstellar froth in irregular galaxies N91-14152
Ar/S N91-14153
Spatially resolved optical and near infrared spectroscopy of I Zw 18 N91-14154
Optical and near-IR study of LMC HII region N11AB N91-14155
HII regions in dwarf irregular galaxies of the local group N91-14156
HII regions in IC 1613: The ISM in a nearby dwarf irregular galaxy N91-14157
Differences in the size-internal velocity relation of galactic and extragalactic HII regions N91-14158
A study of HII regions in spiral galaxies using multiobject spectroscopy N91-14159
The diffuse ionized interstellar medium perpendicular to the plane of NGC 891 N91-14160
Supernova remnants and diffuse ionized gas in M31 N91-14179
Unbound molecular complexes in M33 N91-14201
Deep narrow band imagery of the diffuse ISM in M33 N91-14202
Small-scale star formation at low metallicity N91-14214
High-mass star formation in southern disk galaxies N91-14218
Starburst outflows from nearby galaxies N91-14219
Dense gas and HII regions in the starburst galaxy NGC 253 N91-14220
High spatial resolution studies of galaxies in the far IR: Observations with the KAO, and the promise of SOFIA N91-14229
The molecular spiral arms of NGC 6946 N91-14231
Molecular outflows in the L1641 region of Orion N91-14246
The photoevaporation of interstellar clouds N91-14248

H LINES
Detection of a z = 0.0515, 0.0522 absorption system in the QSO S4 0248+430 due to an intervening galaxy N91-14228

HAIL
A study of the ice-hail charge separation mechanism using a thunderstorm electrification model with explicit microphysics in a kinematic framework N91-13835

HALLEY'S COMET
Laboratory spectra of amorphous and crystalline olivine: An application to comet Halley IR spectrum [DE91-002307] N91-14264

HALOCARBONS
Ultraviolet absorption cross-sections of photoactive species of stratospheric interest. Part 1: The halocarbons [ETN-91-98385] N91-13830

HALOS
The interstellar halo of spiral galaxies: NGC 891 N91-14164

HAMILTONIAN FUNCTIONS
An asymptotic symmetry of the rapidly forced pendulum [DE91-001868] N91-13958
Chaos and order in non-integrable model field theories [DE91-002313] N91-14070

HAZARDS
Hazard studies for solid propellant rocket motors [AGARD-AG-316] N91-13488

HEAD (ANATOMY)
Effects of anthropometric and postural variables on the transmission of whole-body vertical vibration from seat-to-head [ISVR-TR-172] N91-13884

HEARING
Hearing in three dimensions: Sound localization [NASA-CR-187706] N91-13971

HEART
Passive fetal monitoring sensor [NASA-CASE-LAR-14088-1] N91-13686

HEAT AFFECTED ZONE
Study of the tensile strength of the melted zone of vertical welds carried out using electroslag welding on C-Mn steel. Further study on 80 mm thick plate [CETIM-104730] N91-13740

HEAT EXCHANGERS
Research and development of a ceramic fiber composite heat exchanger [DE90-017250] N91-13497
Enhancement of critical heat flux in tubes using staged tangential flow injection [DE90-014935] N91-13659
Heat exchanger fouling: Prediction, measurement, and mitigation [DE91-001997] N91-13661
Thermal power transfer system using applied potential difference to sustain operating pressure difference [NASA-CASE-NPO-18034-1-CU] N91-13796
Carbon dioxide release from Ocean Thermal Energy Conversion (OTEC) cycles [DE89-009504] N91-13809

HEAT FLUX
Enhancement of critical heat flux in tubes using staged tangential flow injection [DE90-014935] N91-13659
Heat exchanger fouling: Prediction, measurement, and mitigation [DE91-001997] N91-13661
Plug-type heat flux gauge and method of producing same [NASA-CASE-LEW-14967-1] N91-13685
Sea ice-atmosphere interaction: Application of multispectral satellite data in polar surface energy flux estimates [NASA-CR-187376] N91-13782
The status-quo and prospect of superconducting digital devices N91-14039

HEAT PIPES
Analytical study of the liquid phase transient behavior of a high temperature heat pipe [NASA-CR-187426] N91-13644
Heat pipe dynamic behavior [NASA-CR-187422] N91-13645
Experiments on bench-scale heat-pipe solar receivers [DE90-013806] N91-13806

HEAT SOURCES
Second law analysis of advanced power generation systems using variable temperature heat sources [DE91-001818] N91-13799

HEAT TRANSFER
Experimental and theoretical determination of the thermomechanical response of inelastic structural materials to high energy thermal inputs [AD-A226671] N91-13496
Flexible thermal apparatus for mounting of thermoelectric cooler [NASA-CASE-NPO-17806-1-CU] N91-13581
Enhancement of critical heat flux in tubes using staged tangential flow injection [DE90-014935] N91-13659
Heat exchanger fouling: Prediction, measurement, and mitigation [DE91-001997] N91-13661
Heat transfer device and method of making the same [NASA-CASE-LEW-14162-1] N91-13668
Supercritical binary geothermal cycle experiments with mixed-hydrocarbon working fluids and a near-horizontal in-tube condenser [DE91-001815] N91-13798
Experiments on bench-scale heat-pipe solar receivers [DE90-013806] N91-13806
Coupled transport processes in semipermeable media. Part 2: Numerical method and results [DE91-004140] N91-14073

HEAT TRANSFER COEFFICIENTS
The effect of condensation in clothing on heat transfer [IZF-1990-B-5] N91-13881

HEAT TREATMENT
The effects of thermal treatment after welding on the functional properties of assemblies. Follow-up of the work on Cr-Mo [CETIM-104720] N91-13739

HEATING
Transition control via boundary layer heating [ARE-TR-88503] N91-13667
Confinement and heating studies of field-reversed configurations [DE91-001965] N91-14008
Kinetic and electromagnetic transport processes in toroidal devices [DE91-001901] N91-14011
Emission from small dust particles in diffuse and molecular cloud medium N91-14137
Origin and dynamics of emission line clouds in cooling flow environments N91-14167

HEAVING
Laboratory investigation of the use of geotextiles to mitigate frost heave [DOT/FAA/RD-90/13] N91-13465

HEAVY ELEMENTS
The onset of galactic winds in early-type galaxies N91-14165

HEAVY IONS
Inclusive inelastic scattering of heavy ions and nuclear correlations [NASA-TP-3026] N91-13985

HELICOPTER CONTROL
Aerodynamic effect of strakes on two-dimensional tail boom models of the OH-58A and the OH-58D helicopters [NASA-TM-4248] N91-13406

HELICOPTER DESIGN
Helicopter structural integrity program (HSIP). Volume 1: Structural test requirements specification [AD-A226520] N91-13444

HELICOPTER PERFORMANCE
Aerodynamic effect of strakes on two-dimensional tail boom models of the OH-58A and the OH-58D helicopters [NASA-TM-4248] N91-13406
Helicopter structural integrity program (HSIP). Volume 1: Structural test requirements specification [AD-A226520] N91-13444
Wind-tunnel survey of an oscillating flow field for application to model helicopter rotor testing [NASA-TM-4224] N91-13462

HELIOSEISMOLOGY
A solar chronometer for climate: Astronomical and geophysical evidence N91-13823

HELIOSPHERE
Temporal variations of cosmic rays in the heliosphere N91-14267

HELIUM IONS
High spatial and temporal resolution visible spectroscopy of the plasma edge in DIII-D [DE91-002718] N91-14023

HELIUM ISOTOPES
Superfluid Stirling refrigerator: A new method for cooling below 1 Kelvin [DE91-002311] N91-13582
Fast Pb-glass neutron-to-light converter for ICF (Inertial Confinement Fusion) target burn history measurements [DE91-002670] N91-14021

HELIUM PLASMA
Measurement of air entrainment in plasma jets [DE91-001943] N91-14013

HELMET MOUNTED DISPLAYS
EMU helmet mounted display [NASA-CASE-MSC-21460-1] N91-13879

HESSIAN MATRICES
Projected quasi-Newton updates [MATHS-REPT-A-135] N91-13920

HETERODYNING
FIRST: Far Infrared and Submillimetre Space Telescope [ESA-BR-69] N91-14095

HETEROJUNCTION DEVICES
Band-gap narrowing and III-V heterostructure FETs (Field-Effect Transistors) [DE91-000401] N91-14056

HETEROJUNCTIONS
A theoretical investigation of effective surface recombination velocity in AlGaAs/GaAs heteroface solar cells [DE91-001754] N91-13795
High-gain AlGaAs/GaAs double heterojunction Darlington phototransistors for optical neural networks [NASA-CASE-NPO-18101-1-CU] N91-13995

HEURISTIC METHODS
An improved exploratory search technique for pure integer linear programming problems [NASA-TM-103517] N91-13910
The mechanism of restructuring in geometry [AD-A224740] N91-13951

HIERARCHIES
Theory and procedure of the hierarchical design rule checking of integrated circuits [ETN-91-98173] N91-13627
Bilevel shared control for teleoperators [NASA-CASE-NPO-17800-1-CU] N91-13724

HIGH ENERGY INTERACTIONS
Elementary particle interactions [DE91-001220] N91-13979
Particle theory and cosmology [DE91-004189] N91-14250

HIGH FREQUENCIES
Ultrasound generation through a fiber optic delivery system using pulsed laser energy [DE91-001914] N91-13970

HIGH LEVEL LANGUAGES
BAG: A programming language for the CESAR buffer address generator
[FFI-90/7022] N91-13923
HIGH PRESSURE
Dynamic high-pressure studies of an electrothermal capillary
[DE91-000966] N91-13617
Variable orifice flow regulator
[NASA-CASE-MSC-21549-1] N91-13657
Viscosity measurements at high temperature and high pressure: A novel technique
[NASA-CR-187239] N91-13967
HIGH RESOLUTION
Methods of analysis for complex organic aerosol mixtures from urban emission sources of particulate carbon
[DE91-001722] N91-13814
High spatial resolution 100 micron observations of the M83 bar N91-14130
A high resolution CO map of M51 N91-14203
High spatial resolution studies of galaxies in the far IR: Observations with the KAO, and the promise of SOFIA N91-14229
High angular resolution mm- and submm-observations of dense molecular gas in M82 N91-14230
HIGH REYNOLDS NUMBER
The IAR high Reynolds number two-dimensional test facility: A description of equipment and procedures common to most 2-D airfoil tests
[AD-A226629] N91-13409
HIGH SPEED
The status-quo and prospect of superconducting digital devices N91-14039
High velocity gas in external galaxies N91-14105
HIGH SPEED CAMERAS
High pulse rate interferometry using a ruby laser and a Cordin model 360 camera
[DE91-001882] N91-13703
HIGH TEMPERATURE
Three point bend creep testing of carbon/epoxy
[DE91-001083] N91-13501
Preparation of polyimides from bis(N-isoprenyl)s of aryl diamides
[NASA-CASE-LAR-14330-1-CU] N91-13560
Water cooled static pressure probe
[NASA-CASE-LAR-14340-1-CU] N91-13684
Viscosity measurements at high temperature and high pressure: A novel technique
[NASA-CR-187239] N91-13967
HIGH TEMPERATURE AIR
Influence of oxide reinforcement materials on high-temperatue oxidation resistance of Ni3Al matrix composites
[DE91-001625] N91-13498
HIGH TEMPERATURE GASES
A survey of the properties of early-type galaxies N91-14109
The hot and cold interstellar matter of early type galaxies and their radio emission N91-14112
Hot interstellar gas and ionization of embedded clouds N91-14161
Radiative thermal conduction fronts N91-14162
Evolution of a superbubble blastwave in a magnetized medium N91-14180
HIGH TEMPERATURE PLASMAS
A rapid relativistic distorted wave approach for calculating cross sections for ionization of highly charged ions
[DE91-002667] N91-14020
HIGH TEMPERATURE SUPERCONDUCTORS
A 15 MeV proton dianostic for DIII-D
[DE91-002717] N91-14022
A compact, low cost, 7 channel polychromator for Thomson scattering measurements
[DE91-002719] N91-14024
A real-time digital control, data acquisition and analysis system for the DIII-D multipulse Thomson scattering diagnostic
[DE91-002720] N91-14025
Applications of Superconductivity to Avionics
[AGARD-CP-481] N91-14030
Progress in high Tc superconductors N91-14031
Physics and applications of low temperature superconductivity N91-14032
High temperature superconducting thin films for microelectronics: Preparation and properties N91-14033
Passive microwave devices using high temperature superconductors N91-14036
Microwave superconducting electronic devices N91-14037
High Tc superconductors for microwave filters N91-14038
Analog superconductive electronics for avionics N91-14040
Fabrication and characterization of high temperature superconducting thin films for sensors and electronics N91-14041
Application of high-temperature superconductors to high-precision accelerometers N91-14042
Superconducting Josephson Junction Gyroscope (JJG) N91-14043
SQUIDs devices made from high Tc superconductors: Results and perspectives N91-14044
Oxide superconductor coils: Present successes, future challenges N91-14046
A liquid nitrogen cooled superconductive electron beam focusing system for improved performance ECM helix traveling wave tubes N91-14047
Synthesis and characterization of high temperature superconductor materials N91-14048
Ultrafast optical electronics center
[AD-A226669] N91-14054
Flux flow pinning and resistive behavior in superconducting networks
[DE91-002756] N91-14064
HIGH VACUUM
Signal processing development
[AD-A226593] N91-14052
HIGH VOLTAGES
Design of high voltage planar devices using SIPOS technology
[LAAS-90237] N91-13629
HILBERT TRANSFORMATION
Modified Hilbert transform pair and Kramers-Kronig relations for complex permittivities
[NASA-TM-102682] N91-13585
HOLDERS
Transducer holder and method of making
[NASA-CASE-LAR-14027-1] N91-13693
HOLMIUM
Theoretical temperature-dependent branching ratios and laser thresholds of the (5)I7 yields (5)I8 levels of Ho3(+) in ten garnets
[NASA-TM-103429] N91-14053
HOLOGRAPHIC INTERFEROMETRY
High pulse rate interferometry using a ruby laser and a Cordin model 360 camera
[DE91-001882] N91-13703
HOLOGRAPHY
X ray holography at Lawrence Livermore National Laboratory
[DE91-002673] N91-13690
Control system for ruling blazed, aberration corrected diffraction gratings
[NASA-CASE-GSC-13240-1] N91-13692
Real-time dynamic holographic image storage device
[NASA-CASE-LAR-13989-1] N91-13694
HOMING DEVICES
Guidance, navigation and control. Digital emulation technology laboratory. Volume 2, Task 2: Seeker emulator development
[AD-A225124] N91-13429
Midcourse guidance technologies for advanced tactical missiles systems N91-13436
HOMOGENEOUS TURBULENCE
Comment on local energy transfer and nonlocal interactions in homogeneous, isotropic turbulence (Phys. Fluids A2, 413 (1990))
[NASA-TM-103263] N91-13638
HOMOPOLAR GENERATORS
The world of superconductive machinery N91-14045
HOOKS
Two fault tolerant toggle-hook release
[NASA-CASE-MSC-21671-1] N91-13723
HORMONES
Localize and identify the gravity sensing mechanism of plants
[NASA-CR-187411] N91-13841
HORNS
The prediction and measurement of the one-parameter behaviour of horns
[ISVR-TR-185] N91-13974
HOT STARS
Starburst outflows from nearby galaxies N91-14219
HOT WORKING
Evaluation of the functional properties of welds on cold finished tubes defined as NF A 49.541
[CETIM-104700] N91-13738
HOVERING
General Rotorcraft Aeromechanical Stability Program (GRASP): Theory manual
[NASA-TM-102255] N91-13762
HUMAN FACTORS ENGINEERING
The poet revealed: A future for human-centered design
[AD-A226648] N91-13878
The human factors of quality and QA in R and D environments
[DE91-001913] N91-13880
Effects of anthropometric and postural variables on the transmission of whole-body vertical vibration from seat-to-head
[ISVR-TR-172] N91-13884
HUMAN PERFORMANCE
AN alternative to suppression: Modeling methodology for assessing indirect effects of weapons and human performance degradation
[AD-A226518] N91-13877
The human factors of quality and QA in R and D environments
[DE91-001913] N91-13880
HUMAN REACTIONS
A subjective rating scale for assessing pilot workload in flight: A decade of practical use
[RAE-TR-90019] N91-13882
HUMAN TOLERANCES
Vestibulo-ocular responses in man to +G sub z hypergravity
[IZF-1989-59] N91-13873
HUMIDITY
Assessments of atmospheric effects on VHF and UHF communications
[AD-A226661] N91-13592
HYDRAULIC EQUIPMENT
Calibration set up for load cells
[PD-ST-8917] N91-13673
Hydraulic lifting device
[NASA-CASE-SSC-00008-1] N91-13733
HYDRAULIC TEST TUNNELS
A review of ice accretion data from a model rotor icing test and comparison with theory
[NASA-TM-103712] N91-13421
HYDROCARBONS
Electrocatalyst surfaces
[PB90-252560] N91-13507
Preparation of polyimides from bis(N-isoprenyl)s of aryl diamides
[NASA-CASE-LAR-14330-1-CU] N91-13560
Supercritical binary geothermal cycle experiments with mixed-hydrocarbon working fluids and a near-horizontal in-tube condenser
[DE91-001815] N91-13798
HYDRODYNAMICS
Polymer/riblet combination for hydrodynamic skin friction reduction
[NASA-CASE-LAR-14271-1-CU] N91-13558
A review of interaction mechanisms in fluid-solid flows
[DE91-000941] N91-13660
Regularized Chapman-Enskog expansion for scalar conservation laws
[NASA-CR-187441] N91-13966
Gas flows in elliptical galaxies N91-14170
A combined N-body and hydrodynamic code for modeling disk galaxies N91-14241
HYDROGEN
Computed potential energy surfaces for chemical reactions
[NASA-CR-186877] N91-13506
The extragalactic radiation field and sharp edges to HI disks in galaxies N91-14101
A comparison of UV surface brightness and HI surface densities for spiral galaxies N91-14102
Neutral hydrogen in the starburst galaxy NGC3690/IC694 N91-14104
High velocity gas in external galaxies N91-14105
Disk mass densities in edge-on spiral galaxies N91-14108
CO aperture synthesis of NGC 4038/9 (ARP 244) N91-14123
CS J = 2 yields 1 emission toward the central region of M82 N91-14128
High resolution sub-millimetre mapping of starburst galaxies: Comparison with CO emission N91-14129
Energy input and HI spin temperatures in low pressure regions N91-14163
NGC 4438: Ram pressure sweeping of a tidally disrupted galaxy N91-14176
NGC 3312: A victim of ram pressure sweeping N91-14177
MHD shocks in the ISM N91-14183
What sort of standard candle is Orion for studying molecular hydrogen line emission in galaxies N91-14184
H2 line emission in three Seyfert nuclei: Evidence against UV-excitation N91-14185
Lyman alpha radiation in external galaxies N91-14186
High brightness neutral hydrogen in M31: A new probe of interstellar pressure N91-14196
Spiral structure of M51: Streaming motions across the spiral arms N91-14206
High-mass star formation in southern disk galaxies N91-14218
Kinetics of hydrogen release from lunar soil
[NASA-CR-187363] N91-14256

HYDROGEN IONS
A linear accelerator in the space: The beam experiment aboard rocket
[DE91-002347] N91-13988
HYDROGEN MASERS
Complete the development and construction of a spaceborne hydrogen maser clock
[NASA-CR-184043] N91-13688
HYDROGEN RECOMBINATIONS
Spectrum formation in SN1987A N91-14243
HYDROGEN SULFIDE
Radio observations of several interstellar molecules N91-14093
HYDROGRAPHY
Colour specifications for the Electronic Chart Display and Information System (ECDIS)
[IZF-1990-A-19] N91-13789
HYDROXYL EMISSION
CS J = 2 yields 1 emission toward the central region of M82 N91-14128
HYPERPLANES
M-dimensional computer memory with M-1 dimensional hyperplane access
[AD-D014615] N91-13886
On hyperplane design techniques for discrete-time variable structure control systems
[MATHS-REPT-A-133] N91-13948
HYPERSONIC AIRCRAFT
Influence of thermodynamical modelization for chemically reacting air flow
[MBB/FE122/S/PUB/400] N91-13418
HYPERSONIC FLOW
Effect of bulk viscosity in low density, hypersonic blunt body flows
[DE90-012756] N91-13419
Shock tunnel studies of scramjet phenomena, supplement 5
[NASA-CR-182096-SUPPL-5] N91-13651
HYPERSONIC SHOCK
Generalized flux vectors for hypersonic shock capturing
[MBB/FE122/S/PUB/397] N91-13423
HYPERSONICS
Thermal and structural assessments of a ceramic wafer seal in hypersonic engines
[NASA-TM-103651] N91-13456
HYPERVELOCITY IMPACT
The origin and evolution of the Uranian dust rings N91-14253
HYSTERESIS
Temporal variations of cosmic rays in the heliosphere N91-14267

I

ICE
A review of ice accretion data from a model rotor icing test and comparison with theory
[NASA-TM-103712] N91-13421
A study of the ice-hail charge separation mechanism using a thunderstorm electrification model with explicit microphysics in a kinematic framework N91-13835
ICE FORMATION
A review of ice accretion data from a model rotor icing test and comparison with theory
[NASA-TM-103712] N91-13421
IDEAL GAS
Superfluid Stirling refrigerator: A new method for cooling below 1 Kelvin
[DE91-002311] N91-13582
IGNITION
Transverse liquid fuel jet breakup, burning, and ignition
[NASA-CR-187423] N91-13510
Modelization of two phase turbulent jet up to its auto ignition in variable pressure and temperature environments
[ETN-91-98341] N91-13665
ITER confinement capability
[DE91-002647] N91-14018
Dependence of CIT (compact ignition tokamak) PF (poloidal field) coil currents on profile and shape parameters using the control matrix
[DE91-002650] N91-14019
ILLUMINATING
EMU helmet mounted display
[NASA-CASE-MSC-21460-1] N91-13879
IMAGE ANALYSIS
SAR detection of topography, vegetation and installations over land
[FFI-90/7016] N91-13600
IMAGE CONTRAST
Multi-scale contrast enhancement with applications to image fusion
[IZF-1990-A-9] N91-14003
IMAGE ENHANCEMENT
Millimeter-wave sensor image enhancement
[NASA-CR-187430] N91-13679
Multi-scale contrast enhancement with applications to image fusion
[IZF-1990-A-9] N91-14003
IMAGE FILTERS
Method for providing a polarization filter for processing synthetic aperture radar image data
[NASA-CASE-NPO-17904-1-CU] N91-13594
IMAGE PROCESSING
Method for providing a polarization filter for processing synthetic aperture radar image data
[NASA-CASE-NPO-17904-1-CU] N91-13594
Data reduction of digitized images processed from calibrated photographic and spectroscopic films obtained from terrestial, rocket and space shuttle telescopic instruments
[NASA-CR-187320] N91-13674
Millimeter-wave sensor image enhancement
[NASA-CR-187430] N91-13679
Real-time dynamic holographic image storage device
[NASA-CASE-LAR-13989-1] N91-13694
Method of selection of TM/LANDSAT color composition for analysis of land use classes
[INPE-5119-TDL/421] N91-13783
The relation between tree physiology and multispectral and color photography: First phase
[BCRS-89-39] N91-13785
Programmable remapper with single flow architecture
[NASA-CASE-MSC-21481-1] N91-13890
NDRE/TAli processor architecture study
[FFI-90/7012] N91-13891
Architecture for electronic imagery interoperability
[AD-A226522] N91-13901
The design of a distributed image processing and dissemination system
[DE91-001835] N91-13909
General method of pattern classification using the two-domain theory
[NASA-CASE-MSC-21737-1] N91-13911
Computed tomography software and standards
[DE91-002573] N91-13914
Multispectral target detection using image processing programs developed on PC's
[FEL-89-B304] N91-13925
A discrepancy within primate spatial vision and its bearing on the definition of edge detection processes in machine vision
[NASA-TM-102739] N91-13941
Communication system test for image transmission
[DE91-001890] N91-13994
Motion detection, novelty filtering, and target tracking using an interferometric technique with a GaAs phase conjugate mirror
[NASA-CASE-NPO-17784-1-CU] N91-13998
Morphological stability and kinetics in crystal growth from vapors
[NASA-CR-187650] N91-14055
Sweeping-vector conversion for polygonal data
[INPE-4558-PRE/1299] N91-14077
Georelational data model: A conceptual vision of a geographical information system
[INPE-4612-PRE/1335] N91-14078
Utilization of IHS transformation for integration of images of differing resolutions: Urban land use study
[INPE-4606-PRE/1329] N91-14086
Methodology to treat stellar images
[IFSI-89-21] N91-14094
IMAGE RECONSTRUCTION
Restoration of solar radio images: Evaluation of poor conditions and resolution by regularization techniques
[INPE-4557-PRE/1298] N91-13587
IMAGE RESOLUTION
High spatial resolution studies of galaxies in the far IR: Observations with the KAO, and the promise of SOFIA N91-14229
IMAGERY
Deep narrow band imagery of the diffuse ISM in M33 N91-14202
IMAGING TECHNIQUES
Restoration of solar radio images: Evaluation of poor conditions and resolution by regularization techniques
[INPE-4557-PRE/1298] N91-13587
Optical shared memory system demonstration model
[AD-A226431] N91-13612
Detection of multiple-bit errors from single-ion tracks in integrated circuits
[NASA-CASE-NPO-18075-1-CU] N91-13622
Millimeter-wave sensor image enhancement
[NASA-CR-187430] N91-13679
High pulse rate interferometry using a ruby laser and a Cordin model 360 camera
[DE91-001882] N91-13703
Multispectral target detection using image processing programs developed on PC's
[FEL-89-B304] N91-13925
Multi-scale contrast enhancement with applications to image fusion
[IZF-1990-A-9] N91-14003
The large-scale space distribution of emission-line galaxies N91-14091
Variable magnification glancing incidence x ray telescope
[NASA-CASE-MFS-28013-2] N91-14096
Imaging spectrophotometry of the nuclear outflow of NGC 1068 N91-14149
Spatially resolved optical and near infrared spectroscopy of I Zw 18 N91-14154
HII regions in dwarf irregular galaxies of the local group N91-14156
The diffuse ionized interstellar medium perpendicular to the plane of NGC 891 N91-14160
High-mass star formation in southern disk galaxies N91-14218
Central star formation in S0 galaxies N91-14223
The Hawaii Imaging Fabry-Perot Interferometer (HIFI) N91-14240
IMMUNOLOGY
JPRS Report: Science and technology. USSR: Life sciences
[JPRS-ULS-89-011] N91-13861
IMPACT DAMAGE
Ion-induced damage and amorphization in Si
[DE91-002358] N91-14061
Abstracts for the International Workshop on Meteorite Impact on the Early Earth
[NASA-CR-185355] N91-14099
IMPACT LOADS
Damage assessment and residual compression strength of thick composite plates with through-the-thickness reinforcements
[NASA-CR-187377] N91-13494
Failure behavior of generic metallic and composite aircraft structural components under crash loads
[NASA-RP-1239] N91-13751
IMPACT RESISTANCE
Impact behavior of composite materials: Exploratory research
[CETIM-101130] N91-13504
IMPACT TESTS
Impact behavior of composite materials: Exploratory research
[CETIM-101130] N91-13504
IMPURITIES
Materials impurity analysis by means of nuclear resonance reactions
[DE91-001758] N91-13520
IN-FLIGHT MONITORING
A flight expert system for on-board fault monitoring and diagnosis
[NASA-CR-187334] N91-13452
INCIDENT RADIATION
Large scale excitation of the ISM in NGC 1068 N91-14150
INCOMPRESSIBLE FLOW
Development of a time-dependent incompressible Navier-Stokes solver based on a fractional-step method
[NASA-CR-182323] N91-13639
Computation of incompressible flow around the DARPA SUBOFF bodies
[AD-A226481] N91-13646
INDEXES (DOCUMENTATION)
Aeronautical engineering: A continuing bibliography with indexes (supplement 258)
[NASA-SP-7037(258)] N91-13399
List of standards to accompany manual of documentation practices applicable to defence-aerospace scientific and technical information. Addendum
[AGARD-AG-235-ADD] N91-14076
INDIUM ALLOYS
An x ray photoelectron spectroscopy study of Au(x)In(y) alloys
[NASA-TM-103659] N91-14050
INDOOR AIR POLLUTION
Environmental projects. Volume 12: Friable asbestos abatement, GDSCC
[NASA-CR-187636] N91-13808
INDUSTRIES
The 1990 JSAE (Society of Automative Engineers of Japan, Inc.) Spring Convention Proceedings 901
[DE91-715185] N91-13579
Overview of European technology in computers, telecommunications, and electronics
[PB90-215773] N91-13610
Federal information inventory/locator systems: From burden to benefit N91-14074

INELASTIC SCATTERING
Inclusive inelastic scattering of heavy ions and nuclear correlations
[NASA-TP-3026] N91-13985
INERTIAL CONFINEMENT FUSION
Laser programs highlights, July - August 1990
[DE91-001056] N91-13709
HYLIFE-2 inertial confinement fusion reactor design
[DE91-000792] N91-14004
Fast Pb-glass neutron-to-light converter for ICF (Inertial Confinement Fusion) target burn history measurements
[DE91-002670] N91-14021
Experimental development, testing, and research work in support of the inertial confinement fusion program
[DE91-002770] N91-14026
INERTIAL NAVIGATION
Midcourse guidance technologies for advanced tactical missiles systems N91-13436
Assured crew return vehicle
[NASA-CASE-MSC-21536-1] N91-13483
INERTIAL UPPER STAGE
All Shuttle Centaur engine and nozzle support plug vibration testing
[NASA-CR-183201] N91-13485
RL10A-3-3B high mixture ratio qualification program
[NASA-CR-183200] N91-13486
INFORMATION
Energy Data Base
[DE90-009278] N91-14081
INFORMATION DISSEMINATION
Technical communications in aerospace: An analysis of the practices reported by US and European aerospace engineers and scientists
[NASA-TM-103441] N91-14079
INFORMATION MANAGEMENT
Communication system test for image transmission
[DE91-001890] N91-13994
Report of foreign travel
[DE91-001732] N91-14082
INFORMATION RETRIEVAL
Energy Data Base
[DE90-009278] N91-14081
INFORMATION SYSTEMS
Validation environment for AIPS/ALS: Implementation and results
[NASA-CR-4340] N91-13930
Flexible cooperation in non-standard application environments
[AD-A226486] N91-13940
Federal information inventory/locator systems: From burden to benefit N91-14074
Information systems supported end-user interaction: Impacts on inter- and intra-organizational connectivity and cooperative behavior N91-14075
List of standards to accompany manual of documentation practices applicable to defence-aerospace scientific and technical information. Addendum
[AGARD-AG-235-ADD] N91-14076
INFORMATION THEORY
Algorithmic information content, Church-Turing thesis, physical entropy, and Maxwell's demon
[DE91-001804] N91-14069
INFORMATION TRANSFER
Design of integrated CMOS circuits for parallel detection and storage of optical data
[AD-A225702] N91-13611
Report of foreign travel
[DE91-001732] N91-14082
INFRARED ASTRONOMY
Physical conditions in photodissociation regions: Application to galactic nuclei N91-14113
INFRARED ASTRONOMY SATELLITE
An ADP proposal to study the formation and evolution of dust-embedded clusters
[NASA-CR-186793] N91-14089
Far-infrared observations of Circinus and NGC 4945 galaxies N91-14131
Spatial analysis of IRAS observations of nearby spirals N91-14133
Evidence against a simple two-component model for the far-infrared emission from galaxies N91-14136
Emission from small dust particles in diffuse and molecular cloud medium N91-14137
IRAS observations of the ISM in the gamma CAS reflection nebula N91-14140
Peering beyond IRAS: The 100 to 350 micron dust emission from galaxies N91-14141
Far-infrared emission from dusty ellipticals N91-14142
Observations of the galactic plane by the zodiacal infrared project N91-14143
High spatial-resolution IRAS images of M51 N91-14207
Are bars essential for starbursts in non-interacting galaxies N91-14208
INFRARED DETECTORS
Evaluation of Raytek infrared pyrometer for continuous propellant temperature measurement
[NASA-CR-184040] N91-13570
INFRARED IMAGERY
An infrared jet in Centaurus A (NGC 5128): Evidence for interaction between the active nucleus and the interstellar medium N91-14175
Are bars essential for starbursts in non-interacting galaxies N91-14208
Near-infrared mapping of spiral barred galaxies N91-14217
INFRARED LASERS
Chromium sensitized garnets for mid-IR lasers
[AD-A226630] N91-13696
INFRARED RADIATION
Physical conditions in photodissociation regions: Application to galactic nuclei N91-14113
The FCRAO extragalactic CO survey: Global properties of galaxies N91-14117
The CO-12 and CO-13 J=2-1 and J=1-0 observations of hot and cold galaxies N91-14126
CS J = 2 yields 1 emission toward the central region of M82 N91-14128
Far infrared luminosity functions of normal galaxies N91-14135
Very small grains in the Milky Way and external galaxies N91-14138
A model for the infrared emission from an OB star cluster environment N91-14139
Far-infrared emission from dusty ellipticals N91-14142
The infrared continuum spectrum of x ray illuminated molecular gas N91-14144
Search for cold gas in clusters with and without cooling flows N91-14174
Infrared analysis of LMC superbubbles N91-14181
Infrared polarimetry and the magnetic field in external galaxies N91-14192
CO observations of southern mergers N91-14197
Global and radial variations in the efficiency of massive star formation among galaxies N91-14215
Near-infrared mapping of spiral barred galaxies N91-14217
Dense gas and HII regions in the starburst galaxy NGC 253 N91-14220
CO excitation in four IR luminous galaxies N91-14234
INFRARED REFLECTION
Very small grains in the Milky Way and external galaxies N91-14138
INFRARED SPECTRA
Far infrared luminosity functions of normal galaxies N91-14135
The infrared continuum spectrum of x ray illuminated molecular gas N91-14144
Near-infrared mapping of spiral barred galaxies N91-14217
Spectrum formation in SN1987A N91-14243
Laboratory spectra of amorphous and crystalline olivine: An application to comet Halley IR spectrum
[DE91-002307] N91-14264
INFRARED SPECTROMETERS
A near infrared spectroscopic study of the interstellar gas in the starburst core of M82 N91-14221
INFRARED SPECTROPHOTOMETERS
COBE's search for structure in the Big Bang
[NASA-TM-102976] N91-14271
INFRARED SPECTROSCOPY
Publications, patents, presentations, honors, and students report. Kinetics of semiconductor processing chemistry: SiGe and GaAs growth on silicon surfaces
[AD-A226639] N91-13514
The 3 micron spectrum of NGC 4565 N91-14132
Ar/S N91-14153
Spatially resolved optical and near infrared spectroscopy of I Zw 18 N91-14154
Infrared spectroscopy of the dwarf starburst galaxy Henize 2-10 N91-14213
A near infrared spectroscopic study of the interstellar gas in the starburst core of M82 N91-14221
INFRARED TELESCOPES
FIRST: Far Infrared and Submillimetre Space Telescope
[ESA-BR-69] N91-14095
Infrared spectroscopy of the dwarf starburst galaxy Henize 2-10 N91-14213
High angular resolution mm- and submm-observations of dense molecular gas in M82 N91-14230
INFRARED WINDOWS
Evaluation of Raytek infrared pyrometer for continuous propellant temperature measurement
[NASA-CR-184040] N91-13570
INHIBITORS
Summary of JAYGO mixing and FSM-1 application of castable inhibitor and liner
[NASA-CR-184030] N91-13569
INJECTION
Analytical and experimental studies for thermal plasma processing of materials
[DE91-000599] N91-13576
Enhancement of critical heat flux in tubes using staged tangential flow injection
[DE90-014935] N91-13659
Simultaneous measurement of Ni-Al particle size, velocity, and temperature in atmospheric thermal plasmas
[DE91-001935] N91-13826
INJECTION MOLDING
Binders used in metal injection molding
[VTT-RR-691] N91-13529
INLET FLOW
Turbulence and pressure loss characteristics of the inlet vanes for the 80- by 120-ft wind tunnel
[NASA-TM-102808] N91-13466
Flow establishment in a generic scramjet combustor
[NASA-CR-187467] N91-13649
INSPECTION
Tissue simulating gel for medical research
[NASA-CASE-LAR-14036-1] N91-13562
Signal processing used in the electromagnetic inspection of long bodies
[CETIM-107270] N91-13749
INSTITUTIONS
Activities report of the Max-Planck Institute for Aeronomy
[ETN-91-98383] N91-14272
INSULATION
An assessment of wind tunnel test data on flexible thermal protection materials and results of new fatigue tests of threads
[NASA-CR-177466] N91-13972
INTEGERS
An improved exploratory search technique for pure integer linear programming problems
[NASA-TM-103517] N91-13910
INTEGRATED CIRCUITS
Optical shared memory system demonstration model
[AD-A226431] N91-13612
Detection of multiple-bit errors from single-ion tracks in integrated circuits
[NASA-CASE-NPO-18075-1-CU] N91-13622
Evaluation and fabrication of GaAs integrated logic circuits
[LAAS-90160] N91-13628
GaAs MMIC mixer for 8-12 GHz, based on 0.5 micrometer gate length D-MESFETS. Volume 1: Design and layout
[FEL-89-B277-VOL-1] N91-13632
High-gain AlGaAs/GaAs double heterojunction Darlington phototransistors for optical neural networks
[NASA-CASE-NPO-18101-1-CU] N91-13995
INTEGRITY
Quality of expert systems: Algorithms for integrity control
[FEL-89-A312] N91-13748
INTELLIGENCE
Architecture for electronic imagery interoperability
[AD-A226522] N91-13901
INTERACTING GALAXIES
High spatial resolution 100 micron observations of the M83 bar N91-14130
Star formation on the leading edge of a ring-like density wave in Arp 143 N91-14198
INTERATOMIC FORCES
Non-empirical interatomic potentials for transition metals, alloys, and semiconductors
[DE91-002396] N91-14062
INTERCEPTION
Interactions between battle management and guidance law design for a strategic interceptor N91-13441
Guidance methods for tactical and strategic missiles N91-13442
INTERFACES
Investigation and development of ISFET type chemical sensors, sensitized by dielectric tying
[ECL-90-18] N91-13630
INTERFACIAL ENERGY
Synchrotron radiation photoemission study of metal overlayers on hydrogenated amorphous silicon at room temperature
[DE91-000740] N91-13525
INTERFERENCE FIT
The United Kingdom contribution to the AGARD fatigue-rated fastener systems program
[RAE-TR-89046] N91-13451

INTERFEROMETERS
High pulse rate interferometry using a ruby laser and a Cordin model 360 camera
[DE91-001882] N91-13703
A high resolution CO map of M51 N91-14203
INTERFEROMETRY
Feasibility study, software design, layout and simulation of a two-dimensional fast Fourier transform machine for use in optical array interferometry
[NASA-CR-186922] N91-13885
Motion detection, novelty filtering, and target tracking using an interferometric technique with a GaAs phase conjugate mirror
[NASA-CASE-NPO-17784-1-CU] N91-13998
Laser optical disk position encoder with active heads
[NASA-CASE-GSC-13175-1] N91-14001
The CO-12 and CO-13 J=2-1 and J=1-0 observations of hot and cold galaxies N91-14126
A high resolution CO map of M51 N91-14203
INTERGALACTIC MEDIA
Intergalactic HI in the NGC5018 group N91-14110
Differences in the size-internal velocity relation of galactic and extragalactic HII regions N91-14158
The onset of galactic winds in early-type galaxies N91-14165
Stripping of gas and dust from the elliptical galaxy M86 N91-14171
Accounting for the dispersion in the x ray properties of early-type galaxies N91-14173
NGC 4438: Ram pressure sweeping of a tidally disrupted galaxy N91-14176
Clues to galaxy activity from rich cluster simulations N91-14222
Ionization in the local interstellar and intergalactic media N91-14249
INTERNAL COMBUSTION ENGINES
Interpretation of engine cycle-to-cycle variation by chaotic time series analysis
[DE91-000729] N91-13955
INTERNAL PRESSURE
The environments of double radiogalaxies N91-14166
INTERNATIONAL COOPERATION
Report of foreign travel
[DE91-001732] N91-14082
Activities report of the Max-Planck Institute for Aeronomy
[ETN-91-98383] N91-14272
INTERPLANETARY DUST
Observations of the galactic plane by the zodiacal infrared project N91-14143
INTERSTELLAR CHEMISTRY
Radio observations of several interstellar molecules N91-14093
Instellar Gas Experiment (IGE): Testing interstellar gas particles to provide information on the processes of nucleosynthesis in the big bang stars and supernova
[NASA-CR-186713] N91-14097
INTERSTELLAR GAS
Instellar Gas Experiment (IGE): Testing interstellar gas particles to provide information on the processes of nucleosynthesis in the big bang stars and supernova
[NASA-CR-186713] N91-14097
NGC 1058: Gas motions in an extended, quiescent spiral disk N91-14103
The ratio of molecular to atomic gas in spiral galaxies as a function of morphological type N91-14119
Ionized interstellar froth in irregular galaxies N91-14152
Hot interstellar gas and ionization of embedded clouds N91-14161
ISM stripping from cluster galaxies and inhomogeneities in cooling flows N91-14172
An infrared jet in Centaurus A (NGC 5128): Evidence for interaction between the active nucleus and the interstellar medium N91-14175
Evolution of a superbubble blastwave in a magnetized medium N91-14180
Lyman alpha radiation in external galaxies N91-14186
One-dimensional cloud fluid model for propagating star formation N91-14211
A near infrared spectroscopic study of the interstellar gas in the starburst core of M82 N91-14221
Detection of a z=0.0515, 0.0522 absorption system in the QSO S4 0248+430 due to an intervening galaxy N91-14228
INTERSTELLAR MAGNETIC FIELDS
Evolution of a superbubble blastwave in a magnetized medium N91-14180
Virial theorem analysis of the structure and stability of magnetized clouds N91-14190
Infrared polarimetry and the magnetic field in external galaxies N91-14192
Granularity in the magnetic field structure of M83 N91-14194
The photoevaporation of interstellar clouds N91-14248
INTERSTELLAR MATTER
Radio observations of several interstellar molecules N91-14093
The Interstellar Medium in External Galaxies: Summaries of contributed papers
[NASA-CP-3084] N91-14100
The extragalactic radiation field and sharp edges to HI disks in galaxies N91-14101
A comparison of UV surface brightness and HI surface densities for spiral galaxies N91-14102
The hot and cold interstellar matter of early type galaxies and their radio emission N91-14112
Physical conditions in photodissociation regions: Application to galactic nuclei N91-14113
Far-infrared spectroscopy of NGC 6946, IC 342, and Arp 299 N91-14114
Empirical relationships between gas abundances and UV selective extinction N91-14116
The 3 micron spectrum of NGC 4565 N91-14132
Contribution of cool dust to the FIR brightness distribution of NGC 6946 Sc(s)2 N91-14134
Far infrared luminosity functions of normal galaxies N91-14135
Evidence against a simple two-component model for the far-infrared emission from galaxies N91-14136
Very small grains in the Milky Way and external galaxies N91-14138
A model for the infrared emission from an OB star cluster environment N91-14139
IRAS observations of the ISM in the gamma CAS reflection nebula N91-14140
Imaging spectrophotometry of the nuclear outflow of NGC 1068 N91-14149
Large scale excitation of the ISM in NGC 1068 N91-14150
Multiband observations of Cygnus A: A study of pressure balance in the core of a powerful radio galaxy N91-14151
Ionized interstellar froth in irregular galaxies N91-14152
HII regions in IC 1613: The ISM in a nearby dwarf irregular galaxy N91-14157
The diffuse ionized interstellar medium perpendicular to the plane of NGC 891 N91-14160
Hot interstellar gas and ionization of embedded clouds N91-14161
Radiative thermal conduction fronts N91-14162
The interstellar halo of spiral galaxies: NGC 891 N91-14164
Origin and dynamics of emission line clouds in cooling flow environments N91-14167
Gas flows in elliptical galaxies N91-14170
NGC 3312: A victim of ram pressure sweeping N91-14177
The violent interstellar medium in Messier 31 N91-14178
Infrared analysis of LMC superbubbles N91-14181
MHD shocks in the ISM N91-14183
What sort of standard candle is Orion for studying molecular hydrogen line emission in galaxies N91-14184
H2 line emission in three Seyfert nuclei: Evidence against UV-excitation N91-14185
Lyman alpha radiation in external galaxies N91-14186
Aspects of the interstellar medium in starburst galaxies N91-14209
Starburst outflows from nearby galaxies N91-14219
Current star formation in S0 galaxies: NGC 4710 N91-14224
Probing the interstellar medium of external galaxies using quasar absorption lines: The 3C 232/NGC 3067 system N91-14227
The evolution of comets and the detectability of Extra-Solar Oort Clouds N91-14242
The photoevaporation of interstellar clouds N91-14248
Ionization in the local interstellar and intergalactic media N91-14249
INTERSTELLAR RADIATION
High spatial resolution 100 micron observations of the M83 bar N91-14130
Evidence against a simple two-component model for the far-infrared emission from galaxies N91-14136
Emission from small dust particles in diffuse and molecular cloud medium N91-14137
A relationship between the integrated CO intensity and the radio continuum emission in spiral galaxies N91-14146
Infrared analysis of LMC superbubbles N91-14181
INVENTORIES
Federal information inventory/locator systems: From burden to benefit N91-14074
INVISCID FLOW
Theory of finite disturbances in a centrifugal compression system with a vaneless radial diffuser
[NASA-CR-187049] N91-13458
Flow establishment in a generic scramjet combustor
[NASA-CR-187467] N91-13649
IODIDES
Development of mercuric iodide uncooled x ray detectors and spectrometers
[NASA-CR-185394] N91-13484
ION BEAMS
The role of chemical interactions in ion-solid processes
[DE91-000763] N91-13977
Inner-shell ionization of lithium-like chromium ions
[DE91-001749] N91-13981
ION EXCHANGING
An exploratory program for using hydrous metal oxide ion exchangers as Fischer-Tropsch catalysts
[DE91-002341] N91-13521
ION IMPACT
Single event upset hardening techniques
[DE91-002337] N91-13625
ION IMPLANTATION
Evaluation and fabrication of GaAs integrated logic circuits
[LAAS-90160] N91-13628
ION SCATTERING
Inclusive inelastic scattering of heavy ions and nuclear correlations
[NASA-TP-3026] N91-13985
ION TEMPERATURE
High spatial and temporal resolution visible spectroscopy of the plasma edge in DIII-D
[DE91-002718] N91-14023
IONIC COLLISIONS
The role of chemical interactions in ion-solid processes
[DE91-000763] N91-13977
Atomic and molecular theory
[DE91-004475] N91-13983
Inclusive inelastic scattering of heavy ions and nuclear correlations
[NASA-TP-3026] N91-13985
IONIZATION
Inner-shell ionization of lithium-like chromium ions
[DE91-001749] N91-13981
A rapid relativistic distorted wave approach for calculating cross sections for ionization of highly charged ions
[DE91-002667] N91-14020
Neutral atomic absorption lines and far-UV extinction: Possible implications for depletions and grain parameters N91-14115
Hot interstellar gas and ionization of embedded clouds N91-14161
Origin and dynamics of emission line clouds in cooling flow environments N91-14167
MHD shocks in the ISM N91-14183
Spectrum formation in SN1987A N91-14243
IONIZATION CROSS SECTIONS
A rapid relativistic distorted wave approach for calculating cross sections for ionization of highly charged ions
[DE91-002667] N91-14020
IONIZED GASES
A model for the infrared emission from an OB star cluster environment N91-14139
Circumnuclear ionized gas in starburst nuclei N91-14148
Imaging spectrophotometry of the nuclear outflow of NGC 1068 N91-14149
Ionized interstellar froth in irregular galaxies N91-14152
Optical and near-IR study of LMC HII region N11AB N91-14155
The diffuse ionized interstellar medium perpendicular to the plane of NGC 891 N91-14160
Supernova remnants and diffuse ionized gas in M31 N91-14179
MHD shocks in the ISM N91-14183
Observations of extended and counterrotating disks of ionized gas in S0 galaxies N91-14187
A multi-wavelength study of the peculiar galaxy NGC 2976 N91-14199
A high resolution CO map of M51 N91-14203
IONIZING RADIATION
The photoevaporation of interstellar clouds N91-14248
IONOSPHERIC DISTURBANCES
Utilization of the HIPAS facility for cooperative experiments related to ionospheric modification
[AD-A226609] N91-13590

IONOSPHERIC ELECTRON DENSITY
Transionospheric propagation calculations for the output of two EMP (Electromagnetic Pulse) simulators
[DE91-001618] N91-13720
IONOSPHERIC PROPAGATION
Transionospheric Propagation Code (TIPC)
[DE91-002435] N91-13597
Transionospheric propagation calculations for the output of two EMP (Electromagnetic Pulse) simulators
[DE91-001618] N91-13720
IONS
Detection of multiple-bit errors from single-ion tracks in integrated circuits
[NASA-CASE-NPO-18075-1-CU] N91-13622
A rapid relativistic distorted wave approach for calculating cross sections for ionization of highly charged ions
[DE91-002667] N91-14020
Circumnuclear ionized gas in starburst nuclei N91-14148
IRRADIATION
Methyl substituted polyimides containing carbonyl and ether connecting groups
[NASA-CASE-LAR-14351-1] N91-13561
Operation of silicon microstrip detectors in a high radiation environment
[DE91-001953] N91-13682
IRREGULAR GALAXIES
Ionized interstellar froth in irregular galaxies N91-14152
HII regions in dwarf irregular galaxies of the local group N91-14156
HII regions in IC 1613: The ISM in a nearby dwarf irregular galaxy N91-14157
ISOTOPE SEPARATION
Laser programs highlights, July - August 1990
[DE91-001056] N91-13709
ISOTOPES
Instellar Gas Experiment (IGE): Testing interstellar gas particles to provide information on the processes of nucleosynthesis in the big bang stars and supernova
[NASA-CR-186713] N91-14097
Observations of CO isotopic emission and the far-infrared continuum of Centaurus A N91-14125
The CO-12 and CO-13 J=2-1 and J=1-0 observations of hot and cold galaxies N91-14126
CS in nearby galaxies: Distribution, kinematics, and multilevel studies N91-14235
Spatial variation of the physical conditions of molecular gas in galaxies N91-14236
ISOTROPIC TURBULENCE
Comment on local energy transfer and nonlocal interactions in homogeneous, isotropic turbulence (Phys. Fluids A2, 413 (1990))
[NASA-TM-103263] N91-13638
ITERATION
Projected quasi-Newton updates
[MATHS-REPT-A-135] N91-13920
The simultaneous integration of many trajectories using nilpotent normal forms
[NASA-CR-187318] N91-13950
IUE
Empirical relationships between gas abundances and UV selective extinction N91-14116

J

JACKS (LIFTS)
Calibration set up for load cells
[PD-ST-8917] N91-13673
JET FLOW
Transverse liquid fuel jet breakup, burning, and ignition
[NASA-CR-187423] N91-13510
Reynolds stress closure in jet flows using wave models
[NASA-CR-185717] N91-13640
JET MIXING FLOW
Large eddy simulations and direct numerical simulations of high speed turbulent reacting flows
[NASA-CR-187674] N91-13656
JOINTS (JUNCTIONS)
Two fault tolerant toggle-hook release
[NASA-CASE-MSC-21671-1] N91-13723
ADENG, adhesive bonding technology for engineering applications: Computer aided design
[CETIM-105070] N91-13917
JOSEPHSON JUNCTIONS
Superconducting Josephson Junction Gyroscope (JJG) N91-14043
Experimental studies of Josephson effect
[AD-A226548] N91-14051
Flux flow pinning and resistive behavior in superconducting networks
[DE91-002756] N91-14064
JUNCTION TRANSISTORS
Radiation effects on JFETs (Junction Field-Effect Transistors), MOSFETs, and dipolar transistors, as related to SSC circuit design
[DE91-001486] N91-13618

K

K LINES
Detection of a z=0.0515, 0.0522 absorption system in the QSO S4 0248+430 due to an intervening galaxy N91-14228
KERR MAGNETOOPTICAL EFFECT
Magnetic field effect transistors
[AD-A226535] N91-13614
KINEMATICS
Midcourse guidance technologies for advanced tactical missiles systems N91-13436
A study of the ice-hail charge separation mechanism using a thunderstorm electrification model with explicit microphysics in a kinematic framework N91-13835
Robust deterministic control for robotic manipulators N91-13937
Imaging spectrophotometry of the nuclear outflow of NGC 1068 N91-14149
The violent interstellar medium in Messier 31 N91-14178
CS in nearby galaxies: Distribution, kinematics, and multilevel studies N91-14235
KINETIC ENERGY
Kinetic and electromagnetic transport processes in toroidal devices
[DE91-001901] N91-14011
KLYSTRONS
Relativistic kylstron simulations using RKTW2D
[DE91-001747] N91-13619
Dual klystron modulator
[DE91-002348] N91-13626
KNOWLEDGE BASES (ARTIFICIAL INTELLIGENCE)
Quality of expert systems: Methods and techniques
[FEL-89-A267] N91-13747
KNOWLEDGE REPRESENTATION
Study of Design Knowledge Capture (DKC) schemes implemented in magnetic bearing applications
[NASA-CR-187394] N91-13677
Knowledge representation into Ada parallel processing
[NASA-CR-187451] N91-13934
KRAMERS-KRONIG FORMULA
Modified Hilbert transform pair and Kramers-Kronig relations for complex permittivities
[NASA-TM-102682] N91-13585
KUIPER AIRBORNE OBSERVATORY
Far-infrared spectroscopy of NGC 6946, IC 342, and Arp 299 N91-14114
High spatial resolution 100 micron observations of the M83 bar N91-14130

L

LABORATORIES
Laser programs highlights, July - August 1990
[DE91-001056] N91-13709
Atmospheric and geophysical sciences division program report, 1988 - 1989
[DE91-001057] N91-13780
LAGEOS (SATELLITE)
Measuring the Lense-Thirring precession using a second Lageos satellite
[NASA-CR-186945] N91-13470
LAMINAR FLOW
Large-eddy simulation of transitional channel flow
[NASA-CR-187465] N91-13410
Spray deflagration
[INPE-5079-TDL/413] N91-13511
Coherent anti-Stokes Raman spectroscopic measurement of air entrainment in argon plasma jets
[DE91-001936] N91-13670
LAMINATES
Use of neutron diffraction methods for the determination of mechanical stresses in metal ceramic laminated composite materials N91-13537
Development of standards for advanced polymer matrix composites: A BPF/ACG overview
[NPL-DMM(A)-8] N91-13568
Free vibrations of thin-walled semicircular graphite-epoxy composite frames
[NASA-TP-3010] N91-13750
Experimental observations and finite element analysis of the initiation of fiber microbuckling in notched composite laminates
[NASA-CR-185354] N91-13756
LAND USE
Method of selection of TM/LANDSAT color composition for analysis of land use classes
[INPE-5119-TDL/421] N91-13783
Utilization of IHS transformation for integration of images of differing resolutions: Urban land use study
[INPE-4606-PRE/1329] N91-14086
LANDFORMS
SAR detection of topography, vegetation and installations over land
[FFI-90/7016] N91-13600
LANDING GEAR
F-106B airplane active control landing gear drop test performance
[NASA-TM-102741] N91-13445
LANDING LOADS
F-106B airplane active control landing gear drop test performance
[NASA-TM-102741] N91-13445
LANDING SITES
Assured crew return vehicle
[NASA-CASE-MSC-21536-1] N91-13483
LANGUAGE PROGRAMMING
Semantic validation of structured theories: Applications to a generic programming language
[ETN-91-98207] N91-13916
LAP JOINTS
Tubular lap joints for wind turbine applications
[DE91-001341] N91-13736
LAPLACE TRANSFORMATION
Frequency-domain analysis of one-dimensional electromagnetic scattering by lossy media
[FEL-90-A112] N91-13607
LARGE SPACE STRUCTURES
Analytical and photogrammetric characterization of a planar tetrahedral truss
[NASA-TM-4231] N91-13473
Multivariable methods for the design, identification, and control of large space structures. Volume 1: Estimator Eigenvalue placement in positive real design
[AD-A226525] N91-13477
Multivariable methods for the design, identification, and control of large space structures. Volume 3: A study of the integrated control/structure design optimization problem for large flexible structures
[AD-A226526] N91-13478
Computational methods and software systems for dynamics and control of large space structures
[NASA-CR-187669] N91-13480
LASER ANEMOMETERS
Fibre-linked miniature laser transit anemometer for complex flow fields N91-13678
LASER APPLICATIONS
Fibre-linked miniature laser transit anemometer for complex flow fields N91-13678
Optical joint correlation for real-time tracking
[NASA-CASE-MSC-21509-1] N91-13997
LASER BEAMS
Twelve signals multiplexed with the LLNL optical streak camera
[DE91-000066] N91-13680
Diagnostics for high-brightness beams
[DE91-001865] N91-13701
High pulse rate interferometry using a ruby laser and a Cordin model 360 camera
[DE91-001882] N91-13703
A multi-laser system for a fast sampling Thomson scattering diagnostic
[DE91-002708] N91-13705
Apparatus for precision focusing and positioning of a beam waist on a target
[NASA-CASE-ARC-11916-1-SB] N91-14002
LASER FUSION
Laser programs highlights, July - August 1990
[DE91-001056] N91-13709
Stimulated Raman scatter from laser-produced plasmas: Merely nonlinear or also chaotic
[DE91-001742] N91-14007
LASER GUIDANCE
Study system concept for a pelotons procedure trainer (PEP-trainer) for the weapon systems YPR-PRAT, YPR-25 mm (EWS) and Leopard 1-5
[FEL-90-A084] N91-13871
LASER HEATING
Experimental and theoretical determination of the thermomechanical response of inelastic structural materials to high energy thermal inputs
[AD-A226671] N91-13496
LASER INDUCED FLUORESCENCE
Progress in the detection of single molecules in levitated droplets
[DE91-000612] N91-13517
Laser-induced fluorescence of phosphors for remote cryogenic thermometry
[DE91-001733] N91-13681

LASER OUTPUTS
Small signal gain based on analytic models of thin intense electron beams
[DE91-001874] N91-13631
Fibre-linked miniature laser transit anemometer for complex flow fields N91-13678
Folded RF-excited CO2 waveguide lasers N91-13695
Diagnostics for high-brightness beams
[DE91-001865] N91-13701
Progress of research on water vapor lidar
[NASA-CR-187673] N91-13837
LASER PLASMAS
Stimulated Raman scatter from laser-produced plasmas: Merely nonlinear or also chaotic
[DE91-001742] N91-14007
LASER RANGE FINDERS
Measuring the Lense-Thirring precession using a second Lageos satellite
[NASA-CR-186945] N91-13470
LASER SPECTROMETERS
Actinide speciation by photothermal spectroscopies: Instrumentation development
[DE91-001854] N91-13700
LASER SPECTROSCOPY
Publications, patents, presentations, honors, and students report. Kinetics of semiconductor processing chemistry: SiGe and GaAs growth on silicon surfaces
[AD-A226639] N91-13514
Actinide speciation by photothermal spectroscopies: Instrumentation development
[DE91-001854] N91-13700
LASER TARGETS
An interactive program for the analysis and design of advanced laser targets
[DE91-002542] N91-13704
Fast Pb-glass neutron-to-light converter for ICF (Inertial Confinement Fusion) target burn history measurements
[DE91-002670] N91-14021
Experimental development, testing, and research work in support of the inertial confinement fusion program
[DE91-002770] N91-14026
LASERS
Use of dome (meniscus) lenses to eliminate birefringence and tensile stresses in spatial filters for the Nova laser
[DE91-002784] N91-13707
Laser optical disk position encoder with active heads
[NASA-CASE-GSC-13175-1] N91-14001
LATTICES (MATHEMATICS)
Lattice Boltzmann methods for some 2-D nonlinear diffusion equations: Computational results
[DE91-004175] N91-13962
LAUNCH VEHICLES
Integrated launch and emergency vehicle system
[NASA-CASE-LAR-13780-1] N91-13481
LAUNCHING SITES
Integrated launch and emergency vehicle system
[NASA-CASE-LAR-13780-1] N91-13481
LAYOUTS
Theory and procedure of the hierarchical design rule checking of integrated circuits
[ETN-91-98173] N91-13627
LEAD OXIDES
Electrocatalysis of anodic oxygen-transfer reactions at modified lead dioxide electrodes
[DE91-000664] N91-13518
LEADING EDGES
Analysis of the leading edge effects on the boundary layer transition
[NASA-CR-187361] N91-13405
LEGIBILITY
Modelling the effects of vibration on visual performance
[ISVR-TR-171] N91-13883
LENSES
Use of dome (meniscus) lenses to eliminate birefringence and tensile stresses in spatial filters for the Nova laser
[DE91-002784] N91-13707
Portable dynamic fundus instrument
[NASA-CASE-MSC-21675-1] N91-13865
LEPTONS
Particle theory and cosmology
[DE91-004189] N91-14250
LEVITATION
Progress in the detection of single molecules in levitated droplets
[DE91-000612] N91-13517
LIBRARIES
Technical communications in aerospace: An analysis of the practices reported by US and European aerospace engineers and scientists
[NASA-TM-103441] N91-14079
LIE GROUPS
Evaluation of expressions involving higher order derivations
[NASA-CR-187319] N91-13949
The simultaneous integration of many trajectories using nilpotent normal forms
[NASA-CR-187318] N91-13950
LIFE SCIENCES
JPRS Report: Science and technology. USSR: Life sciences
[JPRS-ULS-89-011] N91-13861
LIFE SUPPORT SYSTEMS
Business and life in space N91-13854
A personal history of the human exploration initiative with commentary on the pivotal role for life support research N91-13855
LIGANDS
Inorganic concepts relevant to metal binding, activity, and toxicity in a biological system
[DE91-001489] N91-13858
LIGHT BEAMS
Progress of research on water vapor lidar
[NASA-CR-187673] N91-13837
LIGHT EMISSION
Origin and dynamics of emission line clouds in cooling flow environments N91-14167
Narrow band images of suspected cooling flow galaxies N91-14168
Optical emission from cooling flows in distant x ray clusters of galaxies N91-14169
Stripping of gas and dust from the elliptical galaxy M86 N91-14171
Dense gas and HII regions in the starburst galaxy NGC 253 N91-14220
Probing the interstellar medium of external galaxies using quasar absorption lines: The 3C 232/NGC 3067 system N91-14227
Non-steller light from high-redshift radiogalaxies N91-14238
LIGHT MODULATION
Superconducting neural network computer and sensor array
[AD-D014625] N91-13887
LIGHT SCATTERING
Stimulated Raman scatter from laser-produced plasmas: Merely nonlinear or also chaotic
[DE91-001742] N91-14007
LIGHT TRANSMISSION
Injection efficiency of bound modes
[NASA-CR-4333] N91-13991
LIGHTNING
DOPLIGHT 1987 project summary
[PB90-253584] N91-13834
LINCOLN EXPERIMENTAL SATELLITES
Loading the LES-9 wideband UHF transponder
[AD-A226179] N91-13475
LINE OF SIGHT
EMU helmet mounted display
[NASA-CASE-MSC-21460-1] N91-13879
LINE OF SIGHT COMMUNICATION
Extremely High Frequency (EHF) Low Probability of Intercept (LPI) communication applications
[AD-A226653] N91-13591
LINE SPECTRA
Neutral atomic absorption lines and far-UV extinction: Possible implications for depletions and grain parameters N91-14115
Aperture synthesis CO observations of the inner disk of NGC 1068 N91-14122
CS J = 2 yields 1 emission toward the central region of M82 N91-14128
Observations of extended and counterrotating disks of ionized gas in S0 galaxies N91-14187
Probing the interstellar medium of external galaxies using quasar absorption lines: The 3C 232/NGC 3067 system N91-14227
Non-steller light from high-redshift radiogalaxies N91-14238
An imaging and spectroscopic study of low and intermediate power radio galaxies N91-14268
Analysis of gamma ray burst spectra with cyclotron lines
[DE91-001745] N91-14269
LINEAR ACCELERATORS
Dual klystron modulator
[DE91-002348] N91-13626
Diagnostics for high-brightness beams
[DE91-001865] N91-13701
A linear accelerator in the space: The beam experiment aboard rocket
[DE91-002347] N91-13988
NRL compact accelerator theory studies
[AD-A226537] N91-14005
LINEAR ARRAYS
Performance of multiplexed Ge:Ga detector arrays in the far infrared
[NASA-TM-102275] N91-14087
LINEAR PROGRAMMING
An improved exploratory search technique for pure integer linear programming problems
[NASA-TM-103517] N91-13910
LINEAR SYSTEMS
Linear vs nonlinear and infinite vs finite: An interpretation of chaos
[DE91-002522] N91-14072
LINEARITY
Microwave superconducting electronic devices N91-14037
LININGS
Summary of JAYGO mixing and FSM-1 application of castable inhibitor and liner
[NASA-CR-184030] N91-13569
LIQUID COOLING
Water cooled static pressure probe
[NASA-CASE-LAR-14340-1-CU] N91-13684
LIQUID CRYSTALS
The effect of the molecular structure of polymer and low molecular liquid crystals on their electro-optical characteristics at the nematic-isotropic phase transition
[ETN-91-98170] N91-13564
Optical shared memory system demonstration model
[AD-A226431] N91-13612
EMU helmet mounted display
[NASA-CASE-MSC-21460-1] N91-13879
LIQUID FLOW
Polymer/riblet combination for hydrodynamic skin friction reduction
[NASA-CASE-LAR-14271-1-CU] N91-13558
LIQUID FUELS
Transverse liquid fuel jet breakup, burning, and ignition
[NASA-CR-187423] N91-13510
LIQUID HELIUM
Superfluid Stirling refrigerator: A new method for cooling below 1 Kelvin
[DE91-002311] N91-13582
Funds request for 1990. The cryogenic gravitational antenna (T = 2.0 K) ALTAIR
[IFSI-90-2] N91-13615
Cryostat for the gravitational antenna ALTAIR
[IFSI-90-3] N91-13616
The world of superconductive machinery N91-14045
LIQUID LITHIUM
HYLIFE-2 inertial confinement fusion reactor design
[DE91-000792] N91-14004
LIQUID METAL COOLED REACTORS
SP-100 from ground demonstration to flight validation
[DE91-001869] N91-13986
LIQUID NITROGEN
A liquid nitrogen cooled superconductive electron beam focusing system for improved performance ECM helix traveling wave tubes N91-14047
LIQUID PHASE EPITAXY
Study and development of tunable, single mode AlGaAs/GaAs lasers
[DE91-001684] N91-13697
LIQUID PHASES
Analytical study of the liquid phase transient behavior of a high temperature heat pipe
[NASA-CR-187426] N91-13644
LIQUID PROPELLANT ROCKET ENGINES
All Shuttle Centaur engine and nozzle support plug vibration testing
[NASA-CR-183201] N91-13485
RL10A-3-3B high mixture ratio qualification program
[NASA-CR-183200] N91-13486
Shuttle Centaur engine cooldown evaluation and effects of expanded inlets on start transient
[NASA-CR-183198] N91-13487
JANNAF liquid rocket combustion instability panel research recommendations
[NASA-TM-103653] N91-13491
LITERATURE
Spectrum fatigue testing: A literature survey
[FFA-TN-1990-40] N91-13772
LITHIUM
Secondary Li battery incorporating 12-crown-4 ether
[NASA-CASE-NPO-17922-1-CU] N91-13621
Heat pipe dynamic behavior
[NASA-CR-187422] N91-13645
Inner-shell ionization of lithium-like chromium ions
[DE91-001749] N91-13981
LITHIUM ALLOYS
Sustained-load crack growth of 8090 aluminium-lithium alloy plate in dry air at 50-200 C
[RAE-TR-90033] N91-13777
LITHOSPHERE
Mars tectonics and volcanism
[NASA-CR-187351] N91-14254

LOAD TESTS
Mechanical testing of advanced coating system, volume 1
[NASA-CR-186725] N91-13534
Sustained-load crack growth of 8090 aluminium-lithium alloy plate in dry air at 50-200 C
[RAE-TR-90033] N91-13777
LOADS (FORCES)
Wave by wave analysis of in-line force data for fixed cylinders in regular waves
[IC-AERO-89-02] N91-13672
Calibration set up for load cells
[PD-ST-8917] N91-13673
Dual strain gage balance system for measuring light loads
[NASA-CASE-LAR-14419-1] N91-13687
Airfoil design for variable RPM horizontal axis wind turbines
[FFA-TN-1990-02] N91-13801
Connectivity alternatives for remote users of the Maintenance Processor Subsystem (MPS)
[DOT/FAA/CT-90/16] N91-13900
LOCKING
Two fault tolerant toggle-hook release
[NASA-CASE-MSC-21671-1] N91-13723
LOGIC CIRCUITS
Single event upset hardening techniques
[DE91-002337] N91-13625
Evaluation and fabrication of GaAs integrated logic circuits
[LAAS-90160] N91-13628
Auto and hetero-associative memory using a 2-D optical logic gate
[NASA-CASE-NPO-17997-1-CU] N91-13888
LOGIC PROGRAMMING
An object-oriented logic language for modular system specification
[REPT-90-027] N91-13927
LOGICAL ELEMENTS
Logics for the description of processes and their properties: Expressivity and decidability
[ETN-91-98200] N91-13960
LONG DURATION EXPOSURE FACILITY
Instellar Gas Experiment (IGE): Testing interstellar gas particles to provide information on the processes of nucleosynthesis in the big bang stars and supernova
[NASA-CR-186713] N91-14097
LONG TERM EFFECTS
Physiological responses to prolonged bed rest in humans: A compendium of research, 1981-1988
[NASA-TM-102249] N91-13862
LOSSES
ISM stripping from cluster galaxies and inhomogeneities in cooling flows N91-14172
Accounting for the dispersion in the x ray properties of early-type galaxies N91-14173
LOSSY MEDIA
Frequency-domain analysis of one-dimensional electromagnetic scattering by lossy media
[FEL-90-A112] N91-13607
LOUDSPEAKERS
The prediction and measurement of the one-parameter behaviour of horns
[ISVR-TR-185] N91-13974
LOW DENSITY FLOW
Effect of bulk viscosity in low density, hypersonic blunt body flows
[DE90-012756] N91-13419
LOW FREQUENCIES
Effects of anthropometric and postural variables on the transmission of whole-body vertical vibration from seat-to-head
[ISVR-TR-172] N91-13884
LOW NOISE
Analog superconductive electronics for avionics N91-14040
LOW REYNOLDS NUMBER
Comment on local energy transfer and nonlocal interactions in homogeneous, isotropic turbulence (Phys. Fluids A2, 413 (1990))
[NASA-TM-103263] N91-13638
A quiet flow Ludwieg tube for study of transition in compressible boundary layers: Design and feasibility
[NASA-CR-187374] N91-13676
LOW TEMPERATURE
Physics and applications of low temperature superconductivity N91-14032
Contribution of cool dust to the FIR brightness distribution of NGC 6946 Sc(s)2 N91-14134
LOWER ATMOSPHERE
Simulation of the formation and transport of ozone in the atmospheric boundary layer
[DLR-FB-90-25] N91-13827
LUBRICATING OILS
Effect of lubricating oil characteristics on gear vibrations N91-13710
Analysis of single and multi-grade lubricant film thickness in a diesel engine
[AD-A226651] N91-13715
LUMINESCENCE
Dense gas and HII regions in the starburst galaxy NGC 253 N91-14220
LUMINOSITY
Aperture synthesis CO observations of the inner disk of NGC 1068 N91-14122
High spatial resolution 100 micron observations of the M83 bar N91-14130
Far infrared luminosity functions of normal galaxies N91-14135
Peering beyond IRAS: The 100 to 350 micron dust emission from galaxies N91-14141
Far-infrared emission from dusty ellipticals N91-14142
HII regions in dwarf irregular galaxies of the local group N91-14156
The onset of galactic winds in early-type galaxies N91-14165
Origin and dynamics of emission line clouds in cooling flow environments N91-14167
Gas flows in elliptical galaxies N91-14170
Accounting for the dispersion in the x ray properties of early-type galaxies N91-14173
Search for cold gas in clusters with and without cooling flows N91-14174
NGC 3312: A victim of ram pressure sweeping N91-14177
Magnetic collimation of protostellar winds into bipolar outflows N91-14182
What sort of standard candle is Orion for studying molecular hydrogen line emission in galaxies N91-14184
CO observations of southern mergers N91-14197
The morphology-density relation for dwarf galaxies N91-14200
Are bars essential for starbursts in non-interacting galaxies N91-14208
Global and radial variations in the efficiency of massive star formation among galaxies N91-14215
Starburst outflows from nearby galaxies N91-14219
Dense gas and HII regions in the starburst galaxy NGC 253 N91-14220
CO excitation in four IR luminous galaxies N91-14234
LUNAR BASES
Single launch lunar habitat derived from an NSTS external tank
[NASA-TM-4212] N91-14251
Design considerations for lunar base photovoltaic power systems
[NASA-TM-103642] N91-14259
LUNAR LANDING MODULES
Single launch lunar habitat derived from an NSTS external tank
[NASA-TM-4212] N91-14251
LUNAR MINING
Kinetics of hydrogen release from lunar soil
[NASA-CR-187363] N91-14256
LUNAR RESOURCES
Kinetics of hydrogen release from lunar soil
[NASA-CR-187363] N91-14256
LUNAR ROCKS
Kinetics of hydrogen release from lunar soil
[NASA-CR-187363] N91-14256
LUNAR SOIL
Kinetics of hydrogen release from lunar soil
[NASA-CR-187363] N91-14256
LYMAN ALPHA RADIATION
Lyman alpha radiation in external galaxies N91-14186
LYMAN SPECTRA
Interpreting the convergence of Lyman series absorption lines N91-14225

M

MACH NUMBER
A semiempirical method for obtaining fuselage normal areas from fuselage Mach sliced areas
[NASA-TM-4228] N91-13433
MACHINE TOOLS
Study of the time and effort signal in cutting operations
[CETIM-101580] N91-13583
MACHINING
Plug-type heat flux gauge and method of producing same
[NASA-CASE-LEW-14967-1] N91-13685
MAFFEI GALAXIES
High resolution sub-millimetre mapping of starburst galaxies: Comparison with CO emission N91-14129
MAGELLANIC CLOUDS
Neutral atomic absorption lines and far-UV extinction: Possible implications for depletions and grain parameters N91-14115
Observations of CO in the Magellanic irregular galaxy NGC 55 N91-14124
Infrared analysis of LMC superbubbles N91-14181
Starburst outflows from nearby galaxies N91-14219
The stellar content of M101 N91-14244
Properties of the Magellanic-type galaxies N91-14245
MAGMA
Proceedings of the MEVTV Workshop on The Evolution of Magma Bodies on Mars
[NASA-CR-187357] N91-14252
MAGNESIUM OXIDES
Analytical and experimental studies for thermal plasma processing of materials
[DE91-000599] N91-13576
MAGNETIC BEARINGS
Study of Design Knowledge Capture (DKC) schemes implemented in magnetic bearing applications
[NASA-CR-187394] N91-13677
The Improved Three Axis Test Table (ITATT): Program status and recommendation for completion
[AD-A226508] N91-13712
MAGNETIC CLOUDS
Virial theorem analysis of the structure and stability of magnetized clouds N91-14190
Evolution of magnetized, rotating, isothermal clouds N91-14191
MAGNETIC COOLING
Performance comparison of magnetic refrigeration cycles
[DE91-001520] N91-13578
MAGNETIC CORES
Numerical solution of the geoelectrodynamic problem
[NASA-CR-186941] N91-13818
MAGNETIC EFFECTS
Magnetic field effect transistors
[AD-A226535] N91-13614
Evolution of a superbubble blastwave in a magnetized medium N91-14180
MAGNETIC FIELD CONFIGURATIONS
Confinement and heating studies of field-reversed configurations
[DE91-001965] N91-14008
Dependence of CIT (compact ignition tokamak) PF (poloidal field) coil currents on profile and shape parameters using the control matrix
[DE91-002650] N91-14019
Infrared polarimetry and the magnetic field in external galaxies N91-14192
Polarization in the Lagoon nebula N91-14193
Granularity in the magnetic field structure of M83 N91-14194
MAGNETIC FIELDS
Magnetic field effect transistors
[AD-A226535] N91-13614
Laser-induced fluorescence of phosphors for remote cryogenic thermometry
[DE91-001733] N91-13681
Investigation of the uniformity of the magnetic field and flux density in the NPL permeameter
[NPL-DES-101] N91-13968
Magnetic turbulent electron transport in a reversed field pinch
[DE91-001898] N91-14009
Measurement of magnetic fluctuations on ZT-40(M)
[DE91-001899] N91-14010
Kinetic and electromagnetic transport processes in toroidal devices
[DE91-001901] N91-14011
Two-fluid simulations of the reversed-field pinch
[DE91-001961] N91-14014
A 15 MeV proton dianostic for DIII-D
[DE91-002717] N91-14022
Magnetic collimation of protostellar winds into bipolar outflows N91-14182
MHD shocks in the ISM N91-14183
Evolution of magnetized, rotating, isothermal clouds N91-14191
Polarization in the Lagoon nebula N91-14193
MAGNETIC FLUX
Evolution of magnetized, rotating, isothermal clouds N91-14191
MAGNETIC MATERIALS
Performance comparison of magnetic refrigeration cycles
[DE91-001520] N91-13578
MAGNETIC MEASUREMENT
Numerical solution of the geoelectrodynamic problem
[NASA-CR-186941] N91-13818
Measurement of magnetic fluctuations on ZT-40(M)
[DE91-001899] N91-14010

SQUIDs devices made from high Tc superconductors: Results and perspectives N91-14044
MAGNETIC MOMENTS
Particle theory and cosmology [DE91-004189] N91-14250
MAGNETIC PERMEABILITY
Optical characterization techniques applied to ceramic oxides [DE91-001526] N91-13556
Data reduction of digitized images processed from calibrated photographic and spectroscopic films obtained from terrestial, rocket and space shuttle telescopic instruments [NASA-CR-187320] N91-13674
MAGNETIC PROPERTIES
Fabrication and characterization of high temperature superconducting thin films for sensors and electronics N91-14041
MAGNETIC STORMS
Long persistence effects of geomagnetic activity [RAE-TM-SP-376] N91-13829
MAGNETIC SUSPENSION
Magnetic suspension and balance system advanced study, phase 2 [NASA-CR-4327] N91-13463
MAGNETIC VARIATIONS
Measurement of magnetic fluctuations on ZT-40(M) [DE91-001899] N91-14010
MAGNETOACOUSTICS
Method and apparatus for characterizing residual stress in ferromagnetic materials [NASA-CASE-LAR-14239-1] N91-13527
MAGNETOHYDRODYNAMIC FLOW
Plasma properties [DE91-001361] N91-14006
MAGNETOHYDRODYNAMIC STABILITY
NRL compact accelerator theory studies [AD-A226537] N91-14005
Plasma properties [DE91-001361] N91-14006
Stimulated Raman scatter from laser-produced plasmas: Merely nonlinear or also chaotic [DE91-001742] N91-14007
Two-fluid simulations of the reversed-field pinch [DE91-001961] N91-14014
Confinement properties of the RFP (reversed field pinch) [DE91-002322] N91-14015
ITER confinement capability [DE91-002647] N91-14018
Virial theorem analysis of the structure and stability of magnetized clouds N91-14190
MAGNETOHYDRODYNAMIC WAVES
Confinement and heating studies of field-reversed configurations [DE91-001965] N91-14008
MHD shocks in the ISM N91-14183
MAGNETOHYDRODYNAMICS
Evolution of a superbubble blastwave in a magnetized medium N91-14180
Magnetic collimation of protostellar winds into bipolar outflows N91-14182
MHD shocks in the ISM N91-14183
MAGNETOHYDROSTATICS
Virial theorem analysis of the structure and stability of magnetized clouds N91-14190
MAGNETOSPHERIC ION DENSITY
Long persistence effects of geomagnetic activity [RAE-TM-SP-376] N91-13829
MAGNIFICATION
Variable magnification glancing incidence x ray telescope [NASA-CASE-MFS-28013-2] N91-14096
MAINTENANCE
Degradation modeling with application to aging and maintenance effectiveness evaluations [DE91-004004] N91-13746
Three-dimensional cell to tissue assembly process [NASA-CASE-MSC-21559-1] N91-13860
Connectivity alternatives for remote users of the Maintenance Processor Subsystem (MPS) [DOT/FAA/CT-90/16] N91-13900
MAN MACHINE SYSTEMS
The human factors of quality and QA in R and D environments [DE91-001913] N91-13880
MAN-COMPUTER INTERFACE
Adaptable driver-car interfacing and mental workload: A review of the literature [IZF-1990-B-3] N91-13874
Modeling pilot interaction with automated digital avionics systems: Guidance and control algorithms for contour and nap-of-the-Earth flight [NASA-CR-186105] N91-13875
Research into alternative network approaches for space operations [NASA-CR-187015] N91-13894
MANEUVERS
Flight control design issues in bank-to-turn missiles N91-13437
MANGANESE ALLOYS
Study of the metallurgical effects of hammering between passes during C-Mn weld deposition [CETIM-104850] N91-13532
Study of the tensile strength of the melted zone of vertical welds carried out using electroslag welding on C-Mn steel. Further study on 80 mm thick plate [CETIM-104730] N91-13740
MANIPULATORS
The effect of inertial coupling in the dynamics and control of flexible robotic manipulators [NASA-CR-187679] N91-13721
Dynamic modeling, property investigation, and adaptive controller design of serial robotic manipulators modeled with structural compliance [NASA-CR-187678] N91-13722
Modeling and control of a redundant robot manipulator composed of several Stewart platforms [LAAS-90146] N91-13728
Robust deterministic control for robotic manipulators N91-13937
MANNED SPACE FLIGHT
A personal history of the human exploration initiative with commentary on the pivotal role for life support research N91-13855
MANUALS
A preliminary ocean ARM (Atmospheric Radiation Measurements) guide for climatic evaluations [DE91-001120] N91-13811
Microbial ecology laboratory procedures manual NASA/MSFC [NASA-CR-184033] N91-13856
List of standards to accompany manual of documentation practices applicable to defence-aerospace scientific and technical information. Addendum [AGARD-AG-235-ADD] N91-14076
MANUFACTURING
Solar collector manufacturing activity, 1988 [DE90-003539] N91-13797
MANY BODY PROBLEM
Constraint treatment techniques and parallel algorithms for multibody dynamic analysis [NASA-CR-187668] N91-13759
A combined N-body and hydrodynamic code for modeling disk galaxies N91-14241
MAPPING
Programmable remapper with single flow architecture [NASA-CASE-MSC-21481-1] N91-13890
Georelational data model: A conceptual vision of a geographical information system [INPE-4612-PRE/1335] N91-14078
Star formation on the leading edge of a ring-like density wave in Arp 143 N91-14198
Near-infrared mapping of spiral barred galaxies N91-14217
MARINE METEOROLOGY
Cloud properties as deduced from satellite observation [NASA-CR-182851] N91-13833
MARKET RESEARCH
Civil tiltrotor missions and applications [NASA-CR-177452] N91-13424
MARKETING
Solar collector manufacturing activity, 1988 [DE90-003539] N91-13797
Fuel cells [DE90-009686] N91-13805
MARS (PLANET)
Proceedings of the MEVTV Workshop on The Evolution of Magma Bodies on Mars [NASA-CR-187357] N91-14252
Mars tectonics and volcanism [NASA-CR-187351] N91-14254
Exobiology site selection for future Mars missions: Martian paleolake sediments and terrestrial analogs [NASA-CR-187358] N91-14255
MARS OBSERVER
Elemental mapping of planetary surfaces using gamma ray spectroscopy [DE91-001877] N91-14258
MARS SURFACE
Mars tectonics and volcanism [NASA-CR-187351] N91-14254
MARS VOLCANOES
Mars tectonics and volcanism [NASA-CR-187351] N91-14254
MASKS
Distortion-free x ray mask technology [AD-A226524] N91-13993
MASS
Star formation in proto dwarf galaxies N91-14212
MASS BALANCE
Magnetic suspension and balance system advanced study, phase 2 [NASA-CR-4327] N91-13463
MASS DISTRIBUTION
The large-scale space distribution of emission-line galaxies N91-14091
A scaling law of radial gas distribution in disk galaxies N91-14106
MASS FLOW RATE
ISM stripping from cluster galaxies and inhomogeneities in cooling flows N91-14172
MASS SPECTROMETERS
Operation of inductively coupled plasma source mass spectrometers in the peak jumping mode [DE91-001766] N91-13689
MASS SPECTROSCOPY
Materials impurity analysis by means of nuclear resonance reactions [DE91-001758] N91-13520
Operation of inductively coupled plasma source mass spectrometers in the peak jumping mode [DE91-001766] N91-13689
MASS TRANSFER
Heat exchanger fouling: Prediction, measurement, and mitigation [DE91-001997] N91-13661
Coupled transport processes in semipermeable media. Part 2: Numerical method and results [DE91-004140] N91-14073
MASSIVELY PARALLEL PROCESSORS
Computational methods and software systems for dynamics and control of large space structures [NASA-CR-187669] N91-13480
Solving the Fokker-Planck equation on a massively parallel computer [DE91-002795] N91-13915
MATCHING
Algorithms for finding an optimal matching between a given string and a string generated by a regular grammar [MEMO-836] N91-13905
MATERIALS TESTS
Development of standards for advanced polymer matrix composites: A BPF/ACG overview [NPL-DMM(A)-8] N91-13568
MATHEMATICAL LOGIC
A tutorial on the construction of high-performance resolution/paramodulation systems [DE91-001096] N91-13942
MATHEMATICAL MODELS
Analytical aerodynamic model of a high alpha research vehicle wind-tunnel model [NASA-CR-187362] N91-13404
Development of a full potential solver for rotor aerodynamics analysis N91-13407
Analytic formulations of unsteady profile aerodynamics and its application to simulation of rotors [DLR-FB-90-28] N91-13415
Modern robust control for missile autopilot design N91-13435
Guidnace simulation model of antisea-skimmer utilization for weapon system definition N91-13438
Theoretical evaluation of engine auxiliary inlet design for supersonic V/STOL aircraft [NASA-CR-186610] N91-13443
Multivariable methods for the design, identification, and control of large space structures. Volume 3: A study of the integrated control/structure design optimization problem for large flexible structures [AD-A226526] N91-13478
Multiphase carbon and its properties in complex mixtures [DE91-001679] N91-13499
Transverse liquid fuel jet breakup, burning, and ignition [NASA-CR-187423] N91-13510
Spray deflagration [INPE-5079-TDL/413] N91-13511
Modified Hilbert transform pair and Kramers-Kronig relations for complex permittivities [NASA-TM-102682] N91-13585
Dynamic high-pressure studies of an electrothermal capillary [DE91-000966] N91-13617
Small signal gain based on analytic models of thin intense electron beams [DE91-001874] N91-13631
Reynolds stress closure in jet flows using wave models [NASA-CR-185717] N91-13640
The fluid mechanics of continuous flow electrophoresis [NASA-CR-187647] N91-13648
Turbulence modeling for sharp-fin-induced shock wave/turbulent boundary-layer interactions [NASA-TM-102828] N91-13652

Large eddy simulations and direct numerical simulations of high speed turbulent reacting flows
[NASA-CR-187674] N91-13656
Frontogenesis in gravity currents: The effect of endwalls and diffusion
[MATHS-REPT-A-127] N91-13666
Data reduction of digitized images processed from calibrated photographic and spectroscopic films obtained from terrestial, rocket and space shuttle telescopic instruments
[NASA-CR-187320] N91-13674
Field error lottery
[DE91-001875] N91-13702
Effect of lubricating oil characteristics on gear vibrations N91-13710
The effect of inertial coupling in the dynamics and control of flexible robotic manipulators
[NASA-CR-187679] N91-13721
Mathematical modelling of part voltage and weld current in resistance welders
[DE91-002534] N91-13727
Modeling and control of a redundant robot manipulator composed of several Stewart platforms
[LAAS-90146] N91-13728
Degradation modeling with application to aging and maintenance effectiveness evaluations
[DE91-004004] N91-13746
Failure behavior of generic metallic and composite aircraft structural components under crash loads
[NASA-RP-1239] N91-13751
Fracture mechanics of interface cracks between dissimilar anisotropic materials N91-13752
Finite element and boundary element methods for elastoplastic stress analysis of two-dimensional and axisymmetric problems N91-13755
A review of nonlinear constitutive models for metals
[NASA-TM-102727] N91-13761
A comparison of two numerical methods for shocks in one-dimensional elastic-plastic solids
[DE91-001741] N91-13765
Test and model correlation of the atmospheric emission photometric imager fiberglass pedestal
[NASA-TM-103515] N91-13766
Calculations for structures with nonlinear joints
[CETIM-108830] N91-13776
Comparison of NASA Lewis Research Center's performance code's pressure-drop model predictions to Stirling engine working-space flow test data
[NASA-CR-182215] N91-13804
SEPAC data analysis in support of the environmental interaction program
[NASA-CR-184028] N91-13807
Terrestrial ecosystems and climatic change
[DE91-001492] N91-13813
Mesoscale monitoring of the soil freeze/thaw boundary from orbital microwave radiometry
[NASA-CR-185901] N91-13817
Simulation of the formation and transport of ozone in the atmospheric boundary layer
[DLR-FB-90-25] N91-13827
Gravity waves excited by flow over an obstacle
[FFI-90/7017] N91-13828
A study of the ice-hail charge separation mechanism using a thunderstorm electrification model with explicit microphysics in a kinematic framework N91-13835
Evaluation of a wind profile model
[FOA-E-40045-4.5] N91-13839
A primitive equation model for the equatorial Pacific
[KNMI-TR-124] N91-13840
Modelling the effects of vibration on visual performance
[ISVR-TR-171] N91-13883
Specifications extraction and synthesis: Their correlations with preliminary design N91-13936
Robust variable structure control of model reference systems
[MATHS-REPT-A-131] N91-13947
Logics for the description of processes and their properties: Expressivity and decidability
[ETN-91-98200] N91-13960
On the invertibility of Leslie systems
[REPT-90-006] N91-13963
Direct modeling of white noise in stochastic systems
[MEMO-865] N91-13964
Regularized Chapman-Enskog expansion for scalar conservation laws
[NASA-CR-187441] N91-13966
The prediction and measurement of the one-parameter behaviour of horns
[ISVR-TR-185] N91-13974
Real-space multiple scattering theory calculations of LEED (Low-Energy Electron Diffraction) intensities for stepped surfaces
[DE91-000810] N91-13978
The design of phase-only filters for optical correlations
[AD-A225641] N91-13992
Compact Ignition Tokamak project: Localizability of electron-cyclotron heating power
[DE91-002571] N91-14016
A rapid relativistic distorted wave approach for calculating cross sections for ionization of highly charged ions
[DE91-002667] N91-14020
Ionization degree of classical, dense, and highly condensed plasmas
[ETN-91-98174] N91-14027
Flux flow pinning and resistive behavior in superconducting networks
[DE91-002756] N91-14064
U1(prime) dark matter and R-parity violation
[DE91-001792] N91-14068
A scaling law of radial gas distribution in disk galaxies N91-14106
One-dimensional cloud fluid model for propagating star formation N91-14211
Properties of the Magellanic-type galaxies N91-14245
Ionization in the local interstellar and intergalactic media N91-14249

MATRICES (MATHEMATICS)
Practical considerations for the measurement of internal and coupling loss factors on complex structures
[ISVR-TR-182] N91-13778
Computing the eigenvalues and eigenvectors of a general matrix by reduction to general tridiagonal form
[DE91-002523] N91-13959

MATRIX MATERIALS
Development of BEM for ceramic composites
[NASA-CR-187676] N91-13557
Novel polyimide molding powder, coating, adhesive, and matrix resin
[NASA-CASE-LAR-14163-1] N91-13559

MEAN FREE PATH
Magnetic turbulent electron transport in a reversed field pinch
[DE91-001898] N91-14009

MEASURING INSTRUMENTS
Measurement results of the FEL-TNO planar rectangular near field facility (1978-1989)
[FEL-89-B336] N91-13602
Simultaneous measurement of Ni-Al particle size, velocity, and temperature in atmospheric thermal plasmas
[DE91-001935] N91-13826
Investigation of the uniformity of the magnetic field and flux density in the NPL permeameter
[NPL-DES-101] N91-13968
Database management system for instrument data management
[DE91-004300] N91-14084

MECHANICAL DEVICES
Device for applying constant pressure to a surface
[NASA-CASE-GSC-13230-1] N91-13734
The status-quo and prospect of superconducting digital devices N91-14039

MECHANICAL DRIVES
Sheave assembly
[AD-D014605] N91-13711
Heat engine with corrugated shape memory drive belt
[AD-D014640] N91-13716

MECHANICAL ENGINEERING
Miniature closed cycle refrigerators N91-14035

MECHANICAL PROPERTIES
Precision, accuracy, and tectonics from the Global Positioning System N91-13822
Physics and applications of low temperature superconductivity N91-14032
Success criteria for oxide superconductor wires: Measuring the present, predicting the future N91-14034

MEDICAL SCIENCE
Tissue simulating gel for medical research
[NASA-CASE-LAR-14036-1] N91-13562

MEDICAL SERVICES
Passive fetal monitoring sensor
[NASA-CASE-LAR-14088-1] N91-13686

MELTING POINTS
Viscosity measurements at high temperature and high pressure: A novel technique
[NASA-CR-187239] N91-13967

MEMBRANES
Mechanisms of gas permeation through polymer membranes
[DE91-004190] N91-13671

MEMORY (COMPUTERS)
Feasibility study, software design, layout and simulation of a two-dimensional fast Fourier transform machine for use in optical array interferometry
[NASA-CR-186922] N91-13885
M-dimensional computer memory with M-1 dimensional hyperplane access
[AD-D014615] N91-13886
Auto and hetero-associative memory using a 2-D optical logic gate
[NASA-CASE-NPO-17997-1-CU] N91-13888

MENISCI
Use of dome (meniscus) lenses to eliminate birefringence and tensile stresses in spatial filters for the Nova laser
[DE91-002784] N91-13707

MENTAL PERFORMANCE
Cognitive and neural bases of skilled performance
[AD-A226668] N91-13869
General method of pattern classification using the two-domain theory
[NASA-CASE-MSC-21737-1] N91-13911

MERCURY CADMIUM TELLURIDES
Viscosity measurements at high temperature and high pressure: A novel technique
[NASA-CR-187239] N91-13967

MERCURY COMPOUNDS
Development of mercuric iodide uncooled x ray detectors and spectrometers
[NASA-CR-185394] N91-13484

MESONS
Operation of silicon microstrip detectors in a high radiation environment
[DE91-001953] N91-13682
A computer model to determine the primary contributors to relative radiation dose received by astronauts
[DE90-015681] N91-13866
Influence of collective effects on the performance of high-luminosity colliders
[DE91-001797] N91-13982

MESOSCALE PHENOMENA
Mesoscale monitoring of the soil freeze/thaw boundary from orbital microwave radiometry
[NASA-CR-185901] N91-13817

MESOSPHERE
Aeronomic chemistry of ozone
[AERONOMICA-ACTA-A-355-1990] N91-13816

METABOLIC WASTES
The NASA CELSS program N91-13848

METAL CUTTING
Study of the time and effort signal in cutting operations
[CETIM-101580] N91-13583

METAL FILMS
Synchrotron radiation photoemission study of metal overlayers on hydrogenated amorphous silicon at room temperature
[DE91-000740] N91-13525
Interfacial chemistry of titanium films deposited on PMDA-ODA polyimide
[AD-A225730] N91-13550
Distortion-free x ray mask technology
[AD-A226524] N91-13993

METAL FLUORIDES
Method of making carbide/fluoride/silver composites
[NASA-CASE-LEW-14902-1] N91-13503

METAL IONS
An exploratory program for using hydrous metal oxide ion exchangers as Fischer-Tropsch catalysts
[DE91-002341] N91-13521
Reactions of the excited state of polypyridyl chromium(III) ion
[DE91-000741] N91-13526
Inner-shell ionization of lithium-like chromium ions
[DE91-001749] N91-13981

METAL MATRIX COMPOSITES
Influence of oxide reinforcement materials on high-temperatue oxidation resistance of Ni3Al matrix composites
[DE91-001625] N91-13498
Fabrication and properties of powder metallurgically manufactured aluminum products and composites
[VTT-RR-699] N91-13531

METAL OXIDE SEMICONDUCTORS
Radiation effects on JFETs (Junction Field-Effect Transistors), MOSFETs, and dipolar transistors, as related to SSC circuit design
[DE91-001486] N91-13618

METAL OXIDES
An exploratory program for using hydrous metal oxide ion exchangers as Fischer-Tropsch catalysts
[DE91-002341] N91-13521
Interfacial chemistry of titanium films deposited on PMDA-ODA polyimide
[AD-A225730] N91-13550

METAL POWDER
Binders used in metal injection molding
[VTT-RR-691] N91-13529
Fabrication and properties of powder metallurgically manufactured aluminum products and composites
[VTT-RR-699] N91-13531

METAL SPRAYING
Intelligent processing for spray metal manufacturing
[AD-A226499] N91-13523

METAL SURFACES
Electrocatalyst surfaces
[PB90-252560] N91-13507
METALLICITY
Small-scale star formation at low metallicity
N91-14214
METALLIZING
Thin solar cell and lightweight array
[NASA-CASE-LEW-14959-1] N91-13803
METALLOGRAPHY
Micrographic etching of nitrided iron and steel layers
[CETIM-106470] N91-13533
METALS
A review of nonlinear constitutive models for metals
[NASA-TM-102727] N91-13761
Optical properties and electronic structures of d- and f-electron metals and alloys, Ag-In, Ni-Cu, AuGa2, PtGa2, beta'-NiAl, beta'-CoAl, CeSn3, and LaSn3
[DE91-001597] N91-14059
Non-empirical interatomic potentials for transition metals, alloys, and semiconductors
[DE91-002396] N91-14062
METATHESIS
The synthesis of star block copolymers by controlled ring-opening metathesis polymerization
[AD-A225987] N91-13551
METEORITE COLLISIONS
The origin and evolution of the Uranian dust rings
N91-14253
METEORITE CRATERS
Abstracts for the International Workshop on Meteorite Impact on the Early Earth
[NASA-CR-185355] N91-14099
METEORITES
Proceedings of a Workshop on Cosmogenic Nuclide Production Rates
[NASA-CR-185349] N91-14098
Abstracts for the International Workshop on Meteorite Impact on the Early Earth
[NASA-CR-185355] N91-14099
Proceedings of the MEVTV Workshop on The Evolution of Magma Bodies on Mars
[NASA-CR-187357] N91-14252
METEOROLOGICAL PARAMETERS
A preliminary ocean ARM (Atmospheric Radiation Measurements) guide for climatic evaluations
[DE91-001120] N91-13811
METEOROLOGICAL SERVICES
DOPLIGHT 1987 project summary
[PB90-253584] N91-13834
METEOROLOGY
Atmospheric and geophysical sciences division program report, 1988 - 1989
[DE91-001057] N91-13780
A primitive equation model for the equatorial Pacific
[KNMI-TR-124] N91-13840
METHANE
Carbon dioxide reforming of methane in a solar volume-TRIC receiver-reactor: The CAESAR (Catalytically Enhanced Solar Absorption Receiver) project
[DE91-002340] N91-13800
METHOD OF MOMENTS
Resonance region scattering
[AD-A226536] N91-13589
METHYL ALCOHOL
High-alcohol microemulsion fuel performance in a diesel engine
[DE91-001617] N91-13572
Results from the second year of operation of the Federal Methanol Fleet at Oak Ridge National Laboratory
[DE91-000543] N91-13718
Development and initial characterization of a nuclear magnetic resonance dosimetry system
[DE91-001775] N91-13867
Interpretation of engine cycle-to-cycle variation by chaotic time series analysis
[DE91-000729] N91-13955
METHYL COMPOUNDS
Methyl substituted polyimides containing carbonyl and ether connecting groups
[NASA-CASE-LAR-14351-1] N91-13561
METRIC SPACE
General method of pattern classification using the two-domain theory
[NASA-CASE-MSC-21737-1] N91-13911
MICROANALYSIS
Application of parallel computing to the Monte Carlo simulation of electron scattering in solids: A rapid method for profile deconvolution
[DE91-001227] N91-13980
MICROBIOLOGY
Microbial ecology laboratory procedures manual NASA/MSFC
[NASA-CR-184033] N91-13856
MICROCOMPUTERS
Micro based technology: A new tool for missile guidance system design and visualization N91-13440
Implementation of the MAGINT-MAGGRAF code in the microVAX-3600 system
[INPE-5042-PRE/1575] N91-13898
MICROELECTRONICS
Single event upset hardening techniques
[DE91-002337] N91-13625
High temperature superconducting thin films for microelectronics: Preparation and properties
N91-14033
MICROMECHANICS
Development of BEM for ceramic composites
[NASA-CR-187676] N91-13557
MICROORGANISMS
Historical overview of the Biosphere 2 project
N91-13844
Soil bed reactor work of the Environmental Research Lab. of the University of Arizona in support of the research and development of Biosphere 2 N91-13846
Plants and their microbial assistants: Nature's answer to Earth's environmental pollution problems N91-13851
The BioHome: A spinoff of space technology
N91-13852
MICROPHONES
Measurement of waves in flows across a surface
[NASA-CASE-NPO-17479-1-CU] N91-13658
MICROPROCESSORS
Predictive sensor method and apparatus
[NASA-CASE-SSC-00006-1] N91-13691
MICROSCOPY
Calcified-tissue investigations using synchrotron x ray microscopy
[DE91-001729] N91-13859
MICROSTRIP ANTENNAS
Time domain finite difference analysis of antennas
[AD-A226534] N91-13613
MICROSTRIP DEVICES
A design method for an X-band diplexer
[FEL-90-B176] N91-13635
Operation of silicon microstrip detectors in a high radiation environment
[DE91-001953] N91-13682
MICROSTRUCTURE
An investigation of microstructural characteristics of contact-lens polymers
[NASA-TP-3034] N91-13492
Intelligent processing for spray metal manufacturing
[AD-A226499] N91-13523
Research and development for improved toughness aluminides
[AD-A226627] N91-13524
Fabrication and properties of powder metallurgically manufactured aluminum products and composites
[VTT-RR-699] N91-13531
Micrographic etching of nitrided iron and steel layers
[CETIM-106470] N91-13533
Mechanical testing of advanced coating system, volume 1
[NASA-CR-186725] N91-13534
A comparative study of ductile fracture in the 2.25 percent Cr-1 percent Mo and 9 percent Cr-1 percent Mo alloy steels N91-13753
Surfaces and thin films studied by picosecond ultrasonics
[DE91-004167] N91-13973
Modeling and analysis of surface roughness effects on sputtering, reflection, and sputtered particle transport
[DE91-004429] N91-14028
Variable magnification glancing incidence x ray telescope
[NASA-CASE-MFS-28013-2] N91-14096
MICROWAVE EMISSION
Neutral hydrogen in the starburst galaxy NGC3690/IC694 N91-14104
NGC 4438: Ram pressure sweeping of a tidally disrupted galaxy N91-14176
High brightness neutral hydrogen in M31: A new probe of interstellar pressure N91-14196
MICROWAVE EQUIPMENT
Passive microwave devices using high temperature superconductors N91-14036
Microwave superconducting electronic devices
N91-14037
High Tc superconductors for microwave filters
N91-14038
MICROWAVE FILTERS
High Tc superconductors for microwave filters
N91-14038
MICROWAVE INTERFEROMETERS
CO aperture synthesis of NGC 4038/9 (ARP 244)
N91-14123
M51: Molecular spiral arms, GMAs and superclouds
N91-14204
MICROWAVE RADIOMETERS
COBE's search for structure in the Big Bang
[NASA-TM-102976] N91-14271
MICROWAVE SPECTRA
NGC 1058: Gas motions in an extended, quiescent spiral disk N91-14103
MICROWAVES
Free-electron laser experiments in the microwave tokamak experiment
[DE91-001746] N91-13699
Thermoregulatory consequences of resonant microwave exposure
[AD-A226540] N91-13864
Microwave superconducting electronic devices
N91-14037
Experimental studies of Josephson effect
[AD-A226548] N91-14051
MIDCOURSE GUIDANCE
Missile Interceptor Guidance System Technology
[AGARD-LS-173] N91-13434
Midcourse guidance technologies for advanced tactical missiles systems N91-13436
Guidnace simulation model of antisea-skimmer utilization for weapon system definition N91-13438
MILKY WAY GALAXY
Very small grains in the Milky Way and external galaxies N91-14138
The diffuse ionized interstellar medium perpendicular to the plane of NGC 891 N91-14160
Small-scale star formation at low metallicity
N91-14214
The stellar content of M101 N91-14244
MILLIMETER WAVES
Extremely High Frequency (EHF) Low Probability of Intercept (LPI) communication applications
[AD-A226653] N91-13591
Electronic scan at millimetre wave frequencies
[FEL-89-B258] N91-13601
Millimeter-wave sensor image enhancement
[NASA-CR-187430] N91-13679
Monolithic mm-wave phase shifter using optically activated superconducting switches
[NASA-CASE-LEW-14878-1] N91-13996
CO aperture synthesis of NGC 4038/9 (ARP 244)
N91-14123
High angular resolution mm- and submm-observations of dense molecular gas in M82 N91-14230
The molecular spiral arms of NGC 6946 N91-14231
CO mapping of the nuclear region of NGC 6946 and IC 342 with Nobeyama millimeter array N91-14233
MINIATURIZATION
Method of making single crystal fibers
[NASA-CASE-LEW-14921-1] N91-13502
Fibre-linked miniature laser transit anemometer for complex flow fields N91-13678
Miniature closed cycle refrigerators N91-14035
MIRRORS
Motion detection, novelty filtering, and target tracking using an interferometric technique with a GaAs phase conjugate mirror
[NASA-CASE-NPO-17784-1-CU] N91-13998
Wide acceptance angle, high concentration ratio, optical collector
[NASA-CASE-MFS-28295-1] N91-13999
MISS DISTANCE
Advanced missile guidance N91-13439
Interactions between battle management and guidance law design for a strategic interceptor N91-13441
MISSILE CONFIGURATIONS
Flight control design issues in bank-to-turn missiles
N91-13437
MISSILE CONTROL
Missile Interceptor Guidance System Technology
[AGARD-LS-173] N91-13434
Advanced missile guidance N91-13439
Micro based technology: A new tool for missile guidance system design and visualization N91-13440
Interactions between battle management and guidance law design for a strategic interceptor N91-13441
Guidance methods for tactical and strategic missiles
N91-13442
Description of sea wave motion and its influence on the altitude control of sea skimming missiles
[FEL-89-A368] N91-13450
MISSILE DESIGN
Modern robust control for missile autopilot design
N91-13435
MISSILE SYSTEMS
Midcourse guidance technologies for advanced tactical missiles systems N91-13436
MISSILE TRAJECTORIES
Description of sea wave motion and its influence on the altitude control of sea skimming missiles
[FEL-89-A368] N91-13450
MISSILES
Advanced missile guidance N91-13439

MISSION PLANNING
Applications of artificial intelligence to mission planning
[NASA-CR-184994] N91-13939
Exobiology site selection for future Mars missions: Martian paleolake sediments and terrestrial analogs
[NASA-CR-187358] N91-14255
MIXERS
Summary of JAYGO mixing and FSM-1 application of castable inhibitor and liner
[NASA-CR-184030] N91-13569
Evaluation of Raytek infrared pyrometer for continuous propellant temperature measurement
[NASA-CR-184040] N91-13570
MIXING
Summary of JAYGO mixing and FSM-1 application of castable inhibitor and liner
[NASA-CR-184030] N91-13569
MIXING CIRCUITS
GaAs MMIC mixer for 8-12 GHz, based on 0.5 micrometer gate length D-MESFETS. Volume 1: Design and layout
[FEL-89-B277-VOL-1] N91-13632
MIXING LAYERS (FLUIDS)
Zero wavenumber modes of a compressible supersonic mixing layer
[NASA-CR-187476] N91-13669
MIXTURES
Multiphase carbon and its properties in complex mixtures
[DE91-001679] N91-13499
A review of interaction mechanisms in fluid-solid flows
[DE91-000941] N91-13660
MODELS
Influence of thermodynamical modelization for chemically reacting air flow
[MBB/FE122/S/PUB/400] N91-13418
Airport stand assignment model
[TT-9009] N91-13426
Modelization of two phase turbulent jet up to its auto ignition in variable pressure and temperature environments
[ETN-91-98341] N91-13665
Dual strain gage balance system for measuring light loads
[NASA-CASE-LAR-14419-1] N91-13687
Methods for computer-aided design of free-form objects
[MA-56] N91-13921
Superconducting Josephson Junction Gyroscope (JJG) N91-14043
MODEMS
Definition study into the requirements of a data modem for the SYSCOM network
[FEL-90-A116] N91-13892
MODFETS
Band-gap narrowing and III-V heterostructure FETs (Field-Effect Transistors)
[DE91-000401] N91-14056
MODULATORS
Dual klystron modulator
[DE91-002348] N91-13626
MODULUS OF ELASTICITY
Effects of temperature on acoustically-induced strains and damage propagation in CFRP plates N91-13493
MOIRE INTERFEROMETRY
Three dimensional moire pattern alignment
[NASA-CASE-MSC-21416-1] N91-14000
MOISTURE
Tropical Pacific moisture variability: Its detection, synoptic structure and consequences in the general circulation
[NASA-CR-184045] N91-13832
MOLECULAR BEAM EPITAXY
Evaluation and fabrication of GaAs integrated logic circuits
[LAAS-90160] N91-13628
High temperature superconducting thin films for microelectronics: Preparation and properties N91-14033
Method of fabricating germanium and gallium arsenide devices
[NASA-CASE-GSC-13265-1] N91-14066
MOLECULAR CHAINS
A new approach to design of cross-linked second-order nonlinear optical polymers
[AD-A226674] N91-13553
MOLECULAR CLOUDS
A comparison of UV surface brightness and HI surface densities for spiral galaxies N91-14102
A scaling law of radial gas distribution in disk galaxies N91-14106
Physical conditions in photodissociation regions: Application to galactic nuclei N91-14113
Empirical relationships between gas abundances and UV selective extinction N91-14116
The FCRAO extragalactic CO survey: Global properties of galaxies N91-14117
A survey of galaxies in CO N91-14118
The ratio of molecular to atomic gas in spiral galaxies as a function of morphological type N91-14119
Circumnuclear molecular gas in starburst and Seyfert galaxies N91-14120
Aperture synthesis CO observations of the inner disk of NGC 1068 N91-14122
Observations of CO isotopic emission and the far-infrared continuum of Centaurus A N91-14125
The CO-12 and CO-13 J=2-1 and J=1-0 observations of hot and cold galaxies N91-14126
The molecular cloud content of early type galaxies N91-14127
CS J = 2 yields 1 emission toward the central region of M82 N91-14128
High resolution sub-millimetre mapping of starburst galaxies: Comparison with CO emission N91-14129
Evidence against a simple two-component model for the far-infrared emission from galaxies N91-14136
Emission from small dust particles in diffuse and molecular cloud medium N91-14137
Very small grains in the Milky Way and external galaxies N91-14138
A model for the infrared emission from an OB star cluster environment N91-14139
A relationship between the integrated CO intensity and the radio continuum emission in spiral galaxies N91-14146
Magnetic collimation of protostellar winds into bipolar outflows N91-14182
Lyman alpha radiation in external galaxies N91-14186
The gravitational wakefield of a molecular cloud in a disk galaxy N91-14188
The effect of suspended particles on Jean's criterion for gravitational instability N91-14189
Evolution of magnetized, rotating, isothermal clouds N91-14191
Polarization in the Lagoon nebula N91-14193
Unbound molecular complexes in M33 N91-14201
M51: Molecular spiral arms, GMAs and superclouds N91-14204
High angular resolution mm- and submm-observations of dense molecular gas in M82 N91-14230
The molecular spiral arms of NGC 6946 N91-14231
CO excitation in four IR luminous galaxies N91-14234
Molecular outflows in the L1641 region of Orion N91-14246
The photoevaporation of interstellar clouds N91-14248
MOLECULAR COLLISIONS
Atomic and molecular theory
[DE91-004475] N91-13983
MOLECULAR FLOW
Transport properties of dense fluid mixtures using nonequilibrium molecular dynamics
[DE91-000262] N91-13654
MOLECULAR GASES
The ratio of molecular to atomic gas in spiral galaxies as a function of morphological type N91-14119
High resolution CO images of Seyfert Galaxies N91-14121
Aperture synthesis CO observations of the inner disk of NGC 1068 N91-14122
CO aperture synthesis of NGC 4038/9 (ARP 244) N91-14123
Observations of CO in the Magellanic irregular galaxy NGC 55 N91-14124
Observations of CO isotopic emission and the far-infrared continuum of Centaurus A N91-14125
High resolution sub-millimetre mapping of starburst galaxies: Comparison with CO emission N91-14129
Contribution of cool dust to the FIR brightness distribution of NGC 6946 Sc(s)2 N91-14134
The infrared continuum spectrum of x ray illuminated molecular gas N91-14144
A comparison of the radial distribution of molecular gas and non-thermal radio continuum in spiral disks N91-14145
MHD shocks in the ISM N91-14183
What sort of standard candle is Orion for studying molecular hydrogen line emission in galaxies N91-14184
H2 line emission in three Seyfert nuclei: Evidence against UV-excitation N91-14185
CO observations of southern mergers N91-14197
Unbound molecular complexes in M33 N91-14201
A high resolution CO map of M51 N91-14203
Dissociation and ionization of molecular gas in the spiral arms of M51 N91-14205
Infrared spectroscopy of the dwarf starburst galaxy Henize 2-10 N91-14213
Molecular gas and star formation in the centers of Virgo spirals N91-14216
Current star formation in S0 galaxies: NGC 4710 N91-14224
High angular resolution mm- and submm-observations of dense molecular gas in M82 N91-14230
The molecular spiral arms of NGC 6946 N91-14231
The molecular spiral arms of NGC 6946 N91-14232
CO mapping of the nuclear region of NGC 6946 and IC 342 with Nobeyama millimeter array N91-14233
CO excitation in four IR luminous galaxies N91-14234
Spatial variation of the physical conditions of molecular gas in galaxies N91-14236
MOLECULAR ROTATION
Development and evaluation of continuum models for translational-rotational nonequilibrium N91-13403
MOLECULAR STRUCTURE
Electrocatalyst surfaces
[PB90-252560] N91-13507
The effect of the molecular structure of polymer and low molecular liquid crystals on their electro-optical characteristics at the nematic-isotropic phase transition
[ETN-91-98170] N91-13564
The molecular structure of the HAN-based liquid propellants
[AD-A226415] N91-13571
MOLECULAR THEORY
Atomic and molecular theory
[DE91-004475] N91-13983
MOLECULAR WEIGHT
Novel polyimide molding powder, coating, adhesive, and matrix resin
[NASA-CASE-LAR-14163-1] N91-13559
MOLECULES
Emission from small dust particles in diffuse and molecular cloud medium N91-14137
MOLYBDENUM ALLOYS
Creep and creep failure of power plant steels
[VTT-RR-685] N91-13528
The effects of thermal treatment after welding on the functional properties of assemblies. Follow-up of the work on Cr-Mo
[CETIM-104720] N91-13739
MOMENTUM TRANSFER
Inclusive inelastic scattering of heavy ions and nuclear correlations
[NASA-TP-3026] N91-13985
MONATOMIC GASES
Development and evaluation of continuum models for translational-rotational nonequilibrium N91-13403
The ratio of molecular to atomic gas in spiral galaxies as a function of morphological type N91-14119
A model for the infrared emission from an OB star cluster environment N91-14139
A high resolution CO map of M51 N91-14203
MONITORS
Passive fetal monitoring sensor
[NASA-CASE-LAR-14088-1] N91-13686
Biofilm monitoring coupon system
[NASA-CASE-MSC-21585-1] N91-13857
MONTE CARLO METHOD
A computer model to determine the primary contributors to relative radiation dose received by astronauts
[DE90-015681] N91-13866
Application of parallel computing to the Monte Carlo simulation of electron scattering in solids: A rapid method for profile deconvolution
[DE91-001227] N91-13980
Modeling and analysis of surface roughness effects on sputtering, reflection, and sputtered particle transport
[DE91-004429] N91-14028
Morphological stability and kinetics in crystal growth from vapors
[NASA-CR-187650] N91-14055
Spectrum formation in SN1987A N91-14243
MORPHOLOGY
The importance of fracturing in the Pimenta Bueno-Ro Basin structure: A study of the morphostructural elements of the rupture-ductile character through remote sensing techniques and products
[INPE-5004-TDL/398] N91-13825
The ratio of molecular to atomic gas in spiral galaxies as a function of morphological type N91-14119
Molecular outflows in the L1641 region of Orion N91-14246
MOUNTING
Flexible thermal apparatus for mounting of thermoelectric cooler
[NASA-CASE-NPO-17806-1-CU] N91-13581
Post clamp
[NASA-CASE-LEW-14862-1] N91-13730
MOVING TARGET INDICATORS
Observation with stand-off radars
[FEL-90-A022] N91-13606

MULTIPHASE FLOW
A review of interaction mechanisms in fluid-solid flows
[DE91-000941] N91-13660
MULTIPLE ACCESS
M-dimensional computer memory with M-1 dimensional hyperplane access
[AD-D014615] N91-13886
MULTIPLEXING
Twelve signals multiplexed with the LLNL optical streak camera
[DE91-000066] N91-13680
Multiplexer/amplifier test results for SP-100
[DE91-004504] N91-13990
Performance of multiplexed Ge:Ga detector arrays in the far infrared
[NASA-TM-102275] N91-14087
MULTIPROCESSING (COMPUTERS)
The advanced software development and commercialization project
[DE91-002956] N91-13933
MULTISENSOR APPLICATIONS
Sea ice-atmosphere interaction: Application of multispectral satellite data in polar surface energy flux estimates
[NASA-CR-187376] N91-13782
MULTISPECTRAL PHOTOGRAPHY
The relation between tree physiology and multispectral and color photography: First phase
[BCRS-89-39] N91-13785
MULTISTATIC RADAR
Method for providing a polarization filter for processing synthetic aperture radar image data
[NASA-CASE-NPO-17304-1-CU] N91-13594
MUONS
Particle theory and cosmology
[DE91-004189] N91-14250
Feasibility of cosmic-ray muon intensity measurements for tunnel detection
[AD-A223355] N91-14266

N

NARROWBAND
Small particle selective emitter
[NASA-CASE-LEW-14731-1] N91-13802
Narrow band images of suspected cooling flow galaxies N91-14168
Deep narrow band imagery of the diffuse ISM in M33 N91-14202
NASA PROGRAMS
Microgravity strategic plan, 1990
[NASA-TM-103448] N91-13575
NASTRAN
All Shuttle Centaur engine and nozzle support plug vibration testing
[NASA-CR-183201] N91-13485
NATIONAL SEVERE STORMS PROJECT
DOPLIGHT 1987 project summary
[PB90-253584] N91-13834
NAVIER-STOKES EQUATION
Navier-Stokes and Euler solutions for lee-side flows over supersonic delta wings. A correlation with experiment
[NASA-TP-3035] N91-13401
Development and evaluation of continuum models for translational-rotational nonequilibrium N91-13403
Indicial response approach derived from Navier-Stokes equations. Part 1: Time-invariant equilibrium state
[NASA-TM-102856] N91-13408
Large-eddy simulation of transitional channel flow
[NASA-CR-187465] N91-13410
Thrust chamber modeling using Navier-Stokes equations: Code documentation and listings, volume 2
[NASA-CR-183617] N91-13489
Development of a time-dependent incompressible Navier-Stokes solver based on a fractional-step method
[NASA-CR-182323] N91-13639
Nonlinear viscous waves produced by an impulsively moving plate N91-13641
Computation of incompressible flow around the DARPA SUBOFF bodies
[AD-A226481] N91-13646
Turbulence modeling for sharp-fin-induced shock wave/turbulent boundary-layer interactions
[NASA-TM-102828] N91-13652
Regularized Chapman-Enskog expansion for scalar conservation laws
[NASA-CR-187441] N91-13966
NAVIGATION
Guidance, navigation and control. Digital emulation technology laboratory. Volume 2, Task 2: Seeker emulator development
[AD-A225124] N91-13429
Guidance, navigation and control. Digital emulation technology laboratory. Volume 3, Task 3: Special studies
[AD-A225125] N91-13430
NAVIGATION AIDS
Guidance, navigation and control. Digital emulation technology laboratory. Volume 2, Task 2: Seeker emulator development
[AD-A225124] N91-13429
NAVIGATION SATELLITES
System and method for measuring ocean surface currents at locations remote from land masses using synthetic aperture radar
[NASA-CASE-NPO-17937-1-CU] N91-13787
NAVY
Coordinates of a life-cycle model for a software system and communicating the need for software technology
[AD-A226592] N91-13903
NEAR FIELDS
Measurement results of the FEL-TNO planar rectangular near field facility (1978-1989)
[FEL-89-B336] N91-13602
Planar near-field measurement of non-reciprocal antennas
[FEL-90-B092] N91-13604
NEAR INFRARED RADIATION
Emission from small dust particles in diffuse and molecular cloud medium N91-14137
Observations of the galactic plane by the zodiacal infrared project N91-14143
An infrared jet in Centaurus A (NGC 5128): Evidence for interaction between the active nucleus and the interstellar medium N91-14175
Are bars essential for starbursts in non-interacting galaxies N91-14208
A near infrared spectroscopic study of the interstellar gas in the starburst core of M82 N91-14221
NEBULAE
IRAS observations of the ISM in the gamma CAS reflection nebula N91-14140
The effect of suspended particles on Jean's criterion for gravitational instability N91-14189
Polarization in the Lagoon nebula N91-14193
Starburst outflows from nearby galaxies N91-14219
NEGATIVE IONS
A linear accelerator in the space: The beam experiment aboard rocket
[DE91-002347] N91-13988
NEODYMIUM LASERS
Ultra-high brightness (greater than 10(exp 21) W/sq cm) laser facility
[DE91-001685] N91-13698
A multi-laser system for a fast sampling Thomson scattering diagnostic
[DE91-002708] N91-13705
Laser programs highlights, July - August 1990
[DE91-001056] N91-13709
Subnanosecond, high voltage photoconductive switching in GaAs
[DE91-002671] N91-14063
NETWORK ANALYSIS
Definition study into the requirements of a data modem for the SYSCOM network
[FEL-90-A116] N91-13892
NETWORK CONTROL
Applications of neural networks to adaptive control
[AD-A225408] N91-13938
NEURAL NETS
BSB radar pulse classification
[FEL-90-B023] N91-13603
Superconducting neural network computer and sensor array
[AD-D014625] N91-13887
Applications of neural networks to adaptive control
[AD-A225408] N91-13938
High-gain AlGaAs/GaAs double heterojunction Darlington phototransistors for optical neural networks
[NASA-CASE-NPO-18101-1-CU] N91-13995
NEUROPHYSIOLOGY
Cognitive and neural bases of skilled performance
[AD-A226668] N91-13869
NEUTRAL ATOMS
Neutral atomic absorption lines and far-UV extinction: Possible implications for depletions and grain parameters N91-14115
Empirical relationships between gas abundances and UV selective extinction N91-14116
NEUTRAL GASES
The extragalactic radiation field and sharp edges to HI disks in galaxies N91-14101
A comparison of UV surface brightness and HI surface densities for spiral galaxies N91-14102
Neutral hydrogen in the starburst galaxy NGC3690/IC894 N91-14104
High velocity gas in external galaxies N91-14105
Radial profiles of gas in late-type disk galaxies N91-14107
Disk mass densities in edge-on spiral galaxies N91-14108
A survey of the properties of early-type galaxies N91-14109
Intergalactic HI in the NGC5018 group N91-14110
HI and FIR emission from S0 galaxies N91-14111
Peering beyond IRAS: The 100 to 350 micron dust emission from galaxies N91-14141
Far-infrared emission from dusty ellipticals N91-14142
The diffuse ionized interstellar medium perpendicular to the plane of NGC 891 N91-14160
Energy input and HI spin temperatures in low pressure regions N91-14163
NGC 4438: Ram pressure sweeping of a tidally disrupted galaxy N91-14176
NGC 3312: A victim of ram pressure sweeping N91-14177
High brightness neutral hydrogen in M31: A new probe of interstellar pressure N91-14196
High-mass star formation in southern disk galaxies N91-14218
NEUTRINOS
Axions and SN 1987A: Axion trapping
[NASA-CR-186467] N91-13976
Elementary particle interactions
[DE91-001220] N91-13979
NEUTRON DIFFRACTION
Use of neutron diffraction methods for the determination of mechanical stresses in metal ceramic laminated composite materials N91-13537
Determination of residual stresses in ceramics materials using neutron diffraction N91-13538
NEUTRON SPECTRA
Unique features of space reactors
[DE91-001910] N91-13987
NEUTRON STARS
Axions and SN 1987A: Axion trapping
[NASA-CR-186467] N91-13976
Relativistic effects in millisecond pulsars and active galactic nuclei N91-14247
Gamma ray bursts from comet neutron star magnetosphere interaction, field twisting and E(sub parallel) formation
[DE91-002320] N91-14270
NEUTRONS
HYLIFE-2 inertial confinement fusion reactor design
[DE91-000792] N91-14004
NEWTON METHODS
Projected quasi-Newton updates
[MATHS-REPT-A-135] N91-13920
NICKEL ALLOYS
Influence of oxide reinforcement materials on high-temperatue oxidation resistance of Ni3Al matrix composites
[DE91-001625] N91-13498
Simultaneous measurement of Ni-Al particle size, velocity, and temperature in atmospheric thermal plasmas
[DE91-001935] N91-13826
NITROGEN
Computed potential energy surfaces for chemical reactions
[NASA-CR-186877] N91-13506
NITROGEN COMPOUNDS
Ammonia decomposition on silicon surfaces studied using transmission FTIR spectroscopy
[AD-A226625] N91-13513
NOISE REDUCTION
Non-linear dynamic analysis of geared systems
[NASA-CR-4338] N91-13737
Constrained viscoelastic layer damping of thick aluminum plates: Design, analysis, and testing
[AD-A226556] N91-13758
NONDESTRUCTIVE TESTS
Creep and creep failure of power plant steels
[VTT-RR-685] N91-13528
Material degradation of steam turbine rotors in long term operations
[VTT-RR-692] N91-13530
Testing of engineering ceramics, summary
[VTT-RR-678] N91-13567
Analysis of bond quality by resonant ultrasound
[DE91-000439] N91-13743
Calcified-tissue investigations using synchrotron x ray microscopy
[DE91-001729] N91-13859
Surfaces and thin films studied by picosecond ultrasonics
[DE91-004167] N91-13973
NONEQUILIBRIUM FLOW
Development and evaluation of continuum models for translational-rotational nonequilibrium N91-13403
Transport properties of dense fluid mixtures using nonequilibrium molecular dynamics
[DE91-000262] N91-13654

NONLINEAR OPTICS
PBT, PBO-based hybrid polymers with nonlinear optical properties or high electrical conductivity
[AD-A226646] N91-13552
A new approach to design of cross-linked second-order nonlinear optical polymers
[AD-A226674] N91-13553
NONLINEAR PROGRAMMING
Analysis of parallelism for nonlinear programming
[INPE-5121-TDL/422] N91-13899
NONLINEAR SYSTEMS
Nonlinear viscous waves produced by an impulsively moving plate N91-13641
The route to chaos for the Kuramoto-Sivashinsky equation
[NASA-CR-187461] N91-13642
Calculations for structures with nonlinear joints
[CETIM-108830] N91-13776
Evaluation of expressions involving higher order derivations
[NASA-CR-187319] N91-13949
Chaos and order in non-integrable model field theories
[DE91-002313] N91-14070
NONLINEARITY
A nonlinear viscoelastic approach to durability predictions for polymer based composite structures
[NASA-CR-187653] N91-13554
Robust deterministic control for robotic manipulators N91-13937
Microwave superconducting electronic devices N91-14037
Linear vs nonlinear and infinite vs finite: An interpretation of chaos
[DE91-002522] N91-14072
NONTHERMAL RADIATION
Far-infrared emission from dusty ellipticals N91-14142
NORTH ATLANTIC TREATY ORGANIZATION (NATO)
Echocardiography in NATO aircrew
[AGARD-AR-297] N91-13863
NOVA LASER SYSTEM
Ultra-high brightness (greater than 10(exp 21) W/sq cm) laser facility
[DE91-001685] N91-13698
Use of dome (meniscus) lenses to eliminate birefringence and tensile stresses in spatial filters for the Nova laser
[DE91-002784] N91-13707
Fast Pb-glass neutron-to-light converter for ICF (Inertial Confinement Fusion) target burn history measurements
[DE91-002670] N91-14021
NOZZLE DESIGN
A quiet flow Ludwieg tube for study of transition in compressible boundary layers: Design and feasibility
[NASA-CR-187374] N91-13676
NUCLEAR BINDING ENERGY
An x ray photoelectron spectroscopy study of Au(x)In(y) alloys
[NASA-TM-103659] N91-14050
NUCLEAR DEVICES
Semi-custom integrated circuit amplifier and level discriminator for nuclear and space instruments
[DE91-001951] N91-13620
NUCLEAR EXPLOSION EFFECT
Guidance, navigation and control. Digital emulation technology laboratory. Volume 2, Task 2: Seeker emulator development
[AD-A225124] N91-13429
NUCLEAR FISSION
The behavior of fission products during nuclear rocket reactor tests
[DE91-001956] N91-13490
NUCLEAR FUSION
Assessment of ion-atom collision data for magnetic fusion plasma edge modelling
[DE91-001920] N91-14012
NUCLEAR MAGNETIC RESONANCE
Fundamental investigations of supported monometallic and bimetallic catalysts by proton magnetic resonance spectroscopy
[DE91-000610] N91-13516
Development and initial characterization of a nuclear magnetic resonance dosimetry system
[DE91-001775] N91-13867
NUCLEAR PHYSICS
High energy physics program at Texas A&M University
[DE91-001639] N91-13989
NUCLEAR POWER PLANTS
Degradation modeling with application to aging and maintenance effectiveness evaluations
[DE91-004004] N91-13746
NUCLEAR REACTIONS
Materials impurity analysis by means of nuclear resonance reactions
[DE91-001758] N91-13520
Modeling and analysis of surface roughness effects on sputtering, reflection, and sputtered particle transport
[DE91-004429] N91-14028
NUCLEAR REACTORS
Mechanical properties of 1950's vintage Type 304 stainless steel weldment components
[DE91-004328] N91-13774
International Thermonuclear Experimental Reactor physics basis
[DE91-002646] N91-14017
NUCLEAR ROCKET ENGINES
The behavior of fission products during nuclear rocket reactor tests
[DE91-001956] N91-13490
NUCLEATION
Definition study for temperature control in advanced protein crystal growth
[NASA-CR-187346] N91-14029
The morphology-density relation for dwarf galaxies N91-14200
NUCLEONS
A computer model to determine the primary contributors to relative radiation dose received by astronauts
[DE90-015681] N91-13866
NUCLIDES
Proceedings of a Workshop on Cosmogenic Nuclide Production Rates
[NASA-CR-185349] N91-14098
NUMERICAL ANALYSIS
Instability of a supersonic shock free elliptic jet
[NASA-TM-103428] N91-13413
The route to chaos for the Kuramoto-Sivashinsky equation
[NASA-CR-187461] N91-13642
Transionospheric propagation calculations for the output of two EMP (Electromagnetic Pulse) simulators
[DE91-001618] N91-13720
NUMERICAL CONTROL
Missile Interceptor Guidance System Technology
[AGARD-LS-173] N91-13434
Success with an automated computer control system
[DE91-001759] N91-13945

O

O STARS
IRAS observations of the ISM in the gamma CAS reflection nebula N91-14140
OBJECT PROGRAMS
An object-oriented logic language for modular system specification
[REPT-90-027] N91-13927
Applications of artificial intelligence to mission planning
[NASA-CR-184994] N91-13939
OBLIQUE WINGS
Integrated aerodynamic and control system design of oblique wing aircraft N91-13459
OCCULTATION
The origin and evolution of the Uranian dust rings N91-14253
OCEAN SURFACE
System and method for measuring ocean surface currents at locations remote from land masses using synthetic aperture radar
[NASA-CASE-NPO-17937-1-CU] N91-13787
OCEAN THERMAL ENERGY CONVERSION
Carbon dioxide release from Ocean Thermal Energy Conversion (OTEC) cycles
[DE89-009504] N91-13809
OCTANES
Interpretation of engine cycle-to-cycle variation by chaotic time series analysis
[DE91-000729] N91-13955
OFFICE AUTOMATION
Flexible cooperation in non-standard application environments
[AD-A226486] N91-13940
ON-LINE SYSTEMS
About transient stability of power systems: Statistical pattern recognition approach
[LAAS-90192] N91-13889
OORT CLOUD
The evolution of comets and the detectability of Extra-Solar Oort Clouds N91-14242
OPERATING COSTS
UK airlines' cost structure and implications of air transport services fragmentation. Research report on air transport fragmentation
[TT-9011] N91-13427
OPERATORS (MATHEMATICS)
Two-fluid simulations of the reversed-field pinch
[DE91-001961] N91-14014
OPTICAL COMPUTERS
Superconducting neural network computer and sensor array
[AD-D014625] N91-13887
OPTICAL CORRELATORS
Optical joint correlation for real-time tracking
[NASA-CASE-MSC-21509-1] N91-13997
OPTICAL DATA PROCESSING
Optical shared memory system demonstration model
[AD-A226431] N91-13612
OPTICAL DATA STORAGE MATERIALS
Design of integrated CMOS circuits for parallel detection and storage of optical data
[AD-A225702] N91-13611
OPTICAL DISKS
Laser optical disk position encoder with active heads
[NASA-CASE-GSC-13175-1] N91-14001
The extragalactic radiation field and sharp edges to HI disks in galaxies N91-14101
OPTICAL EMISSION SPECTROSCOPY
Prospects of CsJ(Tl)-photodiode detectors for low level spectroscopy
[MPI-PAE/EXP.EL-228] N91-13984
OPTICAL EQUIPMENT
Communication system test for image transmission
[DE91-001890] N91-13994
Apparatus for precision focusing and positioning of a beam waist on a target
[NASA-CASE-ARC-11916-1-SB] N91-14002
OPTICAL FIBERS
Twelve signals multiplexed with the LLNL optical streak camera
[DE91-000066] N91-13680
Apparatus for precision focusing and positioning of a beam waist on a target
[NASA-CASE-ARC-11916-1-SB] N91-14002
OPTICAL FILTERS
The design of phase-only filters for optical correlations
[AD-A225641] N91-13992
OPTICAL MEASUREMENT
Fibre-linked miniature laser transit anemometer for complex flow fields N91-13678
OPTICAL MEMORY (DATA STORAGE)
Optical shared memory system demonstration model
[AD-A226431] N91-13612
Real-time dynamic holographic image storage device
[NASA-CASE-LAR-13989-1] N91-13694
OPTICAL PATHS
Motion detection, novelty filtering, and target tracking using an interferometric technique with a GaAs phase conjugate mirror
[NASA-CASE-NPO-17784-1-CU] N91-13998
OPTICAL PROPERTIES
The design of phase-only filters for optical correlations
[AD-A225641] N91-13992
Fabrication and characterization of high temperature superconducting thin films for sensors and electronics N91-14041
Optical properties and electronic structures of d- and f-electron metals and alloys, Ag-In, Ni-Cu, AuGa2, PtGa2, beta'-NiAl, beta'-CoAl, CeSn3, and LaSn3
[DE91-001597] N91-14059
OPTICAL RADAR
Progress of research on water vapor lidar
[NASA-CR-187673] N91-13837
Lidar as a slant path visio-ceilometer
[FEL-90-A207] N91-13838
OPTIMAL CONTROL
Analysis of the leading edge effects on the boundary layer transition
[NASA-CR-187361] N91-13405
OPTIMIZATION
A minimization method adapted to the finite element technique for turbulent flow simulation with nonlinear boundary conditions in the wall vicinity
[ECL-90-016] N91-13664
On unconstrained conjugate gradient optimization methods and their interrelationships
[MATHS-REPT-A-129] N91-13919
Projected quasi-Newton updates
[MATHS-REPT-A-135] N91-13920
A global convergence result for conjugate gradient methods
[MATHS-REPT-A-134] N91-13961
ORBIT CALCULATION
Local closed orbit bumps in AmPS
[NIKHEF-K/AMPS/90-01] N91-13471
Orbit determination and analysis for Aureole 2 rocket at 27:2 resonance
[RAE-TR-90018] N91-13472
ORBIT DECAY
Orbit determination and analysis for Aureole 2 rocket at 27:2 resonance
[RAE-TR-90018] N91-13472
The origin and evolution of the Uranian dust rings N91-14253

ORBITAL ASSEMBLY
Single launch lunar habitat derived from an NSTS external tank
[NASA-TM-4212] N91-14251
ORBITAL LIFETIME
Orbit determination and analysis for Aureole 2 rocket at 27:2 resonance
[RAE-TR-90018] N91-13472
ORBITAL MANEUVERS
Analytical and experimental research on large angle maneuvers of flexible structures
[AD-A226679] N91-13479
ORBITAL MECHANICS
Generic extravehicular (EVA) and telerobot task primitives for analysis, design, and integration. Version 1.0: Reference compilation for the EVA and telerobotics communities
[NASA-CR-187429] N91-13876
ORBITAL RESONANCES (CELESTIAL MECHANICS)
Orbit determination and analysis for Aureole 2 rocket at 27:2 resonance
[RAE-TR-90018] N91-13472
ORBITAL SERVICING
Telerobotic on-orbit remote fluid resupply system
[NASA-CR-184052] N91-13474
ORBITS
Local closed orbit bumps in AmPS
[NIKHEF-K/AMPS/90-01] N91-13471
ORGANIC COMPOUNDS
Methods of analysis for complex organic aerosol mixtures from urban emission sources of particulate carbon
[DE91-001722] N91-13814
ORGANIZATIONS
Information systems supported end-user interaction: Impacts on inter- and intra-organizational connectivity and cooperative behavior N91-14075
ORGANOMETALLIC COMPOUNDS
Inorganic concepts relevant to metal binding, activity, and toxicity in a biological system
[DE91-001489] N91-13858
ORIFICE FLOW
Variable orifice flow regulator
[NASA-CASE-MSC-21549-1] N91-13657
ORIFICES
Variable orifice flow regulator
[NASA-CASE-MSC-21549-1] N91-13657
ORION NEBULA
What sort of standard candle is Orion for studying molecular hydrogen line emission in galaxies N91-14184
OROGRAPHY
Frontal interactions with orography: Objective cross-sectional analysis of ALPEX data N91-13836
OSCILLATING FLOW
Wind-tunnel survey of an oscillating flow field for application to model helicopter rotor testing
[NASA-TM-4224] N91-13462
OSCILLATIONS
Indicial response approach derived from Navier-Stokes equations. Part 1: Time-invariant equilibrium state
[NASA-TM-102856] N91-13408
An application of oscillation damped motion for suspended payloads to the advanced integrated maintenance system
[DE91-002658] N91-13946
OSMOSIS
Coupled transport processes in semipermeable media. Part 2: Numerical method and results
[DE91-004140] N91-14073
OTTO CYCLE
Interpretation of engine cycle-to-cycle variation by chaotic time series analysis
[DE91-000729] N91-13955
OXIDATION
Oxidation characteristics of Ti-25Al-10Nb-3V-1Mo intermetallic alloy
[NASA-TP-3044] N91-13522
Vinyl capped addition polyimides
[NASA-CASE-LEW-15027-1] N91-13566
OXIDATION RESISTANCE
Influence of oxide reinforcement materials on high-temperatue oxidation resistance of Ni3Al matrix composites
[DE91-001625] N91-13498
OXIDE FILMS
Electrocatalysis of anodic oxygen-transfer reactions at modified lead dioxide electrodes
[DE91-000664] N91-13518
Interfacial chemistry of titanium films deposited on PMDA-ODA polyimide
[AD-A225730] N91-13550
OXIDES
Optical characterization techniques applied to ceramic oxides
[DE91-001526] N91-13556
Success criteria for oxide superconductor wires: Measuring the present, predicting the future N91-14034
Oxide superconductor coils: Present successes, future challenges N91-14046
OXYGEN
Computed potential energy surfaces for chemical reactions
[NASA-CR-186877] N91-13506
OXYGEN PRODUCTION
CELSS research and development program N91-13850
OZONE
Stratospheric ozone conservation by electron attachment to chlorine atoms: The negative-ion chemistry
[DE91-002951] N91-13815
Aeronomic chemistry of ozone
[AERONOMICA-ACTA-A-355-1990] N91-13816
Simulation of the formation and transport of ozone in the atmospheric boundary layer
[DLR-FB-90-25] N91-13827
OZONE DEPLETION
Ultraviolet absorption cross-sections of photoactive species of stratospheric interest. Part 1: The halocarbons
[ETN-91-98385] N91-13830

P

P-I-N JUNCTIONS
Design of an X-band PIN diode phase shifter by computer optimization
[FEL-89-B286] N91-13633
PACIFIC OCEAN
Tropical Pacific moisture variability: Its detection, synoptic structure and consequences in the general circulation
[NASA-CR-184045] N91-13832
A primitive equation model for the equatorial Pacific
[KNMI-TR-124] N91-13840
PANEL METHOD (FLUID DYNAMICS)
Theoretical evaluation of engine auxiliary inlet design for supersonic V/STOL aircraft
[NASA-CR-186610] N91-13443
PANELS
FE analyses of aircraft model with interior trim
[FFA-TN-1990-21] N91-13417
Damage assessment and residual compression strength of thick composite plates with through-the-thickness reinforcements
[NASA-CR-187377] N91-13494
Relationship between voids and interlaminar shear strength of polymer matrix composites
[NASA-TM-103643] N91-13495
PARALLEL COMPUTERS
Analysis of parallelism for nonlinear programming
[INPE-5121-TDL/422] N91-13899
Solving the Fokker-Planck equation on a massively parallel computer
[DE91-002795] N91-13915
The advanced software development and commercialization project
[DE91-002956] N91-13933
PARALLEL PROCESSING (COMPUTERS)
Computational methods and software systems for dynamics and control of large space structures
[NASA-CR-187669] N91-13480
Programmable remapper with single flow architecture
[NASA-CASE-MSC-21481-1] N91-13890
Analysis of parallelism for nonlinear programming
[INPE-5121-TDL/422] N91-13899
Implementing automatic differentiation efficiently
[DE91-002409] N91-13913
Parallel Ada benchmarks for the SVMS
[NASA-CR-182453] N91-13929
Synthetic models of distributed memory parallel programs
[DE91-001058] N91-13931
The advanced software development and commercialization project
[DE91-002956] N91-13933
Knowledge representation into Ada parallel processing
[NASA-CR-187451] N91-13934
Applications of neural networks to adaptive control
[AD-A225408] N91-13938
Application of parallel computing to the Monte Carlo simulation of electron scattering in solids: A rapid method for profile deconvolution
[DE91-001227] N91-13980
PARALLEL PROGRAMMING
Guidance, navigation and control. Digital emulation technology laboratory. Volume 3, Task 3: Special studies
[AD-A225125] N91-13430
Computational methods and software systems for dynamics and control of large space structures
[NASA-CR-187669] N91-13480
Constraint treatment techniques and parallel algorithms for multibody dynamic analysis
[NASA-CR-187668] N91-13759
Synthetic models of distributed memory parallel programs
[DE91-001058] N91-13931
PARAMETERIZATION
A physical parameterization of snow albedo for use in climate models N91-13781
PARITY
U1(prime) dark matter and R-parity violation
[DE91-001792] N91-14068
PARTIAL DIFFERENTIAL EQUATIONS
A fully Sinc-Galerkin method for Euler-Bernoulli beam models
[NASA-CR-187462] N91-13952
PARTICLE ACCELERATORS
Success with an automated computer control system
[DE91-001759] N91-13945
PARTICLE BEAMS
NRL 1989 beam propagation studies in support of the ATA multi-pulse propagation experiment
[AD-A226443] N91-13588
Diagnostics for high-brightness beams
[DE91-001865] N91-13701
A linear accelerator in the space: The beam experiment aboard rocket
[DE91-002347] N91-13988
PARTICLE COLLISIONS
Inner-shell ionization of lithium-like chromium ions
[DE91-001749] N91-13981
Influence of collective effects on the performance of high-luminosity colliders
[DE91-001797] N91-13982
Atomic and molecular theory
[DE91-004475] N91-13983
Assessment of ion-atom collision data for magnetic fusion plasma edge modelling
[DE91-001920] N91-14012
The origin and evolution of the Uranian dust rings N91-14253
PARTICLE INTERACTIONS
The role of chemical interactions in ion-solid processes
[DE91-000763] N91-13977
New phases of D greater than or equal to 2 current and diffeomorphism algebras in particle physics
[DE91-001515] N91-14067
Chaos and order in non-integrable model field theories
[DE91-002313] N91-14070
Research in theoretical physics
[DE91-002458] N91-14071
PARTICLE SIZE DISTRIBUTION
Possibilities of the calculation of stresses and residual stresses in materials with a phase transformation N91-13548
The origin and evolution of the Uranian dust rings N91-14253
PARTICLE THEORY
Particle theory and cosmology
[DE91-004189] N91-14250
PARTICLE TRACKS
Detection of multiple-bit errors from single-ion tracks in integrated circuits
[NASA-CASE-NPO-18075-1-CU] N91-13622
PARTICLE TRAJECTORIES
The fluid mechanics of continuous flow electrophoresis
[NASA-CR-187647] N91-13648
PARTICLES
The effect of suspended particles on Jean's criterion for gravitational instability N91-14189
PARTICULATE SAMPLING
Characterization of rocket propellant combustion products: Description of sampling and analysis methods for rocket exhaust characterization studies
[DE91-002536] N91-13574
The influence of the sampling time on diffusion measurements in the atmosphere N91-13824
PASSIVITY
Dissipative controller designs for second-order dynamic systems
[NASA-CR-187452] N91-13935
PATENTS
Catalogue of ESA patents
[ESA-SP-1131] N91-14083
PATTERN RECOGNITION
Millimeter-wave sensor image enhancement
[NASA-CR-187430] N91-13679
About transient stability of power systems: Statistical pattern recognition approach
[LAAS-90192] N91-13889

General method of pattern classification using the two-domain theory
[NASA-CASE-MSC-21737-1] N91-13911

PAVEMENTS
Literature review on geotextiles to improve pavements for general aviation airports
[DOT/FAA/RD-90/26] N91-13464
Laboratory investigation of the use of geotextiles to mitigate frost heave
[DOT/FAA/RD-90/13] N91-13465

PAYLOAD TRANSFER
Telerobotic on-orbit remote fluid resupply system
[NASA-CR-184052] N91-13474

PAYLOADS
Integrated launch and emergency vehicle system
[NASA-CASE-LAR-13780-1] N91-13481

PECULIAR GALAXIES
The CO-12 and CO-13 J=2-1 and J=1-0 observations of hot and cold galaxies N91-14126
A multi-wavelength study of the peculiar galaxy NGC 2976 N91-14199
Global and radial variations in the efficiency of massive star formation among galaxies N91-14215

PEEK
Experimental observations and finite element analysis of the initiation of fiber microbuckling in notched composite laminates
[NASA-CR-185354] N91-13756

PEENING
Study of the metallurgical effects of hammering between passes during C-Mn weld deposition
[CETIM-104850] N91-13532
Study of the metallurgical consequences of hammering between passes to compensate for the withdrawal of metal caused by welding
[CETIM-104430] N91-13741

PENALTY FUNCTION
Analysis of parallelism for nonlinear programming
[INPE-5121-TDL/422] N91-13899

PENDULUMS
An application of oscillation damped motion for suspended payloads to the advanced integrated maintenance system
[DE91-002658] N91-13946
An asymptotic symmetry of the rapidly forced pendulum
[DE91-001868] N91-13958

PERFORMANCE PREDICTION
AN alternative to suppression: Modeling methodology for assessing indirect effects of weapons and human performance degradation
[AD-A226518] N91-13877

PERFORMANCE TESTS
Hazard studies for solid propellant rocket motors
[AGARD-AG-316] N91-13488
Planar near-field measurement of non-reciprocal antennas
[FEL-90-B092] N91-13604
Feasibility to study of a non-reciprocal latched ferrite phase shifter in the 92-96 GHz band
[FEL-90-B114] N91-13634
Test procedure frequency multiplier 583R936H03/H04
[FEL-90-A089] N91-13636
Bidirectional slapper detonators in spherical explosion systems
[DE91-002399] N91-13662
Tethering sockets and wrenches
[NASA-CR-184032] N91-13675
The Improved Three Axis Test Table (ITATT): Program status and recommendation for completion
[AD-A226508] N91-13712
Passive microwave devices using high temperature superconductors N91-14036
High Tc superconductors for microwave filters N91-14038

PERIOD DOUBLING
The route to chaos for the Kuramoto-Sivashinsky equation
[NASA-CR-187461] N91-13642

PERIODIC VARIATIONS
Centimeter emission variation of Venus: Its second phase
[INPE-5122-TDL/423] N91-14257

PERMAFROST
Mesoscale monitoring of the soil freeze/thaw boundary from orbital microwave radiometry
[NASA-CR-185901] N91-13817

PERMANENT MAGNETS
Magnetic suspension and balance system advanced study, phase 2
[NASA-CR-4327] N91-13463

PERMEABILITY
An investigation of microstructural characteristics of contact-lens polymers
[NASA-TP-3034] N91-13492
A complex permittivity and permeability measurement system for elevated temperatures
[NASA-CR-186916] N91-13609
Mechanisms of gas permeation through polymer membranes
[DE91-004190] N91-13671
Application of high-temperature superconductors to high-precision accelerometers N91-14042
Coupled transport processes in semipermeable media. Part 2: Numerical method and results
[DE91-004140] N91-14073

PERMEATING
Investigation of the uniformity of the magnetic field and flux density in the NPL permeameter
[NPL-DES-101] N91-13968

PERMITTIVITY
Modified Hilbert transform pair and Kramers-Kronig relations for complex permittivities
[NASA-TM-102682] N91-13585
A complex permittivity and permeability measurement system for elevated temperatures
[NASA-CR-186916] N91-13609

PERSONAL COMPUTERS
Micro based technology: A new tool for missile guidance system design and visualization N91-13440
Multispectral target detection using image processing programs developed on PC's
[FEL-89-B304] N91-13925

PERTURBATION
Measurement of waves in flows across a surface
[NASA-CASE-NPO-17479-1-CU] N91-13658
Confinement and heating studies of field-reversed configurations
[DE91-001965] N91-14008

PHASE COHERENCE
Superconducting Josephson Junction Gyroscope (JJG) N91-14043

PHASE CONJUGATION
Motion detection, novelty filtering, and target tracking using an interferometric technique with a GaAs phase conjugate mirror
[NASA-CASE-NPO-17784-1-CU] N91-13998

PHASE SHIFT
Centimeter emission variation of Venus: Its second phase
[INPE-5122-TDL/423] N91-14257

PHASE SHIFT CIRCUITS
Electronic scan at millimetre wave frequencies
[FEL-89-B258] N91-13601
Design of an X-band PIN diode phase shifter by computer optimization
[FEL-89-B286] N91-13633
Feasibility to study of a non-reciprocal latched ferrite phase shifter in the 92-96 GHz band
[FEL-90-B114] N91-13634

PHASE SHIFT KEYING
Multiple symbol differential detection
[NASA-CASE-NPO-17896-1-CU] N91-13596

PHASE TRANSFORMATIONS
Multiphase carbon and its properties in complex mixtures
[DE91-001679] N91-13499
Physical properties of thermosetting polymers
[AD-A225864] N91-13508
Possibilities of the calculation of stresses and residual stresses in materials with a phase transformation N91-13548
The effect of the molecular structure of polymer and low molecular liquid crystals on their electro-optical characteristics at the nematic-isotropic phase transition
[ETN-91-98170] N91-13564
Viscosity measurements at high temperature and high pressure: A novel technique
[NASA-CR-187239] N91-13967

PHASE VELOCITY
Zero wavenumber modes of a compressible supersonic mixing layer
[NASA-CR-187476] N91-13669

PHASED ARRAYS
Utilization of the HIPAS facility for cooperative experiments related to ionospheric modification
[AD-A226609] N91-13590
Electronic scan at millimetre wave frequencies
[FEL-89-B258] N91-13601
Analog superconductive electronics for avionics N91-14040

PHOSPHATES
Optical characterization techniques applied to ceramic oxides
[DE91-001526] N91-13556

PHOSPHORIC ACID FUEL CELLS
Corrosion-resistant catalyst supports for phosphoric acid fuel cells
[DE91-001713] N91-13794

PHOSPHORS
Laser-induced fluorescence of phosphors for remote cryogenic thermometry
[DE91-001733] N91-13681

PHOTOACOUSTIC SPECTROSCOPY
Actinide speciation by photothermal spectroscopies: Instrumentation development
[DE91-001854] N91-13700

PHOTOCHEMICAL REACTIONS
Real-time dynamic holographic image storage device
[NASA-CASE-LAR-13989-1] N91-13694

PHOTOCONDUCTIVITY
Subnanosecond, high voltage photoconductive switching in GaAs
[DE91-002671] N91-14063

PHOTODIODES
A silicon avalanche photodiode detector circuit for Nd:YAG laser scattering
[DE91-002709] N91-13706
Prospects of CsJ(Tl)-photodiode detectors for low level spectroscopy
[MPI-PAE/EXP.EL-228] N91-13984
X ray and charged particle detection with CsI(Tl) layer coupled to a-Si:H photodiode layers
[DE91-001798] N91-14060

PHOTODISSOCIATION
Physical conditions in photodissociation regions: Application to galactic nuclei N91-14113
Far-infrared spectroscopy of NGC 6946, IC 342, and Arp 299 N91-14114

PHOTOELECTRIC EMISSION
Synchrotron radiation photoemission study of metal overlayers on hydrogenated amorphous silicon at room temperature
[DE91-000740] N91-13525

PHOTOELECTRON SPECTROSCOPY
An x ray photoelectron spectroscopy study of Au(x)In(y) alloys
[NASA-TM-103659] N91-14050

PHOTOELECTRONS
The infrared continuum spectrum of x ray illuminated molecular gas N91-14144

PHOTOGEOLOGY
Methodological contribution utilizing TM/LANDSAT-5 imagery in geologic mapping of regions with significant vegetative cover
[INPE-5117-TDL/419] N91-13784

PHOTOGRAMMETRY
Close-range photogrammetric measurement of static deflections for an aeroelastic supercritical wing
[NASA-TM-4194] N91-13400
Analytical and photogrammetric characterization of a planar tetrahedral truss
[NASA-TM-4231] N91-13473

PHOTOGRAPHIC FILM
Data reduction of digitized images processed from calibrated photographic and spectroscopic films obtained from terrestial, rocket and space shuttle telescopic instruments
[NASA-CR-187320] N91-13674
Variable magnification glancing incidence x ray telescope
[NASA-CASE-MFS-28013-2] N91-14096

PHOTOGRAPHS
An interactive program for the analysis and design of advanced laser targets
[DE91-002542] N91-13704

PHOTOINTERPRETATION
Methodological contribution utilizing TM/LANDSAT-5 imagery in geologic mapping of regions with significant vegetative cover
[INPE-5117-TDL/419] N91-13784

PHOTOIONIZATION
Large scale excitation of the ISM in NGC 1068 N91-14150
Hot interstellar gas and ionization of embedded clouds N91-14161
Star formation in proto dwarf galaxies N91-14212
Ionization in the local interstellar and intergalactic media N91-14249

PHOTOLYSIS
Magnetic field effect transistors
[AD-A226535] N91-13614
Radio observations of several interstellar molecules N91-14093

PHOTOMETERS
A silicon avalanche photodiode detector circuit for Nd:YAG laser scattering
[DE91-002709] N91-13706

PHOTOMETRY
Far-infrared observations of Circinus and NGC 4945 galaxies N91-14131
Peering beyond IRAS: The 100 to 350 micron dust emission from galaxies N91-14141
Optical and near-IR study of LMC HII region N11AB N91-14155

Deep narrow band imagery of the diffuse ISM in M33 N91-14202
Are bars essential for starbursts in non-interacting galaxies N91-14208

PHOTONS
Elementary particle interactions
[DE91-001220] N91-13979

PHOTOSYNTHESIS
Terrestrial ecosystems and climatic change
[DE91-001492] N91-13813

PHOTOTRANSISTORS
High-gain AlGaAs/GaAs double heterojunction Darlington phototransistors for optical neural networks
[NASA-CASE-NPO-18101-1-CU] N91-13995

PHOTOVOLTAIC CELLS
Status of concentrator collector and high-efficiency concentrator cell development
[DE91-001260] N91-13793
Small particle selective emitter
[NASA-CASE-LEW-14731-1] N91-13802
Design considerations for lunar base photovoltaic power systems
[NASA-TM-103642] N91-14259

PHOTOVOLTAIC EFFECT
SERI photovoltaic subcontract reports: Abstracts and document control information
[DE90-000378] N91-13792

PHYSIOLOGICAL RESPONSES
Physiological responses to prolonged bed rest in humans: A compendium of research, 1981-1988
[NASA-TM-102249] N91-13862
Thermoregulatory consequences of resonant microwave exposure
[AD-A226540] N91-13864
Cognitive and neural bases of skilled performance
[AD-A226668] N91-13869
Vestibulo-ocular responses in man to +G sub z hypergravity
[IZF-1989-59] N91-13873

PHYSIOLOGY
A discrepancy within primate spatial vision and its bearing on the definition of edge detection processes in machine vision
[NASA-TM-102739] N91-13941

PICOSECOND PULSES
Surfaces and thin films studied by picosecond ultrasonics
[DE91-004167] N91-13973

PIEZOELECTRIC TRANSDUCERS
Design of a mechanical modulator for the planetary Fourier spectrometer experiment of the MARS 94 mission
[IFSI-89-22] N91-13717

PILOT PERFORMANCE
Aircraft accident report: Aloha IslandAir, Inc., Flight 1712, de Havilland Twin Otter, DHC-6-300, N707PV, Halawa Point, Molokai, Hawaii, October 28, 1989
[PB90-910405] N91-13425
Simulator flight as a selection device: Effects of test anxiety on subjective and objective measures of performance
[IZF-1989-57] N91-13468
Time-sharing performance as a factor for success in flight training: Test development and validation
[IZF-1989-58] N91-13872
Modeling pilot interaction with automated digital avionics systems: Guidance and control algorithms for contour and nap-of-the-Earth flight
[NASA-CR-186105] N91-13875
A subjective rating scale for assessing pilot workload in flight: A decade of practical use
[RAE-TR-90019] N91-13882

PILOT SELECTION
Simulator flight as a selection device: Effects of test anxiety on subjective and objective measures of performance
[IZF-1989-57] N91-13468
Time-sharing performance as a factor for success in flight training: Test development and validation
[IZF-1989-58] N91-13872

PIONEER VENUS SPACECRAFT
Pioneer-Venus radio occultation (ORO) data reduction: Profiles of 13 cm absorptivity
[NASA-CR-186986] N91-13584

PIPE FLOW
Analytical study of the liquid phase transient behavior of a high temperature heat pipe
[NASA-CR-187426] N91-13644
Heat pipe dynamic behavior
[NASA-CR-187422] N91-13645

PIPELINING (COMPUTERS)
Pipeline synthetic aperture radar data compression utilizing systolic binary tree-searched architecture for vector quantization
[NASA-CASE-NPO-17941-1-CU] N91-13595

PIPES (TUBES)
Creep and creep failure of power plant steels
[VTT-RR-685] N91-13528
Enhancement of critical heat flux in tubes using staged tangential flow injection
[DE90-014935] N91-13659
Evaluation of the functional properties of welds on cold finished tubes defined as NF A 49.541
[CETIM-104700] N91-13738
Mechanical properties of 1950's vintage Type 304 stainless steel weldment components
[DE91-004328] N91-13774

PITCH (INCLINATION)
Effects of anthropometric and postural variables on the transmission of whole-body vertical vibration from seat-to-head
[ISVR-TR-172] N91-13884

PIXELS
Programmable remapper with single flow architecture
[NASA-CASE-MSC-21481-1] N91-13890

PLANAR STRUCTURES
Design of high voltage planar devices using SIPOS technology
[LAAS-90237] N91-13629

PLANETARY EVOLUTION
The evolution of comets and the detectability of Extra-Solar Oort Clouds N91-14242

PLANETARY GEOLOGY
Proceedings of the MEVTV Workshop on The Evolution of Magma Bodies on Mars
[NASA-CR-187357] N91-14252
Mars tectonics and volcanism
[NASA-CR-187351] N91-14254

PLANETARY MAPPING
Elemental mapping of planetary surfaces using gamma ray spectroscopy
[DE91-001877] N91-14258

PLANETARY SURFACES
Proceedings of a Workshop on Cosmogenic Nuclide Production Rates
[NASA-CR-185349] N91-14098
Elemental mapping of planetary surfaces using gamma ray spectroscopy
[DE91-001877] N91-14258

PLANETARY SYSTEMS
The evolution of comets and the detectability of Extra-Solar Oort Clouds N91-14242

PLANTS (BOTANY)
Localize and identify the gravity sensing mechanism of plants
[NASA-CR-187411] N91-13841
Plants and their microbial assistants: Nature's answer to Earth's environmental pollution problems N91-13851

PLASMA ANTENNAS
Plasma properties
[DE91-001361] N91-14006

PLASMA CONTROL
Free-electron laser experiments in the microwave tokamak experiment
[DE91-001746] N91-13699
Assessment of ion-atom collision data for magnetic fusion plasma edge modelling
[DE91-001920] N91-14012
Confinement properties of the RFP (reversed field pinch)
[DE91-002322] N91-14015
Dependence of CIT (compact ignition tokamak) PF (poloidal field) coil currents on profile and shape parameters using the control matrix
[DE91-002650] N91-14019
A 15 MeV proton dianostic for DIII-D
[DE91-002717] N91-14022

PLASMA CURRENTS
ITER confinement capability
[DE91-002647] N91-14018
Dependence of CIT (compact ignition tokamak) PF (poloidal field) coil currents on profile and shape parameters using the control matrix
[DE91-002650] N91-14019

PLASMA DENSITY
A compact, low cost, 7 channel polychromator for Thomson scattering measurements
[DE91-002719] N91-14024
A real-time digital control, data acquisition and analysis system for the DIII-D multipulse Thomson scattering diagnostic
[DE91-002720] N91-14025
Ionization degree of classical, dense, and highly condensed plasmas
[ETN-91-98174] N91-14027

PLASMA DIAGNOSTICS
A multi-laser system for a fast sampling Thomson scattering diagnostic
[DE91-002708] N91-13705
Compact Ignition Tokamak project: Localizability of electron-cyclotron heating power
[DE91-002571] N91-14016
International Thermonuclear Experimental Reactor physics basis
[DE91-002646] N91-14017
A 15 MeV proton dianostic for DIII-D
[DE91-002717] N91-14022
High spatial and temporal resolution visible spectroscopy of the plasma edge in DIII-D
[DE91-002718] N91-14023
A compact, low cost, 7 channel polychromator for Thomson scattering measurements
[DE91-002719] N91-14024
A real-time digital control, data acquisition and analysis system for the DIII-D multipulse Thomson scattering diagnostic
[DE91-002720] N91-14025

PLASMA EQUILIBRIUM
Plasma properties
[DE91-001361] N91-14006

PLASMA HEATING
Plasma properties
[DE91-001361] N91-14006
Confinement properties of the RFP (reversed field pinch)
[DE91-002322] N91-14015
Compact Ignition Tokamak project: Localizability of electron-cyclotron heating power
[DE91-002571] N91-14016

PLASMA JETS
Analytical and experimental studies for thermal plasma processing of materials
[DE91-000599] N91-13576
Dynamic high-pressure studies of an electrothermal capillary
[DE91-000966] N91-13617
Coherent anti-Stokes Raman spectroscopic measurement of air entrainment in argon plasma jets
[DE91-001936] N91-13670
Measurement of air entrainment in plasma jets
[DE91-001943] N91-14013

PLASMA LAYERS
Fatigue testing of plasma-sprayed thermal barrier coatings, volume 2
[NASA-CR-186726] N91-13535

PLASMA PHYSICS
Plasma properties
[DE91-001361] N91-14006

PLASMA SPRAYING
Composite thermal barrier coating
[NASA-CASE-LEW-14999-1] N91-13500
Simultaneous measurement of Ni-Al particle size, velocity, and temperature in atmospheric thermal plasmas
[DE91-001935] N91-13826

PLASMA TORCHES
Simultaneous measurement of Ni-Al particle size, velocity, and temperature in atmospheric thermal plasmas
[DE91-001935] N91-13826

PLASMAS (PHYSICS)
Modified Hilbert transform pair and Kramers-Kronig relations for complex permittivities
[NASA-TM-102682] N91-13585
Inner-shell ionization of lithium-like chromium ions
[DE91-001749] N91-13981
Plasma properties
[DE91-001361] N91-14006
Confinement and heating studies of field-reversed configurations
[DE91-001965] N91-14008
Magnetic turbulent electron transport in a reversed field pinch
[DE91-001898] N91-14009
Assessment of ion-atom collision data for magnetic fusion plasma edge modelling
[DE91-001920] N91-14012
Experimental development, testing, and research work in support of the inertial confinement fusion program
[DE91-002770] N91-14026
Hot interstellar gas and ionization of embedded clouds N91-14161
Origin and dynamics of emission line clouds in cooling flow environments N91-14167

PLASTIC BODIES
A comparison of two numerical methods for shocks in one-dimensional elastic-plastic solids
[DE91-001741] N91-13765

PLASTIC DEFORMATION
A comparative study of ductile fracture in the 2.25 percent Cr-1 percent Mo and 9 percent Cr-1 percent Mo alloy steels N91-13753

PLATES (STRUCTURAL MEMBERS)
Composite fuselage technology
[NASA-CR-187658] N91-13446

Effects of temperature on acoustically-induced strains and damage propagation in CFRP plates N91-13493
Specifications extraction and synthesis: Their correlations with preliminary design N91-13936

PLATINUM
Signal processing development
[AD-A226593] N91-14052

PLUG NOZZLES
All Shuttle Centaur engine and nozzle support plug vibration testing
[NASA-CR-183201] N91-13485

PLUGS
Improved plug valve computer-aided design of plug element
[DE91-001044] N91-13719

PLY ORIENTATION
Experimental observations and finite element analysis of the initiation of fiber microbuckling in notched composite laminates
[NASA-CR-185354] N91-13756

POINT SOURCES
Research in theoretical physics
[DE91-002458] N91-14071
Spatial analysis of IRAS observations of nearby spirals N91-14133

POLAR REGIONS
Sea ice-atmosphere interaction: Application of multispectral satellite data in polar surface energy flux estimates
[NASA-CR-187376] N91-13782

POLARIMETRY
Method for providing a polarization filter for processing synthetic aperture radar image data
[NASA-CASE-NPO-17904-1-CU] N91-13594
Infrared polarimetry and the magnetic field in external galaxies N91-14192
Polarization in the Lagoon nebula N91-14193

POLARIZATION (CHARGE SEPARATION)
A study of the ice-hail charge separation mechanism using a thunderstorm electrification model with explicit microphysics in a kinematic framework N91-13835

POLICIES
Federal information inventory/locator systems: From burden to benefit N91-14074

POLLUTION CONTROL
Plants and their microbial assistants: Nature's answer to Earth's environmental pollution problems N91-13851

POLOIDAL FLUX
Dependence of CIT (compact ignition tokamak) PF (poloidal field) coil currents on profile and shape parameters using the control matrix
[DE91-002650] N91-14019

POLYCRYSTALS
Design of high voltage planar devices using SIPOS technology
[LAAS-90237] N91-13629

POLYIMIDE RESINS
Interfacial chemistry of titanium films deposited on PMDA-ODA polyimide
[AD-A225730] N91-13550
Vinyl capped addition polyimides
[NASA-CASE-LEW-15027-1] N91-13566

POLYIMIDES
Novel polyimide molding powder, coating, adhesive, and matrix resin
[NASA-CASE-LAR-14163-1] N91-13559
Preparation of polyimides from bis(N-isoprenyl)s of aryl diamides
[NASA-CASE-LAR-14330-1-CU] N91-13560
Methyl substituted polyimides containing carbonyl and ether connecting groups
[NASA-CASE-LAR-14351-1] N91-13561

POLYMER BLENDS
PBT, PBO-based hybrid polymers with nonlinear optical properties or high electrical conductivity
[AD-A226646] N91-13552

POLYMER MATRIX COMPOSITES
Relationship between voids and interlaminar shear strength of polymer matrix composites
[NASA-TM-103643] N91-13495
Development of standards for advanced polymer matrix composites: A BPF/ACG overview
[NPL-DMM(A)-8] N91-13568
Experimental observations and finite element analysis of the initiation of fiber microbuckling in notched composite laminates
[NASA-CR-185354] N91-13756

POLYMER PHYSICS
The effect of the molecular structure of polymer and low molecular liquid crystals on their electro-optical characteristics at the nematic-isotropic phase transition
[ETN-91-98170] N91-13564

POLYMERIC FILMS
PBT, PBO-based hybrid polymers with nonlinear optical properties or high electrical conductivity
[AD-A226646] N91-13552

POLYMERIZATION
The synthesis of star block copolymers by controlled ring-opening metathesis polymerization
[AD-A225987] N91-13551

POLYMERS
Preparation of polyimides from bis(N-isoprenyl)s of aryl diamides
[NASA-CASE-LAR-14330-1-CU] N91-13560

POLYMETHYL METHACRYLATE
Tubular lap joints for wind turbine applications
[DE91-001341] N91-13736

POLYNOMIALS
The simultaneous integration of many trajectories using nilpotent normal forms
[NASA-CR-187318] N91-13950

POLYVINYL CHLORIDE
Hydraulic lifting device
[NASA-CASE-SSC-00008-1] N91-13733

POPULATIONS
On the invertibility of Leslie systems
[REPT-90-006] N91-13963
The large-scale space distribution of emission-line galaxies N91-14091

POROUS MATERIALS
Coupled transport processes in semipermeable media. Part 2: Numerical method and results
[DE91-004140] N91-14073

POSEIDON SATELLITE
Report by the Subcommitee on Intercomparison and Merging of Geodetic Data of the Topex/Poseidon science working team
[LR-638] N91-13791

POSITION (LOCATION)
Local closed orbit bumps in AmPS
[NIKHEF-K/AMPS/90-01] N91-13471
System and method for measuring ocean surface currents at locations remote from land masses using synthetic aperture radar
[NASA-CASE-NPO-17937-1-CU] N91-13787
DOPLIGHT 1987 project summary
[PB90-253584] N91-13834
Hearing in three dimensions: Sound localization
[NASA-CR-187706] N91-13971
Optical joint correlation for real-time tracking
[NASA-CASE-MSC-21509-1] N91-13997
Apparatus for precision focusing and positioning of a beam waist on a target
[NASA-CASE-ARC-11916-1-SB] N91-14002
Influence of the delocalized excitation process on the determination of foreign atom positions using the channeling effect
[ETN-91-98175] N91-14065
Variable magnification glancing incidence x ray telescope
[NASA-CASE-MFS-28013-2] N91-14096

POSITION SENSING
Laser optical disk position encoder with active heads
[NASA-CASE-GSC-13175-1] N91-14001

POSITIONING
Three dimensional moire pattern alignment
[NASA-CASE-MSC-21416-1] N91-14000
Apparatus for precision focusing and positioning of a beam waist on a target
[NASA-CASE-ARC-11916-1-SB] N91-14002

POSTFLIGHT ANALYSIS
An assessment of wind tunnel test data on flexible thermal protection materials and results of new fatigue tests of threads
[NASA-CR-177466] N91-13972
Instellar Gas Experiment (IGE): Testing interstellar gas particles to provide information on the processes of nucleosynthesis in the big bang stars and supernova
[NASA-CR-186713] N91-14097

POTENTIAL ENERGY
Computed potential energy surfaces for chemical reactions
[NASA-CR-186877] N91-13506
Variational transition state theory
[DE91-001253] N91-14058
Non-empirical interatomic potentials for transition metals, alloys, and semiconductors
[DE91-002396] N91-14062

POWDER (PARTICLES)
Method of making single crystal fibers
[NASA-CASE-LEW-14921-1] N91-13502
Novel polyimide molding powder, coating, adhesive, and matrix resin
[NASA-CASE-LAR-14163-1] N91-13559
Analytical and experimental studies for thermal plasma processing of materials
[DE91-000599] N91-13576

POWDER METALLURGY
Method of making carbide/fluoride/silver composites
[NASA-CASE-LEW-14902-1] N91-13503
Binders used in metal injection molding
[VTT-RR-691] N91-13529
Fabrication and properties of powder metallurgically manufactured aluminum products and composites
[VTT-RR-699] N91-13531

POWER AMPLIFIERS
Folded RF-excited CO2 waveguide lasers N91-13695

POWER EFFICIENCY
Injection efficiency of bound modes
[NASA-CR-4333] N91-13991

POWER GAIN
Small signal gain based on analytic models of thin intense electron beams
[DE91-001874] N91-13631

PRECESSION
Measuring the Lense-Thirring precession using a second Lageos satellite
[NASA-CR-186945] N91-13470

PREDICTION ANALYSIS TECHNIQUES
A review of nonlinear constitutive models for metals
[NASA-TM-102727] N91-13761
Comparison of NASA Lewis Research Center's performance code's pressure-drop model predictions to Stirling engine working-space flow test data
[NASA-CR-182215] N91-13804

PREDICTIONS
A review of ice accretion data from a model rotor icing test and comparison with theory
[NASA-TM-103712] N91-13421
Interactions between battle management and guidance law design for a strategic interceptor N91-13441
Guidance methods for tactical and strategic missiles N91-13442
Measurements and predictions of a liquid spray from an air-assist nozzle
[NASA-TM-103640] N91-13455
Relationship between voids and interlaminar shear strength of polymer matrix composites
[NASA-TM-103643] N91-13495
Study of improved methods for predicting chemical equilibria
[DE91-000263] N91-13509
A nonlinear viscoelastic approach to durability predictions for polymer based composite structures
[NASA-CR-187653] N91-13554
Predictive sensor method and apparatus
[NASA-CASE-SSC-00006-1] N91-13691
A physical parameterization of snow albedo for use in climate models N91-13781
Success criteria for oxide superconductor wires: Measuring the present, predicting the future N91-14034
A model for the infrared emission from an OB star cluster environment N91-14139

PREMIXED FLAMES
Topics in physico-chemical hydrodynamics
[DE91-001674] N91-13519

PREPOLYMERS
A new approach to design of cross-linked second-order nonlinear optical polymers
[AD-A226674] N91-13553

PRESSURE DEPENDENCE
Interpretation of engine cycle-to-cycle variation by chaotic time series analysis
[DE91-000729] N91-13955

PRESSURE DISTRIBUTION
Transonic wind tunnel tests on two-dimensional aerofoil sections: Determination of pressure distribution and drag for an aerofoil of type SAAB 7301 in FFA wind tunnel S5
[FFA-TN-1989-47] N91-13416
Nonlinear viscous waves produced by an impulsively moving plate N91-13641
Pressure visualization (PreViz) package version 1.0 user's guide
[NASA-CR-187444] N91-13907

PRESSURE EFFECTS
Simulation of pressure and temperature responses for the 20 Inch Supersonic Wind Tunnel
[NASA-TM-102647] N91-13467
Dynamic high-pressure studies of an electrothermal capillary
[DE91-000966] N91-13617
Device for applying constant pressure to a surface
[NASA-CASE-GSC-13230-1] N91-13734
Thermal power transfer system using applied potential difference to sustain operating pressure difference
[NASA-CASE-NPO-18034-1-CU] N91-13796
NGC 3312: A victim of ram pressure sweeping N91-14177

PRESSURE GRADIENTS
Assessments of atmospheric effects on VHF and UHF communications
[AD-A226661] N91-13592
Coupled transport processes in semipermeable media. Part 2: Numerical method and results
[DE91-004140] N91-14073

PRESSURE MEASUREMENT
Measurement of waves in flows across a surface
[NASA-CASE-NPO-17479-1-CU] N91-13658
Volumetric measurement of tank volume
[NASA-CASE-MSC-21500-1] N91-13683
Probe insertion apparatus with inflatable seal
[NASA-CASE-LEW-14965-1] N91-13732
PRESSURE PULSES
Passive fetal monitoring sensor
[NASA-CASE-LAR-14088-1] N91-13686
PRESSURE REDUCTION
The effect of longitudinal spacer ribs on the minimum pressure drop in a heated annulus
[DE91-000784] N91-13655
Volumetric measurement of tank volume
[NASA-CASE-MSC-21500-1] N91-13683
Comparison of NASA Lewis Research Center's performance code's pressure-drop model predictions to Stirling engine working-space flow test data
[NASA-CR-182215] N91-13804
PRESSURE SENSORS
Water cooled static pressure probe
[NASA-CASE-LAR-14340-1-CU] N91-13684
PRESSURE VESSELS
Material and mechanical characterizations for braided composite pressure vessels
[AD-A226640] N91-13713
Probe insertion apparatus with inflatable seal
[NASA-CASE-LEW-14965-1] N91-13732
PRESSURIZED WATER REACTORS
Potential impact of enhanced fracture-toughness data on pressurized-thermal-shock analysis
[DE91-001493] N91-13763
PREVENTION
Fluid flow effects on electroplating
[DE91-001087] N91-13577
PRIMATES
A discrepancy within primate spatial vision and its bearing on the definition of edge detection processes in machine vision
[NASA-TM-102739] N91-13941
PRIMITIVE EQUATIONS
A primitive equation model for the equatorial Pacific
[KNMI-TR-124] N91-13840
Generic extravehicular (EVA) and telerobot task primitives for analysis, design, and integration. Version 1.0: Reference compilation for the EVA and telerobotics communities
[NASA-CR-187429] N91-13876
PROBABILITY THEORY
On the design of component test plans based on system reliability objectives
[DE90-017034] N91-13745
PROBES
Heat exchanger fouling: Prediction, measurement, and mitigation
[DE91-001997] N91-13661
PROBLEM SOLVING
Development of a full potential solver for rotor aerodynamics analysis N91-13407
The mechanism of restructuring in geometry
[AD-A224740] N91-13951
New techniques for the union-find problem
[RUU-CS-89-12] N91-13954
PROCEDURES
Microbial ecology laboratory procedures manual NASA/MSFC
[NASA-CR-184033] N91-13856
List of standards to accompany manual of documentation practices applicable to defence-aerospace scientific and technical information. Addendum
[AGARD-AG-235-ADD] N91-14076
PROCESS CONTROL (INDUSTRY)
The CELSS breadboard project: Plant production N91-13849
PRODUCT DEVELOPMENT
Development and computer aided residual stress measurements on coated specimen using blind-hole drilling technique N91-13544
PRODUCTION ENGINEERING
Influence of materials structure and production method of Al2O3 ceramic on the x-ray stress measurement N91-13540
PROGRAM VERIFICATION (COMPUTERS)
Comparison of NASA Lewis Research Center's performance code's pressure-drop model predictions to Stirling engine working-space flow test data
[NASA-CR-182215] N91-13804
Software reliability through fault-avoidance and fault-tolerance
[NASA-CR-187646] N91-13904
Validation environment for AIPS/ALS: Implementation and results
[NASA-CR-4340] N91-13930
PROGRAMMING LANGUAGES
An object-oriented logic language for modular system specification
[REPT-90-027] N91-13927
The ISIS project: Fault-tolerance in large distributed systems
[NASA-CR-186625] N91-13928
PROJECT MANAGEMENT
Microgravity strategic plan, 1990
[NASA-TM-103448] N91-13575
Coupling artificial intelligence and a system dynamics simulation to optimize quality assurance and testing in software development
[AD-A226580] N91-13902
PROJECT PLANNING
Civil tiltrotor missions and applications
[NASA-CR-177452] N91-13424
JANNAF liquid rocket combustion instability panel research recommendations
[NASA-TM-103653] N91-13491
Microgravity strategic plan, 1990
[NASA-TM-103448] N91-13575
PROJECTILES
Penetration of yawed projectiles
[DE91-001084] N91-13726
PROPAGATION VELOCITY
Study of static and dynamic fracture using strain measurements N91-13754
PROPELLANT COMBUSTION
Characterization of rocket propellant combustion products: Description of sampling and analysis methods for rocket exhaust characterization studies
[DE91-002536] N91-13574
PROPELLANT MASS RATIO
RL10A-3-3B high mixture ratio qualification program
[NASA-CR-183200] N91-13486
PROPELLER NOISE
Computation of broadband mixing noise from turbomachinery
[AD-A226559] N91-13969
PROPULSION
An AD100 implementation of a real-time STOVL aircraft propulsion system
[NASA-TM-103683] N91-13457
PROPULSION SYSTEM CONFIGURATIONS
Variable orifice flow regulator
[NASA-CASE-MSC-21549-1] N91-13657
PROPULSION SYSTEM PERFORMANCE
Integrated flight-propulsion control concepts for supersonic transport airplanes
[NASA-TM-101728] N91-13460
Dynamic high-pressure studies of an electrothermal capillary
[DE91-000966] N91-13617
Comparison of NASA Lewis Research Center's performance code's pressure-drop model predictions to Stirling engine working-space flow test data
[NASA-CR-182215] N91-13804
PROTEIN CRYSTAL GROWTH
Definition study for temperature control in advanced protein crystal growth
[NASA-CR-187346] N91-14029
PROTEINS
Definition study for temperature control in advanced protein crystal growth
[NASA-CR-187346] N91-14029
PROTOCOL (COMPUTERS)
Echocardiography in NATO aircrew
[AGARD-AR-297] N91-13863
Research into alternative network approaches for space operations
[NASA-CR-187015] N91-13894
The design of a distributed image processing and dissemination system
[DE91-001835] N91-13909
The ISIS project: Fault-tolerance in large distributed systems
[NASA-CR-186625] N91-13928
System and method for a general purpose architecture for intelligent computer-aided training
[NASA-CASE-MSC-21381-1] N91-13944
The mechanism of restructuring in geometry
[AD-A224740] N91-13951
PROTON BEAMS
Diagnostics for high-brightness beams
[DE91-001865] N91-13701
PROTON MAGNETIC RESONANCE
Fundamental investigations of supported monometallic and bimetallic catalysts by proton magnetic resonance spectroscopy
[DE91-000610] N91-13516
PROTON RESONANCE
Development and initial characterization of a nuclear magnetic resonance dosimetry system
[DE91-001775] N91-13867
PROTONS
Elementary particle interactions
[DE91-001220] N91-13979
A 15 MeV proton dianostic for DIII-D
[DE91-002717] N91-14022
Space radiation dose analysis for solar flare of August 1989
[NASA-TM-4229] N91-14265
PSYCHOLOGICAL EFFECTS
AN alternative to suppression: Modeling methodology for assessing indirect effects of weapons and human performance degradation
[AD-A226518] N91-13877
PULLEYS
Sheave assembly
[AD-D014605] N91-13711
Heat engine with corrugated shape memory drive belt
[AD-D014640] N91-13716
PULSARS
Relativistic effects in millisecond pulsars and active galactic nuclei N91-14247
PULSE COMPRESSION
Ultra-high brightness (greater than 10(exp 21) W/sq cm) laser facility
[DE91-001685] N91-13698
PULSE DURATION
Computation of the current density in nonlinear materials subjected to large current pulses
[DE91-001950] N91-13624
PULSE GENERATORS
MPPE (Multiple Pulse Propagation Experiment) results
[DE91-001678] N91-13599
Computational and experimental progress on laser-activated gas avalanche switches for broadband, high-power electromagnetic pulse generation
[DE91-001763] N91-13623
PULSED LASERS
Ultra-high brightness (greater than 10(exp 21) W/sq cm) laser facility
[DE91-001685] N91-13698
Actinide speciation by photothermal spectroscopies: Instrumentation development
[DE91-001854] N91-13700
High pulse rate interferometry using a ruby laser and a Cordin model 360 camera
[DE91-001882] N91-13703
Ultrasound generation through a fiber optic delivery system using pulsed laser energy
[DE91-001914] N91-13970
PULSED RADIATION
MPPE (Multiple Pulse Propagation Experiment) results
[DE91-001678] N91-13599
PUMPS
Complete the development and construction of a spaceborne hydrogen maser clock
[NASA-CR-184043] N91-13688
PURIFICATION
Biosphere 2 test module experimentation program N91-13845
PURSUIT TRACKING
An indexed bibliography on tracking
[AD-A226682] N91-13870
PYROLYTIC GRAPHITE
Heat transfer device and method of making the same
[NASA-CASE-LEW-14162-1] N91-13668

Q

QUADRATIC EQUATIONS
On unconstrained conjugate gradient optimization methods and their interrelationships
[MATHS-REPT-A-129] N91-13919
QUALITY CONTROL
Measurement results of the FEL-TNO planar rectangular near field facility (1978-1989)
[FEL-89-B336] N91-13602
Quality of expert systems: Methods and techniques
[FEL-89-A267] N91-13747
Quality of expert systems: Algorithms for integrity control
[FEL-89-A312] N91-13748
Signal processing used in the electromagnetic inspection of long bodies
[CETIM-107270] N91-13749
The use of satellite data in the ECMWF analysis system
[KNMI-TR-123] N91-13790
Microbial ecology laboratory procedures manual NASA/MSFC
[NASA-CR-184033] N91-13856
Echocardiography in NATO aircrew
[AGARD-AR-297] N91-13863
The human factors of quality and QA in R and D environments
[DE91-001913] N91-13880

Coupling artificial intelligence and a system dynamics simulation to optimize quality assurance and testing in software development
[AD-A226580] N91-13902
Software management guidelines for automated measuring systems
[NPL-DES-99] N91-13926
QUANTUM CHROMODYNAMICS
Status of lattice field theory calculations
[DE91-001141] N91-14057
QUANTUM MECHANICS
New phases of D greater than or equal to 2 current and diffeomorphism algebras in particle physics
[DE91-001515] N91-14067
QUANTUM THEORY
Experimental studies of Josephson effect
[AD-A226548] N91-14051
QUANTUM WELLS
Design of GaAlAs/GaAs GRIN-SCH SQW diode lasers. Analysis of the temperature dependence
[LAAS-90277] N91-13708
Band-gap narrowing and III-V heterostructure FETs (Field-Effect Transistors)
[DE91-000401] N91-14056
QUASARS
Interpreting the convergence of Lyman series absorption lines N91-14225
Radio continuum observations of the quasar-galaxy pair 3C 232-NGC 3067 N91-14226
Probing the interstellar medium of external galaxies using quasar absorption lines: The 3C 232/NGC 3067 system N91-14227
Detection of a z=0.0515, 0.0522 absorption system in the QSO S4 0248+430 due to an intervening galaxy N91-14228
Non-steller light from high-redshift radiogalaxies N91-14238

R

RADAR CROSS SECTIONS
Resonance region scattering
[AD-A226536] N91-13589
RADAR DATA
Pipeline synthetic aperture radar data compression utilizing systolic binary tree-searched architecture for vector quantization
[NASA-CASE-NPO-17941-1-CU] N91-13595
RADAR IMAGERY
Method for providing a polarization filter for processing synthetic aperture radar image data
[NASA-CASE-NPO-17904-1-CU] N91-13594
The importance of fracturing in the Pimenta Bueno-Ro Basin structure: A study of the morphostructural elements of the rupture-ductile character through remote sensing techniques and products
[INPE-5004-TDL/398] N91-13825
RADAR SIGNATURES
BSB radar pulse classification
[FEL-90-B023] N91-13603
RADAR TARGETS
Observation with stand-off radars
[FEL-90-A022] N91-13606
RADIAL DISTRIBUTION
A scaling law of radial gas distribution in disk galaxies N91-14106
The FCRAO extragalactic CO survey: Global properties of galaxies N91-14117
A comparison of the radial distribution of molecular gas and non-thermal radio continuum in spiral disks N91-14145
Global and radial variations in the efficiency of massive star formation among galaxies N91-14215
RADIANT FLUX DENSITY
Feasibility of cosmic-ray muon intensity measurements for tunnel detection
[AD-A223355] N91-14266
RADIATION ABSORPTION
Carbon dioxide reforming of methane in a solar volume-TRIC receiver-reactor: The CAESAR (Catalytically Enhanced Solar Absorption Receiver) project
[DE91-002340] N91-13800
A critical review of charged particle astronomy at Saturn: The evidence for co-orbiting material in the inner satellite system
[NASA-CR-187348] N91-14090
Infrared analysis of LMC superbubbles N91-14181
RADIATION COUNTERS
Elementary particle interactions
[DE91-001220] N91-13979
RADIATION DAMAGE
Operation of silicon microstrip detectors in a high radiation environment
[DE91-001953] N91-13682
RADIATION DETECTORS
Development of mercuric iodide uncooled x ray detectors and spectrometers
[NASA-CR-185394] N91-13484
X ray and charged particle detection with CsI(Tl) layer coupled to a-Si:H photodiode layers
[DE91-001798] N91-14060
Performance of multiplexed Ge:Ga detector arrays in the far infrared
[NASA-TM-102275] N91-14087
Feasibility of cosmic-ray muon intensity measurements for tunnel detection
[AD-A223355] N91-14266
RADIATION DISTRIBUTION
The extragalactic radiation field and sharp edges to HI disks in galaxies N91-14101
High spatial resolution 100 micron observations of the M83 bar N91-14130
Evidence against a simple two-component model for the far-infrared emission from galaxies N91-14136
Emission from small dust particles in diffuse and molecular cloud medium N91-14137
Very small grains in the Milky Way and external galaxies N91-14138
A model for the infrared emission from an OB star cluster environment N91-14139
Far-infrared emission from dusty ellipticals N91-14142
A relationship between the integrated CO intensity and the radio continuum emission in spiral galaxies N91-14146
Large scale excitation of the ISM in NGC 1068 N91-14150
Hot interstellar gas and ionization of embedded clouds N91-14161
Infrared analysis of LMC superbubbles N91-14181
Ionization in the local interstellar and intergalactic media N91-14249
RADIATION DOSAGE
Thermoregulatory consequences of resonant microwave exposure
[AD-A226540] N91-13864
A computer model to determine the primary contributors to relative radiation dose received by astronauts
[DE90-015681] N91-13866
Review of uncertainties in the use of NPL primary standards of x ray exposure for the calibration of secondary standards in terms of exposure and air kerma
[NPL-RS(EXT)-109] N91-13868
Total-dose radiation effects data for semiconductor devices (1989 supplement)
[NASA-CR-187431] N91-14049
Space radiation dose analysis for solar flare of August 1989
[NASA-TM-4229] N91-14265
RADIATION EFFECTS
Radiation effects on JFETs (Junction Field-Effect Transistors), MOSFETs, and dipolar transistors, as related to SSC circuit design
[DE91-001486] N91-13618
Thermoregulatory consequences of resonant microwave exposure
[AD-A226540] N91-13864
Multiplexer/amplifier test results for SP-100
[DE91-004504] N91-13990
Total-dose radiation effects data for semiconductor devices (1989 supplement)
[NASA-CR-187431] N91-14049
RADIATION HARDENING
Single event upset hardening techniques
[DE91-002337] N91-13625
Multiplexer/amplifier test results for SP-100
[DE91-004504] N91-13990
RADIATION MEASUREMENT
A preliminary ocean ARM (Atmospheric Radiation Measurements) guide for climatic evaluations
[DE91-001120] N91-13811
RADIATION PROTECTION
Review of uncertainties in the use of NPL primary standards of x ray exposure for the calibration of secondary standards in terms of exposure and air kerma
[NPL-RS(EXT)-109] N91-13868
RADIATION PYROMETERS
Evaluation of Raytek infrared pyrometer for continuous propellant temperature measurement
[NASA-CR-184040] N91-13570
RADIATION SHIELDING
Space radiation dose analysis for solar flare of August 1989
[NASA-TM-4229] N91-14265
RADIATION SOURCES
Experimental studies of Josephson effect
[AD-A226548] N91-14051
Variable magnification glancing incidence x ray telescope
[NASA-CASE-MFS-28013-2] N91-14096
RADIATION THERAPY
Review of uncertainties in the use of NPL primary standards of x ray exposure for the calibration of secondary standards in terms of exposure and air kerma
[NPL-RS(EXT)-109] N91-13868
RADIATION TOLERANCE
Total-dose radiation effects data for semiconductor devices (1989 supplement)
[NASA-CR-187431] N91-14049
RADIATIVE TRANSFER
Tropical Pacific moisture variability: Its detection, synoptic structure and consequences in the general circulation
[NASA-CR-184045] N91-13832
A study of active regions on RS CVn stars N91-14092
Very small grains in the Milky Way and external galaxies N91-14138
A model for the infrared emission from an OB star cluster environment N91-14139
RADIO ASTRONOMY
Restoration of solar radio images: Evaluation of poor conditions and resolution by regularization techniques
[INPE-4557-PRE/1298] N91-13587
The Interstellar Medium in External Galaxies: Summaries of contributed papers
[NASA-CP-3084] N91-14100
The FCRAO extragalactic CO survey: Global properties of galaxies N91-14117
The CO-12 and CO-13 J=2-1 and J=1-0 observations of hot and cold galaxies N91-14126
CS J = 2 yields 1 emission toward the central region of M82 N91-14128
High angular resolution mm- and submm-observations of dense molecular gas in M82 N91-14230
RADIO EMISSION
The Interstellar Medium in External Galaxies: Summaries of contributed papers
[NASA-CP-3084] N91-14100
The hot and cold interstellar matter of early type galaxies and their radio emission N91-14112
A survey of galaxies in CO N91-14118
Observations of CO in the Magellanic irregular galaxy NGC 55 N91-14124
The CO-12 and CO-13 J=2-1 and J=1-0 observations of hot and cold galaxies N91-14126
A comparison of the radial distribution of molecular gas and non-thermal radio continuum in spiral disks N91-14145
A relationship between the integrated CO intensity and the radio continuum emission in spiral galaxies N91-14146
Radio continuum and far-infrared emission of spiral galaxies: Implications of correlations N91-14147
Supernova remnants and diffuse ionized gas in M31 N91-14179
Star formation on the leading edge of a ring-like density wave in Arp 143 N91-14196
A multi-wavelength study of the peculiar galaxy NGC 2976 N91-14199
M51: Molecular spiral arms, GMAs and superclouds N91-14204
Central star formation in S0 galaxies N91-14223
Radio continuum observations of the quasar-galaxy pair 3C 232-NGC 3067 N91-14226
Molecular outflows in the L1641 region of Orion N91-14246
Centimeter emission variation of Venus: Its second phase
[INPE-5122-TDL/423] N91-14257
RADIO FREQUENCIES
Folded RF-excited CO2 waveguide lasers N91-13695
A linear accelerator in the space: The beam experiment aboard rocket
[DE91-002347] N91-13988
RADIO GALAXIES
The environments of double radiogalaxies N91-14166
Origin and dynamics of emission line clouds in cooling flow environments N91-14167
ISM stripping from cluster galaxies and inhomogeneities in cooling flows N91-14172
An infrared jet in Centaurus A (NGC 5128): Evidence for interaction between the active nucleus and the interstellar medium N91-14175
Non-steller light from high-redshift radiogalaxies N91-14238
An imaging and spectroscopic study of low and intermediate power radio galaxies N91-14268
RADIO JETS (ASTRONOMY)
ISM stripping from cluster galaxies and inhomogeneities in cooling flows N91-14172
An infrared jet in Centaurus A (NGC 5128): Evidence for interaction between the active nucleus and the interstellar medium N91-14175

RADIO OBSERVATION
Radio observations of several interstellar molecules N91-14093
Radio continuum observations of the quasar-galaxy pair 3C 232-NGC 3067 N91-14226
RADIO OCCULTATION
Pioneer-Venus radio occultation (ORO) data reduction: Profiles of 13 cm absorptivity
[NASA-CR-186986] N91-13584
RADIO PHYSICS
Supernova remnants and diffuse ionized gas in M31 N91-14179
RADIO SOURCES (ASTRONOMY)
Multiband observations of Cygnus A: A study of pressure balance in the core of a powerful radio galaxy N91-14151
The environments of double radiogalaxies N91-14166
RADIO STARS
The hot and cold interstellar matter of early type galaxies and their radio emission N91-14112
RADIOACTIVE DECAY
Operation of silicon microstrip detectors in a high radiation environment
[DE91-001953] N91-13682
Prospects of CsJ(Tl)-photodiode detectors for low level spectroscopy
[MPI-PAE/EXP.EL-228] N91-13984
RADIOACTIVE ISOTOPES
Proceedings of a Workshop on Cosmogenic Nuclide Production Rates
[NASA-CR-185349] N91-14098
RADIOACTIVE WASTES
Materials impurity analysis by means of nuclear resonance reactions
[DE91-001758] N91-13520
RAMAN SPECTRA
Progress of research on water vapor lidar
[NASA-CR-187673] N91-13837
Stimulated Raman scatter from laser-produced plasmas: Merely nonlinear or also chaotic
[DE91-001742] N91-14007
RAMAN SPECTROSCOPY
Measurement of air entrainment in plasma jets
[DE91-001943] N91-14013
RANDOM ACCESS MEMORY
Design of integrated CMOS circuits for parallel detection and storage of optical data
[AD-A225702] N91-13611
M-dimensional computer memory with M-1 dimensional hyperplane access
[AD-D014615] N91-13886
RANDOM NOISE
Direct modeling of white noise in stochastic systems
[MEMO-865] N91-13964
RANDOM PROCESSES
Field error lottery
[DE91-001875] N91-13702
RANDOM VIBRATION
Some observations on the Houbolt-Rainey and peak-hold methods of flutter onset prediction
[NASA-TM-102745] N91-13411
RANKINE CYCLE
Second law analysis of advanced power generation systems using variable temperature heat sources
[DE91-001818] N91-13799
RARE EARTH ELEMENTS
Optical characterization techniques applied to ceramic oxides
[DE91-001526] N91-13556
Performance comparison of magnetic refrigeration cycles
[DE91-001520] N91-13578
Theoretical temperature-dependent branching ratios and laser thresholds of the (5)I7 yields (5)I8 levels of Ho3(+) in ten garnets
[NASA-TM-103429] N91-14053
RARE GASES
Proceedings of a Workshop on Cosmogenic Nuclide Production Rates
[NASA-CR-185349] N91-14098
REACTION KINETICS
Study of improved methods for predicting chemical equilibria
[DE91-000263] N91-13509
Publications, patents, presentations, honors, and students report. Kinetics of semiconductor processing chemistry: SiGe and GaAs growth on silicon surfaces
[AD-A226639] N91-13514
Electrocatalysis of anodic oxygen-transfer reactions at modified lead dioxide electrodes
[DE91-000664] N91-13518
Oxidation characteristics of Ti-25Al-10Nb-3V-1Mo intermetallic alloy
[NASA-TP-3044] N91-13522
Variational transition state theory
[DE91-001253] N91-14058
Aperture synthesis CO observations of the inner disk of NGC 1068 N91-14122
Kinetics of hydrogen release from lunar soil
[NASA-CR-187363] N91-14256
REACTOR DESIGN
Tightly coupled simulation utilizing the EBR-II LMR: A real-time supercomputing and AI environment
[DE91-001942] N91-13932
HYLIFE-2 inertial confinement fusion reactor design
[DE91-000792] N91-14004
REACTOR MATERIALS
Mechanical properties of 1950's vintage Type 304 stainless steel weldment components
[DE91-004328] N91-13774
Modeling and analysis of surface roughness effects on sputtering, reflection, and sputtered particle transport
[DE91-004429] N91-14028
REACTOR PHYSICS
International Thermonuclear Experimental Reactor physics basis
[DE91-002646] N91-14017
REACTOR SAFETY
The behavior of fission products during nuclear rocket reactor tests
[DE91-001956] N91-13490
HYLIFE-2 inertial confinement fusion reactor design
[DE91-000792] N91-14004
READ-ONLY MEMORY DEVICES
Design of integrated CMOS circuits for parallel detection and storage of optical data
[AD-A225702] N91-13611
REAL TIME OPERATION
Micro based technology: A new tool for missile guidance system design and visualization N91-13440
An AD100 implementation of a real-time STOVL aircraft propulsion system
[NASA-TM-103683] N91-13457
Restoration of solar radio images: Evaluation of poor conditions and resolution by regularization techniques
[INPE-4557-PRE/1298] N91-13587
Real-time data compression of broadcast video signals
[NASA-CASE-LEW-14945-1] N91-13598
Predictive sensor method and apparatus
[NASA-CASE-SSC-00006-1] N91-13691
Real-time dynamic holographic image storage device
[NASA-CASE-LAR-13989-1] N91-13694
Programmable remapper with single flow architecture
[NASA-CASE-MSC-21481-1] N91-13890
NDRE/TAII processor architecture study
[FFI-90/7012] N91-13891
Research into software executives for space operations support
[NASA-CR-187013] N91-13895
Knowledge representation into Ada parallel processing
[NASA-CR-187451] N91-13934
Optical joint correlation for real-time tracking
[NASA-CASE-MSC-21509-1] N91-13997
A real-time digital control, data acquisition and analysis system for the DIII-D multipulse Thomson scattering diagnostic
[DE91-002720] N91-14025
RECOMBINATION REACTIONS
High spatial and temporal resolution visible spectroscopy of the plasma edge in DIII-D
[DE91-002718] N91-14023
RECOMMENDATIONS
Software management guidelines for automated measuring systems
[NPL-DES-99] N91-13926
RECONNAISSANCE
Architecture for electronic imagery interoperability
[AD-A226522] N91-13901
RECTANGULAR WAVEGUIDES
A complex permittivity and permeability measurement system for elevated temperatures
[NASA-CR-186916] N91-13609
RED SHIFT
The large-scale space distribution of emission-line galaxies N91-14091
Clues to galaxy activity from rich cluster simulations N91-14222
Detection of a z=0.0515, 0.0522 absorption system in the QSO S4 0248+430 due to an intervening galaxy N91-14228
Non-steller light from high-redshift radiogalaxies N91-14238
REDUCED GRAVITY
Microgravity strategic plan, 1990
[NASA-TM-103448] N91-13575
REENTRY VEHICLES
Effect of bulk viscosity in low density, hypersonic blunt body flows
[DE90-012756] N91-13419
REFLECTANCE
Cloud properties as deduced from satellite observation
[NASA-CR-182851] N91-13833
REFLECTION
Modeling and analysis of surface roughness effects on sputtering, reflection, and sputtered particle transport
[DE91-004429] N91-14028
REFLECTION NEBULAE
Very small grains in the Milky Way and external galaxies N91-14138
REFLECTORS
Analytical and photogrammetric characterization of a planar tetrahedral truss
[NASA-TM-4231] N91-13473
REFRIGERATING
Performance comparison of magnetic refrigeration cycles
[DE91-001520] N91-13578
REFRIGERATORS
Superfluid Stirling refrigerator: A new method for cooling below 1 Kelvin
[DE91-002311] N91-13582
Miniature closed cycle refrigerators N91-14035
REGENERATION (ENGINEERING)
The NASA CELSS program N91-13848
REGENERATION (PHYSIOLOGY)
Biological Life Support Technologies: Commercial Opportunities
[NASA-CP-3094] N91-13842
REGRESSION ANALYSIS
Evaluation of a wind profile model
[FOA-E-40045-4.5] N91-13839
REINFORCED PLASTICS
Development of standards for advanced polymer matrix composites: A BPF/ACG overview
[NPL-DMM(A)-8] N91-13568
REINFORCED PLATES
Damage assessment and residual compression strength of thick composite plates with through-the-thickness reinforcements
[NASA-CR-187377] N91-13494
REINFORCING FIBERS
Damage assessment and residual compression strength of thick composite plates with through-the-thickness reinforcements
[NASA-CR-187377] N91-13494
Research and development of a ceramic fiber composite heat exchanger
[DE90-017250] N91-13497
RELATIVISTIC EFFECTS
Experimental studies of Josephson effect
[AD-A226548] N91-14051
Relativistic effects in millisecond pulsars and active galactic nuclei N91-14247
RELATIVISTIC ELECTRON BEAMS
NRL compact accelerator theory studies
[AD-A226537] N91-14005
RELATIVISTIC PARTICLES
Inclusive inelastic scattering of heavy ions and nuclear correlations
[NASA-TP-3026] N91-13985
RELATIVISTIC PLASMAS
An infrared jet in Centaurus A (NGC 5128): Evidence for interaction between the active nucleus and the interstellar medium N91-14175
RELATIVITY
Measuring the Lense-Thirring precession using a second Lageos satellite
[NASA-CR-186945] N91-13470
RELIABILITY
Design reliability engineering
[DE91-001949] N91-13744
RELIABILITY ANALYSIS
Software reliability through fault-avoidance and fault-tolerance
[NASA-CR-187646] N91-13904
RELIABILITY ENGINEERING
Design reliability engineering
[DE91-001949] N91-13744
Security for safety critical space borne systems
[NASA-CR-187656] N91-13906
REMOTE CONTROL
Telerobotic on-orbit remote fluid resupply system
[NASA-CR-184052] N91-13474
REMOTE MANIPULATOR SYSTEM
Telerobotic on-orbit remote fluid resupply system
[NASA-CR-184052] N91-13474
Standard remote manipulator system docking target augmentation for automated docking
[NASA-CASE-MFS-28419-1] N91-13482
REMOTE SENSING
Laser-induced fluorescence of phosphors for remote cryogenic thermometry
[DE91-001733] N91-13681

The relation between tree physiology and multispectral and color photography: First phase
[BCRS-89-39] N91-13785

REMOVAL
Environmental projects. Volume 12: Friable asbestos abatement, GDSCC
[NASA-CR-187636] N91-13808

REQUIREMENTS
Definition study into the requirements of a data modem for the SYSCOM network
[FEL-90-A116] N91-13892

RESEARCH AND DEVELOPMENT
Civil tiltrotor missions and applications
[NASA-CR-177452] N91-13424
JANNAF liquid rocket combustion instability panel research recommendations
[NASA-TM-103653] N91-13491
Microgravity strategic plan, 1990
[NASA-TM-103448] N91-13575
Overview of European technology in computers, telecommunications, and electronics
[PB90-215773] N91-13610
Computational fluid dynamics
[NASA-TM-101197] N91-13637
JPRS Report: Science and technology. USSR: Life sciences
[JPRS-ULS-89-011] N91-13861
The human factors of quality and QA in R and D environments
[DE91-001913] N91-13880
Experimental development, testing, and research work in support of the inertial confinement fusion program
[DE91-002770] N91-14026
Non-empirical interatomic potentials for transition metals, alloys, and semiconductors
[DE91-002396] N91-14062

RESEARCH FACILITIES
Activities report of the Max-Planck Institute for Aeronomy
[ETN-91-98383] N91-14272

RESEARCH MANAGEMENT
Summaries of physical research in the geosciences
[DE91-001043] N91-13779

RESEARCH PROJECTS
JANNAF liquid rocket combustion instability panel research recommendations
[NASA-TM-103653] N91-13491
Summaries of physical research in the geosciences
[DE91-001043] N91-13779
High energy physics program at Texas A&M University
[DE91-001639] N91-13989
Activities report of the Max-Planck Institute for Aeronomy
[ETN-91-98383] N91-14272

RESEARCH VEHICLES
Analytical aerodynamic model of a high alpha research vehicle wind-tunnel model
[NASA-CR-187362] N91-13404

RESERVOIRS
Water cooled static pressure probe
[NASA-CASE-LAR-14340-1-CU] N91-13684

RESIDUAL GAS
Signal processing development
[AD-A226593] N91-14052
Star formation in proto dwarf galaxies N91-14212

RESIDUAL STRESS
Large-eddy simulation of transitional channel flow
[NASA-CR-187465] N91-13410
Method and apparatus for characterizing residual stress in ferromagnetic materials
[NASA-CASE-LAR-14239-1] N91-13527
Residual stresses in ceramics
[JUEL-SPEZ-550] N91-13536
Use of neutron diffraction methods for the determination of mechanical stresses in metal ceramic laminated composite materials N91-13537
Determination of residual stresses in ceramics materials using neutron diffraction N91-13538
Residual stresses analyses in ceramics and metal ceramic composites using x ray methods N91-13539
Influence of materials structure and production method of Al2O3 ceramic on the x-ray stress measurement N91-13540
X ray measurements of residual stresses in thin, hard layers N91-13542
Development and computer aided residual stress measurements on coated specimen using blind-hole drilling technique N91-13544
Residual stresses in Al2O3: Comparison between electromechanical measurements and finite element method calculations N91-13545
Possibilities of the calculation of stresses and residual stresses in materials with a phase transformation N91-13548
Calculations of residual stresses in ceramic soldered joints N91-13549
Finite element and boundary element methods for elastoplastic stress analysis of two-dimensional and axisymmetric problems N91-13755

RESINS
Novel polyimide molding powder, coating, adhesive, and matrix resin
[NASA-CASE-LAR-14163-1] N91-13559

RESONANCE
Materials impurity analysis by means of nuclear resonance reactions
[DE91-001758] N91-13520

RESONANCE SCATTERING
Resonance region scattering
[AD-A226536] N91-13589

RESONANT FREQUENCIES
FE analyses of aircraft model with interior trim
[FFA-TN-1990-21] N91-13417
Distortion-free x ray mask technology
[AD-A226524] N91-13993

RESOURCES MANAGEMENT
Managing the Global Commons Decision Making and Conflict Resolution in Response to Climate Change Research Workshop
[DE91-001018] N91-13810

RESPONSE TIME (COMPUTERS)
Operation of inductively coupled plasma source mass spectrometers in the peak jumping mode
[DE91-001766] N91-13689

RETINA
Portable dynamic fundus instrument
[NASA-CASE-MSC-21675-1] N91-13865

RETINAL IMAGES
Modelling the effects of vibration on visual performance
[ISVR-TR-171] N91-13883

RETURN TO EARTH SPACE FLIGHT
Assured crew return vehicle
[NASA-CASE-MSC-21536-1] N91-13483

REVERSE FIELD PINCH
Confinement and heating studies of field-reversed configurations
[DE91-001965] N91-14008
Kinetic and electromagnetic transport processes in toroidal devices
[DE91-001901] N91-14011
Two-fluid simulations of the reversed-field pinch
[DE91-001961] N91-14014
Confinement properties of the RFP (reversed field pinch)
[DE91-002322] N91-14015

REYNOLDS STRESS
Reynolds stress closure in jet flows using wave models
[NASA-CR-185717] N91-13640

RHODAMINE
Progress in the detection of single molecules in levitated droplets
[DE91-000612] N91-13517

RIBLETS
Polymer/riblet combination for hydrodynamic skin friction reduction
[NASA-CASE-LAR-14271-1-CU] N91-13558

RIBS (SUPPORTS)
The effect of longitudinal spacer ribs on the minimum pressure drop in a heated annulus
[DE91-000784] N91-13655

RING GALAXIES
Star formation on the leading edge of a ring-like density wave in Arp 143 N91-14198

RISK
Hazard studies for solid propellant rocket motors
[AGARD-AG-316] N91-13488

ROBOT ARMS
Robot cable-compliant devices
[NASA-CASE-GSC-13127-1] N91-13735
Robust deterministic control for robotic manipulators N91-13937

ROBOT CONTROL
The effect of inertial coupling in the dynamics and control of flexible robotic manipulators
[NASA-CR-187679] N91-13721
Dynamic modeling, property investigation, and adaptive controller design of serial robotic manipulators modeled with structural compliance
[NASA-CR-187678] N91-13722
Bilevel shared control for teleoperators
[NASA-CASE-NPO-17800-1-CU] N91-13724
Positional estimation techniques for an autonomous mobile robot
[NASA-CR-187689] N91-13725
Modeling and control of a redundant robot manipulator composed of several Stewart platforms
[LAAS-90146] N91-13728
Robot deterministic control for robotic manipulators N91-13937

ROBOT DYNAMICS
The effect of inertial coupling in the dynamics and control of flexible robotic manipulators
[NASA-CR-187679] N91-13721
Dynamic modeling, property investigation, and adaptive controller design of serial robotic manipulators modeled with structural compliance
[NASA-CR-187678] N91-13722
Robot cable-compliant devices
[NASA-CASE-GSC-13127-1] N91-13735

ROBOTICS
An application of multiattribute decision analysis to the Space Station Freedom program. Case study: Automation and robotics technology evaluation
[NASA-CR-187432] N91-13476
Dynamic modeling, property investigation, and adaptive controller design of serial robotic manipulators modeled with structural compliance
[NASA-CR-187678] N91-13722
Positional estimation techniques for an autonomous mobile robot
[NASA-CR-187689] N91-13725
Modeling and control of a redundant robot manipulator composed of several Stewart platforms
[LAAS-90146] N91-13728
Robot cable-compliant devices
[NASA-CASE-GSC-13127-1] N91-13735

ROBOTS
Bilevel shared control for teleoperators
[NASA-CASE-NPO-17800-1-CU] N91-13724
Positional estimation techniques for an autonomous mobile robot
[NASA-CR-187689] N91-13725
Modeling and control of a redundant robot manipulator composed of several Stewart platforms
[LAAS-90146] N91-13728
Robust deterministic control for robotic manipulators N91-13937

ROBUSTNESS (MATHEMATICS)
Robust variable structure control of model reference systems
[MATHS-REPT-A-131] N91-13947
On hyperplane design techniques for discrete-time variable structure control systems
[MATHS-REPT-A-133] N91-13948

ROCKET ENGINE DESIGN
Thrust chamber modeling using Navier-Stokes equations: Code documentation and listings, volume 2
[NASA-CR-183617] N91-13489

ROCKET ENGINES
Integrated launch and emergency vehicle system
[NASA-CASE-LAR-13780-1] N91-13481

ROCKET EXHAUST
Characterization of rocket propellant combustion products: Description of sampling and analysis methods for rocket exhaust characterization studies
[DE91-002536] N91-13574

ROCKET FLIGHT
Observations of the galactic plane by the zodiacal infrared project N91-14143

ROCKET PROPELLANTS
Characterization of rocket propellant combustion products: Description of sampling and analysis methods for rocket exhaust characterization studies
[DE91-002536] N91-13574

RODS
A computational procedure for the dynamics of flexible beams within multibody systems
[NASA-CR-187667] N91-13760

ROLL
The Improved Three Axis Test Table (ITATT): Program status and recommendation for completion
[AD-A226508] N91-13712

ROLLER BEARINGS
Non-linear dynamic analysis of geared systems
[NASA-CR-4338] N91-13737

ROLLING
Device for applying constant pressure to a surface
[NASA-CASE-GSC-13230-1] N91-13734

ROOTS OF EQUATIONS
On the invertibility of Leslie systems
[REPT-90-006] N91-13963

ROTARY WING AIRCRAFT
Periodic trim solutions with hp-version finite elements in time
[NASA-CR-187705] N91-13449
General Rotorcraft Aeromechanical Stability Program (GRASP): Theory manual
[NASA-TM-102255] N91-13762

ROTATING CYLINDERS
Fluid flow effects on electroplating
[DE91-001087] N91-13577

ROTATING DISKS
Fluid flow effects on electroplating
[DE91-001087] N91-13577

Observations of extended and counterrotating disks of ionized gas in S0 galaxies N91-14187
ROTATING MIRRORS
Design of a mechanical modulator for the planetary Fourier spectrometer experiment of the MARS 94 mission
[IFSI-89-22] N91-13717
ROTATING SPHERES
Fluid flow effects on electroplating
[DE91-001087] N91-13577
ROTATION
Spanwise aerodynamic loads on a rotating wind turbine blade
[DE91-002101] N91-13414
Cantilever clamp fitting
[NASA-CASE-MFS-28328-1] N91-13731
Superconducting Josephson Junction Gyroscope (JJG) N91-14043
NGC 1058: Gas motions in an extended, quiescent spiral disk N91-14103
Evolution of magnetized, rotating, isothermal clouds N91-14191
ROTOR AERODYNAMICS
Development of a full potential solver for rotor aerodynamics analysis N91-13407
Analytic formulations of unsteady profile aerodynamics and its application to simulation of rotors
[DLR-FB-90-28] N91-13415
A review of ice accretion data from a model rotor icing test and comparison with theory
[NASA-TM-103712] N91-13421
ROTOR BLADES (TURBOMACHINERY)
Analytic formulations of unsteady profile aerodynamics and its application to simulation of rotors
[DLR-FB-90-28] N91-13415
ROTORS
Development of a full potential solver for rotor aerodynamics analysis N91-13407
A review of ice accretion data from a model rotor icing test and comparison with theory
[NASA-TM-103712] N91-13421
Material degradation of steam turbine rotors in long term operations
[VTT-RR-692] N91-13530
RUBY LASERS
High pulse rate interferometry using a ruby laser and a Cordin model 360 camera
[DE91-001882] N91-13703
RUN TIME (COMPUTERS)
CESAR trap program library
[FFI-90/7023] N91-13924
RUNGE-KUTTA METHOD
Numerical methods for boundary value problems in differential-algebraic equations
[DE91-001748] N91-13956
RUNWAYS
Literature review on geotextiles to improve pavements for general aviation airports
[DOT/FAA/RD-90/26] N91-13464

S

SAFETY DEVICES
Tethering sockets and wrenches
[NASA-CR-184032] N91-13675
SAFETY FACTORS
Hazard studies for solid propellant rocket motors
[AGARD-AG-316] N91-13488
SAMPLING
Microbial ecology laboratory procedures manual NASA/MSFC
[NASA-CR-184033] N91-13856
Biofilm monitoring coupon system
[NASA-CASE-MSC-21585-1] N91-13857
Ground-based studies of emission-line variability: Recent results for NGC 5548 and future plans
[NASA-CR-180433] N91-14088
SAPPHIRE
An interactive program for the analysis and design of advanced laser targets
[DE91-002542] N91-13704
SATELLITE IMAGERY
S-band diplexer for a telecommunication board transponder
[INPE-4540-PRE/1286] N91-13586
Methodological contribution utilizing TM/LANDSAT-5 imagery in geologic mapping of regions with significant vegetative cover
[INPE-5117-TDL/419] N91-13784
Sweeping-vector conversion for polygonal data
[INPE-4558-PRE/1299] N91-14077
SATELLITE OBSERVATION
The use of satellite data in the ECMWF analysis system
[KNMI-TR-123] N91-13790
SATELLITE-BORNE INSTRUMENTS
Gradiometry coexperiments to the gravity probe B and step missions
[NASA-CR-187704] N91-13788
SATURN ATMOSPHERE
A critical review of charged particle astronomy at Saturn: The evidence for co-orbiting material in the inner satellite system
[NASA-CR-187348] N91-14090
SCALARS
Regularized Chapman-Enskog expansion for scalar conservation laws
[NASA-CR-187441] N91-13966
SCALING LAWS
A scaling law of radial gas distribution in disk galaxies N91-14106
SCATTERING
Influence of collective effects on the performance of high-luminosity colliders
[DE91-001797] N91-13982
The diffuse ionized interstellar medium perpendicular to the plane of NGC 891 N91-14160
SCAVENGING
Complete the development and construction of a spaceborne hydrogen maser clock
[NASA-CR-184043] N91-13688
SCHEDULING
Knowledge representation into Ada parallel processing
[NASA-CR-187451] N91-13934
Applications of artificial intelligence to mission planning
[NASA-CR-184994] N91-13939
SCIENTISTS
Technical communications in aerospace: An analysis of the practices reported by US and European aerospace engineers and scientists
[NASA-TM-103441] N91-14079
SEA ICE
Sea ice-atmosphere interaction: Application of multispectral satellite data in polar surface energy flux estimates
[NASA-CR-187376] N91-13782
SEA ROUGHNESS
Description of sea wave motion and its influence on the altitude control of sea skimming missiles
[FEL-89-A368] N91-13450
SEALING
Cantilever clamp fitting
[NASA-CASE-MFS-28328-1] N91-13731
Probe insertion apparatus with inflatable seal
[NASA-CASE-LEW-14965-1] N91-13732
SEALS (STOPPERS)
Thermal and structural assessments of a ceramic wafer seal in hypersonic engines
[NASA-TM-103651] N91-13456
SEATS
Hydraulic lifting device
[NASA-CASE-SSC-00008-1] N91-13733
Effects of anthropometric and postural variables on the transmission of whole-body vertical vibration from seat-to-head
[ISVR-TR-172] N91-13884
SEDIMENTS
The importance of fracturing in the Pimenta Bueno-Ro Basin structure: A study of the morphostructural elements of the rupture-ductile character through remote sensing techniques and products
[INPE-5004-TDL/398] N91-13825
Three-dimensional cell to tissue assembly process
[NASA-CASE-MSC-21559-1] N91-13860
Exobiology site selection for future Mars missions: Martian paleolake sediments and terrestrial analogs
[NASA-CR-187358] N91-14255
SEISMIC WAVES
Comparison of spectral estimators application to ground sensor signals
[FEL-1988-85] N91-13605
SEISMOLOGY
Summaries of physical research in the geosciences
[DE91-001043] N91-13779
Fractals and chaotic dynamics in tectonics: Applications to topography and seismicity N91-13821
SEMANTICS
Semantic validation of structured theories: Applications to a generic programming language
[ETN-91-98207] N91-13916
SEMICONDUCTOR DEVICES
Total-dose radiation effects data for semiconductor devices (1989 supplement)
[NASA-CR-187431] N91-14049
SEMICONDUCTOR DIODES
Design of GaAlAs/GaAs GRIN-SCH SQW diode lasers. Analysis of the temperature dependence
[LAAS-90277] N91-13708
Method of fabricating germanium and gallium arsenide devices
[NASA-CASE-GSC-13265-1] N91-14066
SEMICONDUCTOR LASERS
Study and development of tunable, single mode AlGaAs/GaAs lasers
[DE91-001684] N91-13697
Design of GaAlAs/GaAs GRIN-SCH SQW diode lasers. Analysis of the temperature dependence
[LAAS-90277] N91-13708
Subnanosecond, high voltage photoconductive switching in GaAs
[DE91-002671] N91-14063
SEMICONDUCTORS (MATERIALS)
Publications, patents, presentations, honors, and students report. Kinetics of semiconductor processing chemistry: SiGe and GaAs growth on silicon surfaces
[AD-A226639] N91-13514
Magnetic field effect transistors
[AD-A226535] N91-13614
Ultrafast optical electronics center
[AD-A226669] N91-14054
Non-empirical interatomic potentials for transition metals, alloys, and semiconductors
[DE91-002396] N91-14062
SENSORIMOTOR PERFORMANCE
Time-sharing performance as a factor for success in flight training: Test development and validation
[IZF-1989-58] N91-13872
SENSORS
Superconducting neural network computer and sensor array
[AD-D014625] N91-13887
SEPAC (PAYLOAD)
SEPAC data analysis in support of the environmental interaction program
[NASA-CR-184028] N91-13807
SEPARATED FLOW
A steadying effect of acoustic excitation on transitory stall
[NASA-TM-103689] N91-13420
SEQUENCING
Fractals and chaotic dynamics in tectonics: Applications to topography and seismicity N91-13821
SEQUENTIAL CONTROL
Success with an automated computer control system
[DE91-001759] N91-13945
SERIES EXPANSION
An asymptotic symmetry of the rapidly forced pendulum
[DE91-001868] N91-13958
SERVICE LIFE
Coordinates of a life-cycle model for a software system and communicating the need for software technology
[AD-A226592] N91-13903
SET THEORY
New techniques for the union-find problem
[RUU-CS-89-12] N91-13954
SEYFERT GALAXIES
Circumnuclear molecular gas in starburst and Seyfert galaxies N91-14120
High resolution CO images of Seyfert Galaxies N91-14121
Large scale excitation of the ISM in NGC 1068 N91-14150
H2 line emission in three Seyfert nuclei: Evidence against UV-excitation N91-14185
SHAFTS (MACHINE ELEMENTS)
Sheave assembly
[AD-D014605] N91-13711
SHAPE MEMORY ALLOYS
Heat engine with corrugated shape memory drive belt
[AD-D014640] N91-13716
SHEAR FLOW
Analysis of the leading edge effects on the boundary layer transition
[NASA-CR-187361] N91-13405
SHEAR STRENGTH
Relationship between voids and interlaminar shear strength of polymer matrix composites
[NASA-TM-103643] N91-13495
SHEAR STRESS
Calibration set up for load cells
[PD-ST-8917] N91-13673
Three-dimensional cell to tissue assembly process
[NASA-CASE-MSC-21559-1] N91-13860
SHOCK TESTS
Shock tunnel studies of scramjet phenomena, supplement 5
[NASA-CR-182096-SUPPL-5] N91-13651
SHOCK TUBES
Shock tunnel studies of scramjet phenomena, supplement 5
[NASA-CR-182096-SUPPL-5] N91-13651

A quiet flow Ludwieg tube for study of transition in compressible boundary layers: Design and feasibility
[NASA-CR-187374] N91-13676

SHOCK TUNNELS
Flow establishment in a generic scramjet combustor
[NASA-CR-187467] N91-13649
Shock tunnel studies of scramjet phenomena, supplement 5
[NASA-CR-182096-SUPPL-5] N91-13651

SHOCK WAVES
Instability of a supersonic shock free elliptic jet
[NASA-TM-103428] N91-13413
All hot spots are not equal
[DE91-002303] N91-13573
Turbulence modeling for sharp-fin-induced shock wave/turbulent boundary-layer interactions
[NASA-TM-102828] N91-13652
Bidirectional slapper detonators in spherical explosion systems
[DE91-002399] N91-13662
A comparison of two numerical methods for shocks in one-dimensional elastic-plastic solids
[DE91-001741] N91-13765
Evolution of a superbubble blastwave in a magnetized medium N91-14180
Lyman alpha radiation in external galaxies N91-14186
CO mapping of the nuclear region of NGC 6946 and IC 342 with Nobeyama millimeter array N91-14233

SHORELINES
Precision, accuracy, and tectonics from the Global Positioning System N91-13822

SIDE-LOOKING RADAR
Observation with stand-off radars
[FEL-90-A022] N91-13606

SIDESLIP
A preliminary look at techniques used to obtain airdata from flight at high angles of attack
[NASA-TM-101729] N91-13453

SIGNAL DETECTION
Multiple symbol differential detection
[NASA-CASE-NPO-17896-1-CU] N91-13596
FIRST: Far Infrared and Submillimetre Space Telescope
[ESA-BR-69] N91-14095
Feasibility of cosmic-ray muon intensity measurements for tunnel detection
[AD-A223355] N91-14266

SIGNAL DISTORTION
Twelve signals multiplexed with the LLNL optical streak camera
[DE91-000066] N91-13680

SIGNAL PROCESSING
Multiple symbol differential detection
[NASA-CASE-NPO-17896-1-CU] N91-13596
Transionospheric Propagation Code (TIPC)
[DE91-002435] N91-13597
Real-time data compression of broadcast video signals
[NASA-CASE-LEW-14945-1] N91-13598
Passive fetal monitoring sensor
[NASA-CASE-LAR-14088-1] N91-13686
Actinide speciation by photothermal spectroscopies: Instrumentation development
[DE91-001854] N91-13700
Signal processing used in the electromagnetic inspection of long bodies
[CETIM-107270] N91-13749
Auto and hetero-associative memory using a 2-D optical logic gate
[NASA-CASE-NPO-17997-1-CU] N91-13888
CESAR trap program library
[FFI-90/7023] N91-13924
Microwave superconducting electronic devices N91-14037
Analog superconductive electronics for avionics N91-14040
A liquid nitrogen cooled superconductive electron beam focusing system for improved performance ECM helix traveling wave tubes N91-14047
Signal processing development
[AD-A226593] N91-14052

SIGNATURES
Mesoscale monitoring of the soil freeze/thaw boundary from orbital microwave radiometry
[NASA-CR-185901] N91-13817

SILICA GLASS
Friction and wear of TPS fibers: A study of the adhesion and friction of high modulus fibers
[NASA-CR-187666] N91-13515
Mechanism of mechanical fatigue of silica glass
[DE91-004053] N91-13565

SILICATES
Laboratory spectra of amorphous and crystalline olivine: An application to comet Halley IR spectrum
[DE91-002307] N91-14264

SILICON
Ammonia decomposition on silicon surfaces studied using transmission FTIR spectroscopy
[AD-A226625] N91-13513
Publications, patents, presentations, honors, and students report. Kinetics of semiconductor processing chemistry: SiGe and GaAs growth on silicon surfaces
[AD-A226639] N91-13514
Ion-induced damage and amorphization in Si
[DE91-002358] N91-14061

SILICON CARBIDES
Fabrication and properties of powder metallurgically manufactured aluminum products and composites
[VTT-RR-699] N91-13531
Advanced Materials Development Program: Ceramic Technology for Advanced Heat Engines program plan, 1983--1993
[DE91-000516] N91-13555
Analytical and experimental studies for thermal plasma processing of materials
[DE91-000599] N91-13576

SILICON COMPOUNDS
Signal processing development
[AD-A226593] N91-14052

SILICON DIOXIDE
Friction and wear of TPS fibers: A study of the adhesion and friction of high modulus fibers
[NASA-CR-187666] N91-13515

SILICON FILMS
Synchrotron radiation photoemission study of metal overlayers on hydrogenated amorphous silicon at room temperature
[DE91-000740] N91-13525

SILICON NITRIDES
Advanced Materials Development Program: Ceramic Technology for Advanced Heat Engines program plan, 1983--1993
[DE91-000516] N91-13555

SILICON RADIATION DETECTORS
Operation of silicon microstrip detectors in a high radiation environment
[DE91-001953] N91-13682

SILICON TRANSISTORS
Design of high voltage planar devices using SIPOS technology
[LAAS-90237] N91-13629

SILVER COMPOUNDS
Method of making carbide/fluoride/silver composites
[NASA-CASE-LEW-14902-1] N91-13503

SIMULATION
Tissue simulating gel for medical research
[NASA-CASE-LAR-14036-1] N91-13562
Optical shared memory system demonstration model
[AD-A226431] N91-13612
A minimization method adapted to the finite element technique for turbulent flow simulation with nonlinear boundary conditions in the wall vicinity
[ECL-90-016] N91-13664
Clues to galaxy activity from rich cluster simulations N91-14222

SIMULATORS
Guidance, navigation and control. Digital emulation technology laboratory. Volume 2, Task 2: Seeker emulator development
[AD-A225124] N91-13429
Transionospheric propagation calculations for the output of two EMP (Electromagnetic Pulse) simulators
[DE91-001618] N91-13720

SINGLE CRYSTALS
Method of making single crystal fibers
[NASA-CASE-LEW-14921-1] N91-13502
Ion-induced damage and amorphization in Si
[DE91-002358] N91-14061

SINGLE EVENT UPSETS
Single event upset hardening techniques
[DE91-002337] N91-13625

SINGULARITY (MATHEMATICS)
Vortex collapse from a viewpoint of complex-time singularity
[DE91-001852] N91-13957

SINTERING
Method of making single crystal fibers
[NASA-CASE-LEW-14921-1] N91-13502

SITE SELECTION
A preliminary ocean ARM (Atmospheric Radiation Measurements) guide for climatic evaluations
[DE91-001120] N91-13811
Exobiology site selection for future Mars missions: Martian paleolake sediments and terrestrial analogs
[NASA-CR-187358] N91-14255

SIZE (DIMENSIONS)
Differences in the size-internal velocity relation of galactic and extragalactic HII regions N91-14158

SKIN FRICTION
Polymer/riblet combination for hydrodynamic skin friction reduction
[NASA-CASE-LAR-14271-1-CU] N91-13558

SLIDING
On hyperplane design techniques for discrete-time variable structure control systems
[MATHS-REPT-A-133] N91-13948

SLURRIES
An exploratory program for using hydrous metal oxide ion exchangers as Fischer-Tropsch catalysts
[DE91-002341] N91-13521

SMALL PERTURBATION FLOW
Transonic blade-vortex interactions noise: A parametric study
[NASA-CR-187713] N91-13422
Theory of finite disturbances in a centrifugal compression system with a vaneless radial diffuser
[NASA-CR-187049] N91-13458

SNOW
A physical parameterization of snow albedo for use in climate models N91-13781

SNOW COVER
A physical parameterization of snow albedo for use in climate models N91-13781

SOCIAL FACTORS
Information systems supported end-user interaction: Impacts on inter- and intra-organizational connectivity and cooperative behavior N91-14075

SODAR
Evaluation of a wind profile model
[FOA-E-40045-4.5] N91-13839

SODIUM
Experiments on bench-scale heat-pipe solar receivers
[DE90-013806] N91-13806

SOFIA (AIRBORNE OBSERVATORY)
High spatial resolution studies of galaxies in the far IR: Observations with the KAO, and the promise of SOFIA N91-14229

SOFTENING
A structural constitutive algorithm based on continuum damage mechanics for softening with snapback
[DE90-015841] N91-13773

SOFTWARE ENGINEERING
Coupling artificial intelligence and a system dynamics simulation to optimize quality assurance and testing in software development
[AD-A226580] N91-13902
Coordinates of a life-cycle model for a software system and communicating the need for software technology
[AD-A226592] N91-13903
Software management guidelines for automated measuring systems
[NPL-DES-99] N91-13926
The advanced software development and commercialization project
[DE91-002956] N91-13933
Proceedings of the Workshop on Software Tools for Distributed Intelligent Control Systems
[DE91-001755] N91-13943

SOFTWARE TOOLS
Pressure visualization (PreViz) package version 1.0 user's guide
[NASA-CR-187444] N91-13907
The ISIS project: Fault-tolerance in large distributed systems
[NASA-CR-186625] N91-13928
Proceedings of the Workshop on Software Tools for Distributed Intelligent Control Systems
[DE91-001755] N91-13943

SOIL MOISTURE
Laboratory investigation of the use of geotextiles to mitigate frost heave
[DOT/FAA/RD-90/13] N91-13465

SOIL SCIENCE
Soil bed reactor work of the Environmental Research Lab. of the University of Arizona in support of the research and development of Biosphere 2 N91-13846

SOILS
Mesoscale monitoring of the soil freeze/thaw boundary from orbital microwave radiometry
[NASA-CR-185901] N91-13817

SOLAR ACTIVITY
A solar chronometer for climate: Astronomical and geophysical evidence N91-13823
Solar-geophysical data number 550, June 1990. Part 1: (Prompt reports). Data for May, April 1990 and late data
[PB90-258799] N91-14260
Solar-geophysical data number 549, May 1990. Part 1: (Prompt reports). Data for April, March, 1990, and late data
[PB90-251224] N91-14262

SOLAR ARRAYS
Small particle selective emitter
[NASA-CASE-LEW-14731-1] N91-13802

Design considerations for lunar base photovoltaic power systems
[NASA-TM-103642] N91-14259

SOLAR CELLS
SERI photovoltaic subcontract reports: Abstracts and document control information
[DE90-000378] N91-13792
Status of concentrator collector and high-efficiency concentrator cell development
[DE91-001260] N91-13793
A theoretical investigation of effective surface recombination velocity in AlGaAs/GaAs heteroface solar cells
[DE91-001754] N91-13795
Solar collector manufacturing activity, 1988
[DE90-003539] N91-13797
Thin solar cell and lightweight array
[NASA-CASE-LEW-14959-1] N91-13803

SOLAR COLLECTORS
Solar collector manufacturing activity, 1988
[DE90-003539] N91-13797
Carbon dioxide reforming of methane in a solar volume-TRIC receiver-reactor: The CAESAR (Catalytically Enhanced Solar Absorption Receiver) project
[DE91-002340] N91-13800
Experiments on bench-scale heat-pipe solar receivers
[DE90-013806] N91-13806
Wide acceptance angle, high concentration ratio, optical collector
[NASA-CASE-MFS-28295-1] N91-13999

SOLAR CORONA
Hot interstellar gas and ionization of embedded clouds N91-14161

SOLAR CYCLES
Temporal variations of cosmic rays in the heliosphere N91-14267

SOLAR ENERGY
SERI photovoltaic subcontract reports: Abstracts and document control information
[DE90-000378] N91-13792
Solar collector manufacturing activity, 1988
[DE90-003539] N91-13797
Experiments on bench-scale heat-pipe solar receivers
[DE90-013806] N91-13806

SOLAR ENERGY ABSORBERS
Carbon dioxide reforming of methane in a solar volume-TRIC receiver-reactor: The CAESAR (Catalytically Enhanced Solar Absorption Receiver) project
[DE91-002340] N91-13800

SOLAR ENERGY CONVERSION
SERI photovoltaic subcontract reports: Abstracts and document control information
[DE90-000378] N91-13792

SOLAR FLARES
Solar-geophysical data number 550, June 1990. Part 1: (Prompt reports). Data for May, April 1990 and late data
[PB90-258799] N91-14260
Solar-geophysical data number 550, June 1990. Part 2: (Comprehensive reports). Data for December 1989 and miscellaneous
[PB90-258807] N91-14261
Solar-geophysical data number 549, May 1990. Part 2: (Comprehensive reports). Data for November 1989 and miscellaneous
[PB90-251232] N91-14263
Space radiation dose analysis for solar flare of August 1989
[NASA-TM-4229] N91-14265

SOLAR FLUX
Utilization of the HIPAS facility for cooperative experiments related to ionospheric modification
[AD-A226609] N91-13590

SOLAR MAGNETIC FIELD
Solar-geophysical data number 550, June 1990. Part 1: (Prompt reports). Data for May, April 1990 and late data
[PB90-258799] N91-14260
Solar-geophysical data number 549, May 1990. Part 1: (Prompt reports). Data for April, March, 1990, and late data
[PB90-251224] N91-14262

SOLAR PHYSICS
Solar-geophysical data number 549, May 1990. Part 1: (Prompt reports). Data for April, March, 1990, and late data
[PB90-251224] N91-14262

SOLAR RADIO BURSTS
Solar-geophysical data number 550, June 1990. Part 2: (Comprehensive reports). Data for December 1989 and miscellaneous
[PB90-258807] N91-14261
Solar-geophysical data number 549, May 1990. Part 2: (Comprehensive reports). Data for November 1989 and miscellaneous
[PB90-251232] N91-14263

SOLAR RADIO EMISSION
Solar-geophysical data number 550, June 1990. Part 1: (Prompt reports). Data for May, April 1990 and late data
[PB90-258799] N91-14260

SOLAR ROTATION
Solar-geophysical data number 550, June 1990. Part 2: (Comprehensive reports). Data for December 1989 and miscellaneous
[PB90-258807] N91-14261

SOLAR SYSTEM
Biospheres and solar system exploration N91-13843
The evolution of comets and the detectability of Extra-Solar Oort Clouds N91-14242

SOLAR TERRESTRIAL INTERACTIONS
Research projects including climate, atmospheric chemistry, solar-terrestrial physics, metrology, and storm systems
[PB90-256306] N91-13820
Long persistence effects of geomagnetic activity
[RAE-TM-SP-376] N91-13829

SOLAR WIND
Solar-geophysical data number 550, June 1990. Part 2: (Comprehensive reports). Data for December 1989 and miscellaneous
[PB90-258807] N91-14261
Solar-geophysical data number 549, May 1990. Part 1: (Prompt reports). Data for April, March, 1990, and late data
[PB90-251224] N91-14262
Temporal variations of cosmic rays in the heliosphere N91-14267

SOLAR X-RAYS
Solar-geophysical data number 550, June 1990. Part 2: (Comprehensive reports). Data for December 1989 and miscellaneous
[PB90-258807] N91-14261
Solar-geophysical data number 549, May 1990. Part 2: (Comprehensive reports). Data for November 1989 and miscellaneous
[PB90-251232] N91-14263

SOLDERED JOINTS
Calculations of residual stresses in ceramic soldered joints N91-13549

SOLDERS
Solder dross removal apparatus
[NASA-CASE-MFS-28406-1] N91-13729

SOLID ELECTROLYTES
Secondary Li battery incorporating 12-crown-4 ether
[NASA-CASE-NPO-17922-1-CU] N91-13621

SOLID PROPELLANT ROCKET ENGINES
Hazard studies for solid propellant rocket motors
[AGARD-AG-316] N91-13488

SOLID ROCKET PROPELLANTS
Evaluation of Raytek infrared pyrometer for continuous propellant temperature measurement
[NASA-CR-184040] N91-13570

SOLID SOLUTIONS
Analytical and experimental studies for thermal plasma processing of materials
[DE91-000599] N91-13576

SOLID STATE DEVICES
A liquid nitrogen cooled superconductive electron beam focusing system for improved performance ECM helix traveling wave tubes N91-14047

SOLID STATE LASERS
Chromium sensitized garnets for mid-IR lasers
[AD-A226630] N91-13696
Theoretical temperature-dependent branching ratios and laser thresholds of the (5)I7 yields (5)I8 levels of Ho3(+) in ten garnets
[NASA-TM-103429] N91-14053

SOLID STATE PHYSICS
Atomic and molecular theory
[DE91-004475] N91-13983

SOLID-SOLID INTERFACES
Synchrotron radiation photoemission study of metal overlayers on hydrogenated amorphous silicon at room temperature
[DE91-000740] N91-13525
Fracture mechanics of interface cracks between dissimilar anisotropic materials N91-13752

SOLIDS
A comparison of two numerical methods for shocks in one-dimensional elastic-plastic solids
[DE91-001741] N91-13765
Surfaces and thin films studied by picosecond ultrasonics
[DE91-004167] N91-13973
Application of parallel computing to the Monte Carlo simulation of electron scattering in solids: A rapid method for profile deconvolution
[DE91-001227] N91-13980

SOLITARY WAVES
New phases of D greater than or equal to 2 current and diffeomorphism algebras in particle physics
[DE91-001515] N91-14067

SOLUBILITY
Mechanisms of gas permeation through polymer membranes
[DE91-004190] N91-13671
Definition study for temperature control in advanced protein crystal growth
[NASA-CR-187346] N91-14029

SONIC BOOMS
A semiempirical method for obtaining fuselage normal areas from fuselage Mach sliced areas
[NASA-TM-4228] N91-13433

SOUND FIELDS
Hearing in three dimensions: Sound localization
[NASA-CR-187706] N91-13971
The prediction and measurement of the one-parameter behaviour of horns
[ISVR-TR-185] N91-13974

SOUND LOCALIZATION
Hearing in three dimensions: Sound localization
[NASA-CR-187706] N91-13971
Adaptive inverse filters for stereophonic sound reproduction
[ISVR-TR-187] N91-13975

SOUND WAVES
Comparison of spectral estimators application to ground sensor signals
[FEL-1988-85] N91-13605
Computation of broadband mixing noise from turbomachinery
[AD-A226559] N91-13969
Ultrasound generation through a fiber optic delivery system using pulsed laser energy
[DE91-001914] N91-13970

SPACE CHARGE
A theoretical investigation of effective surface recombination velocity in AlGaAs/GaAs heteroface solar cells
[DE91-001754] N91-13795

SPACE COMMERCIALIZATION
Biological Life Support Technologies: Commercial Opportunities
[NASA-CP-3094] N91-13842

SPACE DEBRIS
A critical review of charged particle astronomy at Saturn: The evidence for co-orbiting material in the inner satellite system
[NASA-CR-187348] N91-14090

SPACE EXPLORATION
Biospheres and solar system exploration N91-13843
Business and life in space N91-13854
A personal history of the human exploration initiative with commentary on the pivotal role for life support research N91-13855

SPACE FLIGHT
Space flight undertakings of present-day china (photo captions on 65 selected pages)
[AD-A222816] N91-13469
A computer model to determine the primary contributors to relative radiation dose received by astronauts
[DE90-015681] N91-13866

SPACE LOGISTICS
The NASA CELSS program N91-13848
Single launch lunar habitat derived from an NSTS external tank
[NASA-TM-4212] N91-14251

SPACE MISSIONS
Earth observing satellite: Understanding the Earth as a system N91-13853

SPACE PERCEPTION
Lidar as a slant path visio-ceilometer
[FEL-90-A207] N91-13838
A discrepancy within primate spatial vision and its bearing on the definition of edge detection processes in machine vision
[NASA-TM-102739] N91-13941

SPACE PLASMAS
Solar-geophysical data number 550, June 1990. Part 2: (Comprehensive reports). Data for December 1989 and miscellaneous
[PB90-258807] N91-14261
Solar-geophysical data number 549, May 1990. Part 2: (Comprehensive reports). Data for November 1989 and miscellaneous
[PB90-251232] N91-14263

SPACE POWER REACTORS
The behavior of fission products during nuclear rocket reactor tests
[DE91-001956] N91-13490
SP-100 from ground demonstration to flight validation
[DE91-001869] N91-13986
Unique features of space reactors
[DE91-001910] N91-13987

Multiplexer/amplifier test results for SP-100
[DE91-004504] N91-13990

SPACE SHUTTLE BOOSTERS
Summary of JAYGO mixing and FSM-1 application of castable inhibitor and liner
[NASA-CR-184030] N91-13569
Evaluation of Raytek infrared pyrometer for continuous propellant temperature measurement
[NASA-CR-184040] N91-13570

SPACE SHUTTLE MAIN ENGINE
Thrust chamber modeling using Navier-Stokes equations: Code documentation and listings, volume 2
[NASA-CR-183617] N91-13489

SPACE SHUTTLE MISSION 31-B
An assessment of wind tunnel test data on flexible thermal protection materials and results of new fatigue tests of threads
[NASA-CR-177466] N91-13972

SPACE SHUTTLE ORBITERS
All Shuttle Centaur engine and nozzle support plug vibration testing
[NASA-CR-183201] N91-13485
RL10A-3-3B high mixture ratio qualification program
[NASA-CR-183200] N91-13486
Shuttle Centaur engine cooldown evaluation and effects of expanded inlets on start transient
[NASA-CR-183198] N91-13487

SPACE SHUTTLES
Business and life in space N91-13854

SPACE STATIONS
Security for safety critical space borne systems
[NASA-CR-187656] N91-13906

SPACE SUITS
Business and life in space N91-13854

SPACEBORNE TELESCOPES
FIRST: Far Infrared and Submillimetre Space Telescope
[ESA-BR-69] N91-14095

SPACECRAFT CHARGING
SEPAC data analysis in support of the environmental interaction program
[NASA-CR-184028] N91-13807

SPACECRAFT CONSTRUCTION MATERIALS
Summary of JAYGO mixing and FSM-1 application of castable inhibitor and liner
[NASA-CR-184030] N91-13569

SPACECRAFT CONTROL
Multivariable methods for the design, identification, and control of large space structures. Volume 1: Estimator Eigenvalue placement in positive real design
[AD-A226525] N91-13477
Multivariable methods for the design, identification, and control of large space structures. Volume 3: A study of the integrated control/structure design optimization problem for large flexible structures
[AD-A226526] N91-13478
Analytical and experimental research on large angle maneuvers of flexible structures
[AD-A226679] N91-13479
Computational methods and software systems for dynamics and control of large space structures
[NASA-CR-187669] N91-13480

SPACECRAFT DESIGN
An application of multiattribute decision analysis to the Space Station Freedom program. Case study: Automation and robotics technology evaluation
[NASA-CR-187432] N91-13476
Multivariable methods for the design, identification, and control of large space structures. Volume 1: Estimator Eigenvalue placement in positive real design
[AD-A226525] N91-13477
Multivariable methods for the design, identification, and control of large space structures. Volume 3: A study of the integrated control/structure design optimization problem for large flexible structures
[AD-A226526] N91-13478
Generic extravehicular (EVA) and telerobot task primitives for analysis, design, and integration. Version 1.0: Reference compilation for the EVA and telerobotics communities
[NASA-CR-187429] N91-13876

SPACECRAFT DOCKING
Standard remote manipulator system docking target augmentation for automated docking
[NASA-CASE-MFS-28419-1] N91-13482

SPACECRAFT INSTRUMENTS
Semi-custom integrated circuit amplifier and level discriminator for nuclear and space instruments
[DE91-001951] N91-13620

SPACECRAFT STABILITY
Analytical and experimental research on large angle maneuvers of flexible structures
[AD-A226679] N91-13479

SPACECREWS
Integrated launch and emergency vehicle system
[NASA-CASE-LAR-13780-1] N91-13481

SPACELAB
SEPAC data analysis in support of the environmental interaction program
[NASA-CR-184028] N91-13807

SPACERS
The effect of longitudinal spacer ribs on the minimum pressure drop in a heated annulus
[DE91-000784] N91-13655

SPACETENNAS
Analytical and photogrammetric characterization of a planar tetrahedral truss
[NASA-TM-4231] N91-13473

SPARK IGNITION
Interpretation of engine cycle-to-cycle variation by chaotic time series analysis
[DE91-000729] N91-13955

SPATIAL DISTRIBUTION
Application of parallel computing to the Monte Carlo simulation of electron scattering in solids: A rapid method for profile deconvolution
[DE91-001227] N91-13980
Spatial analysis of IRAS observations of nearby spirals N91-14133
The morphology-density relation for dwarf galaxies N91-14200
High spatial-resolution IRAS images of M51 N91-14207
CS in nearby galaxies: Distribution, kinematics, and multilevel studies N91-14235
Spatial variation of the physical conditions of molecular gas in galaxies N91-14236
CO distribution in southern S0 galaxies N91-14239

SPATIAL FILTERING
Use of dome (meniscus) lenses to eliminate birefringence and tensile stresses in spatial filters for the Nova laser
[DE91-002784] N91-13707

SPATIAL RESOLUTION
Mesoscale monitoring of the soil freeze/thaw boundary from orbital microwave radiometry
[NASA-CR-185901] N91-13817
High spatial resolution 100 micron observations of the M83 bar N91-14130
High spatial-resolution IRAS images of M51 N91-14207
High spatial resolution studies of galaxies in the far IR: Observations with the KAO, and the promise of SOFIA N91-14229

SPECIFIC HEAT
Optical characterization techniques applied to ceramic oxides
[DE91-001526] N91-13556

SPECIFICATIONS
Helicopter structural integrity program (HSIP). Volume 1: Structural test requirements specification
[AD-A226520] N91-13444
Definition study into the requirements of a data modem for the SYSCOM network
[FEL-90-A116] N91-13892

SPECTRA
The 3 micron spectrum of NGC 4565 N91-14132
Imaging spectrophotometry of the nuclear outflow of NGC 1068 N91-14149
Ionized interstellar froth in irregular galaxies N91-14152
Hot interstellar gas and ionization of embedded clouds N91-14161
CO observations of southern mergers N91-14197

SPECTRAL LINE WIDTH
NGC 1058: Gas motions in an extended, quiescent spiral disk N91-14103

SPECTRAL RESOLUTION
Ground-based studies of emission-line variability: Recent results for NGC 5548 and future plans
[NASA-CR-180433] N91-14088

SPECTROMETERS
Development of mercuric iodide uncooled x ray detectors and spectrometers
[NASA-CR-185394] N91-13484
The fluid mechanics of continuous flow electrophoresis
[NASA-CR-187647] N91-13648
Operation of silicon microstrip detectors in a high radiation environment
[DE91-001953] N91-13682
Design of a mechanical modulator for the planetary Fourier spectrometer experiment of the MARS 94 mission
[IFSI-89-22] N91-13717
Development and initial characterization of a nuclear magnetic resonance dosimetry system
[DE91-001775] N91-13867
Infrared spectroscopy of the dwarf starburst galaxy Henize 2-10 N91-14213

SPECTROPHOTOMETRY
Imaging spectrophotometry of the nuclear outflow of NGC 1068 N91-14149

SPECTROSCOPY
Fundamental investigations of supported monometallic and bimetallic catalysts by proton magnetic resonance spectroscopy
[DE91-000610] N91-13516
Data reduction of digitized images processed from calibrated photographic and spectroscopic films obtained from terrestial, rocket and space shuttle telescopic instruments
[NASA-CR-187320] N91-13674
Development and initial characterization of a nuclear magnetic resonance dosimetry system
[DE91-001775] N91-13867
Far-infrared spectroscopy of NGC 6946, IC 342, and Arp 299 N91-14114
Circumnuclear ionized gas in starburst nuclei N91-14148
Multiband observations of Cygnus A: A study of pressure balance in the core of a powerful radio galaxy N91-14151
Ar/S N91-14153
Differences in the size-internal velocity relation of galactic and extragalactic HII regions N91-14158
A study of HII regions in spiral galaxies using multiobject spectroscopy N91-14159
High-mass star formation in southern disk galaxies N91-14218

SPECTRUM ANALYSIS
Comparison of spectral estimators application to ground sensor signals
[FEL-1988-85] N91-13605
Spectrum fatigue testing: A literature survey
[FFA-TN-1990-40] N91-13772
Mesoscale monitoring of the soil freeze/thaw boundary from orbital microwave radiometry
[NASA-CR-185901] N91-13817
Ground-based studies of emission-line variability: Recent results for NGC 5548 and future plans
[NASA-CR-180433] N91-14088
Relativistic effects in millisecond pulsars and active galactic nuclei N91-14247
Analysis of gamma ray burst spectra with cyclotron lines
[DE91-001745] N91-14269

SPHERES
Bidirectional slapper detonators in spherical explosion systems
[DE91-002399] N91-13662

SPIN TEMPERATURE
Energy input and HI spin temperatures in low pressure regions N91-14163

SPIRAL GALAXIES
A comparison of UV surface brightness and HI surface densities for spiral galaxies N91-14102
High velocity gas in external galaxies N91-14105
Disk mass densities in edge-on spiral galaxies N91-14108
The hot and cold interstellar matter of early type galaxies and their radio emission N91-14112
The ratio of molecular to atomic gas in spiral galaxies as a function of morphological type N91-14119
The CO-12 and CO-13 J=2-1 and J=1-0 observations of hot and cold galaxies N91-14126
High resolution sub-millimetre mapping of starburst galaxies: Comparison with CO emission N91-14129
High spatial resolution 100 micron observations of the M83 bar N91-14130
Spatial analysis of IRAS observations of nearby spirals N91-14133
A comparison of the radial distribution of molecular gas and non-thermal radio continuum in spiral disks N91-14145
A relationship between the integrated CO intensity and the radio continuum emission in spiral galaxies N91-14146
Radio continuum and far-infrared emission of spiral galaxies: Implications of correlations N91-14147
A study of HII regions in spiral galaxies using multiobject spectroscopy N91-14159
The interstellar halo of spiral galaxies: NGC 891 N91-14164
Granularity in the magnetic field structure of M83 N91-14194
Unbound molecular complexes in M33 N91-14201
Deep narrow band imagery of the diffuse ISM in M33 N91-14202
A high resolution CO map of M51 N91-14203
M51: Molecular spiral arms, GMAs and superclouds N91-14204
Dissociation and ionization of molecular gas in the spiral arms of M51 N91-14205
Spiral structure of M51: Streaming motions across the spiral arms N91-14206

High spatial-resolution IRAS images of M51 N91-14207
Gravitational star formation thresholds and gas density in three galaxies N91-14210
Molecular gas and star formation in the centers of Virgo spirals N91-14216
Near-infrared mapping of spiral barred galaxies N91-14217
Probing the interstellar medium of external galaxies using quasar absortion lines: The 3C 232/NGC 3067 system N91-14227
Detection of a z=0.0515, 0.0522 absorption system in the QSO S4 0248+430 due to an intervening galaxy N91-14228
The molecular spiral arms of NGC 6946 N91-14231
The molecular spiral arms of NGC 6946 N91-14232
CO mapping of the nuclear region of NGC 6946 and IC 342 with Nobeyama millimeter array N91-14233
CO excitation in four IR luminous galaxies N91-14234
Detection of CO emission in Hydra 1 cluster galaxies N91-14237
The stellar content of M101 N91-14244

SPIRALS
Fluid flow effects on electroplating
[DE91-001087] N91-13577

SPRAYED COATINGS
Fatigue testing of plasma-sprayed thermal barrier coatings, volume 2
[NASA-CR-186726] N91-13535
Simultaneous measurement of Ni-Al particle size, velocity, and temperature in atmospheric thermal plasmas
[DE91-001935] N91-13826

SPRAYERS
Measurements and predictions of a liquid spray from an air-assist nozzle
[NASA-TM-103640] N91-13455
Spray deflagration
[INPE-5079-TDL/413] N91-13511
Intelligent processing for spray metal manufacturing
[AD-A226499] N91-13523
Tissue simulating gel for medical research
[NASA-CASE-LAR-14036-1] N91-13562

SPUTTERING
Distortion-free x ray mask technology
[AD-A226524] N91-13993
Modeling and analysis of surface roughness effects on sputtering, reflection, and sputtered particle transport
[DE91-004429] N91-14028

SQUID (DETECTORS)
SQUIDs devices made from high Tc superconductors: Results and perspectives N91-14044

STABILITY
A study of confined diffusion flames
[AD-A226552] N91-13512
Vinyl capped addition polyimides
[NASA-CASE-LEW-15027-1] N91-13566
Dissipative controller designs for second-order dynamic systems
[NASA-CR-187452] N91-13935
Influence of collective effects on the performance of high-luminosity colliders
[DE91-001797] N91-13982
The effect of suspended particles on Jean's criterion for gravitational instability N91-14189

STABILIZERS (FLUID DYNAMICS)
Some buffet response characteristics of a twin-vertical-tail configuration
[NASA-TM-102749] N91-13412

STABLE OSCILLATIONS
Real-time dynamic holographic image storage device
[NASA-CASE-LAR-13989-1] N91-13694

STAINLESS STEELS
Mechanical properties of 1950's vintage Type 304 stainless steel weldment components
[DE91-004328] N91-13774

STANDARDIZATION
Development of standards for advanced polymer matrix composites: A BPF/ACG overview
[NPL-DMM(A)-8] N91-13568
Report of foreign travel
[DE91-001732] N91-14082

STANDARDS
Development of standards for advanced polymer matrix composites: A BPF/ACG overview
[NPL-DMM(A)-8] N91-13568
Review of uncertainties in the use of NPL primary standards of x ray exposure for the calibration of secondary standards in terms of exposure and air kerma
[NPL-RS(EXT)-109] N91-13868
List of standards to accompany manual of documentation practices applicable to defence-aerospace scientific and technical information. Addendum
[AGARD-AG-235-ADD] N91-14076

STANDING WAVES
Relativistic kylstron simulations using RKTW2D
[DE91-001747] N91-13619

STAR CLUSTERS
An ADP proposal to study the formation and evolution of dust-embedded clusters
[NASA-CR-186793] N91-14089
A model for the infrared emission from an OB star cluster environment N91-14139
Optical and near-IR study of LMC HII region N11AB N91-14155
Evolution of a superbubble blastwave in a magnetized medium N91-14180
Unbound molecular complexes in M33 N91-14201
Starburst outflows from nearby galaxies N91-14219

STAR DISTRIBUTION
The stellar content of M101 N91-14244
An imaging and spectroscopic study of low and intermediate power radio galaxies N91-14268

STAR FORMATION
The Interstellar Medium in External Galaxies: Summaries of contributed papers
[NASA-CP-3084] N91-14100
Neutral hydrogen in the starburst galaxy NGC3690/IC694 N91-14104
A scaling law of radial gas distribution in disk galaxies N91-14106
The hot and cold interstellar matter of early type galaxies and their radio emission N91-14112
The FCRAO extragalactic CO survey: Global properties of galaxies N91-14117
A survey of galaxies in CO N91-14118
The ratio of molecular to atomic gas in spiral galaxies as a function of morphological type N91-14119
Circumnuclear molecular gas in starburst and Seyfert galaxies N91-14120
Aperture synthesis CO observations of the inner disk of NGC 1068 N91-14122
Observations of CO in the Magellanic irregular galaxy NGC 55 N91-14124
Observations of CO isotopic emission and the far-infrared continuum of Centaurus A N91-14125
The CO-12 and CO-13 J=2-1 and J=1-0 observations of hot and cold galaxies N91-14126
CS J = 2 yields 1 emission toward the central region of M82 N91-14128
High resolution sub-millimetre mapping of starburst galaxies: Comparison with CO emission N91-14129
High spatial resolution 100 micron observations of the M83 bar N91-14130
Contribution of cool dust to the FIR brightness distribution of NGC 6946 Sc(s)2 N91-14134
IRAS observations of the ISM in the gamma CAS reflection nebula N91-14140
A comparison of the radial distribution of molecular gas and non-thermal radio continuum in spiral disks N91-14145
Ionized interstellar froth in irregular galaxies N91-14152
The diffuse ionized interstellar medium perpendicular to the plane of NGC 891 N91-14160
Stripping of gas and dust from the elliptical galaxy M86 N91-14171
Search for cold gas in clusters with and without cooling flows N91-14174
The violent interstellar medium in Messier 31 N91-14178
Infrared analysis of LMC superbubbles N91-14181
Magnetic collimation of protostellar winds into bipolar outflows N91-14182
What sort of standard candle is Orion for studying molecular hydrogen line emission in galaxies N91-14184
H2 line emission in three Seyfert nuclei: Evidence against UV-excitation N91-14185
Lyman alpha radiation in external galaxies N91-14186
Virial theorem analysis of the structure and stability of magnetized clouds N91-14190
Evolution of magnetized, rotating, isothermal clouds N91-14191
Granularity in the magnetic field structure of M83 N91-14194
Thermal instabilities in protogalactic clouds N91-14195
CO observations of southern mergers N91-14197
Star formation on the leading edge of a ring-like density wave in Arp 143 N91-14198
A multi-wavelength study of the peculiar galaxy NGC 2976 N91-14199
Aspects of the interstellar medium in starburst galaxies N91-14209
Gravitational star formation thresholds and gas density in three galaxies N91-14210
One-dimensional cloud fluid model for propagating star formation N91-14211
Star formation in proto dwarf galaxies N91-14212
Infrared spectroscopy of the dwarf starburst galaxy Henize 2-10 N91-14213
Small-scale star formation at low metallicity N91-14214
Global and radial variations in the efficiency of massive star formation among galaxies N91-14215
Molecular gas and star formation in the centers of Virgo spirals N91-14216
High-mass star formation in southern disk galaxies N91-14218
Starburst outflows from nearby galaxies N91-14219
Dense gas and HII regions in the starburst galaxy NGC 253 N91-14220
Clues to galaxy activity from rich cluster simulations N91-14222
Central star formation in S0 galaxies N91-14223
Current star formation in S0 galaxies: NGC 4710 N91-14224
The molecular spiral arms of NGC 6946 N91-14231
The molecular spiral arms of NGC 6946 N91-14232
CO mapping of the nuclear region of NGC 6946 and IC 342 with Nobeyama millimeter array N91-14233
CO excitation in four IR luminous galaxies N91-14234
The photoevaporation of interstellar clouds N91-14248

STAR FORMATION RATE
Contribution of cool dust to the FIR brightness distribution of NGC 6946 Sc(s)2 N91-14134
Radio continuum and far-infrared emission of spiral galaxies: Implications of correlations N91-14147
The interstellar halo of spiral galaxies: NGC 891 N91-14164
Search for cold gas in clusters with and without cooling flows N91-14174
Dissociation and ionization of molecular gas in the spiral arms of M51 N91-14205
Global and radial variations in the efficiency of massive star formation among galaxies N91-14215
The molecular spiral arms of NGC 6946 N91-14232

STARBURST GALAXIES
Circumnuclear molecular gas in starburst and Seyfert galaxies N91-14120
High resolution CO images of Seyfert Galaxies N91-14121
CS J = 2 yields 1 emission toward the central region of M82 N91-14128
High resolution sub-millimetre mapping of starburst galaxies: Comparison with CO emission N91-14129
The infrared continuum spectrum of x ray illuminated molecular gas N91-14144
Circumnuclear ionized gas in starburst nuclei N91-14148
Aspects of the interstellar medium in starburst galaxies N91-14209
Infrared spectroscopy of the dwarf starburst galaxy Henize 2-10 N91-14213
Starburst outflows from nearby galaxies N91-14219
Dense gas and HII regions in the starburst galaxy NGC 253 N91-14220
A near infrared spectroscopic study of the interstellar gas in the starburst core of M82 N91-14221
CO mapping of the nuclear region of NGC 6946 and IC 342 with Nobeyama millimeter array N91-14233

STARS
Methodology to treat stellar images
[IFSI-89-21] N91-14094
A comparison of UV surface brightness and HI surface densities for spiral galaxies N91-14102
CO observations of southern mergers N91-14197
Star formation on the leading edge of a ring-like density wave in Arp 143 N91-14198
Deep narrow band imagery of the diffuse ISM in M33 N91-14202
Aspects of the interstellar medium in starburst galaxies N91-14209
Molecular outflows in the L1641 region of Orion N91-14246

STATE VECTORS
Assured crew return vehicle
[NASA-CASE-MSC-21536-1] N91-13483

STATIC LOADS
Test and model correlation of the atmospheric emission photometric imager fiberglass pedestal
[NASA-TM-103515] N91-13766

STATIC PRESSURE
A preliminary look at techniques used to obtain airdata from flight at high angles of attack
[NASA-TM-101729] N91-13453
Water cooled static pressure probe
[NASA-CASE-LAR-14340-1-CU] N91-13684

Clues to galaxy activity from rich cluster simulations N91-14222

STATISTICAL ANALYSIS
Relationship between voids and interlaminar shear strength of polymer matrix composites
[NASA-TM-103643] N91-13495
Practical considerations for the measurement of internal and coupling loss factors on complex structures
[ISVR-TR-182] N91-13778
About transient stability of power systems: Statistical pattern recognition approach
[LAAS-90192] N91-13889
Linear vs nonlinear and infinite vs finite: An interpretation of chaos
[DE91-002522] N91-14072
Properties of the Magellanic-type galaxies N91-14245

STATISTICAL DISTRIBUTIONS
Evaluation of a wind profile model
[FOA-E-40045-4.5] N91-13839

STATISTICAL MECHANICS
The gravitational wakefield of a molecular cloud in a disk galaxy N91-14188

STEADY FLOW
Computation of incompressible flow around the DARPA SUBOFF bodies
[AD-A226481] N91-13646

STEADY STATE
Predictive sensor method and apparatus
[NASA-CASE-SSC-00006-1] N91-13691

STEAM TURBINES
Material degradation of steam turbine rotors in long term operations
[VTT-RR-692] N91-13530

STEELS
Micrographic etching of nitrided iron and steel layers
[CETIM-106470] N91-13533
Penetration of yawed projectiles
[DE91-001084] N91-13726
Potential impact of enhanced fracture-toughness data on pressurized-thermal-shock analysis
[DE91-001493] N91-13763

STELLAR COMPOSITION
Radio observations of several interstellar molecules N91-14093
Hot interstellar gas and ionization of embedded clouds N91-14161

STELLAR EVOLUTION
An ADP proposal to study the formation and evolution of dust-embedded clusters
[NASA-CR-186793] N91-14089
Circumnuclear ionized gas in starburst nuclei N91-14148
A combined N-body and hydrodynamic code for modeling disk galaxies N91-14241
The evolution of comets and the detectability of Extra-Solar Oort Clouds N91-14242
Molecular outflows in the L1641 region of Orion N91-14246
The photoevaporation of interstellar clouds N91-14248

STELLAR LUMINOSITY
An ADP proposal to study the formation and evolution of dust-embedded clusters
[NASA-CR-186793] N91-14089
Aspects of the interstellar medium in starburst galaxies N91-14209
The stellar content of M101 N91-14244

STELLAR MASS
High resolution CO images of Seyfert Galaxies N91-14121
CO aperture synthesis of NGC 4038/9 (ARP 244) N91-14123
Observations of CO isotopic emission and the far-infrared continuum of Centaurus A N91-14125

STELLAR MODELS
A study of active regions on RS CVn stars N91-14092

STELLAR ROTATION
Relativistic effects in millisecond pulsars and active galactic nuclei N91-14247

STELLAR SPECTRA
Circumnuclear ionized gas in starburst nuclei N91-14148
Aspects of the interstellar medium in starburst galaxies N91-14209

STELLAR STRUCTURE
High spatial resolution 100 micron observations of the M83 bar N91-14130

STELLAR SYSTEMS
A study of active regions on RS CVn stars N91-14092

STELLAR WINDS
The infrared continuum spectrum of x ray illuminated molecular gas N91-14144
Evolution of a superbubble blastwave in a magnetized medium N91-14180
Magnetic collimation of protostellar winds into bipolar outflows N91-14182
One-dimensional cloud fluid model for propagating star formation N91-14211
Molecular outflows in the L1641 region of Orion N91-14246

STELLARATORS
NRL compact accelerator theory studies
[AD-A226537] N91-14005

STEREOPHONICS
Adaptive inverse filters for stereophonic sound reproduction
[ISVR-TR-187] N91-13975

STEREOSCOPIC VISION
The effect of stereoscopic presentation on a simulated air traffic control task
[IZF-1989-53] N91-13431

STIFFNESS
Some buffet response characteristics of a twin-vertical-tail configuration
[NASA-TM-102749] N91-13412

STIRLING CYCLE
Superfluid Stirling refrigerator: A new method for cooling below 1 Kelvin
[DE91-002311] N91-13582

STIRLING ENGINES
Comparison of NASA Lewis Research Center's performance code's pressure-drop model predictions to Stirling engine working-space flow test data
[NASA-CR-182215] N91-13804

STOCHASTIC PROCESSES
Analysis of parallelism for nonlinear programming
[INPE-5121-TDL/422] N91-13899
Direct modeling of white noise in stochastic systems
[MEMO-865] N91-13964

STOICHIOMETRY
Novel polyimide molding powder, coating, adhesive, and matrix resin
[NASA-CASE-LAR-14163-1] N91-13559

STORAGE BATTERIES
Secondary Li battery incorporating 12-crown-4 ether
[NASA-CASE-NPO-17922-1-CU] N91-13621

STORAGE TANKS
Dual diaphragm tank with telltale drain
[NASA-CASE-MSC-21703-1] N91-13580

STRAIN DISTRIBUTION
Study of static and dynamic fracture using strain measurements N91-13754

STRAIN GAGE BALANCES
Dual strain gage balance system for measuring light loads
[NASA-CASE-LAR-14419-1] N91-13687

STRAIN GAGES
Calibration set up for load cells
[PD-ST-8917] N91-13673

STRAIN MEASUREMENT
Mechanical testing of advanced coating system, volume 1
[NASA-CR-186725] N91-13534
Study of static and dynamic fracture using strain measurements N91-13754

STRAIN RATE
Precision, accuracy, and tectonics from the Global Positioning System N91-13822

STRAKES
Aerodynamic effect of strakes on two-dimensional tail boom models of the OH-58A and the OH-58D helicopters
[NASA-TM-4248] N91-13406

STRATEGY
Study of strategies for the determination of deformations from Global Positioning System (GPS) measurements
[ETN-91-98141] N91-13786

STRATOCUMULUS CLOUDS
Cloud properties as deduced from satellite observation
[NASA-CR-182851] N91-13833

STRATOSPHERE
Stratospheric ozone conservation by electron attachment to chlorine atoms: The negative-ion chemistry
[DE91-002951] N91-13815
Ultraviolet absorption cross-sections of photoactive species of stratospheric interest. Part 1: The halocarbons
[ETN-91-98385] N91-13830

STREAK CAMERAS
Twelve signals multiplexed with the LLNL optical streak camera
[DE91-000066] N91-13680
Fast Pb-glass neutron-to-light converter for ICF (Inertial Confinement Fusion) target burn history measurements
[DE91-002670] N91-14021

STRESS (PSYCHOLOGY)
AN alternative to suppression: Modeling methodology for assessing indirect effects of weapons and human performance degradation
[AD-A226518] N91-13877

STRESS ANALYSIS
The United Kingdom contribution to the AGARD fatigue-rated fastener systems program
[RAE-TR-89046] N91-13451
Method and apparatus for characterizing residual stress in ferromagnetic materials
[NASA-CASE-LAR-14239-1] N91-13527
Residual stresses in ceramics
[JUEL-SPEZ-550] N91-13536
Use of neutron diffraction methods for the determination of mechanical stresses in metal ceramic laminated composite materials N91-13537
Determination of residual stresses in ceramics materials using neutron diffraction N91-13538
Residual stresses analyses in ceramics and metal ceramic composites using x ray methods N91-13539
Influence of materials structure and production method of Al2O3 ceramic on the x-ray stress measurement N91-13540
The x ray elastic constants of ceramic materials for the determination of the stresses from lattice expansion measurements N91-13541
Development and computer aided residual stress measurements on coated specimen using blind-hole drilling technique N91-13544
Residual stresses in Al2O3: Comparison between electromechanical measurements and finite element method calculations N91-13545
Determination of stresses in ceramics using ultrasonic methods: Possibilities and limitations N91-13546
Possibilities of the calculation of stresses and residual stresses in materials with a phase transformation N91-13548
Calculations of residual stresses in ceramic soldered joints N91-13549
Nonlinear viscous waves produced by an impulsively moving plate N91-13641
Fracture mechanics of interface cracks between dissimilar anisotropic materials N91-13752
Study of static and dynamic fracture using strain measurements N91-13754
Finite element and boundary element methods for elastoplastic stress analysis of two-dimensional and axisymmetric problems N91-13755
Test and model correlation of the atmospheric emission photometric imager fiberglass pedestal
[NASA-TM-103515] N91-13766

STRESS CORROSION
Material degradation of steam turbine rotors in long term operations
[VTT-RR-692] N91-13530

STRESS INTENSITY FACTORS
Damage tolerance analysis and testing of the fighter aircraft 37 Viggen
[FFA-TN-1990-35] N91-13448
Fracture mechanics of interface cracks between dissimilar anisotropic materials N91-13752
Accurate and reliable computation of complete solutions to the equations of linear elastomechanics on three-dimensional domains: Computation of edge stress intensity functions
[FFA-TN-1989-12] N91-13769
Accurate and reliable determination of edge and vertex stress intensity factors in three-dimensional elastomechanics
[FFA-TN-1990-28] N91-13771

STRESS MEASUREMENT
Determination of stresses in ceramics using ultrasonic methods: Possibilities and limitations N91-13546
Possibilities of stress measurement on ceramic materials using acoustic microscopy N91-13547

STRESS RELIEVING
Distortion-free x ray mask technology
[AD-A226524] N91-13993

STRESSES
Tubular lap joints for wind turbine applications
[DE91-001341] N91-13736

STRING THEORY
Algorithms for finding an optimal matching between a given string and a string generated by a regular grammar
[MEMO-836] N91-13905

STRONGLY COUPLED PLASMAS
Operation of inductively coupled plasma source mass spectrometers in the peak jumping mode
[DE91-001766] N91-13689

STRUCTURAL ANALYSIS
Thermal and structural assessments of a ceramic wafer seal in hypersonic engines
[NASA-TM-103651] N91-13456

Analytical and photogrammetric characterization of a planar tetrahedral truss
[NASA-TM-4231] N91-13473
X ray holography at Lawrence Livermore National Laboratory
[DE91-002673] N91-13690
Free vibrations of thin-walled semicircular graphite-epoxy composite frames
[NASA-TP-3010] N91-13750
A review of nonlinear constitutive models for metals
[NASA-TM-102727] N91-13761
A structural constitutive algorithm based on continuum damage mechanics for softening with snapback
[DE90-015841] N91-13773
Calculations for structures with nonlinear joints
[CETIM-108830] N91-13776
The importance of fracturing in the Pimenta Bueno-Ro Basin structure: A study of the morphostructural elements of the rupture-ductile character through remote sensing techniques and products
[INPE-5004-TDL/398] N91-13825

STRUCTURAL DESIGN
Composite passive damping struts for large precision structures
[NASA-CASE-NPO-17914-1-CU] N91-13767

STRUCTURAL FAILURE
Helicopter structural integrity program (HSIP). Volume 1: Structural test requirements specification
[AD-A226520] N91-13444

STRUCTURAL PROPERTIES (GEOLOGY)
The importance of fracturing in the Pimenta Bueno-Ro Basin structure: A study of the morphostructural elements of the rupture-ductile character through remote sensing techniques and products
[INPE-5004-TDL/398] N91-13825
Feasibility of cosmic-ray muon intensity measurements for tunnel detection
[AD-A223355] N91-14266

STRUCTURAL RELIABILITY
Helicopter structural integrity program (HSIP). Volume 1: Structural test requirements specification
[AD-A226520] N91-13444
Thermal and structural assessments of a ceramic wafer seal in hypersonic engines
[NASA-TM-103651] N91-13456

STRUCTURAL STABILITY
Bolted structural assemblies: Bibliographic analysis
[CETIM-13N061] N91-13742
General Rotorcraft Aeromechanical Stability Program (GRASP): Theory manual
[NASA-TM-102255] N91-13762

STRUCTURAL VIBRATION
Effects of temperature on acoustically-induced strains and damage propagation in CFRP plates N91-13493
The effect of inertial coupling in the dynamics and control of flexible robotic manipulators
[NASA-CR-187679] N91-13721
Free vibrations of thin-walled semicircular graphite-epoxy composite frames
[NASA-TP-3010] N91-13750
Practical considerations for the measurement of internal and coupling loss factors on complex structures
[ISVR-TR-182] N91-13778

STRUTS
Composite passive damping struts for large precision structures
[NASA-CASE-NPO-17914-1-CU] N91-13767

STYRENES
The synthesis of star block copolymers by controlled ring-opening metathesis polymerization
[AD-A225987] N91-13551

SUBMILLIMETER WAVES
High resolution sub-millimetre mapping of starburst galaxies: Comparison with CO emission N91-14129

SUBROUTINE LIBRARIES (COMPUTERS)
CESAR MALU program library
[FFI-90/7010] N91-13922

SUBROUTINES
A physical parameterization of snow albedo for use in climate models N91-13781

SUBSTRATES
The influence of the texture of Al2O3 substrates on the fracture behavior under thermal loading N91-13543

SUDDEN IONOSPHERIC DISTURBANCES
Solar-geophysical data number 550, June 1990. Part 1: (Prompt reports). Data for May, April 1990 and late data
[PB90-258799] N91-14260
Solar-geophysical data number 549, May 1990. Part 1: (Prompt reports). Data for April, March, 1990, and late data
[PB90-251224] N91-14262

SUGAR CANE
Method of selection of TM/LANDSAT color composition for analysis of land use classes
[INPE-5119-TDL/421] N91-13783

SULFIDES
CS in nearby galaxies: Distribution, kinematics, and multilevel studies N91-14235

SULFUR
Ar/S N91-14153

SULFURIC ACID
Pioneer-Venus radio occultation (ORO) data reduction: Profiles of 13 cm absorptivity
[NASA-CR-186986] N91-13584

SUN
A solar chronometer for climate: Astronomical and geophysical evidence N91-13823
Hot interstellar gas and ionization of embedded clouds N91-14161
Temporal variations of cosmic rays in the heliosphere N91-14267

SUPERCONDUCTING FILMS
Fabrication and characterization of high temperature superconducting thin films for sensors and electronics N91-14041
SQUIDs devices made from high Tc superconductors: Results and perspectives N91-14044

SUPERCONDUCTING MAGNETS
Magnetic suspension and balance system advanced study, phase 2
[NASA-CR-4327] N91-13463

SUPERCONDUCTIVITY
Monolithic mm-wave phase shifter using optically activated superconducting switches
[NASA-CASE-LEW-14878-1] N91-13996
Applications of Superconductivity to Avionics
[AGARD-CP-481] N91-14030
Physics and applications of low temperature superconductivity N91-14032
High temperature superconducting thin films for microelectronics: Preparation and properties N91-14033
Success criteria for oxide superconductor wires: Measuring the present, predicting the future N91-14034
Passive microwave devices using high temperature superconductors N91-14036
Microwave superconducting electronic devices N91-14037
High Tc superconductors for microwave filters N91-14038
The status-quo and prospect of superconducting digital devices N91-14039
Fabrication and characterization of high temperature superconducting thin films for sensors and electronics N91-14041
Application of high-temperature superconductors to high-precision accelerometers N91-14042
Superconducting Josephson Junction Gyroscope (JJG) N91-14043
The world of superconductive machinery N91-14045
Oxide superconductor coils: Present successes, future challenges N91-14046
Synthesis and characterization of high temperature superconductor materials N91-14048
Ultrafast optical electronics center
[AD-A226669] N91-14054

SUPERCONDUCTORS
Analytical and experimental studies for thermal plasma processing of materials
[DE91-000599] N91-13576
Superconducting neural network computer and sensor array
[AD-D014625] N91-13887
Success criteria for oxide superconductor wires: Measuring the present, predicting the future N91-14034
The world of superconductive machinery N91-14045

SUPERCRITICAL WINGS
Close-range photogrammetric measurement of static deflections for an aeroelastic supercritical wing
[NASA-TM-4194] N91-13400

SUPERFLUIDITY
Superfluid Stirling refrigerator: A new method for cooling below 1 Kelvin
[DE91-002311] N91-13582

SUPERGIANT STARS
The stellar content of M101 N91-14244

SUPERHIGH FREQUENCIES
S-band diplexer for a telecommunication board transponder
[INPE-4540-PRE/1286] N91-13586
Design of an X-band PIN diode phase shifter by computer optimization
[FEL-89-B286] N91-13633
A design method for an X-band diplexer
[FEL-90-B176] N91-13635

SUPERNOVA REMNANTS
CS J = 2 yields 1 emission toward the central region of M82 N91-14128
Supernova remnants and diffuse ionized gas in M31 N91-14179

SUPERNOVA 1987A
Axions and SN 1987A: Axion trapping
[NASA-CR-186467] N91-13976
Spectrum formation in SN1987A N91-14243

SUPERNOVAE
The infrared continuum spectrum of x ray illuminated molecular gas N91-14144
Radio continuum and far-infrared emission of spiral galaxies: Implications of correlations N91-14147
The interstellar halo of spiral galaxies: NGC 891 N91-14164
Gas flows in elliptical galaxies N91-14170
Evolution of a superbubble blastwave in a magnetized medium N91-14180
Infrared analysis of LMC superbubbles N91-14181
Star formation in proto dwarf galaxies N91-14212

SUPERPLASTICITY
Superplastic deformation properties of Ti-6Al-4V
[DE91-000503] N91-13757

SUPERSONIC COMBUSTION
Shock tunnel studies of scramjet phenomena, supplement 5
[NASA-CR-182096-SUPPL-5] N91-13651

SUPERSONIC COMBUSTION RAMJET ENGINES
Computed potential energy surfaces for chemical reactions
[NASA-CR-186877] N91-13506
Flow establishment in a generic scramjet combustor
[NASA-CR-187467] N91-13649
Shock tunnel studies of scramjet phenomena, supplement 5
[NASA-CR-182096-SUPPL-5] N91-13651

SUPERSONIC FLOW
Navier-Stokes and Euler solutions for lee-side flows over supersonic delta wings. A correlation with experiment
[NASA-TP-3035] N91-13401
Zero wavenumber modes of a compressible supersonic mixing layer
[NASA-CR-187476] N91-13669
One-dimensional cloud fluid model for propagating star formation N91-14211

SUPERSONIC INLETS
Theoretical evaluation of engine auxiliary inlet design for supersonic V/STOL aircraft
[NASA-CR-186610] N91-13443

SUPERSONIC JET FLOW
Instability of a supersonic shock free elliptic jet
[NASA-TM-103428] N91-13413
Large eddy simulations and direct numerical simulations of high speed turbulent reacting flows
[NASA-CR-187674] N91-13656
Water cooled static pressure probe
[NASA-CASE-LAR-14340-1-CU] N91-13684

SUPERSONIC NOZZLES
A quiet flow Ludwieg tube for study of transition in compressible boundary layers: Design and feasibility
[NASA-CR-187374] N91-13676

SUPERSONIC SPEED
Concept development of a Mach 4 high-speed civil transport
[NASA-TM-4223] N91-13432

SUPERSONIC TRANSPORTS
Concept development of a Mach 4 high-speed civil transport
[NASA-TM-4223] N91-13432
Procedure for generating global atmospheric engine emissions data from future supersonic transport aircraft. The 1990 high speed civil transport studies
[NASA-CR-181882] N91-13447
Integrated flight-propulsion - control concepts for supersonic transport airplanes
[NASA-TM-101728] N91-13460

SUPERSONIC WIND TUNNELS
Simulation of pressure and temperature responses for the 20 Inch Supersonic Wind Tunnel
[NASA-TM-102647] N91-13467

SUPPLYING
Integrated launch and emergency vehicle system
[NASA-CASE-LAR-13780-1] N91-13481

SUPPORT SYSTEMS
Research into software executives for space operations support
[NASA-CR-187013] N91-13895
The design of a distributed image processing and dissemination system
[DE91-001835] N91-13909

SUPPORTS
Post clamp
[NASA-CASE-LEW-14862-1] N91-13730

SURFACE ENERGY
Sea ice-atmosphere interaction: Application of multispectral satellite data in polar surface energy flux estimates
[NASA-CR-187376] N91-13782

SURFACE GEOMETRY
Fluid flow effects on electroplating
[DE91-001087] N91-13577
Methods for computer-aided design of free-form objects
[MA-56] N91-13921
SURFACE LAYERS
A theoretical investigation of effective surface recombination velocity in AlGaAs/GaAs heteroface solar cells
[DE91-001754] N91-13795
The evolution of comets and the detectability of Extra-Solar Oort Clouds N91-14242
SURFACE PROPERTIES
Fundamental investigations of supported monometallic and bimetallic catalysts by proton magnetic resonance spectroscopy
[DE91-000610] N91-13516
Heat exchanger fouling: Prediction, measurement, and mitigation
[DE91-001997] N91-13661
SURFACE REACTIONS
Ammonia decomposition on silicon surfaces studied using transmission FTIR spectroscopy
[AD-A226625] N91-13513
SURFACE ROUGHNESS EFFECTS
Modeling and analysis of surface roughness effects on sputtering, reflection, and sputtered particle transport
[DE91-004429] N91-14028
SURFACE TREATMENT
Biofilm monitoring coupon system
[NASA-CASE-MSC-21585-1] N91-13857
SURFACE WAVES
Description of sea wave motion and its influence on the altitude control of sea skimming missiles
[FEL-89-A368] N91-13450
SURGERY
Optical joint correlation for real-time tracking
[NASA-CASE-MSC-21509-1] N91-13997
SURVEILLANCE RADAR
Observation with stand-off radars
[FEL-90-A022] N91-13606
SURVEYS
The large-scale space distribution of emission-line galaxies N91-14091
A survey of the properties of early-type galaxies N91-14109
Empirical relationships between gas abundances and UV selective extinction N91-14116
The FCRAO extragalactic CO survey: Global properties of galaxies N91-14117
A survey of galaxies in CO N91-14118
The molecular cloud content of early type galaxies N91-14127
Molecular outflows in the L1641 region of Orion N91-14246
Design considerations for lunar base photovoltaic power systems
[NASA-TM-103642] N91-14259
SUSPENDING (MIXING)
The effect of suspended particles on Jean's criterion for gravitational instability N91-14189
SWITCHES
Monolithic mm-wave phase shifter using optically activated superconducting switches
[NASA-CASE-LEW-14878-1] N91-13996
Performance of multiplexed Ge:Ga detector arrays in the far infrared
[NASA-TM-102275] N91-14087
SWITCHING
The status-quo and prospect of superconducting digital devices N91-14039
Subnanosecond, high voltage photoconductive switching in GaAs
[DE91-002671] N91-14063
SYMBOLS
Multiple symbol differential detection
[NASA-CASE-NPO-17896-1-CU] N91-13596
SYMMETRY
Evaluation of expressions involving higher order derivations
[NASA-CR-187319] N91-13949
An asymptotic symmetry of the rapidly forced pendulum
[DE91-001868] N91-13958
SYNCHROTRON RADIATION
Synchrotron radiation photoemission study of metal overlayers on hydrogenated amorphous silicon at room temperature
[DE91-000740] N91-13525
Radio continuum and far-infrared emission of spiral galaxies: Implications of correlations N91-14147
SYNCHROTRONS
Calcified-tissue investigations using synchrotron x ray microscopy
[DE91-001729] N91-13859
SYNTHESIS (CHEMISTRY)
A new approach to design of cross-linked second-order nonlinear optical polymers
[AD-A226874] N91-13553
Preparation of polyimides from bis(N-isoprenyl)s of aryl diamides
[NASA-CASE-LAR-14330-1-CU] N91-13560
SYNTHETIC APERTURE RADAR
Method for providing a polarization filter for processing synthetic aperture radar image data
[NASA-CASE-NPO-17904-1-CU] N91-13594
Pipeline synthetic aperture radar data compression utilizing systolic binary tree-searched architecture for vector quantization
[NASA-CASE-NPO-17941-1-CU] N91-13595
SAR detection of topography, vegetation and installations over land
[FFI-90/7016] N91-13600
System and method for measuring ocean surface currents at locations remote from land masses using synthetic aperture radar
[NASA-CASE-NPO-17937-1-CU] N91-13787
CESAR MALU program library
[FFI-90/7010] N91-13922
BAG: A programming language for the CESAR buffer address generator
[FFI-90/7022] N91-13923
CESAR trap program library
[FFI-90/7023] N91-13924
SYNTHETIC APERTURES
Aperture synthesis CO observations of the inner disk of NGC 1068 N91-14122
SYNTHETIC FUELS
An exploratory program for using hydrous metal oxide ion exchangers as Fischer-Tropsch catalysts
[DE91-002341] N91-13521
SYSTEM IDENTIFICATION
Proceedings of the Workshop on Software Tools for Distributed Intelligent Control Systems
[DE91-001755] N91-13943
SYSTEMS ANALYSIS
Guidnace simulation model of antisea-skimmer utilization for weapon system definition N91-13438
Guidance methods for tactical and strategic missiles N91-13442
On the design of component test plans based on system reliability objectives
[DE90-017034] N91-13745
Dissipative controller designs for second-order dynamic systems
[NASA-CR-187452] N91-13935
SYSTEMS ENGINEERING
An improved exploratory search technique for pure integer linear programming problems
[NASA-TM-103517] N91-13910
SYSTEMS INTEGRATION
Integrated flight-propulsion control concepts for supersonic transport airplanes
[NASA-TM-101728] N91-13460
Research into software executives for space operations support
[NASA-CR-187013] N91-13895
SYSTEMS STABILITY
About transient stability of power systems: Statistical pattern recognition approach
[LAAS-90192] N91-13889
SYSTOLIC ARRAYS
Pipeline synthetic aperture radar data compression utilizing systolic binary tree-searched architecture for vector quantization
[NASA-CASE-NPO-17941-1-CU] N91-13595
Feasibility study, software design, layout and simulation of a two-dimensional fast Fourier transform machine for use in optical array interferometry
[NASA-CR-186922] N91-13885

T

TAIL ASSEMBLIES
Aerodynamic effect of strakes on two-dimensional tail boom models of the OH-58A and the OH-58D helicopters
[NASA-TM-4248] N91-13406
Some buffet response characteristics of a twin-vertical-tail configuration
[NASA-TM-102749] N91-13412
TANKS (COMBAT VEHICLES)
Study system concept for a pelotons procedure trainer (PEP-trainer) for the weapon systems YPR-PRAT, YPR-25 mm (EWS) and Leopard 1-5
[FEL-90-A084] N91-13871
TARGET ACQUISITION
Advanced missile guidance N91-13439
Observation with stand-off radars
[FEL-90-A022] N91-13606
An indexed bibliography on tracking
[AD-A226682] N91-13870
Multispectral target detection using image processing programs developed on PC's
[FEL-89-B304] N91-13925
TARGET RECOGNITION
An indexed bibliography on tracking
[AD-A226682] N91-13870
Multispectral target detection using image processing programs developed on PC's
[FEL-89-B304] N91-13925
TARGETS
Standard remote manipulator system docking target augmentation for automated docking
[NASA-CASE-MFS-28419-1] N91-13482
Materials impurity analysis by means of nuclear resonance reactions
[DE91-001758] N91-13520
Bilevel shared control for teleoperators
[NASA-CASE-NPO-17800-1-CU] N91-13724
Penetration of yawed projectiles
[DE91-001084] N91-13726
Motion detection, novelty filtering, and target tracking using an interferometric technique with a GaAs phase conjugate mirror
[NASA-CASE-NPO-17784-1-CU] N91-13998
Apparatus for precision focusing and positioning of a beam waist on a target
[NASA-CASE-ARC-11916-1-SB] N91-14002
TASK COMPLEXITY
A subjective rating scale for assessing pilot workload in flight: A decade of practical use
[RAE-TR-90019] N91-13882
TASK PLANNING (ROBOTICS)
Generic extravehicular (EVA) and telerobot task primitives for analysis, design, and integration. Version 1.0: Reference compilation for the EVA and telerobotics communities
[NASA-CR-187429] N91-13876
TECHNICAL WRITING
Report of foreign travel
[DE91-001732] N91-14082
TECHNOLOGIES
JPRS Report: Science and technology. USSR: Life sciences
[JPRS-ULS-89-011] N91-13861
Technical communications in aerospace: An analysis of the practices reported by US and European aerospace engineers and scientists
[NASA-TM-103441] N91-14079
TECHNOLOGY ASSESSMENT
The third generation of Soviet civilian-use turbofan engines
[AD-A225392] N91-13454
Laser programs highlights, July - August 1990
[DE91-001056] N91-13709
Status of lattice field theory calculations
[DE91-001141] N91-14057
TECHNOLOGY TRANSFER
Activities report of the Max-Planck Institute for Aeronomy
[ETN-91-98383] N91-14272
TECHNOLOGY UTILIZATION
Miniature closed cycle refrigerators N91-14035
TECTONICS
Fractals and chaotic dynamics in tectonics: Applications to topography and seismicity N91-13821
Precision, accuracy, and tectonics from the Global Positioning System N91-13822
Proceedings of the MEVTV Workshop on The Evolution of Magma Bodies on Mars
[NASA-CR-187357] N91-14252
Mars tectonics and volcanism
[NASA-CR-187351] N91-14254
TEETH
Calcified-tissue investigations using synchrotron x ray microscopy
[DE91-001729] N91-13859
TELECOMMUNICATION
S-band diplexer for a telecommunication board transponder
[INPE-4540-PRE/1286] N91-13586
Overview of European technology in computers, telecommunications, and electronics
[PB90-215773] N91-13610
Research into alternative network approaches for space operations
[NASA-CR-187015] N91-13894
The design of a distributed image processing and dissemination system
[DE91-001835] N91-13909
TELEOPERATORS
Bilevel shared control for teleoperators
[NASA-CASE-NPO-17800-1-CU] N91-13724

An application of oscillation damped motion for suspended payloads to the advanced integrated maintenance system
[DE91-002658] N91-13946

TELEROBOTICS
Telerobotic on-orbit remote fluid resupply system
[NASA-CR-184052] N91-13474
Generic extravehicular (EVA) and telerobot task primitives for analysis, design, and integration. Version 1.0: Reference compilation for the EVA and telerobotics communities
[NASA-CR-187429] N91-13876

TELESCOPES
FIRST: Far Infrared and Submillimetre Space Telescope
[ESA-BR-69] N91-14095
CO observations of southern mergers N91-14197
Deep narrow band imagery of the diffuse ISM in M33 N91-14202
High spatial resolution studies of galaxies in the far IR: Observations with the KAO, and the promise of SOFIA N91-14229

TELEVISION SYSTEMS
Optical joint correlation for real-time tracking
[NASA-CASE-MSC-21509-1] N91-13997

TEMPERATURE CONTROL
Definition study for temperature control in advanced protein crystal growth
[NASA-CR-187346] N91-14029

TEMPERATURE DEPENDENCE
Laser-induced fluorescence of phosphors for remote cryogenic thermometry
[DE91-001733] N91-13681
Theoretical temperature-dependent branching ratios and laser thresholds of the (5)I7 yields (5)I8 levels of Ho3(+) in ten garnets
[NASA-TM-103429] N91-14053

TEMPERATURE EFFECTS
Simulation of pressure and temperature responses for the 20 Inch Supersonic Wind Tunnel
[NASA-TM-102647] N91-13467
Effects of temperature on acoustically-induced strains and damage propagation in CFRP plates N91-13493
Experimental and theoretical determination of the thermomechanical response of inelastic structural materials to high energy thermal inputs
[AD-A226671] N91-13496
Oxidation characteristics of Ti-25Al-10Nb-3V-1Mo intermetallic alloy
[NASA-TP-3044] N91-13522
The effect of longitudinal spacer ribs on the minimum pressure drop in a heated annulus
[DE91-000784] N91-13655
Material and mechanical characterizations for braided composite pressure vessels
[AD-A226640] N91-13713
The effects of thermal treatment after welding on the functional properties of assemblies. Follow-up of the work on Cr-Mo
[CETIM-104720] N91-13739
A comparative study of ductile fracture in the 2.25 percent Cr-1 percent Mo and 9 percent Cr-1 percent Mo alloy steels N91-13753
A review of nonlinear constitutive models for metals
[NASA-TM-102727] N91-13761
Sustained-load crack growth of 8090 aluminium-lithium alloy plate in dry air at 50-200 C
[RAE-TR-90033] N91-13777
The effect of condensation in clothing on heat transfer
[IZF-1990-B-5] N91-13881

TEMPERATURE GRADIENTS
Experimental and theoretical determination of the thermomechanical response of inelastic structural materials to high energy thermal inputs
[AD-A226671] N91-13496
Assessments of atmospheric effects on VHF and UHF communications
[AD-A226661] N91-13592
Definition study for temperature control in advanced protein crystal growth
[NASA-CR-187346] N91-14029

TEMPERATURE MEASUREMENT
Evaluation of Raytek infrared pyrometer for continuous propellant temperature measurement
[NASA-CR-184040] N91-13570
Plug-type heat flux gauge and method of producing same
[NASA-CASE-LEW-14967-1] N91-13685

TEMPORAL DISTRIBUTION
Mesoscale monitoring of the soil freeze/thaw boundary from orbital microwave radiometry
[NASA-CR-185901] N91-13817
Temporal variations of cosmic rays in the heliosphere N91-14267

TEMPORAL RESOLUTION
Ground-based studies of emission-line variability: Recent results for NGC 5548 and future plans
[NASA-CR-180433] N91-14088

TENSILE PROPERTIES
Tubular lap joints for wind turbine applications
[DE91-001341] N91-13736
Mechanical properties of 1950's vintage Type 304 stainless steel weldment components
[DE91-004328] N91-13774

TENSILE STRENGTH
Study of the metallurgical effects of hammering between passes during C-Mn weld deposition
[CETIM-104850] N91-13532
Mechanical testing of advanced coating system, volume 1
[NASA-CR-186725] N91-13534
Material and mechanical characterizations for braided composite pressure vessels
[AD-A226640] N91-13713
Study of the tensile strength of the melted zone of vertical welds carried out using electroslag welding on C-Mn steel. Further study on 80 mm thick plate
[CETIM-104730] N91-13740
Study of the metallurgical consequences of hammering between passes to compensate for the withdrawal of metal caused by welding
[CETIM-104430] N91-13741

TENSILE STRESS
Use of dome (meniscus) lenses to eliminate birefringence and tensile stresses in spatial filters for the Nova laser
[DE91-002784] N91-13707

TENSION
Calibration set up for load cells
[PD-ST-8917] N91-13673

TERMINAL GUIDANCE
Midcourse guidance technologies for advanced tactical missiles systems N91-13436

TERMINOLOGY
Report of foreign travel
[DE91-001732] N91-14082

TEST EQUIPMENT
The Improved Three Axis Test Table (ITATT): Program status and recommendation for completion
[AD-A226508] N91-13712

TEST FIRING
RL10A-3-3B high mixture ratio qualification program
[NASA-CR-183200] N91-13486

TETHERING
Tethering sockets and wrenches
[NASA-CR-184032] N91-13675

TETRAHEDRONS
Analytical and photogrammetric characterization of a planar tetrahedral truss
[NASA-TM-4231] N91-13473

TEXAS
High energy physics program at Texas A&M University
[DE91-001639] N91-13989

TEXTURES
The influence of the texture of Al2O3 substrates on the fracture behavior under thermal loading N91-13543

THALLIUM
X ray and charged particle detection with CsI(Tl) layer coupled to a-Si:H photodiode layers
[DE91-001798] N91-14060

THEMATIC MAPPING
Method of selection of TM/LANDSAT color composition for analysis of land use classes
[INPE-5119-TDL/421] N91-13783
Methodological contribution utilizing TM/LANDSAT-5 imagery in geologic mapping of regions with significant vegetative cover
[INPE-5117-TDL/419] N91-13784
The importance of fracturing in the Pimenta Bueno-Ro Basin structure: A study of the morphostructural elements of the rupture-ductile character through remote sensing techniques and products
[INPE-5004-TDL/398] N91-13825

THEOREM PROVING
Semantic validation of structured theories: Applications to a generic programming language
[ETN-91-98207] N91-13916
Dissipative controller designs for second-order dynamic systems
[NASA-CR-187452] N91-13935

THEORETICAL PHYSICS
High energy physics program at Texas A&M University
[DE91-001639] N91-13989
U1(prime) dark matter and R-parity violation
[DE91-001792] N91-14068
Research in theoretical physics
[DE91-002458] N91-14071

THERMAL ANALYSIS
ESATAN: User manual
[ESA-PSS-03-105-ISSUE-1] N91-13897

THERMAL CONDUCTIVITY
Flexible thermal apparatus for mounting of thermoelectric cooler
[NASA-CASE-NPO-17806-1-CU] N91-13581
Transport properties of dense fluid mixtures using nonequilibrium molecular dynamics
[DE91-000262] N91-13654
Heat transfer device and method of making the same
[NASA-CASE-LEW-14162-1] N91-13668

THERMAL CONTROL COATINGS
Composite thermal barrier coating
[NASA-CASE-LEW-14999-1] N91-13500
Fatigue testing of plasma-sprayed thermal barrier coatings, volume 2
[NASA-CR-186726] N91-13535

THERMAL CYCLING TESTS
Influence of oxide reinforcement materials on high-temperatue oxidation resistance of Ni3Al matrix composites
[DE91-001625] N91-13498

THERMAL DECOMPOSITION
Ammonia decomposition on silicon surfaces studied using transmission FTIR spectroscopy
[AD-A226625] N91-13513
Synthesis and characterization of high temperature superconductor materials N91-14048

THERMAL EMISSION
Emission from small dust particles in diffuse and molecular cloud medium N91-14137
Observations of the galactic plane by the zodiacal infrared project N91-14143
The infrared continuum spectrum of x ray illuminated molecular gas N91-14144
H2 line emission in three Seyfert nuclei: Evidence against UV-excitation N91-14185

THERMAL ENERGY
Thermal power transfer system using applied potential difference to sustain operating pressure difference
[NASA-CASE-NPO-18034-1-CU] N91-13796
Small particle selective emitter
[NASA-CASE-LEW-14731-1] N91-13802

THERMAL FATIGUE
Material degradation of steam turbine rotors in long term operations
[VTT-RR-692] N91-13530
The influence of the texture of Al2O3 substrates on the fracture behavior under thermal loading N91-13543

THERMAL INSTABILITY
Thermal instabilities in protogalactic clouds N91-14195

THERMAL PLASMAS
Analytical and experimental studies for thermal plasma processing of materials
[DE91-000599] N91-13576
Simultaneous measurement of Ni-Al particle size, velocity, and temperature in atmospheric thermal plasmas
[DE91-001935] N91-13826

THERMAL PROTECTION
An assessment of wind tunnel test data on flexible thermal protection materials and results of new fatigue tests of threads
[NASA-CR-177466] N91-13972

THERMOCOUPLES
Plug-type heat flux gauge and method of producing same
[NASA-CASE-LEW-14967-1] N91-13685

THERMODYNAMIC CYCLES
Performance comparison of magnetic refrigeration cycles
[DE91-001520] N91-13578

THERMODYNAMIC PROPERTIES
Study of improved methods for predicting chemical equilibria
[DE91-000263] N91-13509

THERMODYNAMICS
Influence of thermodynamical modelization for chemically reacting air flow
[MBB/FE122/S/PUB/400] N91-13418
Experimental and theoretical determination of the thermomechanical response of inelastic structural materials to high energy thermal inputs
[AD-A226671] N91-13496
Study of improved methods for predicting chemical equilibria
[DE91-000263] N91-13509
Second law analysis of advanced power generation systems using variable temperature heat sources
[DE91-001818] N91-13799
Algorithmic information content, Church-Turing thesis, physical entropy, and Maxwell's demon
[DE91-001804] N91-14069

THERMOELECTRICITY
Flexible thermal apparatus for mounting of thermoelectric cooler
[NASA-CASE-NPO-17806-1-CU] N91-13581

THERMOGRAPHY
Laser-induced fluorescence of phosphors for remote cryogenic thermometry
[DE91-001733] N91-13681
THERMONUCLEAR REACTIONS
International Thermonuclear Experimental Reactor physics basis
[DE91-002646] N91-14017
THERMOPLASTICITY
Binders used in metal injection molding
[VTT-RR-691] N91-13529
THERMOREGULATION
Thermoregulatory consequences of resonant microwave exposure
[AD-A226540] N91-13864
THERMOSETTING RESINS
Physical properties of thermosetting polymers
[AD-A225864] N91-13508
THICK PLATES
Constrained viscoelastic layer damping of thick aluminum plates: Design, analysis, and testing
[AD-A226556] N91-13758
THIN FILMS
Magnetic field effect transistors
[AD-A226535] N91-13614
Biofilm monitoring coupon system
[NASA-CASE-MSC-21585-1] N91-13857
Surfaces and thin films studied by picosecond ultrasonics
[DE91-004167] N91-13973
Injection efficiency of bound modes
[NASA-CR-4333] N91-13991
Progress in high Tc superconductors N91-14031
High temperature superconducting thin films for microelectronics: Preparation and properties N91-14033
Fabrication and characterization of high temperature superconducting thin films for sensors and electronics N91-14041
THIN WALLED SHELLS
Analysis of shells as 3D-elasticity problems using the p-version of the FE method
[FFA-TN-1990-25] N91-13770
THOMSON SCATTERING
A multi-laser system for a fast sampling Thomson scattering diagnostic
[DE91-002708] N91-13705
A silicon avalanche photodiode detector circuit for Nd:YAG laser scattering
[DE91-002709] N91-13706
A compact, low cost, 7 channel polychromator for Thomson scattering measurements
[DE91-002719] N91-14024
A real-time digital control, data acquisition and analysis system for the DIII-D multipulse Thomson scattering diagnostic
[DE91-002720] N91-14025
THREE DIMENSIONAL BODIES
On the variation in crack-opening stresses at different locations in a three-dimensional body
[NASA-CR-187722] N91-13768
Accurate and reliable computation of complete solutions to the equations of linear elastomechanics on three-dimensional domains: Computation of edge stress intensity functions
[FFA-TN-1989-12] N91-13769
Analysis of shells as 3D-elasticity problems using the p-version of the FE method
[FFA-TN-1990-25] N91-13770
Accurate and reliable determination of edge and vertex stress intensity factors in three-dimensional elastomechanics
[FFA-TN-1990-28] N91-13771
THREE DIMENSIONAL FLOW
A laser Doppler velocimeter approach for near-wall three-dimensional turbulence measurements
[NASA-TM-102841] N91-13653
THREE DIMENSIONAL MODELS
FE analyses of aircraft model with interior trim
[FFA-TN-1990-21] N91-13417
THRUST CHAMBERS
Thrust chamber modeling using Navier-Stokes equations: Code documentation and listings, volume 2
[NASA-CR-183617] N91-13489
THUNDERSTORMS
DOPLIGHT 1987 project summary
[PB90-253584] N91-13834
A study of the ice-hail charge separation mechanism using a thunderstorm electrification model with explicit microphysics in a kinematic framework N91-13835
TIGHTNESS
Bolted structural assemblies: Bibliographic analysis
[CETIM-13N061] N91-13742
TILES
An assessment of wind tunnel test data on flexible thermal protection materials and results of new fatigue tests of threads
[NASA-CR-177466] N91-13972
TILT ROTOR AIRCRAFT
Civil tiltrotor missions and applications
[NASA-CR-177452] N91-13424
TIME DEPENDENCE
Development of a time-dependent incompressible Navier-Stokes solver based on a fractional-step method
[NASA-CR-182323] N91-13639
TIME FUNCTIONS
Logics for the description of processes and their properties: Expressivity and decidability
[ETN-91-98200] N91-13960
TIME RESPONSE
Time domain finite difference analysis of antennas
[AD-A226534] N91-13613
TIME SERIES ANALYSIS
Interpretation of engine cycle-to-cycle variation by chaotic time series analysis
[DE91-000729] N91-13955
On the invertibility of Leslie systems
[REPT-90-006] N91-13963
TIME TEMPERATURE PARAMETER
Physical properties of thermosetting polymers
[AD-A225864] N91-13508
TISSUES (BIOLOGY)
Calcified-tissue investigations using synchrotron x ray microscopy
[DE91-001729] N91-13859
Three-dimensional cell to tissue assembly process
[NASA-CASE-MSC-21559-1] N91-13860
TITANIUM
Interfacial chemistry of titanium films deposited on PMDA-ODA polyimide
[AD-A225730] N91-13550
TITANIUM ALLOYS
Oxidation characteristics of Ti-25Al-10Nb-3V-1Mo intermetallic alloy
[NASA-TP-3044] N91-13522
Research and development for improved toughness aluminides
[AD-A226627] N91-13524
Superplastic deformation properties of Ti-6Al-4V
[DE91-000503] N91-13757
TOILETS
Hydraulic lifting device
[NASA-CASE-SSC-00008-1] N91-13733
TOKAMAK DEVICES
Free-electron laser experiments in the microwave tokamak experiment
[DE91-001746] N91-13699
A multi-laser system for a fast sampling Thomson scattering diagnostic
[DE91-002708] N91-13705
A silicon avalanche photodiode detector circuit for Nd:YAG laser scattering
[DE91-002709] N91-13706
Plasma properties
[DE91-001361] N91-14006
Confinement properties of the RFP (reversed field pinch)
[DE91-002322] N91-14015
Compact Ignition Tokamak project: Localizability of electron-cyclotron heating power
[DE91-002571] N91-14016
International Thermonuclear Experimental Reactor physics basis
[DE91-002646] N91-14017
ITER confinement capability
[DE91-002647] N91-14018
Dependence of CIT (compact ignition tokamak) PF (poloidal field) coil currents on profile and shape parameters using the control matrix
[DE91-002650] N91-14019
A compact, low cost, 7 channel polychromator for Thomson scattering measurements
[DE91-002719] N91-14024
A real-time digital control, data acquisition and analysis system for the DIII-D multipulse Thomson scattering diagnostic
[DE91-002720] N91-14025
TOLERANCES (PHYSIOLOGY)
The effect of condensation in clothing on heat transfer
[IZF-1990-B-5] N91-13881
TOOLS
Robot cable-compliant devices
[NASA-CASE-GSC-13127-1] N91-13735
TOPEX
Report by the Subcommitee on Intercomparison and Merging of Geodetic Data of the Topex/Poseidon science working team
[LR-638] N91-13791
TOPOGRAPHY
SAR detection of topography, vegetation and installations over land
[FFI-90/7016] N91-13600
Fractals and chaotic dynamics in tectonics: Applications to topography and seismicity N91-13821
TOPOLOGY
New phases of D greater than or equal to 2 current and diffeomorphism algebras in particle physics
[DE91-001515] N91-14067
TOROIDAL PLASMAS
Kinetic and electromagnetic transport processes in toroidal devices
[DE91-001901] N91-14011
International Thermonuclear Experimental Reactor physics basis
[DE91-002646] N91-14017
High spatial and temporal resolution visible spectroscopy of the plasma edge in DIII-D
[DE91-002718] N91-14023
TOUGHNESS
Potential impact of enhanced fracture-toughness data on pressurized-thermal-shock analysis
[DE91-001493] N91-13763
TOXIC HAZARDS
Environmental projects. Volume 12: Friable asbestos abatement, GDSCC
[NASA-CR-187636] N91-13808
TOXICITY AND SAFETY HAZARD
Environmental projects. Volume 12: Friable asbestos abatement, GDSCC
[NASA-CR-187636] N91-13808
TRACE CONTAMINANTS
Soil bed reactor work of the Environmental Research Lab. of the University of Arizona in support of the research and development of Biosphere 2 N91-13846
TRACKING (POSITION)
Positional estimation techniques for an autonomous mobile robot
[NASA-CR-187689] N91-13725
Optical joint correlation for real-time tracking
[NASA-CASE-MSC-21509-1] N91-13997
Motion detection, novelty filtering, and target tracking using an interferometric technique with a GaAs phase conjugate mirror
[NASA-CASE-NPO-17784-1-CU] N91-13998
TRAINING DEVICES
The effect of stereoscopic presentation on a simulated air traffic control task
[IZF-1989-53] N91-13431
Study system concept for a pelotons procedure trainer (PEP-trainer) for the weapon systems YPR-PRAT, YPR-25 mm (EWS) and Leopard 1-5
[FEL-90-A084] N91-13871
TRAINING SIMULATORS
The effect of stereoscopic presentation on a simulated air traffic control task
[IZF-1989-53] N91-13431
TRAJECTORIES
Bilevel shared control for teleoperators
[NASA-CASE-NPO-17800-1-CU] N91-13724
An application of oscillation damped motion for suspended payloads to the advanced integrated maintenance system
[DE91-002658] N91-13946
The simultaneous integration of many trajectories using nilpotent normal forms
[NASA-CR-187318] N91-13950
TRANSDUCERS
Transducer holder and method of making
[NASA-CASE-LAR-14027-1] N91-13693
TRANSFORMATIONS (MATHEMATICS)
Programmable remapper with single flow architecture
[NASA-CASE-MSC-21481-1] N91-13890
Utilization of IHS transformation for integration of images of differing resolutions: Urban land use study
[INPE-4606-PRE/1329] N91-14086
TRANSIENT RESPONSE
Analytical study of the liquid phase transient behavior of a high temperature heat pipe
[NASA-CR-187426] N91-13644
Effect of lubricating oil characteristics on gear vibrations N91-13710
TRANSISTORS
Single event upset hardening techniques
[DE91-002337] N91-13625
Multiplexer/amplifier test results for SP-100
[DE91-004504] N91-13990
TRANSITION FLOW
Large-eddy simulation of transitional channel flow
[NASA-CR-187465] N91-13410
TRANSITION METALS
Non-empirical interatomic potentials for transition metals, alloys, and semiconductors
[DE91-002396] N91-14062

TRANSITION TEMPERATURE
Physical properties of thermosetting polymers
[AD-A225864] N91-13508
TRANSLATIONAL MOTION
Development and evaluation of continuum models for translational-rotational nonequilibrium N91-13403
TRANSMISSION LOSS
Frequency-domain analysis of one-dimensional electromagnetic scattering by lossy media
[FEL-90-A112] N91-13607
TRANSMITTER RECEIVERS
Optical shared memory system demonstration model
[AD-A226431] N91-13612
TRANSONIC FLOW
Transonic blade-vortex interactions noise: A parametric study
[NASA-CR-187713] N91-13422
TRANSONIC WIND TUNNELS
Transonic wind tunnel tests on two-dimensional aerofoil sections: Determination of pressure distribution and drag for an aerofoil of type SAAB 7301 in FFA wind tunnel S5
[FFA-TN-1989-47] N91-13416
TRANSPONDERS
Loading the LES-9 wideband UHF transponder
[AD-A226179] N91-13475
S-band diplexer for a telecommunication board transponder
[INPE-4540-PRE/1286] N91-13586
TRANSPORT AIRCRAFT
Effect of location of aft-mounted nacelles on the longitudinal aerodynamic characteristics of a high-wing transport airplane
[NASA-TP-3047] N91-13402
TRANSPORT PROPERTIES
The coupling of finite methods for transport-diffusion problems
[ETN-91-98172] N91-13663
Aeronomic chemistry of ozone
[AERONOMICA-ACTA-A-355-1990] N91-13816
Progress in high Tc superconductors N91-14031
TRANSPORTATION NETWORKS
Civil tiltrotor missions and applications
[NASA-CR-177452] N91-13424
TRANSPUTERS
NDRE/TAll processor architecture study
[FFI-90/7012] N91-13891
TRAPPED PARTICLES
Axions and SN 1987A: Axion trapping
[NASA-CR-186467] N91-13976
A critical review of charged particle astronomy at Saturn: The evidence for co-orbiting material in the inner satellite system
[NASA-CR-187348] N91-14090
TRAVELING WAVE TUBES
Extremely High Frequency (EHF) Low Probability of Intercept (LPI) communication applications
[AD-A226653] N91-13591
TRAVELING WAVES
Relativistic kylstron simulations using RKTW2D
[DE91-001747] N91-13619
TREES (PLANTS)
The relation between tree physiology and multispectral and color photography: First phase
[BCRS-89-39] N91-13785
TRIANGULATION
Analytical and experimental research on large angle maneuvers of flexible structures
[AD-A226679] N91-13479
Precision, accuracy, and tectonics from the Global Positioning System N91-13822
TRIBOLOGY
Friction and wear of TPS fibers: A study of the adhesion and friction of high modulus fibers
[NASA-CR-187666] N91-13515
Advanced Materials Development Program: Ceramic Technology for Advanced Heat Engines program plan, 1983--1993
[DE91-000516] N91-13555
TRINITROTOLUENE
All hot spots are not equal
[DE91-002303] N91-13573
TRISONIC WIND TUNNELS
The IAR high Reynolds number two-dimensional test facility: A description of equipment and procedures common to most 2-D airfoil tests
[AD-A226629] N91-13409
TRITIUM
An interactive program for the analysis and design of advanced laser targets
[DE91-002542] N91-13704
Tritium method oil consumption and its relation to oil film thickness in a production diesel engine
[AD-A226649] N91-13714
Fast Pb-glass neutron-to-light converter for ICF (Inertial Confinement Fusion) target burn history measurements
[DE91-002670] N91-14021
TROPICAL REGIONS
Tropical Pacific moisture variability: Its detection, synoptic structure and consequences in the general circulation
[NASA-CR-184045] N91-13832
TROPOSPHERE
Aeronomic chemistry of ozone
[AERONOMICA-ACTA-A-355-1990] N91-13816
Review of geography internship of convective wave project
[NASA-CR-187022] N91-13819
TRUSSES
Analytical and photogrammetric characterization of a planar tetrahedral truss
[NASA-TM-4231] N91-13473
TUNABLE LASERS
Study and development of tunable, single mode AlGaAs/GaAs lasers
[DE91-001684] N91-13697
TUNGSTEN
Distortion-free x ray mask technology
[AD-A226524] N91-13993
Modeling and analysis of surface roughness effects on sputtering, reflection, and sputtered particle transport
[DE91-004429] N91-14028
TUNGSTEN ALLOYS
Penetration of yawed projectiles
[DE91-001084] N91-13726
TURBINE BLADES
Spanwise aerodynamic loads on a rotating wind turbine blade
[DE91-002101] N91-13414
TURBOFANS
The third generation of Soviet civilian-use turbofan engines
[AD-A225392] N91-13454
TURBOMACHINERY
Computation of broadband mixing noise from turbomachinery
[AD-A226559] N91-13969
TURBULENCE
Some observations on the Houbolt-Rainey and peak-hold methods of flutter onset prediction
[NASA-TM-102745] N91-13411
Turbulence and pressure loss characteristics of the inlet vanes for the 80- by 120-ft wind tunnel
[NASA-TM-102808] N91-13466
Topics in physico-chemical hydrodynamics
[DE91-001674] N91-13519
A laser Doppler velocimeter approach for near-wall three-dimensional turbulence measurements
[NASA-TM-102841] N91-13653
Frontogenesis in gravity currents: The effect of endwalls and diffusion
[MATHS-REPT-A-127] N91-13666
Magnetic turbulent electron transport in a reversed field pinch
[DE91-001898] N91-14009
Origin and dynamics of emission line clouds in cooling flow environments N91-14167
TURBULENCE EFFECTS
Free-stream turbulence and concave curvature effects on heated, transitional boundary layers, volumes 1 and 2 N91-13643
TURBULENCE MODELS
Reynolds stress closure in jet flows using wave models
[NASA-CR-185717] N91-13640
Toward the large-eddy simulation of compressible turbulent flows
[NASA-CR-187460] N91-13650
TURBULENT BOUNDARY LAYER
Turbulence modeling for sharp-fin-induced shock wave/turbulent boundary-layer interactions
[NASA-TM-102828] N91-13652
TURBULENT DIFFUSION
A study of confined diffusion flames
[AD-A226552] N91-13512
TURBULENT FLOW
Large-eddy simulation of transitional channel flow
[NASA-CR-187465] N91-13410
Topics in physico-chemical hydrodynamics
[DE91-001674] N91-13519
Free-stream turbulence and concave curvature effects on heated, transitional boundary layers, volumes 1 and 2 N91-13643
Toward the large-eddy simulation of compressible turbulent flows
[NASA-CR-187460] N91-13650
Turbulence modeling for sharp-fin-induced shock wave/turbulent boundary-layer interactions
[NASA-TM-102828] N91-13652
A laser Doppler velocimeter approach for near-wall three-dimensional turbulence measurements
[NASA-TM-102841] N91-13653
A minimization method adapted to the finite element technique for turbulent flow simulation with nonlinear boundary conditions in the wall vicinity
[ECL-90-016] N91-13664
Coherent anti-Stokes Raman spectroscopic measurement of air entrainment in argon plasma jets
[DE91-001936] N91-13670
Measurement of air entrainment in plasma jets
[DE91-001943] N91-14013
TURBULENT JETS
Modelization of two phase turbulent jet up to its auto ignition in variable pressure and temperature environments
[ETN-91-98341] N91-13665
TURBULENT MIXING
Large eddy simulations and direct numerical simulations of high speed turbulent reacting flows
[NASA-CR-187674] N91-13656
TURBULENT WAKES
Far field wake velocity measurements with hot film probes
[AD-A226650] N91-13647
TWO DIMENSIONAL MODELS
Transonic wind tunnel tests on two-dimensional aerofoil sections: Determination of pressure distribution and drag for an aerofoil of type SAAB 7301 in FFA wind tunnel S5
[FFA-TN-1989-47] N91-13416
Theoretical evaluation of engine auxiliary inlet design for supersonic V/STOL aircraft
[NASA-CR-186610] N91-13443
Free-stream turbulence and concave curvature effects on heated, transitional boundary layers, volumes 1 and 2 N91-13643
TWO PHASE FLOW
Modelization of two phase turbulent jet up to its auto ignition in variable pressure and temperature environments
[ETN-91-98341] N91-13665

U

U.S.S.R.
JPRS Report: Science and technology. USSR: Life sciences
[JPRS-ULS-89-011] N91-13861
UH-60A HELICOPTER
A review of ice accretion data from a model rotor icing test and comparison with theory
[NASA-TM-103712] N91-13421
ULTRAHIGH FREQUENCIES
S-band diplexer for a telecommunication board transponder
[INPE-4540-PRE/1286] N91-13586
Assessments of atmospheric effects on VHF and UHF communications
[AD-A226661] N91-13592
ULTRASONIC SPECTROSCOPY
Analysis of bond quality by resonant ultrasound
[DE91-000439] N91-13743
ULTRASONIC TESTS
Damage assessment and residual compression strength of thick composite plates with through-the-thickness reinforcements
[NASA-CR-187377] N91-13494
Determination of stresses in ceramics using ultrasonic methods: Possibilities and limitations N91-13546
Testing of engineering ceramics, summary
[VTT-RR-678] N91-13567
Analysis of bond quality by resonant ultrasound
[DE91-000439] N91-13743
ULTRASONICS
Analysis of bond quality by resonant ultrasound
[DE91-000439] N91-13743
Ultrasound generation through a fiber optic delivery system using pulsed laser energy
[DE91-001914] N91-13970
Surfaces and thin films studied by picosecond ultrasonics
[DE91-004167] N91-13973
ULTRAVIOLET ABSORPTION
Ultraviolet absorption cross-sections of photoactive species of stratospheric interest. Part 1: The halocarbons
[ETN-91-98385] N91-13830
H2 line emission in three Seyfert nuclei: Evidence against UV-excitation N91-14185
ULTRAVIOLET RADIATION
The interstellar halo of spiral galaxies: NGC 891 N91-14164
UNDERGROUND STRUCTURES
Feasibility of cosmic-ray muon intensity measurements for tunnel detection
[AD-A223355] N91-14266

UNITED KINGDOM
UK airlines' cost structure and implications of air transport services fragmentation. Research report on air transport fragmentation
[TT-9011] N91-13427
UNIVERSITIES
The CO-12 and CO-13 J=2-1 and J=1-0 observations of hot and cold galaxies N91-14126
UNIVERSITY PROGRAM
High energy physics program at Texas A&M University
[DE91-001639] N91-13989
UNSTEADY AERODYNAMICS
Indicial response approach derived from Navier-Stokes equations. Part 1: Time-invariant equilibrium state
[NASA-TM-102856] N91-13408
Analytic formulations of unsteady profile aerodynamics and its application to simulation of rotors
[DLR-FB-90-28] N91-13415
UNSTEADY FLOW
Nonlinear viscous waves produced by an impulsively moving plate N91-13641
Flow establishment in a generic scramjet combustor
[NASA-CR-187467] N91-13649
UPLINKING
Loading the LES-9 wideband UHF transponder
[AD-A226179] N91-13475
URANUS RINGS
The origin and evolution of the Uranian dust rings N91-14253
USER MANUALS (COMPUTER PROGRAMS)
Temporal scattering and response software: Users' manual
[DE91-001760] N91-13593
ESATAN: User manual
[ESA-PSS-03-105-ISSUE-1] N91-13897
Pressure visualization (PreViz) package version 1.0 user's guide
[NASA-CR-187444] N91-13907
Image 3.3: Tutorial manual
[DE91-001762] N91-13908
BAG: A programming language for the CESAR buffer address generator
[FFI-90/7022] N91-13923
USER REQUIREMENTS
Federal information inventory/locator systems: From burden to benefit N91-14074
Information systems supported end-user interaction: Impacts on inter- and intra-organizational connectivity and cooperative behavior N91-14075

V

V/STOL AIRCRAFT
Theoretical evaluation of engine auxiliary inlet design for supersonic V/STOL aircraft
[NASA-CR-186610] N91-13443
An AD100 implementation of a real-time STOVL aircraft propulsion system
[NASA-TM-103683] N91-13457
VALIDITY
Semantic validation of structured theories: Applications to a generic programming language
[ETN-91-98207] N91-13916
VANADATES
Optical characterization techniques applied to ceramic oxides
[DE91-001526] N91-13556
VANADIUM ALLOYS
Superplastic deformation properties of Ti-6Al-4V
[DE91-000503] N91-13757
VANELESS DIFFUSERS
Theory of finite disturbances in a centrifugal compression system with a vaneless radial diffuser
[NASA-CR-187049] N91-13458
VANES
Turbulence and pressure loss characteristics of the inlet vanes for the 80- by 120-ft wind tunnel
[NASA-TM-102808] N91-13486
VAPOR DEPOSITION
Interfacial chemistry of titanium films deposited on PMDA-ODA polyimide
[AD-A225730] N91-13550
Morphological stability and kinetics in crystal growth from vapors
[NASA-CR-187650] N91-14055
Method of fabricating germanium and gallium arsenide devices
[NASA-CASE-GSC-13265-1] N91-14066
VAPOR PHASES
Measurements and predictions of a liquid spray from an air-assist nozzle
[NASA-TM-103640] N91-13455
Characterization of rocket propellant combustion products: Description of sampling and analysis methods for rocket exhaust characterization studies
[DE91-002536] N91-13574
Heat pipe dynamic behavior
[NASA-CR-187422] N91-13645
Empirical relationships between gas abundances and UV selective extinction N91-14116
VAPOR PRESSURE
The molecular structure of the HAN-based liquid propellants
[AD-A226415] N91-13571
VAPORIZERS
The effect of longitudinal spacer ribs on the minimum pressure drop in a heated annulus
[DE91-000784] N91-13655
VAPORIZING
Supercritical binary geothermal cycle experiments with mixed-hydrocarbon working fluids and a near-horizontal in-tube condenser
[DE91-001815] N91-13798
VAPORS
Morphological stability and kinetics in crystal growth from vapors
[NASA-CR-187650] N91-14055
VARIABILITY
Tropical Pacific moisture variability: Its detection, synoptic structure and consequences in the general circulation
[NASA-CR-184045] N91-13832
Ground-based studies of emission-line variability: Recent results for NGC 5548 and future plans
[NASA-CR-180433] N91-14088
VARISTORS
Computation of the current density in nonlinear materials subjected to large current pulses
[DE91-001950] N91-13624
VECTOR ANALYSIS
BSB radar pulse classification
[FEL-90-B023] N91-13603
On unconstrained conjugate gradient optimization methods and their interrelationships
[MATHS-REPT-A-129] N91-13919
Evaluation of expressions involving higher order derivations
[NASA-CR-187319] N91-13949
VECTOR PROCESSING (COMPUTERS)
Sweeping-vector conversion for polygonal data
[INPE-4558-PRE/1299] N91-14077
VECTOR QUANTIZATION
Pipeline synthetic aperture radar data compression utilizing systolic binary tree-searched architecture for vector quantization
[NASA-CASE-NPO-17941-1-CU] N91-13595
VECTORS (MATHEMATICS)
Evaluation of expressions involving higher order derivations
[NASA-CR-187319] N91-13949
VEGETATION
SAR detection of topography, vegetation and installations over land
[FFI-90/7016] N91-13600
Methodological contribution utilizing TM/LANDSAT-5 imagery in geologic mapping of regions with significant vegetative cover
[INPE-5117-TDL/419] N91-13784
VEGETATION GROWTH
Localize and identify the gravity sensing mechanism of plants
[NASA-CR-187411] N91-13841
VELOCITY
Differences in the size-internal velocity relation of galactic and extragalactic HII regions N91-14158
VELOCITY DISTRIBUTION
Indicial response approach derived from Navier-Stokes equations. Part 1: Time-invariant equilibrium state
[NASA-TM-102856] N91-13408
Instability of a supersonic shock free elliptic jet
[NASA-TM-103428] N91-13413
Far field wake velocity measurements with hot film probes
[AD-A226650] N91-13647
NGC 1058: Gas motions in an extended, quiescent spiral disk N91-14103
Accounting for the dispersion in the x ray properties of early-type galaxies N91-14173
Spiral structure of M51: Streaming motions across the spiral arms N91-14206
VELOCITY ERRORS
Far field wake velocity measurements with hot film probes
[AD-A226650] N91-13647
VELOCITY MEASUREMENT
Far field wake velocity measurements with hot film probes
[AD-A226650] N91-13647
A laser Doppler velocimeter approach for near-wall three-dimensional turbulence measurements
[NASA-TM-102841] N91-13653
VENUS (PLANET)
Centimeter emission variation of Venus: Its second phase
[INPE-5122-TDL/423] N91-14257
VERTICAL FLIGHT
General Rotorcraft Aeromechanical Stability Program (GRASP): Theory manual
[NASA-TM-102255] N91-13762
VERY HIGH FREQUENCIES
Assessments of atmospheric effects on VHF and UHF communications
[AD-A226661] N91-13592
Transionospheric Propagation Code (TIPC)
[DE91-002435] N91-13597
VERY LARGE ARRAY (VLA)
Disk mass densities in edge-on spiral galaxies N91-14108
VERY LARGE SCALE INTEGRATION
Optical shared memory system demonstration model
[AD-A226431] N91-13612
Theory and procedure of the hierarchical design rule checking of integrated circuits
[ETN-91-98173] N91-13627
VERY LOW FREQUENCIES
Utilization of the HIPAS facility for cooperative experiments related to ionospheric modification
[AD-A226609] N91-13590
VESTIBULAR NYSTAGMUS
Vestibulo-ocular responses in man to +G sub z hypergravity
[IZF-1989-59] N91-13873
VESTIBULAR TESTS
Vestibulo-ocular responses in man to +G sub z hypergravity
[IZF-1989-59] N91-13873
VHSIC (CIRCUITS)
Parallel Ada benchmarks for the SVMS
[NASA-CR-182453] N91-13929
VIABILITY
Connectivity alternatives for remote users of the Maintenance Processor Subsystem (MPS)
[DOT/FAA/CT-90/16] N91-13900
VIBRATION DAMPING
Effect of lubricating oil characteristics on gear vibrations N91-13710
Non-linear dynamic analysis of geared systems
[NASA-CR-4338] N91-13737
Antivibration isolation (a practical guidebook)
[CETIM-108220] N91-13775
VIBRATION EFFECTS
F-106B airplane active control landing gear drop test performance
[NASA-TM-102741] N91-13445
Non-linear dynamic analysis of geared systems
[NASA-CR-4338] N91-13737
Free vibrations of thin-walled semicircular graphite-epoxy composite frames
[NASA-TP-3010] N91-13750
Modelling the effects of vibration on visual performance
[ISVR-TR-171] N91-13883
Effects of anthropometric and postural variables on the transmission of whole-body vertical vibration from seat-to-head
[ISVR-TR-172] N91-13884
VIBRATION ISOLATORS
Antivibration isolation (a practical guidebook)
[CETIM-108220] N91-13775
VIBRATION MEASUREMENT
Antivibration isolation (a practical guidebook)
[CETIM-108220] N91-13775
Practical considerations for the measurement of internal and coupling loss factors on complex structures
[ISVR-TR-182] N91-13778
VIBRATION TESTS
All Shuttle Centaur engine and nozzle support plug vibration testing
[NASA-CR-183201] N91-13485
VIDEO SIGNALS
Real-time data compression of broadcast video signals
[NASA-CASE-LEW-14945-1] N91-13598
VIRGO GALACTIC CLUSTER
NGC 4438: Ram pressure sweeping of a tidally disrupted galaxy N91-14176
NGC 3312: A victim of ram pressure sweeping N91-14177
Molecular gas and star formation in the centers of Virgo spirals N91-14216
Detection of CO emission in Hydra 1 cluster galaxies N91-14237

VIRIAL THEOREM
Virial theorem analysis of the structure and stability of magnetized clouds N91-14190
VISCOELASTIC DAMPING
Constrained viscoelastic layer damping of thick aluminum plates: Design, analysis, and testing [AD-A226556] N91-13758
VISCOELASTICITY
A nonlinear viscoelastic approach to durability predictions for polymer based composite structures [NASA-CR-187653] N91-13554
Constrained viscoelastic layer damping of thick aluminum plates: Design, analysis, and testing [AD-A226556] N91-13758
Composite passive damping struts for large precision structures [NASA-CASE-NPO-17914-1-CU] N91-13767
VISCOMETRY
Viscosity measurements at high temperature and high pressure: A novel technique [NASA-CR-187239] N91-13967
VISCOPLASTICITY
Experimental and theoretical determination of the thermomechanical response of inelastic structural materials to high energy thermal inputs [AD-A226671] N91-13496
A review of nonlinear constitutive models for metals [NASA-TM-102727] N91-13761
VISCOSITY
Effect of bulk viscosity in low density, hypersonic blunt body flows [DE90-012756] N91-13419
Nonlinear viscous waves produced by an impulsively moving plate N91-13641
Two-fluid simulations of the reversed-field pinch [DE91-001961] N91-14014
VISCOUS FLOW
Development of a time-dependent incompressible Navier-Stokes solver based on a fractional-step method [NASA-CR-182323] N91-13639
Heat pipe dynamic behavior [NASA-CR-187422] N91-13645
VISCOUS FLUIDS
Transport properties of dense fluid mixtures using nonequilibrium molecular dynamics [DE91-000262] N91-13654
A review of interaction mechanisms in fluid-solid flows [DE91-000941] N91-13660
VISIBILITY
EMU helmet mounted display [NASA-CASE-MSC-21460-1] N91-13879
VISUAL ACUITY
Modelling the effects of vibration on visual performance [ISVR-TR-171] N91-13883
VISUAL PERCEPTION
A discrepancy within primate spatial vision and its bearing on the definition of edge detection processes in machine vision [NASA-TM-102739] N91-13941
VOIDS
Relationship between voids and interlaminar shear strength of polymer matrix composites [NASA-TM-103643] N91-13495
VOLCANOLOGY
Proceedings of the MEVTV Workshop on The Evolution of Magma Bodies on Mars [NASA-CR-187357] N91-14252
Mars tectonics and volcanism [NASA-CR-187351] N91-14254
VOLUME
An investigation of microstructural characteristics of contact-lens polymers [NASA-TP-3034] N91-13492
Volumetric measurement of tank volume [NASA-CASE-MSC-21500-1] N91-13683
VORTEX BREAKDOWN
Free-stream turbulence and concave curvature effects on heated, transitional boundary layers, volumes 1 and 2 N91-13643
Vortex collapse from a viewpoint of complex-time singularity [DE91-001852] N91-13957
VORTICES
Indicial response approach derived from Navier-Stokes equations. Part 1: Time-invariant equilibrium state [NASA-TM-102856] N91-13408
Large-eddy simulation of transitional channel flow [NASA-CR-187465] N91-13410
Toward the large-eddy simulation of compressible turbulent flows [NASA-CR-187460] N91-13650
Large eddy simulations and direct numerical simulations of high speed turbulent reacting flows [NASA-CR-187674] N91-13656
Vortex collapse from a viewpoint of complex-time singularity [DE91-001852] N91-13957
The gravitational wakefield of a molecular cloud in a disk galaxy N91-14188
VORTICITY EQUATIONS
Frontogenesis in gravity currents: The effect of endwalls and diffusion [MATHS-REPT-A-127] N91-13666

W

WAFERS
Thermal and structural assessments of a ceramic wafer seal in hypersonic engines [NASA-TM-103651] N91-13456
Analytical and experimental studies for thermal plasma processing of materials [DE91-000599] N91-13576
Method of fabricating germanium and gallium arsenide devices [NASA-CASE-GSC-13265-1] N91-14066
WAKES
Development of a full potential solver for rotor aerodynamics analysis N91-13407
WALL FLOW
A laser Doppler velocimeter approach for near-wall three-dimensional turbulence measurements [NASA-TM-102841] N91-13653
A minimization method adapted to the finite element technique for turbulent flow simulation with nonlinear boundary conditions in the wall vicinity [ECL-90-016] N91-13664
WALLS
Dual diaphragm tank with telltale drain [NASA-CASE-MSC-21703-1] N91-13580
WARFARE
AN alternative to suppression: Modeling methodology for assessing indirect effects of weapons and human performance degradation [AD-A226518] N91-13877
WARNING SYSTEMS
A flight expert system for on-board fault monitoring and diagnosis [NASA-CR-187334] N91-13452
WASTE TREATMENT
Biosphere 2 test module experimentation program N91-13845
The NASA CELSS program N91-13848
The CELSS breadboard project: Plant production N91-13849
Plants and their microbial assistants: Nature's answer to Earth's environmental pollution problems N91-13851
WASTE WATER
The BioHome: A spinoff of space technology N91-13852
WATER
Mechanism of mechanical fatigue of silica glass [DE91-004053] N91-13565
The molecular structure of the HAN-based liquid propellants [AD-A226415] N91-13571
Biofilm monitoring coupon system [NASA-CASE-MSC-21585-1] N91-13857
WATER TREATMENT
CELSS research and development program N91-13850
The BioHome: A spinoff of space technology N91-13852
WATER TUNNEL TESTS
Transition control via boundary layer heating [ARE-TR-88503] N91-13667
WATER VAPOR
Progress of research on water vapor lidar [NASA-CR-187673] N91-13837
WATER WAVES
Description of sea wave motion and its influence on the altitude control of sea skimming missiles [FEL-89-A368] N91-13450
Nonlinear viscous waves produced by an impulsively moving plate N91-13641
WAVE EQUATIONS
Wave by wave analysis of in-line force data for fixed cylinders in regular waves [IC-AERO-89-02] N91-13672
WAVE EXCITATION
Gravity waves excited by flow over an obstacle [FFI-90/7017] N91-13828
WAVE FUNCTIONS
A rapid relativistic distorted wave approach for calculating cross sections for ionization of highly charged ions [DE91-002667] N91-14020
WAVE PROPAGATION
NRL 1989 beam propagation studies in support of the ATA multi-pulse propagation experiment [AD-A226443] N91-13588
Extremely High Frequency (EHF) Low Probability of Intercept (LPI) communication applications [AD-A226653] N91-13591
MPPE (Multiple Pulse Propagation Experiment) results [DE91-001678] N91-13599
WAVE SCATTERING
Tissue simulating gel for medical research [NASA-CASE-LAR-14036-1] N91-13562
Temporal scattering and response software: Users' manual [DE91-001760] N91-13593
Transionospheric Propagation Code (TIPC) [DE91-002435] N91-13597
WAVEFORMS
Measurement of waves in flows across a surface [NASA-CASE-NPO-17479-1-CU] N91-13658
Actinide speciation by photothermal spectroscopies: Instrumentation development [DE91-001854] N91-13700
WAVEGUIDE LASERS
Folded RF-excited CO2 waveguide lasers N91-13695
WAVEGUIDES
Feasibility to study of a non-reciprocal latched ferrite phase shifter in the 92-96 GHz band [FEL-90-B114] N91-13634
WEAPON SYSTEMS
Guidance, navigation and control. Digital emulation technology laboratory. Volume 2, Task 2: Seeker emulator development [AD-A225124] N91-13429
Guidance, navigation and control. Digital emulation technology laboratory. Volume 3, Task 3: Special studies [AD-A225125] N91-13430
Guidnace simulation model of antisea-skimmer utilization for weapon system definition N91-13438
Study system concept for a pelotons procedure trainer (PEP-trainer) for the weapon systems YPR-PRAT, YPR-25 mm (EWS) and Leopard 1-5 [FEL-90-A084] N91-13871
AN alternative to suppression: Modeling methodology for assessing indirect effects of weapons and human performance degradation [AD-A226518] N91-13877
WEAR
Study of the time and effort signal in cutting operations [CETIM-101580] N91-13583
WEAR TESTS
Friction and wear of TPS fibers: A study of the adhesion and friction of high modulus fibers [NASA-CR-187666] N91-13515
Study of the time and effort signal in cutting operations [CETIM-101580] N91-13583
WEATHER
Aircraft accident report: Aloha IslandAir, Inc., Flight 1712, de Havilland Twin Otter, DHC-6-300, N707PV, Halawa Point, Molokai, Hawaii, October 28, 1989 [PB90-910405] N91-13425
WEATHER FORECASTING
Tropical Pacific moisture variability: Its detection, synoptic structure and consequences in the general circulation [NASA-CR-184045] N91-13832
DOPLIGHT 1987 project summary [PB90-253584] N91-13834
WEIBULL DENSITY FUNCTIONS
Thermal and structural assessments of a ceramic wafer seal in hypersonic engines [NASA-TM-103651] N91-13456
WEIGHT INDICATORS
Magnetic suspension and balance system advanced study, phase 2 [NASA-CR-4327] N91-13463
WEIGHTLESSNESS
Volumetric measurement of tank volume [NASA-CASE-MSC-21500-1] N91-13683
WELD STRENGTH
Study of the metallurgical effects of hammering between passes during C-Mn weld deposition [CETIM-104850] N91-13532
Evaluation of the functional properties of welds on cold finished tubes defined as NF A 49.541 [CETIM-104700] N91-13738
The effects of thermal treatment after welding on the functional properties of assemblies. Follow-up of the work on Cr-Mo [CETIM-104720] N91-13739

Study of the tensile strength of the melted zone of vertical welds carried out using electroslag welding on C-Mn steel. Further study on 80 mm thick plate
[CETIM-104730] N91-13740

WELD TESTS
Study of the metallurgical effects of hammering between passes during C-Mn weld deposition
[CETIM-104850] N91-13532
Evaluation of the functional properties of welds on cold finished tubes defined as NF A 49.541
[CETIM-104700] N91-13738
The effects of thermal treatment after welding on the functional properties of assemblies. Follow-up of the work on Cr-Mo
[CETIM-104720] N91-13739
Study of the tensile strength of the melted zone of vertical welds carried out using electroslag welding on C-Mn steel. Further study on 80 mm thick plate
[CETIM-104730] N91-13740

WELDED JOINTS
Study of the metallurgical effects of hammering between passes during C-Mn weld deposition
[CETIM-104850] N91-13532
Evaluation of the functional properties of welds on cold finished tubes defined as NF A 49.541
[CETIM-104700] N91-13738
The effects of thermal treatment after welding on the functional properties of assemblies. Follow-up of the work on Cr-Mo
[CETIM-104720] N91-13739
Study of the tensile strength of the melted zone of vertical welds carried out using electroslag welding on C-Mn steel. Further study on 80 mm thick plate
[CETIM-104730] N91-13740
Study of the metallurgical consequences of hammering between passes to compensate for the withdrawal of metal caused by welding
[CETIM-104430] N91-13741
Mechanical properties of 1950's vintage Type 304 stainless steel weldment components
[DE91-004328] N91-13774

WEST GERMANY
Activities report of the Max-Planck Institute for Aeronomy
[ETN-91-98383] N91-14272

WETTING
Analysis of single and multi-grade lubricant film thickness in a diesel engine
[AD-A226651] N91-13715

WHEELS
Device for applying constant pressure to a surface
[NASA-CASE-GSC-13230-1] N91-13734

WHISKER COMPOSITES
Fabrication and properties of powder metallurgically manufactured aluminum products and composites
[VTT-RR-699] N91-13531

WHITE NOISE
Direct modeling of white noise in stochastic systems
[MEMO-865] N91-13964

WICKS
Experiments on bench-scale heat-pipe solar receivers
[DE90-013806] N91-13806

WIGGLER MAGNETS
Field error lottery
[DE91-001875] N91-13702

WIND DIRECTION
Aerodynamic effect of strakes on two-dimensional tail boom models of the OH-58A and the OH-58D helicopters
[NASA-TM-4248] N91-13406

WIND PROFILES
Evaluation of a wind profile model
[FOA-E-40045-4.5] N91-13839

WIND TUNNEL APPARATUS
Magnetic suspension and balance system advanced study, phase 2
[NASA-CR-4327] N91-13463
Turbulence and pressure loss characteristics of the inlet vanes for the 80- by 120-ft wind tunnel
[NASA-TM-102808] N91-13466
Probe insertion apparatus with inflatable seal
[NASA-CASE-LEW-14965-1] N91-13732

WIND TUNNEL MODELS
Analytical aerodynamic model of a high alpha research vehicle wind-tunnel model
[NASA-CR-187362] N91-13404
Magnetic suspension and balance system advanced study, phase 2
[NASA-CR-4327] N91-13463

WIND TUNNEL TESTS
Close-range photogrammetric measurement of static deflections for an aeroelastic supercritical wing
[NASA-TM-4194] N91-13400
Analytical aerodynamic model of a high alpha research vehicle wind-tunnel model
[NASA-CR-187362] N91-13404
Aerodynamic effect of strakes on two-dimensional tail boom models of the OH-58A and the OH-58D helicopters
[NASA-TM-4248] N91-13406
The IAR high Reynolds number two-dimensional test facility: A description of equipment and procedures common to most 2-D airfoil tests
[AD-A226629] N91-13409
Some buffet response characteristics of a twin-vertical-tail configuration
[NASA-TM-102749] N91-13412
Transonic wind tunnel tests on two-dimensional aerofoil sections: Determination of pressure distribution and drag for an aerofoil of type SAAB 7301 in FFA wind tunnel S5
[FFA-TN-1989-47] N91-13416
Wind-tunnel survey of an oscillating flow field for application to model helicopter rotor testing
[NASA-TM-4224] N91-13462
Dual strain gage balance system for measuring light loads
[NASA-CASE-LAR-14419-1] N91-13687
Pressure visualization (PreViz) package version 1.0 user's guide
[NASA-CR-187444] N91-13907
An assessment of wind tunnel test data on flexible thermal protection materials and results of new fatigue tests of threads
[NASA-CR-177466] N91-13972

WIND TUNNEL WALLS
Calibration of the 13- by 13-inch adaptive wall test section for the Langley 0.3-meter transonic cryogenic tunnel
[NASA-TP-3049] N91-13461

WIND TUNNELS
Turbulence and pressure loss characteristics of the inlet vanes for the 80- by 120-ft wind tunnel
[NASA-TM-102808] N91-13466
A quiet flow Ludwieg tube for study of transition in compressible boundary layers: Design and feasibility
[NASA-CR-187374] N91-13676
AGARD highlights 90/2, part 2
[AD-A226532] N91-14080

WIND TURBINES
Spanwise aerodynamic loads on a rotating wind turbine blade
[DE91-002101] N91-13414
Tubular lap joints for wind turbine applications
[DE91-001341] N91-13736
Airfoil design for variable RPM horizontal axis wind turbines
[FFA-TN-1990-02] N91-13801

WIND VELOCITY
Review of geography internship of convective wave project
[NASA-CR-187022] N91-13819

WINDING
The world of superconductive machinery N91-14045

WING NACELLE CONFIGURATIONS
Effect of location of aft-mounted nacelles on the longitudinal aerodynamic characteristics of a high-wing transport airplane
[NASA-TP-3047] N91-13402

WINGS
Damage tolerance analysis and testing of the fighter aircraft 37 Viggen
[FFA-TN-1990-35] N91-13448

WIRE
Success criteria for oxide superconductor wires: Measuring the present, predicting the future N91-14034
The world of superconductive machinery N91-14045
Oxide superconductor coils: Present successes, future challenges N91-14046
Synthesis and characterization of high temperature superconductor materials N91-14048

WIRING
The status-quo and prospect of superconducting digital devices N91-14039

WORK CAPACITY
Adaptable driver-car interfacing and mental workload: A review of the literature
[IZF-1990-B-3] N91-13874

WORKING FLUIDS
Supercritical binary geothermal cycle experiments with mixed-hydrocarbon working fluids and a near-horizontal in-tube condenser
[DE91-001815] N91-13798

WORKLOADS (PSYCHOPHYSIOLOGY)
Adaptable driver-car interfacing and mental workload: A review of the literature
[IZF-1990-B-3] N91-13874
A subjective rating scale for assessing pilot workload in flight: A decade of practical use
[RAE-TR-90019] N91-13882

WORKSTATIONS
Research into software executives for space operations support
[NASA-CR-187013] N91-13895

WRENCHES
Tethering sockets and wrenches
[NASA-CR-184032] N91-13675

X

X RAY ANALYSIS
The x ray elastic constants of ceramic materials for the determination of the stresses from lattice expansion measurements N91-13541
Data reduction of digitized images processed from calibrated photographic and spectroscopic films obtained from terrestial, rocket and space shuttle telescopic instruments
[NASA-CR-187320] N91-13674
Calcified-tissue investigations using synchrotron x ray microscopy
[DE91-001729] N91-13859

X RAY DIFFRACTION
Residual stresses analyses in ceramics and metal ceramic composites using x ray methods N91-13539
Influence of materials structure and production method of Al2O3 ceramic on the x-ray stress measurement N91-13540
X ray holography at Lawrence Livermore National Laboratory
[DE91-002673] N91-13690

X RAY IRRADIATION
Review of uncertainties in the use of NPL primary standards of x ray exposure for the calibration of secondary standards in terms of exposure and air kerma
[NPL-RS(EXT)-109] N91-13868

X RAY LASERS
Ultra-high brightness (greater than 10(exp 21) W/sq cm) laser facility
[DE91-001685] N91-13698

X RAY SOURCES
Research in theoretical physics
[DE91-002458] N91-14071
The infrared continuum spectrum of x ray illuminated molecular gas N91-14144
Gas flows in elliptical galaxies N91-14170

X RAY SPECTRA
The onset of galactic winds in early-type galaxies N91-14165

X RAY SPECTROSCOPY
Development of mercuric iodide uncooled x ray detectors and spectrometers
[NASA-CR-185394] N91-13484
Inner-shell ionization of lithium-like chromium ions
[DE91-001749] N91-13981
An x ray photoelectron spectroscopy study of Au(x)In(y) alloys
[NASA-TM-103659] N91-14050

X RAY STARS
Research in theoretical physics
[DE91-002458] N91-14071

X RAY STRESS ANALYSIS
X ray measurements of residual stresses in thin, hard layers N91-13542

X RAY TELESCOPES
Variable magnification glancing incidence x ray telescope
[NASA-CASE-MFS-28013-2] N91-14096

X RAYS
Distortion-free x ray mask technology
[AD-A226524] N91-13993
HYLIFE-2 inertial confinement fusion reactor design
[DE91-000792] N91-14004
X ray and charged particle detection with CsI(Tl) layer coupled to a-Si:H photodiode layers
[DE91-001798] N91-14060
Variable magnification glancing incidence x ray telescope
[NASA-CASE-MFS-28013-2] N91-14096
The infrared continuum spectrum of x ray illuminated molecular gas N91-14144
Multiband observations of Cygnus A: A study of pressure balance in the core of a powerful radio galaxy N91-14151
The onset of galactic winds in early-type galaxies N91-14165
The environments of double radiogalaxies N91-14166
Optical emission from cooling flows in distant x ray clusters of galaxies N91-14169
Stripping of gas and dust from the elliptical galaxy M86 N91-14171
Accounting for the dispersion in the x ray properties of early-type galaxies N91-14173

An infrared jet in Centaurus A (NGC 5128): Evidence for interaction between the active nucleus and the interstellar medium N91-14175
NGC 3312: A victim of ram pressure sweeping N91-14177
Spectrum formation in SN1987A N91-14243

Y

YAG LASERS
A silicon avalanche photodiode detector circuit for Nd:YAG laser scattering
[DE91-002709] N91-13706
A compact, low cost, 7 channel polychromator for Thomson scattering measurements
[DE91-002719] N91-14024
YAW
Penetration of yawed projectiles
[DE91-001084] N91-13726
YTTRIUM COMPOUNDS
Composite thermal barrier coating
[NASA-CASE-LEW-14999-1] N91-13500
YTTRIUM OXIDES
Progress in high Tc superconductors N91-14031
Application of high-temperature superconductors to high-precision accelerometers N91-14042

Z

ZEEMAN EFFECT
Evolution of magnetized, rotating, isothermal clouds N91-14191
ZIRCONIUM OXIDES
Research and development of a ceramic fiber composite heat exchanger
[DE90-017250] N91-13497
Composite thermal barrier coating
[NASA-CASE-LEW-14999-1] N91-13500
ZONE MELTING
Method of making single crystal fibers
[NASA-CASE-LEW-14921-1] N91-13502

Typical Personal Author Index Listing

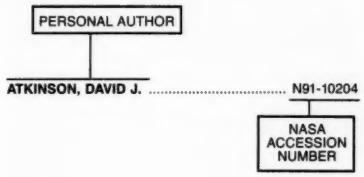

Listings in this index are arranged alphabetically by personal author. The NASA accession number denotes the number by which the citation is identified.

A

ABDELSALAM, M. K. N91-13463
ABEYOUNIS, WILLIAM K. N91-13402
ABRAHAM, M. M. N91-13556
ABRAMS, EVE N91-13734
ADAIR, ELEANOR R. N91-13864
ADAMS, RICHARD R. N91-13400
N91-13473
ADAMSON, A. J. N91-14132
ADKINS, DOUGLAS R. N91-13806
ADKISSON, LORI N91-13900
ADLER, D. S. N91-14146
N91-14203
AGAN, CHRISTOPHER E. N91-13902
AGER, C. N91-13968
AGGARWAL, J. K. N91-13725
AGGARWAL, SURESH K. N91-13455
AHMED, RAFI N91-13896
AKMAN, N. N91-13651
ALBRECHT, DIETMAR N91-13663
ALDE, D. M. N91-13682
ALDERING, GREGORY SCOTT N91-14091
ALEXANDER, J. IWAN D. N91-13967
ALFERDINCK, J. W. A. M. N91-13789
ALFORD, CECIL O. N91-13430
ALFORD, N. MCN. N91-14036
ALI, A. WAHAB N91-13588
N91-14005
ALI, MOONIS N91-13452
ALIYEV, I. D. N91-13861
ALLAART, MARC A. F. N91-13840
ALLEN, DAVID H. N91-13496
N91-13761
ALLEN, G. A. N91-13651
ALLEN, JOHN P. N91-13844
ALLEN, JOSEPH N91-13854
ALLEN, LORI E. N91-14215
ALLEN, R. J. N91-14146
N91-14194
N91-14203
N91-14206
ALLEN, S. L. N91-13699
ALLEY, G. T. N91-13618
ALLING, ABIGAIL N91-13845
ALLISON, MICHAEL J. N91-13908
ALVAREZ-ROMO, NORBERTO N91-13845
ALYESDAFONTOURARODRIGUES, JOSE N91-13664
ANDERSEN, VIDAR S. N91-13891
N91-13922
ANDERSON, D. M. N91-13933
ANDERSSON, BOERJE N91-13769
N91-13771
ANDREASSEN, OYVIND N91-13828
ANNESE, C. N91-13690
ANTONIO, BRIAN KENT N91-13713
APPLETON, A. D. N91-14045
APPLETON, P. N. N91-14198
ARAUJO, THAIS MAIA N91-13511
ARMENTROUT, CHARLES J. N91-14026
ARNOLD, S. N91-13517
ARNOLDSSON, GOERAN N91-13839
ARVAS, ERCUMENT N91-13589
ASCHER, URI M. N91-13956
ASHFORD, N. J. N91-13426
ASLAM, S. N91-13933
ATKINS, D. J. N91-13667
AUERKARI, PERTTI N91-13528
N91-13530
N91-13567
AVERNER, MAURICE M. N91-13848
AWADALLA, N. G. N91-13774
AZEVEDO, S. G. N91-13914

B

BAAS, S. M. N91-13905
BABIKYAN, CAROL N91-13934
BABUSKA, IVO N91-13769
N91-13771
BADO, P. N91-13698
BAFFES, PAUL N91-13944
BAGCHI, ARUNABHA N91-13964
BAIRD, D. C. N91-14032
BALBUS, STEVEN A. N91-14162
BALDETTI, PAOLO N91-13717
BALL, ROGER N91-14133
BANDURSKI, ROBERT S. N91-13841
BANERJEE, P. K. N91-13557
BANKS, BRUCE A. N91-13668
BANNISTER, D. J. N91-13926
BARBARIN, A. N91-13749
BARBER, DAVID G. N91-13932
BARCLAY, REBECCA O. N91-14079
BARD, STEVEN N91-13581
BAREISS, R. N91-13418
BARKER, L. A. N91-13766
BARNES, NORMAN P. N91-14053
BARNES, PAUL R. N91-13862
BARNES, SCOTT P. N91-13598
BARRETT, T. B. N91-14052
BARRY, R. N91-13782
BARTELDREES, ANDREAS N91-14187
BARTON, TIMOTHY J. N91-13894
BASCOM, WILLARD D. N91-13515
BATEMAN, MICHAEL J. N91-13758
BATHA, STEVEN H. N91-14007
BATTRICK, B. N91-14083
BATY, ROY S. N91-13413
BAUMGAERTNER, PAUL N91-13424
BAZEN, G. C. N91-13551
BECK, W. J. C. N91-13605
BEHNKEN, H. N91-13541
BEIERSDORFER, P. N91-13981
BEISSNER, FRED L., JR. N91-13432
BELCHER, ROBERT W. N91-13591
BENSON, D. A. N91-13617
BERBICHE, MONSEF N91-13889
BERG, J. M. N91-13700
BERGER, JOHN ROLAND N91-13754
BERGERON, PIERETTE N91-14074
BERNARD, J. P. N91-14137
BERRY, DENNIS N91-13424
BERTOLDI, FRANK N91-14248
BESHEARS, D. L. N91-13681
BHANDARI, PRADEEP N91-13796
BHASIN, KUL B. N91-13996
BINGEL, BRADFORD D. N91-13907
BINGHAM, PHILLIP R. N91-13430
BIRDSALL, D. N91-13690
BIREMBAUT, Y. N91-13776
BIRMAN, KENNETH P. N91-13928
BISHOP, ANN N91-14074
BISHT, R. S. N91-14131
BISSINGER, NORBERT C. N91-13423
BITTNER, R. D. N91-13649
BJOERCK, ANDERS N91-13801
BJORDAL, HALVOR N91-13922
BLACKBURN, J. F. N91-13610
BLAHA, CYNTHIA ANNE N91-14244
BLANCO, A. N91-14264
BLANCO, P. R. N91-14213
BLAND, JONATHAN N91-14150
N91-14240
BLENKINSOP, S. E. N91-14031
BLIEM, C. J. N91-13798
N91-13799
BLITZ, L. N91-14121
BLOM, ANDERS F. N91-13448
N91-13768
BLOOM, J. N91-14052
BOCKMAN, R. S. N91-13859
BODENHEIMER, P. N91-14212
BOGGS, THOMAS L. N91-13488
BOGREN, JONAS N91-13772
BOHL, RICHARD J. N91-13490
BOISSEVAIN, J. G. N91-13682
BOKOR, PETER C. N91-13490
BOL, J. C. P. N91-13871
BOLES, MICHAEL A. N91-13443
BOMAN, PER OLOF N91-13448
BOND, THOMAS H. N91-13421
BONIFAZI, P. N91-13616
BOOM, R. W. N91-13463
BORIAKOFF, VALENTIN N91-13885
BORIS, JAY P. N91-13588
BORIS, PAUL N91-13588
BORKOWSKI, KAZIMIERZ J. N91-14162
BORNSCHEIN, R. L. N91-13859
BOTHUN, GREG N91-14168
BOUAJJANI, AHMED N91-13960
BOUHELIER, C. N91-13583
BOULANGER, F. N91-14231
BOWERS, K. L. N91-13952
BOWLES, KENNETH J. N91-13495
BOYLE, EDWARD N91-13878
BRACKER, A. S. N91-13513
BRADLEY, WALTER L. N91-13756
BRADSHAW, T. W. N91-14035
BRADSTREET, D. W. N91-13926
BRAHM, DAVID ERNEST N91-14068
BRAMLEY, R. N91-13933
BRAND, P. W. J. L. N91-14129
BRANDHORST, HENRY W. N91-13803
BRASE, J. N91-13690
BRAUN, ROBERT N91-14178
N91-14179
N91-14196
BREAKWELL, J. N91-13788
BREGMAN, JOEL N. N91-14109
N91-14172
BRESCIANINI, C. P. N91-13651
BRINKLEY, P. N91-13612
BRINKS, ELIAS N91-14178
BRINKSMEIER, E. N91-13540
BRINSON, HAL F. N91-13554
BRITTON, C. L., JR. N91-13618
BRITTON, RANDALL K. N91-13421
BRONK, B. V. N91-13517
BROOKS, J. N. N91-14028
BROWN, CHRISTOPHER WILLIAM N91-13723
BROWN, J. D. N91-13653
BROWN, M. D. N91-13699
BROWN, ROBERT M. N91-13811
BRUHWEILER, F. N91-14161
BRYAN, THOMAS N91-13482
BRZEZINSKI, J. N91-13775
BUBENHEIM, DAVID N91-13850
BUCK, REINER N91-13800
BUDEN, DAVID N91-13744
N91-13986
N91-13987
BUENOBUCCI, ELIANA FRANCO N91-13783
BUGG, W. M. N91-13979
BULZAN, DANIEL L. N91-13455
BUMPAS, STANLEY E. N91-13707
BUNGE, HANS JOACHIM N91-13543
BURBIDGE, E. MARGARET N91-14228
BURCHAM, FRANK W., JR. N91-13460
BUREL, F. N91-13438
BURESCH, I. N91-13545
BURGESS, D. W. N91-13834
BURNS, KAREN S. N91-13492
BURNSIDE, W. D. N91-13428
BURRELL, K. H. N91-14023
BURROWS, ADAM N91-13976
BURTON, MICHAEL N91-14184
BUSHNELL, DENNIS M. N91-13558

BUSS, RICHARD H., JR. N91-14140
BUSSOLETTI, E. N91-14264
BUSTIN, ROBERTA N91-14256
BUTLER, RALPH N91-13942
BUTLER, THOMAS A. N91-13988
BUTTERFIELD, ANSEL J. N91-14251
BUTTERFIELD, C. P. N91-13414
BUZASI, DEREK LASZLO N91-14092
BYERS, J. A. N91-13699
BYRDSONG, THOMAS A. N91-13400

C

CABANEL, R. N91-14033
CABLE, M. D. N91-14021
CAFFERTY, MAUREEN M. N91-13620
CAHILL, P. A. N91-13617
CAIN, JOSEPH C. N91-13818
CAMARANETO, GILBERTO N91-14078
CAMBRIDGE, VIVIEN N91-13691
CAMERON, M. N91-14125
CAMPBELL, DAVID K. N91-14070
CAMPBELL, E. M. N91-13698
CAMPBELL, G. L. N91-14025
CANFIELD, T. R. N91-13933
CANTERNA, R. N91-14207
CANZIAN, BLAISE N91-14216
CAO, JICHANG N91-13404
CAPLAN, EDDIE N91-13930
CAPORASO, G. J. N91-13599
CAPPS, G. J. N91-13681
CAPUTO, MICHAEL N91-13865
CARDEN, HUEY D. N91-13750
N91-13751
CARILLI, CHRIS N91-14151
N91-14226
CARLSON, NANCY M. N91-13970
CARLSTROM, J. E. N91-14128
N91-14220
CARLSTROM, T. N. N91-13705
N91-13706
N91-14024
N91-14025
CARNAHAN, CHALON L. N91-14073
CARPENTER, ELISABETH J. N91-13476
CARR, JOHN N91-14221
CARR, STEPHEN H. N91-13552
CASE, JAMES N91-14227
CASEY, R. N91-13651
CASEY, SEAN N91-14141
CASOLI, F. N91-14197
N91-14231
CASPER, T. A. N91-13699
CASS, G. R. N91-13814
CASTELLANO, M. G. N91-13616
CASTLEMAN, WAYNE N91-14042
CATES, M. R. N91-13681
CATTON, I. N91-13645
CAULFIELD, J. N91-14052
CECIL, G. N. N91-14150
CECIL, GERALD N91-14149
N91-14240
CELMINS, AIVARS N91-14266
CERIMELE, CHRISTOPHER J. N91-13483
CHAMBERS, FRANK W. N91-13599
CHANG, CHI-YUNG N91-13595
CHANG, YI-HUA N91-13958
CHAO, TIEN-HSIN N91-13888
CHARENTUS, SYLVIE N91-13728
CHEN, F. C. N91-13578
CHEN, G. L. N91-13578
CHEN, KAI-YOU N91-14247
CHEN, QUARK N91-14042
CHEN, WEI N91-13885
CHEN, Z. N91-13773
CHENG, K.-P. N91-14161
CHENG, KWANG-PING N91-14249
CHENG, LI-JEN N91-13998
CHERMAHINI, R. G. N91-13768
CHERNOFF, D. F. N91-14183
CHERRY, JOHN N91-13900
CHESNUTT, J. C. N91-13524
CHEW, N. G. N91-14031
CHIH, PING PING N91-14267
CHIOU, JIN-CHERN N91-13759
CHITRE, SUSHEEL N91-13455
CHO, G. N91-14060
CHONG, Y. P. N91-13599
CHOW, PAO-LIU N91-13405
CHRIEN, ROBERT E. N91-14008
CHRISTIANSON, ROLLIN N91-13657
CHRISTOPHOROU, L. G. N91-13979
CHUBB, DONALD L. N91-13802
CHUNG, ALAN N91-13930
CHUNG, D. W. N91-14041
CIUFOLINI, I. N91-13470
CLARK, RONALD K. N91-13522
CLARKE, R. N. N91-13926
CLARKE, ROBERT N91-13879
CLAUSSEN, M. N91-14117
CLAUSSET, F. N91-14231
CLAY, BILL N91-13424
CLOSE, F. E. N91-13979
COAKLEY, JAMES A., JR. N91-13833
COCKRELL, C. R. N91-13585
COE, CHARLES F. N91-13972
COFFEY, H. E. N91-14260
N91-14261
N91-14262
N91-14263
COHEN, B. I. N91-13699
COHEN, R. H. N91-13699
COHEN, ROSS D. N91-14228
COLANGELI, L. N91-14254
COLE, STANLEY R. N91-13412
COLEMAN, RODERICK M. N91-13646
COLGAN, SEAN W. J. N91-14114
COLGATE, STIRLING A. N91-14270
COLLARD, PHILIPPE E. N91-13929
COLLIER, MARK D. N91-13895
COLLINS, CHARLES N91-13819
N91-13831
COLWELL, JOSHUA EDWARDS N91-14253
COMBES, F. N91-14197
N91-14231
COMER, C. N91-14052
COMPANION, JOHN A. N91-13562
N91-13693
COMPERE, A. L. N91-13572
CONDO, G. T. N91-13979
CONNER, SAM N91-14151
COOK, A. N91-13451
COOPER, JOHN F. N91-14090
COPELAND, P. P. N91-13892
CORBELLI, E. N91-14163
CORBETT, W. T. N91-13625
CORDES, GAIL A. N91-13932
COSS, JAMES R. N91-14049
COSTA, JOAQUIM E. R. N91-13587
COX, M. G. N91-13926
CRAFT, LEROY H. N91-14049
CREUZET, G. N91-14033
CROPLEY, C. C. N91-13794
CROSS, C. N91-13868
CROSS, JOHN H. N91-13860
CROWELL, CYNTHIA A. N91-13406
CRUSE, T. A. N91-13534
N91-13535
CUCINOTTA, FRANCIS A. N91-13985
CULBERTSON, GARY W. N91-13592
CULLEN, W. H. N91-13774
CUMMINGS, J. C. N91-13699
CURLANDER, JOHN C. N91-13595
CURRAN, CAROL COCKRELL N91-13721
CURTIS, HENRY B. N91-14259
CUTLER, DEBORAH E. N91-14081
CZECK, EDWARD N91-13930

D

DABNEY, RICHARD N91-13482
DAHLQUIST, HANS N91-13839
DALEY, P. L. N91-13489
DAMOTA, ANA CLARA N91-13899
DARGUSH, G. F. N91-13557
DAROU, Y. N91-13741
DAUGHERTY, ROBERT H. N91-13445
DAVARPANAH, MICHAEL M. N91-14049
DAVID, L. P. N91-14165
N91-14170
DAVIES, A. D. N91-13883
DAVIES, MARTIN J. S. N91-13672
DAW, C. S. N91-13955
DEADRICK, F. J. N91-13599
DEASON, V. A. N91-13703
DEBIEZ, S. N91-13532
N91-13739
N91-13741
DEBOO, J. C. N91-13705
N91-13706
N91-14024
N91-14025
DEISSLER, ROBERT G. N91-13638
DEJUN, XUE N91-13859
DELEEUW, G. N91-13838
DELLACORTE, CHRISTOPHER N91-13503
DELOOR, G. P. N91-13606
DELOURDESNEVESDEOLIVEIRAKURKDJIAN, MARIA
N91-14086
DELVIGS, PETER N91-13566
DEMATTEO, MARY B. N91-13901
DERR, RONALD L. N91-13488
DESERT, X. N91-14137
DESOUZAPONTES, CLAYTON N91-13825
DESTEFAN, D. E. N91-13727
DETTMAR, RALF-JUERGEN N91-14124
N91-14160
N91-14187
DEUSTUA, SUSANA N91-14168
DEUTSCH, OWEN L. N91-13441
DEUTSCHE, S. N91-14272
DEVAN, J. H. N91-13498
DEVEREUX, NICHOLAS A. N91-14117
N91-14136
N91-14145
DEVRIES, J. S. N91-13925
DICKEY, JOHN M. N91-14103
N91-14104
DICKSON, T. L. N91-13763
DIEUMEGARD, D. N91-14038
DILLON, A. C. N91-13513
DISTEFANO, SALVADOR N91-13621
DIVADEENAM, M. N91-13866
DIVECHA, A. P. N91-14048
DIVSALAR, D. N91-13596
DIXON, RAYMOND D. N91-13743
DOBSON, CRAIG N91-13817
DODSON, BRIAN W. N91-13977
DOGGETT, ROBERT V., JR. N91-13411
N91-13412
DOLGIN, BENJAMIN P. N91-13767
DOLLYHIGH, SAMUEL M. N91-13432
DOMACK, CHRISTOPHER S. N91-13432
DOMOKOS, G. N91-14071
DONAHUE, MEGAN N91-14169
N91-14227
DONGARRA, J. J. N91-13959
DOPITA, MICHAEL A. N91-14218
DOSCH, R. G. N91-13521
DOSWELL, C. A. N91-13834
DOTY, PHILIP N91-14074
DOWBEN, PETER A. N91-13614
DOWNER, JANICE DIANE N91-13760
DOWNES, DENNIS N91-14234
N91-14236
DOWNS, RAYMOND L. N91-14026
DRABIK, PASCAL N91-13916
DRAKE, A. E N91-13968
DRAKE, DOUGLAS J. N91-14026
DRAKE, R. PAUL N91-14007
DREHER, JOHN N91-14151
DRESSEL, L. L. N91-14223
DREWERY, J. N91-14060
DREWS, MICHAEL N91-13876
DRUCE, ROBERT L. N91-14063
DRUMMOND, COLIN K. N91-13457
DRUMMOND, TIMOTHY J. N91-13795
DUBOIS, PASCALE C. N91-13594
DUDLEY, MICHAEL R. N91-13466
DUONG, HAU N91-14022
DUPRAZ, C. N91-14197
DURAND, A. N91-13742
DUTSCHK, A. N91-13545
DWEK, ELI N91-14181
DYKSTRA, MARK D. N91-13570

E

EALES, STEPHEN A. N91-14136
N91-14238
EASTERLING, ROBERT G. N91-13745
EBERLE, ALBRECHT N91-13423
EBNETER, KATHLEEN ANN N91-14268
ECKART, A. N91-14125
ECKART, ANDREAS N91-14230
N91-14236
ECKMAN, RICHARD MARK N91-13824
ECKOLD, G. N91-13537
EDWARDS, J. A. N91-14031
EFTEKHARI, ABE N91-13492
EGALON, CLAUDIO OLIVEIRA N91-13991
EHN, GOERAN N91-13416
EIGENMANN, B. N91-13539
ELDERING, C. N91-13612
ELFHAG, TORSTEN N91-14118
ELLIOTT, C. JAMES N91-13631
N91-13702
ELLIOTT, S. J. N91-13975
ELLIS, G. A. N91-13882
ELLIS, R. F. N91-14015
ELLZEY, J. L. N91-13512
ELSTON, RICHARD N91-14159
ELTON, BRACY H. N91-13962
EMANUEL, WILLIAM R. N91-13813
ENGARGIOLA, GREG N91-14134
N91-14141

ENGLAND, ANTHONY W. N91-13817
ENGLAND, M. WENDY N91-13858
ENGLERT, PETER A. J. N91-14098
ENGLISH, JAYANNE N91-14214
EPSTEIN, J. S. N91-13703
ERICKSON, EDWIN F. N91-14114
ERLEBACHER, G. N91-13650
ERTHAL, GUARACI JOSE N91-14077
N91-14078
ESKRIDGE, PAUL B. N91-14111
EVANKO, R. N91-14024
EVANS, KURT B. N91-13569
EVERITT, C. W. F. N91-13788
EVES, JOHN W. N91-13684
EVRARD, AUGUST E. N91-14222
EYSSA, Y. M. N91-13463

F

FABBIANO, GIUSEPPINA N91-14112
FABIAN, A. C. N91-14171
FAHY, F. J. N91-13974
FALK, URBAN N91-13769
N91-13771
FANELLI, MICHAEL N. N91-14209
FANG, WAI-CHI N91-13595
FARHAT, C. N91-13480
FARHOOMAND, JAM N91-14087
FARMANESH, SAM N91-14049
FATEMI, NAVID S. N91-14050
FAWLEY, W. M. N91-13599
FEDERMAN, S. R. N91-14102
FEDERSCHMIDT, CLEMENS N91-13627
FEIGELSON, ERIC D. N91-14135
FELIPPA, C. A. N91-13480
FENSTERMACHER, M. E. N91-13699
FERGUSON, H. C. N91-14177
N91-14200
FERNANDODELCIAMPO, LINEU N91-14257
FERNSLER, RICHARD F. N91-13588
FERRANDO, W. A. N91-14048
FERRARIO, LILIA N91-14218
FERRARO, A. J. N91-13590
FERRIERE, KATIA M. N91-14180
FILA, J. N91-13444
FILER, ELIZABETH D. N91-14053
FINCKE, J. R. N91-13670
N91-13826
N91-14013
FISHER, TIMOTHY E. N91-13890
FLANAGAN, DAVID T. N91-13857
FLETCHER, R. N91-14041
FLOYD, STEPHEN A. N91-13939
FLUZIN, GERARD N91-13665
FOGLE, F. R. N91-13910
FONTI, S. N91-14264
FONTIJN, L. A. N91-13838
FOOTE, J. H. N91-13699
FORD, DONNIE R. N91-13939
FORESTI, CELINA N91-14086
FORMAN, W. N91-14165
N91-14170
N91-14171
FORMISANO, VITTORIO N91-14094
FORSTER, J. R. N91-14218
FORSYTH, D. E. N91-13834
FOURNIER, JOSEPH N91-13879
FOURTINE, STEPHANE N91-13708
FRASER, H. L. N91-13524
FRIEDERICH, PAUL N91-13609
FRIMPONG, STEPHEN N91-13495
FRISTROM, CARL C. N91-14162
FROEBEL, RICHARD N91-13683
FRYE, ROBERT N91-13846
FUJIEDA, I. N91-14060
FUJITA, TOSHIO N91-13796

G

GAFFNEY, NIALL N91-14221
GAIER, JAMES R. N91-13668
GAILLARD, R. N91-13532
N91-13738
N91-13739
N91-13740
N91-13741
GALAYDA, THOMAS A. N91-13901
GALEA, STEPHEN C. P. N91-13493
GALLAGHER, JOHN S., III N91-14152
N91-14160
GALLAIS, P. N91-14217
GALLOPOULOS, E. N91-13933
GALWAY, R. D. N91-13409
GARAYEV, P. S. N91-13861
GARRETT, FREDERICK, JR. N91-13404
GARTEN, CHARLES T., JR. N91-13812
GASNIER, J. N91-13583
GAYLE, T. M. N91-13574
GEBALLE, T. R. N91-14185
GEE, JAMES M. N91-13793
N91-13795
GEE, T. N91-14060
GEISELHART, KARL A. N91-13432
GEISSINGER, STEVE K. N91-13684
GEIST, G. A. N91-13959
GELHAUSEN, PAUL A. N91-13460
GENZEL, REINHARD N91-14230
N91-14236
GEORGE, STEVEN M. N91-13513
N91-13514
GEORGE, T. J. N91-13805
GHOSH, S. K. N91-14131
GIBSON, C. ROBERT N91-13865
GIESEKING, STEPHEN R. N91-13429
GILLHAM, JOHN K. N91-13508
GILLOTAY, D. N91-13830
GILMAN, ADA W. N91-13877
GILYARD, GLENN B. N91-13460
GIOIA, ISABELLA N91-14169
GIVI, PEYMAN N91-13656
GLASSMAN, MYRON N91-14079
GOBEN, CHARLES A. N91-14049
GOERANSSON, PETER N91-13417
GOHIL, P. N91-14023
GOLDSTEIN, DAVID N91-13716
GONIS, A. N91-13978
GOODYEAR, S. W. N91-14031
GORSKI, JOSEPH J. N91-13646
GOSULA, R. N91-13612
GOUGH, C. E. N91-14036
GRABELSKY, D. A. N91-14174
GRAF, JUTTA N91-13827
GRAINGER, JOHN L. N91-13527
GRANDIN, GUSTAV N91-13839
GRASDALEN, GARY L. N91-14207
GRAVER, L. N91-13926
GRAVES, MICHAEL J. N91-13446
GRAVES, PHILIP LEE N91-13721
GRAVES, THOMAS JOSEPH N91-13723
GRAY, B. N91-13618
GRAY, J. N91-13690
GRAYSON, MATTHEW A. N91-13950
GREEN, HERBERT J. N91-13809
GREEN, M. C. N91-14047
GREENFIELD, C. M. N91-13705
N91-13706
N91-14024
N91-14025
GREENLEAF, JOHN E. N91-13862
GRIEWANK, ANDREAS N91-13913
GRIFFIN, E. J. N91-13926
GRIFFIN, KENNETH L. N91-14063
GRIFFIN, M. J. N91-13883
N91-13884
GRIFFITH, R. L. N91-13680
GRIFFITH, W. L. N91-13572
GRIGG, LEWIS RANDALL N91-13647
GRISAFFE, SALVATORE J. N91-13500
GROEBNER, R. J. N91-14023
GROLADE, D. N91-13776
GROOTERS, R. N91-13632
GROSCH, C. E. N91-13669
GROSSET, E. N91-13583
GROSSMAN, ROBERT N91-13949
N91-13950
GUENTHER, PETER R. N91-13809
GUERNY, GENE N91-14271
GUESS, T. R. N91-13736
GUETHLEIN, G. N91-13599
GUHATHAKURTA, P. N91-14110
GULLIXSON, CRAIG A. N91-14157
GUNTER, WILLIAM D. N91-14002
GUPTA, P. N91-13513
GUPTA, SHANTI S. N91-13953
GUYNN, E. GAIL N91-13756

H

HAAS, MICHAEL R. N91-14114
HACKWELL, JOHN A. N91-14207
HAHN, SANGKOO F. N91-13620
HALEY, PAMELA J. N91-13907
HAMADA, H. N91-13975
HAMID, SOHAIL N91-13678
HAMMOND, ERNEST C., JR. N91-13674
HAMMOND, P. B. N91-13859
HAMOUDA, M-NABIL H. N91-13462
HANDLER, T. N91-13979
HANNULA, SIMO-PEKKA N91-13531
HANSON, MARGARET MURRAY N91-14103
HARPER, D. A. N91-14134
N91-14141
HARPER, RICHARD N91-13934
HARRIS, ANDREW I. N91-14230
N91-14236
HARRIS, CHARLES E. N91-13761
HART, E. L. N91-13979
HARTEMANN, P. N91-14037
HARTMAN, RICHARD M. N91-13714
HARTMANN, ULRICH N91-13436
HARTSOUGH, CRAIG STEVEN N91-13836
HARVEY, P. M. N91-14130
N91-14175
N91-14229
HASKOVEC, J. N91-13706
HAUK, V. N91-13541
HAUSSLING, HENRY J. N91-13646
HAVENITH, G. N91-13881
HAVENS, STEVEN J. N91-13561
HAWTHORNE, J. R. N91-13774
HAXTHAUSEN, ERIC N91-14226
HAYATI, SAMAD A. N91-13724
HAYNES, RONALD B. N91-13901
HEAVNER, RICHARD L. N91-13443
HEIDBRINK, W. W. N91-14022
HEILES, C. N91-14138
HEITHAUSEN, ANDREAS N91-14124
HEKSTRA, A. D. N91-13431
HELOU, GEORGE N91-14103
HEMENGER, P. M. N91-14041
HENKEL, CHRISTIAN N91-14127
N91-14235
HENKUS, J. C. N91-13635
HENRY, D. P. N91-13557
HENRY, KAREN S. N91-13465
HENSHAW, ANDREW M. N91-13429
HER, SHIUH CHUAN N91-13752
HERGENROTHER, PAUL M. N91-13561
HERGET, CHARLES J. N91-13943
HESS, RONALD A. N91-13875
HESSE, P. W. N91-14048
HESTER, J. JEFF N91-14164
N91-14202
HIBBARD, J. E. N91-14176
HICKMAN, J. MARK N91-14259
HIEL, C. C. N91-13554
HILDEMANN, L. M. N91-13814
HILL, ACQUILLA S. N91-13461
HILL, J. M. N91-14159
HILL, ROBERT N91-14214
HILL, SUSAN G. N91-13880
HILLIS, S. L. N91-13718
HINNANT, HOWARD E. N91-13762
HIROMOTO, DAVID S. N91-13501
HIRSCH, T. N91-13542
HISER, A. L. N91-13774
HIXSON, R. S. N91-13624
HO, D. D.-M. N91-13815
HO, PAUL T. P. N91-14220
N91-14236
HODGDON, M. L. N91-13624
HODGE, PAUL N91-14156
HODGES, DEWEY H. N91-13762
HODGETTS, T. E. N91-13926
HOELTZEL, D. A. N91-13859
HOESCHELE, JAMES D. N91-13858
HOFFMAN, ERIC N91-13404
HOFFMANN, KLAUS A. N91-13419
HOGAN, J. T. N91-14018
HOGAN, ROY E. N91-13800
HOGG, D. E. N91-14109
HOLLAND, K. R. N91-13974
HOLLAND, O. W. N91-14061
HOLLENBACH, DAVID J. N91-14100
N91-14113
N91-14114
N91-14183
HOLLOWAY, J. N91-14252
HOLTKAMP, BERNHARD N91-13940
HOOPER, E. B. N91-13699
HOOVER, RICHARD N91-14096
HOPKINS, A. STEWART N91-13762
HORNADY, R. S. N91-13520
HORSTMAN, C. C. N91-13652
HOU, LIN-JUN N91-13449
HOUGARDY, HANS P. N91-13548
HOUSER, DONALD R. N91-13737
HOWARD, RICHARD N91-13482
HOWELL, M. N91-13498
HOWELL, WILLIAM E. N91-13445
HOWER, LINN N91-13909
HSIAO, YUN-LIN N91-13518
HSIEH, C.-L. N91-13705
N91-13706
N91-14024
N91-14025

HSU, F. N91-13746
HU, Y. F. N91-13919
N91-13920
N91-13961
HUA, GRACE C. N91-13944
HUANG, JIE N91-13821
HUANG, Y. N91-14117
HUBBARD, A. T. N91-13507
HUBBARD, RICHARD F. N91-13588
N91-14005
HUCHTMEIER, W. K. N91-14237
HUFF, TIMOTHY L. N91-13856
HULS, MARY H. N91-13860
HUMPHREYS, R. G. N91-14031
HUNT, GERALD F. N91-13689
HUNT, J. T. N91-13698
HUNT, R. NIALL M. N91-13744
HUNTER, DEIDRE A. N91-14141
N91-14152
HUNTER, NORWOOD N91-13865
HUSAIN, IMAD AHMED N91-13755
HUSSAINI, M. Y. N91-13650
HUYGEN, A. N91-13925
HYLAND, A. R. N91-14175
HYPES, WARREN D. N91-14251

I

IANCU, O. N91-13549
IDE, J. P. N91-13926
INGRAHAM, J. C. N91-14015
INOKUTI, MITIO N91-13983
ISHIGURO, MASATO N91-14233
ISHIZUKI, SUMIO N91-14233
ISOBE, TAKASHI N91-14135
ISRAEL, F. P. N91-14104
ISSACCI, F. N91-13645
IWANCZYK, JAN S. N91-13484
IYENGAR, K. V. K. N91-14131
N91-14147

J

JACKSON, JAMES M. N91-14220
N91-14230
N91-14236
JACKSON, PAUL EDWARD N91-13695
JACKSON, T. L. N91-13669
JACOBS, P. A. N91-13649
N91-13651
JACOBSEN, JANET S. N91-14073
JAFFE, D. T. N91-14230
N91-14236
JAIN, M. H. N91-13834
JANS, W. N91-13785
JARDIN, S. C. N91-14019
JARLAAS, ROLF N91-13770
JAUME, DENIS N91-13629
JAYNE, DOUGLAS T. N91-14050
JEANDREAU, J. P. N91-13917
JENKINS, EDWARD B. N91-14225
JENKINS, R. A. N91-13574
JEPPESEN, R. G. N91-13682
JHABVALA, MURZBAN N91-14066
JIN, WEI-QING N91-13967
JING, T. N91-14060
JOBSON, DANIEL J. N91-13941
JOHNSON, ANNE N91-13852
JOHNSON, D. A. N91-13653
JOHNSON, E. P. N91-13675
JOHNSON, G. N91-13660
JOHNSON, JOHN A. N91-13970
JOHNSON, W. JOEL D. N91-13626
JOHNSTON, B. S. N91-13655
JOKINEN, ANTERO N91-13531
JOKINEN, J. N91-13528
JONES, C. N91-14165
N91-14170
N91-14171
JONES, JACK A. N91-13581
JONES, K. W. N91-13859
JONES, TERRY JAY N91-14192
JORGENSEN, ELDON N. N91-13711
JORNA, P. G. A. M. N91-13468
N91-13872
JOSEPH, CHARLES L. N91-14116
JOY, MARSHALL N91-14175
N91-14221
JOYCE, GLENN N91-13588
N91-14005
JUANG, J. N. N91-13935
JUDAY, RICHARD D. N91-13997
N91-14000
JUEDES, DAVID N91-13913
JULLIEN-DETTMAR, MARLIES N91-14187
JUNGBAUER, DIETMAR N91-13564
JUNKINS, JOHN L. N91-13479
JUNKKARINEN, VESA T. N91-14228

K

KADIRI, M. N91-13776
KAHL, W. K. N91-13955
KAHRAMAN, AHMET N91-13737
KALDEICH, BRIGITTE N91-14095
KALLENBACH, P. A. N91-14083
KALLMAN, ROBERT R. N91-13992
KAMEYA, OSAMO N91-14120
KAMPHUIS, J. N91-14105
KANE, LEOTA S. N91-14081
KANG, CHUL GOO N91-13937
KAPLAN, S. N. N91-14060
KAPUSTINSKY, J. S. N91-13682
KARGATIS, VINCENT N91-14269
KARMARKAR, S. D. N91-14048
KARWACKI, FRANCIS A. N91-14043
KATTENBERG, ARIE N91-13840
KAUFMAN, LLOYD N91-13869
KAUFMANN, W. A. N91-13437
KAUPPINEN, PENTTI N91-13567
KAWABE, RYOHEI N91-14233
KAWABE, USHIO N91-14039
KAY, A. N91-13666
KEANE, C. N91-13698
KEATING, THOMAS N91-14271
KELLEY, HENRY L. N91-13406
KELLEY, THOMAS A. N91-13597
KEMNA, G. J. M. N91-13636
KENDALL, JAMES M., JR. N91-13658
KENNEDY, E. J. N91-13618
KENNEDY, JOHN M. N91-14079
KENNEY, J. D. N91-14117
KENNICUTT, R. C., JR. N91-14154
N91-14210
KEPPEL, JEAN N91-14160
KERLEY, JAMES J., JR. N91-13735
KEY, J. N91-13782
KHANDELWAL, GOVIND S. N91-13985
KHODA, K. M. N91-13918
KILGUS, U. N91-13984
KIM, D.-W. N91-14110
KIM, DONG-WOO N91-14112
KIM, JAE H. N91-13995
KIM, JUNGHO N91-13643
KIM, K. STEVEN N91-13758
KIM, KWANG JOO N91-14059
KIMURA, YOSHIFUMI N91-13957
KING, CHARLES B. N91-14251
KING, DONALD B. N91-13990
KING, RONALD W. N91-13932
KIRK, WILLIAM L. N91-13490
KIRKPATRICK, J. R. N91-13577
KISTLER, DORIS J. N91-13971
KLAASEN, J. J. A. N91-13607
KLEIN, D. B. N91-13645
KLEIN, H. N91-13543
KLEIN, NATHAN N91-13571
KLEM, J. F. N91-14056
KLEM, MARK D. N91-13491
KLUMPERS, F. J. N91-13633
KNAPP, G. R. N91-14110
KNAPP, JILL N91-14142
KNEZEK, PATRICIA M. N91-14117
N91-14119
KNOTT, WILLIAM M. N91-13849
KOCH, JOHN, JR. N91-13685
KOCSIS, FRANK J. N91-13994
KOGER, THOMAS L. N91-13691
KOK, W. J. N91-13786
KOLLENBERG, W. N91-13536
KOOMEN, P. J. N91-13635
KOSEK, J. A. N91-13794
KOTSUBO, V. N91-13582
KOTTHAUS, R. N91-13984
KOVESI-DOMOKOS, S. N91-14071
KOWEL, STEPHEN T. N91-13612
KRALL, J. N91-14005
KRUER, MARK ARTHUR N91-13999
KULKARNI, SHRINIVAS R. N91-14164
N91-14202
N91-14204
KUMER, JAYANT N91-13553
KUNZ, DONALD L. N91-13762
KUNZ, G. J. N91-13838
KUSHNICK, PETER W. N91-13527
KUSMANOFF, ANTONE L. N91-13894
KYRAZIS, DEMOS T. N91-13707

L

LABANCZ, KRISZTINA N91-13790
LACOMBE, F. N91-14217
LACONTI, A. B. N91-13794
LAFLEUR, SHARON S. N91-13694
LAGACE, PAUL A. N91-13446
LAGEN, NICHOLAS T. N91-13684
LALOR, N. N91-13778
LANCASTER, M. J. N91-14036
LANDGRAF, M. N91-13612
LANDIS, GEOFFREY A. N91-14259
LANE, D. W. N91-13682
LANE, S. N91-13690
LANGE, E. N91-13984
LAPOUTRE, J. A. N91-13954
LARSON, KRISTINE MARIE N91-13822
LASKEY, K. J. N91-13512
LAWRENCE, R. V. N91-13439
LAZARETH, O. W. N91-13866
LEE, H. M., III N91-13766
LEE, ILZOO N91-13515
LEE, MYUNG GYOON N91-14155
N91-14156
LEES, J. F. N91-14205
LEGRAND, SUE N91-13906
LEHTO, WAYNE K. N91-13932
LEIGH, LINDA S. N91-13845
LEISAWITZ, D. N91-14139
LEITCH, M. J. N91-13682
LEITENETO, JOAQUIM PAULINO N91-13898
LEMASCON, A. N91-13504
LENTING, J. H. J. N91-13747
N91-13748
LENZ, JAMES N91-14042
LENZ, TERRY G. N91-13509
LERCHE, R. A. N91-13680
N91-14021
LESTER, DAN F. N91-14130
N91-14221
N91-14229
LEVERMORE, C. DAVID N91-13962
LEVIN, RICHARD R. N91-13476
LEVITON, DOUGLAS B. N91-13692
LEVY, YESHAYAHOU N91-13455
LEWIS, MARIAN L. N91-13860
LI, HSI-SHANG N91-13510
LIANG, EDISON P. N91-14269
LIEBERT, CURT H. N91-13685
LILLBERG, J. W. N91-13682
LIN, CHIN S. N91-13807
LIN, D. N. C. N91-14195
N91-14212
LIN, SHYNG-HER N91-13722
LIN, STEVEN H. N91-13995
LIND, DON N91-14097
LINDBERG, STEVEN E. N91-13812
LINDSAY, RICHARD W. N91-13932
LIU, J. C. N91-13697
LIU, TSUEN-HSI N91-13998
LIU, Y. N91-13918
LO, K. Y. N91-14146
N91-14203
N91-14205
LO, R. Y. N91-14133
LOEWENSTEIN, MICHAEL N91-14167
LOFTIN, R. BOWEN N91-13944
LONDON, R. N91-13690
LOPEZ, T. A. N91-13682
LORD, STEVEN D. N91-14114
LOSCHIAVO, VALERIA N91-14094
LOTENS, W. A. N91-13881
LOTT, J. A. N91-14056
LOWNEY, J. R. N91-14056
LUAN, L. N91-14138
LUCASSEN, M. P. N91-13608
LUCKHARDT, RUTH N91-14026
LUDEWIG, H. N91-13866
LUFF, J. N91-13926
LUGTEN, J. B. N91-14230
LUKENS, JAMES N91-14051
LUKER, SPENCER MICHAEL N91-13990
LUMPKIN, FORREST EDWARD, III N91-13403
LUND, J. N91-13952
LUND, PATRICIA N91-13810
LUU, PHUONG B. N91-13862
LYNCH, A. W. N91-13521
LYNCH, DANA H. N91-14002
LYNCH, MICHAEL T. N91-13988
LYNCH, S. P. N91-13777
LYRINTZIS, A. S. N91-13422

M

MA, C. Y. N91-13574
MAARTENSE, I. N91-14041
MAAS, R. N91-13471
MACCALLUM, TABER N91-13845
MACDONALD, ROBERT H. N91-13891
MACK, ROBERT J. N91-13433
MACKE, A. N91-14272
MACLAREN, J. M. N91-13978
MACLEAN, T. S. M. N91-14036
MACLOW, MORDECAI-MARK N91-14180
MADNIA, CYRUS K. N91-13656
MAGE, J. C. N91-14038
MAHIOUT, AMAR N91-13531
MAIANI, M. N91-13616
MAILLARD, A. N91-13583
MAINE, P. N91-13698
MAKINEN, REINO N91-13528
MAKO, F. N91-14005
MAKOWITZ, HENRY N91-13932
MALARIK, DIANE C. N91-13566
MALONEY, PHILIP RICHARD N91-14101
MANDAL, BRAJA K. N91-13553
MANSOUR, A. N. N91-14048
MARAWA, A. N91-13426
MARCUS, J. T. N91-13873
MARIS, HUMPHREY J. N91-13973
MARKS, TOBIN J. N91-13552
MARMOLEJO, JOSE N91-13879
MARQUARDT, B. J. N91-13524
MARRS, R. E. N91-13981
MARSH, A. R. S. N91-13868
MARSHALL, R. N91-14052
MARSHALL, SUSAN ELAINE N91-13781
MARTIN, J. N91-13444
MARTIN, JAMES A. N91-13481
MARTIN, KEITH E. N91-14049
MARTIN, R. N. N91-14128
MARTINELLI, G. N91-13616
MARTINEZ, ERNEST C. N91-13662
MARTZ, H. E. N91-13914
MARZULLO, KEITH N91-13928
MASCARENHAS, NELSON D. A. N91-13587
MASLANIK, J. N91-13782
MASON, STEPHEN F. N91-14157
MASOTTO, TOM N91-13934
MASSOUDI, M. N91-13660
MATLOFF, N. N91-13612
MATTHAEI, E. N91-13547
MATTHEWS, D. N91-13690
MAUERSBERGER, R. N91-14235
MAY, WILLIAM EDGAR N91-13912
MAYFIELD, M. J. N91-13805
MAYHALL, DAVID J. N91-13623
MAYR, P. N91-13542
MAZUMDAR, MAINAK N91-13745
MAZUNDAR, RAVI N91-13964
MAZUREK, M. A. N91-13814
MCALISTER, KENNETH W. N91-14002
MCALLISTER, DAVID F. N91-13904
MCARDLE, JAMES N91-14042
MCCALL, MARSHALL L. N91-14153
N91-14193
N91-14214
MCCLURE, CHARLES R. N91-14074
MCCREIGHT, CRAIG N91-14087
MCDONALD, M. M. N91-13757
MCGAUGHEY, P. L. N91-13682
MCGEHEE, JOHN R. N91-13445
MCGILL, R. N. N91-13718
MCGRAW, MARVIN E., JR. N91-13432
MCGREGOR, P. J. N91-14175
MCGUFFIN, BRUCE F. N91-13475
MCGUIRK, JAMES P. N91-13832
MCINTOSH, G. E. N91-13463
MCKAMEY, C. G. N91-13498
MCKEE, CHRISTOPHER F. N91-14183
N91-14186
MCKENNA, KENNETH F. N91-13988
MCLAREN, M. D. N91-13477
N91-13478
MCLEAN, WILLIAM N91-13879
MCLEOD, ROBERT R. N91-13593
N91-13908
MCMAHON, P. M. N91-14177
MCMILLIN, S. NAOMI N91-13401
MCNIVEN, ULLA N91-13530
MCVEY, BRIAN D. N91-13631
N91-13702
MEEHAN, RICHARD N91-13865
MEI, KENNETH K. N91-13613
MEI, V. C. N91-13578
MEILER, P. P. N91-13603
MEIXNER, M. N91-14121
MELLOMARSHALL, PAULO N91-13586
MELTON, PATRICK B. N91-13731
MELTON, ROY W. N91-13429
MENDELL, WENDELL N91-13855
MENESES, PAULO ROBERTO N91-14086
MESSENGER, A. N91-13884
MEYER, SAM N91-13424
MEYN, ERWIN M. N91-13730
MICHAEL, J. R. N91-13980
MICHEL, ROLF N91-14098
MIESCKE, KLAUS J. N91-13953
MIGLIORI, ALBERT N91-13743
MILLER, GUTHRIE N91-14010
N91-14015
MILLET, P. N91-13917
MINECK, RAYMOND E. N91-13461
MINES, G. L. N91-13798
N91-13799
MING, XIAO N91-13454
MINH, YOUNG CHOL N91-14093
MINKOFF, M. N91-13933
MIRICK, PAUL H. N91-13462
MIRIN, ARTHUR A. N91-13915
MOE, KAREN N91-14271
MOES, TIMOTHY R. N91-13453
MOIR, RALPH W. N91-14004
MONACO, LISA A. N91-14029
MONCUR, KENT N91-14026
MONGIS, J. N91-13533
MONTES, ANTONIO N91-13898
MONTGOMERY, RAYMOND C. N91-13694
MOONEY, L. E. N91-13834
MOORE, F. K. N91-13458
MOORE, T. L. N91-13945
MORAN, ANGELA L. N91-13523
MORFEY, C. L. N91-13974
MORGAN, JAMES ARTHUR N91-14246
MORGAN, R. G. N91-13651
MORITA, KOH-ICHIRO N91-14233
MORRIS, D. E. N91-13700
MORRIS, K. A. N91-13935
MORRIS, PHILIP J. N91-13640
MORRIS, STEPHEN JAMES N91-13459
MORRISON, CLYDE A. N91-14053
MORZENTI, ANGELO N91-13927
MOSES, RONALD W., JR. N91-14009
N91-14011
MOSS, J. M. N91-13682
MOSS, STEVEN W. N91-13412
MOTTER, MARK A. N91-13467
MOUGINIS-MARK, P. N91-14252
MOULTON, PETER F. N91-13696
MOUNTAIN, C. M. N91-14129
MOUROU, GERARD N91-13698
N91-14054
MOYER, SANDRA N91-14026
MUELLER, C. N91-13933
MUIR, JAMES F. N91-13800
MUNSON, C. P. N91-14015
MUNZ, D. N91-13549
MURAD, S. N91-13654
MURATORI, SIMONA N91-13963
MURMAN, EARLL M. N91-13401
MURPHY, R. W. N91-13578
MURRAY, P. T. N91-14041
MURRAY, S. D. N91-14195
MUSIAL, W. N91-13414
MYERS, DAVID R. N91-14056
MYERS, S. T. N91-14122
MYKLEBUST, R. L. N91-13980

N

NAEGELI, WOLFGANG N91-13810
NAGASUBRAMANIAN, GANESAN N91-13621
NAGY, A. N91-13534
N91-13535
NAIDON, A. N91-13776
NAIL, WILLIAM L. N91-13691
NAKAI, NAOMASA N91-14120
N91-14129
NAMKUNG, MIN N91-13527
NANDHAKUMAR, N. N91-13725
NDOH, N. N. N91-13427
NEALY, JOHN E. N91-14251
N91-14265
NEBEL, R. A. N91-14014
NEEDLEMAN, KATHY E. N91-13433
NEFF, J. M. N91-13655
NEILSEN, M. K. N91-13773
NELSON, MARK N91-13842
NELSON, P. A. N91-13975
NENNIE, F. A. N91-13634
NEUFELD, DAVID A. N91-14186
NEUVONEN, A. N91-13528
NEWBURY, D. E. N91-13980
NICOLET, MARCEL N91-13816
NOAKES, M. W. N91-13946
NOOR, AHMED K. N91-13750
NORIEGA-CRESPO, A. N91-14212
NORMAN, MICHAEL L. N91-14182
NORVILLE, KENT WESTON N91-13835
NYCE, THOMAS A. N91-14029

O

OBANNON, B. JIM N91-14063
OCHOA, OZDEN O. N91-13756
OCONNELL, R. W. N91-14223
ODELL, C. R. N91-14158
ODEWAHN, STEPHEN CHARLES N91-14245
OEY, M. S. N91-14210
OHLSSON, STELLAN N91-13951
OKUMURA, SACHIKO K. N91-14233
OLBERG, M. N91-14125
OLECHOWSKI, MARK JOSEPH N91-13715
OLSSON, MATS OLOF N91-13448
ORAN, ELAINE S. N91-13512
N91-13588
ORFORD, G. R. N91-13926
ORLOWSKA, A. H. N91-14035
OROFINO, V. N91-14264
ORTIZ, VANESSA N91-13862
ORZECHOWSKI, T. J. N91-13599
OSBORNE, ERIC P. N91-14001
OSHEA, PATRICK G. N91-13988
OTTENBRITE, RAPHAEL M. N91-13560
OUZTS, PETER J. N91-13457
OVERBEEK, ROSS N91-13942
OVERDUIN, R. N91-13635
OWENS, S. F. N91-13489

P

PAINE, THOMAS O. N91-13843
PALMBERG, BJOERN N91-13448
PANKAKOSKI, PEKKA H. N91-13567
PANTUCEK, P. N91-13544
PAPAGEORGIOU, DEMETRIOS T. N91-13642
PARK, K. C. N91-13480
PARKER, JUNE M. N91-13965
PARKS, ALLEN D. N91-13886
PARKS, W. P., JR. N91-13497
PARSONS, W. M. N91-13624
PATTERSON, JAMES C., JR. N91-13402
PATTON, R. J. N91-13947
PEARCE, S. J. N91-13667
PELLAT, R. N91-14188
PENG, Y.-K. M. N91-14019
PENTECOST, C. G. N91-13670
N91-14013
PERERA, P. A. B. A. R. N91-13710
PEREZ-MENDEZ, V. N91-14060
PERLEY, RICK N91-14151
PERRE, M. N91-13747
N91-13748
PERROT, HUBERT N91-13630
PERRY, CHARLES AUGUST N91-13823
PERRY, JAMES C. N91-13886
PERRY, M. D. N91-13698
PETERS, D. N91-13690
PETERS, DAVID A. N91-13449
PETERS, JEANNE M. N91-13750
PETERSON, BRADLEY M. N91-14088
PETERSON, EVA N91-13839
PETERSON, T. L. N91-14041
PETERSON, WAYNE L. N91-13483
PETRICK, S. WALTER N91-13581
PETTERSON, B. J. N91-13946
PETZOLD, LINDA R. N91-13956
PEYRARD, MICHEL N91-14070
PEYRE, J. P. N91-13533
PFALZNER, SUSANNE N91-14027
PHANEUF, R. A. N91-14012
PHILLION, D. W. N91-14021
PI, JONATHAN N91-13525
PICKRELL, M. M. N91-14015
PICONE, J. MICHAEL N91-13588
PILANT, M. S. N91-13496
PINELLI, THOMAS E. N91-14079
PINKEL, D. N91-13690
PINTSCHOVIUS, L. N91-13538
PIOMELLI, UGO N91-13410
PITKANEN, JORMA N91-13567
PITTS, JOHN H. N91-13707
PLANESAS, P. N91-14122
PLASKACZ, E. N91-13933
PLIMPTON, S. J. N91-13980
PLOUGH, ALAN N91-13879

POCHA, MICHAEL D. N91-14063
POGGE, RICHARD W. N91-14111
POLLOCK, THOMAS C. N91-13479
POMPEA, STEPHEN M. N91-14208
POMPHREY, N. N91-14019
PONGRATZ, MORRIS B. N91-13988
PONTON, MICHAEL K. N91-13413
POPELAR, C. F. N91-13534
N91-13535
POPLAWSKI, DAVID A. N91-13931
POST, D. E. N91-14017
POWELL, J. R. N91-13866
POWERS, ALAN K. N91-13932
PRAMONO, E. N91-13480
PRICE, JILL S. N91-14157
PRICE, S. D. N91-14143
PRICE, WILLIAM E. N91-14049
PRICHARD, DEVON S. N91-13407
PROGAR, DONALD J. N91-13559
PROTOPOPESCU, V. N91-14072
PUCHALSKY, R. N91-14121
PUXLEY, P. J. N91-14213
PUXLEY, PHIL J. N91-14129
N91-14184

Q

QUIMBY, DAVID C. N91-13702

R

RABINOWITZ, M. B. N91-13859
RADEMACHER, KURT R. N91-13819
N91-13831
RADFORD, SIMON J. E. N91-14234
RAFFERTY, PATRICK N91-13909
RAHKA, KLAUS N91-13530
N91-13531
RAHMAN, ZAHIDUL H. N91-13479
RAJAGOPAL, K. R. N91-13660
RAMSAY, JOHN B. N91-13573
RAMSEY, J. M. N91-13517
RAMSEY, JOHN K. N91-13730
RAND, R. J. N91-14164
RAND, RICHARD J. N91-14204
RANDO, BERNARD A. N91-13994
RAO, T. V. GOVINDA N91-13673
RAWLINGS, STEVE N91-14166
N91-14238
RAYNER, STEVE N91-13810
REAUGH, JOHN E. N91-13726
REBER, RON N91-13424
REE, F. H. N91-13499
REECE, GARLAND D. N91-13684
REED, JASON C. N91-13558
REEDY, E. D., JR. N91-13736
REEDY, ROBERT C. N91-14098
N91-14258
REICHERT, ROBERT T. N91-13435
REIMERS, W. N91-13537
REISDORFER, D. N91-13444
RELOU, H. N91-13785
RENBARGER, V. L. N91-13599
RENGARAJAN, T. N. N91-14131
N91-14147
RESSELL, M. TED N91-13976
RHODES, C. G. N91-13524
RHODES, MARVIN D. N91-13473
RIBEIRO, EDSON A. N91-13587
RICHER, MICHAEL G. N91-14193
RICHTER, HERBERT P. N91-13573
RICHTER, O.-G. N91-14177
RICKARD, L. J. N91-14143
RIED, ROBERT C. N91-13483
RIEKE, G. H. N91-14208
RINALDI, SERGIO N91-13963
RINTAMAA, RAUNO N91-13530
RITZ, CH. P. N91-14015
ROBERSON, G. P. N91-13914
ROBERTS, M. L. N91-13945
ROBERTS, M. S. N91-14109
ROBERTS, MORTON S. N91-14160
ROBERTS, PAUL W. N91-13687
ROBINSON, M. B. N91-13513
ROBINSON, MARTHA P. N91-13751
ROCHE, G. L. N91-13645
ROCHE, GREGORY LAWRENCE N91-13644
RODRIGUE, GARRY H. N91-13962
RODRIQUEZ, R. N91-13670
N91-14013
ROGERS, D., JR. N91-13599
ROGERS, JOHN S. N91-13939
ROGERS, R. C. N91-13649
ROGGE, W. F. N91-13814
ROGUIN, P. N91-13532
N91-13738
N91-13739
N91-13740
ROJAS, R. G. N91-13428
ROMANOFSKY, ROBERT R. N91-13996
ROMIG, A. D., JR. N91-13980
ROMINE, C. H. N91-13959
RORVIG, MARK E. N91-13911
ROSCOE, A. H. N91-13882
ROSENBERGER, FRANZ N91-13967
N91-14029
N91-14055
ROSENFELD, MOSHE N91-13639
ROSS, BRIAN N91-13483
ROTHERMEL, H. N91-14125
ROUAN, D. N91-14217
ROUS, P. J. N91-13978
ROUSSEL-DUPRE, ROBERT N91-13597
N91-13720
RUBIN, ROBERT H. N91-14114
RUDBERG, BJORN N91-13891
RUIZENDAAL, P. F. N91-13450
RUPEN, MICHAEL P. N91-14108
RUSS, G. PRICE, III N91-13689
RUSSO, CARL J. N91-14034
N91-14046
RUTLEDGE, WALTER H. N91-13419
RUZIC, D. N. N91-14028
RYAN, RODGER N91-13990
RYDBECK, G. N91-14125
RYNE, ROBERT D. N91-13619

S

SACKETT, JOHN I. N91-13932
SALASALVES, DIOGENES N91-14078
SALMI, JAAKO N91-13529
SALONEN, JORMA N91-13528
SALOUR, M. N91-14052
SALPETER, E. E. N91-14163
SAMANTA, P. K. N91-13746
SAMPATH, K. S. N91-13428
SAMPSON, DOUGLAS H. N91-14020
SANCISI, R. N91-14105
SANDAGE, A. N91-14200
SANDERS, D. B. N91-14123
SANDFORD, MAYNARD C. N91-13400
SANKARAN, SANKARA N. N91-13522
SANPIETRO, PIERLUIGI N91-13927
SARAZIN, CRAIG L. N91-14172
N91-14173
SARGENT, A. I. N91-14123
SATCHELL, J. S. N91-14031
SAUER, HERBERT H. N91-14265
SAUER, RICHARD L. N91-13857
SAULT, A. G. N91-13521
SAVAGE, N. J. N91-13505
SAVILLE, D. A. N91-13648
SAYLES, ANDRE HARDING N91-13611
SCARR, G. K. N91-13524
SCHIDLOVSKY, G. N91-13859
SCHIMEL, DAVID S. N91-13813
SCHIPANI, SALVATORE P. N91-13870
SCHLOERB, F. P. N91-14117
SCHLOERB, F. PETER N91-14126
SCHMATZ, MANFRED A. N91-13423
SCHMITT, MARK N91-13631
SCHNEBERK, D. J. N91-13914
SCHNEIDER, E. N91-13546
SCHNEIDER, STEVEN P. N91-13676
SCHOCHET, STEVEN N91-13966
SCHOENBERG, K. F. N91-14011
N91-14015
SCHOENBERG, KURT F. N91-14009
SCHOLTES, B. N91-13539
SCHREYER, H. L. N91-13773
SCHROCK, R. R. N91-13551
SCHROEDER, MICHAEL CHRISTOPHER N91-14241
SCHUBERT, H. N91-13545
SCHUBERT, T. N91-13612
SCHUHL, A. N91-14033
SCHULER, ALBERT P. N91-13886
SCHWARZ, RAY P. N91-13860
SCHWEIGER, A. N91-13782
SCHWENTEK, H. N91-14272
SCHWENTERLY, S. W. N91-13681
SCOTT, G. N91-13414
SCOTT, ROBERT, JR. N91-13932
SCOTT, RUSSELL W., II N91-13938
SCOVILLE, N. Z. N91-14122
N91-14123
SEGALL, ZARY N91-13930
SEGUR, HARVEY N91-13958
SEINER, JOHN M. N91-13413
SELLGREN, K. N91-14138
SELVADURAI, U. N91-13537
SEPPALA, LYNN G. N91-13707
SERAFIM, P. N91-14005
SERAYDARIAN, R. P. N91-14023
SHAFER, ROBERT E. N91-13701
SHALKHAUSER, MARY J. N91-13598
SHALLENBERGER, KURT N91-13900
SHARPE, STEPHEN R. N91-14057
SHAW, DAVID C. N91-14049
SHIELDS, ELWOOD W. N91-13432
SHIN, YOUNG S. N91-13758
SHINYASHIBATA, CARLOS N91-13898
SHIVASHANKAR, N. N91-13673
SHULL, J. MICHAEL N91-14227
SIEMER, H. N91-13540
SIEWIOREK, DANIEL N91-13930
SILVEIRASOARESFILHO, BRITALDO N91-13784
SILVER, A. H. N91-14040
SIMMONS, C. M. N91-13681
SIMMS, D. N91-13414
SIMON, M. N91-13596
SIMON, P. C. N91-13830
SIMONSEN, LISA C. N91-14251
N91-14265
SIMS, GRAHAM D. N91-13568
SINDELAR, R. L. N91-13774
SINGH, JAG J. N91-13492
SINGH, RAJENDRA N91-13737
SIVASHINSKY, GREGORY N91-13519
SIVERSON, R. J. N91-13815
SKEATE, M. F. N91-13914
SKILLMAN, EVAN D. N91-14154
SKINNER, K. N91-13651
SKOCYPEC, RUSSELL D. N91-13800
SKUBIC, P. L. N91-13618
SLATER, G. L. N91-13477
N91-13478
SLINEY, HAROLD E. N91-13503
SLINKER, S. P. N91-14005
SLINKER, STEVEN P. N91-13588
SMITH, A. D. N91-14040
SMITH, B. J. N91-14130
SMITH, BARRY T. N91-13494
SMITH, C. N91-13486
SMITH, GARY R. N91-14016
SMITH, HENRY I. N91-13993
SMITH, JEFFREY H. N91-13476
N91-13876
SMITH, JOSEPH G., JR. N91-13560
SMITH, P. A. N91-14129
SMITH, R. C. N91-13952
SMITH, STEPHEN N91-13879
SMYRLIS, YIORGOS, ... N91-13642
SNIDER, R. T. N91-13705
N91-13706
N91-14024
N91-14025
SNIEDER, J. N91-13601
SNOW, THEODORE P. N91-14227
SOFFEN, GERALD N91-13842
N91-13853
N91-14271
SOHN, R. A. N91-13447
SOKER, NOAM N91-14172
SOKOLOWSKI, J. N91-14150
SOLOMON, P. M. N91-14234
SOLOMON, SEAN C. N91-14254
SOMORJAI, G. A. N91-13978
SOUVIGNET, R. N91-13742
SOWERS, JENNIFER W. N91-14029
SPANNE, P. N91-13859
SPENCER, FLOYD W. N91-13745
SPENCER, JAMES T. N91-13614
SPEZIALE, C. G. N91-13650
SPRANGLE, P. N91-14005
SPURGEON, S. K. N91-13947
N91-13948
ST.CLAIR, TERRY L. N91-13559
STAGNARO, MICHAEL J. N91-13483
STALFORD, HAROLD N91-13404
STALKER, R. J. N91-13651
STANFORD, S. A. N91-14123
STEELMAN, DENNIS N91-13900
STEFFAN, CARL R. N91-13526
STEFFEN, K. N91-13782
STEFFES, PAUL G. N91-13584
STEIN, WILLIAM E. N91-13626
STEINBERGER, CRAIG J. N91-13656
STEINETZ, BRUCE M. N91-13456
STEMWEDEL, S. W. N91-14143
STEPHAN, RONAN N91-14044
STEPHENS, J. R. N91-14264
STERN, C. N91-14171
STERN, S. ALEXANDER N91-13671
STERN, SOL ALAN N91-14242

STEVENS, RALPH ROBERT N91-13764
STEVENSON, CHRIS N91-14153
STOCKE, JOHN T. N91-14169
N91-14227
STONE, JAMES M. N91-14182
STONER, K. J. N91-13774
STOREY, C. N91-13918
N91-13920
N91-13961
STOREY, M. N91-13919
STREET, R. A. N91-14060
STREHLOW, RICHARD A. N91-14082
STRICKLER, D. J. N91-14019
STROM, C. N91-14102
STROUP, J. W. N91-13447
STRUCK-MARCELL, CURTIS N91 14107
N91-14211
STUTZKI, J. N91-14230
SUBDUHI, M. N91-13746
SUESS, HELMUT N91-13679
SUKUMAR, S. N91-14194
SULLIVAN, TIMOTHY J. N91-13804
SULLIVAN, WALTER N91-14271
SWANK, W. D. N91-13826
SWANSON, EDWARD E. N91-13432
SWIEP, G. N91-13871
SWIFT, G. W. N91-13582
SYGNET, J. F. N91-14188
SZOKE, A. N91-13698
SZU, HAROLD H. N91-13887

T

TABACCHIONI, F. N91-13616
TACCONI-GARMAN, L. N91-14117
TACCONI, L. N91-14117
TACCONI, L. J. N91-14199
N91-14232
TACCONI, LINDA N91-14239
TADMOR, EITAN N91-13966
TAGGER, M. N91-14188
TAIT, C. D. N91-13700
TAM, CHRISTOPHER N91-13969
TANDON, S. N. N91-14131
TANG, C. M. N91-14005
TANIGUCHI, YOSHIAKI N91-14120
N91-14148
TAPLEY, B. D. N91-13470
TAPLEY, M. N91-13788
TATUM, CHARLES P. N91-14084
TAUC, JAN N91-13973
TAYLOR, GERALD N91-13865
TAYLOR, RONALD D. N91-13588
TEITEL, STEPHEN N91-14064
TELESCO, C. M. N91-14223
TENORIO-TAGLE, G. N91-14212
TERRELL, KYLE N91-13733
TESAR, DELBERT N91-13721
N91-13722
THANING, LENNART N91-13839
THEISS, T. J. N91-13763
THERIOS, I. U. N91-13933
THOE, ROBERT N91-13704
THOMAS, JAMES L. N91-13401
THOMASSON, DAVID MICHAEL N91-13867
THOMPSON, C. V. N91-13574
THOMPSON, PETE N91-13424
THRONSON, HARLEY A., JR. N91-14100
N91-14141
TIELENS, A. G. G. M. N91-14113
TIEMAN, T. C. N91-13632
TIGGES, C. P. N91-14056
TILANUS, R. P. J. N91-14206
TITUS, TIMOTHY N. N91-14211
TOBAK, M. N91-13408
TOET, A. N91-14003
TOKERUD, BARD N91-13891
TOLLESTRUP, E. V. N91-14175
TOLSTOY, E. N91-14104
TOMISAKA, KOHJI N91-14191
TOMKINS, B. A. N91-13574
TOMOZAWA, MINORU N91-13565
TONG, MIKE T. N91-13456
TORTORELLI, P. F. N91-13498
TOSUNOGLU, SABRI N91-13722
TOURNIER, C. N91-13533
TOWNSEND, LAWRENCE W. N91-13985
N91-14265
TRANGENSTEIN, JOHN A. N91-13765
TREBES, J. N91-13690
TRIMARCHI, PAUL A. N91-13732
TRIPATHY, SUKANT N91-13553
TROST, P. N91-13706
N91-14024
TROST, P. K. N91-13705
N91-14025
TRUHLAR, DONALD G. N91-14058
TRUONG, K. V. N91-13408
TRUSZKOWSKI, WALT N91-14271
TSANG, K. T. N91-13815
TSUI, H. Y. W. N91-14015
TUCKER, W. N91-14165
TULLY, BRENT N91-14240
TULLY, R. B. N91-14150
TURNER, GREGORY A. N91-14053
TURNER, J. L. N91-14220
TURNER, JAMES E. N91-13858
TURNER, MICHAEL S. N91-13976
TUTHILL, WALLACE C. N91-13580
TVETE, KNUT N91-13891
TZE, CHIA-HSIUNG N91-14067

U

UCKAN, N. A. N91-14017
N91-14018
ULABY, FAWWAZ T. N91-13817
ULMER, M. P. N91-14174
UMARETIYA, JAGDISH R. N91-13936
UNERTL, W. N. N91-13550
UNGER, STEPHEN W. N91-14178
UPCHURCH, BILLY T. N91-13492
UUTTU, TERO N91-13567

V

VALAND, PER ATLE N91-13923
N91-13924
VALLAS, G. N91-13438
VANBEZOUWEN, J. P. N91-13636
VANBUSKIRK, PAUL N91-13683
VANDELINDE, F. J. G. N91-13881
VANDENANCKER, J. A. M. N91-13785
VANDERHULST, J. M. N91-14105
N91-14199
VANDERVOET, H. N91-13785
VANDERWALL, BEREND N91-13415
VANDERWERF, D. C. N91-13785
VANGORKOM, JACQUELINE H. N91-14110
N91-14176
N91-14177
N91-14226
VANHEZEWIJK, J. G. N91-13602
VANHOLTEN, C. R. N91-13873
VANHOVE, M. A. N91-13978
VANMIEGROET, HELGA N91-13812
VANNEL, JEAN-PAUL N91-13628
VANNUCCI, RAYMOND D. N91-13566
VANPATTEN, R. N91-13788
VANSCHAIK, P. N91-13905
VANTHIEL, M. N91-13499
VANWOERDEN, HUGO N91-14239
VANZYL, JAKOB J. N91-13594
VARELLA, D. N91-13486
VAUGHAN, JOHN D. N91-13509
VENKATARAMAN, SUBRAMANIAN T. N91-13724
VENKATESH, C. S. N91-13673
VERMA, R. P. N91-14131
VERTER, FRAN N91-14181
VERWEY, W. B. N91-13874
VESELY, W. E. N91-13746
VESSOT, ROBERT F. C. N91-13688
VETTERS, H. N91-13547
VIALLEFOND, F. N91-14231
VIEIRADUTRA, LUCIANO N91-14086
VILLA, FRANCESCO N91-13623
VISCO, M. N91-13616
VISCUSO, P. N91-14117
VISSCHER, WILLIAM M. N91-13743
VISSER, H. J. N91-13604
VISSER, R. T. B. N91-13468
VISVANATHAN, N. N91-14193
VOGEL, D. A. N91-13981
VOGEL, T. N91-13486
VOGLER, WILLIAM A. N91-13445
VOIT, G. MARK N91-14144
N91-14169
VOLAKIS, JOHN L. N91-13893
VONHUGO, DIRK N91-14065
VOUK, MLADEN A. N91-13904
VRSALOVIC, DALIBOR N91-13930

W

WAIBEL, B. N91-13543
WAKKER, K. F. N91-13791
WALCH, STEPHEN P. N91-13506
WALFORD, ROY N91-13847
WALKER, C. E. N91-14128
WALKER, C. K. N91-14128
WALLACE, TERRYL A. N91-13522
WALLER, WILLIAM H. N91-14219
WALRAVEN, J. N91-13431
N91-13608
N91-13789
WALSH, DUNCAN N91-14142
WALTER, RICHARD T. N91-13683
WALTERBOS, RENE N91-14179
N91-14196
WALTERS, DAVID N91-13900
WANG, LUI N91-13944
WANG, ZHONG N91-14106
WARD, B. F. L. N91-13979
WARD, LEONARD W. N91-13932
WARD, N. R. N91-13651
WARDE, C. N91-14052
WASBERG, CARL ERIK N91-13828
WEAVER, H. T. N91-13625
WEAVER, R. N91-13782
WEBB, WINSTON S. N91-13729
WEBER, D. P. N91-13933
WEBER, P. G. N91-14015
WEBER, WILLIAM N91-13683
WEFEL, JOHN P. N91-14090
WEIDNER, E. H. N91-13649
WEINBERG, IRVING N91-13803
WEIR, J. T. N91-13599
WEITZNER, HAROLD N91-14006
WEIZER, VICTOR G. N91-14050
WELCH, DOUGLAS L. N91-14153
WELTY, DANIEL E. N91-14115
WENDT, M. N91-13651
WERNER, J. C. N91-13946
WERNER, M. W. N91-14138
WERNER, MICHAEL W. N91-14140
WERNER, TOM N91-14042
WESSELIUS, P. R. N91-14199
WEST, B. H. N91-13572
N91-13718
WESTFALL, LEONARD J. N91-13502
WEYDAHL, DAN JOHAN N91-13600
WEZENBEEK, A. M. N91-13603
WHARTON, ROBERT A., JR. N91-14255
WHITE, C. W. N91-14061
WHITE, D. A. N91-14171
WHITE, DAWN R. N91-13523
WHITE, DEWEY W., JR. N91-13464
WHITE, RAYMOND E., III N91-14173
WHITMORE, STEPHEN A. N91-13453
WHITTEN, W. B. N91-13517
WHITTET, D. C. B. N91-14132
WHYTE, WAYNE A., JR. N91-13598
WIEDEMANN, KARL E. N91-13522
WIGHTMAN, FREDERIC L. N91-13971
WIKLIND, T. N91-14125
WIKLIND, TOMMY N91-14127
WILD, W. N91-14125
N91-14230
WILD, WOLFGANG N91-14236
WILDERMUTH, D. N91-14060
WILKERSON, T. D. N91-13837
WILKING, BRUCE A. N91-14089
WILLIAMSON, SAMUEL J. N91-13869
WILSON, CHRISTINE D. N91-14201
WILSON, JOHN W. N91-13985
N91-14265
WILSON, WILLIAM J. N91-13679
WINTERBOTTOM, A. N. N91-13472
WOLF, DAVID A. N91-13860
WOLFIRE, M. G. N91-14113
WOLLKIND, DAVID J. N91-14189
WOLVERTON, B. C. N91-13851
WOMBLE, DONNA S. N91-14228
WONG, A. Y. N91-13815
WONG, ALFRED W. N91-13590
WONG, K. L. N91-13981
WOOD, A. W. N91-14085
WOODRUFF, W. H. N91-13700
WOODWARD, CHARLES N91-13921
WORDEN, P. N91-13788
WORDIN, J. J. N91-13719
WRENN, GORDON L. N91-13829
WRIGHT, M. N91-14121
WROBEL, J. M. N91-14224
WU, A. N91-13618
WU, FRANCIS WOOMIN N91-14075
WU, K. CHAUNCEY N91-13473
WU, XI N91-13516
WU, Z. N91-14036
WURDEN, G. A. N91-14015

X

XIE, S. N91-14232
XIE, SHUDING N91-14126

XU, YUEMING N91-14243
XUE, Y. N91-13422

Y

YANG, SHIH-AN N91-13641
YANG, XIAOPU N91-13589
YATES, KEMBLE R. N91-14189
YEAGER, WILLIAM T., JR. N91-13462
YEE, JICK H. N91-13623
YOST, DAVID J. N91-13435
YOST, WILLIAM T. N91-13527
YOUNG, J. S. N91-14117
N91-14145
YOUNG, JUDITH N91-14126
YOUNG, JUDITH S. N91-14119
N91-14215
YOUNG, LAWRENCE E. N91-13787
YU, P. K. L. N91-13697
YU, SIMON S. N91-13619

Z

ZACCONE, M. A. N91-13757
ZAMAN, K. B. M. Q. N91-13420
ZANG, T. A. N91-13650
ZANG, THOMAS A. N91-13410
ZAPP, JOHN N91-13893
ZARCHAN, PAUL N91-13440
N91-13442
ZARITSKY, DENNIS N91-14159
ZASADZINSKI, R. N91-13981
ZAUGG, THOMAS J. N91-13988
ZHANG, HONG LIN N91-14020
ZHANG, JIAN GUO N91-13753
ZHANG, X.-G. N91-13978
ZINNECKER, H. N91-14125
ZISMAN, MICHAEL S. N91-13982
ZOUTENDYK, JOHN A. N91-13622
ZUERNDORFER, BRIAN N91-13817
ZUPP, GEORGE A., JR. N91-13483
ZUREK, WOJCIECH H. N91-14069
ZWEIBEL, ELLEN G. N91-14180
N91-14190

Typical Corporate Source Index Listing

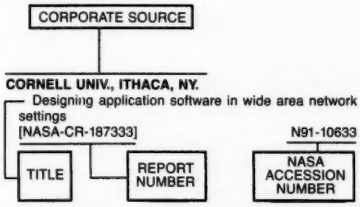

Listings in this index are arranged alphabetically by corporate source. The title of the document provides the user with a brief description of the subject matter. The report number helps to indicate the type of document cited (e.g., NASA report, translation, NASA contractor report). The NASA accession number denotes the number by which the citation is identified. The titles are arranged under each corporate source in ascending accession number order.

A

ABILENE CHRISTIAN UNIV., TX.
Operation of silicon microstrip detectors in a high radiation environment
[DE91-001953] N91-13682

ACADEMIA SINICA, TAIPEI (TAIWAN).
Operation of silicon microstrip detectors in a high radiation environment
[DE91-001953] N91-13682

ADMIRALTY RESEARCH ESTABLISHMENT, GOSPORT (ENGLAND).
Transition control via boundary layer heating
[ARE-TR-88503] N91-13667

ADVISORY GROUP FOR AEROSPACE RESEARCH AND DEVELOPMENT, NEUILLY-SUR-SEINE (FRANCE).
Missile Interceptor Guidance System Technology
[AGARD-LS-173] N91-13434
Hazard studies for solid propellant rocket motors
[AGARD-AG-316] N91-13488
Echocardiography in NATO aircrew
[AGARD-AR-297] N91-13863
Applications of Superconductivity to Avionics
[AGARD-CP-481] N91-14030
List of standards to accompany manual of documentation practices applicable to defence-aerospace scientific and technical information. Addendum
[AGARD-AG-235-ADD] N91-14076
AGARD highlights 90/2, part 2
[AD-A226532] N91-14080

AERONAUTICAL RESEARCH INST. OF SWEDEN, STOCKHOLM.
Transonic wind tunnel tests on two-dimensional aerofoil sections: Determination of pressure distribution and drag for an aerofoil of type SAAB 7301 in FFA wind tunnel S5
[FFA-TN-1989-47] N91-13416
FE analyses of aircraft model with interior trim
[FFA-TN-1990-21] N91-13417
Damage tolerance analysis and testing of the fighter aircraft 37 Viggen
[FFA-TN-1990-35] N91-13448
On the variation in crack-opening stresses at different locations in a three-dimensional body
[NASA-CR-187722] N91-13768
Accurate and reliable computation of complete solutions to the equations of linear elastomechanics on three-dimensional domains: Computation of edge stress intensity functions
[FFA-TN-1989-12] N91-13769
Analysis of shells as 3D-elasticity problems using the p-version of the FE method
[FFA-TN-1990-25] N91-13770
Accurate and reliable determination of edge and vertex stress intensity factors in three-dimensional elastomechanics
[FFA-TN-1990-28] N91-13771
Spectrum fatigue testing: A literature survey
[FFA-TN-1990-40] N91-13772
Airfoil design for variable RPM horizontal axis wind turbines
[FFA-TN-1990-02] N91-13801

AEROSPACE CORP., LOS ANGELES, CA.
High spatial-resolution IRAS images of M51
N91-14207

AIR FORCE HUMAN RESOURCES LAB., WRIGHT-PATTERSON AFB, OH.
The poet revealed: A future for human-centered design
[AD-A226648] N91-13878

AIR FORCE MATERIALS LAB., WRIGHT-PATTERSON AFB, OH.
Fabrication and characterization of high temperature superconducting thin films for sensors and electronics
N91-14041

AIR FORCE SYSTEMS COMMAND, WRIGHT-PATTERSON AFB, OH.
The third generation of Soviet civilian-use turbofan engines
[AD-A225392] N91-13454
Space flight undertakings of present-day china (photo captions on 65 selected pages)
[AD-A222816] N91-13469

ALABAMA UNIV., HUNTSVILLE.
Applications of artificial intelligence to mission planning
[NASA-CR-184994] N91-13939
Viscosity measurements at high temperature and high pressure: A novel technique
[NASA-CR-187239] N91-13967
Definition study for temperature control in advanced protein crystal growth
[NASA-CR-187346] N91-14029
Morphological stability and kinetics in crystal growth from vapors
[NASA-CR-187650] N91-14055
Accounting for the dispersion in the x ray properties of early-type galaxies N91-14173

AMERICAN SUPERCONDUCTOR CORP., WATERTOWN, MA.
Success criteria for oxide superconductor wires: Measuring the present, predicting the future
N91-14034
Oxide superconductor coils: Present successes, future challenges N91-14046

AMES LAB., IA.
Fundamental investigations of supported monometallic and bimetallic catalysts by proton magnetic resonance spectroscopy
[DE91-000610] N91-13516
Electrocatalysis of anodic oxygen-transfer reactions at modified lead dioxide electrodes
[DE91-000664] N91-13518
Synchrotron radiation photoemission study of metal overlayers on hydrogenated amorphous silicon at room temperature
[DE91-000740] N91-13525
Reactions of the excited state of polypyridyl chromium(III) ion
[DE91-000741] N91-13526
Optical properties and electronic structures of d- and f-electron metals and alloys, Ag-In, Ni-Cu, AuGa2, PtGa2, beta'-NiAl, beta'-CoAl, CeSn3, and LaSn3
[DE91-001597] N91-14059

ARGONNE NATIONAL LAB., IL.
Implementing automatic differentiation efficiently
[DE91-002409] N91-13913
The advanced software development and commercialization project
[DE91-002956] N91-13933
A tutorial on the construction of high-performance resolution/paramodulation systems
[DE91-001096] N91-13942
Atomic and molecular theory
[DE91-004475] N91-13983
Modeling and analysis of surface roughness effects on sputtering, reflection, and sputtered particle transport
[DE91-004429] N91-14028

ARIZONA UNIV., TUCSON.
Soil bed reactor work of the Environmental Research Lab. of the University of Arizona in support of the research and development of Biosphere 2 N91-13846
Specifications extraction and synthesis: Their correlations with preliminary design N91-13936
CS J = 2 yields 1 emission toward the central region of M82 N91-14128
A study of HII regions in spiral galaxies using multiobject spectroscopy N91-14159
Are bars essential for starbursts in non-interacting galaxies N91-14208
Gravitational star formation thresholds and gas density in three galaxies N91-14210

ARKANSAS COLL., BATESVILLE.
Kinetics of hydrogen release from lunar soil
[NASA-CR-187363] N91-14256

ARMY AVIATION SYSTEMS COMMAND, MOFFETT FIELD, CA.
General Rotorcraft Aeromechanical Stability Program (GRASP): Theory manual
[NASA-TM-102255] N91-13762

ARMY ENGINEER WATERWAYS EXPERIMENT STATION, VICKSBURG, MS.
Literature review on geotextiles to improve pavements for general aviation airports
[DOT/FAA/RD-90/26] N91-13464

ARNOLD ENGINEERING DEVELOPMENT CENTER, ARNOLD AIR FORCE STATION, TN.
Some buffet response characteristics of a twin-vertical-tail configuration
[NASA-TM-102749] N91-13412

AUTOMETRIC CORP., INC., ROME, NY.
Architecture for electronic imagery interoperability
[AD-A226522] N91-13901

B

BABCOCK AND WILCOX CO., LYNCHBURG, VA.
Research and development of a ceramic fiber composite heat exchanger
[DE90-017250] N91-13497

BALLISTIC RESEARCH LABS., ABERDEEN PROVING GROUND, MD.
The molecular structure of the HAN-based liquid propellants
[AD-A226415] N91-13571
AN alternative to suppression: Modeling methodology for assessing indirect effects of weapons and human performance degradation
[AD-A226518] N91-13877
Feasibility of cosmic-ray muon intensity measurements for tunnel detection
[AD-A223355] N91-14266

BELEIDSCOMMISSIE REMOTE SENSING, DELFT (NETHERLANDS).
The relation between tree physiology and multispectral and color photography: First phase
[BCRS-89-39] N91-13785

BENTLEY COLL., BOSTON, MA.
HII regions in IC 1613: The ISM in a nearby dwarf irregular galaxy N91-14157

BIRMINGHAM UNIV. (ENGLAND).
Passive microwave devices using high temperature superconductors N91-14036

BODENSEEWERK GERAETETECHNIK G.M.B.H., UEBERLINGEN (GERMANY, F.R.).
Midcourse guidance technologies for advanced tactical missiles systems N91-13436

BOEING COMMERCIAL AIRPLANE CO., SEATTLE, WA.
Civil tiltrotor missions and applications
[NASA-CR-177452] N91-13424

BROOKHAVEN NATIONAL LAB., UPTON, NY.
Degradation modeling with application to aging and maintenance effectiveness evaluations
[DE91-004004] N91-13746

A preliminary ocean ARM (Atmospheric Radiation Measurements) guide for climatic evaluations [DE91-001120] N91-13811
Methods of analysis for complex organic aerosol mixtures from urban emission sources of particulate carbon [DE91-001722] N91-13814
Calcified-tissue investigations using synchrotron x ray microscopy [DE91-001729] N91-13859
A computer model to determine the primary contributors to relative radiation dose received by astronauts [DE90-015681] N91-13866

BROWN UNIV., PROVIDENCE, RI.
Fracture of ceramics under farfield cyclic compression [DE90-008417] N91-13563
Surfaces and thin films studied by picosecond ultrasonics [DE91-004167] N91-13973

C

CALIFORNIA INST. OF TECH., PASADENA.
A scaling law of radial gas distribution in disk galaxies N91-14106
The interstellar halo of spiral galaxies: NGC 891 N91-14164
Unbound molecular complexes in M33 N91-14201
Deep narrow band imagery of the diffuse ISM in M33 N91-14202
M51: Molecular spiral arms, GMAs and superclouds N91-14204

CALIFORNIA UNIV., BERKELEY.
Time domain finite difference analysis of antennas [AD-A226534] N91-13613
Robust deterministic control for robotic manipulators N91-13937
U1(prime) dark matter and R-parity violation [DE91-001792] N91-14068
Supernova remnants and diffuse ionized gas in M31 N91-14179
Lyman alpha radiation in external galaxies N91-14186
Dense gas and HII regions in the starburst galaxy NGC 253 N91-14220
Clues to galaxy activity from rich cluster simulations N91-14222
The photoevaporation of interstellar clouds N91-14248
An imaging and spectroscopic study of low and intermediate power radio galaxies N91-14268

CALIFORNIA UNIV., BERKELEY. LAWRENCE BERKELEY LAB.
Operation of silicon microstrip detectors in a high radiation environment [DE91-001953] N91-13682
Influence of collective effects on the performance of high-luminosity colliders [DE91-001797] N91-13982
X ray and charged particle detection with CsI(Tl) layer coupled to a-Si:H photodiode layers [DE91-001798] N91-14060
U1(prime) dark matter and R-parity violation [DE91-001792] N91-14068
Coupled transport processes in semipermeable media. Part 2: Numerical method and results [DE91-004140] N91-14073

CALIFORNIA UNIV., DAVIS.
Optical shared memory system demonstration model [AD-A226431] N91-13612
Modeling pilot interaction with automated digital avionics systems: Guidance and control algorithms for contour and nap-of-the-Earth flight [NASA-CR-186105] N91-13875

CALIFORNIA UNIV., LOS ANGELES.
Transverse liquid fuel jet breakup, burning, and ignition [NASA-CR-187423] N91-13510
Utilization of the HIPAS facility for cooperative experiments related to ionospheric modification [AD-A226609] N91-13590
Analytical study of the liquid phase transient behavior of a high temperature heat pipe [NASA-CR-187426] N91-13644
Heat pipe dynamic behavior [NASA-CR-187422] N91-13645
Enhancement of critical heat flux in tubes using staged tangential flow injection [DE90-014935] N91-13659
Fracture mechanics of interface cracks between dissimilar anisotropic materials N91-13752

CALIFORNIA UNIV., SAN DIEGO.
Precision, accuracy, and tectonics from the Global Positioning System N91-13822
Detection of a z=0.0515, 0.0522 absorption system in the QSO S4 0248+430 due to an intervening galaxy N91-14228

CALIFORNIA UNIV., SAN DIEGO, LA JOLLA.
Parallel Ada benchmarks for the SVMS [NASA-CR-182453] N91-13929

CALIFORNIA UNIV., SANTA CRUZ.
Thermal instabilities in protogalactic clouds N91-14195

CALSPAN-STATE UNIV. OF NEW YORK JOINT VENTURE, BUFFALO, NY.
Development of BEM for ceramic composites [NASA-CR-187676] N91-13557

CANADIAN INST. FOR THEORETICAL ASTROPHYSICS, TORONTO (ONTARIO).
Star formation in proto dwarf galaxies N91-14212

CARNEGIE-MELLON UNIV., PITTSBURGH, PA.
Validation environment for AIPS/ALS: Implementation and results [NASA-CR-4340] N91-13930

CATHOLIC UNIV. OF AMERICA, WASHINGTON, DC.
Hot interstellar gas and ionization of embedded clouds N91-14161
Ionization in the local interstellar and intergalactic media N91-14249

CENTRE TECHNIQUE DES INDUSTRIES MECANIQUES, NANTES (FRANCE).
Impact behavior of composite materials: Exploratory research [CETIM-101130] N91-13504
Study of the metallurgical effects of hammering between passes during C-Mn weld deposition [CETIM-104850] N91-13532
Evaluation of the functional properties of welds on cold finished tubes defined as NF A 49.541 [CETIM-104700] N91-13738
The effects of thermal treatment after welding on the functional properties of assemblies. Follow-up of the work on Cr-Mo [CETIM-104720] N91-13739
Study of the tensile strength of the melted zone of vertical welds carried out using electroslag welding on C-Mn steel. Further study on 80 mm thick plate [CETIM-104730] N91-13740
Study of the metallurgical consequences of hammering between passes to compensate for the withdrawal of metal caused by welding [CETIM-104430] N91-13741

CENTRE TECHNIQUE DES INDUSTRIES MECANIQUES, SENLIS (FRANCE).
Micrographic etching of nitrided iron and steel layers [CETIM-106470] N91-13533
Study of the time and effort signal in cutting operations [CETIM-101580] N91-13583
Signal processing used in the electromagnetic inspection of long bodies [CETIM-107270] N91-13749
Antivibration isolation (a practical guidebook) [CETIM-108220] N91-13775
Calculations for structures with nonlinear joints [CETIM-108830] N91-13776

CENTRE TECHNIQUE DES INDUSTRIES MECANIQUES, SAINT ETIENNE (FRANCE).
Bolted structural assemblies: Bibliographic analysis [CETIM-13N061] N91-13742
ADENG, adhesive bonding technology for engineering applications: Computer aided design [CETIM-105070] N91-13917

CHAM OF NORTH AMERICA, INC., HUNTSVILLE, AL.
Thrust chamber modeling using Navier-Stokes equations: Code documentation and listings, volume 2 [NASA-CR-183617] N91-13489

CHICAGO UNIV., IL.
Operation of silicon microstrip detectors in a high radiation environment [DE91-001953] N91-13682
Neutral atomic absorption lines and far-UV extinction: Possible implications for depletions and grain parameters N91-14115

CINCINNATI UNIV., OH.
Multivariable methods for the design, identification, and control of large space structures. Volume 1: Estimator Eigenvalue placement in positive real design [AD-A226525] N91-13477
Multivariable methods for the design, identification, and control of large space structures. Volume 3: A study of the integrated control/structure design optimization problem for large flexible structures [AD-A226526] N91-13478
Electrocatalyst surfaces [PB90-252560] N91-13507

CITY COLL. OF THE CITY UNIV. OF NEW YORK, NY.
Topics in physico-chemical hydrodynamics [DE91-001674] N91-13519

COE ENGINEERING, INC., MOUNTAIN VIEW, CA.
An assessment of wind tunnel test data on flexible thermal protection materials and results of new fatigue tests of threads [NASA-CR-177466] N91-13972

COLLEGE OF WILLIAM AND MARY, WILLIAMSBURG, VA.
Damage assessment and residual compression strength of thick composite plates with through-the-thickness reinforcements [NASA-CR-187377] N91-13494
Injection efficiency of bound modes [NASA-CR-4333] N91-13991

COLORADO STATE UNIV., FORT COLLINS.
Study of improved methods for predicting chemical equilibria [DE91-000263] N91-13509

COLORADO UNIV., BOULDER.
Computational methods and software systems for dynamics and control of large space structures [NASA-CR-187669] N91-13480
Constraint treatment techniques and parallel algorithms for multibody dynamic analysis [NASA-CR-187668] N91-13759
A computational procedure for the dynamics of flexible beams within multibody systems [NASA-CR-187667] N91-13760
A physical parameterization of snow albedo for use in climate models N91-13781
Sea ice-atmosphere interaction: Application of multispectral satellite data in polar surface energy flux estimates [NASA-CR-187376] N91-13782
Frontal interactions with orography: Objective cross-sectional analysis of ALPEX data N91-13836
An asymptotic symmetry of the rapidly forced pendulum [DE91-001868] N91-13958
NGC 1058: Gas motions in an extended, quiescent spiral disk N91-14103
Optical emission from cooling flows in distant x ray clusters of galaxies N91-14169
Virial theorem analysis of the structure and stability of magnetized clouds N91-14190
Probing the interstellar medium of external galaxies using quasar absortion lines: The 3C 232/NGC 3067 system N91-14227
The evolution of comets and the detectability of Extra-Solar Oort Clouds N91-14242
Spectrum formation in SN1987A N91-14243
The origin and evolution of the Uranian dust rings N91-14253

COLUMBIA UNIV., NEW YORK, NY.
NGC 4438: Ram pressure sweeping of a tidally disrupted galaxy N91-14176
NGC 3312: A victim of ram pressure sweeping N91-14177
Relativistic effects in millisecond pulsars and active galactic nuclei N91-14247

COMMISSARIAT A L'ENERGIE ATOMIQUE, SACLAY (FRANCE).
The gravitational wakefield of a molecular cloud in a disk galaxy N91-14188

COMPUTER SCIENCES CORP., HAMPTON, VA.
Pressure visualization (PreViz) package version 1.0 user's guide [NASA-CR-187444] N91-13907

CONSIGLIO NAZIONALE DELLE RICERCHE, FRASCATI (ITALY).
Funds request for 1990. The cryogenic gravitational antenna (T = 2.0 K) ALTAIR [IFSI-90-2] N91-13615
Cryostat for the gravitational antenna ALTAIR [IFSI-90-3] N91-13616
Design of a mechanical modulator for the planetary Fourier spectrometer experiment of the MARS 94 mission [IFSI-89-22] N91-13717
Methodology to treat stellar images [IFSI-89-21] N91-14094

CONTRAVES GOERZ CORP., PITTSBURGH, PA.
The Improved Three Axis Test Table (ITATT): Program status and recommendation for completion [AD-A226508] N91-13712

CORNELL UNIV., ITHACA, NY.
Theory of finite disturbances in a centrifugal compression system with a vaneless radial diffuser [NASA-CR-187049] N91-13458
Fractals and chaotic dynamics in tectonics: Applications to topography and seismicity N91-13821
The ISIS project: Fault-tolerance in large distributed systems [NASA-CR-186625] N91-13928
Energy input and HI spin temperatures in low pressure regions N91-14163

COUNCIL FOR NATIONAL ACADEMIC AWARDS (ENGLAND).
Fibre-linked miniature laser transit anemometer for complex flow fields N91-13678
Finite element and boundary element methods for elastoplastic stress analysis of two-dimensional and axisymmetric problems N91-13755

D

DAVID TAYLOR RESEARCH CENTER, BETHESDA, MD.
Intelligent processing for spray metal manufacturing [AD-A226499] N91-13523
Computation of incompressible flow around the DARPA SUBOFF bodies [AD-A226481] N91-13646
Constrained viscoelastic layer damping of thick aluminum plates: Design, analysis, and testing [AD-A226556] N91-13758
DELAWARE UNIV., NEWARK.
Particle theory and cosmology [DE91-004189] N91-14250
DEPARTMENT OF ENERGY, MORGANTOWN, WV.
Fuel cells [DE90-009686] N91-13805
DEPARTMENT OF ENERGY, OAK RIDGE, TN.
Energy Data Base [DE90-009278] N91-14081
DEPARTMENT OF ENERGY, WASHINGTON, DC.
Summaries of physical research in the geosciences [DE91-001043] N91-13779
Solar collector manufacturing activity, 1988 [DE90-003539] N91-13797
DEPARTMENT OF THE NAVY, WASHINGTON, DC.
Sheave assembly [AD-D014605] N91-13711
Heat engine with corrugated shape memory drive belt [AD-D014640] N91-13716
M-dimensional computer memory with M-1 dimensional hyperplane access [AD-D014615] N91-13886
Superconducting neural network computer and sensor array [AD-D014625] N91-13887
DESERT RESEARCH INST., RENO, NV.
Exobiology site selection for future Mars missions: Martian paleolake sediments and terrestrial analogs [NASA-CR-187358] N91-14255
DEUTSCHE FORSCHUNGSANSTALT FUER LUFT- UND RAUMFAHRT, BRUNSWICK (GERMANY, F.R.).
Analytic formulations of unsteady profile aerodynamics and its application to simulation of rotors [DLR-FB-90-28] N91-13415
DEUTSCHE FORSCHUNGSANSTALT FUER LUFT- UND RAUMFAHRT, OBERPFAFFENHOFEN (GERMANY, F.R.).
Simulation of the formation and transport of ozone in the atmospheric boundary layer [DLR-FB-90-25] N91-13827
DORTMUND UNIV. (GERMANY, F.R.).
Use of neutron diffraction methods for the determination of mechanical stresses in metal ceramic laminated composite materials N91-13537
DOUGLAS AIRCRAFT CO., INC., LONG BEACH, CA.
Procedure for generating global atmospheric engine emissions data from future supersonic transport aircraft. The 1990 high speed civil transport studies [NASA-CR-181882] N91-13447
DRAPER (CHARLES STARK) LAB., INC., CAMBRIDGE, MA.
Micro based technology: A new tool for missile guidance system design and visualization N91-13440
Interactions between battle management and guidance law design for a strategic interceptor N91-13441
Guidance methods for tactical and strategic missiles N91-13442
Knowledge representation into Ada parallel processing [NASA-CR-187451] N91-13934

E

ECOLE CENTRALE DE LYON (FRANCE).
Investigation and development of ISFET type chemical sensors, sensitized by dielectric tying [ECL-90-18] N91-13630
A minimization method adapted to the finite element technique for turbulent flow simulation with nonlinear boundary conditions in the wall vicinity [ECL-90-016] N91-13664
Modelization of two phase turbulent jet up to its auto ignition in variable pressure and temperature environments [ETN-91-98341] N91-13665
ECOLE NORMALE SUPERIEURE, PARIS (FRANCE).
CO observations of southern mergers N91-14197
The molecular spiral arms of NGC 6946 N91-14231
EDGERTON, GERMESHAUSEN AND GRIER, INC., IDAHO FALLS, ID.
Heat exchanger fouling: Prediction, measurement, and mitigation [DE91-001997] N91-13661
Design reliability engineering [DE91-001949] N91-13744
Supercritical binary geothermal cycle experiments with mixed-hydrocarbon working fluids and a near-horizontal in-tube condenser [DE91-001815] N91-13798
Tightly coupled simulation utilizing the EBR-II LMR: A real-time supercomputing and AI environment [DE91-001942] N91-13932
SP-100 from ground demonstration to flight validation [DE91-001869] N91-13986
Communication system test for image transmission [DE91-001890] N91-13994
EDINBURGH UNIV. (SCOTLAND).
High resolution sub-millimetre mapping of starburst galaxies: Comparison with CO emission N91-14129
Infrared spectroscopy of the dwarf starburst galaxy Henize 2-10 N91-14213
EG AND G ROCKY FLATS, INC., GOLDEN, CO.
Mathematical modelling of part voltage and weld current in resistance welders [DE91-002534] N91-13727
Superplastic deformation properties of Ti-6Al-4V [DE91-000503] N91-13757
ELECTRONIQUE MARCEL DASSAULT, SAINT CLOUD (FRANCE).
Guidnace simulation model of antisea-skimmer utilization for weapon system definition N91-13438
ELORET CORP., SUNNYVALE, CA.
Computed potential energy surfaces for chemical reactions [NASA-CR-186877] N91-13506
EUROPEAN SPACE AGENCY, PARIS (FRANCE).
Catalogue of ESA patents [ESA-SP-1131] N91-14083
FIRST: Far Infrared and Submillimetre Space Telescope [ESA-BR-69] N91-14095
EUROPEAN SPACE AGENCY. EUROPEAN SPACE RESEARCH AND TECHNOLOGY CENTER, ESTEC, NOORDWIJK (NETHERLANDS).
ESATAN: User manual [ESA-PSS-03-105-ISSUE-1] N91-13897

F

FEDERAL AVIATION ADMINISTRATION, ATLANTIC CITY, NJ.
Connectivity alternatives for remote users of the Maintenance Processor Subsystem (MPS) [DOT/FAA/CT-90/16] N91-13900
FEDERAL AVIATION ADMINISTRATION, WASHINGTON, DC.
Literature review on geotextiles to improve pavements for general aviation airports [DOT/FAA/RD-90/26] N91-13464
Laboratory investigation of the use of geotextiles to mitigate frost heave [DOT/FAA/RD-90/13] N91-13465
FERMI NATIONAL ACCELERATOR LAB., BATAVIA, IL.
Operation of silicon microstrip detectors in a high radiation environment [DE91-001953] N91-13682
Axions and SN 1987A: Axion trapping [NASA-CR-186467] N91-13976
FIVE-COLLEGE ASTRONOMY DEPT., AMHERST, MA.
The FCRAO extragalactic CO survey: Global properties of galaxies N91-14117
The ratio of molecular to atomic gas in spiral galaxies as a function of morphological type N91-14119
A comparison of the radial distribution of molecular gas and non-thermal radio continuum in spiral disks N91-14145
Global and radial variations in the efficiency of massive star formation among galaxies N91-14215
FLORIDA STATE UNIV., TALLAHASSEE.
Numerical solution of the geoelectrodynamic problem [NASA-CR-186941] N91-13818
Computation of broadband mixing noise from turbomachinery [AD-A226559] N91-13969
FLORIDA UNIV., GAINESVILLE.
Version control and management in computer-aided design databases N91-13896
FORSCHUNGSZENTRUM JUELICH G.M.B.H. (GERMANY, F.R.).
Residual stresses in ceramics [JUEL-SPEZ-550] N91-13536
Possibilities of the calculation of stresses and residual stresses in materials with a phase transformation N91-13548
FRAUNHOFER-INST. FUER BETRIEBSFESTIGKEIT, DARMSTADT (GERMANY, F.R.).
Development and computer aided residual stress measurements on coated specimen using blind-hole drilling technique N91-13544
FRAUNHOFER INST. FUER WERKSTOFFMECHANIK, FREIBURG (GERMANY, F.R.).
Determination of stresses in ceramics using ultrasonic methods: Possibilities and limitations N91-13546

G

GENERAL ATOMIC CO., SAN DIEGO, CA.
A multi-laser system for a fast sampling Thomson scattering diagnostic [DE91-002708] N91-13705
A silicon avalanche photodiode detector circuit for Nd:YAG laser scattering [DE91-002709] N91-13706
A 15 MeV proton dianostic for DIII-D [DE91-002717] N91-14022
High spatial and temporal resolution visible spectroscopy of the plasma edge in DIII-D [DE91-002718] N91-14023
A compact, low cost, 7 channel polychromator for Thomson scattering measurements [DE91-002719] N91-14024
A real-time digital control, data acquisition and analysis system for the DIII-D multipulse Thomson scattering diagnostic [DE91-002720] N91-14025
GENERAL ELECTRIC CO., CINCINNATI, OH.
Research and development for improved toughness aluminides [AD-A226627] N91-13524
GEORGIA INST. OF TECH., ATLANTA.
Analytical aerodynamic model of a high alpha research vehicle wind-tunnel model [NASA-CR-187362] N91-13404
Development of a full potential solver for rotor aerodynamics analysis N91-13407
Guidance, navigation and control. Digital emulation technology laboratory. Volume 2, Task 2: Seeker emulator development [AD-A225124] N91-13429
Guidance, navigation and control. Digital emulation technology laboratory. Volume 3, Task 3: Special studies [AD-A225125] N91-13430
Periodic trim solutions with hp-version finite elements in time [NASA-CR-187705] N91-13449
Pioneer-Venus radio occultation (ORO) data reduction: Profiles of 13 cm absorptivity [NASA-CR-186986] N91-13584
A complex permittivity and permeability measurement system for elevated temperatures [NASA-CR-186916] N91-13609
GINER, INC., WALTHAM, MA.
Corrosion-resistant catalyst supports for phosphoric acid fuel cells [DE91-001713] N91-13794
GRENOBLE-1 UNIV. (FRANCE).
Logics for the description of processes and their properties: Expressivity and decidability [ETN-91-98200] N91-13960

H

HARRY DIAMOND LABS., ADELPHI, MD.
Millimeter-wave sensor image enhancement [NASA-CR-187430] N91-13679
HARVARD-SMITHSONIAN CENTER FOR ASTROPHYSICS, CAMBRIDGE, MA.
Disk mass densities in edge-on spiral galaxies N91-14108
The hot and cold interstellar matter of early type galaxies and their radio emission N91-14112
The onset of galactic winds in early-type galaxies N91-14165
Gas flows in elliptical galaxies N91-14170
HELSINKI UNIV. OF TECHNOLOGY, ESPOO (FINLAND).
Methods for computer-aided design of free-form objects [MA-56] N91-13921
HITACHI LTD., TOKYO (JAPAN).
The status-quo and prospect of superconducting digital devices N91-14039

HONEYWELL, INC., MINNEAPOLIS, MN.
Application of high-temperature superconductors to high-precision accelerometers N91-14042
HOUSTON UNIV., CLEAR LAKE, TX.
Security for safety critical space borne systems
[NASA-CR-187656] N91-13906
HUGHES AIRCRAFT CO., CANOGA PARK, CA.
Flight control design issues in bank-to-turn missiles N91-13437
HULL UNIV. (ENGLAND).
Folded RF-excited CO2 waveguide lasers N91-13695
HUMAN ENGINEERING LABS., ABERDEEN PROVING GROUND, MD.
An indexed bibliography on tracking
[AD-A226682] N91-13870

I

IDAHO NATIONAL ENGINEERING LAB., IDAHO FALLS.
Coherent anti-Stokes Raman spectroscopic measurement of air entrainment in argon plasma jets
[DE91-001936] N91-13670
High pulse rate interferometry using a ruby laser and a Cordin model 360 camera
[DE91-001882] N91-13703
Second law analysis of advanced power generation systems using variable temperature heat sources
[DE91-001818] N91-13799
Simultaneous measurement of Ni-Al particle size, velocity, and temperature in atmospheric thermal plasmas
[DE91-001935] N91-13826
The human factors of quality and QA in R and D environments
[DE91-001913] N91-13880
The design of a distributed image processing and dissemination system
[DE91-001835] N91-13909
WordPerfect's toolbox: Formatting documents using styles and macros
[DE91-001884] N91-13912
Ultrasound generation through a fiber optic delivery system using pulsed laser energy
[DE91-001914] N91-13970
Unique features of space reactors
[DE91-001910] N91-13987
Measurement of air entrainment in plasma jets
[DE91-001943] N91-14013
ILLINOIS UNIV., CHICAGO.
Transport properties of dense fluid mixtures using nonequilibrium molecular dynamics
[DE91-000262] N91-13654
Evaluation of expressions involving higher order derivations
[NASA-CR-187319] N91-13949
ILLINOIS UNIV., URBANA.
HI and FIR emission from S0 galaxies N91-14111
A relationship between the integrated CO intensity and the radio continuum emission in spiral galaxies N91-14146
A high resolution CO map of M51 N91-14203
ILLINOIS UNIV., URBANA-CHAMPAIGN.
Magnetic collimation of protostellar winds into bipolar outflows N91-14182
IMPERIAL COLL. OF SCIENCE AND TECHNOLOGY, LONDON (ENGLAND).
Wave by wave analysis of in-line force data for fixed cylinders in regular waves
[IC-AERO-89-02] N91-13672
INSTITUT D'AERONOMIE SPATIALE DE BELGIQUE, BRUSSELS.
Aeronomic chemistry of ozone
[AERONOMICA-ACTA-A-355-1990] N91-13816
Ultraviolet absorption cross-sections of photoactive species of stratospheric interest. Part 1: The halocarbons
[ETN-91-98385] N91-13830
INSTITUT DE RADIO ASTRONOMIE MILLIMETRIQUE, GRENOBLE (FRANCE).
CO excitation in four IR luminous galaxies N91-14234
INSTITUT DE SOUDURE, PARIS (FRANCE).
Study of the metallurgical effects of hammering between passes during C-Mn weld deposition
[CETIM-104850] N91-13532
Evaluation of the functional properties of welds on cold finished tubes defined as NF A 49.541
[CETIM-104700] N91-13738
The effects of thermal treatment after welding on the functional properties of assemblies. Follow-up of the work on Cr-Mo
[CETIM-104720] N91-13739
Study of the tensile strength of the melted zone of vertical welds carried out using electroslag welding on C-Mn steel. Further study on 80 mm thick plate
[CETIM-104730] N91-13740
Study of the metallurgical consequences of hammering between passes to compensate for the withdrawal of metal caused by welding
[CETIM-104430] N91-13741
INSTITUT NATIONAL POLYTECHNIQUE, GRENOBLE (FRANCE).
Semantic validation of structured theories: Applications to a generic programming language
[ETN-91-98207] N91-13916
INSTITUTE FOR COMPUTER APPLICATIONS IN SCIENCE AND ENGINEERING, HAMPTON, VA.
Large-eddy simulation of transitional channel flow
[NASA-CR-187465] N91-13410
The route to chaos for the Kuramoto-Sivashinsky equation
[NASA-CR-187461] N91-13642
Flow establishment in a generic scramjet combustor
[NASA-CR-187467] N91-13649
Toward the large-eddy simulation of compressible turbulent flows
[NASA-CR-187460] N91-13650
Zero wavenumber modes of a compressible supersonic mixing layer
[NASA-CR-187476] N91-13669
Dissipative controller designs for second-order dynamic systems
[NASA-CR-187452] N91-13935
A fully Sinc-Galerkin method for Euler-Bernoulli beam models
[NASA-CR-187462] N91-13952
Regularized Chapman-Enskog expansion for scalar conservation laws
[NASA-CR-187441] N91-13966
INSTITUTE FOR PERCEPTION RVO-TNO, SOESTERBERG (NETHERLANDS).
The effect of stereoscopic presentation on a simulated air traffic control task
[IZF-1989-53] N91-13431
Simulator flight as a selection device: Effects of test anxiety on subjective and objective measures of performance
[IZF-1989-57] N91-13468
Evaluation of a simple method for color monitor recalibration
[IZF-1990-B-4] N91-13608
Colour specifications for the Electronic Chart Display and Information System (ECDIS)
[IZF-1990-A-19] N91-13789
Time-sharing performance as a factor for success in flight training: Test development and validation
[IZF-1989-58] N91-13872
Vestibulo-ocular responses in man to +G sub z hypergravity
[IZF-1989-59] N91-13873
Adaptable driver-car interfacing and mental workload: A review of the literature
[IZF-1990-B-3] N91-13874
The effect of condensation in clothing on heat transfer
[IZF-1990-B-5] N91-13881
Multi-scale contrast enhancement with applications to image fusion
[IZF-1990-A-9] N91-14003
INSTITUTE OF ASTRONOMY, CAMBRIDGE (ENGLAND).
Stripping of gas and dust from the elliptical galaxy M86 N91-14171
INSTITUTO DE PESQUISAS ESPACIAIS, SAO JOSE DOS CAMPOS (BRAZIL).
Spray deflagration
[INPE-5079-TDL/413] N91-13511
S-band diplexer for a telecommunication board transponder
[INPE-4540-PRE/1286] N91-13586
Restoration of solar radio images: Evaluation of poor conditions and resolution by regularization techniques
[INPE-4557-PRE/1298] N91-13587
Method of selection of TM/LANDSAT color composition for analysis of land use classes
[INPE-5119-TDL/421] N91-13783
Methodological contribution utilizing TM/LANDSAT-5 imagery in geologic mapping of regions with significant vegetative cover
[INPE-5117-TDL/419] N91-13784
The importance of fracturing in the Pimenta Bueno-Ro Basin structure: A study of the morphostructural elements of the rupture-ductile character through remote sensing techniques and products
[INPE-5004-TDL/398] N91-13825
Implementation of the MAGINT-MAGGRAF code in the microVAX-3600 system
[INPE-5042-PRE/1575] N91-13898
Analysis of parallelism for nonlinear programming
[INPE-5121-TDL/422] N91-13899
Sweeping-vector conversion for polygonal data
[INPE-4558-PRE/1299] N91-14077
Georelational data model: A conceptual vision of a geographical information system
[INPE-4612-PRE/1335] N91-14078
Utilization of IHS transformation for integration of images of differing resolutions: Urban land use study
[INPE-4606-PRE/1329] N91-14086
Centimeter emission variation of Venus: Its second phase
[INPE-5122-TDL/423] N91-14257
INSTITUTO DE RADIOASTRONOMIA, GRANADA (SPAIN).
CS in nearby galaxies: Distribution, kinematics, and multilevel studies N91-14235
INTERNATIONAL BUSINESS MACHINES CORP., YORKTOWN HEIGHTS, NY.
The simultaneous integration of many trajectories using nilpotent normal forms
[NASA-CR-187318] N91-13950
INTERNATIONAL RESEARCH AND DEVELOPMENT CO. LTD., FOSSWAY (ENGLAND).
The world of superconductive machinery N91-14045
IOWA STATE UNIV. OF SCIENCE AND TECHNOLOGY, AMES.
Radial profiles of gas in late-type disk galaxies N91-14107
Star formation on the leading edge of a ring-like density wave in Arp 143 N91-14198
IOWA UNIV., IOWA CITY.
Nonlinear viscous waves produced by an impulsively moving plate N91-13641

J

JET PROPULSION LAB., CALIFORNIA INST. OF TECH., PASADENA.
An application of multiattribute decision analysis to the Space Station Freedom program. Case study: Automation and robotics technology evaluation
[NASA-CR-187432] N91-13476
Flexible thermal apparatus for mounting of thermoelectric cooler
[NASA-CASE-NPO-17806-1-CU] N91-13581
Method for providing a polarization filter for processing synthetic aperture radar image data
[NASA-CASE-NPO-17904-1-CU] N91-13594
Pipeline synthetic aperture radar data compression utilizing systolic binary tree-searched architecture for vector quantization
[NASA-CASE-NPO-17941-1-CU] N91-13595
Multiple symbol differential detection
[NASA-CASE-NPO-17896-1-CU] N91-13596
Secondary Li battery incorporating 12-crown-4 ether
[NASA-CASE-NPO-17922-1-CU] N91-13621
Detection of multiple-bit errors from single-ion tracks in integrated circuits
[NASA-CASE-NPO-18075-1-CU] N91-13622
Measurement of waves in flows across a surface
[NASA-CASE-NPO-17479-1-CU] N91-13658
Millimeter-wave sensor image enhancement
[NASA-CR-187430] N91-13679
Bilevel shared control for teleoperators
[NASA-CASE-NPO-17800-1-CU] N91-13724
Composite passive damping struts for large precision structures
[NASA-CASE-NPO-17914-1-CU] N91-13767
System and method for measuring ocean surface currents at locations remote from land masses using synthetic aperture radar
[NASA-CASE-NPO-17937-1-CU] N91-13787
Thermal power transfer system using applied potential difference to sustain operating pressure difference
[NASA-CASE-NPO-18034-1-CU] N91-13796
Environmental projects. Volume 12: Friable asbestos abatement, GDSCC
[NASA-CR-187636] N91-13808
Generic extravehicular (EVA) and telerobot task primitives for analysis, design, and integration. Version 1.0: Reference compilation for the EVA and telerobotics communities
[NASA-CR-187429] N91-13876
Auto and hetero-associative memory using a 2-D optical logic gate
[NASA-CASE-NPO-17997-1-CU] N91-13888
High-gain AlGaAs/GaAs double heterojunction Darlington phototransistors for optical neural networks
[NASA-CASE-NPO-18101-1-CU] N91-13995
Motion detection, novelty filtering, and target tracking using an interferometric technique with a GaAs phase conjugate mirror
[NASA-CASE-NPO-17784-1-CU] N91-13998
Total-dose radiation effects data for semiconductor devices (1989 supplement)
[NASA-CR-187431] N91-14049

JOHN B. PIERCE FOUNDATION OF CONNECTICUT, NEW HAVEN.
Thermoregulatory consequences of resonant microwave exposure
[AD-A226540] N91-13864
JOHNS HOPKINS UNIV., BALTIMORE, MD.
Research in theoretical physics
[DE91-002458] N91-14071
The morphology-density relation for dwarf galaxies N91-14200
JOHNS HOPKINS UNIV., LAUREL, MD.
Modern robust control for missile autopilot design N91-13435
JOINT ASTRONOMY CENTRE, HILO, HI.
H2 line emission in three Seyfert nuclei: Evidence against UV-excitation N91-14185
JOINT INST. FOR LAB. ASTROPHYSICS, BOULDER, CO.
The infrared continuum spectrum of x ray illuminated molecular gas N91-14144
Origin and dynamics of emission line clouds in cooling flow environments N91-14167
JOINT PUBLICATIONS RESEARCH SERVICE, ARLINGTON, VA.
JPRS Report: Science and technology. USSR: Life sciences
[JPRS-ULS-89-011] N91-13861

K

KANSAS UNIV., LAWRENCE.
A solar chronometer for climate: Astronomical and geophysical evidence N91-13823
KAPTEYN ASTRONOMICAL LAB., GRONINGEN (NETHERLANDS).
High velocity gas in external galaxies N91-14105
Spiral structure of M51: Streaming motions across the spiral arms N91-14206
CO distribution in southern S0 galaxies N91-14239
KARLSRUHE UNIV. (GERMANY, F.R.).
Residual stresses analyses in ceramics and metal ceramic composites using x ray methods N91-13539
Calculations of residual stresses in ceramic soldered joints N91-13549
KERNFORSCHUNGSZENTRUM G.M.B.H., KARLSRUHE (GERMANY, F.R.).
Determination of residual stresses in ceramics materials using neutron diffraction N91-13538
KMS FUSION, INC., ANN ARBOR, MI.
Experimental development, testing, and research work in support of the inertial confinement fusion program
[DE91-002770] N91-14026

L

LABORATOIRE CENTRAL DE RECHERCHES THOMSON-CSF, ORSAY (FRANCE).
High temperature superconducting thin films for microelectronics: Preparation and properties N91-14033
Microwave superconducting electronic devices N91-14037
High Tc superconductors for microwave filters N91-14038
LABORATOIRE D'AUTOMATIQUE ET D'ANALYSE DES SYSTEMES, TOULOUSE (FRANCE).
Evaluation and fabrication of GaAs integrated logic circuits
[LAAS-90160] N91-13628
Design of high voltage planar devices using SIPOS technology
[LAAS-90237] N91-13629
Design of GaAlAs/GaAs GRIN-SCH SQW diode lasers. Analysis of the temperature dependence
[LAAS-90277] N91-13708
Modeling and control of a redundant robot manipulator composed of several Stewart platforms
[LAAS-90146] N91-13728
About transient stability of power systems: Statistical pattern recognition approach
[LAAS-90192] N91-13889
LANCASTER POLYTECHNIC, PRESTON (ENGLAND).
The 3 micron spectrum of NGC 4565 N91-14132
LAWRENCE LIVERMORE NATIONAL LAB., CA.
Multiphase carbon and its properties in complex mixtures
[DE91-001679] N91-13499
Three point bend creep testing of carbon/epoxy
[DE91-001083] N91-13501
Materials impurity analysis by means of nuclear resonance reactions
[DE91-001758] N91-13520
Temporal scattering and response software: Users' manual
[DE91-001760] N91-13593
MPPE (Multiple Pulse Propagation Experiment) results
[DE91-001678] N91-13599
Relativistic kylstron simulations using RKTW2D
[DE91-001747] N91-13619
Computational and experimental progress on laser-activated gas avalanche switches for broadband, high-power electromagnetic pulse generation
[DE91-001763] N91-13623
Twelve signals multiplexed with the LLNL optical streak camera
[DE91-000066] N91-13680
Operation of inductively coupled plasma source mass spectrometers in the peak jumping mode
[DE91-001766] N91-13689
X ray holography at Lawrence Livermore National Laboratory
[DE91-002673] N91-13690
Study and development of tunable, single mode AlGaAs/GaAs lasers
[DE91-001684] N91-13697
Ultra-high brightness (greater than 10(exp 21) W/sq cm) laser facility
[DE91-001685] N91-13698
Free-electron laser experiments in the microwave tokamak experiment
[DE91-001746] N91-13699
An interactive program for the analysis and design of advanced laser targets
[DE91-002542] N91-13704
Use of dome (meniscus) lenses to eliminate birefringence and tensile stresses in spatial filters for the Nova laser
[DE91-002784] N91-13707
Laser programs highlights, July - August 1990
[DE91-001056] N91-13709
Penetration of yawed projectiles
[DE91-001084] N91-13726
A comparison of two numerical methods for shocks in one-dimensional elastic-plastic solids
[DE91-001741] N91-13765
Atmospheric and geophysical sciences division program report, 1988 - 1989
[DE91-001057] N91-13780
Stratospheric ozone conservation by electron attachment to chlorine atoms: The negative-ion chemistry
[DE91-002951] N91-13815
Image 3.3: Tutorial manual
[DE91-001762] N91-13908
Computed tomography software and standards
[DE91-002573] N91-13914
Solving the Fokker-Planck equation on a massively parallel computer
[DE91-002795] N91-13915
Proceedings of the Workshop on Software Tools for Distributed Intelligent Control Systems
[DE91-001755] N91-13943
Success with an automated computer control system
[DE91-001759] N91-13945
Numerical methods for boundary value problems in differential-algebraic equations
[DE91-001748] N91-13956
Lattice Boltzmann methods for some 2-D nonlinear diffusion equations: Computational results
[DE91-004175] N91-13962
Real-space multiple scattering theory calculations of LEED (Low-Energy Electron Diffraction) intensities for stepped surfaces
[DE91-000810] N91-13978
Inner-shell ionization of lithium-like chromium ions
[DE91-001749] N91-13981
HYLIFE-2 inertial confinement fusion reactor design
[DE91-000792] N91-14004
Stimulated Raman scatter from laser-produced plasmas: Merely nonlinear or also chaotic
[DE91-001742] N91-14007
Compact Ignition Tokamak project: Localizability of electron-cyclotron heating power
[DE91-002571] N91-14016
A rapid relativistic distorted wave approach for calculating cross sections for ionization of highly charged ions
[DE91-002667] N91-14020
Fast Pb-glass neutron-to-light converter for ICF (Inertial Confinement Fusion) target burn history measurements
[DE91-002670] N91-14021
Subnanosecond, high voltage photoconductive switching in GaAs
[DE91-002671] N91-14063
Spatial analysis of IRAS observations of nearby spirals N91-14133
Analysis of gamma ray burst spectra with cyclotron lines
[DE91-001745] N91-14269
LEIDEN UNIV. (NETHERLANDS).
The extragalactic radiation field and sharp edges to HI disks in galaxies N91-14101
Neutral hydrogen in the starburst galaxy NGC3690/IC694 N91-14104
LIVERPOOL UNIV. (ENGLAND).
A comparative study of ductile fracture in the 2.25 percent Cr-1 percent Mo and 9 percent Cr-1 percent Mo alloy steels N91-13753
LOS ALAMOS NATIONAL LAB., NM.
The behavior of fission products during nuclear rocket reactor tests
[DE91-001956] N91-13490
All hot spots are not equal
[DE91-002303] N91-13573
Superfluid Stirling refrigerator: A new method for cooling below 1 Kelvin
[DE91-002311] N91-13582
Transionospheric Propagation Code (TIPC)
[DE91-002435] N91-13597
Semi-custom integrated circuit amplifier and level discriminator for nuclear and space instruments
[DE91-001951] N91-13620
Computation of the current density in nonlinear materials subjected to large current pulses
[DE91-001950] N91-13624
Dual klystron modulator
[DE91-002348] N91-13626
Small signal gain based on analytic models of thin intense electron beams
[DE91-001874] N91-13631
Bidirectional slapper detonators in spherical explosion systems
[DE91-002399] N91-13662
Operation of silicon microstrip detectors in a high radiation environment
[DE91-001953] N91-13682
Actinide speciation by photothermal spectroscopies: Instrumentation development
[DE91-001854] N91-13700
Diagnostics for high-brightness beams
[DE91-001865] N91-13701
Field error lottery
[DE91-001875] N91-13702
Transionospheric propagation calculations for the output of two EMP (Electromagnetic Pulse) simulators
[DE91-001618] N91-13720
Analysis of bond quality by resonant ultrasound
[DE91-000439] N91-13743
Mesh considerations for finite element structural dynamic applications
[DE91-001717] N91-13764
Vortex collapse from a viewpoint of complex-time singularity
[DE91-001852] N91-13957
A linear accelerator in the space: The beam experiment aboard rocket
[DE91-002347] N91-13988
Confinement and heating studies of field-reversed configurations
[DE91-001965] N91-14008
Magnetic turbulent electron transport in a reversed field pinch
[DE91-001898] N91-14009
Measurement of magnetic fluctuations on ZT-40(M)
[DE91-001899] N91-14010
Kinetic and electromagnetic transport processes in toroidal devices
[DE91-001901] N91-14011
Two-fluid simulations of the reversed-field pinch
[DE91-001961] N91-14014
Confinement properties of the RFP (reversed field pinch)
[DE91-002322] N91-14015
Algorithmic information content, Church-Turing thesis, physical entropy, and Maxwell's demon
[DE91-001804] N91-14069
Chaos and order in non-integrable model field theories
[DE91-002313] N91-14070
Elemental mapping of planetary surfaces using gamma ray spectroscopy
[DE91-001877] N91-14258
Laboratory spectra of amorphous and crystalline olivine: An application to comet Halley IR spectrum
[DE91-002307] N91-14264
Gamma ray bursts from comet neutron star magnetosphere interaction, field twisting and E(sub parallel) formation
[DE91-002320] N91-14270
LOUGHBOROUGH UNIV. OF TECHNOLOGY (ENGLAND).
Airport stand assignment model
[TT-9009] N91-13426

UK airlines' cost structure and implications of air transport services fragmentation. Research report on air transport fragmentation
[TT-9011] N91-13427
Frontogenesis in gravity currents: The effect of endwalls and diffusion
[MATHS-REPT-A-127] N91-13666
A generalized Polak-Ribiere algorithm
[MATHS-REPT-A-128] N91-13918
On unconstrained conjugate gradient optimization methods and their interrelationships
[MATHS-REPT-A-129] N91-13919
Projected quasi-Newton updates
[MATHS-REPT-A-135] N91-13920
Robust variable structure control of model reference systems
[MATHS-REPT-A-131] N91-13947
On hyperplane design techniques for discrete-time variable structure control systems
[MATHS-REPT-A-133] N91-13948
A global convergence result for conjugate gradient methods
[MATHS-REPT-A-134] N91-13961

LOUISIANA STATE UNIV., BATON ROUGE.
A critical review of charged particle astronomy at Saturn: The evidence for co-orbiting material in the inner satellite system
[NASA-CR-187348] N91-14090

LOWELL OBSERVATORY, FLAGSTAFF, AZ.
Ionized interstellar froth in irregular galaxies N91-14152
The diffuse ionized interstellar medium perpendicular to the plane of NGC 891 N91-14160
Observations of extended and counterrotating disks of ionized gas in S0 galaxies N91-14187

LOWELL UNIV., MA.
A new approach to design of cross-linked second-order nonlinear optical polymers
[AD-A226674] N91-13553

LUNAR AND PLANETARY INST., HOUSTON, TX.
Proceedings of a Workshop on Cosmogenic Nuclide Production Rates
[NASA-CR-185349] N91-14098
Abstracts for the International Workshop on Meteorite Impact on the Early Earth
[NASA-CR-185355] N91-14099
Proceedings of the MEVTV Workshop on The Evolution of Magma Bodies on Mars
[NASA-CR-187357] N91-14252

M

MADISON MAGNETICS, INC., WI.
Magnetic suspension and balance system advanced study, phase 2
[NASA-CR-4327] N91-13463

MAINE UNIV., ORONO.
Interfacial chemistry of titanium films deposited on PMDA-ODA polyimide
[AD-A225730] N91-13550
A combined N-body and hydrodynamic code for modeling disk galaxies N91-14241

MARYLAND UNIV., COLLEGE PARK.
Study of Design Knowledge Capture (DKC) schemes implemented in magnetic bearing applications
[NASA-CR-187394] N91-13677
Study of static and dynamic fracture using strain measurements N91-13754
Progress of research on water vapor lidar
[NASA-CR-187673] N91-13837
High resolution CO images of Seyfert Galaxies N91-14121

MASSACHUSETTS INST. OF TECH., CAMBRIDGE.
Composite fuselage technology
[NASA-CR-187658] N91-13446
Loading the LES-9 wideband UHF transponder
[AD-A226179] N91-13475
The synthesis of star block copolymers by controlled ring-opening metathesis polymerization
[AD-A225987] N91-13551
Far field wake velocity measurements with hot film probes
[AD-A226650] N91-13647
Material and mechanical characterizations for braided composite pressure vessels
[AD-A226640] N91-13713
Tritium method oil consumption and its relation to oil film thickness in a production diesel engine
[AD-A226649] N91-13714
Analysis of single and multi-grade lubricant film thickness in a diesel engine
[AD-A226651] N91-13715
Distortion-free x ray mask technology
[AD-A226524] N91-13993
Observations of CO in the Magellanic irregular galaxy NGC 55 N91-14124
Mars tectonics and volcanism
[NASA-CR-187351] N91-14254

MASSACHUSETTS UNIV., AMHERST.
Radio observations of several interstellar molecules N91-14093
The FCRAO extragalactic CO survey: Global properties of galaxies N91-14117
The ratio of molecular to atomic gas in spiral galaxies as a function of morphological type N91-14119
The CO-12 and CO-13 J=2-1 and J=1-0 observations of hot and cold galaxies N91-14126
Molecular outflows in the L1641 region of Orion N91-14246

MAX-PLANCK-INST. FUER AERONOMIE, KATLENBURG-LINDAU (GERMANY, F.R.).
Activities report of the Max-Planck Institute for Aeronomy
[ETN-91-98383] N91-14272

MAX-PLANCK-INST. FUER EXTRATERRESTRISCHE PHYSIK, GARCHING (GERMANY, F.R.).
High angular resolution mm- and submm-observations of dense molecular gas in M82 N91-14230
Spatial variation of the physical conditions of molecular gas in galaxies N91-14236

MAX-PLANCK-INST. FUER METALLFORSCHUNG, STUTTGART (GERMANY, F.R.).
Residual stresses in Al2O3: Comparison between electromechanical measurements and finite element method calculations N91-13545

MAX-PLANCK-INST. FUER PHYSIK UND ASTROPHYSIK, GARCHING (GERMANY, F.R.).
Prospects of CsJ(Tl)-photodiode detectors for low level spectroscopy
[MPI-PAE/EXP.EL-228] N91-13984
Observations of CO isotopic emission and the far-infrared continuum of Centaurus A N91-14125

MAX-PLANCK-INST. FUER RADIOASTRONOMIE, BONN (GERMANY, F.R.).
Detection of CO emission in Hydra 1 cluster galaxies N91-14237

MCAT INST., SAN JOSE, CA.
Development of a time-dependent incompressible Navier-Stokes solver based on a fractional-step method
[NASA-CR-182323] N91-13639

MESSERSCHMITT-BOELKOW-BLOHM G.M.B.H., MUNICH (GERMANY, F.R.).
Influence of thermodynamical modelization for chemically reacting air flow
[MBB/FE122/S/PUB/400] N91-13418
Generalized flux vectors for hypersonic shock capturing
[MBB/FE122/S/PUB/397] N91-13423

MICHIGAN STATE UNIV., EAST LANSING.
Localize and identify the gravity sensing mechanism of plants
[NASA-CR-187411] N91-13841

MICHIGAN UNIV., ANN ARBOR.
Mesoscale monitoring of the soil freeze/thaw boundary from orbital microwave radiometry
[NASA-CR-185901] N91-13817
Examples of finite element mesh generation using SDRC IDEAS
[NASA-CR-186962] N91-13893
Regularized Chapman-Enskog expansion for scalar conservation laws
[NASA-CR-187441] N91-13966
The large-scale space distribution of emission-line galaxies N91-14091
Narrow band images of suspected cooling flow galaxies N91-14168

MIDWEST RESEARCH INST., GOLDEN, CO.
SERI photovoltaic subcontract reports: Abstracts and document control information
[DE90-000378] N91-13792
Carbon dioxide release from Ocean Thermal Energy Conversion (OTEC) cycles
[DE89-009504] N91-13809

MILITARY ACADEMY, WEST POINT, NY.
Design of integrated CMOS circuits for parallel detection and storage of optical data
[AD-A225702] N91-13611

MINNESOTA UNIV., MINNEAPOLIS.
Transonic blade-vortex interactions noise: A parametric study
[NASA-CR-187713] N91-13422
Analytical and experimental studies for thermal plasma processing of materials
[DE91-000599] N91-13576
Free-stream turbulence and concave curvature effects on heated, transitional boundary layers, volumes 1 and 2 N91-13643
Variational transition state theory
[DE91-001253] N91-14058
Infrared polarimetry and the magnetic field in external galaxies N91-14192
The stellar content of M101 N91-14244

MISSOURI UNIV., SAINT LOUIS.
An ADP proposal to study the formation and evolution of dust-embedded clusters
[NASA-CR-186793] N91-14089

MORGAN STATE UNIV., BALTIMORE, MD.
Data reduction of digitized images processed from calibrated photographic and spectroscopic films obtained from terrestial, rocket and space shuttle telescopic instruments
[NASA-CR-187320] N91-13674

MOUNT STROMLO AND SIDING SPRING OBSERVATORY, CANBERRA (AUSTRALIA).
High-mass star formation in southern disk galaxies N91-14218

MULLARD RADIO ASTRONOMY OBSERVATORY, CAMBRIDGE (ENGLAND).
The environments of double radiogalaxies N91-14166
Non-steller light from high-redshift radiogalaxies N91-14238

N

NATIONAAL INST. VOOR KERNFYSICA EN HOGE ENERGIEFYSICA, AMSTERDAM (NETHERLANDS).
Local closed orbit bumps in AmPS
[NIKHEF-K/AMPS/90-01] N91-13471

NATIONAL AERONAUTICAL LAB., BANGALORE (INDIA).
Calibration set up for load cells
[PD-ST-8917] N91-13673

NATIONAL AERONAUTICS AND SPACE ADMINISTRATION, WASHINGTON, DC.
Aeronautical engineering: A continuing bibliography with indexes (supplement 258)
[NASA-SP-7037(258)] N91-13399
Microgravity strategic plan, 1990
[NASA-TM-103448] N91-13575
Biological Life Support Technologies: Commercial Opportunities
[NASA-CP-3094] N91-13842
The NASA CELSS program N91-13848

NATIONAL AERONAUTICS AND SPACE ADMINISTRATION. AMES RESEARCH CENTER, MOFFETT FIELD, CA.
Indicial response approach derived from Navier-Stokes equations. Part 1: Time-invariant equilibrium state
[NASA-TM-102856] N91-13408
Integrated flight-propulsion control concepts for supersonic transport airplanes
[NASA-TM-101728] N91-13460
Turbulence and pressure loss characteristics of the inlet vanes for the 80- by 120-ft wind tunnel
[NASA-TM-102808] N91-13466
Turbulence modeling for sharp-fin-induced shock wave/turbulent boundary-layer interactions
[NASA-TM-102828] N91-13652
A laser Doppler velocimeter approach for near-wall three-dimensional turbulence measurements
[NASA-TM-102841] N91-13653
General Rotorcraft Aeromechanical Stability Program (GRASP): Theory manual
[NASA-TM-102255] N91-13762
CELSS research and development program N91-13850
Physiological responses to prolonged bed rest in humans: A compendium of research, 1981-1988
[NASA-TM-102249] N91-13862
Apparatus for precision focusing and positioning of a beam waist on a target
[NASA-CASE-ARC-11916-1-SB] N91-14002
Performance of multiplexed Ge:Ga detector arrays in the far infrared
[NASA-TM-102275] N91-14087
The Interstellar Medium in External Galaxies: Summaries of contributed papers
[NASA-CP-3084] N91-14100
Physical conditions in photodissociation regions: Application to galactic nuclei N91-14113
Far-infrared spectroscopy of NGC 6946, IC 342, and Arp 299 N91-14114
Very small grains in the Milky Way and external galaxies N91-14138
IRAS observations of the ISM in the gamma CAS reflection nebula N91-14140
Multiband observations of Cygnus A: A study of pressure balance in the core of a powerful radio galaxy N91-14151
Evolution of a superbubble blastwave in a magnetized medium N91-14180
MHD shocks in the ISM N91-14183

What sort of standard candle is Orion for studying molecular hydrogen line emission in galaxies N91-14184

NATIONAL AERONAUTICS AND SPACE ADMINISTRATION. GODDARD SPACE FLIGHT CENTER, GREENBELT, MD.

Control system for ruling blazed, aberration corrected diffraction gratings [NASA-CASE-GSC-13240-1] N91-13692

Device for applying constant pressure to a surface [NASA-CASE-GSC-13230-1] N91-13734

Robot cable-compliant devices [NASA-CASE-GSC-13127-1] N91-13735

Earth observing satellite: Understanding the Earth as a system N91-13853

Laser optical disk position encoder with active heads [NASA-CASE-GSC-13175-1] N91-14001

Method of fabricating germanium and gallium arsenide devices [NASA-CASE-GSC-13265-1] N91-14066

Emission from small dust particles in diffuse and molecular cloud medium N91-14137

A model for the infrared emission from an OB star cluster environment N91-14139

Infrared analysis of LMC superbubbles N91-14181

A near infrared spectroscopic study of the interstellar gas in the starburst core of M82 N91-14221

COBE's search for structure in the Big Bang [NASA-TM-102976] N91-14271

NATIONAL AERONAUTICS AND SPACE ADMINISTRATION. HUGH L. DRYDEN FLIGHT RESEARCH FACILITY, EDWARDS, CA.

A preliminary look at techniques used to obtain airdata from flight at high angles of attack [NASA-TM-101729] N91-13453

Integrated flight-propulsion control concepts for supersonic transport airplanes [NASA-TM-101728] N91-13460

NATIONAL AERONAUTICS AND SPACE ADMINISTRATION. JOHN C. STENNIS SPACE CENTER, BAY SAINT LOUIS, MS.

Predictive sensor method and apparatus [NASA-CASE-SSC-00006-1] N91-13691

Hydraulic lifting device [NASA-CASE-SSC-00008-1] N91-13733

NATIONAL AERONAUTICS AND SPACE ADMINISTRATION. JOHN F. KENNEDY SPACE CENTER, COCOA BEACH, FL.

The CELSS breadboard project: Plant production N91-13849

NATIONAL AERONAUTICS AND SPACE ADMINISTRATION. LYNDON B. JOHNSON SPACE CENTER, HOUSTON, TX.

Assured crew return vehicle [NASA-CASE-MSC-21536-1] N91-13483

Dual diaphragm tank with telltale drain [NASA-CASE-MSC-21703-1] N91-13580

Variable orifice flow regulator [NASA-CASE-MSC-21549-1] N91-13657

Volumetric measurement of tank volume [NASA-CASE-MSC-21500-1] N91-13683

Two fault tolerant toggle-hook release [NASA-CASE-MSC-21671-1] N91-13723

A personal history of the human exploration initiative with commentary on the pivotal role for life support research N91-13855

Biofilm monitoring coupon system [NASA-CASE-MSC-21585-1] N91-13857

Three-dimensional cell to tissue assembly process [NASA-CASE-MSC-21559-1] N91-13860

Portable dynamic fundus instrument [NASA-CASE-MSC-21675-1] N91-13865

EMU helmet mounted display [NASA-CASE-MSC-21460-1] N91-13879

Programmable remapper with single flow architecture [NASA-CASE-MSC-21481-1] N91-13890

General method of pattern classification using the two-domain theory [NASA-CASE-MSC-21737-1] N91-13911

System and method for a general purpose architecture for intelligent computer-aided training [NASA-CASE-MSC-21381-1] N91-13944

Optical joint correlation for real-time tracking [NASA-CASE-MSC-21509-1] N91-13997

Three dimensional moire pattern alignment [NASA-CASE-MSC-21416-1] N91-14000

NATIONAL AERONAUTICS AND SPACE ADMINISTRATION. LANGLEY RESEARCH CENTER, HAMPTON, VA.

Close-range photogrammetric measurement of static deflections for an aeroelastic supercritical wing [NASA-TM-4194] N91-13400

Navier-Stokes and Euler solutions for lee-side flows over supersonic delta wings. A correlation with experiment [NASA-TP-3035] N91-13401

Effect of location of aft-mounted nacelles on the longitudinal aerodynamic characteristics of a high-wing transport airplane [NASA-TP-3047] N91-13402

Aerodynamic effect of strakes on two-dimensional tail boom models of the OH-58A and the OH-58D helicopters [NASA-TM-4248] N91-13406

Some observations on the Houbolt-Rainey and peak-hold methods of flutter onset prediction [NASA-TM-102745] N91-13411

Some buffet response characteristics of a twin-vertical-tail configuration [NASA-TM-102749] N91-13412

Instability of a supersonic shock free elliptic jet [NASA-TM-103428] N91-13413

Concept development of a Mach 4 high-speed civil transport [NASA-TM-4223] N91-13432

A semiempirical method for obtaining fuselage normal areas from fuselage Mach sliced areas [NASA-TM-4228] N91-13433

F-106B airplane active control landing gear drop test performance [NASA-TM-102741] N91-13445

Calibration of the 13- by 13-inch adaptive wall test section for the Langley 0.3-meter transonic cryogenic tunnel [NASA-TP-3049] N91-13461

Wind-tunnel survey of an oscillating flow field for application to model helicopter rotor testing [NASA-TM-4224] N91-13462

Simulation of pressure and temperature responses for the 20 Inch Supersonic Wind Tunnel [NASA-TM-102647] N91-13467

Analytical and photogrammetric characterization of a planar tetrahedral truss [NASA-TM-4231] N91-13473

Integrated launch and emergency vehicle system [NASA-CASE-LAR-13780-1] N91-13481

An investigation of microstructural characteristics of contact-lens polymers [NASA-TP-3034] N91-13492

Oxidation characteristics of Ti-25Al-10Nb-3V-1Mo intermetallic alloy [NASA-TP-3044] N91-13522

Method and apparatus for characterizing residual stress in ferromagnetic materials [NASA-CASE-LAR-14239-1] N91-13527

Polymer/riblet combination for hydrodynamic skin friction reduction [NASA-CASE-LAR-14271-1-CU] N91-13558

Novel polyimide molding powder, coating, adhesive, and matrix resin [NASA-CASE-LAR-14163-1] N91-13559

Preparation of polyimides from bis(N-isoprenyl)s of aryl diamides [NASA-CASE-LAR-14330-1-CU] N91-13560

Methyl substituted polyimides containing carbonyl and ether connecting groups [NASA-CASE-LAR-14351-1] N91-13561

Tissue simulating gel for medical research [NASA-CASE-LAR-14036-1] N91-13562

Modified Hilbert transform pair and Kramers-Kronig relations for complex permittivities [NASA-TM-102682] N91-13585

Computational fluid dynamics [NASA-TM-101197] N91-13637

Water cooled static pressure probe [NASA-CASE-LAR-14340-1-CU] N91-13684

Passive fetal monitoring sensor [NASA-CASE-LAR-14088-1] N91-13686

Dual strain gage balance system for measuring light loads [NASA-CASE-LAR-14419-1] N91-13687

Transducer holder and method of making [NASA-CASE-LAR-14027-1] N91-13693

Real-time dynamic holographic image storage device [NASA-CASE-LAR-13989-1] N91-13694

Free vibrations of thin-walled semicircular graphite-epoxy composite frames [NASA-TP-3010] N91-13750

Failure behavior of generic metallic and composite aircraft structural components under crash loads [NASA-RP-1239] N91-13751

A review of nonlinear constitutive models for metals [NASA-TM-102727] N91-13761

A discrepancy within primate spatial vision and its bearing on the definition of edge detection processes in machine vision [NASA-TM-102739] N91-13941

Inclusive inelastic scattering of heavy ions and nuclear correlations [NASA-TP-3026] N91-13985

Theoretical temperature-dependent branching ratios and laser thresholds of the (5)I7 yields (5)I8 levels of Ho3(+) in ten garnets [NASA-TM-103429] N91-14053

Technical communications in aerospace: An analysis of the practices reported by US and European aerospace engineers and scientists [NASA-TM-103441] N91-14079

Single launch lunar habitat derived from an NSTS external tank [NASA-TM-4212] N91-14251

Space radiation dose analysis for solar flare of August 1989 [NASA-TM-4229] N91-14265

NATIONAL AERONAUTICS AND SPACE ADMINISTRATION. LEWIS RESEARCH CENTER, CLEVELAND, OH.

A steadying effect of acoustic excitation on transitory stall [NASA-TM-103689] N91-13420

A review of ice accretion data from a model rotor icing test and comparison with theory [NASA-TM-103712] N91-13421

Measurements and predictions of a liquid spray from an air-assist nozzle [NASA-TM-103640] N91-13455

Thermal and structural assessments of a ceramic wafer seal in hypersonic engines [NASA-TM-103651] N91-13456

An AD100 implementation of a real-time STOVL aircraft propulsion system [NASA-TM-103683] N91-13457

JANNAF liquid rocket combustion instability panel research recommendations [NASA-TM-103653] N91-13491

Relationship between voids and interlaminar shear strength of polymer matrix composites [NASA-TM-103643] N91-13495

Composite thermal barrier coating [NASA-CASE-LEW-14999-1] N91-13500

Method of making single crystal fibers [NASA-CASE-LEW-14921-1] N91-13502

Method of making carbide/fluoride/silver composites [NASA-CASE-LEW-14902-1] N91-13503

Vinyl capped addition polyimides [NASA-CASE-LEW-15027-1] N91-13566

Real-time data compression of broadcast video signals [NASA-CASE-LEW-14945-1] N91-13598

Comment on local energy transfer and nonlocal interactions in homogeneous, isotropic turbulence (Phys. Fluids A2, 413 (1990)) [NASA-TM-103263] N91-13638

Heat transfer device and method of making the same [NASA-CASE-LEW-14162-1] N91-13668

Plug-type heat flux gauge and method of producing same [NASA-CASE-LEW-14967-1] N91-13685

Post clamp [NASA-CASE-LEW-14862-1] N91-13730

Probe insertion apparatus with inflatable seal [NASA-CASE-LEW-14965-1] N91-13732

Small particle selective emitter [NASA-CASE-LEW-14731-1] N91-13802

Thin solar cell and lightweight array [NASA-CASE-LEW-14959-1] N91-13803

Monolithic mm-wave phase shifter using optically activated superconducting switches [NASA-CASE-LEW-14878-1] N91-13996

An x ray photoelectron spectroscopy study of Au(x)In(y) alloys [NASA-TM-103659] N91-14050

Design considerations for lunar base photovoltaic power systems [NASA-TM-103642] N91-14259

NATIONAL AERONAUTICS AND SPACE ADMINISTRATION. MARSHALL SPACE FLIGHT CENTER, HUNTSVILLE, AL.

Standard remote manipulator system docking target augmentation for automated docking [NASA-CASE-MFS-28419-1] N91-13482

Laser-induced fluorescence of phosphors for remote cryogenic thermometry [DE91-001733] N91-13681

Solder dross removal apparatus [NASA-CASE-MFS-28406-1] N91-13729

Cantilever clamp fitting [NASA-CASE-MFS-28328-1] N91-13731

Test and model correlation of the atmospheric emission photometric imager fiberglass pedestal [NASA-TM-103515] N91-13766

An improved exploratory search technique for pure integer linear programming problems [NASA-TM-103517] N91-13910

Wide acceptance angle, high concentration ratio, optical collector
[NASA-CASE-MFS-28295-1] N91-13999
Variable magnification glancing incidence x ray telescope
[NASA-CASE-MFS-28013-2] N91-14096
An infrared jet in Centaurus A (NGC 5128): Evidence for interaction between the active nucleus and the interstellar medium N91-14175
Central star formation in S0 galaxies N91-14223

NATIONAL AERONAUTICS AND SPACE ADMINISTRATION. NATIONAL SPACE TECHNOLOGY LABS., BAY SAINT LOUIS, MS.
The BioHome: A spinoff of space technology N91-13852

NATIONAL AERONAUTICS AND SPACE ADMINISTRATION. PASADENA OFFICE, CA.
Flexible thermal apparatus for mounting of thermoelectric cooler
[NASA-CASE-NPO-17806-1-CU] N91-13581
Method for providing a polarization filter for processing synthetic aperture radar image data
[NASA-CASE-NPO-17904-1-CU] N91-13594
Pipeline synthetic aperture radar data compression utilizing systolic binary tree-searched architecture for vector quantization
[NASA-CASE-NPO-17941-1-CU] N91-13595
Multiple symbol differential detection
[NASA-CASE-NPO-17896-1-CU] N91-13596
Secondary Li battery incorporating 12-crown-4 ether
[NASA-CASE-NPO-17922-1-CU] N91-13621
Detection of multiple-bit errors from single-ion tracks in integrated circuits
[NASA-CASE-NPO-18075-1-CU] N91-13622
Measurement of waves in flows across a surface
[NASA-CASE-NPO-17479-1-CU] N91-13658
Bilevel shared control for teleoperators
[NASA-CASE-NPO-17800-1-CU] N91-13724
Composite passive damping struts for large precision structures
[NASA-CASE-NPO-17914-1-CU] N91-13767
System and method for measuring ocean surface currents at locations remote from land masses using synthetic aperture radar
[NASA-CASE-NPO-17937-1-CU] N91-13787
Thermal power transfer system using applied potential difference to sustain operating pressure difference
[NASA-CASE-NPO-18034-1-CU] N91-13796
Auto and hetero-associative memory using a 2-D optical logic gate
[NASA-CASE-NPO-17997-1-CU] N91-13888
High-gain AlGaAs/GaAs double heterojunction Darlington phototransistors for optical neural networks
[NASA-CASE-NPO-18101-1-CU] N91-13995
Motion detection, novelty filtering, and target tracking using an interferometric technique with a GaAs phase conjugate mirror
[NASA-CASE-NPO-17784-1-CU] N91-13998

NATIONAL CENTER FOR ATMOSPHERIC RESEARCH, BOULDER, CO.
Research projects including climate, atmospheric chemistry, solar-terrestrial physics, metrology, and storm systems
[PB90-256306] N91-13820

NATIONAL DEFENCE RESEARCH ESTABLISHMENT, UMEA (SWEDEN).
Evaluation of a wind profile model
[FOA-E-40045-4.5] N91-13839

NATIONAL GEOPHYSICAL DATA CENTER, BOULDER, CO.
Solar-geophysical data number 550, June 1990. Part 1: (Prompt reports). Data for May, April 1990 and late data
[PB90-258799] N91-14260
Solar-geophysical data number 550, June 1990. Part 2: (Comprehensive reports). Data for December 1989 and miscellaneous
[PB90-258807] N91-14261
Solar-geophysical data number 549, May 1990. Part 1: (Prompt reports). Data for April, March, 1990, and late data
[PB90-251224] N91-14262
Solar-geophysical data number 549, May 1990. Part 2: (Comprehensive reports). Data for November 1989 and miscellaneous
[PB90-251232] N91-14263

NATIONAL PHYSICAL LAB., TEDDINGTON (ENGLAND).
Development of standards for advanced polymer matrix composites: A BPF/ACG overview
[NPL-DMM(A)-8] N91-13568
Review of uncertainties in the use of NPL primary standards of x ray exposure for the calibration of secondary standards in terms of exposure and air kerma
[NPL-RS(EXT)-109] N91-13868
Software management guidelines for automated measuring systems
[NPL-DES-99] N91-13926
Investigation of the uniformity of the magnetic field and flux density in the NPL permeameter
[NPL-DES-101] N91-13968

NATIONAL RADIO ASTRONOMY OBSERVATORY, CHARLOTTESVILLE, VA.
A survey of the properties of early-type galaxies N91-14109

NATIONAL RADIO ASTRONOMY OBSERVATORY, SOCORRO, NM.
High brightness neutral hydrogen in M31: A new probe of interstellar pressure N91-14196
Current star formation in S0 galaxies: NGC 4710 N91-14224
Radio continuum observations of the quasar-galaxy pair 3C 232-NGC 3067 N91-14226

NATIONAL RESEARCH COUNCIL OF CANADA, OTTAWA (ONTARIO).
The IAR high Reynolds number two-dimensional test facility: A description of equipment and procedures common to most 2-D airfoil tests
[AD-A226629] N91-13409

NATIONAL SEVERE STORMS LAB., NORMAN, OK.
DOPLIGHT 1987 project summary
[PB90-253584] N91-13834

NATIONAL TRANSPORTATION SAFETY BOARD, WASHINGTON, DC.
Aircraft accident report: Aloha IslandAir, Inc., Flight 1712, de Havilland Twin Otter, DHC-6-300, N707PV, Halawa Point, Molokai, Hawaii, October 28, 1989
[PB90-910405] N91-13425

NAVAL AIR DEVELOPMENT CENTER, WARMINSTER, PA.
Superconducting Josephson Junction Gyroscope (JJG) N91-14043

NAVAL POSTGRADUATE SCHOOL, MONTEREY, CA.
Extremely High Frequency (EHF) Low Probability of Intercept (LPI) communication applications
[AD-A226653] N91-13591
Assessments of atmospheric effects on VHF and UHF communications
[AD-A226661] N91-13592
Constrained viscoelastic layer damping of thick aluminum plates: Design, analysis, and testing
[AD-A226556] N91-13758
Coupling artificial intelligence and a system dynamics simulation to optimize quality assurance and testing in software development
[AD-A226580] N91-13902
Applications of neural networks to adaptive control
[AD-A225408] N91-13938
Flexible cooperation in non-standard application environments
[AD-A226486] N91-13940

NAVAL RESEARCH LAB., WASHINGTON, DC.
A study of confined diffusion flames
[AD-A226552] N91-13512
NRL 1989 beam propagation studies in support of the ATA multi-pulse propagation experimont
[AD-A226443] N91-13588
NRL compact accelerator theory studies
[AD-A226537] N91-14005
Observations of the galactic plane by the zodiacal infrared project N91-14143

NAVAL SURFACE WEAPONS CENTER, SILVER SPRING, MD.
Synthesis and characterization of high temperature superconductor materials N91-14048

NETHERLANDS FOUNDATION FOR RADIO ASTRONOMY, DWINGELO.
A multi-wavelength study of the peculiar galaxy NGC 2976 N91-14199
The molecular spiral arms of NGC 6946 N91-14232

NEW HAMPSHIRE UNIV., DURHAM.
Temporal variations of cosmic rays in the heliosphere N91-14267

NEW YORK UNIV., NEW YORK.
Cognitive and neural bases of skilled performance
[AD-A226668] N91-13869
Plasma properties
[DE91-001361] N91-14006

NEWCASTLE-UPON-TYNE UNIV. (ENGLAND).
Effect of lubricating oil characteristics on gear vibrations N91-13710

NIIGATA UNIV. (JAPAN).
Evolution of magnetized, rotating, isothermal clouds N91-14191

NOBEYEMA SOLAR RADIO OBSERVATORY (JAPAN).
CO mapping of the nuclear region of NGC 6946 and IC 342 with Nobeyama millimeter array N91-14233

NORTH CAROLINA STATE UNIV., RALEIGH.
Theoretical evaluation of engine auxiliary inlet design for supersonic V/STOL aircraft
[NASA-CR-186610] N91-13443
Software reliability through fault-avoidance and fault-tolerance
[NASA-CR-187646] N91-13904

NORTHWESTERN UNIV., EVANSTON, IL.
PBT, PBO-based hybrid polymers with nonlinear optical properties or high electrical conductivity
[AD-A226646] N91-13552
Search for cold gas in clusters with and without cooling flows N91-14174

NORWEGIAN DEFENCE RESEARCH ESTABLISHMENT, KJELLER.
SAR detection of topography, vegetation and installations over land
[FFI-90/7016] N91-13600
Gravity waves excited by flow over an obstacle
[FFI-90/7017] N91-13828
NDRE/TAll processor architecture study
[FFI-90/7012] N91-13891
CESAR MALU program library
[FFI-90/7010] N91-13922
BAG: A programming language for the CESAR buffer address generator
[FFI-90/7022] N91-13923
CESAR trap program library
[FFI-90/7023] N91-13924

O

OAK RIDGE GASEOUS DIFFUSION PLANT, TN.
Fluid flow effects on electroplating
[DE91-001087] N91-13577

OAK RIDGE NATIONAL LAB., TN.
Influence of oxide reinforcement materials on high-temperatue oxidation resistance of Ni3Al matrix composites
[DE91-001625] N91-13498
Progress in the detection of single molecules in levitated droplets
[DE91-000612] N91-13517
Advanced Materials Development Program: Ceramic Technology for Advanced Heat Engines program plan, 1983--1993
[DE91-000516] N91-13555
Optical characterization techniques applied to ceramic oxides
[DE91-001526] N91-13556
High-alcohol microemulsion fuel performance in a diesel engine
[DE91-001617] N91-13572
Characterization of rocket propellant combustion products: Description of sampling and analysis methods for rocket exhaust characterization studies
[DE91-002536] N91-13574
Performance comparison of magnetic refrigeration cycles
[DE91-001520] N91-13578
Radiation effects on JFETs (Junction Field-Effect Transistors), MOSFETs, and dipolar transistors, as related to SSC circuit design
[DE91-001486] N91-13618
Laser-induced fluorescence of phosphors for remote cryogenic thermometry
[DE91-001733] N91-13681
Results from the second year of operation of the Federal Methanol Fleet at Oak Ridge National Laboratory
[DE91-000543] N91-13718
Potential impact of enhanced fracture-toughness data on pressurized-thermal-shock analysis
[DE91-001493] N91-13763
Managing the Global Commons Decision Making and Conflict Resolution in Response to Climate Change Research Workshop
[DE91-001018] N91-13810
Acidic deposition and the environment
[DE91-002352] N91-13812
Terrestrial ecosystems and climatic change
[DE91-001492] N91-13813
Inorganic concepts relevant to metal binding, activity, and toxicity in a biological system
[DE91-001489] N91-13858
Synthetic models of distributed memory parallel programs
[DE91-001058] N91-13931
An application of oscillation damped motion for suspended payloads to the advanced integrated maintenance system
[DE91-002658] N91-13946
Interpretation of engine cycle-to-cycle variation by chaotic time series analysis
[DE91-000729] N91-13955
Computing the eigenvalues and eigenvectors of a general matrix by reduction to general tridiagonal form
[DE91-002523] N91-13959

Assessment of ion-atom collision data for magnetic fusion plasma edge modelling
[DE91-001920] N91-14012
International Thermonuclear Experimental Reactor physics basis
[DE91-002646] N91-14017
ITER confinement capability
[DE91-002647] N91-14018
Dependence of CIT (compact ignition tokamak) PF (poloidal field) coil currents on profile and shape parameters using the control matrix
[DE91-002650] N91-14019
Ion-induced damage and amorphization in Si
[DE91-002358] N91-14061
Linear vs nonlinear and infinite vs finite: An interpretation of chaos
[DE91-002522] N91-14072
Report of foreign travel
[DE91-001732] N91-14082

OBSERVATOIRE DE PARIS-MEUDON (FRANCE).
Near-infrared mapping of spiral barred galaxies N91-14217

OFFICE OF NAVAL RESEARCH EUROPEAN OFFICE, FPO NEW YORK, NY.
Overview of European technology in computers, telecommunications, and electronics
[PB90-215773] N91-13610

OHIO STATE UNIV., COLUMBUS.
Modelling and performance analysis of four and eight element TCAS
[NASA-CR-187414] N91-13428
Non-linear dynamic analysis of geared systems
[NASA-CR-4338] N91-13737
Ground-based studies of emission-line variability: Recent results for NGC 5548 and future plans
[NASA-CR-180433] N91-14088

ONSALA SPACE OBSERVATORY (SWEDEN).
The molecular cloud content of early type galaxies N91-14127

OREGON STATE UNIV., CORVALLIS.
Cloud properties as deduced from satellite observation
[NASA-CR-182851] N91-13833

OWENS VALLEY RADIO OBSERVATORY, PASADENA, CA.
Aperture synthesis CO observations of the inner disk of NGC 1068 N91-14122
Molecular gas and star formation in the centers of Virgo spirals N91-14216

OXFORD POLYTECHNIC (ENGLAND).
ADENG, adhesive bonding technology for engineering applications: Computer aided design
[CETIM-105070] N91-13917

P

PAINE (THOMAS) ASSOCIATES, LOS ANGELES, CA.
Biospheres and solar system exploration N91-13843

PARKE MATHEMATICAL LABS., INC., CARLISLE, MA.
Signal processing development
[AD-A226593] N91-14052

PENNSYLVANIA STATE UNIV., UNIVERSITY PARK.
Utilization of the HIPAS facility for cooperative experiments related to ionospheric modification
[AD-A226609] N91-13590
Reynolds stress closure in jet flows using wave models
[NASA-CR-185717] N91-13640
The influence of the sampling time on diffusion measurements in the atmosphere N91-13824
A study of active regions on RS CVn stars N91-14092
Far infrared luminosity functions of normal galaxies N91-14135

PERA, MELTON MOWBRAY, LEICESTER (ENGLAND).
ADENG, adhesive bonding technology for engineering applications: Computer aided design
[CETIM-105070] N91-13917

PHYSICS AND ELECTRONICS LAB. TNO, THE HAGUE (NETHERLANDS).
Description of sea wave motion and its influence on the altitude control of sea skimming missiles
[FEL-89-A368] N91-13450
Electronic scan at millimetre wave frequencies
[FEL-89-B258] N91-13601
Measurement results of the FEL-TNO planar rectangular near field facility (1978-1989)
[FEL-89-B336] N91-13602
BSB radar pulse classification
[FEL-90-B023] N91-13603
Planar near-field measurement of non-reciprocal antennas
[FEL-90-B092] N91-13604
Comparison of spectral estimators application to ground sensor signals
[FEL-1988-85] N91-13605
Observation with stand-off radars
[FEL-90-A022] N91-13606
Frequency-domain analysis of one-dimensional electromagnetic scattering by lossy media
[FEL-90-A112] N91-13607
GaAs MMIC mixer for 8-12 GHz, based on 0.5 micrometer gate length D-MESFETS. Volume 1: Design and layout
[FEL-89-B277-VOL-1] N91-13632
Design of an X-band PIN diode phase shifter by computer optimization
[FEL-89-B286] N91-13633
Feasibility to study of a non-reciprocal latched ferrite phase shifter in the 92-96 GHz band
[FEL-90-B114] N91-13634
A design method for an X-band diplexer
[FEL-90-B176] N91-13635
Test procedure frequency multiplier 583R936H03/H04
[FEL-90-A089] N91-13636
Quality of expert systems: Methods and techniques
[FEL-89-A267] N91-13747
Quality of expert systems: Algorithms for integrity control
[FEL-89-A312] N91-13748
Lidar as a slant path visio-ceilometer
[FEL-90-A207] N91-13838
Study system concept for a pelotons procedure trainer (PEP-trainer) for the weapon systems YPR-PRAT, YPR-25 mm (EWS) and Leopard 1-5
[FEL-90-A084] N91-13871
Definition study into the requirements of a data modem for the SYSCOM network
[FEL-90-A116] N91-13892
Multispectral target detection using image processing programs developed on PC's
[FEL-89-B304] N91-13925

PITTSBURGH ENERGY TECHNOLOGY CENTER, PA.
A review of interaction mechanisms in fluid-solid flows
[DE91-000941] N91-13660

PITTSBURGH UNIV., PA.
The mechanism of restructuring in geometry
[AD-A224740] N91-13951

POLITECNICO DI MILANO (ITALY).
An object-oriented logic language for modular system specification
[REPT-90-027] N91-13927
On the invertibility of Leslie systems
[REPT-90-006] N91-13963

PRATT AND WHITNEY AIRCRAFT, WEST PALM BEACH, FL.
All Shuttle Centaur engine and nozzle support plug vibration testing
[NASA-CR-183201] N91-13485
RL10A-3-3B high mixture ratio qualification program
[NASA-CR-183200] N91-13486
Shuttle Centaur engine cooldown evaluation and effects of expanded inlets on start transient
[NASA-CR-183198] N91-13487

PRINCETON UNIV., NJ.
Physical properties of thermosetting polymers
[AD-A225864] N91-13508
The fluid mechanics of continuous flow electrophoresis
[NASA-CR-187647] N91-13648
Intergalactic HI in the NGC5018 group N91-14110
Far-infrared emission from dusty ellipticals N91-14142
Imaging spectrophotometry of the nuclear outflow of NGC 1068 N91-14149

PRINCETON UNIV. OBSERVATORY, NJ.
Empirical relationships between gas abundances and UV selective extinction N91-14116
Dissociation and ionization of molecular gas in the spiral arms of M51 N91-14205
Interpreting the convergence of Lyman series absorption lines N91-14225

PURDUE UNIV., WEST LAFAYETTE, IN.
A quiet flow Ludwieg tube for study of transition in compressible boundary layers: Design and feasibility
[NASA-CR-187374] N91-13676
On combining selection and estimation in the search for the largest binomial parameter
[AD-A226595] N91-13953

Q

QUEENSLAND UNIV., SAINT LUCIA (AUSTRALIA).
Shock tunnel studies of scramjet phenomena, supplement 5
[NASA-CR-182096-SUPPL-5] N91-13651

R

RENSSELAER POLYTECHNIC INST., TROY, NY.
Mechanism of mechanical fatigue of silica glass
[DE91-004053] N91-13565

RICE UNIV., HOUSTON, TX.
Large scale excitation of the ISM in NGC 1068 N91-14150
Differences in the size-internal velocity relation of galactic and extragalactic HII regions N91-14158
The Hawaii Imaging Fabry-Perot Interferometer (HIFI) N91-14240

ROCHESTER UNIV., NY.
Ultrafast optical electronics center
[AD-A226669] N91-14054
Flux flow pinning and resistive behavior in superconducting networks
[DE91-002756] N91-14064

ROYAL AEROSPACE ESTABLISHMENT, FARNBOROUGH (ENGLAND).
Advanced missile guidance N91-13439
The United Kingdom contribution to the AGARD fatigue-rated fastener systems program
[RAE-TR-89046] N91-13451
Orbit determination and analysis for Aureole 2 rocket at 27:2 resonance
[RAE-TR-90018] N91-13472
Sustained-load crack growth of 8090 aluminium-lithium alloy plate in dry air at 50-200 C
[RAE-TR-90033] N91-13777
Long persistence effects of geomagnetic activity
[RAE-TM-SP-376] N91-13829
A subjective rating scale for assessing pilot workload in flight: A decade of practical use
[RAE-TR-90019] N91-13882

ROYAL ARMAMENT RESEARCH AND DEVELOPMENT ESTABLISHMENT, WALTHAM ABBEY (ENGLAND).
Work of fracture of composites in axial compression: Measurement and origins
[RARDE-1/90] N91-13505

ROYAL GREENWICH OBSERVATORY, HAILSHAM (ENGLAND).
The violent interstellar medium in Messier 31 N91-14178

ROYAL MILITARY COLL. OF CANADA, KINGSTON (ONTARIO).
Physics and applications of low temperature superconductivity N91-14032

ROYAL NETHERLANDS METEOROLOGICAL INST., DE BILT.
The use of satellite data in the ECMWF analysis system
[KNMI-TR-123] N91-13790
A primitive equation model for the equatorial Pacific
[KNMI-TR-124] N91-13840

ROYAL SIGNALS AND RADAR ESTABLISHMENT, MALVERN (ENGLAND).
Progress in high Tc superconductors N91-14031
The SWORD model of multilevel secure databases
[RSRE-90008] N91-14085

RUTHERFORD APPLETON LAB., CHILTON (ENGLAND).
Miniature closed cycle refrigerators N91-14035

S

SANDIA NATIONAL LABS., ALBUQUERQUE, NM.
Effect of bulk viscosity in low density, hypersonic blunt body flows
[DE90-012756] N91-13419
An exploratory program for using hydrous metal oxide ion exchangers as Fischer-Tropsch catalysts
[DE91-002341] N91-13521
Dynamic high-pressure studies of an electrothermal capillary
[DE91-000966] N91-13617
Single event upset hardening techniques
[DE91-002337] N91-13625
Tubular lap joints for wind turbine applications
[DE91-001341] N91-13736
On the design of component test plans based on system reliability objectives
[DE90-017034] N91-13745
A structural constitutive algorithm based on continuum damage mechanics for softening with snapback
[DE90-015841] N91-13773
Status of concentrator collector and high-efficiency concentrator cell development
[DE91-001260] N91-13793
A theoretical investigation of effective surface recombination velocity in AlGaAs/GaAs heteroface solar cells
[DE91-001754] N91-13795

Carbon dioxide reforming of methane in a solar volume-TRIC receiver-reactor: The CAESAR (Catalytically Enhanced Solar Absorption Receiver) project
[DE91-002340] N91-13800
Experiments on bench-scale heat-pipe solar receivers
[DE90-013806] N91-13806
The role of chemical interactions in ion-solid processes
[DE91-000763] N91-13977
Application of parallel computing to the Monte Carlo simulation of electron scattering in solids: A rapid method for profile deconvolution
[DE91-001227] N91-13980
Multiplexer/amplifier test results for SP-100
[DE91-004504] N91-13990
Band-gap narrowing and III-V heterostructure FETs (Field-Effect Transistors)
[DE91-000401] N91-14056

SCHWARTZ ELECTRO-OPTICS, INC., CONCORD, MA.
Chromium sensitized garnets for mid-IR lasers
[AD-A226630] N91-13696

SMITHSONIAN ASTROPHYSICAL OBSERVATORY, CAMBRIDGE, MA.
Complete the development and construction of a spaceborne hydrogen maser clock
[NASA-CR-184043] N91-13688

SOCIETY OF AUTOMOTIVE ENGINEERS OF JAPAN, TOKYO.
The 1990 JSAE (Society of Automative Engineers of Japan, Inc.) Spring Convention Proceedings 901
[DE91-715185] N91-13579

SOFTECH, INC., HOUSTON, TX.
Security for safety critical space borne systems
[NASA-CR-187656] N91-13906

SOUTH CAROLINA UNIV., COLUMBIA.
Operation of silicon microstrip detectors in a high radiation environment
[DE91-001953] N91-13682

SOUTHAMPTON UNIV. (ENGLAND).
Effects of temperature on acoustically-induced strains and damage propagation in CFRP plates N91-13493
Practical considerations for the measurement of internal and coupling loss factors on complex structures
[ISVR-TR-182] N91-13778
Modelling the effects of vibration on visual performance
[ISVR-TR-171] N91-13883
Effects of anthropometric and postural variables on the transmission of whole-body vertical vibration from seat-to-head
[ISVR-TR-172] N91-13884
The prediction and measurement of the one-parameter behaviour of horns
[ISVR-TR-185] N91-13974
Adaptive inverse filters for stereophonic sound reproduction
[ISVR-TR-187] N91-13975

SOUTHWEST RESEARCH INST., SAN ANTONIO, TX.
Mechanical testing of advanced coating system, volume 1
[NASA-CR-186725] N91-13534
Fatigue testing of plasma-sprayed thermal barrier coatings, volume 2
[NASA-CR-186726] N91-13535
SEPAC data analysis in support of the environmental interaction program
[NASA-CR-184028] N91-13807
Research into alternative network approaches for space operations
[NASA-CR-187015] N91-13894
Research into software executives for space operations support
[NASA-CR-187013] N91-13895

SPACE BIOSPHERES VENTURES, ORACLE, AZ.
Historical overview of the Biosphere 2 project N91-13844
Biosphere 2 test module experimentation program N91-13845
Biomedical program at Space Biospheres Ventures N91-13847

SPACE INDUSTRIES, INC., HOUSTON, TX.
Business and life in space N91-13854

SPACE TELESCOPE SCIENCE INST., BALTIMORE, MD.
Evidence against a simple two-component model for the far-infrared emission from galaxies N91-14136
Granularity in the magnetic field structure of M83 N91-14194

SPECTRA RESEARCH SYSTEMS, INC., HUNTSVILLE, AL.
Telerobotic on-orbit remote fluid resupply system
[NASA-CR-184052] N91-13474

SRI INTERNATIONAL CORP., MENLO PARK, CA.
Spanwise aerodynamic loads on a rotating wind turbine blade
[DE91-002101] N91-13414

STANFORD UNIV., CA.
Development and evaluation of continuum models for translational-rotational nonequilibrium N91-13403
Integrated aerodynamic and control system design of oblique wing aircraft N91-13459
Ammonia decomposition on silicon surfaces studied using transmission FTIR spectroscopy
[AD-A226625] N91-13513
Publications, patents, presentations, honors, and students report. Kinetics of semiconductor processing chemistry: SiGe and GaAs growth on silicon surfaces
[AD-A226639] N91-13514
Gradiometry coexperiments to the gravity probe B and step missions
[NASA-CR-187704] N91-13788

STATE UNIV. OF NEW YORK, BUFFALO.
Large eddy simulations and direct numerical simulations of high speed turbulent reacting flows
[NASA-CR-187674] N91-13656

STATE UNIV. OF NEW YORK, STONY BROOK.
Experimental studies of Josephson effect
[AD-A226548] N91-14051

STIFTUNG INST. FUER WERKSTOFFTECHNIK, BREMEN (GERMANY, F.R.).
X ray measurements of residual stresses in thin, hard layers N91-13542
Possibilities of stress measurement on ceramic materials using acoustic microscopy N91-13547

STOCKHOLM OBSERVATORY (SWEDEN).
A survey of galaxies in CO N91-14118

SVERDRUP TECHNOLOGY, INC., CLEVELAND, OH.
Comparison of NASA Lewis Research Center's performance code's pressure-drop model predictions to Stirling engine working-space flow test data
[NASA-CR-182215] N91-13804

SVERDRUP TECHNOLOGY, INC., HUNTSVILLE, AL.
Microbial ecology laboratory procedures manual NASA/MSFC
[NASA-CR-184033] N91-13856

SYRACUSE UNIV., NY.
Resonance region scattering
[AD-A226536] N91-13589
Magnetic field effect transistors
[AD-A226535] N91-13614
Mechanisms of gas permeation through polymer membranes
[DE91-004190] N91-13671
Federal information inventory/locator systems: From burden to benefit N91-14074

T

TATA INST. OF FUNDAMENTAL RESEARCH, BOMBAY (INDIA).
Far-infrared observations of Circinus and NGC 4945 galaxies N91-14131
Radio continuum and far-infrared emission of spiral galaxies: Implications of correlations N91-14147

TECHNICAL RESEARCH CENTRE OF FINLAND, ESPOO.
Creep and creep failure of power plant steels
[VTT-RR-685] N91-13528
Binders used in metal injection molding
[VTT-RR-691] N91-13529
Material degradation of steam turbine rotors in long term operations
[VTT-RR-692] N91-13530
Fabrication and properties of powder metallurgically manufactured aluminum products and composites
[VTT-RR-699] N91-13531
Testing of engineering ceramics, summary
[VTT-RR-678] N91-13567

TECHNISCHE HOCHSCHULE, AACHEN (GERMANY, F.R.).
The x ray elastic constants of ceramic materials for the determination of the stresses from lattice expansion measurements N91-13541

TECHNISCHE HOCHSCHULE, DARMSTADT (GERMANY, F.R.).
The effect of the molecular structure of polymer and low molecular liquid crystals on their electro-optical characteristics at the nematic-isotropic phase transition
[ETN-91-98170] N91-13564
Theory and procedure of the hierarchical design rule checking of integrated circuits
[ETN-91-98173] N91-13627
The coupling of finite methods for transport-diffusion problems
[ETN-91-98172] N91-13663
Classes of priors in games and decision models
[ETN-91-98171] N91-13965
Ionization degree of classical, dense, and highly condensed plasmas
[ETN-91-98174] N91-14027
Influence of the delocalized excitation process on the determination of foreign atom positions using the channeling effect
[ETN-91-98175] N91-14065

TECHNISCHE UNIV., CLAUSTHAL-ZELLERFELD (GERMANY, F.R.).
The influence of the texture of Al2O3 substrates on the fracture behavior under thermal loading N91-13543

TECHNISCHE UNIV., DELFT (NETHERLANDS).
Study of strategies for the determination of deformations from Global Positioning System (GPS) measurements
[ETN-91-98141] N91-13786
Report by the Subcommitee on Intercomparison and Merging of Geodetic Data of the Topex/Poseidon science working team
[LR-638] N91-13791

TECHNISCHE UNIV., HANOVER (GERMANY, F.R.).
Influence of materials structure and production method of Al2O3 ceramic on the x-ray stress measurement N91-13540

TECHPLAN CORP., SAN DIEGO, CA.
Coordinates of a life-cycle model for a software system and communicating the need for software technology
[AD-A226592] N91-13903

TENNESSEE UNIV., KNOXVILLE.
Elementary particle interactions
[DE91-001220] N91-13979

TENNESSEE UNIV. SPACE INST., TULLAHOMA.
A flight expert system for on-board fault monitoring and diagnosis
[NASA-CR-187334] N91-13452

TEXAS A&M UNIV., COLLEGE STATION.
Analytical and experimental research on large angle maneuvers of flexible structures
[AD-A226679] N91-13479
Experimental and theoretical determination of the thermomechanical response of inelastic structural materials to high energy thermal inputs
[AD-A226671] N91-13496
Experimental observations and finite element analysis of the initiation of fiber microbuckling in notched composite laminates
[NASA-CR-185354] N91-13756
Tropical Pacific moisture variability: Its detection, synoptic structure and consequences in the general circulation
[NASA-CR-184045] N91-13832
High energy physics program at Texas A&M University
[DE91-001639] N91-13989

TEXAS UNIV., AUSTIN.
Measuring the Lense-Thirring precession using a second Lageos satellite
[NASA-CR-186945] N91-13470
The effect of inertial coupling in the dynamics and control of flexible robotic manipulators
[NASA-CR-187679] N91-13721
Dynamic modeling, property investigation, and adaptive controller design of serial robotic manipulators modeled with structural compliance
[NASA-CR-187678] N91-13722
Positional estimation techniques for an autonomous mobile robot
[NASA-CR-187689] N91-13725
Information systems supported end-user interaction: Impacts on inter- and intra-organizational connectivity and cooperative behavior N91-14075
High spatial resolution 100 micron observations of the M83 bar N91-14130
Spatially resolved optical and near infrared spectroscopy of I Zw 18 N91-14154
High spatial resolution studies of galaxies in the far IR: Observations with the KAO; and the promise of SOFIA N91-14229
Properties of the Magellanic-type galaxies N91-14245

TEXAS UNIV., SAN ANTONIO.
A nonlinear viscoelastic approach to durability predictions for polymer based composite structures
[NASA-CR-187653] N91-13554

TEXTRON BELL HELICOPTER, FORT WORTH, TX.
Helicopter structural integrity program (HSIP). Volume 1: Structural test requirements specification
[AD-A226520] N91-13444

THIOKOL CORP., BRIGHAM CITY, UT.
Summary of JAYGO mixing and FSM-1 application of castable inhibitor and liner
[NASA-CR-184030] N91-13569
Evaluation of Raytek infrared pyrometer for continuous propellant temperature measurement
[NASA-CR-184040] N91-13570
Tethering sockets and wrenches
[NASA-CR-184032] N91-13675

THOMSON SINTRA ASM (FRANCE).
SQUIDs devices made from high Tc superconductors: Results and perspectives N91-14044

TOKYO UNIV. (JAPAN).
Circumnuclear molecular gas in starburst and Seyfert galaxies N91-14120
TOKYO UNIV., MITAKE (JAPAN).
Circumnuclear ionized gas in starburst nuclei N91-14148
TOLEDO UNIV., OH.
A comparison of UV surface brightness and HI surface densities for spiral galaxies N91-14102
TRW, INC., REDONDO BEACH, CA.
Analog superconductive electronics for avionics N91-14040

U

UNIVERSITEIT TWENTE, ENSCHEDE (NETHERLANDS).
Algorithms for finding an optimal matching between a given string and a string generated by a regular grammar
[MEMO-836] N91-13905
Direct modeling of white noise in stochastic systems
[MEMO-865] N91-13964
UNIVERSITY OF NORTH TEXAS, DENTON.
The design of phase-only filters for optical correlations
[AD-A225641] N91-13992
UNIVERSITY OF NORTHERN COLORADO, GREELEY.
Review of geography internship of convective wave project
[NASA-CR-187022] N91-13819
Interannual variation of seasonal means and subseasonal variability of cloud streets off the east coast of North America 1984-1987
[NASA-CR-187021] N91-13831
UNIVERSITY OF NORTHERN ILLINOIS, DE KALB.
Operation of silicon microstrip detectors in a high radiation environment
[DE91-001953] N91-13682
UNIVERSITY OF SOUTHERN CALIFORNIA, MARINA DEL REY.
Development of mercuric iodide uncooled x ray detectors and spectrometers
[NASA-CR-185394] N91-13484
UTAH STATE UNIV., LOGAN.
Instellar Gas Experiment (IGE): Testing interstellar gas particles to provide information on the processes of nucleosynthesis in the big bang stars and supernova
[NASA-CR-186713] N91-14097
UTAH UNIV., SALT LAKE CITY.
Friction and wear of TPS fibers: A study of the adhesion and friction of high modulus fibers
[NASA-CR-187666] N91-13515
UTRECHT STATE UNIV. (NETHERLANDS).
New techniques for the union-find problem
[RUU-CS-89-12] N91-13954

V

VARIAN ASSOCIATES, PALO ALTO, CA.
A liquid nitrogen cooled superconductive electron beam focusing system for improved performance ECM helix traveling wave tubes N91-14047
VIRGINIA POLYTECHNIC INST. AND STATE UNIV., BLACKSBURG.
New phases of D greater than or equal to 2 current and diffeomorphism algebras in particle physics
[DE91-001515] N91-14067
VIRGINIA UNIV., CHARLOTTESVILLE.
Radiative thermal conduction fronts N91-14162
ISM stripping from cluster galaxies and inhomogeneities in cooling flows N91-14172
Aspects of the interstellar medium in starburst galaxies N91-14209

W

WASHINGTON STATE UNIV., PULLMAN.
The effect of suspended particles on Jean's criterion for gravitational instability N91-14189
WASHINGTON UNIV., SAINT LOUIS, MO.
Non-empirical interatomic potentials for transition metals, alloys, and semiconductors
[DE91-002396] N91-14062
WASHINGTON UNIV., SEATTLE.
A study of the ice-hail charge separation mechanism using a thunderstorm electrification model with explicit microphysics in a kinematic framework N91-13835
Status of lattice field theory calculations
[DE91-001141] N91-14057
Optical and near-IR study of LMC HII region N11AB N91-14155
HII regions in dwarf irregular galaxies of the local group N91-14156
Starburst outflows from nearby galaxies N91-14219
WAYNE STATE UNIV., DETROIT, MI.
Analysis of the leading edge effects on the boundary layer transition
[NASA-CR-187361] N91-13405
WESTINGHOUSE IDAHO NUCLEAR CO., INC., IDAHO FALLS.
Improved plug valve computer-aided design of plug element
[DE91-001044] N91-13719
WESTINGHOUSE SAVANNAH RIVER CO., AIKEN, SC.
The effect of longitudinal spacer ribs on the minimum pressure drop in a heated annulus
[DE91-000784] N91-13655
Mechanical properties of 1950's vintage Type 304 stainless steel weldment components
[DE91-004328] N91-13774
Database management system for instrument data management
[DE91-004300] N91-14084
WISCONSIN UNIV., MADISON.
Development and initial characterization of a nuclear magnetic resonance dosimetry system
[DE91-001775] N91-13867
CO aperture synthesis of NGC 4038/9 (ARP 244) N91-14123
WISCONSIN UNIV., MILWAUKEE.
Hearing in three dimensions: Sound localization
[NASA-CR-187706] N91-13971
WOLVERTON ENVIRONMENTAL SERVICES, PICAYUNE, MS.
Plants and their microbial assistants: Nature's answer to Earth's environmental pollution problems N91-13851
WORCESTER POLYTECHNIC INST., MA.
Feasibility study, software design, layout and simulation of a two-dimensional fast Fourier transform machine for use in optical array interferometry
[NASA-CR-186922] N91-13885
WYOMING UNIV., LARAMIE.
Peering beyond IRAS: The 100 to 350 micron dust emission from galaxies N91-14141
One-dimensional cloud fluid model for propagating star formation N91-14211

Y

YERKES OBSERVATORY, WILLIAMS BAY, WI.
Contribution of cool dust to the FIR brightness distribution of NGC 6946 Sc(s)2 N91-14134
YORK UNIV., TORONTO (ONTARIO).
Ar/S N91-14153
Polarization in the Lagoon nebula N91-14193
Small-scale star formation at low metallicity N91-14214

Typical Contract Number Index Listing

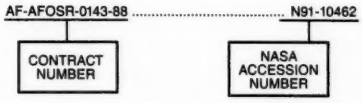

Listings in this index are arranged alphanumerically by contract number. Under each contract number the NASA accession numbers denoting documents that have been produced as a result of research done under that contract are arranged in ascending order. The NASA accession number denotes the number by which the citation is identified.

AF PROJ. 2303 ..... N91-13552
AF PROJ. 2420 ..... N91-13524
AF PROJ. 3005 ..... N91-13696
AF PROJ. 3484 ..... N91-13869
AF PROJ. 4600 ..... N91-14052
AF PROJ. 5581 ..... N91-13612
AF PROJ. 7757 ..... N91-13864
ARPA ORDER 4395 ..... N91-13588
A80/KL/138 ..... N91-13605
A81/KM/126 ..... N91-13468
N91-13872
A84/KM/080 ..... N91-13450
A86/K/012 ..... N91-13607
A87/D/149 ..... N91-14003
A87/KL/072 ..... N91-13892
A87/KL/116 ..... N91-13606
A88/KLU/631 ..... N91-13636
A88/M/318 ..... N91-13873
A89/K/602 ..... N91-13747
N91-13748
A89/KL/606 ..... N91-13871
A89/KLU/654 ..... N91-13838
B87-63 ..... N91-13881
B89-10 ..... N91-13608
CETIM-86-3636 ..... N91-13741
CETIM-88-1352-A N91-13740
CETIM-88-1352-B N91-13739
CETIM-89-9003 ..... N91-13532
CW-0001-85 ..... N91-14115
DA PROJ. 1L1-62211-A-47-A N91-13406
DA PROJ. 1L1-62211-A-47-AB N91-13462
DAAJ02-88-C-0022 ..... N91-13444
DARPA ORDER 4395 ..... N91-13599
DASG60-89-C-0142 ..... N91-13429
N91-13430
DE-AC02-76CH-00016 ..... N91-13746
N91-13811
N91-13814
N91-13859
N91-13866
DE-AC02-76CH-03073 ..... N91-14017
DE-AC02-78ER-05007 ..... N91-14250
DE-AC02-83CH-10093 ..... N91-13414
N91-13792
N91-13809
DE-AC02-89ER-80807 ..... N91-13794
DE-AC03-76SF-00098 ..... N91-13978
N91-13982
N91-14060
N91-14068
N91-14073
DE-AC03-87DP-10560 ..... N91-14026
DE-AC03-89ER-51114 ..... N91-13705
N91-13706
N91-14022
N91-14023
N91-14024
N91-14025
DE-AC04-76DP-00789 ..... N91-13413
N91-13419
N91-13521
N91-13617
N91-13625
N91-13736
N91-13745
N91-13773
N91-13793
N91-13795
N91-13800
N91-13806
N91-13946
N91-13977
N91-13980
N91-13990
N91-14056
DE-AC05-84OR-21400 ..... N91-13498
N91-13517
N91-13555
N91-13556
N91-13572
N91-13574
N91-13578
N91-13618
N91-13681
N91-13718
N91-13763
N91-13810
N91-13812
N91-13813
N91-13858
N91-13931
N91-13946
N91-13955
N91-13959
N91-14012
N91-14017
N91-14018
N91-14019
N91-14061
N91-14072
N91-14082
DE-AC05-84OT-21400 ..... N91-13577
DE-AC07-76ID-01570 ..... N91-13661
N91-13670
N91-13703
N91-13744
N91-13798
N91-13799
N91-13826
N91-13880
N91-13909
N91-13912
N91-13932
N91-13970
N91-13986
N91-13987
N91-13994
N91-14013
DE-AC07-84ID-12435 ..... N91-13719
DE-AC07-84ID-12536 ..... N91-13497
DE-AC09-89SR-18035 ..... N91-13655
N91-13774
N91-14084
DE-AC34-90DP-62349 ..... N91-13727
N91-13757
DE-AI01-85CE-50112 ..... N91-13804
DE-AS05-76ER-03956 ..... N91-13979
DE-AS05-80ER-10713 ..... N91-14067
DE-AS05-81ER-40039 ..... N91-13989
DE-AS06-88ER-40423 ..... N91-14057
DE-FG02-84ER-45130 ..... N91-14062
DE-FG02-84ER-45167 ..... N91-13563
DE-FG02-85ER-13433 ..... N91-13576
DE-FG02-85ER-40211 ..... N91-14071
DE-FG02-85ER-45217 ..... N91-13565
DE-FG02-85ER-53208 ..... N91-14020
DE-FG02-86ER-13579 ..... N91-14058
DE-FG02-86ER-13582 ..... N91-13509
DE-FG02-86ER-25021 ..... N91-13958
DE-FG02-86ER-45267 ..... N91-13973
DE-FG02-86ER-53223 ..... N91-14006
DE-FG02-86ER-60417 ..... N91-13867
DE-FG02-86NE-37966 ..... N91-13722
DE-FG02-87ER-13649 ..... N91-13671
DE-FG02-87ER-13769 ..... N91-13654
DE-FG02-88ER-13822 ..... N91-13519
DE-FG02-89ER-14017 ..... N91-14064
DE-FG02-90ER-80861 ..... N91-13794
DE-FG03-85ER-13360 ..... N91-13659
DE-FG03-88ER-13910 ..... N91-13510
DFG-DE-385/1-1 ..... N91-14187
DFG-DE-385/2-1 ..... N91-14187
DNA001-C-0320 ..... N91-13645
DTFA01-89-Z-02029 ..... N91-13464
EEC-RI1B-0094-UK(H) N91-13917
EPA-R-813277 ..... N91-13814
ESA-4791/81/NL/DK(SC) N91-13897
FMV-82223-72-004 ..... N91-13416
FMV-82250-89-156-73-001 ..... N91-13448
F08635-86-K-0139 ..... N91-13992
F08635-89-C-0297 ..... N91-13712
F19628-84-C-0008 ..... N91-14052
F19628-88-K-0025 ..... N91-13613
F19628-90-C-0002 ..... N91-13475
F30602-87-D-0086 ..... N91-13901
F30602-88-D-0026 ..... N91-13612
F30602-88-D-0027 ..... N91-13589
N91-13614
F33615-85-C-5167 ..... N91-13524
F33615-86-C-3216 ..... N91-13477
N91-13478
F33615-87-C-0607 ..... N91-13864
F33615-88-C-5423 ..... N91-14041
F49620-86-C-0131 ..... N91-13869
F49620-86-K-0016 ..... N91-13496
F49620-87-C-0016 ..... N91-14054
F49620-87-C-0078 ..... N91-13479
F49620-88-C-0046 ..... N91-13696
F49620-88-C-0122 ..... N91-13552
F62400-90-0034 ..... N91-13720
GA PROJ. 3466 ..... N91-13705
N91-13706
N91-14022
N91-14023
N91-14024
N91-14025
GRI-5086-260-1404 ..... N91-13507
NAGW-91 ..... N91-14190
NAGW-674 ..... N91-13651
NAGW-766 ..... N91-14180
NAGW-0097 ..... N91-13841
NAGW-1009 ..... N91-14211
NAGW-1077 ..... N91-14254
NAGW-1231 ..... N91-13807
NAGW-1330 ..... N91-13470
NAGW-1340 ..... N91-13976
NAGW-1401 ..... N91-13484
NAGW-1937 ..... N91-14254
NAGW-2158 ..... N91-13782
NAG1-190 ..... N91-13930
NAG1-460 ..... N91-13405
NAG1-513 ..... N91-13452
NAG1-529 ..... N91-13768
NAG1-657 ..... N91-13413
N91-13640
NAG1-659 ..... N91-13756
NAG1-702 ..... N91-14097
NAG1-730 ..... N91-13750
NAG1-756 ..... N91-13480
N91-13759
N91-13760
NAG1-935 ..... N91-13833
NAG1-959 ..... N91-13404
NAG1-972 ..... N91-14055
NAG1-983 ..... N91-13904
NAG1-991 ..... N91-13446
NAG1-1027 ..... N91-13449
NAG1-1063 ..... N91-13494
NAG1-1122 ..... N91-13656
NAG1-1133 ..... N91-13676
NAG2-134 ..... N91-14141
NAG2-221 ..... N91-13875
NAG2-444 ..... N91-13515
NAG2-513 ..... N91-13949
N91-13950
NAG2-515 ..... N91-13584
NAG2-528 ..... N91-14090

NAG2-541 ..... N91-13893
NAG2-588 ..... N91-13422
NAG2-593 ..... N91-13928
NAG3-349 ..... N91-13458
NAG3-608 ..... N91-13443
NAG3-696 ..... N91-14050
NAG3-773 ..... N91-13737
NAG3-888 ..... N91-13557
NAG3-899 ..... N91-13645
NAG3-972 ..... N91-13609
NAG5-255 ..... N91-14115
NAG5-286 ..... N91-14115
NAG5-616 ..... N91-14225
NAG5-852 ..... N91-13817
NAG5-955 ..... N91-13677
NAG5-1070 ..... N91-13818
NAG5-1115 ..... N91-13819
N91-13831
NAG5-1138 ..... N91-13885
NAG5-1157 ..... N91-14089
NAG5-1366 ..... N91-14088
NAG8-597 ..... N91-13648
NAG8-717 ..... N91-13939
NAG8-790 ..... N91-13967
NAG8-824 ..... N91-14029
NAG9-340 ..... N91-13895
NAG9-360 ..... N91-13721
N91-13722
NAG9-361 ..... N91-13725
NAG9-369 ..... N91-13894
NAG9-474 ..... N91-14256
NASW-4066 ..... N91-14098
N91-14099
N91-14252
NAS1-18279 ..... N91-13463
NAS1-18347 ..... N91-13991
NAS1-18378 ..... N91-13447
NAS1-18565 ..... N91-13934
NAS1-18605 ..... N91-13410
N91-13642
N91-13649
N91-13650
N91-13669
N91-13935
N91-13952
N91-13966
NAS1-19038 ..... N91-13907
NAS2-11420 ..... N91-13972
NAS2-12393 ..... N91-13424
NAS3-22902 ..... N91-13486
N91-13487
NAS3-23791 ..... N91-13485
NAS3-25266 ..... N91-13421
N91-13804
N91-14050
NAS5-28067 ..... N91-13788
NAS5-29293 ..... N91-14228
NAS7-918 ..... N91-13476
N91-13581
N91-13594
N91-13595
N91-13596
N91-13621
N91-13622
N91-13658
N91-13679
N91-13724
N91-13767
N91-13787
N91-13796
N91-13876
N91-13888
N91-13995
N91-13998
N91-14049
NAS8-30490 ..... N91-13569
N91-13570
N91-13675
NAS8-32488 ..... N91-13807
NAS8-32902 ..... N91-14149
N91-14240
NAS8-36552 ..... N91-13489
NAS8-37284 ..... N91-13832
NAS8-37743 ..... N91-13474
NAS8-37752 ..... N91-13688
NAS8-37814 ..... N91-13856
NCA2-279 ..... N91-14138
NCC1-25 ..... N91-13837
NCC2-374 ..... N91-13510
N91-13644
N91-13645
NCC2-478 ..... N91-13506
NCC2-542 ..... N91-13971
NCC2-562 ..... N91-13639
NCC2-577 ..... N91-14255
NCC2-603 ..... N91-13929
NCC2-678 ..... N91-13554
NCC3-89 ..... N91-13534
N91-13535
NCC9-16 ..... N91-13906
NIEHS-ES0156611 ..... N91-13859
NIH-CA-38645 ..... N91-13859
NIH-ES-00138 ..... N91-13859
NIH-H-08945 ..... N91-13859
NIH-HD-17047 ..... N91-13859
NIH-HD-18655 ..... N91-13859
NIH-HD-20381 ..... N91-13859
NIH-P01-NS-12732 ..... N91-13971
NIH-RR-01838 ..... N91-13859
NR PROJ. RR0-4206 ..... N91-13951
NSF AST-86-02698 ..... N91-14142
NSF AST-86-13257 ..... N91-14154
NSF AST-86-15177 ..... N91-14186
NSF AST-87-14721 ..... N91-14220
NSF AST-87-15905 ..... N91-14194
N91-14205
NSF AST-87-17867 ..... N91-14212
NSF AST-88-18606 ..... N91-14223
NSF AST-88-18900 ..... N91-14240
NSF AST-89-15258 ..... N91-14088
NSF ATM-25-06632 ..... N91-14190
NSF CCR-90-00000 ..... N91-13933
NSF DMS-87-17799 ..... N91-13953
NSF DMS-89-04740 ..... N91-13950
NSF DMS-89-14420 ..... N91-13962
NSF DMS-89-23071 ..... N91-13953
NSF PHY-85-15857 ..... N91-14068
NSF R11-87-22796 ..... N91-14190
NSG-1498 ..... N91-13428
NSG-5074 ..... N91-13674
N00014-84-C-0261 ..... N91-14051
N00014-84-K-0021 ..... N91-13508
N00014-86-K-0545 ..... N91-13513
N00014-86-K-0677 ..... N91-13590
N00014-86-K-0691 ..... N91-13642
N00014-88-K-0170 ..... N91-13953
N00014-88-K-2021 ..... N91-14020
N00014-89-J-1314 ..... N91-13550
N00014-89-J-1542 ..... N91-13551
N00014-89-J-1681 ..... N91-13951
N00014-89-J-1836 ..... N91-13969
N00014-90-J-1148 ..... N91-13553
N00014-90-J-1281 ..... N91-13514
N00014-90-K-2018 ..... N91-13993
N00123-89-G-0580 ..... N91-13647
N91-13713
N91-13714
N91-13715
N00167-90-WR-00300 ..... N91-13758
N66001-87-D-0179 ..... N91-13903
R87/KL/097 ..... N91-13925
R87/KM/123 ..... N91-13789
STEV-506-266-4 ..... N91-13801
SWRI PROJ. 05-2881 ..... N91-13895
SWRI PROJ. 05-2921 ..... N91-13894
SWRI PROJ. 06-1778-001 ..... N91-13534
SWRI PROJ. 06-1778-002 ..... N91-13535
SWRI PROJ. 15-4865-009 ..... N91-13807
T0704E N91-13900
W-31-109-ENG-38 ..... N91-13913
N91-13933
N91-13942
N91-13983
N91-14028
W-7405-ENG-36 ..... N91-13490
N91-13573
N91-13582
N91-13597
N91-13620
N91-13624
N91-13626
N91-13631
N91-13662
N91-13682
N91-13700
N91-13701
N91-13702
N91-13720
N91-13743
N91-13764
N91-13957
N91-13988
N91-14008
N91-14009
N91-14010
N91-14011
N91-14014
N91-14015
N91-14069
N91-14070
N91-14258
N91-14264
N91-14270
W-7405-ENG-48 ..... N91-13499
N91-13501
N91-13520
N91-13593
N91-13599
N91-13619
N91-13623
N91-13680
N91-13689
N91-13690
N91-13697
N91-13698
N91-13699
N91-13704
N91-13707
N91-13709
N91-13726
N91-13765
N91-13780
N91-13815
N91-13908
N91-13914
N91-13915
N91-13943
N91-13945
N91-13956
N91-13962
N91-13978
N91-13981
N91-14004
N91-14007
N91-14016
N91-14020
N91-14021
N91-14063
N91-14269
W-7405-ENG-82 ..... N91-13516
N91-13518
N91-13525
N91-13526
N91-14059
188-44-53 ..... N91-14100
199-04-16-11 ..... N91-13985
199-18-12-07 ..... N91-13862
307-51-10 ..... N91-13941
323-51-43-05-00 ..... N91-14049
324-02-00-01 ..... N91-13463
326-22-20-50 ..... N91-14265
326-23-30-01 ..... N91-14251
326-81-10 ..... N91-14259
412-20-26-01 ..... N91-13492
476-30-70-08 ..... N91-13476
505-43-11 ..... N91-14050
505-60-11 ..... N91-13652
N91-13653
505-61-21-03 ..... N91-13461
505-61-51-10 ..... N91-13406
505-61-71 ..... N91-13408
N91-13466
505-61-71-01 ..... N91-13401
505-61-71-07 ..... N91-13907
505-62-21 ..... N91-13420
505-62-40-02 ..... N91-13651
505-62-41 ..... N91-13455
505-62-41-05 ..... N91-13402
505-62-71 ..... N91-13457
505-63-01-05 ..... N91-13761
505-63-01-11 ..... N91-13750
N91-13751
505-63-10-02 ..... N91-13445
505-63-21 ..... N91-13400
505-63-21-02 ..... N91-13412
505-63-50-13 ..... N91-13411
505-63-51 ..... N91-13737
505-63-51-03 ..... N91-13462
505-63-113 ..... N91-13456
505-66-91-01 ..... N91-13585
505-68-11 ..... N91-13421
505-68-91-01 ..... N91-13467
505-69-01-02 ..... N91-13432
N91-13433
505-90-01 ..... N91-13638
505-90-21-01 ..... N91-13410
N91-13642
N91-13649
N91-13650
N91-13669
N91-13935
N91-13952
N91-13966
506-42-00 ..... N91-13491
506-43-11-03 ..... N91-13991
506-43-31 ..... N91-13972
506-43-41-02 ..... N91-13473
506-43-71-01 ..... N91-13522

506-45-31 ..... N91-14087
506-46-21-05 ..... N91-13930
506-48-41 ..... N91-13688
510-01-50 ..... N91-13495
533-02-00 ..... N91-13460
533-02-01 ..... N91-13453
535-05-10 ..... N91-13458
537-01-31-01 ..... N91-13447
549-03-31-03 ..... N91-13934
778-35-13 ..... N91-13804
992-21-01 ..... N91-13762

Typical Report Number Index Listing

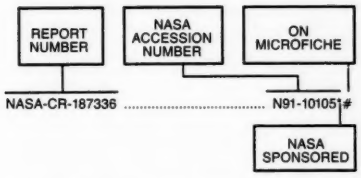

Listings in this index are arranged alphanumerically by report number. The NASA accession number denotes the number by which the citation is identified. An asterisk (*) indicates that the item is a NASA report. A pound sign (#) indicates that the item is available on microfiche.

A-90003 ..... N91-13862* #
A-90014 ..... N91-13762* #
A-90053 ..... N91-14087* #
A-90075 ..... N91-14100* #
A-90123 ..... N91-13466* #
A-90172 ..... N91-13652* #
A-90207 ..... N91-13653* #
A-90258 ..... N91-13408* #

AD-A222816 ..... N91-13469 #
AD-A223355 ..... N91-14266 #
AD-A224740 ..... N91-13951 #
AD-A225124 ..... N91-13429 #
AD-A225125 ..... N91-13430 #
AD-A225392 ..... N91-13454 #
AD-A225408 ..... N91-13938 #
AD-A225641 ..... N91-13992 #
AD-A225702 ..... N91-13611 #
AD-A225730 ..... N91-13550 #
AD-A225864 ..... N91-13508 #
AD-A225987 ..... N91-13551 #
AD-A226179 ..... N91-13475 #
AD-A226415 ..... N91-13571 #
AD-A226431 ..... N91-13612 #
AD-A226443 ..... N91-13588 #
AD-A226481 ..... N91-13646 #
AD-A226486 ..... N91-13940 #
AD-A226499 ..... N91-13523 #
AD-A226503 ..... N91-14079* #
AD-A226508 ..... N91-13712 #
AD-A226518 ..... N91-13877 #
AD-A226520 ..... N91-13444 #
AD-A226522 ..... N91-13901 #
AD-A226524 ..... N91-13993 #
AD-A226525 ..... N91-13477 #
AD-A226526 ..... N91-13478 #
AD-A226532 ..... N91-14080 #
AD-A226534 ..... N91-13613 #
AD-A226535 ..... N91-13614 #
AD-A226536 ..... N91-13589 #
AD-A226537 ..... N91-14005 #
AD-A226540 ..... N91-13864 #
AD-A226548 ..... N91-14051 #
AD-A226552 ..... N91-13512 #
AD-A226556 ..... N91-13758 #
AD-A226559 ..... N91-13969 #
AD-A226580 ..... N91-13902 #
AD-A226592 ..... N91-13903 #
AD-A226593 ..... N91-14052 #
AD-A226595 ..... N91-13953 #
AD-A226609 ..... N91-13590 #
AD-A226625 ..... N91-13513 #
AD-A226627 ..... N91-13524 #
AD-A226629 ..... N91-13409 #
AD-A226630 ..... N91-13696 #
AD-A226639 ..... N91-13514 #
AD-A226640 ..... N91-13713 #
AD-A226646 ..... N91-13552 #
AD-A226648 ..... N91-13878 #
AD-A226649 ..... N91-13714 #
AD-A226650 ..... N91-13647 #
AD-A226651 ..... N91-13715 #
AD-A226653 ..... N91-13591 #
AD-A226661 ..... N91-13592 #
AD-A226664 ..... N91-14053* #
AD-A226668 ..... N91-13869 #
AD-A226669 ..... N91-14054 #
AD-A226671 ..... N91-13496 #
AD-A226674 ..... N91-13553 #
AD-A226679 ..... N91-13479 #
AD-A226682 ..... N91-13870 #

AD-D014605 ..... N91-13711 #
AD-D014615 ..... N91-13886 #
AD-D014625 ..... N91-13887
AD-D014640 ..... N91-13716 #

AERONOMICA-ACTA-A-355-1990 ..... N91-13816

AFATL-TR-90-63 ..... N91-13992 #

AFHRL-TP-90-64 ..... N91-13878 #

AFOSR-90-0861TR ..... N91-13696 #
AFOSR-90-0916TR ..... N91-14054 #
AFOSR-90-0918TR ..... N91-13869 #
AFOSR-90-0919TR ..... N91-13479 #
AFOSR-90-0922TR ..... N91-13496 #
AFOSR-90-1025TR ..... N91-13552 #

AGARD-AG-235-ADD ..... N91-14076 #
AGARD-AG-316 ..... N91-13488 #

AGARD-AR-297 ..... N91-13863 #

AGARD-CP-481 ..... N91-14030 #

AGARD-LS-173 ..... N91-13434 #

AGARD-WG-13 ..... N91-13863 #

AIAA-91-0043 ..... N91-13420* #
AIAA-91-0661 ..... N91-13421* #
AIAA-91-0692 ..... N91-13455* #

ANL-90/30 ..... N91-13942 #

ANL/MCS-TM-140 ..... N91-13913 #

ANL/TM-484 ..... N91-13933 #

AR-0142-90-001-VOL-2 ..... N91-13429 #
AR-0142-90-001-VOL-3 ..... N91-13430 #

ARE-TR-88503 ..... N91-13667 #

AVSCOM-TR-90-B-007 ..... N91-13462* #
AVSCOM-TR-90-B-010 ..... N91-13406* #
AVSCOM-TR-90-C-020 ..... N91-13737* #

BCRS-89-39 ..... N91-13785 #

BHT-699-099-319-VOL-1 ..... N91-13444 #

BN-1120 ..... N91-13837* #

BNL-NUREG-45309 ..... N91-13746 #

BNL-44441 ..... N91-13814 #
BNL-44730 ..... N91-13859 #
BNL-44858 ..... N91-13866 #
BNL-45216 ..... N91-13811 #

BRL-TR-3110 ..... N91-14266 #
BRL-TR-3131 ..... N91-13877 #
BRL-TR-3139 ..... N91-13571 #

BR114106 ..... N91-13451 #
BR114552 ..... N91-14085 #
BR114645 ..... N91-13829 #
BR114653 ..... N91-13472 #
BR114657 ..... N91-13505 #
BR114792 ..... N91-13667 #
BR114794 ..... N91-13882 #
BR114930 ..... N91-13777 #

CETIM-13N061 ..... N91-13742 #
CETIM-101130 ..... N91-13504 #
CETIM-101580 ..... N91-13583 #
CETIM-104430 ..... N91-13741 #
CETIM-104700 ..... N91-13738 #
CETIM-104720 ..... N91-13739 #
CETIM-104730 ..... N91-13740 #
CETIM-104850 ..... N91-13532 #
CETIM-105070 ..... N91-13917 #
CETIM-106470 ..... N91-13533 #
CETIM-107270 ..... N91-13749 #
CETIM-108220 ..... N91-13775 #
CETIM-108830 ..... N91-13776 #

CHAM-2008/3-A-VOL-2 ..... N91-13489* #

CMC-5485-90-1 ..... N91-13496 #

CONF-890870-2 ..... N91-13994 #
CONF-891103-77 ..... N91-13744 #
CONF-891103-78 ..... N91-13986 #
CONF-891159-5 ..... N91-13909 #
CONF-900343-7 ..... N91-13932 #
CONF-900466-91 ..... N91-13670 #
CONF-900505-10 ..... N91-14028 #
CONF-900520-1 ..... N91-13826 #
CONF-900520-1 ..... N91-14013 #
CONF-900557-23 ..... N91-14023 #
CONF-900557-24 ..... N91-14024 #
CONF-900557-25 ..... N91-14025 #
CONF-900557-26 ..... N91-14021 #
CONF-900557-29 ..... N91-13705 #
CONF-900557-31 ..... N91-13706 #
CONF-900557-32 ..... N91-14022 #
CONF-900608-51 ..... N91-13946 #
CONF-900617-18 ..... N91-13774 #
CONF-900791-3 ..... N91-13743 #
CONF-900791-7 ..... N91-13970 #
CONF-900877-9 ..... N91-13980 #
CONF-900917-24 ..... N91-13987 #
CONF-900923-3 ..... N91-13981 #
CONF-900936-11 ..... N91-13977 #
CONF-900936-17 ..... N91-14061 #
CONF-900960-1 ..... N91-13815 #
CONF-900971-1 ..... N91-13499 #
CONF-901007-6 ..... N91-14004 #
CONF-901007-23 ..... N91-14017 #
CONF-901007-24 ..... N91-14018 #
CONF-901007-25 ..... N91-14019 #
CONF-901025-15 ..... N91-13699 #
CONF-901029-1 ..... N91-13578 #
CONF-901029-2 ..... N91-13582 #
CONF-901057-4 ..... N91-14258 #
CONF-901101-43 ..... N91-13625 #
CONF-901105-18 ..... N91-13700 #
CONF-901106-2-EXTD-ABST ..... N91-13794 #
CONF-901116-22 ..... N91-13520 #
CONF-901116-23 ..... N91-13945 #
CONF-901120-1 ..... N91-13521 #
CONF-901155-1 ..... N91-13956 #
CONF-901194-4 ..... N91-13655 #
CONF-901194-6 ..... N91-13799 #
CONF-901244-1 ..... N91-14056 #
CONF-910102-1 ..... N91-13745 #
CONF-910104-1 ..... N91-13736 #
CONF-910116-1 ..... N91-13806 #
CONF-910116-2 ..... N91-13866 #
CONF-910116-4 ..... N91-13490 #
CONF-910116-7 ..... N91-13990 #
CONF-910117-2 ..... N91-13419 #
CONF-910120-1 ..... N91-13773 #
CONF-8907226-1 ..... N91-14070 #
CONF-8908254 ..... N91-13810 #
CONF-8909106-1 ..... N91-13661 #
CONF-8911151-3 ..... N91-13809 #
CONF-9002128-3 ..... N91-13982 #
CONF-9003221-1 ..... N91-14057 #
CONF-9003224-1 ..... N91-13698 #
CONF-9005237-7 ..... N91-13957 #
CONF-9005286-1 ..... N91-13765 #
CONF-9006134-2 ..... N91-13813 #

CONF-9006228-4 ..... N91-13599 #
CONF-9006277-1 ..... N91-13517 #
CONF-9006286-1 ..... N91-13573 #
CONF-9006288-1 ..... N91-14069 #
CONF-9007101-1 ..... N91-14269 #
CONF-9007101-2 ..... N91-14270 #
CONF-9007131-3 ..... N91-13978 #
CONF-9007134 ..... N91-13943 #
CONF-9007136-5 ..... N91-14007 #
CONF-9007181-1 ..... N91-14067 #
CONF-9008139-3 ..... N91-13800 #
CONF-9008162-1 ..... N91-13814 #
CONF-9008164-1 ..... N91-14264 #
CONF-9009107-4 ..... N91-13414 #
CONF-9009123-40 ..... N91-13619 #
CONF-9009123-43 ..... N91-13701 #
CONF-9009123-46 ..... N91-13988 #
CONF-9009123-47 ..... N91-13626 #
CONF-9009153-3 ..... N91-13880 #
CONF-9009166-9 ..... N91-13631 #
CONF-9009166-10 ..... N91-13702 #
CONF-9009235-2 ..... N91-13859 #
CONF-9009235-3 ..... N91-13690 #
CONF-9009248-3 ..... N91-13703 #
CONF-9009267-2 ..... N91-13983 #
CONF-9009269-3 ..... N91-13915 #
CONF-9009278-1 ..... N91-13858 #
CONF-9009283-1 ..... N91-14012 #
CONF-9010105-1 ..... N91-13624 #
CONF-9010146-1 ..... N91-13707 #
CONF-9010185-2 ..... N91-13763 #
CONF-9010185-10 ..... N91-13746 #
CONF-9010205-1 ..... N91-13955 #
CONF-9010205-2 ..... N91-13572 #
CONF-9010209-4 ..... N91-14008 #
CONF-9010212-3 ..... N91-13618 #
CONF-9010212-9 ..... N91-13682 #
CONF-9010220-2 ..... N91-13620 #
CONF-9010223-1 ..... N91-13413* #
CONF-9010226-1 ..... N91-14060 #
CONF-9010230-2 ..... N91-14014 #
CONF-9010230-3 ..... N91-14015 #
CONF-9010230-5 ..... N91-14010 #
CONF-9010230-6 ..... N91-14009 #
CONF-9010230-7 ..... N91-14011 #
CONF-9010239-1 ..... N91-13912 #
CONF-9010256-1 ..... N91-14084 #
CONF-9011115-2 ..... N91-13623 #
CONF-9011118-1 ..... N91-13793 #
CONF-9011118-2 ..... N91-13795 #
CONF-9011119-1-DRAFT ..... N91-13617 #
CONF-9011122-1 ..... N91-13498 #
CONF-9011125-3 ..... N91-14063 #

CRREL-90-6 ..... N91-13465 #

CSR-89-3 ..... N91-13470* #

CU-CSSC-90-17 ..... N91-13480* #
CU-CSSC-90-26 ..... N91-13759* #
CU-CSSC-90-27 ..... N91-13760* #

DE89-009504 ..... N91-13809 #
DE90-000378 ..... N91-13792 #
DE90-003539 ..... N91-13797 #
DE90-008417 ..... N91-13563 #
DE90-009278 ..... N91-14081 #
DE90-009686 ..... N91-13805 #
DE90-012756 ..... N91-13419 #
DE90-013806 ..... N91-13806 #
DE90-014935 ..... N91-13659 #
DE90-015681 ..... N91-13866 #
DE90-015841 ..... N91-13773 #
DE90-017034 ..... N91-13745 #
DE90-017250 ..... N91-13497 #
DE91-000066 ..... N91-13680 #
DE91-000262 ..... N91-13654 #
DE91-000263 ..... N91-13509 #
DE91-000401 ..... N91-14056 #
DE91-000439 ..... N91-13743 #
DE91-000503 ..... N91-13757 #
DE91-000516 ..... N91-13555 #
DE91-000543 ..... N91-13718 #
DE91-000599 ..... N91-13576 #
DE91-000610 ..... N91-13516 #
DE91-000612 ..... N91-13517 #
DE91-000664 ..... N91-13518 #
DE91-000729 ..... N91-13955 #
DE91-000740 ..... N91-13525 #
DE91-000741 ..... N91-13526 #
DE91-000763 ..... N91-13977 #
DE91-000784 ..... N91-13655 #
DE91-000792 ..... N91-14004 #
DE91-000810 ..... N91-13978 #
DE91-000941 ..... N91-13660 #
DE91-000966 ..... N91-13617 #

DE91-001018 ..... N91-13810 #
DE91-001043 ..... N91-13779 #
DE91-001044 ..... N91-13719 #
DE91-001056 ..... N91-13709 #
DE91-001057 ..... N91-13780 #
DE91-001058 ..... N91-13931 #
DE91-001083 ..... N91-13501 #
DE91-001084 ..... N91-13726 #
DE91-001087 ..... N91-13577 #
DE91-001096 ..... N91-13942 #
DE91-001120 ..... N91-13811 #
DE91-001141 ..... N91-14057 #
DE91-001220 ..... N91-13979 #
DE91-001227 ..... N91-13980 #
DE91-001231 ..... N91-13413* #
DE91-001253 ..... N91-14058 #
DE91-001260 ..... N91-13793 #
DE91-001341 ..... N91-13736 #
DE91-001361 ..... N91-14006 #
DE91-001486 ..... N91-13618 #
DE91-001489 ..... N91-13858 #
DE91-001492 ..... N91-13813 #
DE91-001493 ..... N91-13763 #
DE91-001515 ..... N91-14067 #
DE91-001520 ..... N91-13578 #
DE91-001526 ..... N91-13556 #
DE91-001597 ..... N91-14059 #
DE91-001617 ..... N91-13572 #
DE91-001618 ..... N91-13720 #
DE91-001625 ..... N91-13498 #
DE91-001639 ..... N91-13989 #
DE91-001674 ..... N91-13519 #
DE91-001678 ..... N91-13599 #
DE91-001679 ..... N91-13499 #
DE91-001684 ..... N91-13697 #
DE91-001685 ..... N91-13698 #
DE91-001713 ..... N91-13794 #
DE91-001717 ..... N91-13764 #
DE91-001722 ..... N91-13814 #
DE91-001729 ..... N91-13859 #
DE91-001732 ..... N91-14082 #
DE91-001733 ..... N91-13681 #
DE91-001741 ..... N91-13765 #
DE91-001742 ..... N91-14007 #
DE91-001745 ..... N91-14269 #
DE91-001746 ..... N91-13699 #
DE91-001747 ..... N91-13619 #
DE91-001748 ..... N91-13956 #
DE91-001749 ..... N91-13981 #
DE91-001754 ..... N91-13795 #
DE91-001755 ..... N91-13943 #
DE91-001758 ..... N91-13520 #
DE91-001759 ..... N91-13945 #
DE91-001760 ..... N91-13593 #
DE91-001762 ..... N91-13908 #
DE91-001763 ..... N91-13623 #
DE91-001766 ..... N91-13689 #
DE91-001775 ..... N91-13867 #
DE91-001792 ..... N91-14068 #
DE91-001797 ..... N91-13982 #
DE91-001798 ..... N91-14060 #
DE91-001804 ..... N91-14069 #
DE91-001815 ..... N91-13798 #
DE91-001818 ..... N91-13799 #
DE91-001835 ..... N91-13909 #
DE91-001852 ..... N91-13957 #
DE91-001854 ..... N91-13700 #
DE91-001865 ..... N91-13701 #
DE91-001868 ..... N91-13958 #
DE91-001869 ..... N91-13986 #
DE91-001874 ..... N91-13631 #
DE91-001875 ..... N91-13702 #
DE91-001877 ..... N91-14258 #
DE91-001882 ..... N91-13703 #
DE91-001884 ..... N91-13912 #
DE91-001890 ..... N91-13994 #
DE91-001898 ..... N91-14009 #
DE91-001899 ..... N91-14010 #
DE91-001901 ..... N91-14011 #
DE91-001910 ..... N91-13987 #
DE91-001913 ..... N91-13880 #
DE91-001914 ..... N91-13970 #
DE91-001920 ..... N91-14012 #
DE91-001935 ..... N91-13826 #
DE91-001936 ..... N91-13670 #
DE91-001942 ..... N91-13932 #
DE91-001943 ..... N91-14013 #
DE91-001949 ..... N91-13744 #
DE91-001950 ..... N91-13624 #
DE91-001951 ..... N91-13620 #
DE91-001953 ..... N91-13682 #
DE91-001956 ..... N91-13490 #
DE91-001961 ..... N91-14014 #
DE91-001965 ..... N91-14008 #
DE91-001997 ..... N91-13661 #
DE91-002101 ..... N91-13414 #

DE91-002303 ..... N91-13573 #
DE91-002307 ..... N91-14264 #
DE91-002311 ..... N91-13582 #
DE91-002313 ..... N91-14070 #
DE91-002320 ..... N91-14270 #
DE91-002322 ..... N91-14015 #
DE91-002337 ..... N91-13625 #
DE91-002340 ..... N91-13800 #
DE91-002341 ..... N91-13521 #
DE91-002347 ..... N91-13988 #
DE91-002348 ..... N91-13626 #
DE91-002352 ..... N91-13812 #
DE91-002358 ..... N91-14061 #
DE91-002396 ..... N91-14062 #
DE91-002399 ..... N91-13662 #
DE91-002409 ..... N91-13913 #
DE91-002435 ..... N91-13597 #
DE91-002458 ..... N91-14071 #
DE91-002522 ..... N91-14072 #
DE91-002523 ..... N91-13959 #
DE91-002534 ..... N91-13727 #
DE91-002536 ..... N91-13574 #
DE91-002542 ..... N91-13704 #
DE91-002571 ..... N91-14016 #
DE91-002573 ..... N91-13914 #
DE91-002646 ..... N91-14017 #
DE91-002647 ..... N91-14018 #
DE91-002650 ..... N91-14019 #
DE91-002658 ..... N91-13946 #
DE91-002667 ..... N91-14020 #
DE91-002670 ..... N91-14021 #
DE91-002671 ..... N91-14063 #
DE91-002673 ..... N91-13690 #
DE91-002708 ..... N91-13705 #
DE91-002709 ..... N91-13706 #
DE91-002717 ..... N91-14022 #
DE91-002718 ..... N91-14023 #
DE91-002719 ..... N91-14024 #
DE91-002720 ..... N91-14025 #
DE91-002756 ..... N91-14064 #
DE91-002770 ..... N91-14026 #
DE91-002784 ..... N91-13707 #
DE91-002795 ..... N91-13915 #
DE91-002951 ..... N91-13815 #
DE91-002956 ..... N91-13933 #
DE91-004004 ..... N91-13746 #
DE91-004053 ..... N91-13565 #
DE91-004140 ..... N91-14073 #
DE91-004167 ..... N91-13973 #
DE91-004175 ..... N91-13962 #
DE91-004189 ..... N91-14250 #
DE91-004190 ..... N91-13671 #
DE91-004300 ..... N91-14084 #
DE91-004328 ..... N91-13774 #
DE91-004429 ..... N91-14028 #
DE91-004475 ..... N91-13983 #
DE91-004504 ..... N91-13990 #
DE91-715185 ..... N91-13579 #

DLR-FB-90-25 ..... N91-13827 #
DLR-FB-90-28 ..... N91-13415 #

DOE/DP-10560/8 ..... N91-14026 #

DOE/EIA-0174(88) ..... N91-13797 #

DOE/ER-0474T ..... N91-13779 #
DOE/ER-03956/9 ..... N91-13979 #
DOE/ER-05007/27 ..... N91-14250 #
DOE/ER-13360/T1 ..... N91-13659 #
DOE/ER-13433/T1 ..... N91-13576 #
DOE/ER-13579/22 ..... N91-14058 #
DOE/ER-13582/4 ..... N91-13509 #
DOE/ER-13649/4 ..... N91-13671 #
DOE/ER-13769/3 ..... N91-13654 #
DOE/ER-13822/T1 ..... N91-13519 #
DOE/ER-14017/2 ..... N91-14064 #
DOE/ER-25021/T1 ..... N91-13958 #
DOE/ER-40039/46 ..... N91-13989 #
DOE/ER-40211/6 ..... N91-14071 #
DOE/ER-40423/10-P90 ..... N91-14057 #
DOE/ER-45130/5 ..... N91-14062 #
DOE/ER-45167/1 ..... N91-13563 #
DOE/ER-45217/T1 ..... N91-13565 #
DOE/ER-45267/4 ..... N91-13973 #
DOE/ER-53223/148 ..... N91-14006 #
DOE/ER-60417/5 ..... N91-13867 #

DOE/ID-12536/2 ..... N91-13497 #

DOE/METC-90-0268 ..... N91-13805 #

DOE/NASA/5266-1 ..... N91-13804*

DOE/OSTI-4500-R75 ..... N91-13727 #
DOE/OSTI-4649 ..... N91-14081 #

DOE/PETC/TR-90/9 ..... N91-13660 #
DOT/FAA/CT-90/16 ..... N91-13900 #
DOT/FAA/RD-90/13 ..... N91-13465 #
DOT/FAA/RD-90/26 ..... N91-13464 #
DTRC-90/016 ..... N91-13646 #
DTRC/SME-90/54 ..... N91-13523 #
D6-53878 ..... N91-13424* #
E-5696 ..... N91-13638* #
E-5718 ..... N91-13737* #
E-5745 ..... N91-14050* #
E-5821 ..... N91-13455* #
E-5823 ..... N91-14259* #
E-5825 ..... N91-13495* #
E-5826 ..... N91-13491* #
E-5840 ..... N91-13456* #
E-5901 ..... N91-13457* #
E-5908 ..... N91-13420* #
E-5930 ..... N91-13421* #
ECL-90-18 ..... N91-13630 #
ECL-90-016 ..... N91-13664 #
EGG-EP-8800 ..... N91-13798 #
EGG-M-89164 ..... N91-13909 #
EGG-M-89226 ..... N91-13661 #
EGG-M-89227 ..... N91-13994 #
EGG-M-89285 ..... N91-13744 #
EGG-M-89286 ..... N91-13986 #
EGG-M-89448 ..... N91-13932 #
EGG-M-89487 ..... N91-13826 #
EGG-M-89488 ..... N91-14013 #
EGG-M-89489 ..... N91-13670 #
EGG-M-90048 ..... N91-13880 #
EGG-M-90086 ..... N91-13970 #
EGG-M-90309 ..... N91-13987 #
EGG-M-90376 ..... N91-13799 #
EGG-M-90380 ..... N91-13703 #
EGG-M-90394 ..... N91-13912 #
ESA-BR-69 ..... N91-14095 #
ESA-PSS-03-105-ISSUE-1 ..... N91-13897 #
ESA-SP-1131 ..... N91-14083 #
ESA-TT-1234 ..... N91-13827 #
ESA-TT-1244 ..... N91-13415 #
ESD-TR-90-026 ..... N91-13475 #
ESL-TR-716199-15 ..... N91-13428* #
ETDE/JP-MF-1715185 ..... N91-13579 #
ETN-90-97354 ..... N91-13536 #
ETN-90-97688 ..... N91-13785 #
ETN-90-97782 ..... N91-14094 #
ETN-90-97783 ..... N91-13717 #
ETN-90-97785 ..... N91-13615 #
ETN-90-97786 ..... N91-13616 #
ETN-90-97994 ..... N91-13897 #
ETN-90-98097 ..... N91-13905 #
ETN-90-98107 ..... N91-13964 #
ETN-90-98122 ..... N91-13954 #
ETN-91-98141 ..... N91-13786 #
ETN-91-98170 ..... N91-13564 #
ETN-91-98171 ..... N91-13965 #
ETN-91-98172 ..... N91-13663 #
ETN-91-98173 ..... N91-13627 #
ETN-91-98174 ..... N91-14027 #
ETN-91-98175 ..... N91-14065 #
ETN-91-98200 ..... N91-13960 #
ETN-91-98207 ..... N91-13916 #
ETN-91-98213 ..... N91-13728 #
ETN-91-98214 ..... N91-13628 #
ETN-91-98215 ..... N91-13889 #
ETN-91-98216 ..... N91-13629 #
ETN-91-98217 ..... N91-13708 #
ETN-91-98259 ..... N91-13827 #
ETN-91-98260 ..... N91-13415 #
ETN-91-98263 ..... N91-13768* #
ETN-91-98264 ..... N91-13769 #
ETN-91-98265 ..... N91-13416 #
ETN-91-98266 ..... N91-13801 #
ETN-91-98267 ..... N91-13417 #
ETN-91-98268 ..... N91-13770 #
ETN-91-98269 ..... N91-13771 #
ETN-91-98270 ..... N91-13448 #
ETN-91-98271 ..... N91-13772 #
ETN-91-98272 ..... N91-13567 #
ETN-91-98273 ..... N91-13528 #
ETN-91-98274 ..... N91-13529 #
ETN-91-98275 ..... N91-13530 #
ETN-91-98276 ..... N91-13531 #
ETN-91-98277 ..... N91-13921 #
ETN-91-98278 ..... N91-13922 #
ETN-91-98279 ..... N91-13891 #
ETN-91-98280 ..... N91-13600 #
ETN-91-98281 ..... N91-13828 #
ETN-91-98282 ..... N91-13923 #
ETN-91-98283 ..... N91-13924 #
ETN-91-98284 ..... N91-13601
ETN-91-98285 ..... N91-13632
ETN-91-98286 ..... N91-13633
ETN-91-98287 ..... N91-13925
ETN-91-98288 ..... N91-13602
ETN-91-98289 ..... N91-13603
ETN-91-98290 ..... N91-13604
ETN-91-98291 ..... N91-13634
ETN-91-98292 ..... N91-13635
ETN-91-98293 ..... N91-13605
ETN-91-98294 ..... N91-13747
ETN-91-98295 ..... N91-13748
ETN-91-98296 ..... N91-13450
ETN-91-98297 ..... N91-13606
ETN-91-98298 ..... N91-13871
ETN-91-98299 ..... N91-13636
ETN-91-98300 ..... N91-13607
ETN-91-98301 ..... N91-13892
ETN-91-98302 ..... N91-13838
ETN-91-98304 ..... N91-13431
ETN-91-98306 ..... N91-13468
ETN-91-98307 ..... N91-13872
ETN-91-98308 ..... N91-13873
ETN-91-98309 ..... N91-14003
ETN-91-98314 ..... N91-13789
ETN-91-98315 ..... N91-13874
ETN-91-98316 ..... N91-13608
ETN-91-98317 ..... N91-13881
ETN-91-98318 ..... N91-13790
ETN-91-98319 ..... N91-13840
ETN-91-98320 ..... N91-13791 #
ETN-91-98324 ..... N91-13471 #
ETN-91-98325 ..... N91-13738 #
ETN-91-98326 ..... N91-13733 #
ETN-91-98327 ..... N91-13740 #
ETN-91-98328 ..... N91-13532 #
ETN-91-98329 ..... N91-13504 #
ETN-91-98330 ..... N91-13741 #
ETN-91-98331 ..... N91-13917 #
ETN-91-98333 ..... N91-13742 #
ETN-91-98334 ..... N91-13583 #
ETN-91-98335 ..... N91-13533 #
ETN-91-98336 ..... N91-13749 #
ETN-91-98337 ..... N91-13775 #
ETN-91-98338 ..... N91-13776 #
ETN-91-98339 ..... N91-13664 #
ETN-91-98340 ..... N91-13630 #
ETN-91-98341 ..... N91-13665 #
ETN-91-98345 ..... N91-14083 #
ETN-91-98348 ..... N91-14095 #
ETN-91-98349 ..... N91-13666 #
ETN-91-98350 ..... N91-13918 #
ETN-91-98351 ..... N91-13919 #
ETN-91-98352 ..... N91-13947 #
ETN-91-98353 ..... N91-13948 #
ETN-91-98354 ..... N91-13961 #
ETN-91-98355 ..... N91-13920 #
ETN-91-98357 ..... N91-13426 #
ETN-91-98358 ..... N91-13427 #
ETN-91-98359 ..... N91-13667 #
ETN-91-98361 ..... N91-13829 #
ETN-91-98362 ..... N91-13451 #
ETN-91-98363 ..... N91-13472 #
ETN-91-98364 ..... N91-13882 #
ETN-91-98365 ..... N91-13777 #
ETN-91-98367 ..... N91-14085 #
ETN-91-98368 ..... N91-13505 #
ETN-91-98369 ..... N91-13672 #
ETN-91-98370 ..... N91-13926
ETN-91-98371 ..... N91-13968
ETN-91-98372 ..... N91-13568
ETN-91-98373 ..... N91-13868
ETN-91-98374 ..... N91-13883 #
ETN-91-98375 ..... N91-13884 #
ETN-91-98376 ..... N91-13778 #
ETN-91-98377 ..... N91-13974 #
ETN-91-98378 ..... N91-13975 #
ETN-91-98379 ..... N91-13839 #
ETN-91-98380 ..... N91-13423
ETN-91-98381 ..... N91-13418
ETN-91-98382 ..... N91-13984
ETN-91-98383 ..... N91-14272
ETN-91-98384 ..... N91-13816
ETN-91-98385 ..... N91-13830
ETN-91-98386 ..... N91-13963
ETN-91-98387 ..... N91-13927
FEL-89-A267 ..... N91-13747
FEL-89-A312 ..... N91-13748
FEL-89-A368 ..... N91-13450
FEL-89-B258 ..... N91-13601
FEL-89-B277-VOL-1 ..... N91-13632
FEL-89-B286 ..... N91-13633
FEL-89-B304 ..... N91-13925
FEL-89-B336 ..... N91-13602
FEL-90-A022 ..... N91-13606
FEL-90-A084 ..... N91-13871
FEL-90-A089 ..... N91-13636
FEL-90-A112 ..... N91-13607
FEL-90-A116 ..... N91-13892
FEL-90-A207 ..... N91-13838
FEL-90-B023 ..... N91-13603
FEL-90-B092 ..... N91-13604
FEL-90-B114 ..... N91-13634
FEL-90-B176 ..... N91-13635
FEL-1988-85 ..... N91-13605
FERMILAB-PUB-90/81-REV ..... N91-13976* #
FFA-TN-1988-21 ..... N91-13768* #
FFA-TN-1989-12 ..... N91-13769 #
FFA-TN-1989-47 ..... N91-13416 #
FFA-TN-1990-02 ..... N91-13801 #
FFA-TN-1990-21 ..... N91-13417 #
FFA-TN-1990-25 ..... N91-13770 #
FFA-TN-1990-28 ..... N91-13771 #
FFA-TN-1990-35 ..... N91-13448 #
FFA-TN-1990-40 ..... N91-13772 #
FFI-90/7010 ..... N91-13922 #
FFI-90/7012 ..... N91-13891 #
FFI-90/7016 ..... N91-13600 #
FFI-90/7017 ..... N91-13828 #
FFI-90/7022 ..... N91-13923 #
FFI-90/7023 ..... N91-13924 #
FOA-E-40045-4.5 ..... N91-13839 #
FR-19435-1 ..... N91-13486* #
FR-19540-1 ..... N91-13485* #
FR-19545-1 ..... N91-13487* #
FTD-ID(RS)T-0258-90 ..... N91-13454 #
GA-A-20094 ..... N91-13706 #
GA-A-20095 ..... N91-13705 #
GA-A-20097 ..... N91-14025 #
GA-A-20098 ..... N91-14024 #
GA-A-20105 ..... N91-14023 #
GA-A-20111 ..... N91-14022 #
GRI-90/0121 ..... N91-13507 #
H-1673 ..... N91-13460* #
H-1674 ..... N91-13453* #
HDL-TR-2185 ..... N91-14053* #
HEL-TN-6-90 ..... N91-13870 #
IAR-AN-66 ..... N91-13409 #
IC-AERO-89-02 ..... N91-13672 #
ICASE-90-65 ..... N91-13935* #
ICASE-90-68 ..... N91-13966* #
ICASE-90-76 ..... N91-13650* #
ICASE-90-77 ..... N91-13649* #
ICASE-90-78 ..... N91-13642* #
ICASE-90-79 ..... N91-13952* #
ICASE-90-80 ..... N91-13410* #
ICASE-90-82 ..... N91-13669* #
IFSI-89-21 ..... N91-14094 #
IFSI-89-22 ..... N91-13717 #
IFSI-90-2 ..... N91-13615 #
IFSI-90-3 ..... N91-13616 #
INPE-4540-PRE/1286 ..... N91-13586 #
INPE-4557-PRE/1298 ..... N91-13587 #
INPE-4558-PRE/1299 ..... N91-14077 #
INPE-4606-PRE/1329 ..... N91-14086 #
INPE-4612-PRE/1335 ..... N91-14078 #
INPE-5004-TDL/398 ..... N91-13825 #
INPE-5042-PRE/1575 ..... N91-13898 #
INPE-5079-TDL/413 ..... N91-13511 #
INPE-5117-TDL/419 ..... N91-13784 #
INPE-5119-TDL/421 ..... N91-13783 #
INPE-5121-TDL/422 ..... N91-13899 #
INPE-5122-TDL/423 ..... N91-14257 #

INT-PATENT-CLASS-G03H-1/02 ..... N91-13694*

IS-T-1409 ..... N91-13525 #
IS-T-1441 ..... N91-13516 #
IS-T-1442 ..... N91-13526 #
IS-T-1451 ..... N91-13518 #
IS-T-1495 ..... N91-14059 #

IS-23-284 ..... N91-13741 #
IS-24-288 ..... N91-13738 #
IS-25-062 ..... N91-13739 #
IS-25101 ..... N91-13532 #
IS-28843 ..... N91-13740 #

ISBN-0-904947-24-6 ..... N91-13426 #
ISBN-0-904947-26-2 ..... N91-13427 #
ISBN-92-835-0581-6 ..... N91-13488 #
ISBN-92-835-0583-2 ..... N91-14076 #
ISBN-92-835-0586-7 ..... N91-14030 #
ISBN-92-835-0587-5 ..... N91-13434 #
ISBN-92-835-0593-X ..... N91-13863 #
ISBN-92-9092-055-6 ..... N91-14095 #
ISBN-100-05-1131 ..... N91-14083 #
ISBN-951-38-3619-3 ..... N91-13567 #
ISBN-951-38-3706-8 ..... N91-13528 #
ISBN-951-38-3713-0 ..... N91-13529 #
ISBN-951-38-3714-9 ..... N91-13530 #
ISBN-951-38-3781-5 ..... N91-13531 #
ISBN-951-666-313-3 ..... N91-13921 #

ISSN-0065-3713 ..... N91-13816
ISSN-0143-7135 ..... N91-13868
ISSN-0143-7305 ..... N91-13926
ISSN-0143-7305 ..... N91-13968
ISSN-0169-1708 ..... N91-13790
ISSN-0169-1708 ..... N91-13840
ISSN-0169-2690 ..... N91-13905 #
ISSN-0169-2690 ..... N91-13964 #
ISSN-0171-1342 ..... N91-13415 #
ISSN-0171-1342 ..... N91-13827 #
ISSN-0281-9945 ..... N91-13839 #
ISSN-0308-7247 ..... N91-13672 #
ISSN-0343-7639 ..... N91-13536 #
ISSN-0355-2713 ..... N91-13921 #
ISSN-0358-5077 ..... N91-13528 #
ISSN-0358-5077 ..... N91-13529 #
ISSN-0358-5077 ..... N91-13530 #
ISSN-0358-5077 ..... N91-13531 #
ISSN-0358-5077 ..... N91-13567 #
ISSN-0379-4059 ..... N91-13897 #
ISSN-0379-6566 ..... N91-14083 #
ISSN-0802-2437 ..... N91-13600 #
ISSN-0802-2437 ..... N91-13828 #
ISSN-0802-2437 ..... N91-13923 #
ISSN-0802-2437 ..... N91-13924 #
ISSN-0959-2423 ..... N91-13568

ISVR-TR-171 ..... N91-13883 #
ISVR-TR-172 ..... N91-13884 #
ISVR-TR-182 ..... N91-13778 #
ISVR-TR-185 ..... N91-13974 #
ISVR-TR-187 ..... N91-13975 #

IZF-1989-53 ..... N91-13431
IZF-1989-57 ..... N91-13468
IZF-1989-58 ..... N91-13872
IZF-1989-59 ..... N91-13873
IZF-1990-A-9 ..... N91-14003
IZF-1990-A-19 ..... N91-13789
IZF-1990-B-3 ..... N91-13874
IZF-1990-B-4 ..... N91-13608
IZF-1990-B-5 ..... N91-13881

JPL-PUBL-87-4 ..... N91-13808* #
JPL-PUBL-88-27 ..... N91-13679* #
JPL-PUBL-89-17 ..... N91-14049* #
JPL-PUBL-90-10 ..... N91-13876* #
JPL-PUBL-90-12 ..... N91-13476* #

JPRS-ULS-89-011 ..... N91-13861 #

JUEL-SPEZ-550 ..... N91-13536 #

K/CSD/TM-88 ..... N91-13577 #

KMSF-U-2339 ..... N91-14026 #

KNMI-TR-123 ..... N91-13790
KNMI-TR-124 ..... N91-13840

L-16603 ..... N91-13432* #
L-16614 ..... N91-13433* #
L-16720 ..... N91-13400* #
L-16726 ..... N91-13750* #
L-16743 ..... N91-13402* #
L-16744 ..... N91-13751* #
L-16751 ..... N91-13401* #
L-16757 ..... N91-13462* #
L-16758 ..... N91-13473* #
L-16764 ..... N91-14251* #
L-16787 ..... N91-13461* #
L-16793 ..... N91-13985* #
L-16808 ..... N91-13522* #
L-16812 ..... N91-14265* #
L-16817 ..... N91-13492* #
L-16842 ..... N91-13406* #

LA-UR-90-2980 ..... N91-13743 #
LA-UR-90-3373 ..... N91-14070 #
LA-UR-90-3380 ..... N91-13582 #
LA-UR-90-3395 ..... N91-14264 #
LA-UR-90-3413 ..... N91-13573 #
LA-UR-90-3440 ..... N91-13626 #
LA-UR-90-3441 ..... N91-13988 #
LA-UR-90-3457 ..... N91-14015 #
LA-UR-90-3461 ..... N91-14270 #
LA-UR-90-3503 ..... N91-14258 #
LA-UR-90-3511 ..... N91-14010 #
LA-UR-90-3512 ..... N91-14009 #
LA-UR-90-3516 ..... N91-14008 #
LA-UR-90-3534 ..... N91-14014 #
LA-UR-90-3544 ..... N91-13490 #
LA-UR-90-3564 ..... N91-13701 #
LA-UR-90-3568 ..... N91-13624 #
LA-UR-90-3576 ..... N91-13620 #
LA-UR-90-3581 ..... N91-13682 #
LA-UR-90-3589 ..... N91-14011 #
LA-UR-90-3595 ..... N91-13631 #
LA-UR-90-3596 ..... N91-13702 #
LA-UR-90-3641 ..... N91-13700 #
LA-UR-90-3664 ..... N91-13957 #
LA-UR-90-3702 ..... N91-14069 #

LA-11799-MS ..... N91-13597 #
LA-11816-MS ..... N91-13662 #
LA-11900-MS ..... N91-13720 #
LA-11916-MS ..... N91-13764 #

LAAS-90146 ..... N91-13728 #
LAAS-90160 ..... N91-13628 #
LAAS-90192 ..... N91-13889 #
LAAS-90237 ..... N91-13629 #
LAAS-90277 ..... N91-13708 #

LBL-25619-PT-2 ..... N91-14073 #
LBL-28820 ..... N91-13982 #
LBL-28841 ..... N91-14068 #
LBL-29477 ..... N91-14060 #

LPI-CONTRIB-746 ..... N91-14099* #

LPI-TR-90-04 ..... N91-14252* #
LPI-TR-90-05 ..... N91-14098* #

LR-638 ..... N91-13791 #

MA-56 ..... N91-13921 #

MATHS-REPT-A-127 ..... N91-13666 #
MATHS-REPT-A-128 ..... N91-13918 #
MATHS-REPT-A-129 ..... N91-13919 #
MATHS-REPT-A-131 ..... N91-13947 #
MATHS-REPT-A-133 ..... N91-13948 #
MATHS-REPT-A-134 ..... N91-13961 #
MATHS-REPT-A-135 ..... N91-13920 #

MBB/FE122/S/PUB/397 ..... N91-13423
MBB/FE122/S/PUB/400 ..... N91-13418

MCAT-90-001 ..... N91-13639* #

MEMO-836 ..... N91-13905 #
MEMO-865 ..... N91-13964 #

MPI-PAE/EXP.EL-228 ..... N91-13984

NAS 1.15:4194 ..... N91-13400* #
NAS 1.15:4212 ..... N91-14251* #
NAS 1.15:4223 ..... N91-13432* #
NAS 1.15:4224 ..... N91-13462* #
NAS 1.15:4228 ..... N91-13433* #
NAS 1.15:4229 ..... N91-14265* #
NAS 1.15:4231 ..... N91-13473* #
NAS 1.15:4248 ..... N91-13406* #
NAS 1.15:101197 ..... N91-13637* #
NAS 1.15:101728 ..... N91-13460* #
NAS 1.15:101729 ..... N91-13453* #
NAS 1.15:102249 ..... N91-13862* #
NAS 1.15:102255 ..... N91-13762* #
NAS 1.15:102275 ..... N91-14087* #
NAS 1.15:102647 ..... N91-13467* #
NAS 1.15:102682 ..... N91-13585* #
NAS 1.15:102727 ..... N91-13761* #
NAS 1.15:102739 ..... N91-13941* #
NAS 1.15:102741 ..... N91-13445* #
NAS 1.15:102745 ..... N91-13411* #
NAS 1.15:102749 ..... N91-13412* #
NAS 1.15:102808 ..... N91-13466* #
NAS 1.15:102828 ..... N91-13652* #
NAS 1.15:102841 ..... N91-13653* #
NAS 1.15:102856 ..... N91-13408* #
NAS 1.15:102976 ..... N91-14271* #
NAS 1.15:103263 ..... N91-13638* #
NAS 1.15:103428 ..... N91-13413* #
NAS 1.15:103429 ..... N91-14053* #
NAS 1.15:103441 ..... N91-14079* #
NAS 1.15:103448 ..... N91-13575* #
NAS 1.15:103515 ..... N91-13766* #
NAS 1.15:103517 ..... N91-13910* #
NAS 1.15:103640 ..... N91-13455* #
NAS 1.15:103642 ..... N91-14259* #
NAS 1.15:103643 ..... N91-13495* #
NAS 1.15:103651 ..... N91-13456* #
NAS 1.15:103653 ..... N91-13491* #
NAS 1.15:103659 ..... N91-14050* #
NAS 1.15:103683 ..... N91-13457* #
NAS 1.15:103689 ..... N91-13420* #
NAS 1.15:103712 ..... N91-13421* #
NAS 1.21:7037(258) N91-13399*
NAS 1.26:4327 ..... N91-13463* #
NAS 1.26:4333 ..... N91-13991* #
NAS 1.26:4338 ..... N91-13737* #
NAS 1.26:4340 ..... N91-13930* #
NAS 1.26:177452 ..... N91-13424* #
NAS 1.26:177466 ..... N91-13972* #
NAS 1.26:180433 ..... N91-14088* #
NAS 1.26:181882 ..... N91-13447* #
NAS 1.26:182096-SUPPL-5 ..... N91-13651* #
NAS 1.26:182215 ..... N91-13804*
NAS 1.26:182323 ..... N91-13639* #
NAS 1.26:182453 ..... N91-13929* #
NAS 1.26:182851 ..... N91-13833* #
NAS 1.26:183198 ..... N91-13487* #
NAS 1.26:183200 ..... N91-13486* #
NAS 1.26:183201 ..... N91-13485* #
NAS 1.26:183617 ..... N91-13489* #
NAS 1.26:184028 ..... N91-13807* #
NAS 1.26:184030 ..... N91-13569* #
NAS 1.26:184032 ..... N91-13675* #
NAS 1.26:184033 ..... N91-13856* #
NAS 1.26:184040 ..... N91-13570* #
NAS 1.26:184043 ..... N91-13688* #
NAS 1.26:184045 ..... N91-13832* #
NAS 1.26:184052 ..... N91-13474* #
NAS 1.26:184994 ..... N91-13939* #
NAS 1.26:185349 ..... N91-14098* #
NAS 1.26:185354 ..... N91-13756* #
NAS 1.26:185355 ..... N91-14099* #
NAS 1.26:185394 ..... N91-13484* #
NAS 1.26:185717 ..... N91-13640* #
NAS 1.26:185901 ..... N91-13817* #
NAS 1.26:186105 ..... N91-13875* #
NAS 1.26:186467 ..... N91-13976* #
NAS 1.26:186610 ..... N91-13443* #
NAS 1.26:186625 ..... N91-13928* #
NAS 1.26:186713 ..... N91-14097* #
NAS 1.26:186725 ..... N91-13534* #
NAS 1.26:186726 ..... N91-13535* #
NAS 1.26:186793 ..... N91-14089* #
NAS 1.26:186877 ..... N91-13506* #
NAS 1.26:186916 ..... N91-13609* #
NAS 1.26:186922 ..... N91-13885* #
NAS 1.26:186941 ..... N91-13818* #
NAS 1.26:186945 ..... N91-13470* #
NAS 1.26:186962 ..... N91-13893* #
NAS 1.26:186986 ..... N91-13584* #
NAS 1.26:187013 ..... N91-13895* #
NAS 1.26:187015 ..... N91-13894* #
NAS 1.26:187021 ..... N91-13831* #
NAS 1.26:187022 ..... N91-13819* #
NAS 1.26:187049 ..... N91-13458* #
NAS 1.26:187239 ..... N91-13967* #
NAS 1.26:187318 ..... N91-13950* #
NAS 1.26:187319 ..... N91-13949* #
NAS 1.26:187320 ..... N91-13674* #
NAS 1.26:187334 ..... N91-13452* #
NAS 1.26:187346 ..... N91-14029* #
NAS 1.26:187348 ..... N91-14090* #
NAS 1.26:187351 ..... N91-14254* #
NAS 1.26:187357 ..... N91-14252* #
NAS 1.26:187358 ..... N91-14255* #
NAS 1.26:187361 ..... N91-13405* #
NAS 1.26:187362 ..... N91-13404* #
NAS 1.26:187363 ..... N91-14256* #
NAS 1.26:187374 ..... N91-13676* #
NAS 1.26:187376 ..... N91-13782* #
NAS 1.26:187377 ..... N91-13494* #
NAS 1.26:187394 ..... N91-13677* #

NAS 1.26:187411 ..... N91-13841* #
NAS 1.26:187414 ..... N91-13428* #
NAS 1.26:187422 ..... N91-13645* #
NAS 1.26:187423 ..... N91-13510* #
NAS 1.26:187426 ..... N91-13644* #
NAS 1.26:187429 ..... N91-13876* #
NAS 1.26:187430 ..... N91-13679* #
NAS 1.26:187431 ..... N91-14049* #
NAS 1.26:187432 ..... N91-13476* #
NAS 1.26:187441 ..... N91-13966* #
NAS 1.26:187444 ..... N91-13907* #
NAS 1.26:187451 ..... N91-13934* #
NAS 1.26:187452 ..... N91-13935* #
NAS 1.26:187460 ..... N91-13650* #
NAS 1.26:187461 ..... N91-13642* #
NAS 1.26:187462 ..... N91-13952* #
NAS 1.26:187465 ..... N91-13410* #
NAS 1.26:187467 ..... N91-13649* #
NAS 1.26:187476 ..... N91-13669* #
NAS 1.26:187636 ..... N91-13808* #
NAS 1.26:187646 ..... N91-13904* #
NAS 1.26:187647 ..... N91-13648* #
NAS 1.26:187650 ..... N91-14055* #
NAS 1.26:187653 ..... N91-13554* #
NAS 1.26:187656 ..... N91-13906* #
NAS 1.26:187658 ..... N91-13446* #
NAS 1.26:187666 ..... N91-13515* #
NAS 1.26:187667 ..... N91-13760* #
NAS 1.26:187668 ..... N91-13759* #
NAS 1.26:187669 ..... N91-13480* #
NAS 1.26:187673 ..... N91-13837* #
NAS 1.26:187674 ..... N91-13656* #
NAS 1.26:187676 ..... N91-13557* #
NAS 1.26:187678 ..... N91-13722* #
NAS 1.26:187679 ..... N91-13721* #
NAS 1.26:187689 ..... N91-13725* #
NAS 1.26:187704 ..... N91-13788* #
NAS 1.26:187705 ..... N91-13449* #
NAS 1.26:187706 ..... N91-13971* #
NAS 1.26:187713 ..... N91-13422* #
NAS 1.26:187722 ..... N91-13768* #
NAS 1.55:3084 ..... N91-14100* #
NAS 1.55:3094 ..... N91-13842* #
NAS 1.60:3010 ..... N91-13750* #
NAS 1.60:3026 ..... N91-13985* #
NAS 1.60:3034 ..... N91-13492* #
NAS 1.60:3035 ..... N91-13401* #
NAS 1.60:3044 ..... N91-13522* #
NAS 1.60:3047 ..... N91-13402* #
NAS 1.60:3049 ..... N91-13461* #
NAS 1.61:1239 ..... N91-13751* #
NAS 1.71:ARC-11916-1-SB ..... N91-14002* #
NAS 1.71:GSC-13127-1 ..... N91-13735* #
NAS 1.71:GSC-13175-1 ..... N91-14001* #
NAS 1.71:GSC-13230-1 ..... N91-13734* #
NAS 1.71:GSC-13240-1 ..... N91-13692* #
NAS 1.71:GSC-13265-1 ..... N91-14066* #
NAS 1.71:LAR-13780-1 ..... N91-13481* #
NAS 1.71:LAR-14027-1 ..... N91-13693* #
NAS 1.71:LAR-14036-1 ..... N91-13562* #
NAS 1.71:LAR-14088-1 ..... N91-13686* #
NAS 1.71:LAR-14163-1 ..... N91-13559* #
NAS 1.71:LAR-14239-1 ..... N91-13527* #
NAS 1.71:LAR-14271-1-CU ..... N91-13558* #
NAS 1.71:LAR-14330-1-CU ..... N91-13560* #
NAS 1.71:LAR-14340-1-CU ..... N91-13684* #
NAS 1.71:LAR-14351-1 ..... N91-13561* #
NAS 1.71:LAR-14419-1 ..... N91-13687* #
NAS 1.71:LEW-14162-1 ..... N91-13668* #
NAS 1.71:LEW-14731-1 ..... N91-13802* #
NAS 1.71:LEW-14862-1 ..... N91-13730* #
NAS 1.71:LEW-14878-1 ..... N91-13996* #
NAS 1.71:LEW-14902-1 ..... N91-13503* #
NAS 1.71:LEW-14921-1 ..... N91-13502* #
NAS 1.71:LEW-14945-1 ..... N91-13598* #
NAS 1.71:LEW-14959-1 ..... N91-13803* #
NAS 1.71:LEW-14965-1 ..... N91-13732* #
NAS 1.71:LEW-14967-1 ..... N91-13685* #
NAS 1.71:LEW-14999-1 ..... N91-13500* #
NAS 1.71:LEW-15027-1 ..... N91-13566* #
NAS 1.71:MFS-28013-2 ..... N91-14096* #
NAS 1.71:MFS-28295-1 ..... N91-13999* #
NAS 1.71:MFS-28328-1 ..... N91-13731* #
NAS 1.71:MFS-28406-1 ..... N91-13729* #
NAS 1.71:MFS-28419-1 ..... N91-13482* #
NAS 1.71:MSC-21381-1 ..... N91-13944* #
NAS 1.71:MSC-21416-1 ..... N91-14000* #
NAS 1.71:MSC-21460-1 ..... N91-13879* #
NAS 1.71:MSC-21481-1 ..... N91-13890* #
NAS 1.71:MSC-21500-1 ..... N91-13683* #
NAS 1.71:MSC-21509-1 ..... N91-13997* #
NAS 1.71:MSC-21536-1 ..... N91-13483* #
NAS 1.71:MSC-21549-1 ..... N91-13657* #
NAS 1.71:MSC-21559-1 ..... N91-13860* #
NAS 1.71:MSC-21585-1 ..... N91-13857* #
NAS 1.71:MSC-21671-1 ..... N91-13723* #
NAS 1.71:MSC-21675-1 ..... N91-13865* #
NAS 1.71:MSC-21703-1 ..... N91-13580* #
NAS 1.71:MSC-21737-1 ..... N91-13911* #
NAS 1.71:NPO-17479-1-CU ..... N91-13658* #
NAS 1.71:NPO-17784-1-CU ..... N91-13998* #
NAS 1.71:NPO-17800-1-CU ..... N91-13724* #
NAS 1.71:NPO-17806-1-CU ..... N91-13581* #
NAS 1.71:NPO-17896-1-CU ..... N91-13596* #
NAS 1.71:NPO-17904-1-CU ..... N91-13594* #
NAS 1.71:NPO-17914-1-CU ..... N91-13767* #
NAS 1.71:NPO-17922-1-CU ..... N91-13621* #
NAS 1.71:NPO-17937-1-CU ..... N91-13787* #
NAS 1.71:NPO-17941-1-CU ..... N91-13595* #
NAS 1.71:NPO-17997-1-CU ..... N91-13888* #
NAS 1.71:NPO-18034-1-CU ..... N91-13796* #
NAS 1.71:NPO-18075-1-CU ..... N91-13622* #
NAS 1.71:NPO-18101-1-CU ..... N91-13995* #
NAS 1.71:SSC-00006-1 ..... N91-13691* #
NAS 1.71:SSC-00008-1 ..... N91-13733* #
NASA-CASE-ARC-11916-1-SB ..... N91-14002* #
NASA-CASE-GSC-13127-1 ..... N91-13735* #
NASA-CASE-GSC-13175-1 ..... N91-14001* #
NASA-CASE-GSC-13230-1 ..... N91-13734* #
NASA-CASE-GSC-13240-1 ..... N91-13692* #
NASA-CASE-GSC-13265-1 ..... N91-14066* #
NASA-CASE-LAR-13780-1 ..... N91-13481* #
NASA-CASE-LAR-13989-1 ..... N91-13694*
NASA-CASE-LAR-14027-1 ..... N91-13693* #
NASA-CASE-LAR-14036-1 ..... N91-13562* #
NASA-CASE-LAR-14088-1 ..... N91-13686* #
NASA-CASE-LAR-14163-1 ..... N91-13559* #
NASA-CASE-LAR-14239-1 ..... N91-13527* #
NASA-CASE-LAR-14271-1-CU ..... N91-13558* #
NASA-CASE-LAR-14330-1-CU ..... N91-13560* #
NASA-CASE-LAR-14340-1-CU ..... N91-13684* #
NASA-CASE-LAR-14351-1 ..... N91-13561* #
NASA-CASE-LAR-14419-1 ..... N91-13687* #
NASA-CASE-LEW-14162-1 ..... N91-13668* #
NASA-CASE-LEW-14731-1 ..... N91-13802* #
NASA-CASE-LEW-14862-1 ..... N91-13730* #
NASA-CASE-LEW-14878-1 ..... N91-13996* #
NASA-CASE-LEW-14902-1 ..... N91-13503* #
NASA-CASE-LEW-14921-1 ..... N91-13502* #
NASA-CASE-LEW-14945-1 ..... N91-13598* #
NASA-CASE-LEW-14959-1 ..... N91-13803* #
NASA-CASE-LEW-14965-1 ..... N91-13732* #
NASA-CASE-LEW-14967-1 ..... N91-13685* #
NASA-CASE-LEW-14999-1 ..... N91-13500* #
NASA-CASE-LEW-15027-1 ..... N91-13566* #
NASA-CASE-MFS-28013-2 ..... N91-14096* #
NASA-CASE-MFS-28295-1 ..... N91-13999* #
NASA-CASE-MFS-28328-1 ..... N91-13731* #
NASA-CASE-MFS-28406-1 ..... N91-13729* #
NASA-CASE-MFS-28419-1 ..... N91-13482* #
NASA-CASE-MSC-21381-1 ..... N91-13944* #
NASA-CASE-MSC-21416-1 ..... N91-14000* #
NASA-CASE-MSC-21460-1 ..... N91-13879* #
NASA-CASE-MSC-21481-1 ..... N91-13890* #
NASA-CASE-MSC-21500-1 ..... N91-13683* #
NASA-CASE-MSC-21509-1 ..... N91-13997* #
NASA-CASE-MSC-21536-1 ..... N91-13483* #
NASA-CASE-MSC-21549-1 ..... N91-13657* #
NASA-CASE-MSC-21559-1 ..... N91-13860* #
NASA-CASE-MSC-21585-1 ..... N91-13857* #
NASA-CASE-MSC-21671-1 ..... N91-13723* #
NASA-CASE-MSC-21675-1 ..... N91-13865* #
NASA-CASE-MSC-21703-1 ..... N91-13580* #
NASA-CASE-MSC-21737-1 ..... N91-13911* #
NASA-CASE-NPO-17479-1-CU ..... N91-13658* #
NASA-CASE-NPO-17784-1-CU ..... N91-13998* #
NASA-CASE-NPO-17800-1-CU ..... N91-13724* #
NASA-CASE-NPO-17806-1-CU ..... N91-13581* #
NASA-CASE-NPO-17896-1-CU ..... N91-13596* #
NASA-CASE-NPO-17904-1-CU ..... N91-13594* #
NASA-CASE-NPO-17914-1-CU ..... N91-13767* #
NASA-CASE-NPO-17922-1-CU ..... N91-13621* #
NASA-CASE-NPO-17937-1-CU ..... N91-13787* #
NASA-CASE-NPO-17941-1-CU ..... N91-13595* #
NASA-CASE-NPO-17997-1-CU ..... N91-13888* #
NASA-CASE-NPO-18034-1-CU ..... N91-13796* #
NASA-CASE-NPO-18075-1-CU ..... N91-13622* #
NASA-CASE-NPO-18101-1-CU ..... N91-13995* #
NASA-CASE-SSC-00006-1 ..... N91-13691* #
NASA-CASE-SSC-00008-1 ..... N91-13733* #
NASA-CP-3084 ..... N91-14100* #
NASA-CP-3094 ..... N91-13842* #
NASA-CR-4327 ..... N91-13463* #
NASA-CR-4333 ..... N91-13991* #
NASA-CR-4338 ..... N91-13737* #
NASA-CR-4340 ..... N91-13930* #
NASA-CR-177452 ..... N91-13424* #
NASA-CR-177466 ..... N91-13972* #
NASA-CR-180433 ..... N91-14088* #
NASA-CR-181882 ..... N91-13447* #
NASA-CR-182096-SUPPL-5 ..... N91-13651* #
NASA-CR-182215 ..... N91-13804*
NASA-CR-182323 ..... N91-13639* #
NASA-CR-182453 ..... N91-13929* #
NASA-CR-182851 ..... N91-13833* #
NASA-CR-183198 ..... N91-13487* #
NASA-CR-183200 ..... N91-13486* #
NASA-CR-183201 ..... N91-13485* #
NASA-CR-183617 ..... N91-13489* #
NASA-CR-184028 ..... N91-13807* #
NASA-CR-184030 ..... N91-13569* #
NASA-CR-184032 ..... N91-13675* #
NASA-CR-184033 ..... N91-13856* #
NASA-CR-184040 ..... N91-13570* #
NASA-CR-184043 ..... N91-13688* #
NASA-CR-184045 ..... N91-13832* #
NASA-CR-184052 ..... N91-13474* #
NASA-CR-184994 ..... N91-13939* #
NASA-CR-185349 ..... N91-14098* #
NASA-CR-185354 ..... N91-13756* #
NASA-CR-185355 ..... N91-14099* #
NASA-CR-185394 ..... N91-13484* #
NASA-CR-185717 ..... N91-13640* #
NASA-CR-185901 ..... N91-13817* #
NASA-CR-186105 ..... N91-13875* #
NASA-CR-186467 ..... N91-13976* #
NASA-CR-186610 ..... N91-13443* #
NASA-CR-186625 ..... N91-13928* #
NASA-CR-186713 ..... N91-14097* #
NASA-CR-186725 ..... N91-13534* #
NASA-CR-186726 ..... N91-13535* #
NASA-CR-186793 ..... N91-14089* #
NASA-CR-186877 ..... N91-13506* #
NASA-CR-186916 ..... N91-13609* #
NASA-CR-186922 ..... N91-13885* #
NASA-CR-186941 ..... N91-13818* #
NASA-CR-186945 ..... N91-13470* #
NASA-CR-186962 ..... N91-13893* #
NASA-CR-186986 ..... N91-13584* #
NASA-CR-187013 ..... N91-13895* #
NASA-CR-187015 ..... N91-13894* #
NASA-CR-187021 ..... N91-13831* #
NASA-CR-187022 ..... N91-13819* #
NASA-CR-187049 ..... N91-13458* #
NASA-CR-187239 ..... N91-13967* #
NASA-CR-187318 ..... N91-13950* #
NASA-CR-187319 ..... N91-13949* #
NASA-CR-187320 ..... N91-13674* #
NASA-CR-187334 ..... N91-13452* #
NASA-CR-187346 ..... N91-14029* #
NASA-CR-187348 ..... N91-14090* #
NASA-CR-187351 ..... N91-14254* #
NASA-CR-187357 ..... N91-14252* #
NASA-CR-187358 ..... N91-14255* #
NASA-CR-187361 ..... N91-13405* #
NASA-CR-187362 ..... N91-13404* #
NASA-CR-187363 ..... N91-14256* #
NASA-CR-187374 ..... N91-13676* #
NASA-CR-187376 ..... N91-13782* #
NASA-CR-187377 ..... N91-13494* #
NASA-CR-187394 ..... N91-13677* #
NASA-CR-187411 ..... N91-13841* #
NASA-CR-187414 ..... N91-13428* #
NASA-CR-187422 ..... N91-13645* #
NASA-CR-187423 ..... N91-13510* #
NASA-CR-187426 ..... N91-13644* #
NASA-CR-187429 ..... N91-13876* #
NASA-CR-187430 ..... N91-13679* #
NASA-CR-187431 ..... N91-14049* #
NASA-CR-187432 ..... N91-13476* #
NASA-CR-187441 ..... N91-13966* #
NASA-CR-187444 ..... N91-13907* #
NASA-CR-187451 ..... N91-13934* #
NASA-CR-187452 ..... N91-13935* #
NASA-CR-187460 ..... N91-13650* #
NASA-CR-187461 ..... N91-13642* #
NASA-CR-187462 ..... N91-13952* #
NASA-CR-187465 ..... N91-13410* #
NASA-CR-187467 ..... N91-13649* #
NASA-CR-187476 ..... N91-13669* #
NASA-CR-187636 ..... N91-13808* #
NASA-CR-187646 ..... N91-13904* #
NASA-CR-187647 ..... N91-13648* #
NASA-CR-187650 ..... N91-14055* #
NASA-CR-187653 ..... N91-13554* #
NASA-CR-187656 ..... N91-13906* #
NASA-CR-187658 ..... N91-13446* #
NASA-CR-187666 ..... N91-13515* #

NASA-CR-187667 ..... N91-13760* #
NASA-CR-187668 ..... N91-13759* #
NASA-CR-187669 ..... N91-13480* #
NASA-CR-187673 ..... N91-13837* #
NASA-CR-187674 ..... N91-13656* #
NASA-CR-187676 ..... N91-13557* #
NASA-CR-187678 ..... N91-13722* #
NASA-CR-187679 ..... N91-13721* #
NASA-CR-187689 ..... N91-13725* #
NASA-CR-187704 ..... N91-13788* #
NASA-CR-187705 ..... N91-13449* #
NASA-CR-187706 ..... N91-13971* #
NASA-CR-187713 ..... N91-13422* #
NASA-CR-187722 ..... N91-13768* #

NASA-RP-1239 ..... N91-13751* #

NASA-SP-7037(258) N91-13399*

NASA-TM-4194 ..... N91-13400* #
NASA-TM-4212 ..... N91-14251* #
NASA-TM-4223 ..... N91-13432* #
NASA-TM-4224 ..... N91-13462* #
NASA-TM-4228 ..... N91-13433* #
NASA-TM-4229 ..... N91-14265* #
NASA-TM-4231 ..... N91-13473* #
NASA-TM-4248 ..... N91-13406* #
NASA-TM-101197 ..... N91-13637* #
NASA-TM-101728 ..... N91-13460* #
NASA-TM-101729 ..... N91-13453* #
NASA-TM-102249 ..... N91-13862* #
NASA-TM-102255 ..... N91-13762* #
NASA-TM-102275 ..... N91-14087* #
NASA-TM-102647 ..... N91-13467* #
NASA-TM-102682 ..... N91-13585* #
NASA-TM-102727 ..... N91-13761* #
NASA-TM-102739 ..... N91-13941* #
NASA-TM-102741 ..... N91-13445* #
NASA-TM-102745 ..... N91-13411* #
NASA-TM-102749 ..... N91-13412* #
NASA-TM-102808 ..... N91-13466* #
NASA-TM-102828 ..... N91-13652* #
NASA-TM-102841 ..... N91-13653* #
NASA-TM-102856 ..... N91-13408* #
NASA-TM-102976 ..... N91-14271* #
NASA-TM-103263 ..... N91-13638* #
NASA-TM-103428 ..... N91-13413* #
NASA-TM-103429 ..... N91-14053* #
NASA-TM-103441 ..... N91-14079* #
NASA-TM-103448 ..... N91-13575* #
NASA-TM-103515 ..... N91-13766* #
NASA-TM-103517 ..... N91-13910* #
NASA-TM-103640 ..... N91-13455* #
NASA-TM-103642 ..... N91-14259* #
NASA-TM-103643 ..... N91-13495* #
NASA-TM-103651 ..... N91-13456* #
NASA-TM-103653 ..... N91-13491* #
NASA-TM-103659 ..... N91-14050* #
NASA-TM-103683 ..... N91-13457* #
NASA-TM-103689 ..... N91-13420* #
NASA-TM-103712 ..... N91-13421* #

NASA-TP-3010 ..... N91-13750* #
NASA-TP-3026 ..... N91-13985* #
NASA-TP-3034 ..... N91-13492* #
NASA-TP-3035 ..... N91-13401* #
NASA-TP-3044 ..... N91-13522* #
NASA-TP-3047 ..... N91-13402* #
NASA-TP-3049 ..... N91-13461* #

NAVY-CASE-71636 ..... N91-13711 #
NAVY-CASE-72449 ..... N91-13886 #
NAVY-CASE-72787 ..... N91-13716 #

NIKHEF-K/AMPS/90-01 ..... N91-13471 #

NOAA-TM-ERL-NSSL-101 ..... N91-13834 #

NOSC/TD-1881 ..... N91-13903 #

NPL-DES-99 ..... N91-13926
NPL-DES-101 ..... N91-13968

NPL-DMM(A)-8 ..... N91-13568

NPL-RS(EXT)-109 ..... N91-13868

NPS52-90-018 ..... N91-13940 #
NPS69-90-05 ..... N91-13758 #

NRC-32132 ..... N91-13409 #

NRL-MR-6677 ..... N91-13588 #
NRL-MR-6681 ..... N91-14005 #
NRL-MR-6704 ..... N91-13512 #

NTSB/AAR-90/05 ..... N91-13425 #

ONREUR-ESNIB-90-04 ..... N91-13610 #

ORNL-TM-11643 ..... N91-13574 #

ORNL/ATD-44 ..... N91-13681 #

ORNL/FTR-3783 ..... N91-13556 #
ORNL/FTR-3787 ..... N91-13812 #
ORNL/FTR-3800 ..... N91-14082 #

ORNL/M-1248 ..... N91-13555 #

ORNL/TM-11619 ..... N91-13810 #
ORNL/TM-11622 ..... N91-13718 #
ORNL/TM-11634 ..... N91-13931 #
ORNL/TM-11667 ..... N91-14072 #
ORNL/TM-11669 ..... N91-13959 #

PB90-215773 ..... N91-13610 #
PB90-251224 ..... N91-14262 #
PB90-251232 ..... N91-14263 #
PB90-252560 ..... N91-13507 #
PB90-253584 ..... N91-13834 #
PB90-256306 ..... N91-13820 #
PB90-258799 ..... N91-14260 #
PB90-258807 ..... N91-14261 #
PB90-910405 ..... N91-13425 #

PD-ST-8917 ..... N91-13673 #

PEI-994 ..... N91-13675* #

RADC-TR-89-229 ..... N91-14052 #
RADC-TR-90-137 ..... N91-13612 #
RADC-TR-90-139 ..... N91-13613 #
RADC-TR-90-155 ..... N91-13589 #
RADC-TR-90-158 ..... N91-13614 #
RADC-TR-90-257 ..... N91-13901 #

RAE-FM-6 ..... N91-13882 #

RAE-MAT/STR-259 ..... N91-13451 #
RAE-MAT/STR-288 ..... N91-13777 #

RAE-SS-11 ..... N91-13472 #

RAE-TM-SP-376 ..... N91-13829 #

RAE-TR-89046 ..... N91-13451 #
RAE-TR-90018 ..... N91-13472 #
RAE-TR-90019 ..... N91-13882 #
RAE-TR-90033 ..... N91-13777 #

RARDE-1/90 ..... N91-13505 #

REPT-90-006 ..... N91-13963
REPT-90-027 ..... N91-13927
REPT-023921-1-F ..... N91-13817* #
REPT-025921-16-T ..... N91-13893* #

RFP-4218 ..... N91-13727 #
RFP-4253 ..... N91-13757 #

RSRE-90008 ..... N91-14085 #

RUU-CS-89-12 ..... N91-13954 #

SAE-901928 ..... N91-13460* #

SAF/AQT-SR-90-013 ..... N91-14079* #

SAND-90-0179C ..... N91-13413* #
SAND-90-0884C ..... N91-13800 #
SAND-90-0957C ..... N91-13773 #
SAND-90-1064C ..... N91-13745 #
SAND-90-1587C ..... N91-13419 #
SAND-90-1725C ..... N91-13625 #
SAND-90-1779C ..... N91-13806 #
SAND-90-1911C ..... N91-14056 #
SAND-90-1978C ..... N91-13736 #
SAND-90-2440C ..... N91-13977 #
SAND-90-2494C ..... N91-13617 #
SAND-90-2549C ..... N91-13980 #
SAND-90-2553C ..... N91-13521 #
SAND-90-2597C ..... N91-13795 #
SAND-90-2598C ..... N91-13793 #
SAND-90-2730C ..... N91-13990 #

SERI/TP-211-3934 ..... N91-13792 #
SERI/TP-253-3594 ..... N91-13809 #
SERI/TP-257-3983 ..... N91-13414 #

SGD-549-PT-1 ..... N91-14262 #
SGD-549-PT-2 ..... N91-14263 #

SGD-550-PT-1 ..... N91-14260 #
SGD-550-PT-2 ..... N91-14261 #

SRS/STD-TR90-89 ..... N91-13474* #

SU-TR-13 ..... N91-13513 #

TAMURF-AERO-90-5-1 ..... N91-13479 #

TD-89-0345 ..... N91-13605
TD-89-3867 ..... N91-13747
TD-89-3869 ..... N91-13633
TD-89-3870 ..... N91-13925
TD-89-3875 ..... N91-13601
TD-89-3879-VOL-1 ..... N91-13632
TD-89-4466 ..... N91-13450
TD-89-4551 ..... N91-13431
TD-89-4555 ..... N91-13468
TD-89-4556 ..... N91-13872
TD-89-4557 ..... N91-13873
TD-89-4573 ..... N91-13602
TD-89-4578 ..... N91-13748
TD-90-0018 ..... N91-13874
TD-90-0022 ..... N91-14003
TD-90-0029 ..... N91-13608
TD-90-0033 ..... N91-13881
TD-90-0046 ..... N91-13606
TD-90-1224 ..... N91-13871
TD-90-1227 ..... N91-13604
TD-90-1229 ..... N91-13636
TD-90-1230 ..... N91-13634
TD-90-1234 ..... N91-13892
TD-90-1609 ..... N91-13789
TD-90-1714 ..... N91-13607
TD-90-1726 ..... N91-13635
TD-90-2483 ..... N91-13838
TD-90-2780 ..... N91-13603

TELAC-90-19 ..... N91-13446* #

TR-9 ..... N91-13551 #
TR-18-ONR ..... N91-13553 #
TR-90-33C ..... N91-13953 #
TR-882 ..... N91-13475 #
TR-27824 ..... N91-13712 #

TT-9009 ..... N91-13426 #
TT-9011 ..... N91-13427 #

TWR-60119-REV-A ..... N91-13675* #
TWR-60189 ..... N91-13570* #
TWR-60551 ..... N91-13569* #

UCB-PTH-90/10 ..... N91-14068 #

UCLA-ENG-88-28 ..... N91-13645* #

UCRL-CR-104524 ..... N91-13689 #
UCRL-CR-104625 ..... N91-13697 #
UCRL-CR-105109 ..... N91-14020 #

UCRL-ID-103856 ..... N91-13704 #
UCRL-ID-104374 ..... N91-13709 #
UCRL-ID-104835 ..... N91-13501 #
UCRL-ID-104836 ..... N91-13680 #
UCRL-ID-104890 ..... N91-13726 #
UCRL-ID-105132 ..... N91-13914 #
UCRL-ID-105222 ..... N91-14016 #

UCRL-JC-103281 ..... N91-14021 #
UCRL-JC-103354 ..... N91-13698 #
UCRL-JC-103458 ..... N91-13699 #
UCRL-JC-103502 ..... N91-13623 #
UCRL-JC-103798 ..... N91-13619 #
UCRL-JC-103816 ..... N91-14004 #
UCRL-JC-103870 ..... N91-13499 #
UCRL-JC-104150 ..... N91-14007 #
UCRL-JC-104433 ..... N91-13520 #
UCRL-JC-104448 ..... N91-13945 #
UCRL-JC-104691 ..... N91-13962 #
UCRL-JC-104869 ..... N91-13707 #
UCRL-JC-104938 ..... N91-13978 #
UCRL-JC-104969 ..... N91-14063 #
UCRL-JC-104971 ..... N91-13690 #
UCRL-JC-104991 ..... N91-13981 #
UCRL-JC-105024 ..... N91-13765 #
UCRL-JC-105200 ..... N91-13599 #
UCRL-JC-105217 ..... N91-13915 #
UCRL-JC-105225 ..... N91-13815 #
UCRL-JC-106057 ..... N91-14269 #
UCRL-JC-106088 ..... N91-13956 #

UCRL-MA-104860 ..... N91-13908 #
UCRL-MA-104861 ..... N91-13593 #

UCRL-51444-88/89 ..... N91-13780 #

UCSD-90-1041 ..... N91-13929* #

UPITT/LRDC/ONR/KUL-90-04 ..... N91-13951 #

US-PATENT-APPL-SN-193612 ..... N91-13735* #
US-PATENT-APPL-SN-252486 ..... N91-13887
US-PATENT-APPL-SN-317776 ..... N91-13860* #
US-PATENT-APPL-SN-318217 ..... N91-13694*
US-PATENT-APPL-SN-414816 ..... N91-13730* #
US-PATENT-APPL-SN-418372 ..... N91-13562* #
US-PATENT-APPL-SN-431538 ..... N91-13482* #
US-PATENT-APPL-SN-458065 ..... N91-13731* #
US-PATENT-APPL-SN-458258 ..... N91-13683* #
US-PATENT-APPL-SN-458476 ..... N91-13483* #
US-PATENT-APPL-SN-481013 ..... N91-13888* #
US-PATENT-APPL-SN-489997 ..... N91-13691* #
US-PATENT-APPL-SN-493190 ..... N91-13787* #
US-PATENT-APPL-SN-493529 ..... N91-13857* #
US-PATENT-APPL-SN-495969 ..... N91-13803* #
US-PATENT-APPL-SN-501893 ..... N91-13668* #
US-PATENT-APPL-SN-503408 ..... N91-13999* #
US-PATENT-APPL-SN-503486 ..... N91-13802* #
US-PATENT-APPL-SN-506136 ..... N91-13890* #
US-PATENT-APPL-SN-506636 ..... N91-14001* #
US-PATENT-APPL-SN-507264 ..... N91-13711 #
US-PATENT-APPL-SN-507553 ..... N91-13657* #
US-PATENT-APPL-SN-522949 ..... N91-13724* #
US-PATENT-APPL-SN-524110 ..... N91-13729* #
US-PATENT-APPL-SN-531373 ..... N91-14002* #
US-PATENT-APPL-SN-531374 ..... N91-13734* #
US-PATENT-APPL-SN-531433 ..... N91-13685* #
US-PATENT-APPL-SN-540976 ..... N91-13598* #
US-PATENT-APPL-SN-544293 ..... N91-13594* #
US-PATENT-APPL-SN-545177 ..... N91-14000* #
US-PATENT-APPL-SN-545178 ..... N91-13733* #
US-PATENT-APPL-SN-545220 ..... N91-14096* #
US-PATENT-APPL-SN-545235 ..... N91-13944* #
US-PATENT-APPL-SN-550775 ..... N91-13595* #
US-PATENT-APPL-SN-551103 ..... N91-13886 #
US-PATENT-APPL-SN-552670 ..... N91-13686* #
US-PATENT-APPL-SN-554509 ..... N91-13716 #
US-PATENT-APPL-SN-555864 ..... N91-13527* #
US-PATENT-APPL-SN-555865 ..... N91-13622* #
US-PATENT-APPL-SN-560691 ..... N91-13596* #
US-PATENT-APPL-SN-560717 ..... N91-13559* #
US-PATENT-APPL-SN-560908 ..... N91-13581* #
US-PATENT-APPL-SN-560924 ..... N91-13997* #
US-PATENT-APPL-SN-560926 ..... N91-13500* #
US-PATENT-APPL-SN-562095 ..... N91-13865* #
US-PATENT-APPL-SN-567025 ..... N91-13558* #
US-PATENT-APPL-SN-568127 ..... N91-13658* #
US-PATENT-APPL-SN-568128 ..... N91-13560* #
US-PATENT-APPL-SN-568129 ..... N91-13998* #
US-PATENT-APPL-SN-568130 ..... N91-13796* #
US-PATENT-APPL-SN-571058 ..... N91-13503* #
US-PATENT-APPL-SN-571059 ..... N91-13502* #
US-PATENT-APPL-SN-571062 ..... N91-13732* #
US-PATENT-APPL-SN-571344 ..... N91-13692* #
US-PATENT-APPL-SN-575694 ..... N91-14066* #
US-PATENT-APPL-SN-575695 ..... N91-13684* #
US-PATENT-APPL-SN-575697 ..... N91-13767* #
US-PATENT-APPL-SN-575737 ..... N91-13481* #
US-PATENT-APPL-SN-584018 ..... N91-13687* #
US-PATENT-APPL-SN-587880 ..... N91-13693* #
US-PATENT-APPL-SN-587919 ..... N91-13879* #
US-PATENT-APPL-SN-587921 ..... N91-13996* #
US-PATENT-APPL-SN-587922 ..... N91-13911* #
US-PATENT-APPL-SN-589571 ..... N91-13561* #
US-PATENT-APPL-SN-596133 ..... N91-13995* #
US-PATENT-APPL-SN-596139 ..... N91-13621* #
US-PATENT-APPL-SN-603052 ..... N91-13580* #
US-PATENT-APPL-SN-603055 ..... N91-13586* #
US-PATENT-APPL-SN-603337 ..... N91-13723* #

US-PATENT-CLASS-350-3.64 ..... N91-13694*
US-PATENT-CLASS-350-320 ..... N91-13694*
US-PATENT-CLASS-350-354 ..... N91-13694*
US-PATENT-CLASS-505-1 ..... N91-13887

US-PATENT-4,913,534 ..... N91-13694*
US-PATENT-4,943,556 ..... N91-13887

USAAVSCOM-TM-89-A-003 ..... N91-13762* #

USAAVSCOM-TR-90-D-15A ..... N91-13444 #

USAF-STINFO-CONTRIB-90/7 ..... N91-14079* #

USAFSAM-TR-90-7 ..... N91-13864 #

UTSA-DOE/ME-1 ..... N91-13554* #

VTT-RR-678 ..... N91-13567 #
VTT-RR-685 ..... N91-13528 #
VTT-RR-691 ..... N91-13529 #
VTT-RR-692 ..... N91-13530 #
VTT-RR-699 ..... N91-13531 #

WINCO-1080 ..... N91-13719 #

WRDC-TR-89-4133 ..... N91-13524 #
WRDC-TR-90-3037-VOL-1 ..... N91-13477 #
WRDC-TR-90-3037-VOL-3 ..... N91-13478 #

WSRC-MS-90-158 ..... N91-13655 #

WSRC-RP-89-959 ..... N91-13774 #
WSRC-RP-90-186 ..... N91-14084 #

Appendix

NASA SCIENTIFIC AND TECHNICAL INFORMATION PROGRAM PRODUCTS AND SERVICES

The NASA Scientific and Technical Information (STI) program provides for the collection and announcement of aerospace-related reports and literature obtained worldwide through agreements and exchanges. The result of the collection is the comprehensive NASA STI Database that covers aeronautics, space, and supporting disciplines.

The STI Database, documents generated or obtained by NASA, and products and services derived from or supporting the database are made available to the NASA research community and to the public. Descriptions and sources of these items are presented in the following pages.

Scientific and Technical Aerospace Reports (*STAR*) is an abstract journal, listing citations with abstracts for aerospace-related reports obtained from worldwide sources. *STAR* is issued on the 8th and 23rd of each month and announces current documents that have been entered into the NASA STI Database during the previous two weeks. The reports are of the following types:

- NASA, NASA contractor, and NASA grantee reports;
- Reports issued by other U.S. Government agencies, domestic and foreign institutions, universities, and private firms;
- Translations in report form;
- NASA-owned patents and patent applications;
- Other U.S. Government agency and foreign patents and patent applications;
- Domestic and foreign dissertations and theses.

Journal, book, and conference literature, journal translations, and certain foreign dissertations having the same subject scope as *STAR* are announced in a companion journal, *International Aerospace Abstracts* (*IAA*). *IAA* is issued on the 1st and 15th of each month and is available from the American Institute of Aeronautics and Astronautics, Technical Information Service, 555 West 57th Street, 12th Floor, New York, NY 10019.

ELIGIBILITY AND REGISTRATION FOR NASA STI PRODUCTS AND SERVICES

Organizations of the type listed below that have registered with NASA can receive products and services.

- NASA offices and installations, contractors, subcontractors, grantees, and consultants;
- Other U.S. Government agencies and their contractors;
- Libraries in the United States that have arrangements with NASA to maintain collections of NASA documents for public reference;
- Other organizations in the United States having a need for NASA documents in work related to aeronautics and space research;
- Organizations abroad that have established reciprocal documents exchange arrangements with NASA.

Only the central service points or central points of document acquisition and control within qualified organizations are eligible to register for NASA STI products and services. Domestic organizations that may be eligible to receive various classes of NASA publications and services should address their requests for registration or further information to:

NASA Scientific and Technical Information Facility
ATTN: Registration Services
P.O. Box 8757
BWI Airport, MD 21240
301-621-0153

Organizations abroad should direct requests to:

National Aeronautics and Space Administration
Director, Scientific and Technical Information Divison
Code NTT
Washington, DC 20546
USA
703-271-5640

SUBJECT SCOPE

The subject scope of *STAR* and *IAA* includes all aspects of aeronautics and space research and development, supporting basic and applied research, and applications. Aerospace aspects of Earth resources, energy development, conservation, oceanography, environmental protection, urban transportation, and other topics of high national priority are also covered.

HOW TO USE *STAR* SUBJECT CATEGORIES

Abstracts in *STAR* are categorized by 10 major subject divisions that are divided further into 76 specific subject categories. The subject divisions and categories are listed in the Table of Contents together with a note for each that defines its scope and provides any cross-references. For example:

16 SPACE TRANSPORTATION
Includes passenger and cargo space transportation, e.g., shuttle operations; and space rescue techniques. For related information see also *03 Air Transportation and Safety* and *18 Spacecraft Design, Testing and Performance.* For space suits see *54 Man/System Technology and Life Support.*

CROSS-REFERENCES

Individual *STAR* abstracts are not ordinarily cross-referenced, except for certain conference reports or book translations that have had separate abstracts written for their component papers or chapters. Citations and abstracts of the components follow immediately after those of the parent document. When the subject content of a component differs sufficiently from the general content of the parent, a cross-reference citation also is printed at the end of the category to which it normally would have been assigned if it were independent.

DOCUMENTS ON MICROFICHE

Documents available on microfiche are designated by a pound sign (#) following the accession number.

LIMITED REPRODUCIBILITY

A note of limited reproducibility appears in the citation, if there are factors affecting the reproducibility of more than 20% of the document. These factors include faint or broken type, color photographs, black and white photographs, foldouts, dot matrix print, or some other factor that limits the reproducibility of the document. This notation also appears on the microfiche header with the specific factor checked off on a list visible in the second frame.

COLOR COPIES

An increasing number of NASA scientific and technical reports are being produced with color graphs, charts, illustrations, and photographs. An indication that a document has color pages follows the source and pricing (SAP) information in the *STAR* citation.

Registered users of the NASA Scientific and Technical Information Program will receive ordered documents with color at no additional cost, as long as stock copies of the document are available. Otherwise, an additional fee of $2.00 per color page will be charged. The NASA STI Facility staff will contact registered users to determine individual user's needs.

NASA PATENTS AND PATENT APPLICATIONS

Patents and patent applications owned by NASA are announced in *STAR* under appropriate subject categories and are referenced in the *STAR* indexes. In the Report/Accession Number Index, patents are indexed by the NASA Case Number, and the U.S. Patent Class. Patent applications are indexed by the NASA Case Number and the U.S. Patent Application Serial Number.

Printed copies of patents (which are not microfiched) are available for purchase from the U.S. Patent and Trademark Office.

NASA patent application specifications are sold in both paper copy and microfiche by the National Technical Information Service (NTIS). The US-Patent-Appl-SN-number should be used in ordering either paper copy or microfiche from NTIS.

When ordering patents, the U.S. Patent Number should be used, and payment must be remitted in advance, by money order or check payable to the Commissioner of Patents and Trademarks. Prepaid purchase coupons for ordering are also available from the U.S. Patent and Trademark Office.

The patents and patent applications announced in *STAR* are owned by NASA and are available for royalty-free licensing. Requests for licensing terms and further information should be addressed to:

National Aeronautics and Space Administration
Associate General Counsel for Intellectual Property
Code GP
Washington, DC 20546

SOURCES FOR DOCUMENTS

One or more sources from which a document announced in *STAR* is available to the public is given in each citation. The most commonly indicated sources and their acronyms or abbreviations are listed on page A-6. If the publication is available from a source other than those listed, the publisher and address will be displayed on the availability line or in combination with the corporate source line.

Avail: NTIS. Sold by the National Technical Information Service. Prices for hard copy (HC) and microfiche (MF) are indicated by a price code following the letters HC or MF in the *STAR* citation. Current values for the price codes are given in the tables on page A-7.

Initially distributed microfiche under the NTIS SRIM (Selected Research in Microfiche) is available at greatly reduced unit prices. For this service and for information concerning subscription to NASA printed reports, consult the NTIS Subscription Section, Springfield, VA 22161.

NOTE ON ORDERING DOCUMENTS: When ordering NASA publications (those followed by the * symbol), use the N accession number. NASA patent applications (only the specifications are offered) should be ordered by the US-Patent-Appl-SN number. Non-NASA publications (no asterisk) should be ordered by the AD, PB, or other *report number* shown on the last line of the citation, not by the N accession number. It is also advisable to cite the title and other bibliographic identification.

Avail: SOD (or GPO). Sold by the Superintendent of Documents, U.S. Government Printing Office, in hard copy. The current price and order number are given following the availability line. (NTIS will fill microfiche requests, as indicated above, for those documents identified by a # symbol.)

Avail: BLL (formerly NLL): British Library Lending Division, Boston Spa, Wetherby, Yorkshire, England. Photocopies available from this organization at the price shown. (If none is given, address inquiry to the BLL.)

Avail: DOE Depository Libraries. Organizations in U.S. cities and abroad that maintain collections of Department of Energy reports, usually in microfiche form, are listed in *Energy Research Abstracts.* Services available from the DOE and its depositories are described in a booklet, *DOE Technical Information Center - Its Functions and Services* (TID-4660), which may be obtained without charge from the DOE Technical Information Center.

Avail: ESDU. Pricing information on specific data, computer programs, and details on Engineering Sciences Data Unit (ESDU) topic categories can be obtained from ESDU International Ltd. Requesters in North America should use the Virginia address while all other requesters should use the London address, both of which are on page A-6.

Avail: Fachinformationszentrum, Karlsruhe. Sold by the Fachinformationszentrum Energie, Physik, Mathematik GMBH, Eggenstein Leopoldshafen, Federal Republic of Germany, at the price shown in deutschmarks (DM).

Avail: HMSO. Publications of Her Majesty's Stationery Office are sold in the U.S. by Pendragon House, Inc. (PHI), Redwood City, CA. The U.S. price (including a service and mailing charge) is given, or a conversion table may be obtained from PHI.

Avail: NASA Public Document Rooms. Documents so indicated may be examined at or purchased from the National Aeronautics and Space Administration, Public Documents Room (Room 126), 600 Independence Ave., S.W., Washington, DC 20546, or public document rooms located at NASA installations, and the NASA Pasadena Office at the Jet Propulsion Laboratory.

Avail: Univ. Microfilms. Documents so indicated are dissertations selected from *Dissertation Abstracts* and are sold by University Microfilms as xerographic copy (HC) and microfilm. All requests should cite the author and the Order Number as they appear in the citation.

Avail: US Patent and Trademark Office. Sold by Commissioner of Patents and Trademarks, U.S. Patent and Trademark Office, at the standard price of $1.50 each, postage free. (See discussion of NASA patents and patent applications below.)

Avail: (US Sales Only). These foreign documents are available to users within the United States from the National Technical Information Service (NTIS). They are available to users outside the United States through the International Nuclear Information Service (INIS) representative in their country, or by applying directly to the issuing organization.

Avail: USGS. Originals of many reports from the U.S. Geological Survey, which may contain color illustrations, or otherwise may not have the quality of illustrations preserved in the microfiche or facsimile reproduction, may be examined by the public at the libraries of the USGS field offices whose addresses are listed on page A-6. The libraries may be queried concerning the availability of specific documents and the possible utilization of local copying services, such as color reproduction.

Avail: Issuing Activity, or Corporate Author, or no indication of availability. Inquiries as to the availability of these documents should be addressed to the organization shown in the citation as the corporate author of the document.

PUBLIC COLLECTIONS OF NASA DOCUMENTS

DOMESTIC: NASA and NASA-sponsored documents and a large number of aerospace publications are available to the public for reference purposes at the library maintained by the American Institute of Aeronautics and Astronautics, Technical Information Service, 555 West 57th Street, 12th Floor, New York, NY 10019.

EUROPEAN: An extensive collection of NASA and NASA-sponsored publications is maintianed by the British Library Lending Divison, Boston Spa, Wetherby, Yorkshire, England, for public access. The British Library Lending Division also has available many of the non-NASA publications cited in *STAR.*

European requesters may purchase facsimile copy or microfiche of NASA and NASA-sponsored documents, those identified by both the symbols # and * from ESA—Information Retrieval Service, European Space Agency, 8-10 rue Mario-Nikis, 75738 Paris CEDEX 15, France.

FEDERAL DEPOSITORY LIBRARIES: To provide the general public with greater access to U.S. Government publications, Congress established the Federal Depository Library Program under the Government Printing Office (GPO), with 51 regional depositories responsible for permanent retention of material, inter-library loan, and reference services. (These libraries are not sales outlets.) At least one copy of nearly every NASA and NASA-sponsored publication, either in printed or microfiche format, is received and retained by the 51 regional depositories. A list of the regional GPO libraries, appears on page A-8. A local library can contact a regional depository library to help locate specific reports, or direct contact may be made by an individual.

SUBMITTING DOCUMENTS

All users of this abstract service are urged to forward reports to be considered for announcement in *STAR.* This will aid NASA in its efforts to provide the fullest possible coverage of all scientific and technical publications that might support aeronautics and space research and development. If you have prepared relevant reports (other than those you will transmit to NASA, DOD, or DOE through the usual contract- or grant-reporting channels), please send them for consideration to the NASA Scientific and Technical Information Facility, P.O. Box 8757, BWI Airport, MD 21240.

Reprints of journal articles, book chapters, and conference papers are also welcome. These will be considered for announcement in *STAR*'s companion journal, *IAA.*

You may specify a particular source to be included in a report announcement if you wish; otherwise the report will be placed on a public sale at the National Technical Information Service. Copyrighted publications will be announced but not distributed or sold.

PURCHASE OF *STAR*

STAR is publicly available on annual subscription from the Superintendent of Documents, U.S. Government Printing Office, Washington, DC 20402.

STAR is available to registered users on annual subscription from the NASA Scientific and Technical Information Facility, ATTN: Registration Services, P.O. Box 8757, BWI Airport, MD 21240.

Microfiche of the abstract sections of *STAR* are available, on annual subscription only, from NTIS as PB91-911300, Attn: Subscriptions, 5285 Port Royal Road, Springfield, VA 22161. Annual subscription rates are $85.00 North America; $170.00 foreign. Abstract sections for previous years retroactive to 1964 are available at the current rates.

ADDRESSES OF ORGANIZATIONS

American Institute of Aeronautics and Astronautics
Technical Information Service
555 West 57th Street, 12th Floor
New York, New York 10019

British Library Lending Division,
Boston Spa, Wetherby, Yorkshire,
England

Commissioner of Patents and Trademarks
U.S. Patent and Trademark Office
Washington, DC 20231

Department of Energy
Technical Information Center
P.O. Box 62
Oak Ridge, Tennessee 37830

European Space Agency-Information Retrieval Service
ESRIN
Via Galileo Galilei
00044 Frascati (Rome) Italy

Engineering Sciences Data Unit International
P.O. Box 1633
Manassas, Virginia 22110

Engineering Sciences Data Unit International, Ltd.
251-259 Regent Street
London, W1R 7AD, England

Fachinformationszentrum Energie, Physik, Mathematik GMBH
7514 Eggenstein Leopoldshafen
Federal Republic of Germany

Her Majesty's Stationery Office
P.O. Box 569, S.E. 1
London, England

NASA Scientific and Technical Information Facility
P.O. Box 8757
BWI Airport, Maryland 21240

National Aeronautics and Space Administration
Scientific and Technical Information Division (NTT)
Washington, DC 20546

National Technical Information Service
5285 Port Royal Road
Springfield, Virginia 22161

Pendragon House, Inc.
899 Broadway Avenue
Redwood City, California 94063

Superintendent of Documents
U.S. Government Printing Office
Washington, DC 20402

University Microfilms
A Xerox Company
300 North Zeeb Road
Ann Arbor, Michigan 48106

University Microfilms, Ltd.
Tylers Green
London, England

U.S. Geological Survey Library National Center MS 950
12201 Sunrise Valley Drive
Reston, Virginia 22092

U.S. Geological Survey Library
2255 North Gemini Drive
Flagstaff, Arizona 86001

U.S. Geological Survey
345 Middlefield Road
Menlo Park, California 94025

U.S. Geological Survey Library
Box 25046
Denver Federal Center, MS914
Denver, Colorado 80225

NTIS PRICE SCHEDULES

(Effective January 1, 1991)

Schedule A
STANDARD PRICE DOCUMENTS AND MICROFICHE**

PRICE CODE	NORTH AMERICAN PRICE	FOREIGN PRICE
A01	$ 8.00	$ 16.00
A02	11.00	22.00
A03	15.00	30.00
A04-A05	17.00	34.00
A06-A09	23.00	46.00
A10-A13	31.00	62.00
A14-A17	39.00	78.00
A18-A21	45.00	90.00
A22-A25	53.00	106.00
A99	*	*
N01	60.00	120.00
N02	59.00	118.00
N03	20.00	40.00

Schedule E
EXCEPTION PRICE DOCUMENTS AND MICROFICHE**

PRICE CODE	NORTH AMERICAN PRICE	FOREIGN PRICE
E01	$10.00	$ 20.00
E02	12.00	24.00
E03	14.00	28.00
E04	16.50	33.00
E05	18.50	37.00
E06	21.50	43.00
E07	24.00	48.00
E08	27.00	54.00
E09	29.50	59.00
E10	32.50	65.00
E11	35.00	70.00
E12	38.50	77.00
E13	41.00	82.00
E14	45.00	90.00
E15	48.50	97.00
E16	53.00	106.00
E17	57.50	115.00
E18	62.00	124.00
E19	69.00	138.00
E20	80.00	160.00
E99	*	*

* Contact NTIS for price quote.

** Effective January 1, 1991, the microfiche copy of any new document entering the NTIS collection will be priced the same as the paper copy of the document.

IMPORTANT NOTICE

NTIS Shipping and Handling Charges

U.S., Canada, Mexico — ADD $3.00 per TOTAL ORDER

All Other Countries — ADD $4.00 per TOTAL ORDER

Exceptions — Does NOT apply to:

ORDERS REQUESTING NTIS RUSH HANDLING

ORDERS FOR SUBSCRIPTION OR STANDING ORDER PRODUCTS *ONLY*

NOTE: Each additional delivery address on an order requires a separate shipping and handling charge.

FEDERAL REGIONAL DEPOSITORY LIBRARIES

ALABAMA

AUBURN UNIV. AT MONTGOMERY LIBRARY
Documents Department
Montgomery, AL 36193
(205) 279-9110 ext.253

UNIV. OF ALABAMA LIBRARY
Reference Department/Documents
Box S
Tuscaloosa, AL 35486
(205) 348-6046

ARIZONA

DEPT. OF LIBRARY, ARCHIVES, AND PUBLIC RECORDS
Third Floor State Capitol
1700 West Washington
Phoenix, AZ 85007
(602) 255-4121

ARKANSAS

ARKANSAS STATE LIBRARY
Documents Service Section
One Capitol Mall
Little Rock, AR 72201
(501) 371-2090

CALIFORNIA

CALIFORNIA STATE LIBRARY
Govt. Publications Section
914 Capitol Mall
Sacramento, CA 95814
(916) 322-4572

COLORADO

UNIV. OF COLORADO
Norlin Library
Government Publications Division
Campus Box 184
Boulder, CO 80309
(303) 492-8834

DENVER PUBLIC LIBRARY
Govt. Pub. Department
1357 Broadway
Denver, CO 80203
(303) 571-2346

CONNECTICUT

CONNECTICUT STATE LIBRARY
231 Capitol Avenue
Hartford, CT 06106
(203) 566-4971

FLORIDA

UNIV. OF FLORIDA LIBRARIES
Documents Department
Library West
Gainesville, FL 32611
(904) 392-0367

GEORGIA

UNIV. OF GEORGIA LIBRARIES
Government Documents Dept.
Athens, GA 30602
(404) 542-8949

HAWAII

UNIV. OF HAWAII
Hamilton Library
Government Documents Collection
2550 The Mall
Honolulu, HI 96822
(808) 948-8230

IDAHO

UNIV. OF IDAHO LIBRARY
Documents Section
Moscow, ID 83843
(208) 885-6344

ILLINOIS

ILLINOIS STATE LIBRARY
Federal Documents
Centennial Building
Springfield, IL 62756
(217) 782-5012

INDIANA

INDIANA STATE LIBRARY
Serials Section
140 North Senate Avenue
Indianapolis, IN 46204
(317) 232-3686

IOWA

UNIV. OF IOWA LIBRARIES
Government Publications Dept.
Iowa City, IA 52242
(319) 335-5926

KANSAS

UNIVERSITY OF KANSAS
Spencer Research Library
Government Documents
Lawrence, KS 66045
(913) 864-4662

KENTUCKY

UNIV. OF KENTUCKY LIBRARIES
Government Publications/Maps Dept.
Lexington, KY 40506
(606) 257-8400

LOUISIANA

LOUISIANA STATE UNIVERSITY
Middleton Library
Government Documents Dept.
Baton Rouge, LA 70803
(504) 388-2570

LOUISIANA TECHNICAL UNIV.
Prescott Memorial Library
Government Documents Dept.
Ruston, LA 71272
(318) 257-4962

MAINE

UNIVERSITY OF MAINE
Raymond H. Fogler Library
Govt. Documents & Microforms Dept.
Orono, ME 04469
(207) 581-1680

MARYLAND

UNIVERSITY OF MARYLAND
McKeldin Library
Documents/Maps Room
College Park, MD 20742
(301) 454-3034

MASSACHUSETTS

BOSTON PUBLIC LIBRARY
Government Documents Dept.
666 Boylston Street
Boston, MA 02117
(617) 536-5400 ext.226

MICHIGAN

DETROIT PUBLIC LIBRARY
5201 Woodward Avenue
Detroit, MI 48202
(313) 833-1409

LIBRARY OF MICHIGAN
Government Documents
P.O. Box 30007
735 E. Michigan Avenue
Lansing, MI 48909
(517) 373-1593

MINNESOTA

UNIVERSITY OF MINNESOTA
Wilson Library
Government Publications
309 Nineteenth Avenue South
Minneapolis, MN 55455
(612) 373-7813

MISSISSIPPI

UNIV. OF MISSISSIPPI LIB.
Government Documents Dept.
106 Old Gym Bldg.
University, MS 38677
(601) 232-5857

MISSOURI

University of Missouri at Columbia Library
Government Documents
Columbia, MO 65201
(314) 882-6733

MONTANA

UNIV. OF MONTANA
Mansfield Library
Documents Division
Missoula, MT 59812
(406) 243-6700

NEBRASKA

UNIVERSITY OF NEBRASKA - LINCOLN
Love Memorial Library
Documents Department
Lincoln, NE 68588
(402) 472-2562

NEVADA

UNIV. OF NEVADA-RENO LIB.
Govt. Pub. Department
Reno, NV 89557
(702) 784-6579

NEW JERSEY

NEWARK PUBLIC LIBRARY
U.S. Documents Division
5 Washington Street
P.O. Box 630
Newark, NJ 07101
(201) 733-7812

NEW MEXICO

UNIVERSITY OF NEW MEXICO
General Library
Government Publications/Maps Dept.
Albuquerque, NM 87131
(505) 277-5441

NEW MEXICO STATE LIBRARY
325 Don Gaspar Avenue
Santa Fe, NM 87501
(505) 827-3826

NEW YORK

NEW YORK STATE LIBRARY
Documents Sect. Cultural Educ. Ctr.
Empire State Plaza
Albany, NY 12230
(518) 474-5563

NORTH CAROLINA

UNIVERSITY OF NORTH CAROLINA AT CHAPEL HILL
Davis Library 080A
BA/SS Department Documents
Chapel Hill, NC 27514
(919) 962-1151

NORTH DAKOTA

NORTH DAKOTA STATE UNIVERSITY LIBRARY
Government Documents Dept.
Fargo, ND 58105
(701) 237-8352
In cooperation with Univ. of North Dakota, Chester Fritz Library
Grand Forks

OHIO

STATE LIBRARY OF OHIO
Documents Section
65 South Front Street
Columbus, OH 43266
(614) 644-7051

OKLAHOMA

OKLAHOMA DEPT. OF LIBRARIES
Government Documents
200 NE 18th Street
Oklahoma City, OK 73105
(405) 521-2502, ext. 252

OKLAHOMA STATE UNIV. LIB.
Documents Department
Stillwater, OK 74078
(405) 624-0489

OREGON

PORTLAND STATE UNIV.
Millar Library
934 SW Harrison - P.O. Box 1151
Portland, OR 97207
(503) 229-3673

PENNSYLVANIA

STATE LIBRARY OF PENN.
Government Publications Section
Box 1601
Walnut St. & Commonwealth Ave.
Harrisburg, PA 17105
(717) 787-3752

SOUTH CAROLINA

CLEMSON UNIV. COOPER LIB.
Documents Department
Clemson, SC 29634
(803) 656-5174
In cooperation with Univ. of South Carolina, Thomas Cooper Library, Columbia

TEXAS

TEXAS STATE LIBRARY
Public Services Department
P.O. Box 12927 - 1201 Brazos
Austin, TX 78711
(512) 463-5455

TEXAS TECH. UNIV. LIBRARY
Documents Department
Lubbock, TX 79409
(806) 742-2268

UTAH

UTAH STATE UNIVERSITY
Merrill Library & Learning Resources Center, UMC-30
Documents Department
Logan, UT 84322
(801) 750-2682

VIRGINIA

UNIVERSITY OF VIRGINIA
Alderman Library
Government Documents
Charlottesville, VA 22903
(804) 924-3133

WASHINGTON

WASHINGTON STATE LIBRARY
Document Section
Olympia, WA 98504
(206) 753-4027

WEST VIRGINIA

WEST VIRGINIA UNIV. LIB.
Government Documents Section
P.O. Box 6069
Morgantown, WV 26506
(304) 293-3640

WISCONSIN

ST. HIST SOC. OF WISCONSIN LIB.
Government Pub. Section
816 State Street
Madison, WI 53706
(608) 262-2781
In cooperation with Univ. of Wisconsin-Madison, Memorial Library

MILWAUKEE PUBLIC LIBRARY
Documents Division
814 West Wisconsin Avenue
Milwaukee, WI 53233
(414) 278-3065

WYOMING

WYOMING STATE LIBRARY
Supreme Court & Library Bldg.
Cheyenne, WY 82002
(307) 777-5919

TYPICAL CITATION AND ABSTRACT

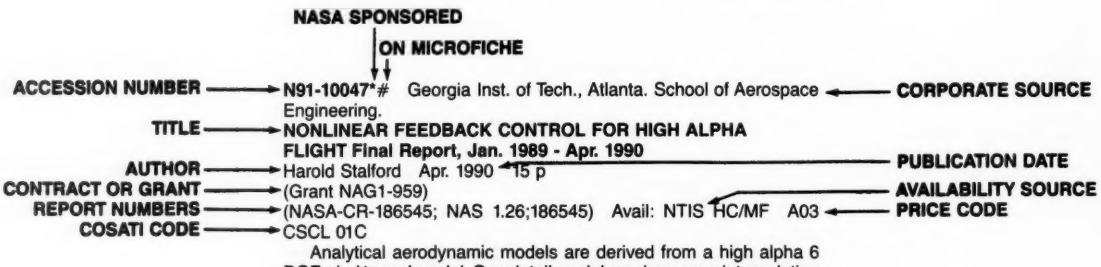

Analytical aerodynamic models are derived from a high alpha 6 DOF wind tunnel model. One detail model requires some interpolation between nonlinear functions of alpha. One analytical model requires no interpolation and as such is a completely continuous model. Flight path optimization is conducted on the basic maneuvers: half-loop, 90 degree pitch-up, and level turn. The optimal control analysis uses the derived analytical model in the equations of motion and is based on both moment and force equations. The maximum principle solution for the half-loop is poststall trajectory performing the half-loop in 13.6 seconds. The agility induced by thrust vectoring capability provided a minimum effect on reducing the maneuver time. By means of thrust vectoring control the 90 degrees pitch-up maneuver can be executed in a small place over a short time interval. The agility capability of thrust vectoring is quite beneficial for pitch-up maneuvers. The level turn results are based currently on only outer layer solutions of singular pertrubation. Poststall solutions provide high turn rates but generate higher losses of energy than that of classical sustained solutions.

Author

National Aeronautics and
Space Administration
Code NTT
Washington, D.C.
20546
Official Business
Penalty for Private Use, $300

SPECIAL FOURTH-CLASS RATE
POSTAGE & FEES PAID
NASA
PERMIT No. G27

POSTMASTER: If Undeliverable (Section 158
Postal Manual) Do Not Return